

AIAA Student Design / Build / Fly Competition

**California Polytechnic State University,
San Luis Obispo**

presents

The Lisa B

CAL POLY

Design Report - Proposal Phase

Designed and Developed by:

**Jonathan Chapman
David House
Julio Hurtado
Joon Kim
Jann Mayer
Jeff Napier
Chad Ward**

March 13, 2000

DISTRIBUTION STATEMENT A
Approved for Public Release
Distribution Unlimited

DTIC QUALITY INSPECTED 4

20001101 019

Table of Contents

Table of Contents	ii
1.0 Executive Summary	1
1.1 Overview	1
1.2 Design Tools	1
1.2.1 AutoCAD R14	1
1.2.2 Microsoft Excel	2
1.2.3 Electri-Calc	2
1.2.4 <u>Theory of Wing Sections</u>	2
1.2.5 <u>Summary of Low-Speed Airfoil Data, Volume 3</u>	2
1.2.6 Daily Journal	2
1.2.7 <u>Fundamentals of Flight</u>	2
1.2.8 <u>Flight Stability and Automatic Control</u>	2
2.0 Management Summary	3
2.1 Team Members	3
2.2 Publicity for the Cal Poly Design/Build/Fly Team	4
2.3 Timeline for The Lisa B	5
<i>Figure 2.1 – Timeline</i>	5
3.0 Conceptual Design	6
3.1 Alternative Concepts Investigated	6
3.2 Analytical Methods	6
3.3 Figures of Merit	7
3.4 Selection of Final Design	7
<i>Table 3.1 – Conceptual Figures of Merit</i>	8
<i>Table 3.2 Estimated Score Based on Payload Capacity</i>	8
4.0 Preliminary Design Processes	9
4.1 Wing	9
4.2 Cargo Bay	10
4.3 Tail Section	10
4.4 Power Plant	11
4.5 Landing Gear	11
4.6 Figures of Merit	12
<i>Table 4.1 – Airfoil Comparisons from <u>Theory of Wing Sections</u></i>	13
<i>Table 4.2 – Airfoil Comparisons from <u>Summary of Low-Speed Airfoil Data, Volume 3</u></i>	13
<i>Table 4.3 – Flap Performance Data</i>	13
<i>Table 4.4 – Motor Comparison</i>	13
<i>Figure 4.1 - Characteristics of the SG6043 Airfoil (Main Wing)</i>	14
<i>Figure 4.2 - Characteristics of the E387 Airfoil (Horizontal Stabilizer)</i>	14
5.0 Detail Design	15
5.1 Flight Performance	15
5.1.1 Take-Off	15
5.1.2 Cruise	15
5.2 Electrical Components	16
5.2.1 Control Systems	16
5.2.2 Power Plant	16
5.3 Structural Details	17

5.3.1 Structure and Component Testing	17
5.3.2 Tail Section	18
5.3.3 Cargo Bay	18
5.3.4 Landing Gear	18
5.4 Stability Analysis	19
Table 5.1 – Take-Off Performance	19
Table 5.2 – Climb To Cruise Performance	19
Table 5.3 – Performance in 180° Turn	19
Table 5.4 – Cruise Performance	20
Table 5.5 – Results of Stability Calculations	20
Figure 5.1 – General Layout	21
Figure 5.2 – Fuselage Structure	22
Figure 5.3 – Bulkheads	23
Figure 5.4 – Wings	24
Figure 5.5 – Spar Construction	25
Figure 5.6 – Tail Structure	26
Figure 5.7 – Joiner and Landing Gear	27
Figure 5.8 – Systems Layout	28
6.0 Manufacturing Plan	29
6.1 Figures of Merit	29
6.2 Manufacturing Processes	31
6.2.1 Fuselage Construction	31
6.2.2 Joiner Construction	31
6.2.3 Wing Spar Construction	32
6.2.4 Wing Construction	32
6.2.5 Stabilizer Construction	32
6.2.6 Landing Gear Construction	33
6.2.7 Motor Mount	33
Table 6.1 – Manufacturing Figures of Merit	34
Figure 6.1 – Manufacturing Timeline	35
7.0 Bibliography	36

Appendix A – Optimizations Calculations and Scoring Estimates

Appendix B - Performance Equations

Appendix C - Performance Calculations

1.0 Executive Summary

1.1 Overview

The rules for the current Design/Build/Fly Competition presented a new spin on previous years. The 1998-99 competition had a simple goal for each entry; carry as much cargo as possible. This year, with the addition of two empty "ferry laps", the rules added an important design consideration; make the plane faster. Top designs from last year were pure heavy lifting airframes with large wing surfaces, or bi-planes with extremely large total wing areas. The wing span restriction on the current competition also demonstrated that more payload capacity might not be the key to a higher overall score. For the empty lap where high speed is the objective, high lifting airfoils and multiple wings create too much drag, overall causing more harm than good. The decision for a low wing aircraft came from the loading and unloading process that must take place during the competition. A high wing design would probably have blocked access to the cargo. On R/C aircraft, contrary to popular belief, a low-wing design is not less stable than a high-wing design; and in spite of the slightly better stability of a high-wing, the low-wing design worked better for this competition.

After studying the top design from last year, a decision was made on how much water The Lisa B should carry. Initially, five liters was chosen based on the idea that more weight would drain battery power too quickly, resulting in fewer laps. After additional calculations of the aircraft's performance, it was decided that more weight could be carried without excess power consumption. As a result, the cargo bay needed to be re-designed. Three separate non-load-bearing cargo bay hatches were built to accommodate different payload volumes. With this design, the amount of cargo carried during the loaded laps may be changed based on remaining battery power. For example, on the first lap The Lisa B might carry eight liters, and then on the second and third laps, she could carry seven and six liters, respectively. The three different cargo bay hatches can accommodate cargos of five, six, seven, or eight liters.

1.2 Design Tools

Throughout the design process, many design tools were used for all the different aspects of the airplane, from the structural design and analysis to the flight performance data.

1.2.1 AutoCAD R14

The structural details of The Lisa B were compiled using *AutoCAD R14*. Full-scale plots from this program were used to visualize every detail of the plane during construction. As one unfortunate team learned last year, lack of a detailed, step-by-step layout of the plane can cause confusion during construction. A master design gave each member a clear image of the completed airframe and also prevented the design from straying far from the original. *AutoCAD R14* made it easy to correct design errors, and to build additional parts identical to the original.

1.2.2 Microsoft Excel

All the performance data for the aircraft was compiled and optimized on a custom *Excel* spreadsheet designed by members of the team. This spreadsheet took into account every flight characteristic of the airplane, from wing efficiency and drag to power usage and flight time.

1.2.3 Electri-Calc

The program *Electri-Calc* (*E-Calc*) was used to find the most efficient combination of batteries, motor, and propeller size. Combined with the *Excel* spreadsheet, *E-Calc* helped determine the power that would be consumed in each part of the mission. Given the number of cells, prop size, and type of motor, the program can estimate thrust available, current draw, and battery life.

1.2.4 Theory of Wing Sections

In selecting an airfoil the team first used the book, Theory of Wing Sections. This book was produced by NACA and is based on experimental wind tunnel tests. This was desirable because the team found that the airfoil programs *PANDA* and *VuFOIL* were inaccurate at certain levels because they are based on inviscid, linear theory, not wind tunnel data. A problem arose when the team realized that all the data in Theory of Wing Sections was based on high Reynolds numbers. This left the team without any useful data, since The Lisa B will operate at low Reynolds numbers.

1.2.5 Summary of Low-Speed Airfoil Data, Volume 3

After an internet search, the team discovered a book from the University of Illinois that contained useful data. This particular volume specialized in low speed airfoils. The team analyzed many airfoils including some with data for different flap deflection angles. This flap data was then used on an airfoil that would be useful for the design of The Lisa B.

1.2.6 Daily Journal

By far the most helpful design tool the team used was a daily journal maintained by one of the team members. The journal was used every day to document discussions and the results of research. It recorded accomplishments of each day, as well as changes made to the design. With this book the team was able to accurately keep track of the meandering thought process. This saved the team from needlessly repeating discussions, kept track of design changes that were made, and helped recall design details for the writing of this report.

1.2.7 Fundamentals of Flight

When calculating the performance data, the team used equations and relationships out of this book. It is used in Cal Poly's aerodynamics courses and, thanks to these classes, each team member is familiar with its contents.

1.2.8 Flight Stability and Automatic Control

This textbook is part of the curriculum in the upper-level aircraft stability and control classes. It was used to predict the stability of The Lisa B during flight operations.

2.0 Management Summary

2.1 Team Members

Personnel assignments were based on each member's previous background. While all team members contributed in every aspect of the design, individual team members had certain strength that was best suited for positions described below

Jonathan "Slash" Chapman, an Aeronautical Engineering Senior, was team captain. Generally credited with putting the team together, he was responsible for organizing meetings, planning work schedules, motivating team members, and keeping everything pointed in the right direction. Jon was also chosen as the team's pilot because of his previous experience with remote-controlled aircraft.

Jann Mayer, an Aeronautical Engineering Senior, was the team's CAD man. Bringing experience from last year's DBF competition, he was a steady source of good ideas. Jann also has extensive knowledge in aerodynamics, which he applied very well to the project. His experience in solid works and CAD produced a very coherent plan that was easy to follow, resulting in a great airframe. Also a previous builder and flyer of gliders, his experience with balsa construction was indispensable.

David House, an Aeronautical Engineering Senior, was the performance guru. He used his knowledge of *Microsoft Excel* to produce several spreadsheets that catalogued every aspect of the airplane's mission. The weights and balances, wing efficiencies, power usage, appropriate speeds, and any other flight characteristic imaginable were calculated on his spreadsheets. His experience with missile design at Raytheon no doubt came in handy.

Jeff Napior, an Aeronautical Engineering Junior, was in all charge of all fundraising, advertising, and public relations. Jeff sent out over 50 letters to various companies asking for support. His acquisitions include donations from Northrop Grumman, X-Acto, AIAA Vandenberg Chapter, Bob Smith Industries, Superior Balsa, and many others. On top of that he produced a web page that tracked the progress of The Lisa B, as well as business cards to pass around campus to get our project known. With all this Jeff also kept a journal recording the team's progress. Lastly, he was the chief editor for the creation of the design report.

Chad Ward, an Aeronautical Engineering Senior, brought a lot of experience in controls and structures. He dreamed up many of the configuration ideas, as well as caught numerous mistakes in small details that the rest of the team had over-looked. Chad also brought perfectionism to the team that nobody could match. During construction, Chad spent many hours cutting out bulkheads and ribs to extremely small tolerances. Extra sanding was not required when Chad was doing the cutting because of his extremely accurate modeling. His preciseness helped the plane achieve all the design requirements.

Julio Hurtado and Joon Kim, Aeronautical Engineering Freshmen, helped a lot during the construction phase. Since their book knowledge was not extensive enough to help in the design process, they did all they could to help out in construction. They put up with Jon's

strict time schedules and a lot of upper-classmen telling them what to do. They were also helpful in pointing out things that an overblown "Aero Ego" can overlook.

All the team members helped with construction. Jonathan, Jann, David, Julio, Jeff, and Chad gave up their entire winter break to stay at school and make this happen. The plane is only as good as the team, and The Lisa B is a great model of the fine people who come from Cal Poly.

A special note about the original "Lisa B" is appropriate. Lisa Barneby is an Aeronautical Engineering Senior who gave the team lots of support and took time out of her very busy schedule to help out in any way she could. She is a dear friend and certainly deserves to be the namesake of this magnificent aircraft.

2.2 Publicity for the Cal Poly Design/Build/Fly Team

The most prominent of all the promotion methods for the team was the Cal Poly Design/Build/Fly 2000 Web Page. Its purpose was to advertise the team's latest accomplishments and also to solicit donations. The Web Page presents a brief background of each team member, the purpose of the contest, and illustrates the team's activities with pictures of the construction and testing phases. The Cal Poly DBF 2000 Web Page may be viewed at:

<http://www.calpoly.edu/~jnapior/dbf.html>

2.3 Timeline for The Lisa B

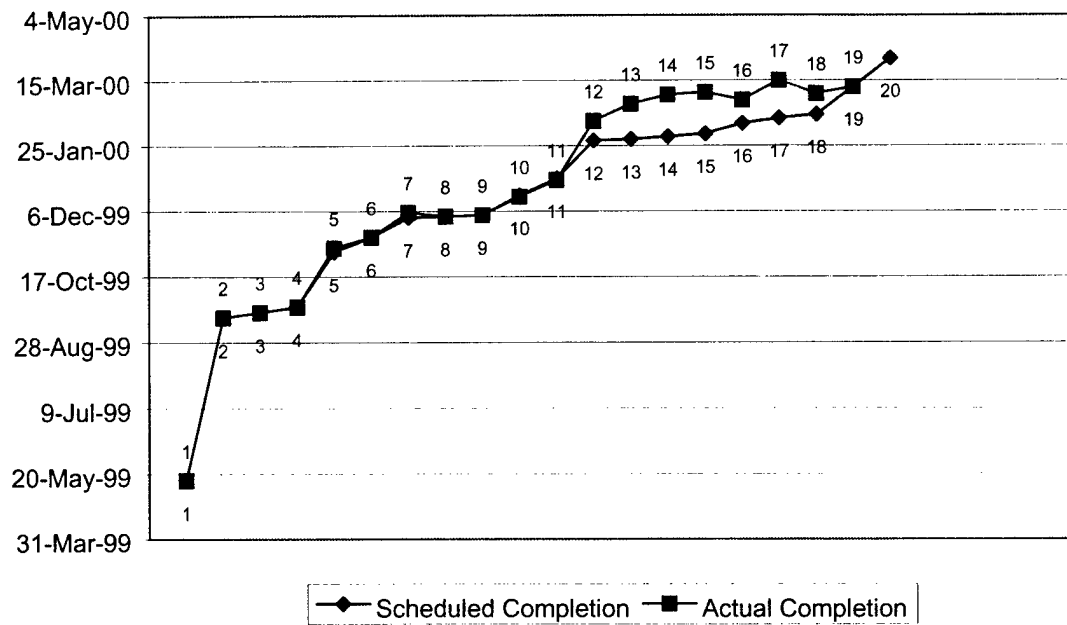


Figure 2.1 –
Timeline

Milestone	Scheduled	Completed	Milestone Description
1	15-May-99	15-May-99	Team Selection
2	16-Sep-99	16-Sep-99	First Meeting, Orientation
3	20-Sep-99	20-Sep-99	Design process begins
4	24-Sep-99	24-Sep-99	Initial configuration chosen
5	5-Nov-99	8-Nov-99	Initial drawings laid out
6	16-Nov-99	16-Nov-99	Design Review
7	1-Dec-99	5-Dec-99	Key components built and tested
8	2-Dec-99	2-Dec-99	Design finalized
9	3-Dec-99	3-Dec-99	Construction begins
10	18-Dec-99	17-Dec-99	Wings completed
11	31-Dec-99	30-Dec-99	Fuselage completed
12	29-Jan-00	13-Feb-00	Final assembly
13	30-Jan-00	26-Feb-00	Ground testing
14	1-Feb-00	4-Mar-00	Maiden voyage
15	3-Feb-00	6-Mar-00	Modifications of design made
16	11-Feb-00	29-Feb-00	First draft of report written
17	15-Feb-00	15-Mar-00	Second plane construction
18	18-Feb-00	5-Mar-00	Final report ready for criticism
19	10-Mar-00	10-Mar-00	Mail in report
20	1-Apr-00	1-Apr-00	Mail in plane

3.0 Conceptual Design

3.1 Alternative Concepts Investigated

The overall aircraft configuration was the team's first concern. Some of the designs that were considered included a flying wing, biplane, twin fuselage or a conventional general-aviation design. A cargo bay blended into the mid section of a wing defined the flying wing. The flying wing would not have any vertical stabilizing surfaces and all maneuvering would be performed by computer-controlled flap deflection. The biplane consisted of two wings positioned parallel to each other and mounted symmetrically to a fuselage. In a twin-fuselage design, a wing would connect the two fuselages. The horizontal stabilizer of this design would also serve as a connection at the tail. The conventional design would look similar to any typical single engine light plane. These considerations are summarized in the Conceptual Figures of Merit, Table 3.1.

An additional consideration was the wing positioning. For stability, the location of the wing must be near the center of gravity. The vertical placement of the wing would affect the structure and the loading and unloading of the cargo bay. The options included mounting the wing high-, low-, or mid-fuselage. There are also many different shapes of wings for low speed aircraft, such as rectangular, tapered, swept, and elliptical. A rectangular wing is the easiest to build due to its constant chord; whereas an elliptical wing is harder to build but more efficient.

3.2 Analytical Methods

For any proper design process, a numerical analysis should precede design. Identifying the key elements in the mission and optimizing them increased the team's chances of remaining competitive. Knowing the parameters to which the aircraft must perform gave way to the conceptual and analytical design.

A spreadsheet was made plotting the flight score versus the payload capacity. This was used in order to find the payload capacity that would score the highest. This approximation was based on the "average" plane from the 1998-99 competition, and is summarized in Table 3.2.

A custom *Microsoft Excel* spreadsheet containing configuration and literal factors was used. The purpose of this spreadsheet was to have the ability to change the parameters of the aircraft and see the effect that the change would have on the aircraft's overall performance. With this ability the team would be able to manipulate the design of the aircraft to improve performance. Equations for lift and drag coefficients, thrust required, lap time, and coefficients of moments were included. The calculations were very accurate, due to built-in redundancies in the spreadsheet that checked for errors.

3.3 Figures of Merit

Rated Aircraft Cost
Modularization
Simplicity of Construction
Performance
Weight

Using the optimization spreadsheet (Appendix A) created at the beginning of the design process, the team was able to quickly evaluate a variety of configurations and sizes. Basic sizes and weights had to be assumed for these initial comparisons. The first parameter inspected was the number of motors. The Rated Aircraft Cost increased dramatically with the addition of a second motor. Since the Total Score is equal to the Report Score multiplied by the Flight Score, and divided by the Rated Aircraft Cost, a low RAC is extremely desirable. After going through similar comparisons between configurations, the team was able to choose one with the lowest Rated Aircraft Cost.

An important stipulation was the shipping of the airplane. Modularization would be a necessity in order to reduce the cost of shipping. Making the wings and the tail surfaces detachable could make the crate narrower.

Simplicity of construction was desirable due to the time restriction. In any working environment, deadlines will always affect the complexity of the project in question.

The competition mandated a seven-foot wing span restriction. So, in order to provide adequate lift, the chord must be large. The wing would have to be effective while flying the loaded sortie, but must also provide efficient cruise performance on the unloaded sortie.

Low weight is desirable not only to improve performance, but also to impart a low Rated Aircraft Cost. In order to run flight performance calculations, the weight of each design was estimated using the known densities of different types of wood. Although the manufacturing material was not yet decided upon, wood was assumed for each configuration in order to accurately compare them.

3.4 Selection of Final Design

The final design was a low wing, single fuselage general aviation aircraft, using a single motor mounted on the nose. This configuration allowed for simple loading and unloading operations between sorties. The basic layout made performance calculations straightforward, as well as simplified the manufacturing process. This configuration was stable in flight, providing more room for pilot error during adverse weather conditions.

The Figures of Merit as discussed above, were given a weighted score and each configuration was analyzed. The results are summarized in Table 3.1. Using the weighted score on the left, each different configuration was rated for each Figure of Merit. The conventional general aviation design received the highest overall score, giving the team an overall airframe layout to work with.

Table 3.1 –
Conceptual Figures of Merit

Weighted Score	Figure of Merit	1	2	3	4
3	Rated Aircraft Cost	2.5	1.0	1.0	2.4
2	Modularization	0.5	0.9	0.5	1.9
2	Simplicity of Construction	0.5	0.4	0.5	1.8
2	Performance	1.6	0.8	0.6	1.6
1	Weight	0.9	0.4	0.1	0.7
10	Totals	6.0	3.5	2.7	8.4

- 1 – Flying Wing
- 2 – Biplane
- 3 – Twin Fuselage
- 4 – Conventional General Aviation

Table 3.2 –
Estimated Score Based on Payload Capacity

Payload/Lap (liters)	Laps	Motors	Total Score	Notes
0.0	0	2	0.00	Albatross - DBF 1998/99
6.9	1	2	6.49	1998/1999 Average plane
1.0	1	2	3.58	1998/1999 Average plane, linear relationships (adjusted for scaling)
2.0	1	2	4.85	
3.0	1	2	5.50	
4.0	1	2	5.90	
5.0	1	2	6.16	
6.0	1	2	6.35	
7.0	1	2	6.50	
8.0	1	2	6.59	
				Max. weight for 2000 competition
1.0	1	1	5.36	
2.0	1	1	7.33	
3.0	1	1	8.35	
4.0	1	1	7.52	
5.0	1	1	9.40	
6.0	1	1	11.28	
7.0	1	1	12.96	
8.0	1	1	13.47	

4.0 Preliminary Design Processes

4.1 Wing

The airfoil dictates the performance of the aircraft. For all airplanes, from heavy lifting aircraft to aerobatic flyers, the airfoil is critical. Initial research was done using the book, Theory of Wing Sections. The focus was on airfoils that had low drag and high maximum coefficients of lift. Listed in Table 4.1 are the airfoils initially studied. In the second column of Table 4.1, a C_L of 0.84 is mentioned. This number was found from an equation for lift found in Fundamentals of Flight, and using known values for air density, velocity, aspect ratio, and weight, a C_L of 0.84 was required for the cruise leg of the mission. From the table, NACA 63₂-615 was chosen for its high $C_{L,max}$ and low angle of attack for the cruise C_L .

However, after further research it was found that all the airfoils in this book were tested at high Reynolds numbers, which meant higher speed aircraft. Since The Lisa B was not designed to fly above a Reynolds number of 3×10^6 , the data found in Theory of Wing Sections was inaccurate and could not be used for the team's purposes. Since there was no initial information on low speed airfoils, *PANDA*, and *VuFoil* were used to create the ideal design. These programs can modify any airfoil as well as find performance data for different conditions. After several modifications, it was found that the programs were only accurate during cruise conditions and didn't accurately predict stall characteristics. The ideal solution to finding the right airfoil was to build some mock-ups and test them in the university's wind tunnel. Unfortunately there was not much time to spend building test models, and taking into account the inaccuracies involved in construction, use of the wind tunnel was not viable.

Finally, a publication was found through the University of Illinois. Summary of Low-Speed Airfoil Data, Volume 3 is a large database of tested, low-speed airfoils. From this database, three airfoils were chosen; their performance data is listed in Table 4.2. The SG6043 was chosen for its low drag and high lift performances (refer to Figure 4.1). The decision for flaps was decided on because they give the option of "morphing" the wing from a standard, higher speed airfoil, to a high lift airfoil. A similar airfoil, the S7062B, had data listed for various flap deflections (refer to Table 4.3). This data was used to estimate a new $C_{L,max}$ for the chosen airfoil, SG6043.

The next decision was the chord length. The initial chord was chosen to be 18" because it was thought that the $C_{L,max}$ would be greatly increased with flaps. Later it was found that the calculated increase in $C_{L,max}$ due to flaps was unreasonable. A new chord length of 24" was chosen to offset the loss of lift found in the real C_L values. After further calculations with *E-Calculator* and the performance spreadsheet, it was found that a chord length of 22.5" was better for both power consumption and lift.

Under the 1998-99 contest rules, a bi-plane would have been the wisest choice given the requirements in the RFP. This year it was clear that a single-wing design would have a higher overall score because of the lower Rated Aircraft Cost. There were a variety of things to consider for the wing's design: dihedral, sweep, chord, span and taper. Since lift was still the key to a successful design, a large amount of wing area was necessary. This had to come

from the chord since a seven-foot span restriction was in the RFP. A tapered wing would only waste usable planform area, and is difficult to construct. Sweep is only important in the transonic region; this was turned down because the plane is not designed to fly close to Mach 1. The last consideration was dihedral. Originally the team was under the impression for a stable low-wing aircraft, some dihedral would be necessary to achieve the same flight characteristics as a high wing. After further research and advice from advanced R/C designers, the use of dihedral was eliminated. A straight, zero dihedral, rectangular wing provided the most area, therefore the most lift, for the given span of seven feet and the calculated chord of 22.5". The other option of an elliptical planform was considered, but the amount of drag saved by reduced wing-tip vortices did not out-weigh the difficulty of an elliptical wing's construction.

4.2 Cargo Bay

The main considerations when designing the cargo bay came with the orientation of the bottles. The first consideration was placing the water bottles standing upright in-line with one another. The advantages of this would be to minimize the fuselage cross-sectional area, thereby reducing parasite drag. The drawback was that having up to eight bottles mounted in a row would extend the length of the fuselage and require special considerations for the additional weight in its construction. It would also create problems in trying to transfer the payload weight onto the landing gear. There was a brief discussion on the topic of using wing pods for part of the cargo, but because of the complexity of loading and unloading the bottles, and the extreme amount of force the wings would have to sustain on a hard landing, the idea was rejected. The final decision was to mount the bottles sideways, one on top of the other, parallel to the thrust line. An additional benefit came from the option of varying the payload without changing the flight characteristics. Four bottles lay in a square configuration centered on the aircraft's center of gravity. The remaining bottles could either mount in groups of two, three, or four on top of the bottom four bottles with just a simple change of a non-load bearing hatch. This gave great flexibility in finding the optimal payload.

4.3 Tail Section

When designing the horizontal stabilizer it was crucial that it counter-act the moment created by the wing. Since the wing alone creates a nose down moment, the horizontal stabilizer had to create an equal and opposite moment. The E387 Airfoil obtained from Summary of Low-Speed Airfoil Data, Volume 3 satisfied this requirement. The airfoil provides the required C_L and is flat on one side, which means no opposing forces would be produced and the vertical surface could be mounted easier. This stabilizer was mounted on The Lisa B to create lift in the downward direction. The performance data for the E387 is shown in Figure 4.2. The force created by that lift multiplied by the moment arm from the quarter-chord of the main wing to the quarter-chord of the stabilizer cancelled out the moment created by the main wing alone. This allows for a balanced aircraft and greater elevator control. The geometry of the stabilizer was based on the required area to produce the above-mentioned moment. The actual aspect ratio was based on construction considerations alone.

Simply dividing the horizontal surface in half chose the vertical stabilizer's dimensions. This was decided on because there were no readily available equations for vertical surfaces. Local R/C designers confirmed that this estimation would be adequate for the design. To improve the efficiency of the vertical tail, the NACA-0012 airfoil was used in its construction. Since this is a symmetrical airfoil, it creates lift equally in both directions, giving it more control than if just a flat surface was used.

4.4 Power Plant

The motor, controller, and batteries are the power systems of The Lisa B; it was also among the most important design considerations. Since this year the batteries were limited to 5 lbs. of NiCad batteries, serious consideration was given to finding an efficient motor and batteries. Two types of batteries were considered. The first, NiCad 5400mAh batteries, were considered for their high capacity. Since any motor that would power The Lisa B would drain any battery quickly, large capacity was required for adequate flight time. The downside to these batteries was their weight. Only 14 cells could be used, thereby reducing the available voltage. This would create a need to increase the current to maintain the same required power. The current needed to do this exceeded all available motor and speed controller specifications. The final batteries chosen were NiCad 3000mAh cells. These have less capacity, but due to their size, 24 cells could be used. This provides sufficient voltage and current for the motor and speed controller.

The next consideration was the motor. There was only one company that could supply a motor with the power and efficiency required: Aveox. Listed in Table 4.4 is the performance data for the two Aveox motors considered, the 1415/2Y and the 1412/2Y. It was clear that the Aveox 1415/2Y motor performed better for the aircraft's requirements. The motor is also equipped with a 3.7:1 planetary gearbox to bring the RPMs down to the required level. On the loaded laps during take-off, the motor will be doing the majority of its work and drawing the most current. The 1415/2Y motor would allow The Lisa B to get to cruise altitude under the current ratings of both the motor and speed controller. Only the H260 controller would work with the 24-cell count and the two different motor options. This controller can run at 60 amps for one minute and 100 amps for ten seconds. These parameters dictated propeller size and thrust for the motors. As a margin of safety, the motor would not pull over 60 amps at any point in the contest.

4.5 Landing Gear

Many different ideas went into the design of the main landing gear. If the wheels were spread too far apart, the ground handling would be erratic and unpredictable. If the gear span was too small, the plane could easily tip over. Straight aluminum struts connected to the outer edge of the wing spar were first considered. This design would eliminate the excess weight in a bow-gear design. Aluminum was chosen because of its high strength-to-weight ratio and ease of construction. After further examination it was found that the forces experienced by the wing spar would be large and designing it to handle such loads would add unnecessary weight. The design changed to an aluminum bow that would connect to the joiner via aluminum L-brackets. This was considered the best connection point because it allowed for the entire load experienced during landing to be distributed to the joiner and spar, which were the strongest parts of the airplane. Two 5-inch, inflatable wheels were

chosen as the main gear wheels because of their low weight and impact absorption characteristics.

The custom nose landing gear was attached to the plane through a single block of wood that attached to the front bulkhead. After additional research and some advice from R/C experts it was found that the single block of wood would not be enough to handle a rough landing. It was also found that the custom-designed landing gear was not able to turn well due to the excessive loads upon it, nor did it absorb much of a load. The Robart Company produces several specialized landing gear. The Robostrut 625 model is rated for aircraft up to 55 lbs, this was the gear installed on The Lisa B. Clamping an aluminum tube over the existing shaft extended the gear to the height required. It was attached by gluing two thrust bearings to two blocks of wood and to the aluminum shaft, one in the center and one at the top, which would be more than adequate for the expected loads. The servo was easily attached to the shaft using two servo arms. In order to reduce the load on the nose gear servo, a roller-blade wheel was used because it doesn't deform when a load is placed on it. The Robostrut's excellent suspension capabilities out-weighed the need for extra absorption by an inflatable wheel.

4.6 Figures of Merit

Handling
Ease of Construction
Weight
Efficiency

The handling characteristics of the plane were crucial in its design. A simple configuration would provide the easiest flight handling traits. The motor is not over-powered for the amount of weight it is carrying and the control surfaces are adequately sized for stable maneuvers. It was decided early on that simplicity would make a successful plane.

Weight is an obvious consideration. It dictates how well the aircraft can perform and how all components need to be sized. There were a number of elements that had to be accepted regardless of their weight, but there were several items there were optimized to save weight. Several carefully planned holes were cut in bulkheads to cut down on material and still maintain strength requirements. Minimum structure was used where strength was not a factor and areas requiring high strength were placed together to cut down on heavy materials.

The motor was the key to efficiency; it had to make a limited power supply last as long as possible. Designing the plane to be aerodynamically sound and light helped the motor overcome much of the drag. Efficiency was also considered in the construction. It was well known that regardless of the design, The Lisa B would take longer to build than expected. It was necessary to be prepared in the construction process to make room for unexpected delays.

Table 4.1 –

Airfoil Comparisons from Theory of Wing Section ($Re = 3 \times 10^6$)

Airfoil	α for $C_L = .84$	C_D	C_L Max	α @ C_L Max
4412	4.5°	.0120	1.40	13°
4415	5.0°	.0135	1.30	12°
65 ₃ -618	4.0°	.0150	1.20	16°
64 ₃ -618	4.5°	.0135	1.30	15°
63 ₃ -618	4.0°	.0130	1.30	14°
63₂-615	4.0°	.0110	1.40	12°
64 ₁ -412	5.0°	.0125	1.35	12°
64 ₂ -415	5.0°	.0135	1.30	13°
64 ₃ -418	5.0°	.0140	1.25	14°
64 ₃ -618	4.0°	.0140	1.30	15°
65 ₁ -412	4.5°	.0125	1.30	11°
65 ₂ -415	5.0°	.0140	1.25	13°

Table 4.2 –

Airfoil Comparisons from Summary of Low-Speed Airfoil Data, Volume 3 ($Re = of 4.0 \times 10^5$)

Airfoil	α for $C_L = .84$	C_D	C_L Max	α @ C_L Max
SD7062B	4.0°	.015	1.65	15°
SG6043	1.0°	.008	1.62	14°
USNPS-4	3.0°	.0095	1.6	14°

Table 4.3 –

Flap Performance Data (S7012B w/ flap data at $Re = 3.0 \times 10^5$)

Flap Deflection	C_L Max
0°	1.10
2.5°	1.20
15°	1.90
20°	2.29
25°	2.59

Table 4.4 –

Motor Comparison

Motor	Max Prop Size	Thrust	Current Draw	Battery Life
1412/2Y	14"x8"	198 oz.	58.4 amps	2.9 min
1415/2Y	16"x8"	215 oz.	55.4 amps	3.1 min

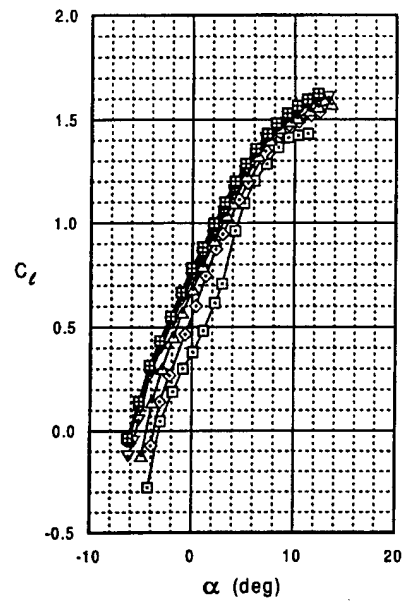
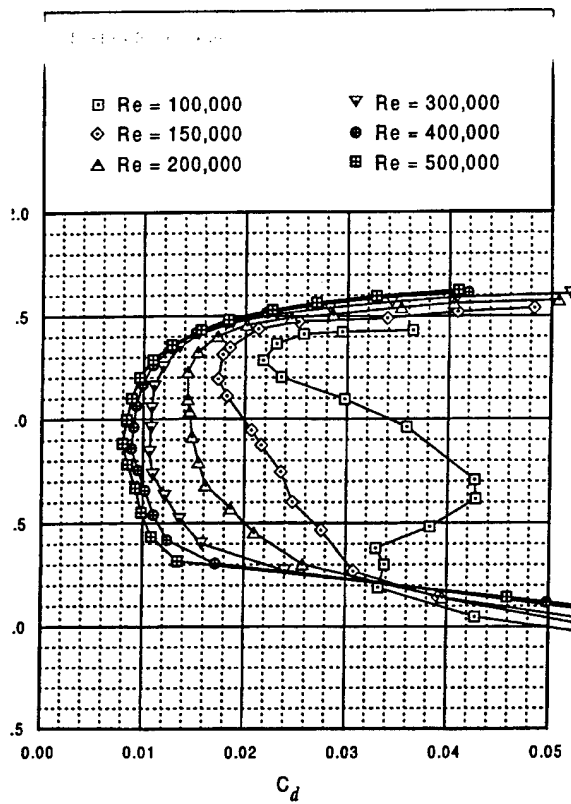


Figure 4.1 –
Characteristics of the SG6043 Airfoil (Main Wing)

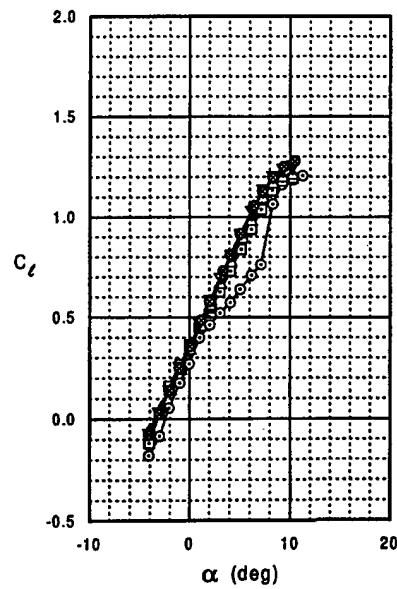
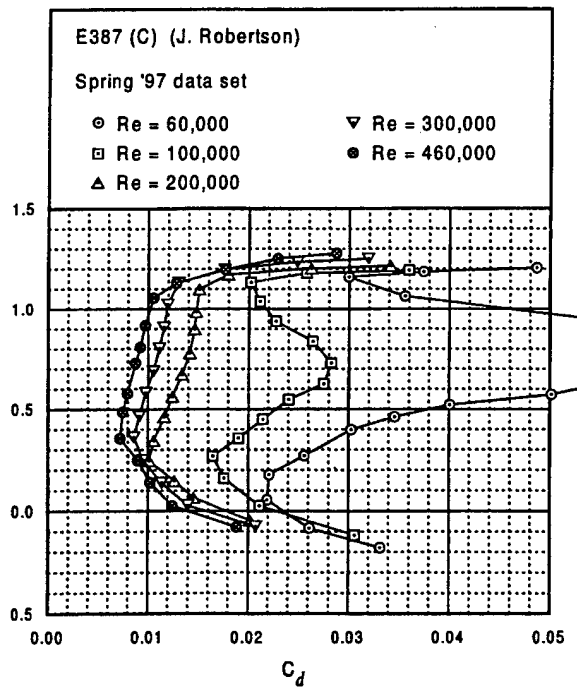


Figure 4.2-
Characteristics of the E387 Airfoil (Horizontal Stabilizer)

5.0 Detail Design

An *Excel* spreadsheet was created to calculate the aerodynamic characteristics of The Lisa B at various speeds. Appendix B lists all formulas used in the creation of this design tool. The main section of the spreadsheet (Appendix C) contains all of the user-defined data for aircraft geometry and desired cruise conditions. A second section calculates drag at different speeds and displays the results on two graphs. These results yielded take off, cruise, and stability characteristics.

5.1 Flight Performance

5.1.1 Take-Off

The RFP states that the aircraft lift off within one hundred feet. The aircraft calculations were done on a requirement of less than ninety feet to allow for a margin of error. The take off speed is the stall speed multiplied by a safety factor of 1.2. Since The Lisa B is designed for a range of payloads, the take off speed must be calculated for each weight. For the calculations several assumptions regarding drag and rolling resistance were made. The average parasite drag for all speeds was used and the rolling resistance due to the landing gear on take-off was neglected. The thrust required was also calculated using the take-off distance, mass, and resistances.

Table 5.1 gives the results for the expected range of weights. For the unloaded lap it was found that a thrust of 4.4 lbf is needed to reach the take off velocity of 22 mph. For a full load of eight litters it was found that the static thrust required to reach a lift off speed of 31 mph was 17.4 lbf.

The next phase of flight is a climb and acceleration to the cruise altitude and speed. The cruise altitude for all laps is 30 ft. From the course diagram in the RFP it was known that the first turn is 500 ft after the start line. After lift off there would be approximately 450 ft before the first turn. The climb rates and cruise speeds varied with different weight configurations. For the unloaded lap the optimum cruise speed was found to be 38 mph. A climb rate of 2.90 ft/s and a thrust of 4.51 lbf is needed to reach this speed and altitude. For the full load of eight litters the optimum cruise speed was found to be 51 mph. A climb rate of 4.00 ft/s and a thrust of 10.9 lbf is needed to reach this speed and altitude. Table 5.2 gives the results for all expected weight ranges. All calculations were made using the spreadsheets in Appendix C.

5.1.2 Cruise

Once in cruise, The Lisa B will have to make two 180-degree turns and a 360-degree turn. These turns will be done at a constant bank angle of 30 degrees, resulting in a G-loading of 1.2. Since all turns are at the same bank angle and speed, the total time turning will be calculated as if the aircraft were making a 180-degree turn four times. The times required for each weight configuration can be seen in Table 5.3. For the unloaded sortie, a 180-degree turn will be completed in 10 seconds with a required thrust of 2.12 lbf. For a full load of eight litters, a 180-degree turn will be completed in 12.6 seconds with a required thrust of 4.2 lbf. These values were all compiled on a spreadsheet using equations from Fundamentals of Flight.

According to the RFP, the total length on both straight sections will be 1000 ft, for a total of 2000 ft of straight flight. Due to the fact that there is a 360-degree turn halfway through the backstretch all cruise calculations were done in increments of 500 ft. The results for all weight configurations can be seen in Table 5.4. For an unloaded sortie, The Lisa B will fly 500 ft in 9 seconds with a required thrust of 1.90 lbf. For a full load of eight liters, The Lisa B will fly 500 ft in 6.70 seconds with a required thrust of 3.7 lbf. Since more time is spent in turns than in straight and level flight, the angle of incidence needed to be optimized. Calculations from the spreadsheet in Appendix C showed that for the 180-degree turn, a C_L of 0.55 was needed, so an incidence angle of 2 degrees was built into the wing.

5.2 Electrical Components

5.2.1 Control Systems

The Lisa B uses rudder, elevator, and flaperons to maintain directional control in flight. In addition, ground control is through a steerable nose-wheel. A Futaba 8 channel PCM radio is used for pilot control. Futaba 3001 servos are used, providing more torque than is available from the standard servos. To compensate for the power drawn by the number of servos and the resistance losses in the long servo leads, a high-capacity 5-cell receiver battery pack was used. This will prevent the receiver from shutting off due to low power.

Due to the requirement for a high coefficient of lift on loaded takeoffs, it was decided to use full span flaps to increase the lift of the wing. By using flaperons, the same surfaces are also capable of performing operations for roll, saving a pair of servos. One servo is required for the flaperon on each wing. Computer mixing on the radio is required to blend the operation of the flaps and ailerons, and this is easily accomplished with the computerized radio. The servos are mounted on the rib nearest to the center of each flaperon. Servo placement is illustrated in Figure 5.8.

One servo each is used for the rudder and the elevator. The similarity of these structures allows for nearly identical mountings for each servo. The servos are mounted between the two spars in the control surface with only the control arm exposed to the free-stream air, minimizing the drag penalty. Control rods and horns are off-the-shelf heavy-duty R/C products.

5.2.2 Power Plant

The Rated Aircraft Cost factor virtually dictates a single motor to avoid excessive cost penalty. The motor selected was the Aveox 1415/2Y. This motor is one of the most efficient electric motors available, and is capable of handling the current required to produce more than 15 lbf of thrust. The motor is geared down by a 3.7:1 gearbox and drives a 16"x8" propeller. This set-up gives a good combination of maximum static thrust and cruise efficiency while minimizing the risk of drawing excessive current. The Aveox H260 speed controller can handle 60 amps continuously.

Twenty-four Sanyo N-3000CR cells in series provide power. The batteries are contained in a compartment in the nose section and are assembled into three packs for flexibility. As a large amount of current is drawn at full throttle, it is expected that the batteries will heat significantly. Cooling is through a series of air intakes on the side of the fuselage, allowing

cooling air to flow over the battery packs. The exact location of the batteries can be adjusted slightly to move the center of gravity of the aircraft to the desired location at the quarter chord of the main wing.

This combination of motor, speed controller, and batteries will provide enough flight time to complete three loaded sorties and two empty sorties. For the performance calculations and estimates of loading time, it is predicted that the ten-minute period will be enough time for three loaded and two empty laps. This is an indication that the power system is properly matched to the aircraft for the expected mission.

5.3 Structural Details

5.3.1 Structure and Component Testing

To save time and money, it was decided to construct the airframe out of wood (see Section 6.1). Construction is of the semi-monocoque type, with plywood bulkheads and spruce stringers supporting a layer of balsa sheeting. This assembly is wrapped with a layer of fiberglass in certain locations for additional strength. A platform in the nose supports the batteries and provides a mount for the motor (see Figures 5.2 & 5.3).

The wings are also of wooden construction. Balsa ribs are attached to a spar (Figures 5.4 & 5.5) consisting of two spruce caps with plywood shear webbing. A thick balsa beam on the rear quarter of the wing provides the mounting surface for the flaperons. Several balsa stringers and leading-edge sheeting help the wing maintain the airfoil shape. The wing is mounted to the fuselage by means of a birch and aluminum joiner beam (Figures 5.5 & 5.7) that slides into the box shaped spar sections. The joiner is directly underneath the cargo bay and is connected directly to the landing gear to transfer landing impacts (see Figure 5.7).

The main spar is required to be the strongest portion of any airplane. As a result, much effort was invested in the design and testing of the spar for The Lisa B. It was found that a distributed load of 90 lbs on each spar would simulate a 5G-loading, far greater than what was anticipated. It was decided to use a top and bottom cap of spruce connected with plywood shear webbing. Several variations of this theme were constructed and tested.

The first design had two spruce caps measuring 0.75" x 0.125". The shear webbing created a box (to contain the joiner; discussed below) for the inboard third of the span and a more typical I beam for the remainder. When tested, this spar sample failed far short of the required load. Analysis of the failure revealed a need for further improvements in the transition of the structure between the I-beam and box sections. The structure was modified to preserve the continuity of the shear loading throughout the span. Various other combinations of spar cap and shear web dimensions were tried until a successful combination was reached. The final spar caps are 0.75" x 0.25" spruce and the webbing is 0.0625" thick for the box section and 0.125" thick for the I-beam. In addition, balsa triangle stock was added to the I-beam and the box section wrapped in a layer of fiberglass. This design was able to hold in excess of 90 lbs; more than sufficient for expected loading.

The first joiner tested was made from 0.5" birch plywood with a layer of balsa on the side to allow for a snug fit into the spar box. The joiner is the piece that will transfer force from the wings to the fuselage. When the final spar design was tested, the 0.5" plywood joiner was

the first portion to fail. The design was revised to incorporate a solid piece of birch with a piece of 0.0625" aluminum stock attached for added rigidity. This design was found to be adequate for the expected loads.

5.3.2 Tail Section

The tail surfaces of The Lisa B were designed using the equations presented in Appendix B. The sizing was not an exact process as long as certain minimums were reached. It was decided that a tail larger than was required would enhance the stability and handling of the aircraft, reducing pilot workload. The size of the horizontal stabilizer is slightly larger than the area required to counter-act the moment produced by the airfoil section. A general rule for R/C aircraft is that the vertical stabilizer be half the size of the horizontal stabilizer. This simple rule was used on The Lisa B.

The structure of the tail surfaces is similar to that of the wings, the main difference being the presence of two equal-sized spars. Both stabilizer surfaces are attached to the fuselage using extended bulkheads in the tail. These bulkheads are 0.125" thick and protrude approximately 8" above the top of the fuselage. Both spars in the vertical stabilizer are hollow and fit snugly over these bulkheads. The horizontal stabilizer's spars also fit over the extended bulkheads and the stabilizer itself is sandwiched in place by the vertical tail. Two bolts hold the two stabilizers to the fuselage. The tail section is illustrated in Figure 5.6.

5.3.3 Cargo Bay

As mentioned earlier, the aircraft was designed to operate with a range of payloads from 6 to 8 liters. The bottles are stored in two layers centered about the wing joiner section at the quarter-chord. The bottom layer consists of four bottles, two wide and two long, aligned axially with the fuselage. Two, three, or four bottles are then stacked on top of this layer. Different shaped hatches fit over the top of the bottles to hold them in place. Due to the different configurations of the top layer of bottles and the need for the hatch to fit snugly over the bottles, three different non-load-bearing hatches are required. The hatches are secured to the fuselage with Velcro straps. Various latching mechanisms were considered, but Velcro was chosen on account of its simplicity.

5.3.4 Landing Gear

To facilitate easy ground handling, The Lisa B is equipped with tricycle type gear with a steerable nose-wheel. The nose-wheel is a single wheel from a pair of inline roller-skates and is mounted on a commercially available Robart 625 strut. The strut is mounted to a bulkhead in the nose using several thrust bearings, and has a dedicated servo for steering. The main landing gear is similar to the landing gear found on most simple R/C aircraft. An aluminum bow is mounted to the wing joiner structure. This is flexible enough to cushion landings without the use of separate shock absorbers. There are no brakes currently, but it will be possible to add them if flight-testing reveals such a need. It is also possible to replace the aluminum main gear with a composite bow to save weight, which will be done if time allows.

5.4 Stability Analysis

Analysis on the modes of the aircraft was performed to predict stability characteristics. With the knowledge obtained from the each mode of flight, accurate assumptions of the quality of the aircraft's flight characteristics were found. The stability and control analysis was performed using the method of small perturbation theory found in the text, Flight Stability and Automatic Control. Equations used in this analysis can be found in Appendix B. Consequently, this analysis was intended to categorize and give a level of flying qualities for the aircraft.

The response of the aircraft depended on the magnitude of the stability coefficients. These results are presented in the Table 5.5. A calculated value for the frequency and dampening of the short-period approximation was conducted. The results showed that for the more important longitudinal approximation, short-period had a high frequency and was well damped. These values suggested the aircraft would respond rapidly to elevator input. This, in turn, would increase the performance in turbulent air conditions. The phugoid approximation determined that the aircraft was a level-one aircraft. Qualification as a level-one aircraft translates into sufficient flight qualities in the loaded and unloaded sorties.

Table 5.1 –

Take Off Performance from Fundamentals of Flight

	Take Off Velocity (mph)	Thrust Required (lbf.)
Unloaded sortie	22	4.4
6 Liters	28	12.3
7 Liters	29	13.9
8 Liters	31	17.4

Table 5.2 -

Climb to Cruise Performance from Fundamentals of Flight

	Rate of Climb (ft/sec)	Cruise Velocity (mph)	Thrust Required (lbf.)	Payload Fraction (%)
Unloaded sortie	2.9	38	4.5	0
6 Liters	3.7	48	9.1	39
7 Liters	3.9	50	10.0	44
8 Liters	4.0	51	10.9	47

Table 5.3 –

Flight Performance During 180° Turns from Fundamentals of Flight

	Thrust Required (lbf.)	Time (sec)
Unloaded sortie	2.1	10.0
6 Liters	3.7	11.9
7 Liters	3.9	12.4
8 Liters	4.2	12.6

Table 5.4 –
Cruise Performance from Fundamentals of Flight

	Thrust Required (lbf.)	Time (sec)
Unloaded sortie	1.9	9.0
6 Liters	3.2	7.1
7 Liters	3.4	6.8
8 Liters	3.7	6.7

Table 5.5 –
Results of Stability Calculations

$C_{l\alpha}$ <input type="text" value="0.8"/>	m <input type="text" value="20"/> lbs 0.622 slugs	$C_{m\alpha}$ <input type="text" value="-0.188"/>	$C_{L\alpha}$ <input type="text" value="0.1166"/> 1/deg 6.6807 1/rad	S_{tail} <input type="text" value="3.03"/> ft ²
Chord <input type="text" value="1.75"/> ft	V <input type="text" value="50"/> mph 73.3 ft/s	η <input type="text" value="0.87"/>	S_{ref} <input type="text" value="12.25"/> ft ²	Q <input type="text" value="6.03"/> lbf/ft ²
I_y <input type="text" value="21.82"/> slugs-ft ²		I_H <input type="text" value="4.5"/> ft	C_{D0} <input type="text" value="0.046"/>	
V_H <input type="text" value="0.636"/>	$Z\alpha$ <input type="text" value="-100.5"/> ft/s ²	M_α <input type="text" value="-1.11"/> 1/s ²	X_u <input type="text" value="-0.149"/> 1/s	C_{mq} <input type="text" value="-19.0"/>
M_q <input type="text" value="-1.34"/> 1/s	Short Period ω_{hsp} <input type="text" value="1.72"/> ζ <input type="text" value="1.11"/>	Phugoid ω_{np} <input type="text" value="1.07"/> ζ <input type="text" value="0.07"/>		Z_u <input type="text" value="-2.59"/> 1/s

THE *Luis* B

California Polytechnic State
University, San Luis Obispo

Scale 1:24

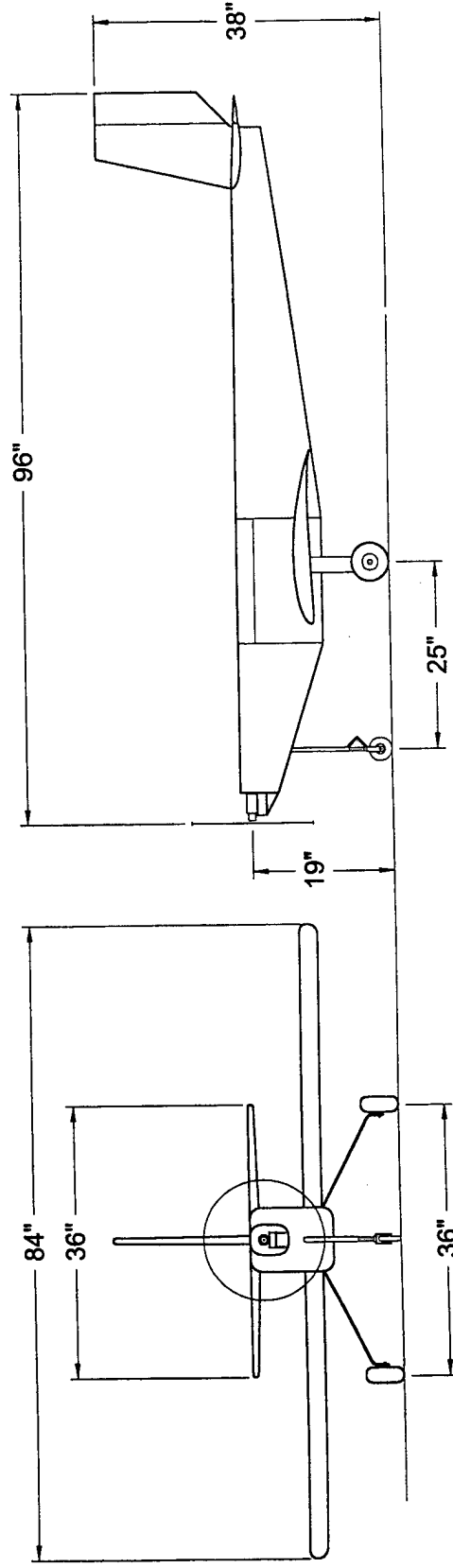
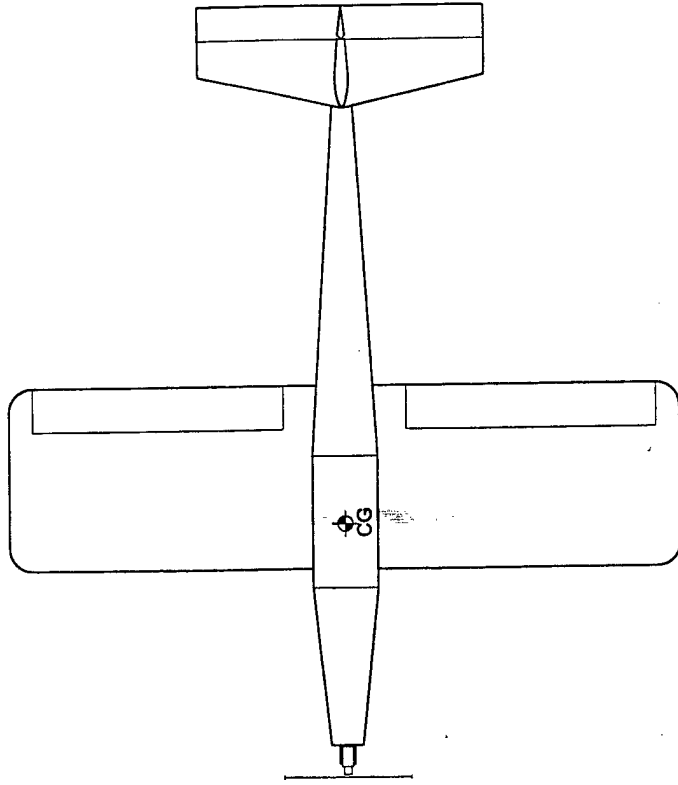
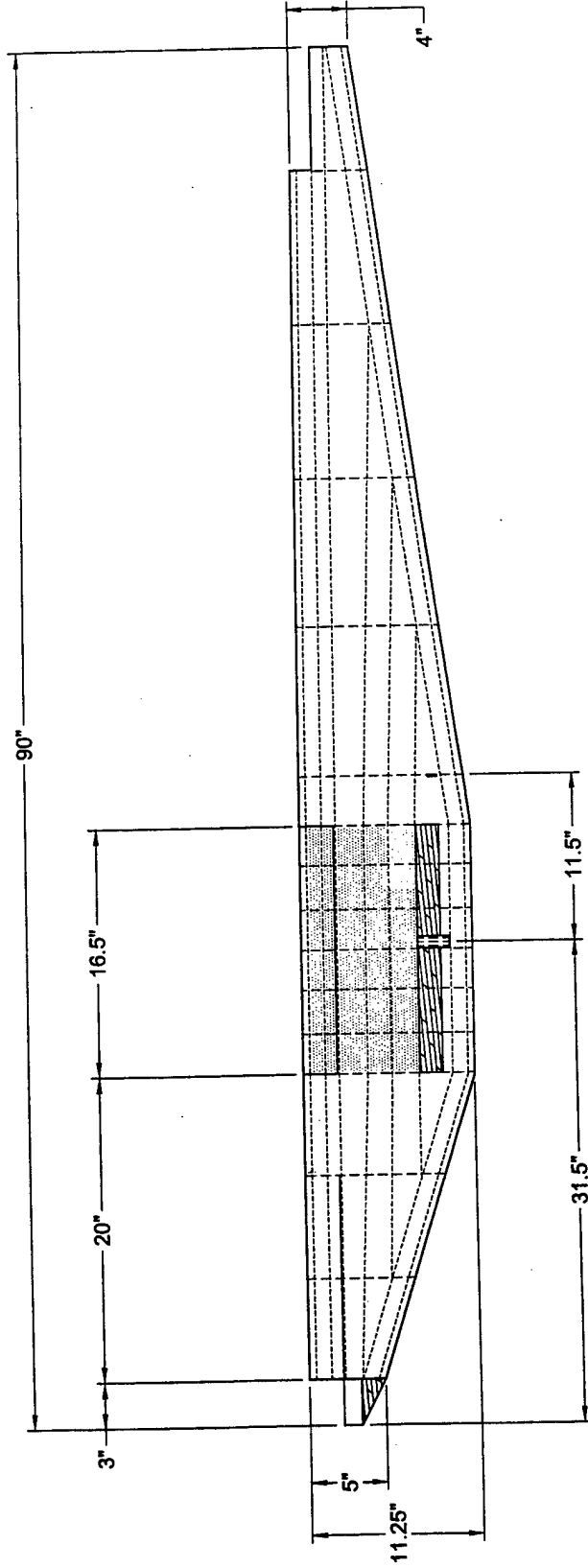


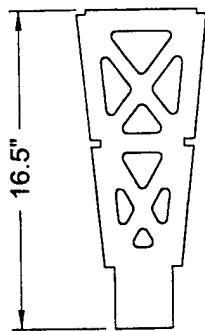
Figure 5.1 - General Layout



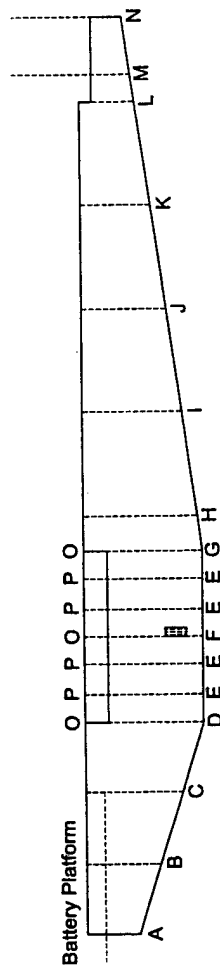
Fuselage Structure Left Side

Scale 1:12

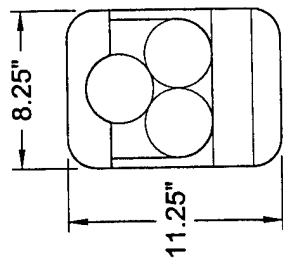
Figure 5.2 - Fuselage Structure



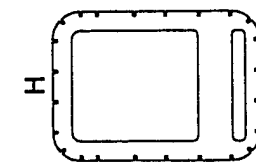
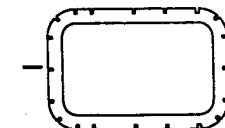
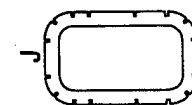
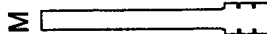
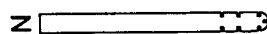
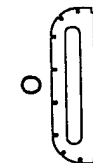
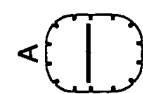
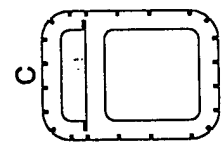
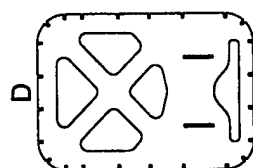
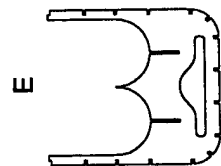
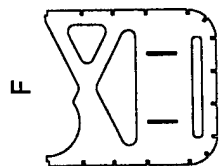
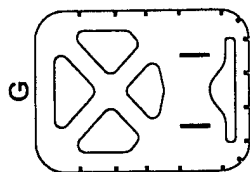
Battery Support Platform
Scale 1:10



Bulkhead Locations
No Scale



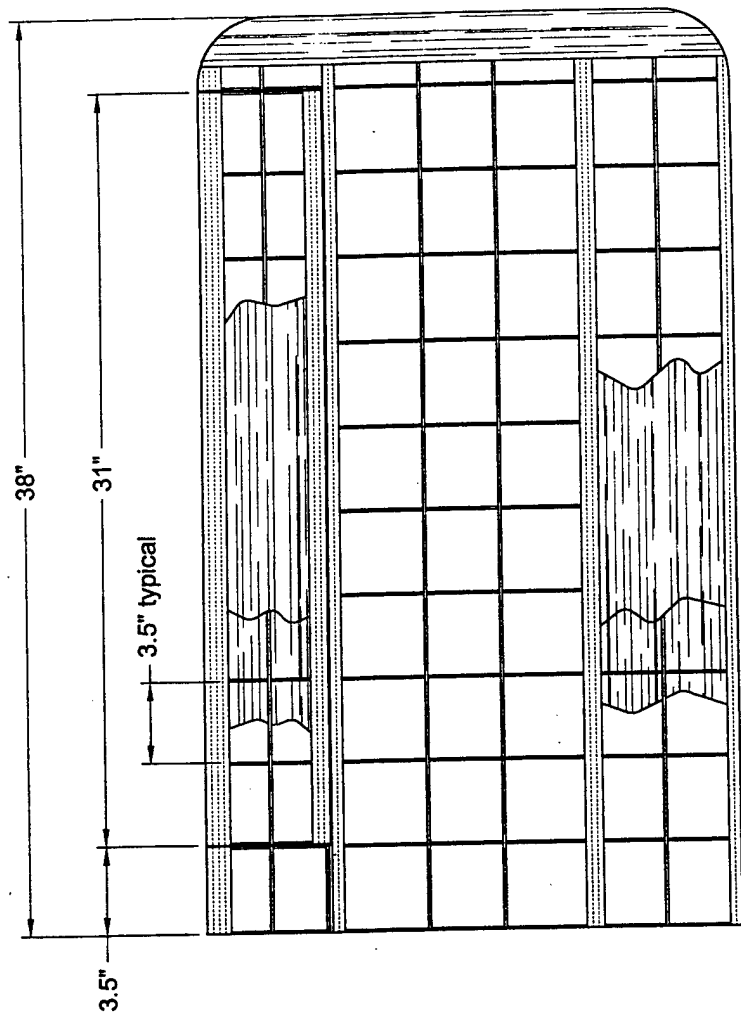
Cross Section
(6 liter configuration)
Scale 1:10



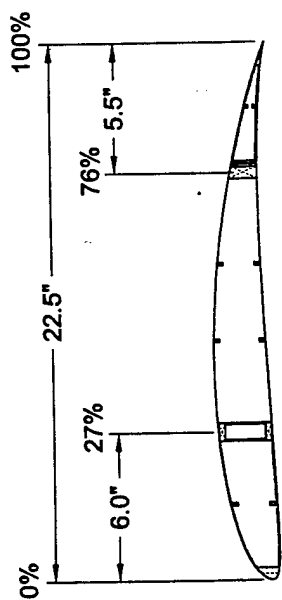
NOTE: Bulkhead P is specific to 6 liter configuration.

Bulkhead Templates
Scale 1:10

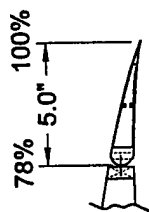
Figure 5.3 - Bulkheads



Left Wing Structure
Scale 1:8

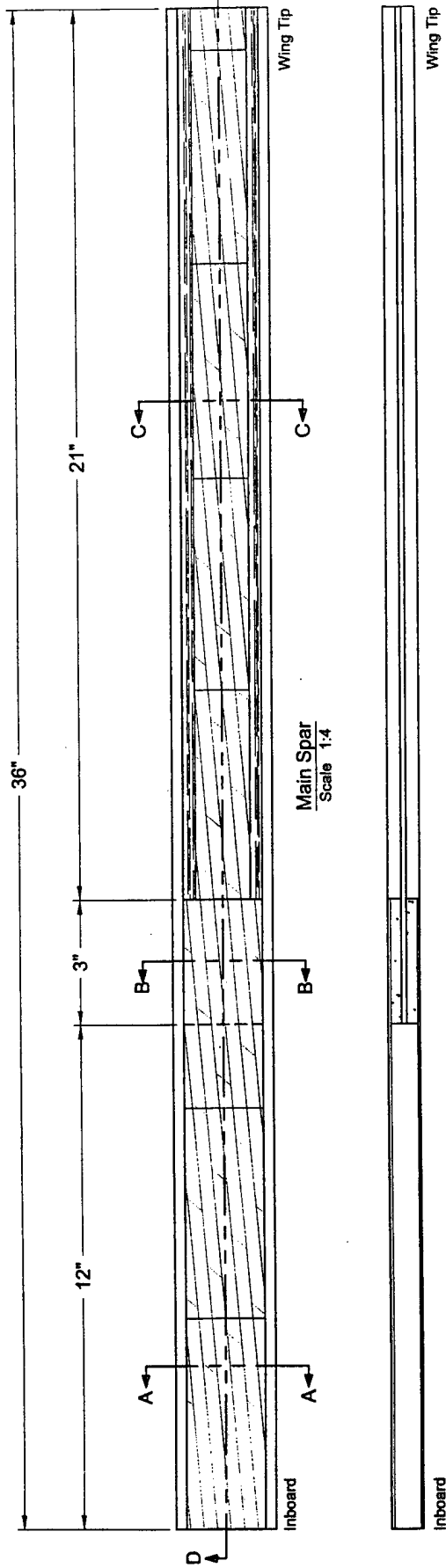


Airfoil and Inboard Structure
Scale 1:8

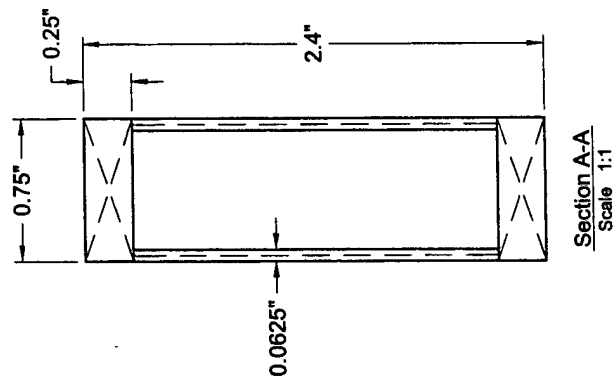


Flap Section
Scale 1:8

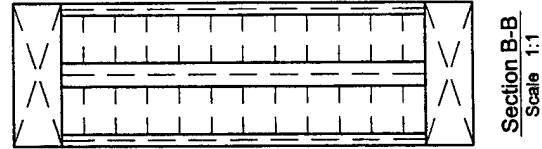
Figure 5.4 - Wings



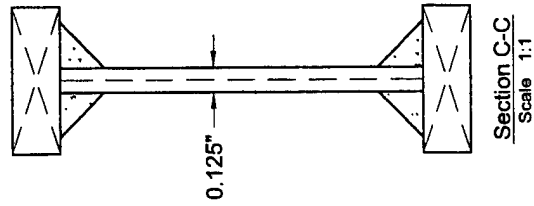
Section D-D
Scale 1:4



Section A-A
Scale 1:1

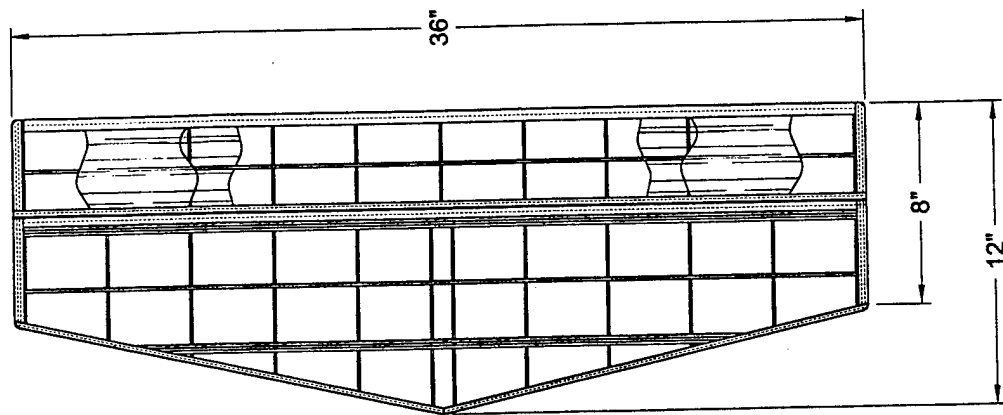


Section B-B
Scale 1:1



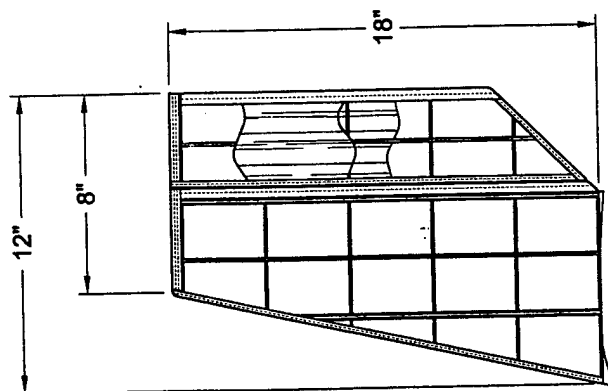
Section C-C
Scale 1:1

Figure 5.5 - Spar Construction



Horizontal Stabilizer

Scale 1:8



Vertical Stabilizer

Scale 1:8

Figure 5.6 - Tail Structure

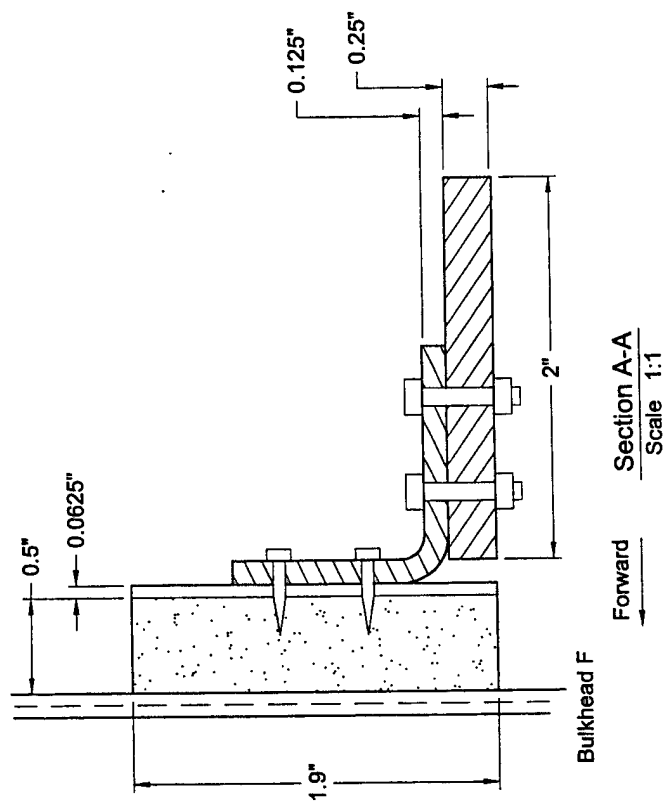
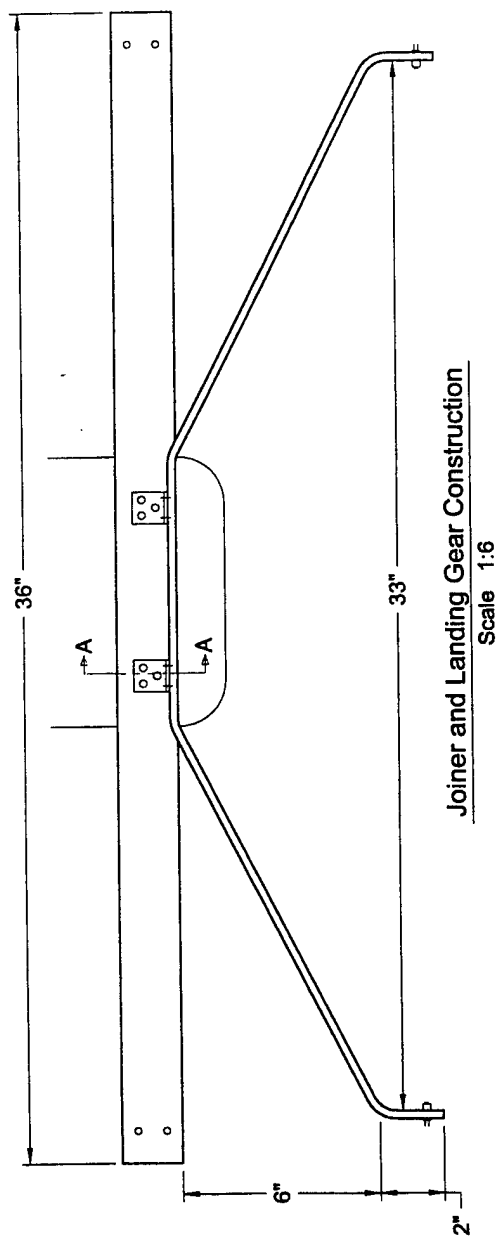
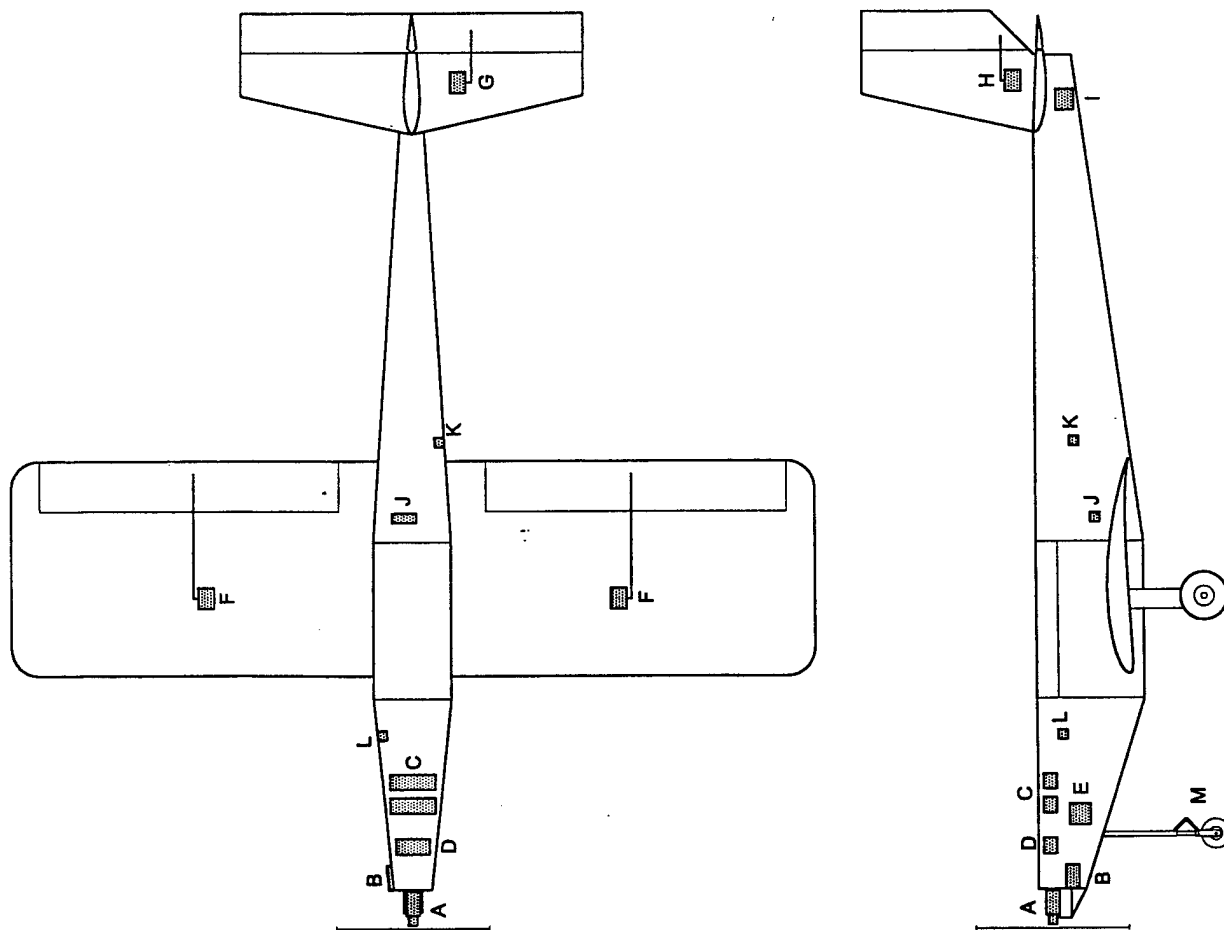


Figure 5.7 - Joiner and Landing Gear



- A. Aveox 1415/2Y brushless electric motor with 3.7:1 gearbox, 16x8 APC propeller
- B. Aveox H260 speed controller with 40A fuse
- C. 9 cell battery pack (Sanyo N3000CR) (x2)
- D. 6 cell battery pack (Sanyo N3000CR)
- E. Nosegear steering servo (Futaba S3001)
- F. Flaperon servo (Futaba S3001) (x2)
- G. Elevator servo (Futaba S3001)
- H. Rudder servo (Futaba S3001)
- I. Receiver battery pack (5 cells)
- J. Futaba receiver
- K. Receiver power switch/charging jack
- L. Motor kill switch
- M. Robart nose landing gear

Scale 1:20

Figure 5.8 - Systems Layout

6.0 Manufacturing Plan

When considering construction materials for The Lisa B, the team members considered all possible options and then narrowed them down to formulate a manufacturing plan.

The most obvious option was wood. Different types of wood would be used for different parts of the airframe: birch plywood for bulkheads, spruce stringers on the fuselage and wings, balsa wood ribs in the wings and for outer sheeting. All of the wooden parts would then be covered in heat-shrink "monocote" fabric to maintain continuity of the shape of the airframe. When several different colors of heat-shrink fabric are used on different parts of the airplane, the pilot can more easily determine the orientation of the plane during flight operations.

The next consideration was a carbon fiber composite design. This would have involved the initial design of the plane and the design of molds in which to "cook" the composite structure for hardening. The internal structure of the airframe would include strong composite spars and bulkheads, with some metal attachment hardware used to mate pieces of cooked carbon fiber together. The outside of the composite airframe would be covered in heat-shrink fabric or painted to lower parasite drag and increase visibility during flight operations.

A foam-core design was also discussed. This would involve cutting the airfoil shapes with a hot-wire foam cutter and shaping the fuselage and control surfaces out of foam blocks. The foam airframe would then be coated in fiberglass or some kind of light fabric and epoxy combination.

6.1 Figures of Merit

- Cost
- Ease of construction
- Durability
- Past experience
- Availability of materials
- Weight

Through the fundraising efforts of the team members, the necessary funds for a properly budgeted airplane were acquired through private donations, and corporate donation of materials. Different types of wood from spruce to balsa were priced and wood design was estimated to cost \$400. Team members largely already owned the tools necessary for wood construction. A carbon fiber design would cost more than \$5,000 for the airframe, including the carbon fiber itself and the machines and tools used for it's construction. Material costs for a foam core design were considerably lower, totaling \$1000, again accounting for the foam itself as well as the construction equipment.

Beginning in the days of the Wright Brothers, the traditional method of airplane construction involves wood. The level of skill necessary for wood construction is minimal, since a modeler is basically gluing one piece of wood to another while taking care not to

adhere one's fingers to the airframe. Since wood is easy to mill and drill, it is a simple matter to correct construction inaccuracies. Wood's simplicity also allows for on-the-fly design modifications. Construction of carbon fiber is very difficult and time consuming because of the layering and cooking time involved. If one actually manages to get past the cooling step, then he or she is faced with the difficulty of working with cured carbon fiber. It is very hard to mill and drill while still maintaining the intrinsic strength of the cured airframe. This makes modifications extremely difficult. Foam core wings and fuselage are relatively easy to make. A hotwire cutter can easily be used to shape these main parts of the airframe as well as the other components. Foam is also very easy to modify during construction.

In the event of a crash, a wooden airframe could potentially be completely destroyed. Depending on the seriousness of the crash and the actual point of impact on the plane, entire sections of the plane would have to be replaced. Conversely, a primary advantage of a carbon fiber design is in its durability; although splintering inside carbon fiber layers are hard to detect before total fracture. A foam core design would probably do very well in a crash. The foam tends to keep the damage localized, rather than distributing the impact loads throughout the entire structure. In many cases, damage to a foam core airframe can be fixed in a few minutes with packaging tape.

Each team member had worked with wood before. Visualization of design details would not be hard because everyone had a working knowledge of how wooden frames work and how loads are transferred from one section to another through joints in the woodwork. Two team members had worked with carbon fiber in last year's DBF competition. Poor planning and even poorer communication led to that team's demise, but another of their major problems was the complete lack of experience in the use of carbon fiber. It takes time and experience to make a carbon fiber design work. As with composites, the team members had very little experience in foam core design.

Wooden modeling parts and tools to implement its construction are available at any hobby store. There are also several companies on the Internet that have a better selection of types and sizes of wood. Materials for carbon fiber are not as readily available, however through the proper channels, they can be acquired. The tools for building such a design are even harder to come by. Many different types of foam can be ordered from various distributing companies. It is not very hard to find.

The types of wood used in construction can control the weight of a wooden airframe. One must also consider the weight of the adhesives that are used to bind the wood together. A wooden airframe (without landing gear) was estimated to be about 13 lbs. The composite design, being considerably lighter would have come out to 11 lbs. A foam design, since the entire fuselage and wing volume is filled with foam, would have been heavier at an estimated 17 lbs.

Based on the results of Figure 6.1, a wooden design was chosen because of its availability, low cost, ease of use in construction, and relatively low weight. The team decided that these advantages far outweighed the disadvantages. A large deciding factor was flight practice for the pilot. The airplane need to be completed several months before the competition so that the pilot could get as many hours as possible flying it, as well allow time for modifications or repairs after a crash.

6.2 Manufacturing Processes

In order to save time, most main components of The Lisa B were manufactured simultaneously. Throughout this time, each component was tested for strength (when appropriate) and components designed to link together were periodically mated together to insure compatibility.

6.2.1 Fuselage Construction

The design program *AUTOCAD R14* was used extensively to insure cohesion between the different components of The Lisa B. In the fuselage section, *AUTOCAD R14* printouts were used to cut bulkheads (see Figure 5.3) by pasting the printout onto 0.125" thick plywood. Then, using a scroll saw, the bulkhead shapes were cut out, leaving notches for the stringers to pass through, and cutting the middle out of most of the bulkheads in order to save weight.

In order to make transportation of The Lisa B easier, the fuselage was designed to split into two parts, the break taking place just aft of the cargo bay. So, the fuselage was built in two pieces and when completed, was put together for flight. When all of the bulkheads were cut out, the spruce stringers (which varied in length from 20" to 48") were mated with the bulkheads to form the fuselage shape. The distances between bulkheads had been previously determined and during construction a full-scale side-view plot of the fuselage made bulkhead spacing a simple matter. A small-scale version of this plot is in Figure 5.2.

The cargo bay was built the same way as the rest of the fuselage, except the bulkhead cutouts were fashioned to accommodate the water bottles. Two "keels" were axially installed below the water bottles to help transfer impact loads from the fuselage to the main landing gear.

In the front section of the fuselage, a battery platform and support structure for the nose gear was installed. The platform is level with the ground and consists of a 0.125" thick plywood platform, 2.5" below the top of the fuselage. The sections of the fuselage above this battery platform are removable hatches to allow access to the battery packs.

High stress areas of the fuselage, namely the sections fore and aft of the cargo bay were then covered in fiberglass, using cyanoacrylate and epoxy as the adhesive matrix.

6.2.2 Joiner Construction

This strong composite member, shown in Figure 5.7 is made of two 0.25" x 2" x 36" pieces of birch glued together, along with a 0.0625" x 2" x 36" aluminum bar glued sandwich style to the wood. When the joiner was originally conceived it was clear that it must be very straight; that is why the birch was glued face to face with the warping of the wood facing in opposite directions. When glued together, clamps and weights were used to keep the member straight. This eliminated the natural warping in the wood. The aluminum bar was adhered to the wood with JB Weld to add to the member's stiffness.

The joiner is the most important component of the entire plane because it transfers the weight of the airframe to the wings in flight. It solidly attaches to the bulkhead in the center of the cargo bay, and protrudes about 15" out from each side of the fuselage to accommodate the wings. Each wing's main spar is hollow, so the joiner may slide down the

length of each spar. At the end of the joiner is an access panel in the wing so that two screws may pass through the joiner and the spar, thus keeping the wings from sliding off of the joiner. These screws also help reduce wing oscillations that may occur during flight.

6.2.3 Wing Spar Construction

Even before the airfoil had been chosen, the team members were working on ways to fabricate the main spar. The final design, shown in Figure 5.5, is a combination of a hollow beam (to accommodate joiner attachment) transitioning to an I-beam. A 0.25" x 0.75" spar cap runs the length of the entire spar on the top and bottom. Beginning from the wing root, plywood shear webbing on each edge of the spar cap run from the wing root, moving 18" outward, forming a box-shaped beam. At this point, the spar transitions into an I-beam. Here, the shear webbing was installed in the middle of the spar caps, forming the I-shape. To reinforce the transition point, the I-section and the box-section overlap, with two pieces of 0.28125" thick plywood filling the gaps between each piece of shear webbing. For the remaining length of the wing spar, the I-beam is reinforced on top, bottom, fore, and aft sides by triangle stock which helps hold the I-beam perpendicular to the spar caps. Once the spar was built, the wing was built around it.

6.2.4 Wing Construction

A warped wing does not have good flight characteristics, so a jig was built to help keep the wings straight during construction. The ribs were cut out using an aluminum mold to help maintain a consistent airfoil design. The ribs were then set up on the jig, along with the completed wing spar, which is located on the quarter chord. In order to accommodate the needed structural continuity of the spar, the airfoils were cut nearly perpendicular to the chord, so that when they were glued to the spar, the desired airfoil shape was still obtained. The stringers, running parallel to the main spar, were made out of 0.125" x 0.125" spruce. A leading-edge-shaped piece of balsa was obtained for the front edge of each wing. Wing tips were sanded down from 2" x 2" blocks that were glued to the end of each wing.

At this point, in order to strengthen the main spar even more, fiberglass was applied to the box-shaped beam section of the spar. Again, cyanoacrylate and epoxy were used as the adhesive matrix.

The area from the leading edge to the quarter chord was then sheeted with 0.0625" thick balsa. The flaperons made up 20% of the length of the chord. They were built at the same time as the wings and were attached using cyanoacrylate hinges. The completed wing is shown in Figure 5.4.

6.2.5 Stabilizer Construction

The horizontal and vertical stabilizers, as shown in Figure 5.6, were built at the same time to ensure cohesion between these two parts. Both were built from 0.0625" thick balsa ribs with 0.125" x 0.125" spruce stringers. The vertical stabilizer has two slots, bordered by 0.0625" thick plywood to accommodate the attachment struts that are attached to the rear of the fuselage. Likewise, the horizontal stabilizer has similar slots so that it may slide onto the attachment struts. Neither piece was sheeted with balsa, but heat-shrink fabric was applied to the outside. As with the flaperons, the elevator and the rudder were attached with cyanoacrylate hinges as well as plastic Robart hinges.

6.2.6 Landing Gear Construction

The main landing gear was fabricated out of a 2" x 0.25" x 40" piece of 6061 aluminum stock. After taking appropriate measurements to ensure an acceptable ground clearance, the aluminum bar was bent in four places (see Figure 5.7). The two wheels for the main gear were then attached to the fuselage via two L-brackets attached to the joiner inside the fuselage. The 5" diameter inflatable wheels were then attached to the vertical faces on the ends of the aluminum bar.

The nose gear consists of an 11" aluminum tube with an outer diameter of 0.75" and an inner diameter of 0.625". One end of this tube was mated to an apparatus of bearings and wood blocks that attached the nose gear to a forward bulkhead. At this attachment point, a control arm extends from a horn on the landing gear to the servo arm, forming a way to steer the plane on the ground using the nose gear. At the other end, a landing gear strut from Robart was inserted into the tube. This strut has internal suspension and since it is hose-clamped to the aluminum tube, the height of the nose gear can be altered if necessary. The nose wheel is a hard roller-blade wheel that was attached to the strut using hardware provided by Robart.

6.2.7 Motor Mount

The Aveox 1415/2Y motor was mounted on the nose of The Lisa B by means of a plywood platform that extends out of the foremost bulkhead (see Figures 5.3 & 5.8). A half-cylindrical block of wood reinforces this platform, with the rounded side facing downward; and two of the flat faces firmly glued to the platform and the forward bulkhead. Two small cross sections of a bicycle inner-tube were wrapped around the motor itself, and the motor was secured to the platform with two hose clamps. The speed controller was mounted to the side of the fuselage with Velcro straps. These components were mounted on the outside of the fuselage to allow as much air as possible to flow over them, facilitating cooling.

Table 6.1 –
Manufacturing Figures of Merit

Weighted Score	Figure of Merit	1	2	3
2	Actual Cost	2.0	0.5	1.0
2	Ease of Construction	1.7	0.8	1.5
2	Durability	1.0	1.5	1.9
2	Past Experience	1.8	1.0	0.8
1	Availability of Materials	1.0	0.3	0.3
1	Weight	0.8	0.9	0.5
10	Totals	8.3	5.0	6.0

- 1 – Wooden Construction
 2 – Composite Construction
 3 – Foam-Core Construction

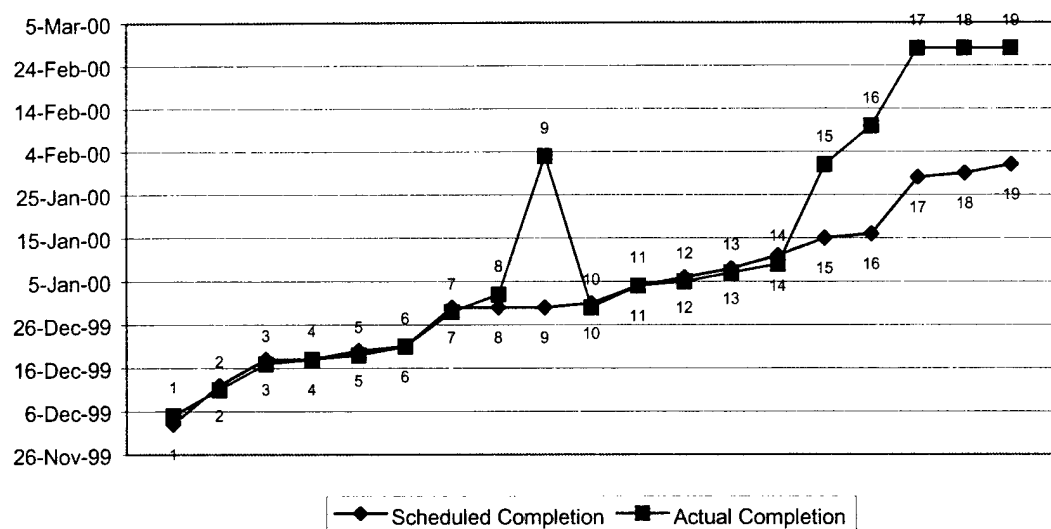


Figure 6.1 –
Manufacturing Timeline

Milestone	Scheduled	Completed	Milestone Description
1	3-Dec-99	5-Dec-99	Prototype Spar
2	12-Dec-99	11-Dec-99	Working Spar
3	18-Dec-99	17-Dec-99	Wing
4	18-Dec-99	18-Dec-99	Empennage
5	20-Dec-99	19-Dec-99	Cargo Bay
6	21-Dec-99	21-Dec-99	Mate Cargo Bay and Empennage
7	30-Dec-99	29-Dec-99	Mate Joiner and Cargo Bay
8	30-Dec-99	2-Jan-00	Front end
9	30-Dec-99	3-Feb-00	Batteries and motor
10	31-Dec-99	30-Dec-99	Mate wing to fuselage
11	4-Jan-00	4-Jan-00	Winter quarter begins
12	6-Jan-00	5-Jan-00	Attach control surfaces
13	8-Jan-00	7-Jan-00	Radio systems
14	11-Jan-00	9-Jan-00	Main gear
15	15-Jan-00	1-Feb-00	Nose gear
16	16-Jan-00	10-Feb-00	Radio ground testing
17	29-Jan-00	28-Feb-00	Systems integration
18	30-Jan-00	28-Feb-00	Ground testing
19	1-Feb-00	28-Feb-00	Maiden voyage

7.0 Bibliography

Abbott, Ira H. & Von Doenhoff, Albert E. Theory of Wing Sections (1958). New York: Dover Publications, Inc.

Broeren, Andy P.; Giguere, Philippe; Gopalarathnam, Ashok; Lyon, Christopher A.; & Selige, Michael S. Summary of Low-Speed Airfoil Data, Volume 3 (1997). Virginia Beach, Virginia, SoarTech Publications

Nelson, Robert C. Flight Stability and Automatic Control (2nd ed.), 1998. Boston, Massachusetts, McGraw-Hill Company, Inc.

Shevell, Richard S. Fundamentals of Flight (2nd ed.), 1989. Englewood Cliffs, New Jersey: Prentice-Hall, Inc.

Appendix A

Optimization Spreadsheets and Scoring Estimates

Cost and Scoring for 2000 DBF Contest

$$\text{Aircraft cost} = A \cdot \text{MEW} + B \cdot \text{REP} + C \cdot \text{MFHR}$$

A = 100
B = 1
C = 20

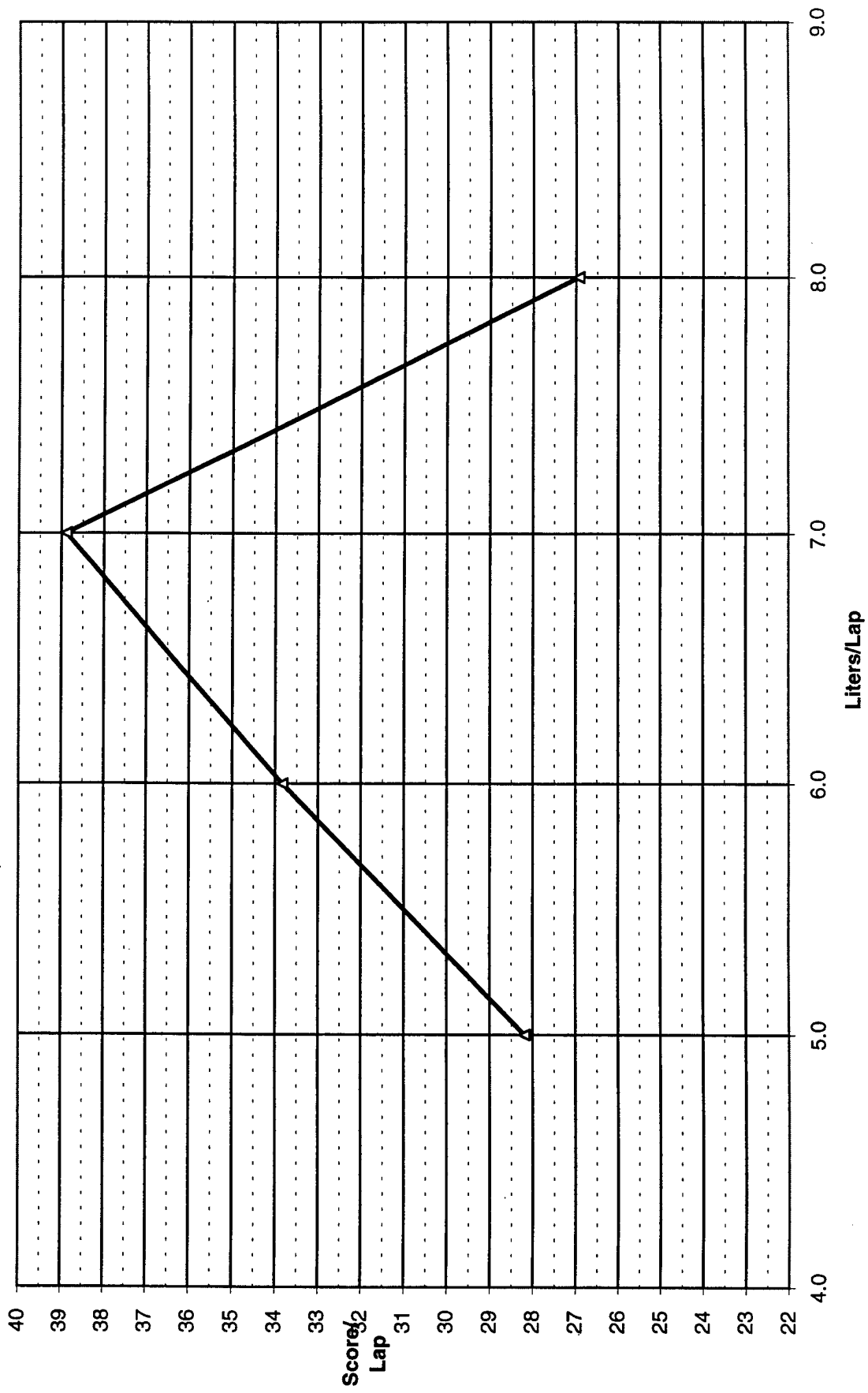
Variables		MEW		REP		MFHR		Costs				Score		Notes	
Payload/Lap (liters)	Laps	Empty Weight (lb)	Weight	Motors	Cells	Wing Area (ft²)	Length (ft)	Servos	MEW	REP	MFHR	Total Cost	Payload Score		Total Score
0.0	0	45.0		2	48	20.0	8.0	5	45.0	5760	172.0	13700	0.0	0.00	Albatross - DBF 1998/99
6.9	2	20.3		2	48	13.1	7.5	4	20.3	5772	141.4	10630	138.0	12.98	
1.0	1	2.9		2	7	3.0	3.0	4	2.9	837	83.0	2791	10.0	3.58	1998/1999 Average plane, linear relationships (adjusted for scaling)
2.0	1	5.9		2	14	5.0	3.5	4	5.9	1673	93.0	4121	20.0	4.85	
3.0	1	8.8		2	21	7.0	4.0	4	8.8	2510	103.0	5452	30.0	5.50	
4.0	1	11.8		2	28	9.0	4.5	4	11.8	3346	113.0	6783	40.0	5.90	
5.0	1	14.7		2	35	11.0	5.0	4	14.7	4183	123.0	8114	50.0	6.16	
6.0	1	17.7		2	42	13.0	5.5	4	17.7	5019	133.0	9444	60.0	6.35	
7.0	1	20.6		2	49	15.0	6.0	4	20.6	5856	143.0	10775	70.0	6.50	Max. weight for 2000 competition
8.0	1	23.5		2	56	17.0	7.0	4	23.5	6692	155.0	12146	80.0	6.59	
1.0	1	2.9		1	7	3.0	3.0	4	2.9	418	78.0	2272	10.0	4.40	
2.0	1	5.9		1	14	5.0	3.5	4	5.9	837	88.0	3185	20.0	6.28	
3.0	1	8.8		1	21	7.0	4.0	4	8.8	1255	98.0	4097	30.0	7.32	
4.0	1	11.8		1	28	9.0	4.5	4	11.8	1673	108.0	5010	40.0	7.98	
5.0	1	14.7		1	35	11.0	5.0	4	14.7	2091	118.0	5922	50.0	8.44	
6.0	1	17.7		1	42	13.0	5.5	4	17.7	2510	128.0	6835	60.0	8.78	
7.0	1	20.6		1	49	15.0	6.0	4	20.6	2928	138.0	7747	70.0	9.04	
8.0	1	23.5		1	56	17.0	7.0	4	23.5	3346	150.0	8700	80.0	9.20	

Graph Liters/Lap	Score
1.0	3.58
2.0	4.85
3.0	5.50
4.0	5.90
5.0	6.16
6.0	6.35
7.0	6.50
8.0	6.59
1.0	4.60
2.0	6.48
3.0	7.50
4.0	8.15
5.0	8.59
6.0	8.91
7.0	9.15
8.0	9.30

Average plane

This was used to demonstrate that the Lisa B is superior to a biplane and such. Only the graph is actually meaningful; this table is scratchwork.

Score Per Lap vs. Payload



6 Liters

Loaded sortie

	Take off	Climb	Turns	Cruise
Thrust (oz)	168.0	136.9	55.7	48.2
Duration (s)	4.33	8.18	23.30	21.76
Capacity (min)	4.50	4.10	7.40	8.40
Power used (%)	1.60	3.33	5.25	4.32

Total time (s):	57.57	Speed (mph):	47
Total power (%):	14.49		

Empty sortie

	Take off	Climb	Turns	Cruise
Thrust (oz)	80.0	71.8	33.4	29.4
Duration (s)	4.66	10.31	18.84	62.80
Capacity (min)	13.90	9.40	15.40	17.00
Power used (%)	0.56	1.83	2.04	6.16

Total time (s):	96.61	Speed (mph):	38
Total power (%):	10.58		

	Both sorties	Two payload, one empty	Three payload, two empty	Four payload, three empty
Total time (min):	2.57	3.53	6.10	8.67
Total power (%):	25.08	39.57	64.65	89.72

7 Liters

Loaded sortie

	Take off	Climb	Turns	Cruise
Thrust (oz)	200.0	154.9	61.5	53.4
Duration (s)	4.05	7.85	24.29	20.87
Capacity (min)	3.40	3.40	6.40	7.20
Power used (%)	1.99	3.85	6.33	4.83

Total time (s):	57.06	Speed (mph):	49
Total power (%):	16.99		

Empty sortie

	Take off	Climb	Turns	Cruise
Thrust (oz)	80.0	69.8	34.6	29.9
Duration (s)	4.88	10.61	17.85	66.29
Capacity (min)	13.30	10.20	16.10	17.80
Power used (%)	0.61	1.73	1.85	6.21

Total time (s):	99.63	Speed (mph):	36
Total power (%):	10.40		

	Both sorties	Two payload, one empty	Three payload, two empty	Four payload, three empty
Total time (min):	2.61	3.56	6.17	8.79
Total power (%):	27.39	44.38	71.77	99.16

8 Liters

Loaded sortie

	Take off	Climb	Turns	Cruise
Thrust (oz)	222.0	191.3	75.5	65.7
Duration (s)	4.09	7.65	25.28	20.05
Capacity (min)	3.00	3.00	5.40	6.20
Power used (%)	2.27	4.25	7.80	5.39

Total time (s):	57.07	Speed (mph):	51
Total power (%):	19.71		

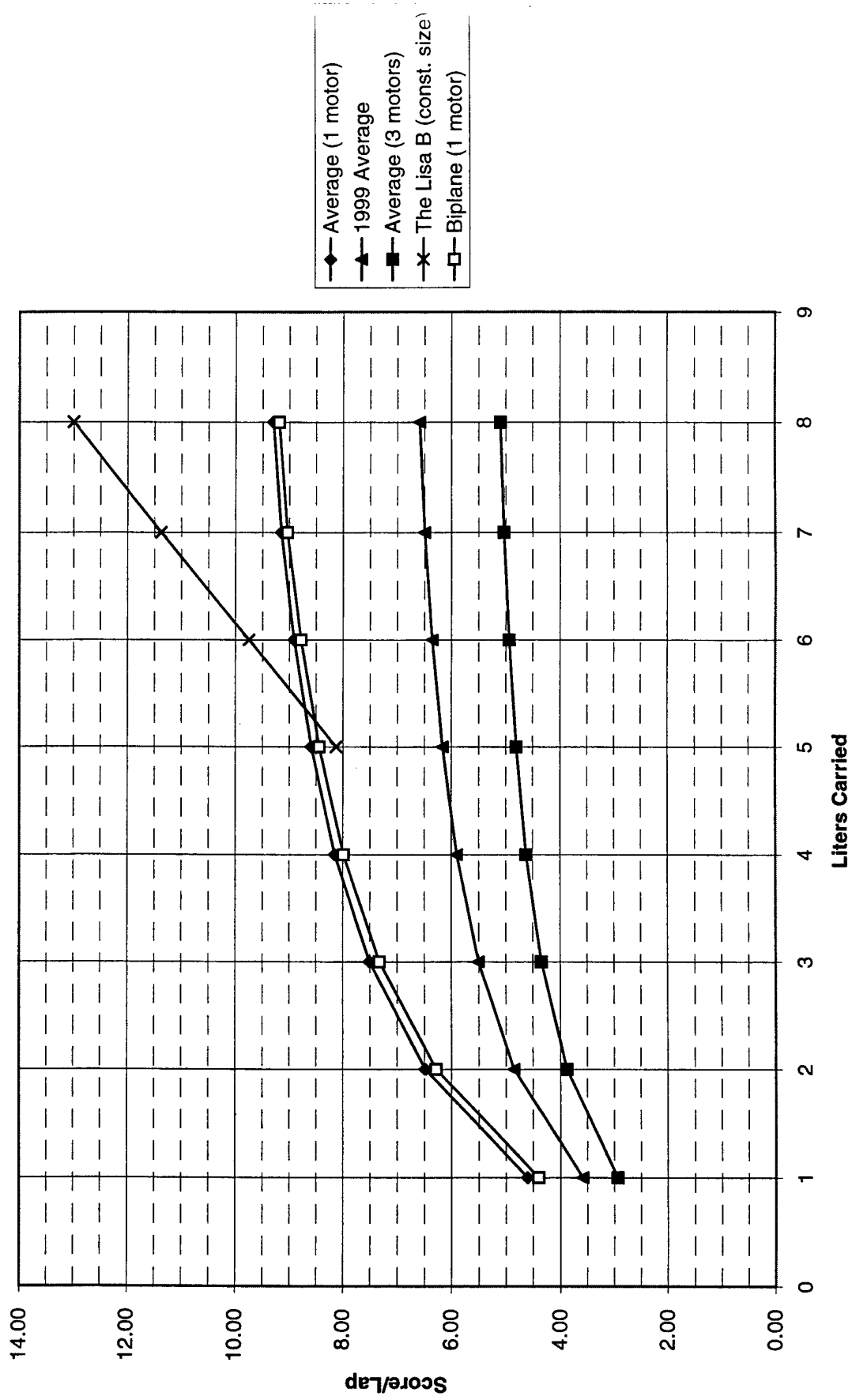
Empty sortie

	Take off	Climb	Turns	Cruise
Thrust (oz)	88.0	86.4	42.4	36.8
Duration (s)	4.96	10.25	18.84	62.80
Capacity (min)	12.10	6.40	12.10	13.30
Power used (%)	0.68	2.67	2.60	7.87

Total time (s):	96.85	Speed (mph):	38
Total power (%):	13.82		

	Both sortie	Two payload, one empty	Three payload, two empty	Four payload, three empty
Total time (min):	2.57	3.52	6.08	8.65
Total power (%):	33.53	53.25	86.78	120.31

Figure 1 - Score vs. Payload



Appendix B

Performance Equations

B.1 General Performance Equations

$$\text{Planform} = \text{Span} * \text{Chord}$$

$$AR = \frac{\text{Span}}{\text{Chord}}$$

$$Re = \frac{c * V_{cruise}}{v}$$

$$C_L = \frac{1}{2} S \rho V^2$$

$$C_{Dp \text{ total}} = C_{Dp \text{ wing}} + C_{Dp \text{ tail}}$$

$$C_{Di} = \frac{C_L^2}{\pi A Re}$$

$$C_{Dtotal} = C_{Dp \text{ total}} + C_{Di}$$

$$S_{vertical} = \text{height} * \text{length}$$

$$S_{fuselage} = \text{length} * \text{diameter} * \pi$$

$$Re_{vertical} = \frac{V * \text{length}}{\gamma}$$

$$Re_{fuselage} = \frac{V * \text{length}}{\gamma}$$

$$C_{fv} = \frac{.664}{\sqrt{Re_v}}$$

$$C_{ff} = \frac{.074}{Re_f^2} - \frac{1700}{Re_f}$$

$$D_{p \text{ vertical}} = .5 * \rho * V^2 * S_v * C_{fv}$$

$$D_{p \text{ fuselage}} = .5 * \rho * V^2 * S_f * C_{ff}$$

$$C_{DiH} = \frac{C_{L \text{ tail}}}{\pi e AR}$$

$$S_H = \text{span} * \text{chord}$$

$$D_{ih} = .5 * \rho * V^2 * S_H * C_{DiH}$$

$$\text{Tail Lift} = .5 * \rho * V^2 * C_L * S_H$$

$$M_W = .5 * C_{Mw} * \rho * V^2 * S_W * c + (.5 * C_{Lw} * \rho * V^2 * S_W * x) \quad x = \text{distance from quarter chord to CG}$$

$$M_H = .5 * C_{LH} * \rho * V^2 * S_H * l_H * \eta \quad l_H = \text{distance from CG to quarter chord of tail}$$

$$M_{CG} = M_W + M_H$$

$$D_i = .5 * C_{Di} * S * \rho * V^2 + D_{i \text{ tail}}$$

$$D_p \text{ cruise} = .5 * \rho * V^2 * C_{Dp \text{ total}} * S + D_p \text{ vertical} + D_p \text{ fuselage}$$

$$D_{\text{total}} = D_i + D_p \text{ cruise}$$

$$D_p \text{ LO} = .5 * \rho * C_{Dp \text{ total}} * S * V_{LO}^2$$

$$D_{\text{total LO}} = D_i + D_p \text{ LO}$$

$$L/D = W/D_{\text{total}}$$

$$T_{\text{cruise}} = D_{\text{total}}$$

$$\text{Power req.} = T * V$$

$$T_{LO} = W * \left(\frac{a}{a_g} \right)$$

$$\text{accel} = V_{LO}^2 / (2 * \Delta X)$$

$$V_s = \sqrt{\frac{W}{.5 * C_{L \text{ max}} * S * \rho}}$$

$$V_{LO} = 1.2 * V_g$$

B.2 Sortie Performance Calculations

B.2.1 Take-Off

$$V_s = \sqrt{\frac{W}{.5 * C_{L_{max}} * S * \rho}}$$

$$V_{LO} = 1.2 * V_g$$

$$accel = T * 32.2 / W$$

$$Dist. = V_{LO}^2 / (2 * a)$$

$$Time = \sqrt{\frac{2 * Dist}{a}}$$

B.2.2 Climb

$$\alpha = \text{climb angle} = \arctan\left(\frac{height}{length}\right)$$

$$accel = \frac{V_f^2 - V_i^2}{2 * length}$$

$$T \text{ for accel} = \frac{W * accel}{32.2}$$

$$T_{req} = D_{total} + (W \sin \alpha)$$

$$T_{total} = T \text{ for accel} + T_{req}$$

$$Time \text{ to climb} \Rightarrow x = x_0 + V_0 t + \frac{1}{2} a t^2 \Rightarrow \frac{-V_i + \sqrt{V_i^2 - 4 \frac{accel}{2} (-length)}}{accel}$$

B.2.3 Turn

$$\text{Lift} = \frac{W}{\sin(\text{bank angle})}$$

$$C_L = \frac{\text{Lift}}{\frac{1}{2} S \rho V^2}$$

$$C_D = C_{Dp \text{ total}} + \frac{C_L^2}{\pi A \text{ Re}}$$

$$\text{Turn radius} = \frac{V^2}{32.2 * \tan(\text{bank angle})}$$

$$\text{Time} = \frac{\pi V}{2 * 32.2 * \tan(\text{bank angle})}$$

$$T_{\text{req}} = .5 * C_D * V^2 * S * \rho + D_{p \text{ vertical}} + D_{p \text{ fuselage}} + D_{i \text{ horizontail}}$$

B.2.4 Cruise

For T_{req} I just took the thrust required from the main sheet

$$\text{Time} = 500 / V_{\text{cruise}} \quad 500 = \text{the distance of half the straight away}$$

B.2.5 Landing

$$T_{\text{req}} = D_{\text{total}} - \frac{W}{16}$$

B.3 Stability Calculations

B.3.1 General Stability

$$V_H = \frac{S_{tail} l_H}{S_{ref} c}$$

$$Z_\alpha = \frac{-(C_{L_\alpha} + C_{D_0}) Q S_{ref}}{m}$$

$$M_\alpha = \frac{C_{m_\alpha} Q S_{ref} c}{I_y} \quad I_y \text{ is the moment of inertia in the y direction}$$

$$X_u = \frac{-(2C_{D_0} Q S_{ref})}{m V_\infty}$$

$$C_{m_q} = -2\eta C_{L_{\alpha_t}} V_H \left(\frac{l_H}{c} \right)$$

$$Z_u = \frac{-(2C_{L_\alpha} Q S_{ref})}{m V_\infty}$$

$$m_q = \frac{C_{m_q} \left(\frac{c}{2V_\infty} \right) Q S_{ref} c}{I_y}$$

B.3.2 Short Period

$$\omega_{nsp} = \sqrt{\frac{Z_\alpha M_q}{V_\infty} - M_\alpha}$$

$$\zeta = \frac{-\left(M_q + M_\alpha + \frac{Z_\alpha}{V_\infty}\right)}{2\omega_{nsp}}$$

B.3.3 Phugoid Period

$$\omega_{np} = \sqrt{\frac{-Z_u g}{V_\infty}}$$

$$\zeta = \frac{-X_u}{2\omega_{np}}$$

Appendix C

Performance Calculations

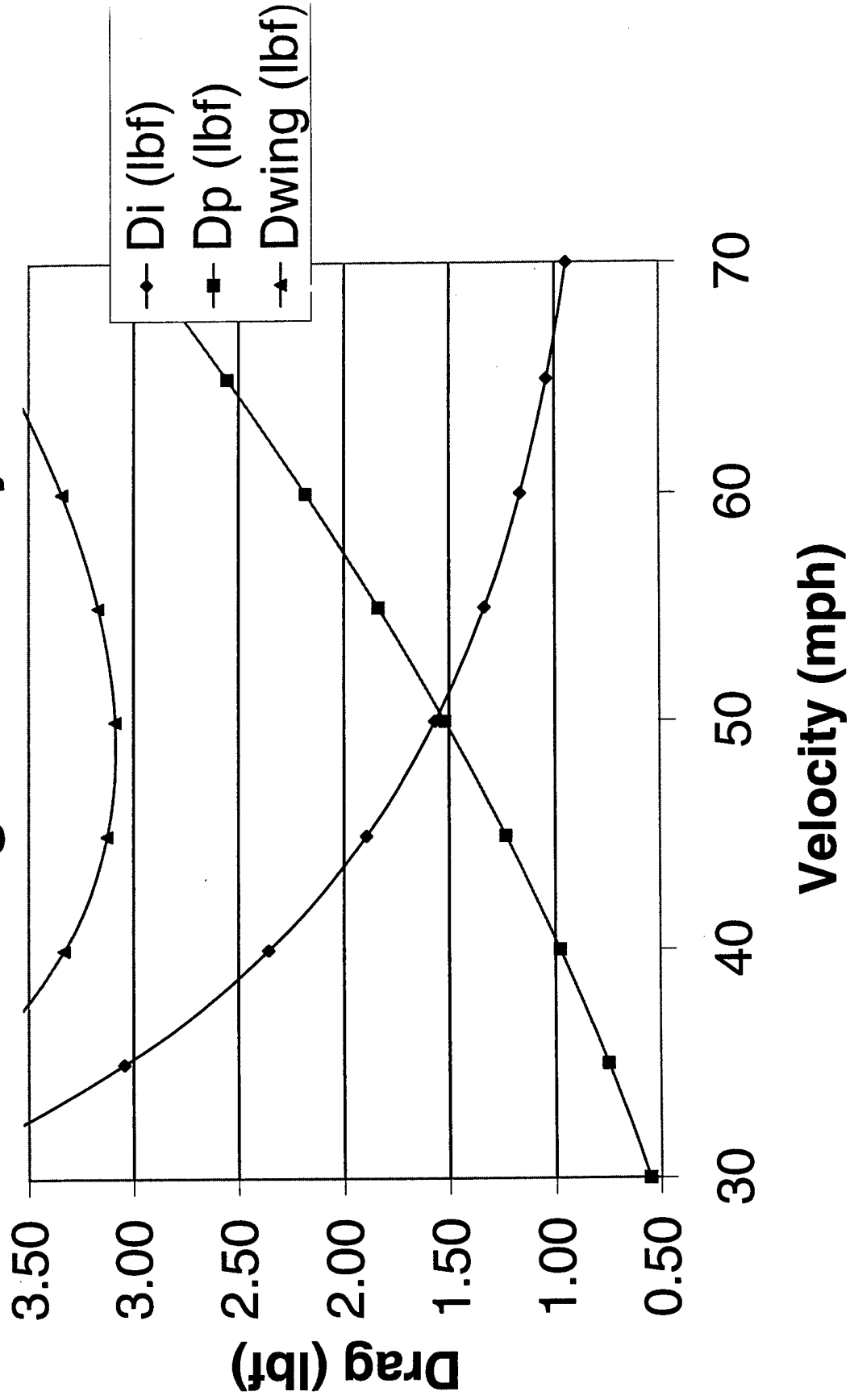
<div> <div>Enter after you get $C_{L_{wing}}$</div> <div> <div>C_{Dp} cruise</div> <div>0.01</div> </div> <div> <div>C_{Dp} Tail</div> <div>0.008</div> </div> <div> <div>C_{Lmax}</div> <div>1.60</div> </div> <div> <div>C_M</div> <div>-0.16</div> </div> </div>		<div> <div>Weight</div> <div>35 lbs</div> </div> <div> <div>Wing loading</div> <div>45.71 oz/ft</div> </div>		<div> <div>Velocity</div> <div>50 mph</div> <div>73.3 ft/s</div> </div>		<div> <div>Horizontal Stabilizer</div> <div> <div>x</div> <div>0 in</div> <div>0.0000 ft</div> </div> <div> <div>C_{LH}</div> <div>-0.29</div> </div> </div>	
<div> <div>Span (b)</div> <div>7 ft</div> </div>		<div> <div>Density</div> <div>0.00224 slug/ft³</div> <div>0.00238 slug/ft³</div> </div>		<div> <div>Span (tail)</div> <div>3.09375 ft</div> </div>		<div> <div>η</div> <div>0.87</div> </div>	
<div> <div>Chord (C)</div> <div>1.75 ft</div> </div>		<div> <div>TO dist</div> <div>90 ft</div> </div>		<div> <div>Chord</div> <div>0.979 ft</div> </div>		<div> <div>Distance from CG to Tail</div> <div>4.5 ft</div> <div>54 in</div> </div>	
<div> <div>Wing Efficiency</div> <div>0.9</div> </div>		<div> <div>Kinematic Viscosity</div> <div>1.650E-04 ft²/s</div> </div>		<div> <div>Vertical Stabilizer</div> <div> <div>length</div> <div>1.61458 ft</div> </div> </div>		<div> <div>Height</div> <div>1.083 ft</div> </div>	
<div> <div>Fuselage length</div> <div>7.5 ft</div> </div>		<div> <div>Fuselage height</div> <div>0.833 ft</div> </div>					

<div> <div>Planform (S)</div> <div>12.25 ft²</div> </div>		<div> <div>AR</div> <div>4.00</div> </div>		<div> <div>R_e</div> <div>7.8E+05</div> </div>		<div> <div>T_{cruise}</div> <div>3.40 lbf</div> </div>		<div> <div>Planform (S_H)</div> <div>3.029 ft²</div> </div>	
<div> <div>C_L</div> <div>0.474</div> </div>		<div> <div>D_i</div> <div>1.64 lbf</div> </div>		<div> <div>$D_{p,cruise}$</div> <div>1.76 lbf</div> </div>		<div> <div>P_{req}</div> <div>249.09 ft-lb/s</div> <div>0.453 hp</div> </div>		<div> <div>M_W</div> <div>-20.67</div> </div>	
<div> <div>C_{Di}</div> <div>0.020</div> </div>		<div> <div>D_{total}</div> <div>3.40 lbf</div> </div>		<div> <div>L/D</div> <div>10.3</div> </div>		<div> <div>T_{Lo}</div> <div>13.86 lbf</div> </div>		<div> <div>M_H</div> <div>20.72</div> </div>	
<div> <div>$C_{Dp,total}$</div> <div>0.018</div> </div>		<div> <div>S_v</div> <div>1.74907809 ft²</div> </div>		<div> <div>Parasite Drag</div> <div>1.74907809 ft²</div> </div>		<div> <div>Tail Lift</div> <div>-5.29 lbf</div> </div>		<div> <div>M_{cg}</div> <div>0.06</div> </div>	
<div> <div>C_{Dtotal}</div> <div>0.0379</div> </div>		<div> <div>S_l</div> <div>19.63 ft²</div> </div>		<div> <div>Re_v</div> <div>4.81E+05</div> </div>		<div> <div>AR horizontal</div> <div>3.160</div> </div>			
<div> <div>V_e</div> <div>27.2 mph</div> </div>		<div> <div>C_v</div> <div>9.57E-04</div> </div>		<div> <div>Re_l</div> <div>3.33E+06</div> </div>					
<div> <div>V_{Lo}</div> <div>32.7 mph</div> </div>		<div> <div>D_{PV}</div> <div>1.01E-02</div> </div>		<div> <div>C_{If}</div> <div>3.54E-03</div> </div>					
<div> <div>47.9 ft/s</div> </div>		<div> <div>Induced Drag</div> <div>0.00941</div> </div>		<div> <div>D_{PF}</div> <div>4.19E-01</div> </div>					
<div> <div>accel</div> <div>12.75 ft/s²</div> </div>		<div> <div>C_{Dh}</div> <div>0.00941</div> </div>							
<div> <div>q</div> <div>6.03 slug/ft-s</div> </div>									

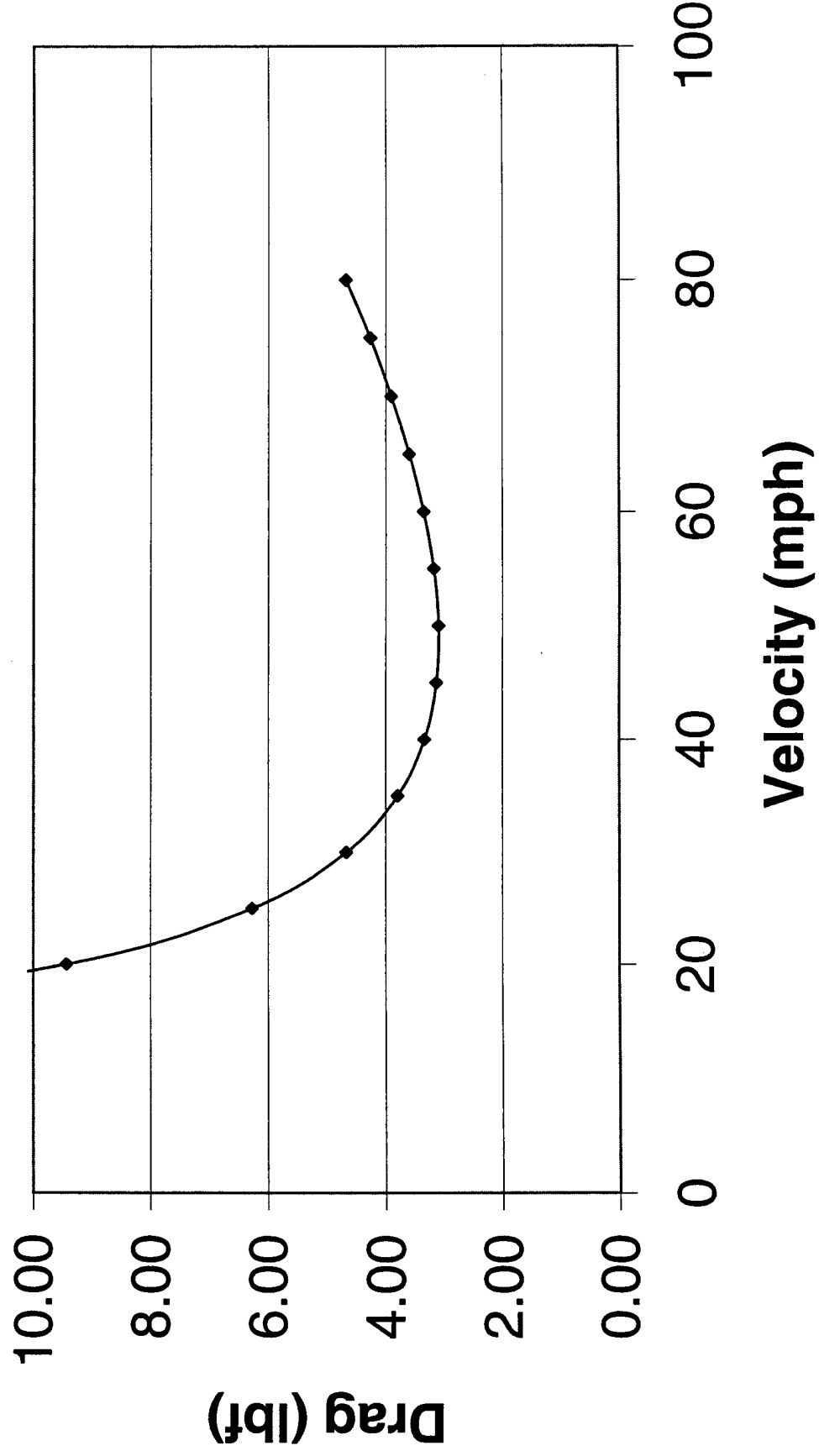
$C_{l\alpha}$	0.8	m	20	lbs	$C_{m\alpha}$	-0.188	$C_{L\alpha t}$	0.1166	1/deg	S_{tail}	3.03
Chord	1.75	ft	0.622	slugs	η	0.87		6.6807	1/rad	Q	6.03
I_y	21.82	slugs-ft ²	50	mph	I_H	4.5	S_{ref}	12.25	ft ²		lb/ft ²
			73.3	ft/s			C_{D0}	0.046			

V_H	0.636	$Z\alpha$	-100.5	ft/s ²	M_α	-1.11	1/s ²	X_u	-0.149	1/s	C_{mq}	-19.0
M_q	-1.34	Short Period	1.72	ω_{sp}	Phugoid	ω_{hp}	1.07		Z_u	-2.59	1/s	
		ζ	1.11	ζ			0.07					

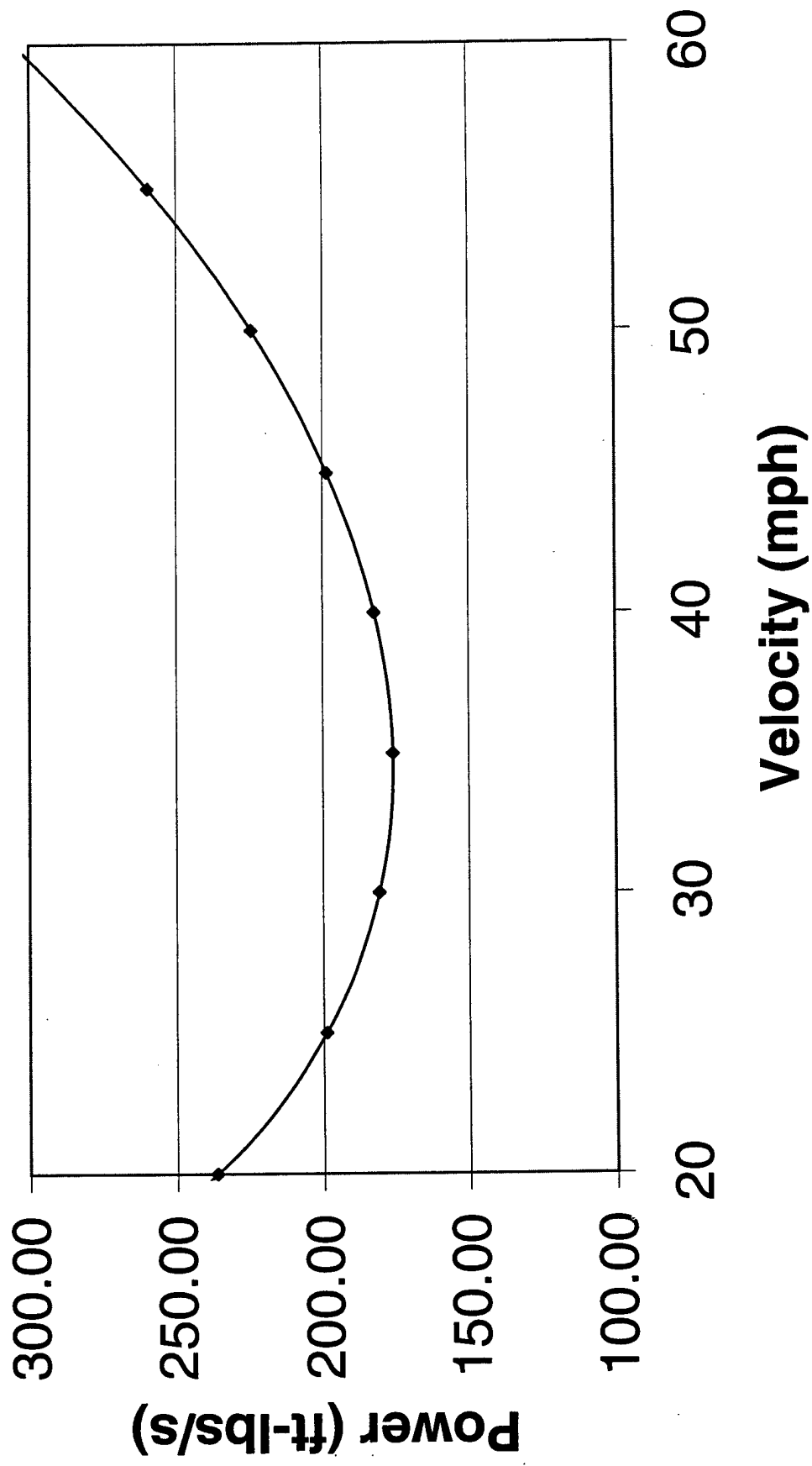
Drag vs. Velocity



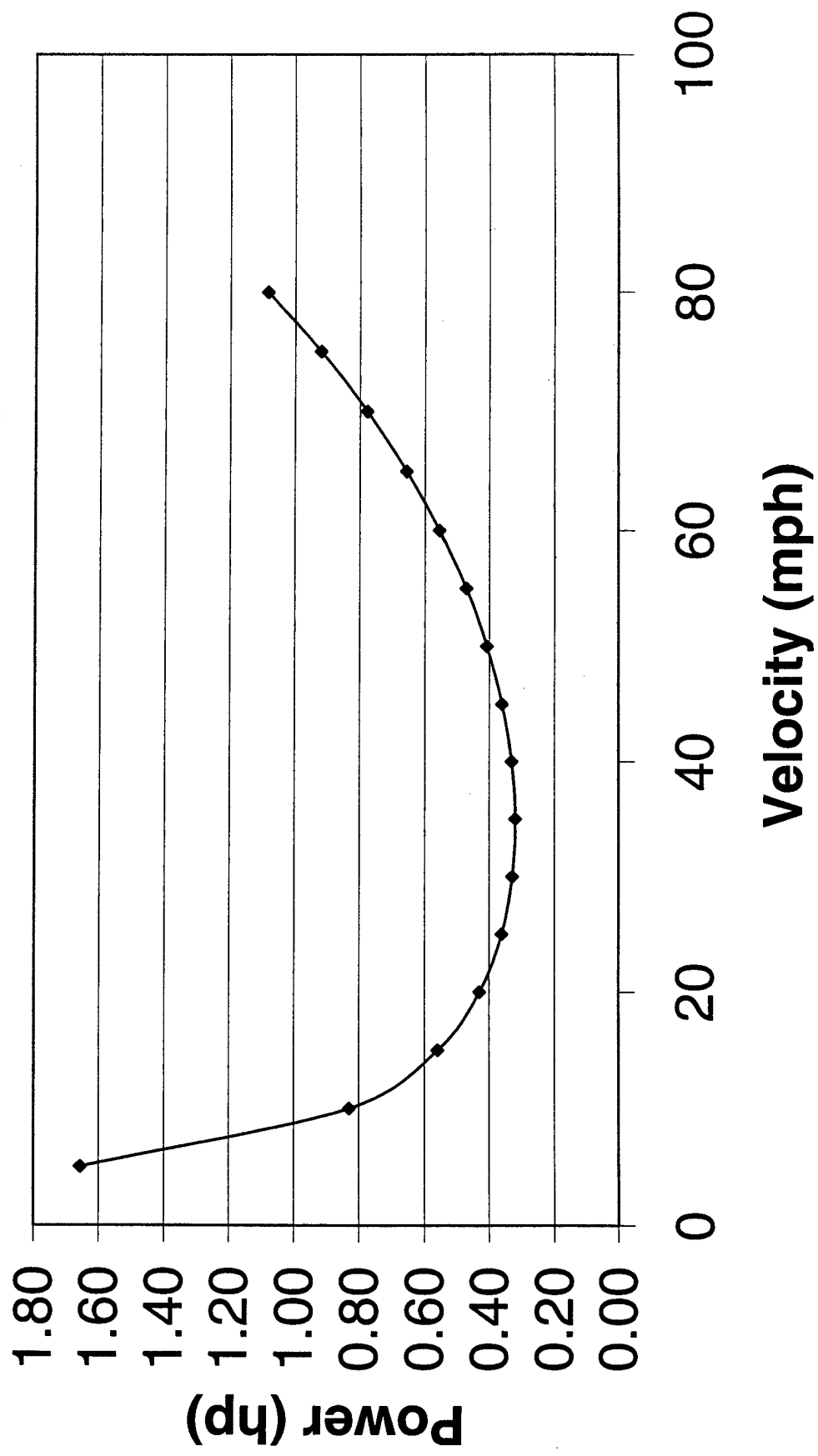
Total Drag vs. Velocity



Power vs Velocity



Power vs Velocity



Take Off	
Weight	35 lb
T _{avg}	13 lbf
V _{cruise}	50 mph
	73.3 ft/s
C _{Lmax}	2
V _s	24.3 mph
	35.7
V _{LO}	29.2 mph
	42.8 ft/s
accel	11.96 ft/s ²
TO dis	76.8 ft
TO time	3.58 s

Climb	
Height reached	30 ft
Length intended	450 ft
V _{cruise}	50 mph
	73 ft/s
climb angle	3.81 deg
	0.067 radians
accel	3.94 ft/s ²
T for accel	4.28 lbf
T _{req}	5.72 lbf
T _{total}	10.00 lbf
Time to climb	7.75 sec

With Water

Turn (180°)	
Bank angle	30 deg
	0.524 radians
V _{cruise}	50 mph
	73 ft/s
Lift	40.4 lbf
Turn radius	289.3 ft
C _L	0.55
Time	12.39 sec
C _D	0.045
T _{req}	3.89 lbf

Cruise (500 ft)	
T _{req}	3.40 lbf
Time	6.8 sec

Take Off	
Weight	19 lb
T _{avg}	4 lbf
V _{cruise}	38 mph
	55.7 ft/s
C _{Lmax}	2
V _s	17.9 mph
	26.3
V _{LO}	21.5 mph
	31.6 ft/s
accel	6.78 ft/s ²
TO dis	73.5 ft
TO time	4.66 s

Climb	
Height reached	30 ft
Length intended	450 ft
V	38 mph
	56 ft/s
climb angle	3.81 deg
	0.067 radians
C _L	0.474
accel	2.34 ft/s ²
T for accel	1.38 lbf
T _{req}	4.66 lbf
T _{total}	6.04 lbf
Time to climb	10.31 sec

With Out Water

Turn (180°)			
Bank angle	30 deg		
	0.524 radians		
V	38 mph		
	56 ft/s		
Lift	21.9 lbf	Turn radius	167.1 ft
C _L	0.51	Time	9.42 sec
C _D	0.04141	T _{req}	2.37 lbf

Cruise (500 ft)	
T _{req}	3.40 lbf
Time	6.8 sec

AIAA Student Design / Build / Fly Competition

**California Polytechnic State University,
San Luis Obispo**

presents

The Lisa B

CAL POLY

Design Report – Addendum Phase

Designed and Developed by:

Jonathan Chapman

David House

Julio Hurtado

Joon Kim

Jann Mayer

Jeff Napior

Chad Ward

April 10, 2000

Table of Contents

Table of Contents	ii
7.0 Lessons Learned	1
7.1 Team Management	1
7.2 Performance	2
7.3 Design Modifications	3
8.0 Rated Aircraft Cost	4
<i>Table 8.1 – Manufacturing Man Hours of the Lisa B</i>	4
<i>Table 8.2 – Rated Aircraft Cost of the Lisa B</i>	5

7.0 Lessons Learned

7.1 Team Management

The team had a simple philosophy in mind from the start of the project; don't delay. Design was started promptly in September, and the construction was done primarily during winter break. Without a doubt, there would be some unforeseen delays. However, the team had not taken into account the reliability (or lack thereof) of sub-contractors. It was assumed that once a product was ordered, in a few days it would be available for use. This was not the case when it came to the propulsion systems of the Lisa B. There were a total of twelve weeks of delays, directly caused by the poor business practices of the manufacturer of the propulsion system. There were many defects that necessitated the return of the product for repair, as well as poor communication between the manufacturer and the team managers. These unfortunate circumstances delayed the Lisa B's maiden flight, and ultimately shortened flight-testing time period from a predicted two months to approximately three weeks.

Throughout the construction of the two models of the Lisa B, construction methods were greatly improved. The first fuselage took three weeks to complete. The second one took only four days. Every component that was built taught the team members new methods of manufacturing subsequent components of the plane.

The cost estimations were also greatly underestimated. It was never thought that a model airplane could cost as much as a new car. Shipping was greatly underestimated, as were many of the unforeseen product needs that arose during construction. Back-up systems were also not accounted for. After the trouble with the power plant, it was decided redundant systems were absolutely necessary, thus doubling the cost of the most expensive parts of the airplane.

While it was known that money was going to have to be raised, the extent of the fundraising campaign came as a surprise. Over fifty letters were sent out, many phone calls were made, as well as many personnel contacts to fund this project. Money management became a necessary and budgeting was essential to the success of the project. This year's team was very fortunate to have almost all expenses funded through corporate and private donations. Many contacts were also made for the next year's team.

Lastly, the value of teamwork was learned. This year's team worked exceedingly well together. Having been close friends before the project began made for a fun and productive work environment. With only seven people on the team, everyone had to do his or her part, though motivation was never a problem. Clearly, a small group such as the current team worked very well for a project of this size.

7.2 Performance

Through flight tests, it was found that some of the calculations used for predicting the Lisa B's performance had some flaws. The following three calculated performance parameters had a drastic effect on the Lisa B:

- C_l max
- Take-off Thrust
- Drag

The SG6043 airfoil was chosen for its high lift coefficient of 1.6. The team was aware of the existence of wingtip vortices, but unfortunately did not know about the effect they really had on the wing, so the 2-D lift coefficient of 1.6 was used in all calculations involving the wing's performance. Through discussions with some professors of aerodynamics at Cal Poly, it was found that the C_l max, when moved from 2-D to a 3-D wing, would decrease by 20 to 30 percent. This meant that the C_l max would be reduced to about 1.2. This drastically changed the amount of water that the Lisa B would be able to carry, dropping from an eight-liter capacity to a four-liter payload. The actual amount of water that the plane would be able to carry was eventually determined by flight-testing.

The thrust needed to take off with no payload was calculated to be 5 pounds. After the first flight it was found that almost 10 pounds of thrust was needed to take off. After talking to some professors at Cal Poly, a new equation was acquired and implemented. The revised calculations then showed that a thrust of a little more than 10 pounds was needed for take off. The new equation was confirmed by the flight test, so the new equation was used for all subsequent calculations. Although the new equation reports a thrust that is slightly higher than needed, it showed what the Lisa B really needed to do to get off the ground.

The drag calculations for the Lisa B originally were lower than what the plane was actually feeling. This caused inaccurate performance calculations for the thrust needed for climb, cruise, and also affected take off. After some discussion, new equations were found and used which gave numbers closer to the actual drag that the Lisa B produced. All drag estimates were made conservatively as a small margin for error is necessary in any performance calculation.

7.3 Design Modifications

After initial flight-testing, it was found The Lisa B was too heavy to perform within the required flight parameters. The Aveox 1415/2Y motor did not perform as was originally expected. To decrease the weight and increase performance, a second fuselage was built with the following changes:

- Motor mount configuration was modified
- Battery configuration was modified
- Propeller dimensions were increased to 18"x6"
- Lighter airframe
- Shorter fuselage

In the initial testing with the 16"x8" propeller, the motor generated exceedingly high operational temperatures. After only two minutes at full throttle the motor had reached unacceptable temperatures of 100°C. To correct the problem the motor mount was re-designed to increase cooling airflow over the motor. Bicycle tubing, which had previously been used to attach the motor, was removed. While it had been known that rubber would insulate the motor, it was believed that enough of the motor remained exposed for sufficient cooling to take place. However, after the removal of this tubing, the motor no longer generated the high temperatures. The mount itself was also re-designed so it would have less contact with the motor, allowing more contact with the cooling airflow.

The battery configuration was changed from three stacks of batteries packs to two 12-cell bars in a two-column configuration. This was done so the packs could be placed farther back in the nose section of the fuselage. By doing this, the center-of-gravity was more easily placed at the quarter-chord without the use of counter weights in the tail section. In addition, with the batteries packed so the positive and negative terminals butted up against each other, there was less power-loss between cells.

The propeller initially used, 16"x8", provided a good testing data for the first flights. However, it only produced 10 pounds of thrust, not nearly close enough to what was required. With the change to an 18"x6" propeller, 50% more power was obtained with just a very small increase in current draw.

The biggest and most important modification was in the construction of the fuselage. By using plywood half the thickness of the original bulkheads and by decreasing the length of the fuselage by 16 inches, over 5 pounds was cut from the original design. Since each bottle weighed 2.2 pounds, this modification allowed two additional bottles to be carried. It was decided not to reduce the frontal cross-section of the fuselage to better accommodate only four bottles, due to time constraints. The Lisa B was known to be stable aircraft, and a drastic re-design would have risked the unintentional creation of an unstable design, and with April looming in the near future, the team decided to make only the previously mentioned modifications and nothing more.

8.0 Rated Aircraft Cost

In previous DBF competitions, the real cost of the aircraft was documented in the addendum phase of the report. For the 2000 contest, a Rated Aircraft Cost model was provided by AIAA to help establish common cost analyses between the different teams. This allowed teams to more accurately document the cost of the respective aircraft, as well as introduced a reliable method of including aircraft cost in the scoring of the contest.

Below, in Table 8.1, the Work Breakdown Structure supplied by AIAA summarizes the manufacturing hours needed to complete the Lisa B. The total Manufacturing Man Hours (MFHR) is the sum of each Work Breakdown Structure (ΣWBS_n), which added up to 128.56 hours.

The Rated Aircraft Cost of the Lisa B is summarized in Table 8.2. The empty weight of 18 lbs, the number of engines, the number of cells, and the total man-hours were the airframe-dependent parameters; the remaining numbers are multipliers set forth by the contest rules. The Rated Aircraft Cost of the Lisa B (in \$ thousands) is 5.811.

Table 8.1 –

Manufacturing Man Hours (MFHR = ΣWBS_n) of the Lisa B

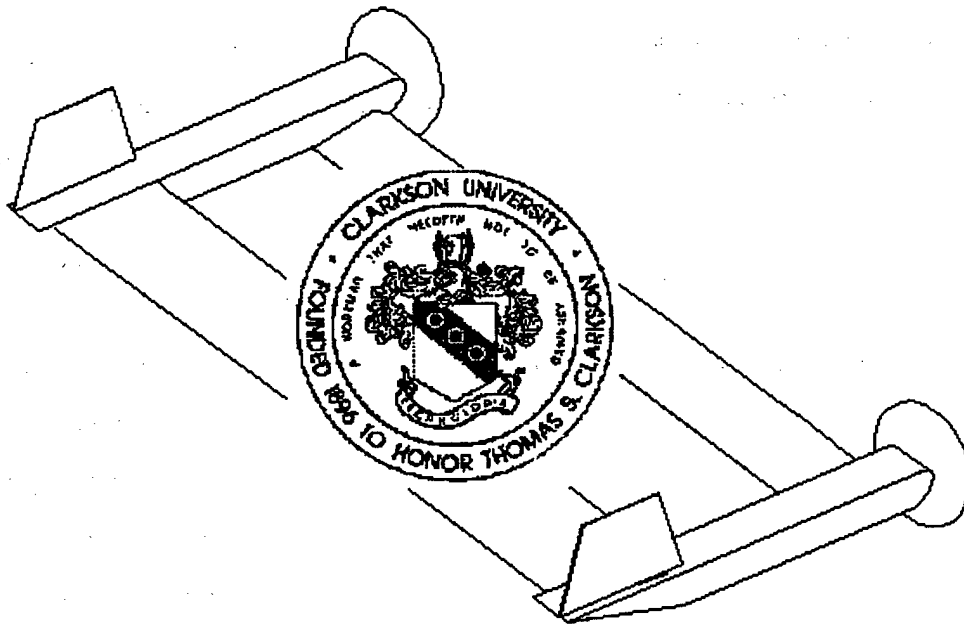
	Multiplier	Parameter	Total Hours
<u>Wing</u> (WBS ₁)	5 hr/wing	1 wing	5
	4 hr/sq ft	13.1 sq ft	52.4
<u>Fuselage & Pods</u> (WBS ₂)	5 hr/body	1 body	5
	4 hr/ft length	6.54 ft	26.16
<u>Empennage</u> (WBS ₃)	5 hr	(basic)	5
	5 hr/vert surface	1 vert surface	5
	10 hr/horz surface	1 horz surface	10
<u>Flight Systems</u> (WBS ₄)	5 hr	(basic)	5
	1 hr/servo	5 servos	5
<u>Propulsion Systems</u> (WBS ₅)	5 hr/engine	1 engine	5
	5 hr/propeller	1 propeller	5
MFHR =			128.56 hours

Table 8.2 –
Rated Aircraft Cost of the Lisa B

Multiplier	Airframe-Dependent Parameter	Value (\$)
\$100/lb.	18 lb.	1800
\$1/watt	(1 engine)*(50A)*(1.2 V/cell)*(24 cells)	1440
\$20/hr	128.56 hr	2571.2
	Total Value (\$)	5811.2
	Rated Aircraft Cost (\$ Thousands) =	5.811

Clarkson University

Golden Flight



1999 – 2000 AIAA Design, Build, and Fly Competition

Clarkson University

1999 – 2000 AIAA Design, Build, and Fly Competition

Design Report - Proposal Phase

Proposal Editors

Matt Duquette
Brent Bartlett
Jim Lychalk

Proposal Contributors

Mark Harrison
Glen Whitehouse
Tom Daugherty

Team Members

Matthew Duquette – *Team Leader*

Controls Team

Dave Kametz – *Team Leader*
Annie B McLaughlin
Thomas Daugherty

Structures Team

J. Wayne Braun - *Team Leader*
Josh Cook
Kevin Meyer
Chris Salter
Matthew Schmigel
Brian G. Kellough

Academic Advisor

Ken Visser, Ph.D.

Aerodynamics Team

Mark Harrison – *Team Leader*
Jason Kuntz
Jim Lychalk
Jun Park
Valeda Scribner

Propulsion Team

Glen Whitehouse – *Team Leader*
Brent Bartlett
Kevin McCutcheon
Matt Vignau
David Young

Other Members

Liz Kenny
Jeffrey Kibler
Rob Preuss
Eric Schlobohm
Joe Tari
Brian Raffa

Table of Contents

List of Figures and Tables	5
I Executive Summary	6
1.1 Design Tools Used	7
II Management Summary	9
III Conceptual Design	11
3.1 Design Parameters Investigated	11
3.2 Figures of Merit	12
3.3 Rated Aircraft Cost	14
3.4 Analytic Methods	14
IV Preliminary Design	17
4.1 Airfoil Selection	17
4.2 Motor Selection	18
V Detailed Design	24
5.1 Flight Analysis and Performance Predictions	24
5.2 Flight Pattern	25
5.3 Stability Analysis	26
5.4 Structural Analysis	27
5.5 Component Selection	27
5.6 Final Aircraft Configuration	29
Drawing Package	39
VI Manufacturing Plan	44
6.1 Wings	46
6.2 Fuselage	46
6.3 Empennage	47
6.4 Landing Gear	47
6.5 Manufacturing Schedule	47
References	50

List of Figures and Tables

Figure 2-1	Milestone Schedule and Completion Chart.....	10
Table 3-1	Weighted Objectives Table	16
Figure 4-1	Characteristics of a NACA 6412 Airfoil (zero flaps)	21
Figure 4-2	Motocalc Analysis of Battery Current (12 X 9 Propeller, 40 cells)	22
Figure 4-3	Motocalc Analysis of Thrust (12 X 9 Propeller, 40 cells)	22
Figure 4-4	Cost function for one fuselage	23
Figure 4-5	Cost function for two fuselages.....	23
Table 5-1	Performance Calculations	30
Table 5-2	Turning Analysis	31
Table 5-3	Endurance Calculations.....	32
Table 5-4	Takeoff Analysis	33
Table 5-5	Spar Analysis.....	34
Table 5-6	Empennage and Control Surface Sizing.....	35
Table 5-7	Aileron Sizing	35
Table 5-8	Rudder Sizing.....	36
Figure 5-1	X-Plane Takeoff Prediction.....	37
Figure 5-2	Longitudinal Motion at 1000 feet and 40 knots	37
Figure 5-3	Three-dimensional Hidden Line Render of Aircraft.	38
Table 6-1	Manufacturing Timeline.....	48
Figure 6-1	Actual and Completed Manufacturing Dates	48
Figure 6-2	Manufacturing Man Hours Breakdown.....	49

Section I

Executive Summary

The production of adequate lift to minimize takeoff distance and maximize payload capacity was the major driving design parameter. To produce an aircraft that has a limited wingspan and limited amount of power available, lifting surface configurations took the highest priority in the design research. Larger wing area would reduce the wing loading, thereby decreasing the stall speed. Since a lower stall speed decreases the takeoff speed, less power is required during the takeoff run. Takeoff is the active constraint when sizing motor power so a smaller motor can be used. The decrease in weight results in less required lift.

Several configurations were chosen for evaluation based on historical cases, namely the tandem wing, canard, conventional biplane, conventional monoplane and flying wing. Primary concerns were lifting area, flight stability, airframe strength, ease of construction and propulsion integration. Other lesser concerns included maneuverability and drag. The team selected the canard configuration during the conceptual design. The possibility was left open for a three-surface configuration. It was believed that a stable, controllable aircraft could be made with the canard or three-surface aircraft. Historical examples of these types of aircraft were cited, particularly ones that use a large canard. Both model and full size aircraft in these configurations have been flown successfully. Andy Lennon's Wild Goose and Henry Mignet's Flying Flea are examples of successful large-canard configurations.

During the preliminary design phase, the airfoil was chosen for both wings, the fuselage layout was constructed and motor research was conducted. During the latter part of the preliminary design phase, a twin fuselage concept was suggested. After a short time of weighing the advantages and disadvantages of the new configuration it was decided that the twin fuselage was a more advantageous design and it was adopted. By moving weight to the outer wings, the moment is reduced on the spar. It also provides a natural

roll damping and reduces drag by increasing the effective wingspan. It was decided that the extra cost applied due to the second pod was outweighed by the advantages.

Detailed design included structural layout of the aircraft, final motor and battery selection and final sizing of control surfaces. It was decided that a hot-wire foam cutting technique would be the easiest manufacturing method and would produce accurate wings. A hot-wire cutter was constructed and tests were carried out to confirm its validity as a construction technique. The hot-wire method produced wings that were within design tolerances in planform and cross-section. The wings were constructed of Styrofoam with a Kevlar-reinforced poplar spar. The fuselages were made primarily of poplar plywood. Nose and tail cones were constructed from Styrofoam and reinforced with fiberglass. Two Aveox 1412/5Y motors were selected for propulsion. Forty sub-C NiCad cells were to be connected in series with the two motors. The final aircraft had a payload capacity of 8 liters, a canard configuration and two vertical fins (one on each fuselage).

1.1 Design Tools Used

Several computer-based design tools were employed to aid in the different stages of the aircraft development. Among them were:

- Microsoft Excel
- Capable Computing MotoCalc
- Computervision DesignView
- Ashlar Vellum 3D
- Martin Hepperle's Calcfoil
- Laminar Research X-Plane

Microsoft Excel was used to compute lift and drag data, set up center of gravity calculations, and size the tail fins and control surfaces.

Motocalc provided an extensive and accurate analysis of different motor and battery combinations that took into account variables such as aircraft weight and drag, the number and type of battery cells, the number and type of motors, the type of motor controller and the diameter, pitch and brand of prop. Motocalc was compared to Aveox's virtual test stand and was found to produce results that were within 10% when given similar data. Motocalc's results underestimated thrust when compared to the virtual test stand.

DesignView is a parametric 2-dimensional drawing program that was used for wing and fuselage layout. Its programming features allowed for the resizing of the airframe by a simple change of one dimension. It was also used to calculate the neutral point for the aircraft.

Vellum 3D was used to provide a 3-dimensional view of parts to be constructed. It aided in the construction process by providing a real-life simulation of part fitting.

Calcfoil is a web-based code created by Martin Hepperle that provides airfoil analysis including C_L - C_D curves and C_L -alpha curves. The validity of Calcfoil was confirmed by running airfoils at similar Reynolds numbers to those tested at University of Illinois at Urbana - Champaign. Calcfoil was within 10% and tended to underestimate the lift and over estimate the drag for a given angle of attack.

Laminar Research X-Plane is a software package that provides a design environment to create an aircraft and a flight simulator to test the aircraft. The software allows for the entry of drag data; airfoils; wing, fuselage and empennage geometry; center of gravity and propulsion placement and size. Using blade element theory the code breaks the aircraft down, performing aerodynamic calculations 15 times per second. The code also includes data output that allows the designer to see the motion of the aircraft. Several variables can be output to determine the stability and performance of the design. Also, many different aircraft views are available to allow the pilot to fly the aircraft from the exterior. The program was used to train students in the operation of model aircraft.

Section II

Management Summary

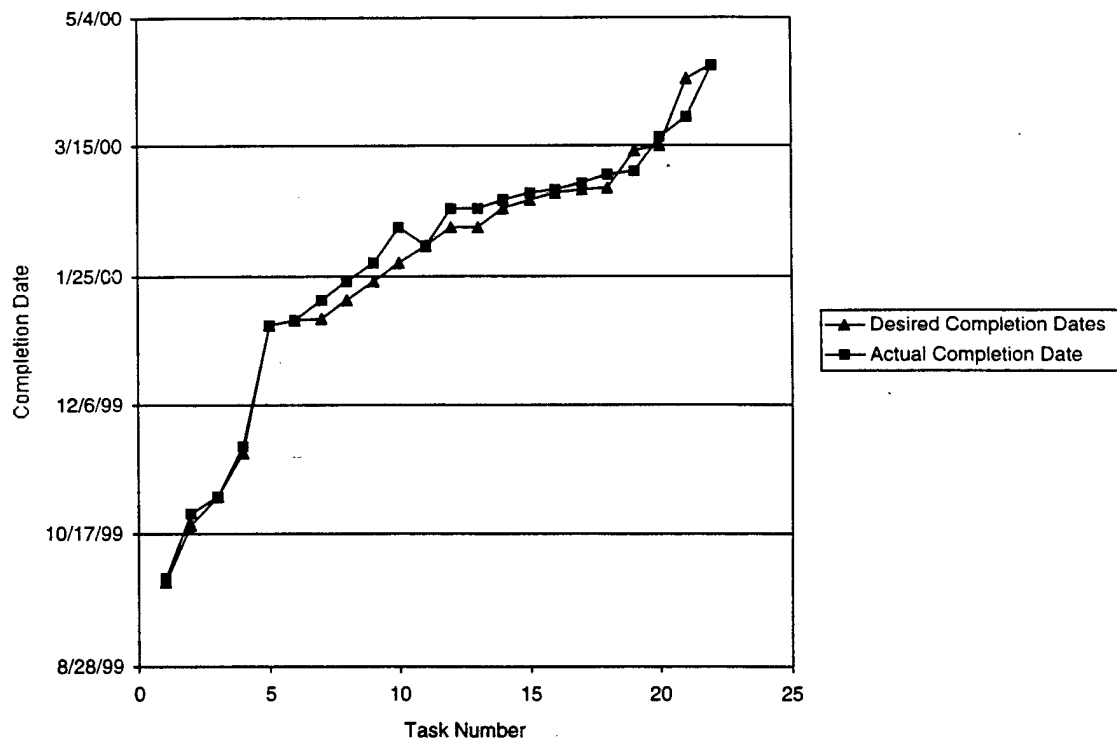
The Clarkson University Design Build and Fly team was broken down into various parts related to the aircraft's design. The team leader was Matthew Duquette. The sub-teams were Controls, Structures, Propulsion and Aerodynamics. While each group within the DBF team was responsible for its own specific aspect of the design, much communication and discussion occurred between groups, and everyone was responsible for the final design and the construction of the aircraft. A milestone schedule and completion chart can be seen in Figure 2-1.

The Controls team was primarily responsible for the control surfaces, center of gravity and flight control of the aircraft. Dave Kametz headed this team.

The Structures team was in charge of the shape and internal design of the wing spars and the fuselage. The team evaluated various shapes and the materials needed for construction. J. Wayne Braun lead the structures group.

The propulsion group, led by Glen Whitehouse, was assigned the task of deciding what engine, what propeller, battery and gearbox should be used on the aircraft. They were also in charge of choosing the propulsion method, i.e. ducted fan, ducted prop or conventional prop.

The aerodynamics team was broken down in a similar method to the previous groups, and was responsible for the shape of the aircraft and the airfoil sections used in the canard and the main wing. This team was lead by Mark Harrison.



Event	Desired Date of Completion	Actual Date of Completion
1 Begin Conceptual Design.	9/29/99	9/30/99
2 Conceptual Design complete. Start Preliminary Design	10/20/99	10/25/99
3 Electronic entry form due	10/31/99	10/31/99
4 Preliminary Design complete. Start Detailed Design	11/17/99	11/20/99
5 Hot-wire Testing Begins	1/6/00	1/6/00
6 Hot-wire Testing Complete	1/8/00	1/8/00
7 Detailed Design Complete. Start Construction	1/9/00	1/16/00
8 Wing Construction and Control Surface Construction Started	1/16/00	1/23/00
9 Control Surface Construction Complete	1/23/00	1/30/00
10 Spar Construction Started and Completed	1/30/00	2/13/00
11 Fuselage Construction Started	2/6/00	2/6/00
12 Wing Construction Complete	2/13/00	2/20/00
13 Fuselage Construction Completed	2/13/00	2/20/00
14 Vertical Stabilizer Construction Started and Completed	2/20/00	2/23/00
15 Landing Gear Construction Started and Completed	2/23/00	2/26/00
16 Final Assembly of Aircraft Started	2/26/00	2/27/00
17 Final Assembly of Aircraft Completed	2/27/00	3/1/00
18 Rollout. Testing begins	2/28/00	3/4/00
19 Written proposal due	3/13/00	3/5/00
20 Testing Complete.	3/15/00	3/18/00
21 Addendum report due.	4/10/00	3/26/00
22 Leave for competition.	4/15/00	4/15/00

Figure 2-1 Milestone Schedule and Completion Chart

Section III

Conceptual Design

The conceptual design phase was an iterative process. The competition requirements were assessed and configurations were considered based on how well the team felt each would meet the requirements. Several configurations were considered.

The configurations considered were as follows:

1. Biplane with a canard
2. Flying wing
3. Three surface
4. Monoplane with a canard
5. Classic biplane

The team felt that these configurations represented a sufficiently diverse pool of aircraft to evaluate and that they had potential to meet the objectives at hand.

3.1 Design Parameters Investigated

The design parameters investigated were:

- Fuselage size
- Motor configuration
- Propulsion type
- Lifting surface design
- Landing gear

Fuselage size was a concern because a larger fuselage would generate more drag, but would ease the layout of internal components as well as accommodate a full load. There was also the possibility of optimizing the fuselage shape in order to generate lift.

Motor configuration was discussed because it affects the center of gravity and the propulsion efficiency. Propellers configured to push tend to have higher efficiencies than the tractor style propellers. However, using pusher propellers would likely use rear mounted engines, which shift the center of gravity back, and this decreases stability. Propeller ground clearance was another topic of concern regarding motor placement. The motors must be placed so that the propellers do not strike the ground. Current losses due to impedance would increase with longer wire lengths between motors and the battery pack, therefore efforts were made to keep the distance between the motors and batteries a minimum. Another consideration was the arrangement of the connection between motor(s) and the battery pack. Analyses for batteries in series and parallel were performed in order to minimize losses in the connections.

Different propulsion systems were considered. The team discussed using pusher and/or tractor propellers, ducted fans, ducted propellers and thrust vectoring. These configurations were evaluated using different numbers and sizes of electric motors being considered. The configuration selected would have to be available commercially. In order to optimize the propulsion system and use commercial products, a propeller was decided to be used.

Airfoil selection was an important factor regarding lifting surface design. An airfoil with high lift and low drag was desired. Wing planform and placement would also affect the lifting efficiency. A large wing would reduce the loading per area, but increase drag. Due to the weight of the fully loaded aircraft, a relatively large wing would have to be used. High lift devices such as flaps and slats were examined. Carrying a payload of 8 liters of water would likely require a high lift system to take off within 100 feet as specified in the competition rules.

3.2 Figures of Merit

The following items were considered in order of importance:

- High lift

- Durability
- Stability & controllability
- Low airframe weight
- Ease of construction

Ground control was not considered a serious design issue. It was decided early in the design process that the landing gear would probably be a steering nose configuration.

The team felt that high lift was of utmost importance in order to maximize the payload of water to be carried and to take off in a short distance. The lift must be equal to the weight of the aircraft for steady-state flight to be possible, and for takeoff the lift force must exceed the weight. It was decided that a greater payload would help maximize the team's overall score as well as reducing the effects of the possible high winds acting on the plane.

A durable aircraft will reduce the chances of damage on landing. If the plane is damaged during landing it may not be possible to ferry the course once a sortie with the payload is completed. It will be possible to fly more than one sortie with a payload if the plane remains intact, which would increase the team's score.

The aircraft must be inherently stable and controllable in order to fly it with success. If the aircraft does not respond as desired it will be difficult to complete the course. With a stable and controllable aircraft the probability of flying successful sorties is increased.

It will be beneficial to reduce the airframe weight as much as possible. The less the plane weighs, the less lift is required, and less drag is created, therefore there is a smaller required thrust for flight. This will increase the range and endurance of the aircraft because less battery power will be used.

It was also decided that ease of construction was of significant importance. With a reduced manufacturing time, the team has more time to resolve unforeseen obstacles in

construction as well as time to test the aircraft. After testing, the aircraft could be modified as necessary to ensure that it will meet the objectives of the competition.

3.3 Rated Aircraft Cost

The aircraft cost was not a determining factor in the team's choice of a configuration since the costs were determined to be relatively similar. A flying wing had the lowest cost, but it would not be worthwhile to reduce the cost and sacrifice the ability to meet the contest objectives.

<u>Configuration</u>	<u>Cost (Thousands of \$)</u>
Biplane with a canard	8.90
Flying wing	8.30
Three surface	8.56
Monoplane with a canard	8.60
Classic biplane	8.90

3.4 Analytic Methods

The majority of the analysis was based on the methods described in R/C Model Aircraft Design by Andy Lennon. These methods were used to help determine the center of gravity, neutral point, aircraft configuration, and to perform a drag analysis. Andy Lennon's methods were preferred over the methods for conventional full sized aircraft because the flight regime is much different between model aircraft and full sized aircraft. Lennon's formulae and rules of thumb are intended for small scale aircraft and have been used with success, therefore his methods should provide adequate accuracy for this design.

The aircraft configuration was chosen by using a weighted objectives table. Weighted values were assigned to the figures of merit according to importance. The different configurations were then given values indicating how well they met a particular FOM and that value is multiplied by the weight value. The numbers were then totaled and the

aircraft with the highest score was chosen. The weighted objectives table is attached following this section as Table 3-1. The monoplane with a canard for the horizontal stabilizer had the highest total score of 161. Hence, this was the design chosen to build for the competition.

Table 3.1 – Weighted Objectives Table

FOM	Weight
High lift	10
Durability	9
Stability & controllability	8
Low airframe weight	7
Ease of construction	6

Definition of values	
Very Good	5
Good	4
Fair	3
Poor	2
Very Poor	1

Configuration	High Lift	Durability	Stability & Control	Low Airframe Weight	Ease of Construction	Total
Biplane w/Canard	5	3	4	4	3	155
Flying Wing	3	5	1	4	4	135
3 Surface	4	2	4	4	3	136
<i>Monoplane w/Canard</i>	4	4	4	5	3	161
Classic Biplane	4	3	4	4	3	145

Section IV

Preliminary Design

Once the monoplane and canard configuration was chosen the preliminary design was initiated. Two areas of the plane were the focus of the design: the wing and propulsion system. The figures of merits used for the wing design were:

- Stall conditions
- Lift to drag ratio
- Thickness of airfoil

The figures of merit for the propulsion system were:

- Thrust generated
- Rated power
- Number of batteries used

These are the major points that were investigated for the design of the aircraft. The empennage was also considered, but was not as rigorously studied because of the lower impact on the overall aircraft.

4.1 Airfoil Selection

Airfoil selection and the wing planform were the focus for the wing design. First the airfoil was selected. In order to select an airfoil that would meet the performance goals of the aircraft, some preliminary calculations were made assuming a 7 foot wingspan and chord lengths of both 1 and 2 feet. A stall speed of approximately 25-mph with a 0° angle of attack was desired. Reynolds numbers of 300000 and 600000 were then examined. A C_{Lmax} of 1.8 was also necessary to provide the desired lift.

Airfoils were chosen from the University of Illinois online airfoil database (http://amber.aae.uiuc.edu/~m-selig/ads/coord_database.html). Several types of airfoils were then analyzed using an online airfoil analysis code written by Martin Hepperle

(<http://beadec1.ea.bs.dlr.de/Airfoils/>). These airfoils included several NACA, Selig, Clark, Drela, Gottingen, and David Fraser airfoils. Desired features looked at included an airfoil that had gentle stall characteristics, low drag, and a fairly high thickness to chord ratio. The high thickness to cord ratio was desired to allow for room in the wing for a spar, servos, batteries and radio equipment, as needed.

Several airfoils that performed close to what was needed were then further analyzed. These included the DAE-11, the Selig 4180, the NACA 6412 and the NACA 6409 airfoils. The NACA 6409 was eliminated because it had the lowest thickness to chord ratio which would result in a wing too thin to store radio equipment in as desired. The DAE-11 and Selig 4180 airfoils where ruled out due to their sharp stall characteristics. The NACA 6412 airfoil was then chosen for its higher $C_{L-\alpha}$ curve and its better drag polar at high values of C_L . As seen in Figure 4-1, the C_L decreases smoothly after it stalls at an angle of attack of 13° . This is advantageous when the plane does start to stall because there is a better chance to recover control of the aircraft. Another aspect of the NACA 6412 is that the coefficient of drag did not increase very much for an increase in C_L . This is beneficial because the lower the drag, the less thrust will be needed so there will be more energy left in the batteries for a longer flight.

4.2 Motor Selection

The motor selection was the next step in the design. There were many restrictions to consider in the motor selection process. The fact that the motors had to be electric and commercially available was a main constraint. Another important limitation was the five-pound weight limit on the battery pack, effectively limiting the power that the motors could use.

A propeller/motor combination was chosen through computational and analytical methods. Motocalc, along with manufacturer's specifications, was used to evaluate the combinations of engines, batteries, gearboxes and propellers. More specifically the software was used to compare the AstroFlight 60 and the Aveox 1412/5Y motors for use

with the wing/canard design. After a brief analysis with different gear ratios and gearboxes, it was decided that there should be no gearbox on the aircraft. Software was used to evaluate propeller and battery configurations for each type of engine. The impact of the number of engines was also evaluated. The engines were chosen to give an optimal thrust while minimizing battery drain for the ten-minute sortie. Before the final propulsion mechanism was chosen, the use of ducted fans and thrust vectored ducted propellers were evaluated. The traditional propeller was chosen for its simplicity and reliability. Also, at the given flight envelope propellers produce thrust most efficiently.

There were already two Aveox motors in the team's inventory so the AstroFlight was evaluated to determine whether the cost of a new motor (or motors) was worthwhile. After a research period, the AstroFlight 60 FAI was determined to be the most suitable competitor based on battery requirements, weight, and cost. The two motors were compared with 12 X 9 propellers, 40 NiCad cells and no gearbox. Results from Motocalc show that the AstroFlight produces thrust that is 10 % greater than the Aveox motor. The AstroFlight draws approximately 10 additional amps compared to the Aveox. By reducing the number of batteries to 32, the AstroFlight draws an equivalent current to the Aveox. The AstroFlight weighs 9 ounces more per motor so the weight decrease from the cells is overcome by the increase in motor weight. The number of cells can not be increased since the maximum battery pack weight occurs at 40 sub-C size cells. Both motors (at full throttle) perform in the 40 – 50 amp range at 0 mph with 12 X 9 propellers. Figures 4-2 and 4-3 at the end of this section show the Motocalc thrust and current draw analysis for the Aveox 1412/5Y and the AstroFlight Cobalt 60 FAI.

Different propeller combinations were tested and the 12-inch diameter propellers delivered the optimal balance between current draw and thrust. The motor controllers, wires and motors were designed for less than 60 amps. The efficiency of the cells decreases with an increase in current draw. Flight time is limited as a linear relationship to current draw. All of these factors are taken into consideration. It was determined that purchasing new AstroFlight motors was unnecessary. There was a marginal, if any,

increase in thrust or propulsive efficiency. It was decided that two Aveox 1412/5Y motors would generate the thrust required.

Throughout the design phase meetings were held to layout the plans of the aircraft. During one of these meetings, a suggestion regarding the configuration was made: aircraft performance might be improved if two fuselages were used, each on the end of the wingtips. There would be several advantages with this concept. By having the payload out on the wingtips, the weight would be better distributed, and would not affect the center of gravity as much as the single fuselage. Also the moment of inertia would increase making the aircraft more stable. By having a single uninterrupted wing, the lift distribution is not disturbed by a fuselage. This would result in a more efficient lift distribution. The fuselage on the wingtips also acts as an endplate so the vortices are pushed farther apart, thus the induced drag is decreased. Regarding structures, creating one solid wing is easier than two smaller sections, and there is an increase in the torsion resistance and shear stress. The motors are easier to mount in the nose section of the two fuselages than it is to integrate them with pods on the wings of the single fuselage section. This lowers the cost function by not needing the pods. Having two compartments for the payload will also shorten the length of the aircraft

There are some disadvantages with this design however. One of them is the fact that there are two fuselages, which increases the cost function. With the single fuselage configuration, the cost function was calculated to be 8.60, while the cost for the double fuselage was 8.70. Though the cost function is greater, it was felt that the dual fuselage was the choice that would give the better chance to achieve the mission objectives. The full cost calculation can be seen in figures 4-4 and 4-5.

Few modifications were made to the baseline design of this new plane. In the first concept a V-tail was going to be used, with the twin fuselage two vertical tails would be used. These were easier to make, decreasing the number of man-hours used. Another change was with the fuselage itself. The old concept had cylindrical fuselages while the newer design was rectangular in shape, so they were easier to build.

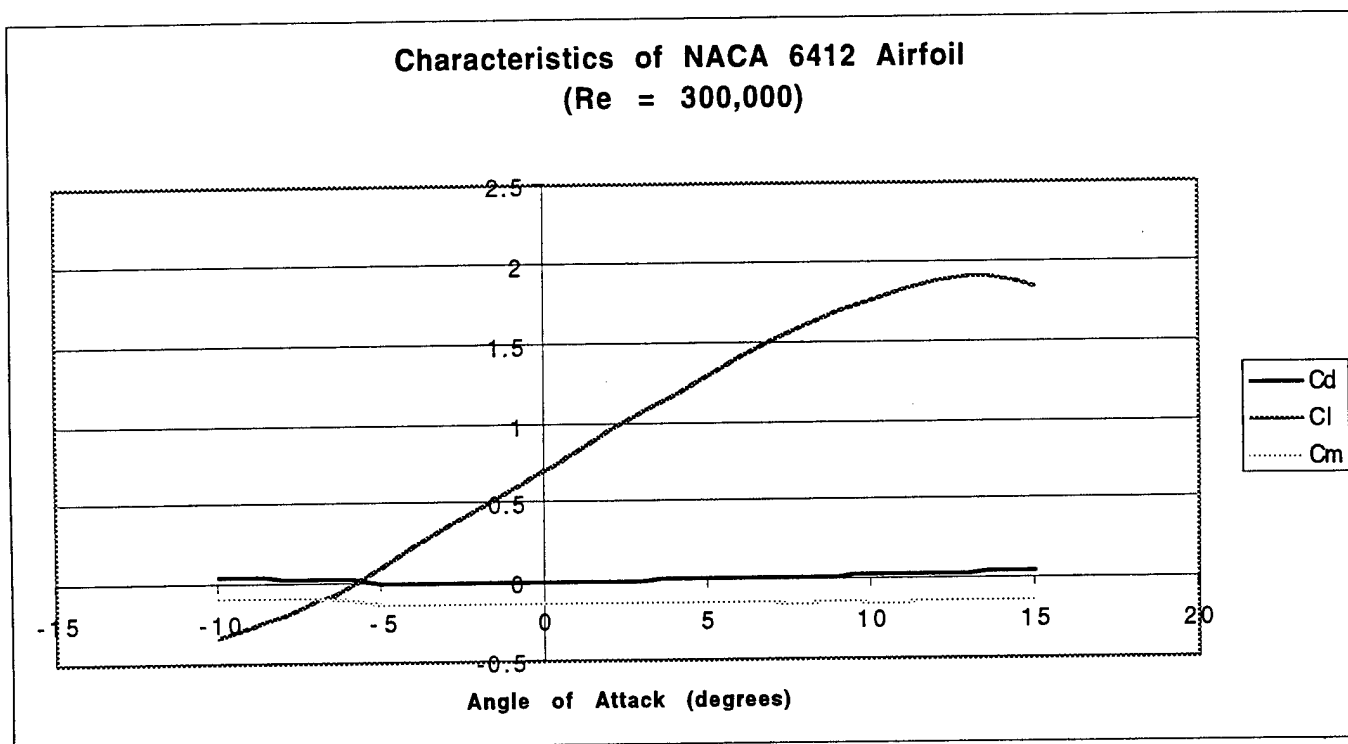


Figure 4-1 Characteristics of a NACA 6412 Airfoil (zero flaps)

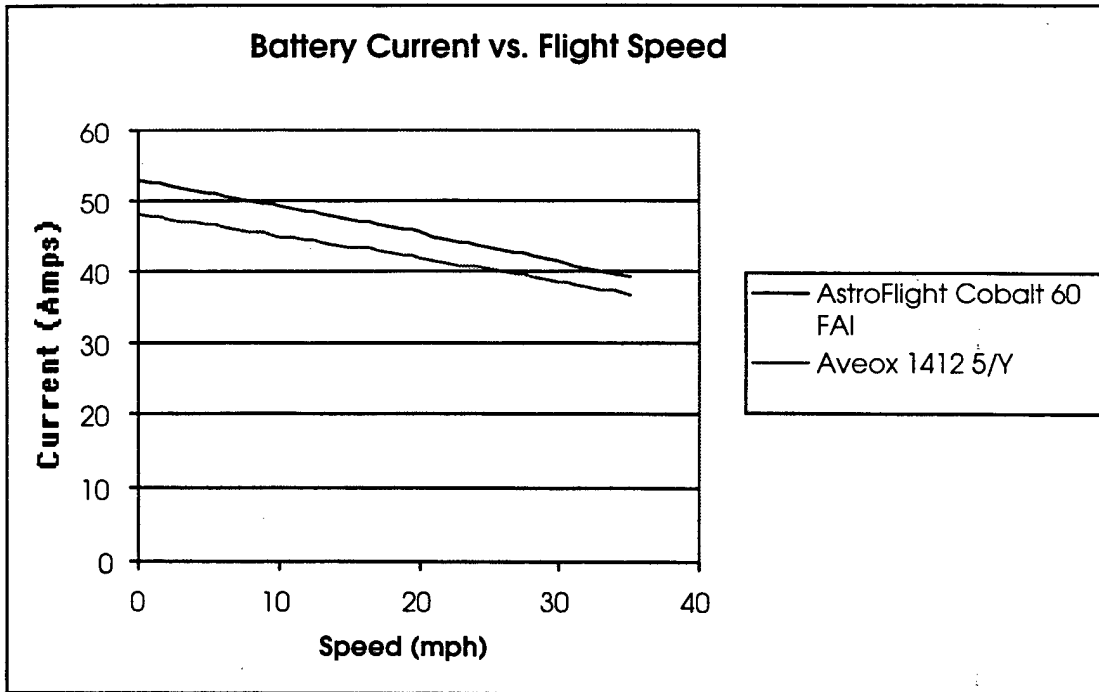


Figure 4-2 Motocalc Analysis of Battery Current (12 X 9 Propeller, 40 cells)

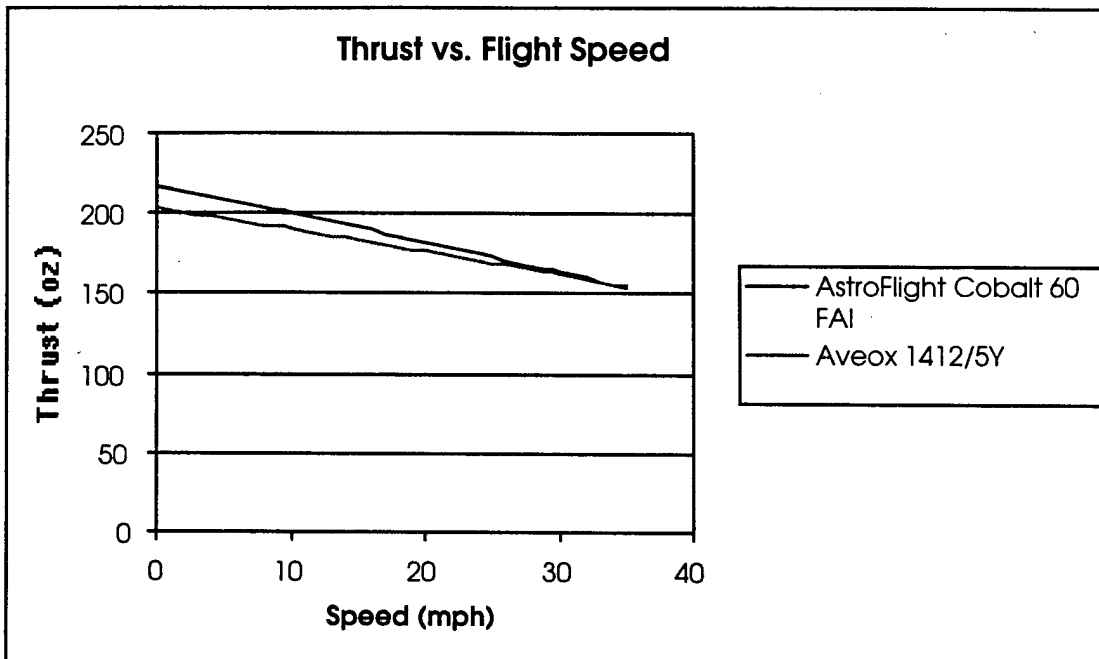


Figure 4-3 Motocalc Analysis of Thrust (12 X 9 Propeller, 40 cells)

Cost Function

				A	Empty Weight Multiplier	100	\$/lb
				B	Engine Power Multiplier	1	\$/Watt
				C	Manufacturing Cost Multiplier	20	\$/hour
REP	Number of Motors	2					
	Number of Cells	40					
	Motor Rated Power	4800	Watts				
	Number of Propellers	2					
				Total MFHR	140	hours	
	Wing Area	14	sq ft				
	No. of Wings	1					
				Total Cost	8.60	\$	
MEW	Empty Weight	10	lbs				
	Number of Fuselage + Pods	1					
	Total Length Fuse + Pods	6	ft				
	No. of Vertical Surfaces	1					
	No. of Horizontal Surfaces	1					
	Number of Servos	5					
Total Cost (A*MEW+B*REP+C*MFHR)/1000							
MEW	Airframe weight without payload or batteries						
MFHR	WING	Charge 5 hours per wing + 4 hours/sq ft area					
	FUSELAGE	Charge 5 hrs/body + 4 hours/ ft length					
	EMPENAGE	5 Hours for Empenage + 5 hours/ vertical surface + 10 hours/ horizontal surface					
	FLIGHT SYS	5 hours (basic) + 1 hour/servo					
	PROP. SYS	5 hours/motor + 5 hours/propeller or fan					

Figure 4-4 Cost function for one fuselage

Cost Function

				A	Empty Weight Multiplier	100	\$/lb
				B	Engine Power Multiplier	1	\$/Watt
				C	Manufacturing Cost Multiplier	20	\$/hour
REP	Number of Motors	2					
	Number of Cells	40					
	Motor Rated Power	4800	Watts				
	Number of Propellers	2					
				Total MFHR	145	hours	
	Wing Area	14	sq ft				
	No. of Wings	1					
				Total Cost	8.70	\$	
MEW	Empty Weight	10	lbs				
	Number of Fuselage + Pods	2					
	Total Length Fuse + Pods	6	ft				
	No. of Vertical Surfaces	1					
	No. of Horizontal Surfaces	1					
	Number of Servos	5					
Total Cost (A*MEW+B*REP+C*MFHR)/1000							
MEW	Airframe weight without payload or batteries						
MFHR	WING	Charge 5 hours per wing + 4 hours/sq ft area					
	FUSELAGE	Charge 5 hrs/body + 4 hours/ ft length					
	EMPENAGE	5 Hours for Empenage + 5 hours/ vertical surface + 10 hours/ horizontal surface					
	FLIGHT SYS	5 hours (basic) + 1 hour/servo					
	PROP. SYS	5 hours/motor + 5 hours/propeller or fan					

Figure 4-5 Cost function for two fuselages

Section V

Detailed Design

5.1 Flight Analysis and Performance Predictions

Drag analysis was performed in order to predict longitudinal dynamic stability, power requirements in cruise flight and takeoff distance. The drag analysis can be seen in its tabulated form in Table 5-1. Fuselage drag data is based off a report published by Hewitt Phillips and Bill Tyler, "Cutting Down the Drag." A series of tests in an MIT wind tunnel provided data for several model aircraft shapes. An interpolation between the different shapes was used to estimate the drag coefficient for the fuselages of the aircraft. Landing gear was assumed to be a flat plate. Vertical tails were considered NACA 0004 airfoils due the leading and trailing edge taper. Wing drag was based on 2-dimensional wing theory as determined by Calcofoil, corrected for 3-dimensional effects. An interference drag addition of 10% was added to the overall drag estimation. The estimated drag in cruise flight at a zero angle of attack is approximately 2.9 lbs at 35 mph. The drag was cross-checked using Motocalc's built-in drag estimation feature. Motocalc's model is limited, not allowing for the analysis of a canard-wing. A model was configured as a monoplane with an equivalent wing area of the canard-wing aircraft. Despite the difference, Motocalc results showed drag within 10% of the analytic values at stall speed.

The stall speed was a major concern throughout the design of the aircraft as it affects the controllability, motor selection, takeoff distance and turning radius. The stall speed was determined using a stall speed equation as provided in Anderson's text. With the full payload of eight liters, The aircraft stalls at 23 mph in straight flight. Carrying no payload the stall speed decreases to 16 mph in straight flight. Both of these estimates assume a zero-flap deflection

A takeoff analysis, based on McCormick's method, shows a zero-flap liftoff occurring at approximately 73 feet. This is assuming a rotation initiation at a distance of 25 feet and a constant rotation throughout the remainder of the takeoff run. This results in an angle of

attack between 7 and 7.5 degrees for both the zero flap and 20 degree flap case. The analysis was performed using drag data obtained from the report mentioned above; drag and lift data from Calcfail, and the takeoff equation and rolling resistance values as presented by McCormick. As calculated, the takeoff roll takes 4 seconds to complete. With flaps deflected 20 degrees the takeoff reduces to approximately 70 feet. Takeoff analysis shows that runway departure speed is approximately 1-2 mph higher than the calculated stall speed. The analysis does not take into account the drag reduction and the lift enhancement from ground effect. The ground roll may be reduced by 5 to 10 percent in reality due to ground effect. Table 5-4 shows the takeoff analysis.

Using turn analysis from Anderson, the turn radius at a load factor of 1.2 is 64 feet. For a load factor of 1.5 is 47 feet. Since stall speed increases by the square root of load factor the stall speed in a fully loaded configuration increases to 25 mph at a load factor of 1.2 and to 28 mph at a load factor of 1.5. The bank angle of a 1.2 g turn is 34 degrees. That increases to 48 degrees at a load factor of 1.5. This analysis was used in the flight pattern analysis described below. A summary of the turning Analysis can be seen in Table 5-2.

5.2 Flight Pattern

A power schedule was defined so that flight endurance on the installed battery pack could be maximized. The analysis was based on the published flight course, the turning analysis performed above and values that are obtained from the program Motocalc. Amperage ratings were used to determine total battery draw to maintain both level flight speed and turning radius. The course assumes a full throttle period of 20 seconds to allow for ground roll and climb-out. Once at altitude, a turn to downwind is performed at 75% power and 1.2 g. Power is kept at 75% to build airspeed for the 360-degree turn. The downwind 360 is performed at 85% power and 1.5 g. The final turn is performed at 25% power for 15 seconds and 1.2 g. The remainder of the flight is flown at gliding power. The total power use during a single sortie is 26 Amp-minutes. The full capacity of the 1800 mAh batteries is 108 Amp-minutes. The analysis is performed for a fully loaded aircraft (8 liters). Twenty-four percent of the battery pack capacity is used in a

single fully loaded water-carrying sortie. The total time aloft is estimated to be 1 minutes, 15 seconds. The estimated distance is 2700 feet. The course is flown at 30 mph except the takeoff run and the gliding phase to landing. An empty sortie would lack the downwind 360-degree turns. This results in a flight path that is 2400 feet. Since two laps are needed for the ferry sortie, the total distance traveled is 4800 feet. Two minutes, ten seconds are needed to complete the full sortie. The energy used is 43 Amp-minutes. This is 40 % of the battery pack capacity. Hence, A full-load sortie and a ferry sortie consume 64 % of the battery pack. By this analysis, the flight periods can be performed in a cargo-ferry-cargo pattern or a ferry-cargo pattern on a single charge. Endurance calculations are included in table 5-3.

5.3 Stability Analysis

Control surface sizing was based on Lennon's method. Nelson's method was used to compare values. Vertical fin, rudder, elevator, and aileron sizing is shown in tables 5-6 to 5-8.

Static Longitudinal Stability was calculated using the method published in Andy Lennon's text R/C Model Aircraft Design. This method calculates the neutral point of a canard-wing aircraft by using a coefficient for the downwash effect of the canard on the wing. The neutral point was calculated using the parametric design program DesignView. This program allows the change of a value such as wing span, area or separation. The neutral point and center of gravity are automatically updated. The center of gravity is placed forward of the neutral point by 5% of the main wing's chord, yielding a static margin of 5% MAC.

Flight performance was tested with the simulation X-Plane. X-Plane allows the input of geometry by the user so that flight analysis can be conducted. After testing several X-plane models the center of gravity was moved forward slightly and an angle of incidence of 4 degrees was given to the canard. After continued testing in the X-plane environment, this configuration is shown to be dynamically stable and offers easy control for the pilot. Several tests were performed from the ground perspective as a radio

controlled pilot. Short period oscillations were not noticeable and stall characteristics show a slump forward at diminishing flight speeds as to be expected with the canard configuration. Sample outputs from X-plane showing longitudinal motion and take-off performance can be seen in figures 5-1 and 5-2.

5.4 Structural Analysis

Structural analysis on a single wing spar was performed. For a box spar that is constructed of poplar plywood the stress in the worst case is 25% of the fracture strength of the spar material. The worst case considered was one which a single wing bears all the weight of a single fuselage. The wing was modeled as a cantilever attached at the mid-span point. The weight of the batteries was included in the analysis so that the stress in the canard is calculated. The analysis does not rely on the structure of the foam wing core or the tensile strength of the covering. The spars alone are designed to withstand a 4 g static load under a no-lift condition. In a dynamic scenario, this can be considered a 2-g landing impact or turbulence. An in-flight load of 4 g would put less stress on the wing though, since the lift decreases the moment created by the fuselages on the end of the aircraft. Table 5-5 shows the structural analysis.

A test to failure was performed on bare wing cores. A 38-inch wing section sustained a weight of 15 lbs. This corresponds to a rupture modulus of 30 PSI. The two wings alone could withstand a landing load of 0.5 g before failure. The commercially advertised tensile strength of Econokote, the film used to cover the wing cores is 25,000 PSI. This enhances the strength of the wing cores significantly, but was not modeled in the structural analysis.

5.5 Component Selection

Two Aveox 1412/5Y 3-phase DC model aircraft motors provide propulsion for the aircraft. Each motor has an Aveox H160 speed controller rated at a maximum current

draw of 60 amps. The motors are connected in series to a series-string of 40 Panasonic 1800 mAh R/P type cells. Each cell is a Sub-C size. Total measured battery pack weight is 4.65 lbs. The batteries are carried as a string in the hollow spar of the canard. This reduces the heat that would be generated by a dense battery pack, allows a connection between the two motors without extra wire and disperses some of the weight towards the center of the aircraft. Possible propellers range from 10 X 6 to 14 X 9. Final propeller selection will be determined from static thrust testing. Analysis shows a 12 X 9 propeller is optimal.

A Futaba 6XAS 6-channel radio controls the airplane. S3003 servos are used for all control surfaces. Each servo produces 44 ounce-inches of torque. Flight-testing will determine if stronger servos are necessary for some or all control surfaces. An R148DP PCM receiver that provides failsafe features on all channels is used. Five channels of the six available are used. Ailerons, elevators, and rudders provide control. The ailerons double as flaps, which reduces weight and complexity. Each flaperon is controlled by a separate servo. The transmitter provides computer mixing that allows flaperon control. Each rudder is controlled by a separate servo. If nose-wheel steering is found to be necessary during ground testing then each rudder servo will also control a nose-wheel. A single servo actuates the elevator.

Stability assistance is provided by the Futaba PA-2 Pilot assist. This system provides wing and pitch stabilization by placing a feedback control loop between the servos and the receiver. Under a zero-input from the pilot the PA-2 stabilizes the aircraft using an optical sensor. The difference between the dark shades of the ground and the light shades of the sky provides a horizon that the aircraft levels to. The gain is adjustable and the pilot can choose to have stabilization on a single or both axes. The sixth channel of the radio will be used to program the PA-2.

5.6 Final Aircraft Configuration

The final aircraft configuration and systems layout are shown in the attached drawing package. The final aircraft configuration is a canard design with identical fuselages attached to the ends of the wings. The empennage consists of two vertical tails that attach to each fuselage. Twin tractor motors located in the nose of each fuselage provide power. Two nose-wheels and two main wheels make up the landing gear. The aircraft has a wingspan of 6 feet, 10 inches, an overall length of 4 feet, 3 1/2 inches and an overall height of 1 foot, 11 1/2 inches. Estimated aircraft empty weight is 9 lbs. Estimated take-off weight is 32 lbs. (fully loaded). A 3-dimensional representation of the aircraft is shown in figure 5-3.

Table 5-1 Performance Calculations

ρ (slug/ft ³)	0.002377
Rolling res.	0.1
W (lbs)	32
e	0.8

Drag Analysis			
	C_{do}	Area (ft ²)	Drag Area
Fuselages	0.3000	0.27778	0.08333
Canard	0.0294	6.20000	0.18228
Wing	0.0294	7.19000	0.21139
Tails	0.0100	0.03878	0.00039
Gear	2.0000	0.04167	0.08333
Sub Total		13.74823	0.56072
Interference	10%		
Total		Drag Area ->	0.61679

Stall Speed		
	ft/s	mph
0 flap	34.39	23.4
20 flap	28.95	19.7

Lift
0 degrees flap

	$C_{l,2d}$	AR	$C_{l,3d}$	$C_{l,\alpha}$	A (ft ²)	Lift Area
Canard	1.18	6.2	1.11	0.1075	6.20	6.90
Wing	0.71	5.3	0.68	0.1075	7.19	4.90
Total					13.39	11.79

20 degrees flap

	$C_{l,2d}$	AR	$C_{l,3d}$	$C_{l,\alpha}$	A (ft ²)	Lift Area
Canard	1.18	6.2	1.11	0.1075	6.20	6.90
Wing	1.5	5.3	1.38	0.1075	7.19	9.89
Total					13.39	16.79

Motor Thrust	
V (ft/s)	T (lbs)
0.00	12.69
1.47	12.61
2.94	12.53
4.41	12.45
5.88	12.37
7.35	12.29
8.82	12.21
10.29	12.13
11.76	12.04
13.23	11.96
14.70	11.88
16.17	11.79
17.64	11.71
19.11	11.63
20.58	11.54
22.05	11.46
23.52	11.38
24.99	11.29
26.46	11.21
27.93	11.12
29.40	11.03
30.87	10.94
32.34	10.86
33.81	10.77
35.28	10.68
36.75	10.59
38.22	10.51
39.69	10.41
41.16	10.33
42.63	10.23
44.10	10.14
45.57	10.05
47.04	9.96
48.51	9.87
49.98	9.78
51.45	9.68
52.92	9.59

Table 5-2 Turning Analysis

n	ϕ (Rad)	ϕ (deg)	V_{stall} Increase (%)
1	0.000	0	0.0
1.1	0.430	25	4.9
1.2	0.586	34	9.5
1.3	0.693	40	14.0
1.4	0.775	44	18.3
1.5	0.841	48	22.5
1.6	0.896	51	26.5
1.7	0.942	54	30.4
1.8	0.982	56	34.2
1.9	1.017	58	37.8
2	1.047	60	41.4

Table 5-3 Endurance Calculations

8 Liter Payload						
n 1.5	n 1.2	Power Level	100%	85%	75%	25%
ϕ (deg) 48.19	ϕ (deg) 33.56	MPH	30	30	30	23
ρ (slugs/ft ³) 0.0023769	ρ (slugs/ft ³) 0.0023769	Amps (ave)	39.7	22.3	15.4	0.5
C_L 1.48	C_L 1.48	t (s)	20	20	20	15
V_s (ft/s) 41.31	V_s (ft/s) 36.95	d (ft)	440	880	880	506
V_s (mph) 28.17	V_s (mph) 25.19	Amp Mins avail	108	Amp mins used		
R (ft) 47.40	R (ft) 63.92			25.93		
		d_{req} (ft)	2699			
Empty Ferry						
n 1.5	n 1.2	Power Level	100%	85%	75%	25%
ϕ (deg) 48.19	ϕ (deg) 33.56	MPH	30	30	30	23
ρ (slugs/ft ³) 0.0023769	ρ (slugs/ft ³) 0.0023769	Amps (ave)	39.7	22.3	15.4	0.5
C_L 1.48	C_L 1.48	t (s)	15	10	30	10
V_s (ft/s) 27.19	V_s (ft/s) 24.32	d (ft)	330	440	1320	337
R (ft) 20.54	R (ft) 27.70	Amp Mins avail	108	Amp mins used		
				21.43		
		d_{req} (ft)	2303			

Table 5-4 Takeoff Analysis

0 degrees Flap									
$\Delta\alpha$ (deg)	t (s)	V (ft/s)	V (mph)	C_{Di}	D (lbs)	L (lbs)	T (lbs)	a (ft/s ²)	D (ft)
0	0.000	0.0	0.0	0.028	0.0	0.0	12.8	9.7	0.0
0	0.125	1.2	0.8	0.028	0.0	0.0	12.8	9.7	0.2
0	0.250	2.4	1.6	0.028	0.0	0.0	12.7	9.6	0.5
0	0.375	3.6	2.4	0.028	0.0	0.1	12.6	9.5	0.9
0	0.500	4.8	3.2	0.028	0.0	0.2	12.5	9.4	1.5
0	0.625	5.9	4.0	0.028	0.0	0.3	12.4	9.3	2.2
0	0.750	7.1	4.8	0.028	0.0	0.5	12.3	9.2	3.1
0	0.875	8.2	5.6	0.028	0.1	0.7	12.2	9.1	4.1
0	1.000	9.3	6.3	0.028	0.1	0.9	12.1	9.0	5.3
0	1.125	10.4	7.1	0.028	0.1	1.2	12.0	8.9	6.6
0	1.250	11.5	7.8	0.028	0.1	1.5	11.9	8.8	8.1
0	1.375	12.6	8.6	0.028	0.2	1.9	11.8	8.7	9.6
0	1.500	13.7	9.3	0.028	0.2	2.2	11.7	8.6	11.3
0	1.625	14.8	10.0	0.028	0.2	2.6	11.6	8.5	13.2
0	1.750	15.8	10.7	0.028	0.3	3.1	11.5	8.4	15.2
0	1.875	16.9	11.5	0.028	0.3	3.5	11.5	8.3	17.3
0	2.000	17.9	12.2	0.028	0.4	4.0	11.4	8.3	19.5
0	2.125	18.9	12.9	0.028	0.4	4.5	11.3	8.2	21.9
1	2.250	19.9	13.5	0.037	0.5	5.6	11.2	8.1	24.4
1.5	2.375	20.9	14.2	0.042	0.6	6.6	11.1	8.0	27.0
2	2.500	21.9	14.9	0.048	0.7	7.6	11.0	7.9	29.7
2.5	2.625	22.9	15.6	0.054	0.9	8.8	10.9	7.8	32.6
3	2.750	23.8	16.2	0.060	1.0	10.0	10.8	7.7	35.5
3.5	2.875	24.8	16.9	0.066	1.2	11.4	10.8	7.6	38.6
4	3.000	25.7	17.5	0.073	1.3	12.8	10.7	7.5	41.9
4.5	3.125	26.6	18.1	0.081	1.5	14.4	10.6	7.3	45.2
5	3.250	27.5	18.7	0.088	1.8	16.0	10.5	7.2	48.6
5.5	3.375	28.4	19.3	0.096	2.0	17.8	10.4	7.1	52.2
6	3.500	29.3	19.9	0.104	2.3	19.6	10.4	6.9	55.8
6.5	3.625	30.1	20.5	0.113	2.6	21.5	10.3	6.7	59.6
7	3.750	30.9	21.0	0.122	2.9	23.6	10.2	6.5	63.5
7.5	3.875	31.7	21.6	0.131	3.2	25.7	10.2	6.4	67.4
8	4.000	32.5	22.1	0.141	3.6	27.9	10.1	6.1	71.5
8.5	4.125	33.2	22.6	0.151	4.0	30.2	10.0	5.9	75.7
9	4.250	33.9	23.1	0.161	4.4	32.5	10.0	5.7	79.9
9.5	4.375	34.6	23.5	0.172	4.8	34.9	9.9	5.4	84.2
10	4.500	35.3	24.0	0.183	5.3	37.3	9.8	5.1	88.6

Table 5-5 Spar Analysis

	W (lbs)	
Engine	1.562	
4L Water	8.8	
Batt. Max	2.5	
Controls (est)	1.562	

Converter	feet (input)	inches
feet to inches	1	12
	inches (input)	feet
inches to feet	12	1

Spar Dimensions		
	Base (in.)	Height (in.)
Outer	1.25	1.25
Inner	1	1
Thickness	0.125	0.125

Wood Selection			
	s_c (psi)	Rupture Mod (psi)	σ_{crush} (psi)
Poplar	500	10100	5540
Basswood	370	8700	4730

Distance from A	in
$W_{batt.con}$	21
W_F	42

I (in ⁴)	0.1201
M (in*lbs)	520.51
σ (psi)	2166.66

Table 5-6 Empennage and Control Surface Sizing

Elevator Sizing							Andy Lennon
Nelson							
W _E (lbs)	t (min)	p (slug/ff ³)	AR _c	C _{Lα=0}	α _{req} (deg)	l _e (ft)	Se (ft ²)
7	8	0.0023769	7	0.39165566	10	4	2.1
W _E (oz)	V _{min} (ft/s)	S _c (ft ²)	AR _w	C _{mαwf}	ΔC _{mαg}	l _e (in)	Se (in ²)
112	20.83	7	3.5	-0.0035	-0.18500	72.00000	302.40000
γ (lbs/liter)	V _{min} (mph)	S _w (ft ²)	C _{Lαc} (/deg)	C _{mαwf}	δ _e (deg)	w _e (ft)	le (ft)
2.2	14.20	14	0.08	-0.05	25	0.2282	6
liters	V _{wind} (mph)	l _c (ft)	C _{Lαw} (/deg)	l _w (deg)	C _{mδe} (/deg)	w _e (in)	le (in)
8	20	1.5	0.08	2	0.00740	2.739	72.00000
W _{IO} (lbs)	V _{min/wind} (mph)	η	C _{mαwfc}	C _{mαc}	†		w _e (ft)
24.6	34.20	1	0.15	0.2	0.29808		0.35000
W _{IO} (oz)	V _{min/wind} (ft/s)	b _c (ft)	V _c	C _{mαwfc}	S _α /S _c		w _e (in)
393.6	50.17	7	0.375	-0.0335	0.130417578		4.2
D/lap (ft)	W/S (lbs/ff ²)	c _c (ft)	C _{Lαwf} (/deg)	ε _o (deg)	S _α (ft ²)		
2500	1.171	1	0.07	4.082	0.912923049		
# of laps	W _c (lbs)	b _w (ft)	δ _w /δ _α	i _c (deg)	S _α (in ²)		
4	8.2	7	0.7295	6.667	131.4609191		
D _{total} (ft)	W _w (lbs)	c _w (ft)	C _{mαc} (/deg)	C _{Lαw} (/rad)			
10000	16.4	2	-0.0300	3.793			

Table 5-7 Aileron Sizing

Nelson		Lennon	
y1 (ft)	l (ft)	w (ft)	
1.8	1.5	0.25	
y2 (ft)	l (in)	w (in)	
3.3	18	3	
Cldareq (/rad)	w (ft)	l (ft)	
0.1	0.262618473	2.625	
t	w (in)	l (in)	
0.168866809	3.151421672	31.5	
Sa/Sw		Sa(ind) (ft2)	
0.056275387		0.65625	
Sa(total) (ft2)		Sa(ind) (in2)	
0.787855418		94.5	
Sa(total) (in2)		Sa(total) (ft2)	
113.4511802		1.3125	
Sa(ind) (ft2)		Sa(total) (in2)	
0.393927709		189	
Sa(ind) (in2)			
56.7255901			

Table 5-8 Rudder Sizing

	Nelson			Lennon
N(per tail) (ft*lbs)	CLv	wv (in)		ARv
6.5	1.108781267	4.27327387		3
lv (ft)	Cn	hv (ft)		ht (ft)
2.3	0.022175625	1.139539699		1.472873032
Yv (lbs)	CLav (/deg)	hv (in)		ht (in)
2.826086957	0.097	13.67447638		17.67447638
Vv	drmax (deg)	bv (ft)		Sv(ind) (ft2)
0.04	20	1.139539699		1.1208334
Sv(total) (ft2)	t	bv (in)		Sv(ind) (in2)
1.704347826	0.571536736	13.67447638		161.4000096
Sv(total) (in2)	Sr/Sv	hr (ft)		Sr(ind) (ft2)
245.426087	0.380779224	1.025585729		0.33625002
Sv(ind) (ft2)	Sr(ind) (ft2)	hr (in)		Sr(ind) (in2)
0.852173913	0.324490121	12.30702874		48.42000289
Sv(ind) (in2)	Sr(ind) (in2)	wr (ft)		
122.7130435	46.72657749	0.316394927		
Qv (slug/s2*ft)	wv (ft)	wr (in)		
2.990965513	0.356106156	3.79673912		

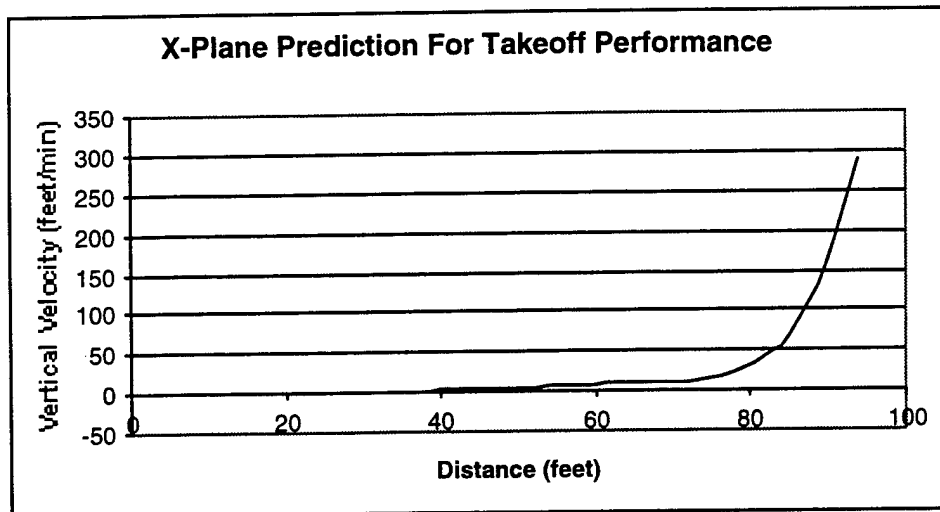


Figure 5-1 X-Plane Takeoff Prediction

(Note that the runway is at a gradient. Takeoff occurs at 70 feet)

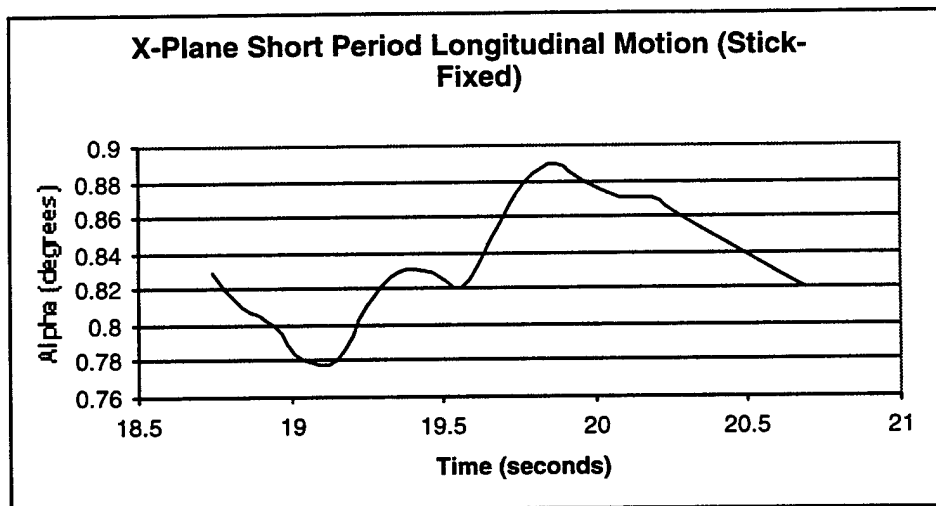


Figure 5-2 Longitudinal Motion at 1000 feet and 40 knots

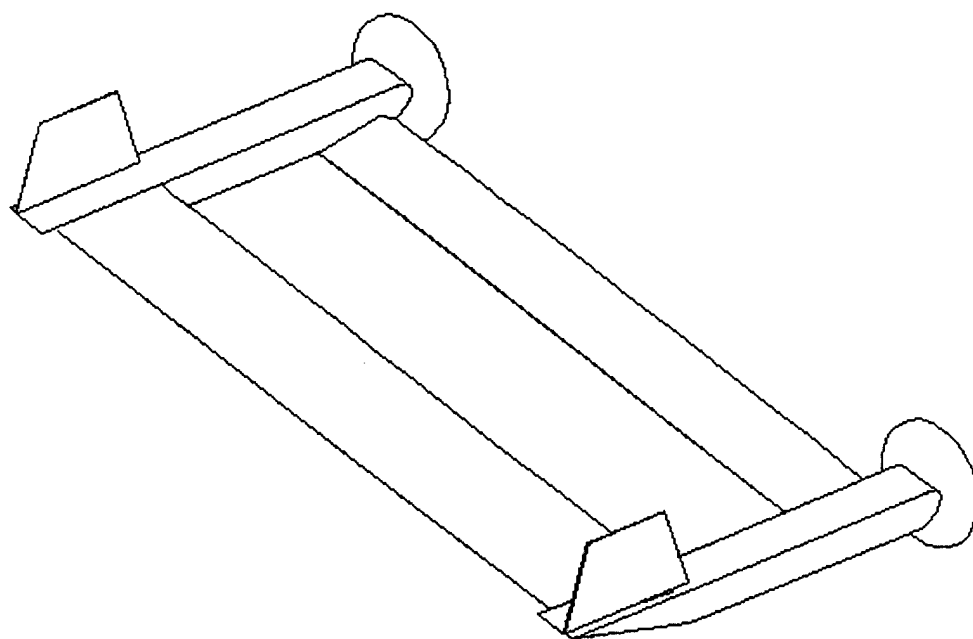
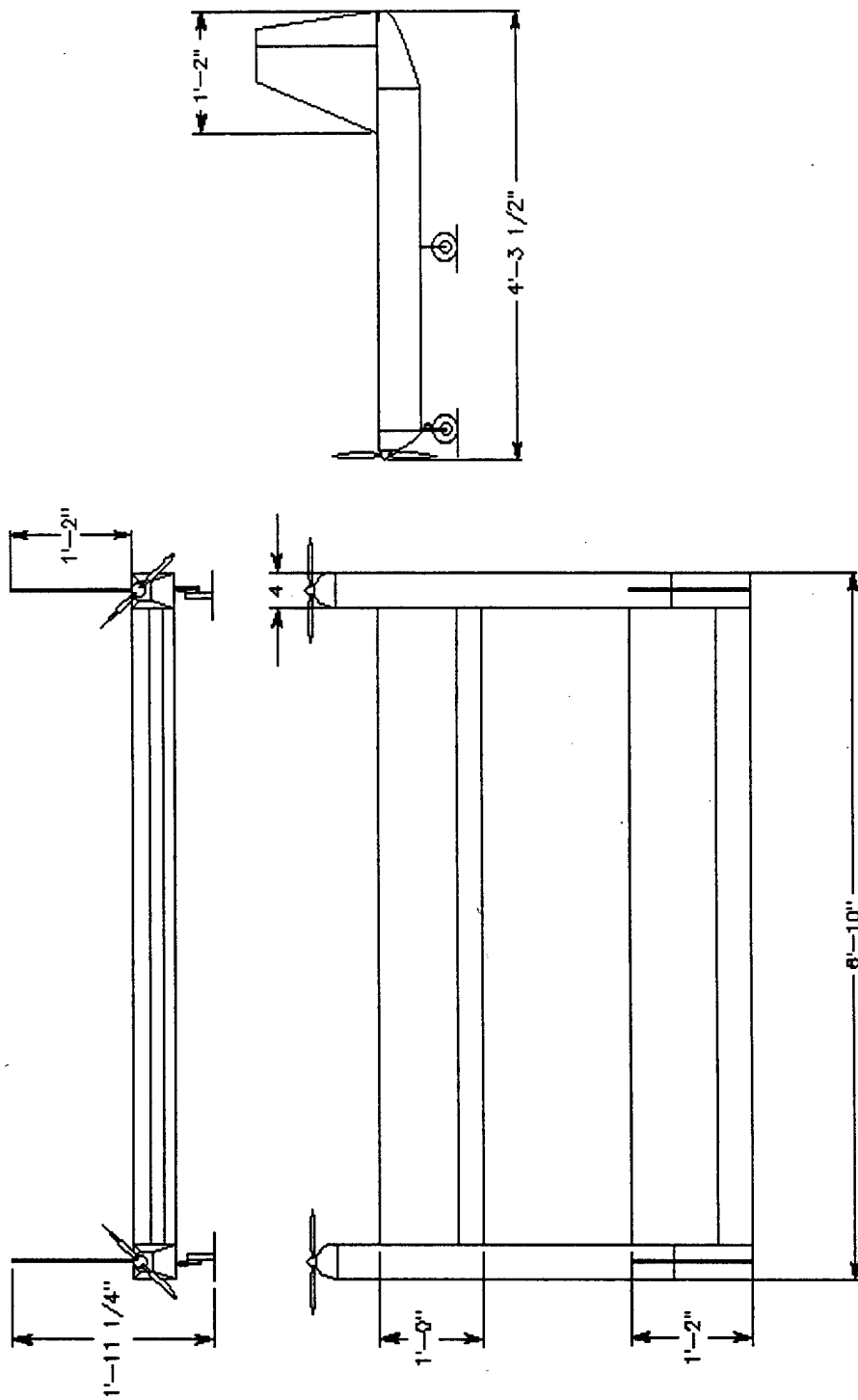
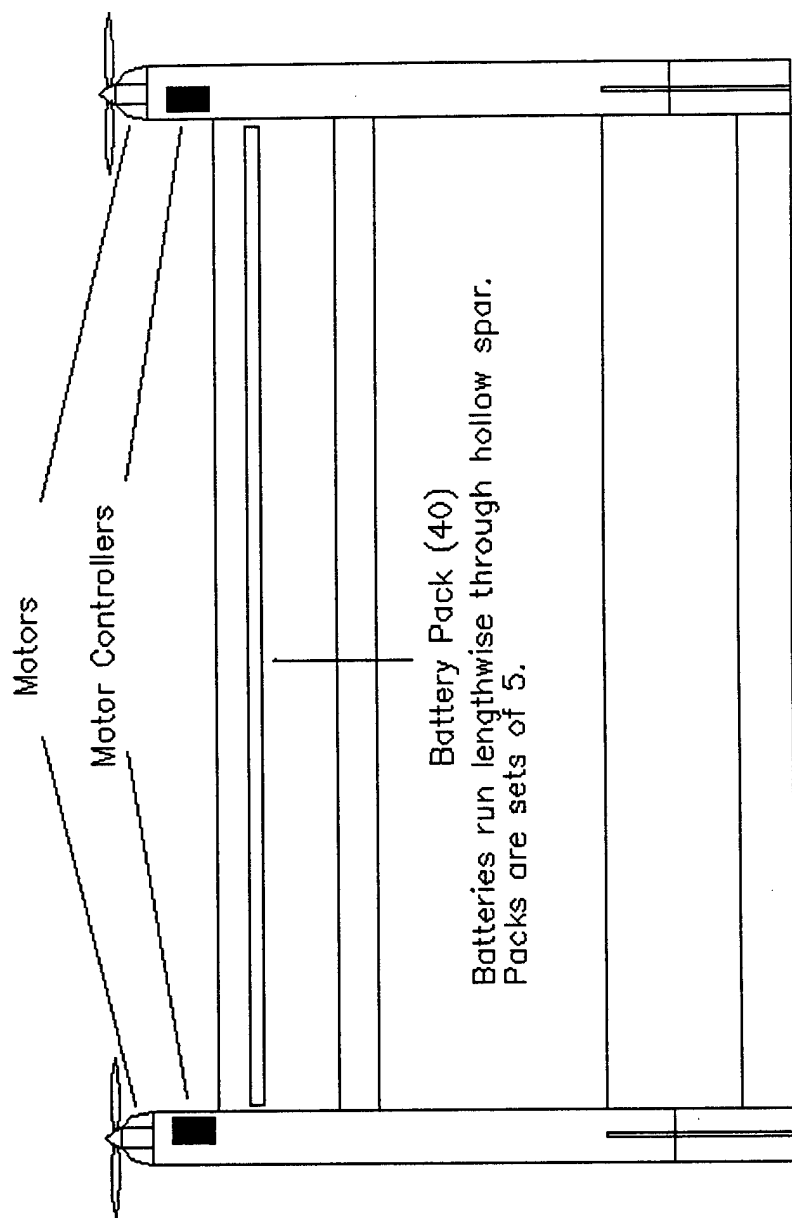


Figure 5-3 Three-dimensional Hidden Line Render of Aircraft.

Drawing Package



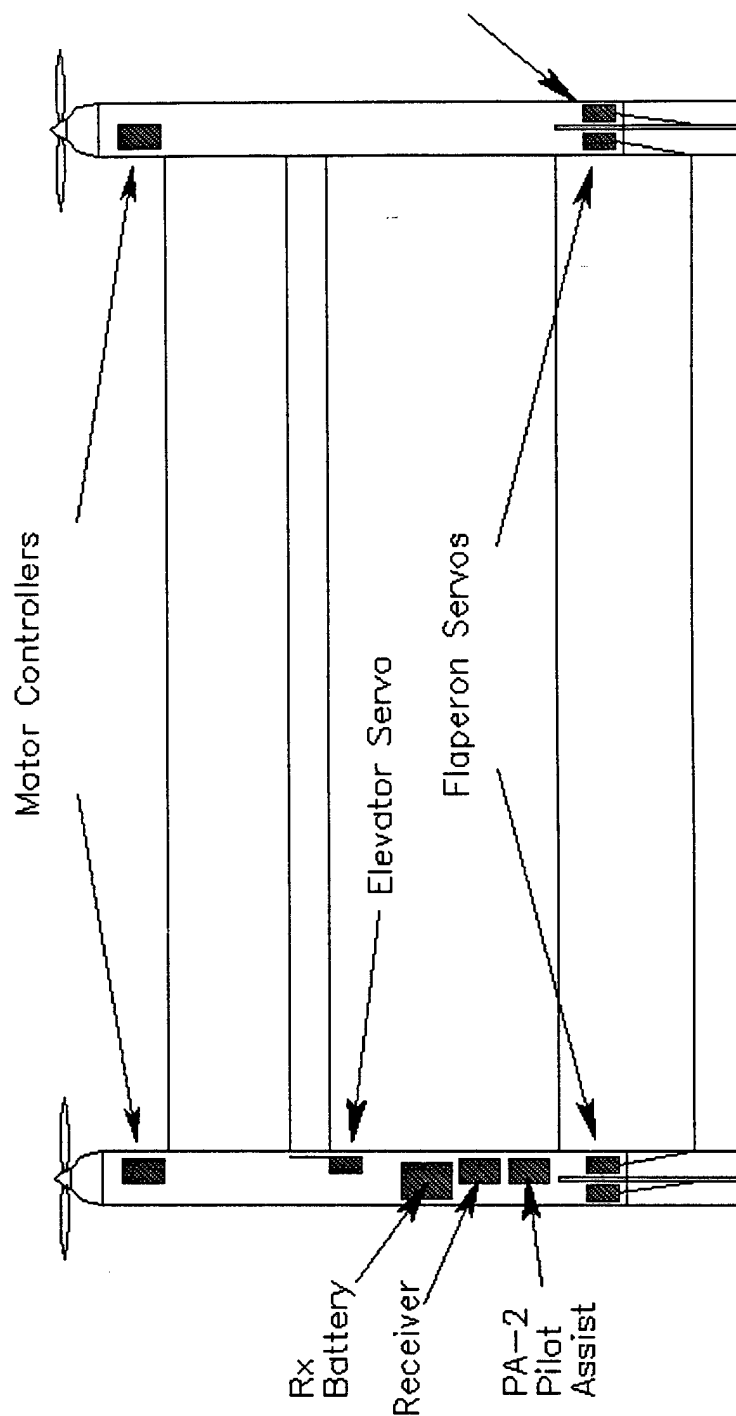
Clarkson University
Golden Flight - 2000
3-view
Drawing 1 of 4



Propulsion System Layout

Motors: Aveox 1412/5Y
 Batteries: Panasonic 1800 mAh
 Sub-C (40)
 Motor Controllers: Aveox H160

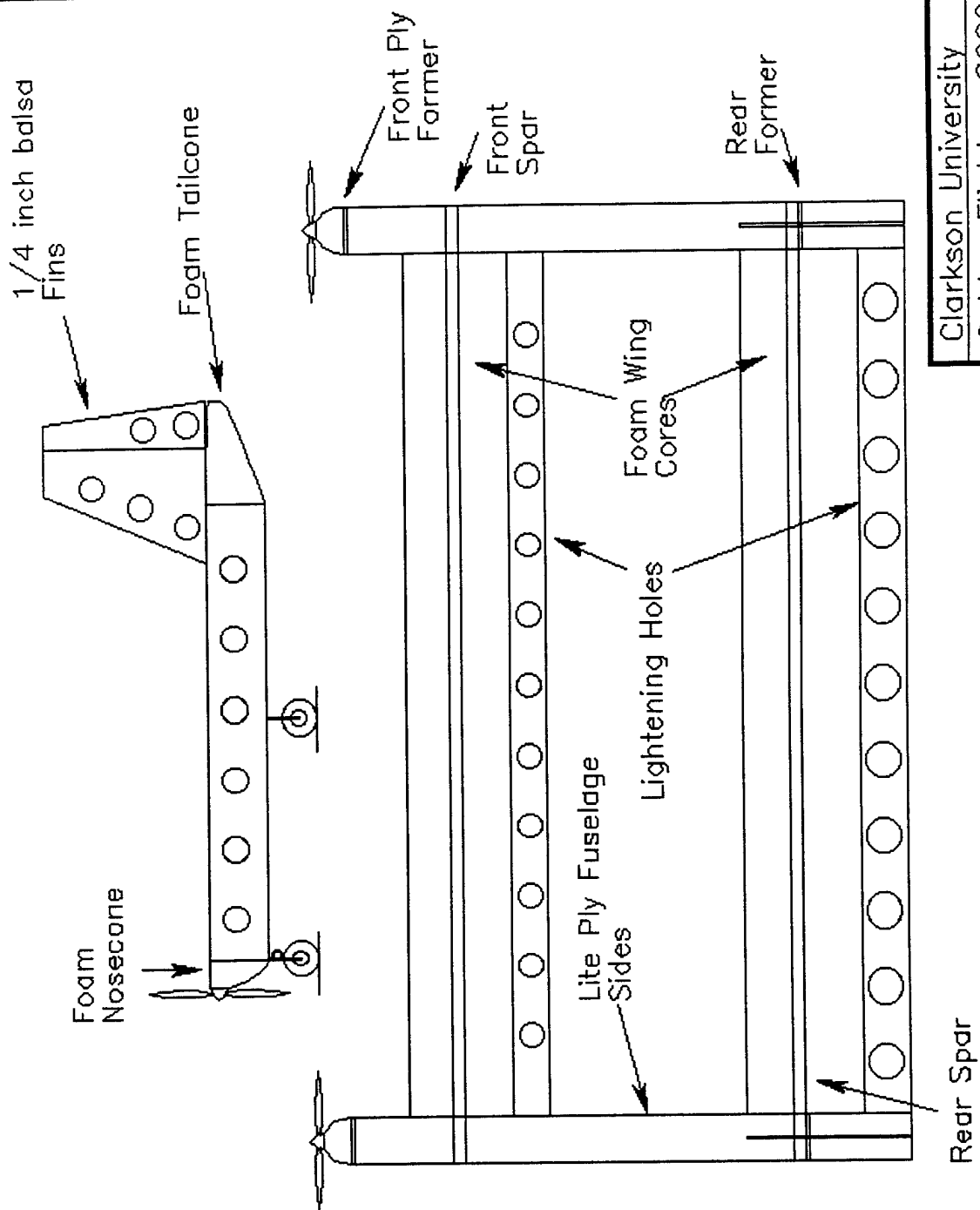
Clarkson University
Golden Flight - 2000
Propulsion System
Drawing 2 of 4



Radio System Layout

Radio system is Futaba 6XAS.
 Receiver is Futaba R148DP.
 All servos are Futaba S3003
 unless otherwise specified.
 Motor controllers are Aveox H160

Clarkson University
Golden Flight – 2000
Radio Gear Layout
Drawing 3 of 4



Clarkson University
Golden Flight - 2000
Structural Layout
Drawing 4 of 4

Section VI

Manufacturing Plan

When considering the materials and process to be used for the manufacture of the aircraft several items were considered. The following describes the figures of merit for manufacturing:

- 1 Ease of Construction
- 2 Cost of Materials
- 3 Weight of Materials/Structures
- 4 Strength of Materials/Structures
- 5 Reparability of Structures

The figure of merit that drove the construction decision was Ease of Construction. Since only three people on the team had experience with model aircraft construction the necessity for a manufacturing process that requires a minimum of skill was apparent. The time to construct the aircraft should also be kept low to allow more time for ground and flight-testing. The cost of the materials was important since the project was run on a limited budget. Weight and strength of the materials is important since the aircraft needs to maintain a lower flight speed to be controllable by inexperienced pilots as well as survive a crash. The reparability of the structures is important since it may be necessary to make repairs on the flight line. Each process was discussed and weighed against each other using the above figures of merit.

The classic approach to small aircraft construction is the "built-up" method. This method uses ribs and spars in the wings; formers and stringers in the fuselage and ribs in the tail section. This method is labor intensive, requiring many man-hours to make parts and assemble them together. Also, the "built-up" method requires an amount of skill that most members on the team do not possess. The cost of the structures is relatively low since the majority of the aircraft is empty space. Structures are made from balsa and polar, both inexpensive materials. These structures are light and can be made strong if constructed correctly. They are hard to repair in a crash. They often require the removal

of the heat-shrink film and hours of repair and replacement of parts to return to a flight-worthy condition.

Another method that spawned from the built-up method is found in many modern-day radio-controlled aircraft kits. It uses balsa or poplar sheets to form the fuselage. The wings are usually built-up as previously described. The fuselage is constructed as a box and the empennage is cut from sheet material. It requires less time and knowledge from the builder. The cost is slightly higher than the built up method since entire sheets of balsa or poplar are used for each side of the fuselage. This method does result in a higher weight than the built-up method but produces a stronger structure. Often the fuselage and the empennage do not rely on the heat-shrink film for added strength. holes can be drilled in the structure to reduce weight. In the event of a crash the structure can be repaired more quickly. A crack in the fuselage side can be reinforced with a small block of wood.

The most advanced form of model aircraft construction uses foam wing cores and composite layup. This method requires more skill and knowledge than any other method although some parts of composite work can be learned easily. Construction of molds is costly and time consuming. Construction of foam wing cores is often easy and requires little time. The strength of this method often exceeds any other method. The weight of composite materials is usually less than a similar wooden structure although is often heavier than the "built-up" structure. Some composite structures can be repaired to like-new condition with some resin and cloth. Foam wings often repair with resin and fiberglass.

By examining the figures of merit, the team decided that no single method was best. The final decision was to combine some composite methods with sheet-wood construction. Alternatives to popular model aircraft materials were explored. Namely, shipping tubes were considered for the fuselage and foam-core presentation board was considered for the empennage and fuselage formers. In the end the final decision was to construct wings from Styrofoam and build the fuselage from polar plywood halves. The nose and tail

cones for the fuselage would be made from Styrofoam and the empennage from balsa sheet material. To reduce weight, lightening holes would be drilled. For strength in critical areas Kevlar cloth would be added. Weight bearing formers would be made from birch plywood.

Once the method of construction was chosen, each component of the aircraft was constructed. The focus during the manufacturing process was to stop at each step and re-evaluate the progress. If a component of the aircraft was substandard or was not constructed as planned, the manufacturing would halt until the problem was rectified.

6.1 Wings

The wings were constructed using the hot wire method as described in Composite Construction for Homebuilt Aircraft, Jack Lambie. Cross-section templates were cut for the canard and the main wing. A hot wire was constructed using PVC tubing and steel wire, which was energized using a battery charger. The wings were cut as halves to keep the hot-wire size to a minimum. Several practice runs were made to find the best method for cutting the wings. A spar channel was cut using the hot wire and a poplar spar was inserted through the length of the wing. The ends of the spar act as the major hold-down points for the wing and canard. Control surfaces were made of balsa sheeting and lightened with two-inch holes throughout the length of the elevator and both flaperons. The wings were joined with foam adhesive and reinforced with Kevlar and fiberglass cloth. The surface was smoothed and filled with microballoons filler. The leading edge was reinforced with fiberglass cloth.

6.2 Fuselage

The fuselage was constructed primarily of 1/8 poplar sheeting. Since there are two identical fuselages, they were constructed at the same time. The bottom and two sides were constructed from poplar sheeting. Poplar formers were attached in the front and rear and birch plywood is used as the wing hold-down blocks. The front former acts as a firewall where the motors attach. The fuselage top hatch was made from balsa since it

bears no weight. The hatch is hinged on one side and uses Velcro straps to clasp it shut. Styrofoam tail and nose blocks were attached and are sanded to shape. Formers throughout the length of the fuselages separate and hold the water bottles in place. Two inch lightening holes were drilled in non structural areas of the fuselages. Kevlar was used to reinforce the joints of the two fuselages.

6.3 Empennage

The empennage consists of vertical tails only. They were constructed of 1/4 inch balsa sheeting that was sanded to a symmetrical airfoil shape. They were attached to the rear of the fuselages. Two-inch lightening holes are cut throughout the surface.

6.4 Landing Gear

The landing gear consists of 4 wheels on separate gear legs. Two front wheels are located on the fuselages below the spar of the canard. The two main wheels are located on the two fuselages just forward of the leading edge of the main wing.

6.5 Manufacturing Schedule

The manufacturing schedule called for both construction and experimentation with different construction methods. As such, there was sufficient time allotted to allow for mistakes to be made and corrected and also allow for a learning curve.

The manufacturing plan was outlined early in the project. As construction techniques were determined, a finalized manufacturing plan was devised. Construction was set to begin January 1, 2000 and end February 28, 2000. Figure 6-1 shows a milestone chart of the planned and actual events in more detail. Figure 6-2 shows the man-hour break down by task.

Table 6-1 Manufacturing Timeline

Manufacturing Milestone Chart			
Event Completed	Planned Date	Actual Date	Man-hours
Build and Test Hotwire	1/4/00	1/6/00	10
Cut Wings from Styrofoam	1/15/00	1/30/00	22
Construct and Assemble Spars	1/30/00	2/15/00	11
Construct Fuselages	2/15/00	2/20/00	8
Construct Empennage	2/20/00	2/20/00	3
Mate Wings and Fuselage	2/20/00	2/28/00	8
Finish Surfaces/Cover	2/28/00	3/5/00	20
Insert Motors/Radio Gear	2/28/00	3/12/00	12

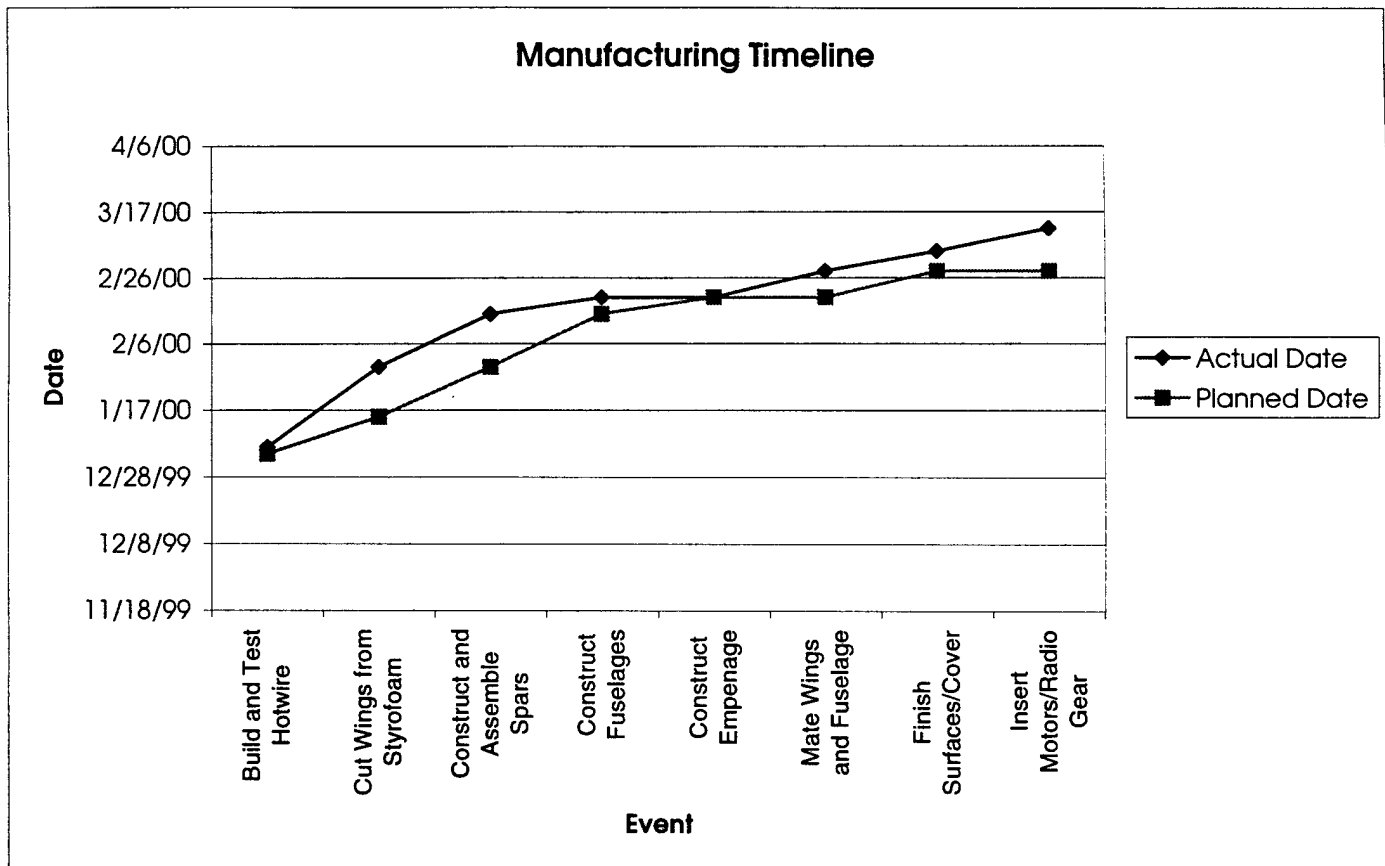


Figure 6-1 Actual and Completed Manufacturing Dates

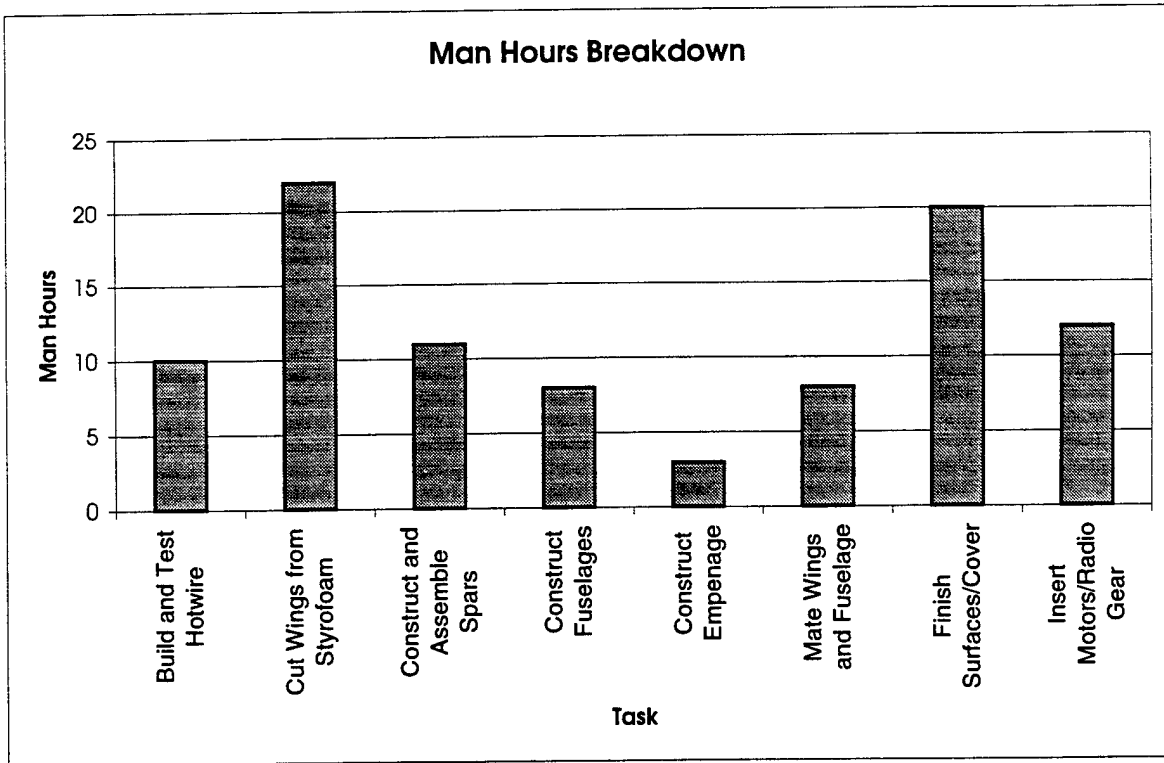


Figure 6-2 Manufacturing Man Hours Breakdown

References

Anderson, John D, *Aircraft Performance and Design*, McGraw-Hill, Boston, 1999.

Lennon, Andy, *R/C Model Aircraft Design*, Air Age, Ridgefield, CT, 1996.

McCormick, Barnes W, *Aerodynamics, Aeronautics, and Flight Mechanics*, John Wiley, New York, 1979.

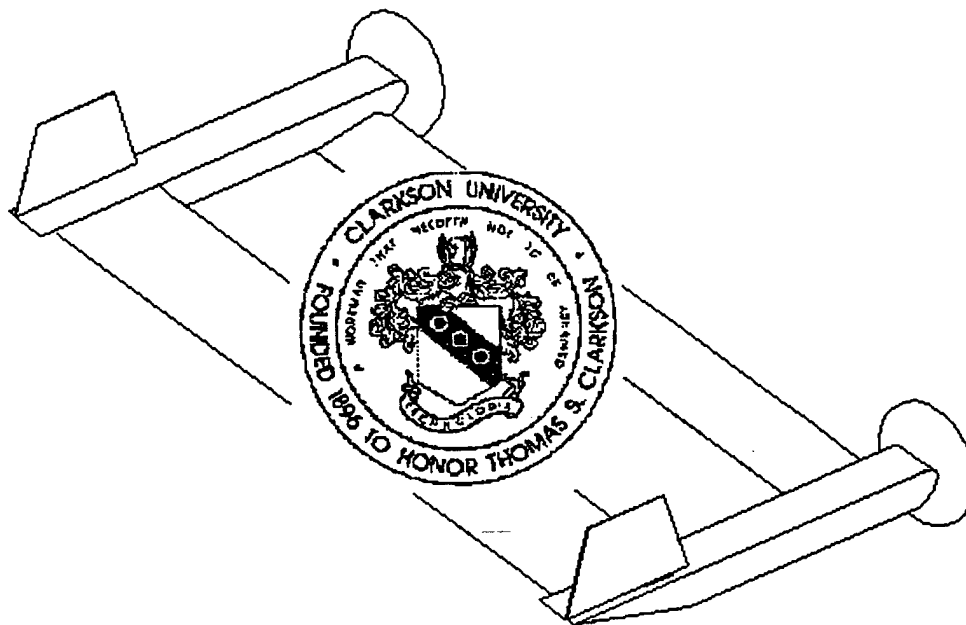
Nelson, Robert C, *Flight Stability and Automatic Control*, McGraw-Hill, Boston, 1998.

Avallone, Eugene A and Theodore Baumeister III, *Marks' Standard Handbook for Mechanical Engineers*, McGraw-Hill, Boston, 1996.

Phillips, Hewitt and Bill Tyler, *Cutting Down the Drag*, Model Airplane News.
Referenced from Lennon.

Clarkson University

Golden Flight



1999 – 2000 AIAA Design, Build, and Fly Competition

Clarkson University

1999 – 2000 AIAA Design, Build, and Fly Competition

Design Report – Addendum Phase

Addendum Editor

Matt Duquette

Academic Advisor

Ken Visser, Ph.D.

Team Members

Matthew Duquette – *Team Leader*

Controls Team

Dave Kametz – *Team Leader*
Annie B McLaughlin
Thomas Daugherty

Structures Team

J. Wayne Braun - *Team Leader*
Josh Cook
Kevin Meyer
Chris Salter
Matthew Schmigel
Brian G. Kellough

Aerodynamics Team

Mark Harrison – *Team Leader*
Jason Kuntz
Jim Lychalk
Jun Park
Valeda Scribner

Propulsion Team

Glen Whitehouse – *Team Leader*
Brent Bartlett
Kevin McCutcheon
Matt Vignau
David Young

Other Members

Liz Kenny
Jeffrey Kibler
Rob Preuss
Eric Schlobohm
Joe Tari
Brian Raffa

Contents

I Lessons Learned	5
1.1 Deviation from Design	5
1.2 Recommendations for Improvement	6
II Rated Aircraft Cost.....	10

Figures and Tables

Figure 1-1 Revised Radio Gear Layout	8
Figure 1-2 Main Landing Gear Structure	9
Table 2.1 – Airframe Dependent Parameters	11
Table 2.2 – Contest Supplied Coefficients used in Equation 2.1	11
Table 2.2 – Work Breakdown Structure	11
Table 2.4 – Rated Aircraft Cost.....	12

Section I

Lessons Learned

1.1 Deviation from Design

The final aircraft does not depart from the proposal design significantly. Few modifications were made as a result of testing. Changes were made to battery placement, servo placement, hatch and former material and landing gear design. These changes are detailed below.

The design called for forty sub-C size nicad cells to be placed in the center of the hollow spar running through the canard. During testing, batteries placed in the canard produced a bending moment that caused an unacceptable deflection. The bending also pulled the fuselages inward, transferring a moment to the front landing gear legs. The team discussed several options including installing a skid or an extra landing gear under the spar in the middle of the canard. This would prevent a damaging deflection on landing but would not prevent deflection from turbulence. The team decided to break the 40-cell pack into two 20-cell sections, each placed in the fuselage of the motor it powered. Less wire was required in this configuration since the pack did not have to span the airplane. Unfortunately, by dividing the pack each motor was connected to a separate power supply, causing the possibility of a One-Engine-Inoperative scenario.

Servos were originally to be placed in the fuselage with linkages connected to the wing's control surfaces. This would minimize the amount of wire that would need to be run for servo actuation. Such a placement would require that linkages be disconnected every time a wing was removed. Furthermore, actuation of long control surfaces from one end requires more torque to overcome torsion from aerodynamic forces. The servos were positioned so that the actuator connects to the midpoint of each control surface. There are 2 servos in the wing, one for each flaperon, and one servo in the canard to actuate the elevator. Also, the rudder servos lie in the tail cone, closer to the fins. All servos are flush to the surface with only the control wheel protruding. Figure 1-1 shows the revised servo layout.

The top hatch for each fuselage is constructed of 1/4-inch foam-core presentation board instead of 3/32-inch balsa as the design calls for. Balsa was not strong enough in torsion or crush strength. The presentation board offers the extra strength without adding weight. The formers that hold the bottles and radio gear in place are also made of presentation board so that they would be more resistant to breakage in an impact.

The landing gear configuration deviates from the design in several ways. After structural testing, the team found that a single rear wheel on each axle did not support the weight of 8 liters of water. A second wheel was added to each axle so to reduce the force on each wheel and to support a bending moment from the fuselage. Since the landing gear axis is on one side of the fuselage, an aluminum support strut was added to reduce the moment on the landing gear hold-down strap. Figure 1.2 shows the main landing gear arrangement. Also, steering pushrods were attached to the nose wheel after testing showed that a castoring nosewheel does not provide adequate ground handling.

1.2 Recommendations for Improvement

As with all projects, the design, build and fly project is a learning experience. There are many ways to solve a given problem and there is no one correct answer. That being said, there is a tenant to design projects that should be followed in order to produce a quality product on time. It is important in a project such as this to maintain a constant workflow through all stages. A schedule for this year's team was set in October but was not adhered to, especially in the design phases. For next year, interest and activity could be kept more consistent through the year by integrating construction and testing into the design phase. For instance, this year's schedule called for construction to begin in January and complete by the beginning of March. Next year, perhaps constructing a set of wings during first semester as well as a test glider would help students keep interest and provide a better understanding of the project. Also, by constructing the wings there is a fixed design, allowing the project to track more steadily and prevent a "last-minute" radical design change. Future teams should plan for deadlines to be broken and allow a buffer between stages. For instance, allow sufficient time between the end of the construction

phase and the competition date so that a lag in construction will not impede adequate testing.

Aside from project timing and organization, there are several ways in which the aircraft could differ. The project can be approached from the perspective of maximizing payload or minimizing rated aircraft cost. A simpler, smaller design that carries less payload but decreases cost more than payload score could gain a larger overall score.

Methods in construction should also be re-examined. The use of stressed-skin design would reduce weight while maintaining the same wing strength. The merits of foam construction were evident in this year's construction. Next year's design could employ a foam core fuselage as well as wing(s).

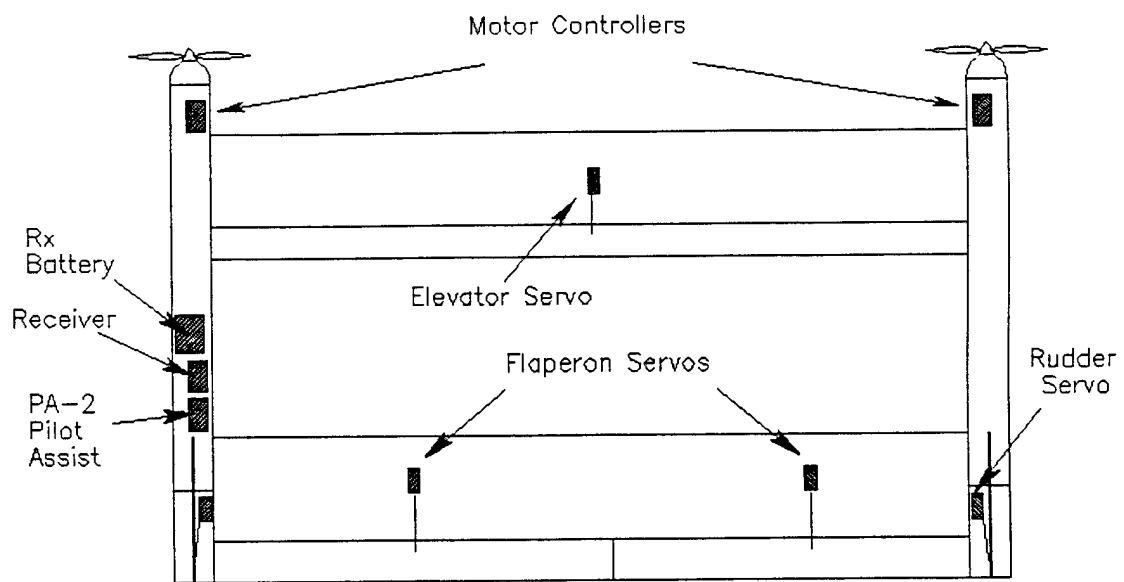


Figure 1-1 Revised Radio Gear Layout

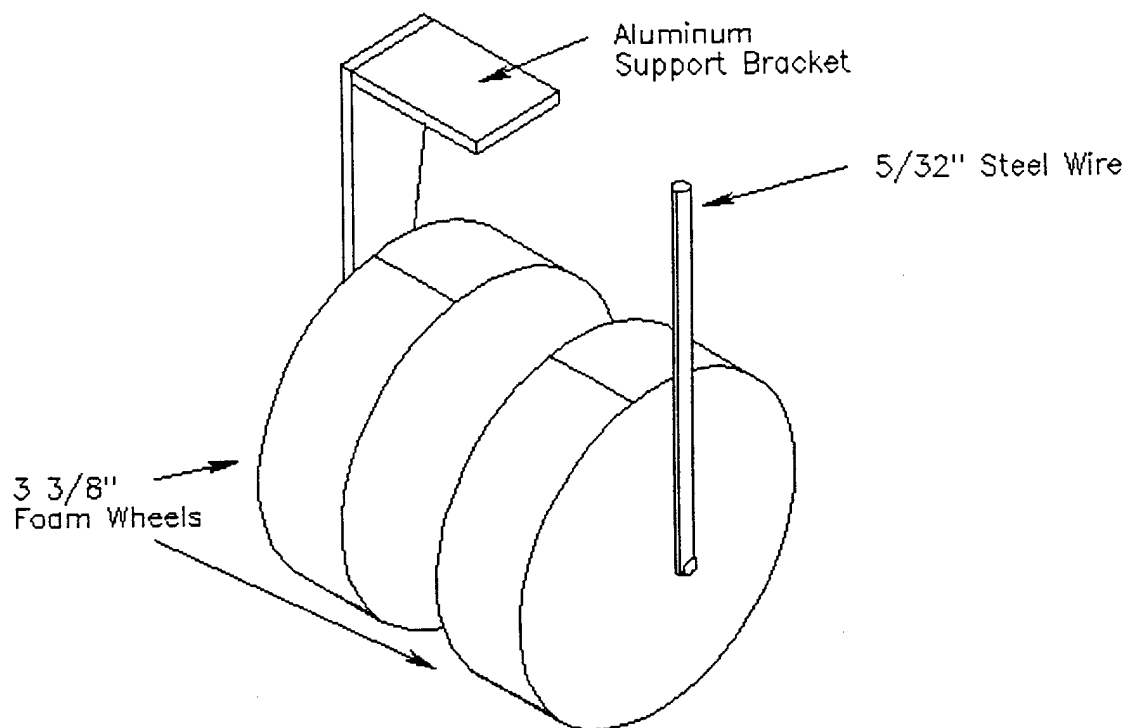


Figure 1-2 Main Landing Gear Structure

Section 2

Rated Aircraft Cost

The total rated cost is \$8.64. Equation 2.1, as supplied by the competition coordinators was used to determine the rated cost. The aircraft consists of two pods totaling 8.92 feet long; a single wing of 8.48 ft²; a single horizontal stabilizer; two vertical stabilizers, two motors; a total of 40 Nicad cells; 5 servos; and two propellers. Its empty weight is 11.5 lbs. Table 2.1 shows the airframe dependent parameters. Table 2.2 shows the coefficients used in equation 1 to develop values for manufacturer's empty weight, rated engine power, and manufacturing man-hours.

$$\text{Rated Cost} = (A * \text{MEW} + B * \text{REP} + C * \text{MFHR})/1000 \quad (2.1)$$

The work breakdown structure (WBS) shows that the most rated man-hours were spent on the fuselage. The wings take up the second most time. The total number of rated man-hours was 134.58. Table 2.3 shows the WBS, organized into the separate construction categories as specified by the contest administrators.

Table 2.4 shows the sum of each component of equation 1 and the final rated aircraft cost. Rated engine power contributes the most to the cost at \$4800.00. Manufacturing hours and empty weight are second and third, respectively.

To ensure the aircraft is within the contest rules, the battery pack was measured as 4.74 lbs., the wingspan is 6 feet, 10 1/2 inches, and the gross takeoff weight is 34 lbs.

Designation	Airframe Component	Value	Unit
REP	Number of Motors	2	Watts
	Number of Cells	40	
	Motor Rated Power	4800	
	Number of Propellers	2	
MEW	Total Wing Area	8.48	sq ft
	Number of Wings	1	
	Empty Weight	11.5	lbs
	Number of Fuselage + Pods	2	ft
	Total Length Fuse + Pods	8.92	
	No. of Vertical Surfaces	1	
	No. of Horizontal Surfaces	1	
	Number of Servos	5	

Table 2.1 – Airframe Dependent Parameters

A	Empty Weight Multiplier	100 \$/lb
B	Engine Power Multiplier	1 \$/Watt
C	Manufacturing Cost Multiplier	20 \$/hour

Table 2.2 – Contest Supplied Coefficients used in Equation 2.1

Work Breakdown Structure	Hours	Rated Labor Cost
1.0 Wings	38.92	\$778.33
2.0 Fuselage/Pods	45.67	\$913.33
3.0 Empenage	20	\$400.00
4.0 Flight Systems	10	\$200.00
5.0 Propulsion	20	\$400.00
Total	134.58	\$2,691.67

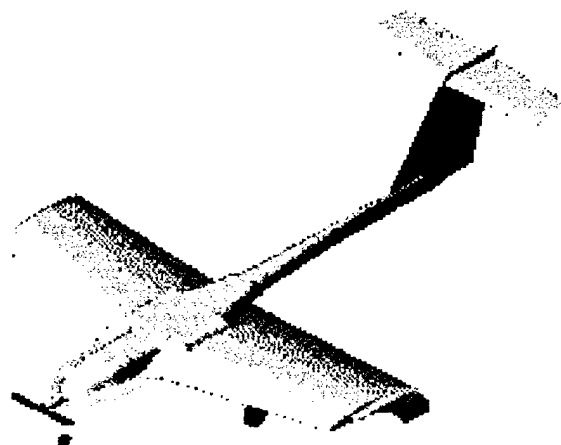
Table 2.2 – Work Breakdown Structure

Designation	Cost Component	Value	Unit	Cost
REP	Rated Engine Power	4800	Watts	\$4,800.00
MEW	Manufacturer Empty Weight	11.5	lbs	\$1,150.00
MFHR	Total Manufacturing Hours	134.58	hours	\$2,691.67
	Total Rated Cost (Thousands)			\$8.64

Table 2.4 – Rated Aircraft Cost

**The American Institute of Aeronautics
and Astronautics, Cessna, and the Office
of Naval Research**

Design, Build and Fly Competition 2000



Cleveland State University

“The Attitude”

The Team

John "Danger" Sustersic	Electrical Engineer - Graduate
Charles "Einstein" Alexander	Electrical Engineer - Junior
Michele "Fuzzy" Beachler	Civil Engineer - Senior
Dave "Dante" Wladyka	Electrical Engineer - Junior
Ray "X-Ray" Still	Mechanical Engineer - Graduate
Paul "Whoop! There It Is!" Weyandt	Mechanical Engineer - Freshman
Marcelo "The Weasel" Gonzalez	Electrical Engineer - Graduate
Maria "Giggles" Laios	Chemical Engineer - Senior
Fred "Red Baron" Glatz	Electrical Engineer - Junior
Anup "The Ghost" Khant	Electrical Engineer - Graduate
Jeff "Stinky N" Rubinski	Mechanical Engineer - Senior
Steve "The Lush" Frydrych	Mechanical Engineer - Senior
Andy "Babyface" Kis	Mechanical Engineer - Sophomore
Bill "Plane Crazy" Tracy	Lorain County Radio Control Club Ace

Table of Contents

Table of Contents	3
Proposal Phase	7
1.0 Executive Summary	8
1.1 Major Development Areas	8
1.2 Overview of Design Tools	10
2.0 Management Summary	11
2.1 Design Team Architecture	11
2.2 Management Overview	11
2.3 Project Milestones	12
3.0 Conceptual Design	14
3.1 Design Parameters	14
3.2 Figures of Merit (FOMs)	15
3.2.1 Rated Aircraft Cost Assignments	17
3.2.2 Importance Factors	17
3.3 Methods of Analysis	17
3.4 Final Concept Selection	18
3.4.1 Final FOM Ranking Chart	18
4.0 Preliminary Design	22
4.1 Design Parameters and Methods of Analysis	22
4.1.1 Take-Off Gross Weight	22
4.1.2 C_L of Main Wing Airfoil	23
4.1.3 Wing Area	24
4.1.4 Tail Volume	25
4.2 Summary of Final Configuration	26
5.0 Detail Design	29
5.1 Design Modeling	29
5.2 Performance Prediction	29
5.3 Component Selection	31
5.4 Systems Architecture	33
5.4.1 Propulsion System	33
5.4.2 Landing Gear	33
5.4.3 Radio System	34

5.4.4	Payload System	35
5.5	Drawing Package	42
6.0	Manufacturing Plan	46
6.1	Investigated Manufacturing Processes	46
6.1.1	Figures of Merit (FOMs)	46
6.1.2	Analysis of Investigated Processes	46
6.2	Selected Manufacturing Process	48
6.2.1	Hot Wire Foam Cutting	48
6.2.2	Internal Structure Construction	49
6.2.3	Component Assembly	50
6.2.4	Final Assembly Process	50
6.2.5	Manufacturing Schedule	50

ADDENDUM PHASE

7.0 Lessons Learned

8.0 Aircraft Cost

Index of Figures

Figure 1	Expected and Actual Milestones for the Cleveland State 1999-2000 DBF	13
Figure 2	Final FOM Ranking Chart	19
Figure 3	Lift – Drag Polar for SG6043 Airfoil	27
Figure 4	SG6043 Airfoil	27
Figure 5	ElectriCalc Screen Shot	36
Figure 6	Thrust and Drag versus Airspeed, 100% Throttle	37
Figure 7	Thrust and Drag versus Airspeed, 58% Throttle (contest cruise)	37
Figure 8	System Efficiency, 100% Throttle	38
Figure 9	System Efficiency, 58% Throttle (contest cruise)	38
Figure 10	Thrust and Drag versus Airspeed, 100% Throttle (unloaded)	39
Figure 11	Thrust and Drag versus Airspeed, 65% Throttle (unloaded)	39
Figure 12	System Efficiency, 100% Throttle (unloaded)	40
Figure 13	System Efficiency, 65% Throttle (unloaded)	40
Figure 14	Rate of Climb versus Airspeed	41
Figure 15	Rate of Climb versus Airspeed (unloaded)	41
Figure 16	Radio System Placement	42
Figure 17	Three View Drawings	43
Figure 18	Internal Structure Configuration	44

Index of Tables

Table 1	Preliminary Weight Breakdown	22
Table 2	Summary of Key Features of Final Configuration	28
Table 3	Manufacturing Time Line	51

Appendix A: Photos of Manufacturing Process.

Proposal Phase

1.0 Executive Summary

Cleveland State University's 1999-2000 entry in the AIAA, Cessna, and Office of Naval Research's Design, Build, and Fly Competition began as the logical extension of last year's entry. That entry resulted in a respectable tenth place finish and left the core of the design team anxious to try their hand again in the 1999-2000 contest. This core of students wanted to take the lessons and the experiences of the previous year's efforts, add some additional key members to the design team, and pursue additional sources of funding for the 1999-2000 design. These efforts have several important objectives. First, last year's design team used a simple, inexpensive, and labor-intensive construction process. This year's team desired to reduce the labor requirements in the construction process, as the key team members expected to be busy with full schedules, etc. Furthermore, last year's design team concluded that advanced composite materials offered considerable advantages over simple, traditional model construction techniques. However, the team also concluded that, as constituted last year, the team lacked the technical expertise and practical experience to attempt any advanced manufacturing process. Therefore, this year's design team strove to recruit additional team members to bring this needed knowledge and experience. Finally, the design team sought external financial support to allow these advanced manufacturing processes to be seriously considered for the construction of the aircraft.

1.0 Major Development Areas

The design team began the concept development with a careful evaluation of the rules for this competition, emphasizing the differences between these rules and the rules of the previous competition. Since many members of the design team were active in the previous year's effort, they were familiar with the analyses that led to the selected concept for that competition. The design team concluded the following:

1. The requirement to fly empty sorties further emphasizes the flight performance and handling characteristics of a successful design.
2. The restriction on battery pack size requires the design to be optimally efficient.

3. The aircraft standard cost metric weights certain elements of the conceptual development; specifically, concepts involving multiple wings, twin tails, etc., are more expensive than a simple monoplane. Other factors being equal, any concept with a higher standard cost will score lower in the competition and therefore be less desirable than a less expensive design.

With these thoughts under consideration, the design team proceeded to investigate several contending concepts. In each case, the conceptual development began with the payload. Previous competitions allowed for square or round cross-section bottles to carry the water payload; this fact was used in previous designs to minimize the volume required to carry a given payload by packing square bottles in a rectangular payload bay. Since the rules of this year's competition require round cross-section bottles only, it became clear that the best way to carry this payload would be in cylindrical bays with central axes aligned with the longitudinal axis of the aircraft. This approach minimizes the frontal area of the payload.

The design team had several brainstorming sessions to consider as many practical or impractical concepts as possible. The design team considered concepts with various features such as V-Tails, tandem wings, and canard configurations. Additionally, a twin-boom, twin tail configuration was evaluated that featured dual payload bays off the centerline of the airplane. Tractor and pusher configurations were also evaluated. After developing several of the more promising concepts, the design team evaluated each concept against the figures of merit (FOM) that were developed for the conceptual design phase and ranked the concepts accordingly. This process resulted in 'The Attitude'.

The design team selected the name of its entry long before the concept that bears the name was developed. One of the design team members, while considering artwork for a student organization contest, thought of an 'in your face' approach to the contest. This artwork was eventually adopted for that contest and resulted in a second-place prize for the group. However, the design team was asked by several people, including an assistant dean of the college, about the 'attitude' in the artwork. It was observed that many things in life revolve around attitude, whether good or bad. Certainly, attitude is all-important in aeronautics. The design team felt that the analogy was sufficient to select 'The Attitude' as the name of this plane.

1.1 Overview of Design Tools

In all areas of development, the design team used Microsoft Excel 2000 and Aveox's Virtual Test Bench website to quickly gage a concept's merit. Additional tools were used in the following specific areas of development:

- **Conceptual Design**

The conceptual design effort made extensive use of ElectriCalc to screen competing concepts. ElectriCalc is a software package developed for the Electric RC model airplane hobby to estimate model flight performance.

- **Preliminary Design**

During this design phase Maple and Matlab software, in addition to the aforementioned spreadsheet software, was used extensively for modeling and design analysis.

- **Detail Design**

In addition to the software used in the previous two design phases, SolidWorks 98, AutoCAD R14, and Algor were employed. These software packages allowed the design team to model the airplane as a 3D solid model and to export the model to Algor for certain finite element analysis investigations. Additionally, the solid model sketches provide a simple means to extract the CAD files necessary for the manufacturing phase of the project.

2.0 Management Summary

2.1 Design Team Architecture

The design team for Cleveland State's 1999-2000 Design, Build, and Fly Competition has the following structure:

John Sustersic, Team Leader and Chief Designer	
Charles Alexander Materials, Aircraft Structure, and Funding	David Wladyka Hot Wire Foam Cutting
Michele Beachler	Construction
Ray Still	Machining, tooling, and construction
Marcelo Gonzalez	Construction
Paul Weyandt	Construction
Maria Laios	Construction
Fred Glatz	Construction
Jeff Rubinski	Landing Gear and Construction
Steve Frydrych	Landing Gear and Construction
Andy Kis	Construction

2.2 Management Overview

This structure was developed largely from the experiences gained from the 1998-1999 entry and from the abilities and time availability of the team members. The highlighted team members were mostly responsible for last year's design, and John was last year's team leader. David was extremely active in last year's design and reliable in keeping deadlines. Charles was a new team member for this year and brought with him a strong physics background in which he has performed research on carbon fiber materials in the Space Materials Research Laboratory at Cleveland State University. He brought to the team the expertise necessary to attempt the advanced composite construction processes employed in this design. Additionally, Charles was responsible for seeking the sponsors needed to fund these more expensive construction techniques.

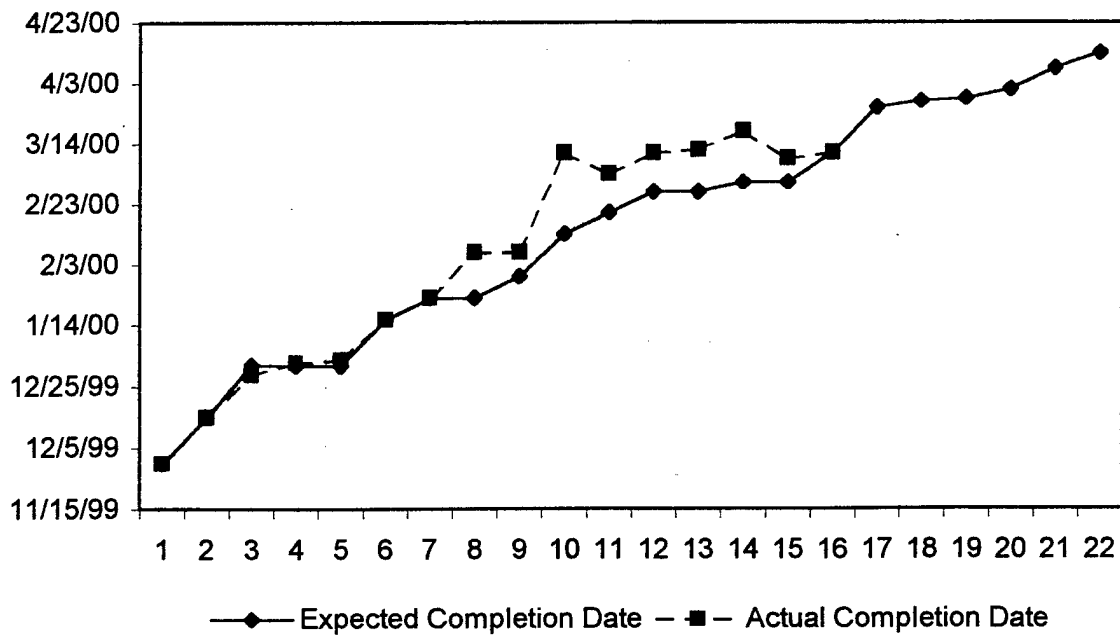
For these reasons, John, David, and Charles were designated as managers for the construction lab. Since the materials used in the aircraft construction are toxic and hazardous, no one was permitted to work in the lab unless one of the managers was present. This not only helped reduce the risk of accidents in the lab, it also provided a mechanism to ensure the quality of the work done in the lab.

The remainder of the team worked in various phases of the construction. Since the managers all know the details of the design and are familiar with the techniques needed in the construction of the plane, they assigned construction tasks based on the individuals who attended that particular construction session. The manager provided whatever training and guidance was needed for the assigned construction task. During building sessions in which all three managers were present, John stepped back and supervised all the work under way. This maximized the efficiency of the construction, as John could reassign labor resources to best fit the needs of the other managers. Additionally, this allowed the construction processes to be parallel. Charles and David could then concentrate on their particular assignment areas while John ensured the quality of the work and orchestrated the timing of the two main thrusts of the construction.

The parallel construction processes employed were structured to allow fine-tuning of the final configuration during final assembly, where the internal structural members were mated with the hot-wire foam cut aerodynamic surfaces. This allowed the accuracy of the final configuration to be determined mostly by the accuracy with which this final assembly stage is completed.

2.3 Project Milestones

The milestone chart attached following this management summary indicates the target and actual milestone dates for this project. Please note that the target dates were intentionally ambitious to help prevent the team from falling too far behind in its work.



#	Milestone	Expected Completion Date	Actual Completion Date
1	Conceptual Design Completed	11/30/99	11/30/99
2	Preliminary Design Stage Completed	12/15/99	12/15/99
3	Detailed Design Completed	1/1/00	12/29/99
4	List of Materials Generated	1/1/00	1/2/00
5	Materials Ordered	1/1/00	1/3/00
6	Jigs and Forms Completed	1/16/00	1/16/00
7	Horizontal Tail Cut	1/23/00	1/23/00
8	Structural Foam Cut	1/23/00	2/7/00
9	Main Wing Cut	1/30/00	2/7/00
10	Final Assembly Complete	2/13/00	3/11/00
11	Control Surfaces Completed	2/20/00	3/4/00
12	Radio Systems Installed	2/27/00	3/11/00
13	Propulsion Systems Installed	2/27/00	3/12/00
14	Initial Test Flight	3/1/00	3/18/00
15	Proposal Phase Draft Due	3/1/00	3/9/00
16	Proposal Phase Sent	3/11/00	3/11/00
17	Test Flights Completed	3/26/00	
18	Final Design Changes Completed	3/28/00	
19	Final Shakedown Flight	3/29/00	
20	Addendum Phase Draft Due	4/1/00	
21	Addendum Phase Sent	4/8/00	
22	Leave for Competition	4/13/00	

Figure 1: Expected and Actual Milestones for the Cleveland State 1999-2000 DBF

3.0 Conceptual Design

The conceptual design team began the process of selecting the vehicle configuration by first evaluating, and then concisely enumerating, what were considered to be the essential parameters of the competition. Primarily, the competition is a payload-carrying competition; specifically, the mission requires the maximum possible payload carried over a closed-course in *a ten-minute period*. While this may superficially seem a rather trivial detail, the design team considered this a crucial point. The team therefore concluded there were two possible dissimilar approaches to this problem: either the plane should be designed to carry the maximum possible payload (i.e. highest weight fraction) or the plane should carry the minimum possible payload in the shortest possible time to allow for the highest number of sorties. Each approach has its advantages and its disadvantages. The design team used several parameters to evaluate the relative merits of each approach.

3.1 Design Parameters

In a payload-carrying competition, the most significant parameter is one representing the absolute payload capacity of the aircraft. Clearly, this parameter is significant in that it is directly used to determine the final score for the competition. For this purpose, it was apparent that maximizing this parameter was most desirable. The only case where it would make sense not to maximize this value would occur if doing so would allow for more overall payload to be carried in the 10 minute competition time limit. However, the design team was unable to identify a case where a minimally loaded plane would be able to carry more payload overall than a heavier loaded plane. The analysis proceeds as follows: a plane that carries half as much payload as a given plane must have at least twice the momentum to carry as much payload overall. Since the kinetic energy of the plane and the energy of the losses of the plane are directly proportional to the square of the momentum, one must conclude that maximizing the payload capacity of the aircraft is most desirable.

A critical parameter to the design of any airplane is the configuration of the main wing. Clearly, an efficient wing is necessary in any successful design. By the rules of the competition, the wing must have a span of 7 feet or less and be stressed for the mandatory

2.5g static load test. However, there are additional factors in the main wing. Of these factors, wing area and aspect ratio are two critical factors. Additionally, the Rated Aircraft Cost metric used in the scoring further complicates the analysis. This metric presses unusual (by today's standards) configurations such as biplanes or tandem-wing planes to perform better than a simple monoplane to offset the additional cost incurred by the additional wing structures.

An additional configuration parameter investigated in this design process was the stabilizer configuration. Of the possible types of stabilization investigated, three principle types received serious consideration: A simple tail stabilizer, a V-Tail stabilizer, and a Canard stabilizer. Flying wing configurations were eliminated early in the conceptual design phase due to insufficient take-off performance and more complicated flight dynamics. The stabilizer design parameter was considered to be almost as important as the design of the main wing since it greatly affects the flying qualities of the aircraft. As with the parameters associated with the main wing, the Rated Aircraft Cost metric further complicates the analysis. However, the effect of the Rated Aircraft Cost metric is less pronounced on the configuration of the stabilizer. The principle difference between the three types of stabilization under investigation is a single control surface.

The final configuration parameter investigated was the propulsion configuration. Principally, the design team evaluated single and twin motor configurations for their effectiveness in combination with each of the aforementioned design parameters. Again, the Rated Aircraft Cost metric greatly influences the analysis of these parameters, especially in the case of the propulsion configuration. The Rated Aircraft Cost exacts a price, not only in the number of propellers and motors, but also in the weight of the additional propulsion components.

3.2 Figures of Merit (FOMs)

Obviously, there is a significant interaction between the great number of permutations in these design parameters. One would be hard-pressed to objectively evaluate the relative merits of these variations without an analytical, quantitative approach. To analyze these concepts, the following figures of merit (FOM) were used:

1. Payload Capacity (PC) – Quantified on a scale from 2 to 8, corresponding to the concept's useful payload capacity. The limits of this FOM were determined by design requirements. The former was determined by the requirement that all planes carry a minimum of two liters of water; the later by the requirement that all planes carry at most eight liters of water. This is a deterministic quantity.
2. Estimated Cycle Time (ECT) – Quantified on an open scale in minutes as the time from take-off to take-off of payload-carrying ferry flights, including landing, payload removal time, take-off to landing of the non-payload flight, and payload loading time. This FOM is really a composite number derived from several factors, including the vehicle's cruise capabilities, maximum rate of turn, ground and air handling characteristics, ease of payload loading and unloading and the reliability of a particular design. This is a probabilistic quantity.
3. Rated Aircraft Cost (RAC) – Quantified on an open scale in thousands of dollars as the standardized cost of the concept. This FOM is derived directly from the formula stipulated in the contest rules as indicated here:

$$(A * MEW + B * REP + C * MFHR) / 1000$$
, where A equals 100 \$/lb., B equals 1 \$/lb., C equals 20 \$/hour, MEW is the Manufacturer's Empty Weight, REP is the Rated Engine Power, and MFHR is the Manufacturing Man Hours. For the Conceptual Design phase, MEW, REP, and MFHR were estimated based on known characteristics of the concept under evaluation. This FOM is an estimate of a deterministic quantity.
4. Score Multiplier (SM) – Quantified on an open scale in 1/\$1000 as the probable score multiplier. This FOM is derived directly from the official scoring formulation as follows: $SM = PC \left[\frac{10}{ECT} \right] / RAC$. This metric was designed to indicate a given concept's performance in maximizing the competition score. This FOM is an estimate of a probabilistic quantity.

Of the first three FOMs, the ECT is probabilistic while the PC and RAC are deterministic. However, any design will be subject to the random processes of chance and weather; therefore, unless otherwise specified, the ECT figure of merit should be considered as evaluated under ideal conditions. (i.e. as an absolute maximum value)

The SM FOM is the final measure used in selecting a concept. This metric is defined as a function of the first three FOMs, and its accuracy is determined solely on the accuracy of the constituent FOMs. Clearly, the effectiveness of these analytical devices will be limited by the accuracy with which the RAC parameter is determined and by minimizing the assumptions necessary to determine the ECT parameter.

3.2.1 Rated Aircraft Cost Assignments

The Rated Aircraft Cost FOM was assigned to each concept under evaluation by carefully determining the Manufacturer's Empty Weight, Rated Engine Power, and the Manufacturing Man Hour parameters. The RAC formula is then evaluated using these values. For those aspects of the MEW, REP, and MFHR FOMs that require physical dimensions, the design team used a benchmark size for the single engine, simple tail monoplane at maximum payload. The parameters for other configurations were then adjusted from this benchmark based on the differences between the baseline configuration and the variant. In this way, the design team hoped to get a truer comparison of the merits of the competing concepts without unnecessarily complicating the analysis. The assigned values are listed in the final ranking chart later in this section.

3.2.2 Importance Factors

The design team generated a set of FOMs that, it was hoped, would best estimate a given concept's performance during the competition. It should be clear that the Score Multiplier FOM summarizes all the other FOMs in a manner similar to the scoring system used in the contest. Therefore, the design team exclusively used this FOM in its final evaluation of the competition concepts.

3.3 Methods of Analysis

The methods employed by the design team to evaluate the concepts under consideration were straightforward. In the beginning, the design team met in brainstorming sessions to discuss potential concepts. These concepts were qualitatively

assessed, then refined. This process was continued through several iterations until the concept had matured into a serious contender, or had been discarded as impractical. Most exotic, esoteric designs were discarded early in the conceptual design phase as either being unsuitable for the competition or being beyond the analytical ability of the design team. This left mostly simple, traditionally configured aircraft as the principle contenders.

As the concepts grew in number and in maturity, the design team began assigning appropriate FOMs to these concepts. After completing the FOM assignments for all the concepts, a final rank was established and the concept with the highest Score Multiplier FOM was selected for construction.

3.4 Final Concept Selection

The design team's final concept selection was simplified by using the FOMs outlined previously. Using these measures, the concept of a heavily loaded monoplane with a simple tail and a single motor/propeller pair was clearly superior for this competition. Thus, any advantage that might be gained through the use of additional wings and motors cannot offset the increase in the Rated Aircraft Cost FOM and the corresponding reduction in the expected competition score.

3.4.1 Final FOM Ranking Chart

The assigned FOMs for each concept considered may be found on the following chart:

Payload Capacity	Main Wing Configuration	Stabilizer Configuration	Propulsion	PC (# Liters)	ECT (minutes)	MEW Estimated	REP Estimated	MFHR Estimated	RAC (\$ Thousands)	SM
Maximum Payload	Monoplane	Simple Tail	Single Motor	8	1.5	10.0	1560.0	129.6	\$5	10.35
			Dual Motor	8	1.5	11.0	3120.0	149.6	\$7	7.40
		V-Tail	Single Motor	8	1.6	11.0	1560.0	124.6	\$5	9.70
			Dual Motor	8	1.6	12.0	3120.0	144.6	\$7	6.93
	Biplane / Tandem Wing	Canard	Single Motor	8	1.9	11.0	1560.0	129.6	\$5	8.02
			Dual Motor	8	1.9	12.0	3120.0	149.6	\$7	5.76
		Simple Tail	Single Motor	8	1.8	15.0	1560.0	134.6	\$6	7.73
			Dual Motor	8	1.8	16.0	3120.0	154.6	\$8	5.69
		V-Tail	Single Motor	8	2.1	16.0	1560.0	129.6	\$6	6.62
			Dual Motor	8	2.1	17.0	3120.0	149.6	\$8	4.88
Moderate Payload	Monoplane	Canard	Single Motor	8	2.2	16.0	1560.0	134.6	\$6	6.21
			Dual Motor	8	2.2	17.0	3120.0	154.6	\$8	4.60
		Simple Tail	Single Motor	4	1.4	9.0	1248.0	114.6	\$4	6.44
			Dual Motor	4	1.4	10.0	2496.0	134.6	\$6	4.62
		V-Tail	Single Motor	4	1.7	10.0	1248.0	109.6	\$4	5.30
			Dual Motor	4	1.7	11.0	2496.0	129.6	\$6	3.80
	Biplane / Tandem Wing	Canard	Single Motor	4	1.8	10.0	1248.0	114.6	\$5	4.89
			Dual Motor	4	1.8	11.0	2496.0	134.6	\$6	3.53
		Simple Tail	Single Motor	4	1.7	14.0	1248.0	119.6	\$5	4.67
			Dual Motor	4	1.7	15.0	2496.0	139.6	\$7	3.47
Minimum Payload	Monoplane	V-Tail	Single Motor	4	2.0	15.0	1248.0	114.6	\$5	3.97
			Dual Motor	4	2.0	16.0	2496.0	134.6	\$7	2.95
		Canard	Single Motor	4	2.1	15.0	1248.0	119.6	\$5	3.71
			Dual Motor	4	2.1	16.0	2496.0	139.6	\$7	2.77
		Simple Tail	Single Motor	2	1.3	8.0	780.0	99.6	\$4	4.31
			Dual Motor	2	1.3	9.0	1560.0	119.6	\$5	3.17
	Biplane / Tandem Wing	V-Tail	Single Motor	2	1.7	9.0	780.0	94.6	\$4	3.29
			Dual Motor	2	1.7	10.0	1560.0	114.6	\$5	2.42
		Canard	Single Motor	2	1.8	9.0	780.0	99.6	\$4	3.03
			Dual Motor	2	1.8	10.0	1560.0	119.6	\$5	2.24
	Biplane / Tandem Wing	Simple Tail	Single Motor	2	1.6	13.0	780.0	104.6	\$4	3.00
			Dual Motor	2	1.6	14.0	1560.0	124.6	\$5	2.29
		V-Tail	Single Motor	2	1.9	14.0	780.0	99.6	\$4	2.52
			Dual Motor	2	1.9	15.0	1560.0	119.6	\$5	1.93
		Canard	Single Motor	2	2.0	14.0	780.0	104.6	\$4	2.34
			Dual Motor	2	2.0	15.0	1560.0	124.6	\$6	1.80

Figure 2: Final FOM Ranking Chart

From the data presented in the final ranking chart, it is clear that all dual-motor configurations scored considerably less than their single-motor counterparts did. Additionally, the biplane and tandem wing concepts suffered not only in the RAC FOM, but also in the ECT FOM, where the additional drag of the second wing reduced top cruise speed. Clearly, the simple, single-motor monoplane concept proved most suitable for this competition.

4.0 Preliminary Design

The preliminary design phase of this project required a detailed analysis of the requirements of the competition and the specifications for the design provided by the conceptual design team. As outlined in the previous sections, the chosen design concept consisted of a simple monoplane configuration with the payload carried in a central, embedded fuselage. The single motor was mounted in a tractor configuration using a motor mount integrated with the nose gear-mounting bracket. At this point, the design team broke into two distinct groups: The fluid dynamics team and the structural design team. The fluid dynamics team considered these parameters with regard to the flight performance requirements of the competition. The structural design team was concerned with the physical construction of a structure that would conform to the physical requirements specified by both the fluid dynamics and the conceptual design teams, while providing the required structural capacity over the flight regime. To analytically determine the preliminary aircraft size and estimate its performance, several design parameters were identified.

4.1 Design Parameters and Methods of Analysis

The design teams were interested in several preliminary design parameters: Take-off gross weight, wing area, C_L of main wing airfoil, and tail volume.

4.1.1 Take-off Gross Weight

The design teams estimated the take-off gross weight by beginning with known quantities. These quantities are documented in the following table:

Payload	20.5 pounds
Batteries	5.0 pounds
Radio	2.0 pounds
Total	27.5 pounds

Table 1: Preliminary Weight Breakdown

An estimate of the airframe weight requires some knowledge of the materials used in its construction. The design team researched several construction techniques, and considered three potentially advantageous. The first and simplest was a traditional construction process involving balsa woods, bass woods, plywoods, CA glues, and epoxy. This technique had the advantage of having been employed in the previous year's entry. Therefore, the returning members of the construction team had considerable experience in these techniques.

A second construction technique considered was one employing machined aluminum spars and ribs. This process would require a moderate learning curve for the construction team in the operation of machine shop equipment. The plane would likely weigh less than one constructed with traditional techniques and would undoubtedly be stronger.

The third construction technique evaluated was a carbon fiber composite process. The returning design team realized that there was significant merit in using composite materials in the construction of the aircraft. This design represented an ideal candidate for such construction processes. A plane constructed using carbon fiber composites could be stronger than one made of aluminum and lighter than one made of balsa wood.

During the preliminary design stage, it was not strictly necessary to determine the exact manufacturing processes to be used, only to determine roughly what the final take-off gross weight (TOGW) one might expect. With this brief background, it was determined that the construction would likely employ composite techniques. Therefore, the design teams were able to agree upon an estimated airframe weight of eight pounds. Consequently, the estimated TOGW of the selected concept at this preliminary design phase was determined to be approximately 35.5 pounds.

4.1.2 C_L of Main Wing Airfoil

When the conceptual design process indicated a vehicle near the TOGW of about 35.5 pounds, it was clear to the fluid dynamics team that a high-lift airfoil would be required. The team began with a search for suitable high lift, low Reynolds number airfoil among existing airfoil databases. It was clear that the resources of time and equipment were insufficient to perform independent tests of prospective or original airfoils. The

team's search of internet and published literature identified the University of Illinois at Urbana-Champaign (UIUC) as one of the world leaders in the low-speed, low Reynolds Number airfoil research relevant to model aircraft. Using this database, a freeware Polar Exchange Format (PEF) Browser and a freeware Airfoil Plotting program, the design team was able to select the SG6043 airfoil as a suitable candidate. (See Figures 3,4) The airfoil features a maximum coefficient of lift of around 1.6 that is relatively independent of the Reynolds Number, and a region of intermediate angles of attack where the coefficient of drag is relatively independent of the angle of attack. Additionally, the airfoil performed similarly over a broad range of Reynolds Numbers, differing chiefly in the drag coefficient. These factors will combine to make the handling of the aircraft predictable and reasonably uniform over a broad range of the flight envelope while providing the required lift.

4.1.3 Wing Area

With a tentative airfoil selected, the design team could begin to look at some other design parameters. Of chief concern to the design team at this point were the specification of the maximum take-off distance and the stall speed of the design as functions of the parameters of the wing that directly influence them. Clearly, it is impossible to consider each separately. An application of basic fluid mechanics will result in the following equations:

$$V_{\min} = \sqrt{\frac{2M_{\text{gross}}g}{\rho_{\text{air}}C_{L_{\max}}A_p}} \quad \text{Equation 1}$$

$$d_{\text{take-off}_{\max}} = \frac{1}{2} \frac{M_{\text{gross}}V_{\min}^2}{F_{\text{thrust}} - F_{\text{friction}}} \quad \text{Equation 2}$$

From the equation for minimum velocity, one may determine that, for a given mass and a given coefficient of lift, the minimum velocity varies inversely with the planform area. Therefore, maximizing the planform area will minimize the minimum velocity¹. At this preliminary stage, there is no simple way to quantify the effects of using flaps on the

¹ This analysis assumes the airfoil does not stall at this speed. This may be verified from the lift-drag polar.

airfoil; therefore, the design team used a conservative value of 1.32 for the coefficient of lift. Of course, this analysis considered the TOGW of 35.5 pounds. Using conservative values in this analysis served as a 'factor of safety' in the design to ensure that the developing design would meet or exceed the required performance specifications. It became evident that a reasonable minimum flight speed would require a considerable wing area. The design team concluded that a wingspan at or near the maximum specified span would be required to construct a wing with a reasonable aspect ratio that would provide the required planform area. After performing several iterations, the team concluded that an average chord of about 25 inches would generate a planform area of 2100 square inches and a corresponding aspect ratio of 3.36. Using these values, the minimum velocity was determined to be 27.58 miles per hour. The design team concluded that this configuration yields the best combination of the two parameters. Without the wingspan limit, the team might have endeavored to increase the wingspan, and therefore the aspect ratio. With the wingspan limit and the necessity to reduce the minimum flight speed as much as possible, the design team chose instead to employ STOL-style wing tips to help reduce the tip vortices generated by the relatively large pressure gradient at the wingtips. It was determined that the minimum flight speed had to be minimized for two critical reasons. First, the vehicle specifications require that the take-off distance be at most 100 feet. From Equation 2, the maximum take-off distance varies with the square of the minimum velocity for a given thrust. This requires that, for the same take-off distance, the thrust required must also vary with the square of the minimum speed. Second, the design of the competition places air and ground handling at a premium; specifically, the ability to land easily and reliably is considered an essential quality of any aircraft contending for this contest. Both factors clearly indicate that a minimized minimum velocity is highly desirable in this design.

4.1.4 Tail Volume

One of the most important parameters in the design of any aircraft is the plane's tail volume. Tail volume is the product of the Tail Moment Arm (TMA) and the horizontal stabilizer area. For this preliminary design phase, the design teams utilized an approximate sizing formula based on several measures. The main wing's Mean Aerodynamic Chord (MAC), the main wing's planform area (A_p), and the TMA are the

values used to determine the Horizontal Tail Area. Using this analysis, the design team estimated the required size and location of the horizontal tail. The analysis indicated that a TMA of 54 inches and a horizontal stabilizer area of 440 square inches would be required in this concept. Finally, the design teams specified that the mean aerodynamic chord of the horizontal tail must be at least eight inches to avoid unfavorable effects at low Reynold's Numbers.

4.2 Summary of Final Configuration

The final configuration selected by the design team has several key features. First, the plane will have a wingspan of the maximum allowed (seven feet.) The aircraft will have a tail moment arm of 54 inches and a horizontal stabilizer of 440 square inches. The main wing will utilize a SG6043 airfoil in a simple taper configuration. This wing will have a planform area of approximately 2100 square inches and a MAC of about 25 inches. Table 2 enumerates these and additional design features.

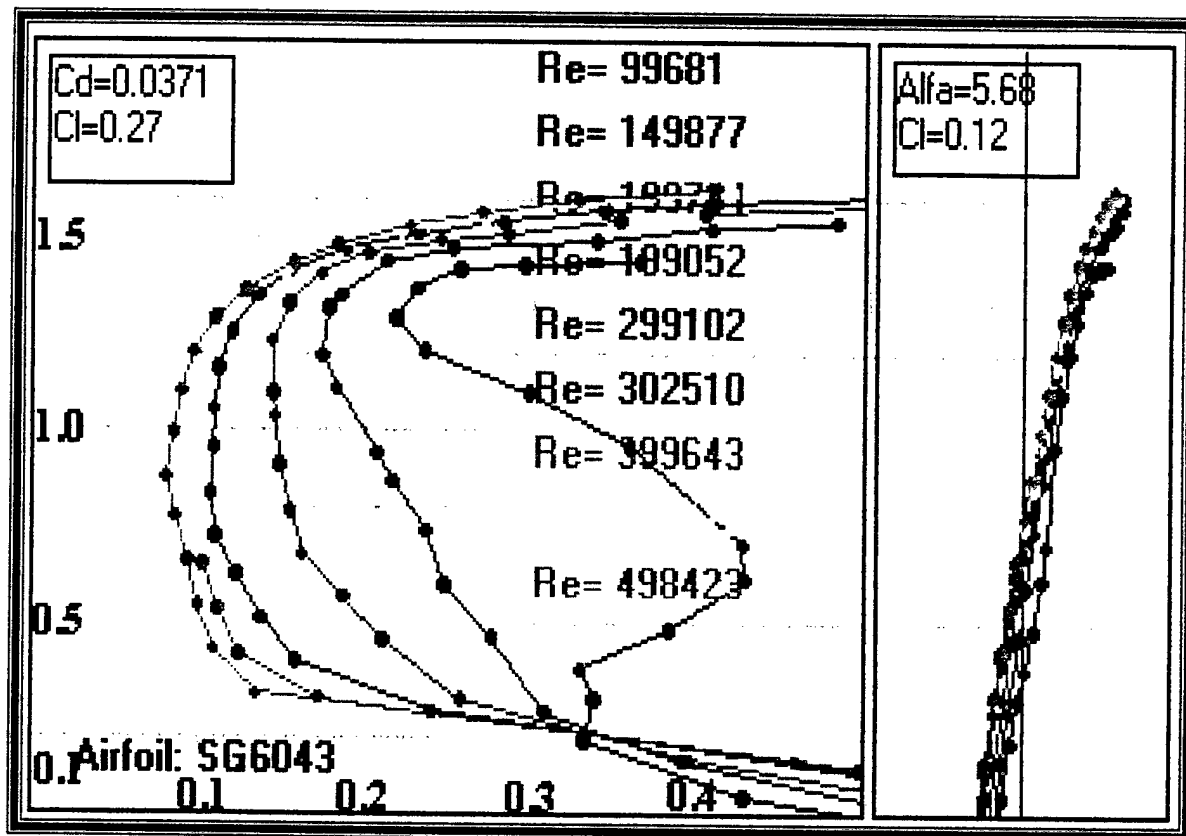


Figure 3: Lift - Drag Polar for SG6043 Airfoil

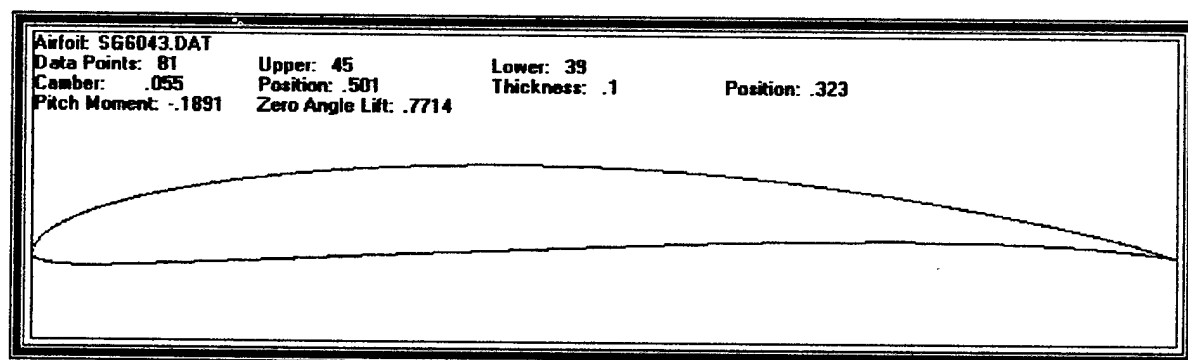


Figure 4: SG6043 Airfoil

Final Configuration	
Wingspan	7 feet
Payload Capacity	8 liters
TOGW	35.5 pounds
Empty Weight (no batteries)	10.5 pounds
Payload Fraction	.563
Main Wing Airfoil	SG6043
Chord at centerline	30 inches
Chord at wingtip	19.5 inches
Tail	Full flying stabilizer
Horizontal Stabilizer Airfoil	SD8020
Motor	Aveox F27L brushless DC motor
Motor Controller	Aveox H160C
Propeller	Master Airscrew 16x8 inch
Batteries	Sanyo N-3000CR cells 26 cell pack 31.2 volts, 3.0 amp-hour

Table 2: Summary of Key Features of Final Configuration

5.0 Detail Design

5.1 Design Modeling

The detail design work for this project was accomplished mainly using CAD software. Principally, the design team used SolidWorks 98 for this purpose; however, the team quickly realized that it was difficult to enter the scaled airfoil coordinates directly into this development environment. Therefore, the team devised a procedure that began by using Microsoft Excel to scale the normalized coordinates to the desired chord and thickness ratio. These scaled coordinates were copied into a script file that was executed in AutoCAD R14. This file could be opened in SolidWorks as a drawing, and the drawing object could then be copied into a sketch and extruded into a three-dimensional piece.

SolidWorks offers the ability to specify material densities; the software can then calculate the volume of the designed three-dimensional part and determine the part weight as well as the moments of inertia. Parts may be combined into assemblies, and assemblies may be incorporated into other assemblies. The software will also determine the center of gravity and the moments of inertia of these complex assemblies. This capability greatly simplifies the design process by automating these simple, though tedious, calculations. Additionally, modeling the design in this environment simplified the construction process by allowing full-size templates to be printed directly from the CAD files. This fact is used extensively in the construction process to generate templates needed for the hot-wire foam cutting and the structural foam bulkheads.

SolidWorks 98 supports the export of its CAD files into the standard IEGS file format compatible with finite element analysis programs such as Algor. This capability allowed the structural design team to investigate several aspects of the design. In particular, the landing gear design was scrutinized using these analysis techniques.

5.2 Performance Predictions

The performance data for this design was determined largely by using a commercially available software package called ElectriCalc (See Figure 5). This program includes a database of many commercial RC motors, propellers, and batteries, and allows

the user to add to these databases' custom entries. The design team used this tool to select a preliminary cruise speed of 45 MPH at a throttle setting of 58% when fully loaded.² Additionally, the tool was used to generate plots of the thrust and drag forces versus airspeed. (See Figures 6 and 7) System efficiency may also be charted from this tool, as illustrated in Figures 8 and 9 for throttle settings of 100% and 58%.

Figure 6 shows the developed thrust over the operating range of airspeeds, and quantifies the thrust at 25 MPH as 240 ounces, or 15 pounds. Using this value in equation 2, the maximum take-off distance was determined to be 91.90 feet. This predicted value allows for a considerable margin of error for this design requirement.

Additionally, the rules of this year's competition require the plane to fly unloaded. Therefore, the design team analyzed these flight parameters. Under this loading condition, the preliminary cruise speed was selected as 50 MPH at a throttle setting of 65%. Figures 10 and 11 show the thrust and drag plots of the aircraft in its unloaded configuration at full power and at cruise power, respectively. Figures 12 and 13 indicate the system efficiencies at the same respective power settings.

Climb capabilities of the fully loaded aircraft may also be determined through the ElectriCalc tool. Figure 14 shows the predicted rate of climb of the fully loaded aircraft at 100% and 58% throttle. Figure 15 shows the predicted rate of climb of the unloaded aircraft at 100% and 65% throttle settings.

The aircraft is predicted to handle well throughout the flight envelope. The fully loaded aircraft has 75% of its mass evenly distributed about the aircraft's center of lift. This results in a relatively small moment of inertia; this effect combines with the large control surfaces to produce an excellent roll rate.

The aircraft's internal structure was designed to support the full payload through a load factor of 3 g's. This load rating, while satisfying the minimum load rating required for this competition, will allow for bank angles of 75 degrees. This will allow for excellent maneuverability and turning capabilities. Furthermore, the design team's analysis of the structural integrity of the aircraft is necessarily conservative. The aircraft

² This value subject to change during the flight-testing phase

uses a stressed-skin, carbon fiber composite structure that is difficult to concisely model analytically. Therefore, the final structural capacity of the aircraft is expected to exceed these load figures. Consequently, the turning ability of the aircraft should also exceed these expectations.

The design team's analysis indicates that the fully loaded aircraft's endurance will be 33.4 minutes. The maximum range of the final aircraft will be 13.36 miles.

With a TOGW of 35.5 pounds and a payload capacity of 20 pounds, the payload fraction of the final aircraft will be 0.563.

5.3 Component Selection

Component selection in this design process has been tightly integrated into appropriate phases of the design process. This integration was employed in the iterative design process to ensure the best possible performance of the final design. Consider the following summary of the component selections specified in previous phases of the design process:

- Motor: Aveox F27L Brushless DC Motor
- Sanyo N-3000CR NiCad Batteries in a 26 cell pack

Closely related to these component specifications, the motor controller was selected to provide the best performance of these components. The H160C motor controller, manufactured by Aveox, provides the best match to these components and to the design specifications of this competition. Specifically, this controller offers a peak current capability of 120 amps for 10 seconds and a continuous current capability of 70 amps.³ These values fall well within the flight parameters of 98.4 amps at full throttle and 25 amps at contest cruise⁴ throttle as specified in this design.

To allow for the necessary heat dissipation required by these components, the design team strategically located these devices in practical, but effective, locations in the airframe. The structures of this assembly were designed not only to handle the considerable loads imposed by the forces and moments generated by the motor and the

³ When properly cooled.

⁴ Throttle setting of 58%.

nose gear, but also to integrate tightly with the thermodynamic devices required. The motor mount was designed to effectively increase the heat conduction from the motor to the slipstream by increasing the wetted surface area. Furthermore, the design allows for the addition of heat sink fins should the flight test process indicate additional heat dissipation capability is required for the aircraft to meet the necessary performance specifications.

The placement of the motor controller is equally critical to the success of the design. The controller resides below the aluminum mounting face of the motor mount, directly behind the nose gear. This configuration allows the controller heat sink surface to be completely exposed to the slipstream. Additional cooling airflow is captured by a scoop between the nose gear and the motor controller housing. This bleed air continues through the airframe and the battery compartment before being vented back to the atmosphere. As with the motor configuration, the design allows for additional heat dissipation by the addition of heat-sink fins.

The selection of the required radio system was straightforward, driven by a contest requirement and the channel requirement of the aircraft. Most importantly, the design specifications of the contest require that all radios be equipped with a fail-safe mode; specifically, the receiver must place all control surfaces to a known, specific location upon loss of signal. This functionality is available only in pulse code modulation (PCM) receivers. Typically, this encoding method is available only on higher-end computerized radios. Additionally, the design of this aircraft offered considerable functional improvements and additional performance capabilities by using such a radio. Specifically, computerized radios offer channel mixing, where distinct but related control channel inputs are combined to affect two or more physical channels (i.e. control surfaces.) This functionality is commonly employed by RC hobbyists to realize 'flaperon' control displacement. Normally, the aileron control surfaces operate in opposite sense in response to lateral input to the control stick; this provides roll axis controllability. Traditionally, flaps can be mechanically similar to ailerons (simple flaps), but since flaps operate in the same sense in each wing, incorporating both functions into one mechanical control element complicates the design and adds weight to the design. The computerized radio, with its mixing ability, allows this functionality with no weight penalty by using

two radio channels for the flaperons – one for each flaperon. The transmitter may then mix the two control inputs. This implements the flaperon functions with no added complexity to the aircraft itself.⁵

The minimum radio requirements of this design indicate that a 6 channel, PCM radio system is necessary. After researching available radio systems, the design team chose a Futaba⁶ 8-channel PCM system. The design team chose a radio with two additional channels to allow for the possible use of mechanical wheel-brakes should flight and taxi testing indicate the small additional weight penalty warrant this function.

5.4 Systems Architecture

5.4.1 Propulsion System

As outlined previously, the motor and motor controller are placed in strategic locations in the airframe- the motor as dictated by the required thrust location, and the controller by the motor location. Both of these configurations are shaped by the cooling requirements of these components.

It was desired to place the batteries as closely as possible to the motor controller to minimize Ohmic wiring losses. At the time this paper was finished, the final installation of these components was not completed. The preliminary weight and balance data from the SolidWorks98 solid modeling software indicated that the batteries must be placed closer to the aerodynamic center of the aircraft. This requires a longer wire path than originally desired. However, the final battery placement will be dictated by the full-size balance tests. The design team may employ two battery locations, one corresponding to a conservative, forward CG location and one corresponding to a less stable, neutral CG location. Finally, the required mechanical arming switch will be placed on top of the fuselage directly behind the motor controller.

5.4.2 Landing Gear

⁵ Assuming two servos were already being used for the ailerons; this is common in large-scale model aircraft as the torque requirements of the control surfaces are greater. In addition, the physical linkages used to control two ailerons with a single servo become necessarily more complicated in larger aircraft.

⁶ <http://www.futaba-na.com/>

The design of the landing gear for this aircraft was one of the biggest points of contention to the design team. Both the numerical analysis of the aircraft and the voices of experience at the local RC model flying field indicated that a considerable performance increase would be realized through the use of retractable landing gear. Furthermore, the contest requirement of flying an empty, non-scoring sortie in between payload carrying sorties emphasized the need to minimize the time required to perform the empty laps. Clearly, the analysis indicated that retractable landing gear would result in a 10% increase in top speed and a 5% increase in the contest cruise speed. However, there was significant resistance to the use of retractable gear for several reasons. First, the additional weight and complexity of pneumatic retracts was a concern. Second, the reliability of the retracts was a serious concern. This was especially disconcerting to hear from the experienced fliers at the RC flying field. Their experiences had shown that no matter how well designed the gear was, they never endured well or functioned particularly reliably. The design team did not want to risk a belly landing or a one-gear up landing with a 35-pound airplane.

The original solution to this problem was to design the landing gear mounting structure to accommodate either fixed gear or retractable gear. However, during the construction of the aircraft, the design team decided to produce this aircraft slightly on the conservative side by fitting the plane only with fixed landing gear. Appropriately sized Robart Robostruts were selected for this purpose.

Finally, the ground handling requirements of this contest and the possibility of having to conduct flight operations in potentially strong winds dictated the use of steerable nose gear. Therefore, the design team fabricated a piano-wire nose gear that mounts on the aft of the motor mount.

5.4.3 Radio System

As outlined previously, the aircraft employs a Futaba PCM radio for control. The radio receiver and its battery pack are located behind the aft-most payload bulkhead, where the tail joins the fuselage. This location serves two purposes: First, it minimizes the total wire lengths required for the tail mounted, wing mounted, and nose mounted

control components. Second, it minimizes the possibility of EMI interference from the high-power DC motor in the nose.

5.4.4 Payload System

The contest requirement to carry 1-liter bottles of water payload is not as straightforward as it may seem. Not only must the aircraft support this payload, it also must allow quick and simple exchanges of the payload. Furthermore, determining the best way to carry the payload in the aircraft is complicated. Therefore, much time was spent in determining the optimum location and functionality of the payload system.

The selected system contains several important features. First, the payload is arranged in such a way that any even combination of bottles (i.e. 0, 2, 4, 6, or 8) may be carried with exactly the same center of gravity location. This is significant in that it minimizes trim changes between payload bearing and non-payload bearing sorties. Second, the bottles are accessible from a single large door on the top of the aircraft. This allows the bottles to be taped together, and loaded and unloaded together, which greatly reduces the ground time required between sorties. The payload is supported directly by the principal structural members of the aircraft, reducing the required strength of the main spars. Finally, since the top of the aircraft is principally in compression, and since the payload bottles are form-fitted into the payload bay, the bottles provide additional structural support to the aircraft. The payload door is opened via a single latch on the top of the aircraft.



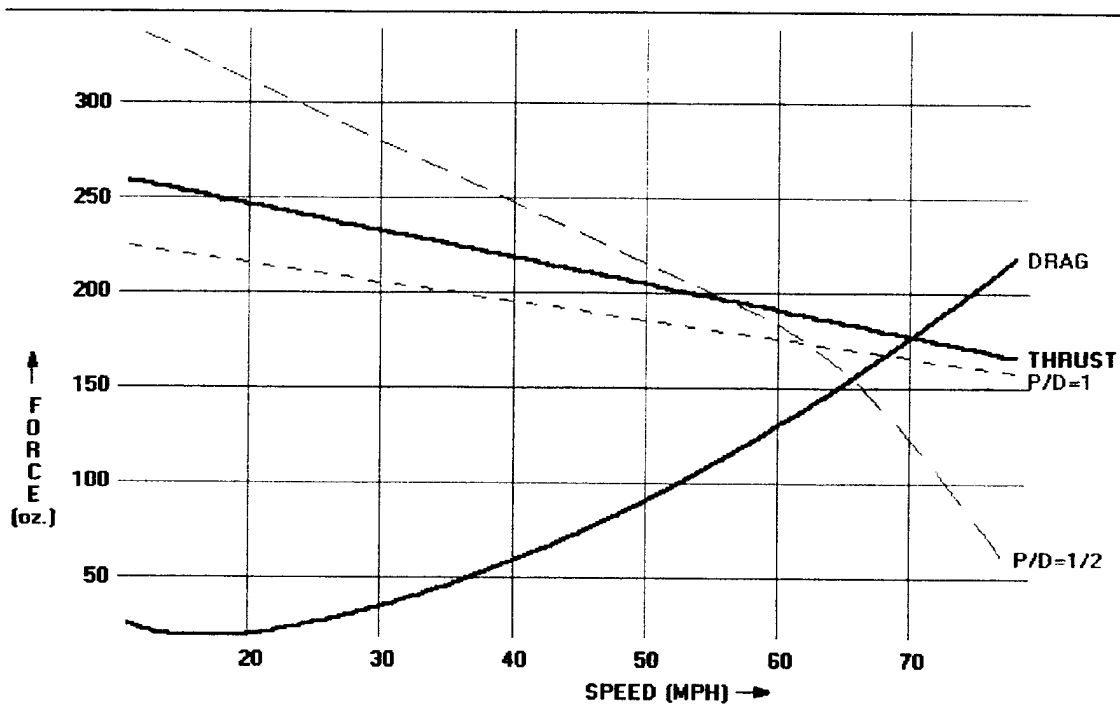


Figure 6: Thrust and Drag versus Airspeed, 100% Throttle

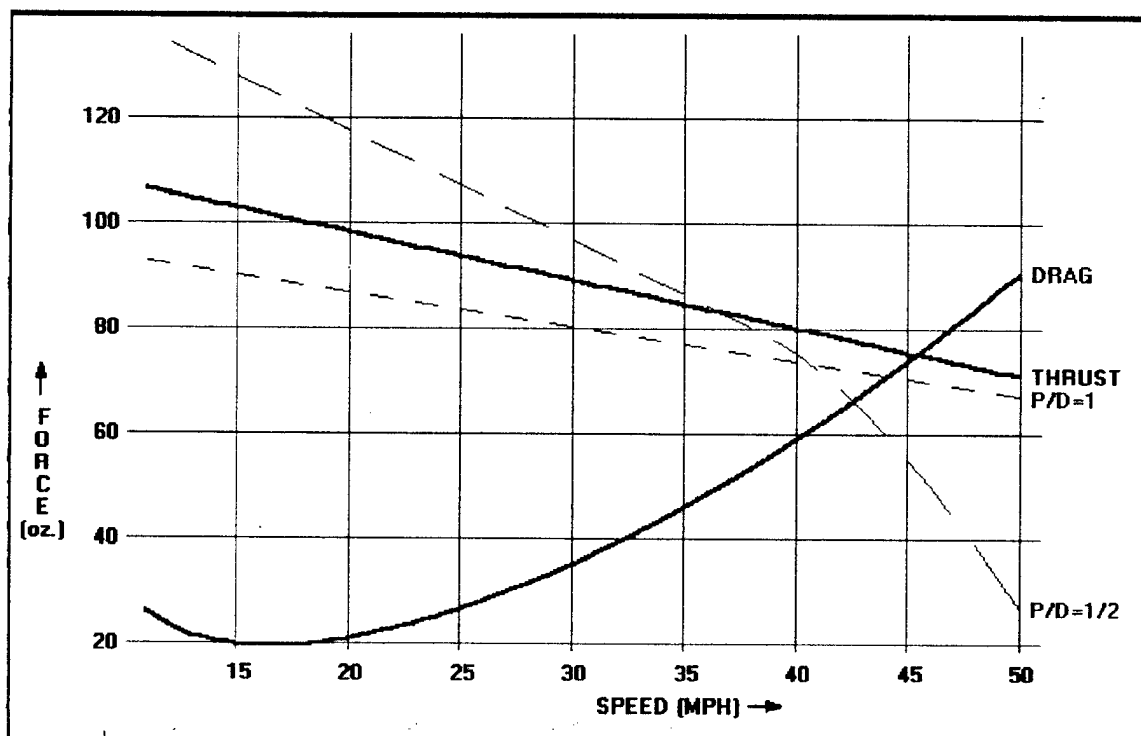


Figure 7: Thrust and Drag versus Airspeed, 58% Throttle (contest cruise)

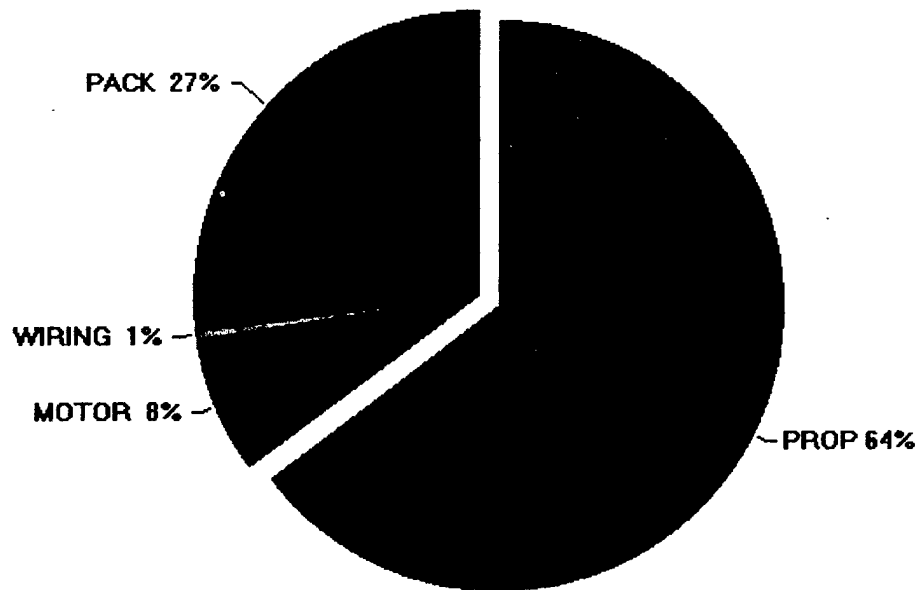


Figure 8: System Efficiency, 100% Throttle

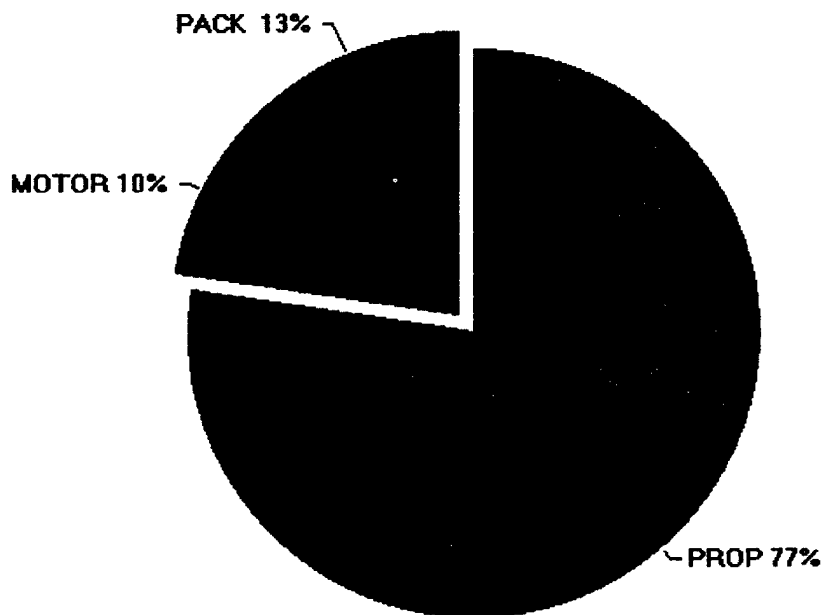


Figure 9: System Efficiency, 58% Throttle (contest cruise)

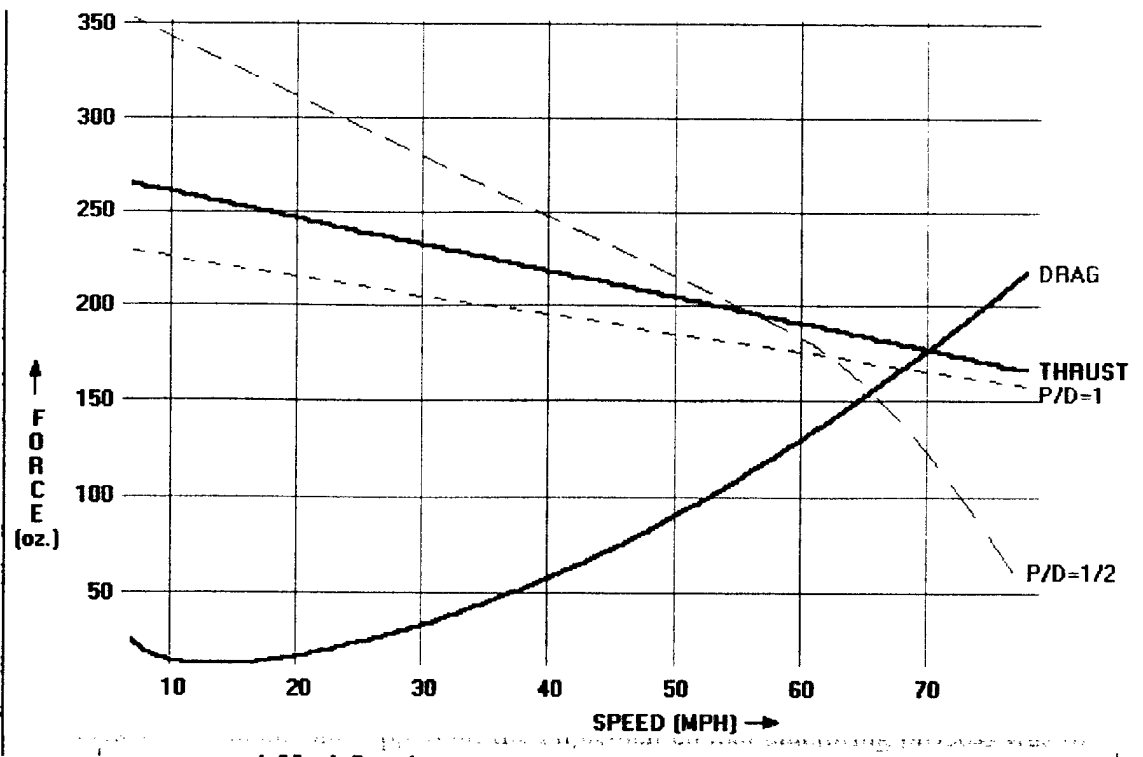


Figure 10: Thrust and Drag versus Airspeed, 100% Throttle (unloaded)

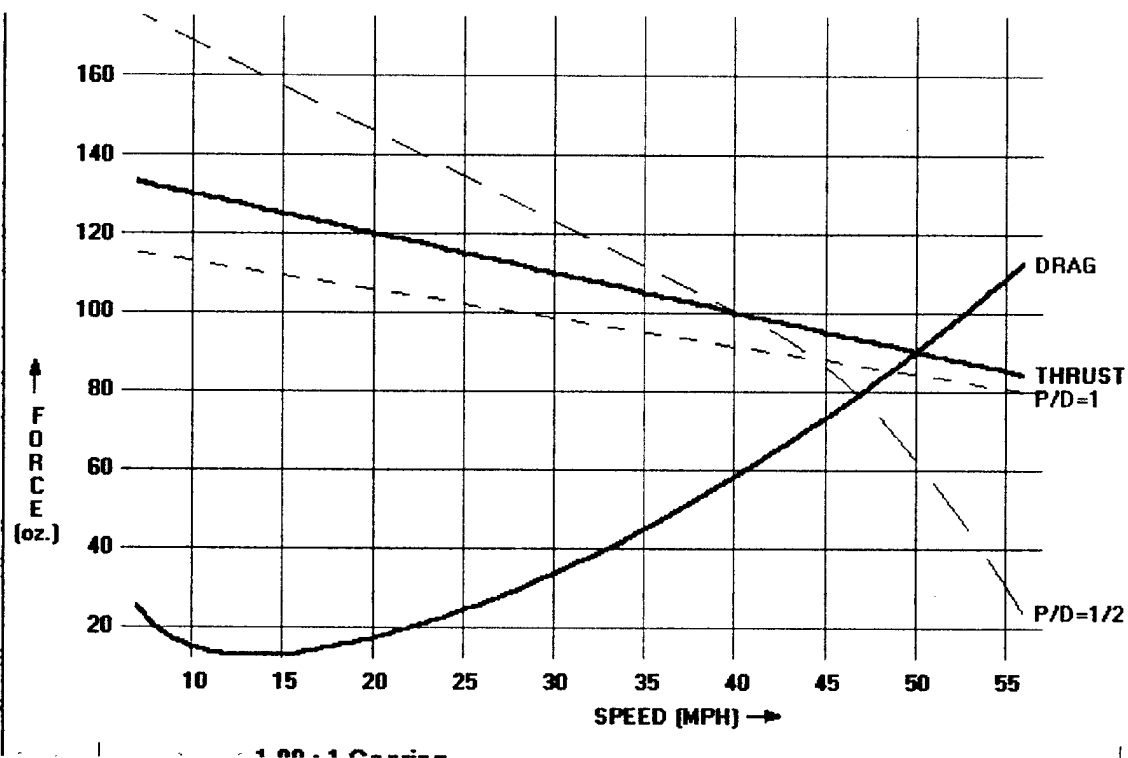


Figure 11: Thrust and Drag versus Airspeed, 65% Throttle (unloaded)

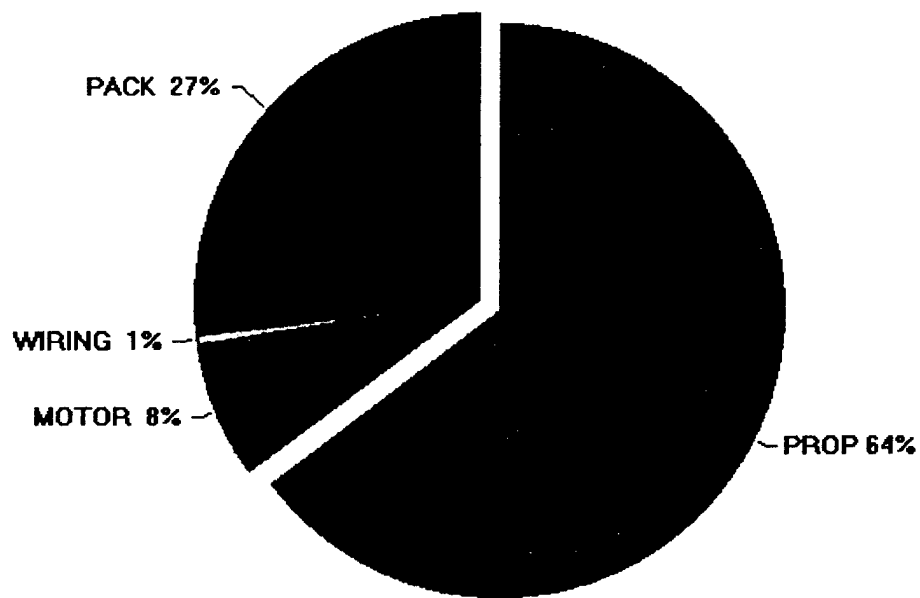


Figure 12: System Efficiency, 100% Throttle (unloaded)

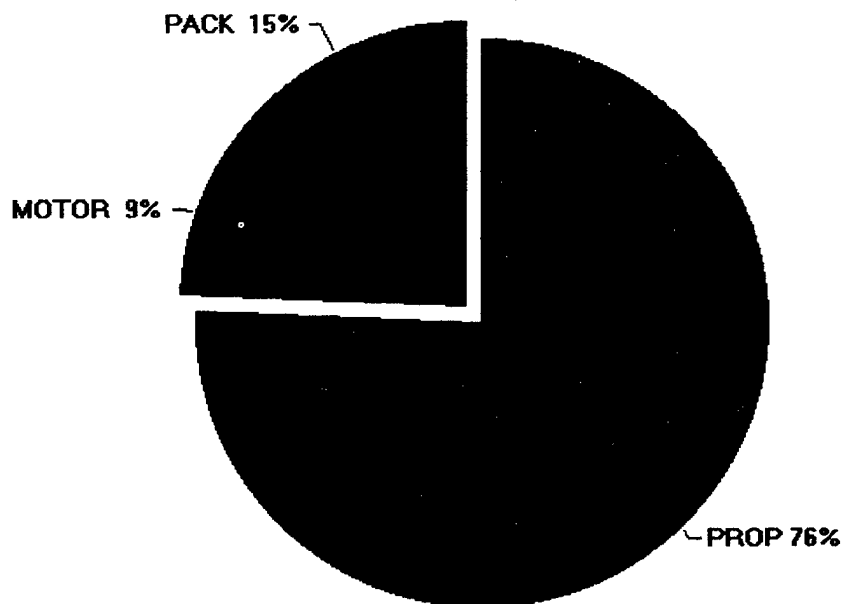


Figure 13: System Efficiency, 65% Throttle (unloaded)

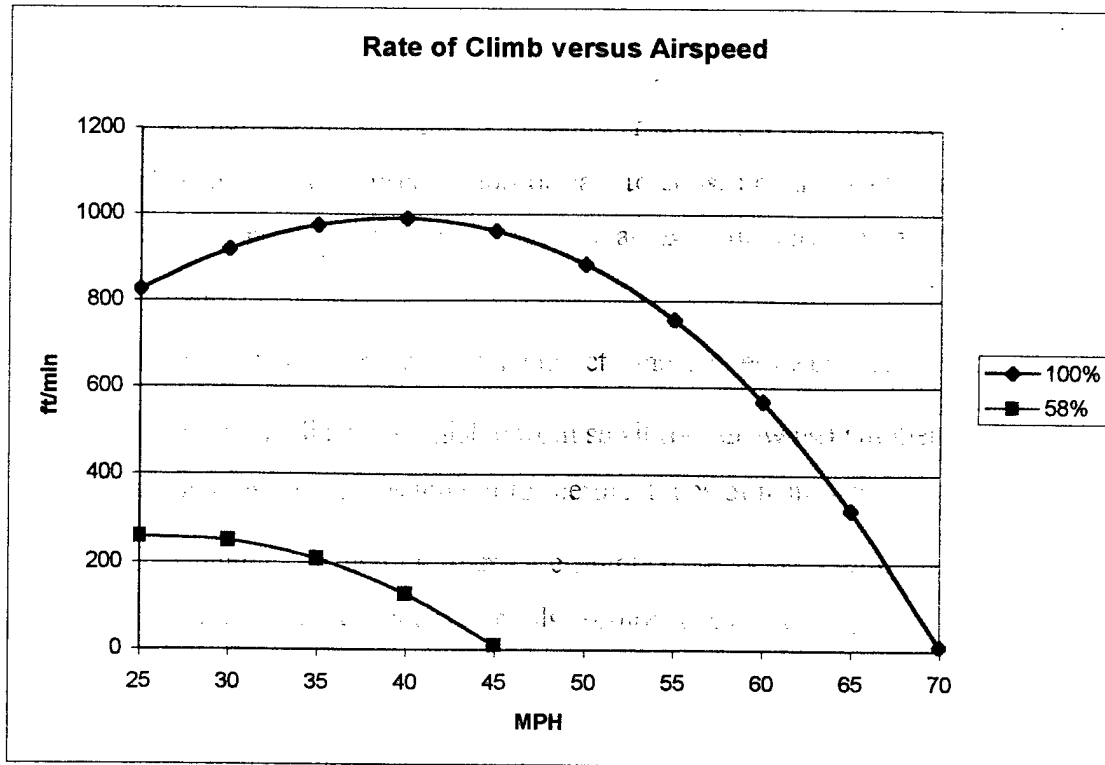


Figure 14: Rate of Climb versus Airspeed (loaded)

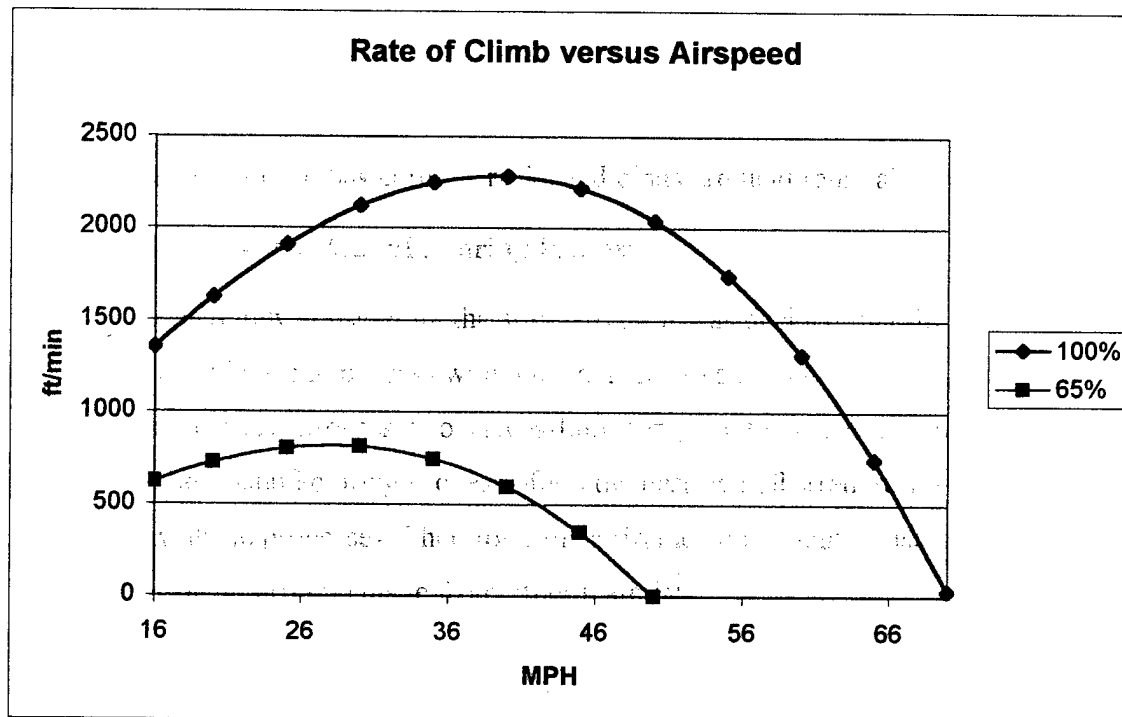


Figure 15: Rate of Climb versus Airspeed (unloaded)

5.5 Drawing Package

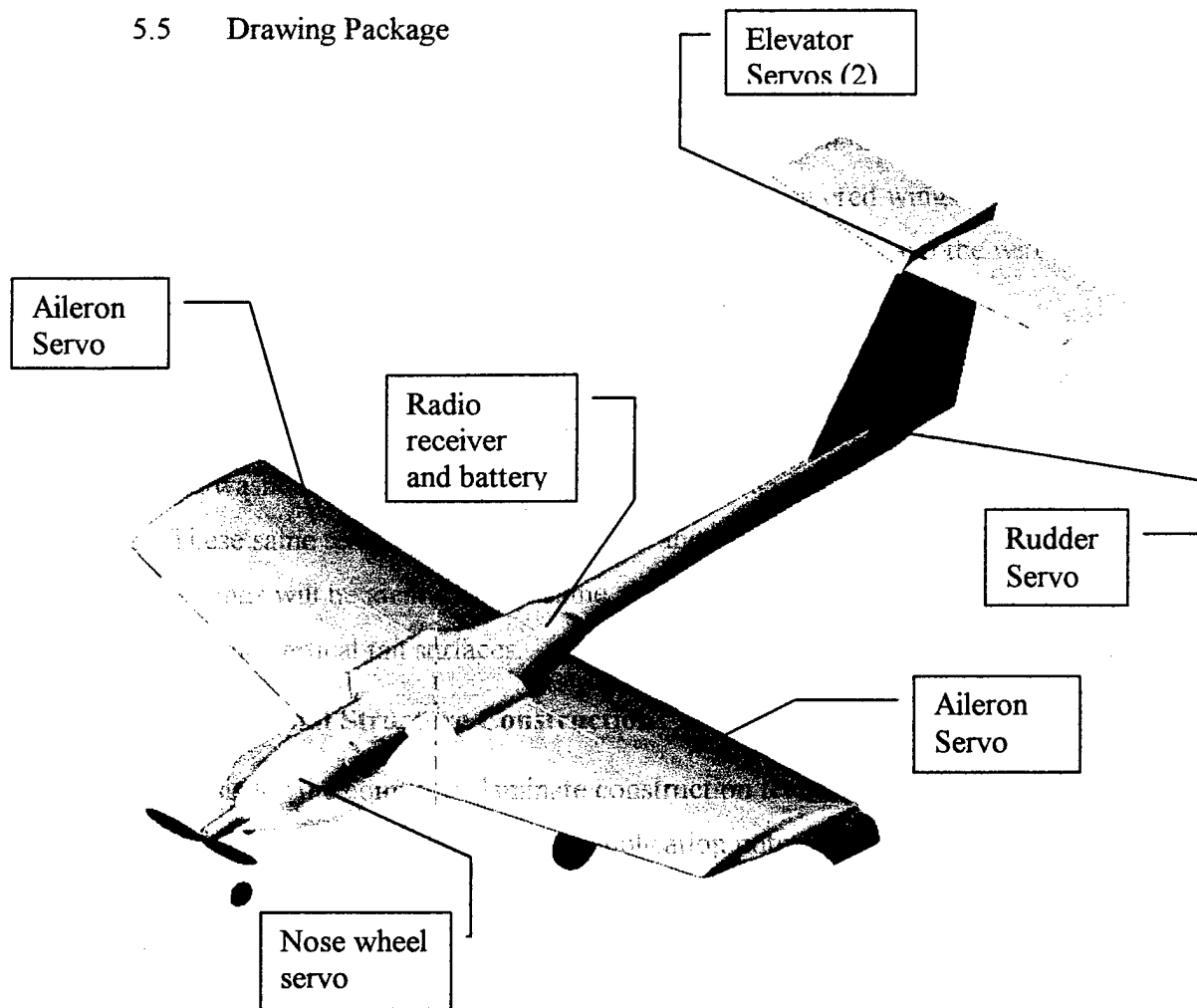


Figure 16: Radio System Placement

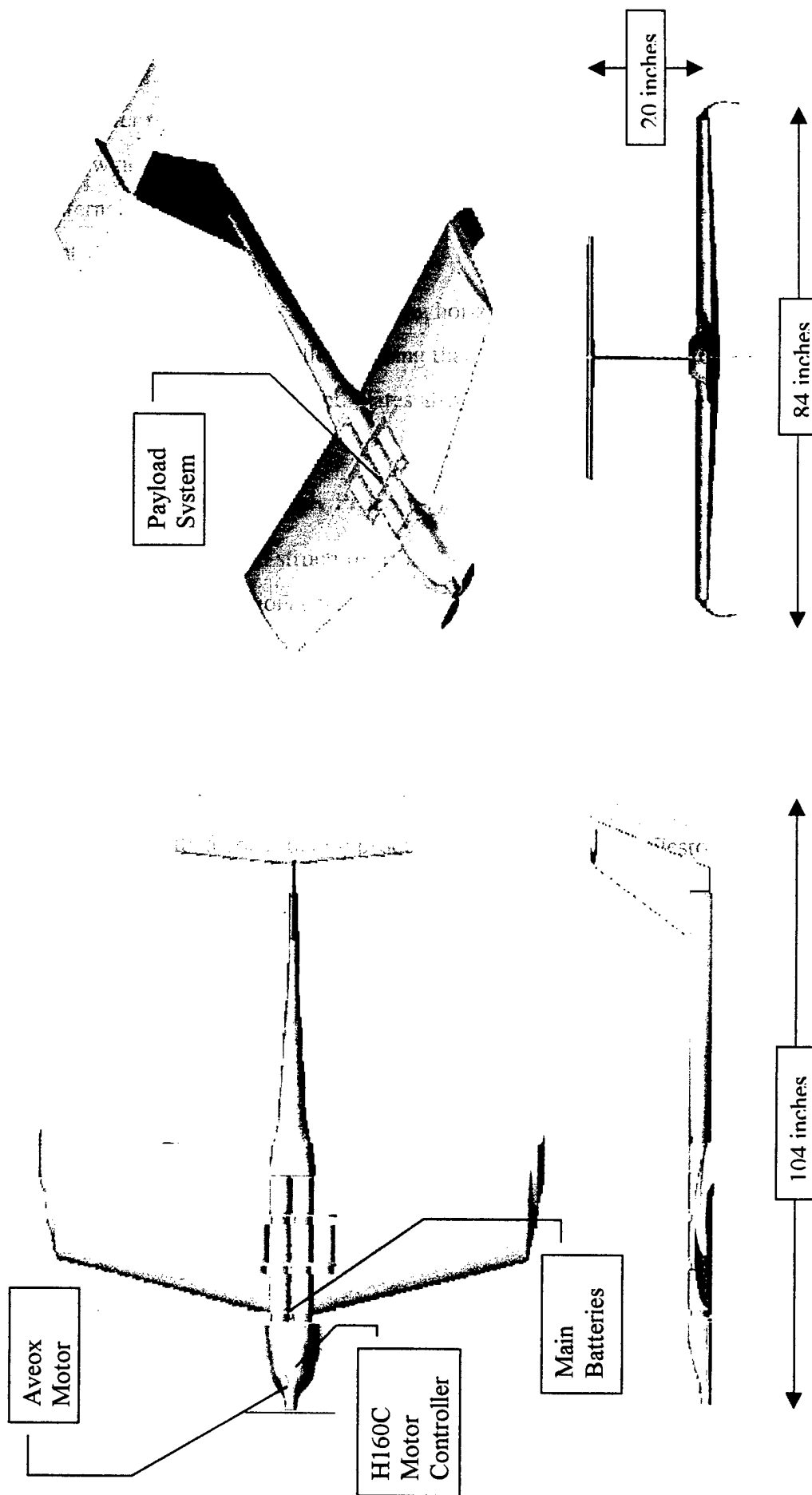


Figure 17: Three view Drawings

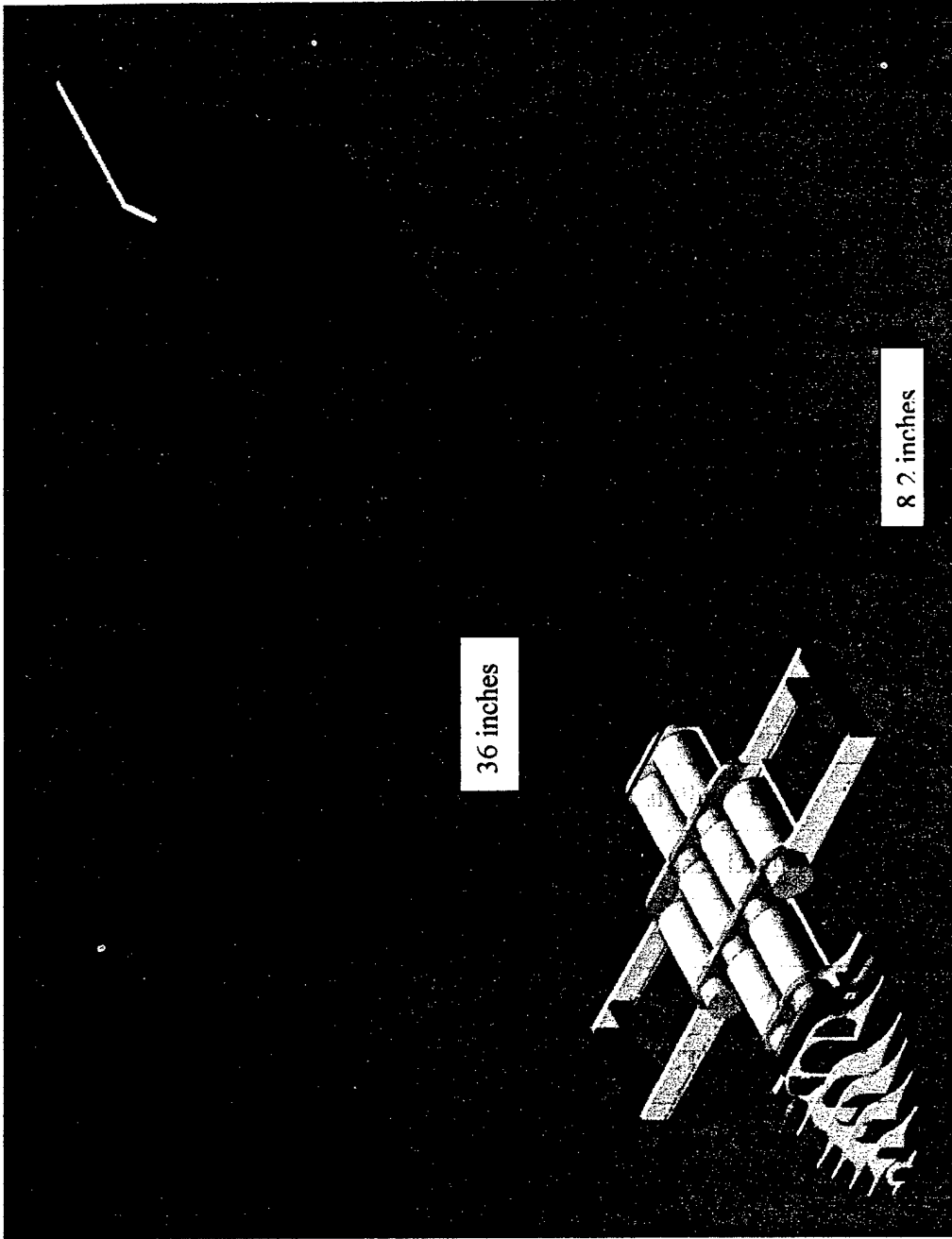


Figure 18: Internal Structure Configuration

6.0 Manufacturing Plan

6.1 Investigated Manufacturing Processes

The design team investigated three principal manufacturing methods. First, the team considered the traditional manufacturing methods that employ lightwoods with cloth or plastic skin. Second, the design team considered utilizing aluminum and other metals to construct the principal aircraft structure. Third, the team considered employing carbon fiber composites in the aircraft manufacturing process.

6.1.1 Figures of Merit (FOMs)

The manufacturing process was considered by employing the basic figures of merit (FOMs): Availability (AV), Required Skill Level (RSL), Available Skill Level (ASL), Cost (CST), Suitability to the Design Concept (SDC), and Reparability (RA). These figures were considered somewhat abstractly, with generalized figures applied in the analysis. As will become apparent, the implemented manufacturing process was the one most suitable for this design team and the one that would result in the highest performance aircraft.

6.1.2 Analysis of Investigated Processes

First, the design team considered the traditional wood and covering technologies commonly used in the RC Hobby industry. These materials are inexpensive and easy to work. Furthermore, an individual with little formal training can easily contribute to the manufacturing process. Since the materials are inexpensive, construction team members may practice procedures that are more complicated. Mistakes are also easily overcome.

Additionally, structures of these materials are tolerant of accidents and mishaps; repairs can often be affected in minutes.

There were two questions facing the construction team. Was the developed concept suitable for these traditional manufacturing processes? Simply put, the airframe specified in the concept is highly contoured, with few flat areas. Additionally, was the structural integrity required by the loading specifications questionable in a purely traditional construction?

The FOMs for this manufacturing process were assigned as follows:

1. AV: High – Material available from many sources in a large variety of shapes and sizes, weights, and strengths.
2. RSL: Low – Material and processes easily workable and learnable.
3. ASL: Medium – Construction team possessed prior experience in almost all phases of the manufacturing process.
4. CST: Low – Most materials are cheap.
5. SDC: Medium – Complex 3-dimensional contours are difficult to realize in wood, but possible. These difficulties are alleviated by the excellent flexibility of Balsa woods and the Mylar covering used in the RC hobby industry.
6. RA: Very High – The CA glues used in this manufacture process set nearly instantly. The low cost of the materials make it possible to have a greater supply of repair materials. The Mylar covering can be patched with simple duct tape if necessary.

Next, the design team considered an aluminum manufacturing approach. These materials would easily provide the necessary strength for the aircraft. Furthermore, these materials are commonly used throughout industry.

The FOMs for this manufacturing process were assigned as follows:

1. AV: Medium – Materials are available from many places with small lead times.
2. RSL: Medium – Easy to work with; requires a minimum of training in use of power tools and machining equipment.
3. ASL: Low to Medium – Several team members had prior machine shop experience. Others needed training.
4. CST: Medium – Can be expensive in non-standard shapes and sizes.
5. SDC: Medium – Can be difficult to machine complex shapes.
6. RA: Low – Serious repairs must be made in machine shop. Primary structure is difficult to patch in the field.

Finally, the carbon fiber composite manufacturing process was evaluated for this concept. This process involves using structural and hot-wire foams to provide shape and compressive strength to the structure. Carbon fiber laminates provide exceptional tensile strength. These materials are used as appropriate to construct laminates that are bound with carbon fiber tape and epoxy. This results in an exceptionally light and strong structural member.

The FOMs for the carbon fiber manufacturing process were assigned as follows:

1. AV: Low to medium – Available from small (but growing) number of vendors. Availability is sometimes limited for certain types of materials.
2. RSL: Medium – Structural foams are simple to work. Hot wire foams slightly more difficult. Carbon fiber materials require special handling.
3. ASL: Medium – Sufficient knowledge base in design team.
4. CST: Medium to high – Prices range to several hundred dollars for a large piece of carbon fiber. Foam costs are high as well.
5. SDC: High – Easy to form into complex shapes, especially to form wing with hot-wire foam cutting machine.
6. RA: Low to Medium – Surface finish is epoxy-coated carbon fiber. It is difficult to reopen after it has cured. Cracks and dings are field repairable with epoxy.

6.2 Selected Manufacturing Process

After carefully considering the alternatives, it was decided that the carbon fiber composite manufacturing process would be ideal for this design. The design team has sufficient skill in these processes to successfully complete the process. Most importantly, the carbon fiber manufacturing process offers the best overall strength-to-weight ratio of any of the available processes. Therefore, the airframe will be lighter using carbon fiber than an equivalent airframe made from other materials.

6.2.1 Hot Wire Foam Cutting

Complex three-dimensional shapes can be simply manufactured using a hot wire foam cutting machine. This device consists of a NiChrome wire that is electrically heated

to a controlled temperature. The operator constructs templates out of Formica or other material that can easily be shaped and sanded to a smooth finish and that will not burn easily when in contact with the hot wire. The wire is then drawn through the foam over the templates. This process is ideal for constructing simple, tapered wings. One simply creates templates for the two end pieces, places them appropriately, and the wire interpolates the cut for the wing.

In the case of this design, the wing has a 30-inch chord at the aircraft centerline and 19.5-inch wing tip chords. Additionally, the design specifies a dihedral angle of 3 degrees and a washout angle of 2 degrees. Both of these angles were constructed into two templates. These same templates cut both the left and the right wing panels; this ensures that the two wings will be identical. The same approach was used to construct the horizontal and the vertical tail surfaces.

6.2.2 Internal Structure Construction

The basis for the composite laminate construction techniques employed in this design was found in The Composite Store's application note on the construction of a super-strong spar. As outlined previously, this process requires a laminate of structural foam and carbon fiber wrapped with carbon fiber tape and epoxied. The design team employed a variation of this process in its construction of this aircraft. The design team employed this process in three-space instead of two. This allowed the structure of the aircraft to contain long strips of uncut carbon fiber laminates, both laterally in the main spars and longitudinally through the central tail longeron. Carbon laminates used in this structure were 60 mil unidirectional fibers in one-half inch strips. At the materials rated tensile strength of 360 KSI, the tensile strength of these strips is roughly 10,000 pounds each.

To construct the internal structure, a jig was produced conforming to the required shape of the bottom of the structure. The structural foam pieces and carbon fiber strips were then cut to shape and assembled on the jig. After epoxying the pieces in place, the structure was wrapped in bi-directional carbon fiber tape and epoxied.

6.2.3 Component Assembly

After the hot wire process was completed on the wings, clearance cuts were made and the wings were fitted to the internal aircraft structure. The vertical tail was fitted to the internal structure as well, incorporating structural support for the horizontal tail assembly of the T-Tail configuration.

The two sections of the full-flying horizontal tail were assembled with a single aluminum shaft bearing on teflon bushing that rest plywood reinforcing plates on the vertical tail surface. The plywood plates also serve as mounting plates for the horizontal tail servos.

6.2.4 Final Assembly Process

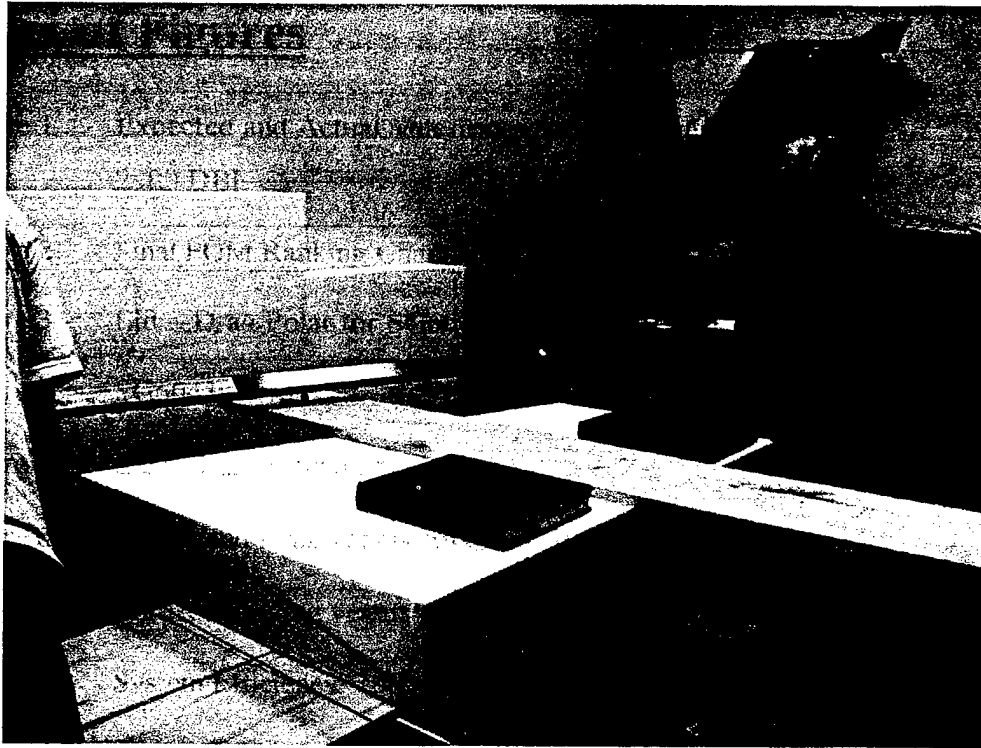
After the principal structures of the aircraft were completed, the entire airframe was wrapped in bi-directional carbon fiber cloth and epoxied. Color pigments were added to the visible sections of the cloth to produce the final color scheme. Finally, the propulsion and radio systems were installed, the control surfaces hinged, and the landing gear mounted. This completes the assembly process.

6.2.5 Manufacturing Schedule

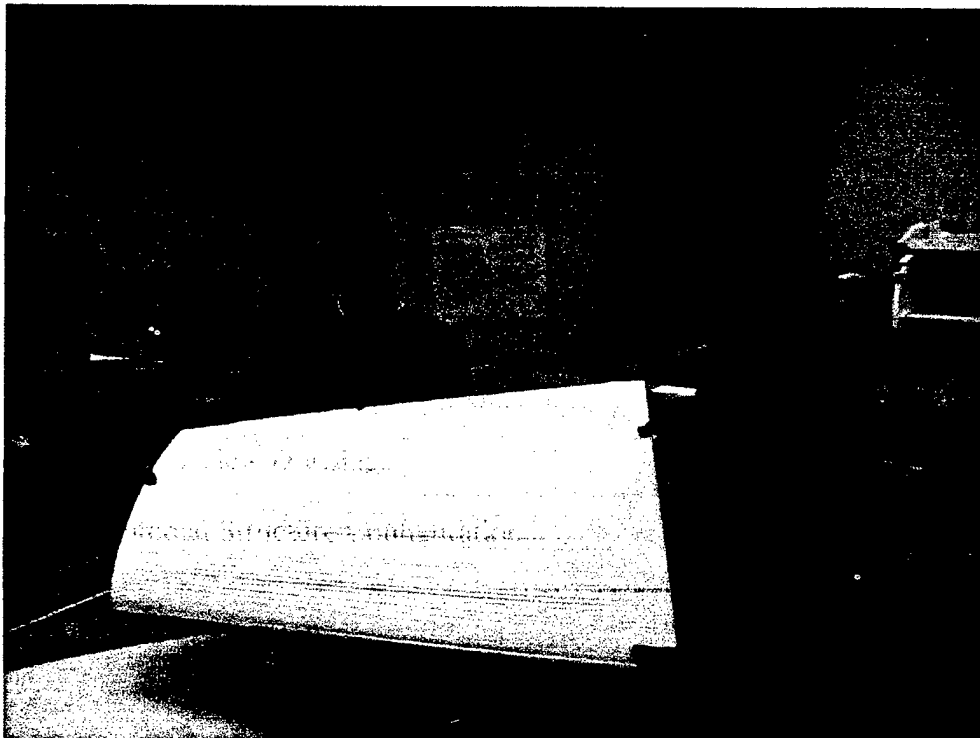
The specified construction process and manufacturing milestone timing data is contained in Table 3. This chart represents the scheduled manufacturing events. The actual timing of some of these events is included in Figure 1.

	Dave	Charles	Jeff	John
Jan. 16	Practice cut done	All jigs finished	Preliminary landing gear analysis report	Help wherever possible
Jan. 23	Horizontal tail cut	All structural foam cut	Design update	Coordinate Recruit help
Jan. 30	Main Wings cut	Final structure assembly	Design completed	Quality control
Feb. 1	Final assembly preparations complete			
Feb. 13	Final assembly complete – ready to cover			
Feb. 20	Control surfaces complete and hinged			
Feb. 27	Systems installation – radio and propulsion			
Mar. 1	First Flight Proposal Phase Draft Due			
Mar. 15	Proposal Phase Due			
Apr. 2	Addendum Phase Draft Due			
Apr. 10	Addendum Phase Due			
Apr. 13	Leave for competition			
Apr. 14-16	COMPETITION			

Table 3: Manufacturing Time Line



Preparing for a hot-wire cut.



Dave and Charles with a wing panel.



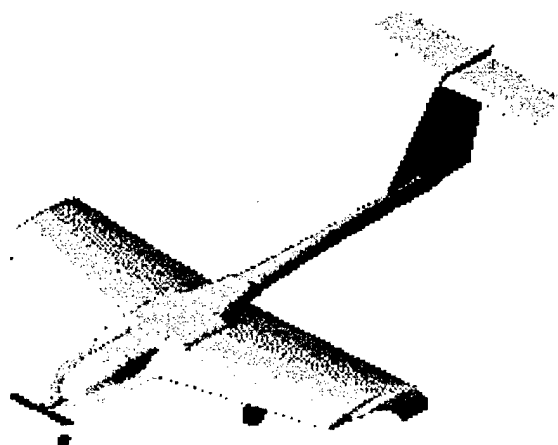
The design team hard at work.



Assembly of the internal structure.

**The American Institute of Aeronautics
and Astronautics, Cessna, and the Office
of Naval Research**

Design, Build and Fly Competition 2000



Cleveland State University

“The Attitude”

The Team

John "Danger" Sustersic	Electrical Engineer - Graduate
Charles "Einstein" Alexander	Electrical Engineer - Junior
Michele "Fuzzy" Beachler	Civil Engineer - Senior
Dave "Dante" Wladyka	Electrical Engineer - Junior
Ray "X-Ray" Still	Mechanical Engineer - Graduate
Paul "Whoop! There It Is!" Weyandt	Mechanical Engineer - Freshman
Marcelo "The Weasel" Gonzalez	Electrical Engineer - Graduate
Maria "Giggles" Laios	Chemical Engineer - Senior
Fred "Red Baron" Glatz	Electrical Engineer - Junior
Anup "The Ghost" Khant	Electrical Engineer - Graduate
Jeff "Stinky N" Rubinski	Mechanical Engineer - Senior
Steve "The Lush" Frydrych	Mechanical Engineer - Senior
Andy "Babyface" Kis	Mechanical Engineer - Sophomore
Bill "Plane Crazy" Tracy	Lorain County Radio Control Club Ace

Table of Contents

Table of Contents	3
Proposal Phase	7
1.0 Executive Summary	8
1.1 Major Development Areas	8
1.2 Overview of Design Tools	10
2.0 Management Summary	11
2.1 Design Team Architecture	11
2.2 Management Overview	11
2.3 Project Milestones	12
3.0 Conceptual Design	14
3.1 Design Parameters	14
3.2 Figures of Merit (FOMs)	15
3.2.1 Rated Aircraft Cost Assignments	17
3.2.2 Importance Factors	17
3.3 Methods of Analysis	17
3.4 Final Concept Selection	18
3.4.1 Final FOM Ranking Chart	18
4.0 Preliminary Design	22
4.1 Design Parameters and Methods of Analysis	22
4.1.1 Take-Off Gross Weight	22
4.1.2 C_L of Main Wing Airfoil	23
4.1.3 Wing Area	24
4.1.4 Tail Volume	25
4.2 Summary of Final Configuration	26
5.0 Detail Design	29
5.1 Design Modeling	29
5.2 Performance Prediction	29
5.3 Component Selection	31
5.4 Systems Architecture	33
5.4.1 Propulsion System	33
5.4.2 Landing Gear	33
5.4.3 Radio System	34

5.4.4	Payload System	35
5.5	Drawing Package	42
6.0	Manufacturing Plan	46
6.1	Investigated Manufacturing Processes	46
6.1.1	Figures of Merit (FOMs)	46
6.1.2	Analysis of Investigated Processes	46
6.2	Selected Manufacturing Process	48
6.2.1	Hot Wire Foam Cutting	48
6.2.2	Internal Structure Construction	49
6.2.3	Component Assembly	50
6.2.4	Final Assembly Process	50
6.2.5	Manufacturing Schedule	50
	ADDENDUM PHASE	54
7.0	Lessons Learned	55
7.1	Introduction	55
7.2	Aircraft Balance and Weight	56
7.3	Propulsion System	59
7.4	Potential Improvements	59
8.0	Aircraft Cost	61
8.1	Computation of the Standard Aircraft Cost	62

Index of Figures

Figure 1	Expected and Actual Milestones for the Cleveland State 1999-2000 DBF	13
Figure 2	Final FOM Ranking Chart	19
Figure 3	Lift – Drag Polar for SG6043 Airfoil	27
Figure 4	SG6043 Airfoil	27
Figure 5	ElectriCalc Screen Shot	36
Figure 6	Thrust and Drag versus Airspeed, 100% Throttle	37
Figure 7	Thrust and Drag versus Airspeed, 58% Throttle (contest cruise)	37
Figure 8	System Efficiency, 100% Throttle	38
Figure 9	System Efficiency, 58% Throttle (contest cruise)	38
Figure 10	Thrust and Drag versus Airspeed, 100% Throttle (unloaded)	39
Figure 11	Thrust and Drag versus Airspeed, 65% Throttle (unloaded)	39
Figure 12	System Efficiency, 100% Throttle (unloaded)	40
Figure 13	System Efficiency, 65% Throttle (unloaded)	40
Figure 14	Rate of Climb versus Airspeed	41
Figure 15	Rate of Climb versus Airspeed (unloaded)	41
Figure 16	Radio System Placement	42
Figure 17	Three View Drawings	43
Figure 18	Internal Structure Configuration	44

Index of Tables

Table 1	Preliminary Weight Breakdown	22
Table 2	Summary of Key Features of Final Configuration	28
Table 3	Manufacturing Time Line	51
Table 4	Summary of Key Features of Production Configuration	60
Table 5	Airframe Dependent Parameters of Cost Model	62
Table 6	Manufacturing Hours Breakdown	63

Appendix A: Photos of Manufacturing Process.

Addendum Phase

7.0 Lessons Learned

7.1 Introduction

After two years of attempting the Design, Build, and Fly competition, it is interesting to note that there are still many lessons to be learned from attempting a design project of this magnitude. In the first year, the design team tried to incorporate an innovative airframe with simple construction techniques and was successful in producing a unique, though flawed, aircraft. Drawing on those experiences, and driven by the rated aircraft cost metric that penalizes more complicated designs, the design team strove to incorporate a more straightforward airframe with advanced manufacturing techniques. In this effort, the team was quite successful in both reducing the total man-hours required for the aircraft's construction and also in producing an aircraft that was potentially superior to a similar design that employed more basic manufacturing techniques. The rationale for this approach was simple: the actual manufacturing techniques used in the aircraft construction were not considered in the rated aircraft cost formula. Therefore, any design that could find advantages in this area would benefit from enhanced performance without suffering a penalty in the competition scoring through an increase in its rated aircraft cost. Interestingly enough, after completing two aircraft for this competition – one for last year using simple balsa construction and one for this year using state-of-the-art carbon fiber materials and specialty foams, the design team found that the process of constructing an aircraft using these advanced techniques was much simpler than the basic approach. Additionally, the team found that the accuracy with which the aircraft could be constructed was greater using the advanced techniques. These conclusions depend upon one necessary condition: the manufacturing team must possess some basic information on the proper handling of these materials and in the use of these materials in an appropriate fashion. The reason for this result is simple. The foams are quite easy to work and shape into complex shapes, while the great strength to weight ratio of carbon fiber materials allows the structural engineers to place the necessary strength where it is needed. Basically, the foam provides the shape and the carbon fiber provides the strength. Epoxy is utilized to bind the structure together. The design team highly recommends this approach for all competition aircraft.

7.2 Aircraft Balance and Weight

Early during the manufacturing process of this aircraft, it was clear that the plane was tail heavy. Of course, it is difficult to gage exactly how far the longitudinal center of gravity (CG) would differ from the design point. As construction progressed it became clear that the balance was incorrect. The design team anticipated this balance problem since there were some elements of the design not included in the SolidWorks solid model and CAD design work; however, the design team was not planning on selecting the final location of the battery pack until after the aircraft was completed. The CAD work indicated that the batteries should be placed approximately 3-4 inches ahead of the required CG location for proper balancing. As it became clear that no possible placement of the battery packs would result in a properly balanced aircraft, the team leaders began reinforcing the wing and nose structures of the airframe. This was done for a simple reason: if it was strictly necessary to add weight to the aircraft, that weight may as well serve another purpose; However, the team did not want to simply add five pounds of lead to the nose for a proper balance. Despite the efforts to increase the forward structural weight of the aircraft, the final airframe as documented in the proposal phase required nearly six pounds of weight sitting just aft of the propeller to properly balance. The design team found this unacceptable for two reasons. First, the required weight would seriously affect the aircraft's ability to meet the required take-off performance and negatively affect its endurance and other flight performance characteristics. Second, there simply was no place in the narrow taper of the nose to place six pounds of lead. Even more weight would have been required with a reduced moment arm farther aft in the airframe.

After much debate, it was decided that it was feasible to reduce the tail length to reduce the positive pitching moment of the tail assembly. This was possible, and actually quite simple, for several reasons. First, in analyzing the performance of last year's aircraft, it was determined that the principle flaw in that design was insufficient tail volume. Therefore, the design team added a generous factor of safety in the tail design. In addition to designing a tail with a large tail volume, the design team placed the horizontal stabilizer in a high T-Tail configuration to eliminate any possible interference between the main wing and the horizontal stabilizer. In short, the additional factor of safety

incorporated into the tail design was partly responsible for the imbalanced condition of the proposal aircraft because it further lengthened the tail moment arm. When it became clear that large weights would be required to properly balance the aircraft, the design team re-evaluated the tail volume specification and concluded that eight inches could be safely removed from the tail without seriously jeopardizing the stability of the aircraft. Second, the physical structure of the tail was easily modified. This structure consists of three 0.5 inch by 60 mil thick strips of carbon fiber laminate sandwiching structural foam cores. There are 0.5-inch thick structural foam bulkheads that shape the tail surface. The tail is covered by carbon fiber cloth and reinforced in key modes by 7 mil thick strips of unidirectional carbon laminates. Furthermore, the only control elements in the length of the tail are the wiring for the two tail mounted servos. Most importantly, however, was the fact that this primary structure was rectangular, so removing a section of the tail required only splicing two ends together of the same dimensions. Therefore, it was quite simple to cut the tail off at a point just before the rudder, remove the specified eight inches of tail length, and then splice the carbon fiber laminates with two-inch long strips of carbon fiber. The wiring was then reinstalled and the carbon fiber surface refinished. The entire modification required less than two hours of work and took one day to complete (allowing for epoxy curing time).

After completing the tail modification, the balance was re-checked. This test indicated that, while the weight needed to balance the aircraft was reduced, it was still tail heavy. The design team proceeded to lighten the tail structure as much as possible, removing all unnecessary foam and cutting lightening holes in both horizontal stabilizers. This was done for a simple reason: the tail moment arm was still almost twice the moment arm to the area where any balancing weight would be carried. Therefore, reducing the weight of the tail by even 8 ounces would reduce the balancing weight by an entire pound, consequently reducing the total weight of the final aircraft by 1.5 pounds. After completing all lightening techniques practical, the aircraft required slightly more than three pounds to balance.

Finally, it was suggested by an advisor that the nose be lengthened to increase the both its moment arm and to allow for a more forward location of the battery packs. This idea actually was considered earlier by several team members and rejected as

unnecessarily complicated. Initially, it was thought that this modification would be too complicated because this relatively thin structure was required to support potentially large transient loads on a hard landing. This is especially true in a case where the tail or main wheels hit hard, causing the plane to pivot about its wheels and land hard on the nose gear. Therefore, a considerably stronger structure was designed for this area. This structure utilizes ten pieces of 0.5 inch by 60 mil carbon laminates, providing a total tensile strength of nearly 100,000 pounds. Additionally, this structure, unlike the rectangular structure of the tail, was tapered into the aluminum motor mount. Therefore, the design team originally thought it would be necessary to completely reconstruct the nose of the aircraft. However, after the advisor suggested the alteration, the team leaders reconsidered the idea, and found a feasible and simple way of accomplishing the modification.

The design team determined that the nose could be cut directly in front of the forward payload bay bulkhead. At this location, the contour of the surface was relatively flat. Extending this area an additional four or six inches would not disrupt the airflow in that area, and only modestly increase parasitic drag over this additional wetted area. Furthermore, the design team spliced the nose section back to the aircraft using simple rectangular section. This extension allowed for a rectangular area large enough to accommodate the complete battery pack. Additionally, making the cut in this location left the entire propulsion system installation unaffected by the modification. The modification did weaken the structure somewhat, since the triangular truss that had been constructed was altered into a hybrid shape. However, since the structure was originally much stronger than actually required, the loss in structural capacity did not adversely affect the aircraft's performance. Finally, the more forward location of the battery packs reduced the wiring required to power the aircraft, resulting in a reduction of copper losses in the overall propulsion system.

In the end, the design team was forced to add an additional one pound weight to the nose of the aircraft to properly balance the craft. In total, the modifications to the aircraft, including the necessary balancing weight, added 1.2 pounds to the total airframe weight. The problem with the original balance point was traced to the CAD model; the complex 3-D shapes were modeled only as surfaces. This meant that the model

underestimated the total mass of the tail and of the main wings. However, since there are considerable structural elements in the main wing, and the mass of the wing is approximately uniformly distributed about the specified center of gravity, the error in the estimation of the tail more severely affected the balance point. Furthermore, the underestimation of the weight of the plane resulted in an airframe weight more than six pounds greater than expected.

7.3 Propulsion System

After in-flight testing and bench running of the power plant, the propeller specified in the proposal phase was changed to a 15-10 APC prop. This change was driven by a repeating thermal shutdown condition of the motor controller during flight; this resulted in successful deadstick landings on the first three flight tests. Additionally, two heat sinks were added to the motor controller and one to the motor mount to help cool these devices during periods of sustained high power operation and/or low airflow conditions.

7.4 Potential Improvements

Clearly, a team's first attempt at the construction of any complicated mechanical device will not be optimum. After having completed an advanced composite structure of this magnitude, the design team found numerous areas in which to improve its processes. Indeed, considerable progress was made even during the construction process; this is especially evident in the quality with which the carbon fiber cloth was applied. It is obvious which sections were first installed and which sections were applied later.

As documented previously in this addendum, the empty weight of this aircraft is somewhat higher than expected. Part of the reason for this is the complications caused by the balancing difficulties. Probably an even greater reason for this is the generous application of epoxy and the added structural elements that were included both to help the balance situation and to ensure that the aircraft would meet its structural integrity tests during the technical inspections. Certainly, a second prototype aircraft would be quite superior to this prototype both in quality of workmanship and in reduced airframe weight.

Final Production Configuration	
Wingspan	7 feet
Payload Capacity	8 liters
TOGW	46 pounds
Empty Weight (no batteries)	20.5 pounds
Payload Fraction	.4457
Main Wing Airfoil	SG6043
Chord at centerline	30 inches
Chord at wingtip	19.5 inches
Tail	Full flying stabilizer
Horizontal Stabilizer Airfoil	SD8020
Motor	Aveox F27L brushless DC motor
Motor Controller	Aveox H160C
Propeller	APC 15 x 10 inch
Batteries	Sanyo N-3000CR cells 26 cell pack 31.2 volts, 3.0 amp-hour

Table 4: Summary of Key Features of Production Configuration

(red letters indicated variation from proposal aircraft)

8.0 Aircraft Cost

The 2000 Design, Build and Fly Competition employs a standard aircraft cost model to better model the engineering atmosphere in a real-world design project. Clearly, an engineer may not use unlimited resources in time and money to find optimal solutions to simple problems. the rated aircraft cost provides a uniform way of gauging a concept's expense; this metric is used in the competition scoring to rank simpler, more economic designs above equally-performing sophisticated designs. Therefore, the contest designers instituted an aircraft cost model based on the following formula:

$$\text{RatedAircraftCost}(\$,\text{Thousands}) = \frac{A * \text{MEW} + B * \text{REP} + C * \text{MFHR}}{1000} \quad \text{Equation 3}$$

Where MEW is the Manufacturer's Empty Weight metric, REP is the Rated Engine Power metric, and the MFHR is the Manufacturing Man Hours metric. The coefficients A, B, and C are multipliers defined as follows:

$$\begin{aligned} A &= \$100/\text{pound} \\ B &= \$1/\text{Watt} \\ C &= \$20/\text{Hour} \end{aligned} \quad \text{Equation 4}$$

By definition, MEW is the actual airframe weight, in pounds, and does not include the payload or the batteries. The REP metric is defined by the following formula:

$$\text{REP} = (\# \text{Engines}) * 50A * \left(1.2V/\text{cell}\right) * (\# \text{cells}) \quad \text{Equation 5}$$

Finally, the MFHR is defined as the prescribed assembly hours by Work Breakdown Structure (WBS). This metric is computed from the following formula:

$$\begin{aligned}
MFHR = & \left(5hr/wing\right)(\# wings) + \left(4hr/ft^2\right)(Projected_Area) \\
& + \left(5hr/body\right)(\# fuselages) + \left(4hr/ft\right)(ft_length) \\
& + 5hr + \left(5hr/VerticalSurface\right)(\# VerticalSurfaces) \\
& + \left(10hr/HorizontalSurface\right)(\# HorizontalSurfaces) \\
& + 5hr + \left(1hr/servo\right)(\# servos) \\
& + \left(5hr/Engine\right)(\# engines) + \left(5hr/Propellers\right)(\# Propellers)
\end{aligned}
\tag{Equation 6}$$

8.1 Computation of the Standard Aircraft Cost

The calculations for the standard aircraft cost begin with the airframe dependent parameters. These parameters are listed in table 5 as follows:

Airframe Weight (Measured April 8, 2000)	20.5 pounds
Number of Engines	1 engine
Number of Cells	26 cells
Number of Wings	1 wing
Projected Area	15.3958 ft ²
Number of Fuselages	1 Fuselage
Length of Fuselages	7.2083 feet
Number of Vertical Surfaces	1 Vertical Surface
Number of Horizontal Surfaces	1 Horizontal Surface
Number of Servos	5 Servos
Number of Propellers	1 Propeller

Table 5: Airframe Dependent Parameters of Cost Model

These parameters are used to calculate the Rated Aircraft Cost. First, the design team computed the Work Breakdown Structure. These calculations are summarized in table 6 as follows:

Wing(s)	$= \left(\frac{5hr}{wing} \right) (1) + \left(\frac{4hr}{ft^2} \right) (15.3598 ft^2)$	66.5833 hours
Fuselage(s)	$= \left(\frac{5hr}{body} \right) (1) + \left(\frac{4hr}{ft} \right) (7.2083)$	33.8333 hours
Empennage	$= 5hr + \left(\frac{5hr}{VerticalSurface} \right) (1) + \left(\frac{10hr}{HorizontalSurface} \right) (1)$	20.0000 hours
Flight Systems	$= 5hr + \left(\frac{1hr}{servo} \right) (5)$	10.0000 hours
Propulsion Systems	$= \left(\frac{5hr}{Engine} \right) (1) + \left(\frac{5hr}{Propellers} \right) (1)$	10.0000 hours
Total Manufacturing Hours		140.4166 hours

Table 6: Manufacturing Hours Breakdown

One may determine the Rated Engine Power as follows:

$$REP = (1Engine) * 50A * \left(\frac{1.2V}{cell} \right) * (26cells) = 1560Watts \quad \text{Equation 7}$$

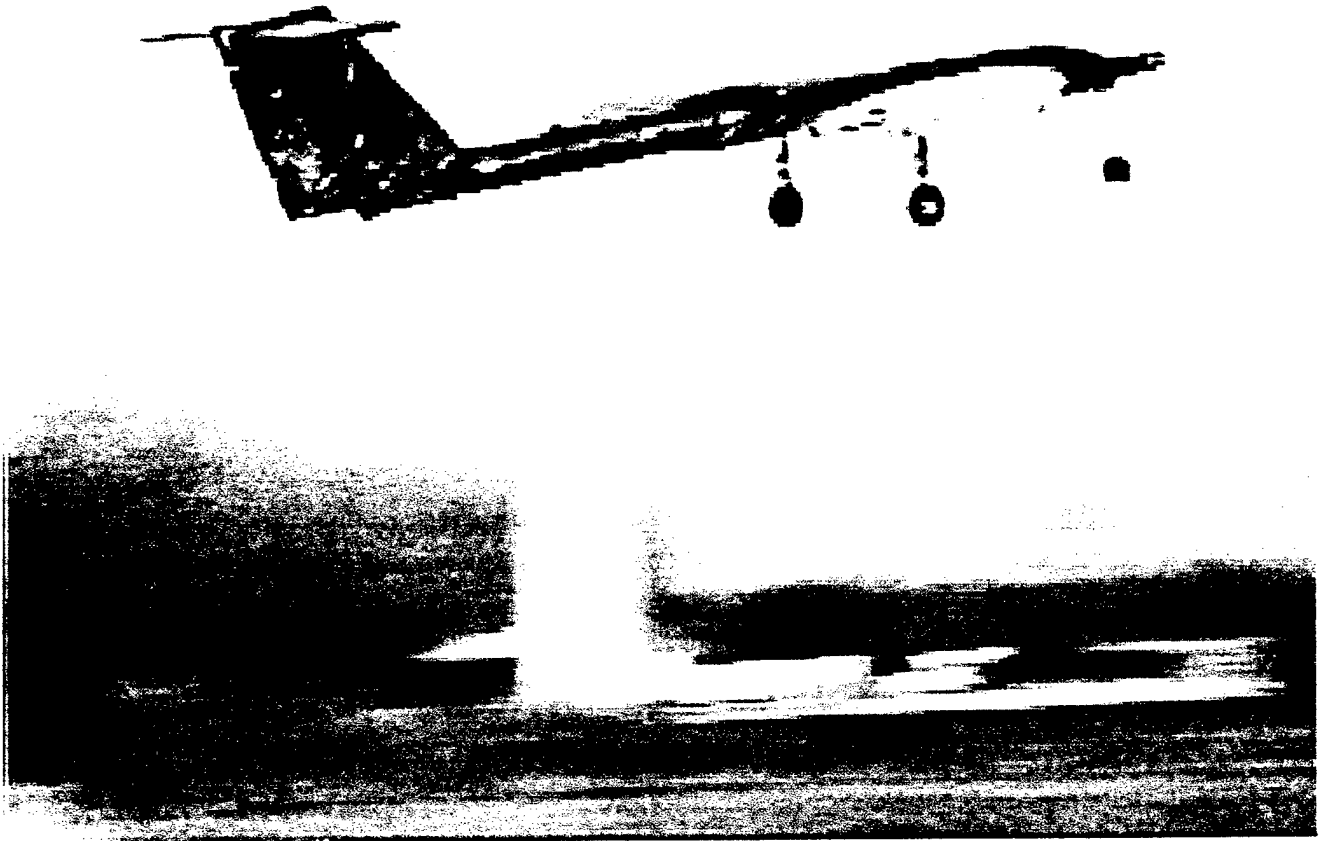
Using these data, one may then calculate the Rated Aircraft Cost for Cleveland State University's entry as follows:

$$RAC(\$, Thousands) = \frac{\$100/pound * 20.5lb + \$1/Watt * 1560watts + \$20/Hour * 140.4166hours}{1000}$$

$$\therefore \text{Rated Aircraft Cost} = 6.4183(\$, Thousands)$$

Equation 8

Therefore, the RAC of this aircraft is 6.4183 Thousand Dollars.



The Attitude in Flight



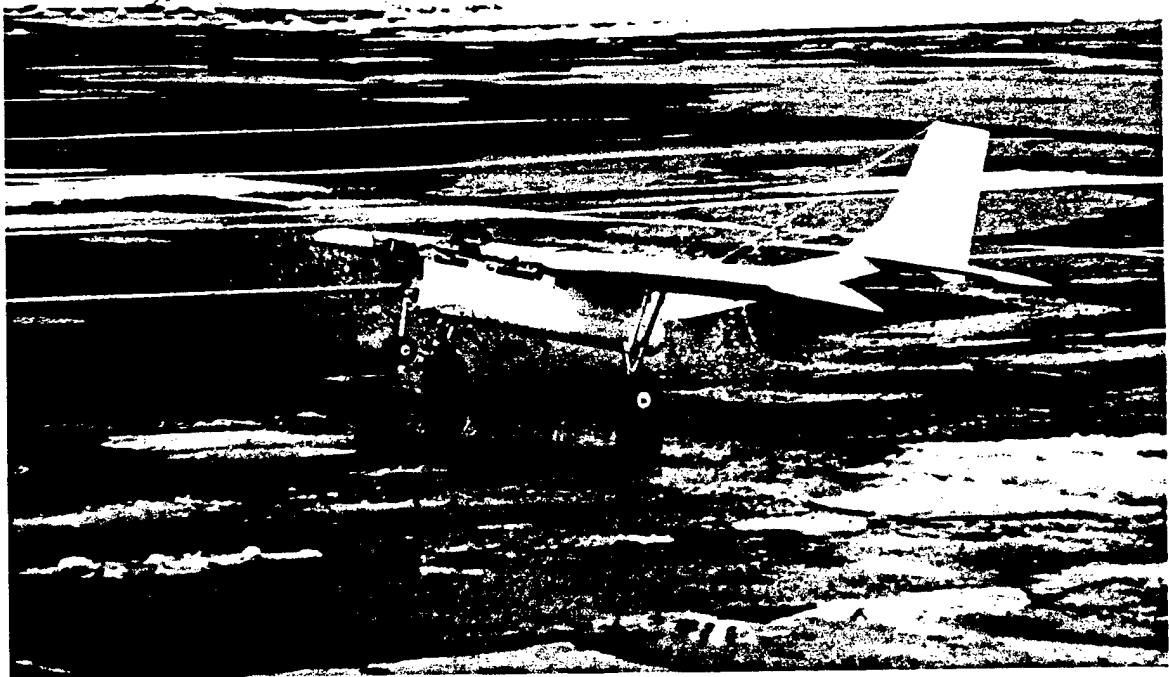
The Attitude in high alpha landing



**East Stroudsburg University
of Pennsylvania**

**2000 Cessna/ONR
Student Design/Build/Fly
Competition**

Design Report



Proposal Phase

Contest Date: April 15-16

Contest Site: Wichita, KA

Electric Airplane Project
c/o Physics Department
East Stroudsburg University
East Stroudsburg Pa, 18301

Phone: 570-422-3341
Fax: 570-422-3505
Email: dlarrabee@po-box.esu.edu

Table of Contents

Executive Summary

Management Summary

Conceptual Design

Preliminary Design

Detailed Design

Manufacturing Plan

Executive Summary

Executive Summary

With intent to compete in the Cessna/ONR 2000 Student Design/Build/Fly Competition, the team from East Stroudsburg University has prepared an original entry that satisfies the specified contest criteria. The entry has already demonstrated capable mission performance and efficient operation in accordance with its modest rated aircraft cost. It is believed that the design shall serve to be far more competitive than the aircraft that was fielded by the team during the previous event.

The final design, dubbed the **Impulse II**, was chosen as a result of the factors arising from team debriefing after the 1999 contest and the new mission/contest requirements. The team did not have to begin from scratch as it did before. It had the benefit of data acquisition and valuable experience gained from the ESU Javelin. Though the new aircraft bares no resemblance to its 42-pound, aluminum predecessor, it was possible to keep a small number of aircraft components that were "contest proven" and required no alteration. This promoted rapid prototyping as the primary means by which the final design would be ultimately frozen. Prototype flights were logged at least four months ahead of the contest and the final variants were flying at least one month before the scheduled event.

A broad range of alternatives was investigated during the conceptual stage of design. The team used a figure of merit exercise to select a conservative planform that reflected our desire to effectively improve upon last year's entry while still retaining any successful equipment. Because battery-weight, span, takeoff distance, and rated aircraft cost posed considerable constraints, primary emphasis was directed toward reduction in empty airframe weight through careful selection of materials. Composite materials were used in stark contrast to the ESU Javelin. A higher skill matrix was necessitated with the incorporation of fiberglass construction, but this was deemed acceptable in order to avoid the high weight penalty of aluminum.

With respect towards sizing, a tiny aircraft with 2-liter capacity relying on a high number of sorties was considered as well as a large aircraft that could carry 8 liters infrequently. The final design is a compromise that operates between the aforementioned extremes of minimal \$/liter ratios, yet maintains solid flight characteristics. The Impulse

II is a 18lb aircraft (including 5lb of batteries) that possesses a 7' span and is powered by one Astro Cobalt 60 motor on 27 cells. Depending on contest weather conditions, it can carry up to 3 liters of cargo.

In the preliminary and detailed stage of design, MS-Works spreadsheets were used to calculate performance predictions and sizing optimization techniques. Math Soft's Mathcad 8 was used for longitudinal stability analysis and 2-D lifting line load distribution studies. Drafix Quick CAD and CAD Key were employed for engineering drawing-based project applications.

The Impulse II represents design, fabrication, and operation an "order of magnitude" greater than was possible with the ESU Javelin. We are confident that the team has produced the best pragmatic design under the imposed system of constraints and we are anxious to demonstrate its advertised capabilities at the 2000 contest.

Management Summary

Management Summary

One of our major hurdles this year was the financial aspect of the project. Not only would we need to build a competition worthy aircraft, but also we would need to transport it along with team members to the contest site.

We were very fortunate to receive a grant from the ESU Foundation to help with the building/materials cost. A donation from the Alumni Association along with individual contributions will enable our team to travel to Wichita for the competition.

Our six-member team consists of students majoring in physics and physics related fields.

Herb Ziegler is the team leader, chief designer and the pilot of the aircraft. He is a graduate student in the General Science Masters Degree Program. Having participated in the competition last spring, Herb brings insight and expertise to the team. As chief aircraft designer, he chose the wing design and the construction materials to make the airplane lighter and more durable. He is also responsible for the electronic components of the aircraft. Herb is responsible for writing the Executive Summary, Detail Design and Preliminary Design Reports.

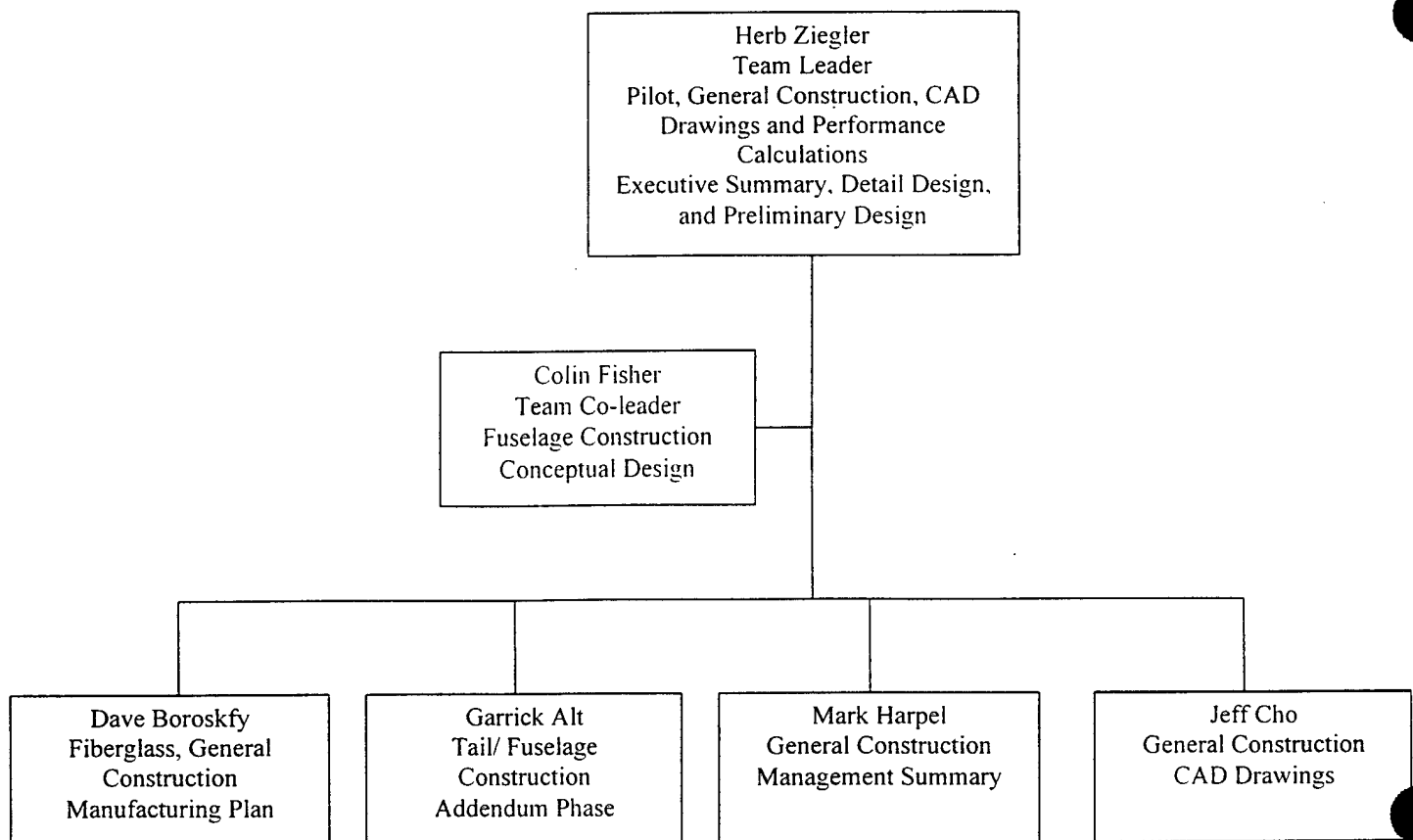
Mark Harpel leads the ground crew and is majoring in Physical Science. He constructed part of the wing and was responsible for the installation of the radio system. Mark has written the Management Summary.

Dave Borofsky is majoring in Earth and Space Science/Secondary Education. Dave is a returning team member and is part of the ground crew. He has done part of the construction on the fuselage as well as working on the tail section of the aircraft. Dave is responsible for writing the Manufacturing Plan.

Colin Fisher, a Physics Major, has done construction work on the fuselage and contributed to the conceptual design of the aircraft. Colin wrote the Conceptual Design Report.

Garrick Alt is a sophomore majoring in Physics. He has worked on component construction. Garrick is a recent addition to our team and will contribute to the Addendum Report.

Our most recent addition to the team is Jeff Cho. He is enrolled in our engineering transfer program. Jeff has done some of the CAD drawings.



East Stroudsburg University
Written by Colin Fisher

Milestones	Planned Date	Actual Date
Conceptual Design Stage	7/1/99	7/15/99
Preliminary Design Stage	7/31/99	7/20/99
Wing Assembly	8/31/99	7/28/99
Detailed Design Stage	8/4/99	8/20/99
Central Fuselage Assembly	8/31/99	7/20/99
Report Preparation	2/10/00	3/5/00
Test Flights	1/15/00	11/27/00

Conceptual Design

Conceptual Design

After having competed in the 1999 Cessna/ONR Competition, and not yet knowing the contest rules for the 2000 competition, the team brainstormed and decided the best approach for preparing for the 2000 competition was to improve on the design used in the previous competition. Believing the 2000 competition would be similar to the previous competition regarding contest rules and objectives, the idea was to have a flyable plane well before the competition, which then could be modified to compete in the contest.

The **Impulse**, the plane flown in the 1999 contest, was an extremely over built two-engine plane. It was a great starting point because the design had already proven to be air worthy and there was much room for improvement. The **Impulse** was very large and heavy, almost exceeding the AMA maximum for weight and having the largest allowed wing span of 9ft. Two Astro Flight Pattern Cobalt 60s, which were the most powerful motors the team could afford, powered the **Impulse**. The airframe consisted of much metal and plastic, which contributed greatly to the weight; not mentioning the two 32-cell battery packs. The goal was to reduce the weight of the plane by replacing the metal and plastic components of the airframe with lighter materials such as balsa wood, blue foam, and fiberglass. Modifications were to be made on the landing gear, along with testing of different props to determine the optimum size prop to use on the Astro Flight Pattern Cobalt 60s.

Upon receiving the 2000 contest rules and objectives, the team agreed the **Impulse** would not be a suitable design. Due to the limit on the weight of the battery pack and the newly imposed Rated Aircraft Cost formula, which benefits a small lightweight single engine plane, the team decided a multi-engine plane would not be advantageous and therefore a single engine airframe design was chosen to be the best option. The **Impulse** could not be easily modified to use only one engine. Therefore, the team's new goal was to design a single engine airframe that would meet contest regulations.

The team developed two different strategies, both trying to maximize the total score ($\text{Score} = \text{Written Report Score} * \text{Total Flight Score} / \text{Rated Aircraft Cost}$). One thought

was to design a small, lightweight plane with an adequate motor capable of carrying a minimal amount of water (1-2 liters), but able to perform a high number of sorties within the time allotted. The advantage to this design is it would keep the Rated Aircraft Cost formula to a minimum. The disadvantage being the amount of water it is able to carry. Alternatively, the second thought was to design a large plane that was capable of carrying much more water (4-6 liters) that relied on making only a few number of sorties. Obviously the advantage to this design being the amount of water it is able to carry, with the disadvantage being its performance in the Rated Aircraft Cost formula. The question being which strategy would be more beneficial to the final score.

A conceptual design was drawn up for the **Mosquito**, which was to carry a maximum two liters of water. An Astro Cobalt 40 Geared motor was chosen to power the **Mosquito**, which was believed to be the smallest motor that would produce enough thrust to power the Plane. The advantage of a smaller motor being the low power it will draw, fewer number of cells needed to power it, and the lighter weight of the motor and battery pack. All of which will help keep the Rated Aircraft Cost to a minimum. The length of the fuselage was also to be kept to a minimum in order to reduce the Rated Aircraft Cost. The goal for this plane was to have a fully loaded plane weight between 10-12lbs, wingspan of 7ft to give a high aspect ratio, and a fuselage length of 3-4ft. The Rated Aircraft Cost was estimated to be about 2.2.

The disadvantages to the **Mosquito** would be its small size and weight. At times during the competition the plane will be over 500ft away from the controller, making it very difficult to see because of its small size. Also, it will only be able to carry a maximum of 2 liters of water. So if it only makes a few sorties, the flight score will be severely lowered. Its stability in strong winds is also a disadvantage due to its small size and lightweight. If a strong wind gust were to come along it could conceivably send the plane out of control and destroy the plane.

The second strategy was to design a single engine plane that could carry 4-6 liters of water. The goal of this design was to keep the Rated Aircraft Cost relatively low by using only one motor, but try to maximize the total Flight Score by carrying as much water as possible. The most powerful motor the team could find, Astro Flight Pattern Cobalt 60, was chosen to power the plane. Published data on this motor suggests that it is

capable of providing 12lb of static thrust. This design would also have the maximum wing span allowed, 7ft. to create the most lift possible. With the length of the wing, the goal was to have the weight of the plane fully loaded to be 20-25lbs and have a Rated Aircraft Cost of about 5.0. The advantage of this design would be its high Flight Score, stability due to large wing span and weight, and high visibility due to size. Although large wing span and weight are advantages when it comes to the actual flying, they are also disadvantages when factored into the cost formula. The large wing span and fuselage add to the cost total, as does the larger motor which has a higher power rating, and more number of cells needed to power it. Although, the team believed the extra points gained in the Flight Score would outweigh the points lost in the Rated Aircraft Cost.

Two conceptual designs were submitted with the basic difference being the method of storage of the water. The first design, **Impulse II**, consisted of a long fuselage where the round 1-liter water bottles were laid horizontally end to end in the fuselage. Because of its length the tail was pitched at angle so it would not hit the ground on take-off. The second design, **Carrier**, had a cargo area that mimicked that of a traditional cargo plane such as the Lockheed-Martin C-130 *Hercules*. The bottles were to lie horizontally, two abreast, widening the fuselage. Both designs were equal in the amount of water they are able to carry and both have an estimated Rated Aircraft Cost of 5.5.

All three designs were compared and the team decided the **Impulse II** would be the better of the two designs. The designs were compared using a figure of merit chart, which clearly shows the **Impulse II** to be the best choice. One of the main advantages it has over the **Carrier** is its aerodynamic shape. The **Impulse II** has a long narrow fuselage whereas the **Carrier** has a short bulkier fuselage. At high speeds in the air the drag would be much greater on the **Carrier** which has a wider fuselage than the **Impulse II**. Also, the **Impulse II** fuselage would be much easier to construct. A round aluminum heating duct, found at a hardware store, was the right diameter to hold the water bottles and could be used as the fuselage. After further consideration of the **Mosquito**, the team decided it would not be a good competition plane mainly due to the fact of where the competition is to be held. Wichita, Kansas is known for windy conditions, and it was determined the **Mosquito** would not fair well if conditions were poor. The team agreed it was not worth building a plane that had a high risk factor in

windy conditions. Therefore the **Impulse II** was chosen as the design to build for the competition plane.

A prototype of the **Impulse II** was quickly built to determine one, if the design would fly, and two, to find strengths and weaknesses of the design. The prototype was successfully tested, although there were many weaknesses. The major drawback was that the plane was too heavy to carry 4 liters of water. The plane's weight was 25lb, without water, and had a Rated Aircraft Cost of 5.3. The team decided at this point it was best to design a plane much like the prototype but to reduce the maximum water capacity to 3 liters, and reduce the weight of the plane as much as possible. So at this point the goal of the team was to come up with an airframe design that mimicked the prototype and could carry three liters of water.

The following is a description of the figures of merit used to evaluate the three designs. Figure of merit points were assigned based on team responses and assessment of each design's theoretical capabilities. The higher the number, the more prowess was judged to be evident in a particular category. Thus the design with the higher summative total was voted to be the best entry.

- **General Aircraft Requirements**

- Could the design in question comply with all AIAA competition & AMA requirements regarding safety and competitive performance?
- Could the design in question be completed by and be ready for the competition?

- **Mission Suitability**

- How well will the design in question perform during the competition?
- How well will the design in question perform in the Rated Aircraft Cost?
- Are there elaborate measures needed to ensure success?
- What are the advantages/risks of the design in question?
- How well will the design in question cope with unforeseen variables such as weather variations?
- Can a pilot of average skill pilot the design in question?
- Is there undo concern necessitated over stability and control?

-Is the design in question adaptable to modified sortie allocation?

- **Manufacturing Suitability**

- How difficult will it be to build the design in question?

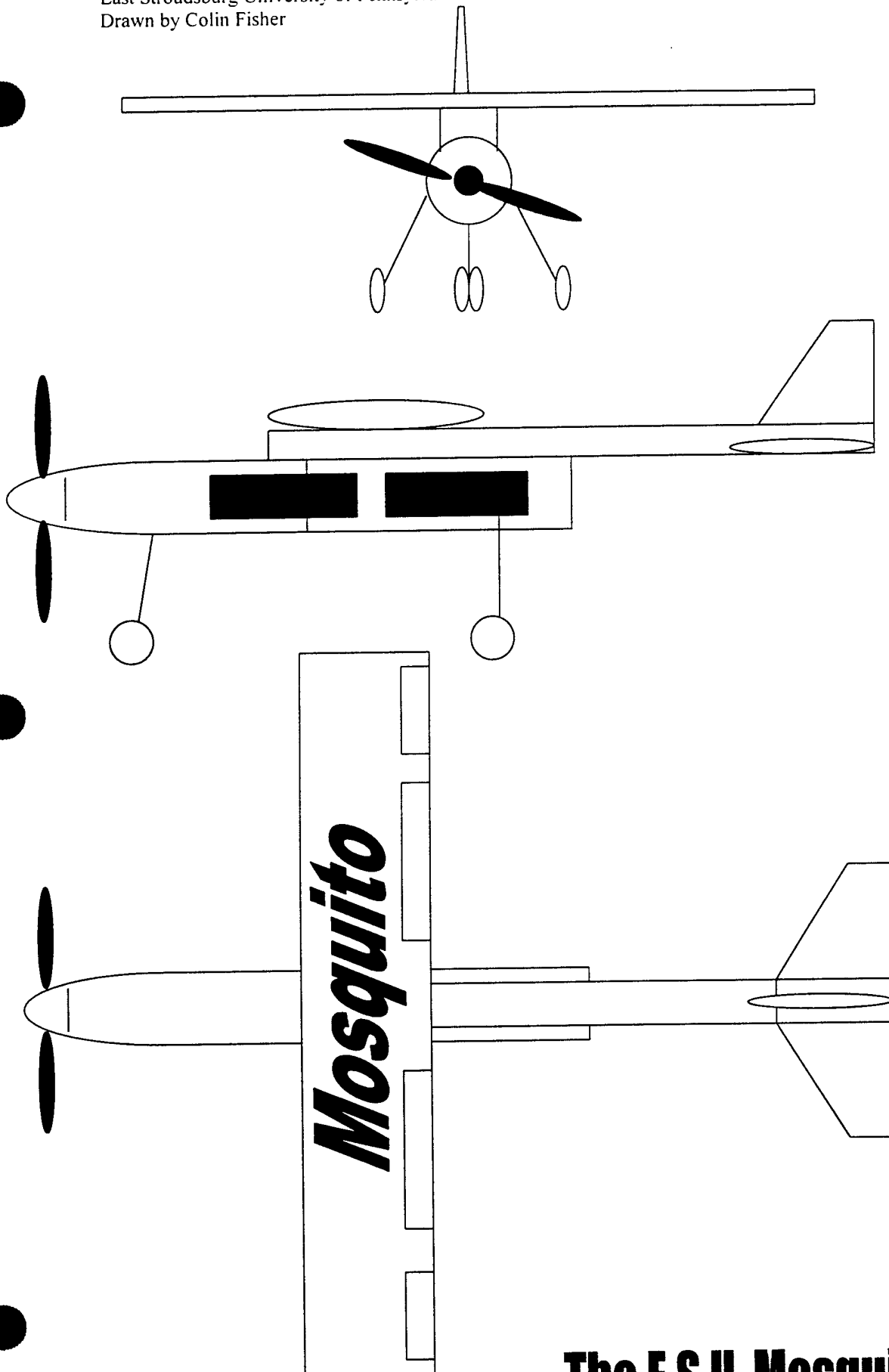
- Can the design in question be built with the team skills available?

- Can the design in question be built with readily obtainable materials?

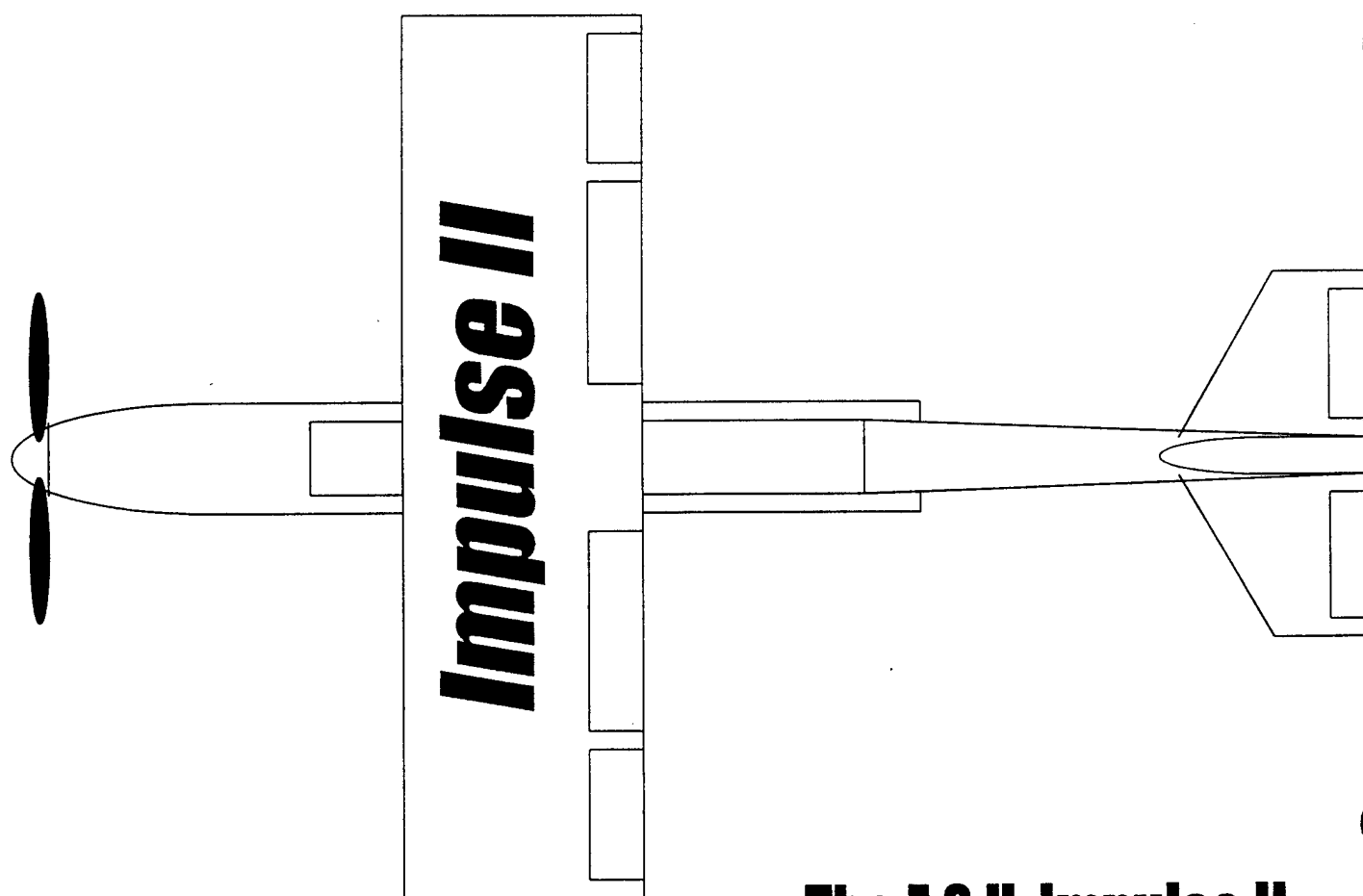
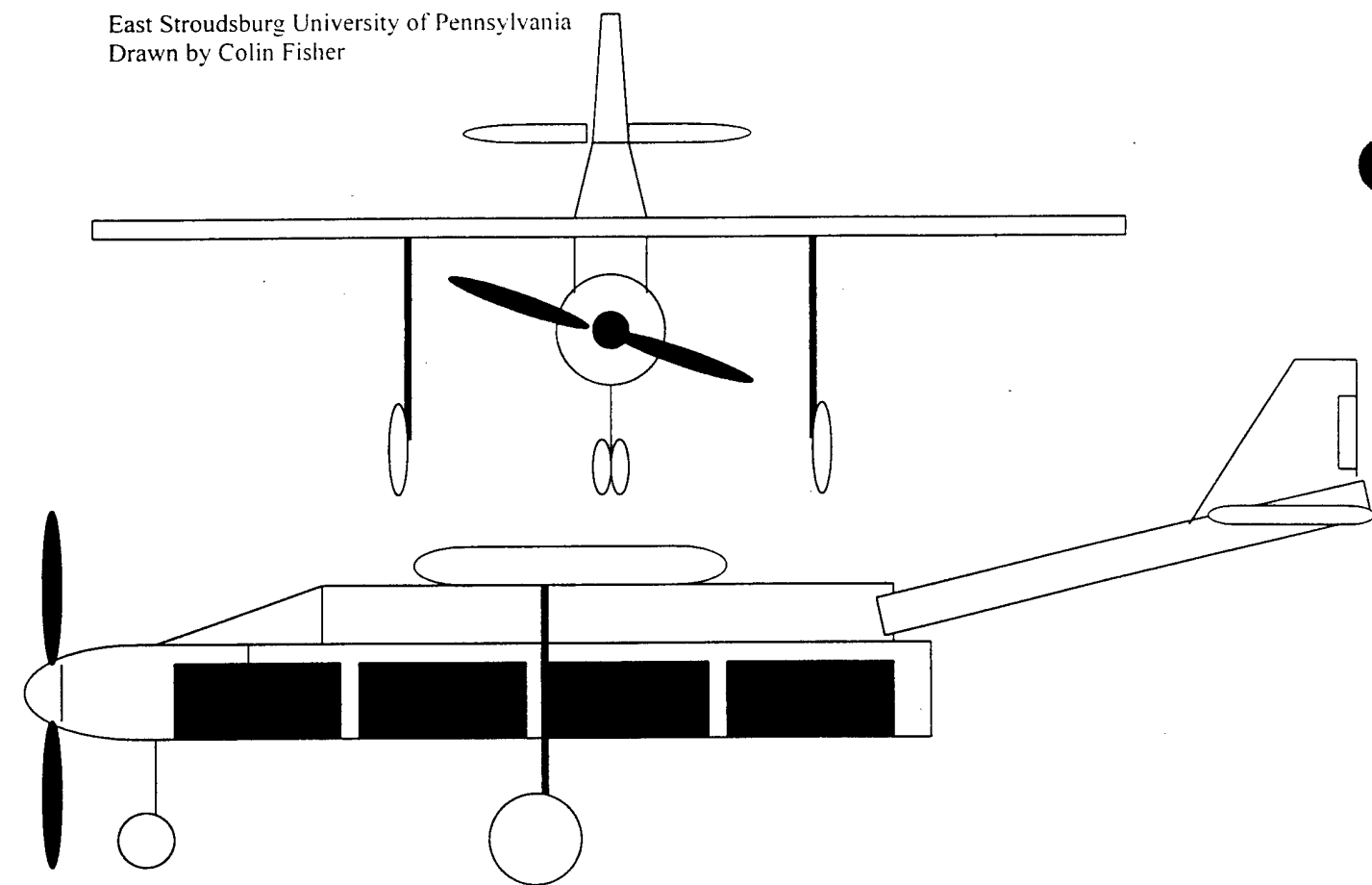
- Can the design in question be built within team cost constraints?

General Aircraft Requirements	Mosquito	Impulse II	Carrier
• Could the design in question comply with all AIAA competition & AMA requirements regarding safety and competitive performance?	10	10	10
• Could the design in question be completed by and be ready for the competition?	9	9	9
Mission Suitability			
• How well will the design in question perform during the competition?	6	8	7
• How well will the design in question perform in the Rated Aircraft Cost?	9	7	7
• Are there elaborate measures needed to ensure success?	9	9	9
• What are the advantages/risks of the design in question?	6	8	7
• How well will the design in question cope with unforeseen variables such as weather variations?	4	7	7
• Can a pilot of average skill pilot the design in question?	7	9	8
• Is there undo concern necessitated over stability and control?	6	9	9
• Is the design in question adaptable to modified sortie allocation?	9	9	9
Manufacturing Suitability			
• How difficult will it be to build the design in question	8	8	6
• Can the design in question be built with the team skills available?	8	8	7
• Can the design in question be built with readily obtainable materials?	8	8	7
• Can the design in question be built within team cost constraints?	9	9	8
Total FOM Points Awarded	108	118	110

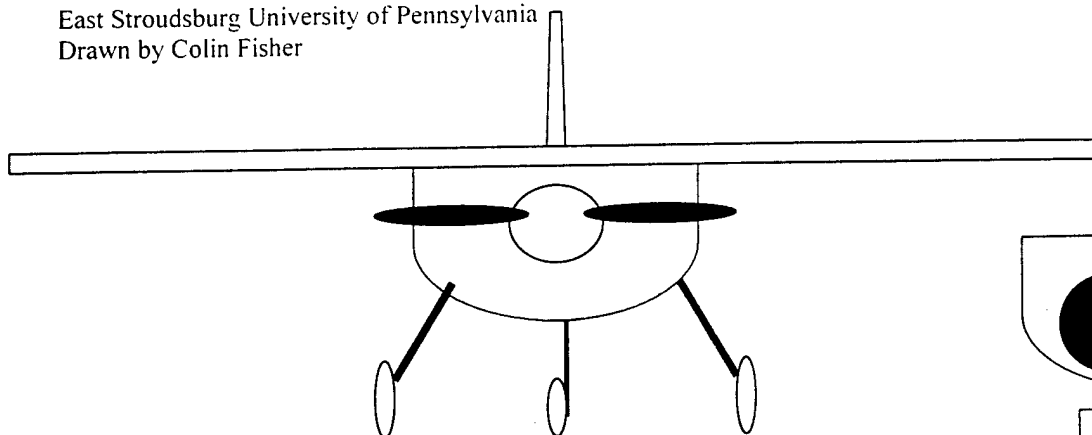
East Stroudsburg University of Pennsylvania
Drawn by Colin Fisher



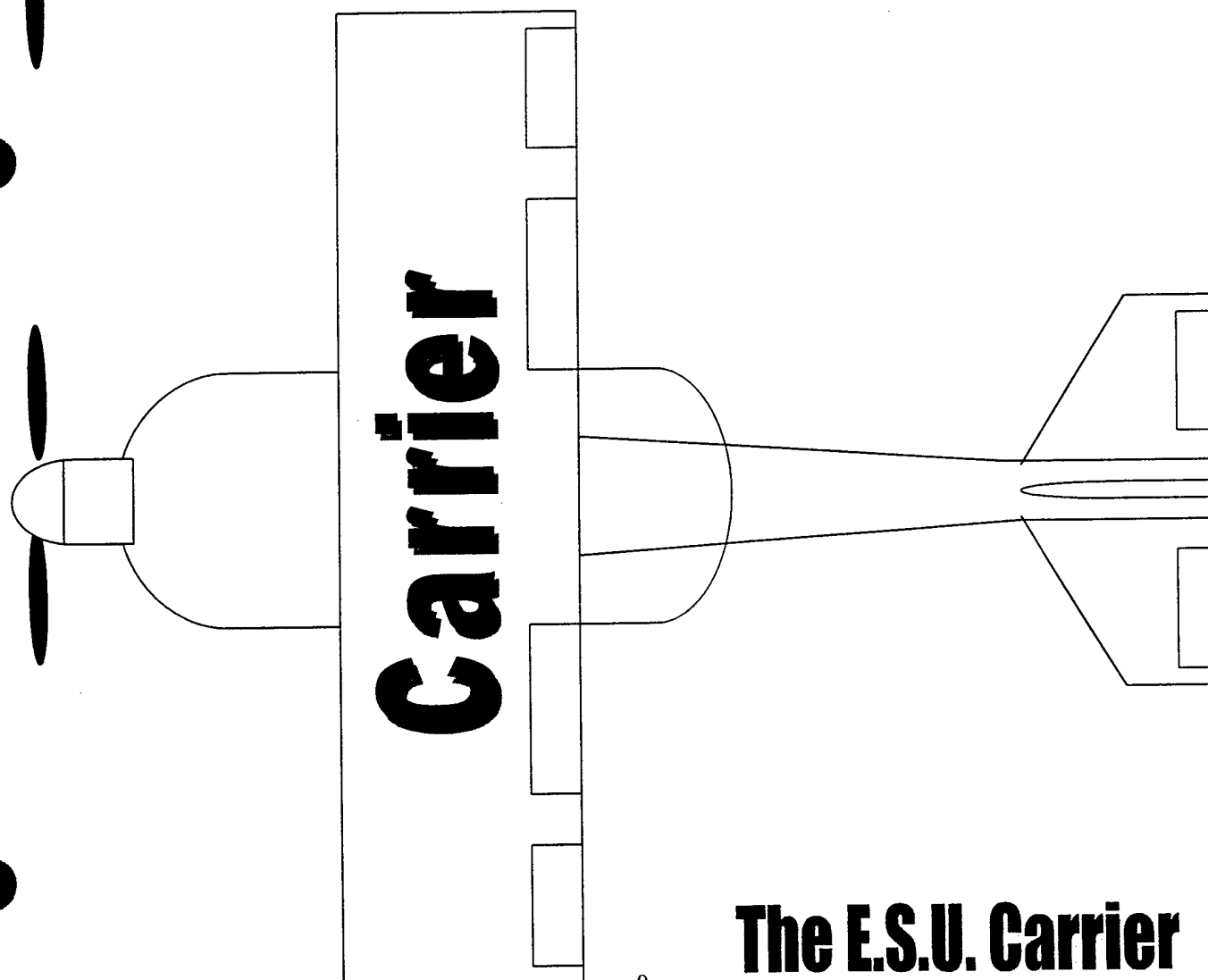
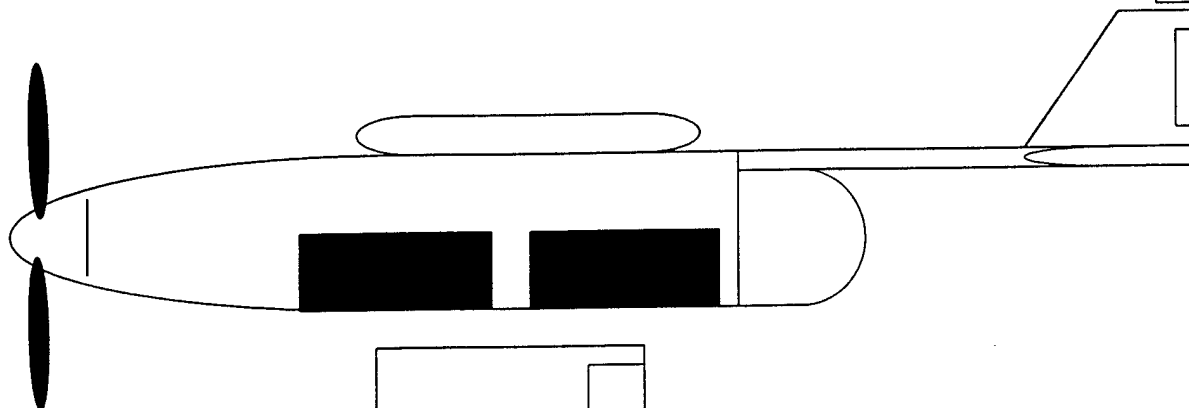
The E.S.U. Mosquito



East Stroudsburg University of Pennsylvania
Drawn by Colin Fisher



Water storage



The E.S.U. Carrier

Preliminary Design

Preliminary Design

The preliminary design phase incorporated spreadsheet-based optimization studies for the final design. Cells were programmed with the traditional list of performance requirements such as takeoff distance, W/S, T/W, load factor, payload fraction, Ps, stall speed, maximum speed, Re, rate of climb, L/D, ... etc. Results were then compiled from the automatic calculation properties of the spreadsheets. Primary aircraft traits were altered until the fundamental constraints were met or exceeded. The contest-imposed constraints addressed in our optimization techniques were primarily the 100ft-takeoff distance and the RAC formula. A sizing matrix plot is included at the end of this report section to quantitatively show the sizing parameters.

It was clear that the ultimate design would need to possess short-field operation capability, multiple sortie endurance, high payload fraction, and minimal RAC. It was also foreseen that the probable contest weather conditions would mandate superb flying qualities in addition. Herein was the dangerous compromise of minimizing the RAC without sacrificing the notion of pragmatic radio-controlled flight. In order to find the "edge" of the RAC envelope, it was decided that a prototype would need to be flown as a test-bed. Aside from analytical calculations, our preliminary stage of design was typified by actual fabrication of the Impulse. The Impulse was the aircraft that decisively dominated the FOM ranking in the conceptual stage of development and as such, it was chosen to be the perceptual manifestation of the alpha-stage performance calculations.

The Impulse relied on several existing components taken from the ESU Javelin. The propulsion system was altered only to accommodate the 5lb pack restrictions and a slight propeller change, thus 27 Sanyo 2000mah cells were used on an AstroCobalt 60 with an APC 15 x 8 propeller. The radio system was unchanged and 1/4-scale servos were used on all control surfaces. In an effort to reduce empty weight, fiberglass and balsa/plywood construction was utilized while techniques involving their application were explored. The rectangular wing was made with an experimental E-glass tape/epoxy rectangular spar laid around pink Styrofoam, while balsa was employed for ribs/sheeting. The same Gottingen 798 airfoil as used on the ESU Javelin was chosen, specifically because of its high lift coefficient and gentle stall characteristics at expected Re. Ease of

bottle loading was considered desirable and so fuselage room for 4L was provided with 4"-diameter aluminum dryer vent into which the bottles could be slid (due to unexpected weight distribution only 3L could be carried without upsetting longitudinal stability). An all-flying stabilator was developed as a result of fuselage lofting, extreme tail ramp angle, and downwash considerations. Tricycle gear comprised of radically stroked, levered mains and dual nose wheels was included to provide excessive stability with respect to turnover angle and vertical descent rate. Final takeoff weight (no water) was approximately 25lb, a reduction of over 13lb from the empty weight of the ESU Javelin.

Test flights of the Impulse began in late November with promising results. The first stage of testing involved high-speed ground runs with more speed being added to each attempt. The aircraft seemed to be stable at high alphas in ground effect, and its pitch response was very predictable with small deflections of the stabilator. The ailerons were effective under these conditions, albeit mildly. The tricycle gear performed well on the rough, grassy terrain and handled abrupt descents and bouncing with ease. Stall speed was close to the predicted values.

The first major flight occurred in early December with less than ideal fruition. After several taxi-runs, the same takeoff conditions could not be duplicated and it seemed like there was much less power available. There were no head winds whatsoever. Once liftoff was eventually obtained, the Impulse remained aloft for approximately one minute, all the time lumbering on the verge of stall. It could not seem to climb any higher than 100ft and the pilot was forced to make an abrupt turn to narrowly miss a tree line. A stall, followed by spiral divergence resulted in a serious crash.

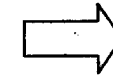
The conclusions drawn afterward primarily implied that the Impulse was still too heavy (too strong) since there was actually no irreparable damage (nothing should have survived that impact!). Secondly, although bad solder connections were ultimately blamed for the lethargic motor performance, the team realized that the design could barely fly with 7lb of thrust in the 25lb condition and this became the maximum allowable takeoff weight. This meant that the Impulse could not fly with any water unless it could drastically lose airframe weight. These and other changes were to be considered for the competition variant, the Impulse II.

The final design variant Impulse II will bear a strong resemblance to its predecessor. Aluminum dryer-vent will again be used for bottle storage. Fuselage propeller blockage will be reduced. One Astro-Cobalt 60 with approximately 27 cells will be used for propulsion. The 7ft-span, parasol, cantilevered wing will incorporate a rectangular E-glass spar, plain flaps and ailerons. No change in wetted area is expected. The wing's airfoil will be from the same family, but with a lower t/c ratio and hence, less drag. An all-flying stabilator will be again be used to eliminate the need for precise rigging of the tail downwash angle. Tricycle gear configuration and the trailing-link levered main gear will be retained. Empty weight is to be reduced by a targeted %36. Payload fraction will be increased accordingly.

The following is a description of the FOM's that were utilized in the overall preliminary design process along with their general design implications. Ranking is accomplished by color. Red arrows signify maximum necessitated design attention followed by yellow and green arrows.

General Aircraft Requirements

- Can the design comply with all AIAA & AMA requirements regarding safety and competitive performance?
- Can the design be completed in accordance with the time constraints of the manufacturing and management milestone charts?
- Can the design be flown well in advance of the competition?
- Can the design be disassembled easily for transport to the specified contest site?



Design Implications of FOM

Limits on span, weight, propulsion, structural quality, crew and spectator safety must be implemented.

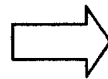
Charts reflect realistic goals toward design completion.

Team experience is paramount.

Considerations for travel must be carefully devised.

Mission Suitability

- How well can the design cope with unforeseen variables caused by weather?
- Can a pilot of average skill operate the design?
- Can the design possess a relatively low RAC?
- Can the design adapt to different sortie strategies at the contest?








Wind is expected to pose a problem in Kansas.

The design should offer predictable flight qualities.

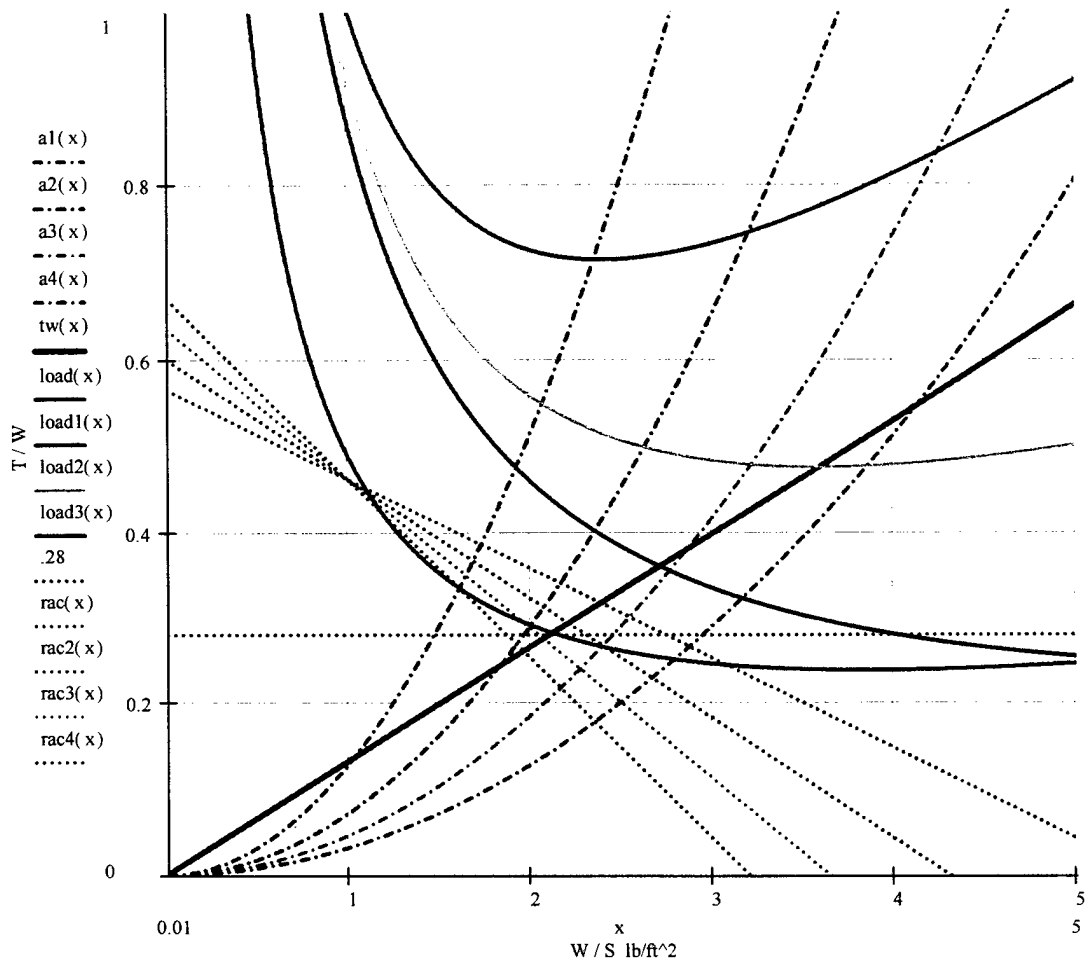
The design should have low RAC, but flight performance comes first.

The design may carry different numbers of water bottles depending on weather.

Manufacturing Suitability

- How difficult will it be to fabricate the design?  Construction ease, though higher MFHR's than last year are acceptable.
- Can several copies of the design be built to serve as replacements?  The team would like redundancy with its entry, though it is not essential
- Can the design be built using the current team skill matrix?  The team has been able to expand its skills significantly since last year.
- Can the design be built with readily obtainable resources?  Composites have been added to our inventory, but not the full spectrum.
- Can the design be built within funding constraints?  Funding is a concern, but it will not force us to compromise our design.

Sizing Matrix Plot

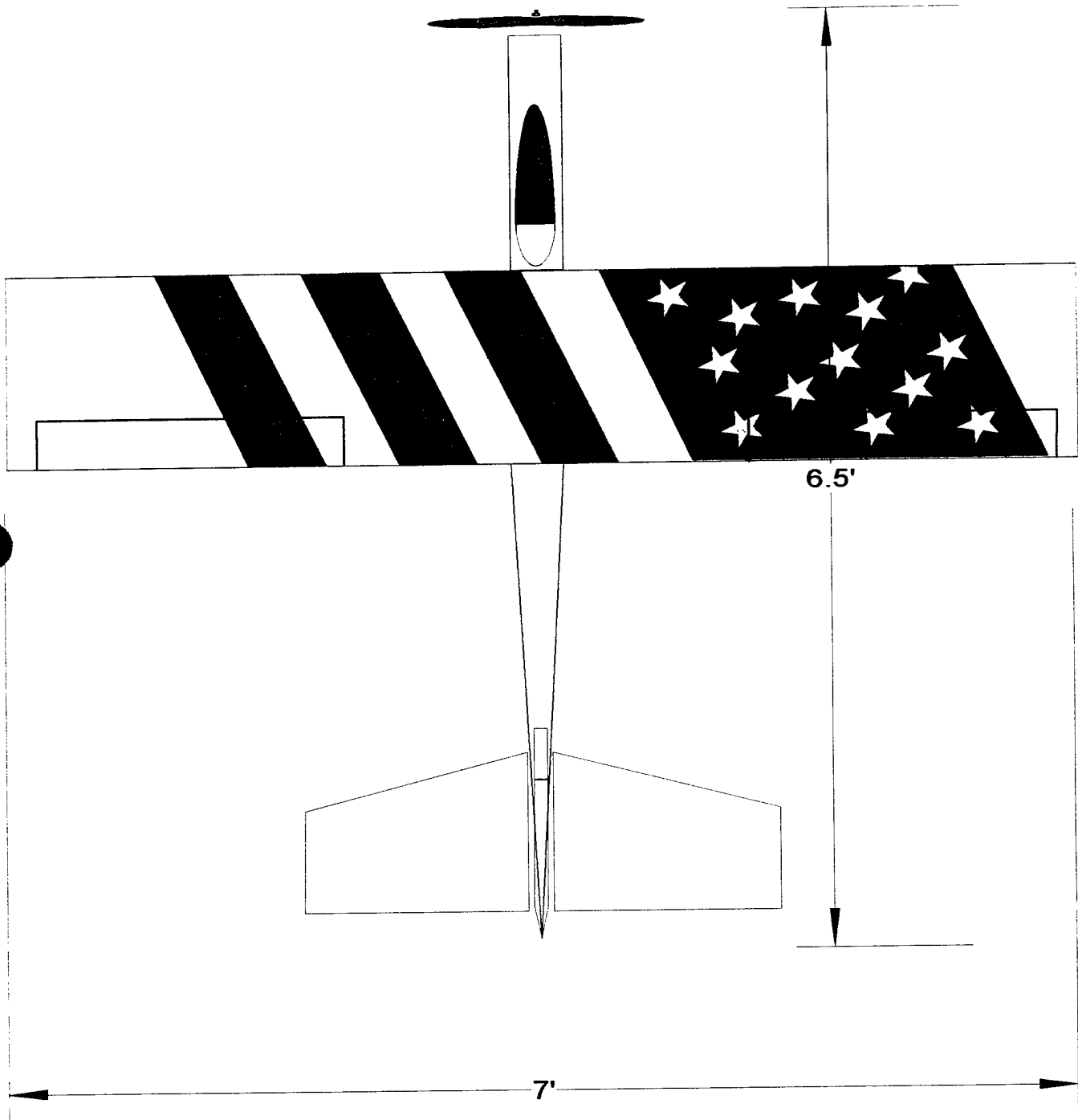


- $W_o=15$ Impulse- T/W & W/S characteristics
- $W_o=20$
- $W_o=25$
- $W_o=30$ lb
- 100ft Takeoff Parameter $TOP=6$
- 1 g at 30 mph (must reside above curve for flight)
- 1g@40mph, $P_s=0$
- 2g@40mph
- 3g@40mph
- Min desirable T/W (assuming worst case 7lb thrust & $W_o=25$ lb)
- 6.6 RAC @ $W_o=15$ lb
- 6.6 RAC @ $W_o=20$ lb
- 6.6 RAC @ $W_o=25$ lb
- 6.6 RAC @ $W_o=30$ lb

East Stroudsburg University of Pennsylvania
"Impulse" Primary Dimensions

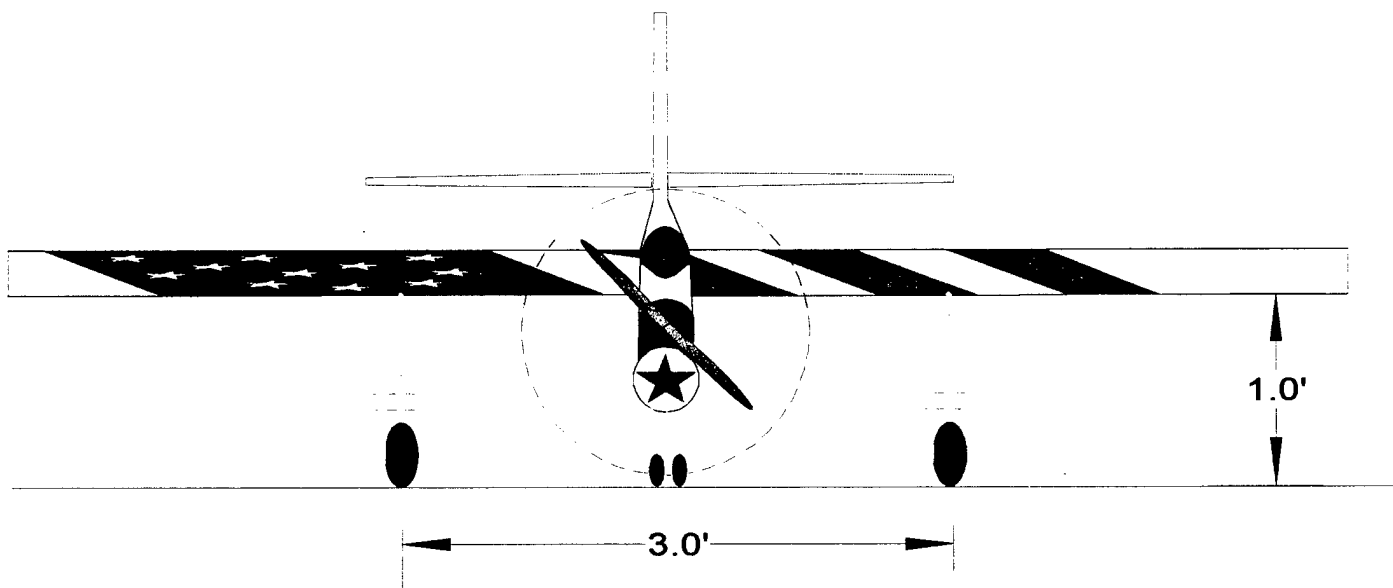
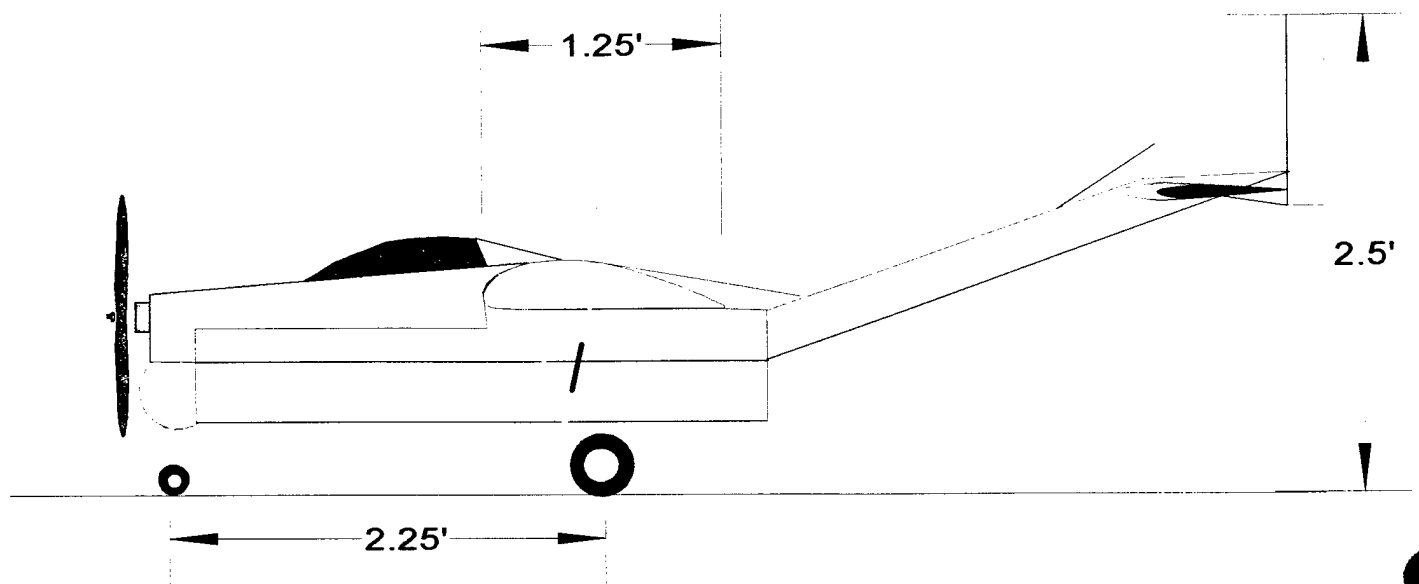
Scale: 1":1'

Drawn by: Herb W. Ziegler



East Stroudsburg University of Pennsylvania
"Impulse" Primary Dimensions
Scale: 1":1'

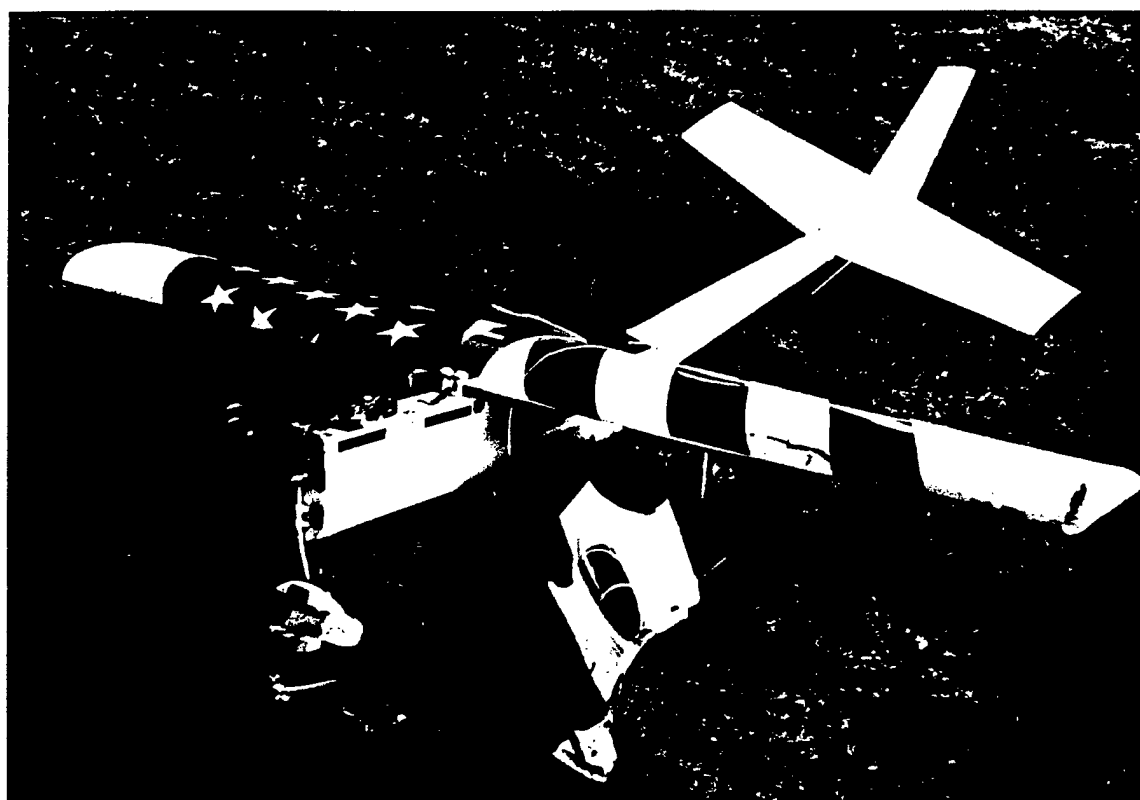
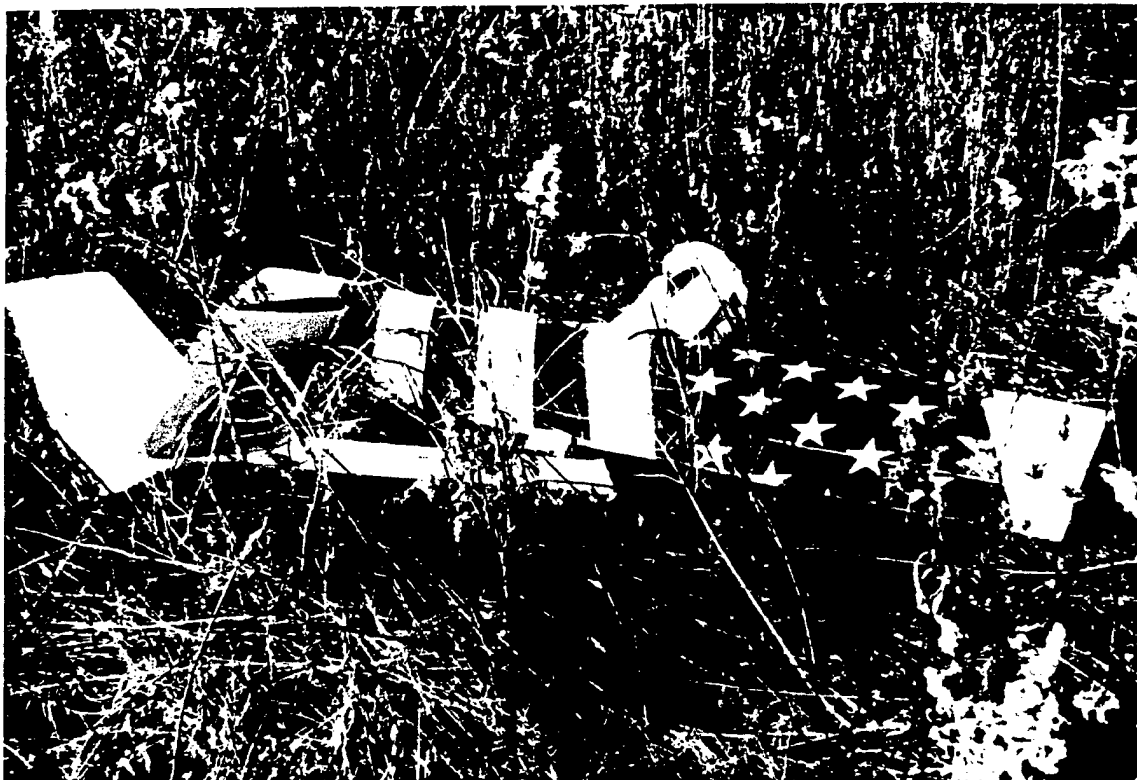
Drawn by: Herb W. Ziegler



East Stroudsburg University of Pennsylvania
Photos courtesy of Professor Mike Orleski







Detail Design

Detail Design

The Impulse II represents the contest variant of the prototype that can be fielded before April. It has already demonstrated capable flight performance and the ability to fly successfully with a payload fraction of .28. Any revisions in the actual contest aircraft will be slight, essentially encompassing further weight reduction in the manufacturing process to drive the payload fraction upwards.

The Göttingen 797 was chosen as the wing section because of its known high lift characteristics at expected vehicle Re. Flaps were added to aid in takeoff and landing operations. It is possible for slight flap deflection to yield a ΔCl such that the 797 will lift as well as the 798. This Cl of 1.55 can be used on takeoff and the flaps may be fully retracted whereby the clean 797 will deliver lower drag than the 798. It has been possible to put excessive flap movement in the design so that full deflection (60°) may be used to provide high lift and drag so crucial in the landing process. Spoilers have also been incorporated so as to permit higher landing approach speeds in gust environments. No wing dihedral was needed because of the high wing location and its inherent equivalent dihedral effects. It was also realized that roll inertial would be greatly increased with payload carried below the roll axis and that geometric dihedral would further degrade roll responsiveness.

The primary contest constraint was viewed as the 100 ft take off distance. The plane was designed to takeoff fully loaded within this distance even with no head wind. In the event that higher winds are expected we will use the increase in takeoff performance as a safety margin rather than an opportunity to carry more water. This is not due to structural inadequacy of the spar, but rather the inability to significantly shift mass within the length of the fuselage without upsetting balance. The fiberglass spar easily passed the contest-type structural verification test and it is not likely that any flight maneuvers can exceed its limits in bending, shear, or torsion. Specific excess power curves show that it is not possible to attain high-g pulls from level flight and predicted top speed seems to limit ultimate loading to approximately 5 g (in a very non-contest-like dive!)

The battery-span loading concept has been dropped on this wing design, which has slightly increased the structural requirements of the spar in flight. In so doing however, the battery inertia loads associated with landing have been isolated primarily to the fuselage (along with water inertia loads), thus saving the wing from such damage. The main gear were placed in the wing to reduce turnover angle in ground operations. They are comprised of a levered trailing arm arrangement and have generous stroke to absorb landing loads. As installed in the wing, the main gear have show the ability to tolerate a static drop from 1.5ft corresponding to a gear load factor of 1.2 and a rate of sink equal to 3 ft/s. Failure of the system is predicted at a gear load factor of approximately 2.5, essentially a static drop from 3 ft with a vertical descent of 5 ft/s. The gear are designed to shear from the spar before it breaks.

The propulsion unit was chosen based entirely upon its successful use demonstrated in the previous year. The AstroFlight Cobalt 60 pattern #661 can provide close to 1 hp within the battery limitations specified in this contest. On 27 Sanyo 2000mah cells swinging an APC 15x8 prop it can deliver over 9 lb. of static thrust while drawing 39 A. No abnormal motor or battery heating has been observed under operating conditions. APC 14x10 and 15x10 props may also be used based on thrust requirements in head winds. We are currently considering the use of an "wind emergency" pack made of 36 1300mah cells that operates the motor at peak power for a shorter duration. This will be used only if the contest weather mandates a low pragmatic number of scoring sorties. Endurance of the primary pack is 4-5min at medium to full throttle settings. Depending on contest weather it may be possible to incorporate some gliding into the flights to help extend this. It is expected that propeller unloading at cruise will also increase run time. Rough range estimates predict that at cruise with full load, a flight segment of 2.5 miles is possible.

With respect to handling performance, more analysis was devoted to control response than was previously possible. The longitudinal pitching mode was analytically modeled so that $\partial C_m / \partial \alpha$ would be negative. The horizontal tail volume coefficient was then adjusted to this effect. Since an all-flying stabilator was employed, the center of pressure was determined and utilized as the lateral hinge axis location so aerodynamic loads could produce no excessive torque against the single 1/4 scale servo. Mass counter

balances were incorporated to balance the stabilator mass aft of the hinge axis, but they were found to be superfluous and detrimental to servo response time. The stabilator pivot mechanism was derived from ball bearing pulleys (taken from force tables) which allowed infinite adjustment in determining the correct stabilator incidence angle. Due to the extreme tail ramp of the fuselage and this feature, it was unnecessary to precisely determine wing downwash characteristics and their effects on the empennage.

The vertical tail volume coefficient and ailerons were sized according to historic data plots of full-scale aircraft values. The control deflection was determined by the practical limit of servo torque. Primary emphasis was toward maximizing movement but avoiding servo stall and high current drain.

The team employed a new simulation program for pilot training and prediction of design performance in variable weather conditions. Great Planes' *Real Flight Standard Edition* software provided a valuable simulation capability never before possible. With the aircraft input parameters adjusted to those of the Impulse II, virtually any foreseeable contest scenario could be flown. The Impulse II underwent "virtual" testing in countless conditions ranging from 0 to 30mph winds with heavy gusting. Sortie strategies for flying in these conditions were explored and potential problems were identified. The program was also used to verify general handling predictions and takeoff performance within the specified distance. We were able to test our addition of spoilers and flaps not found on the Impulse during its preliminary flights. Though the software only allows the use of glow-powered engines, we were able to modify the torque and propeller selection of each to reflect the performance of our AstroFlight Cobalt 60. We even adjusted the fuel tank size so that it would be expended in accordance with our battery duration. We highly recommend this software and know that it has significantly aided our contest design development.

Table of Graphical Contents

Graphs

- General Specifications
- Drag Polar
- Maximum Rate of Climb
- Power Required
- Critical Velocities
- Endurance
- Takeoff Distance
- Specific Excess Power
- Wing Shear
- Wing Bending Moment
- Gear Load Factor

Cad Package

- Primary Component Structure
- Internal Semispan
- Primary Systems Location
- Payload Allocation
- Airframe views
- Nose Strut
- Main Gear

Impulse II General Specifications

Class

Type-	Radio-controlled electric UAV
Max. gross weight-	26.00lb
Empty airframe weight-	14.00lb
Empty weight plus batteries-	19.00lb
Max. liters of water-	3.0L
Total wetted area-	27.6ft ²
Frontal area-	2.0ft ²
Construction type-	65% E-glass/epoxy ,10% aluminum 20% balsa/plywood, 5% other
Rated aircraft cost-	5.3

Fuselage

Length-	6.5 ft
Height (no gear)-	2.2ft
Width-	.3ft

Wing

Planform type-	Rectangular
Airfoil type-	Göttingen 797
Span-	7.0ft
Mean chord-	1.25ft
Max thickness-	0.2ft
Area-	8.75ft ²
Aspect ratio-	5.6:1
Thickness ratio-	0.17
Lift curve slope-	6.4
Max. L/D-	17.0
C _{di} -	0.06
C _{do} -	0.015
Max. C _l -	1.35
Max. Alpha-	15°

Powerplant

Configuration-	Single electric direct drive
Motor type-	Astro Cobalt 60 Pattern #661
Speed controller type-	AstroFlight 204D
Propeller type-	APC 15 x 8
Max. power-	1.0Hp
Static thrust-	9.0lb at 7,800 rpm
Mean dynamic thrust-	6.0lb
Max current draw-	39.0A

Battery pack

Battery type-	Sanyo Cadnica 2000mah x 27
Pack weight-	5.0lb
Pack voltage-	33.0V
Endurance-	4-5min

Undercarriage

Type-	Tricycle, levered mains, dual-tire nose
Track-	3.16ft
Wheelbase-	2.25ft
Nose strut geometry	0.0° caster
Main strut geometry-	0.0° camber, 3.0° toe-in, 2"-4" trail
Stroke-	0.18ft
Maximum descent velocity-	3.0ft/s
Load factor-	1.2
Longitudinal turnover angle-	20°
Later turnover angle-	25° (full), 29°(empty)
Brakes-	Nose dual drum, stabilator actuated
Main tires-	5" diameter
Nose gear tires-	3" diameter

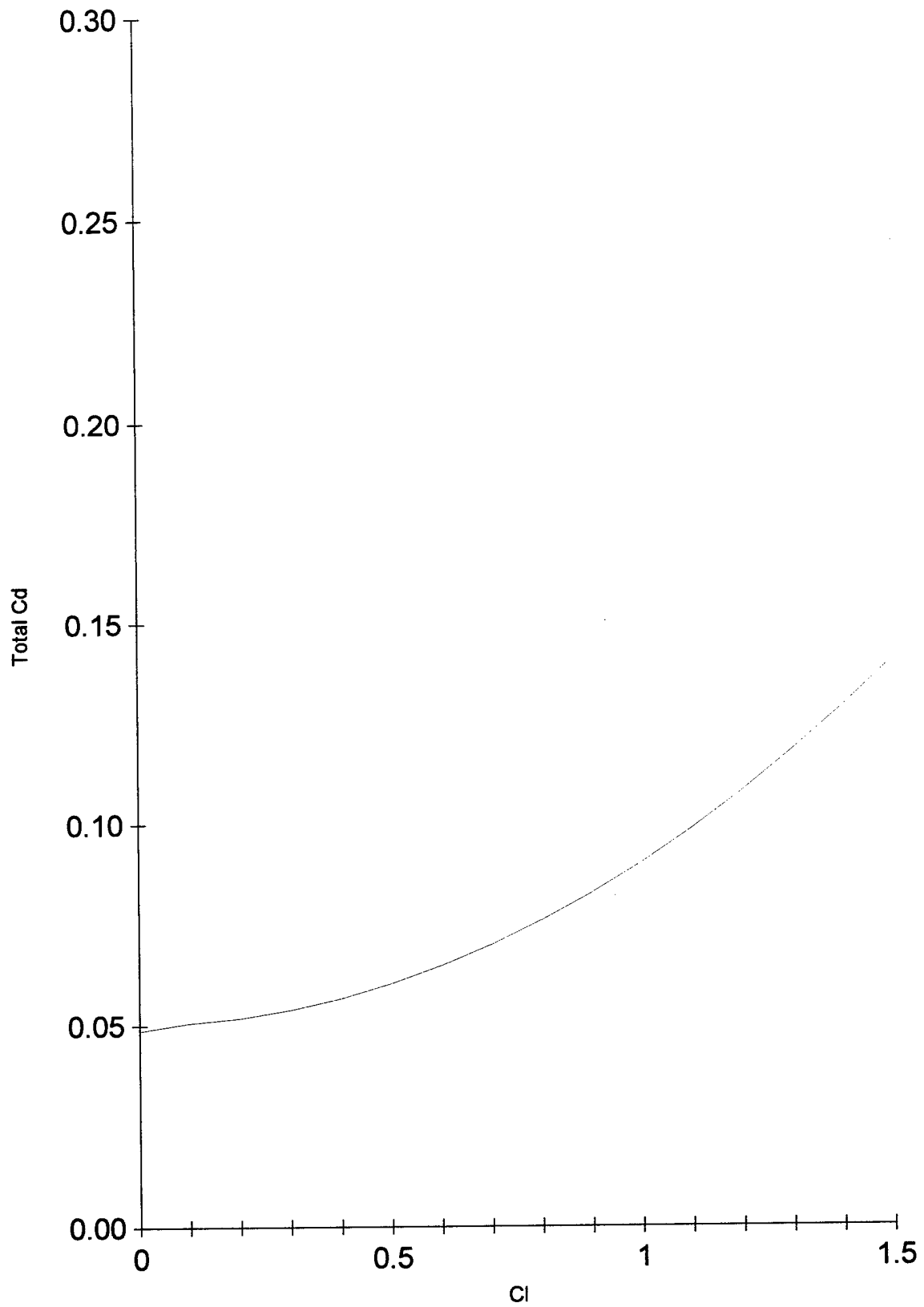
Radio Equipment

Radio type-	Futaba T6XA PCM; Ch 48
Channels used-	6 total 1-aileron 2-stabilator/parking brake 3-throttle 4-rudder/nose steering 5-spoilers 6-flaps

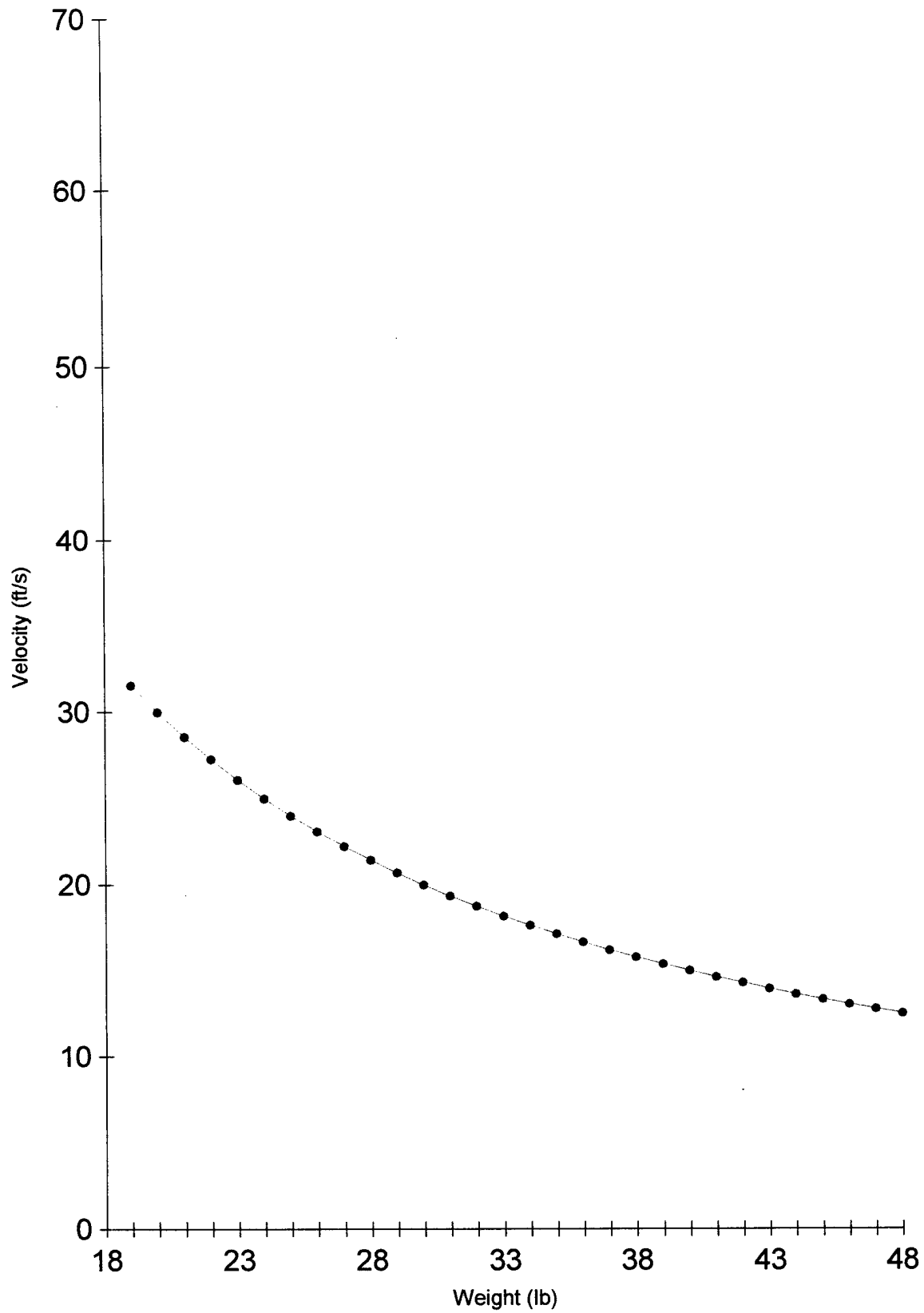
Servo type-	3 Tower 1/4scale:stabilator, flaps, & nose gear 3 Futaba S3003; rudder & ailerons 1 Tower micro, spoilers
-------------	--

Flap deflection-	- 60°
Spoiler deflection-	+35°
Aileron deflection-	+20° -15°
Rudder deflection-	± 30°
Nose gear deflection-	± 30°
Stabilator deflection-	± 30°

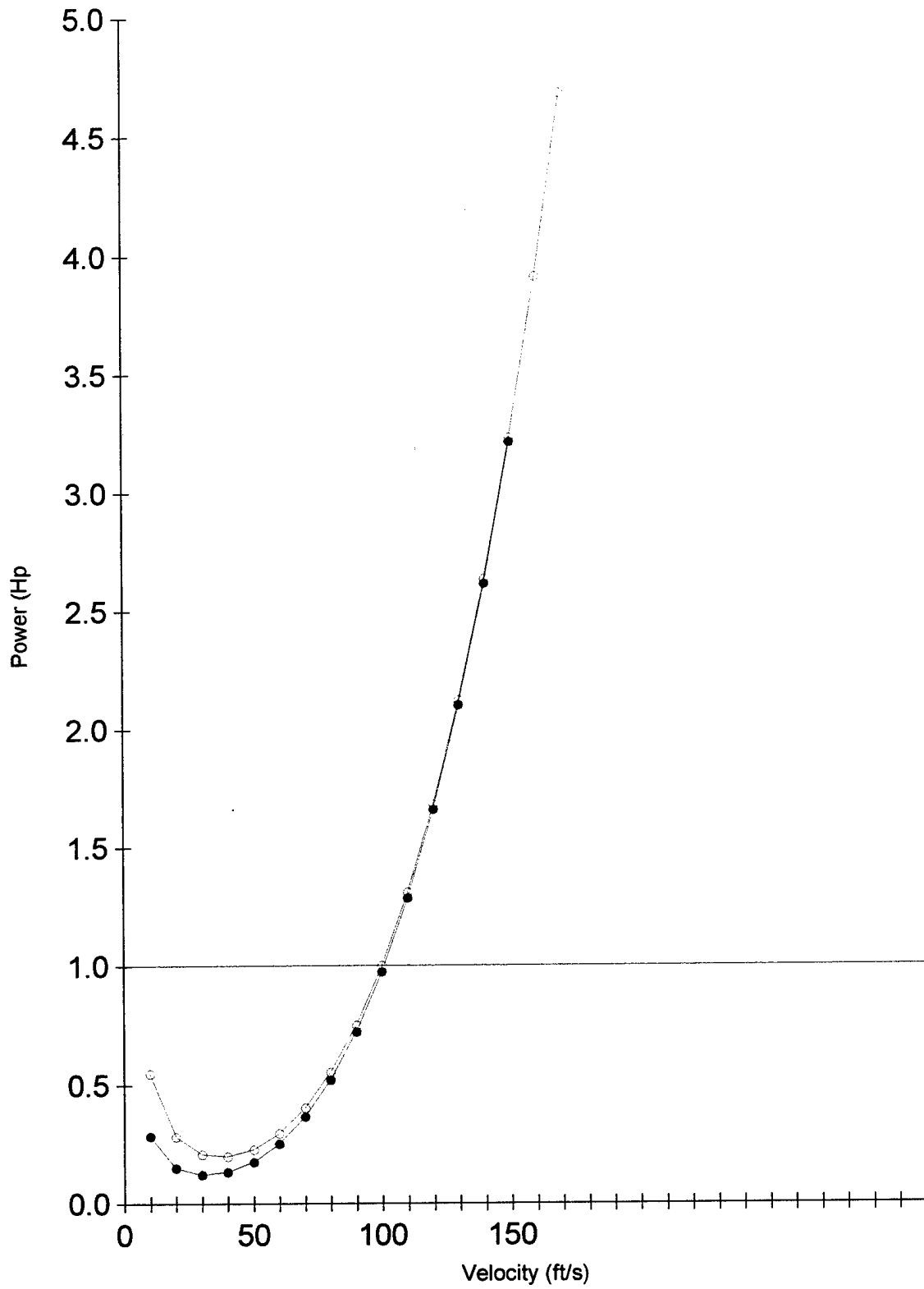
Drag Polar



Maximum Rate of Climb vs. Weight

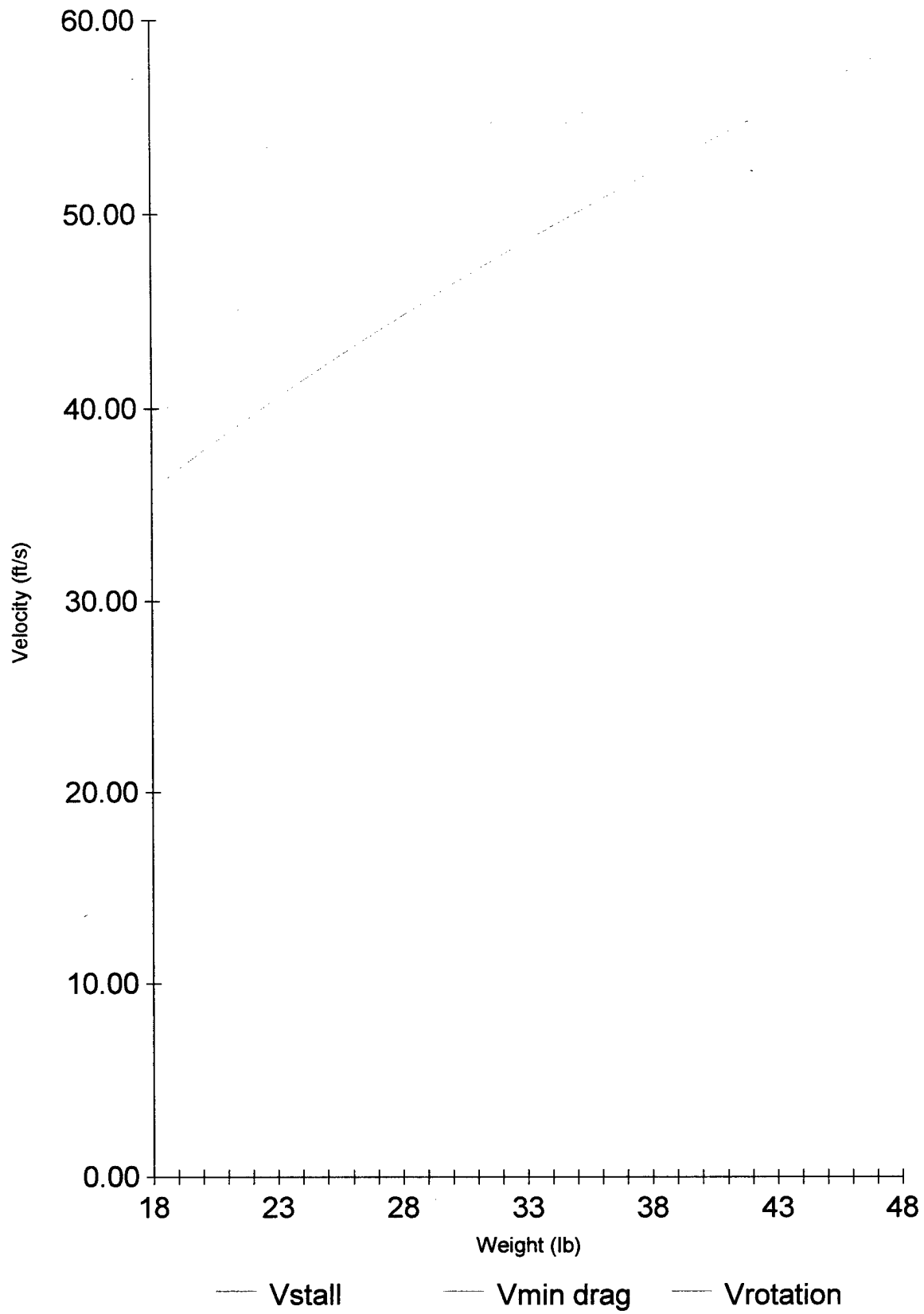


Power Required vs. Velocity

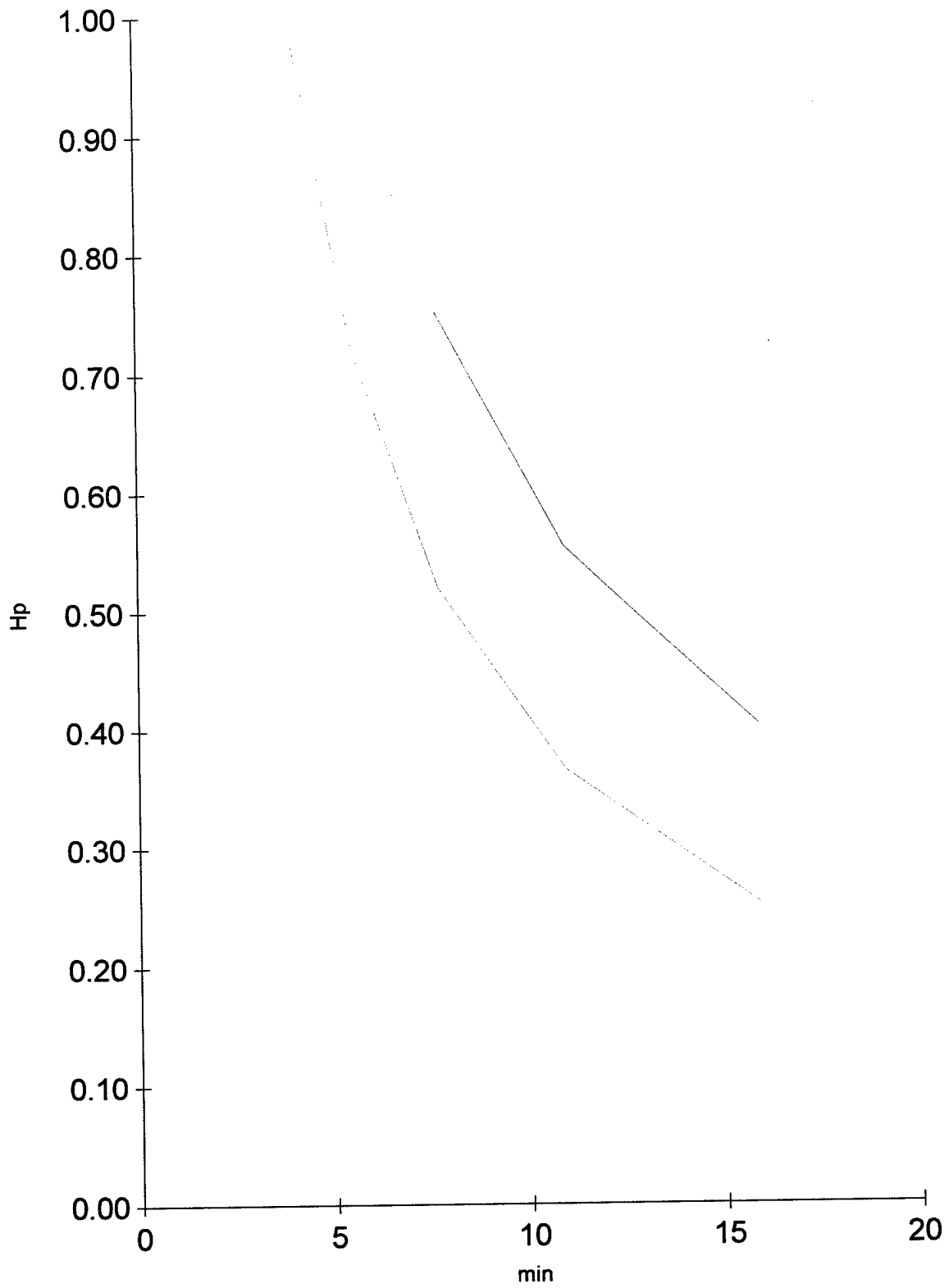


— Power Availab —•— Power req. at —○— Power req. at 2

Critical Velocities vs. Weight

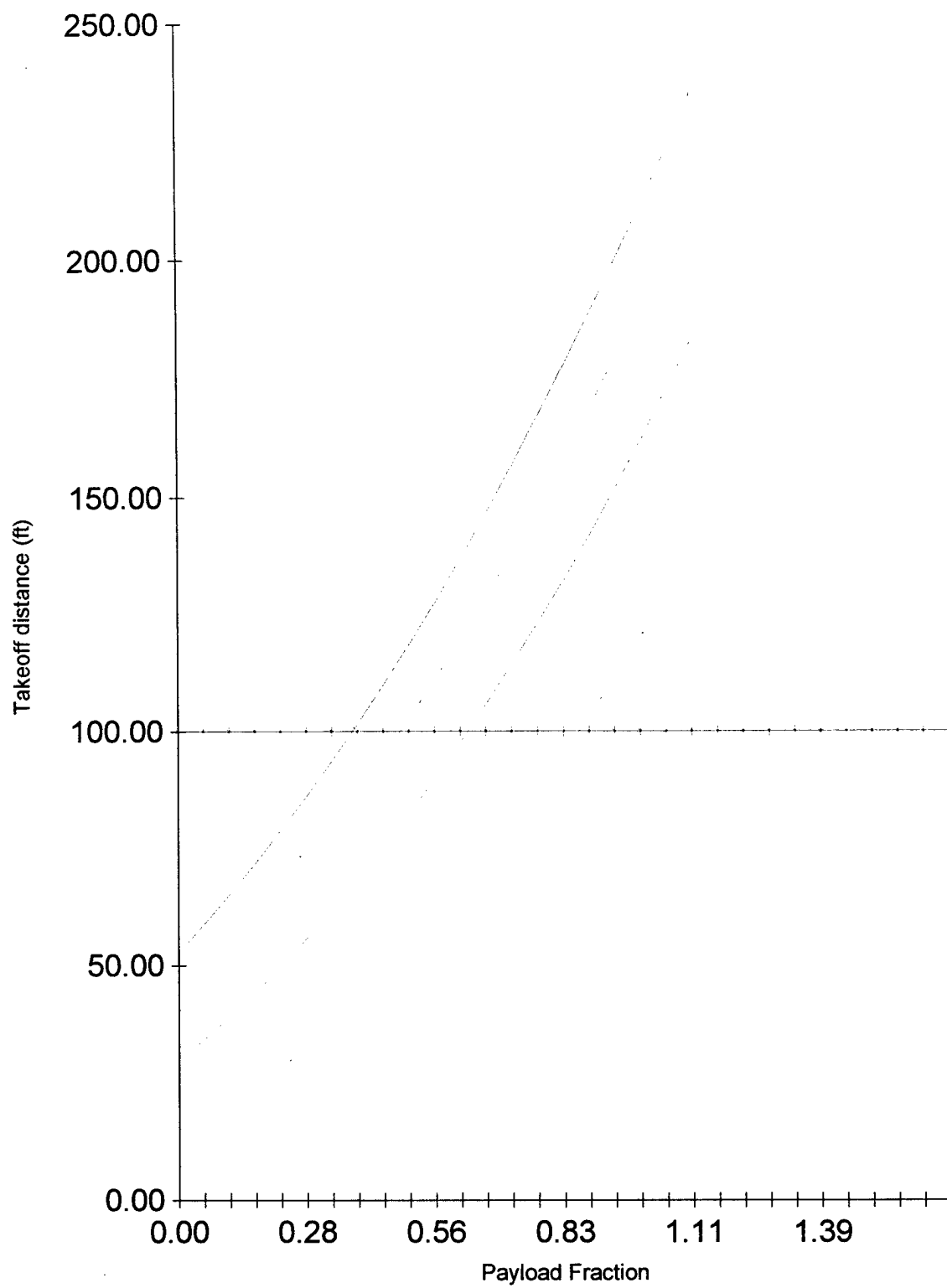


Endurance

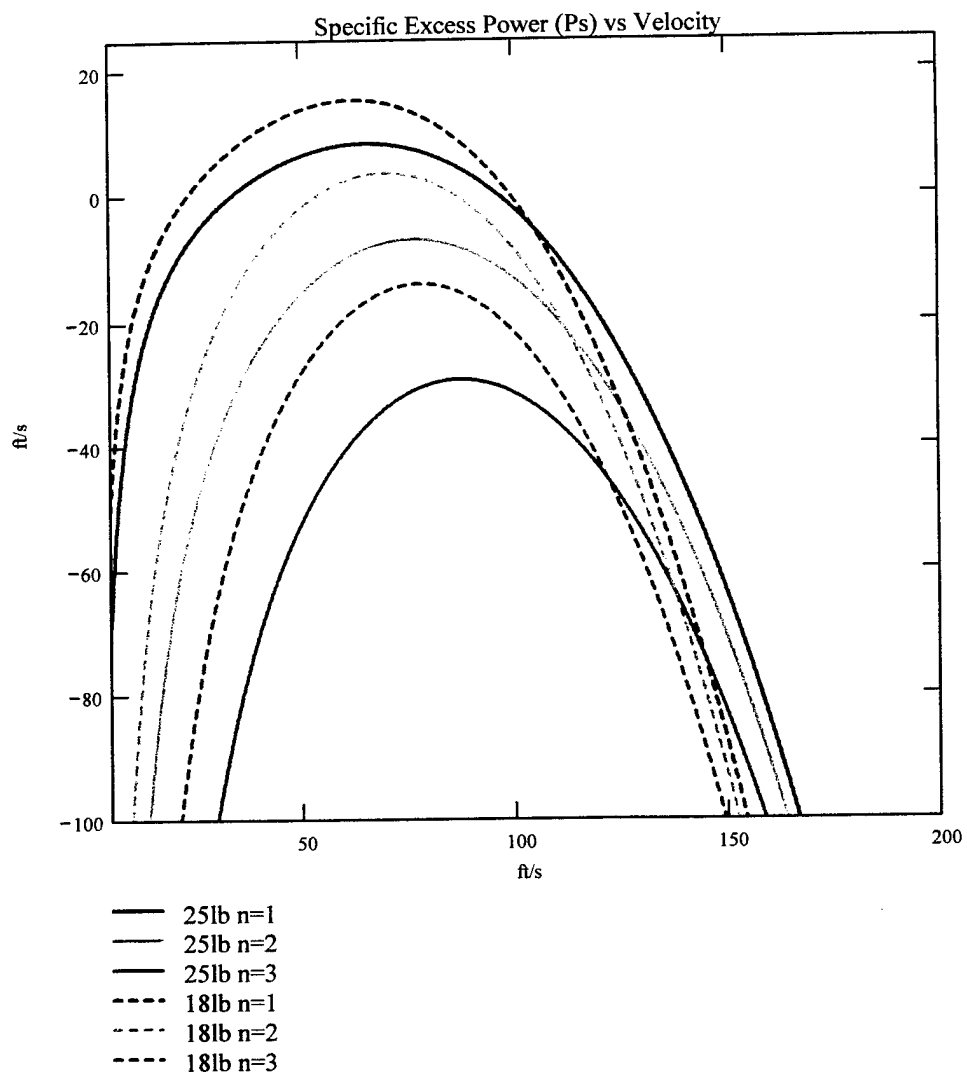


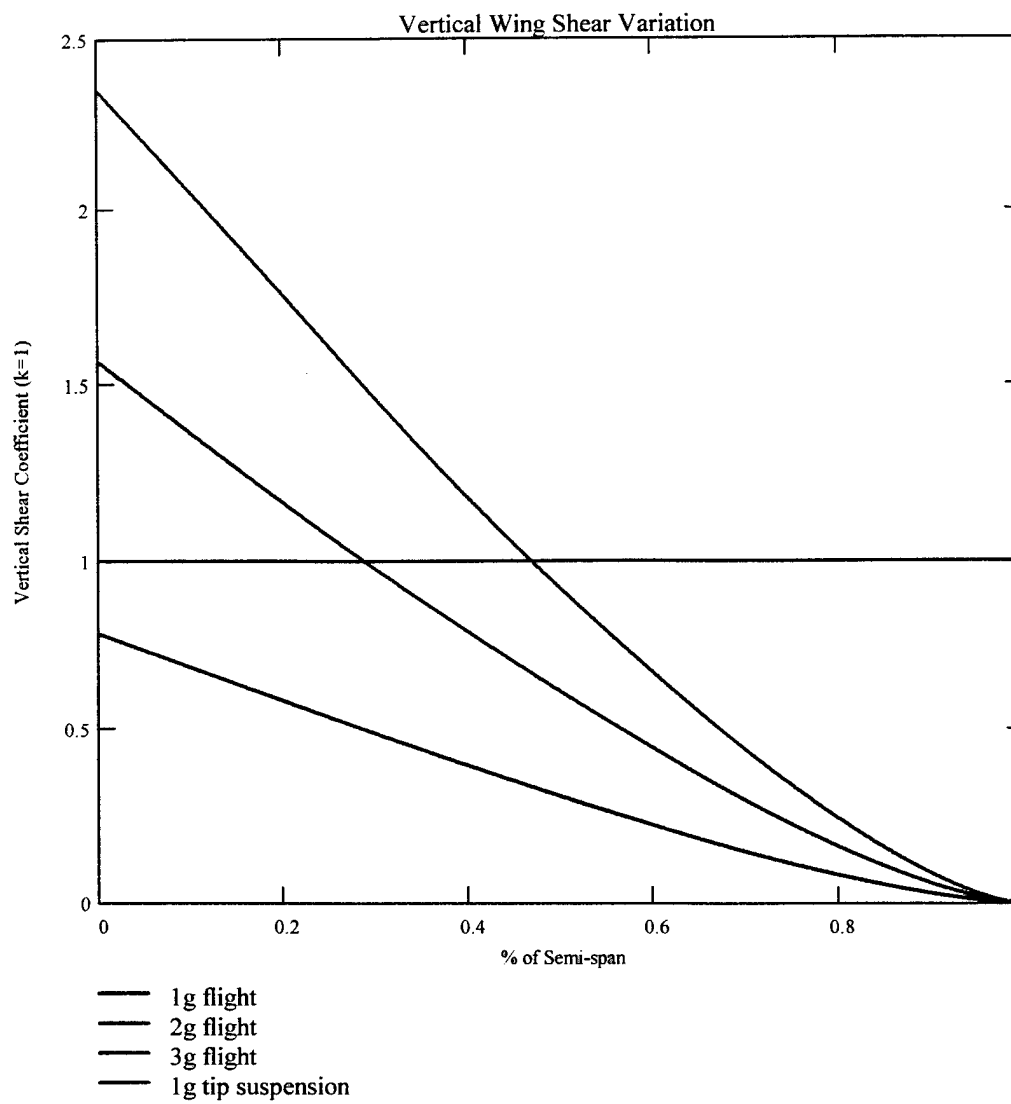
— Endurance at 25 lb — Endurance at 18 lb

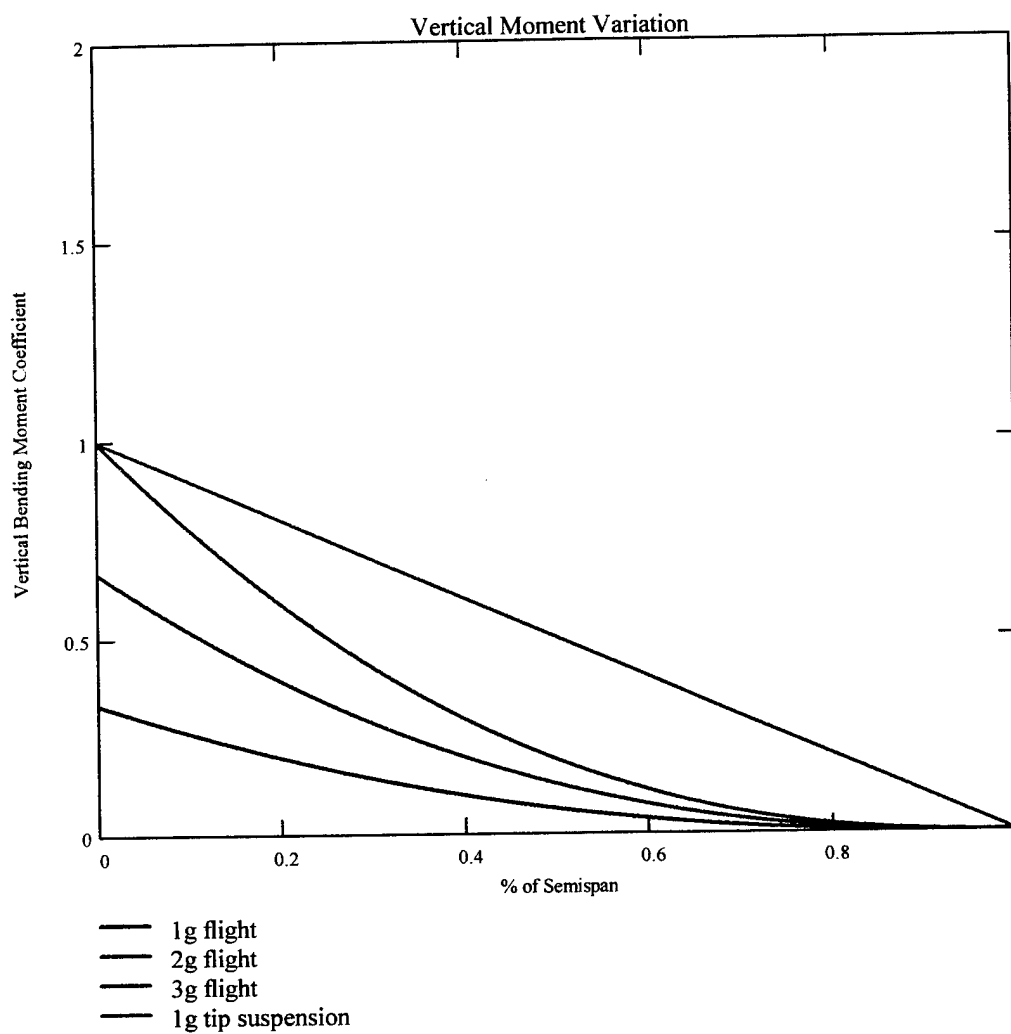
Takeoff Distance vs. Payload Fraction

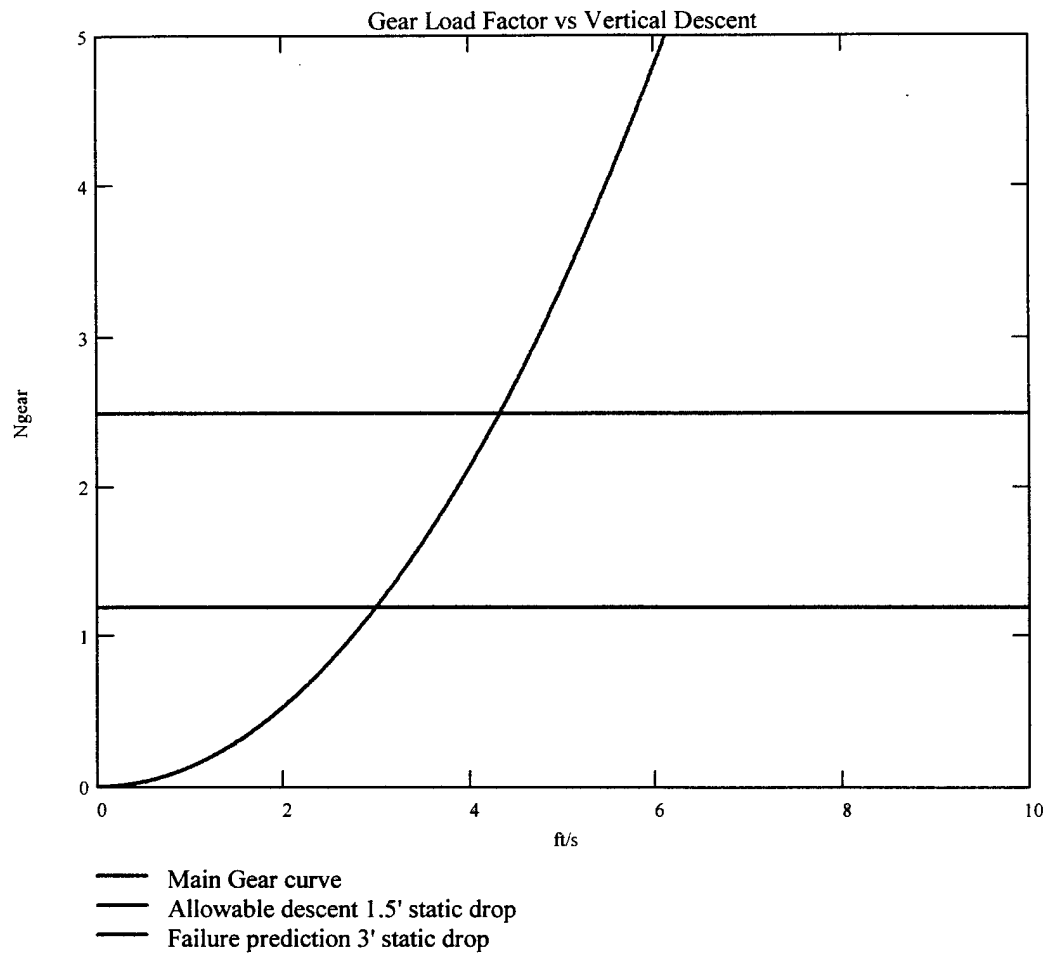


— 0 mph Wind — 5 mph Wind — 10 mph Wind
— 15 mph Wind — 20 mph Wind — 100 ft tod



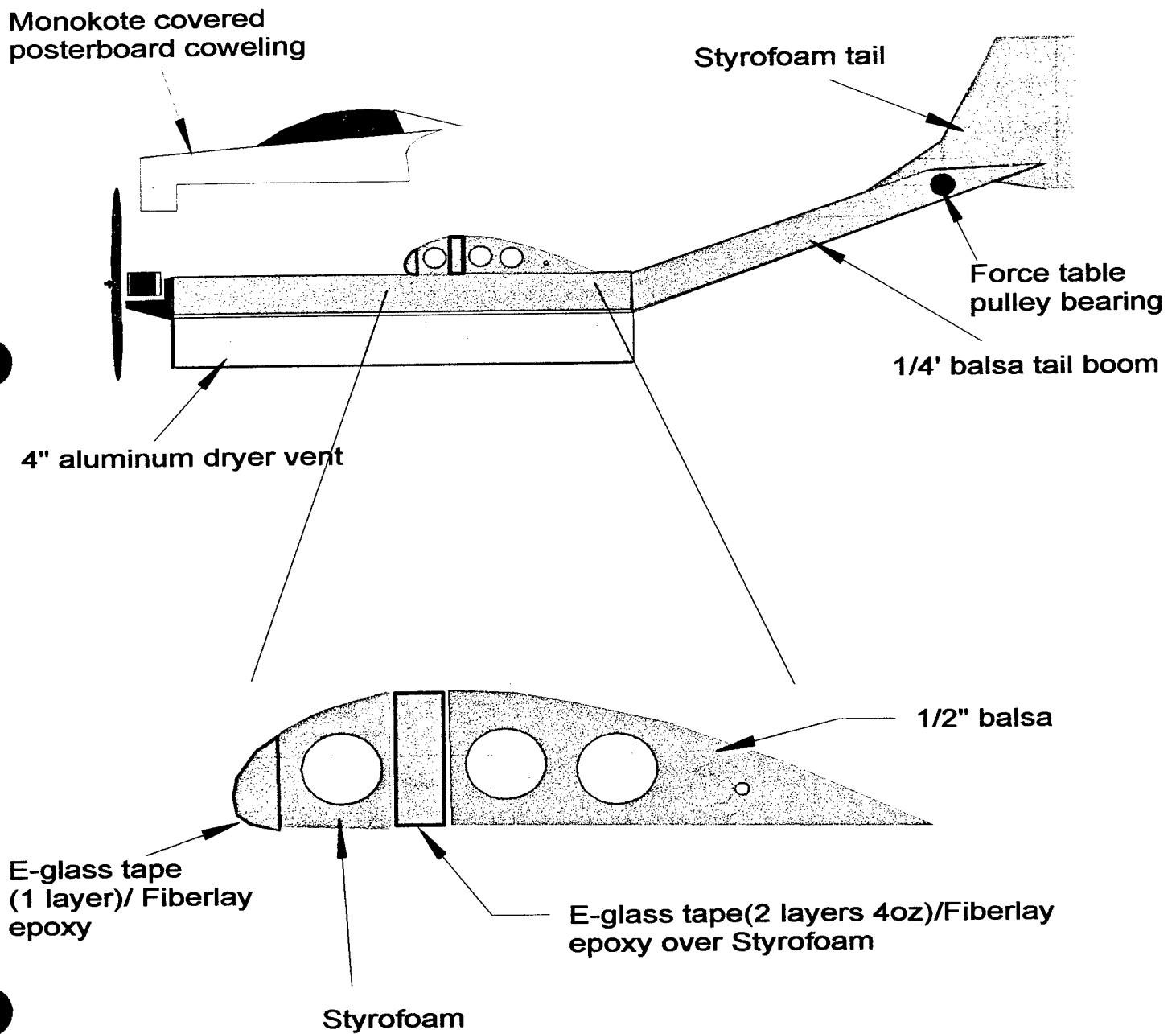






East Stroudsburg University of Pennsylvania
"Impulse" Primary Component Structure
Scale: 1":1'

Drawn by: Herb W. Ziegler

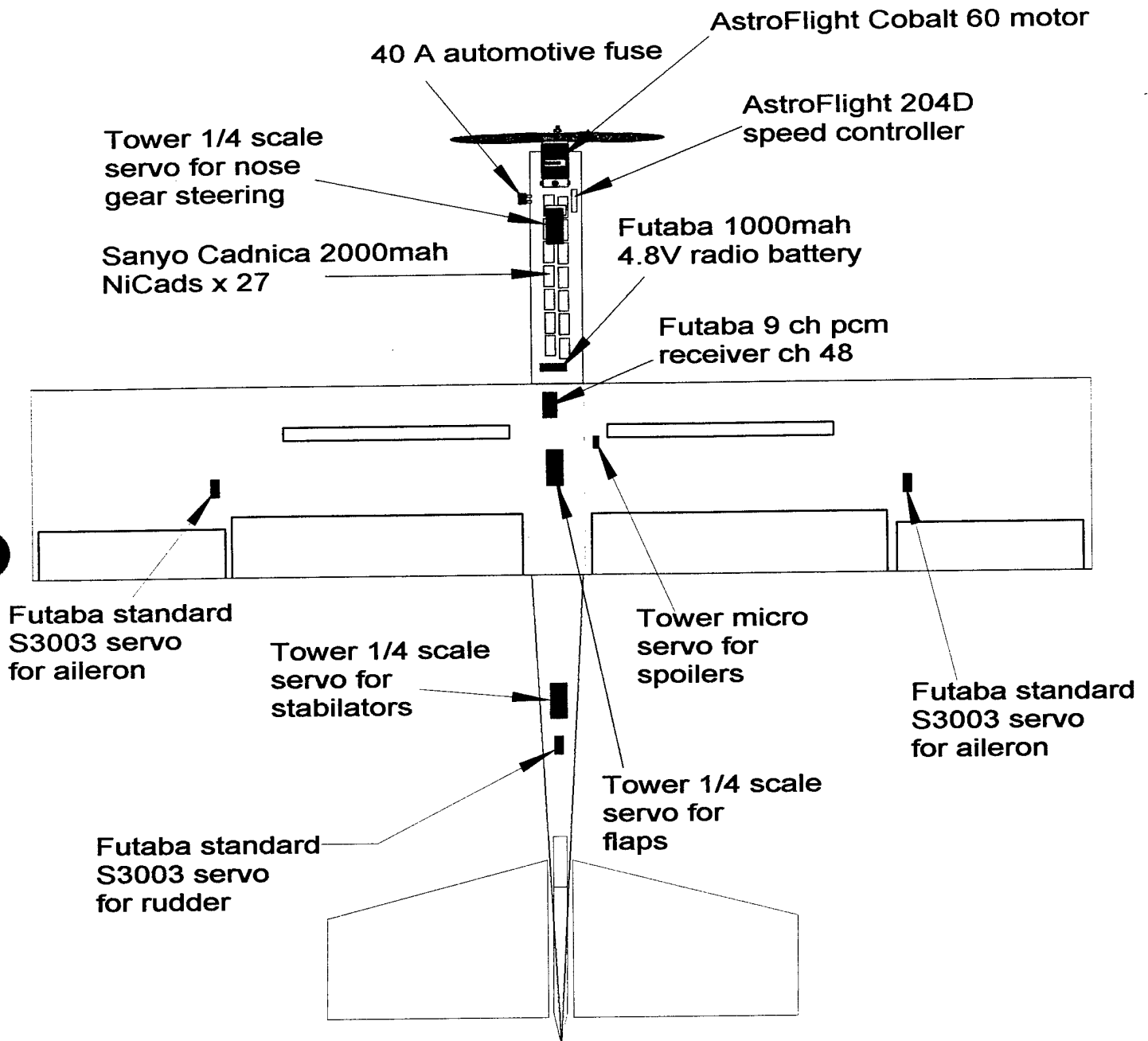


[illegible]

EAST STROUDSBURG UNIVERSITY	TITLE: INSIDE WING		SCALE: 1:1
ENGINEERING GRAPHICS	DRAWN BY: HAN CHANG	DATE: 03/03/00	DWG. NO. 5

East Stroudsburg University of Pennsylvania
"IMPULSE II" Primary Systems Locations
Scale: 1":1'

Drawn by: Herb W. Ziegler

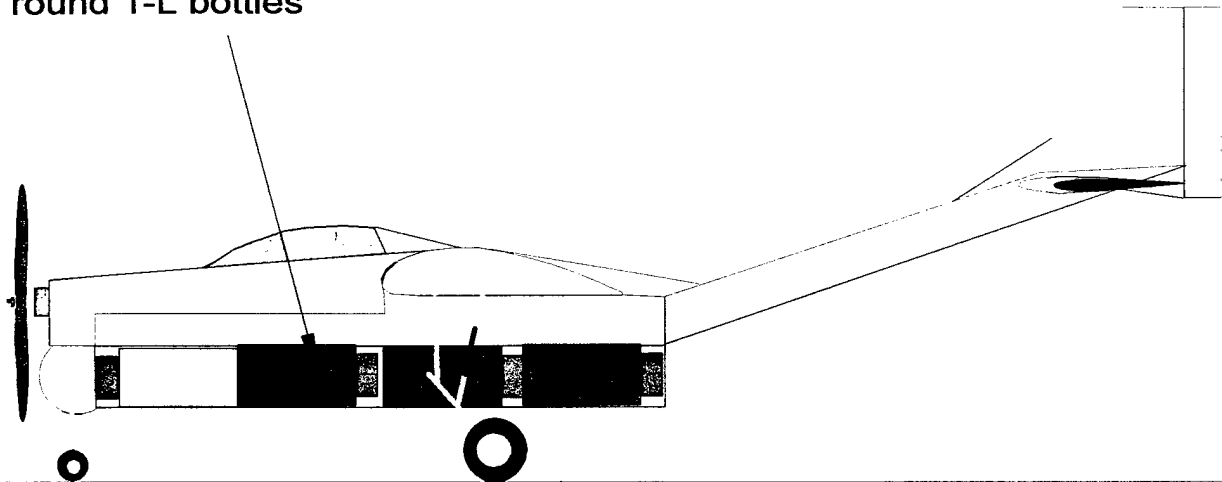


East Stroudsburg University of Pennsylvania
" Impulse II " Payload Allocation

Scale: 1":1'

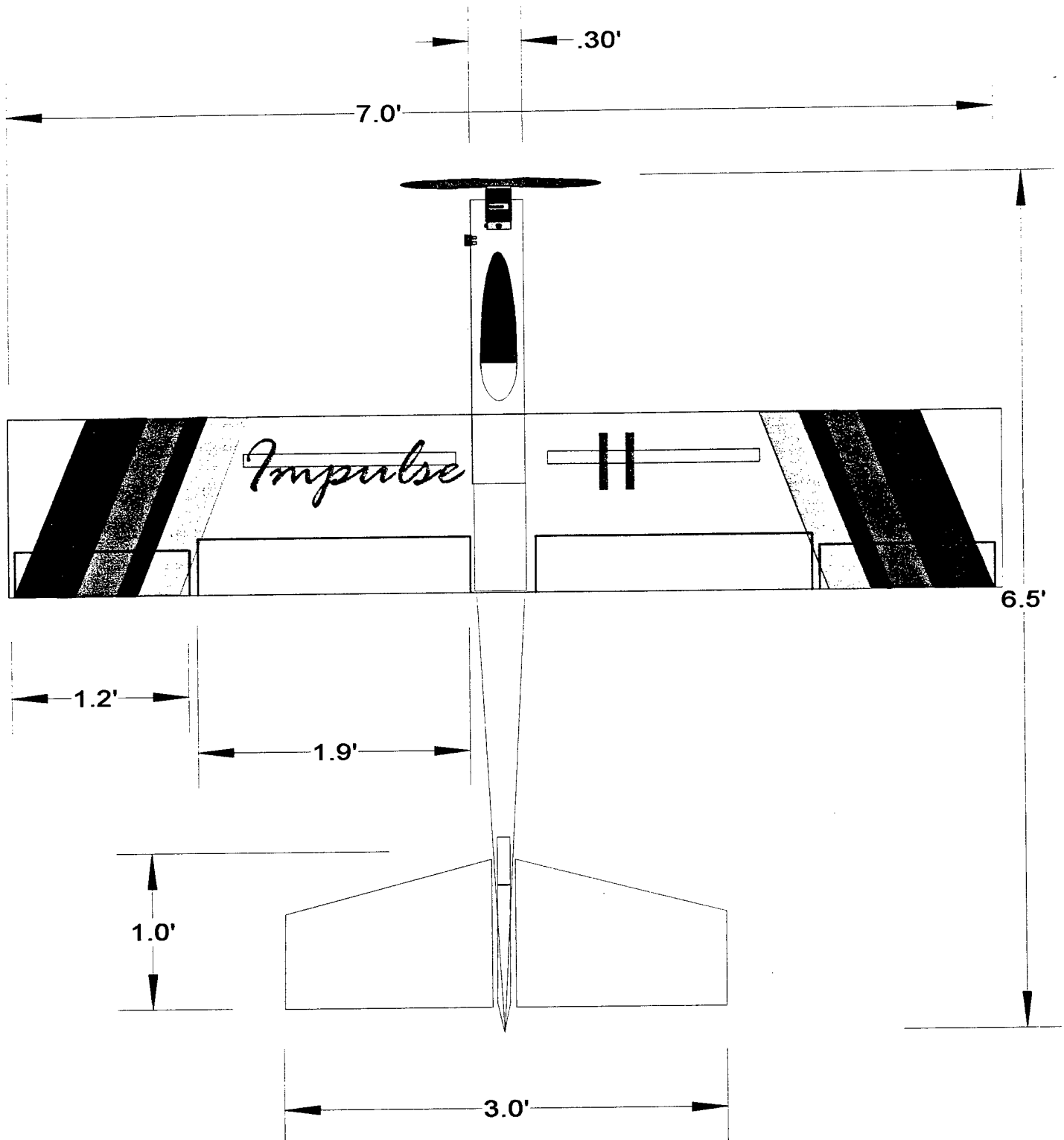
Drawn by: Herb W. Ziegler

3 full McMaster-Carr
round 1-L bottles

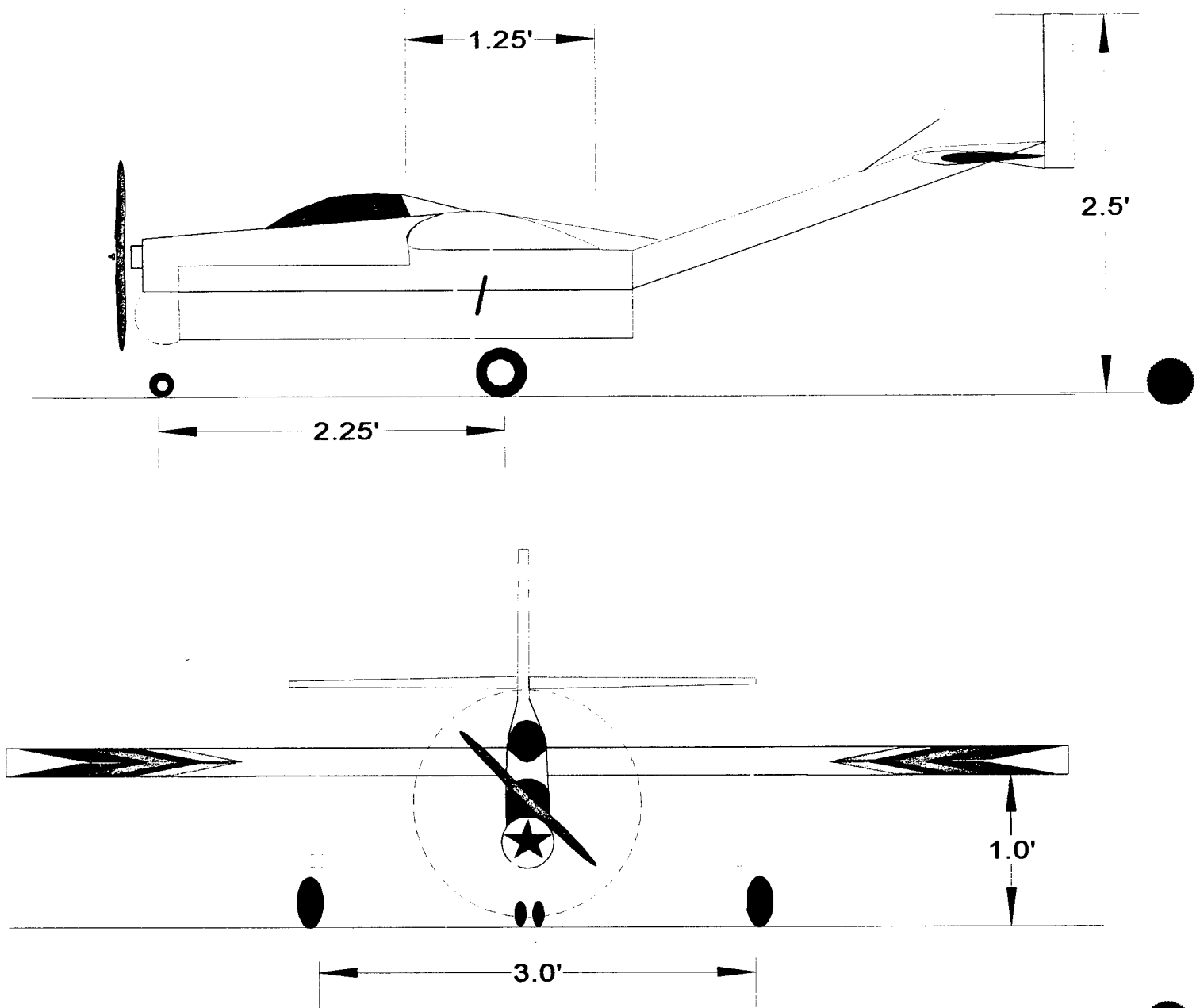


East Stroudsburg University of Pennsylvania
"IMPULSE II" Primary Dimensions
Scale: 1":1'

Drawn by: Herb W. Ziegler



East Stroudsburg University of Pennsylvania
"Impulse II" Primary Dimensions
Scale: 1":1'
Drawn by: Herb W. Ziegler



IN ENTRY

3/16 WHEEL COLLARS
60° ALL TOTAL

30 LB/IN SPRING CONSTANT

1/4" FUEL HOSE

3/16 AXEL THROUGH THE TIRE

R 2 3/8

0 1 7/8

3/4

1 3/8

AST STROUDSBURG UNIVERSITY	TITLE: REAR LANDING GEAR		SCALE: 1:1
ENGINEERING GRAPHICS	DRAWN BY: HAN CHUN CHOI (JEFF)	DATE: 03/03/00	DWG. NO: 13

Manufacturing Plan

Manufacturing Plan

East Stroudsburg University is anxious to get another plane off the ground at the 2000 competition in Wichita, Kansas.

Last Year, we felt that we accomplished a great deal. It was our first time entering the Cessna/ONR/AIAA event. Our budget was extremely small and our team inexperienced. No one on our team had ever been involved in such an endeavor. We were proud to build a plane worthy of the competition. We felt we contributed to the overall competition with our innovative use of home improvement products incorporated into the construction of our plane. We had encountered many difficulties along the way that would force us to continually revise our design until it became successful. These revisions served as the directive for last year's progress as well as this year's construction. As we strive to build a winning entry, we are taking a new approach toward construction by seeking a reduction in weight. Unfortunately, this also meant we had less opportunity to employ C.O.T.S.N.D.I. Nonetheless we are replacing our aluminum with a proven composite material, E-glass/epoxy. The switch gave us the ability to employ a higher strength/weight ratio and a custom manufacturing capability independent of store-bought airframe components.

At the end of last year, members of the team began working on the construction of a prototype. It was completed by mid-summer and tests were conducted. In the beginning of the fall semester the team began work on the contest variant using the prototype as a perceptual aid. Throughout the construction process we considered the use of several materials. We quickly ruled out the use of carbon fiber and graphite because of their expense and the risks they pose as health hazards. Aluminum sheet was heavy and precluded complex designs unless extensive metalworking could be employed. We decided to try making major components E-glass/epoxy. It seemed as though the fiberglass cloth tape was abundant, and when laid down over Styrofoam and covered with epoxy, it formed a splendid laminate.

The wing's spar was constructed in a similar manner: the prototype's first wing was sheeted with balsa wood while balsa and plywood ribs were glued to a fiberglass spar. We later considered using a monocoque structure, an all foam core sheeted with fiberglass but decided that too much glass would be necessary.

Satisfied with the design of this prototype, we proceeded to improve upon it by further reducing its weight in the final Impulse II contest variant. We decided to construct the wing using less balsa wood, more foam ribs, and less fiberglass on the spar. The wing was then covered in a monokote skin. Balsa sheeting was eliminated along with the plywood. We used minimal amounts of balsa wood compared to the wing of the prototype. Our wing weighs considerably less than last year's wing that consisted of 70% aluminum.

The upper portion of the fuselage is constructed of balsa wood and foam. Which will house the wing and NiCad batteries. The lower portion (the cargo hold) consists of a 4" aluminum dryer vent, which will hold 3 of the 4" liter water bottles. The entire fuselage is wrapped in fiberglass with a monokote skin.

The last major component of our plane's construction was the landing gear. Our first design was not streamlined. We later refined the heavy landing gear with a sleeker, lighter and less redundant set up. For shock absorption on the prototype, crushable rubber washers were used. We later replaced the rubber washers with the springs that made them more adjustable. We switched the wheels to foam, thus saving weight as opposed to the heavier rubber tires.

There were many things we had to take in account while we were building our plane. First, we were trading strength for weight reduction. We had to find new ways to construct a sturdy plane. Last year, the construction of the wing was relatively simple as we folded some sheets of aluminum roof flashing over an aluminum spar. The method worked fine; however, it left us with a heavy load to bear. This year we are using pink foam and fiberglass. Working with the fiberglass was a learning experience. We found that the fiberglass tape does not like to make 90-degree angles; hence, when covering a foam core it can de-laminate and it takes on the shape of an I beam.

We have encountered several new learning experiences in building our prototype working with fiberglass and epoxy. We learned by trial and error. Some of the mixing ratios were accidentally mismatched and didn't work out. Sometimes it would not dry or it wasn't a strong enough bond. We relied on a trial and error method. We found the best procedure for applying the fiberglass to the foam was to saturate the fiberglass tape with epoxy. We were surprised to find that the fiberglass adhered to aluminum so well.

Another problem we found with the fiberglass was bubbles. They were eliminated in later trials, due to more experience. If we planned to work with the epoxy we would have to schedule to do it at the end of day. The epoxy took a good six hours, to dry completely.

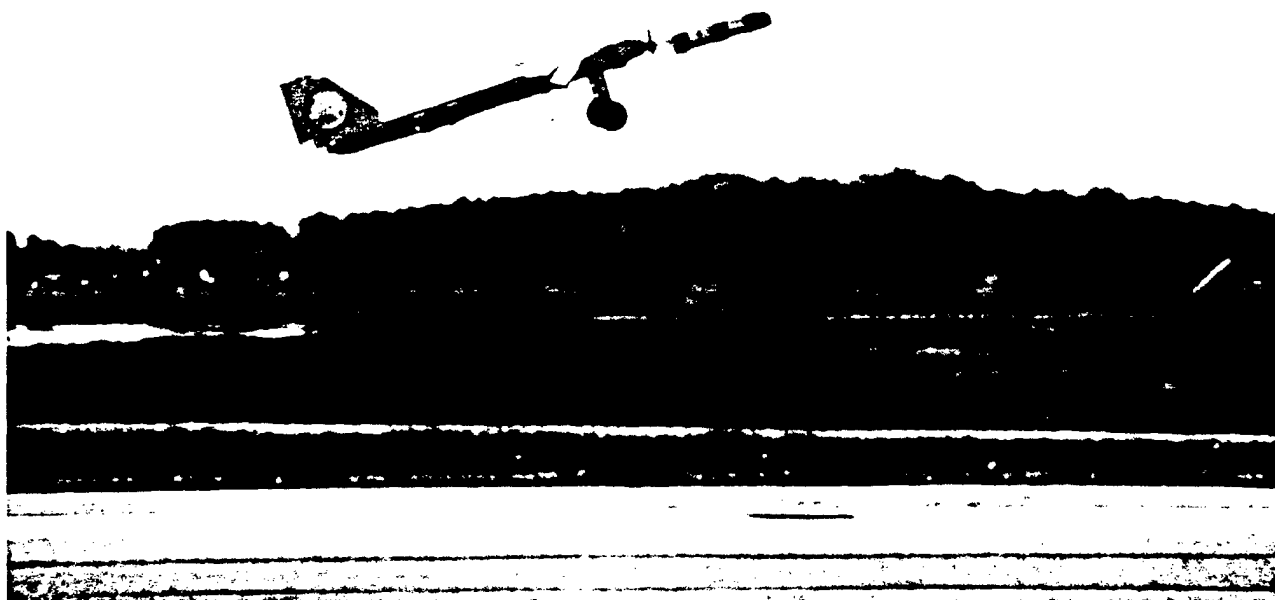
The equipment used to construct our plane was: super-glue, fiberglass tape, epoxy (FiberLay), Styrofoam, hot Ni-Chrome wire, Aluminum screws, exacto-knife, and screwdrivers.

This year's plane will be much lighter than last. Our main objective this year is to make our plane light enough, but durably acceptable.

Wing Construction	Durability	Weight	Ease of construction	Total
Concept 1: Balsa sheeting & shear webs/ Spruce spar caps/ Intermittent Plywood ribs	6	7	6	19
Concept 2: Plywood ribs/ Balsa wood sheeting/fiberglass laminated spar	10	5	7	22
Concept 3: All Aluminum skin & spar	15	2	3	20

Fuselage	Durability	Weight	Ease of construction	Total
Concept 1: Fiberglass covering Plywood Aluminum dryer vent.	7	8	5	20
Concept 2: Solid Fiberglass	5	15	5	25
Concept 3: All Aluminum	8	3	5	16

ESU Javelin 1998-99 Entry



ESU Impulse I 1999-2000 Entry



East Stroudsburg University
of Pennsylvania

2000 Cessna/ONR
Student Design/Build/Fly
Competition

Design Report



Addendum Phase

Contest Date: April 15-16

Contest Site: Wichita, KA

Electric Airplane Project
c/o Physics Department
East Stroudsburg University
East Stroudsburg Pa, 18301

Phone: 570-422-3341
Fax: 570-422-3505
Email: dlarrabee@po-box.esu.edu

Table of Contents

- **Lessons Learned**
- **Rated Aircraft Cost Documentation**

Lessons Learned

Lessons Learned

The Impulse II has flown several times since the submission of the proposal phase of our design report. We are pleased with its demonstrated handling qualities (It has been successfully flown in 90° crosswinds topping 10 knots!) and have seen significant improvement in our ability to field a contest-worthy vehicle. Slight difficulties have been encountered but there does not seem to be any insurmountable performance obstacle. Nonetheless, it is expected that testing and optimization of the aircraft will continue until the contest date.

The first noticeable problems arose with the flap drive, which allowed the flaps to move to an unintended spoiler-like position. Photographs later revealed that they raised approximately 1.5" *above* the wing during takeoff attempts. This was evidenced by an inability to climb out of ground effect and a severe pitching oscillation resulting in a series of "abnormally bouncy" landings. Replacing the servo cable pull-pull arrangement with a fiberglass pushrod solved the detrimental flap divergence.

Although the nose gear is lightly loaded, slight rearward deflection of its strut was detected and the diameter of music wire was increased. Because the ensuing strut weight necessitated the addition of 90g of mass to the tail, it has been changed back to the original 3/16" diameter. The pilot must take care to not over-stress this component but undue concern is not needed. Main strut geometry is adjustable, but it still seems to allow subtle variations in camber and toe. This has lead to abnormal tire wear, in addition to the wear experienced in strong crosswinds when the plane is heavily pressed sideways. Since our foam tires are viewed as expendable, this is a nuisance rather than a problem. We have tried 72mm roller-blade wheels on the Impulse II and have found that they significantly reduce the takeoff distance, though they are over twice the weight of the foam wheels and they allow minimal lateral grip in crosswinds. We would like to use either wheel depending on the prevailing crosswind conditions at the contest.

These are the only faults with the gear. In general, they are otherwise superb!

The main gear have unofficially surpassed the failure predictions found in our proposal phase. They have demonstrated the ability to handle landing in rough field conditions that would destroy other undercarriages. In one instance during flight tests, the pilot flared about 2 seconds late (because of optical illusion in picking landing spot

amidst runway threshold paint lines) allowing the plane to bounce over 3 ft back into the air. There was no damage to the gear or the aircraft. Ground handling in crosswinds (with foam tires) is excellent. As mentioned earlier, an excessive turnover angle was built into the airplane. This permits wonderful maneuverability and will facilitate taxiing back to the starting line if it is missed on landing. The nose wheel brake was never added to the aircraft because we did not want to add another servo.

At time of writing we are still trying to optimize the battery configuration. We have flown continuously for over 2.5 min with 27 Sanyo 2000mah cells, and it is highly probable that this will be our competition pack. We made a 3.4lb pack of 32 Sanyo 1500mah cells in hopes that we could save a pound of weight and simultaneously add a pound of thrust at a slight expense of run-time. Unfortunately the internal resistance of the smaller cells seemed to be significantly higher than expected. Pack heating during charging and discharging was deemed to be excessive. This totally negated the increase in pack voltage and we measured less drawn current than with the 27-cell pack. Ideas of its use have been abandoned. We have found a 2300mah Ni-Cad from Panasonic that is also lighter than the Sanyo product. We hope to have a pack of these for evaluation prior to the contest. If these batteries perform as advertised, we will be able to employ the voltage maximum for the Astro Cobalt 60, increase our run-time by %15, and be well below the imposed 5lb pack restriction.

Weight reduction methodology is an ongoing process. The configuration of the Impulse II will remain unchanged except for slight variations in material selection. Two copies of the aircraft will be brought to the contest, thus providing the opportunity to completely replace damaged sections if necessary. Our lightest fuselage employs fiberglass more extensively than does its predecessor, which contains an aluminum and balsa mold as an integral component. With the weight savings realized by these methods, it is marginally possible to carry 4 liters of water instead of our proposed 3 liter maximum.

Regarding the next design and manufacturing process implementation for the Impulse II, we recommend the use of composites with even higher strength-to-weight ratios than fiberglass. This would allow the true structural optimization of the vehicle albeit at the fiscal expense of material. The epoxy lamination technique works well with

fiberglass and other materials and provides virtually unlimited design freedom, but we have not yet explored the entire spectrum of composites. This has been our primary manufacturing limitation.

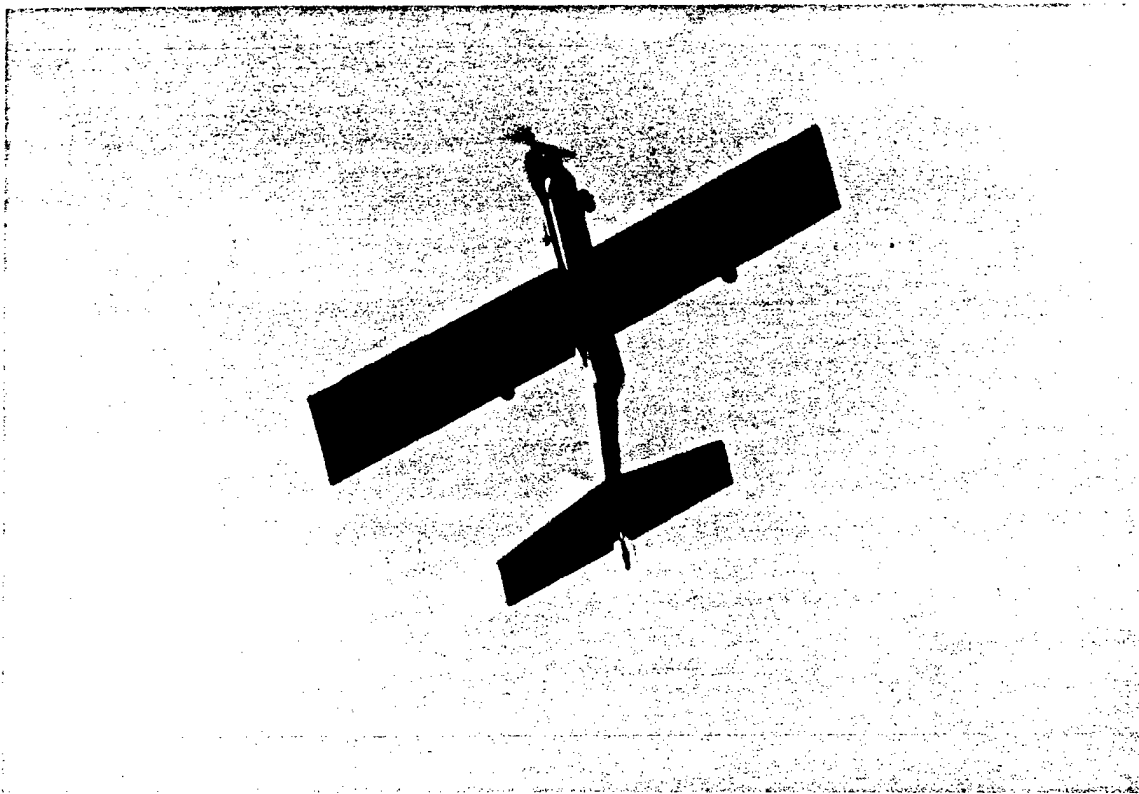
Additionally, we realize the need for additional flight-testing. We have been fortunate to have actual prototype flights 4 months prior to the competition and final variant flights 1 month beforehand. However we have not been able to test *every* conceivable contest scenario (other than on the simulator) because of weather, scheduling, obtaining a flying site etc.... This is the area of development that requires more effort, though it is much improved from last year's contest preparation period (the ESU Javelin flew just 4 *days* before the 1998-1999 contest).

Finally, we recognize the need for more congruency between our analytical modeling and the fruition of our work in applied aerodynamics. Since our aircraft has been extremely successful, it would be beneficial to compile an extensive list of data from static and dynamic tests. It is conceivable that telemetry research should be conducted to verify all performance limitations on the aircraft for correlation with design equations and future reference. This is one area that must be addressed if we are to further advance our entry in the next Cessna/ONR student DBF contest.

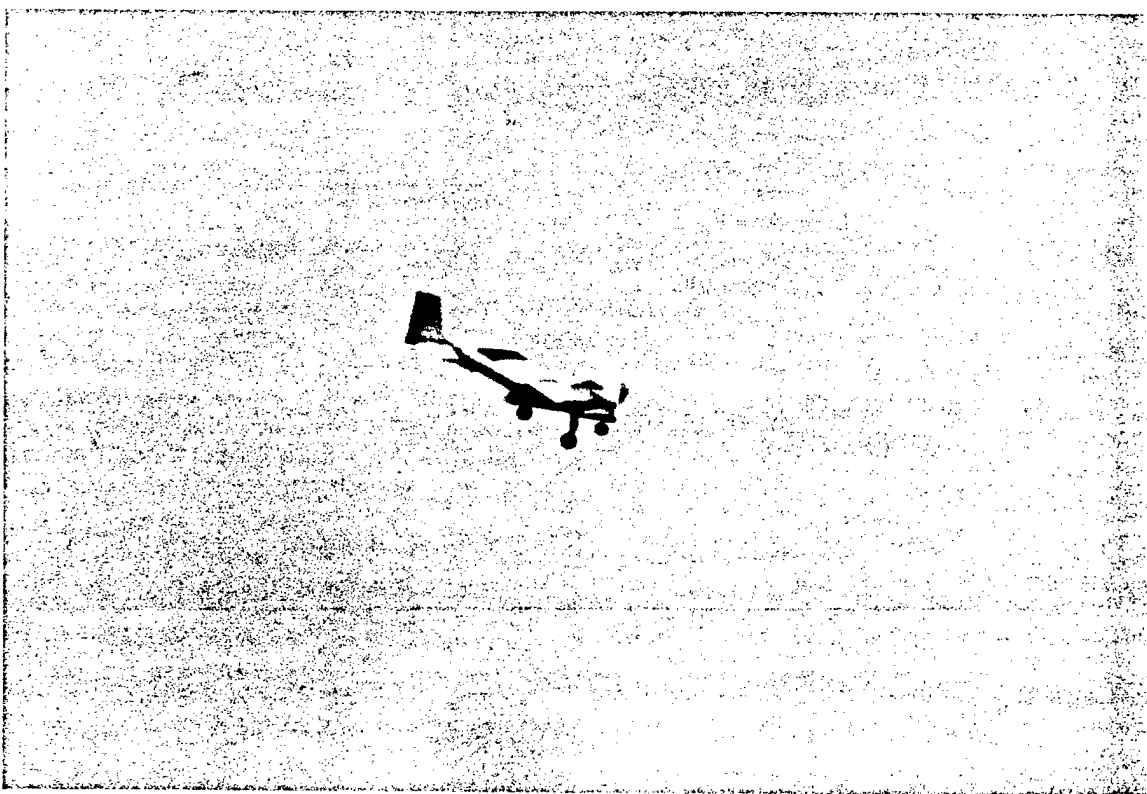
Rated Aircraft Cost

Rated Aircraft Cost Documentation

<u>RAC Component</u>	<u>Description</u>	<u>Value</u>	<u>Cost</u>
MEW	Aircraft weight, no cargo/batteries	13.8 lb.	\$1,380
REP	1 engine x 50A x 1.2V x 27 Cells	1620 W	\$1,600
MFHR	Wing 5 x 1 wing + 4 x 8.60 ft.	39.4 hr	\$788
	Fuselage 5 x 1 + 4 x 6.75 ft.	32 hr	\$640
	Empenage 5 + 5 x 1 fin + 10 x 1 stablato	20 hr	\$400
	Flight Systems 5 + 1 x 8 servos	13 hr	\$260
	Propulsion Systems 5 x 1 engines + 5 x 1 propeller	10 hr	\$200
		Total Cost	\$5,268
		R.A.C.	5.27

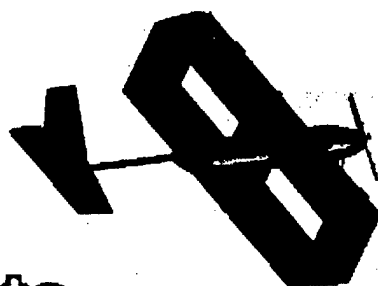
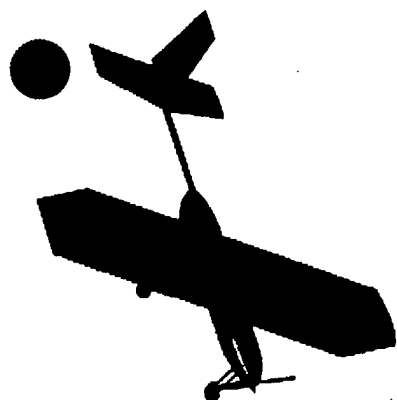
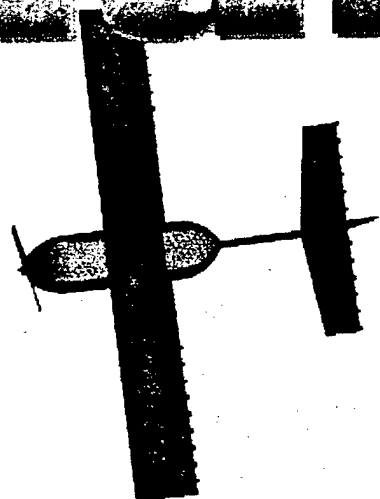


East Stroudsburg University of Pennsylvania
Photos courtesy of Professor Mike Orleski



● 99/2000 AIAA Design/Build/Fly Contest Proposal

PLAN B



TITLE PAGE

**The Georgia Institute of Technology
Presents**

PLAN B

**1999-2000
AIAA Design/Build/Fly Competition**

**School of Aerospace Engineering
Georgia Institute of Technology
Atlanta, GA 30332**

Advisor:

Dr. Dimitri Mavris

Team Members:

Jason Zumstein

Adam Broughton

Karen Feigh

Mike Penland

Kevin Wagahoff

Harlan McCullough

Brian Dolan

Josh Hardy

Alisa Hawkins

Michael Matthews

Phillip Frye

Darius Moore

Elizabeth Walden

ACKNOWLEDGEMENTS

The Georgia Tech DBF team would like to thank:

- ❖ Dr. Dimitri Mavris and the members of the Aerospace Design Laboratory for their dedicated support of all our endeavors
- ❖ Mr. Danny Rockett and Promark Electronics for his battery expertise and his generosity toward academic pursuits
- ❖ National Hobby Supply, who's sponsorship enabled so many team members to attend the competition
- ❖ Newton County RC Flyers, for their generous donation and support
- ❖ The National Science Foundation for providing funds for this multidisciplinary design project

TABLE OF CONTENTS

1.0 EXECUTIVE SUMMARY	2
2.0 MANAGEMENT SUMMARY	8
3.0 CONCEPTUAL DESIGN	12
3.1 PROBLEM DEFINITION	12
DESIGN DRIVING FACTORS	12
MISSION FEATURES	12
3.2 FIGURE OF MERIT DEFINITION	13
3.3 PRESCREENING ANALYSIS	13
3.4 CONFIGURATION IDENTIFICATION	14
CONVENTIONAL	14
BIPLANE	14
DELTA WING	14
3.5 CONFIGURATION ANALYSIS	15
ANALYTICAL TOOLS	15
INDEPENDENT ANALYSIS	15
ANALYSIS CONCLUSIONS	18
3.6 CONFIGURATION EVALUATION	18
QUANTITATIVE FOM EVALUATION	18
QUALITATIVE FOM EVALUATION	18
CONFIGURATION RANKING	19
CONCLUSIONS	19
4.0 PRELIMINARY DESIGN	26
4.1 POWER PLANT SELECTION	26
BATTERY SELECTION	26
MOTOR SELECTION	27
4.2 AIRCRAFT SIZING	29
SPREADSHEET ANALYSIS	30
SPREADSHEET RESULTS	30
5.0 DETAILED DESIGN	36
5.1 WINGS	36
AIRFOIL SELECTION	36
FLAP DESIGN	36
WING STRUCTURE	37
WING ATTACHMENT	38
5.2 FUSELAGE	38
BOTTLE LAYOUT AND STRUCTURE	38
TAIL BOOM	39
5.3 EMPENNAGE	40
SIZING	40
ATTACHMENT	40
5.4 LANDING GEAR	40
SELECTION	40
PLACEMENT	41
TYPE	41
ATTACHMENT	41

5.5 AIRCRAFT STABILITY AND CONTROL	42
5.6 HANDLING QUALITIES	43
5.7 PERFORMANCE	43
6.0 MANUFACTURING PLAN	60
6.1 PRELIMINARY CONSTRUCTION	60
MATERIALS SELECTION	60
6.2 FUSELAGE	61
6.3 EMPENNAGE	62
6.4 WING AND LANDING GEAR	63

NOMENCLATURE

Symbol	Definition	Dimension
AR	Aspect Ratio	
b	Wing Span	ft.
c	Chord	ft.
e	Span Efficiency	
C_D	Coefficient of Drag	
C_{D0}	Coefficient of Parasite Drag	
C_l	Coefficient of Lift (2-D)	
C_{l0}	Coefficient of Lift (2-D) at Zero Angle of Attack	
C_L	Coefficient of Lift (3-D)	
CG	Center of Gravity	
L/D	Lift to Drag Ratio	
MAC	Mean Aerodynamic Chord	ft.
n	load factor	
NACA	National Advisory Committee for Aeronautics	
S	Wing Area	ft ²
T	Thrust	lbs.
T/c	thickness-to-chord ratio	
T/W	Thrust to Weight Ratio	
V	Velocity	ft./sec.
W	Weight	lbs.
W/S	Wing Loading	psf
Greek Symbols	Definition	Dimension
ρ	Air Density	slugs/ft ³
α	Angle of Attack	degrees
Λ	Wing Sweep	degrees

1.0

EXECUTIVE SUMMARY

When classes began at Georgia Tech in August, 1999, work on the design 1999/2000 AIAA Design/Build/Fly project was began immediately. First, the guidelines of the contest were outlined. Teams from around the country are tasked with designing and building a fully operational air vehicle. The vehicle's sole propulsive power has to result from an electric motor and five pound battery pack. The wing span can not exceed seven feet and the gross takeoff weight must be less than 55 pounds. As an added challenge, the aircraft must be able to fly a duel mission around a predetermined course: a cargo sortie with one liter water bottles and a ferry sortie without any cargo at all. During the cargo sortie, the water bottle payload must be completely contained within an aircraft with a minimum capacity of two liters and maximum capacity of no more than eight liters. The overall objective is to transport as many liters of water as possible around the course in a 10 minute time period using multiple sorties that alternate between cargo and ferry. The final evaluation criteria will be based on the sum of the number of liters of water carried during the best three 10 minute flight routine attempts. To add to the excitement of the design strategy, each team's flight score will be penalized based on the size and complexity of their aircraft by a rated aircraft cost model.

After the problem at hand was identified, the team determined the importance of each of the mission features and the figures of merit that could be used to determine the type of aircraft would be best suited for the contest. Some of the areas that were considered most important included minimal structural weight, low design complexity, fast cargo loading/removal, and good handling qualities in windy conditions.

Additionally, the team analyzed the rated aircraft cost model using hypothetical aircraft to determine if a small, minimal aircraft would be able to outperform a larger aircraft with greater payload capacity. The conclusion was that the rated aircraft cost penalty does not scale proportionally with cargo capacity and therefore a small aircraft can not fly fast enough to perform the extra cargo sorties that would be needed to compensate for carrying a smaller amount of cargo.

With the important aircraft characteristics realized, three distinct, yet relatively broad, aircraft configurations were chosen for comparative analysis: conventional monoplane, biplane, delta wing. The design team divided up into subgroups; each subgroup did an in-depth analysis of a different aircraft configuration. The conventional monoplane was selected as a candidate because its dominating presence in aviation. Monoplanes can be designed to be very stable, can use high lift devices, and the team has a level of familiarity based on past experience. The biplane was selected because of lift and drag benefits that are inherent with biplanes when a wingspan limitation is imposed. The delta wing configuration was chosen because of its simplicity; the lack of a fuselage and horizontal stabilizer will reduce the aircraft complexity penalty. Additionally, a delta wing has an enormous amount of natural cargo space because of the large root chord.

In order for the subgroups to tangibly compare the aircraft alternatives at this early stage of the design process, certain aircraft parameters were standardized across the board. First, it was assumed that all of the configurations would utilize the same power plant. Second, all alternatives would have the maximum allowable wingspan of seven feet. Third, all of the aircraft would be sized to carry the same amount of cargo. This allowed assumptions in speed

and airframe weight between the designs to be held to similar standards and accurate engineering decisions could more easily be made.

Each subgroup sized its respective aircraft based on takeoff performance. One of the requirements of the competition is that the aircraft must be off the ground in 100 feet. Through the use of a spreadsheet based around Newton's second law of motion made in Microsoft Excel, the wing area of each of the configurations was sized accordingly such that the aircraft could meet takeoff criteria at a ground roll distance of 100 feet. This was an iterative process because the thrust available and drag, which drive the acceleration, are functions of velocity.

During the takeoff analyses, values of each aircraft's three dimensional lift coefficient was assumed. Because a biplane has two wings with individually high aspect ratios when compared to a conventional monoplane of similar wing area, the maximum lift coefficient for a biplane is slightly higher than for a monoplane. A delta wing aircraft must use a reflexed airfoil, and thus can not attain a very high value for the three dimensional lift coefficient. Additionally, a delta wing can not utilize high lift devices. As a result, the lift coefficient used for the delta wing was considerably lower than it was for the other two designs.

After all of the aircraft were analyzed and sized accordingly, the concepts were compared to one another objectively using the rated aircraft cost model and subjectively using engineering judgement. As expected from its low lift coefficient, the delta wing required an enormous amount of wing area, so much in fact that the benefits of not having a fuselage or horizontal stabilizer in the rated aircraft cost model were negated. The monoplane and biplane were easy to compare to one another because many of the aircraft substructures were nearly identical, thus the only area left for comparison was the wings. Because of a higher lift coefficient, the biplane was able to have less wing area than the monoplane, enough to outweigh the associated cost of an extra wing. Also, the monoplane had a very low aspect ratio wing because of the wing area needed to achieve the takeoff distance requirement. When the induced drag between the biplane and the monoplane was compared, the biplane's was expected to be less. Based on each concept's rated aircraft cost model and ability to meet the mission features, the biplane was selected as the best design for the contest.

Before more detailed sizing of the biplane could be performed, the power plant had to be selected. To begin power plant selection, the battery pack options were investigated. Sanyo batteries were chosen because of their market dominance in NiCad battery technology. In order to maximize the power available, a five pound battery pack would be used. Battery packs of various cell sizes, with the correct number of cells to meet the five pound weight requirement, were investigated. Power available, pack impedance, and tradeoffs between capacity and voltage were realized during the battery selection process. The optimal battery pack from a power, efficiency, and rated aircraft cost standpoint was 26 Sanyo N-3000CR battery cells.

Once the battery pack was selected, the most appropriate motor could be determined. To aid the motor selection process the team used ECALC, an electric flight system evaluation tool, the AveoxTM electric motor company web site, and an experimental test stand. Both ECALC and the web site allowed the virtual comparison of different motor/battery pack combinations. However, from past experience, these tools overestimated the power plant performance. To calibrate ECALC, an experimental test stand was built.

The team chose AveoxTM as the motor manufacturer because their brushless electric motor products outperform the competition. Knowing the expected run time and power setting of the motor based on the competition flight profile, the peak current available from the battery pack

was determined. A motor that is capable of producing the greatest amount of thrust throughout the flight profile while meeting the current requirements would be selected. The Aveox 1415-3Y motor with a 3.7-1 gear reduction unit was determined to be the optimal motor. When combined with an 18" diameter 12" pitch propeller, the power plant is capable of producing eight pounds of static thrust.

Using the thrust information provide by ECALC for the power plant, the aircraft sizing process could begin. Since the thrust curve was very similar to what had been used in the conceptual design phase, the basic aircraft sizing was all ready complete. More detailed weight and drag analyses were performed using Excel spreadsheets. It was determined that the optimal cargo for the aircraft remained at 6 liters and the optimal wing area is 14 ft². The wing will use a Selig 2091 airfoil with full length flaperons. The airfoil was analyzed using a two dimensional web based airfoil analysis package and was chosen because of all the airfoils researched, it came the closest to meeting the lift requirements for the flight phases of both the ferry and cargo sorties.

From the outset of the project, speculation about the how the bottles would be arranged, exchanged, and secured was a driving consideration of the design process. However, it was not until the detailed design phase that a final bottle configuration was determined. Once it was decided that the bottles would load from the rear of the aircraft and reside along the sides of a center fuselage structure, the remaining details of the design were worked out. To aid the detailed design process, Ideas, a three dimensional modeling package was used extensively. Virtual building is a must when working with many subassemblies to ensure that everything goes as planned and a feasible design results

With the aircraft subsystems designed, the expected performance of the aircraft was calculated. The empty weight is anticipated to be 15 lb., which results in a gross takeoff weight of 30 lb. During a single 10 minute flight period, the plane will be able to complete three cargo sorties and two ferry sorties. Each of the cargo sorties will carry 6 liters of water.

Originally, the aircraft was to be completely built by the middle of February, but the team was subjected to a "real" world experience with unavoidable budgeting problems that pushed the building phase back. This caused the plane construction to overlap with the report writing section. Obviously the report writing took precedence, and the aircraft building has been delayed further. However, the details of the manufacturing process are worked out and it is expected that the plane will be complete in time for flight testing and fine tuning before the contest date of April 15.

COMPLIANCE MATRIX

RFP Specifications	Constraint	Plan B		Section Discussed
Mission	As much total weight as possible in 10 minutes	3 Cargo Sorties, 6 Liters		5.7
Propulsion	Off-the-shelf, electric	Aveox 1415-3Y		4.1
Payload	Minimum 2 Liters of Water ~ 4.4 lbs & 106 in ³	6 Liters ~ 15lbs		4.2
Situation	Inside Faired Fuselage	Fuselage		5.2
Accessibility	Must unload payload after each cargo sortie and reload after each ferry sortie	Aft Hatch		5.2
Takeoff/Landing	Under 100 ft	80 ft		5.7
General Performance Parameters		6 Liter Payload	No Payload	
Maximum Endurance	-	7.5 min	21.7 min	5.7
Maximum Range	-	3.66 mi.	7.92 mi.	5.7
Payload Weight Fraction	-	50%	0%	5.7
Cruise Velocity	-	42 fps	55 fps	5.7
Stall Speed, 30° Flaps	-	29 fps	20.5 fps	5.7
L/D max	-	7.32	7.32	5.7
Speed for L/D max	-	46 fps	34 fps	5.7
Maximum Rate of Climb	-	2.75 fps	10.6 fps	5.7
Turn Rate at Cruise Velocity	-	36 deg/sec	84 deg/sec	5.7
Max G loading	-	6	12	5.1

WING SPAN	84"
CHORD LENGTH	12"
TOTAL LENGTH	68"
HORIZONTAL TAIL SPAN	36"
VERTICAL TAIL HEIGHT	16"
TIPBACK ANGLE	15
TAKEOFF WEIGHT	301b
PAYLOAD CAPACITY	6L
PAYLOAD FRACTION	0.5

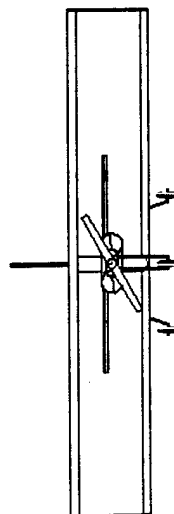
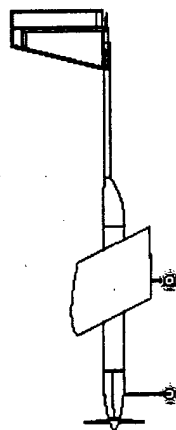
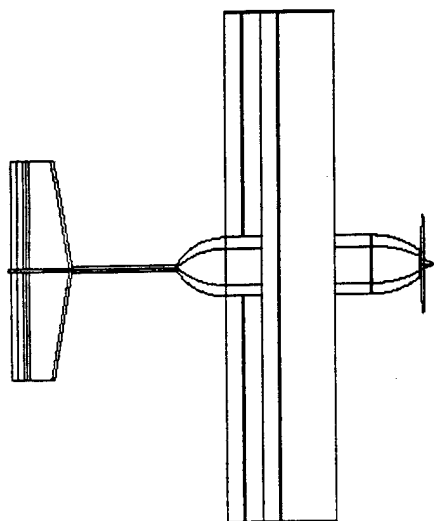
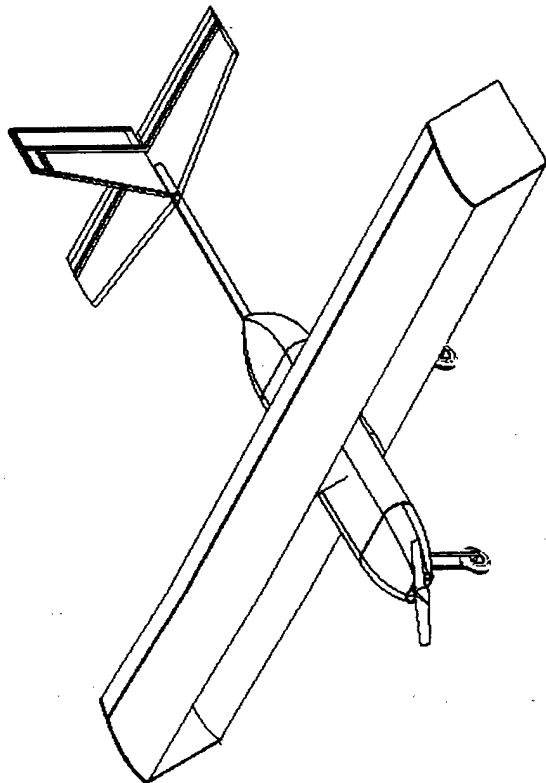


PLATE B

GEORGIA INSTITUTE OF TECHNOLOGY

1999/2000 DBF COMPETITION

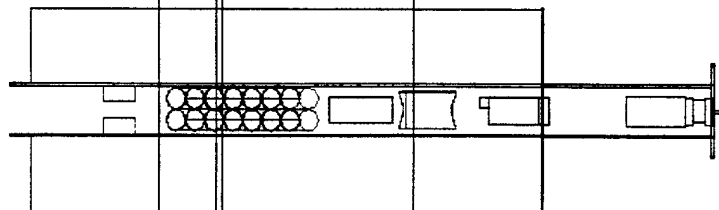
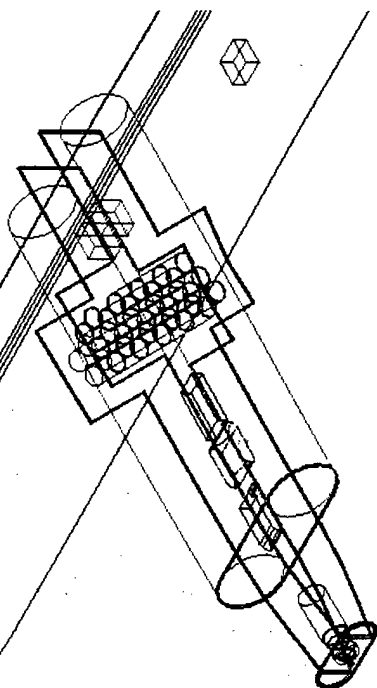
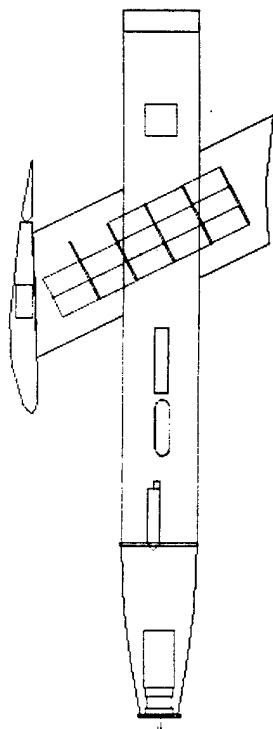
DRAWN BY: BRIAN DOLAN

ALISA HAWKINS

CHECKED BY: JASON ZUMSTEIN

COMPONENTS VIEW

FUSELAGE EXTERIOR, PROPELLOR ASSEMBLY, BOTTOM WING, AND EMPANAGE REMOVED FOR VISIBILITY.



MOTOR	AVEOX 1415-3Y
SPEED CONTROLLER	AVEOX H160C
MOTOR BATTERIES	SANYO N-3000CR (26 CELLS)
SERVOES	FUTABA S9303
RECEIVER	FUTABA PCM

2.0

MANAGEMENT SUMMARY

Before any managerial task could be accomplished, a team had to be formed. Several team members from the 1998/99 competition returned for the fun and excitement one more time, but the desire to introduce more students to an application oriented design project is always present; thus, fliers were posted around campus. This resulted in over 30 students in attendance at the first meeting.

After the second meeting, the design team had streamlined down to a more manageable 13 members. The team is advised by the Director of the Aerospace Systems Design Lab at Georgia Tech, Dr. Dimitri Mavris. Jason Zumstein, an aerospace engineering graduate student, was tasked with managing the undertakings of the design project and overseeing the disciplinary groups. Approximately half of the team has prior aircraft design and or building experience, which made the job of assigning disciplinary leaders easy. Figure 2.1 shows the team organizational structure that is based around a hierarchical subgroups.

During the Fall semester, the entire group met once a week at a time that was convenient to all of the group members. At the first few meetings, the method of approaching the design problem was discussed, which included the development of a timeline by which the team planned to follow. Figure 2.2 shows the amount of time scheduled for each major phase of the design project. Each of the three major design phases, conceptual, preliminary, and detailed, were allocated four weeks for completion. The schedule had all design work to be finished during the fall semester and left building the aircraft and flight testing to be done during the spring semester.

Once the initial stages of Conceptual Design were accomplished and it was time to evaluate feasible aircraft alternatives, the team divided into subgroups. Karen Feigh, an aerospace engineering senior and returning DBF participant, was responsible for leading the conventional monoplane group. Michael Penland, another aerospace engineering senior, took lead of the group that was tasked to evaluate a biplane configuration. Jason Zumstein headed up the delta wing group. These subgroups scheduled times to work on their individual designs and met weekly with the entire group to discuss current progress. By having all of the group members participate in small design groups, each person was able to see all of the different aircraft disciplines interacting together. This was considered very important; when each person went to a specific discipline to work on the chosen concept, that person would better understand the big picture.

After the conceptual phase, group members that felt confident heading up one of the disciplinary areas were placed in charge of keeping the other groups aware of their groups current design parameters. Email was an extremely valuable way to communicate between all group members and have the current design data available to all. The structures and weights group researched construction materials and performed simple stress analyses for the major structural components using ranges of values for weights and loads. Airfoil data research and the design of a performance spreadsheet made of the responsibilities of the aerodynamics and performance groups respectively. The propulsion group was responsible for locating manufacturers of electric motors, batteries, and propellers as well as attaining data for candidate products. The solid modeling group became very busy during the detailed design phase keeping the model up to date with current configuration.

When the building process began in the spring semester, times were set aside throughout the week for groups to meet and build. The building process was divided up into three main

groups: fuselage, wings, and empennage. Each of these groups contained 3 to 4 team members that were solely responsible for their assembly. By having each building group small, the level of congestion in the construction facility was kept to a minimum. Additionally, an all hands meeting was scheduled every Tuesday night to discuss the current construction process and the goals for the next week.

One difficulty that was ever present during the early stages of construction was that the design was somewhat fluid. Design decisions were often made just to meet a deadline rather than because the team felt confident about the solution. When an obviously better way of doing something was discovered, the team could not keep the original idea anymore. Thus, work that had already been done towards the construction of the aircraft was sometimes lost. From inspection of Figure 2.2, the fluid design is evident by the continuation of the detailed design phase along side the manufacturing plan.

Throughout the design process, group members came and went. Several of the members on the team are coop students who work to far away from school to participate during either the Fall or Spring semesters. The students that participate in the Fall understand why the aircraft design is the way it is, but these students are not present with that knowledge during the building and flight testing phase. Students that participate in the Spring suffer the hardships of trying to build an aircraft that is not completely familiar to them. Most of the seniors on the team are involved in Georgia Tech's demanding senior design project. During the Fall semester, the seniors were able to contribute to the DBF cause, but when the Spring semester began, their work load was too overwhelming for them to continue as active team members, and the younger members of the team were forced to take on more active leadership positions.

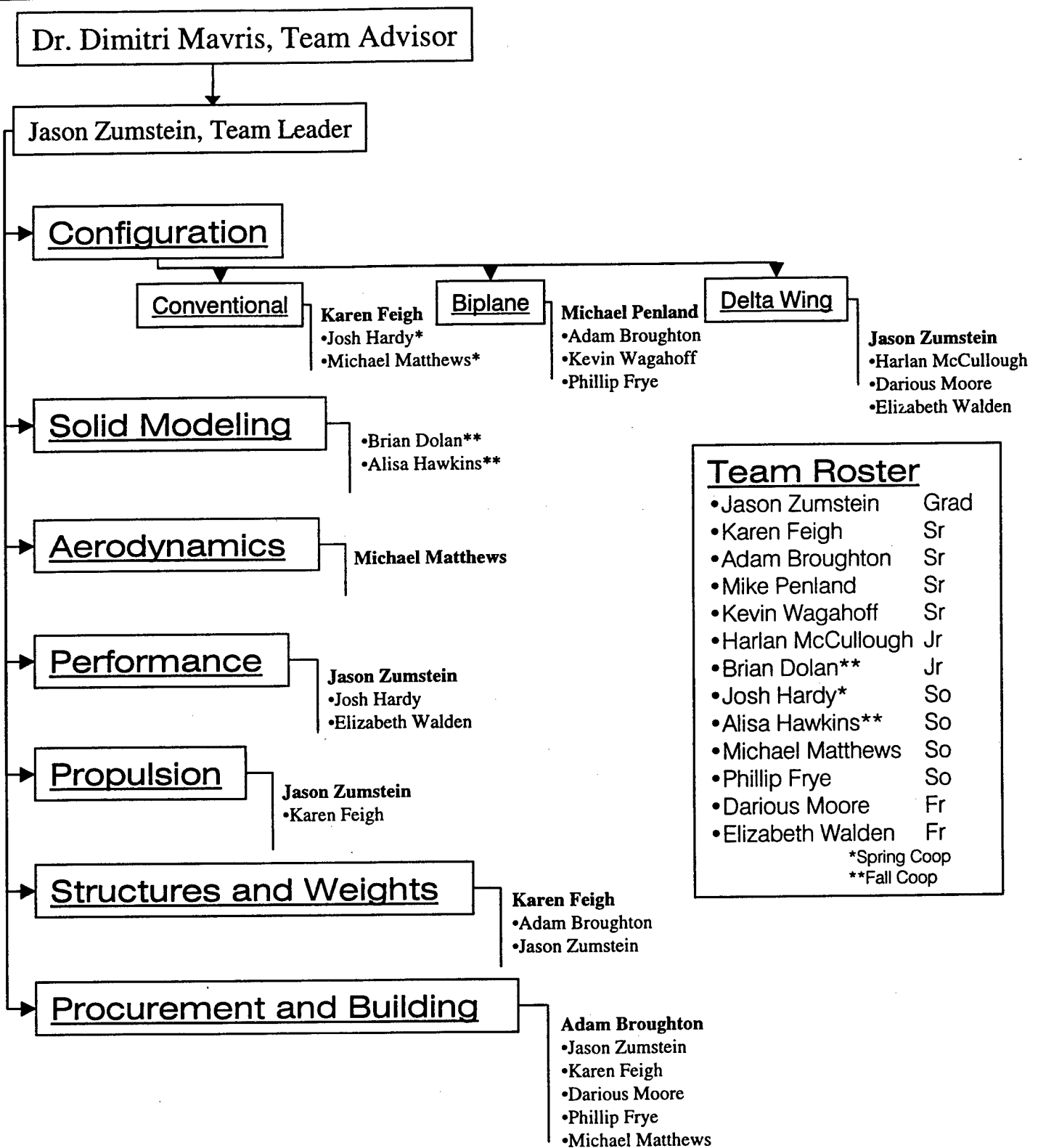
TEAM STRUCTURE

Figure 2.1: Design Team Organizational Structure

TIMELINE

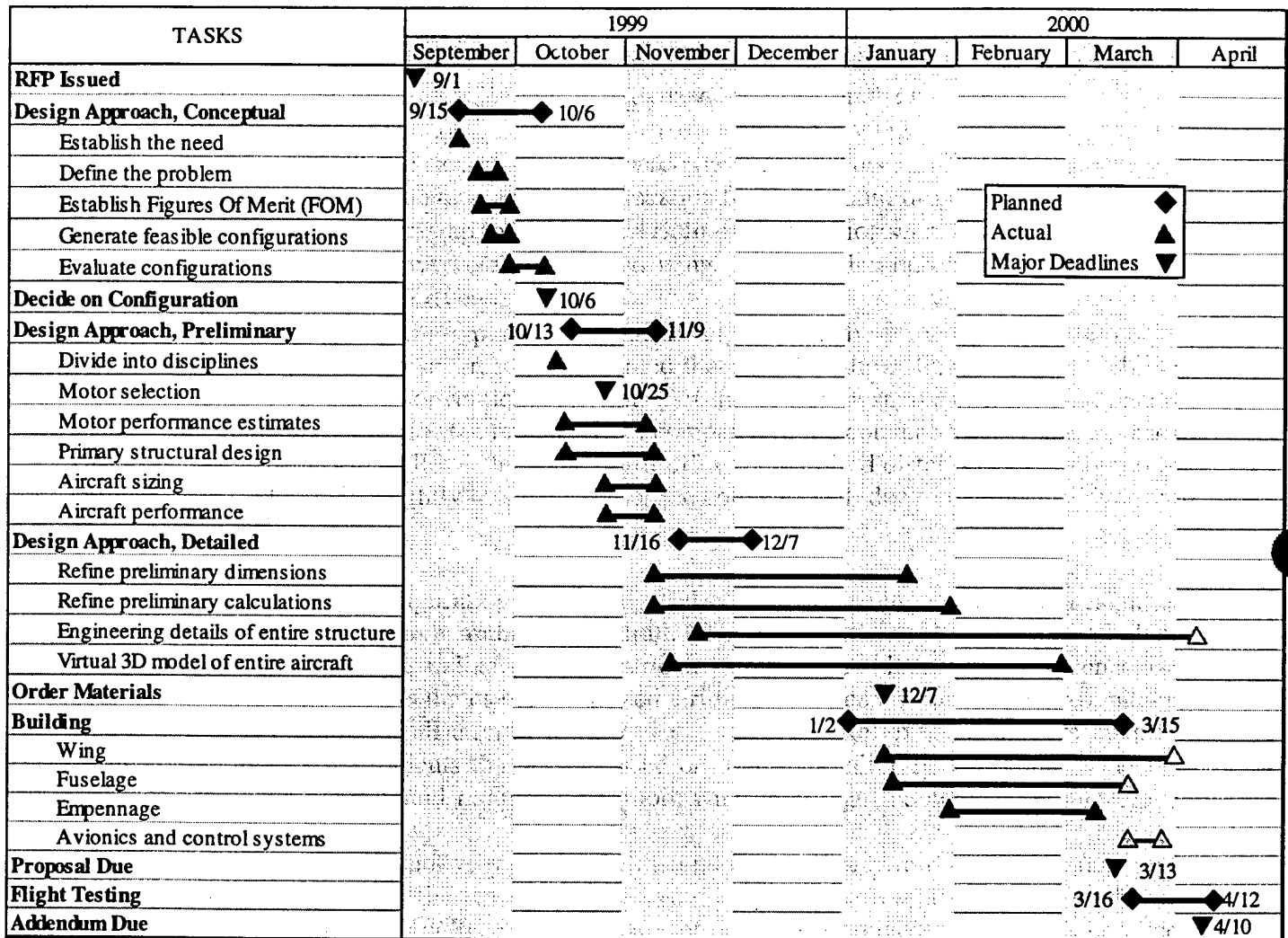


Figure 2.2: Planned and Actual Schedule

3.0

CONCEPTUAL DESIGN

3.1 Problem Definition

The first step in the design process was to define the problem presented in the request for proposal (RFP). The RFP was examined for the major features of the contest. The plane specifications include a limited wing span of only seven feet, a battery pack limitation of five pounds, and a requirement for fully fared cargo bay. The contest location is in Wichita, Kansas, which indicated windy weather conditions. The total flight score takes into account an extensive rated cost model, the number of liters of water carried in the allotted time period, and the report score.

Mission

The RFP indicated that the aircraft mission was to carry as many liters as possible around a specified course in a ten minute time period. This year the mission was to consist of cargo sorties and ferry sorties, which were to be flown alternately, with only the cargo sortie providing score. Both sorties are described in detail in Figure 3.1 and Table 3.1. In the cargo sortie, the aircraft was to carry between two and eight liters, and be given a score based on how many liters were successfully carried in the time period. In the ferry sortie, the aircraft was to carry no cargo and awarded no score. Thus the aircraft would have to be designed to fly a dual mission.

Design Driving Factors

Next, the RFP was analyzed to determine the factors which would impose the most constraints on the design, or in other words, the factors which most drive the design. The obvious design driver, was the rated aircraft cost model (RAC). Due to its large and direct impact on the total flight score, the cost model was carefully analyzed to determine how each aspect of the design contributed to it. This information was later used to help pare down initial concepts. The next significant design driver was the limited electric motor. This limitation results in a tradeoff between thrust and powerplant endurance, and consequently the ability to takeoff with the desired cargo in the specified distance during later sorties. Another major concern was the takeoff field length coupled with the limited wing span. The cargo capacity of the aircraft is directly related to the wing area, therefore reduced wing span was a significant concern. The last design driving factor was the time limit. The time limit would greatly affect the overall mission strategy, because the alternating sorties reduce the number of sorties which will count for score. If there will not be enough time to fly five cargo sorties, then the powerplant can be designed to provide more thrust and less endurance to allow for greater cargo capacity.

Mission Features

The overriding mission feature was the Total Flight Score (TFS) it encompassed virtually every aspect of the design. Due to the dominance of the TFS important key features of the mission were tracked which contributed to the total flight score. The key mission features considered were:

- | | |
|-----------------------|--------------------------------|
| ◆ Wingspan Limitation | ◆ TOGW Limitation |
| ◆ Time Limit | ◆ Commercially Available Parts |
| ◆ Electric Power | ◆ Cargo Location |

- ◆ TOFL Limitation
- ◆ Rated Aircraft Cost Model
- ◆ Cargo Sortie
- ◆ Ferry Sortie
- ◆ Minimum Cargo Capacity

3.2 Figure of Merit Definition

The figures of merit (FOM) were chosen to compare the different configurations based upon the mission features stated earlier. (See Figure 3.2) While compiling the figures of merit, it was assumed that the final design would be able to complete the minimum mission requirements regardless the configuration chosen. Additionally the best power plant available would be used in all configurations, because once the power plant was determined the aircraft would be designed around it. The FOMs are broken into nine categories, and those used in the conceptual design phase are as follows:

- ◆ Rated Aircraft Cost
- ◆ C_{Lmax}
- ◆ Turn Around Time
- ◆ Takeoff Field Length (TOFL)
- ◆ Complexity
- ◆ Turn Rate
- ◆ Side-profile Area
- ◆ Height of Center of Gravity
- ◆ Cruise Velocity (V_{cr})

The rated aircraft cost (RAC) directly affected the total flight score, and was computed using the model stated in the RFP. C_{Lmax} was defined by the airfoil and wing during takeoff configuration. TOGW is the weight of the aircraft at takeoff and included the design parameters payload weight and empty weight. Cruise velocity is the velocity at half throttle, which is assumed velocity at cruise. Turning rate is the rate of a level, sustained turn at cruise velocity and full power. Takeoff field length is the distance needed to go from a complete stop to all wheels off the ground. Side profile area is the wetted area of the aircraft when viewed from its side. The height of the center of gravity is the distance from the ground to the aircraft's center of gravity. Turn around time is the time between sorties, in which the payload must be either loaded or unloaded and the plane repositioned for takeoff. Complexity was defined as the amount of time necessary to build the aircraft, and the number of components necessary to build the aircraft.

The interaction between the mission features and the figures of merit were investigated and summarized in Figure 3.2. The FOMs in bold are used in the conceptual design phase to compare the different configurations.

3.3 Prescreening Analysis

Before the configuration selection began, a preliminary analysis of the Total Flight Score (TFS) was conducted since this was determined to be the overriding mission feature. This analysis was intended to give the team direction during the configuration identification, analysis, and selection, and was conducted via an Excel model. A TFS workbook was constructed to accurately compare different configurations. The workbook consisted of three worksheets: rated aircraft cost model (RAC) spreadsheet, performance spreadsheet, and total flight score spreadsheet. The RAC spreadsheet calculated the costs based on configuration parameters such as number of wings, number of engines, wing area, etc. The performance spreadsheet was linked to the RAC spreadsheet and calculated the number of laps and thus the number of liters it was

possible to carry in the time period. All of this data was imported into the TFS spreadsheet, so that based on a given report score different configurations of aircraft could be compared.

After running several test configurations through the TFS spreadsheet the following conclusions were gleaned. First, because of the initial cost per part, the RAC spreadsheet illustrated the penalties for multiple motors, wings, servos, etc. It was clear that the simpler and the smaller the design, the lower the RAC for the aircraft would be.

Based on these findings, a comparison between a smaller, faster aircraft and a larger, slower aircraft was conducted. This comparison is illustrated in Figure 3.3 and Table 3.2. From this study it was determined to be impossible to carry the same number of liters with a smaller aircraft unless the aircraft could fly much faster than the larger aircraft, at unfeasible. The analysis also indicated that due to the time limitation in combination with the ferry sortie requirement, a bigger, slower aircraft would provide a higher total flight score. Thus efforts were focused to identify a configuration for an aircraft which could carry six liters of water. Six liters of water was chosen as the maximum amount of water that could be realistically carried by this size of aircraft.

3.4 Configuration Identification

Based on the contest objectives and the FOMs, common design points were chosen for all configurations. All alternative configurations were based around these common design points to normalize all configurations, thereby ensuring an equal comparison between alternatives. The configurations would have a propulsion system weighing seven pounds, including only one motor, capable of producing eight pounds of thrust. It would have a seven foot wingspan, and be capable of carrying six liters of water. It would have an endurance of four cargo sorties fully loaded in addition to three unloaded ferry sorties, aircraft speed permitting. From these common design points three different configurations were identified: conventional monoplane, biplane, and delta wing. See Figure 3.4 for a picture of each concept. Justification for each of the three configurations is summarized below.

Conventional

The conventional aircraft was chosen as a potential configuration because of the historical familiarity with the design. A conventional aircraft is stable with either high or low wing variations, and it is simple and easy to build. A conventional aircraft provides ease of access to payload, especially with a low wing configuration. In addition a conventional aircraft allows for the use of high lift devices, crucial to providing the lift necessary for the cargo sorties while maintaining a high cruise velocity necessary for the ferry sorties.

Biplane

A biplane was chosen as a possible configuration because of its unique adaptation to limited wing span situations. It is possible for a biplane to obtain a higher amount of lift for a given wing area and aspect ratio than a conventional plane of similar area and aspect ratio because the individual wings of the biplane have higher aspect ratios. A higher aspect ratio in turn produces a better three dimensional lift coefficient.

Delta Wing

A delta wing aircraft configuration was considered because it lacks both a fuselage and a horizontal tail, thus greatly reducing its rated aircraft cost. The delta wing also has the added bonus of being extremely simple to build, and has a large cargo bay standard. A thin streamlined cross section makes it desirable from a cross wind stand point.

3.5 Configuration Analysis

Due to the nature of the rated aircraft cost, identifying the right configuration was crucial early in the design process. In order to do this, however, a relatively detailed analysis of each different configuration had to be carried out to adequately compare the configurations. The analysis was broken into three subgroups, one for each configuration. The different configuration's design characteristics were further researched, and each configuration was taken through an initial sizing iteration based on the common design points established earlier. From there basic performance calculations to obtain values for FOMs and design parameters were carried out, and the configurations were compared. During this analysis and comparison several analytical methods and tools were used. These methods and tools included a cost model spreadsheet, a takeoff distance spreadsheet, and a drag buildup spreadsheet. Derived from the baseline design points, some of the design parameters had been standardized, while others were allowed to vary. Again, this allowed the different configurations to be normalized and therefore equally compared.

Analytical Tools

Cost model spreadsheet

The cost model spreadsheet, which was described in detail in the prescreening analysis, was used again during this phase of the design. This time the spreadsheet was used to compare designs, and many more details were investigated such as the number of servos, and the size of the wings and fuselage.

Takeoff Distance Spreadsheet

The takeoff distance spreadsheet was based on Newton's second law and involved an iterative process to calculate velocity, thrust, and acceleration over a given time step. The inputs to the spreadsheet are the aircraft take off gross weight, the max lift coefficient of the wing, the wing area, and the estimated parasite drag coefficient. The output of the spreadsheet is the takeoff distance. Using this spreadsheet, the configurations were sized to meet the takeoff requirement by changing the wing dimensions. This spreadsheet was used to size the different wings configurations.

Drag Spreadsheet

The drag buildup spreadsheet was based on basic induced and parasite drag calculations. This spreadsheet was used to compare the conventional to the biplane, because it only compared the wings of the two configurations. All other aspects of the two aircraft were considered comparable, because the biplane and the conventional configurations were assumed to have the same fuselage and empennage. The inputs for the spreadsheet were wing area, aspect ratio, chord length, thickness to chord and velocity. The outputs were parasite drag and induced drag. In this spreadsheet care was taken to account for the additional drag terms associated with a biplane. This spreadsheet was used to compare the drag associated with the biplane and the conventional designs.

Independent Analysis

Conventional

The conventional group was initially faced with what type of configuration to choose for their aircraft, mainly high wing or low wing. A high wing aircraft is more stable than a low wing, especially in the absence of dihedral. However, a low wing will allow easier accessibility to the water bottle payload. At closer inspection, it was realized that at this point in the design

process, the differences between low wing and high wing were negligible. The main issue with the conventional aircraft came down to the efficiency and lifting capabilities of a single 7 ft wing.

Using the generic thrust model that was provided to all of the conceptual design groups, a drag coefficient of .05 was assumed and the aircraft weight and wing area were varied to find the maximum weight that could lift off in the 100 foot field requirement. It was found that a 14 square foot low aspect ratio wing would be required to lift a 30 pound plane off the ground within the field requirements if a C_L of 1.7 could be obtained.

From this analysis, several questions were raised. First, how much does aspect ratio affect lift and drag? Research showed that the three dimensional lift coefficient decreases at a given angle of attack as the aspect ratio of a wing decreases. Also, induced drag increases significantly as the aspect ratio decreases. To make the wing more efficient, winglets or endplates would be required. These devices could effectively increase the aspect ratio, thus increasing the three dimensional lifting capabilities of the wing and reduce the induced drag. An optimal taper ratio for a straight taper wing is .43 (Anderson⁵), which means that the tip chord is 43% of the root chord. This type of taper will result in a nearly elliptical lift distribution for the wing, thus increasing the efficiency. Although maximizing the wing efficiency seems like good idea, on closer inspection of the desired wing area and given wing span, the resulting wing would have a root chord of nearly 3 feet! This would result in a very high volume wing with considerable unnecessary weight.

Uncertainty abounded with the aerodynamic behavior of the low aspect ratio wing required of the conventional aircraft. Nonetheless, the conventional plane was designed as well as could be given the stage of the design process. Table 3.3 shows the final aircraft parameters and rated aircraft cost. The weight of the conventional aircraft was determined based on experience obtained during last years competition and from contemporary model aircraft in this size category.

Biplane

The wings of a biplane aircraft work together with a given amount of interference to produce an increased amount of lift over a similarly designed monoplane. According to Munk⁶ a certain small increase in drag over the monoplane design also exists; however, this drag is significantly smaller than the lift produced by the wings giving merit to the biplane design philosophy. On the contrary, Raymer⁴ indicates that a biplane produces 30% less drag due to lift than a conventional monoplane of equal span. This is due to the fact that induced drag is dependent upon lift squared, and in the case of a biplane, each wing is producing half of the lift of the wing on a monoplane, thus resulting in half of the induced drag. However, this half reduction of drag is not completely realized because of some interference effects between the wings. Some parameters that determine the efficiency of a biplane's wings are the weight of the wings, the stagger of the wings, and the gap distance between the two biplane wings.

The biplane has significant advantages over other configurations in terms of the weight of the finished aircraft. If span-wise, as well as vertical bracing are used between the wings, the combined pair can be treated much like single beam with each individual wing carrying bending loads and the bracing carrying shear loads. If lateral inter-wing bracing is not used, smaller weight advantages can still be realized. The use of only inboard and outboard inter-wing struts/plates gives the aircraft wings much higher torsion stiffness compared to unbraced wings of comparable weight and design. This is because the wings and bracing now form an open box when viewed from the aircraft front. If the end plates/braces on the wings can carry bending

moments at the wing/brace joint then some additional weight savings can be realized because now the braces carry shear loads between the two wings.

Stagger is another important quantity that helps change the aerodynamic efficiency of a biplane and restrict the motion of the center of pressure. Stagger is measured by the position of the top wing in front of or behind the lower wing along the longitudinal axis. In a biplane design, the influence of the lower wing on the upper wing is significant. Due to interaction with the flow around the lower wing the upper wing operates in a region of turbulence. Thus, the forces on the upper wing are reduced over those of the lower wing. In order to increase the effectiveness of the upper wing, a positive stagger (upper wing forward of the lower wing) can be introduced to some extent without losing the benefits of the biplane design. Increasing the stagger in the positive direction also tends to equalized the loads on the two wings.

Another important factor in the efficiency of a biplane's wings is the wing spacing, or gap ratio. The gap is the vertical distance between the wings. This is affected by the angle of attack of the wings. Again there is an optimal location for the amount of gap. It is dependent on the gap to chord ratio and the gap to span ratio. Both of these ratios seem to be a good measure of the interaction of the flows between the two wings and are also dependent on the angle of attack at which the wings are flying.

When investigating flight performance of the biplane, many of the biplanes strengths are not directly quantifiable; however, it was assumed that a higher three dimension lift coefficient could be achieved over the conventional aircraft. For this reason, a smaller wing would result in an equivalent amount of lift for the biplane when compared to the conventional. Table 3.3 shows the biplane parameters that allows the plane to lift off in the required distance. The weight of the biplane is expected to be slightly less than that of the conventional, due to the much lighter wing construction.

Delta wing

The delta wing configuration has a low level of complexity involved in the design, and fewer components than a more traditional aircraft. These features result in an aircraft that is easier to build. However, unlike more traditional aircraft, the delta wing's absence of a horizontal stabilizer warrants the use of a reflexed airfoil to produce a positive, nose up, pitching moment that is required of all aircraft to have static stability. Reflexed airfoils are unable to achieve the high lift coefficients that airfoils used on traditional aircraft can obtain. Due to of this fact, the delta wing would require much more wing area than the convention and biplane configurations.

High lift devices are not very feasible with delta wing aircraft from a stability stand point. When flaps are deflected, the camber of a wing is increased, which increases the lift. Additionally, when flaps are deflected, a negative, or nose down, pitching moment is produced. This negative pitching moment produced by flaps will negate the effects of a reflexed airfoil used on a delta wing and will make the aircraft statically unstable.

To provide control authority for a delta wing, control surfaces located on the trailing edge of the wing are used. If it is desired to pitch the aircraft up, then the trailing edge control surfaces must be deflected upward, reflexing the airfoil further, to produce a positive pitching moment. This is equivalent to deflecting a wing flap upward, which of course will decrease the amount of lift produced. This pitch/lift coupling is very important during takeoff when maximum lift is desired, but the aircraft must rotate, or pitch up, to get to the proper attitude to obtain the desire lift, thus decreasing lift.

Using lift coefficient data obtained from typical reflexed airfoils, and ignoring the adverse pitch/lift effects, the delta wing was sized to meet the takeoff field requirements. Table 3.3 shows the large required wing area and the resulting high rated aircraft cost for a delta wing aircraft that is capable of lifting a six liter payload. The airframe weight for the delta wing was estimated to be close to the weight of the conventional aircraft, although the enormous wing area would most likely result in an even greater airframe weight.

Analysis Conclusions

From the analyses performed, several lessons were learned. First, the delta plane had too much wing area to be economically feasible. It cost fifteen percent more than the conventional aircraft configuration. Second, the cost of a biplane configuration was actually less than that of the conventional configuration. The same number of servos could be used, and the cost of the two thin wings was comparable to the cost for the one large wing. Third, the drag of the biplane with out struts and wires, was similar drag to a thick wing conventional aircraft. Lastly, from the takeoff spreadsheet it was discovered that the conventional plane's wing must be tapered and have winglets, in addition to having a two and a half foot root wing chord in order to meet the takeoff distance requirement. The final sizes of the different configurations can be found in Table 3.3. The drawbacks to each configuration discovered by each analysis are summarized below.

3.6 Configuration Evaluation

Quantitative FOM Evaluation

The quantitative figures of merit of each of the configurations were calculated and inserted into the top of Table 3.4 for a comparison. The rated aircraft cost comparison was conducted using the cost model spreadsheet. The specifications for each configuration were entered and both the rated aircraft cost and the total flight score were computed. From Table 3.4 it is obvious that the cost of the delta wing far outweighs the cost of either the biplane or conventional configuration. The $C_{L_{max}}$ and the height of the center of gravity were estimated independently due to special considerations specific to each configuration. The conventional and delta wing configurations proved to be the simplest to calculate $C_{L_{max}}$ with basic aerodynamic equations from Anderson⁵ for swept wing being used. The biplane used several rules-of-thumb and correction factors to modify traditional aerodynamic equations. (Munk⁶) Both the RAC and the TOFL were directly calculated by the analytical tools mentioned previously.

Qualitative FOM Evaluation

The last five figures of merit in Table 3.4 were qualitatively analyzed by as a whole. Each configuration was presented and the turn rate, turn around time, side profile area, cruise velocity and the complexity were all thoroughly compared. After the comparison each configuration was ranked against one the others for each figure of merit. The rankings for turn rate and cruise velocity FOMs were estimated for each configuration based on past experience and the outputs of the analytical tools. Turn around time was ranked based on the ease of access to the cargo each configuration provided, in addition to the ease of repositioning the aircraft before each sortie. Side profile area was ranked by visually comparing the different configuration's profile. Complexity was rather straight forward, the more components and special situations which a configuration required the more difficult it would be to build.

Configuration Ranking

After the evaluation phase was complete, the values of the different figures of merit for each configuration were ranked, in Table 3.5 with a score of three being most desirable, and one being least desirable. Next weights were assigned to each figure of merit to help show quantitatively which configuration best met the needs of the mission. The ranking of each figure of merit was multiplied by its assigned weight and then the total for each configuration was computed. These totals were then normalized by the highest possible total, and are located in Table 3.6

Conclusions

As can be seen in Table 3.5 the figures of merit for the biplane and the conventional configurations rated very similarly. The delta wing, however, did not rate as well. Although the delta wing configuration had a low level of complexity, it required an airfoil with a positive pitching moment, which limited its C_{Lmax} . Thus, at least twice as much wing area as a conventional configuration was needed to provide the same amount of lift. When this was factored into the cost model, the benefits of not having a fuselage or horizontal stabilizer were negated and the cost of a delta wing configuration was actually significantly more than either the conventional or biplane configurations. For this reason the delta wing was not chosen as the final configuration.

As seen in Table 3.6 the Biplane configuration had the highest score at 0.79, significantly more than the conventional configuration, which had a score of 0.71. At first this is surprising because it was originally thought that the biplane would not rate as well as the conventional configuration in the RAC. After the sizing and analysis, however, it was discovered that the biplane actually cost less to build than the conventional plane because the single large wing cost more than two smaller wings, and that both planes would use the same number of servos. The biplane configuration also had some other advantages over the conventional plane. The biplane has a greater effective aspect ratio, and therefore produced less drag and allowed the possibility to size the design up for eight liters if necessary. The biplane also allows more room for propeller clearance, which was especially important to maximize the propulsion system efficiency. It was concluded that although either the conventional or the biplane could complete the mission carrying six liters per sortie, that the biplane configuration had a higher probability of success. Therefore the biplane configuration was chosen to proceed to preliminary design.

Table 3.1: Tabular Sortie Description

Ferry Sortie

Segment	Description
Takeoff	Stop to all wheels off the ground in 100 ft.
Upwind Leg	500 ft. from start
Turn	180° Turn
Downwind Leg	1000 ft.
Turn	180° Turn
Upwind Leg	1000 ft.
Turn	180° Turn
Downwind Leg	500 ft.
Turn	180° Turn
Upwind Leg	500 ft.
Land	Must land with in 100 ft. of starting point.

Cargo Sortie

Segment	Description
Takeoff	Stop to all wheels off the ground in 100 ft.
Upwind Leg	500 ft. from start
Turn	180° Turn
Downwind Leg	500 ft.
Turn	360° Turn
Downwind Leg	500 ft.
Turn	180° Turn
Upwind Leg	500 ft.
Land	Must land with in 100 ft. of starting point.

Table 3.2: Comparison of Large v. Small Aircraft

	4 Liters	6 Liters	6 Liters	8 Liters
Average Speed Cargo (ft/s)	87	44	59	38
Average Speed Ferry (ft/s)	94	53	70	40
Total Number of Sorties	9	5	7	5
Score	200	180	240	240

Table 3.3: Final Configuration Parameters

	Conventional	Biplane	Delta Wing
C_{Lmax}	1.8	2	1
$C_{D,0}$	0.5	0.5	0.5
Wing Area (ft. ²)	16	14	36
Fuselage Length (ft.)	5	5	--
Empty Weight (lbs.)	9	8	9
Payload Capacity (liters)	6	6	6

Table 3.4: Figure of Merit Data

		Conventional	Biplane	Delta Wing	
Figures of Merit	Quantitative	Rated Aircraft Cost	5.43	5.31	6.424
		C_{Lmax}	1.5	1.7	0.8
		TOFL (ft)	95	90	98
		Height of CG (in.)	12	14	11
	Qualitative	Turn Rate (fps)	2	1	3
		Turn Around Time	2	1	3
		Side Profile Area	2	2	3
		Cruise Velocity	3	2	1
		Complexity	2	1	3

1 Worst 2 Average 3 Best

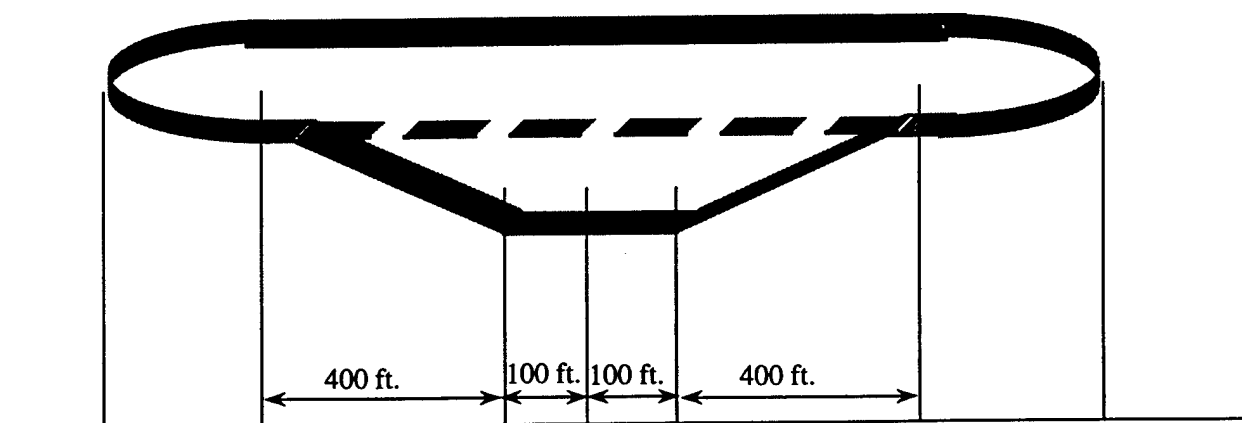
Table 3.5: Figure of Merit Comparison

		Conventional	Biplane	Delta Wing
Figures of Merit	Rated Aircraft Cost	2	3	1
	C_{Lmax}	2	3	1
	TOFL	2	3	1
	Height of CG (in.)	2	1	3
	Turn Rate (fps)	2	3	1
	Turn Around Time	2	1	3
	Side Profile Area	2	1	3
	Cruise Velocity	3	2	1
	Complexity	2	1	3

Table 3.6: Weighted Configuration Comparison

		Conventional	Biplane	Delta Wing	Rating
Figures of Merit	Rated Aircraft Cost	2	3	1	10
	C_{Lmax}	2	3	1	5
	TOFL	2	3	1	5
	Turn Around Time	2	1	3	5
	Cruise Velocity	3	2	1	5
	Turn Rate (fps)	2	3	1	4
	Height of CG (in.)	2	1	3	2
	Side Profile Area	2	1	3	2
	Complexity	2	1	3	1
	Normalized Total	0.71	0.79	0.50	

Ferry Sortie



Cargo Sortie

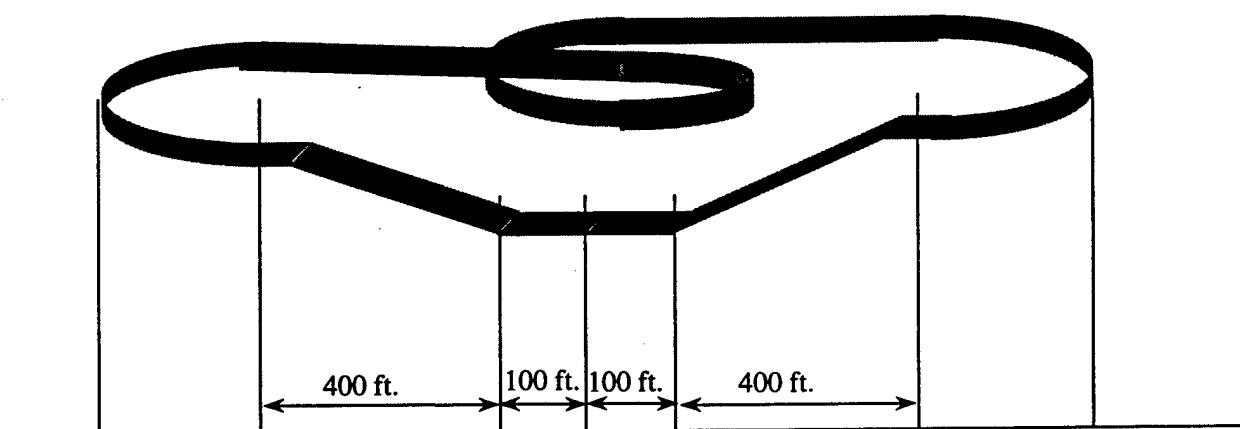


Figure 3.1: Graphical Sortie Description

DIRECTION OF IMPROVEMENT												IMPORTANCE												COMPETITIVE ANALYSIS																																																																																																																																																																																																																																																																																																																																																																																																																																																																																																																																																																																																																																																																																																																																																																																																																																																																																																																																																																																																																																																																																																																																											
Figures of Merit						Mission Features						Performance						Stability and Control																																																																																																																																																																																																																																																																																																																																																																																																																																																																																																																																																																																																																																																																																																																																																																																																																																																																																																																																																																																																																																																																																																																																																	
Mission Specifications		Propulsion		Empennage		Fuselage		Wing		Landing Gear		Procurement and Production		Operation and Support		Performance						Stability and Control		Conventional	Biplane																																																																																																																																																																																																																																																																																																																																																																																																																																																																																																																																																																																																																																																																																																																																																																																																																																																																																																																																																																																																																																																																																																																																										
		Weight	Number of Motors	Current Draw	Configuration	Horizontal Stabilizer	Vertical Stabilizer	Structures	Cargo	Accessability	Batteries	Rated Cost	Engines	Shape	Flaps	Structure	Configuration	Brakes	Loads	Damping	Time Constraint	Complexity	Spare			Accessability	Repairability	Wing Attachment	Transportability	Takeoff Distance	Landing Distance	Turn Rate	Cruise Velocity	L/D max	Rate of Climb	Endurance	Stall Speed	TMT	Height of c.g.	Side Profile Area	Good Handling	Control Power																																																																																																																																																																																																																																																																																																																																																																																																																																																																																																																																																																																																																																																																																																																																																																																																																																																																																																																																																																																																																																																																																																																									
Max. 7ft. Wingspan		5	5	5	5	5	5	5	5	5	5	5	5	5	5	5	5	5	5	5	5	5	5	5	5	5	5	5	5	5	5	5	5	5	5	5	5	5	5	5	5	5	5	5	5	5	5	5	5	5	5	5	5	5	5	5	5	5	5	5	5	5	5	5	5	5	5	5	5	5	5	5	5	5	5	5	5	5	5	5	5	5	5	5	5	5	5	5	5	5	5	5	5	5	5	5	5	5	5	5	5	5	5	5	5	5	5	5	5	5	5	5	5	5	5	5	5	5	5	5	5	5	5	5	5	5	5	5	5	5	5	5	5	5	5	5	5	5	5	5	5	5	5	5	5	5	5	5	5	5	5	5	5	5	5	5	5	5	5	5	5	5	5	5	5	5	5	5	5	5	5	5	5	5	5	5	5	5	5	5	5	5	5	5	5	5	5	5	5	5	5	5	5	5	5	5	5	5	5	5	5	5	5	5	5	5	5	5	5	5	5	5	5	5	5	5	5	5	5	5	5	5	5	5	5	5	5	5	5	5	5	5	5	5	5	5	5	5	5	5	5	5	5	5	5	5	5	5	5	5	5	5	5	5	5	5	5	5	5	5	5	5	5	5	5	5	5	5	5	5	5	5	5	5	5	5	5	5	5	5	5	5	5	5	5	5	5	5	5	5	5	5	5	5	5	5	5	5	5	5	5	5	5	5	5	5	5	5	5	5	5	5	5	5	5	5	5	5	5	5	5	5	5	5	5	5	5	5	5	5	5	5	5	5	5	5	5	5	5	5	5	5	5	5	5	5	5	5	5	5	5	5	5	5	5	5	5	5	5	5	5	5	5	5	5	5	5	5	5	5	5	5	5	5	5	5	5	5	5	5	5	5	5	5	5	5	5	5	5	5	5	5	5	5	5	5	5	5	5	5	5	5	5	5	5	5	5	5	5	5	5	5	5	5	5	5	5	5	5	5	5	5	5	5	5	5	5	5	5	5	5	5	5	5	5	5	5	5	5	5	5	5	5	5	5	5	5	5	5	5	5	5	5	5	5	5	5	5	5	5	5	5	5	5	5	5	5	5	5	5	5	5	5	5	5	5	5	5	5	5	5	5	5	5	5	5	5	5	5	5	5	5	5	5	5	5	5	5	5	5	5	5	5	5	5	5	5	5	5	5	5	5	5	5	5	5	5	5	5	5	5	5	5	5	5	5	5	5	5	5	5	5	5	5	5	5	5	5	5	5	5	5	5	5	5	5	5	5	5	5	5	5	5	5	5	5	5	5	5	5	5	5	5	5	5	5	5	5	5	5	5	5	5	5	5	5	5	5	5	5	5	5	5	5	5	5	5	5	5	5	5	5	5	5	5	5	5	5	5	5	5	5	5	5	5	5	5	5	5	5	5	5	5	5	5	5	5	5	5	5	5	5	5	5	5	5	5	5	5	5	5	5	5	5	5	5	5	5	5	5	5	5	5	5	5	5	5	5	5	5	5	5	5	5	5	5	5	5	5	5	5	5	5	5	5	5	5	5	5	5	5	5	5	5	5	5	5	5	5	5	5	5	5	5	5	5	5	5	5	5	5	5	5	5	5	5	5	5	5	5	5	5	5	5	5	5	5	5	5	5	5	5	5	5	5	5	5	5	5	5	5	5	5	5	5	5	5	5	5	5	5	5	5	5	5	5	5	5	5	5	5	5	5	5	5	5	5	5	5	5	5	5	5	5	5	5	5	5	5	5	5	5	5	5	5	5	5	5	5	5	5	5	5	5	5	5	5	5	5	5	5	5	5	5	5	5	5	5	5	5	5	5	5	5	5	5	5	5	5	5	5	5	5	5	5	5	5	5	5	5	5	5	5	5	5	5	5	5	5	5	5	5	5	5	5	5	5	5	5	5	5	5	5	5	5	5	5	5	5	5	5	5	5	5	5	5	5	5	5	5	5	5	5	5	5	5	5	5	5	5	5	5	5	5	5	5	5	5	5	5	5	5	5	5	5	5	5	5	5	5	5	5	5	5	5	5	5	5	5	5	5	5	5	5	5	5	5	5	5	5	5	5	5	5	5	5	5	5	5	5	5	5	5	5	5	5	5	5	5	5	5	5	5	5	5	5	5	5	5	5	5	5	5	5	5	5	5	5	5	5	5	5	5	5	5	5	5	5	5	5	5	5	5	5	5	5	5	5	5	5	5	5	5	5	5	5	5	5	5	5	5	5	5	5	5	5	5	5	5	5	5	5	5	5	5	5	5	5	5	5	5	5	5	5	5	5	5	5	5	5	5	5	5	5	5	5	5	5	5	5	5	5	5	5	5	5	5	5	5	5	5	5	5	5	5	5	5	5	5	5	5	5	5	5	5	5	5	5	5	5	5	5	5	5	5	5	5	5	5	5	5	5	5	5	5	5	5	5	5	5	5	5	5	5	5	5	5	5	5	5	5	5	5	5	5	5	5	5	5	5	5	5	5	5	5	5	5	5	5	5	5	5	5	5	5	5	5	5	5	5	5	5	5	5	5	5	5	5	5	5	5	5	5	5	5	5	5	5	5	5	5	5	5

Strong +
Medium ○
Weak △

Figure 3.2: Quality Function Deployment Matrix

4 Liters (Fast)		6 Liters (Slow)	
Lift		Lift	
Number of Sorties	9	Number of Sorties	5
Cargo Sortie		Cargo Sortie	
Average Speed (ft/s)	108	Average Speed (ft/s)	44
Takeoff Velocity (ft/s)	32	Takeoff Velocity (ft/s)	32
Ground Time (s)	25	Ground Time (s)	25
Turning Rate (ft/s)	46	Turning Rate (ft/s)	46
Turning Radius (ft)	48	Turning Radius (ft)	48
Gross Weight (lbs)	32	Gross Weight (lbs)	32
Cargo (liters)	4	Cargo (liters)	6
Cargo Weight (lbs)	10	Cargo Weight (lbs)	15
Ferry Sortie		Ferry Sortie	
Average Speed (ft/s)	130	Average Speed (ft/s)	53
Takeoff Velocity (ft/s)	23	Takeoff Velocity (ft/s)	23
Ground Time (s)	25	Ground Time (s)	25
Turning Rate (ft/s)	48	Turning Rate (ft/s)	48
Turning Radius (ft)	41	Turning Radius (ft)	41
Gross Weight (lbs)	15	Gross Weight (lbs)	15

6 Liters (Fast)		8 Liters (Slow)	
Lift		Lift	
Number of Sorties	7	Number of Sorties	5
Cargo Sortie		Cargo Sortie	
Average Speed (ft/s)	59	Average Speed (ft/s)	38
Takeoff Velocity (ft/s)	32	Takeoff Velocity (ft/s)	32
Ground Time (s)	25	Ground Time (s)	25
Turning Rate (ft/s)	46	Turning Rate (ft/s)	46
Turning Radius (ft)	48	Turning Radius (ft)	48
Gross Weight (lbs)	32	Gross Weight (lbs)	32
Cargo (liters)	6	Cargo (liters)	8
Cargo Weight (lbs)	15	Cargo Weight (lbs)	20
Ferry Sortie		Ferry Sortie	
Average Speed (ft/s)	70	Average Speed (ft/s)	40
Takeoff Velocity (ft/s)	23	Takeoff Velocity (ft/s)	23
Ground Time (s)	25	Ground Time (s)	25
Turning Rate (ft/s)	48	Turning Rate (ft/s)	48
Turning Radius (ft)	41	Turning Radius (ft)	41
Gross Weight (lbs)	15	Gross Weight (lbs)	15

Figure 3.3: Large Versus Small Aircraft Comparison

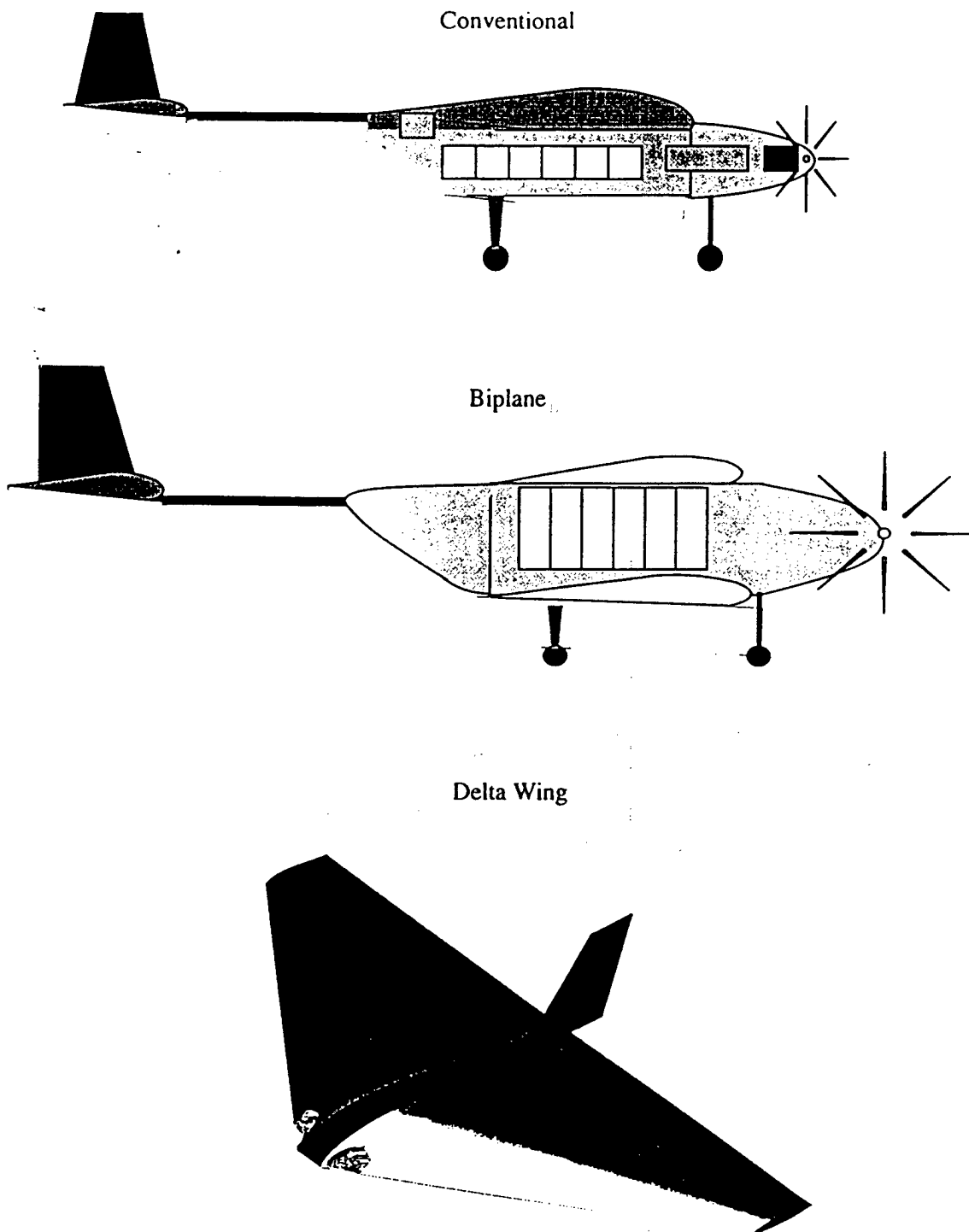


Figure 3.4: Different Configuration Concepts

4.0

PRELIMINARY DESIGN

After an exhaustive search of aircraft configurations during the conceptual design phase, definitive arguments were made in favor of a biplane design. The next steps in the project involved researching specific biplane dimensions such as wing cords, tail moment arm, tail size, and fuselage size that would optimize flight performance.

These flight performance characteristics are directly dependent on the thrust and lift that can be produced and are essentially limited by the duration of that thrust, weight of the aircraft, and drag. Without knowing how much thrust could be realized for less than five lbs. of battery, and without knowing how long that thrust would be adequately available, it was not possible to determine the optimal biplane dimensions. Therefore it was clear that determination of the power plant was the first factor to be clarified in the preliminary design phase. Other design features would later be researched with respect to those findings.

4.1 Power Plant Selection

Battery Selection

Arguments for battery selection revolved around the fact that power(P) is current(I) multiplied times voltage(V), but as current increases, temperature increases and battery output decreases. The temperature increase is due mainly to internal impedance, and it was found that Sanyo™, the industrial leader in battery production, provides batteries with very low internal impedance.

To further the battery research, Sanyo™ dealers were consulted and obtained an Engineers Data Book for Sanyo™ batteries. The "R" Series Sanyo™ batteries (Rapid charge) are best suited to withstand the fast charging and discharging necessary in a competition environment. From the Engineers Data Book it was seen that as the discharge rate increases (specifically, the current out of the battery), the percent available capacity is slightly higher for larger cells than smaller cells (refer to Figure 4.1 for capacity charts of the batteries that were analyzed). However, simple capacity was not adequate to identify the best battery because power is lost due to impedance and impedance varies with battery size.

Power loss was calculated in the following manner. The weights for 1000 and 4000 mAh batteries were divided into 5 lb. to get the number of cells (left as a fraction for comparison). The impedance data from Sanyo™ was multiplied by the number of cells to get the impedance for an entire battery pack. Voltage is 1.2 V per cell, and current is calculated assuming each battery pack is capable of 1000W of power. Power loss is then calculated from $-\Delta P = I^2 \Omega$.

Capacity	#cells (5lbs)	Impedance/cell	Impedance/pack	Voltage	Current	Power Loss
1000mAh	55.17	4.5 mΩ	0.2482 Ω	66.2 V	15.1 A	56.5 W
4000mAh	14.18	2.8 mΩ	0.0397 Ω	17.0 V	58.8 A	134.8 W

As where capacity arguments favor larger batteries, it is clear here that smaller batteries loose less power to impedance. However, smaller batteries cost more in the RAC and also imply potentially huge voltages.

Three battery pack configurations, selected from the best candidates listed in the Engineers Data Book, were analyzed for power output. Pack "A" contains 40 N-1900SCR cells, pack "B" contains 26 N-3000CR cells, and pack "C" contains 14 N-4000DRL cells (cell capacities are the four digit number in mAh). The number of cells for each pack was chosen to get as close to 5 lbs. as possible. At 1.2 volts per cell, pack "A" provides 48 Volts, pack "B"

provides 31.2 volts, and pack "C" provides 16.8 volts. This means that pack "A" could provide 91.2 watts/hr, pack "B" could provide 93.6 watts/hr, and pack "C" could provide 67.2 watts/hr. Clearly pack "C" does not have sufficient energy as compared to pack "A" or "B".

The following arguments were made comparing pack "A" and "B". Higher currents increase the generation of heat, which increases resistance, which further increases heat, compounding the problem. The current in the 40-cell pack "A" is 40% lower than that in the 26-cell pack "B" if the same power is produced; favoring pack "A". Although impedance is higher for smaller (pack "A") cells, as seen above, it does not necessarily mean a greater loss in power. One might now identify the tradeoff between available capacity and impedance.

In order to charge a battery pack, the potential across the pack must be significantly high enough to "push" the energy into it. Which means that a 40-cell pack that needs 1.5+ volts per cell, would require a 60+ volt DC charging device, which is readily available. It was also noted that in the RAC, current is assumed fixed at 50 Amperes, implying that packs that operate closer to 50 Amperes are not penalized as much and can realize higher power; favoring pack "B". For these and similar arguments, it was decided that pack "B" at 26 cells of 3000 mAh each was the best pack. However, due to risks concerning the possibility of decreased performance for the sake of the RAC, both packs were carried into the motor selection phase.

Motor Selection

The first step in selecting a motor was to determine the highest current that might be drawn from each pack during the course of the competition. The mission profile that was developed during the conceptual design phase was used in the current draw analysis. The mission profile consisted of a 6-minute overall flight time; 2 minutes of which were full throttle during climbing and turning maneuvers, and 4 minutes at half throttle during straight level flight. From a simple algebraic equation, the peak current draw at any one instant for pack "A" (40 cells at 1520 mAh each) is 22.8 Amperes, and pack "B" (26 cells at 2400 mAh each) is 36 Amperes. Notice that the capacities used in the calculations is the "available" capacity.

The second step was to identify suitable motors for the given voltage and current. Aveox™ brushless motors were found to be more efficient at high RPM's than conventional commutator-type electric motors in terms of current draw to torque output. These motors are bought with the gearbox, and a low-resistance speed control.

One of the benefits of using an Aveox™ motor is that the company provides their Virtual Test Stand on the Internet (refer to Figure 4.2 for example). The Virtual Test Stand allows users to evaluate the performance of different combinations of gearboxes, propellers, and battery packs on any motor that Aveox™ has available. Outputs of the program (Figure 4.2) include current draw, thrust, RPM, pitch, speed, and motor efficiency. The accuracy of the program is questionable, but it makes motor comparison and selection possible.

In addition to the Virtual Test Stand, a motor/battery/propeller analysis software package called ECALC was purchased. This package gave more freedom with the propulsion system parameters than the Virtual Test Stand (refer to Figure 4.3). However the it was immediately noticed that the thrust values from ECALC were much greater than what had been physically measured from the previous year's competition using Aveox™ motors. Therefore, a static thrust test stand was constructed to measure thrust and RPM of the Aveox™ 1412-4Y motors used in last year's competition.

Figure 4.4 shows the completed test stand used to calibrate ECALC. Using various propellers and a fully charged battery pack, the thrust and rpm in static air were recorded. These values were then compared to those values that resulted from ECALC using the same set-up. On

average, the motor rpm was within 4-5% but the thrust measurements varied 30 to 50%. Close inspection of ECALC revealed the default cell voltage as 1.25 volts, rather than 1.2 volts. Correcting this voltage resulted in nearly identical rpm values.

Actual thrust measurements and those given in the ECALC program were still different. By reducing the propeller efficiency variable in ECALC to between .55 and .7 (depending on brand of propeller) the thrust measurements were matched to the values from the experimental test stand within 5% error.

It is important to note that propeller efficiency changes with airspeed and RPM. Also, the motor, propellers, and batteries used in the experimental test stand were not those chosen for the aircraft. However the experiment was sufficient to calibrate ECALC within acceptable levels of confidence.

During Aveox™ motor evaluation using ECALC, three parameters were considered most important. First, in order for the battery pack to last for the duration of the competition, the current draw could not exceed the maximum current allowed for those batteries as calculated earlier. Second, propellers that gave high thrust across a wide range of airspeeds had to be selected. Within the current limits of each motor, propellers with high static thrust (low pitch propellers) and propellers with higher dynamic thrust (high pitch propellers) could be selected. Propellers with high static thrust loose efficiency as airspeed increases, while propellers with high dynamic thrust have lower static thrust but produce thrust more consistently. The ideal propeller for takeoff will be the one with the greatest average thrust across the velocity range from zero to takeoff velocity. Third, with all other parameters held constant, motor/battery combinations for multiple Aveox™ motors must show acceptable system efficiency.

Motor analysis revealed that for the 40-cell pack "A", the best motor is the Aveox 1415-4Y. For the 26-cell pack "B", the best motor is the Aveox 1415-3Y. The difference between the two motors is the number of windings that make up the electromagnet. The '4Y motor uses 4 windings, and the '3Y motor uses 3. Since the '4Y has more windings, it has higher inductance, which means higher impedance and therefore lower current draw. Voltage held constant, the '4Y will pull less current than the '3Y if they are both under the same load, but the '3Y will produce more power.

Both motors are equipped with a 3.7-1 planetary gear box in order to provide the torque needed to swing a 16 to 20 inch propeller with acceptable thrust. For optimal performance the aircraft needs to operate with the that largest diameter propeller possible while remaining within the current limits of the battery pack and yielding an acceptable thrust verses airspeed relationship in order to maximize both thrust and efficiency. The performance for the motors is shown in Figure 4.5. As seen in the Figure, the two motors are very similar in performance, with the '3Y generally providing more thrust at various velocities. As far as system efficiency goes, the '4Y is operating at 80% and the '3Y is operating at 75% according to ECALC. But, since the '3Y has slightly better performance, uses the battery pack with fewer cells and a slightly higher energy density, the 1415-3Y motor is the obvious choice.

From Figure 4.5, a thrust verse velocity equation was developed that greatly aided the takeoff performance analysis of the aircraft, which will be required when choosing the amount of cargo. The equation is:

$$Thrust(lb_f) = 132 - \%_{11} * Velocity(\frac{ft}{s})$$

This equation was taken from the thrust curve that had the best compromises between static thrust and thrust at 40 ft/s. In the same manner, a thrust equation for half current was

developed. It is important to realize that the thrust equations are rough estimates and that actual flight testing will be required to determine the most appropriate propeller.

4.2 Aircraft Sizing

To evaluate the takeoff and flight performance of different sized biplane designs, the team modified the Excel iterative takeoff distance spreadsheet from the conceptual design phase. Newton's Second Law of motion, is the centerpiece of this spreadsheet. The sum of the forces acting on the plane are thrust, parasite drag, induced drag, rolling resistance, aircraft weight, and lift.

The thrust model now uses the equation developed from the calibrated ECALC test results, and rolling resistance is conservatively assumed to be a constant value of 0.5 lbs. The parasite drag coefficient (C_{D0}) was estimated using a component build-up model which resulted in a low C_{D0} of around .03 when interference estimates and gap estimates were not used. The interference and gap factors were then estimated in a round about way. It did not really make sense to estimate the drag to begin with because in the end the interference and gap factors were modified so that the total parasite drag coefficient came out to be some likely value of around .06. Past experience has shown that this is a good estimate for a clean model aircraft.

Induced drag is dependent upon Oswald efficiency, effective aspect ratio, lift, and ground effect. Of these four quantities, none were known with certainty. The Oswald efficiency could be closely estimated, but the effective aspect ratio contains a level of uncertainty that can have large effects on the drag. The aspect ratio of this aircraft was calculated by dividing the square of the wingspan (effectively, one wing) by the *total* wing area (both wings). There will be less pressure spill over at the wing tips if end plates are added between the biplane wings, which means weaker vortices, and thus lower induced drag. Increasing the aspect ratio of the wing in the induced drag calculation will account for these endplates. However, the interactions of the vortices produced by two wings tend to increase the vortex strength and thus raise the induced drag as was discussed in the conceptual design section on biplanes. The use of a scalar "k-factor" that increases C_D as well as the C_L accounts for wing tip vortex interaction (k-factor is typically defined as 1.11)⁶. K-factor effects and end plate effects were treated independently during performance analyses. The effective aspect ratio used for the aircraft performance analysis is 1.3 times the actual aspect ratio and the C_D and C_L equations are multiplied by a k-factor of 1.11.

Ground effect alone will normally have a strong difference on the takeoff performance of the aircraft because the close proximity of the wings to the ground reduces the vortex strength. However, in this special case where end plates are already used to reduce the vortex strength, the reduction in drag due to ground effect is less than it would be without endplates. Rather than trying to estimate something further of which the team was not certain, ground effect was ignored in the takeoff analysis. Since ground effect *reduces* drag, ignoring its effects it will only add to a margin of safety in calculating takeoff distance.

Flight performance analysis was performed in a rather simple manner. Using the drag equations developed for the takeoff spreadsheet, the parasite drag, induced drag, and total drag of the aircraft are plotted against velocity. When a thrust curve for a given power setting is plotted on top of the drag curve, the steady state aircraft velocity can be determined, assuming that flight is feasible. Figure 4.6 is the performance chart used in the analysis. This is an extremely useful tool because it allows quick determination of L/D_{max} speed by locating the velocity where the induced drag and parasite drag are equal, maximum velocity, and whether or not the aircraft has

enough thrust to climb out after rotation. This is a very important point for the following reason. The power plant on the plane may be able to get the craft to takeoff speed within the distance requirement, but the drag may actually exceed the available thrust when the plane rotates to the attitude required to produce enough lift to takeoff. Thus the airplane would stall and return to the runway.

Spreadsheet analysis

Initially, chord lengths and weights were chosen pseudo-randomly to get indication of what the basic size and capabilities of the aircraft would be. From this familiarization technique, it was noticed that induced drag is independent of C_L and AR when two designs have the same weight and the same Oswald efficiency. This is a very valuable observation because it shows that the most efficient design will use an airfoil with a very high C_L max so that a wing of as little area can be used. A wing of little area has two main advantages. First, it will result in minimum parasite drag. Second, it will result in a lower manufacturing cost.

The aircraft sizing process was an iterative analysis. First, a C_L max of 1.7 was chosen. Then the wing chord was selected so that the aircraft could take off at 1.1 times stall speed in under 100 feet at a given weight. Next, the flight performance chart was inspected to make sure the configuration was feasible from an energy stand point. The power plant is not designed to operate at full power during the entire competition. During level flight, the aircraft will need to be able to fly at half power.

Because of this power limitation, it was easy to find the upper limit on aircraft weight that was feasible. Using Figure 4.6 as a guide, the aircraft weight was increased until the total drag exceeded the half power thrust available. The wing chord was then reduced until the half power thrust curve and total drag curve were tangent. Then, the C_L max was varied until the takeoff distance was met. If this was an unrealistic value for C_L , then weight was reduced and the process started over again.

Things that were taken into account during this process were aircraft empty weight and bottle weight. Since there would be minimally more structure required to carry six liters than four liters, and since the fuselage length and tail size depends heavily upon wing span, which was held at seven feet regardless of the aircraft weight, the aircraft empty weight was expected to change minimally with cargo capacity. Therefore, when weight was changed in the analysis process, it was done in 2.5 lb. increments, the weight of 1 liter of water. Based on past knowledge, the current aircraft is expected to weigh 15 lbs. empty.

Spreadsheet Results

Some interesting discoveries were made from the spreadsheet analysis. The most important was that takeoff distance is not the active constraint on aircraft size. The active constraint is the requirement that the loaded aircraft must cruise at half power. An eight liter cargo, 35 lb. gross takeoff weight, is feasible from the takeoff analysis, but full power is required during flight. This would not only cause the battery power to run out prematurely, but it would also result in a low to nonexistent rate of climb and all turns would be descending.

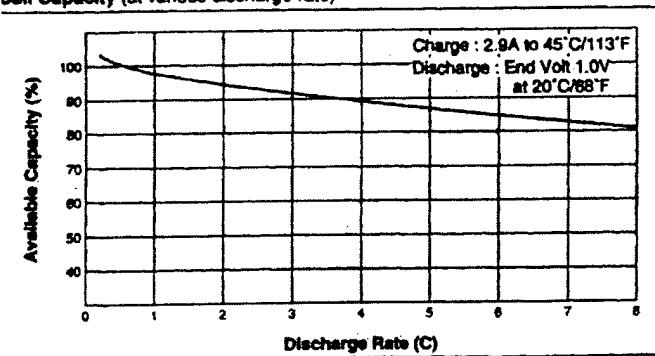
The optimal configuration found has a chord of 12 inches, and a cargo capacity of 6 liters. This design can make the takeoff distance requirement if a flapped airfoil with a very reasonable C_L max of 1.85 is used. Table 4.1 shows the performance of the aircraft during the payload and ferry sorties along with the C_L that the aircraft is operating at during each phase. The C_L data will be used for airfoil selection in the detailed design section of the report.

Table 4.1: Aircraft performance and lift requirements

Aircraft Performance		
	Empty	6 Liters
<u>Weight(lb)</u>	15	30
<u>Takeoff Velocity (ft/s)</u>	43	35
<u>Takeoff CL</u>	0.6	1.85
<u>Cruise Velocity (ft/s)*</u>	55	42
<u>Cruise CL</u>	0.32	1.05
<u>L/D max Velocity (ft/s)</u>	34	46
<u>L/D max CL</u>	0.9	0.88
<u>Maximum Velocity (ft/s)</u>	68	64
<u>Maximum Velocity CL</u>	0.2	0.45

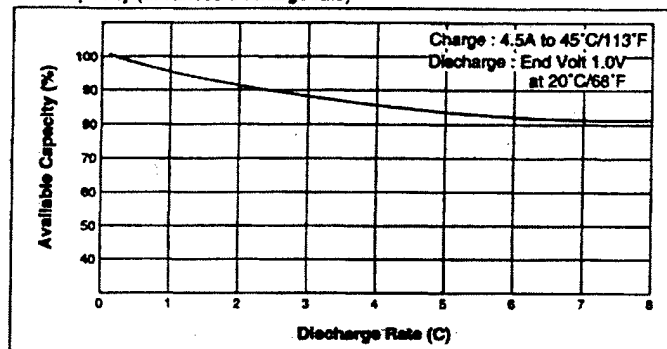
N-1900SCR

Cell Capacity (at various discharge rate)



N-3000CR

Cell Capacity (at various discharge rate)



N-4000DRL

Cell Capacity (at various discharge rate)

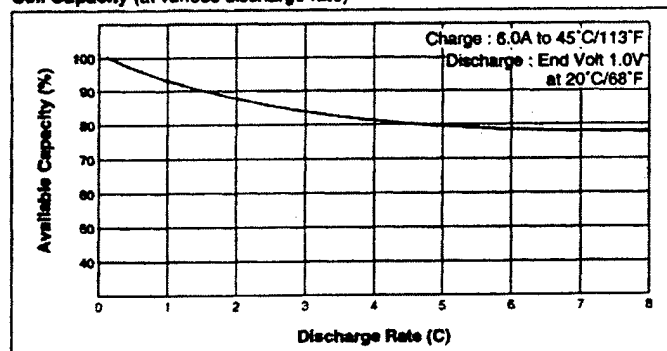


Figure 4.1: Sanyo battery capacity data

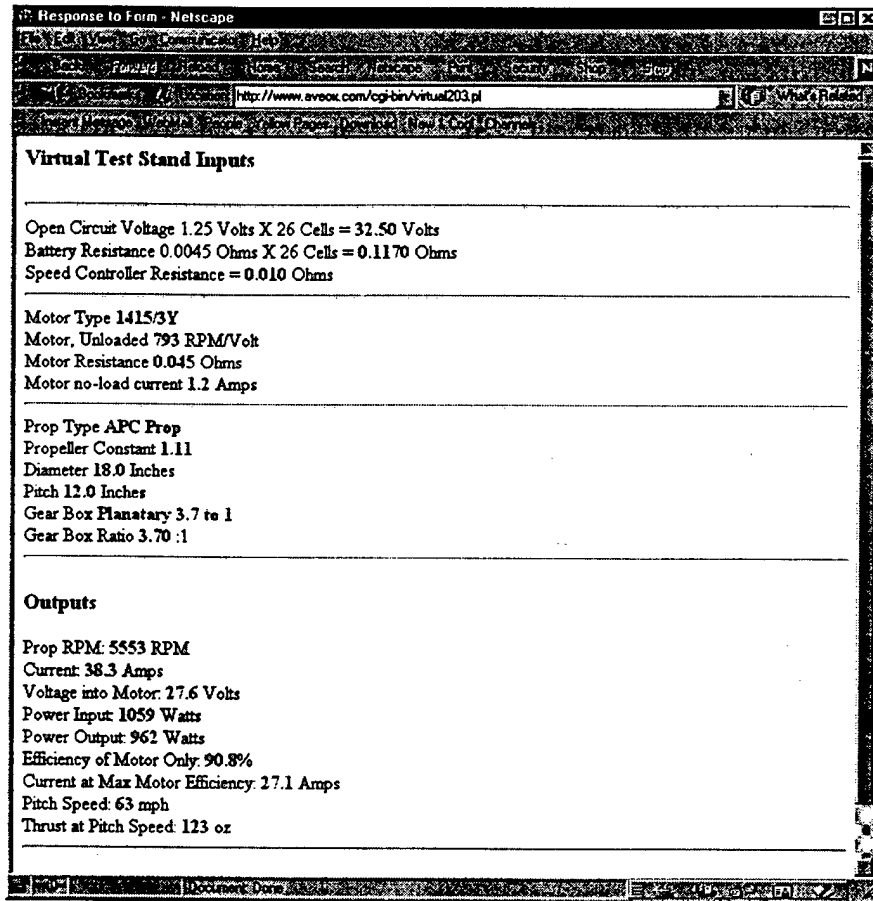


Figure 4.2: Aveox™ online Virtual Test Stand

ElectriCalc

Power Parameters	Motor Parameters	Drive Parameters	Flight Parameters
26 Cell Count	795 KV/RPM/V	18.00 Diameter	468 Pitch
1.20 Cell Volts	50 Rm mohm	12.00 Pitch	38.1 Vmax Load
3.24 Cell mAh	1.2 to amps	1.00 K prop	20.16 Vmax Alt
16 ESC mohm	38.7 Amps	0.72 K eff	0.060 Disc
3000 VAF	AVRox Min	3.70 Gearing	1.00 Motor
N=0006R	1075V	APP	0.00000
1 Edit	1 Motor	1 Prop	1 Pitch
30.7 Battery amps	20.08K Motor RPM	5.43K Prop RPM	35.11/min
4.1 Minutes	90.2 Motor Eff	89.9 Prop Watts	11.1 climbout
5.2 System Eff	10.5 Watts lost	36 Watts per lb	Max climb 1646 ft
120.7 Watts created	10.5 Motor Watts	4.9 Gearbox Watts	Max climb 1646 ft
1.55 Watts lost	27.2 Motor Volts	52 MPH pitch spd	22 MPH stall spd
7.6 oz package	7.5 Motor Constant	106 oz thrust	47 MPH max spd
Max Eff 0.156A	Max Eff 0.251A	21 oz drag	4.2 Minutes Cruise
100% throttle			22 MPH

Figure 4.3: ECALC input/output user interface

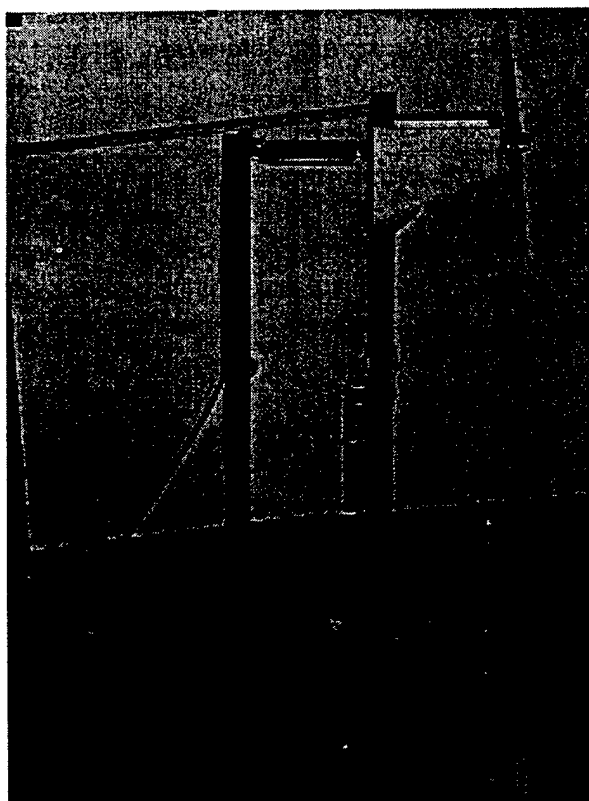


Figure 4.4: Experimental motor/propeller test stand

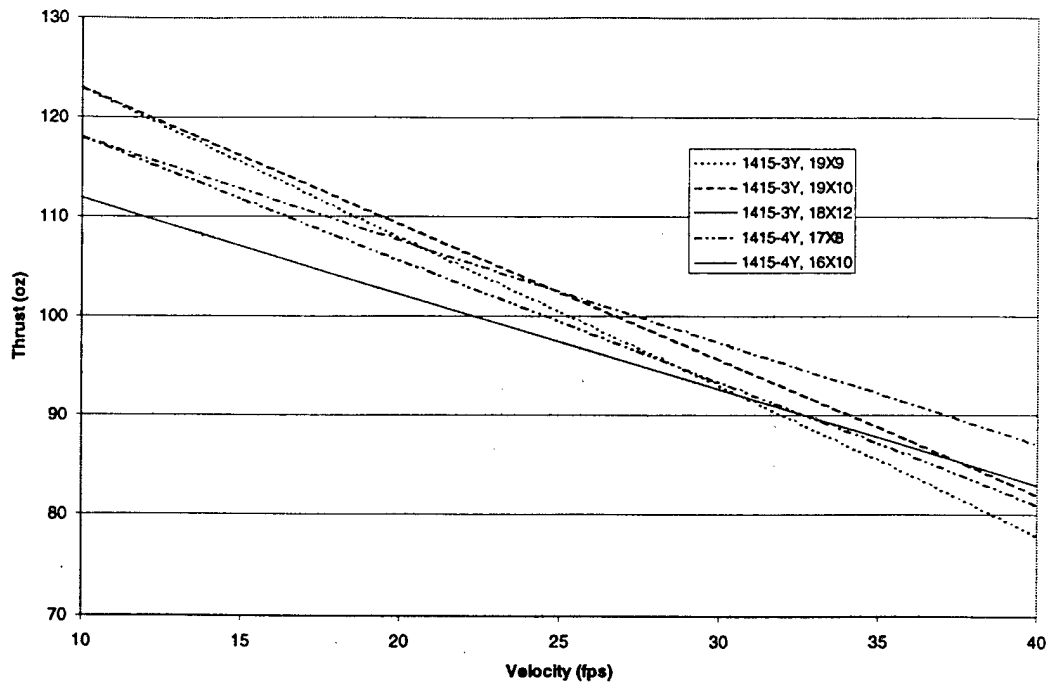


Figure 4.5: Calibrated ECALC motor performance with various propellers

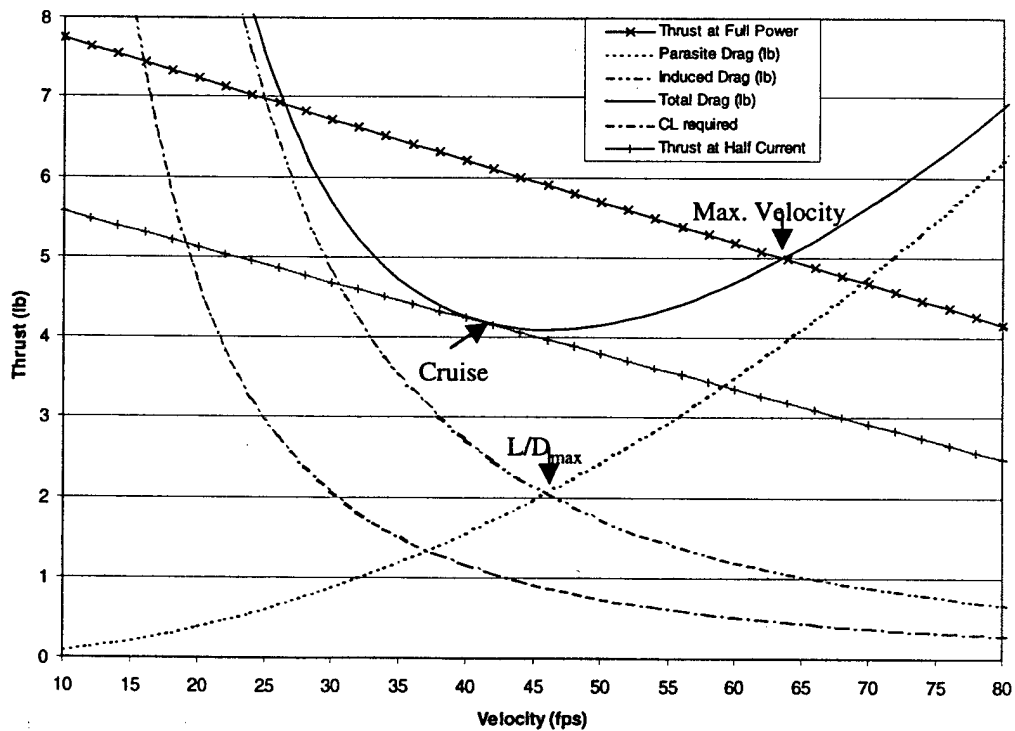


Figure 4.6: Performance chart for 6 liter capacity, 30 lb. GTOW

5.0

DETAILED DESIGN

At the conclusion of the Preliminary Design Phase, the biplane has a seven foot wingspan, a twelve inch chord, a wing spacing of one chord with a half chord positive stagger. The plane will carry a payload of six liters while being powered by 26 Sanyo N-3000CR batteries driving an Aveox 1415-3Y motor. Now the details of the design have to be worked through. The areas of further consideration include: wings, fuselage, empennage, landing gear, aircraft control, handling qualities, and aircraft performance. To aid the detailed design process Ideas, a three dimensional modeling package, and Microsoft Excel were used extensively

5.1 Wings

Airfoil Selection

Based on the preliminary design analysis, the performance that would be required from the wing and corresponding airfoil was known. The required C_L at each stage of flight is shown in Table 5.1. Because of the distinct differences in C_L required for the cargo and ferry sorties, it was evident that the wing final would require flaps.

Extensive airfoil research was conducted to determine an airfoil that could most closely match the requirements. An airfoil data site² in conjunction with an airfoil analysis package³ provided the bulk of the information for the airfoil research. The most efficient way to tackle this problem was to start with an airfoil that worked for a certain situation and then modify the qualities of the airfoil to have them best fit the current situation. As a starting point, the GOE615 was chosen and modified to meet the requirements.

The GOE 615 was over 15% thick, which would cause too much drag for the ferry sortie. Also, the GOE 615 has a C_{l_0} of 0.8, which is too high because of the ferry sortie low lift requirements. Therefore, thin airfoils with less camber were selected for analysis. To provide high lift with a low camber airfoil, 25% chord flaps were analyzed. The candidate airfoils were analyzed at a Reynolds number of 200,000 for takeoff and 400,000 for cruise.

The airfoil that most closely matches the requirements of Table 5.2 is the Selig 2091, shown in Figure 5.1. The airfoil has a thickness of approximately 10% and has a C_l of 0.43 at zero angle of attack. The value of C_{l_0} is slightly higher than was desired for the cruise segment of the ferry sortie. To compensate for this, a slightly negative angle of attack or reflexed control surfaces will be required to decrease the lift and allow level flight. Because the high lift requirements during the cargo sortie were considered more important than a slight increase in drag during the ferry sortie associated with a negative angle of attack, the airfoil requirements were compromised. Table 5.1 shows the wing configurations, wing angle of attach and flap settings, that are required to satisfy the different mission phases for the empty and six liter cases.

Flap design

The three dimensional C_L values in Table 5.1 assume full length flaperons. Full length flaps were chosen for several reasons. First, the lift to drag ratio will be better for a wing that produces the same amount of lift with full length flaps than a wing does with only half span flaps this is due to the fact that the flap deflection required will be less in the full length flap case, resulting in lower drag. Second, the number of control surfaces is reduced, and therefore the number of servos is reduced. Flaperons are often discouraged because they use existing ailerons which are located near the wing tips. Turning existing ailerons in to flaps loads the lift distribution at the wing tips which can lead to poor handling qualities. Additionally, the roll

control authority is generally reduced normally when flaperons are deflected because there is limited control surface travel left for ailerons. If full length flaperons are used, the wing lift distribution will uniformly increase when the flaps are lowered and the control throw for roll will be very small due to the large control surfaces.

When designing flaps, several options exist. The flaps can be plain, split, slotted, or Fowler. To maximize lift while minimizing drag and complexity, slotted flaps are usually chosen. However, since the flaperons must deflect up and down, the biplane must use plain flaps.

Wing Structure

Since the wingspan is only seven feet, it is advantages from a weight and complexity standpoint to make it one piece. Past experience has shown that foam core wings are simple to build and are very precise, therefore one lb/ft³ foam was selected as the wing core material. Typically, foam wings are completely sheeted with some sort of material such as balsa wood, fiberglass, or carbon fiber to provide the required bending stiffness and strength. This method of completely sheeting the core usually results in a wing that is overly strong and heavy. To avoid any excess weight, several options for the wing structure were investigated. All of the options leave most of the wing foam without any structural sheeting, thus the wing will be covered only with typical model aircraft heat shrink covering.

The first concept for the wing uses a foam core spar. Foam acts as the shear web and carbon fiber strips are adhered to the core for bending strength. Because the mechanical properties of the foam are not known, a test spar was built and tested. Figure 5.2 shows the spar after testing. The thin strips of carbon buckled under the compressive load on the top of the wing. This occurred because the foam was unable to withstand the compressive force where the wing would intersect the fuselage.

The second wing concept was very similar to the first, but rather than carbon fiber on both sides of the spar, carbon was only used on the bottom and 3/8 in. thick bass wood was used on top to carry the compressive load. When tested, this spar failed, but not in the same manner as the first spar. This time, the carbon fiber sheared off of the foam, then the bass wood spar broke since it was carrying the entire load. Figure 5.3 shows the end result of this catastrophic test.

A two point bending test was used in both of the spar tests. In actuality, a three point bending test should have been done. If a three point bending test had been performed on the second spar, the carbon fiber would not have sheared off of the foam because tension would have been pulling it in the opposite direction. However, permanent compressive deformation was evident in the foam core between the carbon fiber strip and the basswood. This deformation would have occurred even in a three point bending test, and would not be acceptable in an actual wing.

Next, an analysis of a built-up spar was conducted. The previous two spar concepts were desirable because neither one required the wing to be sectioned, they were simply adhered on top of the foam core using epoxy. A built-up spar requires that the wing be cut along its maximum thickness. Table 5.2 show the spar design and analysis. A balsa shear web sandwiched between two quarter inch square spruce sticks topped off with carbon fiber tape constitutes the spar's structure. When the spar is subjected to a 7.5-pound load at a distance of 42 inches, or half span, all of the stresses are within the allowable limits. This load is equivalent to lifting the plane from the wing tips when it is fully loaded.

Figure 5.4 shows a test built spar. Problems with the carbon delaminating from the spruce sticks and fear of the foam wing core's weakness in torsion drew skepticism about the spar's robustness. Also, with further analysis, it was shown that although the spar could withstand the wing tip lifting test, it could not even withstand a 3g aerodynamic load. Under gusty conditions, structural loadings of more than 3g's are common, this spar was not acceptable.

The final wing structure design combined all of the previous designs together. The first wing spar design with the upper and lower surface carbon fiber would be used. Now the strips were separated by a balsa shear web that would prevent the foam from compressing and the carbon fiber from shearing off. In addition, the carbon fiber would be laid out in a diamond pattern, providing strength in torsion and compression to the wing. Figure 5.5 shows the final spar design. The width of the carbon fiber "diamond" is two inches at the center of the spar and ½ in. at the spar tip. This amount of carbon fiber is more than adequate to support a 6g load during the cargo sortie. While only comparing the tensile and compressive strength of the carbon fiber, the spar can support a 14g loading according to beam theory. This however, ignores buckling, which will be the most likely failure mode of the spar.

The entire wing structure is shown in Figure 5.6. The leading edges and trailing edges of the wing and flaperons are made from lightweight balsa. The wing core is made from one lb/ft³ foam. The wing spar is as described above. Throughout the wing structure, light plywood ribs exist to provide mounting for servos and to distribute landing gear loads throughout the wing.

To add to the structural and aerodynamic efficiency, end plates will connect the top wing to the bottom wing. These will consist of lightweight balsa truss covered with model aircraft covering. Initially, these will not extend above the top wing or below the bottom wing. After flight testing though, the design may be changed by extending the plates to gain further drag and lift benefits. Also, the plates can be made to double as wingtip skids if they are extended below the bottom wing.

Wing attachment

During the aircraft subsystem design process, special care was taken to ensure that all subsystems would interface well with each other to form the complete aircraft. Each wing fits into a specially shaped cradle cut out in the fuselage sides. The wings are then secured to the fuselage with lightweight nylon bolts that screw into spruce blocks that span the small 2¼ in. width of the fuselage. To add strength to the wings at this juncture, carbon fiber is wrapped around the wings and laminated with epoxy.

5.2 Fuselage

Bottle layout and structure

The centerpiece of the fuselage design is the bottle configuration. From the outset of the project, speculation about the how the bottles would be arranged, exchanged, and secured was a driving consideration of the design process. However, it was not until the detailed design phase that a final bottle configuration was decided upon.

The bottle arrangement is crucial to minimizing the turn around time between sorties and must be situated as to have no effect on the center of gravity of the airplane. Modular bottle insertion and withdrawal is very important. Because the plane will carry six liters, and there are three ground crew members, it was thought best to group the bottles into two sets of three. This way one ground crew member can be responsible for turning off the plane and disconnecting the

motor as required by the competition rules while the other two crew members unload/load the payload.

The biplane configuration leads to some minor difficulties in determining the best way to access the cargo. If it is loaded from the side, the crew members must get down between the wings and take the risk of dropping the bottles and damaging the plane. Additionally, there must be some lightweight means of enclosing the bottles once they are in place. If the plane is loaded from the top, the top wing must be sectioned to allow for bottles to be quickly pasted through it and into the fuselage.

Neither of these alternatives were acceptable and it was decided upon to load the plane from the rear. This allows the bottles to be taped together in two tube configurations. These tubular bottles would be 3.5 in. in diameter and 24 in. long. If the bottles slid up through the center of the fuselage, the internal structural layout of the fuselage would be rather complicated, so it seemed best to fit the bottles on the sides of the fuselage.

A fuselage concept that could feasibly carry the cargo with a minimal surface area and structural weight was finally developed. Figure 5.7 shows the basic concept, which consists of a center structural channel made from light weight plywood that houses the power plant and electronics. The bottles slide up from the tail of the aircraft and fit on the outside of this channel in a type of saddlebag arrangement. To allow the bottles to have plenty of clearance from the fuselage and to save unneeded structural weight, a simple boom connects the fuselage to the empennage.

The fuselage could be suspended between the two wings using one of the methods in Figure 5.8. The first method is the simplest. The fuselage sides are extended upward as wing mounting pylons. The second option uses two vertical struts that add wing to wing rigidity along with complexity. The third option uses A-frame cross bracing to suspend the fuselage while adding stiffness to the wing above the landing gear. Of the three fuselage concepts, the first was chosen because of its simplicity and low weight. The final light plywood fuselage structure design of the chosen method is shown in Figure 5.9.

Initially, the bottles were to be contained in thin walled cardboard tubes that were attached to the sides of the fuselage. However, this was not feasible because cardboard tubes of the desired diameter and thickness are not available. Carbon fiber tubes were also investigated, but in the end a design that uses aluminum flashing wrapped around the fuselage to support the bottles was chosen. Figure 5.10 shows the flashing on a fuselage mockup that was constructed. This method turned out to be lighter and simpler than using a tubes structure.

To enhance the aerodynamic efficiency of the biplane, low density foam was shaped to form a cowl, fuselage end cap, and wing pylon fairing. The end cap, as shown in Figure 5.11, rotates down to allow access to the bottles, holds the bottles in place, and aerodynamically tapers down the fuselage in the rear. To add or remove the bottles, the end cap is unlatched, the bottles are removed or inserted, and then the end cap is flipped back into place.

Tail Boom

Initially, the tail boom was to be one in. in diameter and made from carbon fiber. This would cost approximately \$80.00 for the length that was required. Structural analysis showed that an aluminum tube with a 0.035 in. wall thickness would be strong enough, but would not be quite as stiff. The aluminum tube cost is \$9.00 for a six foot length. Also, the carbon tube wall thickness is 0.060 in., which leads to a tube of higher volume. Since the aluminum tube was less expensive and the weight savings from the carbon tube were small due to the higher volume, the

aluminum tube was selected as the boom for the aircraft. Table 5.3 shows the stress analysis of the tail boom.

To secure the tail boom in the fuselage, yet maintain a modular design, the boom is pinned between two fuselage bulkheads rather than being glued into place. If flight testing proves that the boom is not long enough for adequate stability, a longer boom can easily be added.

5.3 Empennage

Sizing

Based mostly on historical data for tail volume coefficients, the vertical and horizontal stabilizer were sized according to the wing area, wing chord, and wingspan. Additional work was done for the sizing of the horizontal stabilizer to ensure that it could produce enough force to compensate the pitching moment produced by the wings when the flaperons are deflected a full 30 degrees. To be able to attain the required force, a NACA 2409 airfoil section was selected for the horizontal stabilizer. The airfoil section is inverted so as to provide force in the appropriate direction. Figures 5.12 and 5.13 show the vertical and horizontal tails respectively with their final dimensions.

The vertical stabilizer is built-up from lightweight balsa sticks as shown in Figure 5.12. The rudder extends across the top of the vertical to gain aerodynamic balancing. The size of the rudder is based on previous model aircraft knowledge and is replaceable if its size proves to be inadequate.

The horizontal stabilizer is made from a lightweight 1 lb/ft³ foam core. The core is fitted with balsa leading and trailing edges for the stabilizer and elevator as shown in Figure 5.13. Initially, a spar was to be added to the stabilizer; however, once the leading and trailing edges were added, it was found that the horizontal stabilizer was strong enough without the added weight of an additional spar.

Attachment

Keeping with the desire to make the aircraft design as modular as possible, the horizontal and vertical stabilizers are removable. A cradle allows the horizontal to fit solidly upon the round tail boom. The bottom of the vertical is formed so that it cradles against the top of the horizontal. The base of the vertical is threaded for 2 bolts that are inserted from the bottom of the tail boom. As a result, the horizontal is clamped into place. This attachment method is shown in Figure 5.14.

5.4 Landing Gear

Selection

From the beginning of the project, it was known that tricycle landing gear would be used on the aircraft. Tricycle landing gear is superior to conventional landing gear with respect to ground handling characteristics. Also, tricycle landing gear keeps the airplane in its lowest drag attitude during takeoff roll, and thus yields better acceleration. When it is time for the aircraft to rotate to take off, tricycle gear allows the aircraft to tip back 15 degrees, if it is designed properly. This 15 degree tip back angle lets the wing operate at or around its maximum lift coefficient so that the aircraft can lift off in the shortest distance possible.

Placement

Ideal placement of the main landing gear will allow the plane to tip back a minimum of 15 degrees before the tail touches the ground. When the plane is in this position, the center of gravity should be directly over the main landing gear wheel axles. By having the landing gear positioned in such a manner, the force required to rotate the aircraft is minimized. This results in an aircraft that can takeoff easily; a very valuable characteristic when the runway length is limited.

The wheel track, or distance between the main landing gear should be at a distance that will not allow the plane to tip to the side easily. A rule of thumb is that the main gear should be more than 25 degrees to the side of the aircraft's vertical center of gravity. This results in a rather small wheel track, so for this aircraft, the mains are placed so that the three wheels of the landing gear form an equilateral triangle, or close to it. The main gear has a wheel track of 18 in. and the wheel base is 18 in. as well.

The nose gear is normally positioned so that it supports between 8% and 15% of the total aircraft weight. Because most of the aircraft design is dictated by other constraints, the nose gear was positioned behind the motor, as far forward as possible. This resulted in the nose gear being located 15 inches ahead of the center of gravity. The main gear is three inches aft of the center of gravity to allow a 15 degree tip back angle. This configuration results in the nose gear supporting a little over 16 % of the total aircraft weight. Given the possibility of strong cross winds at the competition site, the added nose gear authority during takeoff is an added benefit.

Type

Because of the minimal fuselage design, the nose gear has to be very long to allow adequate propeller clearance. Given this, the nose gear needs to be rather sturdy. A Folts duel strut was chosen as the nose gear. The Folts strut is made from $\frac{1}{4}$ in. music wire and has a coiled spring at the top to help with shock absorption during takeoff and landing. With a 3 in. nose wheel, over 3 inches of propeller clearance is available for a 18 in. propeller.

For the main landing gear, Robart struts were considered at first, however simple homemade $\frac{1}{4}$ in. diameter music wire gear was chosen because of the cost savings and anticipated weight savings. Additionally, wire gear can give better shock absorbing characteristics than Robart spring struts because the Robart struts have a limited travel of $\frac{3}{4}$ in. where as the wire gear can be designed to flex much more, resulting in lower g landings. Figure 5.15 shows the wire main landing gear configuration. This configuration design has a wheel to wing clearance of 3 in. when a 3.5 in. wheel is used.

Sullivan Skylite wheels will be used on the plane because of their lightweight and low rolling resistance that is inherent with their solid foam core construction. Some common model aircraft wheels are air filled but not sealed, and deform severely during takeoffs and landings resulting in unwanted drag.

Attachment

The nose gear mounts to a $\frac{1}{8}$ in. birch ply bulkhead behind the motor. Figure 5.15 shows the main landing gear mounting in the wing of the aircraft. Ribs are added to carry the torsional loading through the wing. Each main landing gear attaches to two spruce blocks that are embedded in the foam wing and sandwiched between the light ply torsional ribs. The main wing spar carries the bending loads from landings, and the torsional loads are distributed throughout the wing.

To assure that the main spar could support the landing loads, a 2g landing was analyzed. When fully loaded, the aircraft will weigh approximately 30 lb. Assuming that the mains carry the entire load, a 2g landing results in a 30 lb. load on each main gear. Given the wheel track of 18 in., a bending moment of 270 in-lbs. results. This is well within the structural limit of the wing spar as was calculated in the wing spar subsection.

5.5 Aircraft Stability and Control

Throughout the design process, care was taken to ensure that the center of gravity of the entire aircraft is in the correct location for stability purposes. To do this, a spreadsheet was developed to keep track of all of the component weights. The motor battery pack and receiver battery packs have some freedom of movement to allow fine tuning of the center of gravity location. This spreadsheet allowed the determination of the aircraft empty weight. Table 5.4 lists the aircraft components and their respective locations. The total airframe weight, excluding the battery pack, is approximately 10 lbs. as was expected in the preliminary design phase.

All of the aircraft systems are shown in their correct locations in the three view fold out located after the Executive Summary report section. The flaperons are actuated by two Futaba s9303 servos. Each servo is responsible for the upper and lower flaperons on one side of the aircraft. To accomplish this, high torque servos are used and a coupling rod connects the upper and lower wing surfaces. The flaperon servos are located at half span along the wing to reduce torsion in the control surfaces. Both the rudder servo and elevator servo are located just in front of the tail boom in the fuselage. This location allows for directly push rod linkage through the inside of the tail boom to actuate the elevator and rudder. Also, by locating the servos in the fuselage rather than in the tail, it is easier to achieve the desired center of gravity location and the nose wheel can be coupled to the rudder servo, thus reducing the number of servos.

Control of the aircraft will be accomplished with a Futaba 9Z flight radio and PCM receiver. The 9Z is a computer radio that will allow the mixing functions to be accomplished that are required by the flaperon setup. The PCM receiver will allow a fail safe mode to be used in the rare case that the plane loses contact with the pilot transmitter.

In conjunction with the 9Z radio, stability gyros will be used on the roll and yaw axes. Stability gyros are commonly used on the tail rotors of radio controlled helicopters to help maintain heading and reduce the pilot's work load. In the likely gusty conditions at the contest site, this feature will help the pilot maintain the aircraft flying as smoothly and precisely as possible. Also, since the wings are design with zero dihedral, the stability gyro on the roll axis will compensate for this inherent lack of stability. The gyros will be rigidly mounted in the fuselage of the aircraft as close to the center of gravity as allowed by the other components.

No detailed stability analysis was done to determine the longitudinal dynamic stability of the long and short period modes or the lateral dynamic stability of the Dutch roll and spiral modes for the aircraft design. Since the basic configuration of the aircraft closely resembles historical planes, good dynamic stability is expected. However, in the unlikely case that the frequency or period of any of these modes is unacceptable, the modular empennage design will allow the problem to be corrected. Also, the stability gyros will contribute to the reduction of any lateral aircraft oscillations.

5.6 Handling qualities

This aircraft is designed for a utility mission, therefore extreme maneuverability is not required. The aircraft is expected to be stable as to reduce the pilot's work load, yet responsive enough to compensate for gusty conditions.

For this aircraft, a static margin of around 0.06 would make it stable, yet allow the pilot to actively control the craft. The smallest static margin possible, without excessively increasing the pilot's work load, would be best for the aircraft because this would reduce the amount of down force required from the horizontal stabilizer to trim the aircraft. This reduction in down force would result in additional weight the aircraft could lift.

Because the aircraft was not modeled using a paneling code and no wind tunnel testing was performed, the exact location of the neutral point was not known and the CG location for the desired static margin could not be calculated. It was therefore decided to start out with the CG a 20 % MAC, and determine its best location from flight testing based on handling qualities.

All control surfaces were made slightly on the large side to ensure that adequate control power would always be available when required. With large control surfaces, throw can always be decreased if the aircraft is over controlled or touchy. However, if the control surfaces are small and the control throws are already at their maximums, additional control authority will not be an option.

5.7 Performance

Because the weight of the aircraft remained nearly the same as was expected in the preliminary design section, the takeoff performance of the aircraft only differs because of the more definite airfoil/wing performance. With 30 degree flap deflection, the aircraft can takeoff in 80 feet when it is fully loaded with six liters of cargo. Table 5.5 shows the takeoff performance with different flap settings and payloads. In order to investigate the aircraft's capabilities in windy conditions, Figure 5.16 was made. This figure is linked to an Excel spreadsheet that allows the headwind to be selected, and shows the takeoff distance for a given aircraft weight and average net thrust during takeoff. The tables and figures, which are linked to spreadsheets, will be used during flight testing and the contest to determine what the aircraft is capable of given the existing conditions.

Using the flight performance chart, Figure 5.16, it is easy to determine cruise velocity, maximum velocity, and L/D max speed for any configuration. Table 5.5 summarizes these quantities for zero through six liters of cargo by two liter increments. Notice that the maximum velocity changes very little regardless of cargo. Since the aircraft is estimated to weight only 15 pounds without cargo, a payload fraction of 50% results when six liters of water are loaded. One liter of water weights 2.2 lbs., but when the weight of the bottle is added, the total weight is 2.5 lbs. per liter.

In order to estimate the time required to complete a cargo sortie and a ferry sortie, the turn rate and climb rate of the plane had to be calculated. The turn rate of an aircraft is limited by the power plant, maximum C_L , and structural limit of the wing. The turn rate for a level turn is dependent upon the velocity the aircraft is moving through the air. Rather than determining the best turning speed was found at the design cruise velocity and full throttle. Table 5.5 shows the turn rate and cruise velocity for the aircraft with four payload options. The table also includes the total time estimate for the ferry and cargo sorties. These times were calculated using the sortie breakdown from the conceptual design phase.

Maximum endurance and maximum range were calculated for each of the payload configurations with the help of the flight performance chart and are tabulated in Table 5.5. Maximum endurance occurs when flying at minimum power. Maximum range occurs when flying at L/D max. The amount of time that the aircraft can fly at these power settings was determined using ECALC.

Maximum rate of climb was calculated using a simple equation that multiplies the flight velocity by the difference in the thrust available and aircraft drag at that flight velocity; this quantity is then divided by the aircraft weight to yield rate of climb. If rate of climb is plotted versus velocity, the maximum rate of climb along with its associated velocity can be easily determined. Figure 5.17 shows the rate of climb for the design aircraft with the maximum six liter payload.

Using the data of Table 5.5, and assuming a turn around time between each sortie of 30 seconds, the greatest number of cargo sorties possible will be three, regardless of the amount of payload. If six liters is carried during three cargo sorties, with two ferry sorties in between, a total flight time of seven minutes results. This is more than the anticipated six minute flight time used in the preliminary design phase; however, this knowledge does not affect any of the design work that has been completed. If there is not sufficient power available by the 3rd cargo sortie to lift six liters then the payload will be reduced to make the 3rd sortie possible.

Table 5.1: Aircraft C_L requirements and resulting wing configurations

Aircraft Performance		
	Empty	6 Liters
Weight(lb)	15	30
<u>Takeoff Velocity (ft/s)</u>	43	35
<u>Takeoff CL</u>	0.6	1.85
<u>Flaps (deg.)</u>	0	30
<u>Alpha (deg.)</u>	3	8
<u>Cruise Velocity (ft/s)*</u>	55	42
<u>Cruise CL</u>	0.32	1.05
<u>Flaps (deg.)</u>	0	20
<u>Alpha (deg.)</u>	-1	0
<u>L/D max Velocity (ft/s)</u>	34	46
<u>L/D max CL</u>	0.9	0.88
<u>Flaps (deg.)</u>	10	10
<u>Alpha (deg.)</u>	1	1
<u>Maximum Velocity (ft/s)</u>	68	64
<u>Maximum Velocity CL</u>	0.2	0.45
<u>Flaps (deg.)</u>	0	0
<u>Alpha (deg.)</u>	-2	1

Table 5.2: Spar design and stress analysis

Note: All are referenced to Part C

Parameter	Part A	Part B	Part C	Part D	Part E
Material	Composit	Spruce	Balsa	Spruce	Composit
b	0.25	0.25	0.25	0.25	0.25
h	0.01	0.25	0.73	0.25	0.01
E	8.10E+06	1.20E+06	400000	1.20E+06	8.10E+06
Location (y) [in]	0.62	0.49	0	-0.49	-0.62
area [in ²]	0.0025	0.0625	0.1825	0.0625	0.0025
I _{xc} [in ⁴]	2.08333E-08	0.000326	0.008105	0.000325521	2.08E-08
I _{xx} [in ⁴]	0.000961021	0.015332	0.008105	0.015331771	0.000961
Centroid (y)	9.02E-18	-5.00E-03	-1.30E-01	-4.95E-01	-6.20E-01
I _{xx_sys} [in ⁴]	5.56E+04				
Bending Moment [lb-in]	475				
Max distance [in]	0.625	0.615	0.365	-0.615	-0.625
Max Stress (B) [lb/in ²]	4.32E+04	6.30E+03	1.25E+03	-6.30E+03	-4.32E+04
Max Stress Allow [lb/in ²]	8.00E+04	1.05E+04	1.25E+03	1.05E+04	8.00E+04

Table 5.3: Tail boom stress analysis

Parameter						
Material	Aluminum					
d [in]	1					
L [in]	35					
t [in]	0.035					
E	1.00E+07					
I _{xxc} [in ⁴]	0.013744					
Weighted I _{xxc} [in ⁴]	1.37E+05					
Centroid (y)	0.00E+00					
I _{xx_sys} [in ⁴]	1.37E+05					
Bending Moment [lb-in]	70	140	210	280	350	420
Tip Load [lbs]	2	4	6	8	10	12
Max distance [in]	0.5					
Max Stress (B) [lb/in ²]	2.55E+03	5.09E+03	7.64E+03	1.02E+04	1.27E+04	1.53E+04
Max Stress Allow [lb/in ²]	3.00E+04					
	OK	OK	OK	OK	OK	OK
Deflection of Tip [in]	0.21	0.42	0.62	0.83	1.04	1.25

Table 5.4: Aircraft weight build-up

Component	Weight (lb.)
Payload	
Water	13.200
Bottles	1.800
Section Weight	15.000
Propulsion	
Motor	0.906
Propeller	0.130
Prop Nut	0.045
Battery Pack	5.000
Speed Controller	0.270
Wire	0.100
Section Weight	6.351
Flight Controls	
Receiver	0.125
Receiver Battery	0.325
Flaperon Servos (2)	0.220
Elevator Servo	0.110
Rudder Servo	0.110
Wire	0.050
Section Weight	0.940
Landing Gear	
Nose Wheel	0.100
Main Wheels (2)	0.200
Nose Strut	0.600
Main Struts (2)	0.800
Section Weight	1.700
Fuselage	
Light Ply	1.800
Fairings	0.500
Cowling	0.125
Section Weight	2.425
Wings	
Spars (2)	0.750
Ribs	0.125
Foam Core (2)	1.250
Endplates	0.250
L.E. & T.E. Balsa (2)	0.850
Hard Points	0.125
Section Weight	3.350
Tail Section	
Horizontal	0.340
Vertical	0.180
Boom	0.250
Push rods (2)	0.004
Section Weight	0.774
Total Weight	30.539

Table 5.5: Complete aircraft performance for various payloads

Aircraft Performance				
<u>Liters of Payload</u>	0	2	4	6
<u>Weight(lb)</u>	15	20	25	30
<u>Payload Fraction</u>	0	0.25	0.4	0.5
<u>Takeoff distance (ft) no flaps</u>	32	60	100	150
<u>10 deg. Flaps</u>	27	49	80	119
<u>20 deg. Flaps</u>	22	40	69	105
<u>30 deg. Flaps</u>	20	32	54	80
<u>Cruise Velocity (ft/s)*</u>	55	55	52	42
<u>L/D max Velocity (ft/s)</u>	34	38	42	46
<u>Maximum Velocity (ft/s)</u>	68	67	66	64
<u>Turn Rate at Cruise (deg /s)</u>	84	60	45	36
<u>Bank Angle at Cruise (deg)</u>	68	60	52	40
<u>Maximum Rate of Climb (ft/min)</u>	636	416	271	165
<u>Ferry Time (s)</u>	90.38961	-----	-----	-----
<u>Cargo Time (s)</u>	-----	57.45455	64.07692	79.52381
<u>Maximum Endurance (min)</u>	21.7	13.9	9.5	7.5
<u>Endurance at L/D max (min)</u>	20.6	13.4	9.5	7
<u>Maximum Range (ft)</u>	42024	30552	23940	19320
<u>Maximum Range (mile)</u>	7.959091	5.786364	4.534091	3.659091

*Cruise is defined as half current throttle setting

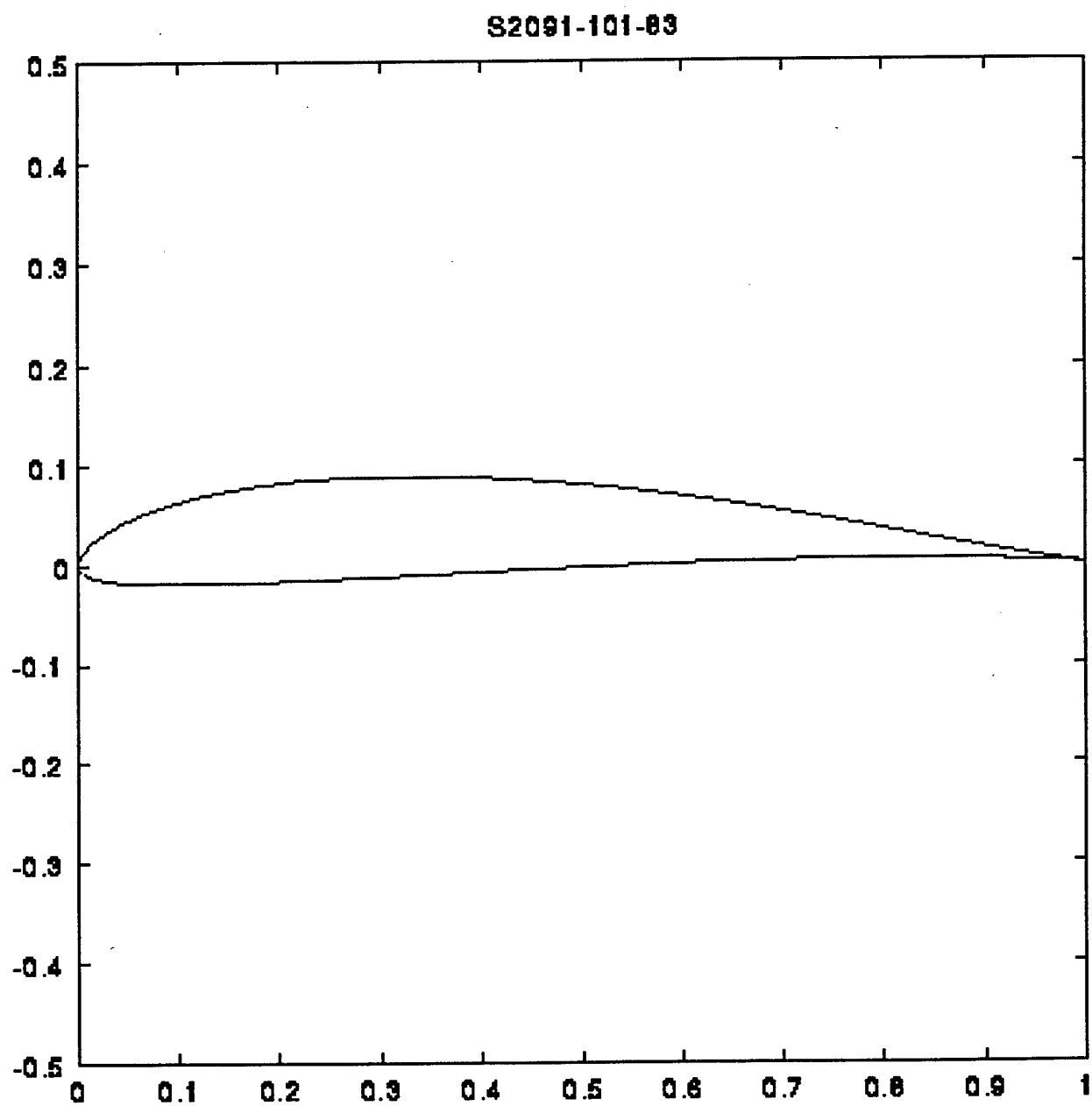


Figure 5.1: Selig 2091 airfoil

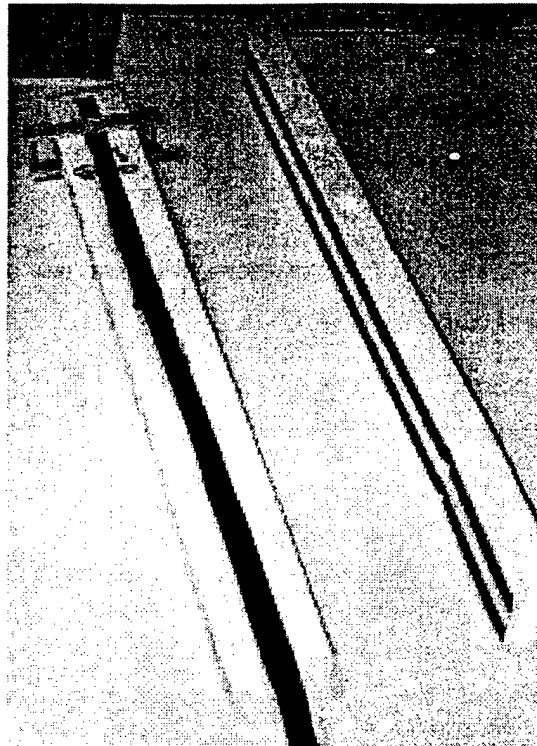


Figure 5.2: Carbon fiber strip only spar test

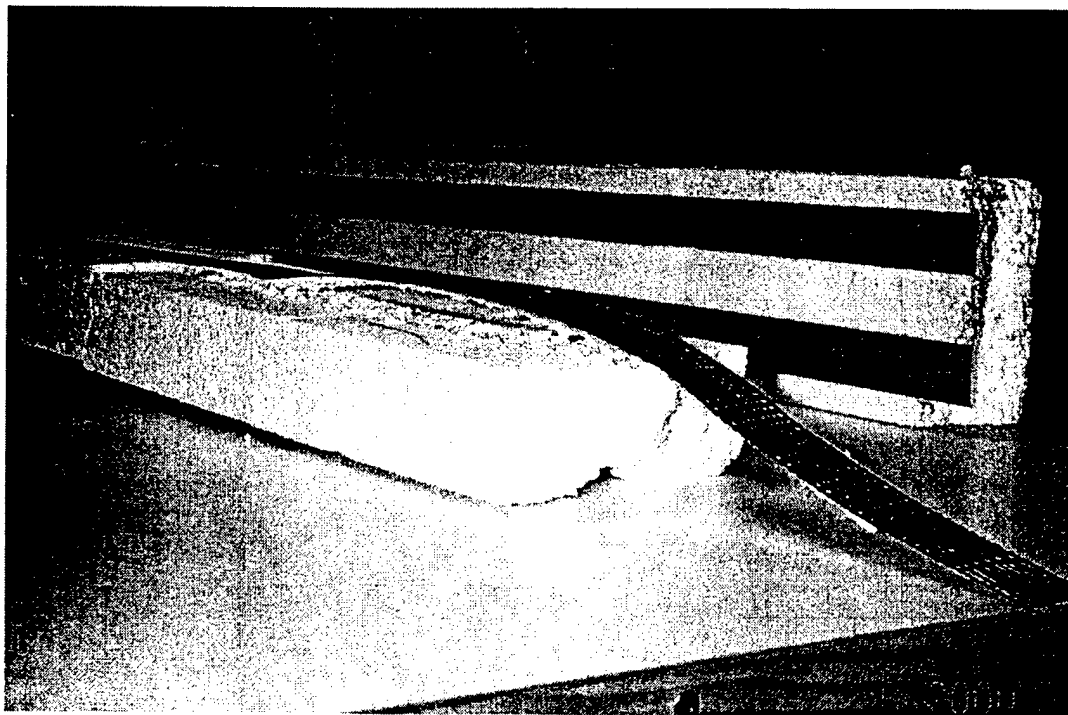


Figure 5.3: Carbon fiber and basswood spar test

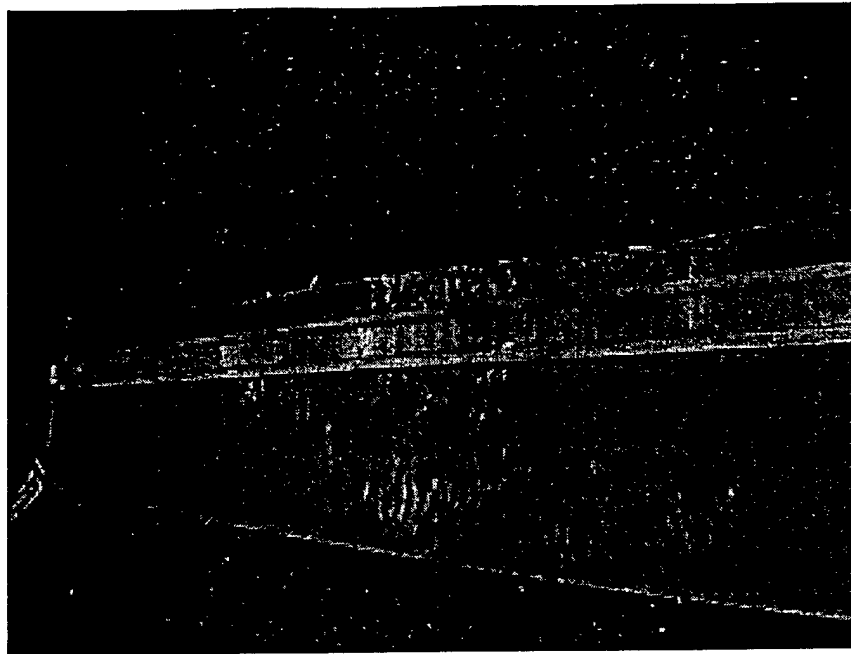


Figure 5.4: Carbon fiber built-up spar

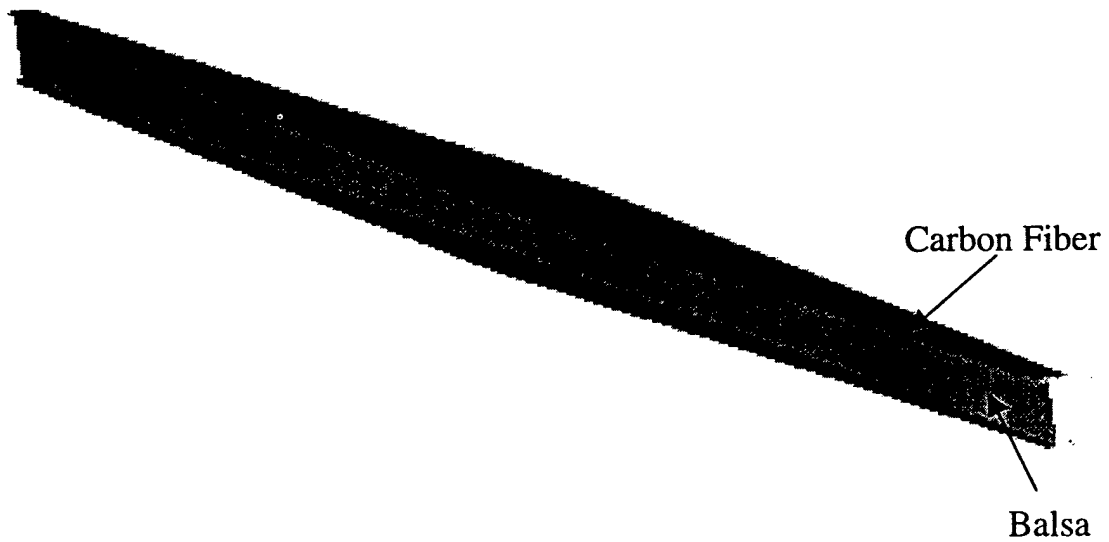


Figure 5.5: Final spar design

ALL DIMENSIONS ARE IN INCHES
BALSA LEADING AND TRAILING EDGES
SPRUCE AND BALSA SPAR

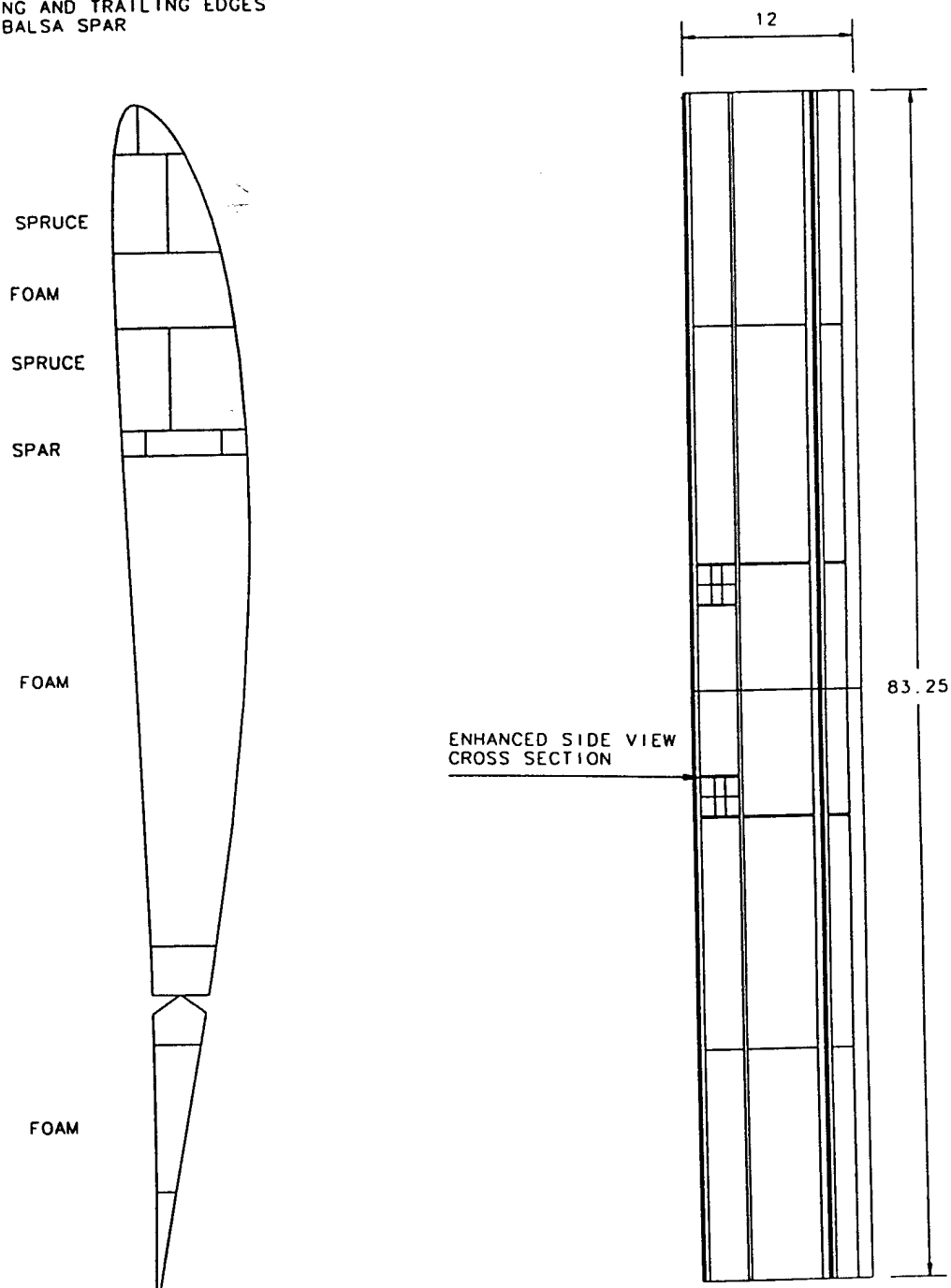


Figure 5.6: Wing structure

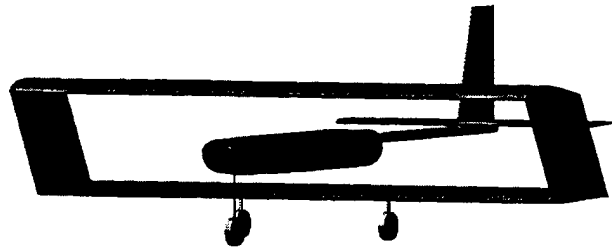
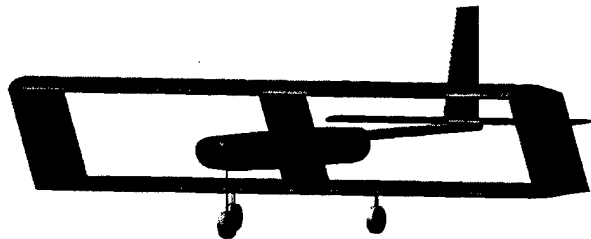
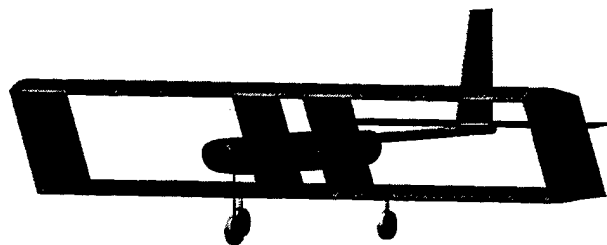


Figure 5.7: Basic fuselage concept

Option 1



Option 2



Option 3

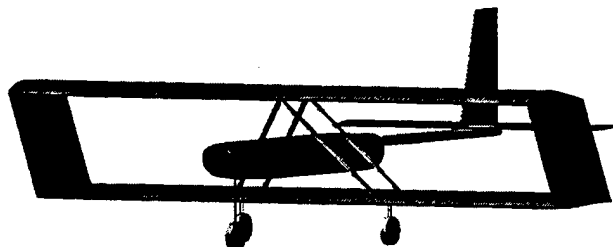


Figure 5.8: Fuselage options

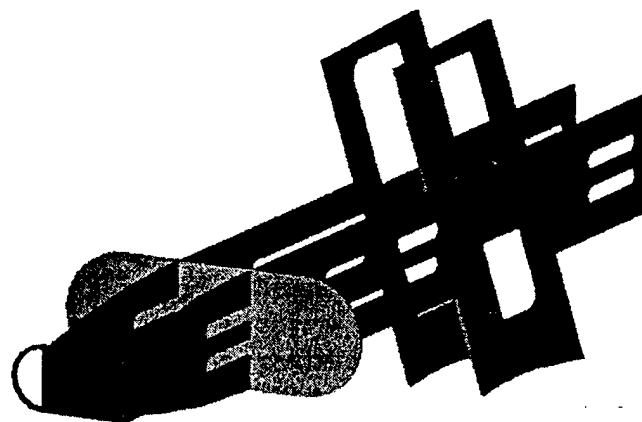


Figure 5.9: Final fuselage structural design

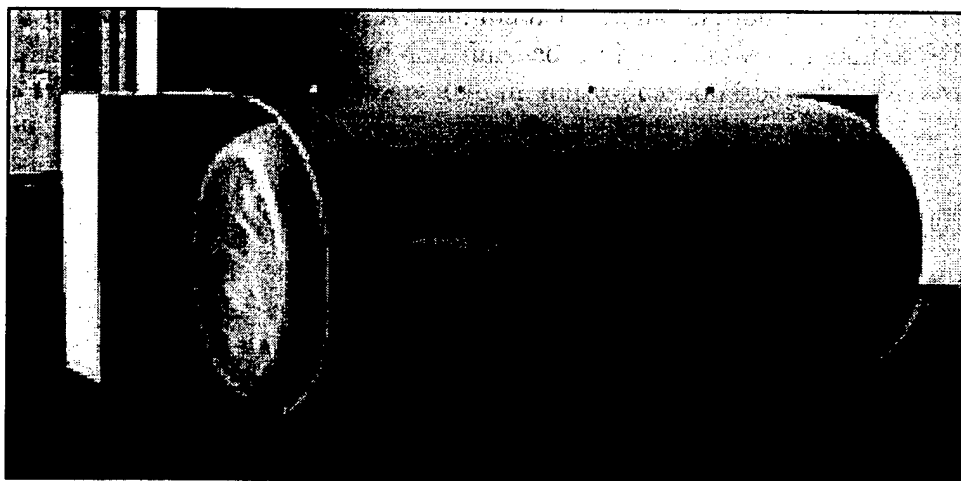


Figure 5.10 Fuselage payload bay mock up

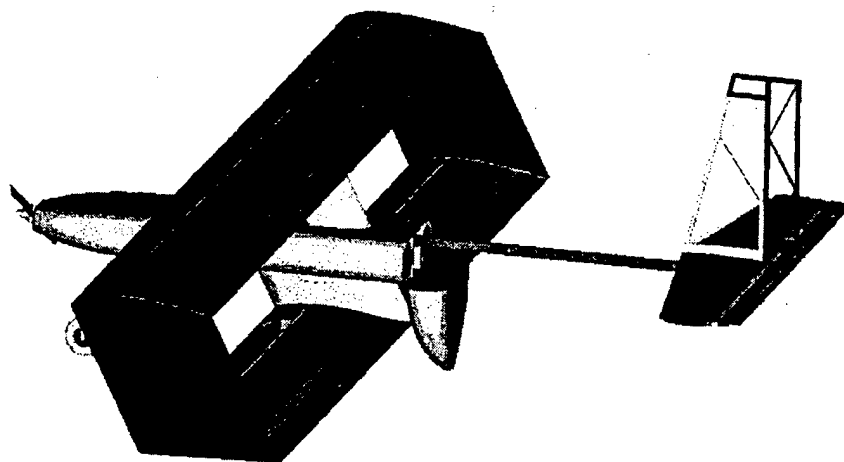


Figure 5.11: Bottle loading and unloading access

ALL DIMENSIONS ARE IN INCHES
TRUSS MEMBERS ARE $1/8" \times 3/8"$
LEADING AND TRAILING EDGES ARE $3/8" \times 3/8"$

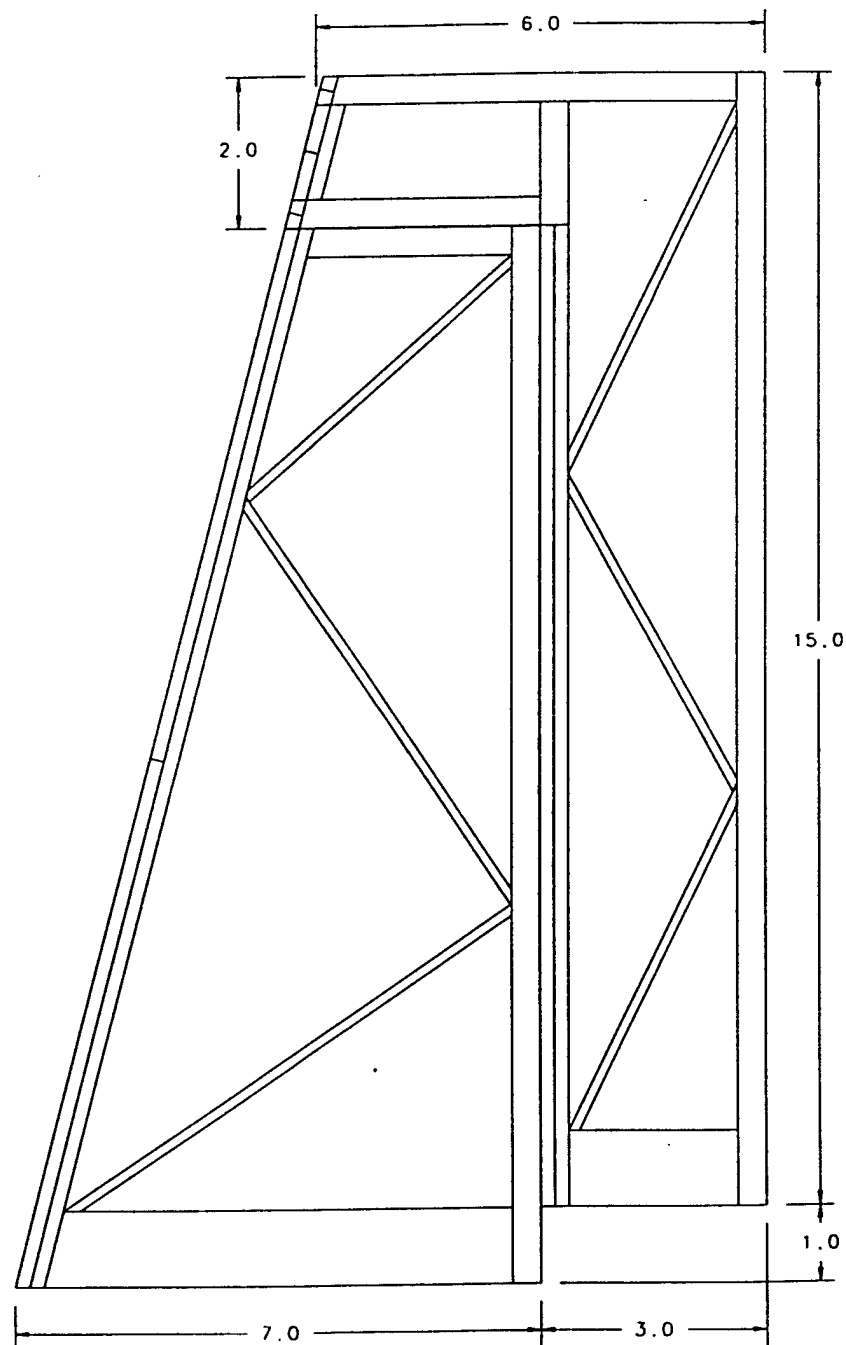


Figure 5.12: Vertical stabilizer structure

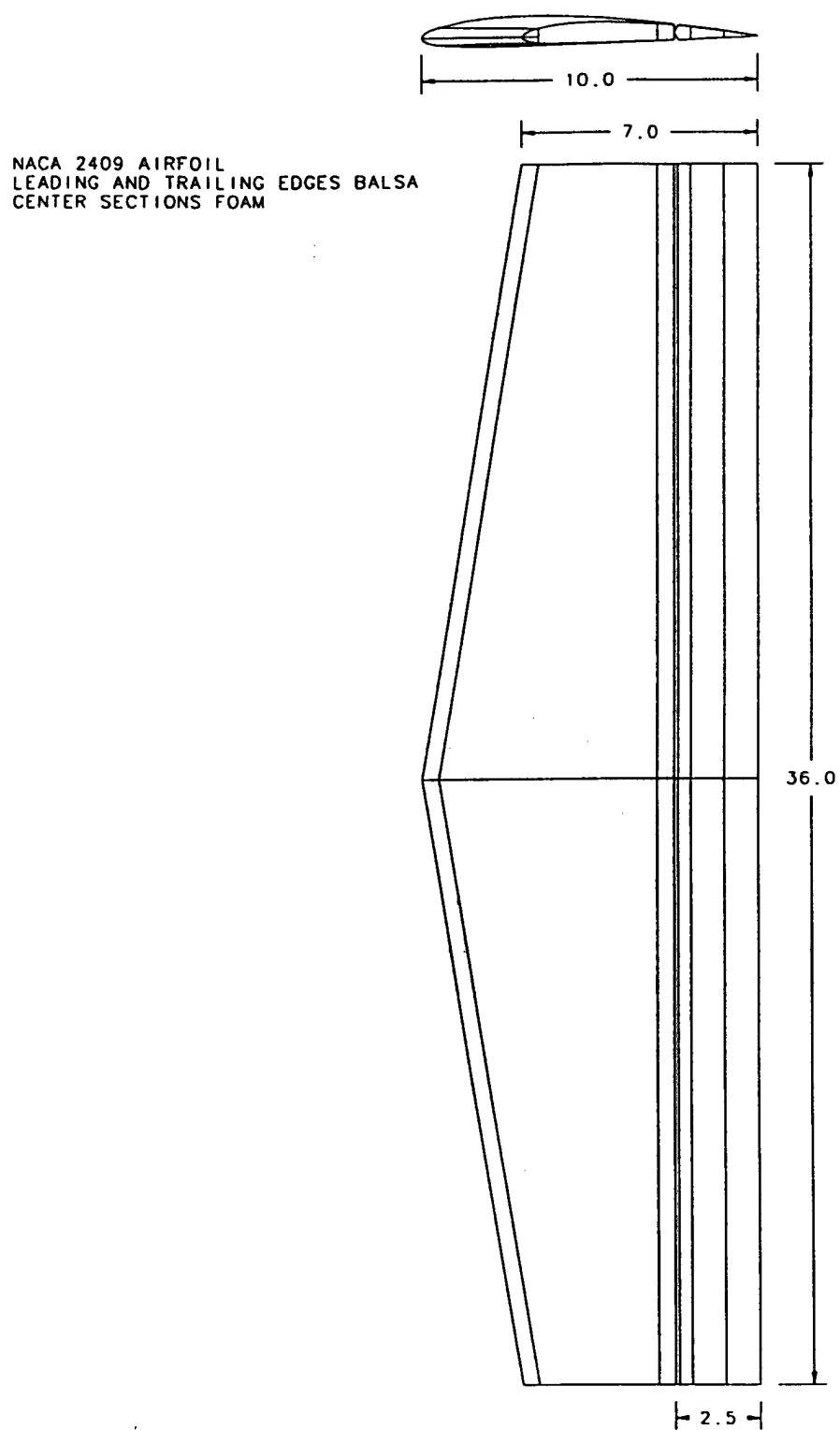


Figure 5.13 Horizontal stabilizer structure

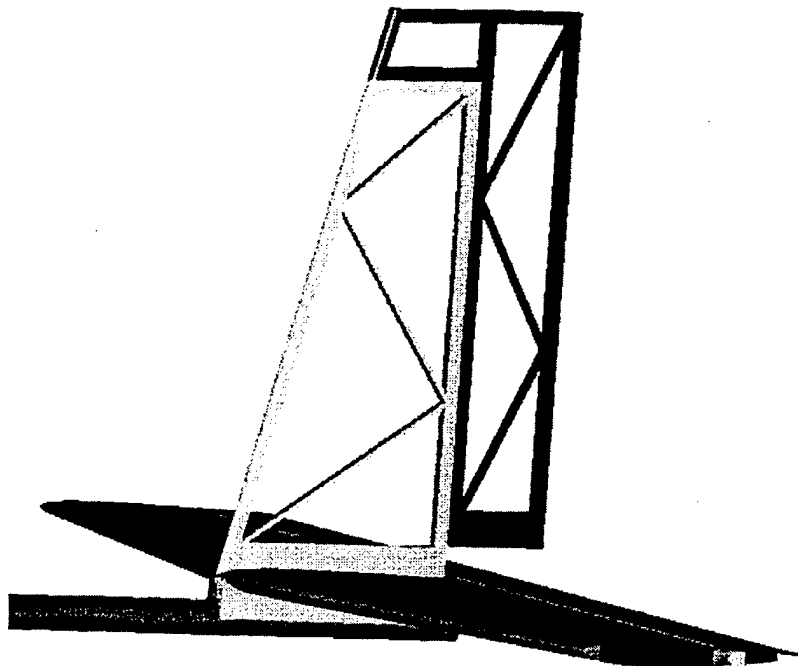


Figure #5.14: Empennage attachment

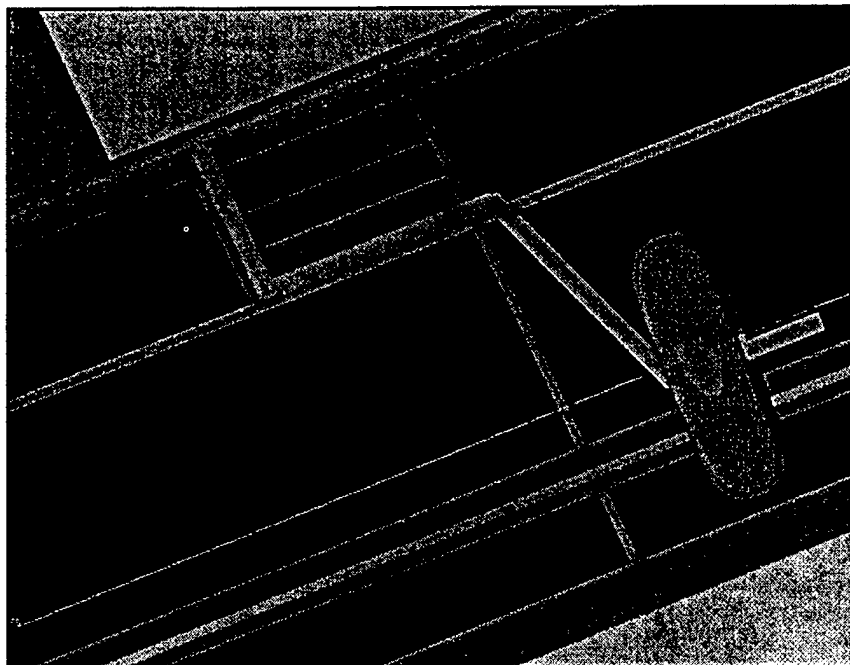


Figure 5.15: Main landing gear

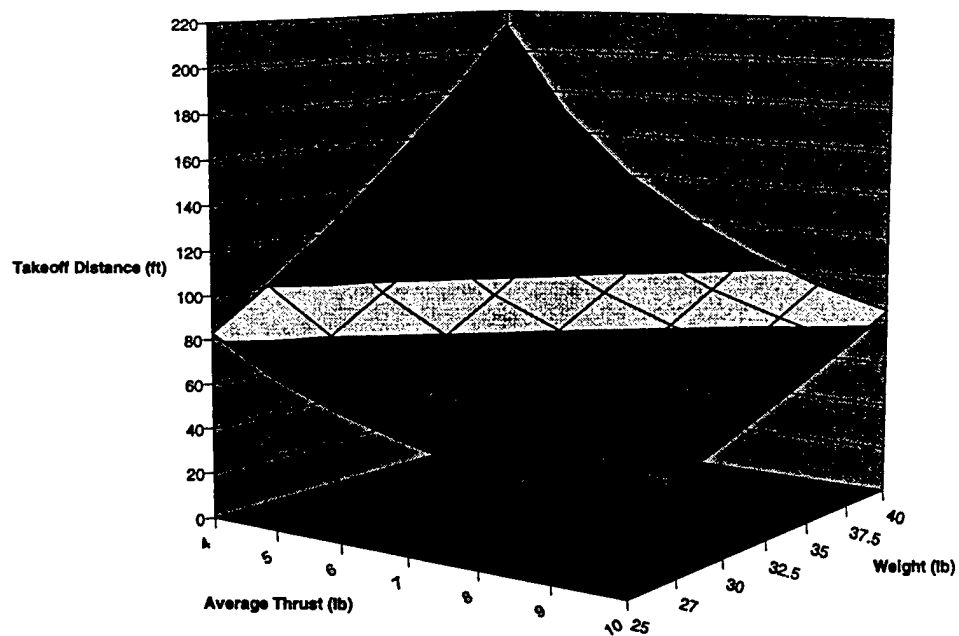


Figure 5.16: Airplane takeoff performance with headwind

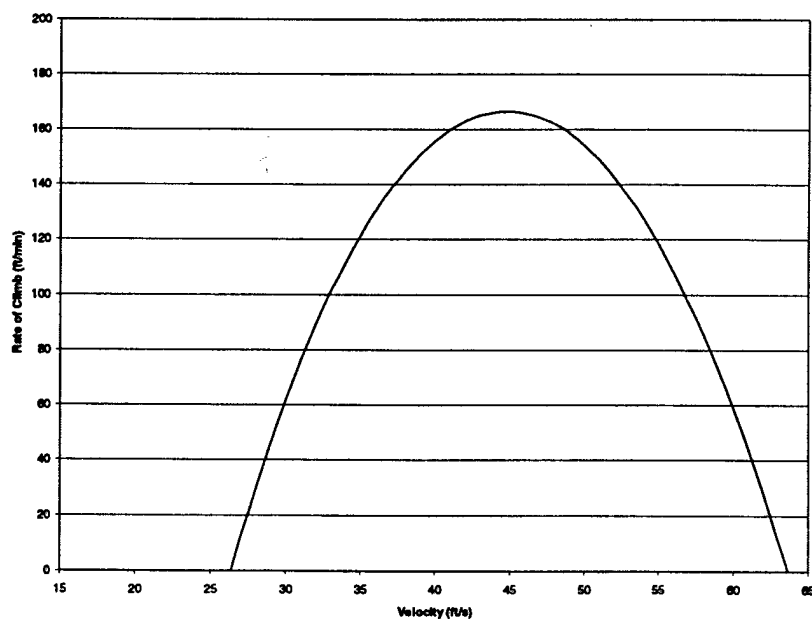


Figure 5.17: Rate of climb verse velocity for 6 liter payload

6.0

MANUFACTURING PLAN

Development of the assembly was planned with a high degree of testing and experimentation. The aircraft was divided into the three traditional modules that typically make up an airplane. These were the fuselage, empennage, and wings. Most of the individual parts that composed the modules were drawn with local CAD software and printed to scale. Although a similar aircraft could have been assembled in just a few weeks, each module was tested for strength and performance over the course of three months. Final aircraft components will be flight tested, evaluated, and possibly replaced between the time of this report and the flight competition.

6.1 Preliminary Construction Planning

The aircraft needed to be assembled in a structured environment dedicated to the project tasks and void of outside influences or exposure. The DBF design team felt that a dedicated room or laboratory would facilitate the needs of construction planning and assembly most efficiently in terms of consistent thinking. The Georgia Tech Aerial Robotics (GTAR) laboratory has traditionally been the research center for remotely operated aircraft and was approved to be dedicated solely to DBF aircraft during the duration of the project.

In addition to the extensive array of equipment already in place, DBF team members renovated the GTAR lab in order to cater to the needs of the project. With a \$10,000 grant from the National Science Foundation for research and development, and with sponsorship from outside organizations, the Georgia Tech team made extensive improvements from the previous year's project. Improvements include additional lighting, new work tables, a conference table and chairs, increased storage facilities, a new band saw, new drafting equipment, and new drilling equipment.

During the assembly of the aircraft, the team decided that the following principles guiding the construction would result in the best aircraft:

RANK	FIGURE OF MERIT
1.	Safety---during use of power tools an operation of the aircraft
2.	Weight---every fraction of an ounce removed will add up to significant savings
3.	Strength---wing loadings expected 4g's max, hard landings expected w/full carg
4.	Assembly Difficulty---all skill levels could contribute over duration of project
5.	Modular---plane should easily disassemble for transport and storage
6.	Cost---DBF cost score and monetary costs were kept to a minimum
7.	Feedback---practical construction may override optimal conceptual designs

Refer to Figure 6.1 for the Milestone Chart for Manufacturing Phases. This figure shows the planned and actual schedule for the construction process. Many of the components of the aircraft were not complete by the time of this report, but anticipated assembly of the aircraft is been indicated.

Materials Selection

Some of the factors that influenced the design of the aircraft were those materials that are readily available and those materials that suit the needs of the aircraft. Materials used were also required to be strong, yet lightweight and easily manipulated. Most of the aircraft was

constructed using balsa wood, basswood, polystyrene, aluminum, carbon fiber, hobby-grade poplar light plywood, birch plywood, and a heavier basswood. The adhesives used were essentially two-part epoxy and cyanoacrylate ester (CA's or "Super Glue") type glues.

Per weight, balsa wood is one of the strongest of all woods. However, its light density makes it impractical to be used in places where high stress is concentrated in small areas. Balsa and foam were therefore used in the construction of the wings and tail surfaces where loads are distributed over larger areas. Denser than balsa, poplar light plywood was used for the majority of the fuselage construction for a rigid yet light fuselage. In places where stress was highly concentrated, solid basswood or birch plywood was used.

The shear and bulk modulus characteristics of carbon fiber and aluminum are very similar, but carbon fiber has a slightly higher modulus of elasticity (Young's Modulus, referred to as "E-value") making it more resistive to deformation. In an Excel spreadsheet, the bending strength and tip displacement for both aluminum and carbon fiber booms were compared under various loads. Although carbon fiber is less dense than aluminum, and therefore lighter than aluminum, it is much more expensive. A 1 in. diameter round carbon fiber tube, such as would be used on the tail boom, has to be laid and finished by hand. As a comparison, 48 in. tube in Aluminum will cost around \$6.70, as where a 48 in. tube of carbon fiber will cost around \$84.00. It was argued that the slightly lower weight and slightly higher resilience were advantages that were too small to offset the extremely high cost of carbon fiber.

6.2 Fuselage

The fuselage was the first component of the aircraft to undergo construction. The fuselage design integrated the vertical support with the main body of the fuselage. Referring to Figure 5.9, one can see that the vertical support gave the correct "stagger" for the wings while simultaneously enclosing the massive battery pack. The interior body of the fuselage, which is rectangular in shape, houses the radio equipment, holds the nose gear, holds the tail boom, and provides support for the cargo bays. Most of the interior fuselage body is composed of poplar light plywood, with the exception of balsa sheeting for streamlining on the top and bottom. For simplicity and weight, the fuselage sides and vertical support sides were integrated into one piece that reduced unnecessary material as seen in Figure 5.9.

The development of the cargo bays took several months before arrival at a simple solution. Very early designs of the biplane fuselage were simply two rigid tubes connected closely with batteries and radio gear on top in the crevice between the tubes and the tail boom tightly secured here and extending toward the rear. These designs were simple, lightweight, rigid, and had a small cross-sectional surface area meeting the oncoming flow of air. However, the makeup of the tubes themselves eluded the capabilities of the design team. Cardboard tubes were investigated, but at 3½ in. inside diameter, most tubes had walls that were ¼ in. thick or larger, which made the fuselage much heavier than was necessary. Carbon fiber tubes were too expensive to have custom made by a professional, and the amateur craftsmanship of design team members was not acceptable for the purposes of the aircraft. Architect's map tubes often had ridges that added strength to the tube but destroyed the streamlined look that was desired. There was also the problem of connecting the two tubes to the wings, attaching the tail boom to them, and providing enough strength to adequately hold the nose gear on a hard landing.

The solution to the fuselage problem was twofold. First, the two tubes were displaced approximately 2 in. in order to provide for an internal structure to hold the nose gear and tail boom while simultaneously inclosing the radio gear. This structure was to be the main body of

the fuselage in the final design. Secondly, the two tubes were replaced with cargo bays formed from rolled sheet aluminum.

The sheet aluminum was thin enough to be lightweight, yet strong enough to hold the bottles in place on a rough landing. Aluminum also gave the smooth streamlined sides that the team had envisioned for the aircraft. A mock up of the aluminum fuselage was built for design feasibility purposes and is shown in Figure 5.10.

Both ends of the cargo bays and the wing support had to be faired in order to streamline the aircraft. Later in the development of the aircraft, it was decided that the same foam used to construct the wings could be easily shaped to form the structure that was needed. The front of the aircraft was divided into two halves by the fuselage; essentially one cowl on either side (see Figure 6.2). The two "nose-end" cowls were shaped on the inside to channel the incoming flow of air around the motor (the inner fuselage has an air return port on its underside) because it is known that high currents and high temperatures are a likely situation. These two halves were glued in permanently, but the rear of the aircraft had to be movable.

In order for the bottles to be removed, the rear cowling had to be moved out of the way, yet the structure had to be strong enough to hold the weight of the bottles at high angles of attack. After a long deliberation about the best means to accomplish this function, it was decided that the rear cowl could be hinged to swing down out of the way to access the bottles. The cowl could be firmly attached to the boom while "shut" in order to keep the bottles securely in the cargo bays. In order to facilitate one hinge and one latch for retaining two cargo bays, the rear cowl obviously had to be constructed from one piece of foam. The rear cowl was fitted with a small rim cut inward at an angle that would push into the cargo bays and shape the rolled aluminum to a perfect contour. The joints between the three cowls, as well as all intersections of the aircraft were diligently constructed to minimize gaps and ensure smooth transitions between pieces.

6.3 Empennage

In addition to the basic aerodynamic qualities, the design team wanted to meet two main requirements for the tail feathers of the aircraft:

1. Create an empennage that is sufficiently rigid in flex and torsion, while retaining light weight.
2. Create a modular empennage that can be easily replaced in the event of damage or for experimentation.

The alignment of the tail to the fuselage was not a problem because the tube could be twisted to match the tail to the plane of the aircraft. However, attaching the lower cambered airfoil of the horizontal stabilizer to the round tube presented some formidable challenges. The case on the top of the where the fin met the shallow camber of the stabilizer was similar and equally challenging. In both places, the intersections had to be rigid when attached (1), yet able to be taken apart in order to be modular (2). The intersections could easily be glued for rigidity, but then they would not be modular. The intersections could be simply bolted together for modularization, but where and how would the bolts be placed so that the entire structure remained rigid?

The first option presented was to put a plug into the tube and mount to tail section on the plug and behind the end of the tube. Two bolts simultaneously through the tube and the plug would make it very easy to remove the entire tail section. There were concerns that the

horizontal stabilizer could not be made strong enough to resist the twisting caused by uneven loads since the "plug" could be, at most, 1 in. wide.

The alternative proposal was to mount the tail to the outside of the tube so that the attaching structure could "grab" the outside of the tube with a joining section that is wide enough to prevent twisting. After several designs were investigated, the design team developed a clever idea that would meet all requirements. The final design was to insert into the stabilizer two wooden "blocks" that are shaped as in Figure 6.3. The block arms are long enough to displace loads into the foam, and the cradle securely fits onto the tail boom tube. To keep the blocks lightweight, they were constructed of a ¼" wide balsa block of the shape desired and laminated with 1/32 in. birch plywood for strength. One block was placed in the front and one near the hinge point of the trailing edge. The fin was attached through these blocks with very long bolts. The bolts were threaded deep enough into the fin so that the rigidity of the bolts themselves gave rigidity to the fin (see Figure 6.3).

6.4 Wing and Landing Gear

Extruded polystyrene (commonly referred to under the Dow Chemicals name, Styrofoam®) was chosen to construct the wing for several reasons. The polystyrene could be cut easily with a hot wire, and the team could experiment with different densities to determine the tradeoff between weight and strength (1-lb/ft² was used in the final aircraft). Another advantage was that it could be cut to hold an exact airfoil shape by using wood templates cut from CAD printouts. The team could cheaply obtain polystyrene in large quantities, which meant that if a cut was done improperly, it was quite easy to simply throw out the piece and make another. Some disadvantages that the team had to work around were the following:

1. A structure made with foam is only as strong as the local glue joint---which meant that large spans of the material had to be reinforced with wood or multidirectional carbon fiber laminate.
2. Polystyrene is susceptible to melting at fairly low temperatures---which meant that special low temperature vinyl covering had to be used for covering.
3. Polystyrene is susceptible to deformation or failure when loads are localized---which meant that it was used only to fill structural members that could support themselves without the polystyrene in place.

The upper and lower wings shared the same airfoil and were therefore cut from the same templates. The top wing was made from two 3½ ft. sections and then joined in the middle. The bottom wing was made in three sections; two outboard from the main landing gear and one providing a platform for the fuselage support. The leading edge was capped in balsa wood to hold the leading edge shape. The trailing edge of the wing that was ahead of the control surface was also capped in balsa wood so that hinges could be mounted securely in the wing. The control surfaces themselves were constructed in the same manner. Each wing has a ¼ in. wide balsa spar running through the thickest part of the airfoil. The balsa spar will be capped with bi-directional carbon fiber as shown in Figure 5.5.

This spar is an essential structural member in the wings, since applied loads could be as much as 90 lbs. (15 lb. airplane in 6g's). Upper and lower spars will share identical but are currently still under research. The lower wing must be significantly reinforced because of the loads it would be required to support on rough landings. Spars and other internal support members will be constructed as discussed in the Detailed Design Phase.

As discussed in the Detailed Design Phase, the upper and lower wings were joined at the ends with end plates. Aside from providing an aerodynamic advantage, they greatly increased the rigidity of the wings. The endplates will be constructed from birch light plywood and balsa, and will be covered in heat transfer vinyl covering. A large hole will be cut in each endplate to lighten the structure.

Multidirectional carbon fiber laminate was used on the top and bottom of each wing. At the center of the wing, the carbon fiber is 4 in. wide and tapers to 2 in. at the wing tips. The curvature of the top strip of carbon fiber gives the wing strength from compression and the lower strip of carbon fiber give the wing strength in tension. The wing spar is to be glued to theses carbon fiber strips along the entire length.

The landing gear was positioned to sit under the lower wings and just behind the center of gravity (CG). Fastening the gear to the underside of the wing meant that the structure had to be engineered not to damage the wing upon landing. Since the wing is made of foam, the design team had to find a solution that displaced the torque that the wire landing gear placed on the wing. One of the reasons the lower wing was divided into three sections was to facilitate this need. Two ribs run along the length of the chord-separated 3 in. Between the ribs is a hard basswood runner that supports the main gear (Figure 5.15). The inboard rib has a basswood block that holds the end of the gear and keeps the gear from twisting fore to aft. The nose gear is simply attached to a rectangular rib of the inner fuselage. It is hinged to turn the aircraft while on the ground and is operated by the rudder servo.

Although the design team does not have a working aircraft at this point, most of the conceptual work has been done. The remainder of the aircraft is currently under construction and will be completed for flight testing in the next ten days.

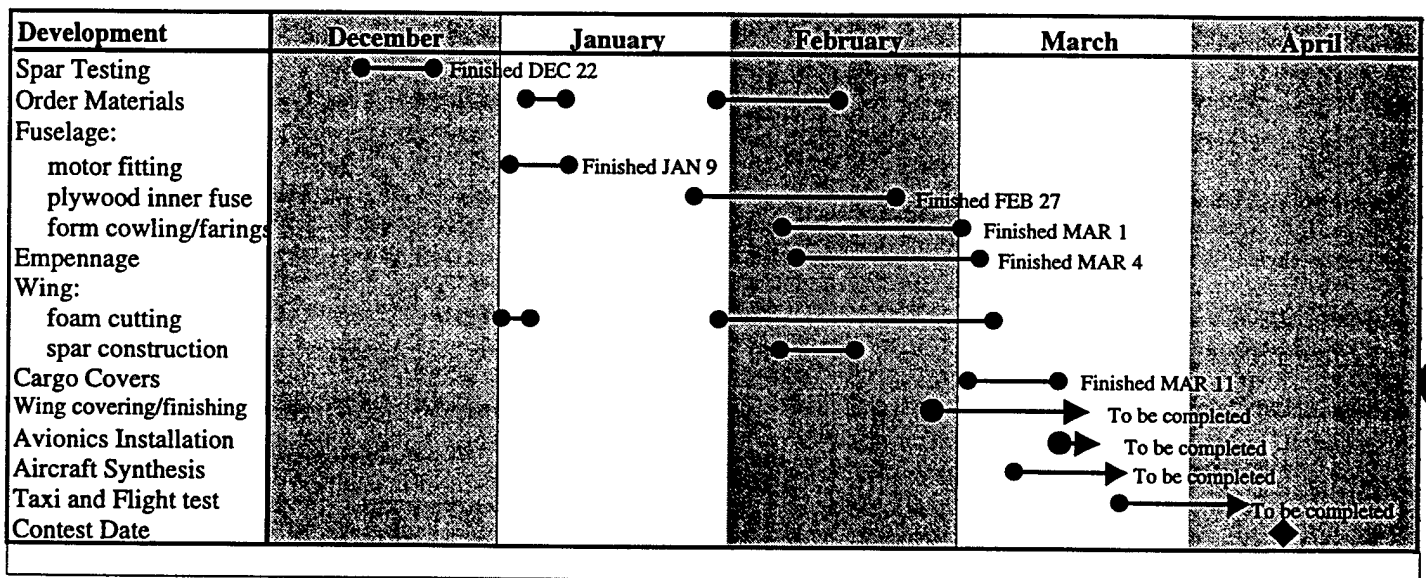


Figure 6.1: Manufacturing Milestones

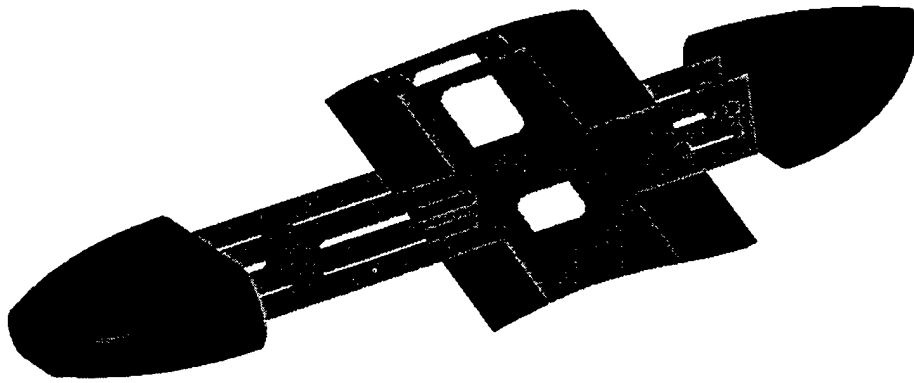


Figure 6.2: Fuselage Fairing

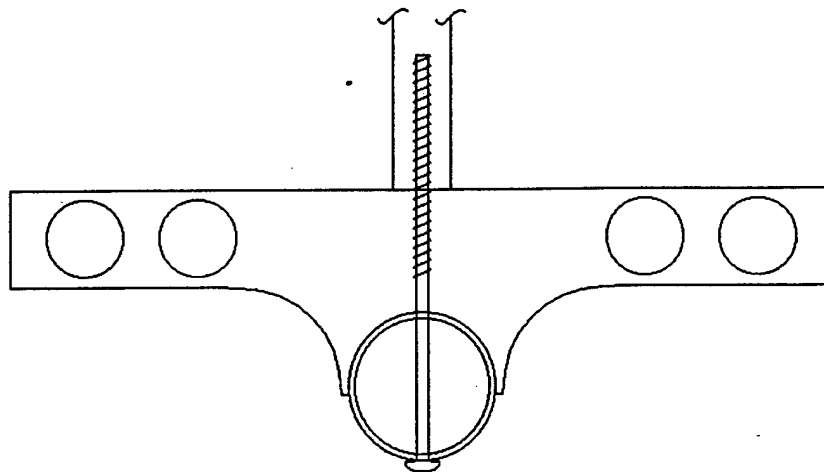


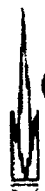
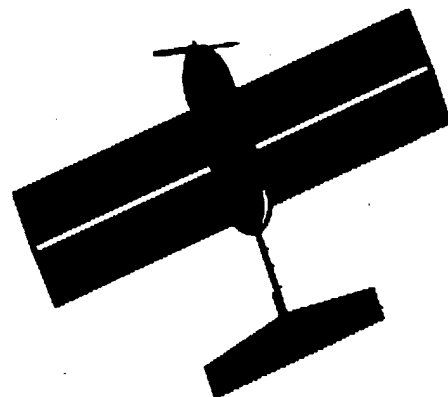
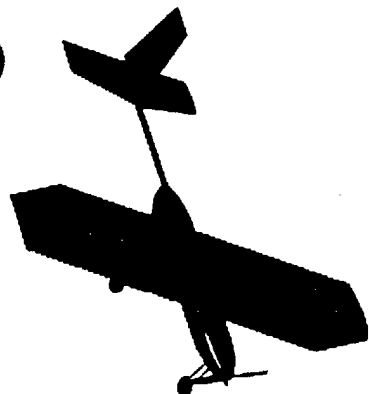
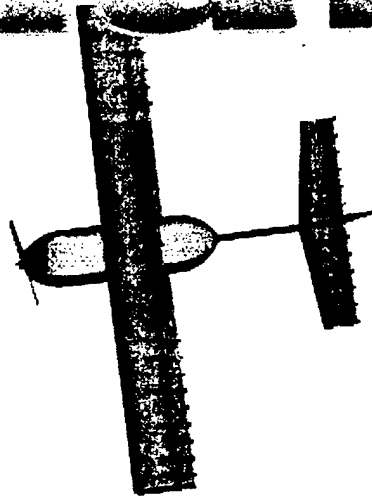
Figure 6.3: Stabilizer Blocks

REFERENCE PAGE

1. Aveox Virtual Test Stand, <http://www.Aveox.com/virtual.html>
2. UIUC Airfoil Coordinates Database, <http://amber.aae.uiuc.edu/~m-selig/ads.html>
3. Analyze on Airfoil, <http://beadec1.ea.bs.dlr.de/Airfoils/calcfoil.htm>
4. Raymer, Daniel P., Aircraft Design: A Conceptual Approach. AIAA Education Series, AIAA 1989
5. Anderson, John D., Jr., Introduction to Flight 3rd Edition. McGraw-Hill Series in Aeronautical and Aerospace Engineering, McGraw-Hill Inc., New York, 1989
6. Munk, Max M. "General Biplane Theory." National Advisory Committee For Aeronautics Report No. 151.

1999/2000 AIAA Design/Build/Fly Contest Addendum

PLAN B



**Georgia Institute
of Technology**

TITLE PAGE

**The Georgia Institute of Technology
Presents**

PLAN B

**1999-2000
AIAA Design/Build/Fly Competition**

**School of Aerospace Engineering
Georgia Institute of Technology
Atlanta, GA 30332**

**Advisor:
Dr. Dimitri Mavris**

**Team Members:
Jason Zumstein
Adam Broughton
Karen Feigh
Mike Penland
Kevin Wagahoff
Harlan McCullough
Brian Dolan
Josh Hardy
Alisa Hawkins
Michael Matthews
Phillip Frye
Darius Moore
Elizabeth Walden**

TABLE OF CONTENTS

TABLE OF CONTENTS	2
1.0 EXECUTIVE SUMMARY	2
2.0 MANAGEMENT SUMMARY	8
3.0 CONCEPTUAL DESIGN	12
3.1 PROBLEM DEFINITION	12
DESIGN DRIVING FACTORS	12
MISSION FEATURES	12
3.2 FIGURE OF MERIT DEFINITION	13
3.3 PRESCREENING ANALYSIS	13
3.4 CONFIGURATION IDENTIFICATION	14
CONVENTIONAL	14
BIPLANE	14
DELTA WING	14
3.5 CONFIGURATION ANALYSIS	15
ANALYTICAL TOOLS	15
INDEPENDENT ANALYSIS	15
ANALYSIS CONCLUSIONS	18
3.6 CONFIGURATION EVALUATION	18
QUANTITATIVE FOM EVALUATION	18
QUALITATIVE FOM EVALUATION	18
CONFIGURATION RANKING	19
CONCLUSIONS	19
4.0 PRELIMINARY DESIGN	26
4.1 POWER PLANT SELECTION	26
BATTERY SELECTION	26
MOTOR SELECTION	27
4.2 AIRCRAFT SIZING	29
SPREADSHEET ANALYSIS	30
SPREADSHEET RESULTS	30
5.0 DETAILED DESIGN	36
5.1 WINGS	36
AIRFOIL SELECTION	36
FLAP DESIGN	36
WING STRUCTURE	37
WING ATTACHMENT	38
5.2 FUSELAGE	38
BOTTLE LAYOUT AND STRUCTURE	38
TAIL BOOM	39
5.3 EMPENNAGE	40
SIZING	40
ATTACHMENT	40
5.4 LANDING GEAR	40
SELECTION	40
PLACEMENT	41
TYPE	41

ATTACHMENT	41
5.5 AIRCRAFT STABILITY AND CONTROL	42
5.6 HANDLING QUALITIES	43
5.7 PERFORMANCE	43
6.0 MANUFACTURING PLAN	60
6.1 PRELIMINARY CONSTRUCTION PLANNING	60
MATERIALS SELECTION	60
6.2 FUSELAGE	61
6.3 EMPENNAGE	62
6.4 WING AND LANDING GEAR	63
7.0 LESSONS LEARNED	67
7.1 DESIGN ALTERATIONS	67
7.2 AREAS FOR IMPROVEMENT	69
8.0 AIRCRAFT COST	74
8.1 RATED AIRCRAFT COST	74
8.2 ACTUAL EXPENDITURES	75

7.0

LESSONS LEARNED

On April 5, at approximately 6pm, the Plan B, under its own power, departed from the paved airstrip of the Newton County RC Flyer's field and flew for the first time. This beautiful blend of artwork and engineering represented over nine months of intense dedication to the project. Although not perfect, the Plan B has taught the Georgia Tech DBF members a tremendous amount about aircraft design, light aircraft construction, UAV electronics, project planning, and project development, just to name a few.

The process of engineering was once thought to be a discrete discipline; every one problem had one proper solution. However, during the development of this project it has been realized that there may be infinitely many solutions to a problem, and many solutions may be equally feasible. The problem itself may not be easily defined, and group members have often had to take several steps "backwards" before being able to proceed to a solution. In order to develop what is considered the best solutions to complex problems, the engineering process was kept as fluid as possible. There were no members that dominated with the "best" ideas. Each problem was solved as a group effort, with brainstorming sessions that sometimes went on for hours until a proper solution of which everyone agreed upon was acquired.

It was also realized that some solutions could be over-engineered. Often times, the best solutions to complex problems were those that were the most simple in design. The simple solutions were the most direct, and because they were less complicated than more clever engineering designs, they reduced the potential for additional problems.

Engineering was realized as an ongoing process. Engineering was realized as not only the development of solutions, but the realization of problems, the acceptance of complexities, and the recognition that another's idea may be better than your own. This sometimes humbling experience was a constant process, and the nature of engineering in this context was the core of what made the *PLAN B* what it is today.

Engineering pushes us toward perfection without ever acquiring perfection. It is now known that the final aircraft, to be flown in competition on April 15th, 2000, could still be improved beyond its current state of construction. Excellent in design or not, this aircraft will represent the engineering, dedication, and creative efforts of the DBF team of Georgia Tech.

7.1 Design Alterations

The aircraft proposed in the design report presented earlier does not significantly differ from what has been ultimately constructed. The majority of the development since that time has been on the wing spar. The wing spar was to be the main structural member of the wing, and it was very important that the spar be designed to withstand the stress of wing testing and normal flight loads, yet maintaining light weight.

Once the airfoil shape was chosen and cut from foam, several spars were constructed and tested. The wing core was cut with the intent of a 1-¼ by ¼ inch spar to run the length of the wingspan. It was thought that the first spar constructed would be the final spar used in the competition aircraft (Figure 7.1A.). This design made use of a light balsa center section (essentially a balsa spar), capped with bi-directional carbon fiber laminate on top and bottom. The carbon fiber on the top of the wing would support compressive loads, while the lower strip would support tension loads. The balsa spar was intended to resist compressive and shear forces. The internal rigidity of the carbon fiber was intended to resist torsion effects. The carbon fiber

strips were 2 inches wide with the spar running along the center. The laminating medium used was two-part 5minute epoxy. After failing the stress test, the spar was analyzed by a materials expert. It was then learned that 5minute epoxy is too viscous to wick into the fiber elements of the carbon fiber, therefore even after fully cured it was "mushy" at best. It was also learned that unidirectional carbon fiber would have been more appropriate for our application, since the fibers running parallel to the wing chord did not add to the structural rigidity of the wing. In order to obtain true rigidity from multidirectional carbon fiber, a proper laminating epoxy, with viscosity similar to water, would have to be used. This type of epoxy requires heat treatment and several days to cure. The design team then decided that composite working was beyond the scope of the skills of the team members, and other spars were investigated.

It was decided that the first design failed because there was no significantly rigid member to give strength to the wing. In the second spar (Figure 7.1B.) the balsa center section was maintained for the reasons mentioned above, but this time the balsa was capped in $\frac{1}{4}$ by $\frac{1}{4}$ inch spruce hardwood. Two-ton epoxy (2-hour cure time) was used as the primary adhesive for this spar. It was thought that the glue joints between the wood would be the strongest points in the structural member. Unfortunately, the quality of the 2-ton epoxy did not match what had been realized with the 5minute epoxy. Spruce joints, which were cut at 45° angles were matched on top and bottom (Figure 7.1E.) which left an extremely weak point in the spar. This joint was so poor that the spar was never tested.

It was assumed that 5-minute epoxy used on the same design would provide the proper strength. However, in the interest of time, other designs were investigated. Some team members felt that balsa, although giving a weight advantage, would never provide the strength needed to support the extreme stress of 15lbs of weight in the center of a 7-foot spar only $1\frac{1}{4}$ inch tall by $\frac{1}{4}$ inch wide. Therefore the balsa was removed from the design and replaced by $\frac{1}{16}$ inch birch light plywood as the shear webbing (Figure 7.1C.). Although very strong, the spar was asymmetrical, and prone to twisting under load.

The simple solution to the spar problem was to create a spar with $\frac{1}{4}$ by $\frac{1}{4}$ inch spruce hardwood strips separated by a $\frac{3}{4}$ inch gap of empty space. Both sides were laminated in $\frac{1}{16}$ inch birch light plywood, giving a total spar width of $\frac{3}{8}$ of an inch (Figure 7.1D.). This spar design was constructed using cyanoacrylate-type (CA) glue instead of epoxy. This adhesive is stronger and lighter than epoxy. The 7-foot spar was installed in the wing and tested well beyond the test minimum of 15 lb. At 25 lb. the spar/wing combination only deflected 2 inches at the center, indicating that the wing may be able to support loads well in excess of design specifications.

As mentioned earlier, the wing cores were cut for a $\frac{1}{4}$ inch wide spar. The final spar used had a total width of $\frac{3}{8}$ inch. One of the high priorities of the design team was to maintain the exact airfoil across the entire wingspan, which is the reason that polystyrene was chosen to construct the wings. If the spar had been designed before the wing cores were cut, the $\frac{1}{8}$ inch discrepancy could have been avoided. It was decided that this small error would not significantly alter the flight performance of the aircraft, and was essentially ignored.

The only other significant change to the wing design from what was described in the proposal phase of the design report was the elimination of two wing ribs. It was decided that the strength of the spar was adequate to resist torsion effects. The current wings only have three wing sections, separated by only two ribs.

The tail cone attachment had not been decided upon at the time of the design report. It was only known that the tail cone was to hinge at its lower edge to allow access to the cargo bays. Currently the tail cone is attached with small aileron hinges, and is held in place by a small wire catch at the tail-end of the cone.

Instead of a toggle switch used to disarm the motor from the battery, a small connector between the speed controller and battery pack was routed to the outside of the fuselage. To disarm the aircraft, one simply unplugs the speed controller from the battery pack. This design came about because of difficulties in finding a light weight switch that would be able carry the high currents of the propulsive unit.

Development of the endplates was delayed until completion of the wings. Originally, the endplates were going to be solid, flat plates joining the lower and upper wings. However, because the wing plates are 3- 1/2 feet away from the center of gravity, they can significantly affect the flight performance of the aircraft in strong crosswind conditions. Discussions about the purpose of the endplates revealed that the design team wanted the endplates to provide additional strength to the pair of wings, while simultaneously reducing the spillover effect that causes induced drag. The endplates were initially cut from 1/16 birch light plywood; making a complete surface from the top of the upper wing to the bottom of the lower wing. Then, to allow crosswind airflow through the plates, a large hole was cut as shown in Figures 7.2 through 7.5. This hole was shaped so that the plate was thicker at the trailing edge to still aid in the reduction of wingtip vortex strength.

Final empty flying weight of the aircraft was 15.5 lb., 0.5 lb. over our original estimation. Every effort was made to reduce weight as much as possible. Lightening holes were cut in every component that could sustain holes, and materials were chosen to maximize strength for the smallest amount of weight. Some design team members feel that the current wing spar is the reason for the extra half pound and that a lighter spar could be made that would still be structurally adequate. Other weight concerns were that the nose and tail cones could have been covered in vinyl film rather than painted, but counter arguments held that aesthetic qualities were important for representing Georgia Tech and the difference in weight was negligible. Ultimately, it is felt by the team that although weights are slightly above estimations, a significantly lighter aircraft could not be realized without altering the overall design of the aircraft.

Further weight investigation found that the center of gravity was nearly 2 inches behind the optimal location of 1/4 mean aerodynamic chord. After shifting the internal components of the aircraft as far forward as possible, the CG was still around 1 inch too far aft. Further movement of the CG would require the addition of weight to the nose of the aircraft. Although team members had strong objections to this solution, there is no compromise to having a stable aircraft and 1 pound of weight was added to the nose for the initial flight tests while the aircraft's handling characteristics are discovered.

7.2 Areas for Improvement

The previous entry into the 1998-1999 DBF competition gave this year's team useful insight into the nature of the competition. Much of the research done on airfoils, electronics, and motor selection were carried over into the development of this year's aircraft. Having placed a proud 4th place in last year's competition, this year's team feels that the new aircraft is much better suited for the purpose of this year's competition. One would like to think that as long as Georgia Tech places an entry into the DBF competition, Georgia Tech will become more of a contender as the year's progress. However, much of the credit for major developments of the

project can be contributed to key members of the team whom were able to culminate a multitude of skills and talents and focus on engineering greatness. The success or failure of the DBF entry in the future depends upon recruiting new people like these that can be competitive in national competition. For those members in this year's team that will contribute to the DBF effort in the future, it is imperative that they learn as much as possible now while the proper people are available. Those people that will be moving on after this year's competition have the obligation to recruit valuable new members that may take their place.

Improvement in the DBF program at Georgia Tech began with the onset of the project last fall. The Georgia Tech Aerial Robotics (GTAR) laboratory was extensively renovated for this year's entry. Professors and research assistants recognized the magnitude of the effort going into the project and have scheduled to move the GTAR lab into a larger, better suited facility for next year. Students involved in this year's project were long term focussed, and purchased many new tools and equipment that will remain part of GTAR for future use.

The contest rules to be released for next year's competition will determine the design for future DBF entries. However, if the rules do not change greatly, then next year's aircraft may be similar in design, yet much closer to perfection. There were always many questions that could only be accurately answered with physical test, which are expensive and time consuming. It is possible that another year on the same project may lend itself towards dramatically different results.

To summarize an entire discourse on the possible improvements to physical entities of the aircraft would be futile. Every effort has been made to refine the aircraft as much as possible. Every last detail of the aircraft has been fine tuned to the purpose of the competition. Improvements beyond what has already been created are still arguable and not clearly defined. The Design, Build, Fly team of Georgia Tech looks forward to measuring up against other teams who have met the same challenge.

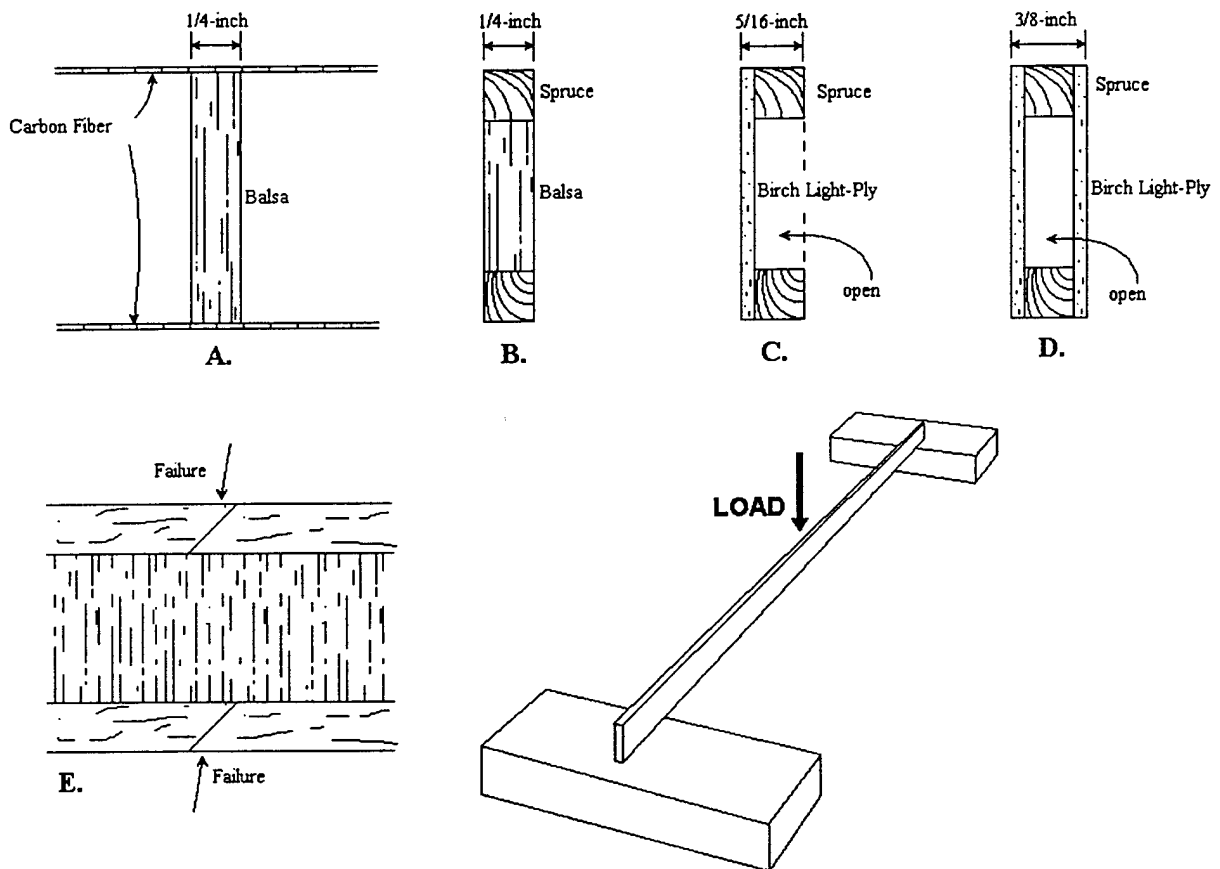


Figure 7.1: Wing spar evolution



Figure 7.2: Eight future aircraft designers

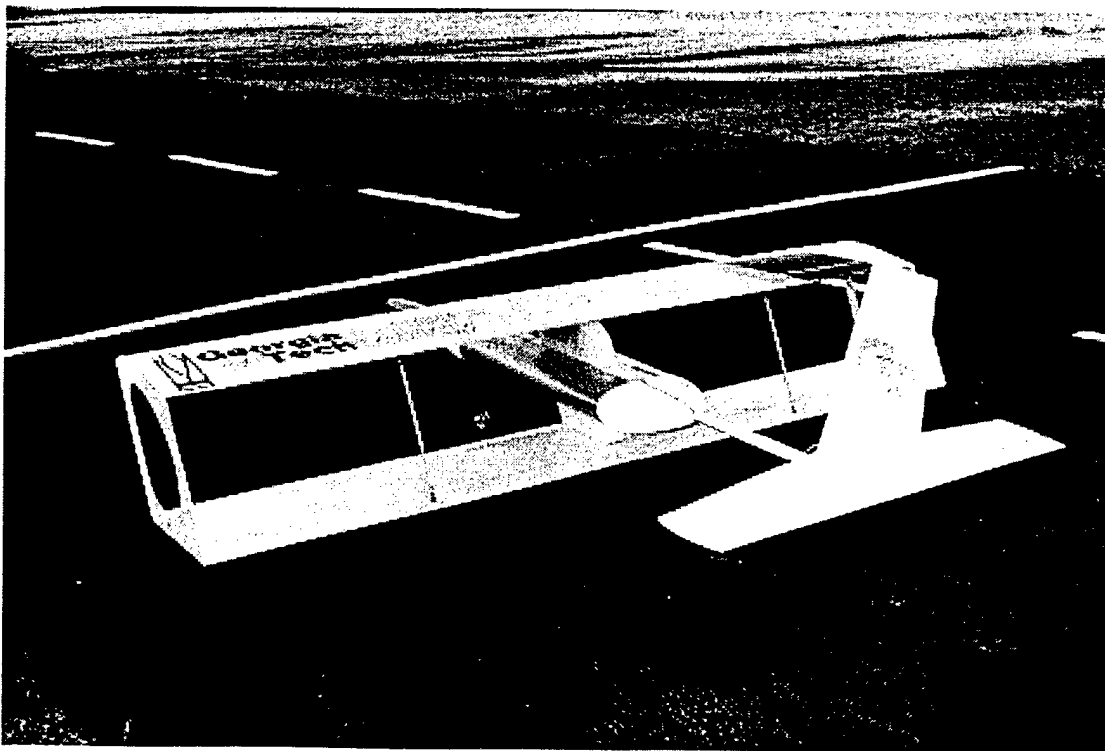


Figure 7.2: Aircraft prepared for first flight

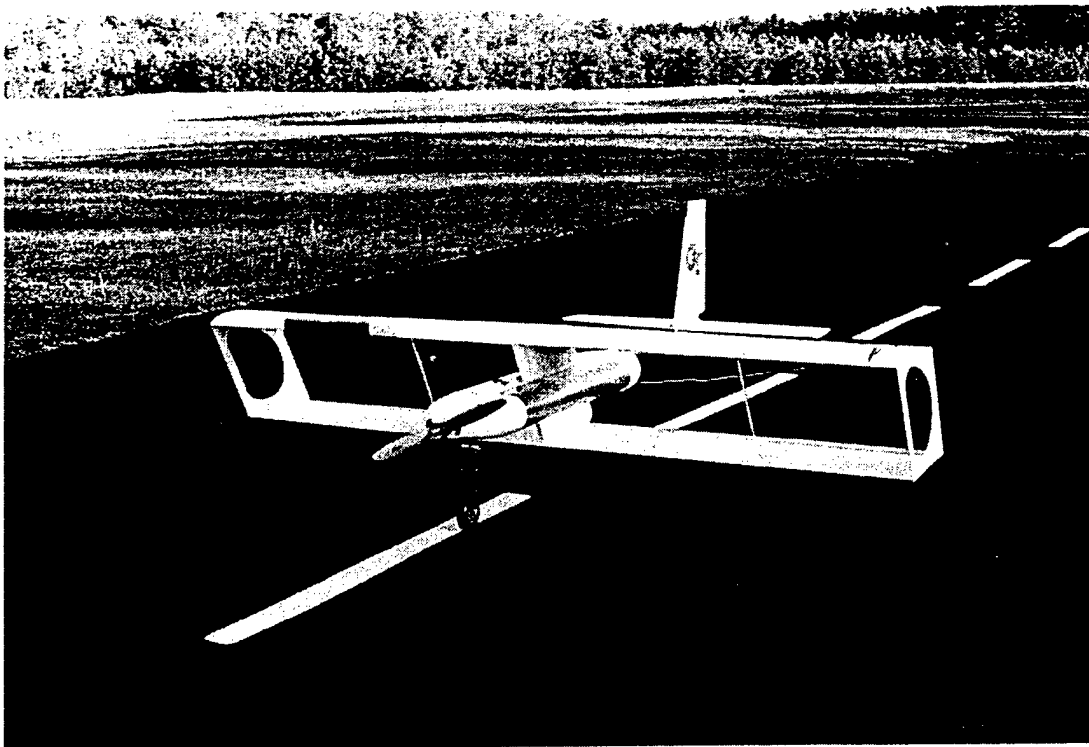


Figure 7.4: Three, Two, One

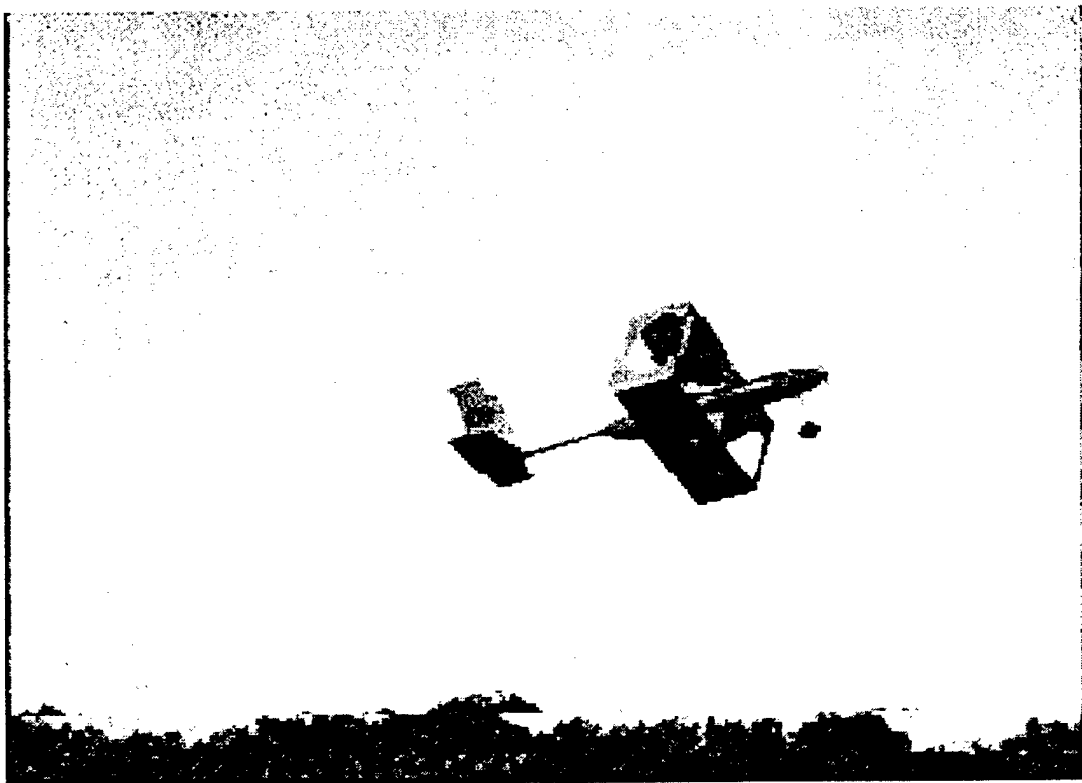


Figure 7.5: ...Liftoff!

8.0

AIRCRAFT COST

8.1 Rated Aircraft Cost

One of the major additions to the 1999/2000 AIAA Design Build Fly contest total score calculation was the rated aircraft cost model. Each of the participating teams in the contest will be scored in the following manner:

$$\text{SCORE} = (\text{Written Report Score} * \text{Total Flight Score}) / \text{Rated Aircraft Cost.}$$

The total flight score is calculated by multiplying the total number of liters of water carried during the best three 10 minute flight routines by a factor of 10. As can be seen in the Score calculation, the rated aircraft cost can have a very significant impact.

The rated aircraft cost is composed of three main areas. These areas are the Manufacturers Empty Weight (MEW), the Rated Engine Power (REP), and the Manufacturing Man Hours (MFHR). The MEW is the weight of the aircraft less any payload and less the propulsive battery pack. The REP is only dependent on the number of motors and number of battery cells used. The MFHR is a manufacturing model that attempts to capture the amount of man hours required to build the aircraft. Thus, as the complexity and size of the aircraft increase, the projected amount of time required increases in the manufacturing model.

Each of the factors that make up the rated aircraft cost have an associated cost with them respectively. For every pound of aircraft weight in the MEW, a \$100.00 cost is modeled. Each watt of motor power calculated from the REP is acquired at the cost of \$1.00. Although students do work for free, each man hour spent on the aircraft comes at the price of \$20.00 in the MFHR model. After the cost of each of the rated aircraft cost contributors is multiplied by its respective cost, the total cost is calculated and the divided by one thousand. This results in the value for the rated aircraft cost that is used in the overall score calculation.

For Georgia Tech's *PLAN B* aircraft, the rated aircraft cost was calculated and is shown in Table 8.1. At the top of the table, the rated aircraft cost is defined and the calculated values for the contributing factors are shown. The MEW value of 10.5 lb. was simply obtained by weighing the entire empty aircraft with the propulsive battery pack removed. The REP was only slightly more complicated to calculate since it is composed of the number of motors multiplied by the battery pack voltage and a generalized current of 50A. For *PLAN B*, only one motor is used and the battery pack is composed of 26 cells. This results in a REP of 1560 watts. The calculation of the REP is shown in the middle of Table 8.1.

The rated aircraft cost factor that has the most complexity is the MFHR. Each component of the aircraft is contained in the MFHR, which is broken down into five subgroups: wing(s), fuselage/pods, empennage, flight systems, and propulsion systems. The wing subgroup has a basic cost of 5 man hours for each wing. Additionally, the size of the wing(s) is taken into account by charging 4 man hours for each square foot of wing area. Since *PLAN B* is a biplane with 14 square feet of wing area, the time required to build the wings is approximated at 66 hours. Each fuselage, or pod, is charged a base fee of 5 man hours. Each foot of fuselage length is then charged 4 hours. Since *PLAN B* only has one fuselage with a total length from the tip of the rudder to the tip of the nose cone of 67 inches, or 5.7 feet, the estimated build time is 27.8 hours. The empennage subgroup is subjected to a base cost of 5 hours, and then an 5 hours for

each vertical and 10 hours for each horizontal stabilizer. *PLAN B* has only one vertical and one horizontal, thus 20 hours is the total time estimated for empennage construction. The control system subgroup bases the complexity of the flight controls and required linkage solely on the number of servos. Each servo is expected to require one man hour for installation in addition to a basic control system time of 5 hours. Because *PLAN B* only has four servos, one for elevator, one for rudder and nose gear, one for the left flaps, and one for the right flaps, the total time for the control system is 9 hours. The final subgroup that makes up the MFHR is the propulsion system. Five man hours are charged for each motor and each propeller. With *PLAN B* being a single engine, single propeller aircraft, the total time for the propulsion system manufacturing is 10 hours. The total man hours for the aircraft when all of the subgroups are added together is 132.8. The bottom section of Table 8.1 shows the MFHR subgroups and resulting values associated with *PLAN B*.

When the *PLAN B* values for MEW, REP, and MFHR are used in the rated aircraft cost model, a value of \$5.266 results and can be used to estimate the total flight score. From the design proposal, *PLAN B* is anticipated to carry 6 liters of water during each cargo sortie. If three cargo sorties are performed during each of the three required 10 minute competition runs, a total of 54 liters of water will be carried. When the number of liters of water and the rated aircraft cost are combined with a mildly optimistic report score of 98, an anticipated total flight score of 10,049 results! However, if only 4 liters of water are carried during each cargo sortie and a written report score of 90 is received with all other parameters remaining the same, then a total flight score of 6,152 results. The team feels that either of these scenarios is possible, so there is a rather large amount of variability in the expected flight score.

8.2 Actual Expenditures

Because this is the second year Georgia Tech has entered the AIAA Design Build Fly Contest, some of the components and support equipment used on the 1998/1999 aircraft, such as the flight control system and battery charger, will be used on *PLAN B*. However, there were still many items that had to be purchased. The main areas of additional purchases include building materials and supplies, propulsive system, field equipment, and report expenses. All of the expenses for this project excluding travel expenses to and from the competition are shown in Table 8.2. Battery packs are not shown in Table 8.2 because the propulsion system battery packs were donated by Promark Electronics.

Table 8.1: Calculation of Rated Aircraft Cost

Aircraft Cost Model		
Rated Aircraft Cost, \$ (Thousands) = (A*MEW + B*REP + C*MFHR)/1000		
<u>Coef.</u>	<u>Description</u>	<u>Value</u>
A	Manufacturers Empty Weight Multiplier	\$100 / lb.
B	Rated Engine Power Multiplier	\$1 / watt
C	Manufacturing Cost Multiplier	\$20 / hr.
MEW	Manufacturers Empty Weight (lb.)	10.5
REP	Rated Engine Power (watts)	1560
MFHR	Manufacturing Man Hours (hr.)	132.4
Rated Aircraft Cost, \$ (Thousands) =		5.258

REP Calculation	
<u>Description</u>	
Rated Engine Power (REP), watts = # motors * 50A * 1.2 V/cell * # cells	
Number of Motors = 1	
Number of Cells = 26	
Rated Engine Power (watts) =	
1560	

MFHR Calculation	
<u>Description</u>	
1.0 Wing(s), 5 hr./wing + 4 hr./sq. ft. Projected Area	
Number of wings = 2	
Total wing area = 14	
Hours = 66	
2.0 Fuselage, 5 hr./body + 4 hr./ft of length	
Number of bodies = 1	
Length = 5.6	
Hours = 27.4	
3.0 Empennage, 5 hr. + 5 hr./vertical + 10 hr./horizontal	
Number of verticals = 1	
Number of horizontals = 1	
Hours = 20	
4.0 Flight Systems, 5 hr. + 1 hr./servo	
Number of Servos = 4	
Hours = 9	
5.0 Propulsion Systems, 5 hr./motor + 5 hr./propeller	
Number of motors = 1	
Number of Propellers = 1	
Hours = 10	
Manufacturing Man Hours (MFHR) =	
132.4	

Table 8.2: Actual project expenditures

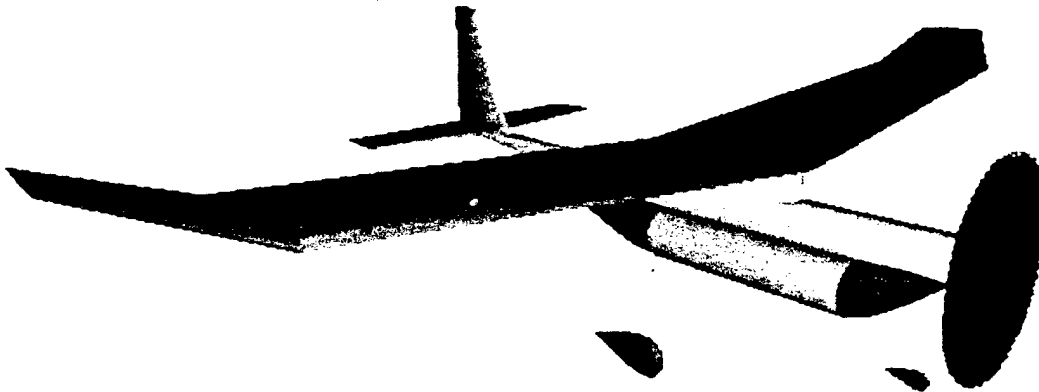
<u>Desert Aircraft Purchases</u>				
Description	Date	Quantity	Unit Price	Total
Menz "standard" 2-blade wood 18X8	Feb. 8 2000	1	16.00	16.00
Menz "standard" 2-blade wood 18X10	Feb. 8 2000	1	16.00	16.00
Menz "standard" 2-blade wood 18X12	Feb. 8 2000	1	16.00	16.00
Menz "standard" 2-blade wood 19X8	Feb. 8 2000	1	17.00	17.00
Menz "standard" 2-blade wood 19X10	Feb. 8 2000	1	17.00	17.00
Menz "standard" 2-blade wood 20X8	Feb. 8 2000	1	19.00	19.00
<u>Aveox Purchases</u>				
Description	Date	Quantity	Unit Price	Total
1415-3Y Brushless Electric Motor	Feb. 28 2000	1	225.00	225.00
H160C Competition Speed Control	Feb. 28 2000	1	240.00	240.00
Robbe 4197 3.7:1 All metal Gearbox	Feb. 28 2000	1	115.00	115.00
<u>Lone Star Balsa Purchases</u>				
Description	Date	Quantity	Unit Price	Total
Misc. Balsa and Spruce	Jan. 17 2000			62.28
<u>Hobby Haven Purchases</u>				
Description	Date	Quantity	Unit Price	Total
Hobbico Rate Gyro	Apr. 5 2000	3	58.30	174.90
Balsa wood and paint	Mar. 25 2000			20.18
Epoxy and Covering	Mar. 27 2000			27.57
Balsa wood and zap CA	Mar. 1 2000			16.48
Astroflight zero loss connectors	Mar. 9 2000	4	6.80	27.20
Screws, button head	Feb. 17.2000	11	1.35	14.85
<u>The Container Store</u>				
Description	Date	Quantity	Unit Price	Total
1 liter polyethylene round bottle	Mar. 29 2000	10	2.99	29.90
<u>Home Depot Purchases</u>				
Description	Date	Quantity	Unit Price	Total
Misc. building hardware	Mar. 29 2000			32.07
Misc. building hardware	Mar. 20 2000			20.84
Delta Band saw	Feb. 14 2000	1	149.99	149.99
Wood and supplies to for table	Jan. 20 2000			118.54
<u>Report Expenses</u>				
Description	Date	Quantity	Unit Price	Total
Kinko's, color copies	Mar. 12 2000			99.72
Fedex same day delivery	Mar. 13 2000			189.00
Fedex overnight delivery	Apr. 7 2000			30.00
Kinko's, color copies	Apr. 7 2000			24.58
Office Depot report materials	Mar. 12 2000			22.56
<u>National Hobby Supply Purchases</u>				
Description	Date	Quantity	Unit Price	Total
Dave Brown Carbon Fiber Tape	Feb. 11 2000	4	5.95	23.80
Pacer Zap a Gap, 1 oz	Feb. 11 2000	2	4.95	9.90
Pacer 5-minute epoxy, 4 oz	Feb. 11 2000	1	5.95	5.95
2-hour Ex-Slow-Cure epoxy, 4.5 oz	Feb. 11 2000	1	5.99	5.99
Hobbico Ball point Hex L-wrench	Feb. 11 2000	1	5.95	5.95
X-Acto Block Plane	Feb. 11 2000	1	5.95	5.95
JR servos, DS 8231	Mar. 15 2000	2	89.95	179.90
JR 24" gold extensions	Mar. 15 2000	2	8.95	17.90
K&S Mighty Wire Bender	Mar. 15 2000	1	15.99	15.99
Hobbico AccuCycle battery cycler	Mar. 15 2000	1	79.99	79.99
Hobbico Deluxe Heat Gun	Mar. 15 2000	1	13.99	13.99
White Ultracote	Mar. 15 2000	4	10.75	43.00



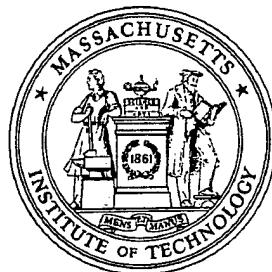
AIAA Student Design/Build/Fly Competition

MIT Fire & Water

Design Report- Proposal Phase



Larry Baskett
Jacob Markish
Larry Pilkington
Bernard Ahyow
Dan Benhammou
Adam Diedrich
Carol Cheung
Allen Chen



Massachusetts Institute of Technology
Cambridge, Massachusetts

Table of Contents

1	Executive Summary.....	4
1.1	<i>Conceptual Design Summary.....</i>	4
1.2	<i>Preliminary Design Summary.....</i>	4
1.3	<i>Detailed Design Summary.....</i>	5
2	Management Summary	6
2.1	<i>Personnel and Tasking.....</i>	6
2.2	<i>Management Structure and Scheduling.....</i>	6
3	Conceptual Design	8
3.1	<i>System Configurations Investigated.....</i>	8
3.2	<i>Analytic Methods Used.....</i>	9
3.3	<i>Final Configuration Decision.....</i>	11
3.4	<i>Configuration Refinement</i>	11
4	Preliminary Design.....	15
4.1	<i>Design parameters investigated.....</i>	15
4.2	<i>Figures of merit</i>	15
4.3	<i>Analytic methods used.....</i>	16
4.3.1	Xfoil	16
4.3.2	Athena Vortex Lattice (AVL)	16
4.3.3	Plane Geometry (PG).....	17
4.3.4	Electricalcalc and MotoCalc.....	17
4.4	<i>Preliminary sizing and key features</i>	17
4.4.1	Wing planform and sizing.....	17
4.4.2	Empennage size and shaping.....	18
4.4.3	Motor configuration and size	18
5	Detailed Design	22
5.1	<i>Component selection and systems architecture</i>	22
5.1.1	Propulsion System.....	22
5.1.2	Control System.....	22
5.1.3	Braking System	23
5.1.4	Configuration Improvements	24
5.2	<i>Final Performance Data</i>	24
5.2.1	Takeoff Performance	24
5.2.2	Handling Qualities and G-Load Capability.....	25
5.2.3	Cruise Performance	25
5.2.4	Weight Budget	25
5.3	<i>Drawing Package</i>	25

6	Manufacturing Plan.....	29
6.1	<i>Material Selection and Manufacturing Process.....</i>	29
6.2	<i>Figures of Merit.....</i>	30
6.3	<i>Construction.....</i>	30
6.3.1	Wing construction	31
6.3.2	Tail Construction.....	31
6.3.3	Fuselage Construction	31
Appendix A	35
Appendix B	40
Appendix C	42

1 Executive Summary

The Fire & Water aircraft is the result of several months of design and construction effort on the part of a dedicated team of eight students. The team combined the volumes of model aircraft-related design, construction, and flying experience of some members with the new enthusiasm of the others. Guided by our advisors, we also brought together a host of analytic methods and software packages to optimize as many aspects of the aircraft as possible. The attributes of analysis methods mentioned in this section will be described fully in the following sections.

1.1 Conceptual Design Summary

After a variety of highly creative ideas with varying levels of practical and competitive merit, the team settled upon two configurations, a conventional single-engine plane with a payload of four water bottles and a twin-engine biplane with a six-bottle capacity. For quantitative analysis of the relative performance of each configuration, an Excel spreadsheet used estimates of aircraft size and speed to calculate projected contest scores. The size and speed estimate came from a MATLAB physical flight simulation running on MotoCalc data, with the takeoff distance requirement serving as the limiting performance factor.

The single-engine plane proved to be the superior concept. It had a slightly greater projected score as well as expected advantages in handling qualities and simplicity of fabrication and operation. The specific configuration includes a load-bearing main tube containing the motor and batteries and supporting the wing, empennage, and landing gear. The payload tube is mounted to the underside of the main tube, with water tube access at the rear. A "keel," or lengthwise bulkhead inside the fuselage, centralizes structural loads and holds internal components. We chose all-composite fabrication for its versatility and high strength-to-weight ratio. RCCAD allowed us to quickly visualize configuration and overall sizing choices.

1.2 Preliminary Design Summary

The team extensively investigated and developed the aerodynamic and structural properties of our fledgling aircraft. The use of Xfoil aided in the design of an airfoil capable of performing well during all phases of the flight. For takeoff, the airfoil has high amount of camber, while for cruise the trailing edge reflexes to reduce the camber, thereby minimizing high-speed drag. AVL assisted in assessing wing loading and stability while distributing lift elliptically along the span, thus resulting in an optimal wing planform. The Plane Geometry program was utilized to finalize the tail sizing and positioning, by balancing low drag and control authority. At this point, battery and motor selection took place. These decisions were based upon experience and analytical modeling, while MotoCalc simulations were used to choose an appropriate propeller.

Experimental data from a spar failure test provided the basis for spar sizing. A failure test of the landing gear material helped to finalize the gear strut size. A design review, consisting of a presentation to the team's advisors, followed by an open

discussion, was the culmination of the preliminary design process. After exhaustive analysis of the aircraft's aerodynamic and structural design parameters, the team turned to detailed configuration and system design.

1.3 Detailed Design Summary

The team made improvements to the basic design as we considered potential difficulties in flight and opportunities to increase performance. A single payload tube became two parallel tubes, the wing moved above the fuselage with a pylon to support it, and the core tube became modular, with removable nose and tail sections. The RCCAD model evolved with these changes, but at this stage, a full-size pencil drawing became absolutely essential and served as the guide for construction. For presentation purposes, RCCAD exported a wireframe drawing for final manipulation in AutoCAD.

2 Management Summary

2.1 Personnel and Tasking

The MIT team consists of 8 members, all in the aeronautics and astronautics department. Larry Baskett, a first-year graduate student, serves as team leader and contributes some model rocket construction and team building experience. Bernard Ahyow, a junior, brings to the team extensive competitive Academy of Model Aeronautics experience in both composite aircraft fabrication and piloting skills. Larry Pilkington, also a junior with some model airplane and composites experience, deals mainly with the landing gear and composites fabrication in general. Jacob Markish, a senior, primarily contributes mathematical performance analysis and experience on MIT's team of two years prior.

Two freshmen, Adam Diedrich and Dan Benhammou, help extensively with construction tasks of all kinds. Carol Cheung, a second-year graduate student, learned from Ahyow how to operate the CNC hot wire foam cutter, and she helps coordinate the report. Allen Chen, a senior, manages the report and keeps tabs on our computer resources.

Our project advisor, Col. Peter Young (Air Force Ret.), provides practical advice and model aircraft equipment expertise and industry contacts. Prof. Mark Drela also helps considerably in an advisory role with aerodynamic design and analysis as well as composites fabrication details.

2.2 Management Structure and Scheduling

Baskett manages personnel tasking and scheduling. The team as a whole contributes to configuration control, although Baskett coordinates the overall configuration. Subsystem construction tasking goes to Ahyow for the wing and tail surfaces and Pilkington for the landing gear.

We held a design review at the end of November to set a benchmark for the design process and to provide a forum for advisor feedback on all aspects of the design. The schedule slipped considerably from the original intent due to a longer than anticipated design phase, a construction slowdown during the January inter-semester timeframe, and delays in the fabrication process. As of the writing of this report, only final composite layups and component installation remain to be completed before flight test can begin. Figure 1 on the next page is a planning milestone chart.

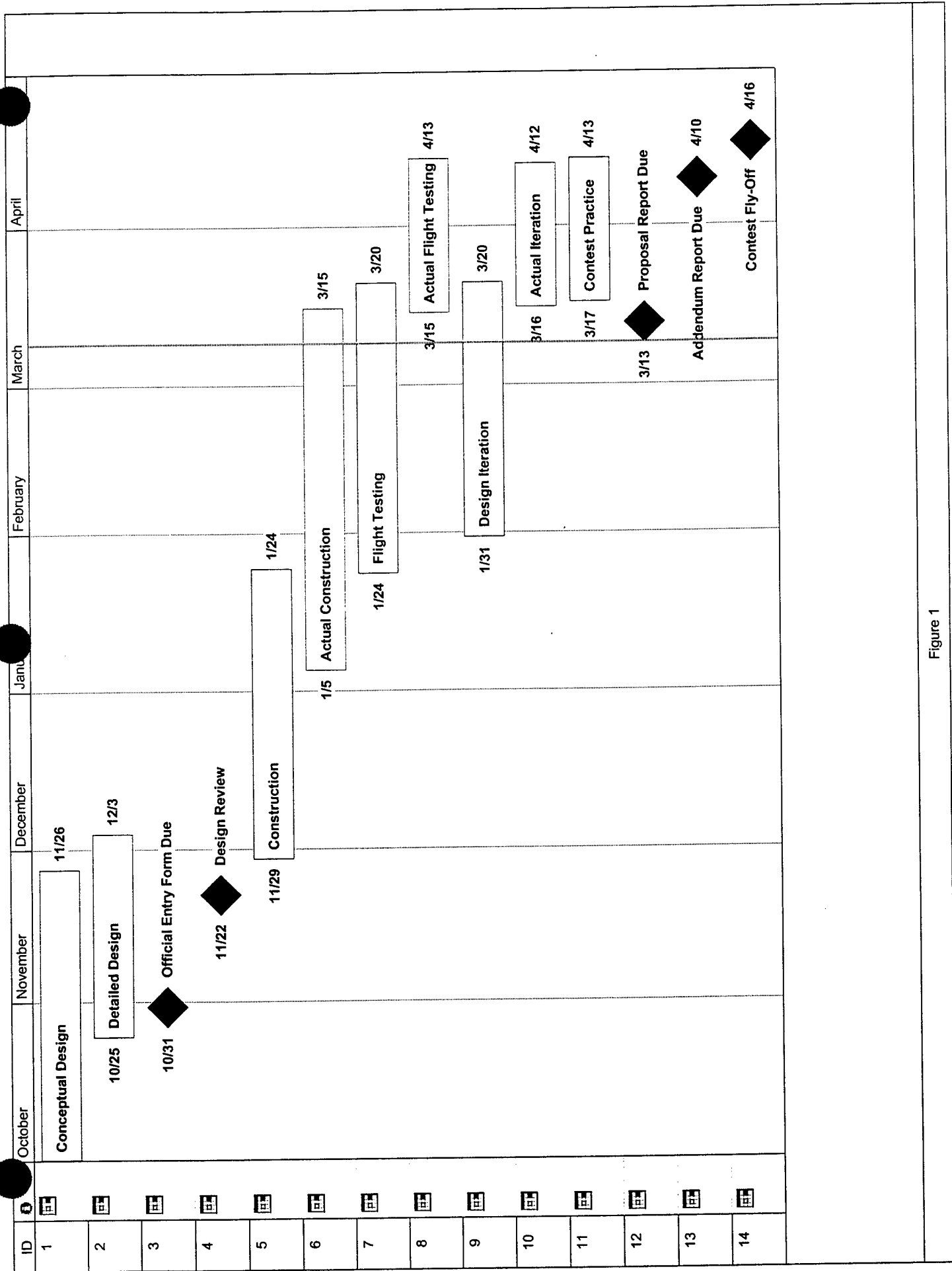


Figure 1

3 Conceptual Design

3.1 System Configurations Investigated

The team followed an evolutionary approach to configuration design where the first step was to brainstorm many configuration concepts, then examine and flesh out the practical details involved in each concept. The primary design parameters were: number of engines, payload capacity, ease of payload loading/unloading, number of lifting surfaces, and aircraft scoring cost. Secondary parameters included landing gear configuration, propeller ground clearance, airframe sturdiness, and handling in turbulent conditions. Based on these design parameters, the team down-selected to one concept for the remainder of the design process. With the exception of the projected contest score, the figures of merit (FOMs) were qualitatively considered as described in the following design process.

During the brainstorm phase, possible designs included conventional fuselage-and-wing aircraft, flying wings, and canard configurations. Ease of payload access and control in windy conditions drove the competing designs toward the more conventional layouts. The final candidate aircraft configurations were:

- Single-engine conventional
- Twin-engine conventional with the engines on the wing
- Twin-engine twin-fuselage
- Twin-engine multiple wing (staggered wing or joined wing)

Due to its higher cost, a twin-engine (twin) plane would have to carry more payload than a single-engine plane to achieve the same score for an equal number of laps flown. Therefore, the single-engine plane minimized cost, while the twin maximized payload.

In consideration of twin engine configurations, the fabrication cost formula drove the design away from certain configurations. The cost formula penalizes designs with multiple large scale body components, such as fuselages and nacelles. Consequently, a single fuselage with two full length engine-carrying nacelles would be charged as three fuselages, according to the cost formula. A slightly lower cost could be achieved by a two full-length fuselage design with an engine mounted in each fuselage; however, the even lower cost of a single fuselage, twin engine pod design eliminated any twin fuselage designs.

Twin engine configurations, because of the added weight of the associated structure and propulsion hardware, require much greater wing area than single engine planes. Additionally, the contest rules dictated a 7 ft. maximum wing span. A twin engine, single wing design would require a very low aspect ratio to achieve a reasonable wing loading. Unfortunately, low aspect ratio designs suffer from large induced drag losses. Multiple wing configurations divide the wing area into multiple sections, each with higher aspect ratio than those possible with a single wing design. Due to the belief that most of the drag of the wing results from induced losses, this became a critical

design issue. As a result of these considerations, the only feasible twin engine configurations were multiple wing designs.

Thus, the two main configurations left for comparative evaluation were the single engine conventional and the twin engine multiple wing aircraft. These two candidate configurations were weighed against each other through an analytical quantitative comparison that projected their probable performance and contest score. The analysis was performed using a suite of analysis packages and team-developed algorithms for calculating performance given the contest requirements. The analytical methods developed are discussed below in section 3.2. Using the results of the analytical models and non-quantitative design strategy preferences of the team, the single engine conventional architecture was selected. This decision is discussed further in section 3.3.

In addition to the overall system architecture configurations investigated, various component configurations were also considered. In the case of landing gear, a tricycle configuration proved to be a better design than both a taildragger configuration, for ground handling reasons, and to a tandem configuration with outrigger gear (like the AV-8B Harrier), for simplicity and sturdiness. An extended brainstorm of water bottle loading and unloading methods led to a "shotgun tube" slide-in approach that allows the easiest and simplest access for the minimum structure. The tube structure provides a simple, sturdy, and easy to manufacture payload compartment.

Although various figures of merit (FOMs), such as expected energy consumption, payload loading/unloading ease, and rough-air handling qualities, were extensively discussed during the configuration selection portion of the conceptual design phase, the dominant FOM was the projected contest score. Since the contest score formula is already an amalgamation of other design considerations, it essentially serves as the ideal combination of the relevant FOMs.

3.2 Analytic Methods Used

During the investigation of alternative design concepts, several analytic tools were employed to generate quantitative comparisons of alternate configurations. A wide range of parameters was considered and a number of trade studies were conducted.

At the vehicle component level, the MotoCalc software package generated powerplant performance estimates. At the mission level, a MATLAB simulation was written to generate flight performance estimates. Finally, at the vehicle configuration level, Excel was used to conduct high-level trade studies, integrating the results of the MotoCalc and MATLAB analysis tools.

MotoCalc is a software package commercially available for use on the PC, designed to provide estimates of electric-powered R/C aircraft performance. For a given motor, propeller, electronics, and airframe configuration; the software generates predicted performance data for a range of vehicle operating speeds and a user-specified range of propellers.

For a preliminary trade study, engineering estimates provided inputs to the MotoCalc software for several vehicle parameters. The parameters are summarized for an Aveox F27 motor test case in Table 1. Given these input parameters (see Table 1), MotoCalc generated predicted performance data for each of the propeller sizes that were considered. Candidate propeller diameters ranged from 14 in. to 18 in., and pitch values ranged from 8 in. to 12 in. For each propeller, the primary output was a table of thrust as a function of velocity, with the motor operating at full throttle. In addition, several other important performance indicators were recorded for each propeller, such as current and voltage levels, static thrust, predicted maximum cruise speed, and predicted duration with the selected battery configuration.

The results of the MotoCalc analysis were used as input data for an integrated mission simulation developed in MATLAB. The simulation consisted of several modules: takeoff, climb, cruise, and land. At conceptual design stage, the most critical performance factor was the 100 ft takeoff requirement. Therefore, the initial focus of the MATLAB simulation was the vehicle takeoff distance. See Appendix A for the source code corresponding to this module of the simulation.

Figure 1 illustrates sample output from the simulation takeoff module, taken from a 16 x 10 propeller configuration. The sample takeoff module was composed of two payload configurations: a 4L and 6L configuration. For the 4L configuration, the takeoff run is a little over 20 m (67 ft), while the 6L variant cannot meet the 100 ft takeoff requirement.

The range of propellers analyzed in MotoCalc was also modeled in the MATLAB simulation and resulted in predicted takeoff run for each propeller. A summary of the information collected through MotoCalc is in Table 2, and the MATLAB simulation results are in Figure 2. Note that the thrust, current, voltage, and duration values are taken at the 100% throttle setting. The MATLAB vehicle simulation was later expanded to cover other parts of the flight envelope and used for final design performance predictions.

Finally, throughout the conceptual design process, Excel was extensively used to compile and compare data and to conduct high level trade studies. For example, a cost model was constructed based on the costing equations presented by the contest rules and on the various characteristics of the candidate concept vehicles. The predicted cost and the predicted flight performance from MotoCalc and MATLAB were used to conduct parametric studies varying the payload flown, number of laps flown, and number of motors used. The results of these studies may be seen in plot form in Figure 3. In the comparison between a one and two-motor configuration, it was noted that a twin-motor configuration would have to carry 6 water bottles to be competitive with the one-motor design. Because of the expected decrease in cruise speed associated with the heavier twin-motor design, it was predicted that although capable, the twin motor design would have more difficulty completing the same number of laps as the single-motor design (projected as 4 laps). Based on these considerations, as well as the team preferences and

non-quantitative reasoning cited in the previous section, the twin-motor concept was eliminated in favor of a single motor.

3.3 Final Configuration Decision

For justification of the projected time performance, see section 5.2.3. Assuming a flawless 10-minute round in each case, the single-engine, four bottle plane with four laps and 120.19 points is projected to outscore the six bottle twin biplane with three laps and 102.90 points (point scoring before the report score is taken into account). Since score was the overriding figure of merit, the quantitative analysis supports the single-engine configuration, though the performance is quite similar.

Although the performance advantages of the single engine conventional configuration were apparent after the analytical examination was made, they did not overwhelmingly suggest the use of that configuration; often, the secondary advantages of the single engine conventional configuration were counterbalanced by other advantages provided by the two engine configuration, thus resulting in a somewhat flat trade space. The single engine plane would be a faster aircraft, but would have to run more laps due to a smaller payload capability. The twin engine concept would be slower and less maneuverable, but could run fewer laps due to the higher payload capability. In the end, secondary FOMs, such as simplicity and ease of fabrication, reinforced the analytical conclusion that the single engine conventional configuration was more desirable. Additionally, non-quantitative team preferences and team goals led the team to lean more towards a faster smaller aircraft that would also be faster and more maneuverable in harsh weather conditions.

3.4 Configuration Refinement

RCCAD, a simple computer-aided design program geared toward model aircraft design, proved to be a valuable design tool. It displays a three-dimensional rendered image of the design (VRML format) that updates simultaneously with each dimension alteration input. The speed and ease of visualization that it allowed compensated for its output format and geometric limitations. RCCAD was most useful for determining component sizing and placement as well as for facilitating intuitive configuration decisions. A sample view of the RCCAD environment is in Figure 4.

Table 1 Sample Motorcalc Design Parameter Inputs

	Model	Specifications
Motor	Aveox F27 w/o gearbox	1480 RPM/V 2.5 A zero load current 0.02 ohms internal resistance 11.22 oz total mass
Batteries	Sanyo 3000 SCR	3000 mAh 0.005 ohms internal resistance 2.76 oz per cell 26 total cells
Gearbox	Aveox/Robbe 3.7:1	3.7 to 1 gear ratio 1 prop
Speed Controller	Aveox H160C/CM	0.0057 ohms internal resistance 70 A maximum continuous current 2 oz total mass
Airframe	CAD design input to Motorcalc	84" wingspan 1100 in ² wing area 210 oz empty weight 293 oz total weight 38.3 oz/ft ² wing loading

Table 2 Performance and Design Parameters Output by Quantitative Models for Various Propeller Configurations

Propeller diam. x pitch	Max speed	Thrust	Current	Voltage	Battery Life	Takeoff Run
(in)	(mph)	(oz)	(A)	(V)	(min:sec)	(ft)
14 x 8	60	69.4	24.4	29	7:22	93
15 x 8	62	73.2	27.3	28.6	6:36	86
15 x 10	70	96	35	27.5	3:09	71
16 x 8	63	77.4	30.5	28.1	5:54	79
16 x 10	72	99.3	38.4	27	4:41	67
17 x 8	64	80.5	33.4	27.7	5:23	75
17 x 10	73	102.9	42	26.5	4:17	65
18 x 8	65	82.3	35.9	27.3	5:00	70
18 x 10	74	105.1	45.2	26	3:59	62
18 x 12	81	126.2	53.8	24.8	3:21	59

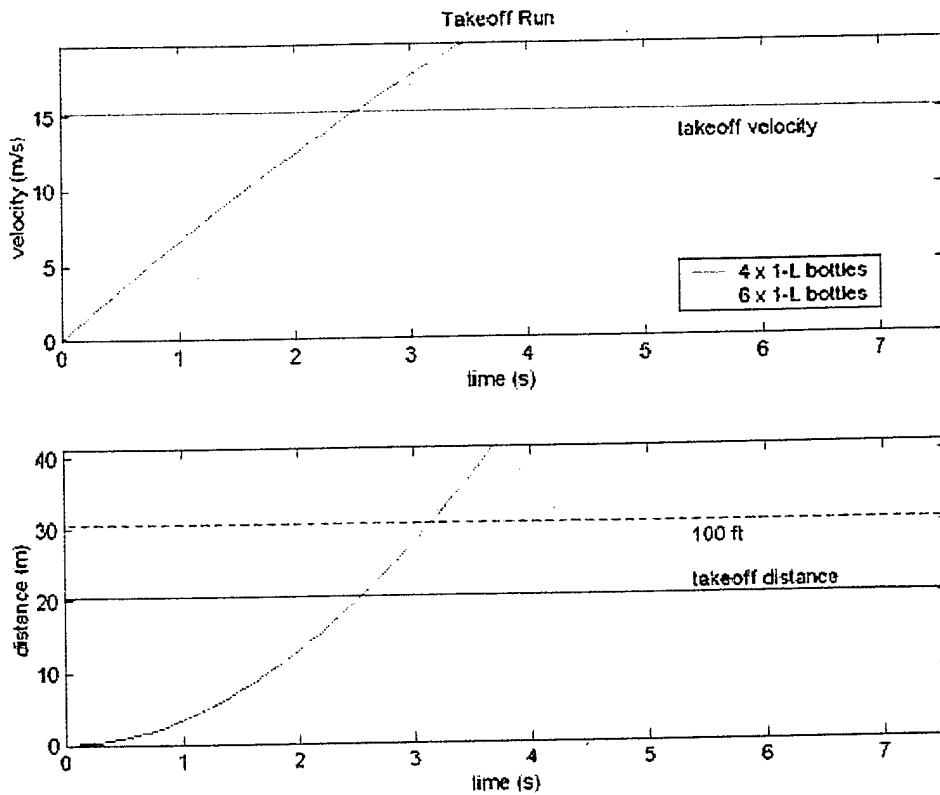


Figure 2 Takeoff Model Results for Two Payload Configurations

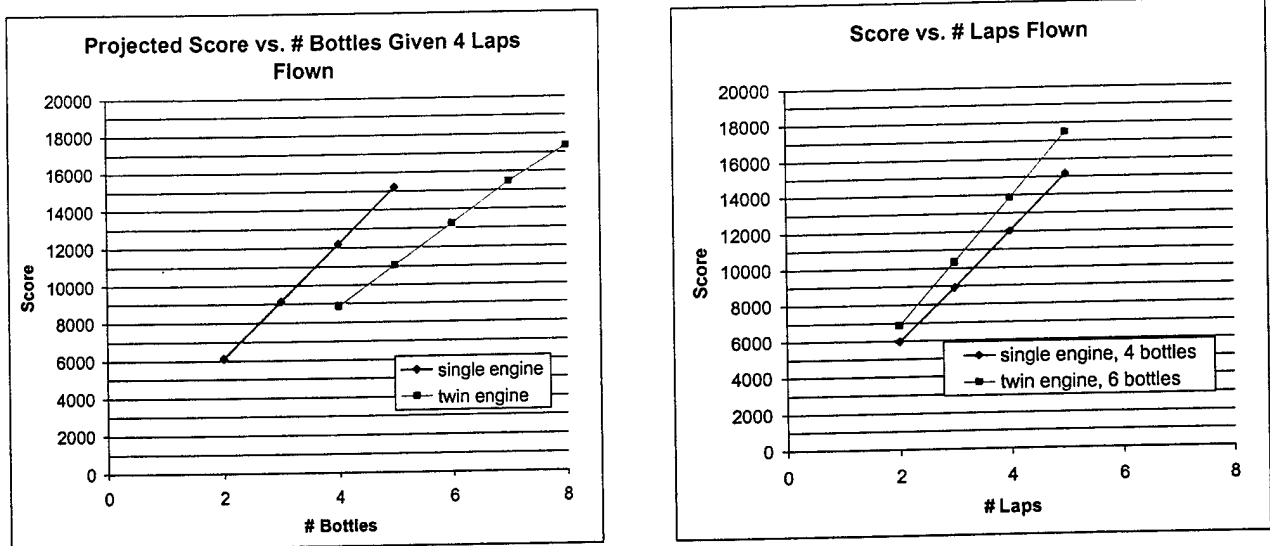


Figure 3 Parametric Study Analyzing Performance of One and Two Motor Configurations

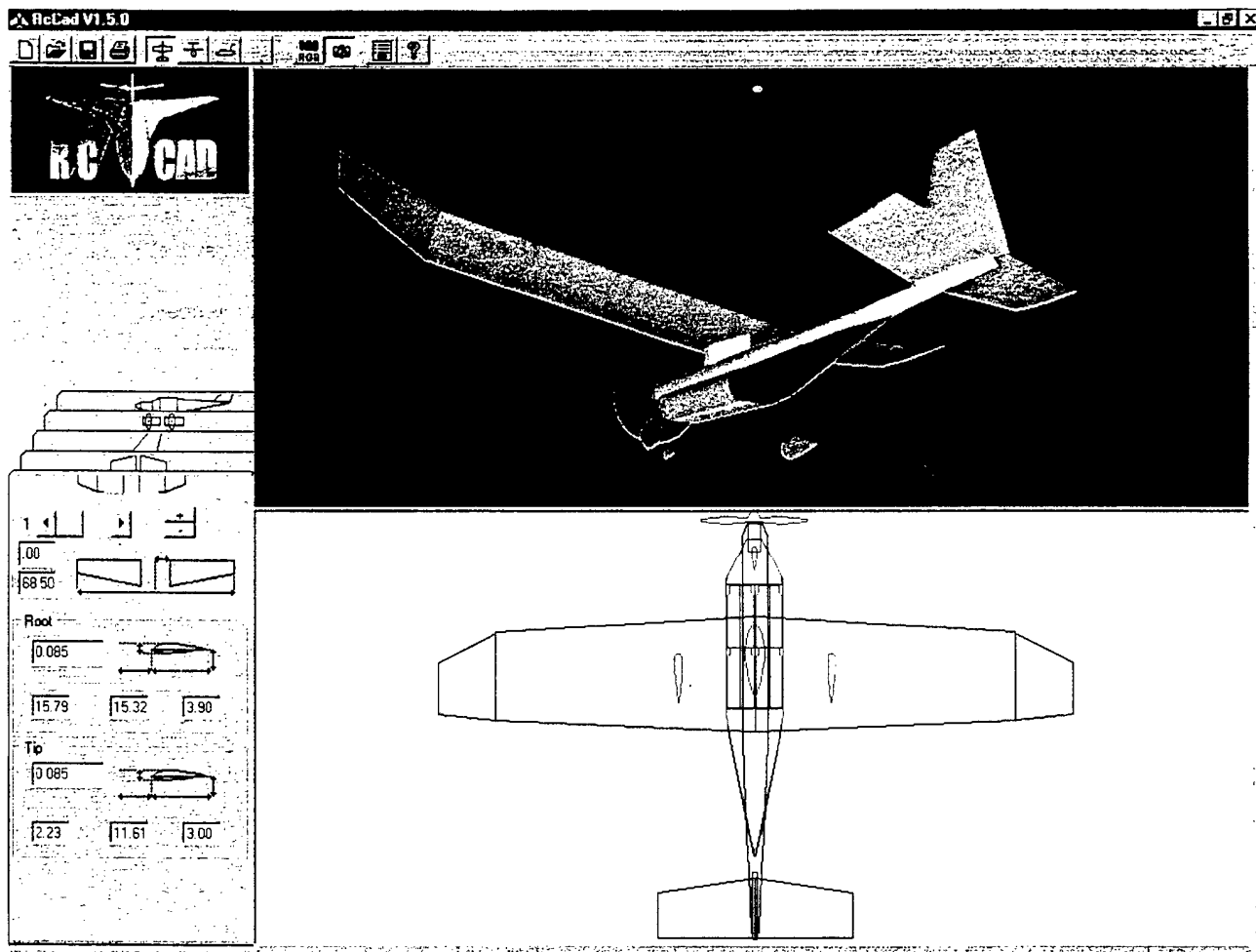


Figure 4 RCCAD Screen Shot

4 Preliminary Design

4.1 Design parameters investigated

During the preliminary design phase, the team considered many parameters. The large list was then distilled into distinct design parameters:

- Wing loading
- Wing planform
- Tail volumes
- Thrust and power to weight ratio
- Fuselage shape and size
- Payload size
- Landing gear configuration

The wing parameters studied were the wing loading and planform. Wing loading affects the handling characteristics of the aircraft primarily with regard to stall speed. Wing loading was chosen to allow a reasonable stall speed while not being so light as to be strongly influenced by gusts and high sustained wind. The wing planform encompassed taper ratio, area, and aspect ratio. It dictated the lift distribution created by the wing. With careful design, a nearly elliptic loading was achieved while providing resistance to tip stall.

The empennage was a critical part of the design. The horizontal and vertical tail sizing affects the handling, drag, and overall weight of the aircraft. The empennage was optimized for a lightweight tail section with low drag and positive handling characteristics.

Two primary design parameters were considered in propulsion. The thrust to weight ratio directly corresponds to takeoff distance. The driving factor for determining this parameter was the maximum takeoff distance of 100 feet. The power loading, expressed as power to weight ratio, correlates to climb rate. This was less critical for our planned tasks, since climb performance was not as crucial as takeoff distance.

Payload size and fuselage layout were essentially one design parameter. The amount of payload that can be carried directly sized the aircraft not only in physical dimension but also in wing loading. To ensure good handling, wing area increases with added payload to maintain reasonable loading. The required payload water bottles dictated the fuselage size and shape. By carefully arranging the payload and other items, a low drag, high volume shape was created.

The landing gear configuration was perhaps one of the most important design parameters. Not only did it have to be robust and resilient, it had to be aerodynamic as well. The geometry of the gear had to allow aircraft stability and good ground handling qualities.

4.2 Figures of merit

During the preliminary design phase, the team considered the following figures of merit.

- Payload access
- Structural integrity and resilience
- Ease of transportation
- Ease of construction

Payload access was a primary concern during the design phase. The configuration had to accommodate quick payload changes while maintaining a rigid structure for flight. A good design would permit team members to spend a minimal amount of time safely loading/unloading the payload.

A mockup spar test was done for wing structural testing (see section 5.2.2). Since the airplane has to be able to support its maximum weight while supported from the wingtips, the loading conditions are different than for pure flight. The simulated testing, to model the competition, required multiple sorties and takeoffs and landings. The aircraft must be properly designed to withstand any loading conditions it experienced during all segments of the flight runs.

Ease of transportation drove the team towards a modular design, which allows a high degree of portability. While space limitations are not a serious issue, the modular design allows easy transportation and field reassembly. This not only reduces the probability for damaging the aircraft during transportation, but also allows us to comply with the airlines shipping regulations en route to Wichita, KS. Additionally, easy disassembly makes transport much less cumbersome than dealing with a fully assembled aircraft.

Ease of construction was the last main consideration for the team during the preliminary design phase. Extremely complicated designs or manufacturing methods were weighed against the extra time and cost required. A more straightforward design would also enable more time for flight testing, final design iterations, and ground crew training.

4.3 Analytic methods used

Analytic methods using Xfoil, Athena Vortex Lattice, Plane Geometry, Electricalc and MotoCalc were used to aid in determining the propulsion system and the aerodynamic configuration of the aircraft. These methods allowed easy design implementation and iteration, thus allowing the effects of multiple design parameter changes to be understood and noted.

4.3.1 Xfoil

Xfoil, an interactive airfoil analysis code written by Professor Mark Drela, was used to create a unique airfoil for the Fire & Water. Xfoil is a typical 2-D inviscid vortex panel method program that uses a viscous integral formulation, thus permitting accurate prediction of separation and separation bubbles. Reynolds numbers and angles of attack were inputs, resulting in C_l and C_d values that were graphed in polar form. The Mach number scaling correction function was ignored since the aircraft operates in the slow speed regime only.

An airfoil unique to the Fire & Water aircraft was developed to accommodate its wide range of operating conditions. The aircraft needs to generate high lift at low speeds during take-off and landing, but also needs to have a good L/D for the high speed cruise and unloaded flight segments. These requirements exceed the realms of most common airfoils. It was decided that varying the trailing edge camber via flaps and ailerons during different phases of flight would shift the airfoils polar favorably. Hence, an airfoil was designed to work both with the trailing edge down in the high lift configuration and with the trailing edge reflexed up in the high speed dash configuration.

The airfoil was based off the Selig S1210, a known high lift airfoil. It was reshaped in Xfoil first by changing the geometry of the airfoil section to accommodate the flap deflection with no sharp corners. Afterwards, the C_p distribution was cleaned up to look for any problematic points that would cause transition and/or separation. The resulting C_p changed the overall shape of the airfoil. These steps were iterated upon, evaluating the airfoil along the way. All evaluations were done at a fixed Reynolds number. See the drag polars in Figure 5 for an illustration.

4.3.2 Athena Vortex Lattice (AVL)

Athena Vortex Lattice is a 3-D vortex lattice solver written by Harold Youngren for MIT in the late 1980's. Professor Mark Drela has implemented recent improvements. By specifying a geometry file of the aerodynamic surfaces, the stability derivatives were easily found. Also, the team used AVL primarily to determine the wing planform. Based on the input geometry and angle of attack, the program produced loading in chord times local C_l , $c \cdot C_l$, and drag losses.

For minimum induced drag, the $c \cdot C_l$ loading should be elliptical; however, if a purely elliptical loading is chosen, potential tip stall problems could result. Hence, the wingtips needed to operate at a lower C_l than the elliptical loading permitted. This trade became the driving force behind the wing planform.

The wing planform took a low aspect ratio triple taper design. The triple taper was to allow for both separate flaps and ailerons while keeping a good planform for a near-elliptic loading. The outer taper or tiplet was raised at a dramatic angle to give stability and help with the induced drag losses by its winglet effect.

4.3.3 *Plane Geometry (PG)*

Plane Geometry, written by Blaine Beron-Rawdon, is a spreadsheet program based in Microsoft Excel. The program analyzes the geometry of the airplane for stability and evaluates control effectiveness. Accurate prediction of the static margin enabled the center of gravity to be determined. This allowed the sizing of the empennage to be conducted in a scientific fashion.

Final configuration had the tail volumes set at 0.452 and 0.033 for the horizontal and vertical respectively. This, along with other stability data, was compared to the database that accompanies Plane Geometry and favorably relates (see Table 3).

4.3.4 *Electricalc and MotoCalc*

Electricalc and MotoCalc were used in parallel to size the propulsion system. Results from each program were compared against each other and gave close results. Both use inputs of the type of motor, motor controllers, and battery types to create a model of the propulsion system. Any combination of these components resulted in battery life, thrust, speed ranges, power, and current draw data plots at different throttle settings and flight speeds.

As the analysis became more specified, the team used MotoCalc exclusively because it outputs discretized data in a table form. This data could readily be incorporated into spreadsheet programs along with MATLAB and allowed ease of interpretation and analysis. This permitted optimization of a given propulsion system after only a few iterative cycles.

The motor system selection was made more as a result of experience rather than numerical analysis. The aircraft needed to fly at high velocities, implying larger current draws. A motor was selected that would perform efficiently at these current values. An Aveox motor was chosen based upon past experience, although many manufacturers of model aircraft electric motors exist for this high current requirement. The brushless motor concept was far more efficient than comparable brushed motors in addition to being virtually maintenance free. Aveox motors are the leading competition-grade motors in the US and are more easily available than comparable European brushless motors. Aveox designs can take high current levels and have been proven in model airplane competitions for a number of years.

Along with the motor choices, the battery cell count of the propulsive system had to be determined. Initially, existing 19-cell 2000 mAh packs, which were used in competition by MIT two years ago, were considered. To use them, the packs had to be run in parallel since the airplane configuration has only one motor. That led to extremely long run times and a rather large propeller, approximately 24 inches in diameter. Eventually, new battery packs were procured and were based on the 26-cell 3000 mAh battery packs. The new cells from Sanyo Electronics had lower impedance than the old 2000 mAh pack. Moving for more current draw and more efficient system overall. Purchasing the cells from Divers Model Aircraft allowed the team to obtain "zapped" cells. This proprietary method further decreased the impedance, allowing greater power to be drawn (see Figure 6).

4.4 Preliminary sizing and key features

4.4.1 *Wing planform and sizing*

Since it is advantageous to use the full allotted wingspan of 7 feet, only the aspect ratio and taper ratio of the panels were evaluated to vary the wing area and thus, the wing loading. Each panel had a different taper ratio to provide a near elliptic lift distribution. The weighted average taper ratio was 0.85 and an aspect ratio of 6.9. Aileron and flaps were based on 25 percent of the chord. 47.6 percent of the

wing was flapped while ailerons actuated 42.9 percent of the wing. Calculations were performed primarily in Xfoil and Plane Geometry. The large flaps and ailerons permit precise control response of the large aircraft, in addition to the ability to increase drag dramatically for landings.

4.4.2 Empennage size and shaping

The tail surfaces were modeled after other successful model aircraft contained in the Plane Geometry database. The team decided that a fairly long fuselage would make the plane easier to fly by lengthening the moment arm and creating more damping. The resulting tail horizontal area was 144 square inches with a 39.75 in. moment arm (distance from the aerodynamic center of tail to the aerodynamic center of wing). The data used in Plane Geometry allowed a rough downwash calculation to be made and at the center of gravity, 7 inches back from the leading edge, a static margin of 0.1 percent was deemed appropriate.

Similar methods determined the calculation of vertical surface areas and moment arms. The final vertical area is 69.75 square inches at a moment arm of 40.06 inches. The control surfaces on both horizontal and vertical tails were set at 2 inch chords to give ample control, especially during the high drag settings of the flaps for landings. The tail airfoil chosen is the HD800 designed by Hannes Delago. It is characterized by lower drag and more linear lift curve slope than a standard NACA0008 and is no longer difficult to build.

4.4.3 Motor configuration and size

The most important issue regarding motor choice is thrust to weight ratio. The most critical requirement driving motor choice is the 100 ft. maximum take-off distance; inability to provide the thrust necessary for take-off in under 100 ft. would disqualify the team. In addition to meeting the take-off requirement, the motor had to have a suitable power to weight ratio to keep the overall mass of the airplane low. These considerations were factors in deciding on the highly specialized competition motors of the Aveox line.

A single motor configuration was chosen, as it traditionally is the most efficient as well as easiest to implement. Also, the cost measurement scale of this year's contest penalized designs with multiple motors. As mentioned previously, the team carefully considered a two engine biplane in the early stages of design, yet it was disregarded due to complexity and lower performance as predicted by analytical models..

The F27 Light was finally chosen due to its light weight and developed power. It is at least 0.25 lbs. lighter than other motors with gearboxes. It has been proven in competition since it is based upon the 1412-2y but includes an integrated gearbox, thereby cutting down weight. Many teams have used the 1412-2y in previous years with success. Other motors would have less efficiency. Additionally, the F27 is tuned for high current draw situations, so it can take the large power demands placed on it with ease.

26 Sanyo 3000cr cells power the F27 Light through a 16x8 APC composite propeller. The APC propeller was chosen for its past performance in model airplane competitions. It is well designed, available, and inexpensive when compared to exotic European composite propellers. The motor simulations also had the APC propeller constants built in, so experimental data gathering was unnecessary.

At full throttle, this hardware combination created 15 lbs of thrust at 2.76 horsepower. The expected run time was around 2.2 minutes, which was rather short due to the current draw of 82.9 amps. Still, the motor is 91 percent efficient at this power level. As the flight profile is only using full throttle for take-offs and climbs, careful throttle management must provide the aircraft with enough battery energy to complete the desired task.

BA8	Re _{YCL} = 280000	Ma _{YCL} = 0.000	Ncrit = 9.000
BA8 -4°	Re _{YCL} = 280000	Ma _{YCL} = 0.000	Ncrit = 9.000
BA8 -8°	Re _{YCL} = 280000	Ma _{YCL} = 0.000	Ncrit = 9.000

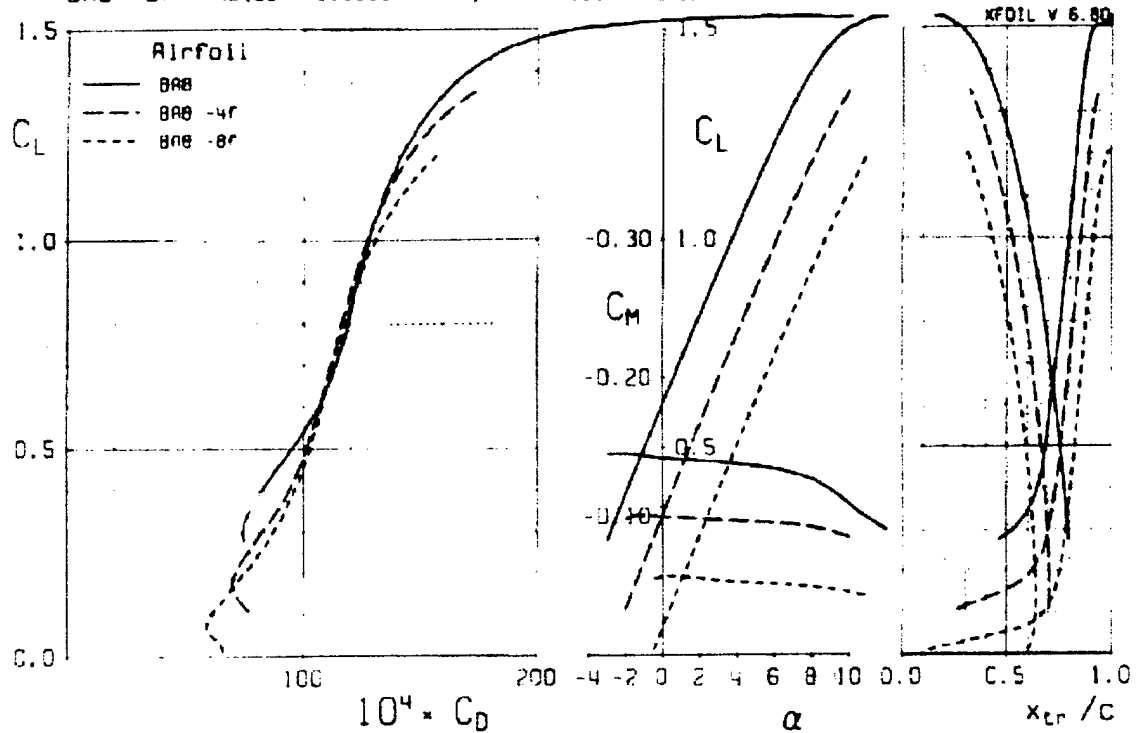


Figure 5 Sample Xfoil Drag Polars

Table 3 Plane Geometry Program Output

STABILITY DATA					
Downwash angle ratio K @ Hh=0		2.12			
K @ Hh=0.2		1.66			
Height of stab over wing wake Hh/b		-0.02			
K @ Hh		2.16			
Effective H Stab area (sq in)		63.31			
Sh eff / Sh		0.44			
Y neutral point, wing-tail (in)		8.17			
N.P. on Cmac, wing-tail (Cmac)		0.45			
Measured Y of CG (in)		8.00			
CG on Cmac		0.44			
N.P. change for fuse + sweep (Cmac)		0.019			
Y neutral point, aircraft (in)		8.40			
N.P. on Cmac, aircraft (Cmac)		0.47			
Static Margin (Cmac)		0.03			
Cl alpha wing (Cl/)		0.0846			
Cl alpha horizontal (Cl/)		0.0725			
Cl alpha vertical (Cl/)		0.0573			
d epsilon / d alpha		0.4820			
Cm alpha wing (1/radian)		0.8971			
Cm alpha fuselage (1/radian)		-0.0925			
Cm alpha tail (1/radian)		-0.9731			
Cm alpha total (1/radian)		-0.1685			
Neutral Point, Cmac		0.4699			
Cm alpha dot (1/)		-0.1014			
Cm q horizontal (1/)		-0.2104			
Cm alpha dot + Cm q horizontal (1/)		-0.3117			
Cm delta elevator (1/)		-0.0150			
CL delta elevator (1/)		0.0047			
Elevator deflection per Cl ()		2.3458			
Cn r vertical (1/)		-0.0018			
Cn delta rudder (1/)		-0.0007			
DOWNWASH ANGLE TABLE					
(from Hoerner, Fluid Dynamic Lift 1965)					
relative to downwash at C/4 as a function of distance aft of C/4 in spans					
Lh/b	K	Slope	K@ Hh/b =0.2	Slope	
	@Hh/b=0				
0.20	2.84	-4.20	1.97	-1.70	
0.30	2.42	-2.10	1.80	-1.00	
0.40	2.21	-1.20	1.70	-0.50	
0.50	2.09	-0.60	1.65	-0.40	
0.60	2.03	-0.50	1.61	-0.20	
0.70	1.98	-0.50	1.59	-0.20	
0.80	1.93	-0.50	1.57	-0.20	
0.90	1.88	-0.30	1.55	-0.10	
1.00	1.85	-0.30	1.54	-0.10	
1.10	1.82	-0.20	1.53	-0.10	
1.20	1.80	0.00	1.52	0.00	

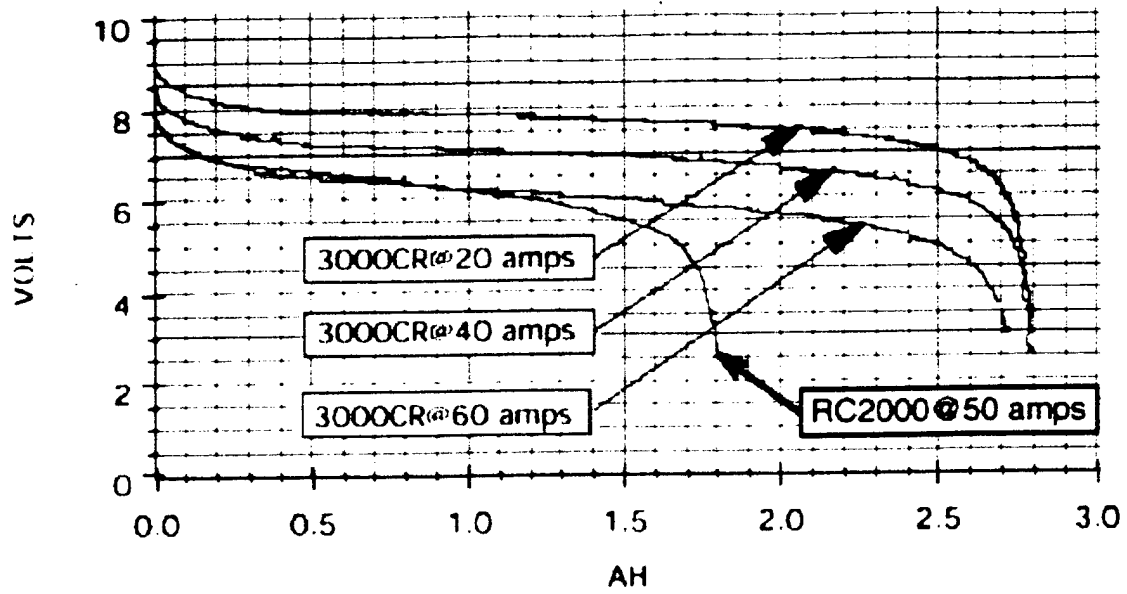


Figure 6 Battery Discharge Curves for Various Current Outputs

5 Detailed Design

5.1 Component selection and systems architecture

5.1.1 *Propulsion System*

The single motor in the Fire and Ice propulsion system is the Aveox F27 Light. With an integrated 3.7:1 gear box and an extremely high current handling capability, the motor puts out tremendous power. It is powered by 26 Sanyo 3000 mAh cells, which create over 2.7 horsepower at full throttle. The power is harnessed by an APC composite 16 x 8 propeller. A corresponding Aveox speed controller, the Aveox H260c, manages the power and is rated for 4 to 32 cells at a maximum continuous current of 70 amps. All propulsion system components were commercially available, thus meeting the stipulation in the contest rules.

The battery packs were supplied by Diversity Model Aircraft at a discounted cost. We purchased three sets, each consisting of two 13 cell packs. The batteries were "zapped," the vendor's proprietary method of increasing voltage output while decreasing internal cell impedance. As this method is available on order, this falls within the limits set by the contest rules.

5.1.2 *Control System*

The Airtronics Stylus 8 channel PCM system was chosen as the Fire & Ice radio controller for several reasons. The use of a PCM radio system makes it possible to meet the contest fail-safe requirements. Furthermore, team member Ahyow and advisor Col. Young have experience with the Stylus programming interface and are confident in its abilities. The most critical reason for the selection of the Stylus 8 lies in the amount of computerized mixing features available with the system. The Stylus has nearly unlimited mixing and flight modes that allow for trim compensation during trailing edge camber changes and landing configurations. The flight mode switch would be used for takeoff, cruise, and landing configurations. By having computer compensation for trim when changing the airfoil, pilot mental workload is greatly reduced. This becomes critical when the mixing features are used for the landing configuration. In landing mode ("crow"), the flaps can pivot down to 90 degrees, while the ailerons move upwards to a lesser angle. This effectively slows the airplane down on final approach. Often used on competition radio controlled sailplanes, "crow" has been shown to be a highly effective means of glideslope control and energy management.

One five-cell 1200 mAh battery pack was used for the on-board control flight pack. The battery pack was deemed appropriate for the size and number of servos utilized in the aircraft. The use of a five-cell pack improved servo response and torque over the capabilities of a smaller pack. The aircraft's large control surfaces tax the servos, so the use of five-cell pack was a prudent added precaution. The battery voltage will be carefully checked before each flight as an indicator of the expected maximum time aloft.

All of the servos selected for the aircraft control surfaces are ball bearing-supported and metal-gearred. The ball bearings reduce output shaft play and virtually eliminate wear. As the aircraft has a high top speed and large surfaces, ball bearings were deemed necessary to ensure good control centering as well as resistance to possible flutter.

The flap servos are expected to take the most abuse due to deployment the large flaps almost perpendicular to the freestream. As a result Airtronics 94141 servos were selected. These are robust, all metal-gearred servos that make 45 ounce-inches of torque at 4.8 volts. Additionally, the travel rate of 0.2 seconds per 60° is suitable for the flaps. From experience with large (3 meter span) remote control sailplanes, these servos have proven to be more than adequate. The ailerons have smaller travel throws, thus lessening torque requirements. The Hitec HS-85MG servos were chosen to actuate the ailerons. They create 38 oz-inches of torque at 4.8 volts and 45 oz-inches of torque at 6.0 volts. The travel rate of 0.18 sec per 60° matched the flap servos well and was considered adequate for aileron deflection. While the matching of travel rates is not that significant, it is useful when the flaps are mixed with the ailerons to increase roll rate. The main driving force behind the aileron servo selection was weight. Less weight further out on the wings meant a lower moment of inertia, thus allowing more maneuverability. The HS-85MGs were 0.84 oz compared to the 94141's 1.17 oz weight.

The elevator and rudder are actuated by the same servos as the ailerons, the HS-85MG. While the smaller empennage surfaces require much less torque than the ailerons, the robustness of the HS-85MG geartrain, small size, and light weight made it the obvious choice.

The nosewheel is steered through a Hitec HS-225MG mini servo. This servo, despite its small size and relatively light weight, can produce 55 oz-inches of torque at 4.8 volts and 67 oz-inches of torque at 6.0 volts. The torque and light weight were the driving factors in the selection of the steering servo. The HS-225MG geartrain can readily handle rough loading conditions. This feature is important since the servo will see the most impact loads. A response time of 0.14 sec/60° is the second fastest of all the servos used and provides a comfort factor to the pilot.

Finally, the servo controlling the brake cables is a Hitec HS-81. Its small size, light weight (0.59 oz), and decent torque (36 oz-inches) make it a good candidate for brake actuation. Though the geartrain is less robust than the HS-85MGs, it is not a major concern as the brake cable loads were deemed to be lightly loaded and free of sudden shocks. The fastest servo response time of 0.11 sec/60° is unnecessary for the brake actuation, though it could prove useful in panic stops.

5.1.3 Braking System

The aircraft's weight and approach speed when loaded meant that a effective braking system would save precious ground time. Manufactured by Rocket City, the

brakes selected can easily be integrated into the aircraft's composite wheels. They rely on a wound spring that tightens around a cylinder when placed under tension. This cylinder is attached to the wheel hub. The design is simple, easy to implement, and very lightweight compared to commonly used pneumatic systems. By using aerodynamic braking, "crow" to slow the descent, and wheel brakes upon touchdown, the need to taxi back to the start line should be eliminated. This would save crucial seconds on the ground, thus allowing the aircraft to spend more of the ten minute working time airborne and scoring points.

5.1.4 Configuration Improvements

The team made several substantial design changes, one for aerodynamic reasons, one for dynamic reasons, and one for practical issues. The aerodynamic improvement had to do with bringing the wing out of the fuselage's adverse influence. With the wing up on a pylon, the leading edge does not encounter the fuselage's boundary layer, so the wing maintains a centerline flow profile nearer to that of an isolated (fuselage-free) wing. Thus the dip in lift at the centerline is attenuated, and the lift distribution becomes more elliptical, enhancing efficiency.

The high moment of inertia of four water bottles in line led to dynamic concerns. They made the pitch and yaw moments of inertia high enough to potentially cause control response lags. The design now has a pair of payload tubes with two bottles in each, such that the mass becomes concentrated toward the balance point as much as possible.

The practical issue concerned modularity, which was noted in section 4.2, and which was not fully resolved until the detailed design stage. The distinct sections are: core fuselage tube/payload tubes/main landing gear/pylon lower half, keel/nose/nose gear, tail cone, payload tube aft fairing, wing center section/pylon upper half, wing outboard sections, horizontal tail, and vertical tail. The sections assemble with brass pins and tape, requiring no tools. This arrangement allows for simple maintenance and field repair as well as easy break-down for transport.

5.2 Final Performance Data

5.2.1 Takeoff Performance

As described in Section 3.2, a Matlab vehicle simulation was used to model and predict takeoff performance. As the design converged and vehicle parameters were exactly specified, simulation outputs became more meaningful as indicators of actual expected performance. With the final propeller, motor, battery, and wing configuration as described in Section 5.1, the expected zero headwind takeoff run is 85.2 ft, with a takeoff speed of 49.8 ft/s. Immediately following takeoff, the climbout segment of the mission was also modeled by the Matlab vehicle simulation. To reach a desired cruising altitude of 55 ft at a flight path angle of 20° , the vehicle is required to climb for 6 s at full throttle at a climb velocity of 19.3 ft/s. For the source code of the Matlab climb module simulation, refer to Appendix B.

5.2.2 *Handling Qualities and G-Load Capability*

Prof. Drela conducted a four-point loading test on a spar similar to the one used in the Fire & Water plane. His results indicated that the spar caps broke in shear at 18000 pounds per square inch while withstanding a 90000 psi axial load. These figures give our spar an approximate load factor maximum of 12, corresponding to a 12-g pullout.

Handling qualities are expected to be very good given the plane's reasonably high cruise speed and long empennage moment arm. The most serious concern is crosswind landing capability, since the large tiplets may inhibit the plane's ability to sideslip. Taking an approach of greater competitiveness at some potential loss of handling capability, the efficiency boost offered by the tiplets was deemed more important than the loss in sideslip capability.

5.2.3 *Cruise Performance*

The vehicle was designed with the specific goal of flying four scoring laps within the allotted ten minutes. To validate these design goals, the mission was run in its entirety with the Matlab vehicle simulation. The source code for the cruise module is presented in Appendix C. This analysis indicates a projected cruise speed of 95.3 ft/s (65 mph). With an estimated level turn radius of 50 ft, the vehicle will execute a 3.2-g turn at a rate of 68.8°/s. The net computed time for a loaded flight (with water), counting takeoff, straight and turning flight, and landing, is 51 s. The computed time for an unloaded flight, counting takeoff, two laps, and landing, is 72 s. Adding 2 loading/unloading pit stops at 15 s each, the total projected time for 1 scoring cycle is 153 s. Therefore, during the allocated ten minute competition time, the vehicle is expected to complete four scoring laps.

5.2.4 *Weight Budget*

The vehicle will carry four one-liter water bottles as payload, with a corresponding maximum gross takeoff weight of 288 ounces (18 pounds). Figure 7 presents a graphical breakdown of the components of the vehicle by weight.

5.3 *Drawing Package*

The AutoCAD three-view of the final configuration is in Figure 8. It is followed in Figure 9 by a series of RCCAD screen shots that provide an overview of the design's evolution. Note that full-size plans drawn in pencil, not included here, were by far the most useful tools for practical issues such as component placement, component interference avoidance, fairing design, and construction in general. The utility of such plans is evident in that they require no scaling and that team members can change them instantly without leaving the lab.

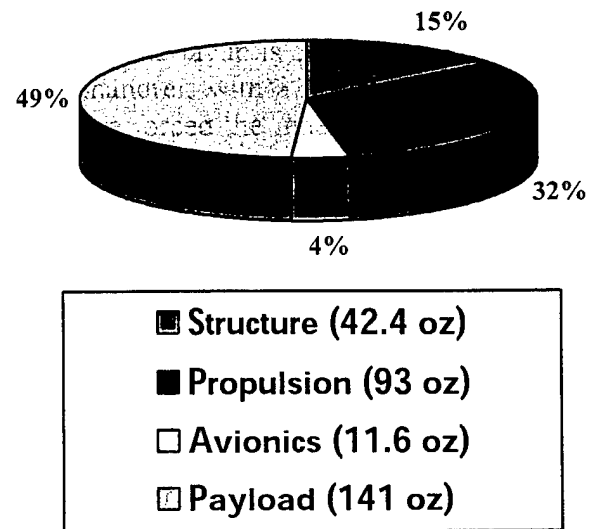
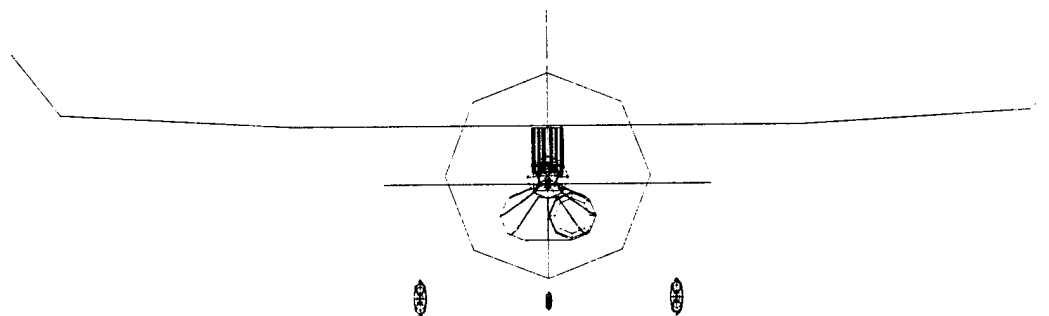
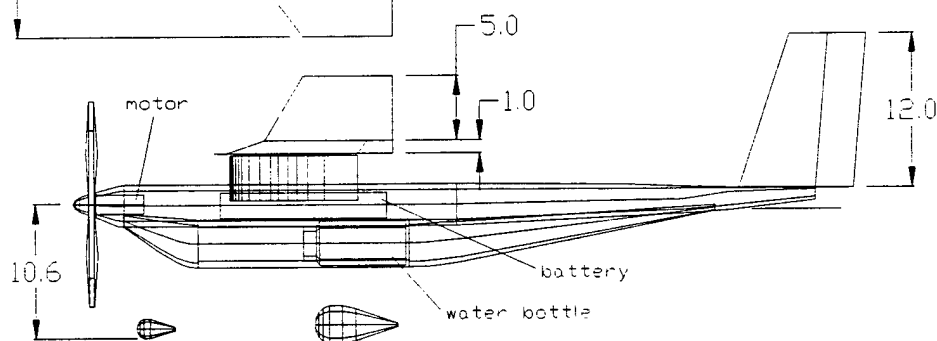
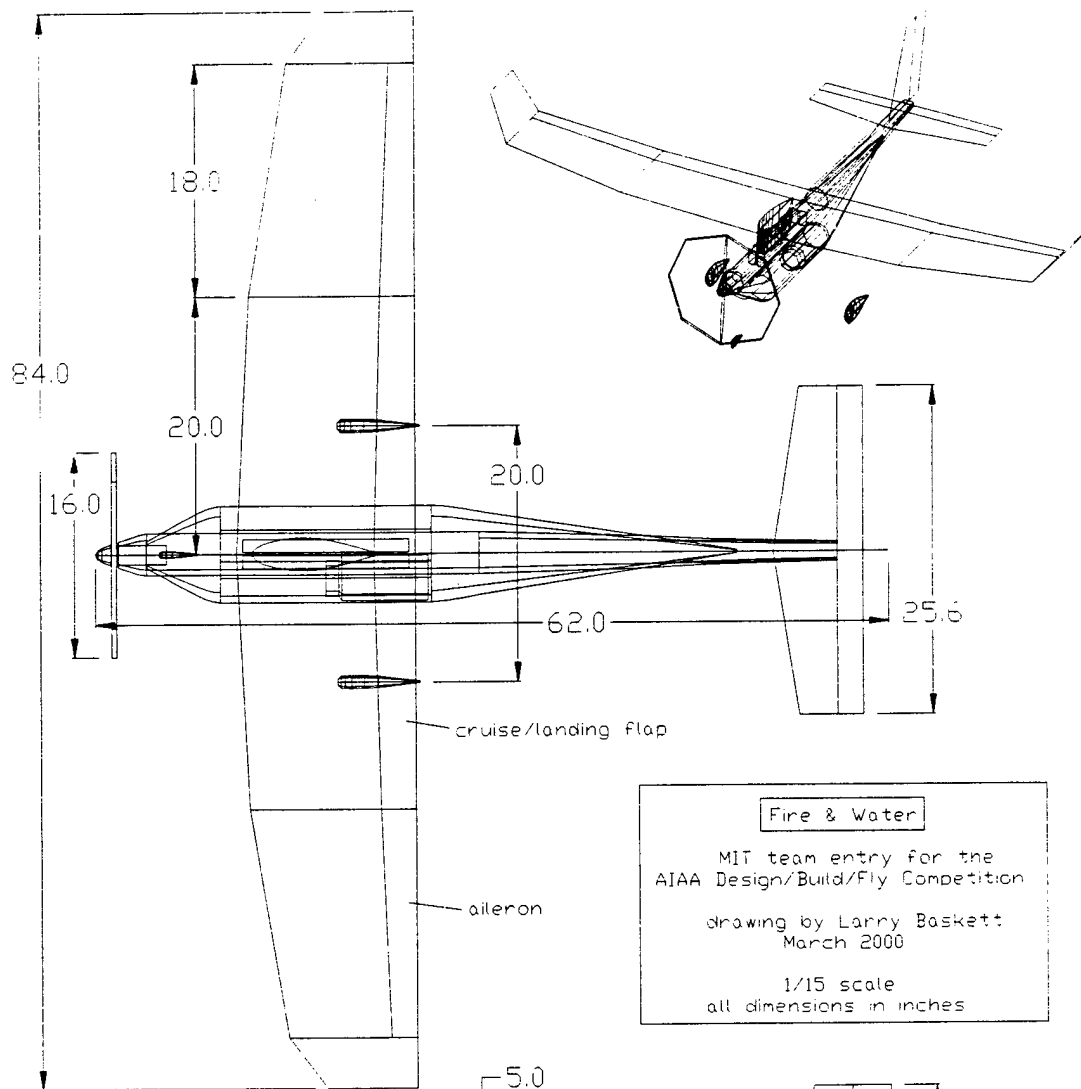


Figure 7 Vehicle Component Weight Breakdown



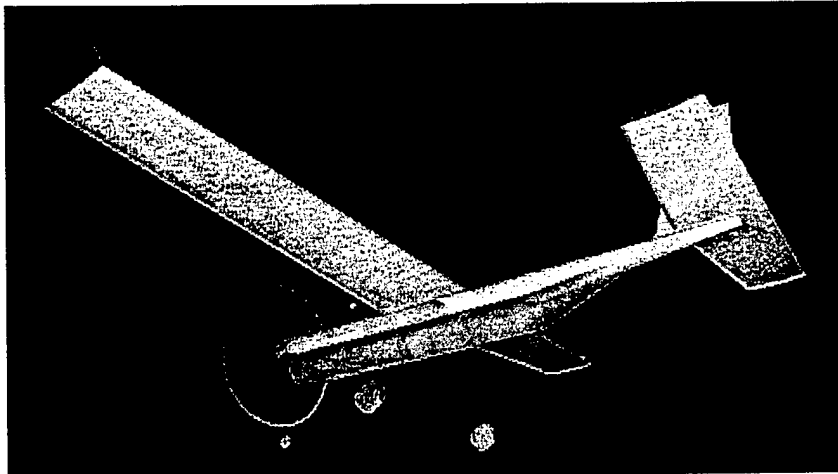


Figure 9A Preliminary Configuration

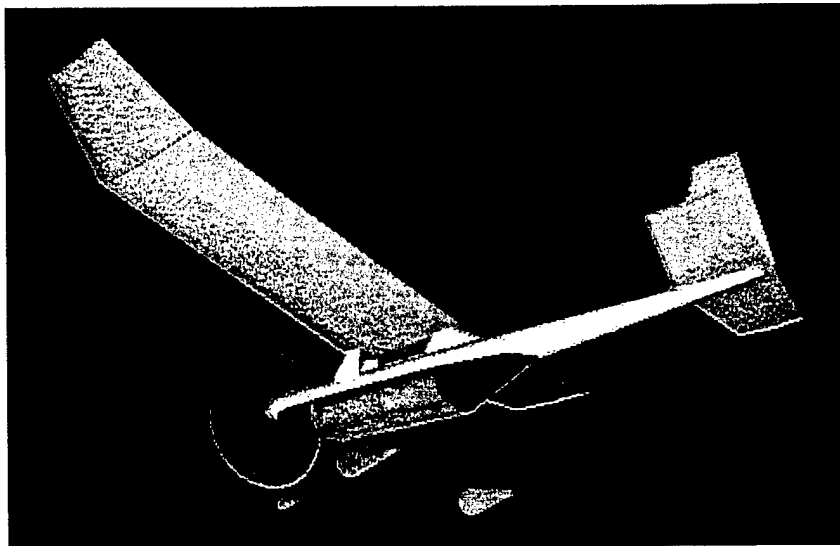


Figure 9B Intermediate Configuration

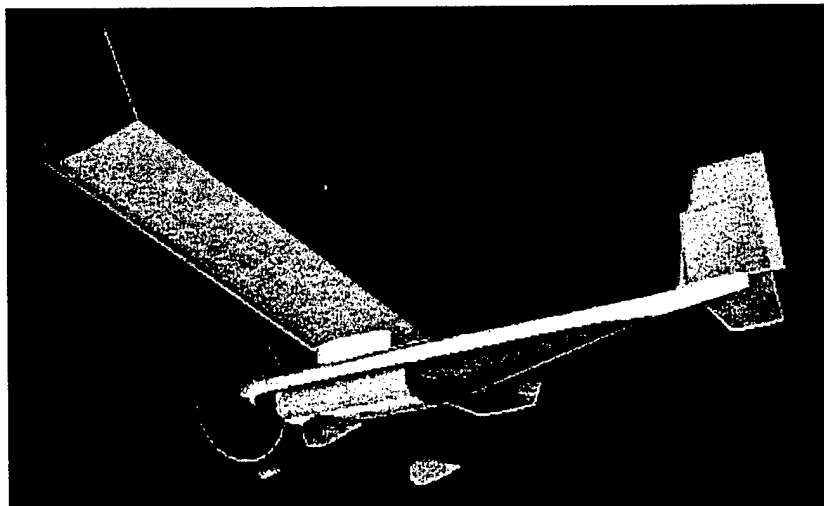


Figure 9C Final Configuration

6 Manufacturing Plan

6.1 Material Selection and Manufacturing Process

The team's contest strategy centers around the design and construction of a relatively light, high speed aircraft that can carry a moderate number of water bottles (4). To realize this strategy, the aircraft's structural weight must be minimized while maintaining the strength necessary to withstand the loads imposed by aggressive maneuvering and landing. The desire for a high strength, low weight airframe led to the selection of composites as the primary structural material.

Composite materials, such as fiberglass, carbon fiber, and kevlar, are generally more expensive to purchase and harder to fabricate than traditional R/C aircraft materials, such as balsa and plywood; however, the performance advantages provided by composite construction have been proven in competition. Composites also enable greater geometric freedom in load-bearing structures as well as high degree of precision for surface contours. Additionally, figures of merit that weigh against composites, such as cost and difficulty of fabrication, have been mitigated by a number of factors specific to this design team:

- Team personnel have extensive experience in composites
- Labs and equipment for composite fabrication are available for use by the team
- Material costs were covered by the team's sponsor, the MIT Aeronautics and Astronautics Department

These considerations (discussed in further in section 6.2), in concert with the team's design strategy, have led to team to design an aircraft that relies heavily on composite materials.

The selection of composites for the major structural components dictates the manufacturing processes put into practice by the team. Most components were produced using a wet layup technique. In a composite wet layup, the fiber is first cut to an appropriate shape. Epoxy is then mixed and spread into the fiber. The fiber is then applied to a mold, typically blue foam or some other former covered in a non-stick surface such as teflon or packing tape, and allowed to cure.

Large, even surfaces like wings and stabilizers require vacuum bagging after layup to ensure a smooth finish after the curing process. The body tube and water tubes are simple cylinders, so an appropriately sized aluminum mandrel is used in their layup. The irregularly shaped nose and tail cones presented problems initially, since they could not be formed on pre-made shapes. The team lathed custom-shaped molds from foam for their construction.

While composite structural components have an involved, time consuming manufacturing process, their high strength to weight ratio provide the aircraft with a performance edge in the contest.

6.2 Figures of Merit

Given the selection of composites as the primary structural material, candidate manufacturing plans were evaluated using four figures of merit:

- Type of composite selected
 - strength
 - resilience
- Required manufacturing skill level
- Precision of construction
- Freedom of design

As discussed in the previous section, composites certainly posed some challenges to the team, but their potential performance payoffs were deemed necessary to the creation of a competitive airframe. One of the requirements of composite construction is craftsmanship skill. The team included several members experienced in composite construction. In addition, the ready availability of a composites lab helped immensely, as the storage and use of composites and epoxies requires such equipment as vacuum pumps, fume hoods, and storage areas for composite cloth.

A second tradeoff that the team considered was the potential cost savings of other materials. This became extraneous in light of the adequate budget for the project and the lack of other choices in materials capable of meeting the design criteria.

The main materials decisions then became the choice of fiber. Kevlar was most appropriate for the primary structure due to its extremely high strength and impact resistance. Carbon fiber, also very strong but stiffer and more brittle, excelled as a means of reinforcement. Fiberglass, which falls between the above materials in resilience and is slightly weaker, is also available in a much wider variety of thicknesses. It was best suited to covering foam surfaces.

6.3 Construction

The large tubes, including the payload compartment and the main body tube of the fuselage, were built first because they are large simple shapes that did not require very precise construction. This allowed the team to refine the fabrication process and complete the detailed design of the more complex aircraft components. Additionally, by working on the main assembly first, subsequent components could be fitted to the main body to ensure good part interfaces.

6.3.1 *Wing construction*

Most of the wing's structural loading is carried by a spar that runs the full length of the wing. The wing spar bisects a foam core, and the whole assembly is wrapped in fiberglass. The spar consists of a carbon fiber/end-grain balsa sandwich. The upper and lower surfaces of carbon fiber take compressive and tensile loads, while the balsa web keeps the carbon surfaces equally spaced. This arrangement handles the bending load generated by wing lift in an I-beam fashion and utilizes the best attributes of both materials.

To make the structural connection between the center and outboard wing sections, a carbon joiner plate fits into fiberglass-wrapped plywood slots at the end each section's spar. This configuration is highly resistant to bending stresses. Once joined in this fashion, the wing sections become one rigid piece. The spar tapers in width toward the wingtips, taking advantage of the diminishing bending loads to save weight.

The spar is sealed in fiberglass and glued in between the front and back halves of the wing. The two halves of the wing are initially made as one continuous airfoil using a computer numeric centering (CNC) hot wire foam cutter. The foam cutter uses a MATLAB model of the airfoil to control the movement of a hot wire through foam, thus cutting the specified wing shape. Once the full airfoils are made, they are cut in half and material is removed to make room for the spar. The spar is then bonded in place between the wing sections. All of the wing panels are constructed in this manner, except for the tip sections which do not require a spar. Each one is then covered with a layer of fiberglass cloth. The layup is done under vacuum pump, with thick mylar applied over the wing surface to ensure a smooth finish, reducing drag.

6.3.2 *Tail Construction*

The tail surfaces are done in a manner similar to that for the wing. Both the vertical and horizontal stabilizers are cut from foam on the CNC wire cutter. Although they do not feature a spar, they are similarly laid up under vacuum pump with mylar over fiberglass surfaces.

6.3.3 *Fuselage Construction*

The aircraft fuselage consists of six main components: main body tube, nose and tail cones, payload tubes, landing gear struts, and wing pylon.

The main body tube of the aircraft consists mainly of kevlar. There are a number of high stress areas that require additional structural support. These areas include:

- Interfaces with the nose and tail cones
- Landing gear mounting area
- Wing pylon mounting area

Due to the stresses at the nose and tail interfaces, induced by the motor in the front and the control surfaces via a long tail cone in the back, the body tube is reinforced with unidirectional carbon fiber at the ends. This process creates rings in the tube that are very resistant to deformation and cracking. The landing gear and wing bolt areas are deemed to be the areas of greatest stress; consequently, they receive a two-layer application of bi-directional carbon fiber weave. The layup is accomplished by wrapping all of the layers of fabric onto an aluminum mandrel, with a layer of waxed sheet acrylic between. A vacuum bag applied during cure forced the inner surface to conform to the mandrel and squeezed out excess epoxy. We thought the tube would then easily slide off the mandrel. It turned out that, due to epoxy's tendency to shrink during cure, the tube bound itself tightly to the mandrel, even resisting our attempts to pound it off in a piledriver-like manner. We solved this issue by dousing the entire assembly with liquid nitrogen, which shrank the aluminum more than the fiber and allowed the tube to slide off.

The nose and tail cones are constructed in a manner similar to the construction of the main body tube. The mandrels are fashioned out of foam on a lathe. The nose and tail cones are constructed of kevlar with carbon fiber reinforcement. The nose cone features a reinforcing ring at the front at the motor mounting area. The tail cone, in contrast, features carbon fiber bands running its full length. These provide bending strength.

The body tube and the nose and tail cones all transfer forces to the keel of the aircraft. The keel is constructed of a composite sandwich, similar to the spar. Bi-directional carbon fiber runs along the sides of a vertically positioned $\frac{1}{4}$ " balsa sheet, which extends between the top and bottom inside surfaces of the main tube. The keel features five-layer aircraft plywood bulkheads, which center it inside the body tube and ensure that forces transfer to the keel. The keel extends into the nose cone, where the motor mounts to it. Bulkheads inside the nose cone, bonded between the keel and the cone surface, ensure that motor mounting is also structurally sound.

The payload tubes, used to carry the water bottles, are mounted below the main body tube. They are also kevlar-carbon fiber layups. Since they are not structural members when empty and are stiffened by the water bottles when full, they need not be as strong as the other parts of the structure. They are composed of a single wrap of kevlar, as opposed to the two layers of the body tube, and feature sparse use of carbon fiber reinforcement. The same construction methods as the main tube were used, although this time several water bottles wrapped in acrylic served as a mandrel, and no vacuum was necessary.

The main landing gear struts are composed of excess material from carbon fiber test sections. They are multi-ply carbon fiber, which are cut in a trapezoidal shape with a width of two inches at the mounting point and one inch at the wheel end. The gear struts are attached to the body tube with kevlar fiber lashings. Plywood brackets are also lashed into place and maintain the angle the struts make in relation to the body tube. The last step in landing gear fabrication is to make carbon disc wheels.

The wing pylon and enclosed wing bolt secure the wing to the fuselage. The pylon is a foam-core structure, cut on the CNC wire cutter. Its upper and lower surfaces are shaped to match the wing and fuselage respectively. It features internal bulkheads to ensure that it can handle the compressive stress applied to it between the wing and fuselage. It also encases the wing bolt, which links the wing to the keel.

A manufacturing planning timeline follows in Figure 10.

Appendix A

Matlab Integrated Vehicle Simulation

Takeoff Module

The takeoff module of the simulation consists of 3 Matlab scripts: takeoff.m, which is the main script; TO_deriv.m, which computes the net acceleration on the vehicle; and inputs.m, which contains all the input parameters for the simulation. All 3 files are presented below.

Takeoff.m

```
inputs;

[ t, s ] = ode23( 'TO_deriv', [ t0:0.05:tf ], s0 );

TO_index = find( s(:,1) > TO_vel );
TO_distance = s( TO_index(1), 2 )           % in m
disp( 'meters' );
TO_mah = s(TO_index(1), 4)/3600*1000        % in mA-hrs
TO_time = t( TO_index(1) )                  % in s
disp( 'seconds' );

% PLOTS
% -----

subplot(2,1,1)
plot( t(1:TO_index(1)), s(1:TO_index(1), 1) )
hold on;
plot( [t0, tf], [TO_vel TO_vel], '--' );
title('Takeoff Run');
xlabel('time (s)');
ylabel('velocity (m/s)');
axis( [ 0, t( TO_index(1) ) + 5, 0, 1.3*TO_vel ] );
grid;

subplot(2,1,2)
plot( t(1:TO_index(1)), s(1:TO_index(1), 2) )
hold on;
plot( [t0, tf], [TO_distance TO_distance], '--' );
xlabel( 'time (s)' );
ylabel('distance (m)' );
axis( [ 0, t( TO_index(1) ) + 5, 0, 2*TO_distance ] );
grid;
```

TO_deriv.m

```
function sdot = TO_deriv( t, s )

% define input variables/parameters
inputs;

% define expression for thrust:
index = round( s(1)+1 );
if (index > length(thrust))
    index = length(thrust);
end

T = thrust( index );

I = current( index );

% define expression for drag:
D = rho/2 * (s(1))^2 * ( S*Cd_o(1) + phi * S * (Cl_TO)^2 / ( pi * AR *
e ) + S_f*Cd_Af );

% define expression for ground resistance:
R = mu_r * ( m*g - rho/2 * (s(1))^2 * S * Cl_TO );

% define expression for sdot, the derivative of the state vector [s1 s2
% s3]
sdot = [ 1/m * ( T - D - R ); s(1); 0; I ];
```

Inputs.m

```
% inputs.m
% =====

% Environmental Parameters
% =====

% freestream density:
% (kg/m^3)
rho = 1.225;

% coefficient of ground friction:
mu_r = 0.02;

% gravity:
g = 9.81;

% POWERPLANT Characteristics
% =====

% NO LONGER USED:
% available power:
% (W)
AP = 300;

% propeller efficiency:
```

eta = 0.85;

STRUCTURAL/PHYSICAL Characteristics

* total mass = a/c mass + cargo mass:
* (kg)
m = 10.16;

* ground clearance of wing:
* (m)
h = 0.2032;

AERODYNAMIC Characteristics

* fuselage drag:
Cd_Af = 0.02;

* fuselage cross-sectional area:
* (m^2)
S_f = 0.02;
* wing span:
* (m)
b = 2.134;

* wing area:
* (m^2)
S = 0.7097;

* Oswald's efficiency factor:
e = 0.9;

* coefficient of parasitic drag:
* (values at takeoff, climb, cruise, and landing configurations)
Cd_o = [0.012 0.012 0.012 0.2];

* coefficient of lift during takeoff roll:
* (based on incidence angle):
Cl_TO = 0.51;

* maximum coefficient of lift:
* (used for takeoff point--rotation)
Cl_max = 1.15;

* derived parameters:

* aspect ratio:

AR = b^2/S;

* ground effect correction:

phi = ((16*h/b)^2)/(1+(16*h/b)^2);

* takeoff speed: (1.2 * stall speed)

TO_vel = 1.2 * sqrt((2*m*g) / (rho*S*Cl_max));

TAKEOFF Flight Parameters

```

% initial state: (velocity, x-position, z-position, battery amp-hours
consumed)
s0 = [0 0 0 0];

% initial time:
t0 = 0;

% final time:
tf = 30;

% CLIMB Flight Parameters
% -----

% flight path angle gamma
% (rad)
gma_climb = 20*pi/180;

% desired cruising altitude
% (m)
h_cruise = 17;

% LEVEL Flight Parameters
% -----

% turn radius of aircraft
% (m)
turn_radius = 50 * 0.3048;

% ground track distance for 1 lap
% (m)
lap_distance = 2000*0.3048 + 2*pi*turn_radius;

% SORTIE SWITCH: 1 = loaded sortie; 2 = empty sortie
h2o_sortie = 1;

% LANDING Flight Parameters
% -----

% desired landing glideslopes (2 phases)
% (rad)
gma_land1 = 20*pi/180;
gma_land2 = 10*pi/180;

% altitude where to switch from phase 1 to phase 2
% (m)
h_crit = 3;

% expected descent distance
descent_dist = ( h_crit/tan(gma_land2) ) + ( (h_cruise -
h_crit)/tan(gma_land1) );

```

```

% -----
% Thrust-Velocity and Power-Velocity data
load vel_thrust.txt -ascii;          load data from Motocalc
thrust-velocity analysis
vel_data = vel_thrust(:,1)*0.44704;    % converting from MPH to
METERS/SECOND
thrust_data = vel_thrust(:,15)*0.278;  % converting from OZ to NEWTONS
current_data = vel_thrust(:,6);        % current is in AMPS

thrust = interp1( vel_data, thrust_data, [0:vel_data(length(vel_data))]
);
current = interp1( vel_data, current_data,
[0:vel_data(length(vel_data))] );

```

Appendix B

Matlab Integrated Vehicle Simulation

Climb Module

The climb module of the simulation consists of 3 Matlab scripts: climb.m, which is the main script; climb_deriv.m, which computes the net acceleration of the vehicle; and inputs.m, which contains all the input parameters for the simulation. The former 2 files are presented below; the latter (inputs.m) may be found in Appendix A.

Climb.m

```
% climb.m

% accelerating climb flight phase

[ t, s ] = ode23( 'climb_deriv', [ TO_time:0.05:TO_time+30 ], [ TO_vel,
TO_distance, 0, TO_mah] );

climb_index = find( s(:,3) > h_cruise );

climb_time = t( climb_index(1) )
climb_mah  = s(climb_index(1), 4)/3600*1000      % mA-hrs
climb_vel  = s( climb_index(1), 1)                % m/s
climb_distance = s( climb_index(1), 2)            % m


% PLOTS
% -----

figure;
subplot(2,1,1)
plot( t(1:climb_index(1)), s(1:climb_index(1), 3) )
hold on;
plot( [TO_time, TO_time+30], [h_cruise h_cruise], '--' );
title('Climbout');
xlabel('time (s)');
ylabel('altitude (m)');
axis([TO_time, climb_time+1 0 5+h_cruise])
grid;

subplot(2,1,2)
plot( t(1:climb_index(1)), s(1:climb_index(1), 1) )
hold on;
plot( [ climb_time climb_time ], [ 0 climb_vel+3 ], '--' );
axis( [TO_time climb_time+1 TO_vel-1 climb_vel+3] );
xlabel( 'time (s)' );
ylabel('velocity (m/s)' );
grid;
```

Climb_deriv.m

```
function sdot = climb_deriv( t, s )

% define input variables/parameters
inputs;

% define expression for thrust:
index = round( s(1)+1 );
if (index > length(thrust))
    index = length(thrust);
end

T = thrust( index );

I = current( index );

% find current lift coefficient from  $mg \cos(\gamma) = L = q \cdot S \cdot C_l$ 
Cl_climb = m*g*cos(gma_climb) / ( 0.5*rho*(s(1))^2*S );

% define expression for drag:
D = rho/2 * (s(1))^2 * ( S*Cd_o(2) + S * (Cl_climb)^2 / ( pi * AR * e )
+ S_f*Cd_Af );

% define expression for sdot, the derivative of the state vector [s1 s2
s3 s4]
% note s = [ velocity; x-position; z-position; battery power consumed ]

sdot = [ 1/m * ( T - D - m*g*sin(gma_climb) ); s(1)*cos(gma_climb);
s(1)*sin(gma_climb); I ];
```


Appendix C

Matlab Integrated Vehicle Simulation

Cruise Module

The cruise, or level flight, module of the simulation consists of 3 Matlab scripts: level.m, which is the main script; level_deriv.m, which computes the net acceleration of the vehicle; and inputs.m, which contains all the input parameters for the simulation. The former 2 files are presented below; the latter (inputs.m) may be found in Appendix A.

Level.m

```
* level.m

% level flight segment

[ t, s ] = ode23( 'level_deriv', [ climb_time:0.05:climb_time+60 ], ...
    [ climb_vel, climb_distance, h_cruise, climb_mah] );

if ( h2o_sortie )
    flight_distance = lap_distance + 2*pi*turn_radius - descent_dist;
else
    flight_distance = 2*lap_distance - descent_dist;
end

level_index = find( s(:,2) > flight_distance );

level_time = t( level_index(1) )
level_mah  = s(level_index(1), 4)/3600*1000    % mA-hrs
level_vel  = s( level_index(1), 1)             % m/s
level_distance = s( level_index(1), 2)         % m

figure;
plot( t, s(:,1) )
title('Level Flight');
xlabel('time (s)');
ylabel('velocity (m/s)');
axis([ TO_time level_time+1 0 level_vel+7 ]);
grid;
```

Level_deriv.m

```
function sdot = level_deriv( t, s )

% define input variables/parameters
inputs;

% define expression for thrust:
index = round( s(1)+1 );
if (index > length(thrust))
    index = length(thrust);
end

T = thrust( index );
I = current( index );

% find current lift coefficient from  $W = L = \rho \cdot S \cdot C_l$ 
 $C_l = m \cdot g / ( 0.5 \cdot \rho \cdot (s(1))^2 \cdot S );$ 

% define expression for drag
 $D = \rho / 2 \cdot (s(1))^2 \cdot ( S \cdot C_{d_o}(3) + S \cdot C_l^2 / ( \pi \cdot AR \cdot e ) + S_f \cdot C_{d_{Af}} );$ 

% define expression for sdot, the derivative of the state vector [s1 s2
s3 s4]
% note s = [ velocity; x-position; z-position; battery power consumed ]

sdot = [ 1/m * ( T - D ); s(1); 0; I ];
```

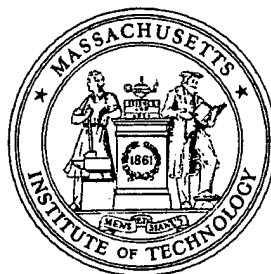
AIAA Student Design/Build/Fly Competition

MIT Fire & Water

Design Report- Addendum Phase



Larry Baskett
Jacob Markish
Larry Pilkington
Bernard Ahyow
Dan Benhammou
Adam Diedrich
Carol Cheung
Allen Chen



Massachusetts Institute of Technology
Cambridge, Massachusetts

Table of Contents

1	Executive Summary.....	4
1.1	<i>Conceptual Design Summary.....</i>	4
1.2	<i>Preliminary Design Summary.....</i>	4
1.3	<i>Detailed Design Summary.....</i>	5
2	Management Summary	6
2.1	<i>Personnel and Tasking.....</i>	6
2.2	<i>Management Structure and Scheduling.....</i>	6
3	Conceptual Design	8
3.1	<i>System Configurations Investigated.....</i>	8
3.2	<i>Analytic Methods Used.....</i>	9
3.3	<i>Final Configuration Decision.....</i>	11
3.4	<i>Configuration Refinement</i>	11
4	Preliminary Design	15
4.1	<i>Design parameters investigated.....</i>	15
4.2	<i>Figures of merit</i>	15
4.3	<i>Analytic methods used.....</i>	16
4.3.1	Xfoil	16
4.3.2	Athena Vortex Lattice (AVL)	16
4.3.3	Plane Geometry (PG).....	17
4.3.4	Electricalcalc and MotoCalc.....	17
4.4	<i>Preliminary sizing and key features</i>	17
4.4.1	Wing planform and sizing.....	17
4.4.2	Empennage size and shaping.....	18
4.4.3	Motor configuration and size	18
5	Detailed Design	22
5.1	<i>Component selection and systems architecture</i>	22
5.1.1	Propulsion System.....	22
5.1.2	Control System.....	22
5.1.3	Braking System	23
5.1.4	Configuration Improvements	24
5.2	<i>Final Performance Data</i>	24
5.2.1	Takeoff Performance	24
5.2.2	Handling Qualities and G-Load Capability.....	25
5.2.3	Cruise Performance	25
5.2.4	Weight Budget	25
5.3	<i>Drawing Package</i>	25

6	Manufacturing Plan.....	29
6.1	<i>Material Selection and Manufacturing Process.....</i>	29
6.2	<i>Figures of Merit.....</i>	30
6.3	<i>Construction.....</i>	30
6.3.1	Wing construction.....	31
6.3.2	Tail Construction.....	31
6.3.3	Fuselage Construction.....	31
	Appendix A.....	35
	Appendix B.....	40
	Appendix C.....	42

7	Lessons Learned	45
7.1	<i>Design Updates.....</i>	45
7.2	<i>Improvements in Next Design</i>	45
7.3	<i>Improvements in Manufacturing Process</i>	45
7.4	<i>Improvements in Design Process.....</i>	46
7.5	<i>Improvements in Team Organization.....</i>	46
8	Aircraft Cost.....	46

7 Lessons Learned

7.1 Design Updates

The final version of the aircraft differs little from the configuration presented in the preliminary report. Minor alterations account for reinforcement and accessibility issues.

The nose/fuselage tube junction, through which the internal keel carries structural loads, sees a good deal of torque from the motor reaction forces and from any lateral bending on the nose gear strut. In anticipation of these stresses, the nose/fuselage junction now includes an additional layer of carbon fiber on each side of the keel as well as slip-fit pins connecting the nose shell to the fuselage shell.

The main landing gear struts will see considerable bending moments on landing. In their current installation, the strut/fuselage junction may not be able to handle the rigors of repeated hard landings. A "training wheel" bracing strut connects the two main gear struts to form a tough structural A-frame. This strut may be removed to reduce drag for contest flights.

Because the plane features modular assembly, control wiring that crosses junctions between airplane pieces must be broken by connectors. To reduce the number of connectors, the receiver moved from the tailcone to the internal keel, which is more centrally located.

The original configuration called for very short battery wires that connect directly to the speed controller. While short wires are certainly desirable, this configuration meant that a battery change would require the removal of the internal keel, which would in turn require removal of the wing and tailcone. In the revised configuration the speed control wires run to the back of the keel. This way the batteries can be accessed simply by removing the tailcone.

7.2 Improvements in Next Design

In next year's design the team intends to, if possible, reduce the number of specialized parts. Unique custom-shaped composite components, necessitating mold fabrication and creative layup methods, absorbed a lot of fabrication time.

7.3 Improvements in Manufacturing Process

The original manufacturing plan called for making enough spare components to make up essentially two aircraft. This plan would allow bulk change-out of components should they become damaged during practice or at the contest. Unfortunately, the team did not have time to implement this plan. Next year this will be a priority.

Another manufacturing priority for next year is to fabricate only what cannot be purchased or modified. The team adhered to this principle to some extent, but specialized performance-improving components such as lightweight carbon disc wheels need to fall behind the rest of the plane on the construction priority hierarchy.

7.4 Improvements in Design Process

Next year will see changes aimed at smoothing out and speeding up the design process. One or two baseline configurations should be set very early in the process. Design parameters will be defined and prioritized more explicitly.

The most practical lesson from this year's project is that full-scale pencil drawings proved absolutely essential to the finalization of the design and to all stages of fabrication. The scale of this project makes full-size drawings convenient. Such drawings are intuitive and facilitate understanding of component positioning and interference issues. Pencil drawings supersede CAD drawings in terms of ease of changes for this type of project. Once the plane's overall size is finalized, hand-drawn plans should be made up immediately.

7.5 Improvements in Team Organization

The most difficult challenges to the team occurred in the areas of coordination, organization and scheduling. Definitions of working times were not formal enough, and project milestones consistently slipped. Specific improvements for next year should include a more regular meeting schedule and class credit offered for team members. At MIT, the month of January is designated an "Independent Activities Period" (IAP) a time between semesters when short classes are offered both on academic and on purely fun topics. IAP is an excellent opportunity to do the majority of the construction, so next year this project should be an officially designated IAP activity. Additional organizational improvements include setting out financial specifics early in an itemized budget as well as having a team member with a unique skill teach that skill to teammates as early as possible.

Although this project faced substantial delays in all phases of design and fabrication, the team believes it has a competitive entry.

8 Aircraft Cost

The total aircraft cost came to \$4663.11. See the following tables for the cost breakdown.

Aircraft Dependent Parameters for Cost Model			
Coefficient	Description	Equation	Value
A	Manufacturer's Empty Weight Multiplier	MEW* \$100/lb	711.70
B	Rated Engine Power Multiplier	REP* \$1/lb	1560.00
C	Manufacturing Cost Multiplier	MFHR* \$20/hr	6670.00
MEW	Manufacturer's Empty Weight	Total Aircraft Weight in Pounds	7.12
REP	Rated Engine Power	# engines* 50A* 1.2 V/cell* # cells	1560.00
MFHR:	Manufacturing Man Hours	Sum of Work Breakdown Structures	333.50
	WBS 1.0: Wings	5 hr/wing + 4 hr/sq.ft. Projected Area	33.50
	WBS 2.0: Fuselage and Pods	5 hr/body + 4 hr/ft of Length	257.00
	WBS 3.0: Empenage	5 hr + 5 hr/ Vertical Surface + 10 hr/ Horizontal Surface	20.00
	WBS 4.0: Flight Systems	5 hr + 1 hr/Servo	13.00
	WBS 5.0: Propulsion Systems	5 hr + 5 hr/Propeller	10.00
Total Aircraft Cost			\$4,663.11

Aircraft Weight		
Part	Qty (if >1)	Total [grams]
Fuselage		
710		
153		
163		1026
Wing		
818		
210		
42		1322
Electroincs		
Servos		
34	2	
21	6	194
Motor		
369		369
Controller		
76		76
Receiver		
46		46
Receiver Batt		
100		100
Switch harness		
45		45
Wire		
57		57
Total Weight		3235 grams 7.117 pounds

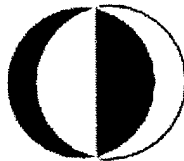
Aircraft Cost		4663.11
MEW	7.117	
REP	1560	
MFHR	333.5	
A	711.7	
B	1560	
C	6670	
REP		
Engines	1 motor	
Bateries	26 cells	
MFHR		
	WBS 1.0	
Wing area	33.5	
1026 in^2		
WBS 2.0		
Fuselage	257	
63 in		
Pods		
0 in		
WBS 3.0		
Vertical Stabilizer	20	
1		
Horizontal Stabilizer		
1		
WBS 4.0		
Servos	13	
8		
WBS 5.0		
Engine	10	
1		
Propeller		
1		
Total		333.5



**AIAA/CESSNA/ONR
STUDENT DESIGN/BUILD/FLY
COMPETITION**

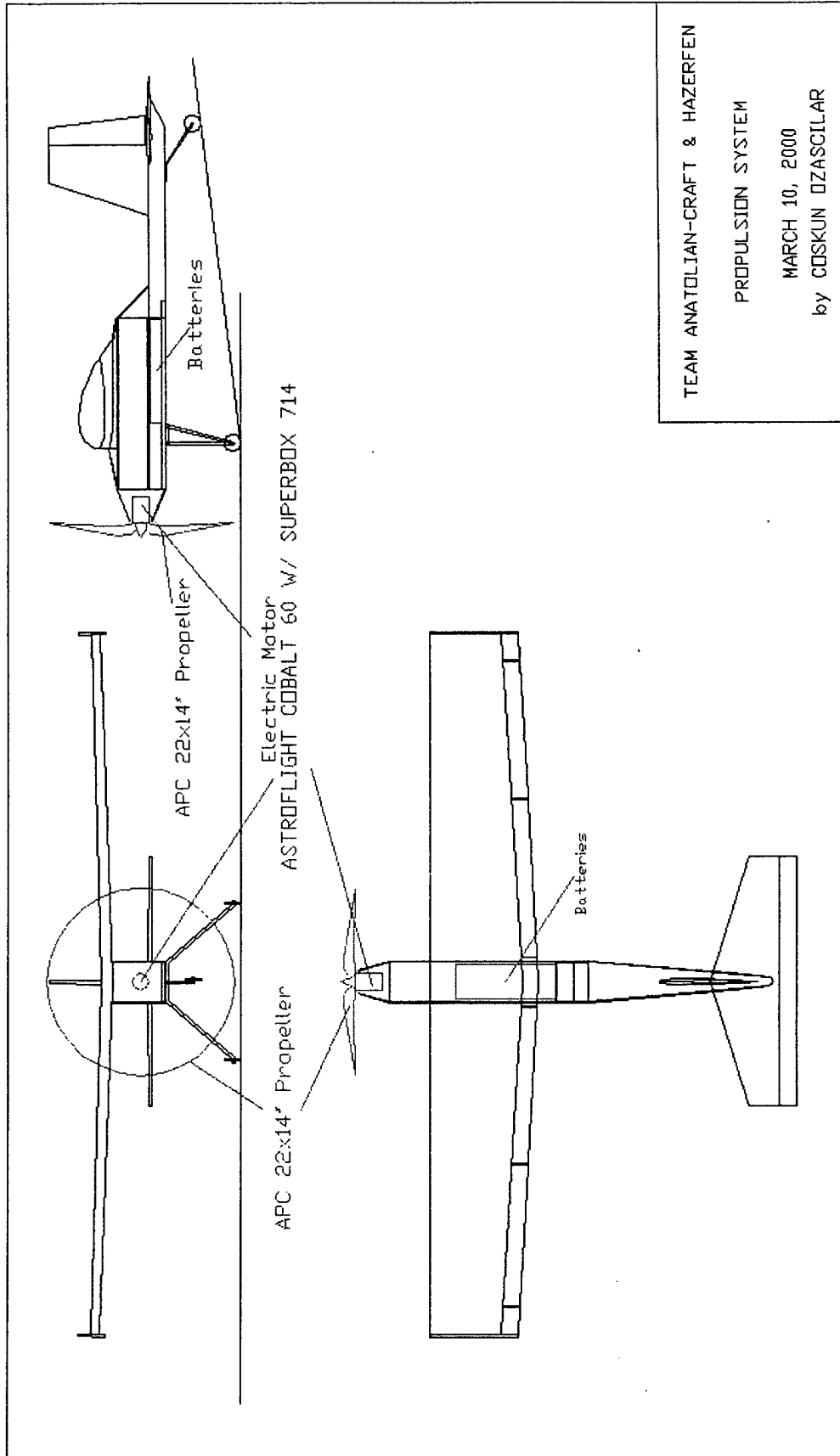
PROPOSAL REPORT

DESIGN OF A UAV CLASS AIRCRAFT

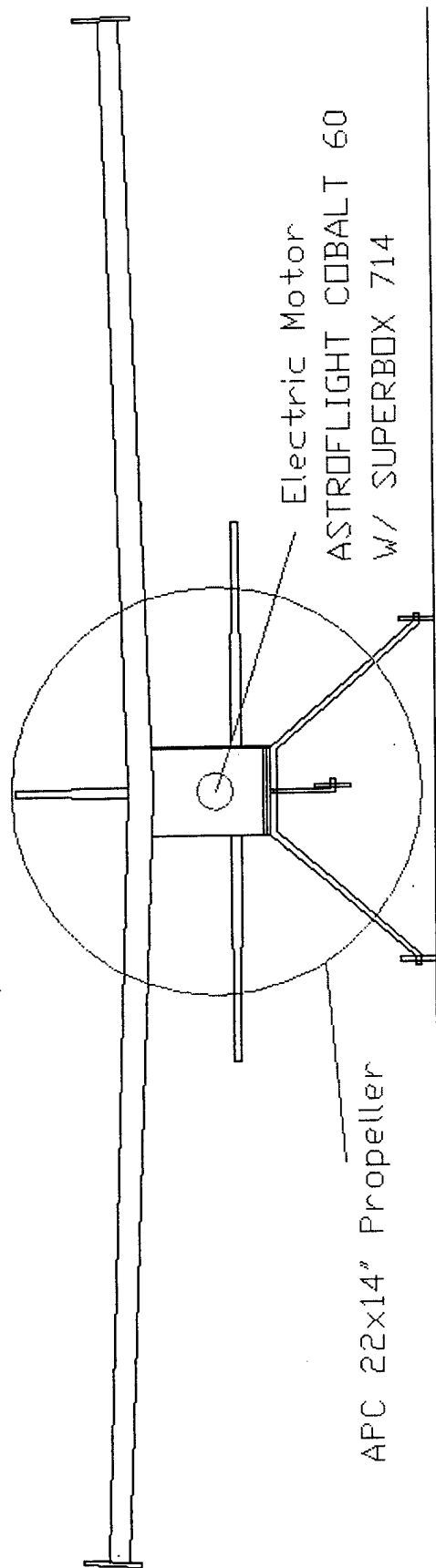


METU

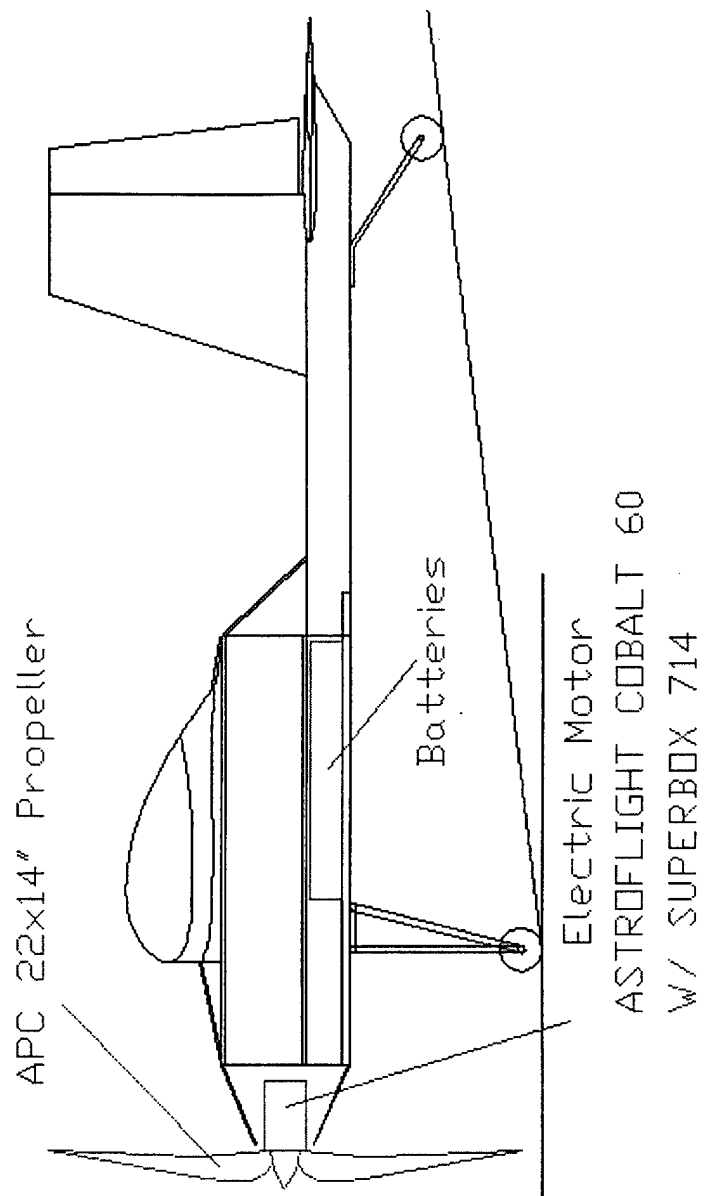
TEAM ANATOLIAN-CRAFT AND HAZERFEN



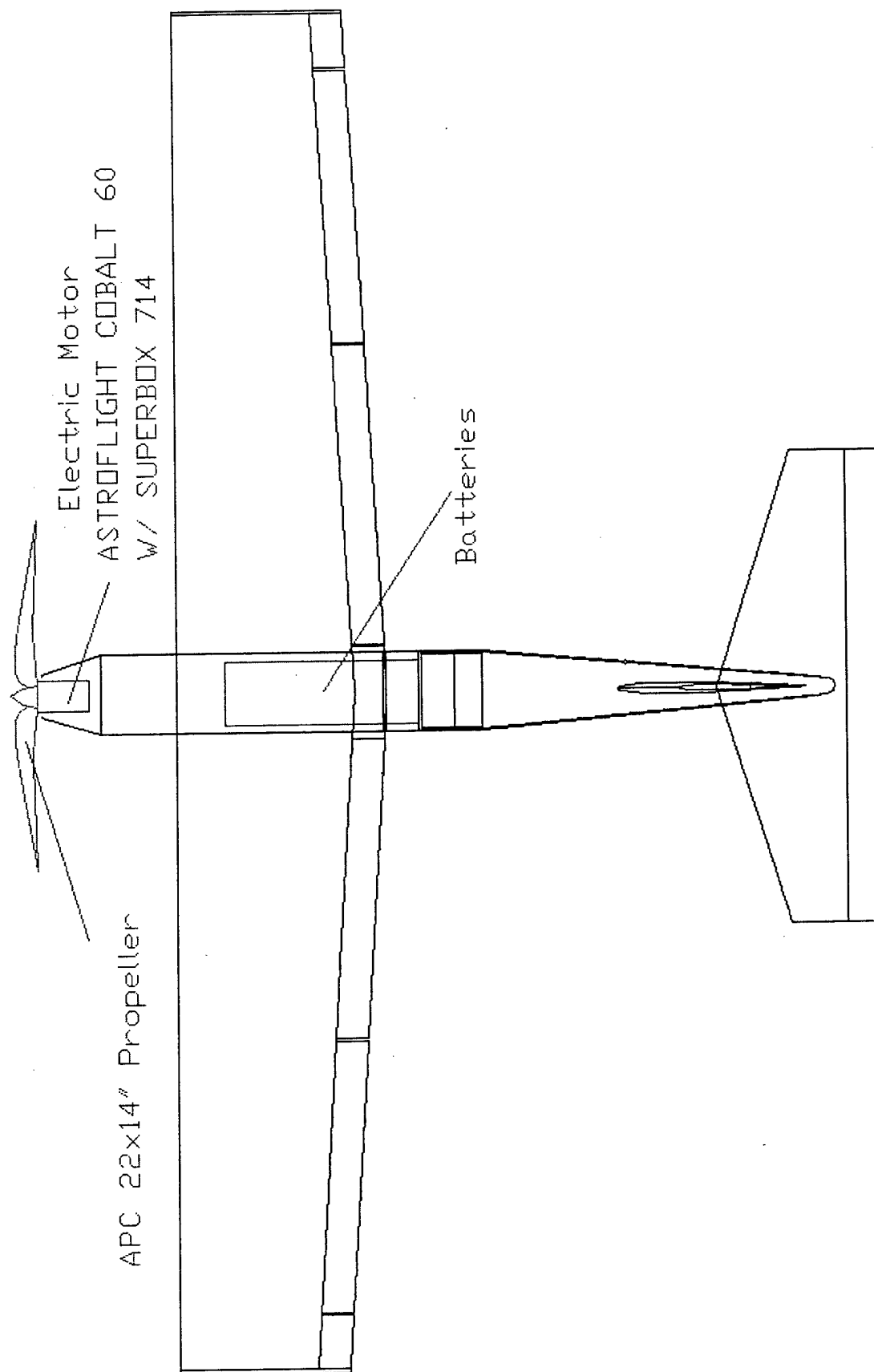
Drawing 5, Propulsion system



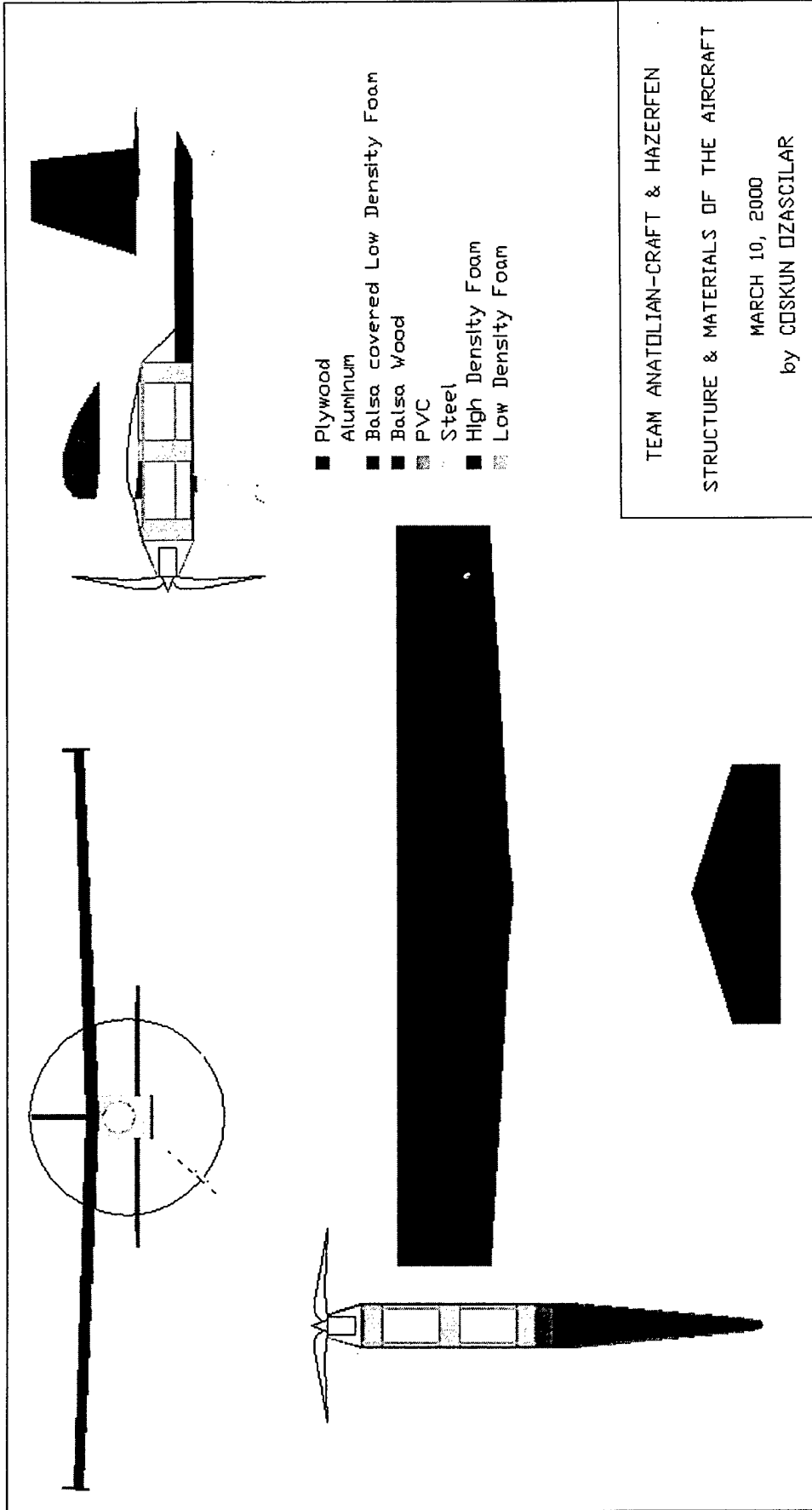
Drawing 5-1, Propulsion system (front view)



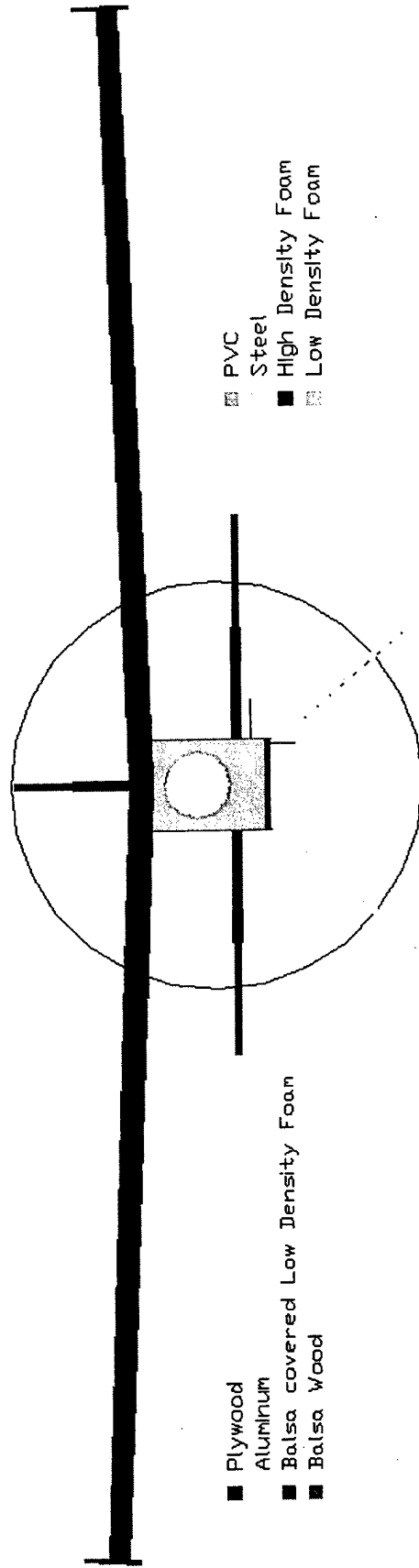
Drawing 5-2, Propulsion system (side view)



Drawing 5-3, Propulsion system (top view)



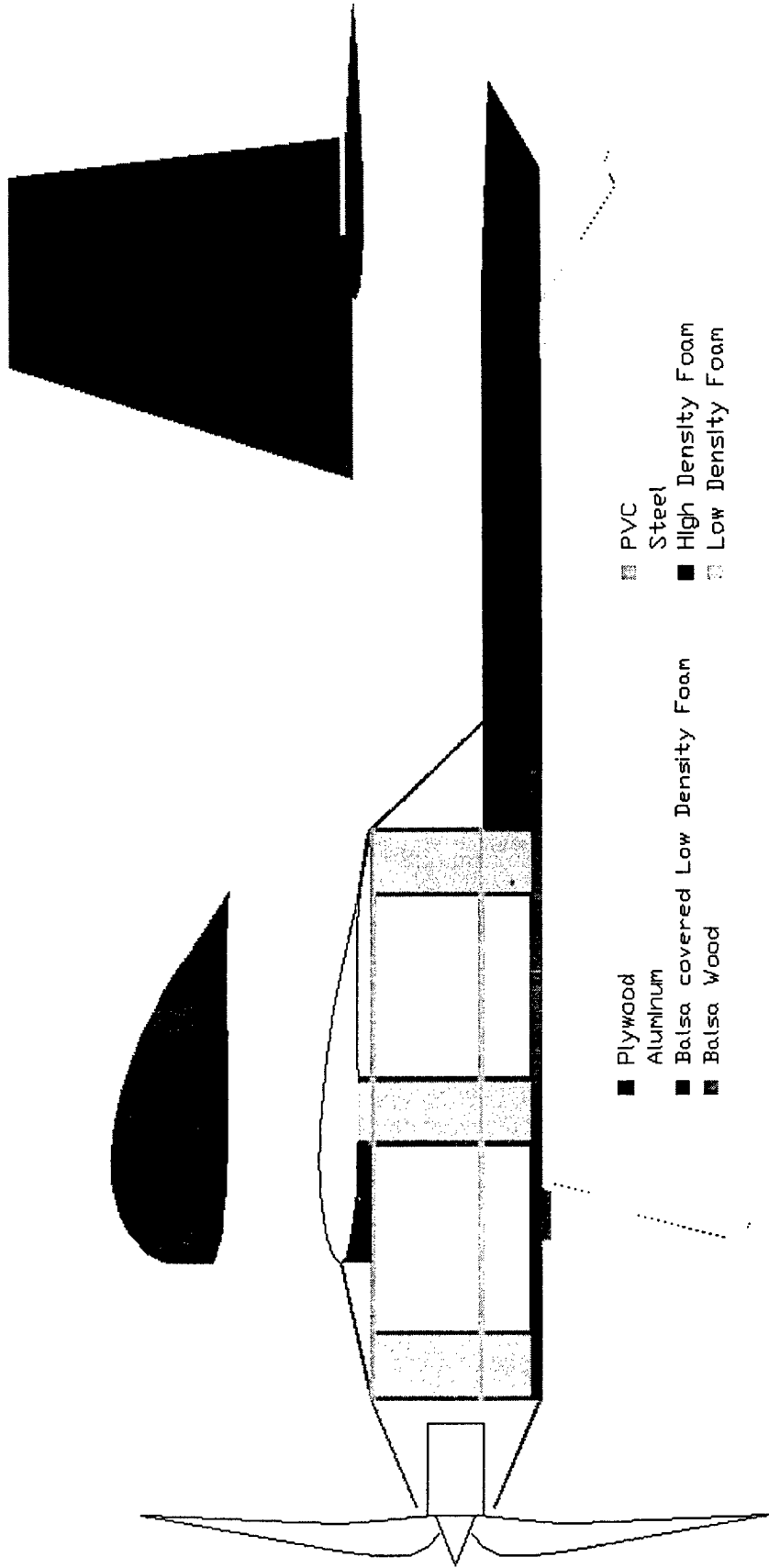
Drawing 6, Structure & Materials of the aircraft



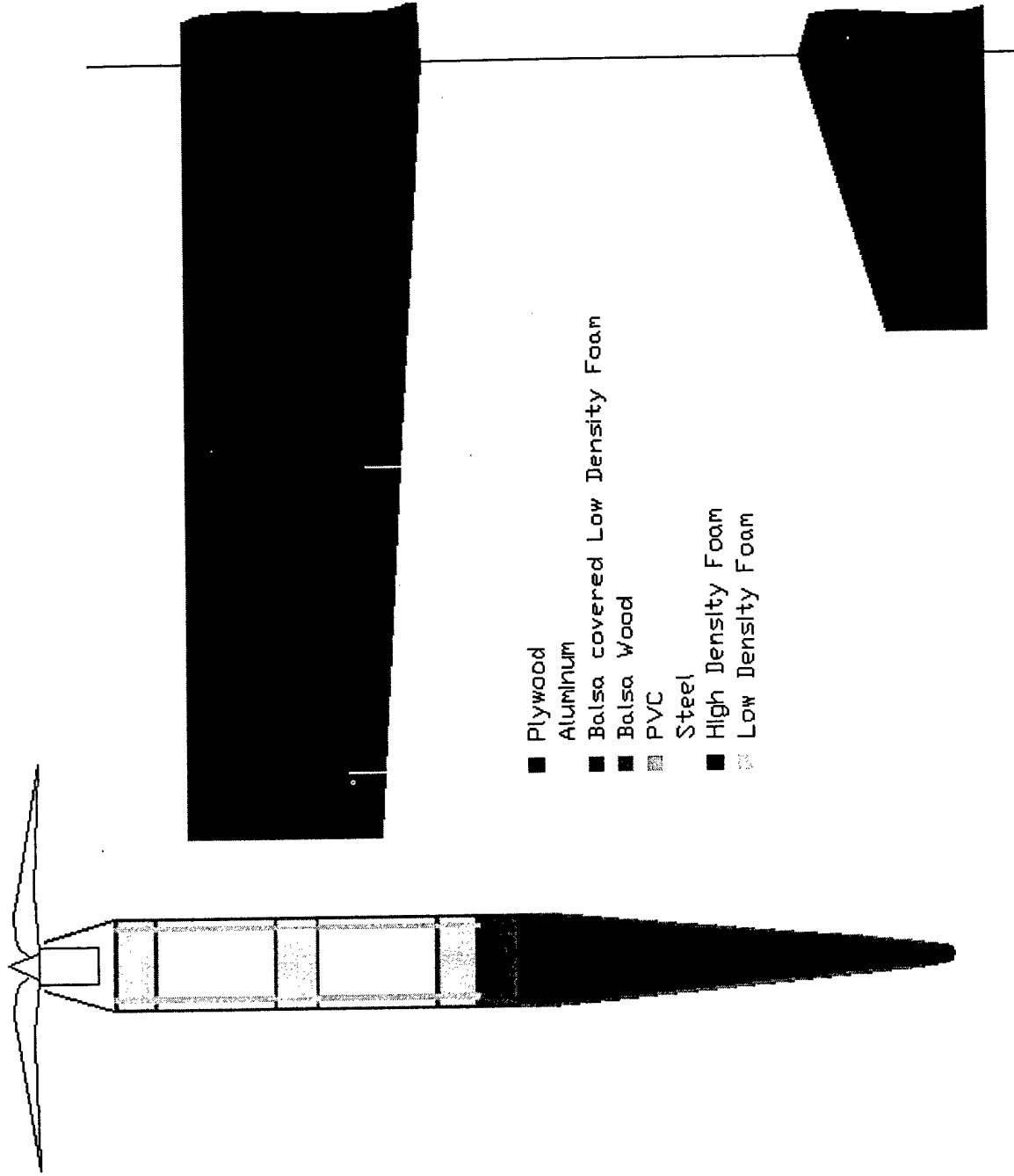
■ PVC
 ■ Steel
 ■ High Density Foam
 ■ Low Density Foam

■ Plywood
 ■ Aluminum
 ■ Balsa covered Low Density Foam
 ■ Balsa Wood

Drawing 6-1, Structure & Materials of the aircraft (front view)



Drawing 6-2, Structure & Materials of the aircraft (side view)



Drawing 6-3, Structure & Materials of the aircraft (top view)

CHAPTER 6

MANUFACTURING PLAN

6.1 INTRODUCTION

In this chapter, the basic steps for manufacturing the major components and assemblies of the final design will be explained. Furthermore, investigated manufacturing processes are detailed and the figures of merit used for their selection will be described.

6.2 MANUFACTURING PROCESSES INVESTIGATED

At first, our team considered using low density wood for the construction of all structural components. Balsa wood will be used for most of the structure –which is a light and stiff kind of wood- while birch plywood or a composite plate will be used for high-stress areas, like joining parts. Balsa sticks can be used as spars on wings to increase their endurance. Using foam inside the wing can be a possibility to obtain lighter wings. Plastic or fabric covering materials can be used to cover Balsa for smoothness. In addition, a wooden boom will be used to combine tail and fuselage, which is the most widely used method for lighter, small UAV construction.

Using carbon fiber and kevlar for construction is another method that was considered. This method uses mold for each component and then covers the molds with fiber and kevlar cloth. This method also requires usage of some wood and composite plates for the production of the boom, wing mountings, motor holders and other electrical equipment mountings. Usage of fiberglass is another alternative for this method.

Using of aluminum was another alternative method for production of our UAV. This method would require some specific tools like CNC machines for processing. However this method is not widely used for UAV type light aircraft.

Finally, a combination of the above stated methods is considered to satisfy the figures of merit for each structural component. Balsa will be used to cover the foam wing and tail which will then be covered with plastic or fabric material. Carbon fiber and kevlar cloth will be used as stiffeners for spars. Carbon fiber and Balsa wood combination will be used to manufacture a stiff and light fuselage, and carbon fiber will be used to manufacture the boom. Components requiring more strength or endurance (like wing mountings, boom mountings, electrical equipment cases etc.) will be stiffened by fiber plates. If more strength is needed, aluminum plates will be used.

6.3 FIGURES OF MERIT

Five figures of merit are used to screen the competing the concepts proposed for manufacturing. These are;

- ➔ Availability of materials
- ➔ Levels of required skill
- ➔ Time of construction
- ➔ Cost of materials
- ➔ Interference with radio frequency reception

It is important that the materials, which will be used, must be readily available and can be purchased easily and rapidly. Aluminum is not very easy to find as compared to other choices. Also it is not very easy to process aluminum. However Balsa wood can easily be found from hobby shops. Fiber or Kevlar clothes can also be found from small companies that are specialized in composite materials. Production and processing with fiber and Balsa wood are also fast.

All the team members are already familiar with how to built a wooden light aircraft, and has developed the skills to produce a modal a/c with Balsa wood. Some of the team members also knew how to make molds for fiber and how to produce parts using fibers and kevlar.

Since our time for building the a/c was running short and we had to spare some time for flight testing before it was ready to fly, we have to optimize our time as much as possible. During this testing period, the aircraft might be broken or major aerodynamic problems may arise. So a period for development and improvement must be foreseen ample time before the competition. These estimations are provided from professionals and their ptractical observations. Wing construction will not take more than 20 hours since the wings will be produced from foam and and will be covered Balsa wood. This is a relatively easy and rapid process. Fiberglass, carbon fiber, or kevlar production depends on mold production. After producing the molds, it only takes a couple of days to produce in desired shape. But at least, production of molds will take more time than wood production from wood. Finally, machining and assembling parts from aluminum airframe is estimated to take at least twice as long as building our UAV out of wood.

Cost is another important dividing factor for the choice of production method for the UAV. Balsa wood is the cheapest material among all the choices, and aluminum is the most expensive one. Also Kevlar and fiber is a good choice as compared in cost since they are not expensive. So fiber and wood combination will also be a low cost choice.

We have finally considered the electromagnetic compatibility problems. We found that aluminum will create electromagnetic compatibility problems for radio control

frequencies and the risk of losing radio reception can never be taken in this design project.

6.4 FINAL SELECTION AND JUSTIFICATION OF MANUFACTURING PROCESSES

The team considered all of these figure of merits and decided to manufacture the UAV from combination of Balsa wood, foam and composite materials for all major parts except the landing gears which will be made from aluminum. This decision is taken as a result of stated figures of merit and the advantages. All of the FOM drives us to use wood and composite mainly for stiffness, low cost, easy and fast manufacturing. It is easy to produce the wing and tail from wood covered foam, a composite boom, and a composite fuselage. This main construction will be finished before the end of March 2000 so there will be enough time to test our UAV.

6.5 MANUFACTURING PROCESS

All the parts of the aircraft will be produced carefully and following a production plan. Completion of each assembly will be followed by the integration with the major assembly and alignment with the rest of the components. First wings will be produced followed by fuselage manufacturing. Tail assembly will be joined to these with a boom. Production of extra wings are planned in case of aircraft..

Throughout the construction process, epoxy and carpenter's wood glue will be used.

6.5.1 WING CONSTRUCTION

The basic structure of the wing panels is formed by cutting the foams to their desired shape.

To satisfy the structural integrity requirements of having the fully loaded aircraft picked up by its wingtips, 3/4"-wide unidirectional carbon fiber tape is applied as spar caps. The carbon fiber is applied symmetrically (top and bottom) as follows: Two layers are applied over the full span of each panel. One layer spanned the inboard 75% of each wing panel, while the fourth layer spanned the inboard half of each wing. A physical test, as described in the detailed design phase, using this identical spar structure showed that the spar alone, without any additional structure such as leading edge sheeting, satisfied the structural requirement for an aircraft weighing 43 pounds. To further increase the safety factor, the aircraft was built with one additional layer of carbon fiber tape capping the top and bottom of the entire spar.

Knowing the fragility of Balsa, the team realized that it will not be feasible to have sharp trailing edges from just 3/32" Balsa sheeting. For this reason, 3/4"-wide strips of 1/64" 3-ply birch plywood were glued between the top and bottom trailing edge pieces. When sanded, this produced a sharp, durable trailing edge.

The 3/32" Balsa leading edge sheeting completed the D-tube structure of the wing panels, yielding high torsional rigidity for the wing.

Cap strips made of 3/8"-wide strips of 3/32" thick Balsa wood are epoxied to the ribs in the wing. These provided more surface area for the covering material to adhere. This was important since the wing panels relied on the high tensile strength of the covering material to provide more structural rigidity.

Ailerons and flaps are cut from the trailing edge and hinged to a false spar installed along the cut in each wing panel. The hinge-line for the ailerons was at the top surface of the wing, but the hinge-line for flaps was at the bottom. This is done in order to allow maximum movement for each surface when deflected for "crow" mixing as described in the detailed design phase. The resulting gaps in the surfaces of the wing were sealed with plastic strips anchored along the hinge-line of the wing.

One servo is used for each aileron and flap to simplify linkage for the two wing panels. Since the wing is separated at the fuselage, only a wire from each servo had to be plugged into the receiver to make the ailerons and the flaps operational.

A 4-40 threaded push-rod coupled with a control horn mounted on each aileron and flap provided the control from each servo.

6.5.2 TAIL SURFACE CONSTRUCTION

Since the horizontal and vertical stabilizers has airfoil sections, as opposed to flat surfaces, they are built using the similar technique as for the wing. Ribs were cut from 3/32" Balsa and assembled to two 1/4" square Balsa spars running the entire span of each stabilizer. These surfaces also used cap strips to increase the adhesion area provided for the covering material.

Sheeting was applied to the roots of the stabilizing surfaces in order to provide solid mounting surfaces for the fuselage. The sheeting at the roots also increased the torsional rigidity of the surfaces.

Construction of the rudder and elevators were similar to the construction of the ailerons in that the trailing edge had strips of 1/64" 3-ply birch plywood between the 1/16" Balsa sheeting. The elevator was hinged at the upper surface and sealed on the bottom, similar to the ailerons. Rudder hinges were put along the centerline of the cross section.

Two carbon tubes solidly mounted to the fin provided vertical fin removal for transportation. The fuselage housed two carbon tubes to accept the vertical fin. To keep the vertical stabilizer in place during flight, two 8-32 bolts were inserted from the inside of the fuselage through its upper surface into the fin.

6.5.3 FUSELAGE CONSTRUCTION

Lite plywood was the primary material used for the construction of the fuselage. Both sides, along with the top and bottom of the fuselage were cut from 1/8" lite plywood. The nose was rounded by building up the top and bottom with Balsa sanded to shape.

Four major bulkheads/formers were assembled in the fuselage. The first one used 1/4" aircraft quality spruce plywood for the nose-gear mount. The next two formers were two 1/8" aircraft quality spruce plywood pieces that accepted the main wing spar for assembly. Triangle stock was used generously when attaching these formers to the fuselage walls since failure of these joints would be catastrophic. The last former was simply in place behind the payload bay to keep the fuselage shape. Lite ply was suitable for the fabrication of this former.

The main payload bay cover was the last major structural element of the fuselage. Again, 1/8" lite plywood was used to produce the hatch cover. Strips of plywood were attached perpendicular to the hatch cover to support aluminum railings to which the water bottles would attach. Each of the ten bottles had a support disk near the cap so that they could be stored on rails such as what is shown in Figure 6.1. Each bottle was moved into place on the rails and secured by cotter pins.

6.5.4 LANDING GEAR CONSTRUCTION

Composite construction was used exclusively for the fabrication of the main landing gear. Twenty-two layers of unidirectional carbon fiber surrounded a 1/8" core of Balsa, birch plywood, and aluminum. Table 6.1 explains the arrangement of carbon layers relative to the core. The resin-laden lay-up was secured over a blue foam template to form its elliptical shape. Figure 6.3 depicts the blue foam template along with the core of the landing gear. Vinyl sheets placed around the lay-up allowed the landing gear to cure with a smooth finish. Six 1/4 x 20 bolts attached the final main landing gear to the fuselage.

The nose-gear was purchased since the appropriate size was already available. Another issue that warranted the purchase, rather than construction of the nose-gear, was that its failure would probably cause extensive damage, which was less likely with a commercially available nose-gear.

6.6 CONCLUSION

This chapter was devoted to the manufacturing plan and to the processes selected for manufacturing of the major components and assemblies of the final design. Manufacturing processes are described according to their figures of merit

REFERENCES

1. *Spot. F* , Fortran Programming Code developed by Dr. Kevin Jones, Dept of Aeronautics and Astronautics, Naval Post Graduate School, Monterey, CA. 93943
2. "*Aircraft Design: A Conceptual Approach*", by Raymer D.P., AIAA Education Series, Second Edition
3. "*Arplane Design*" by Roskam J., Parts: 1-8, Roskam Aviation and Engineering Corporation, second printing, 1989
4. Math-CAD⁴
Math-CAD 7 Professional, © 1986-1997 MathSoft Inc.
5. AutoCAD R14⁵
AutoCAD Release 14.0, Copyright©1982-1997 Autodesk, Inc.
6. 3D Studio⁶
7. Aveox's Virtual Motor Test Stand⁷
Aveox Virtual Motor Test Stand , Copyright ©1999 Aveox Inc.
8. Advanced Aircraft Analysis (AAA)⁸
Advanced Aircraft Analysis Version 2.2, Copyright©1999 DARcorporation
9. Microsoft Excel, Word⁹
Microsoft®Excel 97, Copyright©1985-1996 Microsoft Corporation
Microsoft®Word 97, Copyright© 1983-1996 Microsoft Corporation
10. Microsoft Power Point¹⁰
Microsoft®PowerPoint® 97, Copyright©1987-1996 Microsoft Corporation
11. "*Introduction to Aeronautics: A Design Perspective*" by Brandt S.A., Stiles R.J., Bertin J.J., Whitford R., AIAA Edycation Series, 1992
12. "*Theory of Wing Section*" by I.H. Abbott, A.E. Von Doenhoff, Dover Publications, 1959
13. "*Airfoil Design and Data*" R. Epplerr, Springer-Verlag, 1990
14. "*Airplane Aerodynamics and Performance*" by Chuan-Tau Edward Lan, Jan Roskam.

APPENDIX 1

```

program main
c
      parameter( npx = 101 )
c
c----- All common blocks listed here.
c
      common/bod   / nlower, nupper, noddot, npl, ss,
&                  x(npx+1), y(npx+1), xm(npx), ym(npx),
&                  costhe(npx), sinthe(npx)
      common/cof   / a(npx,npx+10), kutta
      common/cpd   / cp(npx), xp
      common/infl  / aan(npx,npx), bbn(npx,npx)
      common/sing  / q(npx), gamma
      common/forces/ cl, cm
c
      pi = acos(-1.0)
c
c----- Retrieve parameters from the command line.
c
      read*, naca
      read*, noddot
      read*, alpi
c
c----- Valid parameter check.
c
      if (( naca .gt. 25999 ).or.( naca .lt. 1 )) naca = 12
      if ( noddot .lt. 20 ) noddot = 20
      if ( noddot .gt. 100 ) noddot = 100
      if ( alpi .gt. 90.0 ) alpi = 90.0
      if ( alpi .lt. -90.0 ) alpi = -90.0
c
      nlower = noddot / 2
      nupper = noddot - nlower
      npl = noddot + 1
c
      alpi = alpi*pi/180
c
c----- Generate the airfoil coordinates.
c
      call airfoil(naca)
c
c----- Compute a steady solution at AOA = alpi.
c
      call steady(alpi)
c
c----- Hardwire ppm output for now.
c
      call print_cp(naca,alpi)
c
      stop
      end
c-----

```

```

      subroutine airfoil(naca)
c
      parameter( npx = 101 )
c
      common/bod   / nlower, nupper, nodtot, npl, ss,
&                x(npx+1), y(npx+1), xm(npx), ym(npx),
&                costhe(npx), sinthe(npx)
c
c----- Compute the airfoil coordinates and panel angles.
c
      pi = acos( -1.0 )
c
c----- Decompose the NACA number to determine airfoil coefficients.
c
      iep = naca / 1000
      iptmax = naca / 100 - 10 * iep
      itau = naca - 1000 * iep - 100 * iptmax
c
c----- Compute the coefficients.
c
      epsmax = iep * 0.01
      ptmax = iptmax * 0.1
      tau = itau * 0.01
c
c----- Error correction for bogus NACA numbers.
c
      if ( ( naca .le. 9999 ) .and. ( epsmax .gt. 0 ) .and.
&        ( ptmax .eq. 0 ) ) ptmax = .1
c
c----- If NACA 5 digit coding is used, make necessary changes.
c
      if ( iep .ge. 10 ) then
        if ( iep .eq. 21 ) then
          ptmax = 0.0580
          ak1 = 361.4
        elseif ( iep .eq. 22 ) then
          ptmax = 0.1260
          ak1 = 51.64
        elseif ( iep .eq. 23 ) then
          ptmax = 0.2025
          ak1 = 15.957
        elseif ( iep .eq. 24 ) then
          ptmax = 0.2900
          ak1 = 6.643
        elseif ( iep .eq. 25 ) then
          ptmax = 0.3910
          ak1 = 3.230
        endif
        epsmax = ak1 * ptmax**3 / 6
      endif
c
c----- initialize indexing for lower surface.
c
      npoint = nlower

```

```

      nstart = 0
c
c----- Loop over lower surface.
c
      do n = 1, npoint
        z = ( 1 + cos( pi * ( n-1 ) / npoint )) / 2
        i = nstart + n
        call naca45(naca,tau,epsmax,ptmax,z,thick,camber,beta)
        x(i) = body_x(thick,beta,z,-1.0)
        y(i) = body_y(thick,camber,beta,-1.0)
      enddo
c
c----- Reinitialize indexing for upper surface
c
      npoint = nupper
      nstart = nlower
c
c----- Loop over upper surface.
c
      do n = 1, npoint
        z = ( 1 - cos( pi * ( n-1 ) / npoint )) / 2
        i = nstart + n
        call naca45(naca,tau,epsmax,ptmax,z,thick,camber,beta)
        x(i) = body_x(thick,beta,z,1.0)
        y(i) = body_y(thick,camber,beta,1.0)
      enddo
c
c----- Load final point.
c
      x(np1) = x(1)
      y(np1) = y(1)
c
c----- Compute slopes of panals and arc length of airfoil skin.
c
      ss = 0.0
      do i = 1, ntot
c
c----- Control points.
c
        xm(i) = ( x(i+1) + x(i) ) / 2
        ym(i) = ( y(i+1) + y(i) ) / 2
c
c----- Arc length.
c
        dx = x(i+1) - x(i)
        dy = y(i+1) - y(i)
        dist = sqrt( dx**2 + dy**2 )
        ss = ss + dist
c
c----- Slope.
c
        sinthe(i) = dy / dist
        costhe(i) = dx / dist
      enddo

```

```

c      return
      end

```

```

c-----

      function body_x(thick,beta,z,sign)
c
c---- Compute the x coordinate of an airfoil point.
c
      body_x = z - sign * thick * sin( beta )
c
      return
      end

```

```

c-----

      function body_y(thick,camber,beta,sign)
c
c---- Compute the y coordinate of an airfoil point.
c
      body_y = camber + sign * thick * cos( beta )
c
      return
      end

```

```

c-----

      subroutine cofish(alpha)
c
      parameter( npx = 101 )
c
      common/bod   / nlower, nupper, noddot, np1, ss,
&                  x(np1+1), y(np1+1), xm(np1), ym(np1),
&                  costhe(np1), sinthe(np1)
      common/cof   / a(np1,np1+10), kutta
      common/infl  / aan(np1,np1), bbn(np1,np1)
c
      pi = acos( -1.0 )
      pi2inv = 0.5 / pi
      kutta = noddot + 1
      cosalf = cos( alpha )
      sinalf = sin( alpha )
c
c---- Initialize coefs.
c
      do 10 j = 1, kutta
        a(kutta,j) = 0.0
      10 continue
c
c---- Set vn = 0 at midpoint of ith panel.
c
      do 30 i = 1, noddot
        a(i,kutta) = 0.0

```

```

c
c----- Find contribution of jth panel.
c
      do 20 j = 1, nodtot
        if ( j .eq. i ) then
          flog = 0.0
          ftan = pi
        else
          dxj = xm(i) - x(j)
          dxjp = xm(i) - x(j+1)
          dyj = ym(i) - y(j)
          dyjp = ym(i) - y(j+1)
          flog = alog( ( dxjp**2 + dyjp**2 )
&                  / ( dxj**2 + dyj**2 ) ) / 2
          ftan = atan2( dyjp * dxj - dxjp * dyj,
&                  dxjp * dxj + dyjp * dyj )
          endif
          ctimtj = costhe(i) * costhe(j) + sinthe(i) * sinthe(j)
          stimtj = sinthe(i) * costhe(j) - costhe(i) * sinthe(j)
          a(i,j) = pi2inv * ( ftan * ctimtj + flog * stimtj )
          bbn(i,j) = pi2inv * ( flog * ctimtj - ftan * stimtj )
          a(i,kutta) = a(i,kutta) + bbn(i,j)
          if (( i .eq. 1 ) .or. ( i .eq. nodtot )) then
            a(kutta,j) = a(kutta,j) - bbn(i,j)
            a(kutta,kutta) = a(kutta,kutta) + a(i,j)
          endif
        endif
      20 continue
c
c----- Load aan and bbn values now so that they don't have to be
c----- recomputed in infl.
c
      aan(i,j) = a(i,j)
c
c----- Fill in known sides.
c
      a(i,kutta+1) = sinthe(i) * cosalf - costhe(i) * sinalf
30 continue
      a(kutta,kutta+1) = -( costhe(1) + costhe( nodtot ) ) * cosalf
&      -( sinthe(1) + sinthe( nodtot ) ) * sinalf
c
      return
      end

c-----
      subroutine formom(alpha)
c
      parameter( npx = 101 )
c
      common/bod / nlower, nupper, nodtot, npl, ss,
&               x(npx+1), y(npx+1), xm(npx), ym(npx),
&               costhe(npx), sinthe(npx)
      common/cpd / cp(npx), xp
      common/forces/ cl, cm

```

```

C
  cosalf = cos( alpha )
  sinalf = sin( alpha )
  cfx = 0.0
  cfy = 0.0
  cm = 0.0

C
  do i = 1, nodtot
C
C----- Moment coefficient is computed about the elastic axis.
C
    xmid = xm(i) - xp
    ymid = ym(i)
    dx = x(i+1) - x(i)
    dy = y(i+1) - y(i)
    cfx = cfx + cp(i) * dy
    cfy = cfy - cp(i) * dx
    cm = cm + cp(i) * ( dx * xmid + dy * ymid )
  enddo

C
C----- Compute lift.
C
  cl = cfy * cosalf - cfx * sinalf
C
  return
  end

```

```

C-----
      subroutine gauss(nrhs,m,nitr)
C
      parameter( npx = 101 )
C
      common/cof / a(npx,npx+10), neqns
C
C----- Performs Gaussian elimination of matrix a.
C
      np = neqns + 1
      ntot = neqns + nrhs
C
      if (( m .le. 1 ) .and. ( nitr .eq. 0 )) then
C
C----- Do full matrix elimination sequence.
C
        do 10 i = 2, neqns
          im = i - 1
C
C----- Eliminate the (i-1)th unknown from i-th through
C----- neqns-th equations.
C
          do 10 j = i, neqns
            r = a(j,im) / a(im,im)
            do 10 k = i, ntot
              a(j,k) = a(j,k) - r * a(im,k)

```



```

10    continue
    else
c
c----- Elimination on RHS only.
c
        do 20 i = 2, neqns
            im = i - 1
            do 20 j = i, neqns
                r = a(j,im) / a(im,im)
                do 20 k = np, ntot
                    a(j,k) = a(j,k) - r * a(im,k)
20    continue
        endif
c
c----- Back substitution.
c
        do 40 k = np, ntot
            a(neqns,k) = a(neqns,k) / a(neqns,neqns)
            do 40 l = 2, neqns
                i = neqns + 1 - l
                do 30 j = i+1, neqns
                    a(i,k) = a(i,k) - a(i,j) * a(j,k)
30    continue
                a(i,k) = a(i,k) / a(i,i)
40    continue
c
        return
    end

c-----
        subroutine naca45(naca,tau,epsmax,ptmax,z,thick,camber,beta)
c
c----- Compute the thickness, camber, and angular location of an
c----- airfoil point.
c
c----- Thickness, corrected when z is very small.
c
        if ( z .lt. 1.0e-10. ) then
            thick = 0.0
        else
            thick = tau * 5 * ( 0.2969 * SQRT(Z)
&                - Z * ( 0.1260
&                + Z * ( 0.3537
&                - Z * ( 0.2843
&                - Z * 0.1015))))
        endif
c
        if ( epsmax .eq. 0.0 ) then
c
c----- For NACA 4-digit symmetrical airfoils.
c
            camber = 0.0
            beta = 0.0

```

```

      else
        if ( naca .gt. 9999 ) then
c
c-----      For NACA 5 digit numbers.
c
c-----      Ptmax = m and epsmax = (k_1*m^3)/6 from Abbott and Doenhoff.
c
          if ( z .gt. ptmax ) then
            camber = epsmax * ( 1.0 - z )
            dcamdx = - epsmax
          else
            w = z / ptmax
            camber = epsmax * ( w**3 - 3*w**2 +(3.-ptmax)*w)
            dcamdx = epsmax/ptmax*(3*w**2 - 6*w + ( 3.0-ptmax))
          endif
        else
c
c-----      For NACA 4 digit airfoils.
c
          if ( z .gt. ptmax ) then
            camber = epsmax / ( 1.0 - ptmax )**2
            &      * ( 1. + z - ptmax * 2 ) * ( 1. - z )
            dcamdx = epsmax * 2 / ( 1.0 - ptmax )**2
            &      * ( ptmax - z )
          else
            camber = epsmax / ptmax**2 * ( ptmax**2 - z ) * z
            dcamdx = epsmax * 2 / ptmax**2 * ( ptmax - z )
          endif
        endif
c
        beta = atan( dcamdx )
      endif
c
      return
      end

c-----

      subroutine print_cp(naca,alpi)
c
      parameter( npx = 101 )
c
      common/bod / nlower, nupper, nodtot, npl, ss,
      &      x(npx+1), y(npx+1), xm(npx), ym(npx),
      &      costhe(npx), sinthe(npx)
      common/cpd / cp(npx), xp
c
c-----      Write out data.
c
      open(8,file='cp.fmt',form='formatted',status='unknown')
      do n=1,nodtot
        write(8,*) xm(n), ym(n), cp(n)
      enddo
      close(8)

```

```

c      return
c      end

c-----

      subroutine steady(alpha)
c
c-----  alpha is angle of attack in radians, positive clockwise.
c
c      call cofish(alpha)
c      call gauss(1,0,0)
c      call veldis(alpha)
c      call formom(alpha)
c
c      return
c      end

c-----

      subroutine veldis(alpha)
c
c      parameter( npx = 101 )
c
c      common/bod / nlower, nupper, nodtot, npl, ss,
&                x(npx+1), y(npx+1), xm(npx), ym(npx),
&                costhe(npx), sinthe(npx)
c      common/cof / a(npx,npx+10), kutta
c      common/cpd / cp(npx), xp
c      common/infl / aan(npx,npx), bbn(npx,npx)
c      common/sing / q(npx), gamma
c
c      cosalf = cos( alpha )
c      sinalf = sin( alpha )
c
c-----  Retrieve solution from a matrix.
c
c      sum = 0.0
c      do i = 1, nodtot
c         q(i) = a(i,kutta+1)
c         ds = sqrt((x(i+1)-x(i))**2 + (y(i+1)-y(i))**2)
c      enddo
c      gamma = a(kutta,kutta+1)
c
c-----  Find vt and cp at mid-point of i-th panel.
c
c      do i = 1, nodtot
c         vtfree = cosalf * costhe(i) + sinalf * sinthe(i)
c         vtang = vtfree
c
c-----  Add contribution of j-th panel.
c
c      do j = 1, nodtot
c         vtang = vtang - bbn(i,j) * q(j) + gamma * aan(i,j)

```

```
        enddo  
        cp(i) = 1.0 - vtang**2  
    enddo  
c  
    return  
end
```

APPENDIX 2

RATED AIRCRAFT COST MODEL FOR CONVENTIONAL TYPE AIRCRAFT

$w = 22$ Weight of the aircraft in lb
 $ep = 1300$ Engine power in watt.
 $h = 50$ Manufacturing time in hour
 $en = 1$ Engine number
 $cn = 62$ Cell number
 $nw = 1$ Number of wings
 $pa = 6.706$ Projected area of wing in ft²
 $nb = 1$ Number of bodies
 $lf = 4.429$ Length of fuselage in ft
 $vs = 1$ Number of vertical surface
 $hs = 1$ Number of horizontal surface
 $s = 5$ Number of servos
 $p = 1$ Number of propellers

$MEW = 12$ Manufacturers Empty Weight

$A = 100 \cdot w$

$B = 1 \cdot ep$

$C = 20 \cdot h$

$REP = en \cdot 50 \cdot 1.2 \cdot cn$ Rated Engine Power

$MFHR = (5 \cdot nw + 4 \cdot pa) + (nb \cdot 5 + 4 \cdot lf) - (5 + 5 \cdot vs + 10 \cdot hs) + (5 + 1 \cdot s) + (5 \cdot e + 5 \cdot p)$

$RAC = \frac{A \cdot MEW + B \cdot REP + C \cdot MFHR}{1000}$

$$RAC = 4.966 \cdot 10^3$$

CHAPTER 5

DETAIL DESIGN

5.1 INTRODUCTION

Detail design starts with analyzing the final performance data, including the take-off and landing performances, handling qualities and g load capability, range and endurance, and payload fraction, including the component selection and systems architecture.

5.2 PERFORMANCE ANALYSIS

A table consisting of weight estimates and takeoff, climb, cruise, turning and landing performance data of the AC-H was prepared for visual presentation. All of the calculations were performed following the procedures suggested by the books; *Aircraft Design, A Conceptual Approach*, by Daniel P. Raymer and *Airplane Aerodynamics and Performance*¹⁴, by Chuan-Tau Edward Lan, Jan Roskam.

Considering the available power from the motor, and deciding that the a/c will carry two bottles of water at one time, with this configuration the empty weight was estimated to be 5 kg and the payload fraction was 0.3.

The first part of the mission is the takeoff. At take-off, the flaps and ailerons are positioned fully down in order to have enough lift. It is calculated that the aircraft take off after 17.6 m from initial point, with a speed of 16.23 m/s.

After takeoff, AC-H starts to climb with a rate of 3.5 m/s and an angle of 12°. During climbing, the same flap and aileron configuration as in take off phase is used. Therefore its lift and drag coefficients are the same with those experienced as during the take-off phase, 1.1 and 0.2 respectively.

The next part is the turning part. AC-H experiences a 180° turn with a speed of 26.4m/s and a radius of 63.61m.

Between the 180° and 360° turns, there will be a cruise phase. For this phase, cruise, stall and maximum speeds are calculated as 21.55 m/s, 14.11 m/s, and 30.27 m/s respectively. Also, for a range of 304.8 m (1000 ft), 20.3 mAh charge will be used for a total period of 14.2 sec.

After the 360° and 180° turn, AC-H will start landing. When it touches down, it will have a speed of 18.34 m/s and the landing ground roll will be 31.22 m, assuming a friction

RANGE FORMULA

AC-H has an electric motor so we have to derive an equation like Breguet range equation. We define a constant C that

$$i \times \varepsilon = P$$

where "i" is the current of the electric motor which is :

$$i = \frac{dq}{dt} = \frac{P}{\varepsilon}$$

since $T=D$ and $W=L$

$$T = \frac{W}{L/D}$$

Substituting

$$dq = \frac{W}{L/D} \frac{V}{\varepsilon} dt$$

integrating it results in

$$\Delta t = \frac{L/D}{W} \frac{\varepsilon}{V} \Delta q$$

since $R=Vt$

$$R = \frac{L/D}{W} \varepsilon \Delta q$$

ENDURANCE FORMULA

We will use our previous formula for range again to find the equation of endurance because we have electrical engine.

$$E = \Delta t = \frac{L/D}{W} \frac{1}{VC} \Delta q$$

5.4 COMPONENT SELECTION AND SYSTEMS ARCHITECTURE

5.4.1 Propulsion system

Astro Flight Cobalt 60 Electric Motor with Model 714 Super Box 3:1 ratio is used for the propulsion system of our UAV. 62 Panasonic P-160AS A size (KR17/50) Type S batteries will be used to supply the necessary power to the motor. Our motor will turn a glass-filled/composite APC 22x14 2-blade replacement propeller. The motor and the propeller assembly will be placed in front of the fuselage and will therefore function as a tractor type (not a pusher) propeller. The propeller has thinner and less-noise profile with 11" radius (each half), reinforced by carbon fibers to maintain its true constant pitch at any rpm with high output and longer time. The motor gives 3000 static rpm, 26 Volts, 21 Amps, 550 Watts, 70 oz. thrust and 39 mph speed ideally with this propeller. This motor is one of the high output power motors available in the market which will function with the stated number of batteries (since battery weight is limited by the contest rules). Astro Flight 204D Speed Control ESC Airplane Futaba is used. The ESC must be a high quality device that our UAV will have a high temperature increase because of high power motor, so our ESC is heat-protected. But this high quality ESC unfortunately increases the cost. This ESC works in a range of 6-36 NiCad Cells, with max 50 Amps, 2800 switching rate, weighs 30 gram (54 gram with wires) and connectors supplied with zero loss. All of the components of the designed UAV are commercial of the shelf equipment and can easily be found from any hobby shops.

5.4.2 Control system

Our control system is a Futaba Digital proportional radio control unit, with nine-channel PCM 1024Z transmitters. It is a good choice with respect to the contest rules since it has the fail-safe feature for any fail condition. It also satisfies all of our needs in controlling our UAV. It has a dual mode gyro function, which allows to select two different settings within one flight condition. These capabilities will help us in landing and take-off because it increases the usage of ailerons and flaps. It has a frequency synthesizer that allows to fly on any unused channel where we must fly on an unused channel. This radio control is also programmable and has the ability of servo reversing. It has the capability to reverse the rotation of a servo with a flip of a switch. It is easy to use and has flexibility during installation.

We have used 2 Futaba S-3102 micro-servos, which are micro-sized, metal gear, and 5-pole motor, has 51.4 oz. of torque and 5 Futaba S-9202 servos, which are gold plated and deliver 69.5 oz. of torque. We have used two servos for ailerons, one for flaps, one to ESC, one for the rudder and one for the elevator. Micro-servos are used to control the ailerons only. They all have ball bearing supported output shafts. It is known (from our previous experiences) that these torque are large enough for driving the control surfaces.

LATERAL-DIRECTIONAL STATIC STABILITY AND CONTROL

Cn β Calculation:

Wing Terms:

for cruise condition,

$$CL = 0.6$$

$$\Lambda = 0$$

$$A = 7$$

$$b = 2.1 \text{ m}$$

$$X_{acw} = 0.35 \text{ m}$$

$$X_{cg} = 0.4 \text{ m}$$

$$Cn_{\beta w} = (CL)^2 \cdot \left[\frac{1}{4\pi \cdot A} - \left[\frac{\tan(\Lambda)}{\pi \cdot A \cdot (A + 4 \cdot \cos(\Lambda))} \right] \cdot \left[\cos(\Lambda) - \frac{A}{2} - \frac{A^2}{8 \cdot \cos(\Lambda)} + 6 \cdot \frac{(X_{acw} - X_{cg}) \cdot \sin(\Lambda)}{b \cdot A} \right] \right]$$

$$Cn_{\beta w} = 4.093 \cdot 10^{-3}$$

Fuselage Terms:

$$\text{volume} = 0.011 \text{ m}^3$$

$$D_f = 0.15 \text{ m} \quad (\text{depth of fuselage})$$

$$W_f = 0.12 \text{ m} \quad (\text{width of fuselage})$$

$$S_w = 0.623 \text{ m}^2$$

$$Cn_{\beta f} = -1.3 \cdot \frac{\text{volume}}{S_w \cdot b} \cdot \frac{D_f}{W_f}$$

$$Cn_{\beta f} = -0.014$$

Vertical Tail Terms:

$$CL_{\alpha} = 5$$

$$CF_{\beta v} = CL_{\alpha}$$

$$S_v = .068 \text{ m}^2$$

$$Z_{wf} = .065 \text{ m} \quad (\text{ver. heigth of the wing above the fuselage centerline})$$

$$X_{acv} = 1.11 \text{ m}$$

$$k = 0.724 \cdot \frac{3.06 \cdot \frac{S_v}{S_w}}{1 - \cos(\Lambda)} - 0.4 \cdot \frac{Z_{wf}}{D_f} - 0.009 A \quad (k = (\delta\beta/\delta\beta)^* \eta_v)$$

$$k = 0.781$$

Table 5.1 Weight Estimates

Payload weight	2 kg
Empty weight	5 kg
Electrical components weight	3 kg
Takeoff weight	10 kg
Payload fraction	0.3

Table 5.2 Takeoff Performance Data

Density at takeoff altitude	1.134 kg/m ³
Takeoff ground roll	17.6 m
Takeoff rolling friction coefficient	0.04
Velocity at liftoff	16.23 m/s
Drag at liftoff	9.07 N
Thrust at liftoff	85.83 N
Takeoff lift coefficient	1.1
Takeoff drag coefficient	0.2

Table 5.3 Climb Performance Data

Climb angle	12°
Climb rate	3.5 m/s
Total distance traveled to clear 10m obstacle	60m
Climb lift coefficient	1.1
Climb drag coefficient	0.2

Table 5.4 Turning Performance Data

Load factor	1.5
Turn speed	26.4 m/s
Turn radius	63.61 m
Time to turn 360°	15.14 s
Turn lift coefficient	0.6
Turn drag coefficient	0.1

Table 5.5 Cruise Performance data

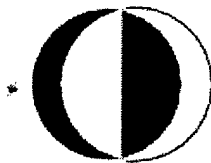
Cruise speed	21.55 m/s
Stall speed	14.11 m/s
Maximum speed	30.27 m/s
Range	304.8 m
Endurance	14.2 sec
Cruise lift coefficient	0.6
Cruise drag coefficient	0.1
Charge used	20.3 mAh



**AIAA/CESSNA/ONR
STUDENT DESIGN/BUILD/FLY
COMPETITION**

PROPOSAL REPORT

DESIGN OF A UAV CLASS AIRCRAFT



METU

TEAM ANATOLIAN-CRAFT AND HAZERFEN

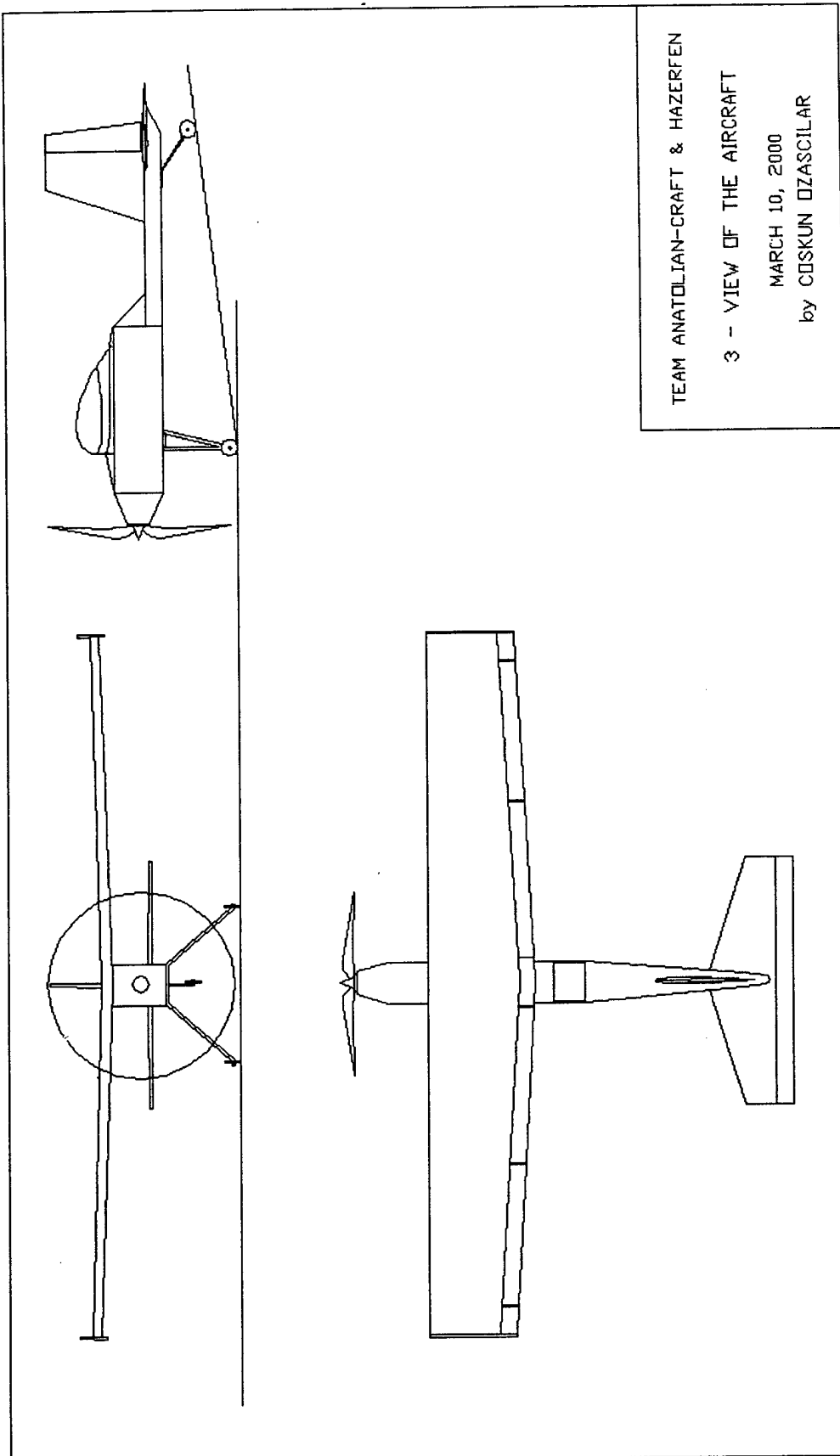
DRAWING PACKAGE

ACKNOWLEDGEMENT

Conceptual and preliminary design of this project was performed as a study in AE 451 'Aerounautical Engineering Design' course offered by Aerounatical Engineering Department of Middle East Technical University. This course was given at the fall semester of 1999-2000 academic year by Dr. Mehmet Şerif Kavsaoğlu and the course assistant was Ms. Özlem Armutçuoğlu.

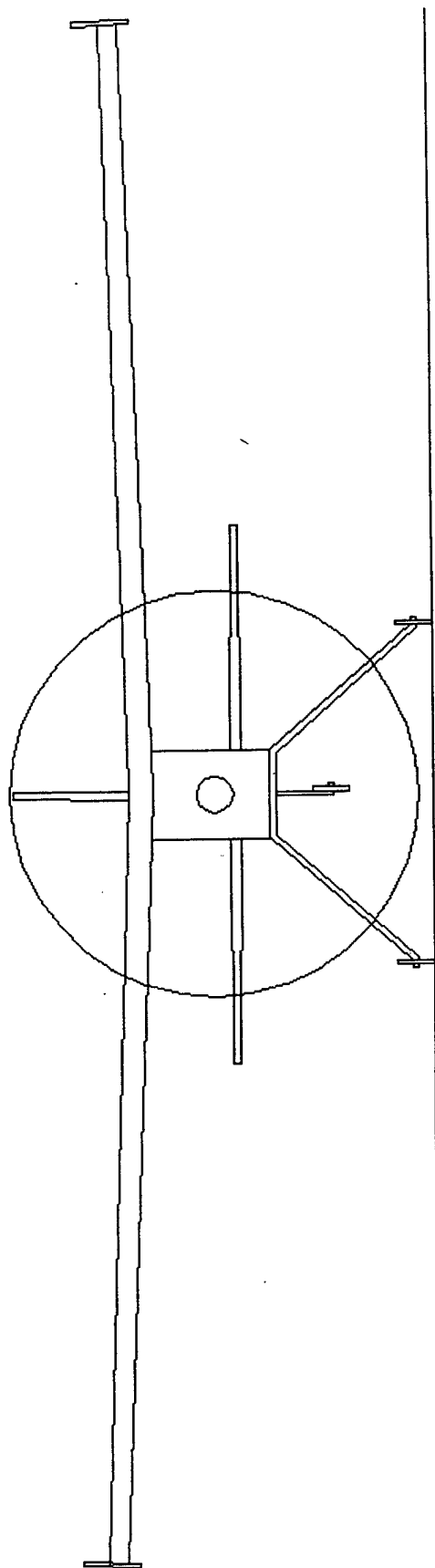
Detail design of the project and manufacturing of the aircraft was performed as a study of a course AE 452 'Aerounatical Engineering Design 2 ' offered by Aerounatical Engineering Deparyment of Middle East Technical University. This course was given at the spring semester of 1999-2000 academic year by Prof. Dr. Nafiz ALEMDAROĞLU and Dr. Mehmet Şerif KAVSAOĞLU.

This project was supported financially by, METU, TUBITAK TIDEB, ASELSAN, TUBITAK BILTEN and TAI.



Drawing 1, 3 views of the aircraft

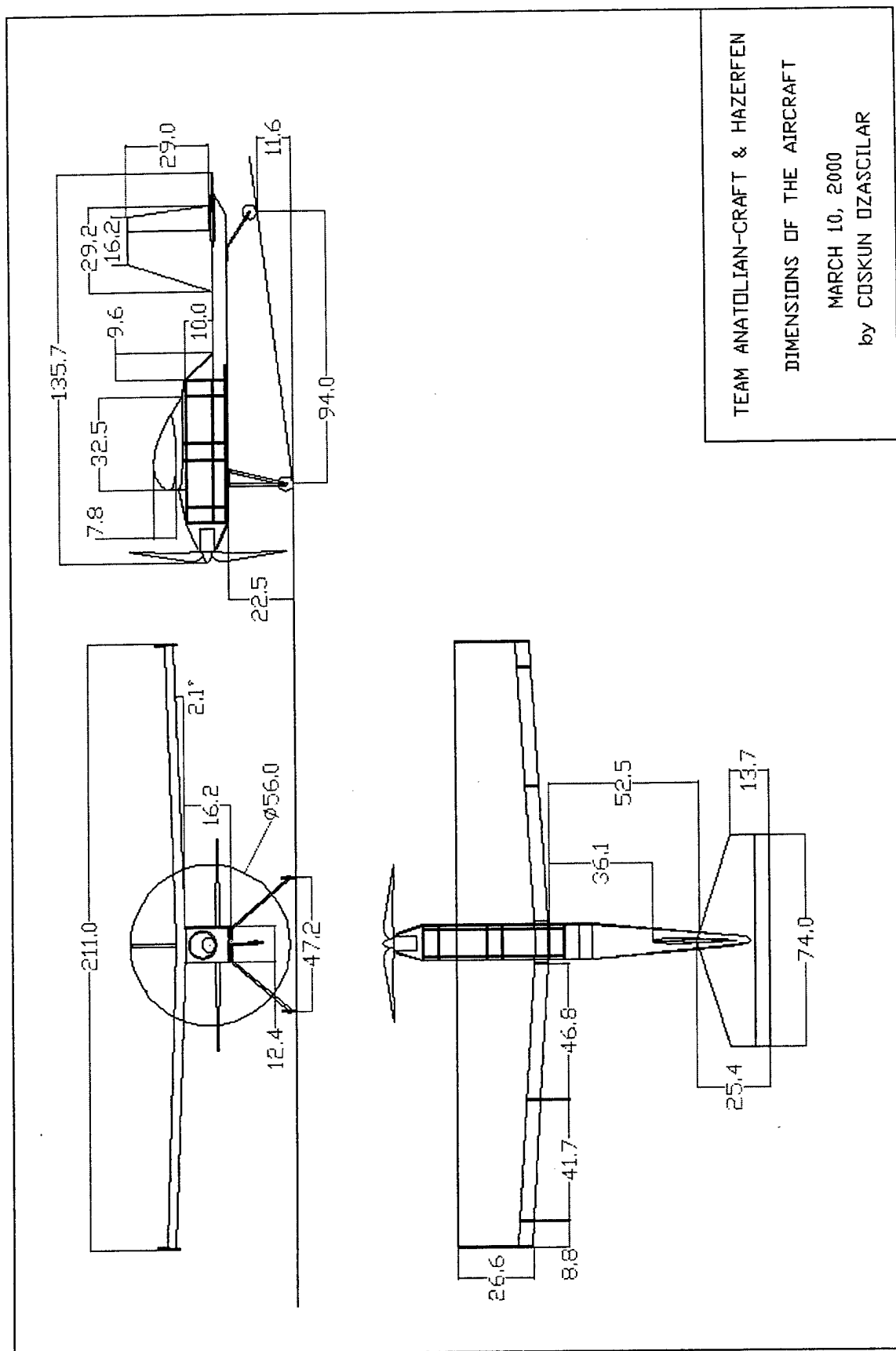
4.5.2 Tail Shape and Sizing	20
4.5.3 Motor Selection and Location	21
4.6 CONCLUSION	21
Table 4.1 Control Surfaces	22
Figure 4.1 NACA0006	23
Figure 4.3 E222	24
 5 DETAIL DESIGN	 25
5.1 INTRODUCTION	25
5.2 PERFORMANCE ANALYSIS	25
5.3 STABILITY ANALYSIS	26
5.4 COMPONENT SELECTION AND SYSTEM ARCHITECTURE	27
5.4.1 Propulsion System	27
5.4.2 Control System	27
5.5 CONCLUSION	28
Table 5.1 Weight Estimates	29
Table 5.2 Take-off Performance Data	29
Table 5.3 Climb Performance Data	29
Table 5.4 Turning Performance Data	29
Table 5.5 Cruise Performance Data	29
Table 5.6 Landing Performance Data	30
DRAWING PACKAGE	
 6 MANUFACTURING PLAN	 31
6.1 INTRODUCTION	31
6.2 MANUFACTURING PROCESSES INVESTIGATED	31
6.3 FIGURES OF MERIT	32
6.4 FINAL SELECTION AND JUSTIFICATION OF MANUFACTURING PROCESSES	33
6.5 MANUFACTURING PROCESS	33
6.5.1 WING CONSTRUCTION	33
6.5.2 TAIL SURFACE CONSTRUCTION	34
6.5.3 FUSELAGE CONSTRUCTION	35
6.5.4 LANDING GEAR CONSTRUCTION	35
6.6 CONCLUSION	35
 REFERENCE	 36
 APPENDIX 1	 37
APPENDIX 2	48
APPENDIX 3	50
APPENDIX 4	52



Drawing 1-2, Front view of the aircraft

W_{uav}	Uninstalled avionics weight
Y	MAC location from the centerline

a	Acceleration
a.c	Aerodynamic center
c	Chord length
c.g	Center of gravity
c_{HT}	Horizontal tail volume coefficient
c_{VT}	Vertical tail volume coefficient
d	Diameter
e	Oswald efficiency
g	Gravitational acceleration
n	Load factor
t	Thickness or time
BFL	Balanced field length
$\Lambda_{c/4}$	Sweep angle at quarter chord
Λ_{LE}	Sweep angle at leading edge
Λ_{TE}	Sweep angle at trailing edge
α	Angle of attack
β	Sideslip angle
δ_f	Flap deflection
ϵ	Downwash angle
ϵ_u	Upwash angle
γ	Angle of climb
μ	Aircraft rolling resistance
σ	Density ratio
λ	Taper ratio
η_p	Propeller efficiency
ρ	Density of the air
ψ	Instantaneous turn
q	Dynamic pressure
t/c	thickness to chord ratio
C_l	Lift coefficient
C_d	Drag coefficient
C_{d0}	Zero lift drag coefficient
C_m	Pitching moment coefficient
$C_{l\alpha}$	Slope of the lift curve



arrangements were eliminated. In order to minimize the loading and unloading times, it was decided to carry the entire payload in one sortie while placing them horizontally in the central fuselage. It was thought that a canard configuration might be necessary but further analysis showed that it was closely placed towards the front part of the fuselage. Conventional tail arrangement was chosen since it provided the adequate stability and control for the aircraft at its minimum weights.

After an initial drawing of the configuration and performing comparisons with similar designs, a first estimate of sizing was made (wing area, TOGW...). Landing gear locations, engine position were the other important design parameters which were considered for the overall shaping of the aircraft. A configuration layout was then drawn after all these steps that would best meet the required design profiles. Then initial analysis of performances, aerodynamics, weights, propulsion system were performed.

1.3 DESIGN TOOLS

Various design tools were used during each phase of our design process. Our basic reference tool used was *Aircraft Design: A Conceptual Approach*² by Daniel P RAYMER which was also the main book of our Aircraft Design course. However, for the build-up phase of the project, other references (such as *Airplane Design*³ by J. ROSKAM) were also investigated.

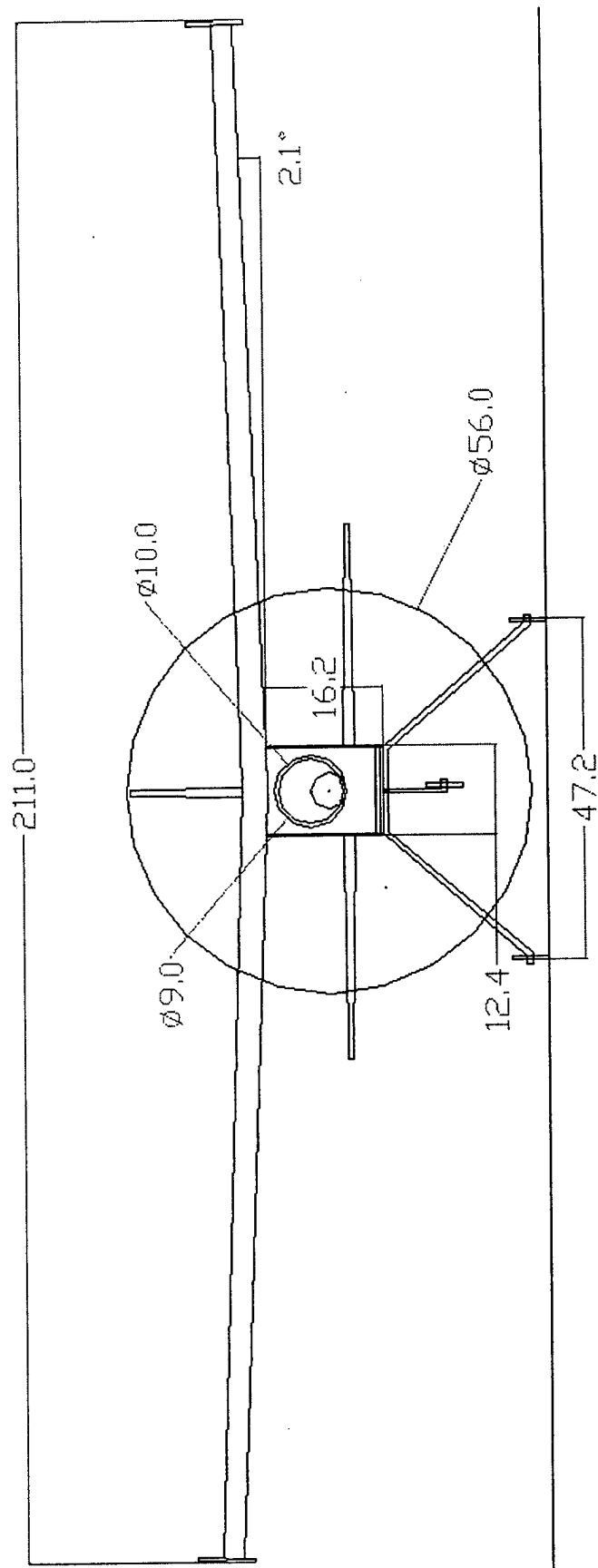
Various software were also used during the conceptual, preliminary and detailed design phases. These were:

- Math-CAD⁴
- AutoCAD R14⁵
- 3D Studio⁶
- Aveox's Virtual Motor Test Stand⁷
- Advanced Aircraft Analysis (AAA)⁸
- Microsoft Excel⁹
- Microsoft Power Point¹⁰

Math-CAD⁴ was used for the longitudinal and directional-lateral stability analysis of the aircraft. Since many different configurations were examined, the package program was very suitable for the stability analysis. Furthermore, Advanced Aircraft Analysis (AAA)⁸ programming of Roskam was used to check the outputs of stability and performance analysis.

Fortran 90 programming language "Spot.f"¹ was used to apply a panel method to calculate the aerodynamic coefficients of the airfoil profiles used in AC-H.

All the configuration layouts and 2D, 3D drawings were done using the AutoCAD R14⁵. AutoCAD can share data with the 3D Studio⁶ software, given some differences between



Drawing 2-1, Dimensions of the aircraft (front view)

CHAPTER 2

MANAGEMENT SUMMARY

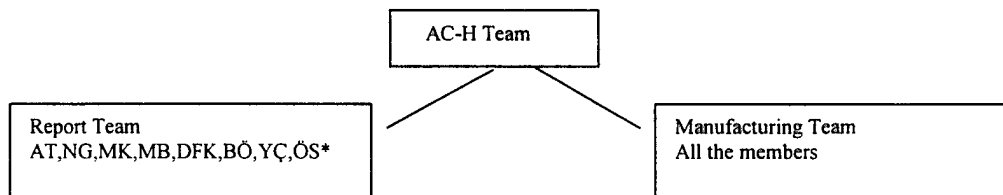
2.1 INTRODUCTION

The design team resulted from the merger of the two design teams; the Anatolian-Craft team and the Hazerfen team. This chapter on "Management Summary" presents the information about the managerial structuring of the design team and the scheduling of the whole design and manufacturing procedure of AC-H.

2.2 DESIGN PERSONNEL AND ASSIGNMENT AREAS

All the team members listed below are METU Aeronautical Engineering Department Students. The complete list of team members is presented in Table 2.1.

2.3 MANAGEMENT STRUCTURE

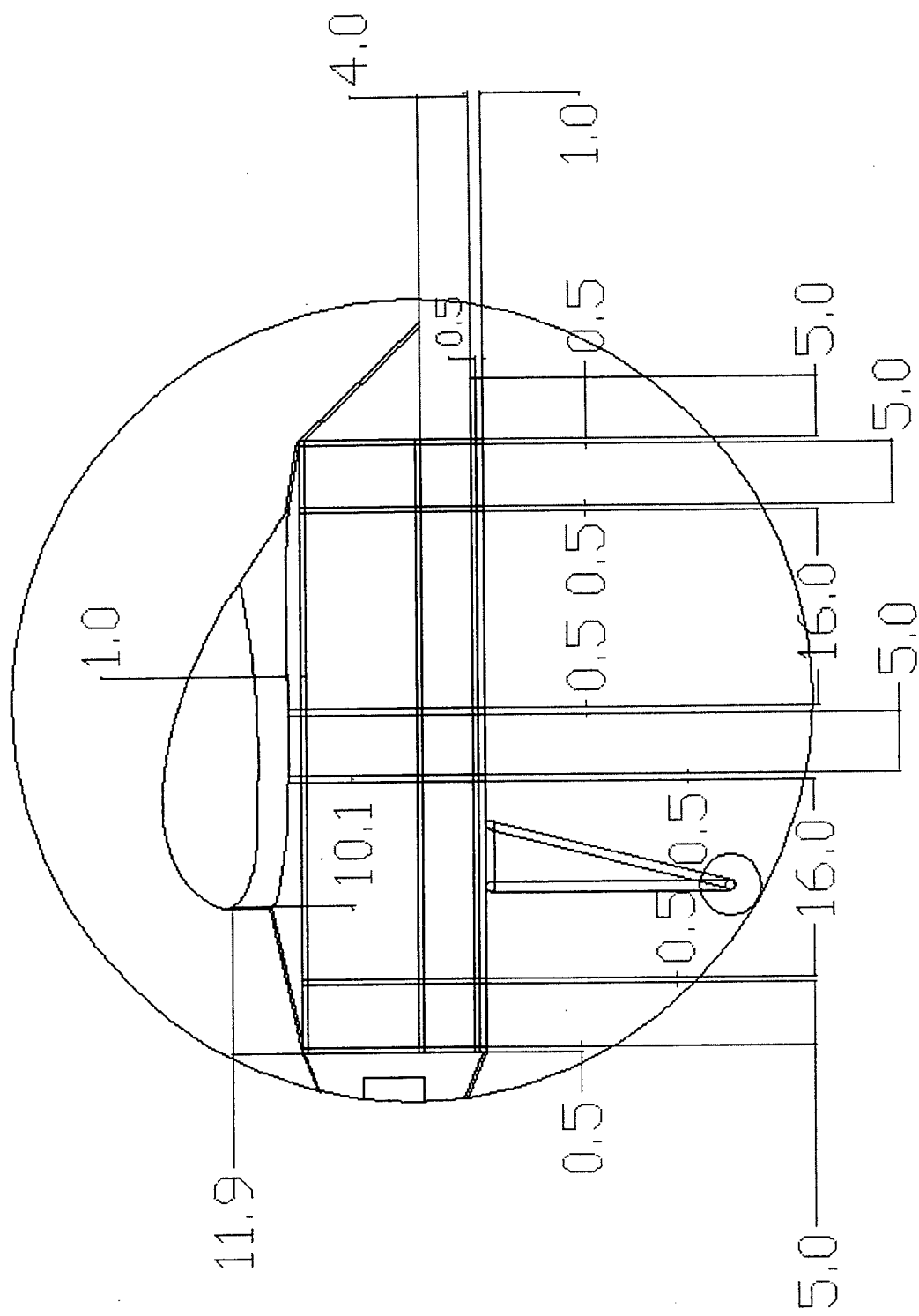


*: indicates the first letters of the team members' names

As an organization the AC-H team was divided into 2 sub-groups; one group responsible from the total report for sharing the responsibility from organizational point of view, whereas the other responsible from a/c manufacturing. Such an organization was thought to be necessary since the time frame to prepare both the report and the a/c was very limited. The list of team members and generalization of them are given in Table 2.1 and in Table 2.2 respectively.

2.4 SCHEDULE

The schedule for the development of the project is represented in Table 2.3 and in Fig. 2.1. This figure compares the actual and planned timing of the design process.



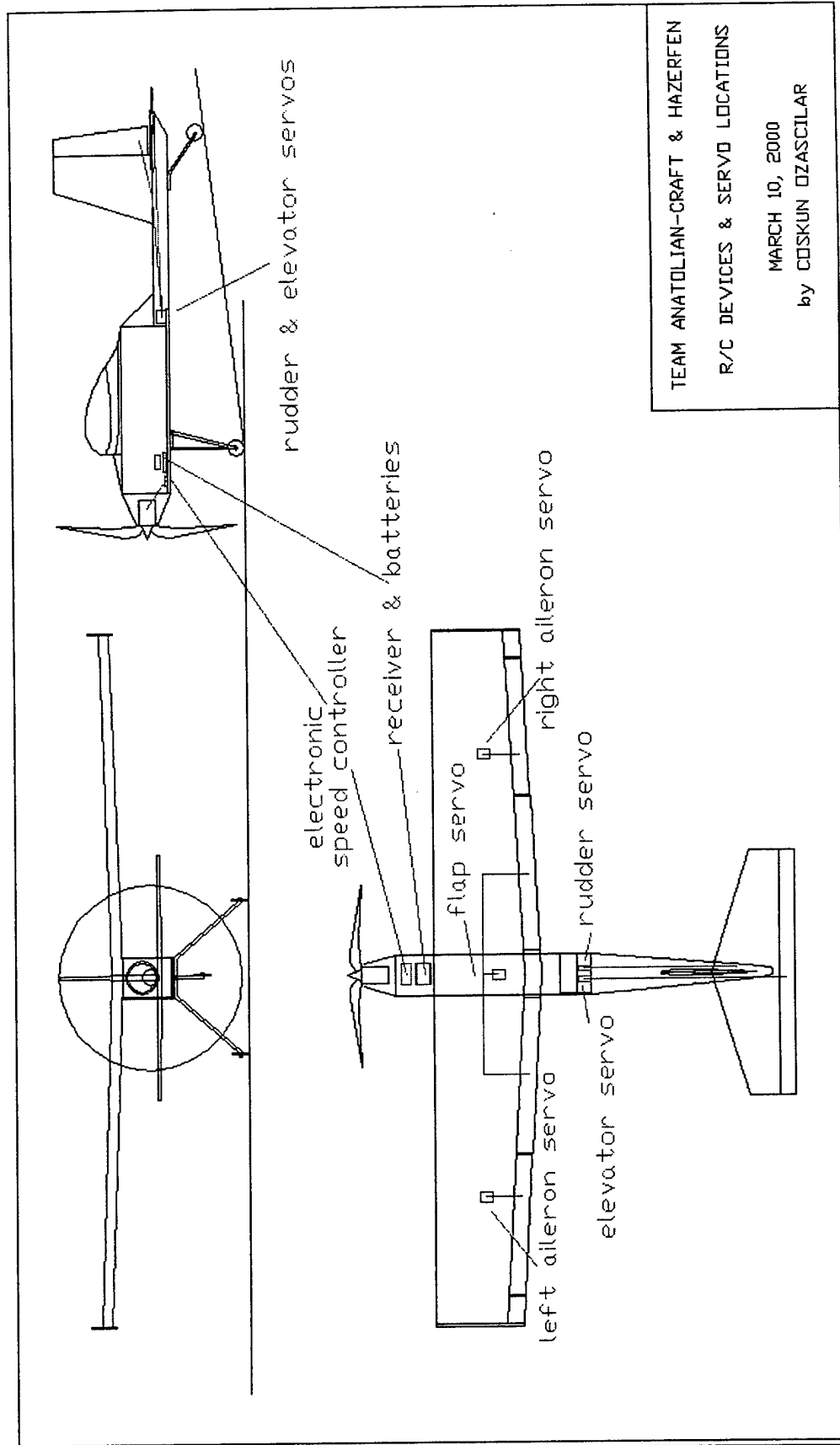
Ms. B.Azra TİMUR	Senior Student. She organized the team meetings and the final report. She participated in conceptual design, manufacturing plan and material selection.
Mr. Gökhan TURSUN	Sophomore Student. He participated in propulsion system integration.
Ms. Ayça YETERE	Junior Student. She participated in propulsion system integration and sponsorship studies.

Table 2.2 Generalization of team members

Students	Boys	Girls
Seniors	7	5
Juniors	6	1
Sophomores	1	0
Freshmen	2	0
Total	16	6

Table 2.3 Schedule

No	Stages	Planned Schedule (last day) (Day/Month/Year)	Actual Schedule (last day) (Day/Month/Year)
1	Conceptual Design Process	10.10.1999	12.10.1999
2	Application to Competition	31.10.2000	31.10.2000
3	Preliminary Design Process	01.11.1999	10.11.1999
4	Detailed Design Process	01.12.1999	15.12.1999
5	Material List Selection	01.12.1999	01.12.1999
6	Finding Sponsorships	01.12.1999	01.02.2000
7	Order of Materials	15.01.2000	19.01.2000
8	Teams' Union	Not planned	21.02.2000
9	Final Drawings(3D)	15.02.2000	29.02.2000
10	Start construction of AC-H	15.02.2000	01.03.2000
11	First flight of model	01.03.2000	
12	Proposal Phase of design report	01.03.2000	10.03.2000
13	Proposal Phase of design report given to advisors	09.03.2000	11.03.2000



Drawing 3, Remote control devices and servo locations on the aircraft

CHAPTER 3

CONCEPTUAL DESIGN

3.1 INTRODUCTION

Aircraft design is a separate discipline of aeronautical engineering, different from the analytical disciplines such as aerodynamics, structures, controls, and propulsion, where most of the analytical knowledge acquired in these courses are brought together to make up a synthesis of ideas which will yield to a new product that will serve the purpose and will meet the requirements that are set. Aircraft design is based on requirements which include parameters such as the range the a/c will fly, the payload the a/c will carry, take-off and landing distances that are necessary, the maneuverability of a/c, the speed of a/c, etc. The conceptual design for AC-H is started with analyzing the design requirements including parameters such as the aircraft payload, takeoff and landing distances, and its maneuverability.

3.2 ALTERNATIVE CONCEPTS

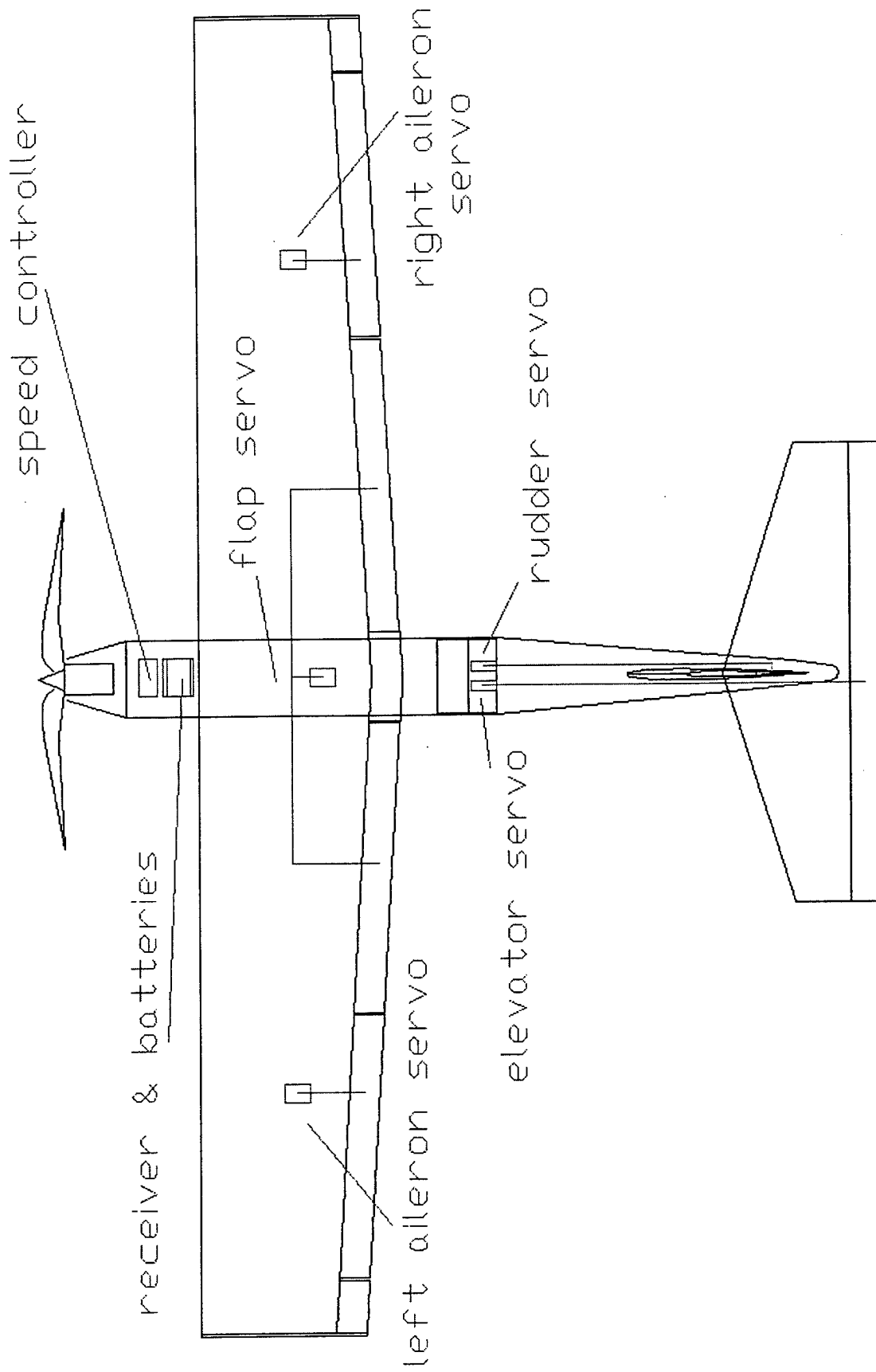
According to the given requirements, in order to achieve the best design performance, following alternative concepts were investigated during the conceptual design phase:

- Delta-wing configuration
- Double-boom configuration
- Single-boom configuration
- Conventional configuration
- Canard configuration

First, delta-wing configuration was investigated because of the stall characteristics of this type. Due to the reduced effective angle of attack at the tips, a lower-aspect-ratio wing would stall at a higher angle of attack than a higher-aspect-ratio wing. As it is known that delta wings have low aspect-ratio thus has an ability to stall at higher angles of attack which was an advantage for the small UAV design.

Secondly, double boom configuration was taken into account. For the pusher type engine, double boom had an advantage for placing the propulsion system and had the best configuration for reducing the propeller's wake on wing. Also, reduction of the total weight would be possible.

Then, single boom configuration was taken into consideration because of its easier stability analysis with respect to double boom type. With this configuration, it will be



Drawing 3-2, Remote control devices and servo locations on the aircraft (side view)

3.4 FIGURES OF MERIT

In the conceptual design phase, the following figures of merit are taken into consideration:

- ➔ Safety
- ➔ Stability
- ➔ Battery Weight
- ➔ Lifting Efficiency
- ➔ Pilot Control
- ➔ Cost of Manufacturing

Safety: From engineering point of view, safety is our primary concern. Therefore in our design project, safety is given the highest priority. Although safety is to be considered during all phases of the mission profile, particular importance must be given to loading and unloading phases of the mission during which human intervention to the a/c will be made. Maximum security and ease of access for loading/unloading must be realized when human intervention is involved to the a/c while its propeller rotating at a very high speed.

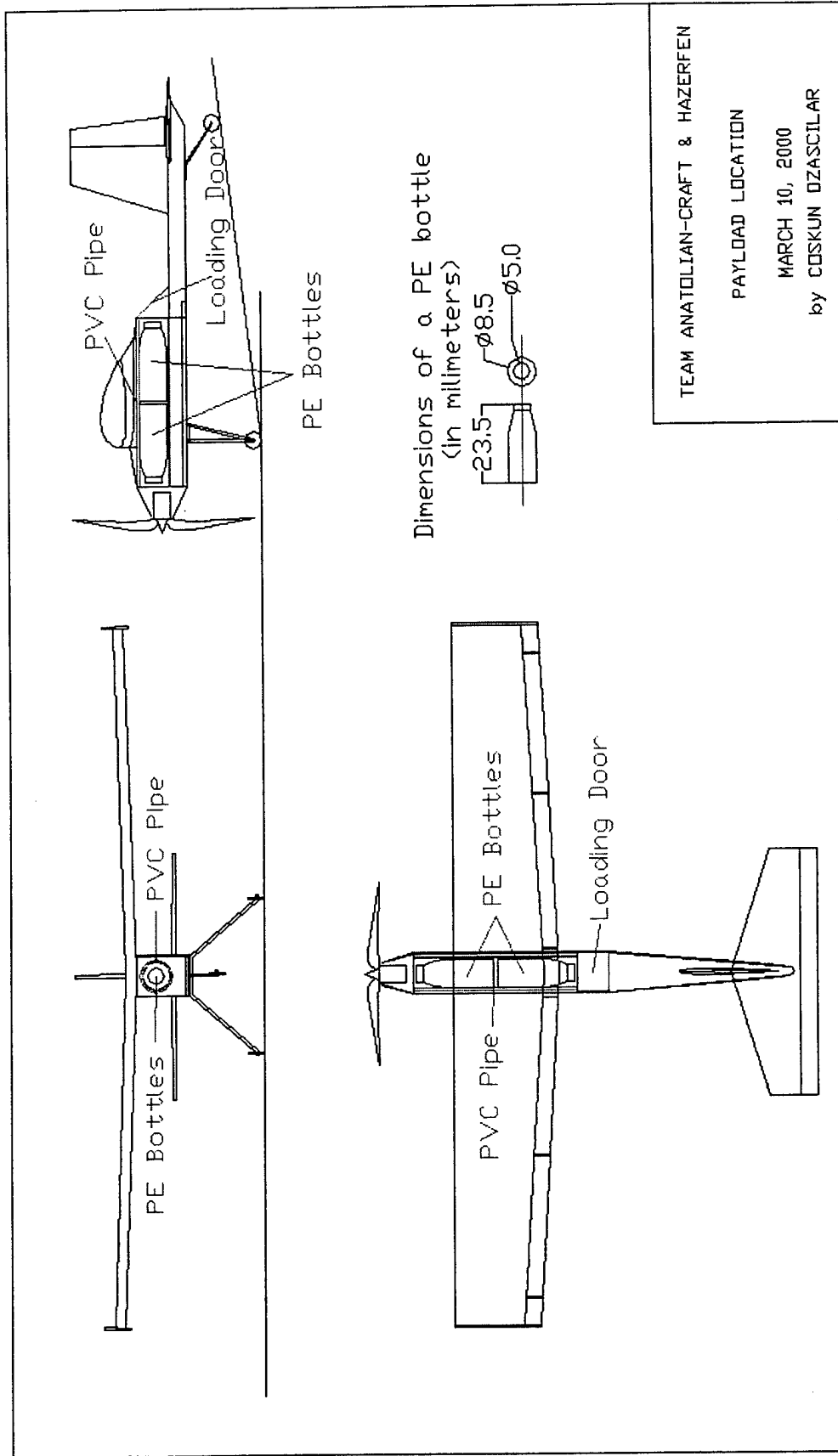
Stability: Stability is of major concern since it is much easier to fly and control a stable a/c than an unstable a/c. An a/c is stable if it returns to its original state followed by a disturbance (pitch, roll, yaw, etc.). Therefore, stability is considered to be a vital property for the a/c to be designed and is therefore assigned a high FOM score evaluation.

Lifting Efficiency: Lifting efficiency is an important feature of the design according to the competition requirements, which brings limitations on take-off distance and battery weight. The take-off distance was limited to 100 ft, which imposes a high lifting efficiency for the design. The battery weight is limited to a maximum of 5 lb, which in turn restricts the velocity. To overcome this, high lifting efficiency is needed.

Battery Weight: The estimation of the weight of a conceptual aircraft is a critical part of its design process. The restriction imposed on the battery weight puts limitations on the motor selection. As a result, the desired power can not be achieved which in turn limits the payload and the configuration selection.

Pilot Control: Pilot control is a very important factor for this competition since; many sorties are to be realized hence the safety of the audience and the a/c must be secured by a very eligible pilot, and time is an important factor, hence the pilot must be very well trained not to loose extra time during take-off and landing phases.

Cost of Manufacturing: Cost of manufacturing is another important factor that must be considered since it is directly proportional with the complexity of the design. According to the rated aircraft cost model, which is one of the parameters for judging the design, the cost of manufacturing must be taken into consideration as a figure of merit.



Drawing 4, Payload location

From the design methodology point of view, it can be concluded that the weight estimation of the aircraft is a critical part of the conceptual design process. Thus battery weight is put on the second place; since, during the design period it really brought limitations on the studies. It is known that there is a limitation on the battery weight to be used. This, in turn brought limitations on motor selection. All the calculations of the power system are done according to this requirement. After the power system is selected, the payload weight is determined according to the performance of the power system selected. Furthermore; the final configuration, especially the wing plan-form area and the fuselage shape, is re-determined while taking into account the power system selected.

In the third place, the lifting efficiency is considered. Since the design is for an electrical power system, there is a problem on the take-off period with payload. According to the analytic methods used, the necessity for high lift capability arose. To achieve a high lift efficiency, different airfoils are investigated and their generated lifts are compared. And as a result, the most suitable airfoils are chosen.

The stability came in the fourth place since it is directly related to the control and maneuver capabilities of the aircraft. It is stated that the competitor aircraft must complete a 360-degree turn in the direction opposite of the base and final turns on each downwind leg. To achieve this turn successfully, the stability becomes the first priority. Also, from the pilot's point of view, in order to achieve the required maneuvering capability for the aircraft, stability of the aircraft must be considered as one of the most important parameters.

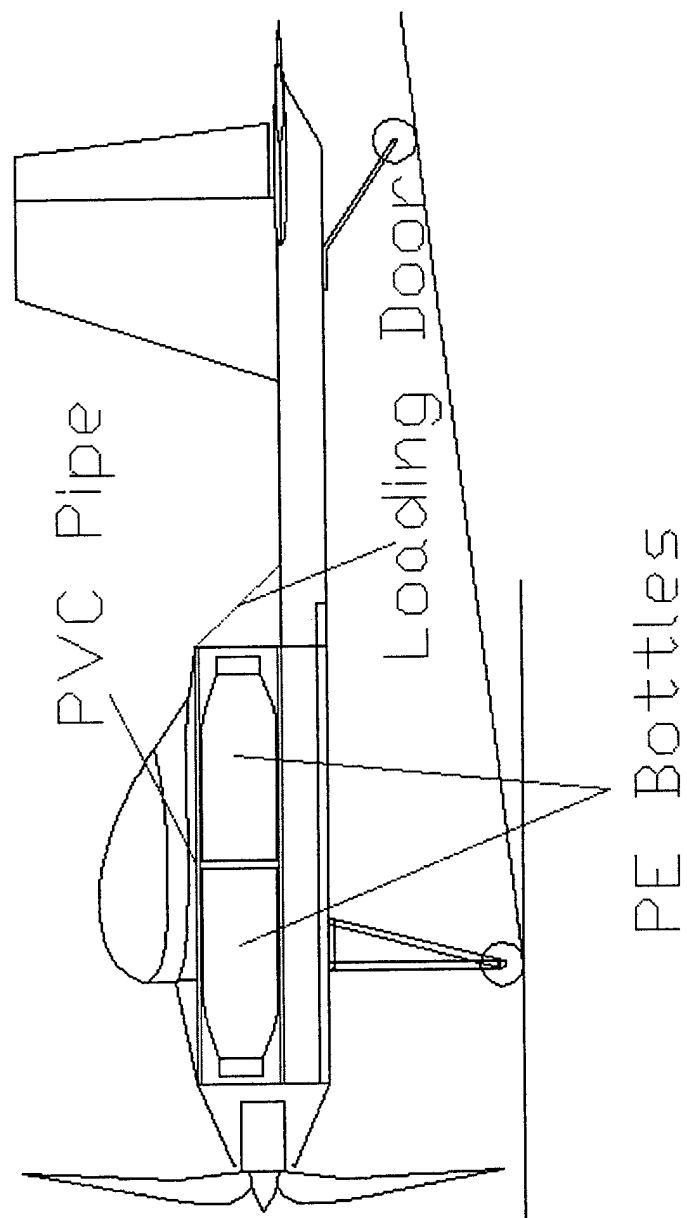
Pilot control is considered as the fifth figure of merit. During the competition, many sorties are to be performed. So the pilot control becomes an important factor that effects the safety of the audience and the aircraft. Furthermore; time, being another constraint for this competition, pilot control, especially during the take-off and landing periods is an important figure of merit.

Another figure of merit is the cost of manufacturing for the a/c. According to the rated aircraft cost model, which is a parameter for judging the cost of manufacturing must be taken into consideration as another important figure of merit for the design.

In addition to the above figures of merit, the pilot control must also be taken into consideration. In reality, if designing and manufacturing of the aircraft is half of the job, preparing and flying it is the other rest. Since during the competition, many sorties are to be performed, pilot control becomes an important factor which effects the safety of the audience and the aircraft itself. Furthermore, time being another constraint for this competition, gives an important role to the pilot control, especially during the take-off and landing phases.

Hence, according to the previous discussion the relative importance of the factors to be considered during the design are listed as follows;

➔ Safety



Drawing 4-2, Payload location (side view)

Table 3.1 Rated Aircraft Cost model for alternative concepts investigated

	Conventional	Delta Wing	Single Boom	Twin Boom	Canard
Weight (lb)	22	26	18	24	25
Engine Power (watt)	1300	1350	1250	1350	1350
Manuf. Time (hour)	50	75	50	70	80
Cell Number	62	65	60	65	65
Area of the Wing (ft²)	6.706	7.5	6	7	7
Length of the Fus. (ft)	4.429	4	4.5	4.5	5
Empty Weight (lb)	12	16	8	14	15
RAC (*10³)* (\$)	4.966	5.463	4.615	5.445	5.473

* Rated Aircraft Cost Model (described in RFP of the competition) can be seen in APPENDIX 2.

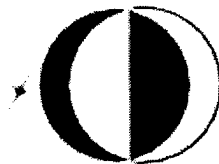
Table 3.2 Ranking Chart for Alternative Concepts Investigated

	%	Twin Boom	Single Boom	Conventional	Delta Wing	Canard
Overall	100	5	5	5	5	5
Safety	30	4	4.5	4.5	2	3
Stability	25	2	3	4	4.5	2
Lifting Eff.	15	3.5	4.5	4	3	2
Weight	15	3	5	4.5	2	2.5
Pilot Control	10	4	3	4.5	2	2.5
Finance	5	3.5	4	4.5	2	3
Total		3.25	4.025	4.3	2.775	2.475



**AIAA/CESSNA/ONR
STUDENT DESIGN/BUILD/FLY
COMPETITION**

DESIGN OF A UAV CLASS AIRCRAFT



ADDENDUM PHASE

this point of the design it is not easy to choose the best tail arrangement which will satisfy the requirements. What is done during preliminary design, was just to compare the possible configurations which are currently used by the available.

Another design parameter was the thrust-to-weight ratio which is directly related to the engine performance. Thrust-to-weight ratio is one of the most important parameters which affects the takeoff distance. Since the takeoff distance must be less than 100 ft. (requiring a high thrust), a careful study was made for the most optimum value of the thrust-to-weight ratio.

The payload to be carried and the fuselage shape are two closely related design parameters. The desired payload depends almost on the wing loading investigated. As for the fuselage shape, it influences the size of the payload, that is, the stacking of the water bottles which will be used as payload for this particular design.

Landing gear is another design parameter which is studied during the preliminary design phase. It must be chosen to have the least possible minimum drag while satisfying all the needs on the ground.

4.3 FIGURES OF MERIT

The figures of merit considered during the preliminary design are listed as follows:

- Ease of construction
- Structural integrity
- Payload access

Ease of construction is the major consideration for the team. Manufacturing an extremely complicated design can easily exceed the capability of the team. This design should not require excessive time for manufacturing. Large delays in manufacturing must be avoided as much as possible in order to have a flying a/c by the date of competition. Therefore, the configuration must be as simple as possible for manufacturing purposes while fulfilling all the design requirements and no risks must be undertaken by involving the team in complicated design concepts.

A spar test is to be conducted on each air-plane at the competition. The air-plane has to support its own weight when lifted by the wingtips. Therefore, structural integrity is a significant figure of merit during the preliminary design phase. In addition, the competition requires repetitive take-offs and landings. Structural integrity must be ensured such that the aircraft will withstand all the loads it will experience during its designated flight profile.

Payload access is also considered because of the time constraint for loading and unloading. Team members must be able to access the payload quickly and safely. A conveniently placed payload will significantly reduce the ground time of the a/c.

This project was supported financially by METU, METU-EBI, METU M. PARLAR Foundation, TUBITAK-TIDEB, ASELSAN, TUBITAK-BILTEN and M-Air. Without their support the airplanes could never be finished.

guide on our way to the last design. Preliminary sizing includes various parameters which should be considered separately. They will be given in more detail in the coming sections.

4.5.1 Wing Shape and Sizing

Main parameters forming the wing are its span, aspect ratio, taper ratio and the wing sweep. Wing span is limited to 7 feet by the requirements of the contest so it wasn't possible to use a longer span wing. 6.89 ft is chosen (210 cm) as the span. Taper ratio is chosen as 0.8 in order to obtain an elliptical lift distribution. Choosing the aspect ratio (AR) is not as easy as the other parameters. We know that it is of primary concern since it has an important effect on most of the performance calculations. Smaller the AR, smaller the lift curve slope($C_{L\alpha}$) which we do not want since high lift is needed at small angle of attacks. So we decided to keep AR at least 6. Later, our calculations which are done simply at that moment showed that in order to have a sufficient wing area and AR, an AR of 7 was needed. Wing sweep was nearly zero degrees at 25%-chord. This value is chosen in order to have a better performance. For subsonic aircraft like ours, smaller this angle, better the performance of the wing. The final estimation of the control surfaces are stated in Table 4.1.

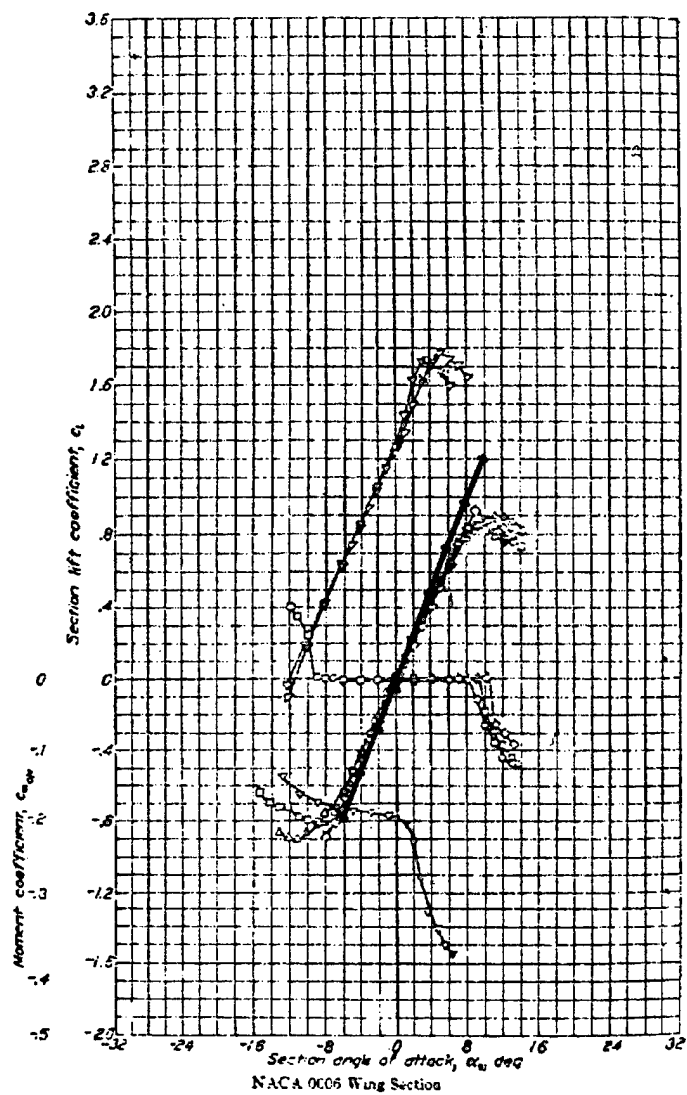
4.5.2. Tail Shape and Sizing

Horizontal tail and vertical tail area and size are initially estimated using simple formulas obtained from historical trends. Mainly moment arm method is used. The aerodynamic center of the a/c is estimated to be at 25% location of the MAC (mean aerodynamic chord) and the moment arm is estimated to be 60% percent of the total length of the a/c. Since a length estimation is done before, areas are calculated accordingly. Taper ratios and AR (aspect ratio) are chosen again considering the competitors. For both 0.55 is chosen as the taper ratio. Aspect ratio for horizontal tail is 3.79 and 1.27 for vertical tail. We examined the historical tail arrangements (i.e. conventional, T-tail, cruciform, H-tail etc.) the most suitable one to begin with was the conventional tail. For most aircraft designs, the conventional tail provides adequate stability and control at the lightest weight. The thickness of the horizontal and vertical stabilizers are determined by again considering historical trends. It is obvious to use a symmetrical section but the thickness of it is not known exactly. 10% NACA 4 digit airfoil is chosen at the first step but then it is realized that it would be thicker than needed especially at the roots. Then after analyzing the size of the servos, it is decided to use a 6% thickness throughout the vertical and the horizontal tails.

4.5.3 Motor Size and Location

The horsepower to weight ratio (hp/W) and the wing loading (W/S) are the two most important parameters affecting the aircraft performance. Wing loading and horsepower to weight ratio are interconnected for a number of performance calculations, such as takeoff distance, which is frequently a critical design factor. Because of this relation between (hp/W) and (W/S), it is difficult to use historical data for independently choosing initial

Drawing 1: The 3-view of the aircraft	70
Drawing 2: The front view of the aircraft	71
Drawing 3: The side view of the aircraft	72
Drawing 4: The top view of the aircraft.....	74

Figure 4.1 NACA0006¹²

———— Calculated by Spot

◆◆◆◆◆◆◆◆ Published Data

- The aft fuselage which was originally designed to be made of high density foam is replaced by two composite hollow booms.
- The tail surfaces are placed to a higher position.
- The flaps and ailerons are replaced by a pair of flaperons.
- The battery location is enlarged.
- the locations for the servo control units on the tail and the electronic speed controller are re-arranged to provide more space for the batteries.
- The attachment regions for the wing attachment and the landing gear are reenforced and improved.

The reason why the material used in the main landing gear was changed was simply due to weight considerations. The weight of aluminum (Aluminum 2025) was much less than that of the steel. The same reason was also valid for the aft fuselage booms. In both cases, the new structures were strong enough to carry the loads. Moreover, the manufacturing of the aft fuselage part made of high density foam would be very difficult, and the fuselage would require structural improvements in this area. Therefore, this complex structure was replaced by a pair of simple, pre-manufactured composite booms used in fishing rods. However, this replacement required that the tail surfaces would be placed in a higher position. We have chosen manufacturing methods as simple as possible, materials as light as possible but as strong as required.

The original design had flaps which would be used only during the take-off to increase the lift and ailerons for aircraft control. It was thought the ailerons may not be powerful enough to roll the aircraft. Therefore, the flaps and the ailerons are combined into one control surface, "flaperons", which will provide the necessary lift increase during the

CHAPTER 5

DETAIL DESIGN

5.1 INTRODUCTION

Detail design starts with analyzing the final performance data, including the take-off and landing performances, handling qualities and g load capability, range and endurance, and payload fraction, including the component selection and systems architecture.

5.2 PERFORMANCE ANALYSIS

A table consisting of weight estimates and takeoff, climb, cruise, turning and landing performance data of the AC-H was prepared for visual presentation. All of the calculations were performed following the procedures suggested by the books; *Aircraft Design, A Conceptual Approach*, by Daniel P. Raymer and *Airplane Aerodynamics and Performance*¹⁴, by Chuan-Tau Edward Lan, Jan Roskam.

Considering the available power from the motor, and deciding that the a/c will carry two bottles of water at one time, with this configuration the empty weight was estimated to be 5 kg and the payload fraction was 0.3.

The first part of the mission is the takeoff. At take-off, the flaps and ailerons are positioned fully down in order to have enough lift. It is calculated that the aircraft take off after 17.6 m from initial point, with a speed of 16.23 m/s.

After takeoff, AC-H starts to climb with a rate of 3.5 m/s and an angle of 12°. During climbing, the same flap and aileron configuration as in take off phase is used. Therefore its lift and drag coefficients are the same with those experienced as during the take-off phase, 1.1 and 0.2 respectively.

The next part is the turning part. AC-H experiences a 180° turn with a speed of 26.4 m/s and a radius of 63.61 m.

Between the 180° and 360° turns, there will be a cruise phase. For this phase, cruise, stall and maximum speeds are calculated as 21.55 m/s, 14.11 m/s, and 30.27 m/s respectively. Also, for a range of 304.8 m (1000 ft), 20.3 mAh charge will be used for a total period of 14.2 sec.

After the 360° and 180° turn, AC-H will start landing. When it touches down, it will have a speed of 18.34 m/s and the landing ground roll will be 31.22 m, assuming a friction

Another suggestion may be related to the selection of materials and components for the aircraft. The availability of materials and components for building a model is a major issue. These materials should be determined right from the start, during the conceptual and preliminary design phases, and these selected materials and components need to be ordered and obtained as soon as possible.

5.4 COMPONENT SELECTION AND SYSTEMS ARCHITECTURE

5.4.1 Propulsion system

Astro Flight Cobalt 60 Electric Motor with Model 714 Super Box 3:1 ratio is used for the propulsion system of our UAV. 62 Panasonic P-160AS A size (KR17/50) Type S batteries will be used to supply the necessary power to the motor. Our motor will turn a glass-filled/composite APC 22x14 2-blade replacement propeller. The motor and the propeller assembly will be placed in front of the fuselage and will therefore function as a tractor type (not a pusher) propeller. The propeller has thinner and less-noise profile with 11" radius (each half), reinforced by carbon fibers to maintain its true constant pitch at any rpm with high output and longer time. The motor gives 3000 static rpm, 26 Volts, 21 Amps, 550 Watts, 70 oz. thrust and 39 mph speed ideally with this propeller. This motor is one of the high output power motors available in the market which will function with the stated number of batteries (since battery weight is limited by the contest rules). Astro Flight 204D Speed Control ESC Airplane Futaba is used. The ESC must be a high quality device that our UAV will have a high temperature increase because of high power motor, so our ESC is heat-protected. But this high quality ESC unfortunately increases the cost. This ESC works in a range of 6-36 NiCad Cells, with max 50 Amps, 2800 switching rate, weighs 30 gram (54 gram with wires) and connectors supplied with zero loss. All of the components of the designed UAV are commercial of the shelf equipment and can easily be found from any hobby shops.

5.4.2 Control system

Our control system is a Futaba Digital proportional radio control unit, with nine-channel PCM 1024Z transmitters. It is a good choice with respect to the contest rules since it has the fail-safe feature for any fail condition. It also satisfies all of our needs in controlling our UAV. It has a dual mode gyro function, which allows to select two different settings within one flight condition. These capabilities will help us in landing and take-off because it increases the usage of ailerons and flaps. It has a frequency synthesizer that allows to fly on any unused channel where we must fly on an unused channel. This radio control is also programmable and has the ability of servo reversing. It has the capability to reverse the rotation of a servo with a flip of a switch. It is easy to use and has flexibility during installation.

We have used 2 Futaba S-3102 micro-servos, which are micro-sized, metal gear, and 5-pole motor, has 51.4 oz. of torque and 5 Futaba S-9202 servos, which are gold plated and deliver 69.5 oz. of torque. We have used two servos for ailerons, one for flaps, one to ESC, one for the rudder and one for the elevator. Micro-servos are used to control the ailerons only. They all have ball bearing supported output shafts. It is known (from our previous experiences) that these torque are large enough for driving the control surfaces.

already available in our department's stocks which decreased the manufacturing cost with respect to the actual case.

8.3

Table 5.1 Weight Estimates

Payload weight	2 kg
Empty weight	5 kg
Electrical components weight	3 kg
Takeoff weight	10 kg
Payload fraction	0.3

Table 5.2 Takeoff Performance Data

Density at takeoff altitude	1.134 kg/m ³
Takeoff ground roll	17.6 m
Takeoff rolling friction coefficient	0.04
Velocity at liftoff	16.23 m/s
Drag at liftoff	9.07 N
Thrust at liftoff	85.83 N
Takeoff lift coefficient	1.1
Takeoff drag coefficient	0.2

Table 5.3 Climb Performance Data

Climb angle	12°
Climb rate	3.5 m/s
Total distance traveled to clear 10m obstacle	60m
Climb lift coefficient	1.1
Climb drag coefficient	0.2

Table 5.4 Turning Performance Data

Load factor	1.5
Turn speed	26.4 m/s
Turn radius	63.61 m
Time to turn 360°	15.14 s
Turn lift coefficient	0.6
Turn drag coefficient	0.1

Table 5.5 Cruise Performance data

Cruise speed	21.55 m/s
Stall speed	14.11 m/s
Maximum speed	30.27 m/s
Range	304.8 m
Endurance	14.2 sec
Cruise lift coefficient	0.6
Cruise drag coefficient	0.1
Charge used	20.3 mAh

Table 8.1 Rated Aircraft Cost

$$\text{RAC \$ (Thousands)} = (A * \text{MEW} + B * \text{REP} + C * \text{MFHR}) / 1000$$

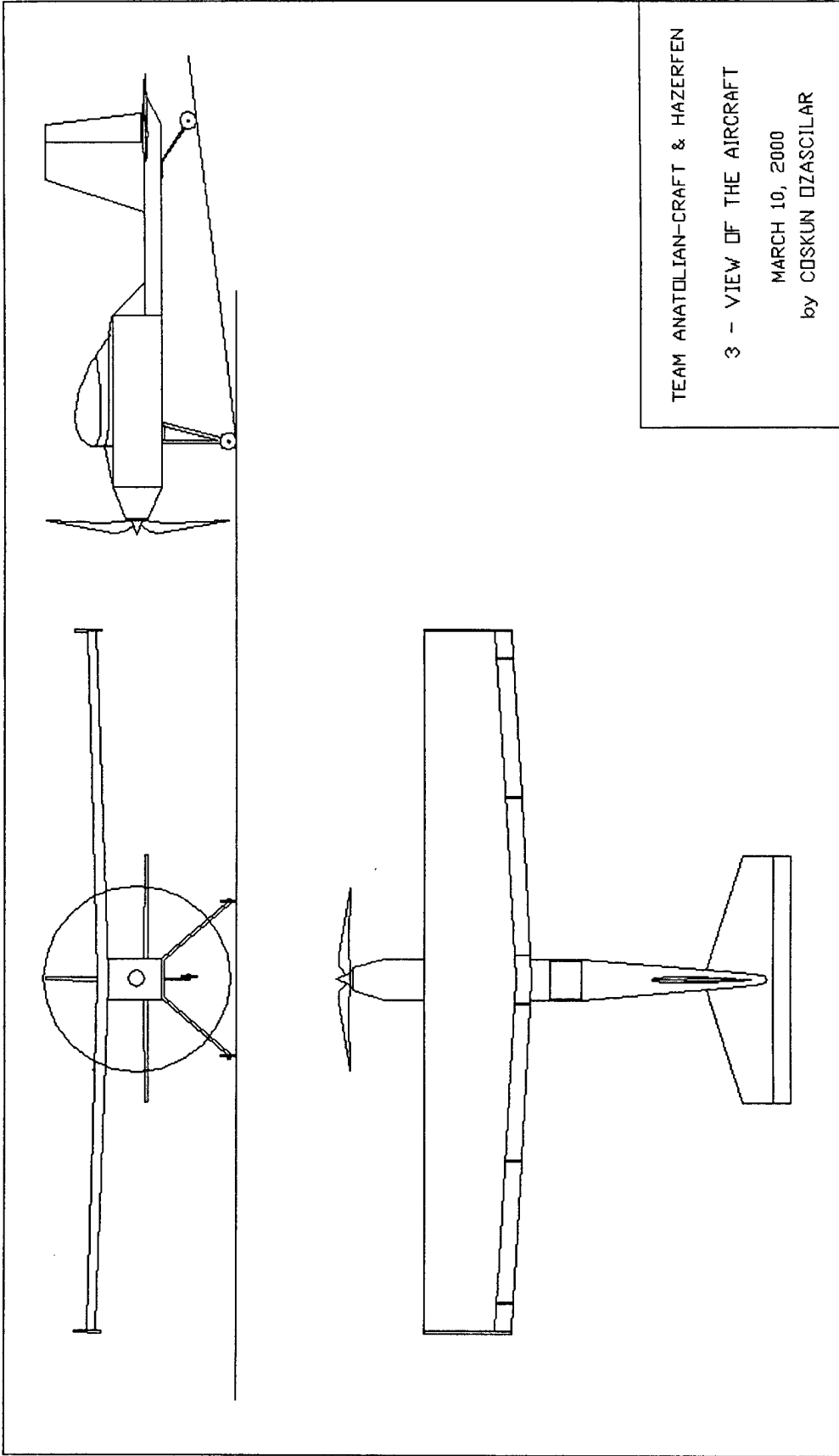
Coefficient	Description	Value
A	Manufacturers Empty Weight Multiplier	\$100 / lb.
B	Rated Engine Power Multiplier	\$1 / watt
C	Manufacturing Cost Multiplier	\$20 / hour
MEW	Manufacturers Empty Weight	Actual airframe weight, lb., without payload or batteries
REP	Rated Engine Power	# engines * 50A * 1.2 V/cell * # cells

DRAWING PACKAGE

Adhesives	\$ 70.00
(epoxy and aliphatic resin)	
Miscellaneous hardware	\$ 40.00
(hinges, control horns, clevises, screws, etc.)	
Subtotal	\$ 262.00

Table 8.3, Landing Gear Costs

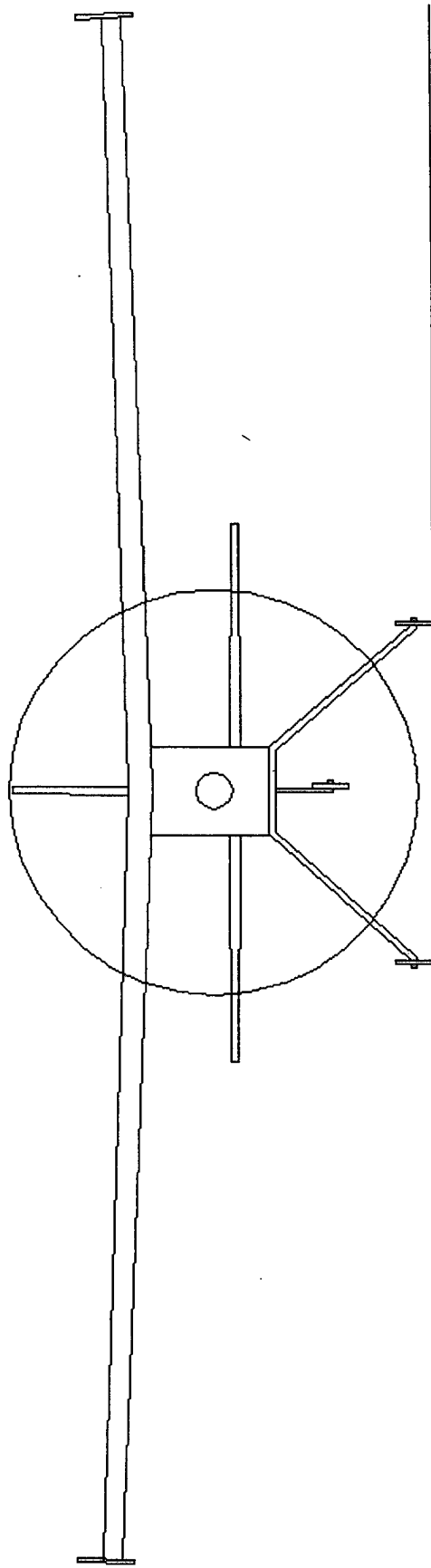
Component	Cost
Wheels	\$ 39.00
Nosegear strut	\$ 1
Main Landing Gear	\$ 3
Subtotal	\$ 43



Drawing 1, 3 views of the aircraft

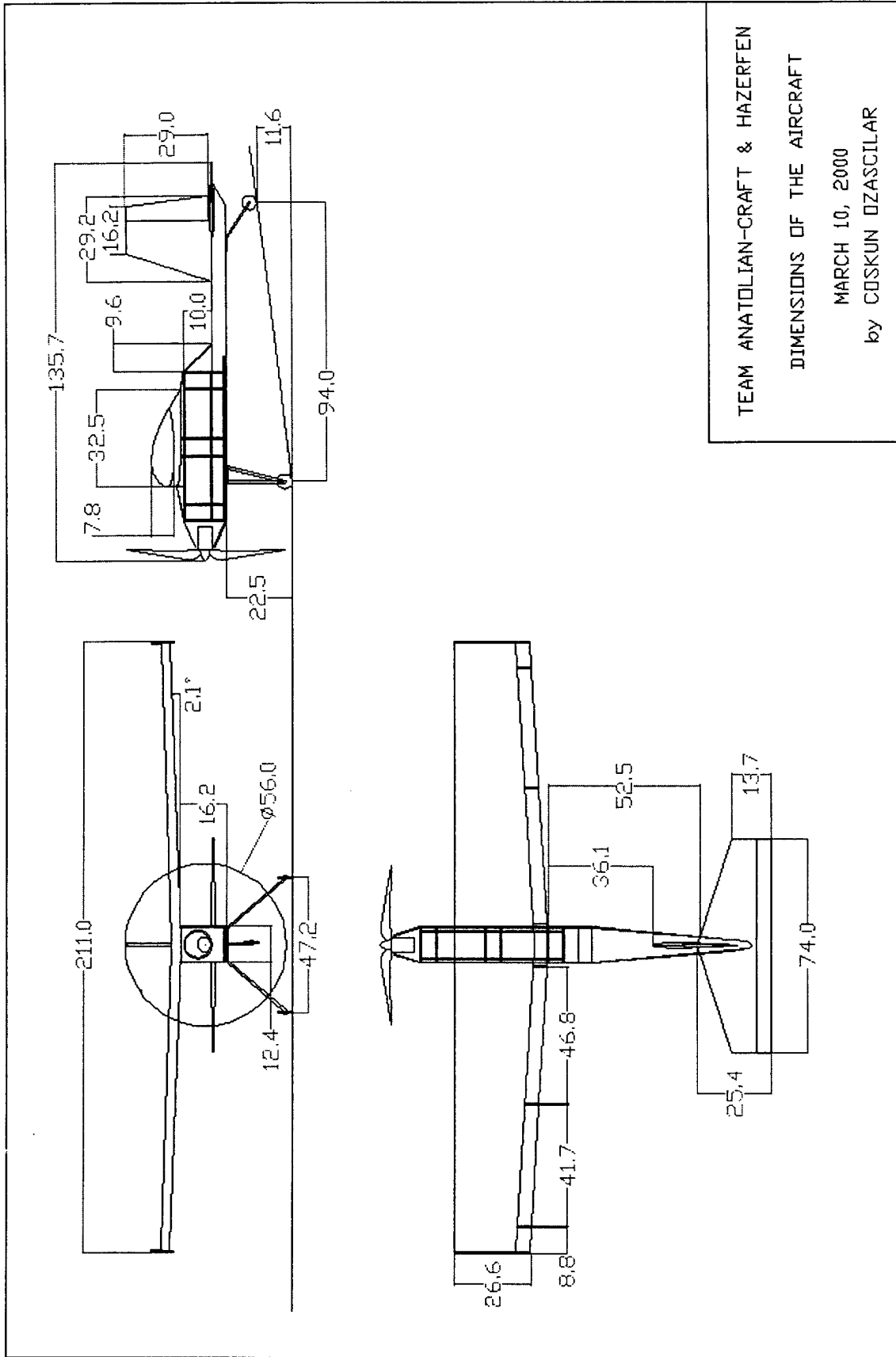
Rudder servos (1)*	\$ 75
Futaba S9202	
Subtotal	\$ 1217.5

*Donated or reused materials

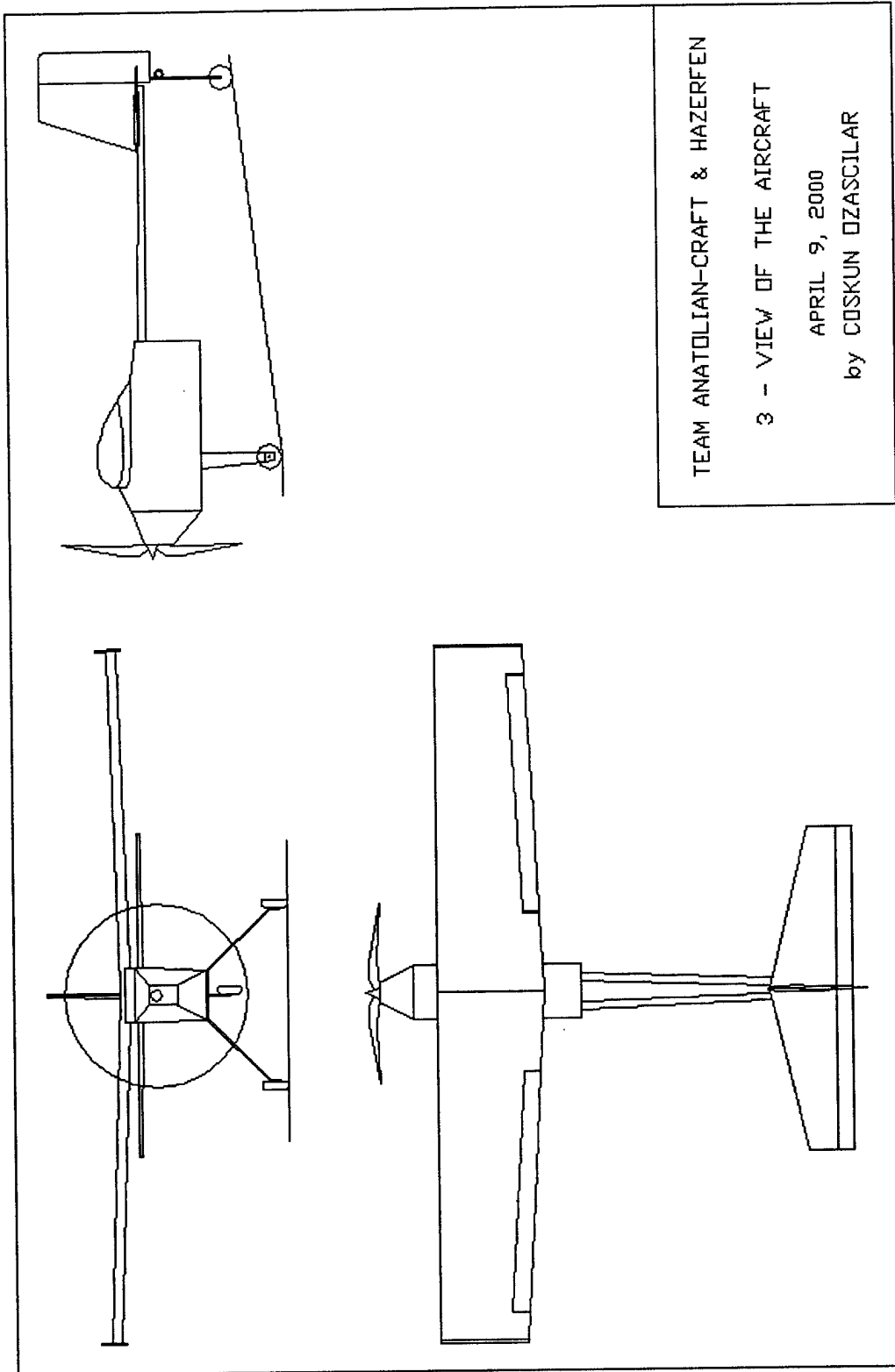


Drawing 1-2, Front view of the aircraft

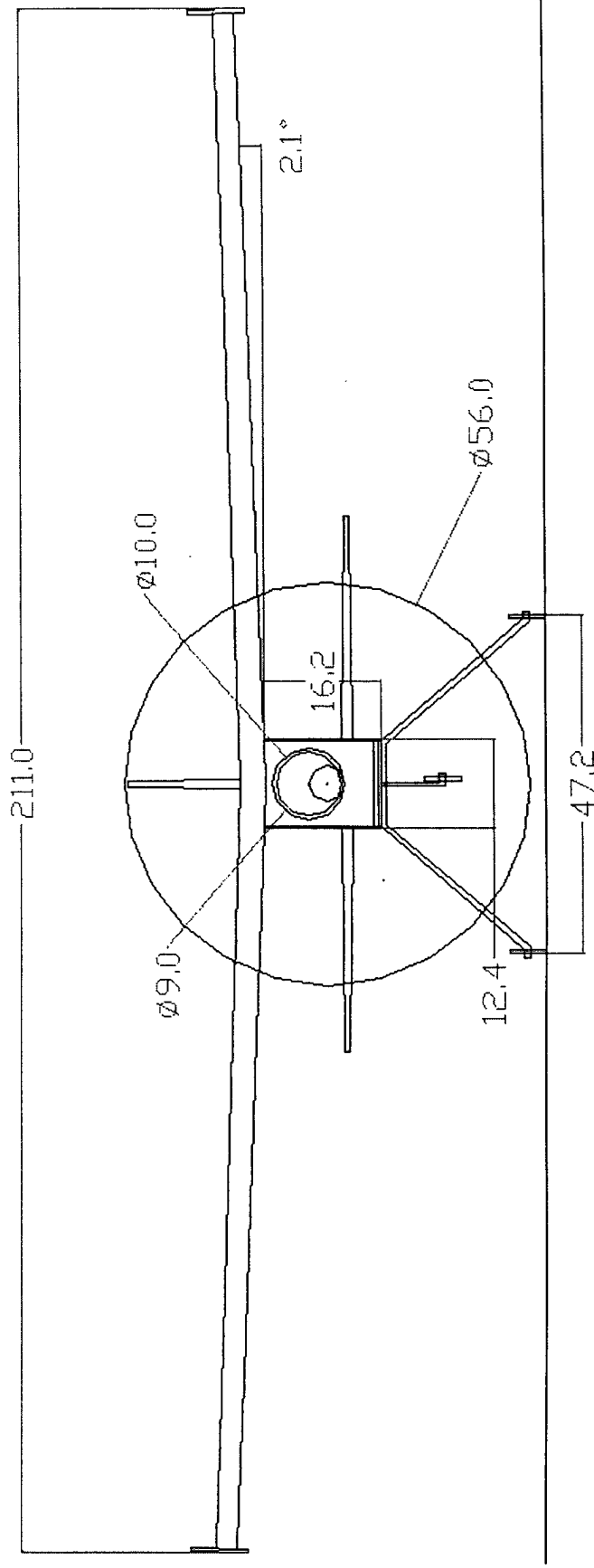
Payload	\$ 2
Subtotal	\$ 2517.5
Donated or Reused Items	-\$ 1172
Total	\$ 1345.5



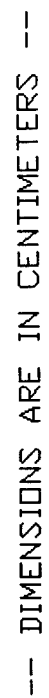
Drawing 2, Dimensions of the aircraft



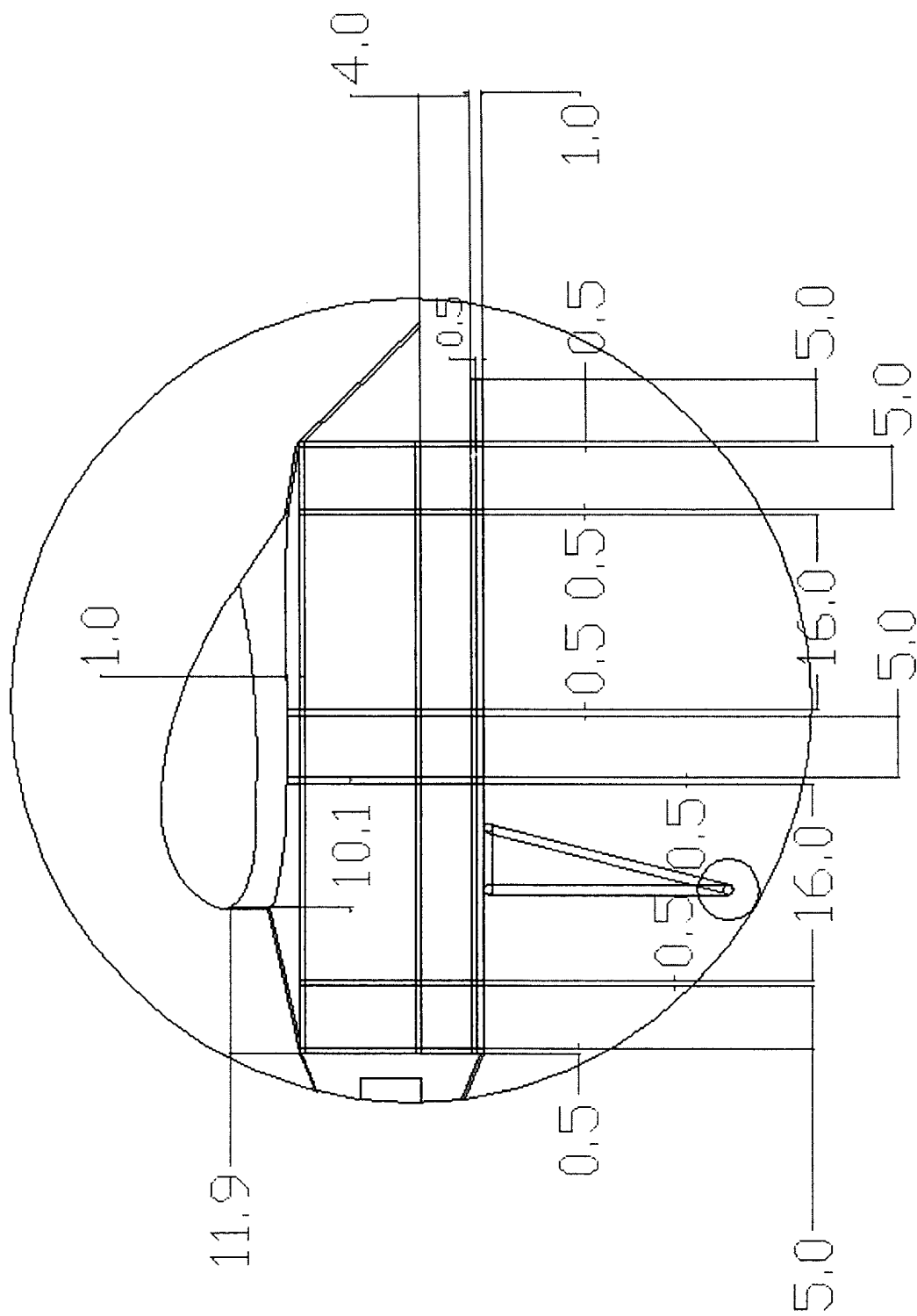
Drawing 1: The 3-view of the aircraft



Drawing 2-1, Dimensions of the aircraft (front view)

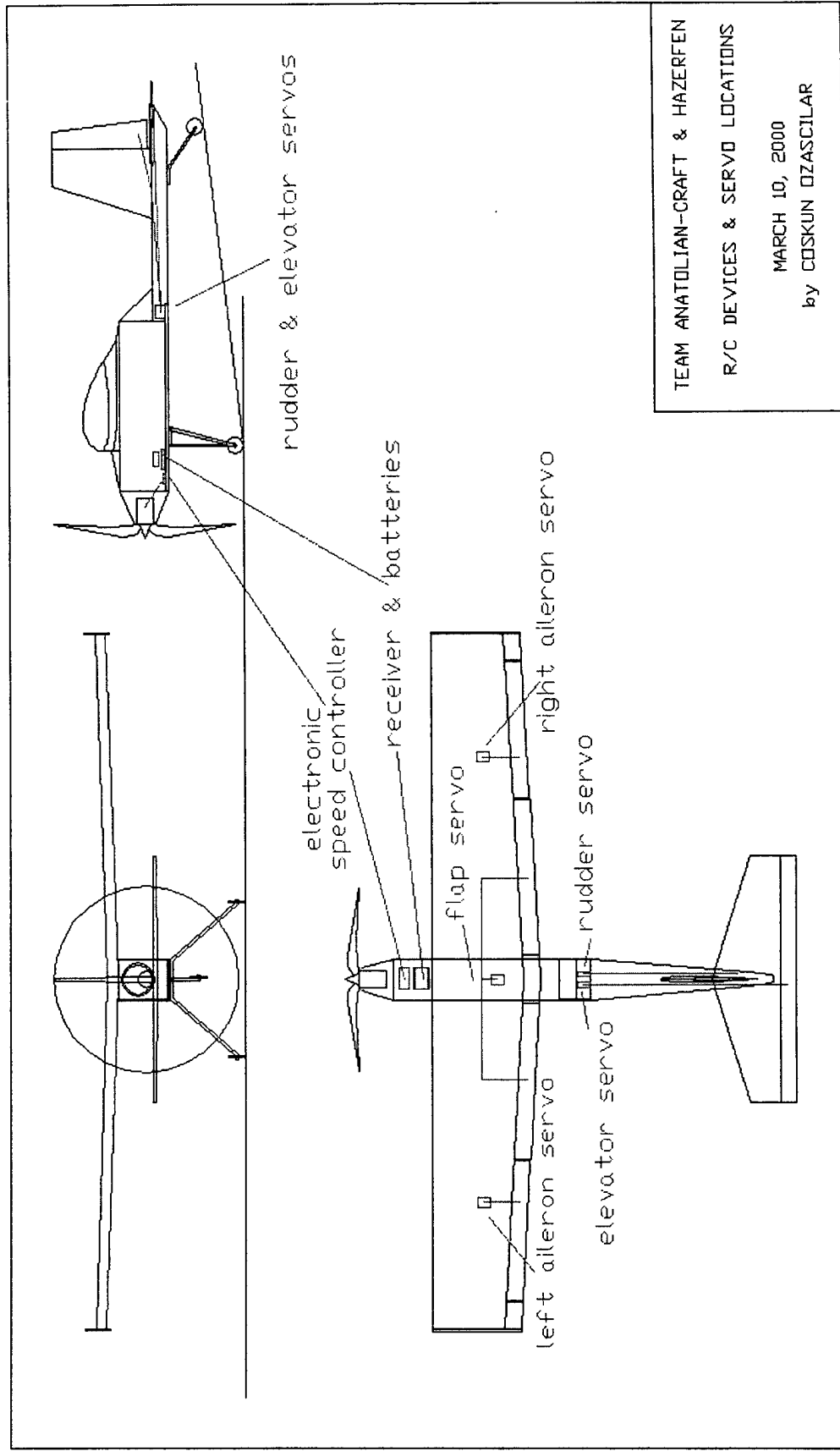


Drawing 3: The side view of the aircraft

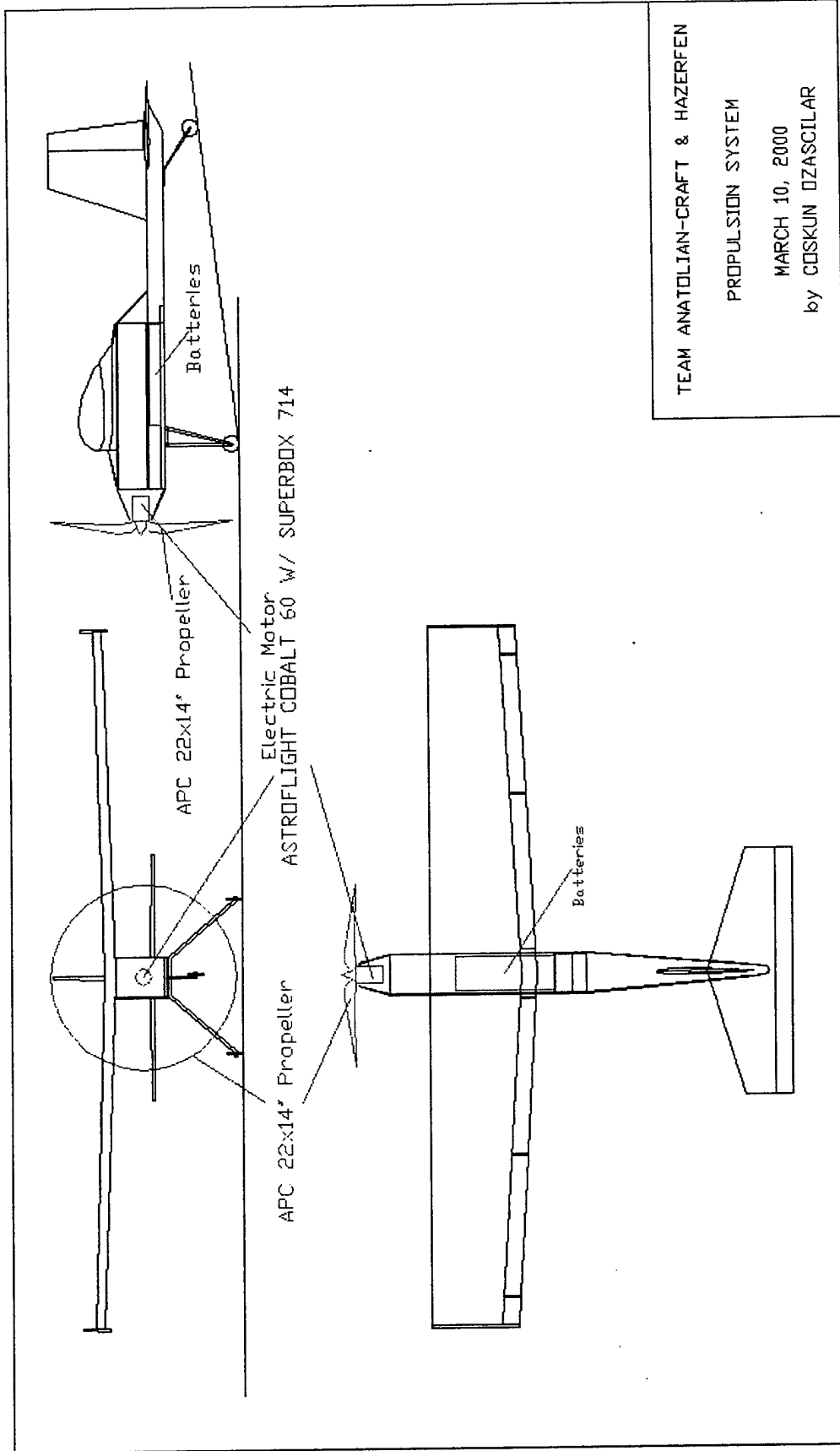


Drawing 2-3, Dimensions of the aircraft (focus on the fuselage)

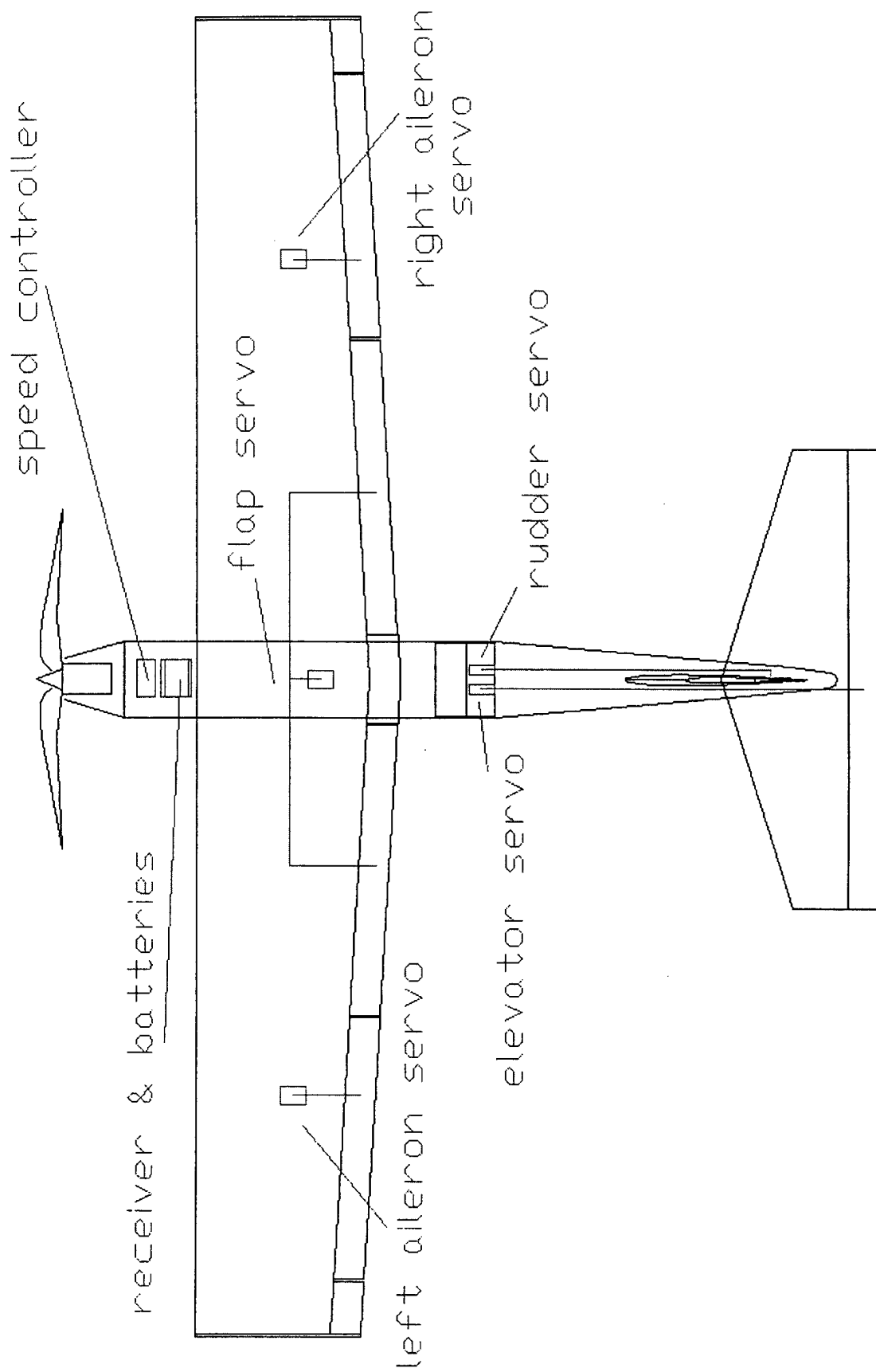
Drawing 4: The top view of the aircraft



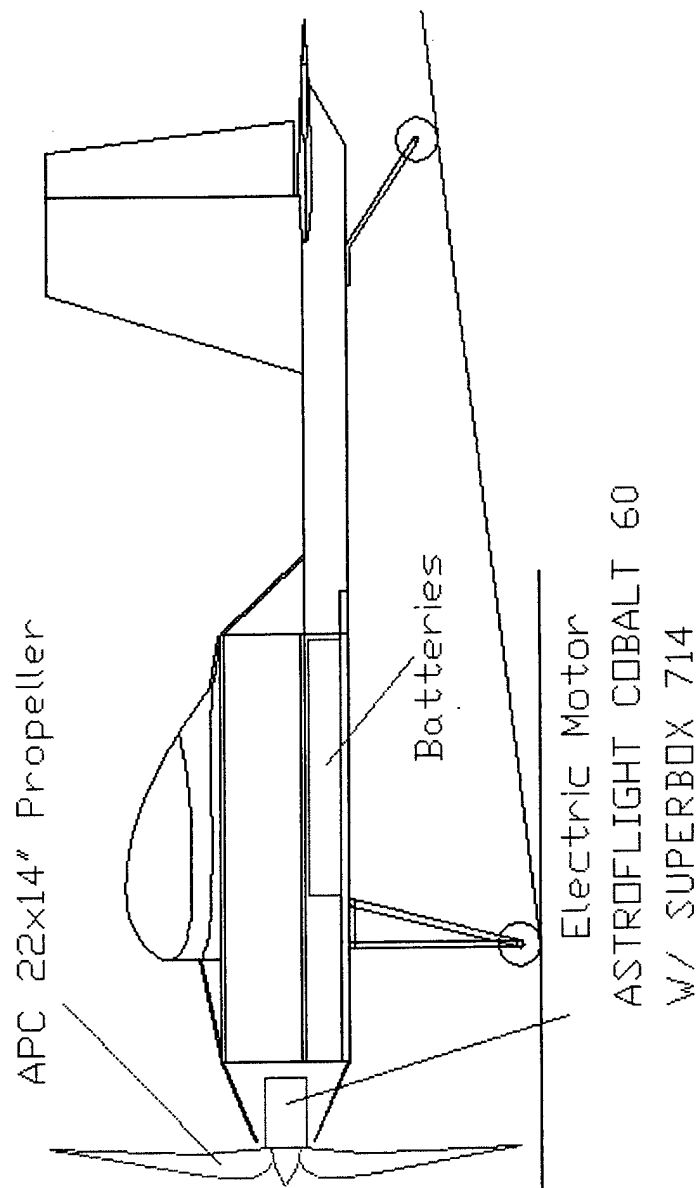
Drawing 3, Remote control devices and servo locations on the aircraft



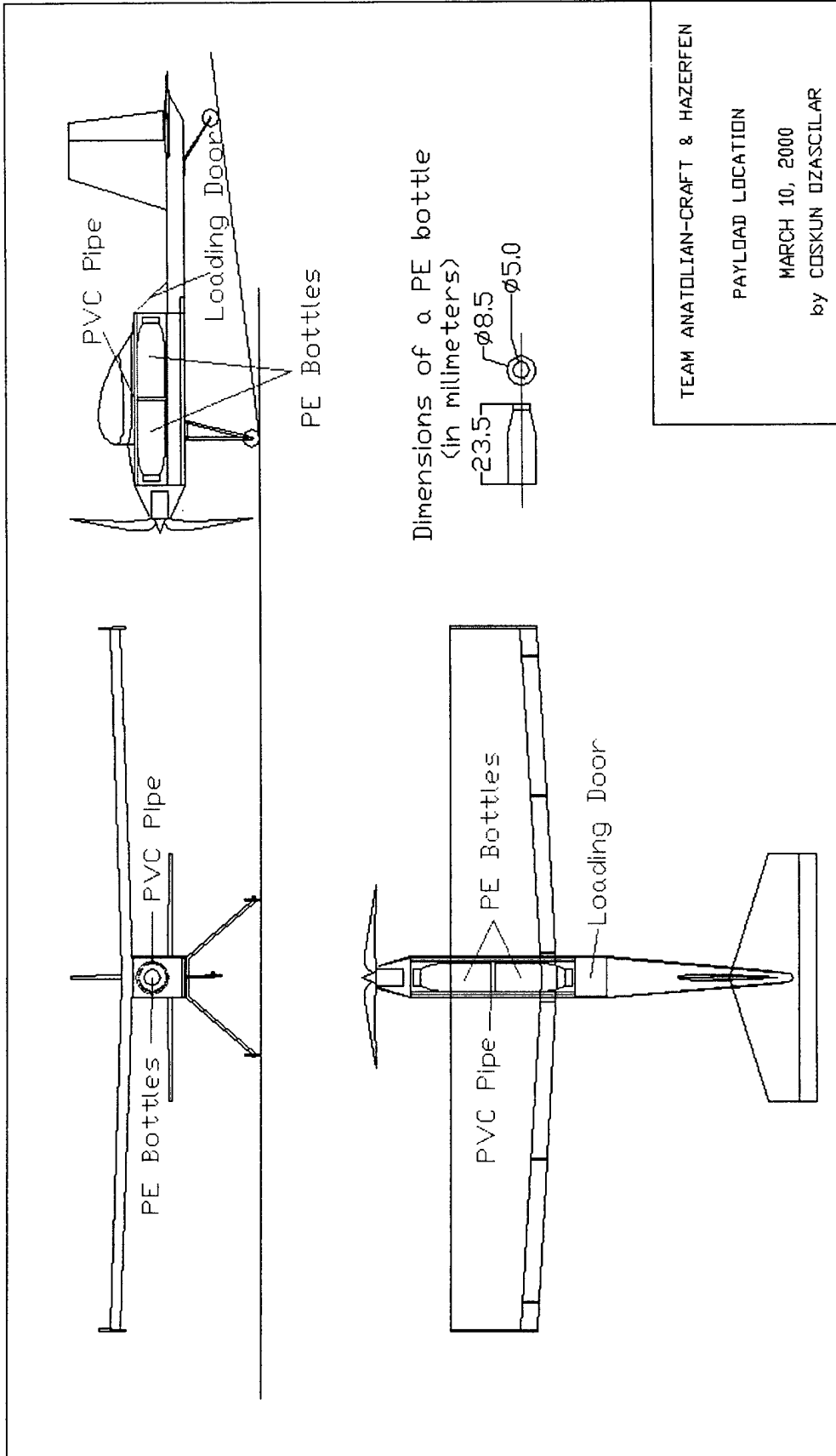
Drawing 5, Propulsion system



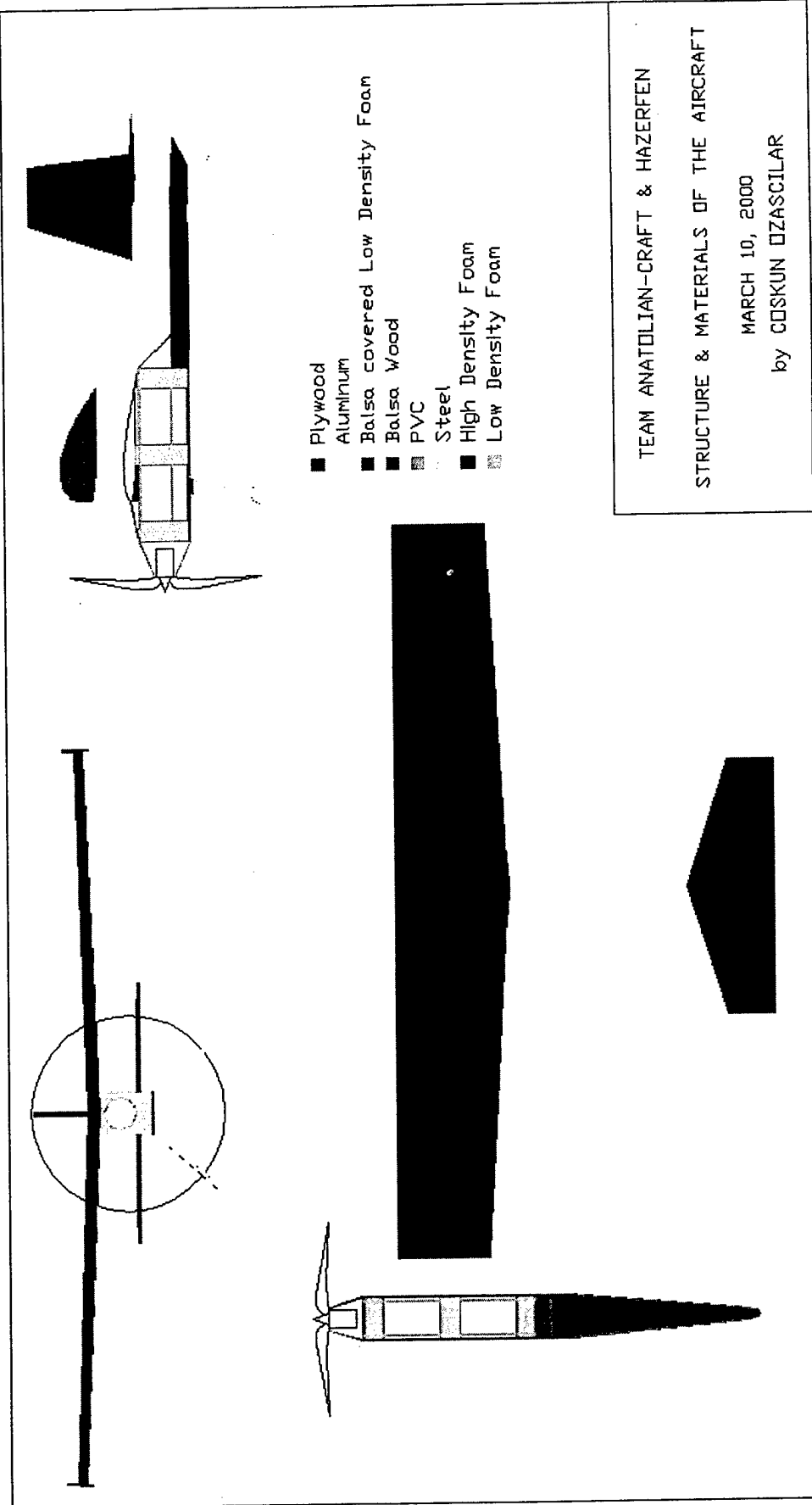
Drawing 3-2, Remote control devices and servo locations on the aircraft (side view)



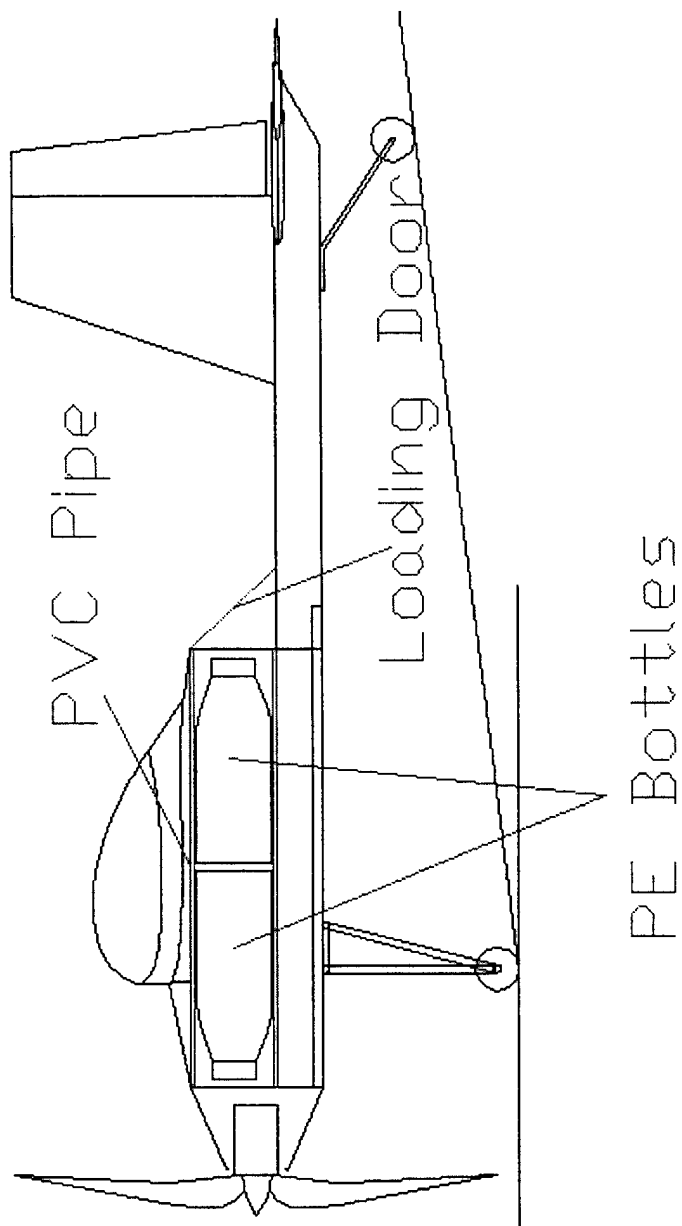
Drawing 5-2, Propulsion system (side view)



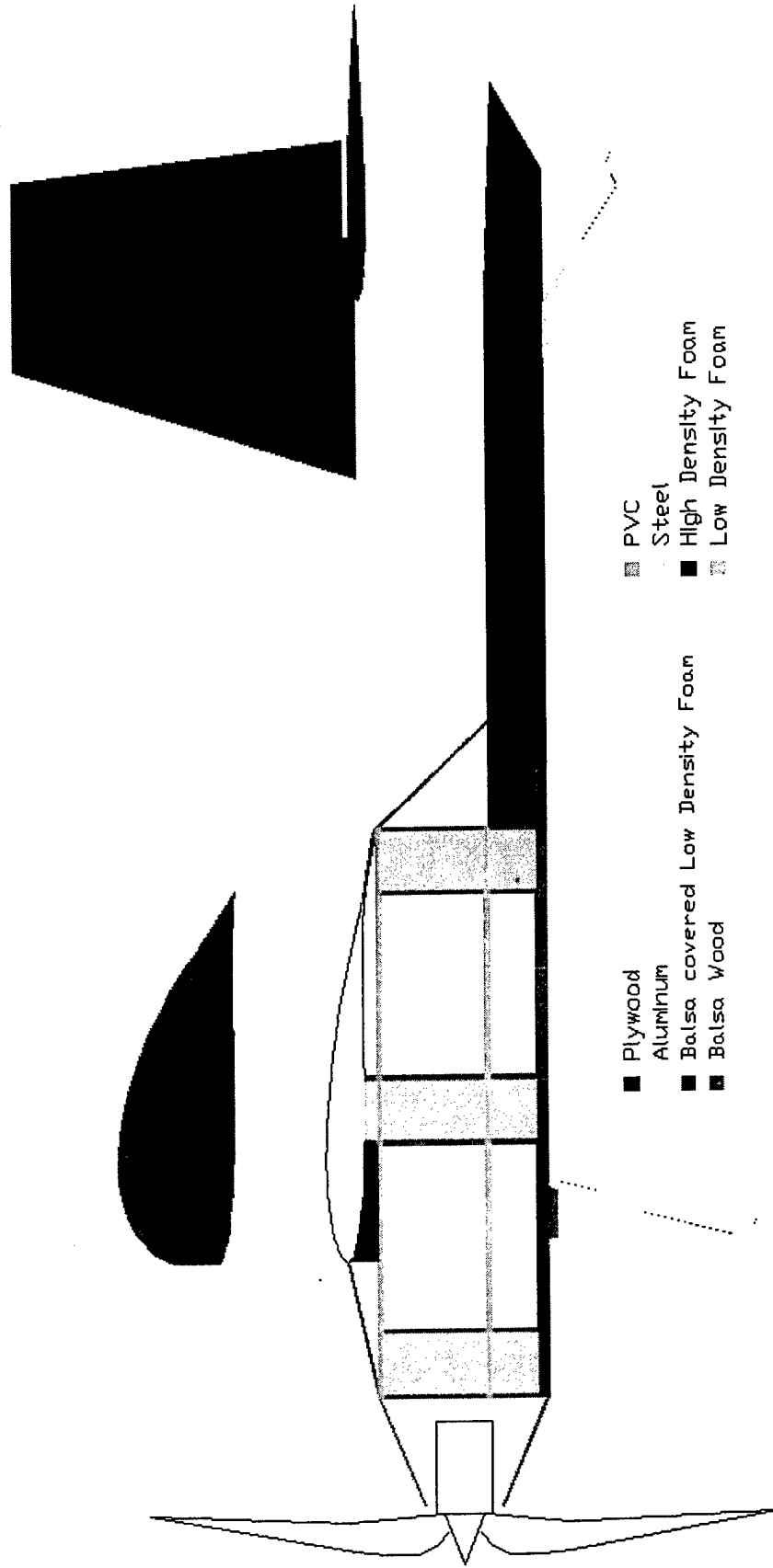
Drawing 4, Payload location



Drawing 6, Structure & Materials of the aircraft



Drawing 4-2, Payload location (side view)

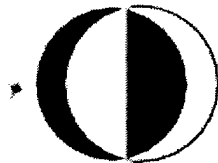


Drawing 6-2, Structure & Materials of the aircraft (side view)



**AIAA/CESSNA/ONR
STUDENT DESIGN/BUILD/FLY
COMPETITION**

DESIGN OF A UAV CLASS AIRCRAFT



ADDENDUM PHASE

CHAPTER 6

MANUFACTURING PLAN

6.1 INTRODUCTION

In this chapter, the basic steps for manufacturing the major components and assemblies of the final design will be explained. Furthermore, investigated manufacturing processes are detailed and the figures of merit used for their selection will be described.

6.2 MANUFACTURING PROCESSES INVESTIGATED

At first, our team considered using low density wood for the construction of all structural components. Balsa wood will be used for most of the structure –which is a light and stiff kind of wood- while birch plywood or a composite plate will be used for high-stress areas, like joining parts. Balsa sticks can be used as spars on wings to increase their endurance. Using foam inside the wing can be a possibility to obtain lighter wings. Plastic or fabric covering materials can be used to cover Balsa for smoothness. In addition, a wooden boom will be used to combine tail and fuselage, which is the most widely used method for lighter, small UAV construction.

Using carbon fiber and kevlar for construction is another method that was considered. This method uses mold for each component and then covers the molds with fiber and kevlar cloth. This method also requires usage of some wood and composite plates for the production of the boom, wing mountings, motor holders and other electrical equipment mountings. Usage of fiberglass is another alternative for this method.

Using of aluminum was another alternative method for production of our UAV. This method would require some specific tools like CNC machines for processing. However this method is not widely used for UAV type light aircraft.

Finally, a combination of the above stated methods is considered to satisfy the figures of merit for each structural component. Balsa will be used to cover the foam wing and tail which will then be covered with plastic or fabric material. Carbon fiber and kevlar cloth will be used as stiffeners for spars. Carbon fiber and Balsa wood combination will be used to manufacture a stiff and light fuselage, and carbon fiber will be used to manufacture the boom. Components requiring more strength or endurance (like wing mountings, boom mountings, electrical equipment cases etc.) will be stiffened by fiber plates. If more strength is needed, aluminum plates will be used.

This project was supported financially by METU, METU-EBI, METU M. PARLAR Foundation, TUBITAK-TIDEB, ASELSAN, TUBITAK-BILTEN and M-Air. Without their support the airplanes could never be finished.

frequencies and the risk of losing radio reception can never be taken in this design project.

6.4 FINAL SELECTION AND JUSTIFICATION OF MANUFACTURING PROCESSES

The team considered all of these figure of merits and decided to manufacture the UAV from combination of Balsa wood, foam and composite materials for all major parts except the landing gears which will be made from aluminum. This decision is taken as a result of stated figures of merit and the advantages. All of the FOM drives us to use wood and composite mainly for stiffness, low cost, easy and fast manufacturing. It is easy to produce the wing and tail from wood covered foam, a composite boom, and a composite fuselage. This main construction will be finished before the end of March 2000 so there will be enough time to test our UAV.

6.5 MANUFACTURING PROCESS

All the parts of the aircraft will be produced carefully and following a production plan. Completion of each assembly will be followed by the integration with the major assembly and alignment with the rest of the components. First wings will be produced followed by fuselage manufacturing. Tail assembly will be joined to these with a boom. Production of extra wings are planned in case of aircraft..

Throughout the construction process, epoxy and carpenter's wood glue will be used.

6.5.1 WING CONSTRUCTION

The basic structure of the wing panels is formed by cutting the foams to their desired shape.

To satisfy the structural integrity requirements of having the fully loaded aircraft picked up by its wingtips, 3/4"-wide unidirectional carbon fiber tape is applied as spar caps. The carbon fiber is applied symmetrically (top and bottom) as follows: Two layers are applied over the full span of each panel. One layer spanned the inboard 75% of each wing panel, while the fourth layer spanned the inboard half of each wing. A physical test, as described in the detailed design phase, using this identical spar structure showed that the spar alone, without any additional structure such as leading edge sheeting, satisfied the structural requirement for an aircraft weighing 43 pounds. To further increase the safety factor, the aircraft was built with one additional layer of carbon fiber tape capping the top and bottom of the entire spar.

Knowing the fragility of Balsa, the team realized that it will not be feasible to have sharp trailing edges from just 3/32" Balsa sheeting. For this reason, 3/4"-wide strips of 1/64" 3-ply birch plywood were glued between the top and bottom trailing edge pieces. When sanded, this produced a sharp, durable trailing edge.

Drawing 1: The 3-view of the aircraft	70
Drawing 2: The front view of the aircraft	71
Drawing 3: The side view of the aircraft	72
Drawing 4: The top view of the aircraft.....	74

6.5.3 FUSELAGE CONSTRUCTION

Lite plywood was the primary material used for the construction of the fuselage. Both sides, along with the top and bottom of the fuselage were cut from 1/8" lite plywood. The nose was rounded by building up the top and bottom with Balsa sanded to shape.

Four major bulkheads/formers were assembled in the fuselage. The first one used 1/4" aircraft quality spruce plywood for the nose-gear mount. The next two formers were two 1/8" aircraft quality spruce plywood pieces that accepted the main wing spar for assembly. Triangle stock was used generously when attaching these formers to the fuselage walls since failure of these joints would be catastrophic. The last former was simply in place behind the payload bay to keep the fuselage shape. Lite ply was suitable for the fabrication of this former.

The main payload bay cover was the last major structural element of the fuselage. Again, 1/8" lite plywood was used to produce the hatch cover. Strips of plywood were attached perpendicular to the hatch cover to support aluminum railings to which the water bottles would attach. Each of the ten bottles had a support disk near the cap so that they could be stored on rails such as what is shown in Figure 6.1. Each bottle was moved into place on the rails and secured by cotter pins.

6.5.4 LANDING GEAR CONSTRUCTION

Composite construction was used exclusively for the fabrication of the main landing gear. Twenty-two layers of unidirectional carbon fiber surrounded a 1/8" core of Balsa, birch plywood, and aluminum. Table 6.1 explains the arrangement of carbon layers relative to the core. The resin-laden lay-up was secured over a blue foam template to form its elliptical shape. Figure 6.3 depicts the blue foam template along with the core of the landing gear. Vinyl sheets placed around the lay-up allowed the landing gear to cure with a smooth finish. Six 1/4 x 20 bolts attached the final main landing gear to the fuselage.

The nose-gear was purchased since the appropriate size was already available. Another issue that warranted the purchase, rather than construction of the nose-gear, was that its failure would probably cause extensive damage, which was less likely with a commercially available nose-gear.

6.6 CONCLUSION

This chapter was devoted to the manufacturing plan and to the processes selected for manufacturing of the major components and assemblies of the final design. Manufacturing processes are described according to their figures of merit

- The aft fuselage which was originally designed to be made of high density foam is replaced by two composite hollow booms.
- The tail surfaces are placed to a higher position.
- The flaps and ailerons are replaced by a pair of flaperons.
- The battery location is enlarged.
- the locations for the servo control units on the tail and the electronic speed controller are re-arranged to provide more space for the batteries.
- The attachment regions for the wing attachment and the landing gear are reenforced and improved.

The reason why the material used in the main landing gear was changed was simply due to weight considerations. The weight of aluminum (Aluminum 2025) was much less than that of the steel. The same reason was also valid for the aft fuselage booms. In both cases, the new structures were strong enough to carry the loads. Moreover, the manufacturing of the aft fuselage part made of high density foam would be very difficult, and the fuselage would require structural improvements in this area. Therefore, this complex structure was replaced by a pair of simple, pre-manufactured composite booms used in fishing rods. However, this replacement required that the tail surfaces would be placed in a higher position. We have chosen manufacturing methods as simple as possible, materials as light as possible but as strong as required.

The original design had flaps which would be used only during the take-off to increase the lift and ailerons for aircraft control. It was thought the ailerons may not be powerful enough to roll the aircraft. Therefore, the flaps and the ailerons are combined into one control surface, "flaperons", which will provide the necessary lift increase during the

APPENDIX 1

Another suggestion may be related to the selection of materials and components for the aircraft. The availability of materials and components for building a model is a major issue. These materials should be determined right from the start, during the conceptual and preliminary design phases, and these selected materials and components need to be ordered and obtained as soon as possible.

```

      subroutine airfoil(naca)
c
      parameter( npx = 101 )
c
      common/bod   / nlower, nupper, ntot, npl, ss,
&                x(npx+1), y(npx+1), xm(npx), ym(npx),
&                costhe(npx), sinthe(npx)
c
c----- Compute the airfoil coordinates and panel angles.
c
      pi = acos( -1.0 )
c
c----- Decompose the NACA number to determine airfoil coefficients.
c
      ieys = naca / 1000
      iptmax = naca / 100 - 10 * ieys
      itau = naca - 1000 * ieys - 100 * iptmax
c
c----- Compute the coefficients.
c
      epsmax = ieys   * 0.01
      ptmax   = iptmax * 0.1
      tau     = itau   * 0.01
c
c----- Error correction for bogus NACA numbers.
c
      if ( ( naca .le. 9999 ) .and. ( epsmax .gt. 0 ) .and.
&        ( ptmax .eq. 0 ) ) ptmax = .1
c
c----- If NACA 5 digit coding is used, make necessary changes.
c
      if ( ieys .ge. 10 ) then
        if ( ieys .eq. 21 ) then
          ptmax = 0.0580
          ak1 = 361.4
        elseif ( ieys .eq. 22 ) then
          ptmax = 0.1260
          ak1 = 51.64
        elseif ( ieys .eq. 23 ) then
          ptmax = 0.2025
          ak1 = 15.957
        elseif ( ieys .eq. 24 ) then
          ptmax = 0.2900
          ak1 = 6.643
        elseif ( ieys .eq. 25 ) then
          ptmax = 0.3910
          ak1 = 3.230
        endif
        epsmax = ak1 * ptmax**3 / 6
      endif
c
c----- initialize indexing for lower surface.
c
      npoint = nlower

```

already available in our department's stocks which decreased the manufacturing cost with respect to the actual case.

8.3

```

c
      return
      end

```

```

c-----
      function body_x(thick,beta,z,sign)
c
c----- Compute the x coordinate of an airfoil point.
c
      body_x = z - sign * thick * sin( beta )
c
      return
      end

```

```

c-----
      function body_y(thick,camber,beta,sign)
c
c----- Compute the y coordinate of an airfoil point.
c
      body_y = camber + sign * thick * cos( beta )
c
      return
      end

```

```

c-----
      subroutine cofish(alpha)
c
      parameter( npx = 101 )
c
      common/bod   / nlower, nupper, noddot, npl, ss,
&                 x(npx+1), y(npx+1), xm(npx), ym(npx),
&                 costhe(npx), sinthe(npx)
      common/cof   / a(npx,npx+10), kutta
      common/infl  / aan(npx,npx), bbn(npx,npx)
c
      pi = acos( -1.0 )
      pi2inv = 0.5 / pi
      kutta = noddot + 1
      cosalf = cos( alpha )
      sinalf = sin( alpha )
c
c----- Initialize coefs.
c
      do 10 j = 1, kutta
         a(kutta,j) = 0.0
      10 continue
c
c----- Set vn = 0 at midpoint of ith panel.
c
      do 30 i = 1, noddot
         a(i,kutta) = 0.0

```

Table 8.1 Rated Aircraft Cost

$$\text{RAC \$ (Thousands)} = (A * \text{MEW} + B * \text{REP} + C * \text{MFHR}) / 1000$$

Coefficient	Description	Value
A	Manufacturers Empty Weight Multiplier	\$100 / lb.
B	Rated Engine Power Multiplier	\$1 / watt
C	Manufacturing Cost Multiplier	\$20 / hour
MEW	Manufacturers Empty Weight	Actual airframe weight, lb., without payload or batteries
REP	Rated Engine Power	# engines * 50A * 1.2 V/cell * # cells

```

C
  cosalf = cos( alpha )
  sinalf = sin( alpha )
  cfx = 0.0
  cfy = 0.0
  cm = 0.0
C
  do i = 1, nodtot
C
C----- Moment coefficient is computed about the elastic axis.
C
    xmid = xm(i) - xp
    ymid = ym(i)
    dx = x(i+1) - x(i)
    dy = y(i+1) - y(i)
    cfx = cfx + cp(i) * dy
    cfy = cfy - cp(i) * dx
    cm = cm + cp(i) * ( dx * xmid + dy * ymid )
  enddo
C
C----- Compute lift.
C
  cl = cfy * cosalf - cfx * sinalf
C
  return
  end

```

```

C-----
      subroutine gauss(nrhs,m,nitr)
C
      parameter( npx = 101 )
C
      common/cof / a(npx,npx+10), neqns
C
C----- Performs Gaussian elimination of matrix a.
C
      np = neqns + 1
      ntot = neqns + nrhs
C
      if (( m .le. 1 ) .and. ( nitr .eq. 0 )) then
C
C----- Do full matrix elimination sequence.
C
        do 10 i = 2, neqns
          im = i - 1
C
C----- Eliminate the (i-1)th unknown from i-th through
C----- neqns-th equations.
C
          do 10 j = i, neqns
            r = a(j,im) / a(im,im)
            do 10 k = i, ntot
              a(j,k) = a(j,k) - r * a(im,k)

```

Adhesives	\$ 70.00
(epoxy and aliphatic resin)	
Miscellaneous hardware	\$ 40.00
(hinges, control horns, clevises, screws, etc.)	
Subtotal	\$ 262.00

Table 8.3, Landing Gear Costs

Component	Cost
Wheels	\$ 39.00
Nosegear strut	\$ 1
Main Landing Gear	\$ 3
Subtotal	\$ 43


```

      else
        if ( naca .gt. 9999 ) then
c
c----- For NACA 5 digit numbers.
c
c----- Ptmax = m and epsmax = (k1*m3)/6 from Abbott and Doenhoff.
c
          if ( z .gt. ptmax ) then
            camber = epsmax * ( 1.0 - z )
            dcamdx = - epsmax
          else
            w = z / ptmax
            camber = epsmax * ( w**3 - 3*w**2 + (3.-ptmax)*w )
            dcamdx = epsmax/ptmax*(3*w**2 - 6*w + ( 3.0-ptmax))
          endif
        else
c
c----- For NACA 4 digit airfoils.
c
          if ( z .gt. ptmax ) then
            camber = epsmax / ( 1.0 - ptmax )**2
            &      * ( 1. + z - ptmax * 2 ) * ( 1. - z )
            dcamdx = epsmax * 2 / ( 1.0 - ptmax )**2
            &      * ( ptmax - z )
          else
            camber = epsmax / ptmax**2 * ( ptmax**2 - z ) * z
            dcamdx = epsmax * 2 / ptmax**2 * ( ptmax - z )
          endif
        endif
c
        beta = atan( dcamdx )
      endif
c
      return
      end

c-----
      subroutine print_cp(naca,alpi)
c
      parameter( npx = 101 )
c
      common/bod / nlower, nupper, nodtot, npl, ss,
      &      x(npx+1), y(npx+1), xm(npx), ym(npx),
      &      costhe(npx), sinthe(npx)
      common/cpd / cp(npx), xp
c
c----- Write out data.
c
      open(8,file='cp.fmt',form='formatted',status='unknown')
      do n=1,nodtot
        write(8,*) xm(n), ym(n), cp(n)
      enddo
      close(8)

```

Rudder servos (1)*	\$ 75
Futaba S9202	
Subtotal	\$ 1217.5

*Donated or reused materials

```
        enddo  
        cp(i) = 1.0 - vtang**2  
    enddo  
c  
    return  
end
```

Payload	\$ 2
Subtotal	\$ 2517.5
Donated or Reused Items	-\$ 1172
Total	\$ 1345.5

RATED AIRCRAFT COST MODEL FOR CONVENTIONAL TYPE AIRCRAFT

$w = 22$ Weight of the aircraft in lb
 $ep = 1300$ Engine power in watt.
 $h = 50$ Manufacturing time in hour
 $en = 1$ Engine number
 $cn = 62$ Cell number
 $nw = 1$ Number of wings
 $pa = 6.706$ Projected area of wing in ft²
 $nb = 1$ Number of bodies
 $lf = 4.429$ Length of fuselage in ft
 $vs = 1$ Number of vertical surface
 $hs = 1$ Number of horizontal surface
 $s = 5$ Number of servos
 $p = 1$ Number of propellers

$MEW = 12$ Manufacturers Empty Weight

$$A = 100 \cdot w$$

$$B = 1 \cdot ep$$

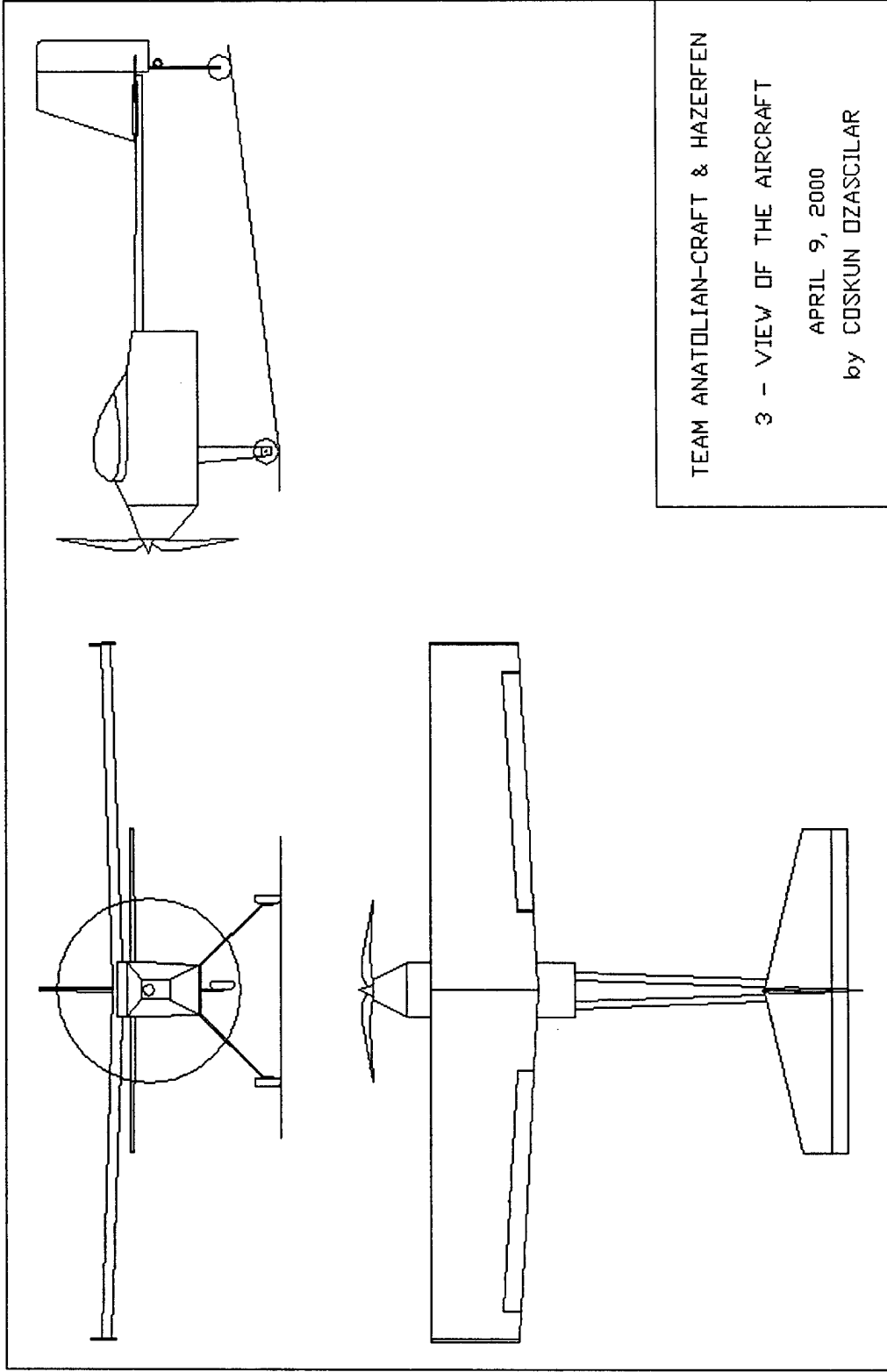
$$C = 20 \cdot h$$

$REP = en \cdot 50 \cdot 1.2 \cdot cn$ Rated Engine Power

$$MFHR = (5 \cdot nw + 4 \cdot pa) + (nb \cdot 5 + 4 \cdot lf) + (5 + 5 \cdot vs + 10 \cdot hs) + (5 + 1 \cdot s) + (5 \cdot e + 5 \cdot p)$$

$$RAC = \frac{A \cdot MEW + B \cdot REP + C \cdot MFHR}{1000}$$

$$RAC = 4.966 \cdot 10^3$$



Drawing 1: The 3-view of the aircraft

RANGE FORMULA

AC-H has an electric motor so we have to derive an equation like Breguet range equation. We define a constant C that

$$i \times \varepsilon = P$$

where "i" is the current of the electric motor which is :

$$i = \frac{dq}{dt} = \frac{P}{\varepsilon}$$

since $T=D$ and $W=L$

$$T = \frac{W}{L/D}$$

Substituting

$$dq = \frac{W}{L/D} \frac{V}{\varepsilon} dt$$

integrating it results in

$$\Delta t = \frac{L/D}{W} \frac{\varepsilon}{V} \Delta q$$

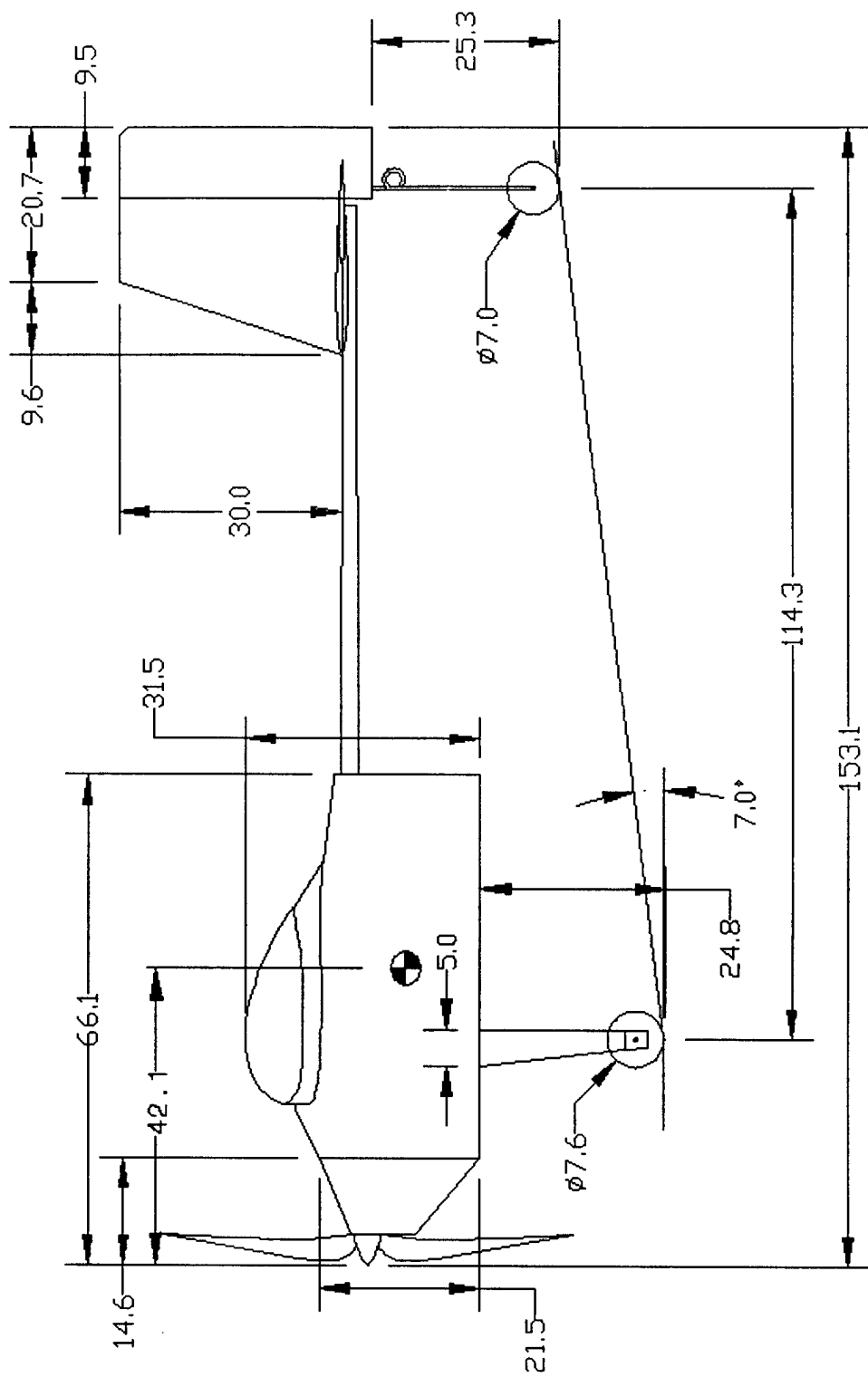
since $R=Vt$

$$R = \frac{L/D}{W} \varepsilon \Delta q$$

ENDURANCE FORMULA

We will use our previous formula for range again to find the equation of endurance because we have electrical engine.

$$E = \Delta t = \frac{L/D}{W} \frac{1}{VC} \Delta q$$



--- DIMENSIONS ARE IN CENTIMETERS ---

Drawing 3: The side view of the aircraft

LATERAL-DIRECTIONAL STATIC STABILITY AND CONTROL

Cn_β Calculation:

Wing Terms:

for cruise condition,

$$CL = 0.6$$

$$\Lambda = 0$$

$$A = 7$$

$$b = 2.1 \text{ m}$$

$$X_{acw} = 0.35 \text{ m}$$

$$X_{cg} = 0.4 \text{ m}$$

$$Cn_{\beta w} = (CL)^2 \cdot \left[\frac{1}{4\pi \cdot A} - \left[\frac{\tan(\Lambda)}{\pi \cdot A \cdot (A + 4 \cdot \cos(\Lambda))} \right] \cdot \left[\cos(\Lambda) - \frac{A}{2} - \frac{A^2}{8 \cdot \cos(\Lambda)} + 6 \cdot \frac{(X_{acw} - X_{cg}) \cdot \sin(\Lambda)}{b \cdot A} \right] \right]$$

$$Cn_{\beta w} = 4.093 \cdot 10^{-3}$$

Fuselage Terms:

$$\text{volume} = 0.011 \text{ m}^3$$

$$Df = 0.15 \text{ m} \quad (\text{depth of fuselage})$$

$$Wf = 0.12 \text{ m} \quad (\text{width of fuselage})$$

$$Sw = 0.623 \text{ m}^2$$

$$Cn_{\beta f} = -1.3 \cdot \frac{\text{volume}}{Sw \cdot b} \cdot \frac{Df}{Wf}$$

$$Cn_{\beta f} = -0.014$$

Vertical Tail Terms:

$$CL_{\alpha} = 5$$

$$CF_{\beta v} = CL_{\alpha}$$

$$Sv = .068 \text{ m}^2$$

$$Z_{wf} = .065 \text{ m} \quad (\text{ver. height of the wing above the fuselage centerline})$$

$$X_{acv} = 1.11 \text{ m}$$

$$k = 0.724 \cdot \frac{3.06 \cdot \frac{Sv}{Sw}}{1 - \cos(\Lambda)} - 0.4 \cdot \frac{Z_{wf}}{Df} + 0.009 A \quad (k = (\delta\beta/\delta\beta)^* \eta)$$

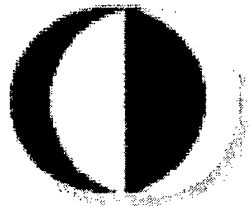
$$k = 0.781$$

Drawing 4: The top view of the aircraft

AIAA
AMERICAN INSTITUTE OF
AERONAUTICS AND ASTRONAUTICS

**AIAA/CESSNA /ONR
STUDENT DESIGN/BUILD/FLY COMPETITION
PROPOSAL REPORT**

“ Design of an Electric UAV Class Aircraft ”



METU - Team ETİ

Middle East Technical University (METU), Ankara, TURKEY

13, March 2000

TEAM ETI AIAA STUDENT DESIGN/BUILD & FLY COMPETITION PROPOSAL REPORT

Designed and developed by,

Team Leader	: Selim Solmaz
Consultant and Pilot	: Oğuz Doğanşoy
Team Members	: Ömer Onur Candaş Bozkurt Aycan Okan Özlem Armutçuoğlu Adem Çalık Monir El-Farra Ramez Bou-Dargham Demet Fatma Ülker Erdem Yavuzbalkan Sedat Doğru Murat Çat Fatih Karakaya Ümit Yusuf Oğraş Eray Özçelik
Advisors	: Prof. Dr. Ersin Tulunay* Dr. Mehmet Şerif Kavsaoğlu† Dr. Ozan Tekinalp†

* Professor, Department of Electrical and Electronics Engineering, METU.

† Assoc. Professor, Department of Aeronautical Engineering, METU.

ACKNOWLEDGEMENT

We would like to express our gratitude to our advisors; Prof. Dr. E. Tulunay, Dr. M. Ş. Kavsaoglu, Dr. O. Tekinalp for their supervision, guidance, encouragement and patience during all the stages of this project.

We would also like to thank to Prof. Dr. N. Alemdaroğlu, chairman of the Aeronautical Engineering Department, for his encouragement

Finally, we would like to thank to our consultant and pilot Oğuz Doğanşoy for his invaluable guidance and help in modeling and manufacturing.

The conceptual and preliminary design studies of this aircraft were mostly performed as student projects in AE 451 "Aeronautical Engineering Design" course instructed by Dr. M. Ş. Kavsaoglu at the Department Aeronautical Engineering, Middle East Technical University (METU) during the Fall Semester of 1999.

Detail design and manufacturing is being evaluated within the AE 452 "Aeronautical Engineering Design" course offered at the Department, currently, which is being instructed by Prof. Dr. N. Alemdaroğlu and Dr. M. Ş. Kavsaoglu.

It should also be mentioned that the facilities of the Aerospace Systems Simulation, Control and Avionics Laboratory of the Department of Aeronautical Engineering as well as Process Control Laboratory of the Department of Electrical and Electronics Engineering of the Middle East Technical University are used during the course of this project.

SPONSORS

This project is supported by the following persons and/or organizations:

An anonymous donation

\$ 3500

Note: The other sponsors that will appear after this date will be listed in the addendum phase of the design report.

NOMENCLATURE

a_{mass}	Aircraft mass
AR	Wing aspect ratio
Arvt	Aspect ratio of the vertical tail
Arw	Aspect ratio of the wing
B,b	Wing span
Beta	Interpolation variable used to determine $claw3d$ and $clavt3d$
b_{ht}	Horizontal tail length
b_{vt}	Vertical tail length
c	Mean aerodynamic chord length
C:G	Center of gravity
Cbar, cbar	Mean aerodynamic chord
C_{D0}	Design aircraft zero lift drag coefficient
CD_{α}	Aircraft drag curve slope
C_{DL}	Design landing drag coefficient
$C_{D_{TO}}$	Design takeoff drag coefficient
C_{Du}	Drag coefficient due to compressibility effects
$C_{L\alpha}$	Design lift curve slope
CL_0	Reference aircraft lift coefficient
CL_{α}	Aircraft lift curve slope
$CL_{\alpha \dot{\alpha}}$	Aircraft unsteady lift curve slope
$Clavt2D$	2-d vertical tail lift curve slope
$Claw2D$	2-d wing lift curve slope
$C_{l\beta}$	Dihedral effect coefficient
C_{LL}	Design landing lift coefficient
$C_{L_{max}}$	Design aircraft maximum clean lift coefficient
Cl_0	Reference aircraft lift coefficient
C_{lp}	Damping coefficient in roll
CL_q	Aircraft lift curve slope with respect to pitch rate
C_{lr}	Rolling moment coefficient due to yaw
$C_{L_{TO}}$	Design takeoff lift coefficient
CL_u	Lift coefficient due to compressibility effects
$C_{l\dot{\beta}}$	Rolling moment derivative
$C_{m\alpha}$	Pitching moment coefficient
CM_{α}	Aircraft moment curve slope
$CM_{\alpha \dot{\alpha}}$	Aircraft unsteady moment curve slope
CM_q	Aircraft moment curve slope with respect to pitch rate
CM_u	Moment coefficient due to compressibility effects
$C_{n\beta}$	Weathercock effect coefficient
$C_{n\beta_{fuse}}$	Weathercock effect due to the fuselage
CNC	Computer numerically controlled
C_{np}	Yawing moment coefficient due to roll
C_{nr}	Damping coefficient in yaw
$C_{n\dot{\beta}}$	Yawing moment derivative
CTOL	Conventional take-off and landing

Cybeta	Side force coefficient due to sideslip
Cybetatail	Side force coefficient due to sideslip caused by the vertical tail
Cyp	Side force coefficient due to roll rate
Cyr	Side force coefficient due to yaw rate
DR_DR	Damping ratio for the dutch roll mode oscillations
Dsigmadbeta	Change in sidewash due to change in angle of sideslip
EtaV	Efficiency factor of the vertical tail
G	Gravity
grav	Gravitational acceleration
Hatwingroot	Height of the fuselage at the wing root
Ix	Moment of inertia about the x-axis of the aircraft
Iyy	Moment of inertia about the y-axis of the aircraft
Iz	Moment of inertia about the z-axis of the aircraft
K	Design lift drag factor
K _n	Static margin
Kt	Interpolation variable used to determine cl _{vt3d}
Kw	Interpolation variable used to determine cl _{w3d}
L	Fuselage length
Lbeta	Dihedral effect
LFL	Landing field length
Lp	Damping in roll
Lr	Rolling moment due to yaw
Lv	Distance from aircraft center of gravity to vertical tail quarter chord
M	Mach number, using a temperature of 75°F
Mq	Aircraft moment as a function of pitch rate
Mu	Moment due to compressibility effects
Mw	Moment due to vertical velocity
Mwdot	Moment due to vertical acceleration
n	Load factor
N _{1/2}	Number of cycles to half-amplitude
Nbeta	Weathercock effect
Nhalf_DR	Number of oscillations for the amplitude of the dutch roll mode oscillations to half
Np	Yawing moment due to roll
Nr	Damping in yaw
Omega_DR	Natural frequency of the dutch roll mode oscillations
Omega_roll	Natural frequency of the roll mode oscillations
Omega_spiral	Natural frequency of the spiral mode oscillations
P _{req}	Required turn power
P _{req}	Required maximum speed power
Q	Dynamic pressure
Rho	Density of air at sea level (altitude of contest site)
Rpm	Revolution per minute
S	Wing reference area
S _G	Takeoff ground roll , Landing ground roll
S _{ht}	Horizontal tail surface area
S _T	Horizontal distance during climbing to 15 feet

S_v	Surface area of the vertical tail
S_{vt}	Vertical tail surface area
Sweepvt	Sweep of the vertical tail quarter chord
Sweepw	Sweep of the wing quarter chord
T_{DR}	Period of the dutch roll mode oscillations
$t_{1/2}$	Time to half-amplitude
Thalf_DR	Time for the amplitude of the dutch roll mode oscillations to half
Thalf_roll	Time for the amplitude of the roll and spiral mode oscillations to half
TOFL	Takeoff field length
UAV	Unmanned air vehicle
U_o	Velocity
V_{cruise}	Velocity
V_h	Climb horizontal velocity
V_{max}	Aircraft maximum level speed
Volumefuse	Volume of the fuselage
V_{stall}	Design stall velocity
V_{TD}	Landing touchdown velocity
V_{TO}	Aircraft liftoff velocity
VTOL	Vertical take-off and landing
$V_{turning}$	Aircraft turning velocity
V_v	Best rate of climb
V_v	Vertical tail volume
W	Weight of the aircraft
$W/S)_{ms}$	Maximum speed wing loading
W_A	Accessory weights (batteries, control, etc.)
W_E	Estimated aircraft empty weight
Widthfuse	Average width of the fuselage
W_P	Specified payload weight
W_{TO}	Design aircraft takeoff weight
X_{CGload}	Loaded c.g. location
$X_{CGunload}$	Unloaded c.g. location
X_{np}	Neutral point location from a/c nose
X_u	Force in x-direction due to compressibility effects
X_w	Force in x-direction due to vertical velocity
Y_{beta}	Side force due to sideslip
Y_p	Side force due to roll rate
Y_r	Side force due to yaw rate
Z_u	Force in z-direction due to compressibility effects
Z_v	Distance from fuselage centerline to vertical tail aerodynamic center
Z_w	Force in z-direction due to vertical velocity

α_{0L}	Zero lift angle of attack
α_{Clmax}	Maximum lift coefficient angle of attack
ψ_{ins}	Instantaneous turn rate
α_{rot}	Angle of attack for takeoff rotation at sea level
ψ_{sust}	Sustained turn rate
$2\pi/\omega$	Period
γ	Best angle of climb
$\Delta\alpha_{Clmax}$	Delta maximum lift coefficient angle of attack
δ_r	Rudder deflection for one engine out case trim
δ_r	Rudder deflection for crosswind case trim
ζ	Damping ratio
μ_{TO}	Rolling friction coefficient
ρ_L	Density at landing altitude
ρ_{ms}	Density at maximum speed altitude
ρ_{TO}	Density at takeoff altitude
$\rho_{turning}$	Density at turning altitude
ω_n	Undamped natural frequency

TABLE OF CONTENTS

ACKNOWLEDGEMENT	i
SPONSORS	ii
NOMENCLATURE	iii
TABLE OF CONTENTS.....	vii
 1. EXECUTIVE SUMMARY	 1
1.1. Major Development Phase.....	1
1.2. Design Tools Overview	3
 2. MANAGEMENT SUMMARY	 4
2.1. Architecture and Assignment Areas of the Design Team.....	4
2.2. Management Structures and Timing.....	5
Figure 2.1 Network Representation of the Events of the Project.....	6
Figure 2.2 Gantt Chart of Project Phases.....	7
Figure 2.3 Gantt Chart of the Manufacturing Process	7
 3. CONCEPTUAL DESIGN.....	 8
3.1. Alternative Concepts Investigated	8
3.2. Design Parameters Investigated.....	8
3.2.1 Airfoil Selection for Wing and Tail.....	8
3.2.2 Wing Selection.....	9
3.2.3 Tail Selection	9
3.2.4 Engine Location.....	10
3.2.5 Wing Tips Selection.....	10
3.2.6 Landing Gear Configuration.....	11
3.3. Figures of Merit	11
3.3.1 Safety	11
3.3.2 Stability	11
3.3.3 Speed of Loading	12
3.3.4 Pilot Control.....	12
3.3.5 Ground Handling	12
3.4. Analytic Methods.....	12
3.4.1 Rubber Engine Sizing	12
3.4.2 Empty Weight Estimation Method	12
3.4.3 Estimation of Hp/W Ratio From Take-Off Distance Requirements....	12
3.4.4 Component Build-Up Method	13
3.4.5 Approximate Group Weights Method	13
3.5. Final Ranking of Figures of Merit	13
3.6. Final Configuration.....	13

4. PRELIMINARY DESIGN	14
4.1. Design Parameters Investigated	14
4.1.1 Wing Geometry	14
4.1.2 Wing Loading	14
4.1.3 Tail Geometry	14
4.1.4 Power Loading and Thrust-to-Weight Ratio	15
4.1.5 Fuselage Shape and Size and Specified Payload	15
4.1.6 Landing Gear Shape and Wheel Size	15
4.1.7 Payload Weight	15
4.1.8 Motor Location	15
4.2. Figures of Merit	15
4.2.1 Ease of Construction	15
4.2.2 Ease of Transportation	16
4.2.3 Structural Integrity	16
4.2.4 Payload Access	16
4.3. Analytic Methods	16
4.3.1 Aveox's Virtual Motor Test Stand	16
4.4. Preliminary Sizing and Key Features	16
4.4.1 Wing Shape and Sizing	17
4.4.2 Tail Shape and Sizing	17
4.4.3 Motor Size and Location	17
Table 4.1 Result of Aveox's Virtual Motor Test Stand	19
Table 4.2 Aircraft Geometry and Stability Parameters	19
Figure 4.1 E 407 Airfoil Published Data	20
Figure 4.2 Calculated C_L - α Curve	21
Figure 4.3 NACA 64 ₁ -012 Airfoil Published Data (C_l - α and C_m - α curves)	22
Figure 4.4 NACA 64 ₁ -012 Airfoil Published Data (C_d - C_l & C_m - C_l curves)	23
Figure 4.5 Weight Trade-off	24
5. DETAIL DESIGN	25
5.1. Final Performance Data	25
5.2. Final Stability and Control Analyses Data	26
5.3. Components Selection and System Architecture	27
5.3.1 Propulsion System	27
5.3.2 Control System	29
5.4. Drawing Package	30
Table 5.1 General Properties of ETi	31
Table 5.2 Weight Estimations	31
Table 5.3 Design Drag and Lift Performance Parameters	31
Table 5.4 Design Takeoff and Climb Performance Parameters	32
Table 5.5 Design Turning Performance Parameters	32
Table 5.6 Design Landing Performance Parameters	33
Table 5.7 Maximum Speed Estimations	33
Table 5.8 Stability Analysis Parameters	33
Table 5.9 Longitudinal Modal Characteristics	34
Table 5.10 Lateral/Directional Modal Characteristics	34

6. MANUFACTURING PLAN	35
6.1. Manufacturing Process Investigated.....	35
6.2. Figures of Merit	35
6.2.1 Applicability of the Process.....	35
6.2.2 Availability of Materials	36
6.2.3 Cost of Materials.....	36
6.2.4 Required Skill Levels.....	36
6.2.5 Ease of Machining the Materials	36
6.2.6 Required Time of Construction	36
6.2.7 Radio Frequency Reception.....	36
6.3. Final Selection of Manufacturing Process	37
6.4. Manufacturing Plan.....	37
6.4.1 Wing Construction.....	37
6.4.2 Tail Construction	38
6.4.3 Fuselage Construction.....	38
6.4.4 Landing Gear Construction.....	38
6.5. Manufacturing Timig.....	38
Figure 6.1 Manufacturing Progress	39
Table 6.1 Manufacturing Milestones	39
REFERENCES	40
APPENDIX A: COMPETITOR STUDY	41
Table A.1 Some VTOL-UAV Aircraft.....	41
Table A.2 Some UAV Aircraft.....	42
APPENDIX B: AVEOX'S VIRTUAL MOTOR TEST STAND	45
Table B.1 Test 1	45
Table B.2 Test 2.....	46
Table B.3 Test 3.....	47
Table B.4 Test 4.....	48
APPENDIX C: STABILITY ANALYSIS	49
Longitudinal Stability Analysis	49
Table C.1 Longitudinal Modal Characteristics.....	50
Table C.2 Nomenclature for Longitudinal Stability Calculations	51
Lateral / Directional Stability Analysis	52
Table C.3 Lateral/Directional Modal Characteristics.....	53
Table C.4 Nomenclature for Lateral/Directional Stability Calculations	54

1. EXECUTIVE SUMMARY

1.1. Major Development Phase

The ETİ, was first started as a student design project, for “AE-451 Aeronautical Engineering Design Course” offered in the 7th semester of the Aeronautical Engineering Department of Middle East Technical University. The idea behind this design was very much different from what came out from the workshop at the end. At first, this aircraft was designed to be a V/STOL aircraft test stand. The predecessor of the V/STOL configuration used in this design comes from the M.Sc. Theses of Research Assistants Aycahan Okan and Özlem Armutçuoğlu. They are still working on their theses and this design would be a test bed for their calculations and also for the new ideas proposed by us.

Initially, this aircraft was going to have tilted ducts, which would allow both vertical take-off and after tilting, horizontal flight. An auxiliary third engine was to be placed at the tail, which would provide both pitch and yaw control with the help of guide vanes at the exit of the vane of this auxiliary engine. The roll motion at hover was going to be provided with differential speed control of the engines. For the ease of control, manufacture and reduced cost constant pitch propellers were to be used.

After we heard about the DBF competition of the AIAA, we decided to enter the competition with the motivation and support of our instructors. This would be first in Turkey to attend an international competition in this field, which constitutes the highest point of technology. We know that many countries are well ahead of Turkey in this field, but by entering this competition we wanted to show that we are determined to come to the point where the others are. This gave us a great motivation. Even if we cannot achieve our goal, we will be an example to the others like us, who are determined to catch the technology level of the many other developed countries and also to prove that we are a strong country. All of us are determined to reach to the aims shown us by the founder of Turkish Republic, the savior, and the first leader, M. Kemal ATATÜRK. Our work is just a small stride in this effort. As he said in 1920's “The future is in the skies.”

Then, we started to modify our conceptual design according to the requirements of the design competition. We are very much troubled with the constraints of the design competition. At first, our V/STOL idea was irrelevant (in better words “too much”) for the requirements of the design competition. According to our calculations, we found out that the required power for vertical take-off operation is too much, which reduces the maximum effective operation time. There were also other crucial problems related with VTOL. Since we had to use constant pitch propellers, there would be a thrust-matching problem. Then came the question: Should we optimize the aircraft for VTOL or for cruise? If we optimized it for cruise, the generated thrust might not be sufficient for VTOL, or if it was sufficient, we would have redundant excess power, which could only be obtained with very powerful engines and, which in turn induces more loss of energy, more weight and less operation time. If we optimized the aircraft for VTOL, again the propeller setting wouldn't be suitable for cruise operation and would cause excessive

drag. What's more, the extra mechanisms required for V/STOL configuration like duct tilt actuator mechanism, extra bearings, links, a third electric motor, guide vanes and all the controllers and servos meant additional weight. Instead of this extra weight we could carry more cargo and make the aircraft less heavy. In conclusion, we decided to postpone the V/STOL idea for another competition. However, instead of changing the whole conceptual and preliminary design, we decided to use the same configuration, without any V/STOL mechanism. If we succeed in CTOL configuration, later we can modify the aircraft for V/STOL operation. So that we are planning to modify and advance this design in the near future (possibly after the competition.)

At first, we started the design by aiming to carry the maximum specified cargo weight of eight bottles. Later, in order to have a safe flight and improved flight performance, we decided to reduce the cargo to an optimum value of four bottles. By reducing the cargo by one half, the cross sectional area of the aircraft became half of the cross sectional area of the eight-bottled configuration, with our choice of cargo placement. For us, a safe success is more important than taking risk by trying to carry the maximum load.

The loading and unloading process was first to be from the aft body of the aircraft. But later we saw that, making the fuselage in two pieces, which can be attached and detached, would destroy the structural integrity and cause problems. Then we decided to make the loading and unloading from the nose, which is not very much important for the structural stiffness. What's more, since there are no controls and/or mechanisms in the nose, attaching and detaching is easier than that of the aft body mounted configuration.

Battery limitation was one of the greatest obstacles in our design. In order to minimize the power usage, many modifications were made to the original design. In order to reduce the power usage, horsepower-to-weight ratio (hp/W) had to be decreased. Any decrease in horsepower-to-weight ratio should be compensated, again, by a decrease in wing loading (W/S). In order to decrease the wing loading, we had to increase the wing area.

The basis behind the bi-plane wing configuration is that, since we have a limited span, which is further increased by the presence of ducts at the ends of the wing tips, we had to increase the wing area by some means. Some plausible solutions were;

- A wing with a very large chord,
- Tandem wing. One of the wings are placed to the fore-body and the other to the rear-body,
- Bi-plane configuration.

A wing with a very large chord would be very inefficient. Induced drag would be too high, and since we are short of power, this choice would cause an increased power requirement. So, we had to find a configuration, which will increase the effective wing area with a limited wing span, while keeping the aerodynamic wing efficiency, as high as possible. Tandem wing would be an answer to this, but this configuration has some problem associated with the control of the aircraft. The last choice was the bi-plane configuration. This configuration was used extensively during the first years of

aviation, and there are still many successful aircraft flying with this configuration. Also a previous successful design, which was flown in 1996/1997 DBF contest, inspired us in our decision. Finally, we decided on the bi-plane configuration.

1.2. Design Tools Overview

The main design tool employed for this project, especially at the conceptual and preliminary design phase is the book, "*Aircraft Design: A Conceptual Approach*" by Daniel P. Raymer, which is used as the textbook for the design course mentioned before (Ref. 1). Also some other reference was used for the assessment of the calculations. One of them is "*Airplane Design*" series by Jan Roskam, (Ref. 2) for performance calculations and justification of the results.

Our pilot and consultant provided us with the necessary information on manufacturing techniques and criticized our work and made positive suggestions. Also, our professors have always been in charge, controlled and assessed our work.

Computational methods used as design tools included the following software:

- AutoCAD R14 (Ref. 3)
- Aveox's Virtual Motor Test Stand (Ref. 4)
- Microsoft Excel (Ref. 5)
- Microsoft Word (Ref. 6)
- Matlab 5.2 (Ref. 7)
- Various airfoil analysis software

Ref. 4 was used to select the propulsion system for the aircraft. Various motor, battery, and propeller combinations were entered into this program to determine the effects of each parameter and their optimization for the ETI.

Personally developed spreadsheets in Ref. 5 were used throughout the conceptual and preliminary design phases. The first one was used to examine the tradeoffs between thrust-to-weight ratios, horse power-to-weight ratios, aspect ratios, and desired payload. This approach formed the basis of the initial sizing of the ETI.

In the stability and control analyses of the aircraft, modal characteristics for longitudinal and lateral/directional stability were examined by a Matlab program.

2. MANAGEMENT SUMMARY

2.1. Architecture and Assignment Areas of the Design Team

Our design team was organized such that the required task could be achieved as fast as possible. We had some difficulty in finding financial support for our design project. This problem is one of the reasons for the delay in the starting time of the manufacture. What's more, non-of us had a previous experience in such a group project, other than class projects. So the organization of such a team was not an easy task.

The team leader, Selim Solmaz, a junior Aeronautical Engineering major had no professional experience himself, other than his previous personal efforts in aircraft modeling and a great motivation in leading such a design team and carrying such a responsibility. He worked on the conceptual and preliminary design phases with Monir, during the early stages of the design. Selim's efforts in the design earned him the position of team leader. Ayca, a graduate research assistant in Aeronautical Engineering was in charge of organization of the meetings and ordering of materials. He was also the contact person for our design team. Özlem, another graduate research assistant in Aeronautical Engineering, who was also the teaching assistant for the design course AE-451, checked the conceptual and preliminary design made by Selim and Monir.

The number of team members increased, when we passed to the detail design phase. With the increased number of people, the progress of the project accelerated. All of the new team members together with the old ones shared the work of report writing and the manufacturing.

For the report, Selim worked on the executive summary and the management summary. Monir and Ramez worked on the conceptual design section. Also, Selim studied on the final form of the preliminary design section. Candaş and Ömer prepared the detail design section. Adem worked on the manufacturing section. And the final format to the report was given by Ömer.

Sedat, Murat, Ümit, Eray and Fatih worked mainly on the electric motor selection. They also made several analyses on Ni-Cad battery packages. Also they are concentrated on the implementation of the electrical systems and subsystems.

The final drawings were prepared by Özlem, Selim, Ömer and Candaş using Ref. 3.

The manufacturing was accomplished by the joint efforts of all team members.

2.2. Management Structures and Timing

Aycan and Selim organized the team together. Aycan usually did meeting arrangements. Because of the lack of experience, we had some difficulty in organizing the team and the working schedules.

Figure 2.1 shows the network representation of the events without schedule. A schedule of project completion deadlines decided by Selim is presented in Figure 2.2 and Figure 2.3. Since the manufacturing is not completed yet, the actual completion dates of the events cannot be displayed here. But when our current level of progress is considered, it seems that we can catch up with the deadlines. But a revision of the report will be made in a more complete form during the addendum phase.

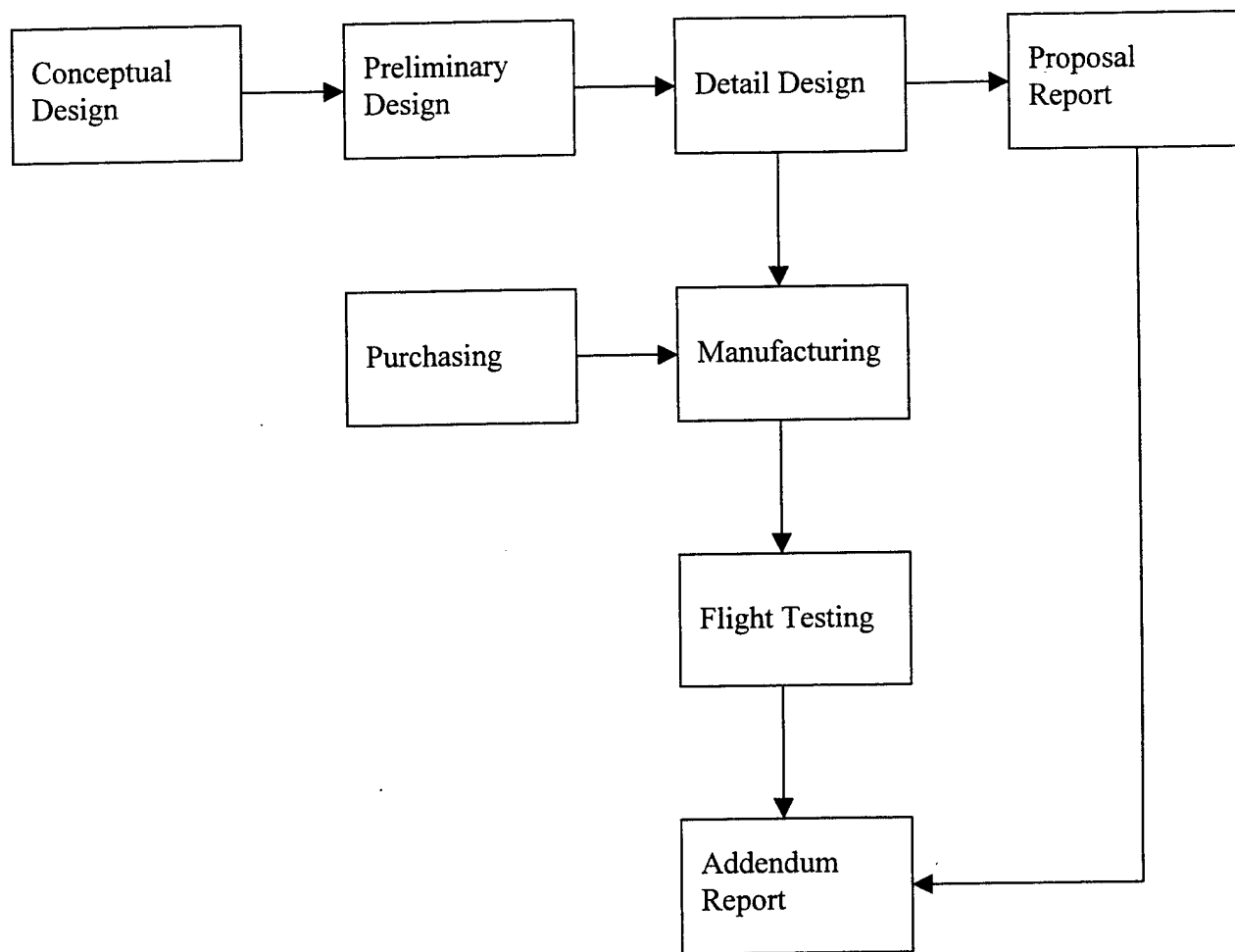


Figure 2.1 Network Representation of the Events of the Project

	February			March			April		
Purchasing									
Detail Design									
Manufacturing									
Proposal Report									
Addendum Report									
Flight Test									

Figure 2.2 Gannt Chart of Project Phases

Weeks	February	March				April
	4 th	1 st	2 nd	3 rd	4 th	1 st
Main Wing Assembly						
Tail Assembly						
Fuselage Assembly						
Final Assembly						
Flight Testing						
Modification						

Figure 2.3 Gannt Chart of the Manufacturing Process

3. CONCEPTUAL DESIGN

3.1. Alternative Concepts Investigated

Various alternative concepts were investigated during the conceptual design stage. More alternatives would provide greater opportunities for choosing a configuration, which has a better efficiency in performing the required mission.

Firstly, the team evaluated the V/STOL design concept. The V/STOL design included a single fuselage, a bi-plane wing, and an empennage located behind the wing. When looking at the concept, stability of the configuration was of most concern. A competitor study of some VTOL-UAV and UAV airplanes similar to the design, which was made during that stages, is given in Appendix A.

After examining the above design, a difficulty of finding an electric motor, which is able to perform VTOL capability, hindered the progress of the design. Consequently, the team decided on adopting the conventional take-off.

3.2. Design Parameters Investigated

The following design parameters were investigated during the conceptual design stage:

3.2.1. Airfoil Selection for Wing and Tail

Below, a number of wing airfoils are described considering Ref. 8 and Ref. 9, out of which the required airfoil is selected that satisfies the flight mission:

- E 403 is the airfoil of the *Phoebus sailplane* and it has a remarkably low drag.
- E 417 is another sailplane airfoil that has a longer laminar region on the upper surface, less drag and a more negative pitching moment coefficient when compared to E 403.
- E 604 has long ramps and a less concave pressure recovery on the upper surface. In addition it has a very low critical Reynolds number due to the very high thickness ratio.
- GA(W)-1 has maximum lift coefficient and its stall characteristics are generally gradual and of trailing-edge type when compared to many 65 series NACA airfoils.
- E 407 is a modernized version of E 403, it has the same low drag at low lift coefficient, less bubbles on the lower surface, and the upper end of the laminar bucket is higher. The moment coefficient, however, is slightly more negative.

Thus from the above mentioned characteristics of the airfoils, E 407 airfoil

seems to be best when compared to the previous airfoils, therefore it was chosen for the designed UAV aircraft. In fact the GA(W)-1 was a promising airfoil, however E 407 was chosen because of the Reynolds number penalty of GA(W)-1 airfoil.

In the case of tail airfoil selection, NACA 64₁-012 airfoil was selected. The basis for this choice is that, it has gradual stall characteristics, which are very important for a tail wing. Another reason is that, this airfoil can be used in the predicted Reynolds number spectrum.

3.2.2. Wing Selection

As have been mentioned before, a bi-plane wing configuration was chosen for this aircraft design. This type of wing geometry is considered when low structural weight is more important to the design than the aerodynamic efficiency, or when low speed is required without complicated high lift devices or excessive wing span. There is a reduction of 30% in drag due to lift for a bi-plane when compared to a monoplane of equal span.

3.2.3. Tail Selection

Conventional tail provides adequate control and stability at the lightest weight for most aircraft designs (Ref. 1). However the biggest drawback of the conventional tail is its poor spin recovery characteristics. Spin recovery requires adequate rudder control even at high angles of attack. For conventional tail geometry, the rudder will be blanketed with the wake of the horizontal tail surfaces. Shifting the horizontal tail forward or backward is necessary and this still cannot fully save the vertical tail from the wake.

Although T-tail has many drawbacks, spin recovery characteristics are good because of the fact that, the flow coming out of the horizontal tail surface does not intersect with the vertical tail surfaces. There is always uniform, fresh airflow coming to the vertical tail surfaces since they are situated at the tips of the horizontal tail. These advantages are accompanied with an increased structural weight and a stall recovery problem.

H-tail is used primarily to position the vertical tails in an undisturbed air during high angle of attack conditions or to position the rudder in the prop-wash on a multi-engine aircraft to enhance one-engine-out control. The H-tail is heavier than the conventional tail, but its endplate effect allows a smaller horizontal tail. Also for H-tail configuration, the area of each vertical tail that is attached to the tips of the horizontal tail is smaller than the area of a single vertical tail. With this configuration, the possibility of the tail to go into the turbulent wake of the wing is almost zero, which provides good stall recovery characteristics. In addition to that, the spin recovery characteristic of the H-tail is quite well.

For this design, H-tail arrangement was chosen because of the reasons stated

above. Another reason for this decision was that, none of the successful tilt-rotor concepts in the market was using a conventional tail arrangement.

3.2.4. Engine Location

The location of the motors affected various parameters of the aircraft such as wing configuration, size and shape of the fuselage. Although the upper wing tip was considered firstly, then the ducted propellers were located between the tips of the wings. This choice was made for many reasons that are listed below:

- Being at the tips of the wings, the electric motors are very close to the center of gravity (C.G.) location. This eliminates the problem of having an engine at the nose or tail, which creates moment about the C.G. location, and requires more aerodynamic force to balance.
- Since they are at the tips, they are not affected by the non-uniform flow around the fuselage, as would be the case with a pusher type of propeller configuration.
- Since the propellers are mounted between the upper and lower wings, they are structurally well supported. Also, being above the ground sufficiently, they are less susceptible to the rocks and debris coming from the ground. The lower wing and the ducts also help protecting the propeller and the motor.
- For multi engine aircraft, wing mounted engines are usually preferred. Wing mounting of engines reduces wing structural weight through a span loading effect, and reduces fuselage drag by removing the fuselage from the propeller wake.

In contrast to the above advantages, there are also some disadvantages. Wing mounting of engines introduces engine-out controllability problems that require an increase in the size of the rudder and vertical tail.

3.2.5. Wing Tips Selection

In the case of wing tips, different types are mentioned:

- Hoerner wing tip is a sharp-edged wing tip with the upper surface continuing the upper surface of the wing. The lower surface is under cut and canted.
- Winglet type wing tip offers lower drag than the Hoerner wing tip and almost equal increase in wing span.

Since there exist ducts at the end of the wing tips of this designed aircraft, the best wing tip type that can be used is the cut-off edge.

Actually, most of the new low-drag wing tips use some forms of sharp edge. In fact, even a simple cut-off tip offers less drag than a rounded-off tip due to the sharp

edge were the upper and lower surfaces end. Thus the wing tips of the designed aircraft are considered as the one with endplates. Endplate effect is only employed when the span must be limited. The presence of the duct at the tips creates the effect of an endplate, consequently there is less flow sweep and increased wing efficiency.

3.2.6. Landing Gear Configuration

The landing gear configuration had a direct effect on the ground handling characteristics of the aircraft. Landing gear configuration became an important parameter as the team realized that multiple take-off and landings would be a demanding part of the competition. In order to suit the design mission, a proper landing gear configuration is assigned. Hence, two types of landing gear arrangements were discussed and compared below:

- Tail-dragger wheel provides more propeller clearance, has less drag and weight, and allows the wing to generate more lift for rough-field operation. However this landing gear configuration is inherently unstable. If the aircraft starts to turn, the location of the C.G. behind the main gear causes the turn to get tighter until a ground loop is encountered, and the aircraft drags a wing tip, collapses the landing gear, or runs off the side of the runway.
- Tricycle wheel arrangement makes the aircraft more stable on the ground because the C.G. is ahead of the main wheel and can be landed at a fairly large crab angle. Also, tricycle gear arrangement improves forward visibility on the ground and permits a flat cabin floor for cargo loading (Ref. 2).

Therefore, for this design the most appropriate selection of the landing gear arrangement is the tricycle.

3.3. Figures of Merit

The figures of merit considered during the conceptual design phase were safety, speed of loading, stability, pilot control, and ground handling.

3.3.1. Safety

Throughout the conceptual design phase of ETI, safety is a primary concern of the team. Safety supports the mission feature of payload loading and unloading. Also a safety switch will be placed on the aircraft, which will provide safe ground maintenance.

3.3.3. Stability

Another feature of the figures of merit is the stability of the aircraft, which influences the ability of the aircraft to fly within its given mission. A stable aircraft is not only easier to fly but also easier to maneuver within the given course of flight. Thus being able to fly the course, the team could avoid any unnecessary penalties.

3.3.2. Speed of loading

Speed of loading is significant for minimizing the time spent on the ground between sorties. Speed of loading supports the mission feature of the ten-minute flight period. A good design is to be the one that could be loaded, unloaded, and flown as fast as possible during the competition.

3.3.4. Pilot Control

The pilot control was chosen as a figure of merit to support the mission feature of being able to satisfy the course of flight. In addition, pilot control plays a significant role during take-off and landings. When the safety of the team members, the audience, and the aircraft is considered during take-off and landings, the pilot control is vital.

3.3.5. Ground Handling

Ground handling is essential because the pilot needs to land within a specified area before the team members can approach the aircraft for reloading. This is because, it supports the repeated take-off and landings for cargo loading and unloading. In addition, a good ground handling ensures that the pilot would be more comfortable in the given 100-ft take-off distance limit.

3.4. Analytic Methods

During the conceptual design phase, two analytical methods were utilized in Ref. 1 and Ref. 2 had proven to be a solid starting point. In addition, it had been extremely helpful for this competition. For this design, the following methods are used:

3.4.1. Rubber Engine Sizing

This method is devoted to calculate the take-off gross weight of the aircraft. In this method, a relation between the gross weight of the aircraft and the empty weight fraction is estimated using Equation 6.1 of Ref 1.

3.4.2. Empty Weight Estimation Method

The empty weight fraction is calculated from the improved statistical equations given in Table 6.2 of Ref. 1.

3.4.3. Estimation of Hp/W Ratio From Take-Off Distance Requirements

This method is an approximate method for determining the ground roll distance, which can be taken the basis for estimating the horsepower to weight ratio. By using this method, a plausibly reasonable result was obtained.

3.4.4. Component Build-Up Method

This method estimates the subsonic parasite drag of each component of the aircraft using a calculated flat-plate skin friction drag coefficient and a component form factor that estimates the pressure drag due to viscous separation. The interference between the components was also taken into consideration. The subsonic parasite drag is given by Equation 12.24 of Ref.1, which includes sums both of miscellaneous drag, the leakage and protuberances drag, and the total.

3.4.5. Approximate Group Weights Method

This method is used considering Table 15.2 of Ref 1. In order to estimate both the total empty and gross weights of the aircraft from which the center of gravity (C.G.) is calculated. This method gives approximate values, which can be used as an initial data.

3.5. Final Ranking of Figures of Merit

After the analytical methods described helped to determine the final ranking of the figures of merit, the final ranking of the figures of merit is as follows:

1. Safety
2. Speed of loading
3. Stability
4. Pilot Control
5. Ground handling

3.6. Final Configuration

It is decided that the final configuration would include the following features:

- A bi-plane wing configuration
- One horizontal and two vertical tails (H-tail) behind the wing
- A single fuselage
- A tricycle landing gear configuration

A bi-plane wing configuration was felt to be the best configuration for the

reasons stated previously. It was also decided to have one horizontal and two vertical tails behind the wing in order to provide the necessary stability and control for ETI. A single fuselage was chosen in order to reduce drag and to consolidate the payload storage to one location on the aircraft. The tricycle landing gear was chosen to ensure that the aircraft would handle well without risks of ground loop or tip-over on the ground. Lastly, the aircraft was designed to be symmetric.

4. PRELIMINARY DESIGN

4.1. Design Parameters Investigated

The following design parameters were considered during the preliminary design study.

- Wing geometry
- Wing Loading
- Tail Geometry
- Power Loading and Thrust to Weight Ratio
- Fuselage shape, size and specified payload
- Landing gear type and size
- Payload access
- Motor location

4.1.1. Wing Geometry

In this stage of the design, wing parameters were studied to determine the best possible wing configuration for the aircraft. The wing section was decided before as E 407 properties of which is given in Figure 4.1. The wing aspect ratio affects the gliding, and stall characteristics of the aircraft. Since the wing has a low aspect ratio, it will stall at a higher angle of attack than a higher aspect ratio wing. In the same manner the taper ratio of the wing was included as a design parameter since it affects the lift distribution of the wing. As proven by Prandtl wing theory, minimum drag due to lift occurs when the lift is distributed in an elliptical fashion. However, the selected untapered wing geometry was chosen solely for the ease of manufacture, ignoring the loss of aerodynamic efficiency caused by the lateral distribution of lift over the plain rectangular wing. The calculated lift coefficient vs. angle of attack curve is given in Figure 4.2.

4.1.2. Wing Loading

Wing loading was examined, since it affects the handling characteristics of the aircraft such as stall speed, climb rate, take-off and landing distances, and turn performance. Wing loading has a strong effect upon size aircraft gross weight.

4.1.3. Tail Geometry

The tail airfoil NACA 64₁-012 was selected. The properties are given in Figure 4.3 and Figure 4.4. The stabilizing surfaces were located and sized for a better handling, less weight and a minimum possible drag. The choice and sizing of these surfaces depends on the historical trends and statistical data, instead of an optimization procedure.

4.1.4. Power Loading and Thrust-to-Weight Ratio

The thrust-to-weight ratio and the power loading were also considered to be design parameters. These two parameters directly affect the aircraft's performance. The thrust-to-weight ratio directly affects the take-off distance thus a careful calculation and selection was performed. The power loading, or power-to-weight ratio, was important because it affects the climb rate of the aircraft. Since aircraft should climb quickly after take-off, a high power loading was also necessary.

4.1.5. Fuselage Shape and Size and Specified Payload

The specified payload, and the fuselage size and shape were two closely related design parameters. The payload weight was an important parameter since it directly affects the wing loading. The wing loading directly affects the performance and handling characteristics of the aircraft. In addition, the shape of the bottles has an importance on deciding the fuselage shape and size.

4.1.6. Landing Gear Shape and Wheel Size

The landing gear shape and wheel size was one of the important components that must be defined as an aircraft layout. The landing gear properties must be selected in order to provide good handling characteristics on the ground and minimum drag.

4.1.7. Payload Weight

Since the payload weight is one of the major design parameters, trade-off studies were made in order to analyze its effect on the total weight of the aircraft. The resultant curves are given in Figure 4.5.

4.1.8. Motor Location

The motor location was decided considering the minimum interference between the fuselage and the propellers. The selection should keep the propellers well away from the turbulent wake of fuselage and wings, therefore increasing the propulsion system efficiency.

4.2. Figures of Merit

The figures of merit considered during the preliminary design phase were:

4.2.1. Ease of Construction

Ease of construction was a major consideration during the preliminary design phase. It was decided that, if complicated design had been applied for this competition, the time to be spent in detail design and manufacturing would be higher. Since the design group is inexperienced in modelling, a complex design would cause big trouble for them.

4.2.2. Ease of Transportation

Ease of transportation was a significant design parameter. This has an effect up on flight-testing. For flight testing, the aircraft should be transported from the workshop to the airfield and from the airfield to the workshop. In addition, the packing of the aircraft was of great concern, when the transportation of it from Turkey to the United States is concerned

4.2.3. Structural Integrity

A spar test will be conducted on each aircraft at the competition as written in the rules section. This test will include the lifting of the aircraft with one lift point at each wing tips to verify in adequate wing strength. So the aircraft had to lift its own weight when lifted as described above. Thus, structural integrity was a significant figure of merit.

4.2.4. Payload Access

The importance of the payload access shows itself during the operation of the aircraft. Since the mission period is limited, the payload should be easy to access with minimum risk.

4.3. Analytic Methods Used

Analytic tools were selected to determine the appropriate propulsion systems.

4.3.1. Virtual Motor Test Stand

Since only Aveox motors were evaluated, the Aveox website; <http://www.aveox.com> was accessed to find more information. On this page, Aveox offers their "*Virtual Motor Test Stand*" (Ref. 4). Although not quite extensive when inputs and outputs are concerned, this virtual motor test stand proved to be a valuable analytical tool.

Hence, several possible configurations for the motor, battery, and the propeller were input into the Aveox virtual motor test stand and comparison between the results was made, which was important in the selection of the appropriate motor. After several tests given in Appendix B, the results in Table 4.1 were obtained.

4.4. Preliminary Sizing and Key Features

The following sizing and key features are determined during the preliminary design phase and the results are tabulated in Table 4.2.

4.4.1. Wing Shape and Sizing

The wingspan was limited to seven feet by contest rules. In order to have more flexibility in changing the wing loading and the wing area, the bi-plane wing configuration was selected. The aspect ratio could also be arranged to control wing loading and the wing area. The taper ratio and wing sweep were the key features in determining the planform of the wing.

In this design, an untapered rectangular wing was chosen. Therefore the taper ratio was set to 1. This would decrease the cost of manufacture and result in an easy-to-built design.

Since the designed aircraft is a low-subsonic one, no sweep was given to the wing, which resulted in the rectangular planform of the wing. This decision was also dependent on the ease of manufacture of the rectangular wings.

Because of the advantages of positive dihedral on the stability of the aircraft, the bottom wing was designed to be with a two degree positive dihedral. It was considered on the bottom wing because, with the V/STOL configuration a straight top wing would allow a single shaft joining the two ducts passing through the wing. This configuration was kept, and it was assumed that the dihedral on the bottom wing would be enough when the stability is concerned.

Ailerons constituted 20% of the chord for 45% of the span of the upper wing and flaps weren't used because of the high lift coefficient provided by the airfoil selected. Percentage chord values came from the competitor study.

4.4.2. Tail Shape and Sizing

The horizontal tail size and location were estimated by performing required calculations. Running simple stability calculations to achieve a reasonable static margin while keeping the centre of gravity location on the main spar of the wing refined the parameters. The horizontal tail area was 1.929 ft^2 with its aerodynamic centre 2.5 feet behind the wing mean aerodynamic chord leading edge.

A similar method of performing required calculations for the vertical tail areas and locations was used to narrow down these parameters. The area of the each vertical surface was estimated as 0.67 ft^2 . The thickness of the horizontal and vertical stabilisers was determined by the aerodynamic considerations such as high stall angle-of-attack and a low parasite drag. NACA symmetrical 64-series sections were used on the tail surfaces, with a 12% thickness throughout the vertical and horizontal tails.

4.4.3. Motor Size and Location

The parameters of most concern when selecting the propulsion system were the power-to-weight ratio and the thrust-to-weight ratio. Since these values would ultimately determine climb rate and take-off distance, they were recorded for every case run in Ref. 4. These values also formed the basis of the performance calculations carried out during the detail design phase. Availability of the motor having the required

characteristic was another concern.

After examining several combinations and analyzing the power-to-weight and thrust-to-weight ratios, it became apparent that multiple motors would be required to achieve the performance demanded. This was partially due to the contest requirement of using only commercially available components in the propulsion system. Thus, the final decision concerning the propulsion system was to use propellers running on two Aveox motors powered by eighteen-cell battery packs.

Initially the ducts were to be placed at the tips of the top wing. But after considering the structural problems arising from connection of the ducts at a single point, the ducts were moved from the top wing to a lower position that is between the bi-plane wings. The two Aveox 1415/3Y motors were placed inside ducts located between the wing tips of the aircraft with their thrust lines located at the wing centerline. This placement allowed the elimination of having a heavy engine at the tip of the top wing, which creates more moment around the center of gravity (C.G.) location than the final selection.

The basis for using ducts was that, they eliminate the non-uniformity of the flow coming to the propellers and increase the propeller efficiency. Therefore the thrust could be increased further. Another advantage is that having a duct around propeller minimises the risk of an accident during ground operation, so that ground crew could work on the aircraft more safely. The risk of debris coming onto the propeller is also reduced by the presence of a duct around it.

Parameter	Value
Virtual Test Stand Inputs	
Open Circuit Voltage 1.25 Volts X 20 Cells (V)	25.00
Battery Resistance 0.0045 Ohms X 20 Cells (ohm)	0.0900
Speed Controller Resistance (ohm)	0.010
Motor Type	1415/3Y
Motor, Unloaded (rpm/V)	793
Motor Resistance (ohm)	0.045
Motor no-load current (amp)	1.2
Prop Type	Master Aircscrew
Propeller Constant	1.31
Propeller Diameter (in)	11.0
Propeller Pitch (in)	7.0
Gear Box	Planetary 3.7 to 1
Gear Box Ratio	3.70: 1
Outputs	
Prop RPM (rpm)	5223
Current (amp)	4.4
Voltage into Motor (V)	24.6
Power Input (W)	107
Power Output (W)	77
Efficiency of Motor Only	71.9%
Current at Max Motor Efficiency (amp)	25.6
Pitch Speed (mph)	35
Thrust at Pitch Speed (oz)	18

Table 4.1 Result of Aveox's Virtual Motor Test Stand (Ref. 4)

Parameter	Symbol	Value
Fuselage length (ft)	L	5.28
Wing surface area (ft ²) (for each wing)	S	5.67
Wing span (ft)	B	5.0
Horizontal tail surface area (ft ²)	S _{ht}	1.93
Horizontal tail length (ft)	b _{ht}	2.2
Vertical tail surface area (ft ²) (for each)	S _{vt}	0.67
Vertical tail length (ft)	b _{vt}	0.97
Unloaded C.G. location (ft) from the nose	X _{CGunload}	2.143
Loaded C.G. location (ft) from the nose	X _{CGload}	2.044
Neutral point location from a/c nose (ft)	X _{np}	2.284
Static margin	K _n	0.094

Table 4.2 Aircraft Geometry and Stability Parameters

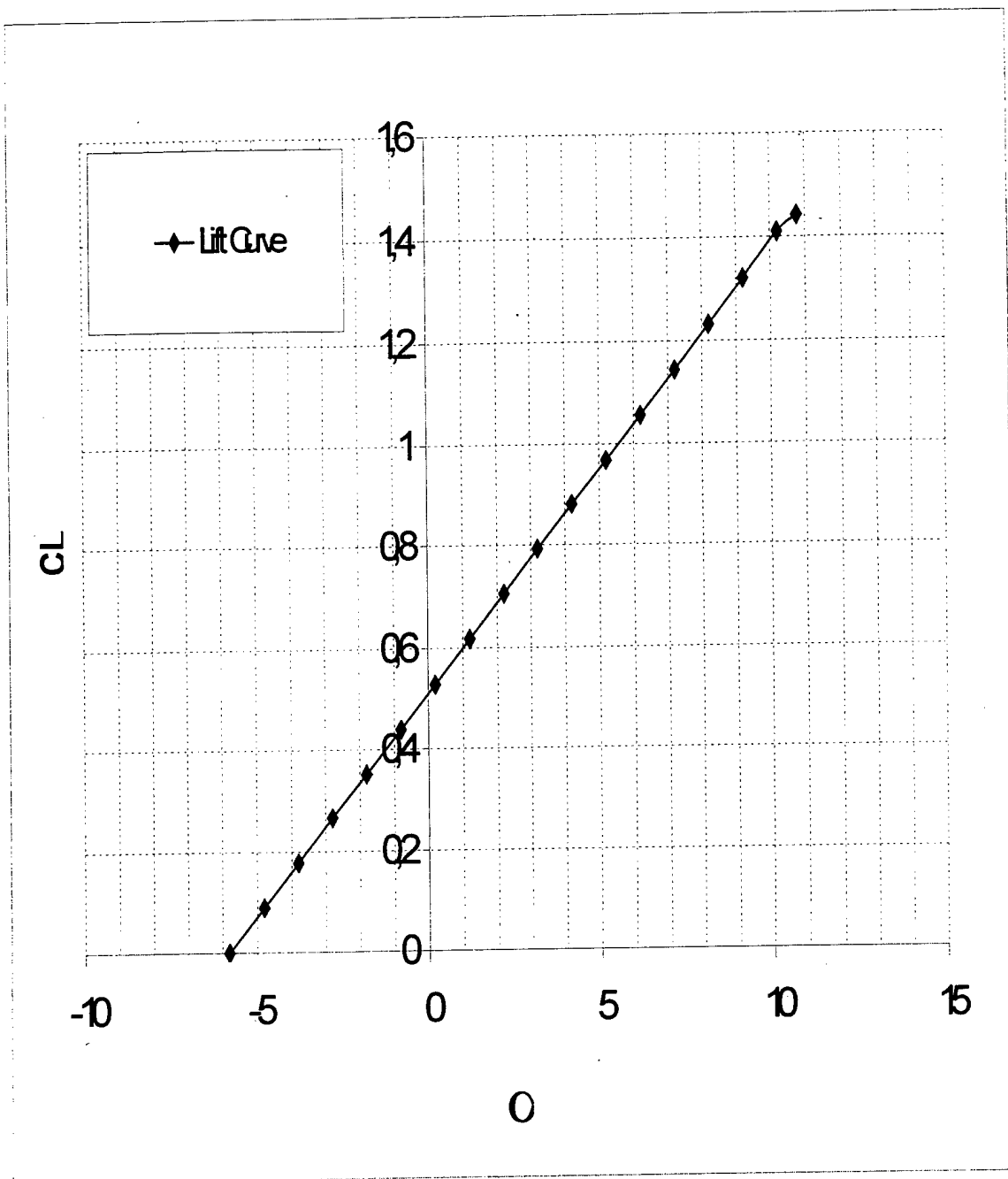


Figure 4.2 Calculated C_L - α Curve

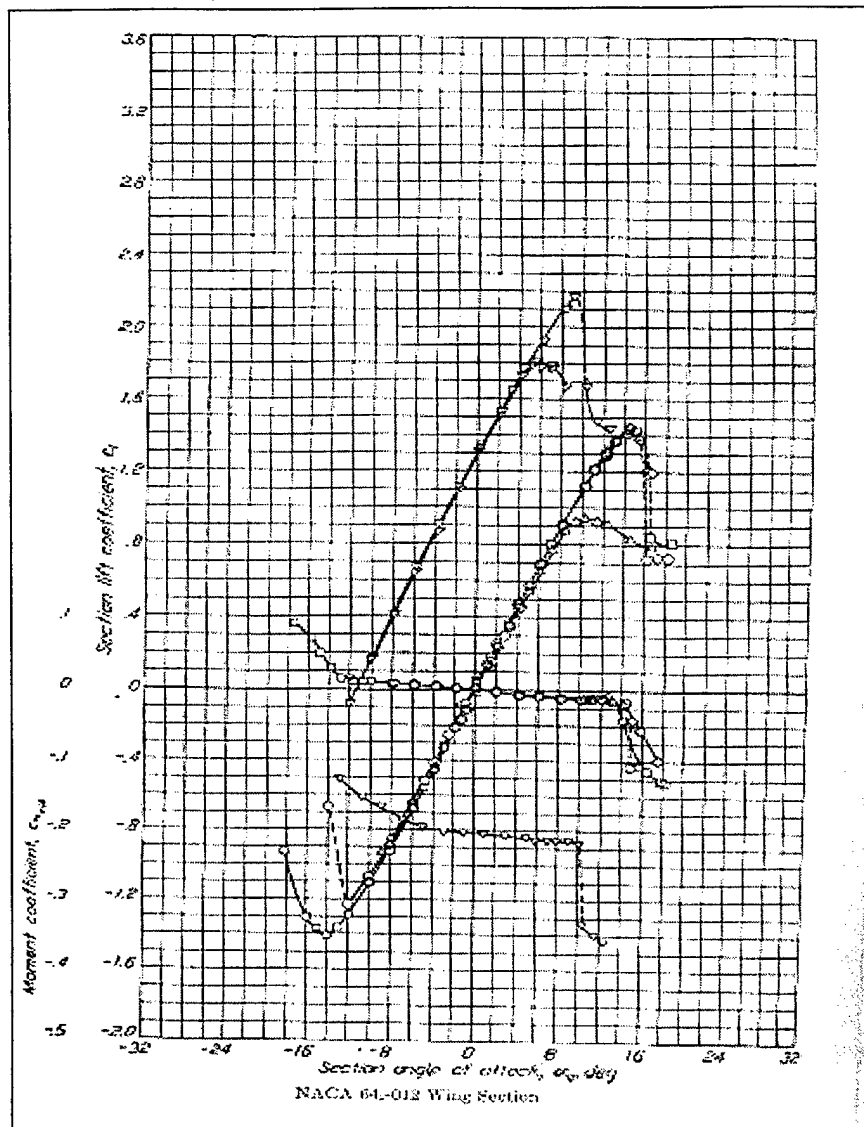


Figure 4.3 NACA 64₁-012 Airfoil published data (C_l - α and C_m - α curves) (Ref. 10)

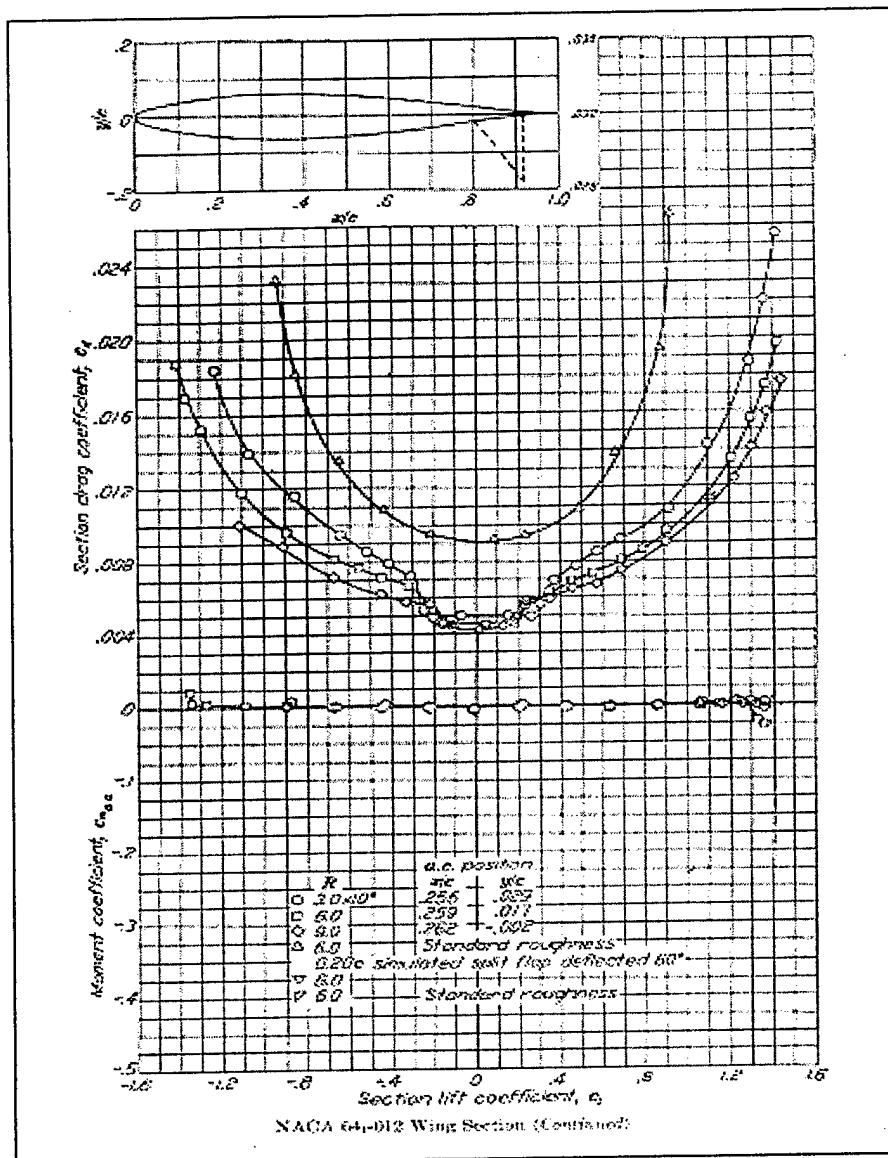


Figure 4.4 NACA 64₁-012 Airfoil Published Data (C_d - C_l & C_m - C_l curves) (Ref. 10)

Wo, We vs. Wpayload

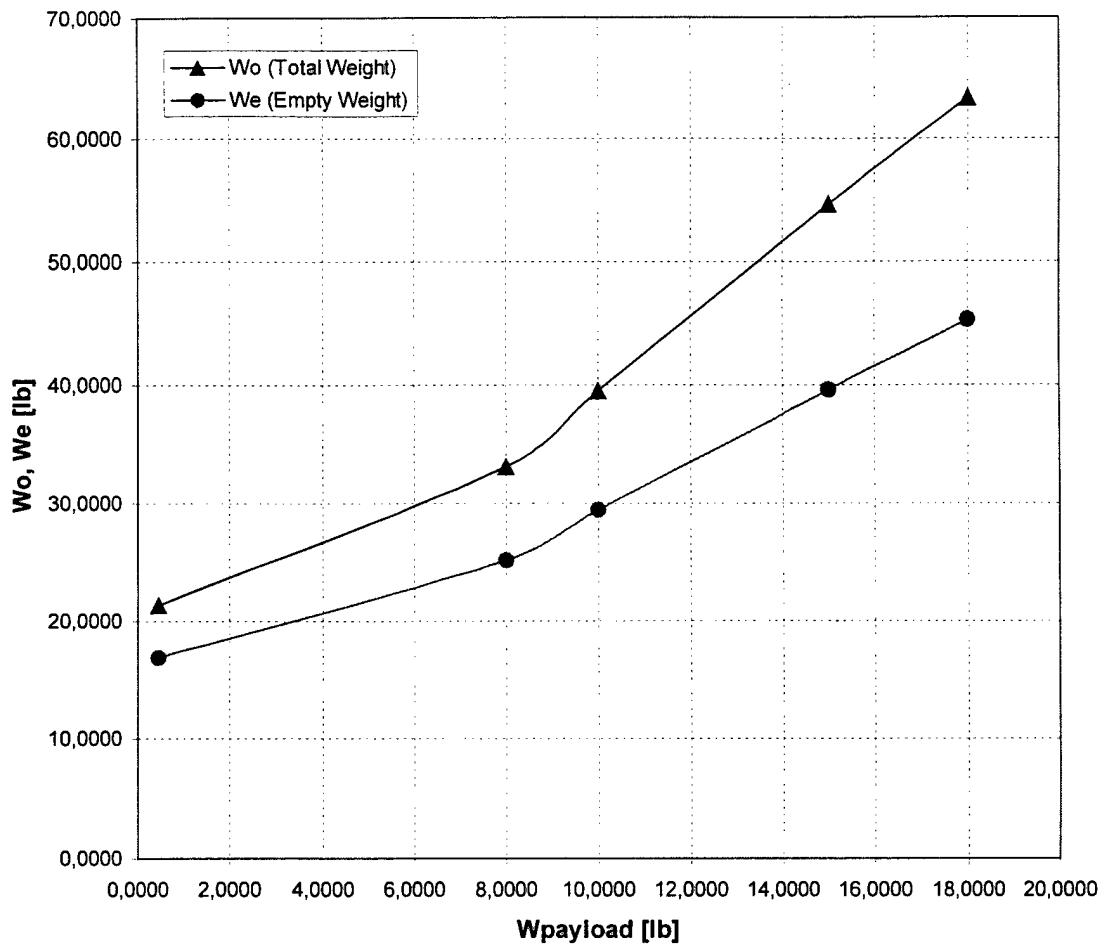


Figure 4.5 Weight Trade-off

5. DETAIL DESIGN

5.1. Final Performance Data

After several studies in the conceptual and preliminary design phases of ETI by using the methods discussed in Ref. 1, the final performance data given in Tables 5.1-5.6 were obtained.

As given in Table 5.1, the aircraft has a design takeoff horsepower to weight ratio of 0.0735 hp/lb, and wing loading of 4.5 lb/ft². With an estimated empty weight of 19 lbs including the batteries and carrying 4 bottles being 2.205 lb each as payload, ETI has a design payload fraction of 0.32 which are shown in Table 5.2.

As the drag and lift performance parameters indicated in Table 5.3, the design zero lift drag coefficient and the maximum lift coefficient of the aircraft were found to be 0.0261 and 1.44 respectively.

With the calculated lift-off velocity of 55.7 ft/sec and takeoff run of 79.6 ft (appropriate to short field takeoff requirement being 100 ft max.), it was seen that the takeoff performance estimation is satisfactory. For the climb performance, in order to get the aircraft from takeoff to an altitude about 100 ft, the best rate of climb was found as 24.5 ft/sec with a 10-sec motor run. The takeoff and climb performance data are given in Table 5.4.

In order to realize the complete 360° turn during the 'Short Field Cargo Sortie', the maximum power generated by the propulsion system being 2065.085 ft.lb/sec was sufficient. As shown in Table 5.5, a level 2.32-g turn with a 47.13 deg/sec turn rate was provided with that power value.

According to the landing performance data given in Table 5.6, the landing run was estimated to be 174.2 ft. Since no flaps were used in the aircraft structure, ETI is to be slowed down to the touchdown velocity of 55.7 ft/sec with decreasing power. If necessary, a drogue chute mechanism was planned to be used for braking. As the flight-testing is realised, the real landing distance and the slowing down procedure would be examined better.

During cruising around the course, a maximum speed of 181.7 ft/sec could be reached with a power value of 2065 ft.lb/sec. Since sufficient value of the lift could be achieved at this speed with zero degree angle of attack for wing sections used (Eppler E 407), the chord line of the biplane wing was constructed parallel to the centerline of the fuselage.

5.2. Final Stability and Control Analyses Data

According to the approach given in Ref. 1, longitudinal, lateral, directional stability analyses of ETI were performed. As given in Tables 5.8, the neutral point location and the static margin of the aircraft were found to be 2.284 ft and 0.094 respectively.

With the trim analysis, the rudder and elevator deflections for several cases were calculated. Since ETI was not supposed to operate at high angle of attack and has a H-tail, the spin recovery analysis was not performed.

As a result, all the stability criteria were satisfied showing that the aircraft would be able to cruise and manoeuvre around the course within the skills of the pilot.

Also, in order to analyze some important points of both longitudinal and lateral/directional stability of the aircraft, small perturbation theory given in Ref. 11 is used. MATLAB code was written to find modal characteristics of the ETI. The code itself is presented in Appendix C.

The longitudinal stability and control analysis is very important in order to determine the requirement of stability augmentation system (SAS). Phugoid (long period) and short period eigenvalues of the aircraft can be given as following;

$$\lambda_{1,2} = -0.012394 \pm 0.38862i \quad (\text{phugoid mode})$$

$$\lambda_{3,4} = -5.2735 \pm 4.7858i \quad (\text{short period mode})$$

where $\lambda_{i,j} = -\eta \pm wi$, $\eta = -\zeta\omega_n$, $\omega = \omega_n \sqrt{1-\zeta^2}$

$$\omega_n = \text{undamped natural frequency (rad / s)}, \quad \zeta = \text{damping ratio}$$

The period, time and number of cycles to half-amplitude, undamped natural frequency and damping ratio are readily obtained once the eigenvalues are known. They are tabulated in Table 5.9. It can be seen from the above eigenvalues, the linearized longitudinal equations are stable and the ETI behaves in a classical manner with short period and phugoid modes in the longitudinal direction.

The aircraft would be able to complete the course by the help of the flight experience of the pilot. Lateral/directional stability was investigated by using the approach given in Ref. 11 and Ref. 12. The values found from necessary calculations are given in Table 5.10.

5.3. Components Selection and System Architecture

5.3.1. Propulsion System

According to the propulsion requirements described below, the propulsion system is limited to an electric driven motor.

"The aircraft must be propeller driven and electrically powered with an unmodified, over the counter model, electric motor. Multiple motors and/or propeller may be used. They might be driven directly or with a gear or belt reduction. For safety, each aircraft uses a commercially produced propeller. The team may modify the propeller diameter by clipping the tip."

Some of the advantages of the electric driven motors can be listed as follows:

- Considerably lighter than an equivalent power gasoline engine.
- Very high RPM values can be obtained. Has more RPM than an equivalent power gasoline engine.
- Relatively simple. Since has less moving parts, it is more reliable.
- Speed control is achieved by changing the current, only.
- Since there is no fuel burnt, no weight change is observed during the flight. Hence, this makes the analysis of the flight far easier.

However, still there are some disadvantages of using electric drive. Such disadvantages are explained below:

- RPM values may be too high, so reduction may be necessary for optimum propeller performance, which in turn causes losses due to friction in reduction elements.
- Since the energy source is a pack of battery, the flight period will be in orders of minutes only (very limited). This is true, because the flight period is directly proportional to the number of batteries used.
- Very high power requires the usage of impractical motor size, which is not applicable always. So max power range is limited.

With these requirements and properties, the most important parameter for the choice was the power output of the engine. With a value of 1400 W for each, two Aveox 1415/3Y motors with 3.7:1 gear reduction were selected as the base of the propulsion system of ETI.

For the motors, thirty 2000 mA-h NiCad cells were sufficient. Also, an Aveox H-260 speed control rated for 8 to 18 cells was considered to operate each motor.

According to the battery requirements described below, with a single cell weight of 50 g, maximum 42 NiCad batteries that is enough for motor and the speed controller, could be carried.

"Over the counter NiCad batteries must be used. For safety, battery packs must have shrink-wrap or other protection over all electrical conduct points. The individual cells must be commercially available, and the manufactures label must be readable. (i.e. clear shrink-wrap is preferred). Maximum battery peek weight is 5.0 lb. Battery

pack must power propulsion and payload systems. Servos may be on a separate battery pack."

Each motor ran 11x7 or 11x8 wooden four-blade ducted propellers. The use of duct was decided after obtaining a significant difference from the results of *the linear momentum (Rendine-Froude) theory of propellers* given in Ref. 13, applied to ducted and unducted propellers. From Equations 3-7.3 to 3-7.11 of Ref. 13, it is found that the ducted propeller diameter is about "71 %" of that of the unshrouded propeller of equal static thrust.

This advantage in favour of the ducted fan will tend to be lost as forward speed builds up due to the increase in external drag of the duct nacelle. Nevertheless, the smaller diameter, combined with the enclosing presence of the duct itself, presents the possibility of significant reduction in noise, and containment of a shed blade.

A comparison of ducted and unducted propellers could be given as follows:

- For the same static thrust, static power, and static efficiency: $A_p = 2A_f$
- For the same static thrust, static power, and area: $M_p = \sqrt{2} M_f = 1.414 M_f$
- For the same static efficiency, static power, and area: $T_f = \sqrt[3]{2} T_p = 1.26 T_p$

where A_f is the ducted fan area, A_p is the propeller area, M is figure of merit or static efficiency, and T is the static thrust.

So, having a duct is far more advantageous than an unducted propeller. The drag penalty was eliminated by the fact that, our aircraft was a model one and it would fly at a comparatively low velocity.

The ducted propellers were considered to be at the tips of the biplane wing. Although it was planned that they would be at the tips of the upper wing firstly, for the structural strength and providing no need to an endplate at the lower wing, the ducts were placed at the interval between the wings. The motors would be placed just after the propeller, inside the duct. So, the airstream passing through the duct will provide enough cooling.

Although stated before, the advantages of the engines to be at the tips of the biplane wing could be listed as follows:

- The motors would be very close to the center of gravity location eliminating the problem of having a heavy engine at the tip or tail, which creates moment about the C.G. location.
- They would not be affected by the non-uniform flow around the fuselage as in the pusher type of propeller configuration.
- The propellers would be structurally well supported with being mounted between the upper and lower wings.
- Wing mounting of engines would reduce wing structural weight through a span loading effect, and reduces fuselage drag by removing the fuselage from the propeller wake.

Since the airflow coming into the propeller was not affected by the turbulent wake of the fuselage, it would automatically provide enough cooling rate for the elective motors. Also, since we don't have burning or similar reactions, heat dissipated will be less than that of a gasoline engine. So, probably, the cooling will not be a major concern for us.

5.3.2. Control System

For the aircraft ETI, JR PROPO X-3810 eight-channel SPCM/PPM selectable radio control system and JR PROPO NET72-FM transmitter was chosen because of some reasons. Firstly, it has satisfied the safety requirements of the competition, it features automatic fail-safe feature that can be selected in case of loss of transmit signal. Secondly, the control stick offer adjustable spring tension length and the throttle stick offers a ratchet for smooth travel. Also, this transmitter had a property named "mixing capability" which provides an option to use ailerons to act as spoilers. This option was important for our aircraft. Since, we have no flaps, we must use other techniques to decelerate quickly on the landing. So, we can use this option to increase the drag and decelerate the aircraft more quickly.

One receiver, with its own switch harness and battery pack, was used to provide control to the servos in the ETI. Receiver was connected to all ailerons, elevators, rudder and nose wheel steering.

In the mission, the recharging of the battery packs would not be allowed, so, combination of batteries was chosen as a one-cell 2000 mA-h battery pack. Four or six sorties were expected with this combination of batteries. Battery packs were combined to satisfy the needs of the receivers that were operating different number and size of servos.

Ball bearing supports was used between servos and the shafts to prevent the problems that can be occurred in handling qualities. Unless this support was made stiff enough, there could be problem between servos and the control surface link when aircraft was in the air.

The primary control surfaces of ETI were the ailerons (roll), elevator (pitch) and rudder (yaw). We have one servo for each aileron, one servo for elevator, one servo for rudder and one for the nose wheel steering, totally made five servos for all aircraft.

In all of the control surfaces Graupner DS 8201 Digital Precision servo was used. This was a microprocessor controlled, twin ball raced, high-performance servo with high-modulus plastic gearbox, JR low-profile plug, working with 4.8 V.

For elevators, this servo was chosen because of its small size providing a big advantage. Graupner DS 8201 has a torque of 48.6 ounce-inches and this was enough because elevators didn't need so much torque because of their 0.774 ft² wing area. Also, at the rudders, same servo was used. The speed of servos was 0.26 sec/60° and this was suitable to control the tail surfaces.

Aileron was controlled by the same Graupner DS 8201 servo. For 0.511 ft² ailerons, the torque and the speed provided by this servo was enough for controlling of ailerons.

Graupner DS 8201 Digital Precision servo was providing nose wheel steering. Another servo could be chosen to provide greater torque, but it would be very heavy when compared with the other servos of ETI to provide such greater torques.

5.4. Drawing Package

Final drawings of ETI were drawn with Ref. 3, and are presented in Autocad R. 14 format. The package includes the three-view drawing of the aircraft and several top, side and front views showing the dimensions, structures, propulsion and control systems, and payload. The drawings are given through Figure 5.1-5.7.

Parameter	Symbol	Value
Design takeoff horsepower to weight ratio (hp/lb)	hp/W	0.074
Design wing loading (lb/ft ²)	W/S	4.5
Wing aspect ratio	AR	4.5
Wing reference area (ft ²)	S	5.83
Wing span (ft) (excluding ducts)	b	5.2
Mean aerodynamic chord length (ft)	c	1.134
Design stall velocity	V _{stall}	50.6

Table 5.1 General Properties of ETI

Parameter	Symbol	Value
Specified payload weight (lb)	W_P	8.82
Accessory weights (batteries, control, etc.) (lb)	W_A	6.5
Design payload fraction (lb)	W_P/W_{TO}	0.32
Estimated aircraft empty weight (lb)	W_E	19
Design aircraft takeoff weight (lb)	W_{TO}	27.82

Table 5.2 Weight Estimations

Parameter	Symbol	Value
Design aircraft zero lift drag coefficient	C_{D0}	0.0261
Design aircraft maximum clean lift coefficient	C_{Lmax}	1.44
Design lift curve slope	$C_{L\alpha}$	0.088
Zero lift angle of attack (deg)	α_{0L}	-5.8
Maximum lift coefficient angle of attack (deg)	$\alpha_{C_{Lmax}}$	10.764
Delta maximum lift coefficient angle of attack (deg)	$\Delta \alpha_{C_{Lmax}}$	0.2
Design lift drag factor	K	0.088

Table 5.3 Design Drag and Lift Performance Parameters

Parameter	Symbol	Value
Aircraft liftoff velocity (ft/sec)	V_{TO}	55.7
Density at takeoff altitude (lb.sec ² /ft ⁴)	ρ_{TO}	$23.769 \cdot 10^{-4}$
Takeoff ground roll (ft)	S_G	79.6
Takeoff field length (ft)	$TOFL$	280.4
Rolling friction coefficient	μ_{TO}	0.04
Design takeoff horsepower to weight ratio (hp/lb)	hp/W	0.074
Design takeoff lift coefficient	C_{LTO}	1.44
Design takeoff drag coefficient	C_{DIO}	0.209
Best angle of climb (deg)	Γ	22.44
Best rate of climb (ft/sec)	V_V	24.5
Climb horizontal velocity (ft/sec)	V_h	59.4
Horizontal distance during climbing to 15 feet (ft)	S_T	200.8

Table 5.4 Design Takeoff and Climb Performance Parameters

Parameter	Symbol	Value
Aircraft turning velocity (ft/sec)	$V_{turning}$	82
Density at turning altitude (lb.sec ² /ft ⁴)	$\rho_{turning}$	$22.840 \cdot 10^{-4}$
Instantaneous turn rate (deg/sec)	ψ_{ins}	47.13
Sustained turn rate (deg/sec)	ψ_{sust}	60.27
Load factor	n	2.32
Required turn power (ft.lb/sec)	P_{req}	2065

Table 5.5 Design Turning Performance Parameters

Parameter	Symbol	Value
Landing touchdown velocity (ft/sec)	V_{TD}	55.7
Density at landing altitude (lb.sec ² /ft ⁴)	ρ_L	$23.769 \cdot 10^{-4}$
Landing ground roll (ft)	S_G	174.2
Landing field length (ft)	LFL	201.8
Rolling friction coefficient	μ_{TO}	0.04
Design landing lift coefficient	C_{LL}	0.074
Design landing drag coefficient	C_{DL}	1.44

Table 5.6 Design Landing Performance Parameters

Parameter	Symbol	Value
Aircraft maximum level speed (ft/sec)	V_{max}	181.7
Density at maximum speed altitude (lb.sec ² /ft ⁴)	ρ_{ms}	$21.570 \cdot 10^{-4}$
Maximum speed wing loading (lb/ft ²)	W/S_{ms}	4.5
Required maximum speed power (ft.lb/sec)	P_{req}	2065

Table 5.7 Maximum Speed Estimations

Parameter	Symbol	Value
Neutral point location (ft) from a/c nose	X_{np}	2.284
Static margin	K_n	0.094
Angle of attack for takeoff rotation at sea level (deg)	α_{rot}	13.14
Pitching moment coefficient (1/rad)	$C_{m\alpha}$	-0.475
Yawing moment derivative (1/rad)	$C_{n\beta}$	0.676
Rolling moment derivative (1/rad)	$C_{l\beta}$	-0.297
Rudder deflection for one engine out case trim (deg)	δ_r	6.126
Rudder deflection for crosswind case trim (deg)	δ_r	-0.437

Table 5.8 Stability Analysis Parameters

Parameter	Symbol	Value	
		Phugoid	Short Period
Time to half-amplitude (sec)	$t_{1/2}$	55.64	0.1308
Period (sec)	$2\pi/\omega$	16.168	1.313
Number of cycles to half-amplitude	$N_{1/2}$	3.442	0.0996
Undamped natural frequency (rad/sec)	ω_n	0.389	7.1213
Damping Ratio	ζ	0.03188	0.74

Table 5.9 Longitudinal Modal Characteristics

Parameter	Symbol	Value		
		Roll	Spiral	Dutch Roll
Time to half-amplitude (sec)	$t_{1/2}$	3.3202	37.194	10.756
Natural frequency (Hz)	ω_n	0.207	0.01855	1.4291
Number of cycles to half-amplitude	$N_{1/2}$			2.444
Period (sec)	$2\pi/\omega$			4.401
Damping Ratio	Z			0.044888

Table 5.10 Lateral/Directional Modal Characteristics

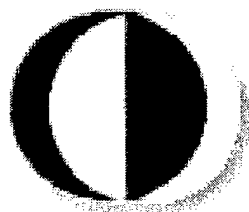


AMERICAN INSTITUTE OF
AERONAUTICS AND ASTRONAUTICS

**AIAA/CESSNA /ONR
STUDENT DESIGN/BUILD/FLY
COMPETITION**

ADDENDUM REPORT

“ Design of an Electric UAV Class Aircraft ”



METU - Team ETÝ

Middle East Technical University (METU), Ankara, TURKEY

04, April 2000

TEAM ETI

AIAA STUDENT DESIGN/BUILD & FLY COMPETITION

ADDENDUM REPORT

Designed and developed by,

Team Leader	:	Selim Solmaz
Consultant and Pilot	:	Ođuz Dođansoy
Team Members	:	Ömer Onur
		Canda° Bozkurt

Advisors

Aycan Okan
Özlem Armutçuoğlu
Adem Çalýk
Monir El-Farra
Ramez Bou-Dargham
Demet Fatma Ülker
Erdem Yavuzbalkan
Sedat Dođru
Murat Çat
Fatih Karakaya
Ümit Yusuf Ođrap
Eray Özçelik
: Prof. Dr. Ersin Tulunay¹
Dr. Mehmet Berif Kavsaođlu
Dr. Ozan Tekinalp²

¹ Professor, Department of Electrical and Electronics Engineering, METU.

² Assoc. Professor, Department of Aeronautical Engineering, METU.

ACKNOWLEDGEMENT

We would like to express our gratitude to our advisors; Prof. Dr. E. Tulunay, Dr. M. p. Kavsaoğlu, Dr. O. Tekinalp for their supervision, guidance, encouragement and patience during all the stages of this project.

We would also like to thank to Prof. Dr. N. Alemdaroğlu, chairman of the Aeronautical Engineering Department, for his encouragement

Finally, we would like to thank to our consultant and pilot Oğuz Doğanşoy for his invaluable guidance and help in modeling and manufacturing.

The conceptual and preliminary design studies of this aircraft were mostly performed as student projects in AE 451 "Aeronautical Engineering Design" course instructed by Dr. M. p. Kavsaoğlu at the Department Aeronautical Engineering, Middle East Technical University (METU) during the Fall Semester of 1999.

Detail design and manufacturing is being evaluated within the AE 452 "Aeronautical Engineering Design" course offered at the Department, currently, which is being instructed by Prof. Dr. N. Alemdaroğlu and Dr. M. p. Kavsaoğlu.

Additionally, we would like to thank to Research Assistant Utku Dincer for his useful ideas, great help and motivation.

It should also be mentioned that the facilities of the Aerospace Systems Simulation, Control and Avionics Laboratory of the Department of Aeronautical Engineering as well as Process Control Laboratory of the Department of Electrical and Electronics Engineering of the Middle East Technical University are used during the course of this project.

SPONSORS

This project is supported by the following persons and/or organizations:

An anonymous donation (\$ 3500)

Middle East Technical University (METU)

TÜBİTAK-BİLTEN (3 Tickets)

METU-EBİ

GEMSA Machine Industry Corp. (1 Ticket)

Turkish Petroleum Foundation (TPV) (1 Ticket)

METU Mustafa Parlar Foundation

AŞELSAN

TÜBİTAK-TİDEB

TABLE OF CONTENTS

ACKNOWLEDGEMENT	i
SPONSORS	ii
TABLE OF CONTENTS.....	iii
 7. LESSONS LEARNED	 56
7.1. Final Configuration.....	56
7.2. Areas of Improvement	57
Table 7.1 General Properties of ETŸ	58
8. AIRCRAFT COST.....	59
8.1. Rated Aircraft Cost	59
Table 8.1 Aircraft Cost Model	59
Table 8.2 Manufacturing Man Hours.....	60
8.2. Manufacturing and Component Price Lists	60
Table 8.3 Airframe Costs of ETŸ	61
Table 8.4 Propulsion System Costs of ETŸ.....	61
Table 8.5 Control System Costs of ETŸ	61
Table 8.6 Ground Support Costs of ETŸ	62
Table 8.7 Payload Costs of ETŸ	62
Table 8.8 Total Costs of ETŸ	62

7. LESSONS LEARNED

7.1. Final Configuration

Since we have less performance than we have expected from the aircraft given in the Proposal Phase of the competition report, some important design features were changed radically as following:

- *Ducts were removed.* Since the ducts have an important weight on wing tips, they increase empty weight of the aircraft. It was thought that using duct would increase the magnitude of thrust compared with unducted configuration. Also we have planned to prevent side wind effect to the propellers. However, after the manufacturing process, it was seen that the ducts became more heavier than expected because of the usage of two and/or three layers of fiber glass and epoxy. Additionally, ducts located on the wing tips affected roll maneuvering characteristics badly during the flight. Finally, removing the ducts was realized.
- *Engines were replaced.* After removing the ducts, engines were mounted to the middle parts of wing in order to decrease the length of the cable connecting batteries to the engines.
- *Biplane configuration changed to single wing.* After ducts had been removed from the wing tips, it was decided that single wing configuration would be used. Because of the removal of the ducts, we had a chance to extend up wing to 7 ft. This change gave an opportunity to get sufficient wing surface area for this aircraft. Also with removing down wing we could reduce empty weight of the aircraft.
- *Landing gears were relocated.* Nose landing gear was changed to tail landing gear configuration. To shift c.g. location forward, the main landing gear was shifted in forward direction. Additionally, the runway distance would decrease.
- *Horizontal and vertical stabilizers were reconfigured.* The H-tail configuration was changed to conventional tail configuration. To be able to increase the payload capacity of aircraft by decreasing the empty weight.

All modifications are shown in Fig. 7.1 through Fig.7.7.

The construction of 'ETV' developed faster than expected due to the team members' work with devotion strengthened with an amateur spirit. During the manufacturing process, some small modifications were made on the proposal design.

Blade number vs. propeller diameter trade-off study was done. The number of propeller blades was reduced to 2. Various tests were performed with different combinations of blade material, number of blades, as with gears and without gears. The following results were obtained:

- (3.7:1) Gear + 4 blade, 11×8 airscrew propeller → 4,300- 4,600 rpm.
- No Gear + 2 blade, 11×8 airscrew propeller → 9400 rpm.
- No Gear + 2 blade, 11×5 wooden propeller → 9600 rpm.
- No Gear + 2 blade, 11×7 Zinger propeller → 10,000 rpm.

The results showed that, as the gear-box is removed, the engine rpm and thrust increased. The 4-blade propeller configuration was changed to 2-blade configuration. This modification was done due to the undesired balance and vibration problems observed as the engine was operated at high rpm's, when the gear-box was removed.

Various types of propellers were tested in order to achieve best performance in thrust.

The properties of the final configuration of 'ETŸ' are given in Table 7.1.

7.2. Areas of Improvement

It was the first time for Middle East Technical University, participating in AIAA Design/Build/Fly competition. Thus, with the lack of experience, more complex configuration, i.e ducted propeller configuration was thought to be realized easily. Although design process showed that this type of aircraft could be produced, some serious problems occurred in manufacturing. As given in the Proposal Design report, the origin of the previous design was VTOL configuration. It was understood that simpler configurations were more suitable for this type of competition.

Simpler the configuration, lighter the aircraft. This is the general rule in aviation. With our new design as represented in Section 7.1, the empty weight of the aircraft was reduced quietly.

As given in section 7.1, ducts were heavier than expected after manufacturing process. With a lighter and smoother duct, the thrust advantage could be achieved effectively. To obtain more smooth surface on the ducts, advanced techniques in mould structures can be used. Firstly, producing mould of the duct can be achieved. Then using vacuum the final shape can be obtained.

By using tail gear configuration, the servo of the nose gear became unnecessary. The tail wheel was connected to the rudder directly by the help of the spring. So removing this servo decreased the weight of the aircraft.

After changing biplane configuration to single wing, the height of the fuselage was reduced by removing parts of the fuselage used in connecting bottom wing to the fuselage.

In the extension of the wing, extra parts were joined to the wing with an angle 7 degree in order to increase the gliding performance of the aircraft.

The extra parts for the wing were obtained from the bottom wing of the previous aircraft. The vertical tails of the previous H-tail configuration were used as the horizontal tails of the new aircraft. Only a new vertical tail for the conventional tail of the new configuration was produced. So not much extra time was spent on the new aircraft and this process cost not much.

The cooling fins were realized. In order to prevent the overheating of the Ni-Cad battery packages located in the fuselage, cooling fins were realized on the right and left sides of the front fuselage as shown in Fig. 7.4. By this way, one of the dominant sources of aircraft cost, Ni-Cad battery packages were prevented from damages.

Parameter	Symbol	Value
Wing Aspect Ratio	AR	6.155
Wing Reference Area (ft ²)	S	7.915
Wing Span (ft)	b	2.130
Mean Aerodynamic Chord Length (ft)	C	1.134
Fuselage length (ft)	L _f	5.572
Fuselage Width (ft)	W _f	0.361
Fuselage Height (ft)	H _f	0.777
Propeller Diameter (ft)	D _p	0.959
Aileron Span (ft)	b _a	1.903
Elevator Span (ft)	b _e	2.212
Vertical Tail chord length (ft)	c _{VT}	0.884
Horizontal Tail chord length (ft)	c _{HT}	0.880
Main Landing Wheel Diameter (ft)	D _{ML}	0.213
Tail Landing Wheel Diameter (ft)	D _{R.L.}	0.164

Table 7.1 General Properties of ETY

8. AIRCRAFT COST

8.1. Rated Aircraft Cost

The Rated Aircraft Cost model given in the Rules section can be tabulated as follows:

$$\text{Rated Aircraft Cost, \$ (Thousands)} = (A * \text{MEW} + B * \text{REP} + C * \text{MFHR}) / 1000$$

Coefficient	Description	Value
A	Manufacturers Empty Weight Multiplier	\$100 / lb.
B	Rated Engine Power Multiplier	\$1 / watt
C	Manufacturing Cost Multiplier	\$20 / hour
MEW	Manufacturers Empty Weight	Actual airframe weight, lb., without payload or batteries
REP	Rated Engine Power	# engines * 50A * 1.2 V/cell * # cells

MFHR	Manufacturing Man Hours	Prescribed assembly hours by WBS (Work Breakdown Structure). MFHR = Σ WBS hours
		WBS 1.0 Wing(s): 5 hr./wing. + 4 hr/sq. ft. Projected Area
		WBS 2.0 Fuselage and/or pods 5 hr/body. 4 hr/ft of length
		WBS 3.0 Empenage 5 hr.(basic) + 5 hr./Vertical Surface + 10 hr./Horizontal Surface
		WBS 4.0 Flight Systems 5 hr.(basic) + 1 hr./servo
		WBS 5.0 Propulsion Systems 5 hr./engine + 5 hr./propeller or fan

Table 8.1 Aircraft Cost Model

The calculations were made for the last configuration of the contest aircraft.

- *Manufacturers Empty Weight*

MEW = 7.143 lb

- *Rated Engine Power*

REP = # engines \cdot 50A \cdot 1.2 V/cell \cdot # cells = 2 \cdot 50 \cdot 1.2 \cdot 36 = 4320

- *Manufacturing Man Hours*

Coefficient	Value
WBS 1.0	5.1 + 4. (7.915) = 36.661
WBS 2.0	5.1 + 4. (5.572) = 27.288

$$\text{WBS 3.0} \quad 5 + 5.1 + 10.1 = 20$$

$$\text{WBS 4.0} \quad 5 + 1.4 = 9$$

$$\text{WBS 5.0} \quad 5.2 + 5.2 = 20$$

$$\text{MFHR} \quad \sum \text{WBS} = 36.661 + 27.288 + 20 + 9 + 20 = 112.949$$

Table 8.2 Manufacturing Man Hours

- *Rated Aircraft Cost*

$$\begin{aligned} \text{Rated Aircraft Cost, \$ (Thousands)} &= (\text{A. MEW} + \text{B. REP} + \text{C. MFHR}) / 1000 \\ &= (100.7143 + 1.4320 + 20.112.949) / 1000 \end{aligned}$$

$$\text{Rated Aircraft Cost, \$ (Thousands)} = 7.406$$

8.2. Manufacturing and Component Price Lists

The lists of the real prices of the aircraft components are given in Tables 8.3 - 8.8. The main sources for the total aircraft cost can be listed as; airframe, propulsion system, control system, ground support, and payload. The dominant ones were the propulsion and control system cost. The total cost for the ETY was \$ 3939. Although this was the first time for Middle East Technical University participating in such a competition. having aircraft cost lower than expected was a good point. This situation will be a good motivation for future studies.

Component	Cost (\$)
Wood for Airframe	120
Covering Material: Oracover (4 rolls)	61
Adhesives: Epoxy, Cyano, Contact Spray	56
Miscellaneous Hardware: Hinges, screws, etc.	40
Landing Gear	20
	297
Subtotal	

Table 8.3 Airframe Costs of ETY

Component	Cost (\$)
Motors: 2 x Aveox 1415/3Y	2 x 260
Speed Controls: 2 x Aveox H 260 up	2 x 195
Battery Packs: 2 x 18 Sanyo 2000 cells	735
Propellers: 2 x (11x7) Zinger (wooden)	2 x 5
Collets: 2 x Graupner (5 mm)	2 x 15
	1685
Subtotal	

Table 8.4 Propulsion System Costs of ET^Y

Component	Cost (\$)
Radio Control : JR Propo 10X PCM	1350
Aileron Servos: 2 x JR DS 8201	2 x 90
Elevator Servo: 1 x JR DS 8201	90
Rudder Servo: 1 x JR DS 8201	90
	1710
Subtotal	

Table 8.5 Control System Costs of ET^Y

Component	Cost (\$)
Propulsion Battery Charger: Graupner MC Ultra Duo plus II	200
Source Battery Charger: Yŷldŷrym 7 Amp 12 V DC Source	20

Tachometer: GloBee

25
245

Subtotal

Table 8.6 Ground Support Costs of ETY

Component	Cost (\$)
-----------	-----------

Water Bottles: 4 x Ülker-Çım Süt Milk bottles

2
2

Subtotal

Table 8.7 Payload Costs of ETY

Component	Cost (\$)
-----------	-----------

Airframe

297

Propulsion System

1685

Control System

1710

Ground Support

245

Payload

2

3939

TOTAL

Table 8.8 Total Costs of ETY

1999-2000
AIAA Design/Build/Fly
Competition Design
METU ETI

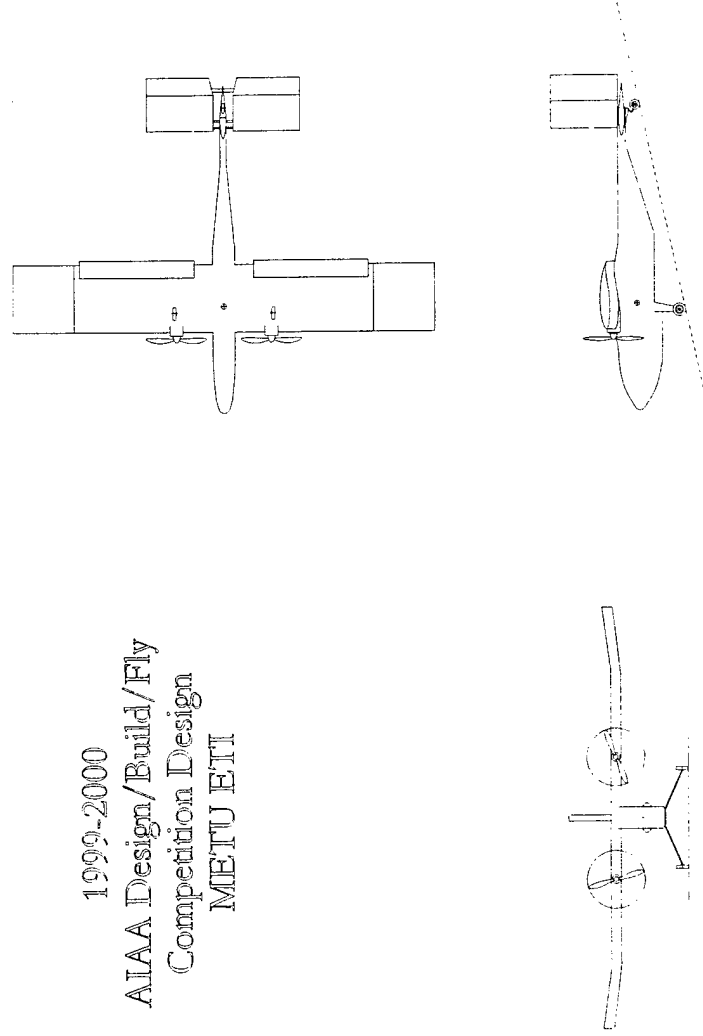


Figure 7.1

Three View

All units in inches

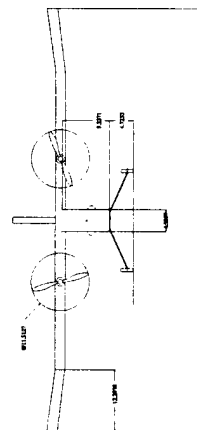
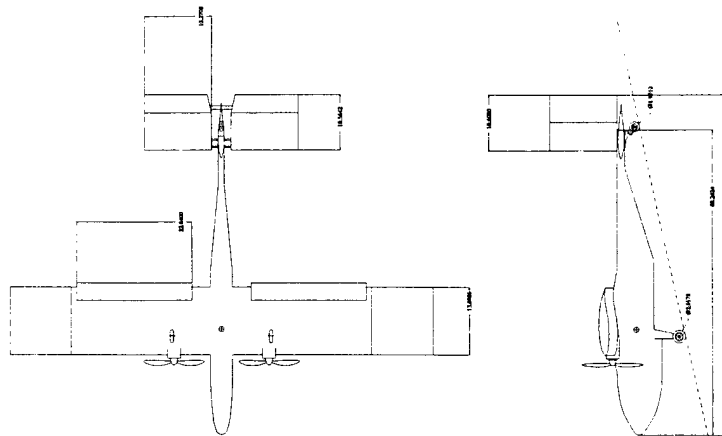
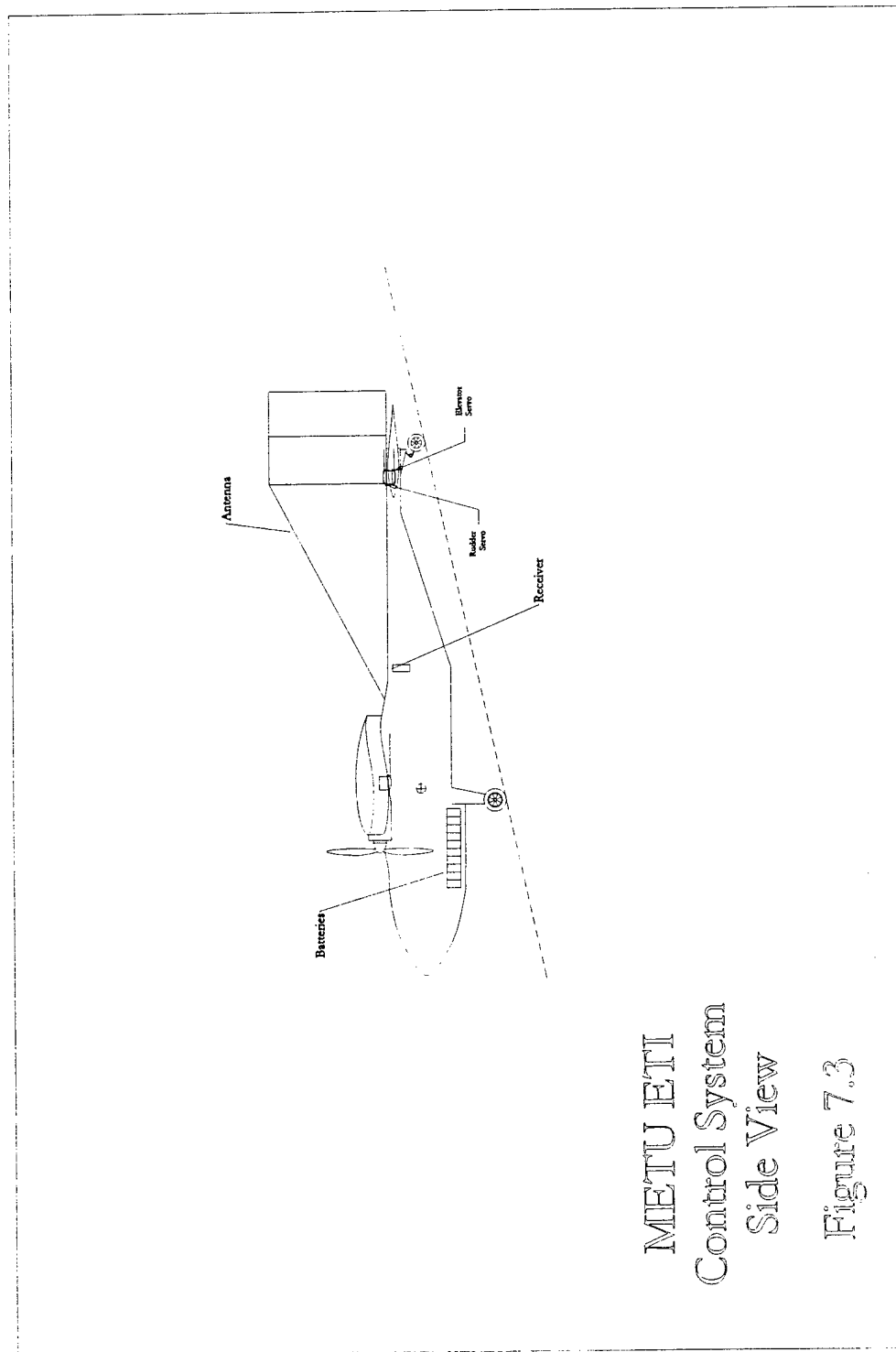
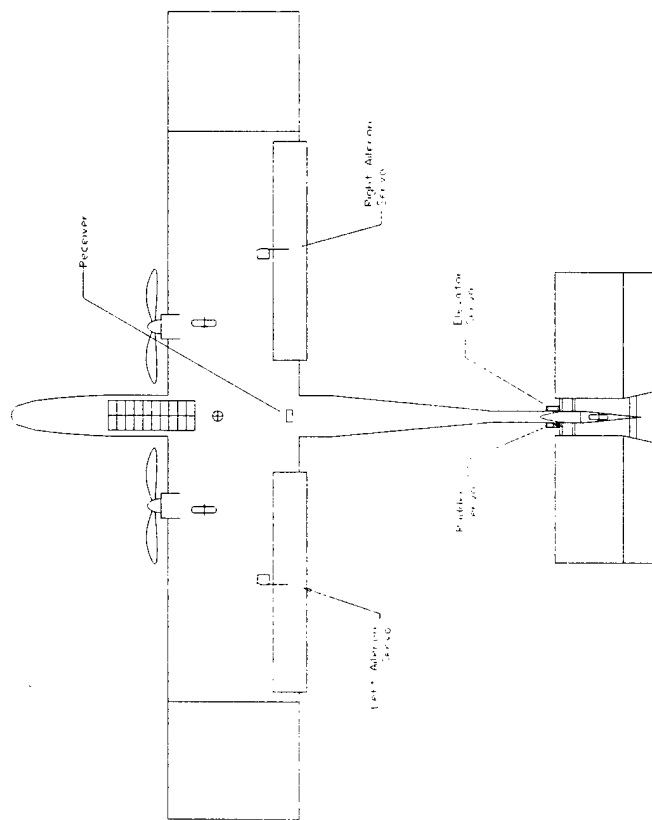


Figure 1

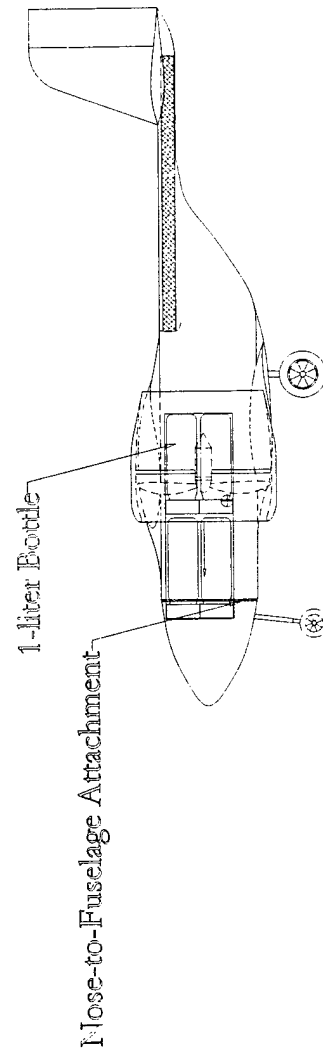


METU ETI
Control System
Side View
Figure 7.3



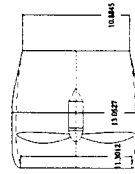
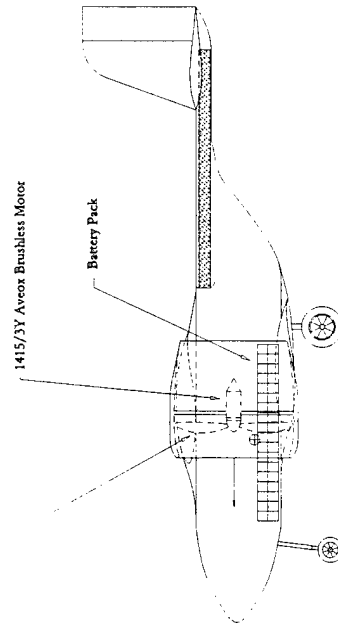
METU ETI
Control System
Top View

Figure 74



METU ETI
Payload Location
Side View
Figure 5.5

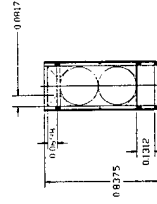
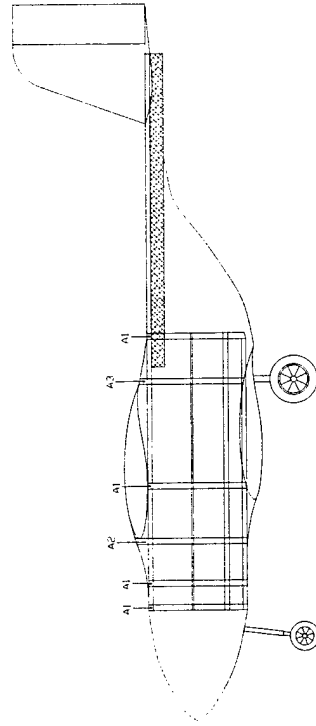
11 x 6 Propeller



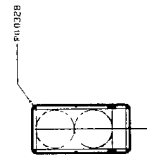
METU ETI
Propulsion System
Side View

Figure 5.6

METU ETI
Structure with
Cross-sections
Title View



A2



A1

Figure 5.7

1999-2000
AIAA Design/Build/Fly
Competition Design
METU ETI

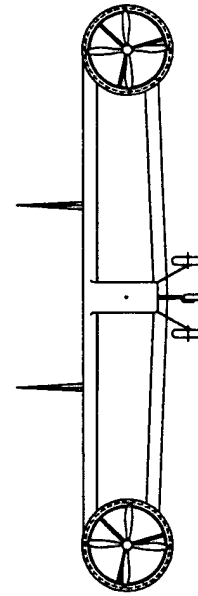
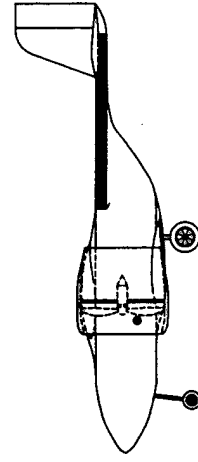
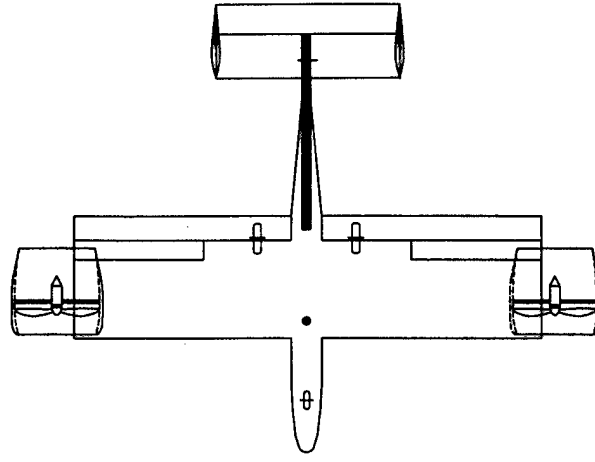


Figure 5.1

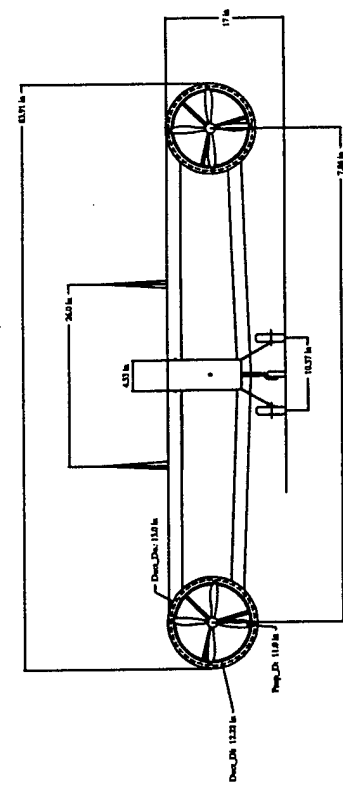
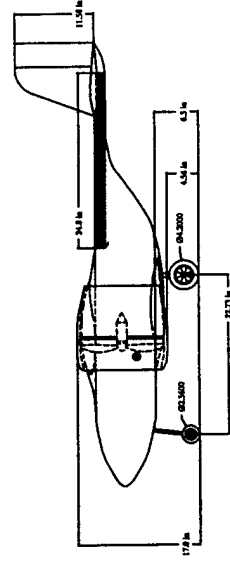
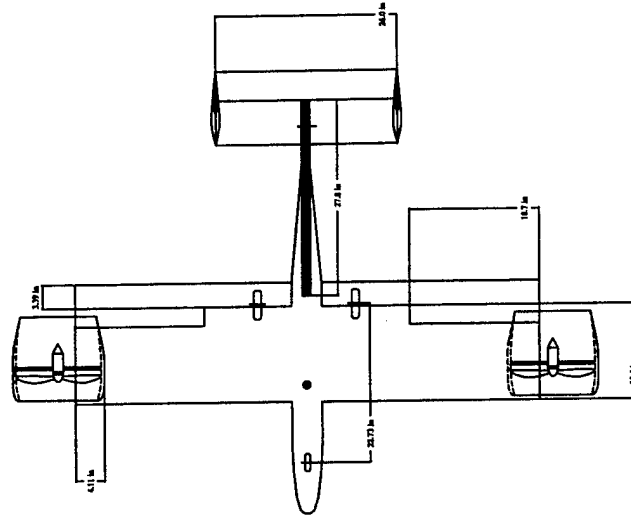


Figure 5.2

METU ETI Control System Side View

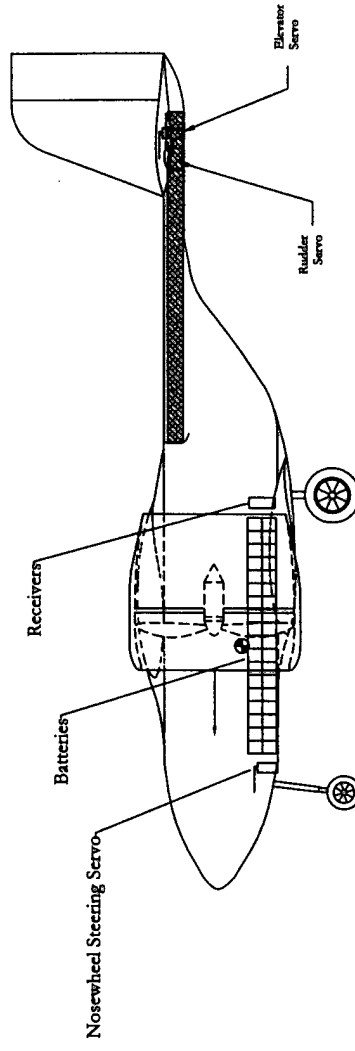
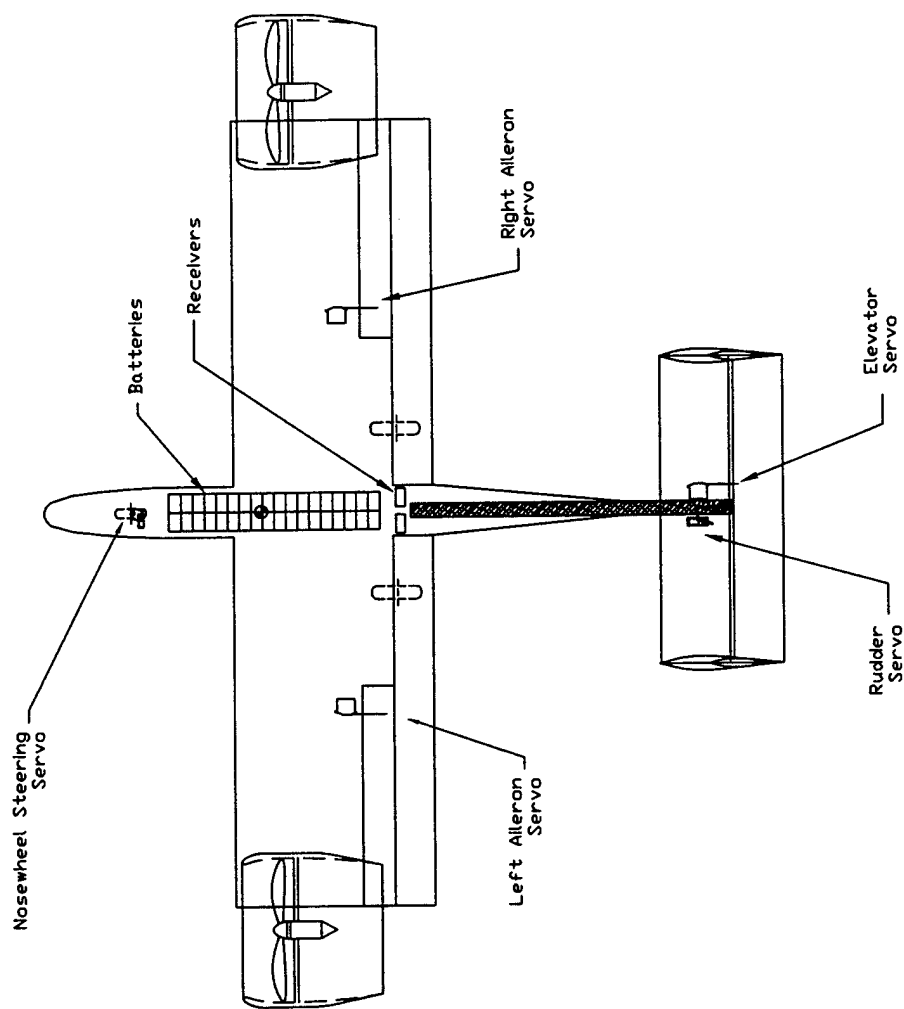
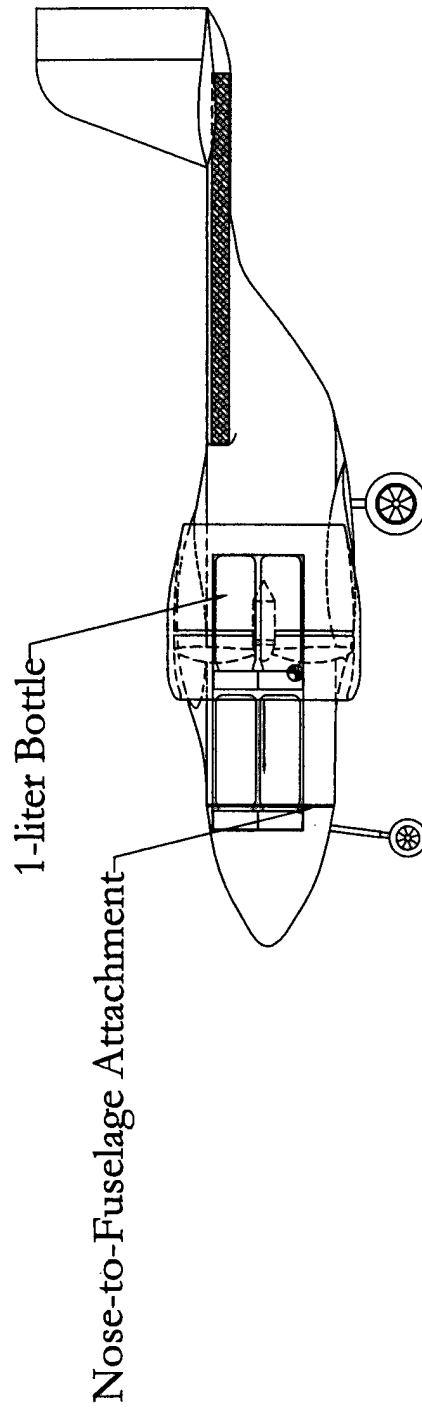


Figure 5.3



METU ETI
Control System
Top View

Figure 5.4



METU ETI
Payload Location
Side View

Figure 5.5

METU ETI Propulsion System Side View

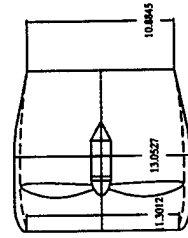
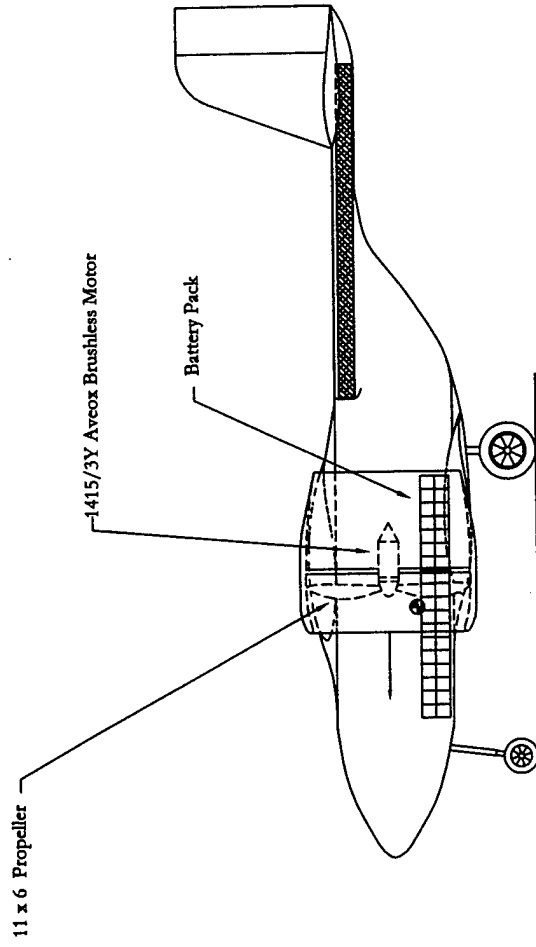
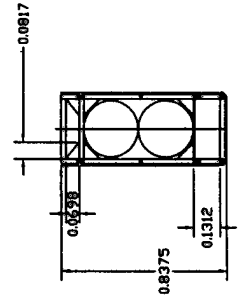
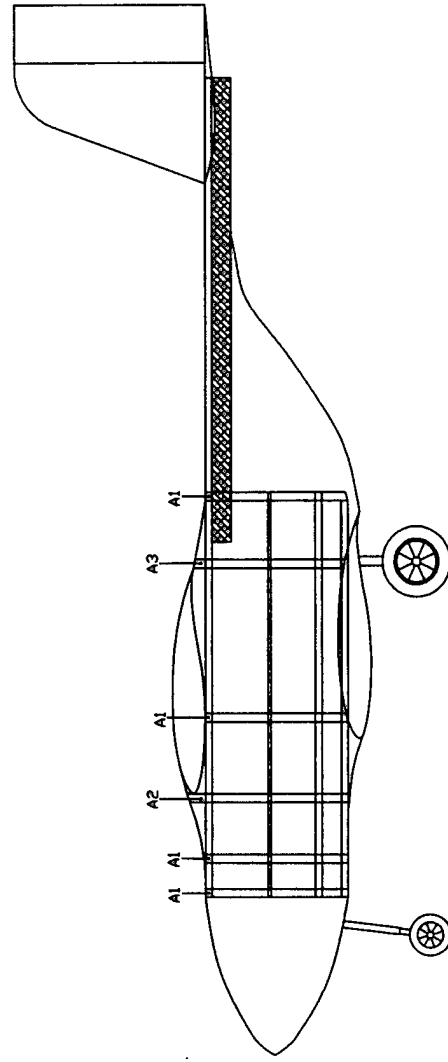


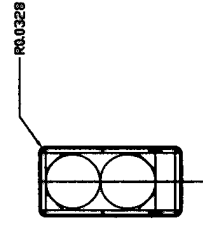
Figure 5.6

METU ETI Structure with Cross-sections Side View

Figure 5.7



A2



A1

6. MANUFACTURING PLAN

6.1. Manufacturing Process Investigated

Completing the design of ETI, the expected problem come to face, which is the manufacturing process type. Different kinds of manufacturing processes had been discussed, and for every part of the aircraft the best process was chosen considering the possible problems that can occur for this local part such as stall, local weight, any sudden impact etc.

As usual, for the construction of all structural parts, wood usage was considered. However, it is discussed and decided that this will cause some unnecessary usage and weight problems. In order to get rid of this problem balsa would be used. However, this manufacturing process needs some additional covering for the located weight parts like motor mounts, and this will again increase weight. The covering material could be plastic, fabric or metallic.

Secondly, foam core panel construction process was considered. By this manufacturing process, the main structural parts of the aircraft could be easily produced. Also, the difficulties of using spars, stringers etc could be rid of and rigid, strong and continuous structural components could be obtained.

Thirdly, aluminum was used for the basic structural lines, which will be loaded by stresses most. Machining aluminum blocks in CNCs would give perfect structural parts, which are stronger than wood.

Also, fiberglass construction process was considered. By this process, most of the structural components of the aircraft could be produced by forming fiberglass in suitable molds for different and complex parts. In some components, some of the manufacturing processes mentioned could be used by taking care of the materials.

6.2. Figures of Merit

The six figures of merit used during the manufacturing plan were:

6.2.1. Applicability of the Process

The manufacturing process chosen must be applicable to our case. This figure of merit puts the top limit to the manufacturing process. The tools and the technology available should satisfy the manufacturing process and the process must be applicable to reach the result.

6.2.2. Availability of Materials

The materials that are used in the manufacturing must be available. This figure of merit puts some limits on some structural parts and some electronic components. However, most of the structural parts are available in Turkey by means of companies that are importing such goods. The parts that are not available could be ordered from outside.

6.2.3. Cost of Materials

The most expensive parts of the aircraft were the propulsion and control system integration. Both were around 2600\$. Since the price of these systems is fixed, the expense of structural components must be kept at the minimum. Wood for this kind of aircraft would cost approximately \$100-\$150. The foam panels were the cheapest parts that were used in the manufacturing process. An estimation of \$400 to \$600 was given as the cost of an entire fiberglass airframe.

6.2.4. Required Skill Levels

Since the summer practice given in 2nd year of the Aeronautical Engineering Department of METU is modeling at Türkkuşu facility, all the team members have some skills about airplane modeling. One of the team members had advanced skills about using carbon fiber, balsa and fiberglass in modeling. Another one had some experience about machining that could be essential to machine the metallic parts of the structural components.

6.2.5. Ease of Machining the Materials

The handled material must be machined easily. Here, machining means both for metallic, wooden, composite and foam material, using a very hard metallic component could create some difficulties in machining and also using some sensitive materials also cause some problems since they can be broken very easily in the production.

6.2.6. Required Time of Construction

Because of some financial difficulties, materials were handled very late. Therefore the time for the wood construction was estimated approximately as 30 hours. Machining any aluminum part would be fast after making the drawings. The most of the time in production of fiberglass or carbon fiber is required for mold preparation.

6.2.7. Radio Frequency Reception

Finally, radio frequency reception is taken as a figure of merit. Since any radio frequency that is prevented or distorted by any metallic portion could cause danger for the airplane, too much use of aluminum in the structure was not considered.

6.3. Final Selection of Manufacturing Process

All of the figures of merit are considered and the final manufacturing process was decided. Out of the figures of merit, required time of construction was the most effective one in choosing the manufacturing process type. The main structural parts, such as wings, tail, were decided to be produced from foam by machining foam in CNC machines and to make the structure more stronger it is decided to cover foam with balsa. Steel was chosen to build the landing gears since it is strong enough in any strike. Carbon rod, which is used in tail structure of helicopter modeling, is used in tail assembly.

6.4. Manufacturing Plan

A time scheduling was put down for the manufacturing. All components were tried to be finished before its dead line shown in the schedule.

All construction and integration of the parts to main body were done by following the gannt chart given in Figure 2.3.

6.4.1. Wing Construction

The main structure of the wings was produced from foam and balsa covering the foam. And oracover is used to get the final configuration of the wings. For the main wings 0.05 kg/m^3 foam was used. In this process, first the template was produced and then the cores were cut. The general process in foam cutting is described below. More information can be get from Ref. 14.

"Hairs are wiped (produced by cutting the foam) from the edges of the foam. These are tough for the wire to melt through and can build up on the wire a major problem that the wire is tried to be traveled smoothly. Bottom template is positioned on the edge of the foam blank and secured with rivets. The cut is done from the leading edge to trailing edge. After the bottom surface is cut, hairs are wiped from both surfaces. When wiping the hairs it is taken care to not let the hairs boll up. Because, any ball is wiped across the surface, it rolls a through into the surface. Since the wire is cooler at the panel edges then the interior of the cut, it is seem that the foam is right up at the same level as the template near the template, but about half inch away, it is actually a little lower then the template surface because the wire is hotter and has melted a little more foam (i.e. the kerf is wider leading to over melt). Then by using a long sanding bar, the core bed and both edges of the core are flattened."

After all of this process, the foam was ready to be used as the wing structural part. Then, the foam was covered by 1.5 mm thick, 10x80 cm balsa sheets. The junctions of the balsa sheets were glued by using cyanoacrylate. Balsa sheets were attached to the foam by using Bison-Spray Adhesive. After gluing, the component was left under a heavy piece (around 440 lb) for a day to make the attachment stronger.

Finally, the wing components were trimmed with sand paper to create a polished surface. Some of the servos were put into the wing by cutting out some pieces from the wings.

By this manufacturing process, a more stronger, lighter and rigid components were produced. And a considerable time of production was saved since there was no need to consider any spars, stringers, stiffeners, ribs etc in manufacturing.

Also, since no flaps were used there was no need to consider any structural changes in the wings.

6.4.2. Tail Construction

Since the tail assembly was very similar to the wings (airfoil section), the same manufacturing process used in wing construction was employed for the tails. For the tail surfaces 0.05 kg/m^3 foam was used.

The control surfaces, elevator and rudder, were produced by cutting pieces from the tail surfaces. They were hinged to the main tail assembly and controlled by the linkages, which are controlled by the servos put into the tail boom.

6.4.3. Fuselage Construction

Balsa and plywood were the main materials used in fuselage construction. Fuselage was manufactured in box-shape. First six frames were cut from 1 mm plywood sheets. Then, four stringers were manufactured from wood and located to the top and bottom of the fuselage. Also four stiffeners were used to strength the structure. The sides, top and bottom of the fuselage were all covered with 1.5 mm balsa sheet. The nose was manufactured from foam and covered by epoxy.

6.4.4. Landing Gear Construction

After buying the landing gear system as a package, steal beams were used in connecting them to the fuselage. The beams were tightened to the fuselage by using steal wires. Also the junctions of the landing gear assembly and the fuselage were covered by epoxy.

6.5. Manufacturing Timing

Because of some problems occurred in handling the materials, the time left for manufacturing process of the ETI was so limited. Therefore, the construction process was needed to be completed so fast. It was started on February 21, 2000 and estimated to be finished on March 25, 2000. In the time that this report was written, the manufacturing process was still in progress. In 145 hours, the manufacturing of ETI was planned to be finished and a total of 65 hours was spent up to now. In Table 6.1 and Figure 6.1 the detailed data for the manufacturing process is given.

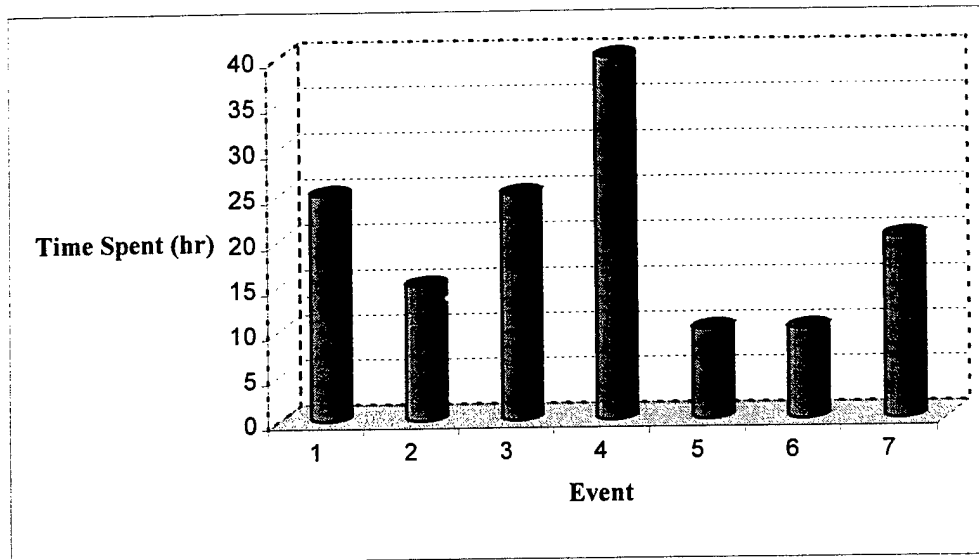


Figure 6.1 Manufacturing Progress

Event	Stating Date	Completion Date	Time Spent (hr)
1.Wing	2/25/00	2/28/00	25
2.Landing Gear	2/25/00	2/27/00	25
3.Enpannage Surfaces	2/25/00	2/27/00	15
4.Fuselage	3/16/00	In progress	40 (Estimated)
5.Component Joining	3/18/00	In progress	10 (Estimated)
6.Airframe Covering	3/19/00	In progress	10 (Estimated)
7.Propulsion, control, and radio system installation	3/17/00	In progress	20 (Estimated)
Complete manufacturing	3/25/00	In progress	145

Table 6.1 Manufacturing Milestones

REFERENCES

1. Raymer D. P., "*Aircraft Design: A Conceptual Approach*", AIAA Education Series, Second Edition, 1992.
2. Roskam J., "*Airplane Design*", Parts: 1-8, Roskam Aviation and Engineering Corporation, Second Printing, 1989.
3. AutoCAD Release 14.0, Copyright© 1982-1997, Autodesk, Inc.
4. Aveox's Virtual Motor Test Stand v2.03, Copyright©, 1999, Aveox Inc., <http://www.aveox.com/virtual.html>.
5. Microsoft® Excel 97, Copyright© 1985-1996, Microsoft Corporation.
6. Microsoft® Word 97, Copyright© 1983-1996, Microsoft Corporation.
7. MATLAB®, "The Language of Technical Computing", Version 5.2.0.3084., Copyright 1984-1998, The MathWorks, Inc.
8. Eppler R., "*Airfoil Design and Data*", Springer-Verlag, 1990.
9. Mc Ghee R. J. and Beasley D., "*NASA Report No:L-9132*".
10. Abbott I. H. and Von Doenhoff A. E., "*Theory of Wing Sections*", Dover Publications, 1949, 1959.
11. Nelson R. C., "*Flight Stability and Automatic Control*", McGraw-Hill Book Company, 1989.
12. Texas A&M University, Texas Flash Food Team (participant of the AIAA 98/99 DBF Competition), "*AIAA 98/99 DBF Competition Best Written Report*", 1999.
13. Archer R. D. and Saarlus M., "*Introduction to Aerospace Propulsion*", Prentice Hall, 1996.
14. CompuFoil Airfoil Plotting and Support Site, Foam Cutting Tutorial, <http://www.compufoil.com/howtofoam.htm>.
15. Editor-in-chief Jackson P. , Deputy editor Munson K., Editor emeritus Dr. Taylor J. W. R., "*JANE's All The World's Aircraft*".
16. "*Unmanned Vehicles Handbook*", Shephard.
17. Okan A., Tekinalp O., Kavsaoglu M. Ş., Armutcuoglu Ö. and Tulunay E., "*Flight Mechanics Analysis of a Tilt Rotor UAV*", AIAA Paper No: 99-4255, AIAA Atmospheric Flight Mechanics Conference and Exhibit, 9-11 August 1999.

APPENDIX A : COMPETITOR STUDY

Aircraft	Camcopter 5.1	Heliot	Tilt Rotor UAV
Country	Austria	Italy-France	USA
Accommodation	0	0	0
Payload Weight, W_p (kg)	25 ¹ (payload+fuel)	120	34 ¹ (payload+fuel)
Empty Weight, W_e (kg)	27	230	68.7
Fuel Weight, W_f (kg)	12.5 ²	100	17 ²
Take-Off Weight, W_o (kg)	52	450	102.7
Powerplant	Two-stroke petrol engine with rope starter	Hirth F30A26AK	3 two-cylinder, two-stroke, piston engines
Power (h.p.)	10	105	24
Wing Span (m)	-	-	3.2
Wing Area (m ²)	-	-	1.75
Wing AR	-	-	6
Cruising Speed (knots)	48.56	70	73.834
Stalling Speed (knots)	-	-	-
Wing Loading, W/S (lb/ft ²)	-	-	21.04
Power Loading, (lb/h.p.)	11.5	9.45	9.435
Service Ceiling (m)	-	1828.8	-
Take Off Distance (m)	0	0	0
Landing Distance (m)	0	0	0
Range (nm)	86.9	-	464.36
Rate of Climb (ft/min)	990	-	-

Table A.1 Some VTOL-UAV Aircraft

¹ The payload weights for Camcopter5.1 and Tilt-rotor UAV are assumed to be half of these values

² Assumed to be half of the "payload + fuel" weight, since not explicitly given.

Aircraft	Brevel	Half Scale UAV Trainer	Crecerelle
Country	France-Germany	USA	France
Accommodation	0	0	0
Payload Weight, W_p (kg)	-	4.5	35
Empty wt. W_e (kg)	-	12.7	45.4
Fuel wt. W_f (kg)	-	0.9	39.6
Take Off wt. W_0 (kg)	150	18.1	120
Powerplant	1 piston engine, Sachs SF 2/350	1x25cc single cylinder, 2-stroke engines	1 piston engine
Power (h.p.)	29.5	4.5	26
Wing Span (m)	3.4	2.5	3.3
Wing Area (m²)	-	-	-
Wing AR	-	-	-
Cruising Speed (knots)	81	80	135
Stalling Speed (knots)	-	-	-
Wing Loading, W/S (lb/ft²)	-	-	-
Power Loading (lb/h.p.)	11.22	8.89	10.19
Service Ceiling (m)	4000	-	3500
Take Off Distance (m)	-	-	-
Landing Distance (m)	-	-	-
Range (nm)	110	-	86.4
Rate of Climb (ft/min)	-	-	-

Table A.2 Some UAV Aircraft

Aircraft	Fox AT1 and AT2	Hellfox	Hermes 450s
Country	France	USA	Israel
Accommodation	0	0	0
Payload Weight, W_p (kg)	25	22.2	150
Empty wt. W_e (kg)	65	-	-
Fuel wt. W_f (kg)	25	-	-
Take Off wt. W_0 (kg)	115	105.8	450
Powerplant	1x Limbach L275E piston engine	1x Arrow A 400s reciprocating engine	Single rotor wankel
Power (h.p.)	22	45	52
Wing Span (m)	3.6	3.3	10
Wing Area (m^2)	-	-	6.9
Wing AR	-	-	14.5
Cruising Speed (knots)	97	125	70
Stalling Speed (knots)	-	-	-
Wing Loading, W/S (lb/ft²)	-	-	13.33
Power Loading (lb/h.p.)	11.52	5.3	19.04
Service Ceiling (m)	4000	4924	7000
Take Off Distance (m)	-	-	-
Landing Distance (m)	-	-	-
Range (nm)	135	54	-
Rate of Climb (ft/min)	-	1200	800

Table A.2 Continued

Aircraft	Mart Mk II	Micro V
Country	France	Israel
Accommodation	0	0
Payload Weight, W_p (kg)	25	8
Empty wt. W_e (kg)	81	-
Fuel wt. W_f (kg)	5	-
Take Off wt. W_o (kg)	110	45
Powerplant	1x TTL WAE 342-30A piston engine	Twin piston engines
Power (h.p.)	25	4
Wing Span (m)	3.4	3.6
Wing Area (m²)	-	-
Wing AR	-	-
Cruising Speed (knots)	48	90
Stalling Speed (knots)	-	-
Wing Loading, W/S (lb/ft²)	-	-
Power Loading (lb/h.p.)	9.7	25
Service Ceiling (m)	3000	5000
Take Off Distance (m)	-	-
Landing Distance (m)	-	-
Range (nm)	54	54
Rate of Climb (ft/min)	1083	1100

Table A.2 Continued

Note: The competitor study is based on Ref. 15, Ref. 16 and Ref. 17.

APPENDIX B : AVEOX'S VIRTUAL MOTOR TEST STAND

The following tests are evaluated using Ref. 4.

Virtual Test Stand Inputs	
Open Circuit Voltage 1.25 Volts X 20 Cells (V)	25.00
Battery Resistance 0.0045 Ohms X 20 Cells (ohm)	0.0900
Speed Controller Resistance (ohm)	0.010
Motor Type	1415/3Y
Motor, Unloaded (rpm/V)	793
Motor Resistance (ohm)	0.045
Motor no-load current (amp)	1.2
Prop Type	Master Aircsrew
Propeller Constant	1.31
Propeller Diameter (in)	11.0
Propeller Pitch (in)	7.0
Gear Box	Planetary 3.7 to 1
Gear Box Ratio	3.70: 1
Outputs	
Prop RPM (rpm)	5223
Current (amp)	4.4
Voltage into Motor (V)	24.6
Power Input (W)	107
Power Output (W)	77
Efficiency of Motor Only	71.9%
Current at Max Motor Efficiency (amp)	25.6
Pitch Speed (mph)	35
Thrust at Pitch Speed (oz)	18

Table B.1 Test 1

Virtual Test Stand Inputs

Open Circuit Voltage 1.25 Volts X 20 Cells (V)	25.00
Battery Resistance 0.0045 Ohms X 20 Cells (ohm)	0.0900
Speed Controller Resistance (ohm)	0.010
Motor Type	1415/3Y
Motor, Unloaded (rpm/V)	793
Motor Resistance (ohm)	0.045
Motor no-load current (amp)	1.2
Prop Type	Master Aircscrew
Propeller Constant	1.31
Propeller Diameter (in)	11.0
Propeller Pitch (in)	8.0
Gear Box	Planetary 3.7 to 1
Gear Box Ratio	3.70: 1

Outputs

Prop RPM (rpm)	5209
Current (amp)	4.8
Voltage into Motor (V)	24.5
Power Input (W)	117
Power Output (W)	87
Efficiency of Motor Only	74.3%
Current at Max Motor Efficiency (amp)	25.6
Pitch Speed (mph)	39
Thrust at Pitch Speed (oz)	18

Table B.2 Test 2

Virtual Test Stand Inputs

Open Circuit Voltage 1.25 Volts X 20 Cells (V)	22.50
Battery Resistance 0.0045 Ohms X 20 Cells (ohm)	0.0810
Speed Controller Resistance (ohm)	0.010
Motor Type	1415/3Y
Motor, Unloaded (rpm/V)	793
Motor Resistance (ohm)	0.045
Motor no-load current (amp)	1.2
Prop Type	Master Airscrew
Propeller Constant	1.31
Propeller Diameter (in)	11.0
Propeller Pitch (in)	7.0
Gear Box	Planetary 3.7 to 1
Gear Box Ratio	3.70: 1

Outputs

Prop RPM (rpm)	4712
Current (amp)	3.8
Voltage into Motor (V)	22.2
Power Input (W)	83
Power Output (W)	56
Efficiency of Motor Only	67.6%
Current at Max Motor Efficiency (amp)	24.3
Pitch Speed (mph)	31
Thrust at Pitch Speed (oz)	15

Table B.3 Test 3

Virtual Test Stand Inputs

Open Circuit Voltage 1.25 Volts X 20 Cells (V)	22.50
Battery Resistance 0.0045 Ohms X 20 Cells (ohm)	0.0810
Speed Controller Resistance (ohm)	0.010
Motor Type	1415/3Y
Motor, Unloaded (rpm/V)	793
Motor Resistance (ohm)	0.045
Motor no-load current (amp)	1.2
Prop Type	Master Airscrew
Propeller Constant	1.31
Propeller Diameter (in)	11.0
Propeller Pitch (in)	8.0
Gear Box	Planetary 3.7 to 1
Gear Box Ratio	3.70: 1

Outputs

Prop RPM (rpm)	4702
Current (amp)	4.1
Voltage into Motor (V)	22.1
Power Input (W)	91
Power Output (W)	64
Efficiency of Motor Only	70.3%
Current at Max Motor Efficiency (amp)	24.3
Pitch Speed (mph)	36
Thrust at Pitch Speed (oz)	14

Table B.4 Test 4

APPENDIX C : STABILITY ANALYSIS

Longitudinal Stability Analysis

Code Written in Matlab

```
% Inputs

% Aircraft properties (ETI)
%
% S = Wing Area [ft2] , cbar = mean aerodynamic chord [ft] ,
% amass = mass [slug] , Iyy = Pitch Axis Inertia [lb.ft2] ,
% grav= gravitational acceleration [lb/ft2] ,
% AR=Aspect Ratio, e=Oswald Efficiency Factor

S=7.5; cbar=1.134; grav=32.2; amass=27.82/grav;

Iyy=0.92; Rad2Deg=57.29578; AR=4.5; e=0.8;

% Aerodynamics (found from Design Study)

CLalpha=5.042; CDalpha=0.241; CDCLS=1/(pi*AR*e);

CMalpha=-0.47445; CMq=-9.465; CMalphadot=-4.278;

CL0=0.3784; CD0=0.0261; Cm0=0.12; CDu=0.0; CLu=0.0024;

% Aircraft cruise flight conditions
%
% Vcruise=[ft/s] and Altitude=h=[ft]
% At these conditions, the air density can be found easily as follows:
% Air Density=Ro=[slug/ft3]

Vcruise=82.021; h=2000; Ro=0.002213;

% Dynamic Pressure, Q=[lb/ft2]

Q=0.5*Ro*Vcruise^2; QS=Q*S; QScbar=Q*S*cbar;

% The longitudinal derivatives can be estimated from the
% following formulas in Table 4.2 of Ref. 2.

% U-Derivatives
Xu=-(CDu+2*CD0)*QS/(Vcruise*amass);
Zu=-(CLu+2*CL0)*QS/(Vcruise*amass); Mu=0;

% W derivatives
Xw=-(CDalpha-CL0)*QS/(Vcruise*amass);
Zw=-(CLalpha+CD0)*QS/(Vcruise*amass);
Mw=(CMalpha*QScbar)/(Vcruise*Iyy)

% Wdot derivatives
Xwdot=0; Zwdot=0;
Mwdot=(CMalphadot*cbar/(2*Vcruise))*QScbar/(Vcruise*Iyy);

% q derivatives
Xq=0; Zq=0;
Mq=(CMq*cbar*QScbar)/(2*Vcruise*Iyy);

% Substituting the numerical values of
```

% the stability derivatives into equation 4.51 of Ref. 2.,
 % The stability matrix can be obtained as follows:

```
A=[Xu Xw 0 -grav; Zu Zw Vcruise 0; Mu+Mwdot*Zu Mw+Mwdot*Zw
Mq+Mwdot*Vcruise 0; 0 0 1 0];
```

```
eigenvalues=eig(A)
```

Output of the Matlab Code

$$A = \begin{bmatrix} -0.041125 & 0.10825 & 0 & -32.2 \\ -0.59813 & -3.9928 & 82.021 & 0 \\ 0.014841 & -0.2989 & -6.5377 & 0 \\ 0 & 0 & 1 & 0 \end{bmatrix}$$

$$\lambda_{1,2} = -0.012394 \pm 0.38862i \quad (\text{phugoid mode})$$

$$\lambda_{3,4} = -5.2735 \pm 4.7858i \quad (\text{short period mode})$$

where $\lambda_{i,j} = -\eta \pm wi$, $\eta = -\zeta\omega_n$, $\omega = \omega_n\sqrt{1-\zeta^2}$

$\omega_n = \text{undamped natural frequency}$, $\zeta = \text{damping ratio}$

The period, time and number of cycles to half-amplitude are readily obtained once the eigenvalues are known.

Phugoid (long period)	Short period
$t_{1/2} = 0.69/ \eta $, $t_{1/2} = 55.645s$	$t_{1/2} = 0.69/ \eta $, $t_{1/2} = 0.1308s$
Period = $2\pi/\omega$, Period = 16.168 s	Period = $2\pi/\omega$, Period = 1.313 s
$N_{1,2} = t_{1/2} / \text{Period}$, $N_{1,2} = 3.442$	$N_{1,2} = t_{1/2} / \text{Period}$, $N_{1,2} = 0.0996$
$\omega_n = 0.389 \text{ rad/s}$	$\omega_n = 7.1213 \text{ rad/s}$
$\zeta = 0.03188$	$\zeta = 0.74$

Table C.1 Longitudinal Modal Characteristics

Note: The longitudinal stability analysis study is based on the approach given in Ref. 11.

Symbol	Description
V_{cruise}	Velocity (ft/s)
W	Weight of the aircraft (lb)
g_{rav}	Gravitational Acceleration (ft/s ²)
a_{mass}	Aircraft Mass (slugs)
S	Surface area of the wing (ft ²)
AR	Aspect ratio of the wing
c_{bar}	Mean aerodynamic chord (ft)
CD_u	Drag coefficient due to compressibility effects
CM_u	Moment coefficient due to compressibility effects
R_o	Density of air at sea level (altitude of contest site) (slug/ft ³)
Q	Dynamic pressure (lb/ft ²)
CD_0	Reference drag coefficient
I_{yy}	Moment of inertia about the y-axis of the aircraft (slug-ft ²)
CL_{α}	Aircraft lift curve slope
CM_{α}	Aircraft moment curve slope
CD_{α}	Aircraft drag curve slope
CL_u	Lift coefficient due to compressibility effects
$CL_{\alpha \dot{\alpha}}$	Aircraft unsteady lift curve slope
$CM_{\alpha \dot{\alpha}}$	Aircraft unsteady moment curve slope
CL_q	Aircraft lift curve slope with respect to pitch rate
CM_q	Aircraft moment curve slope with respect to pitch rate
CL_0	Reference aircraft lift coefficient
M_q	Aircraft moment as a function of pitch rate (ft-lbs)
X_u	Force in x-direction due to compressibility effects (lbs)
Z_u	Force in z-direction due to compressibility effects (lbs)
M_u	Moment due to compressibility effects (ft-lbs)
$M_{w \dot{w}}$	Moment due to vertical acceleration (ft-lbs)
X_w	Force in x-direction due to vertical velocity (lbs)
Z_w	Force in z-direction due to vertical velocity (lbs)
M_w	Moment due to vertical velocity (ft-lbs)

Table C.2 Nomenclature for Longitudinal Stability Calculations

Lateral / Directional Stability Analysis

Code written in Matlab

```
Uo =82.021;
M=Uo/1115.486;
rho=0.002213;
S=7.5;
W=27.82;
g=32.174;
m=W/g;
Ix=14;
Iz=15;
ARw=4.5
ARvt=0.441;
Claw2D=5.28;

Clavt2D=6.03;
etaV =1;
Sv=0.378;
dsigmadbeta=0.32;
Zv = 0.8728;
Lv = 3.5;
b = 5.5;
Cbar = 1.134;
Vv =(Sv/S)*Lv/Cbar;
Q=0.5*rho*Uo^2;

%Fuselage stuff

volumefuse=0.8
widthfuse=0.716
Hatwingroot = 1.13

Cnbetafuse = -1.3*volumefuse*Hatwingroot/(S*b*widthfuse)
Clo = W / (Q*S)
Sweepw = 0.0
Sweepvt = 20
Beta = sqrt (1 - M^2)
kw = Claw2D / (2 * 3.1416)
kt = Clavt2D / (2 * 3.1416)
ClalphaW = 2 * 3.141 * ARw / (2 + sqrt(ARw^2 * Beta^2 / kw^2 * (1 +
(tan(Sweepw/57.3))^2 / Beta^2) + 4))
ClalphaV = 2 * 3.141 * ARvt / (2 + sqrt(ARvt^2 * Beta^2 / kt^2 * (1
+ (tan(Sweepvt/57.3))^2 / Beta^2) + 4))
Cybetatail = ClalphaV
Q = .5 * rho * Uo^2

% Stability Coefficients

Cybeta = - etaV * (Sv/S) * ClalphaV * (1 + dsigmadbeta)
Cyp = - 2 * etaV * (Sv/S) * ClalphaV * (Zv/b)
Cyr = 2 * etaV * Vv * ClalphaV
Clbeta = 0.0
Clp = - ClalphaW / 12 * (1 + 3 * Sweepw) / (1 + Sweepw) - 2 * etaV
* (Sv/S) * (Zv/b)^2 * ClalphaV
Clr = Clo / 4 - 2 * (Lv/b) * (Zv/b) * Cybetatail
Cnbeta = Cnbetafuse + etaV * Vv * ClalphaV * (1 + dsigmadbeta)
Cnp = - Clo / 8 + 2 * etaV * Vv * ClalphaV * (Zv/b)
Cnr = - 2 * etaV * Vv * (Lv/b) * ClalphaV

% Directional Derivatives
```

```

Ybeta = Q*S*Cybeta / m
Yp = Q*S*b*Cyp / (2*m*Uo)
Yr = Q*S*b*Cyr / (2*m*Uo)
Lbeta = Q*S*b*Clbeta / Ix
Lp = Q*S*b^2*Clp / (2*Ix*Uo)
Lr = Q*S*b^2*Clr / (2*Ix*Uo)
Nbeta = Q*S*b*Cnbeta / Iz
Np = Q*S*b^2*Cnp / (2*Iz*Uo)
Nr = Q*S*b^2*Cnr / (2*Iz*Uo)

% Set up the matix for the lateral/directional equations of motion
A = [Ybeta/Uo Yp/Uo -(1-Yr/Uo) g/Uo; Lbeta Lp Lr 0; Nbeta Np Nr 0;
0 1 0 0]
[evect,eval] = eig(A)

% Roll mode
Omega_roll = norm (eval(3,3))
Thalf_roll = 0.69 / abs(real(eval(3,3)))

% Spiral mode
Omega_spiral = norm (eval(4,4))
Thalf_spiral = 0.69 / abs(real(eval(4,4)))

% Dutch roll mode
Omega_DR = norm (eval(1,1))
DR_DR = abs(real(eval(1,1)))/Omega_DR
Thalf_DR = 0.69 / abs(real(eval(1,1)))
T_DR = 2 * pi / abs(imag(eval(1,1)))
Nhalf_DR = Thalf_DR / T_DR

```

Output of the Matlab Code

The natural frequency, time of cycles to half-amplitude of the modes are obtained as follows:

Roll	Spiral	Dutch Roll
$\omega_n = 0.207 Hz$	$\omega_n = 0.01855 Hz$	$\omega_n = 1.4291 Hz$
$t_{1/2} = 3.3202 s$	$t_{1/2} = 37.194 s$	$t_{1/2} = 10.756 s$
		$\zeta = 0.044888$
		Period = 4.401s
		$N_{1,2} = 2.444$

Table C.3 Lateral/Directional Modal Characteristics

Note: The lateral stability analysis is based on the approach given in Ref. 11 and Ref. 12.

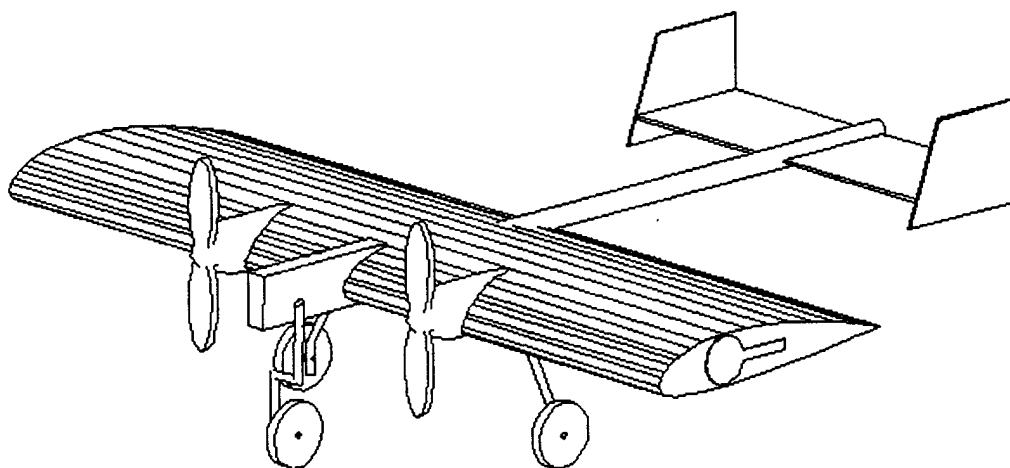
Symbol	Description
U_o	Velocity (ft/s)
M	Mach number, using a temperature of 75°F
Rho	Density of air at sea level (altitude of contest site) (slug/ft ³)
S	Surface area of the wing (ft ²)
W	Weight (lbs)
G	gravity (ft/s ²)
M	mass (slugs)
I_x	Moment of inertia about the x-axis of the aircraft (slug-ft ²)
I_z	Moment of inertia about the z-axis of the aircraft (slug-ft ²)
Ar_w	Aspect ratio of the wing
Ar_v	Aspect ratio of the vertical tail
$Claw_{2D}$	2-D wing lift curve slope
$Clav_{2D}$	2-D vertical tail lift curve slope
Eta_V	Efficiency factor of the vertical tail
S_v	Surface area of the vertical tail (ft ²)
$D\sigma_{\beta}$	Change in sidewash due to change in angle of sideslip
Z_v	Distance from fuselage centerline to vertical tail aerodynamic center
L_v	Distance from aircraft center of gravity to vertical tail quarter chord
B	Wingspan (ft)
$Cbar$	Mean aerodynamic chord (ft)
V_v	Vertical tail volume (ft ³)
Q	Dynamic pressure (lb/ft ²)
$Volume_{fuse}$	Volume of the fuselage (ft ³)
$Width_{fuse}$	Average width of the fuselage (ft ³)
$Hat_{wingroot}$	Height of the fuselage at the wing root (ft)
$Cn_{\beta_{fuse}}$	Weathercock effect due to the fuselage
C_{l_o}	Reference aircraft lift coefficient
$Sweep_w$	Sweep of the wing quarter chord (degrees)
$Sweep_v$	Sweep of the vertical tail quarter chord (degrees)
$Beta$	Interpolation variable used to determine CL_{w3D} and CL_{v3D}
K_w	Interpolation variable used to determine Cl_{w3D}
K_t	Interpolation variable used to determine Cl_{v3D}
$Cy_{\beta_{tail}}$	Side force coefficient due to sideslip caused by the vertical tail
Cy_{β}	Side force coefficient due to sideslip

<i>Cyp</i>	Side force coefficient due to roll rate
<i>Cyr</i>	Side force coefficient due to yaw rate
<i>Clbeta</i>	Dihedral effect coefficient
<i>Clp</i>	Damping coefficient in roll
<i>Clr</i>	Rolling moment coefficient due to yaw
<i>Cnbeta</i>	Weathercock effect coefficient
<i>Cnp</i>	Yawing moment coefficient due to roll
<i>Cnr</i>	Damping coefficient in yaw
<i>Ybeta</i>	Side force due to sideslip (lbs)
<i>Yp</i>	Side force due to roll rate (lbs)
<i>Yr</i>	Side force due to yaw rate (lbs)
<i>Lbeta</i>	Dihedral effect (ft-lbs)
<i>Lp</i>	Damping in roll (ft-lbs)
<i>Lr</i>	Rolling moment due to yaw (ft-lbs)
<i>Nbeta</i>	Weathercock effect (ft-lbs)
<i>Np</i>	Yawing moment due to roll (ft-lbs)
<i>Nr</i>	Damping in yaw (ft-lbs)
<i>Omega_roll</i>	Natural frequency of the roll mode oscillations (Hz)
<i>Thalf_roll</i>	Time for the amplitude of the roll mode oscillations to half (sec)
<i>Omega_spiral</i>	Natural frequency of the spiral mode oscillations (Hz)
<i>Thalf_roll</i>	Time for the amplitude of the spiral mode oscillations to half (sec)
<i>Omega_DR</i>	Natural frequency of the dutch roll mode oscillations (Hz)
<i>DR_DR</i>	Damping ratio for the dutch roll mode oscillations
<i>Thalf_DR</i>	Time for the amplitude of the dutch roll mode oscillations to half (sec)
<i>T_DR</i>	Period of the dutch roll mode oscillations (sec)
<i>Nhalf_DR</i>	Number of oscillations for the amplitude of the dutch roll mode oscillations to half

Table C.4 Nomenclature for Lateral/Directional Stability Calculations

Cessna ONR Student Design, Build, Fly Competition

The MUX-2000



By: The Miami University Aircraft Design Team
Miami University
Oxford Ohio, 45056

Table of Contents

1. Executive Summary.....	1
2. Management Summary.....	3
3. Conceptual Design.....	6
4. Preliminary Design	22
5. Detail Design.....	29
6. Manufacturing Plan.....	47
7. Lessons Learned.....	
8. Aircraft Cost.....	

1. Executive Summary

1.1 Major Development Areas

The Miami University design team is comprised of students from various educational fields. We began meeting in September of 1999 and used our diverse backgrounds combined with our knowledge of flight, physics, and mechanics to design a competitive aircraft. Our team developed a timeline that determined when major tasks should be completed, and we met weekly to discuss progress and future work. Through brainstorming, research, and analysis, our team has chosen our final design from our preliminary ideas.

When our team began developing preliminary designs, many factors were considered. These factors included cost, take off distance, landing survivability, simplicity of construction, ease of transportability, and air stability and performance. Weather reports of Wichita were also researched to determine the past wind conditions in April.

The preliminary designs our team considered include a biplane design, a sport plane design, a cargo plane design and a span loader design. The biplane design employs the use of two wings to give the plane greater lift, which is important since the plane could be carrying up to 18 lbs of water. However, given the expected Wichita weather conditions, the plane's handling could have been a problem. The sport plane design has a short body and tight structure, which make it ideal for good handling and maneuverability. This plane introduces a single propeller used on the nose of the plane, and the water bottles are carried in both the wings and inside the body. The bottles placed in the wings would remain close to the body however, keeping any moments to a minimum. Cargo planes are often used to carry heavy loads. The design places all the bottles in the fuselage, eliminating any worry about bending moments created by storing the bottles in the wings. Placing all the bottles in the fuselage does however create the need for a much larger body. The bottles are laid on their sides and placed in a circular ring similar to a gun barrel. The wing runs across the top of the plane and a propeller is placed in the middle of each side.

Our team decided that the span loader design provided the most advantages and would be the best choice for the competition. The span loader design gets its name from the arrangement of bottles across the wing. The bottles are placed end to end in a hollowed out portion of the wing. This design is able to meet the maximum seven-foot wing requirement, with the bottles taking up approximately five and a half feet of the total span. Placing the bottles along the wingspan is useful because it puts them along the center of gravity of the plane. The plane uses two motors on each side, which run two propellers on the wing. By using two propellers in the design we are able to produce better air movement across the wings.

1.2 Design Tools Overview

Many of the design tools our team used for the analysis of our aircraft were determined from the previous competition. Our university had a team that was involved

in the AIAA Competition last year, so we had experience in determining the analytical tools needed to analyze the various components of the aircraft. Other design tools were also used, and these were added to ensure the stability of the aircraft. These tools included ElectiCalc, Finite Element Analysis, Microsoft Excel and AutoCAD.

ElectriCalc enabled our team to determine the aircraft's propulsion system. It was used to find the optimal motor, battery, and propeller combination. We plugged in parameters such as weight of the airplane, surface area of the wing, the type of motors, etc. (there are about thirty-five variables to enter). Then, Electricalc determined a whole list of information as well as plot out graphs, as desired. Some of the important things it determined are the thrust and drag and the life of the batteries, to name a few. The life of the batteries is important because the maximum flight we could have is 10 minutes.

As stated in the Competition Rules (AIAA 3), our airplane will be lifted with one lift point at each wing tip to verify adequate wing strength (which is equivalent to a 2.5 gram load). In order to make sure our airplane passes this test, we needed a method to verify the strength our airplane. To accomplish this, we decided to use the method of finite element analysis. Finite element analysis enables its user to take an object, in our case, the wing of our airplane, and divide it up into tiny, finite sections. This enables the user to calculate variables such as stress, strain, and deformation, to name a few. For our purposes, we are most concerned with the deformation of the wing. We want to make sure that the wing will deform less than the maximum allowable deformation (the deformation required before the wing breaks).

Microsoft Excel and AutoCAD were other design tools that were used throughout our project. Microsoft Excel was used throughout each stage of our design to develop graphs and spreadsheets. AutoCAD was used to develop detailed drawings of each of our preliminary designs, as well as our final design.

2. Management Summary

During the first few months of our team meetings, we decided to split our team up into four specialized teams, as shown in the chart below. The groups we split into include the propulsion team, wing analysis team, wing design team, and the tail/landing gear team. We decided that by splitting our large group into smaller groups, each member would be able to focus on a certain aspect of the airplane design. Even though we split into smaller teams, we all worked together in order to determine the overall structure of the airplane and make sure that all of the individual designs meshed to create a robust aircraft.

Advisors:	
Dr. Richard Walker (Aeronautics)	Tom Schroeder (Aeronautics)
Dr. Jim Stenger (Engineering)	
Propulsion Group	Skills/Tasks
Brady Ruck (Sr., Finance)	<ul style="list-style-type: none"> - Team Leader - Propulsion / Motor Analysis - Propulsion mount designs / Construction - Electricalc Analysis
Scott Foster (Jr., Chemistry)	<ul style="list-style-type: none"> - Team Leader - Propulsion/Motor Analysis - Builder - Order Parts / Communication with Suppliers
Jill Christiansen (Sr., Manufacturing Engineering)	<ul style="list-style-type: none"> - Electricalc Analysis - Finite Element Analysis - Cost Analysis
Wing Design Team	Skills/Tasks
Eric Ilse (Sr., Manufacturing Engineering)	<ul style="list-style-type: none"> - AutoCAD drawings - Finite Element Analysis - Wing Construction
Jon Yang (Soph., Architecture)	<ul style="list-style-type: none"> - Wing Design
Dave Knight (Soph., ROTC)	<ul style="list-style-type: none"> - Wing Design
Wing Analysis Team	Skills/Tasks
Kara Hammelrath (Sr., Manufacturing Engineering)	<ul style="list-style-type: none"> - Aileron Design - Wing Testing
Eric Dickman (Sr., Management Information Systems)	<ul style="list-style-type: none"> - Wing Building - Wing Testing
Tyler Martin (Sr., Economics)	<ul style="list-style-type: none"> - Wing Building - Wing Testing
Tail / Landing Gear Team	Skills/Tasks
Ben Kessing (Sr., Manufacturing Engineering)	<ul style="list-style-type: none"> - Knowledge of Materials - Manufacturing Processes - Tail / Landing Gear Analysis
James Murray (Sr., Psychology)	<ul style="list-style-type: none"> - Aeronautics Experience
Ashwin Janakiram (Soph., Political Science)	<ul style="list-style-type: none"> - Bottle Selection - Aeronautics Experience

Each Monday at 5:00 p.m., the entire team met to discuss our objectives for the week, our accomplishments from the previous week, and our future work. Also, a member of each of the four specialized teams would give a brief report of what they had accomplished in the previous week. Then, during the week of the large team meeting, each of the four smaller groups would set up meeting times to work on their assigned tasks. In order to make sure we were on schedule with deadlines and our own goals, we made and referred to our Gantt chart, which can be seen on the following page. It is split up into the first and second semester's progress.

TABLE 2.1

1st Semester Gantt Chart

	Week of 9/12/99	Week of 9/9/99	Week of 9/26/99	Week of 10/3/99	Week of 10/10/99	Week of 10/17/99	Week of 10/24/99	Week of 10/31/99	Week of 11/7/99	Week of 11/14/99	Week of 11/21/99	Week of 11/28/99	Week of 12/5/99	Week of 12/12/99	Week of 12/19/99	Week of 12/26/99
Review Competition Rules/ Review Past Reports																
Preliminary Design Ideas																
Break into four specialized groups																
Analysis of Top Designs																
Selection of Final Design																
Detailed Analysis of Final Design																
Building Airplane																
Testing of Airplane																
Competition in Wichita																
Work on Final Report																
Work on Addendum																

2nd Semester Gantt Chart

	Week of 1/2/00	Week of 1/9/00	Week of 1/16/00	Week of 1/23/00	Week of 1/30/00	Week of 2/6/00	Week of 2/13/00	Week of 2/20/00	Week of 2/27/00	Week of 3/5/00	Week of 3/12/00	Week of 3/19/00	Week of 3/26/00	Week of 4/2/00	Week of 4/9/00	Week of 4/16/00	Week of 4/23/00	Week of 4/30/00
Review Competition Rules/ Review Past Reports																		
Preliminary Design Ideas																		
Break into four specialized groups																		
Analysis of Top Designs																		
Selection of Final Design																		
Detailed Analysis of Final Design																		
Building Airplane																		
Testing of Airplane																		
Competition in Wichita																		
Work on Final Report																		
Work on Addendum																		

3. Conceptual Design

3.1 Alternative concepts investigated

We began the conceptual design phase of the project by brainstorming various airplane configurations. Using a "back of the napkin" approach we developed many interesting and imaginative ideas, drawing quick sketches when an idea came to mind. In the long run we wanted a design that would meet all the mission requirements as set forth by the contest rules, but at this point we were willing to look at every design with an open mind. Starting with a broad range of different designs gave our team a large pool of ideas to draw from later.

One of the first designs we evaluated was the biplane. The team from Miami that entered the design contest last year used a biplane to meet the contest requirements so this design seemed like a logical place to start. The biplane design employs the use of two parallel wings, one above the other. This design is used to give the plane greater lift.(Drawing No. 1)

Another design that we investigated was a cargo plane. Actual cargo planes are often used to carry extremely heavy loads. This idea was presented due to the fact that the water bottles certainly are a heavy load, making up approximately half the aircrafts total weight when fully loaded. The design places all the bottles in the fuselage, in a circular pattern, attempting to keep the bottles near the plane's center of gravity.(Drawing No.2)

The sport plane highlights the type of design that model plane enthusiasts often fly, and therefore was looked into as a possible solution. The short body and tight frame make it ideal for good handling and maneuverability. The design for this plane introduces a single propeller used on the nose of the plane, as well as a unique bottle carrying plan, placing bottles both underneath the wings and inside the fuselage.(Drawing No. 3)

The last design we looked at was the span loader. This design gets its name from the arrangement of bottles across the wing. The bottles are placed end to end in a hollowed out portion of the wing. This design is able to meet the maximum seven-foot wing requirement, with the bottles taking up approximately five and a half feet of the total span. Placing the bottles along the wingspan is useful because it puts them along the center of gravity of the plane. Even when the bottles are removed, the center of gravity remains constant. (Drawing No. 4)

3.2 Design parameters investigated

We investigated several design parameters during the conceptual design phase of our project.

- Bottle Storage / Accessibility

- Wing Configuration
- Propulsion System
- Landing Gear Configuration
- Total Weight

It was extremely important that our design have the capability of carrying the maximum number of bottles as specified by the contest rules. As seen in our comparison of scoring values, decreasing the number of bottles carried has an extreme effect on the final team score. We also wanted a design that would allow us to access the bottles easily. Quick and easy loading and unloading of the bottles between sorties is one of the keys to a successful run.

Wing configuration is also extremely important to the design. We want to use a wing setup that allow for maximum lift, ensuring that our plane makes it off the ground. The wing may also be needed to provide some bottle storage area. It will also be vital that the wing be able to support the weight of the plane when the structural verification test is performed.

To achieve the necessary air flow across the wing for lift off and sustained flight the propulsion system must be designed appropriately. Our motors are limited by the power given by the specified 5lb of batteries.

Landing gear configuration will have a direct bearing on the ground handling characteristics of our airplane. The configuration is also an important element of a safe and successful landing. With multiple takeoffs and landings the landing gear will play a vital role in the success of our airplane.

The total weight of the airplane is an important aspect of our airplane design. While we are limited to a maximum weight with payload of 55lbs, we would like to stay well below this value. The airframe weight effects handling characteristics as well as the rated aircraft cost. Keeping airframe weight low without sacrificing structural stability will be an important aspect of our design.

3.3 Figures of merit

In order to evaluate these designs, we needed to determine what "figures of merit" our design needed to address. These figures of merit were determined by the requirements our plane needed to meet as well as our own goals for the airplane we are to build. Basically, they determine what criteria we will use to select the best design. Our figures of merit are:

- Safety
- Speed of Loading / Unloading
- Carrying Capability
- Maneuverability
- Takeoff Distance
- Ground Handling

Safety must always be the primary focus of any design. It is necessary that the airplane function in a manner which does not jeopardize the safety of those people operating the plane or those who are watching its flight. This FOM supports the mission features of loading/unloading the plane as well as the flight pattern. Due to the number of people who may come in contact with this plane throughout the course of the contest, safety is paramount.

The loading and unloading of water bottles should not consume an excessive amount of time. The ten-minute time limit sets definite boundaries on the amount of sorties our plane will be able to complete. We do not want ground time taking up a major portion of the time. A minimum number of steps should be required to either load or unload the bottles and get the plane back into the air.

It is extremely important that the plane be able to hold a maximum number of bottles. The number of bottles carried per sortie has an extremely large effect on the final score. A plane carrying less than the maximum number of bottles may have trouble competing with teams that are able to carry all eight.

Maneuverability will be an important aspect of the contest. While in the air the plane must follow the set course outline, taking turns as tight as possible to eliminate wasted flight time. The 360 degree turn during the loaded sortie will be a major test of the turning capability of our plane.

The takeoff distance of our aircraft is an important aspect of contest requirements. One aspect of the mission is that the airplane must takeoff within 100 feet of the start line. This limiting factor will affect the selection of our propulsion system, as well as the overall size of our airplane.

Our final figure of merit is the ground handling of our aircraft. The mission feature this FOM supports is the repeated takeoffs and landings the plane will make during the contest. It will be necessary for the plane to return to the start line for loading/unloading can begin.

3.4 Rated Aircraft Costs

To analyze the basic merits of our conceptual designs a cost and score analysis spreadsheet has been created. This spreadsheet will allow our team to get some idea of a possible scores that will be received at the competition. Important data such as airframe weight, surface areas, number of motors, number of bottles carried, and number of completed sorties all play an integral part in this analysis. While these values are just an estimation, they do give us a good feeling of how varying factors will contribute to the final score.

Span Loader: In the analysis of the Span Loader we estimated an airframe weight of 12 lbs. We would like our final plane to weigh approximately 35 lbs so we simply

subtracted the 18 lbs of water as well as the 5lbs of batteries to arrive at this desired weight. This weight remains constant for the analysis of all our plane designs. Surface areas were calculated from the airplane sketch and entered into the spreadsheet as well. With this data entered we arrived at a rated aircraft cost of 6.6004. We will now look at some more design possibilities and see how they compare.(Table 3.1)

Cargo Plane: The cost and score analysis spreadsheet was used once again for this model. This design saw an increase in the wing and tail surface area. Due to these changes in the design the rated aircraft cost jumped to 7.043. This design also saw a drop in the total number of bottles to be carried, which will be discussed later.(Table 3.2)

Sport Plane: The rated aircraft cost for this design was the lowest, with a value of 5.03. This low cost was due to the fact that the plane had minimum surface area and only used one propeller.(Table 3.3)

Biplane: Once again we will use the cost and score analysis spreadsheet to judge the merits of the design. Before using the spreadsheet we had concerns about adding a second wing to the design, however the spreadsheet showed little effect on the rated aircraft cost. This information could be invaluable if a second wing becomes necessary to get the plane off the ground. When the calculations were complete, a rated aircraft cost of 5.57 was returned. This was the second lowest cost of the four designs, even with the addition of a second wing. (Table 3.4)

3.5 Analytic Methods

To test the validity of various designs we set up a few mathematical models to test the capabilities of various designs. While these models were not necessarily complex they did return results that gave us a good estimation of the characteristics of the different designs.

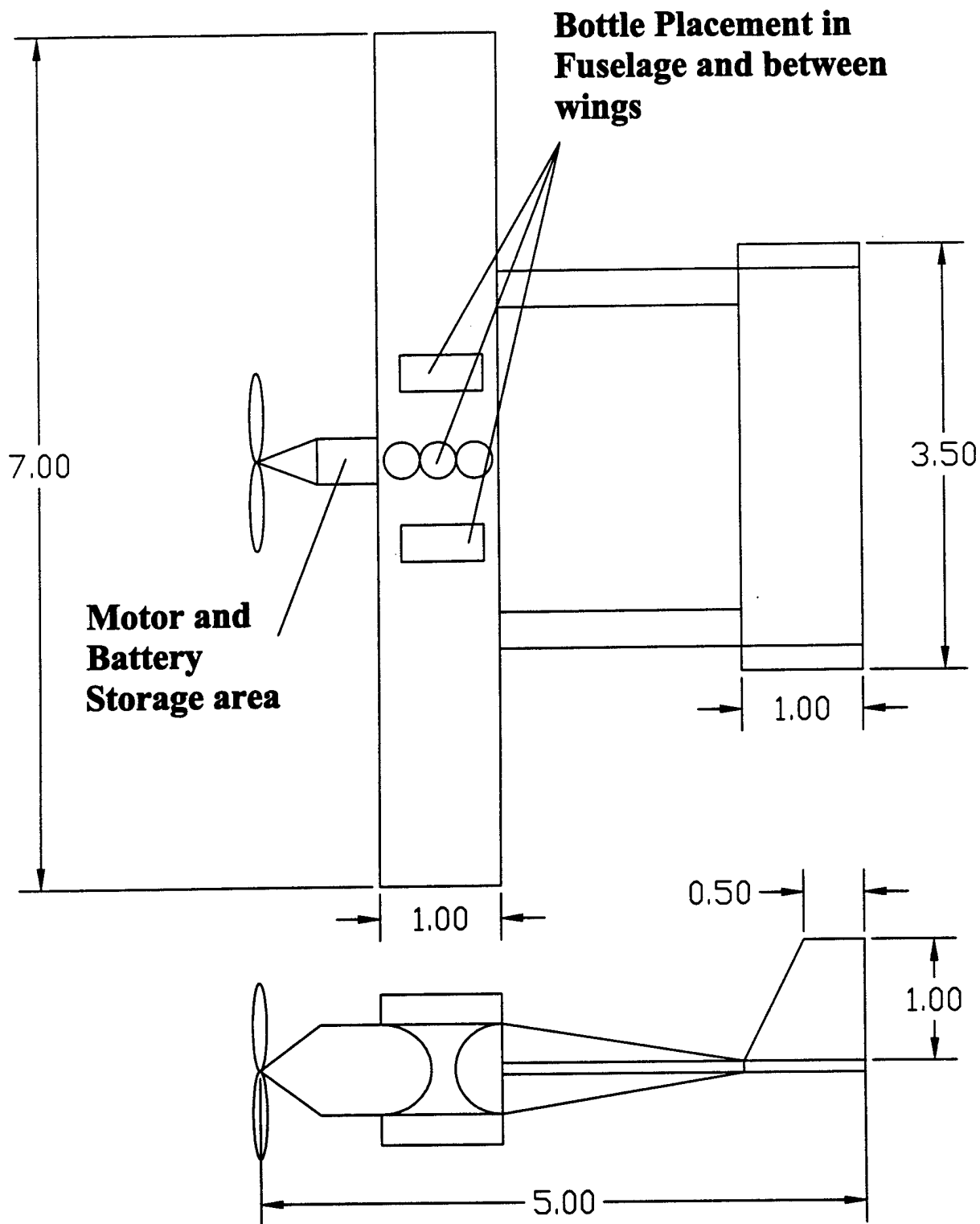
One mathematical model that we used was shear and bending moment diagrams. Due to the simplistic nature of our preliminary designs, we had to make certain assumptions about the various designs to create shear and bending moment diagrams that would hold some degree of merit. The Sport, Biplane, and Cargo designs shared basically the same layout for bottle placement. For this reason we were able to construct one shear and bending moment diagram to represent all three designs. For the Span Loader design we used a similar model but distributed the bottle weight across the entire wing surface. We assumed standard weights for each element of the plane and placed them at locations that would closely model the final design. Following is a list of assumptions that were made:

Component	Location(from edge)	Weight
Motor & Propeller	2.625 ft, 4.375 ft	1 lb
Tail	3.5 ft	5 lb
Nose & Batteries	3.5 ft	5 lb
Water Bottles (standard)	3.5 ft	18 lb
Water Bottles (span loader)	Entire Length	18 lb

With these assumptions made, we were able to construct the diagrams. (See Table 3.5 & 3.6) Of greatest concern was the maximum moment on the wing. The diagram for the Sport, Cargo, and Biplane designs returned a maximum moment of 51.625 ft-lb, while the diagram for the span loader design returned a maximum moment of 36.3 ft-lb. This drastic difference in bending moments was due mainly to the weight distribution across the entire wing. While these may not be exact values for the maximum moment experienced by the wing, this estimation does clearly show the benefit of distributing the force across the entire wing.

3.6 Final Configuration Selection

The final configuration for our plane was determined using several factors. First we looked at the figure of merit ranking chart as shown in Table 3.7. This figure helped us visualize the strengths and weaknesses of the various designs. The design that scored the best was the span loader design. Our second method of evaluation was looking at the Score spreadsheets that we created. The score spreadsheets took into account the Rated Aircraft Cost as well as the number of bottles the plane could carry. This method of evaluation ranked the sport plane first and the span loader second. Finally we looked at the bending moment diagrams. It was clear from these diagrams that the distributed load was the best loading configuration. It returned the smallest moment, leading to lower stresses in the wing during flight and during the structural verification test. With these results we decided to proceed with the Span Loader as our final design.



Dimensions are in feet and are used in the Cost Model.

Miami University

Aeronautics & Manufacturing Engineering Depts.

Oxford Ohio 45056

Title

Biplane Design

The Miami University Aircraft Design Team

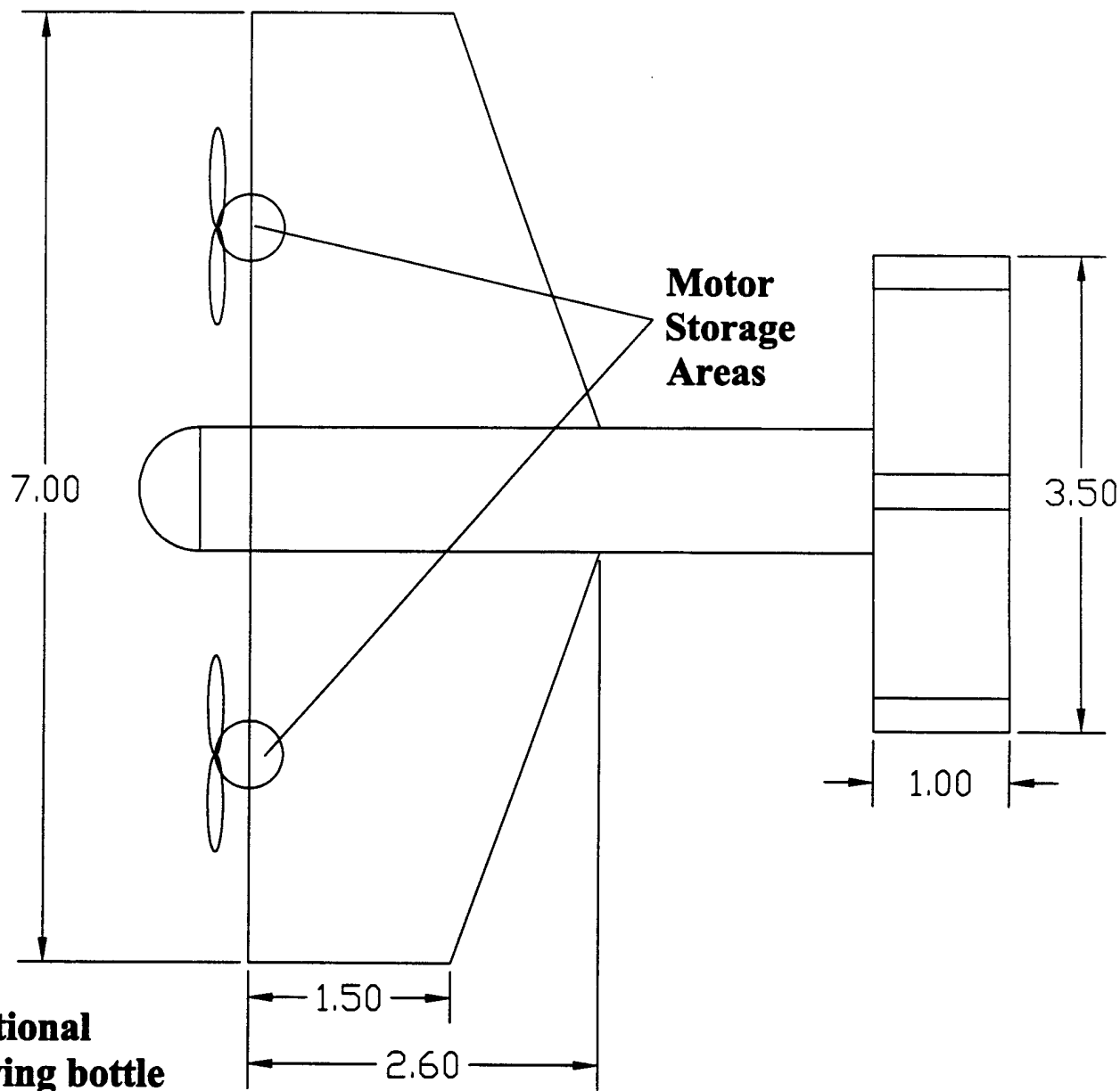
AIAA Cessna/ONR Design Build and Fly Competition

NTS

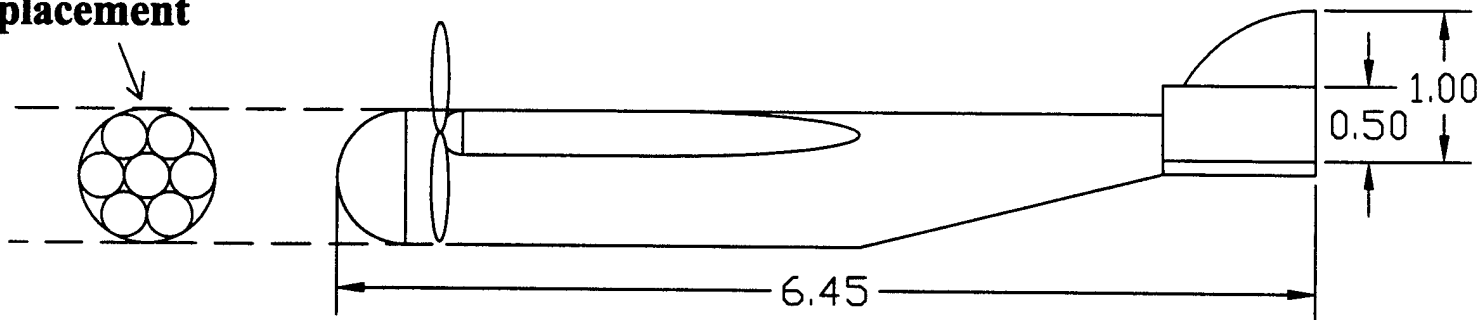
Sheet 1 of 1

Drawing No.

1



**Cross Sectional
view showing bottle
placement**



Dimensions are in feet and are used in the Cost Model.

Miami University

Aeronautics & Manufacturing Engineering Depts.

Oxford Ohio 45056

Title

Cargo Plane Design

The Miami University Aircraft Design Team

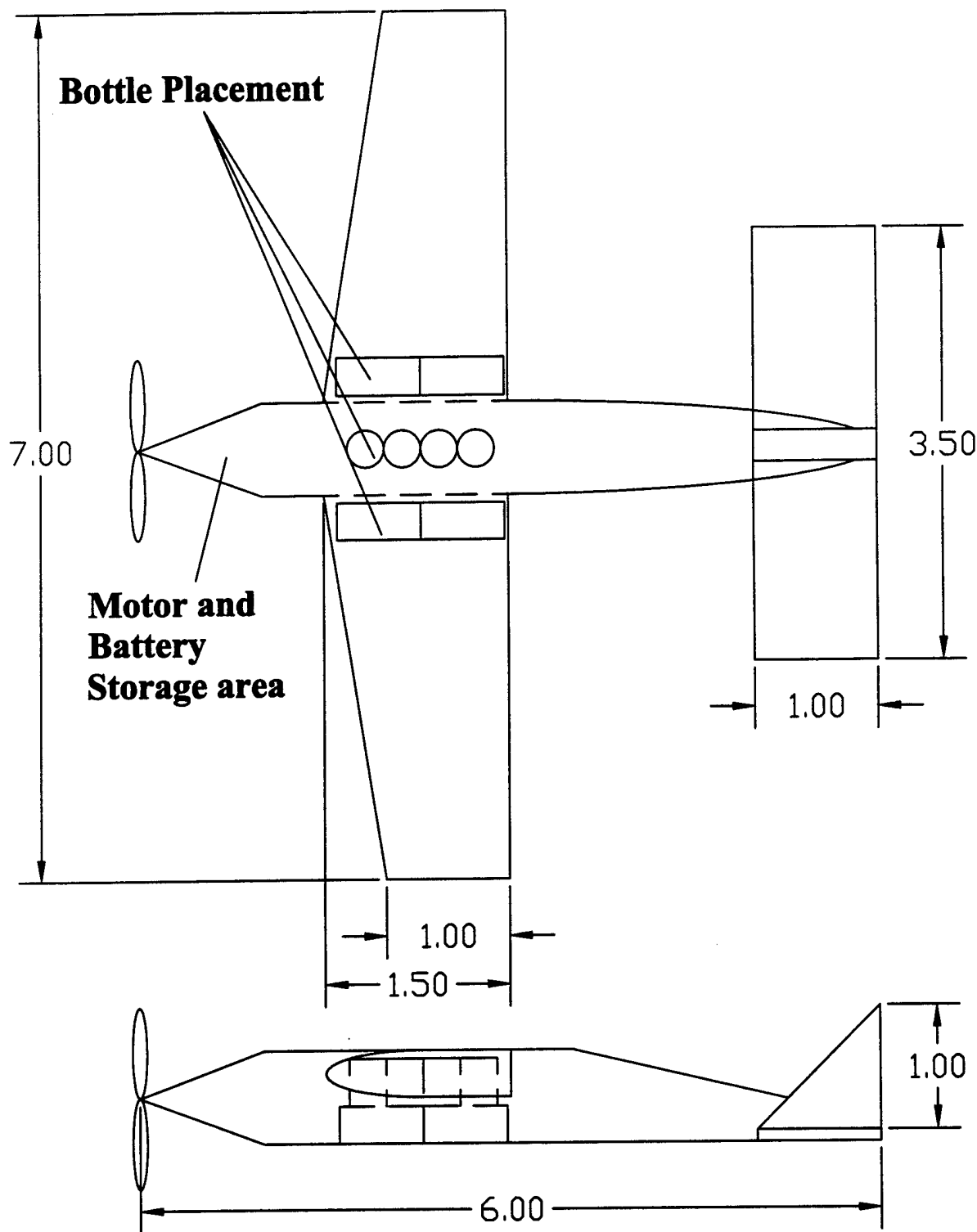
AIAA Cessna/ONR Design Build and Fly Competition

NTS

Sheet 1 of 1

Drawing No.

2



Dimensions are in feet and are used in the Cost Model.

Miami University

Aeronautics & Manufacturing Engineering Depts.

Oxford Ohio 45056

Title

Sport Plane Design

The Miami University Aircraft Design Team

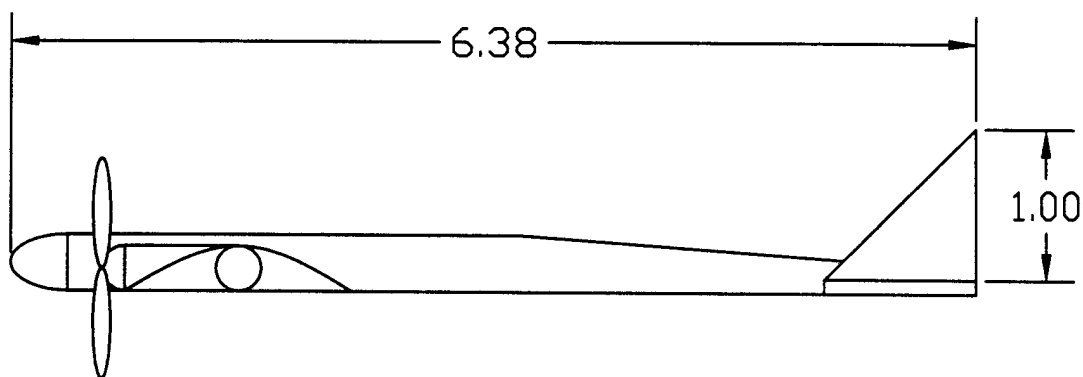
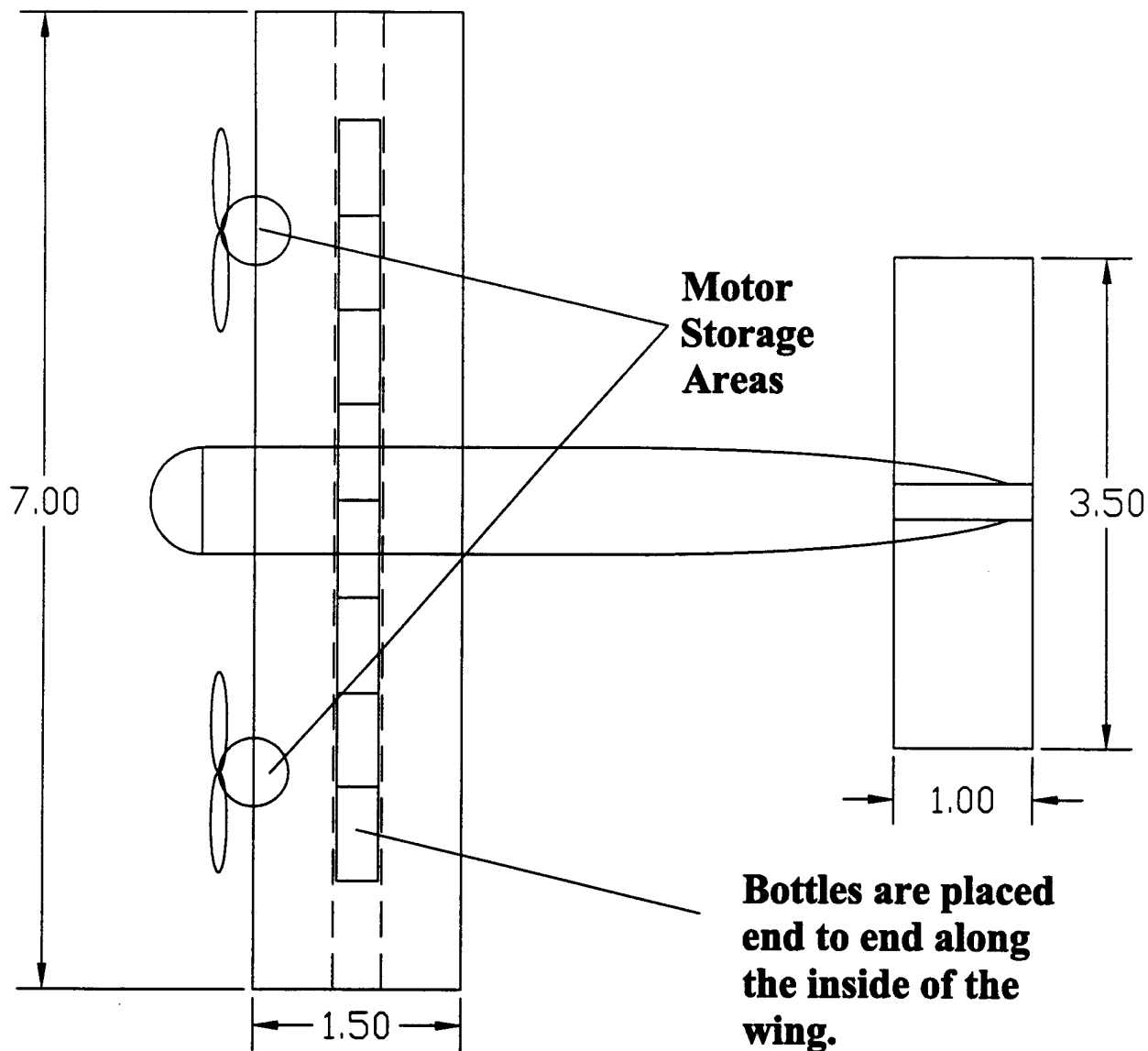
AIAA Cessna/ONR Design Build and Fly Competition

NTS

Sheet 1 of 1

Drawing No.

3



Dimensions are in feet and are used in the Cost Model.

Miami University

Aeronautics & Manufacturing Engineering Depts.

Oxford Ohio 45056

Title

Span Loader Design

The Miami University Aircraft Design Team

AIAA Cessna/ONR Design Build and Fly Competition

NTS

Sheet 1 of 1

Drawing No.

4

Table 3.2: Cost and Score Estimation for Cargo Plane Design

Coef.	Description	Multipliers	Value
A =	Manufacturers Empty Weight Multiplier	\$100 / lb	
B =	Rated Engine Power Multiplier	\$1 / Watt	
C =	Manufacturing Cost Multiplier	\$20 / hr	
MEW =	Manufacturers Empty Weight	Airframe weight without payload or batteries	12 *
REP =	Rated Engine Power	# engines	2 *
		# Cells	20 *
		# engines * 50 A * 1.2 V/cell * # cells	2400
WBS 1.0	Wing(s)	5 hr/ wing	1 *
WBS 2.0	Fuselage and/or pods	4 hr/ sq. ft. projected area	14.35 *
		5 hr/body	1 *
WBS 3.0	Empenage	4 hr/ ft of length	6.45 *
		5 hr (basic)	1
		5 hr./ Vertical Surface	1.79 *
WBS 4.0	Flight Systems	10 hr./ Horizontal Surface	3.5 *
		5 hr. (basic)	1
WBS 5.0	Propulsion System	1 hr / servo	5 *
		5 hr/engine	2
MFHR =	Total WBS hours	5 hr/propeller or fan	2 *
			172.15

# of liters carried during sortie =	3 *
Single Flight Score =	3 *

Rated Aircraft Cost = (A * MEW + B * REP + C*MFHR)/1000 =	7.043 *
Written Report Score =	85
Total Flight Score =	630

Overall Score = 7603

Table 3.3: Cost and Score Estimation for Sport Plane Design

Coef.	Description	Multipliers	Value
A =	Manufacturers Empty Weight Multiplier	\$100 / lb	
B =	Rated Engine Power Multiplier	\$1 / Watt	
C =	Manufacturing Cost Multiplier	\$20 / hr	
MEW =	Manufacturers Empty Weight	Airframe weight without payload or batteries	12*
REP =	Rated Engine Power	# engines	1*
		# Cells	20*
		# engines * 50 A * 1.2 V/cell * # cells	1200
WBS 1.0	Wing(s)	5 hr/ wing	1*
		4 hr/ sq. ft. projected area	8.75*
WBS 2.0	Fuselage and/or pods	5 hr/body	1*
		4 hr/ ft of length	6*
WBS 3.0	Empenage	5 hr (basic)	1*
		5 hr./ Vertical Surface	0.5*
		10 hr./ Horizontal Surface	3.5*
WBS 4.0	Flight Systems	5 hr. (basic)	1*
		1 hr / servo	5*
WBS 5.0	Propulsion System	5 hr/engine	1*
		5 hr/propeller or fan	1*
MFHR =	Total WBS hours		131.5
Total (hrs)			
			5
			35
			5
			24
			5
			2.5
			35
			5
			5
			5
			5
			5
			131.5
Total (hrs)			
			5
			35
			5
			24
			5
			2.5
			35
			5
			5
			5
			5
			5
			131.5
Total (hrs)			
			5
			35
			5
			24
			5
			2.5
			35
			5
			5
			5
			5
			5
			131.5
Total (hrs)			
			5
			35
			5
			24
			5
			2.5
			35
			5
			5
			5
			5
			5
			131.5
Total (hrs)			
			5
			35
			5
			24
			5
			2.5
			35
			5
			5
			5
			5
			5
			131.5
Total (hrs)			
			5
			35
			5
			24
			5
			2.5
			35
			5
			5
			5
			5
			5
			131.5
Total (hrs)			
			5
			35
			5
			24
			5
			2.5
			35
			5
			5
			5
			5
			5
			131.5
Total (hrs)			
			5
			35
			5
			24
			5
			2.5
			35
			5
			5
			5
			5
			5
			131.5
Total (hrs)			
			5
			35
			5
			24
			5
			2.5
			35
			5
			5
			5
			5
			5
			131.5
Total (hrs)			
			5
			35
			5
			24
			5
			2.5
			35
			5
			5
			5
			5
			5
			131.5
Total (hrs)			
			5
			35
			5
			24
			5
			2.5
			35
			5
			5
			5
			5
			5
			131.5
Total (hrs)			
			5
			35
			5
			24
			5
			2.5
			35
			5
			5
			5
			5
			5
			131.5
Total (hrs)			
			5
			35
			5
			24
			5
			2.5
			35
			5
			5
			5
			5
			5
			131.5
Total (hrs)			
			5
			35
			5
			24
			5
			2.5
			35
			5
			5
			5
			5
			5
			131.5
Total (hrs)			
			5
			35
			5
			24
			5
			2.5
			35
			5
			5
			5
			5
			5
			131.5
Total (hrs)			
			5
			35
			5
			24
			5
			2.5
			35
			5
			5
			5
			5
			5
			131.5
Total (hrs)			
			5
			35
			5
			24
			5
			2.5
			35
			5
			5
			5
			5
			5
			131.5
Total (hrs)			
			5
			35
			5
			24
			5
			2.5
			35
			5
			5
			5
			5
			5
			131.5
Total (hrs)			
			5
			35
			5
			24
			5
			2.5
			35
			5
			5
			5
			5
			5
			131.5
Total (hrs)			
			5
			35
			5
			24
			5
			2.5
			35
			5
			5
			5
			5
			5
			131.5
Total (hrs)			
			5
			35
			5
			24
			5
			2.5
			35
			5
			5
			5
			5
			5
			131.5
Total (hrs)			
			5
			35
			5
			24
			5
			2.5
			35
			5
			5
			5
			5
			5
			131.5
Total (hrs)			
			5
			35
			5
			24
			5
			2.5
			35
			5
			5
			5
			5
			5
			131.5
Total (hrs)			
			5
			35
			5
			24
			5
			2.5
			35
			5
			5
			5
			5
			5
			131.5
Total (hrs)			
			5
			35
			5
			24
			5
			2.5
			35
			5
			5
			5
			5
			5
			131.5
Total (hrs)			
			5
			35
			5
			24
			5
			2.5
			35
			5
			5
			5
			5
			5
			131.5
Total (hrs)			
			5
			35
			5
			24
			5
			2.5
			35
			5
			5
			5
			5
			5
			131.5
Total (hrs)			
			5
			35
			5
			24
			5
			2.5
			35
			5
			5
			5
			5
			5
			131.5
Total (hrs)			
			5
			35
			5
			24
			5
			2.5
			35
			5
			5
			5
			5
			5
			131.5
Total (hrs)			
			5
			35
			5
			24
			5
			2.5
			35
			5
			5
			5
			5
			5
			131.5
Total (hrs)			
			5
			35
			5
			24
			5
			2.5
			35
			5
			5
			5
			5
			5
			131.5
Total (hrs)			
			5
			35
			5
			24

Table 3.4: Cost and Score Estimation for Biplane Design

Coef.	Description	Multipliers	Value
A =	Manufacturers Empty Weight Multiplier	\$100 / lb	
B =	Rated Engine Power Multiplier	\$1 / Watt	
C =	Manufacturing Cost Multiplier	\$20 / hr	
MEW =	Manufacturers Empty Weight	Airframe weight without payload or batteries	
		# engines	12 *
		# Cells	1 *
REP =	Rated Engine Power	# engines * 50 A * 1.2 V/cell * # cells	20 *
			1200
WBS 1.0	Wing(s)	5 hr/ wing	2 *
WBS 2.0	Fuselage and/or pods	4 hr/ sq. ft. projected area	14 *
		5 hr/body	1 *
WBS 3.0	Empenage	4 hr/ ft of length	5 *
		5 hr (basic)	1
		5 hr./ Vertical Surface	1.5 *
		10 hr./ Horizontal Surface	3.5 *
WBS 4.0	Flight Systems	5 hr. (basic)	1
		1 hr / servo	5 *
WBS 5.0	Propulsion System	5 hr/engine	1
		5 hr/propeller or fan	1 *
MFHR =	Total WBS hours		158.5

of liters carried during sortie = 8 *

Single Flight Score = 240

of sorties = 3 *

of flights = 3 *

Rated Aircraft Cost = (A * MEW + B * REP + C*MFHR)/1000 = 5.57 *

Written Report Score = 85

Total Flight Score = 720

Overall Score = 10987

Table 3.5
Basic Shear Force & Bending Moment
Diagrams for Sport, Cargo, Biplane Designs

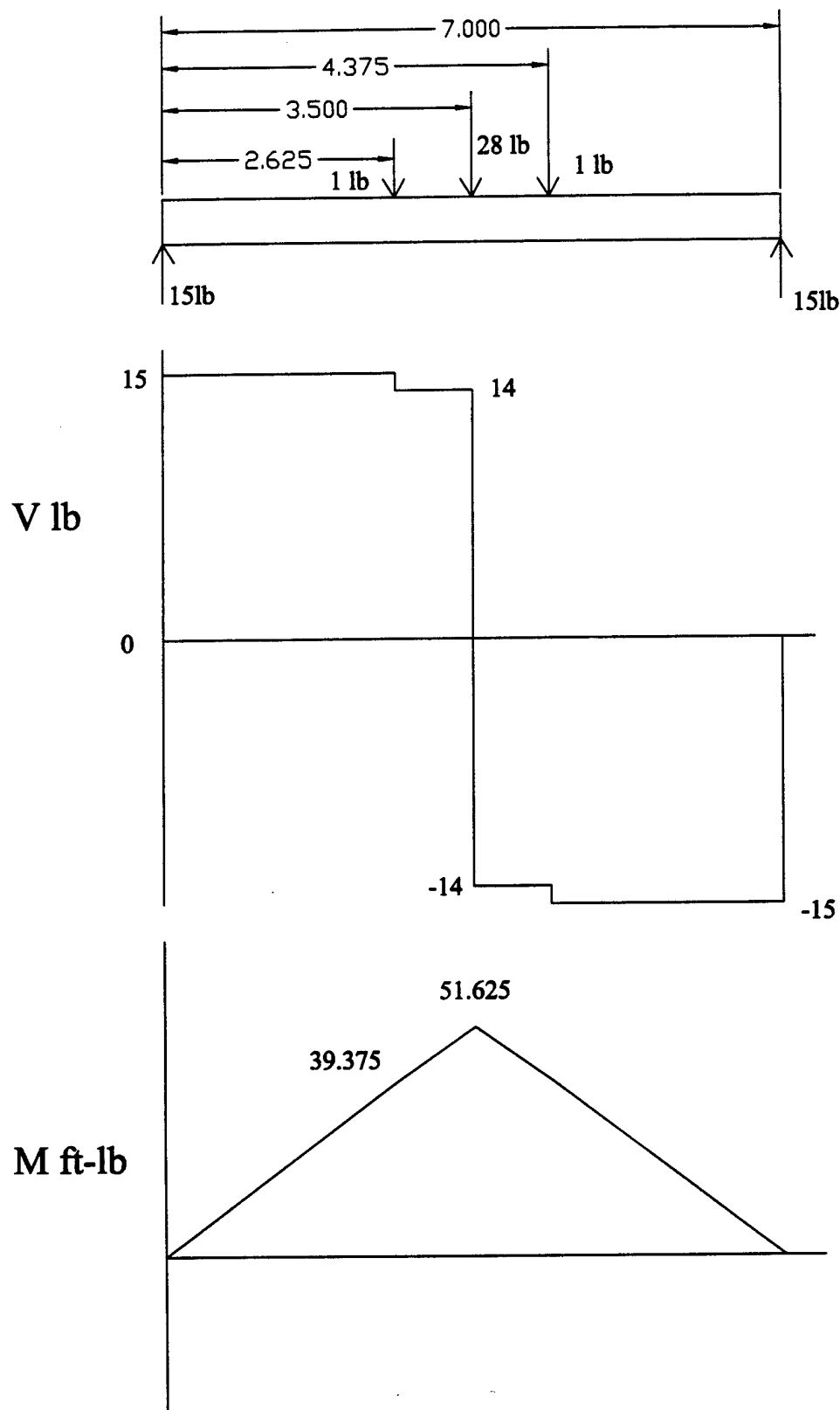


Table 3.6
Basic Shear Force & Bending Moment
Diagrams for Span Loader Design

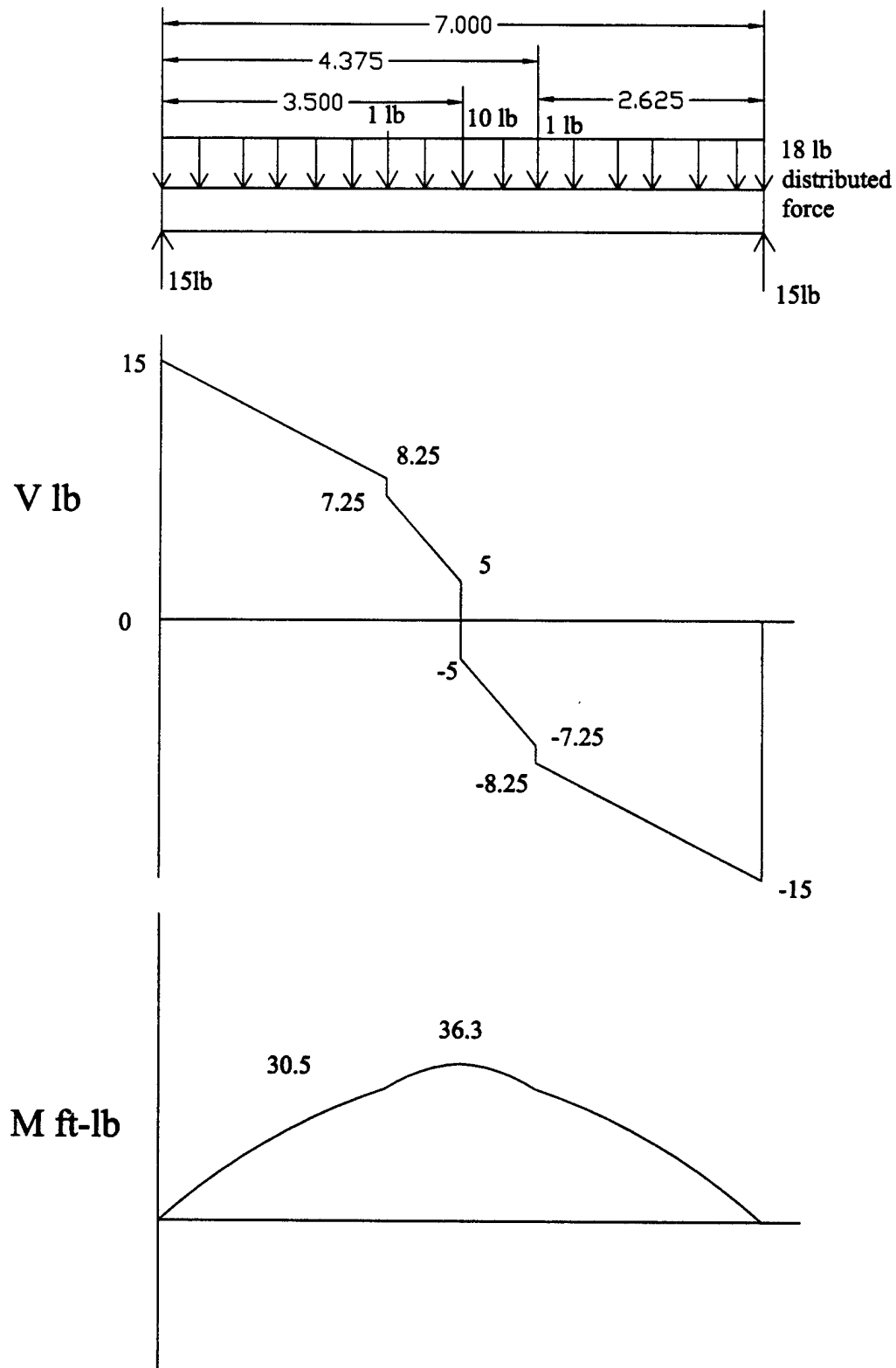


Table 3.7: Ranking Chart for Various Airplane Designs

Rank Multiplier	FOM	1	2	3	4
3	Safety	9	7	8	7
2	Speed of Loading	9	6	4	8
2	Carrying Capability	10	7	10	7
1	Takeoff Distance	6	6	8	9
1	Ground Handling	6	6	9	7
1	Manuverability	6	6	9	9
Total		83	65	78	76

of a possible 100 points

Design 1	Span Loader
Design 2	Cargo Plane
Design 3	Sport Plane
Design 4	Biplane

4. Preliminary Design

4.1 Airfoil Analysis

In determining the best airfoil to meet our requirements (FOM's), we looked at the airfoil database at the University of Illinois – Urbana-Champaign campus' website. We were looking for a high lift airfoil that could accomplish the 100 ft takeoff distance. We narrowed those choices down to a Clark Y airfoil, due to its ease of construction. The chord would be of decent proportion since it would need to be high enough to include the bottles. Other choices wouldn't be stable enough after hollowing out the wing for the payload.

4.2 Test Wing

To see if the airfoil the team had picked would actually produce lift we decided to do a pressure test. The procedure we used goes as follows. The first step was building a wooden "U" shaped box to hold the airfoil during the test. Next the team covered the airfoil with balsa wood to give it a smooth finish. Now we were ready to cut the airfoil in half to allow us to install the static ports. Installing the static ports was accomplished by attaching latex tubes to brass fixtures that were aligned perpendicular with the surface. We placed the static ports at every 1/10 of the length of the cord; starting at .1 and ending at .8 of the cord length. The next step involved gluing the wing back together with 30-minute epoxy. Once that was done we attached inch long red threads to the airfoil, which would eventually enable to see the flow of air over the wing.

The next major phase of this test was to setup the equipment. Now we had to attach the tubes, which are connected to the static ports, to the pressure read out. This is then attached to a laptop computer that collected the data into Visual Basic. To test the airfoil we now inserted the airfoil into the box, which was strapped onto the top of a truck. We needed to use a truck to get the velocity needed for the test because the airfoil was too large to fit into our wind tunnel.

The first run we made had the following parameters: velocity = 25mph, wing angle of attack = 5° , and flaps = 0° . The data that we collected seemed to fit a nicely shaped pressure difference between the top and bottom static ports. The data shows that at the very beginning of the airfoil the pressure difference was the greatest, which should be expected. Then as the air moves towards the trailing edge the pressure difference becomes less. The red threads were flat and straight back along the wing. This result shows that the air is flowing nicely over the wing without stalling.

The second run we made had the following parameters: velocity = 25mph, wing angle of attack = 5° , and flaps = 5° . The data collect during this test gave similar results at the front static ports. However, at the last static port, .8-cord length, the 5° flap caused the pressure to drop significantly from the first test. However, the last two red threads were flapping in the wind, which could be that the airflow was stalling over the wing.

It should be noted that some disturbance might have taken place during the test for the following reason. The air flowing over the windshield of the truck came into the airflow being tested by airfoil. Essentially this created a convergent nozzle, which would cause the pressure to decrease significantly. This can be fixed for future tests by raising the wing further from the truck.

4.3 Tail Design

Proper tail design is essential in allowing us good stability and control in our aircraft's flight. The primary purpose of the tail in an aircraft is to counter unwanted movements generated by the wing. For this reason, large amounts of our tail design are based on the size and volume of the wing. Due to the fact that our wing is quite large, one would expect to have a large tail volume as well. Indeed, when calculating initial tail sizing requirements, we see that not only does the tail volume required depend on wing sizing, but also heavily upon the tail arm length, which in our case, will be a carbon fiber rod which extends from the quarter chord point of the wings to the quarter chord point on the tail. For initial tail sizing, we utilized two separate equations. The first allows us to estimate the size of vertical tail volume required to maintain stability, and this equation is as follows:

$$S_{VT} = (c_{vt} * b_w * S_w) / L$$

Where c_{vt} is equal to a coefficient which is based upon an aircraft type (ranges from .02 to .09), b_w is wing span, S_w is equal to wing span, and L is equal to the length of the tail arm. From this equation, we can see that as wing area increases, as should our vertical tail volume required. We can also see that as our tail arm length increases, the vertical tail volume decreases. Similarly, the equation for the horizontal tail volume required is as follows:

$$S_{HT} = (h_{vt} * C_w * S_w) / L$$

Where h_{vt} is equal to the horizontal tail volume coefficient (typically .05 – 1.0), C_w is the mean wing chord, S_w is the wing area, and L is equal to the length of the tail arm. Once again, we see that as wing area increases, as must the tail volume required. We also see that as the tail arm increases in length, we will need less tail size. For more in depth description of these lengths, see figure following, which provides a drawing for representation. Once we have calculated approximate tail sizing, we can then plug these numbers into a more sophisticated equation that will give us more in depth analysis.

One other aspect we looked at is that of the static margin. The main variable in calculating this was the length of the tail boom. Table 4.3 shows the $C_{N-\beta}$ and static margin associated with the various tail lengths.

4.4 Landing Gear Design

In order to begin to design our landing gear, we needed to know what type of gear was available for us to either purchase or manufacture ourselves. In order to gain a start in this endeavor, we did two main things. First, we performed research on types of landing gear normally employed on model aircraft. Secondly, we used experience gained from last year's aircraft as an example of one type of system that could be used.

From last year's plane, we were able to gain a lot of useful information. The landing gear from last year's plane utilized smaller wheels, with a shock absorber that deflected forwards and backwards from a fixed point on the leg of the gear. While this type of deflection did provide a large amount of shock absorption, it was not without its drawbacks. When large loads were applied to the gear upon landing, it would deflect backwards, and the wheels would constantly come into contact with the fuselage or wings. This resulted in unwanted damage to the aircraft. The large amount of deflection that occurred also made it difficult to estimate the required landing gear height to allow for enough clearance for the propellers. With this year's plans including the possibility of a longer propeller, it is very important that we have the knowledge of how far in the vertical direction our gear will deflect so that we will have enough propeller clearance.

In order to begin the selection and design of landing gear for our plane, we also needed to decide upon which gear arrangement to utilize. After studying different types of arrangements, we chose a "tricycle" landing gear arrangement. In this arrangement, there are two main gear located aft of the center of gravity as well as an auxiliary gear forward of the center of gravity. Because the center of gravity is ahead of the main wheels, the aircraft is very stable on the ground. This feature also makes the aircraft easier to land than other configurations. Because of the work that needed to be performed on our aircraft in between flights, it was very important that our aircraft handle well on the ground and be safe to taxi around the runway.

With knowledge of the types of landing gear arrangement we wanted to utilize, information gained from internet research, and experience gained from last year's plane, it was time to begin designing and selecting specific gear for our aircraft. For our front gear, we chose to utilize an "oleo-shock strut" design, which we could obtain from Robards free of charge. This type of gear will only displace in the vertical dimension, thus avoiding the problems encountered in last year's aircraft, and making it easy for us to estimate the amount of propeller clearance needed.

For the main gear we also had several design options from which to choose from. We could utilize an "oleo-shock strut" system like we plan to employ with the forward landing gear, which would only deflect vertically, or choose a landing gear design that would flex horizontally as well as vertically. After considerations, we chose to go with solid spring struts gear. This type of gear will flex in both directions, and as opposed to the shock absorber used for the front gear, we can more effectively distribute the force that this type of gear will apply to the aircraft body or wing.

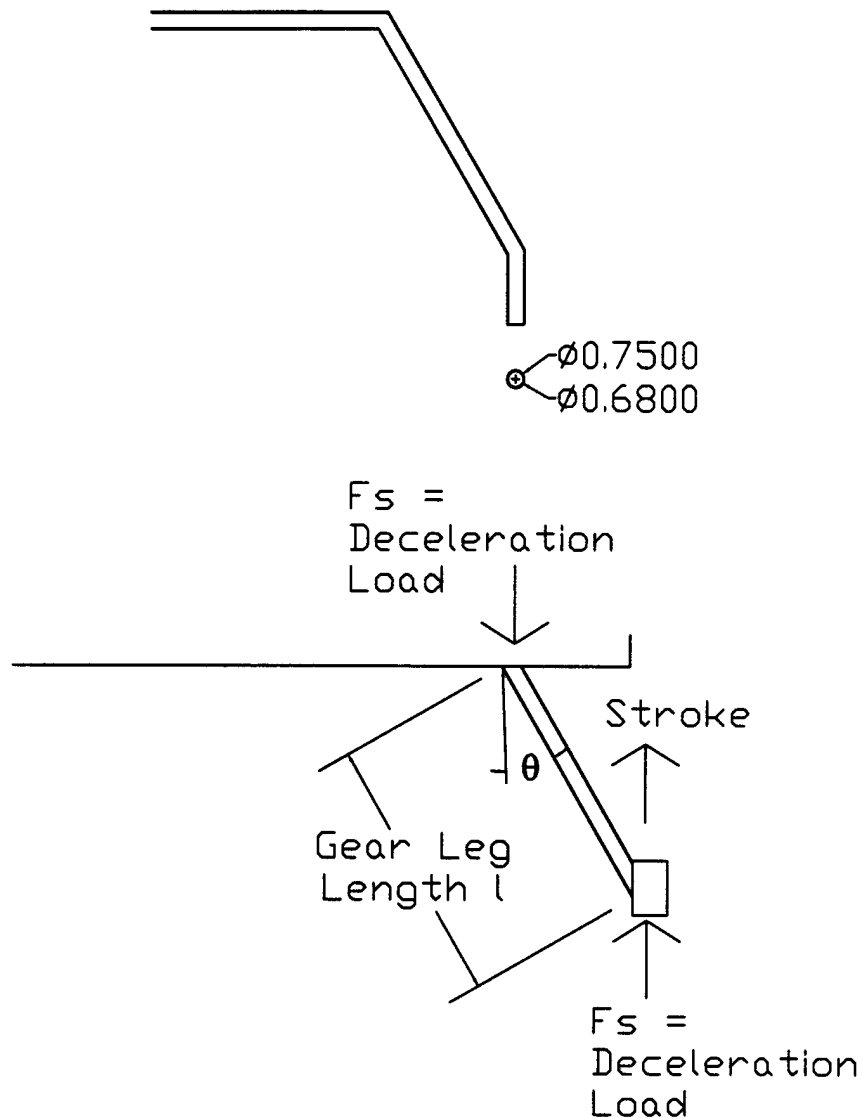
Throughout the landing gear selection process, one very important design factor that we needed to consider was the fact that our landing gear would be responsible for absorbing the force of our landing, and needed to offer enough stroke to counter this, but not enough stroke that we will be in danger of striking the propeller into the ground or causing other damage.

4.5 Propulsion

Another key factor to look at in the design of the aircraft is that of the propulsion system. We decided upon the Aveox 1412/4Y primarily because we had two left over from last year's competition. We ran various propellers and gear boxes through Electricalc 2.0 to find the optimum combination. We were trying to keep the amperage as close to the recommended 22 amps, given by Aveox, while maximizing thrust. Figure 4. shows various propellers with the 1412/4Y motor.

Our choices were narrowed down to an 18x10 and a 20x10 propeller. After further testing, the 18x10 proved incompetent. The thrust was less than the drag at a speed below the stall speed. The 20x10 proved to create more than enough thrust (see figure 5.10).

Figure 4-1 Rear Landing Gear Design



$$\text{Stroke} = F_s (\sin^2 \theta) (l^3) / (3EI)$$

where l = Gear Leg Length

E = Material Modulus of Elasticity (10000 ksi)

$$I = \pi/4 * (.375^4 - .34^4)$$

With Assumption that Aircraft Weight = 36 lbs
and $N_{\text{gear}} = 3$

$$\text{STROKE} = .135$$

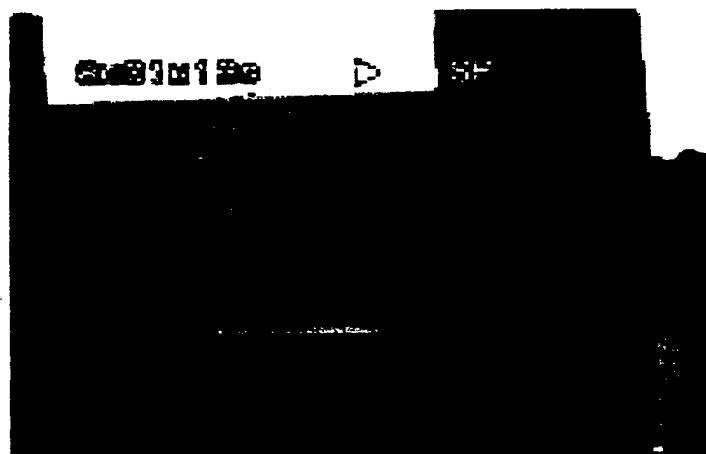
Photos from Airfoil Testing



Airfoil Fastened to Top of Vehicle



Students Ready Electronics



Airfoil "Flying" Down Runway

Table 4.3

Tail Length Analysis

Tail Boom Length	$C_{N-\beta}$	Static Margin
6 ft	.15	.166
5 ft	.12	.119
4 ft	.10	.081
3 ft	.06	.043

5. Detailed Design

Using both TK Solver and Microsoft Excel, we tested many aspects of performance mentioned in Daniel Raymer's *Aircraft Design: A Conceptual Approach*. Among the tested features were the wing characteristics, landing gear, horizontal and vertical tails, and overall flight conditions. We assumed the full payload of 8 liters and a velocity of 35 mph. The results of the TK Solver calculations are listed in tables 5.1-5.8.

5.1 Takeoff Performance

With the aircraft fully loaded, the takeoff distance has been calculated as 78.97 ft. This is well under the maximum distance of 100 ft. Liftoff velocity was also calculated to be 32.32 mph, and an indicated stall speed of 29.38 mph. With a full payload, wing loading was calculated at 2.207 lb/ft².

5.2 Propulsion

Using Electricalc 2.0, we tested the Aveox 1412/4Y using a 20x10 propeller. At full throttle, each motor will be drawing 28.2 amps, and is calculated to last 4.0 minutes. The results at 90 percent create enough thrust to produce ample lift when the aircraft is fully loaded at 35.2 pounds. At 80 percent throttle proved to be just under the power curve but will provide more than enough without the payload. This estimation comes from the data given in Electricalc.

5.3 Payload Fraction

The payload fraction of the aircraft is approximately 48.9 percent, using the actual weight of 35.2 pounds, assuming that eight fully filled, 1liter bottles will be carried.

5.4 Stability

Using TK Solver, we found the static margin of the aircraft to be 11.98 percent. According to *Aircraft Design: A Conceptual Approach*, the target range for a static margin is 5-15 percent. With these results, we should have good pitch stability. The stability results are in table 5.2, with $C_{L-\alpha}$, $C_{M-\alpha}$, and $C_{N-\beta}$ information located in tables 5.12, 5.13, and 5.14, respectively.

5.5 Landing Gear

Another key factor discussed in *Aircraft Design: A Conceptual Approach*, was that of landing gear. With the wind conditions of Wichita, KS, in mind, we decided that it would be in our best interest to keep a decent percent of the aircraft's total weight over the nose gear. This would keep the aircraft from being affected too much by the wind while on the ground. According to Raymer, the optimal percentage range is between 8-15 percent. Our aircraft's nose will be holding 15.56 percent, which is in the upper portion of that range.

5.6 Power Required / Available

Tables 5.9 thru 5.11 show power required, thrust, and rate of climb vs. velocity. These are all key graphs in figuring the aircraft's performance. We have used Electricalc 2.0 and the power curve from table 5.9 to estimate what percent we will need to keep the throttle at to sustain lift during flight and how much we may pull it back during decent.

5.7 Drawing Package

Drawings of our plane were created using AutoCAD 14. Using this program we were able to create a solid model of the airplane, with the ability to modify the design as necessary. Drawings 1 – 3 present 3 views of the airplane giving overall dimensions. Drawing 4 shows the layout of the flight propulsion and control units. Drawing 5 shows a pictorial of the aircraft with important design aspects labled.

Take-Off and Climb Performance

Table 5.1

				Flight Conditions
35	V		mph	Velocity
.002377	rho		slug/ft ³	Density
.00015723	nu		ft ² /s	Kinematic viscosity
	q	3.1319719	lbf/ft ²	Dynamic pressure
				Configuration
				Weight data
8	numbot			Number of full bottles
	Wpay	17.6	lbf	Payload water + bottles
18	Wempty		lbf	Weight empty
	W	35.6	lbf	Total lift-off weight
	W/S	2.18271	lbf/ft ²	Wing loading
	Xcg	1.58	ft	Distant from nose(datum) to cg (cwg/4)
				Performance data
	dlo	83.981722	ft	Lift off distance
	Vlo	32.140292	mph	Lift off Velocity 1.1*Vstall
	Vstall	29.218447	mph	Stall Velocity
	Vrms	22.498204	mph	Root mean Velocity for dlo calculation
	tp20Vrm	13.297466	lbf	Thrust at Vrms 2 1412/4Y's 20 in prop
	Dtot	6.5917724	lbf	Total Aircraft drag wo winglets
	Dtotip	5.8903013	lbf	Total Aircraft drag with winglets
	Cdo	.06471759		Parasite drag coefficient
	Do	3.305934	lbf	Parasite drag
	Di	3.2858384	lbf	Induced drag wo winglets
	Ditip	2.5843673		Induced drag with winglets
	Pav20	678.87543	watt	Thrust Power 2 1412/4Y's 20 in props
	Prq	458.97357	watt	Power required wo winglets
	Prqtip	410.13137	watt	Power required with winglets
	RC20	273.24612	ft/min	Rate of climb wo winglets
	RC20tip	333.93658	ft/min	Rate of climb with winglets

Table 5.2

Stability data				
	SM	.1198044		Static Margin (Xcg-Xac)/cwg
-.49	CMalpha		1/rad	Slope of CM vs alpha
4.09	CLalpha		1/rad	Slope of CL vs alpha
	CL	.69691238		Lift coefficient
	alpfltd	7.7618851	deg	Level flight angle-of attack

Wing- Clark-Y, Rectangular Planform

Table 5.3

	Xwg	1	ft	Distant from nose(datum) to le of wing
7	bwg		ft	Span
2.33	cwg		ft	Chord
.18	t*c			Thickness
	Swg	16.31	ft^2	Planform Area
1	CLmax			Maximum Lift Coefficient- clean
1	ht		ft	Height of winglets
1.3	CLmaxla			Maximum Lift Coefficient- landing flap
1.1	CLmaxto			Maximum Lift Coefficient-take off flap
.8	e			Efficiency factor Hoerner page 7-6
	AR	3.0042918		Aspect ratio
	delAR	.81545064		Delta aspect ratio due to winglets
	AREff	3.8197425		Effective AR due to winglets- Hoerner
	Cftwg	.00470743		Wing turbulent skin friction coeff
	RNcwg	760728.77		Wing Reynolds number
	Dfwg	.48093389	lbf	Wing skin friction drag
	Dswg	.684362	lbf	Wing parasite drag- Hoerner
	CDsec	.0133972		Wing parasite drag coeff- Hoerner
	CDi	.0643242		Induced drag coefficient
	CDitip	.05059207		Induced drag coefficient with winglets

Horizontal Tail

Table 5.4

	Xht	5	ft	Distant from nose(datum) to le of ht
3	bht		ft	Tail span
1	cht			Tail chord
	Sht	3		Tail planform area -rectangular
	RNcht	326493.04		Horizontal tail Reynolds number
	Cftht	.00555972		H-tail turbulent skin friction coeff
	Dfht	.10447729	lbf	H-tail skin friction drag

Vertical Tail (2)

Table 5.5

	Xvt	5	ft	Distant from nose(datum) to le of vt
.8125	cvt		ft	Average chord(each)
1	bvt		ft	Span(each)
	Svt	1.625	ft^2	Total planform area(2)
	RNcvt	265275.59		Vertical tail Reynolds number
	Cftvt	.00580135		V-tail turbulent skin friction coeff
	Dfvt	.05905142	lbf	V-tail skin friction drag(2)

Table 5.6

Landing gear struts, main+nose (3 ft)

3	Lstruts	ft	Length of main+nose struts
.75	Diastru	in	Diameter of landing gear struts
	RNstrut	20405.815	Reynolds number of strut
1.2	Cdstrut		Drag coeff of struts -cylinder Hoerner
	Sprostr	.1875 ft ²	Projected area of struts
	Dstrut	.70469368 lbf	Drag of struts

Main gear tires

3.5	Lmain	in	Distance from cg to main wheels
	Wmain	30.062222 lbf	Weight on main wheels (2)
1.5	bm	in	Tread width
5	dm	in	Height
	Spromn	1.25 ft ²	Projected area of tires(2)
.35	Cdmain		Drag coefficient Hoerner
	Dmain	1.3702377 lbf	Drag of tires(2)

Nose gear tire

19	Lnose	in	Distance from nose wheel to cg
1.25	bn	in	Tread width
	Wnose	5.5377778 lbf	Weight on nose wheel
	Wn%W	.15555556	Percent weight on nose wheel
3.25	dn	in	Diameter
.35	Cdnose		Drag coefficient Hoerner
	Sprons	.33854167 ft ²	Projected area of tire
	Dng	.37110605 lbf	Drag of tire

Table 5.7

Engine nacelles (2)

1.75	dnac	in	Diameter of each nacelle
.039	Cdnac		Nacelle drag coefficient Hoerner
	Spronac	.03340669 ft ²	Projected area of nacelles (2)
	Dnac	.00408052 lbf	Drag of nacelles (2)

Table 5.8

Fuselage

4.6	hfus	in	Height of fuselage
2	wfus	in	Height of fuselage
	Lfus	12 in	Length of fuselage
.06	CDfus		Drag coefficient Hoerner
	Sprofus	.06388889	Projected area of fuselage
	Dfus	.01200589 lbf	Drag of fuselage

Figure 5-9

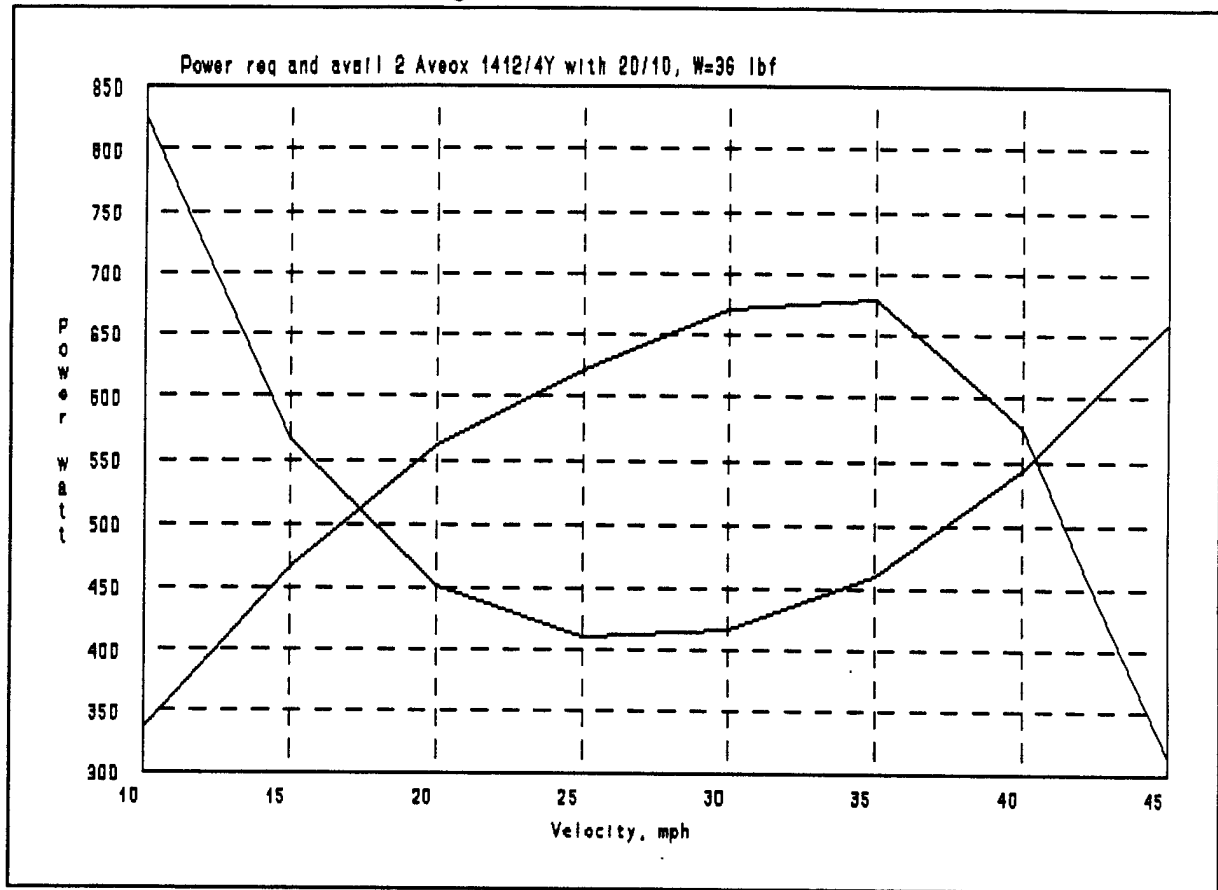


Figure 5-10

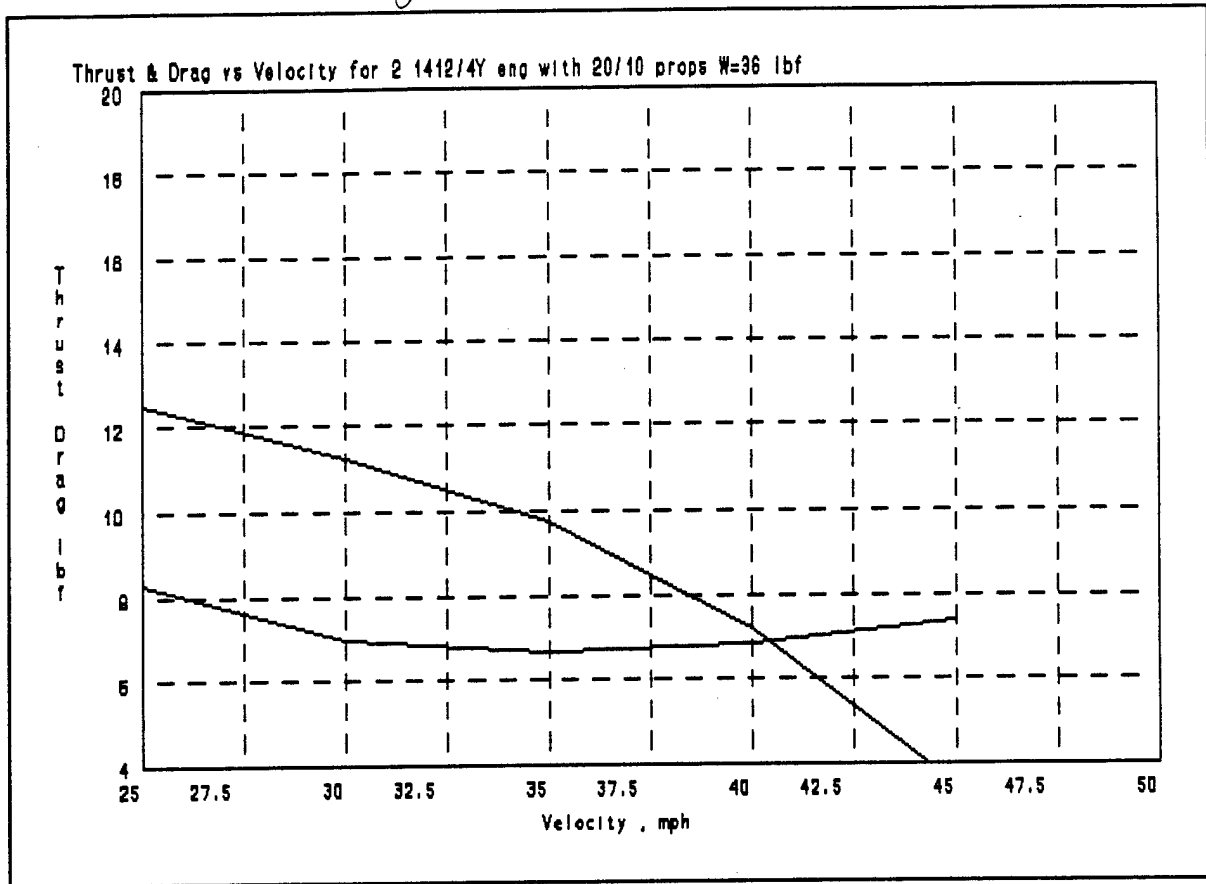


Figure 5-11

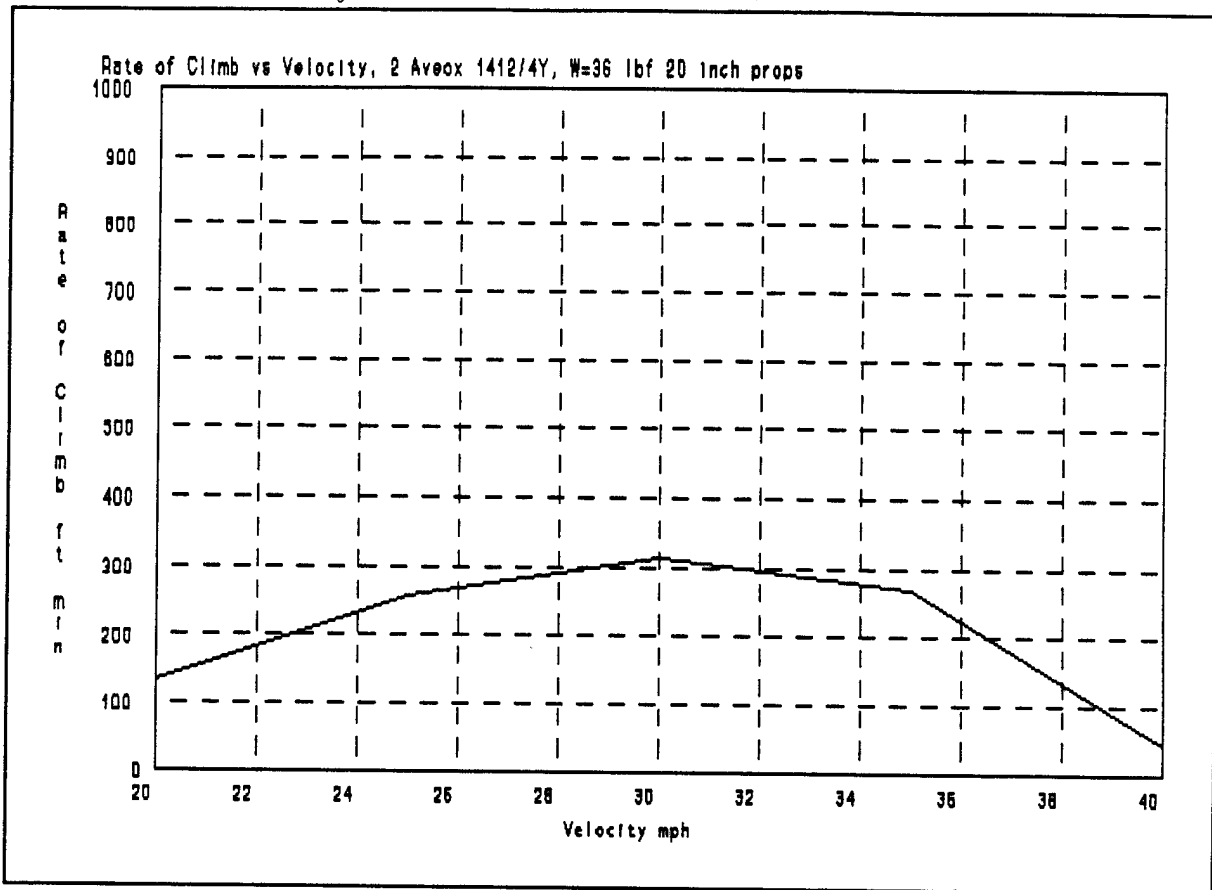


Figure 5-12

C-L-ALPHA TABLE

MACH NO>0.010000	0.020000	0.030000	0.040000	0.050000
ALPHA				
0.00	4.11546	4.11546	4.11546	4.11546
2.00	4.09307	4.09307	4.09307	4.09307
4.00	4.10291	4.10291	4.10291	4.10291
6.00	4.11782	4.11782	4.11782	4.11782
8.00	4.12914	4.12914	4.12914	4.12914
10.00	4.13631	4.13631	4.13631	4.13631
12.00	4.13872	4.13872	4.13872	4.13872
14.00	4.13581	4.13581	4.13581	4.13581
1	C-M-ALPHA TABLE			

MACH NO>0.010000 0.020000 0.030000 0.040000 0.050000

+ Buffer: SACPOUT.LIS
CTRL-Z Save&Exit CTRL-F Abort CTRL-D Command PF2 KeyMap | Write | Insert | Forward

698 lines read from file SYS_USERS:[AER.WALKER.SACP]SACPOUT.LIS;244

Figure 5-13

C-M-ALPHA TABLE				
MACH NO>0.010000	0.020000	0.030000	0.040000	0.050000
ALPHA				
0.00	-0.63385	-0.63385	-0.63385	-0.63385
2.00	-0.63040	-0.63040	-0.63040	-0.63040
4.00	-0.63192	-0.63192	-0.63192	-0.63192
6.00	-0.63421	-0.63421	-0.63421	-0.63421
8.00	-0.63596	-0.63596	-0.63596	-0.63596
10.00	-0.63706	-0.63706	-0.63706	-0.63706
12.00	-0.63743	-0.63743	-0.63743	-0.63743
14.00	-0.63699	-0.63699	-0.63699	-0.63699
C-M-Q TABLE				
MACH NO>0.010000	0.020000	0.030000	0.040000	0.050000
ALPHA				
Buffer: SACPOUT.LIS				
CTRL-Z Save&Exit	CTRL-F Abort	CTRL-D Command	Write Insert Forward	PF2 KeyMap

698 lines read from file SYS_USERS:[AER.WALKER.SACP]SACPOUT.LIS;245

C-N-BETA-TOTAL TABLE

1

MACH NO>0.010000	0.020000	0.030000	0.040000	0.050000
ALPHA				
0.00	0.14667	0.14643	0.14630	0.14620
2.00	0.14921	0.14897	0.14883	0.14874
4.00	0.15248	0.15224	0.15210	0.15201
6.00	0.15648	0.15624	0.15610	0.15600
8.00	0.16119	0.16095	0.16081	0.16070
10.00	0.16660	0.16636	0.16621	0.16610
12.00	0.17268	0.17243	0.17229	0.17217
14.00	0.17941	0.17916	0.17901	0.17889

1

C-N-BETA-WING TABLE

MACH NO>0.010000	0.020000	0.030000	0.040000	0.050000
------------------	----------	----------	----------	----------

+

ALPHA
Buffer: SACPOUT.LIS
CTRL-Z Save&Exit CTRL-F Abort CTRL-D Command PF2 KeyMap
Write | Insert | Forward

698 lines read from file SYS_USERS:[AER.WALKER.SACP]SACPOUT.LIS;245

Figure 5-15

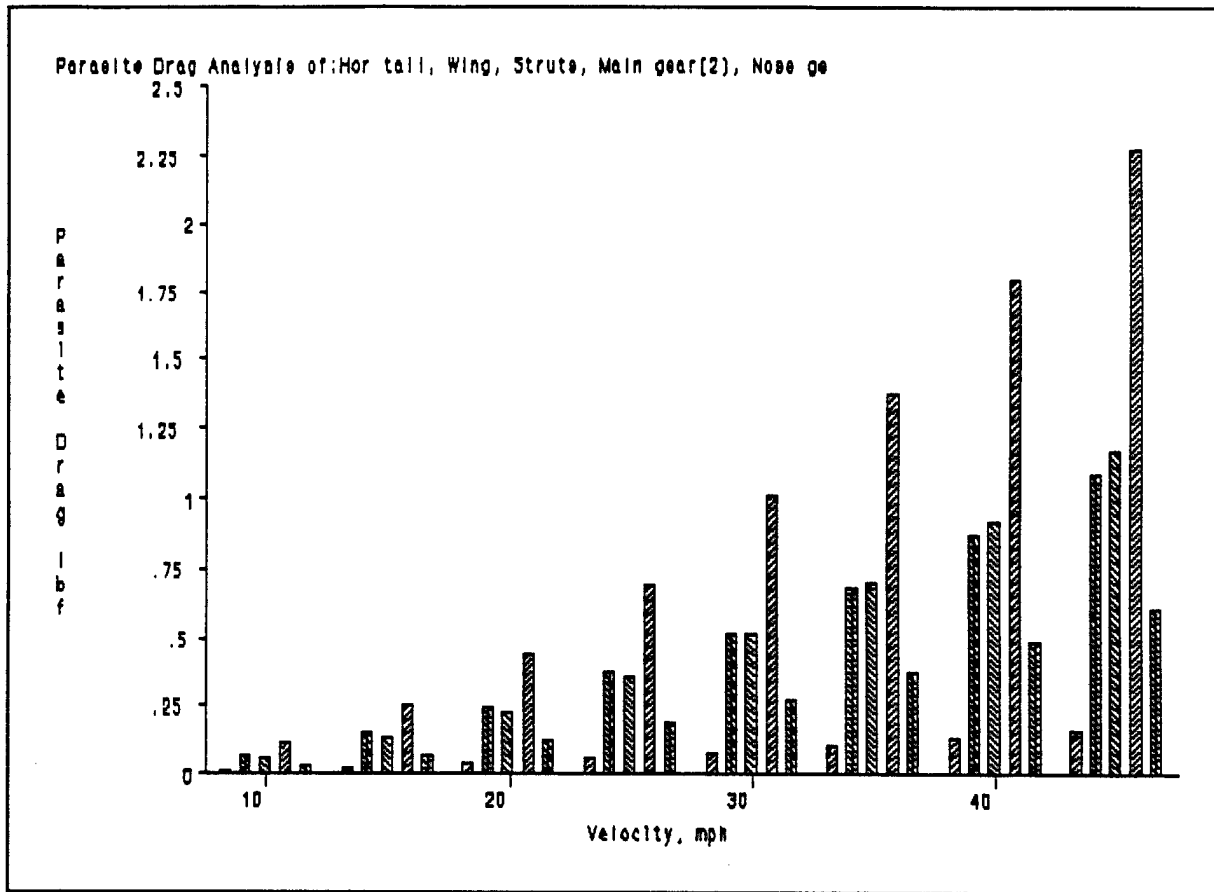
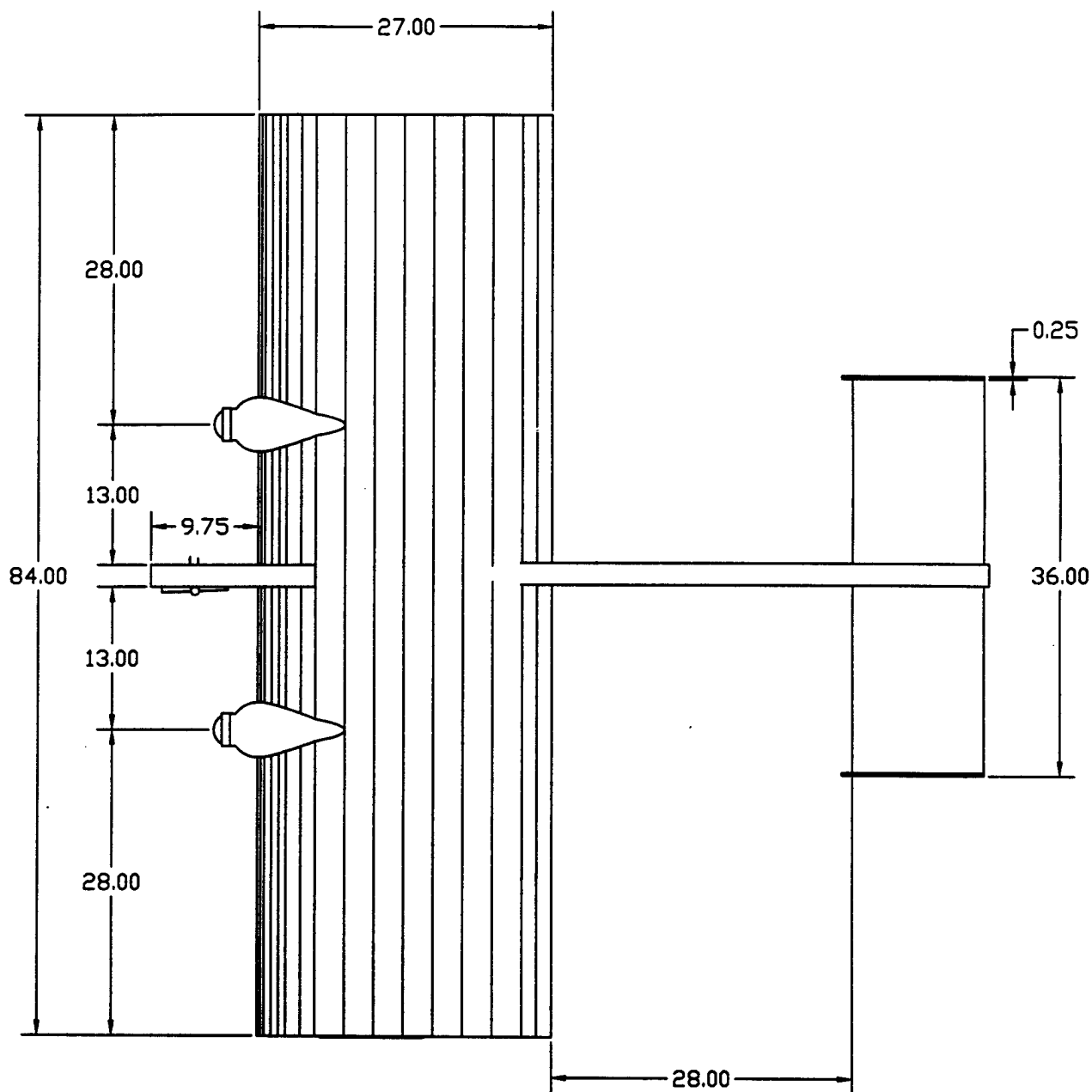


Figure 5-16

Setup	
Prop KRPM	3.62
Motor KRPM	13.45
Prop Watts	486
Motor Watts	575
Motor Amps	28.2
Motor Volts	20.4
Battery Amps	28.2
Run	2000
Minutes	4.0
% Throttle	100
% System Eff.	72
% Motor Eff.	89
Prop Diameter	20.00
Prop Pitch	10.00
Pitch MPH	34
Plane oz	282
Wing sq.in.	1174
Wing oz/sqft	34.6
Drag coeff.	0.121
Watts/pound	33
Climb ft/min	570
Climb angle	17
Max ft/min	570
@ angle	17
Max climb ft	2306
Cruise Minutes	6.7
Stall MPH	19
Max. MPH	38
Speed MPH	22
Thrust oz	108
Drag oz	24
Motor	1412/4Y
Type	
Mfr	AVEOX
Kv	725
	65
	0.7
Km	7.30
Gearing	3.71
Motor Config.	1
Prop	MAS Electric
Type	
K prop	1.58
K pitch	-0.04
K eff	1.05
Cell Type	SR 2000 max
Cell Count	19
Pack Wgt oz	35.1
Cell Volts	1.25
Cell mohm	5.5
ESC mohm	15

ElectriCalc 03-09-2000 08:40:59

Electricalc 2.0 Calculations
for Avox 1412/4Y with
19 cells and 20x10 propeller



Miami University

Aeronautics & Manufacturing Engineering Depts.

Oxford Ohio 45056

Title
Span Loader Top View

The Miami University Aircraft Design Team

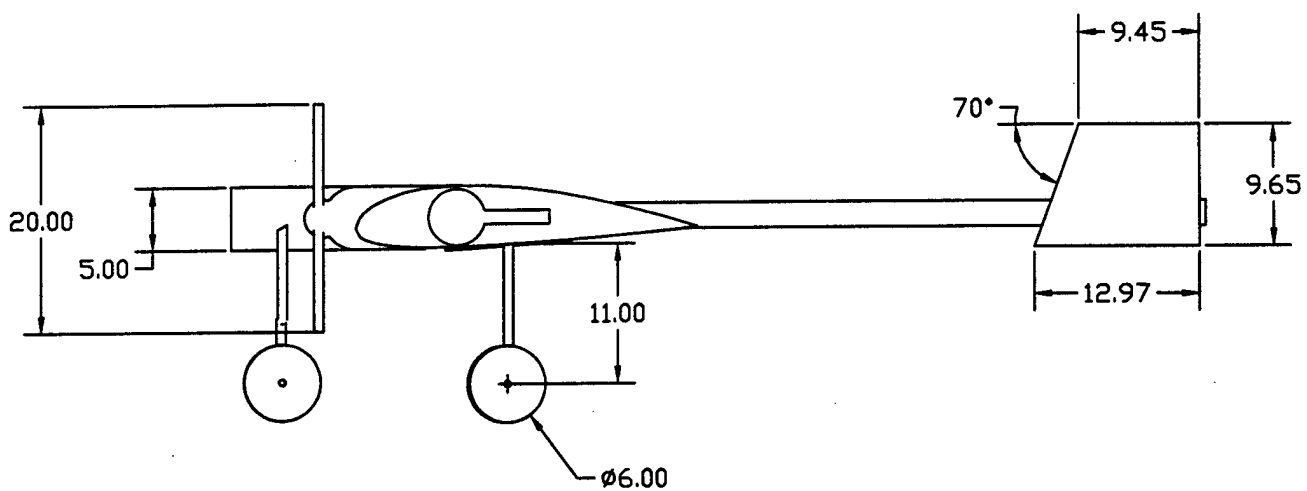
AIAA Cessna/ONR Design Build and Fly Competition

Scale: 1:15

Drawing No.

Sheet 1 of 1

1



Miami University

Aeronautics & Manufacturing Engineering Depts.

Oxford Ohio 45056

Title
Span Loader Side View

The Miami University Aircraft Design Team

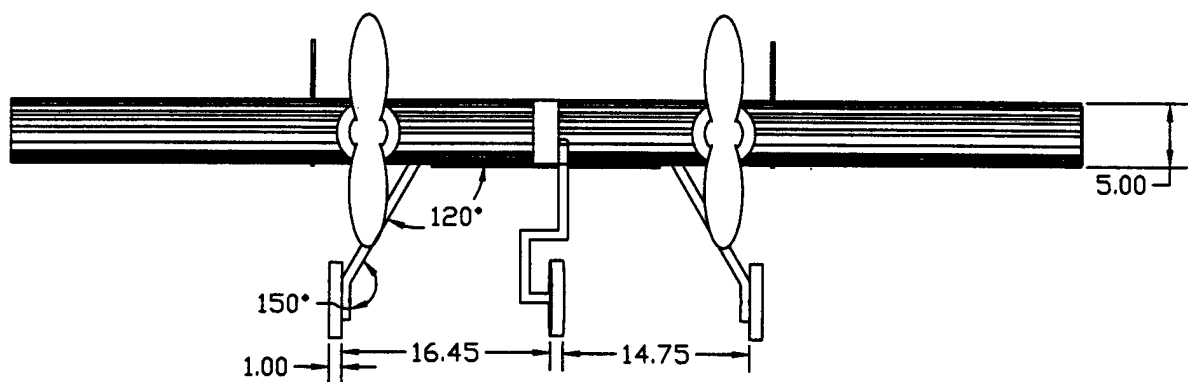
AIAA Cessna/ONR Design Build and Fly Competition

Scale: 1:15

Drawing No.

Sheet 1 of 1

2



Miami University

Aeronautics & Manufacturing Engineering Depts.

Oxford Ohio 45056

Title
Span Loader Front View

The Miami University Aircraft Design Team

AIAA Cessna/ONR Design Build and Fly Competition

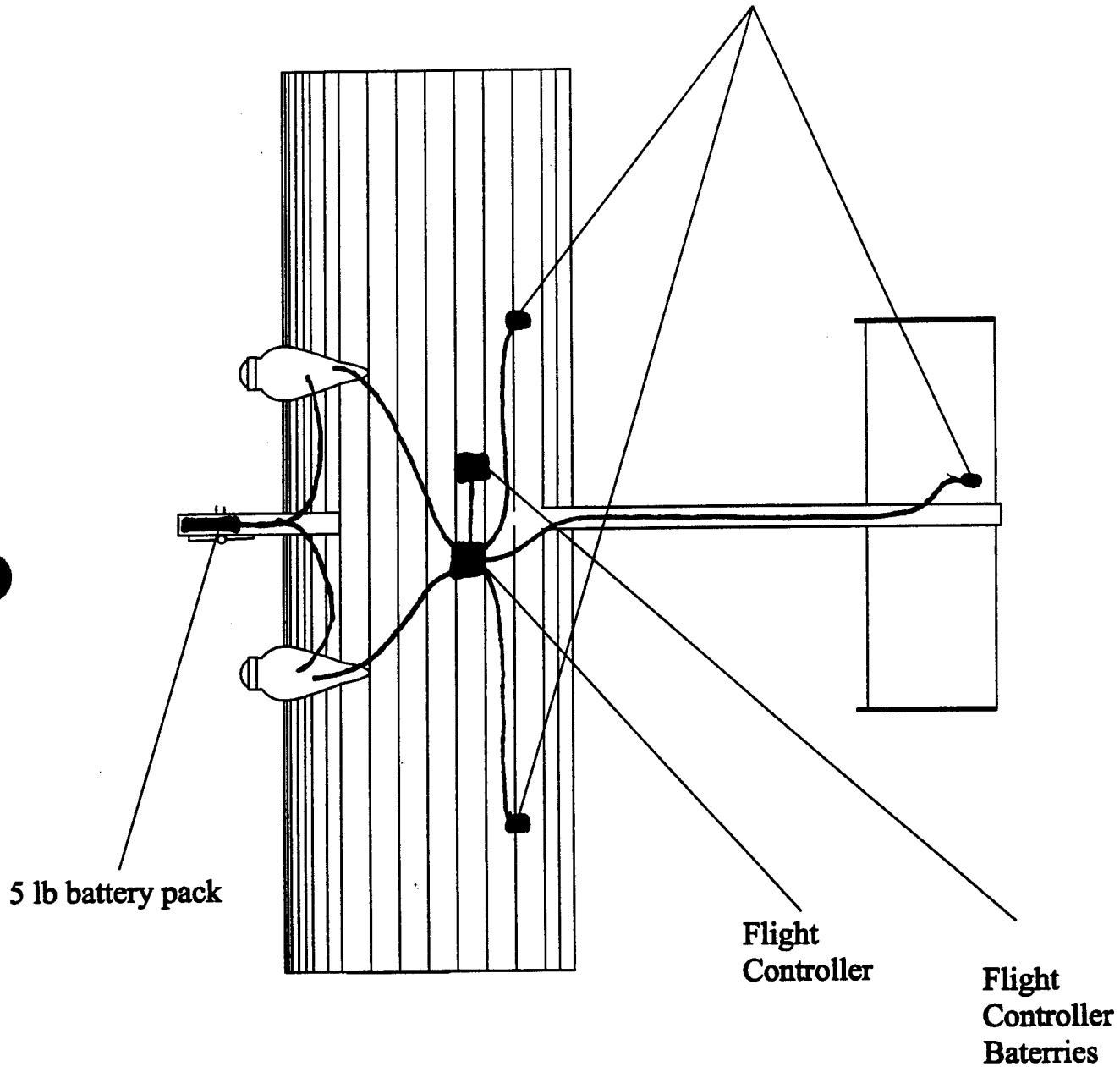
Scale: 1:15

Drawing No.

Sheet 1 of 1

3

Servo Locations



Miami University

Aeronautics & Manufacturing Engineering Depts.

Oxford Ohio 45056

Title
Span Loader Propulsion
System

The Miami University Aircraft Design Team

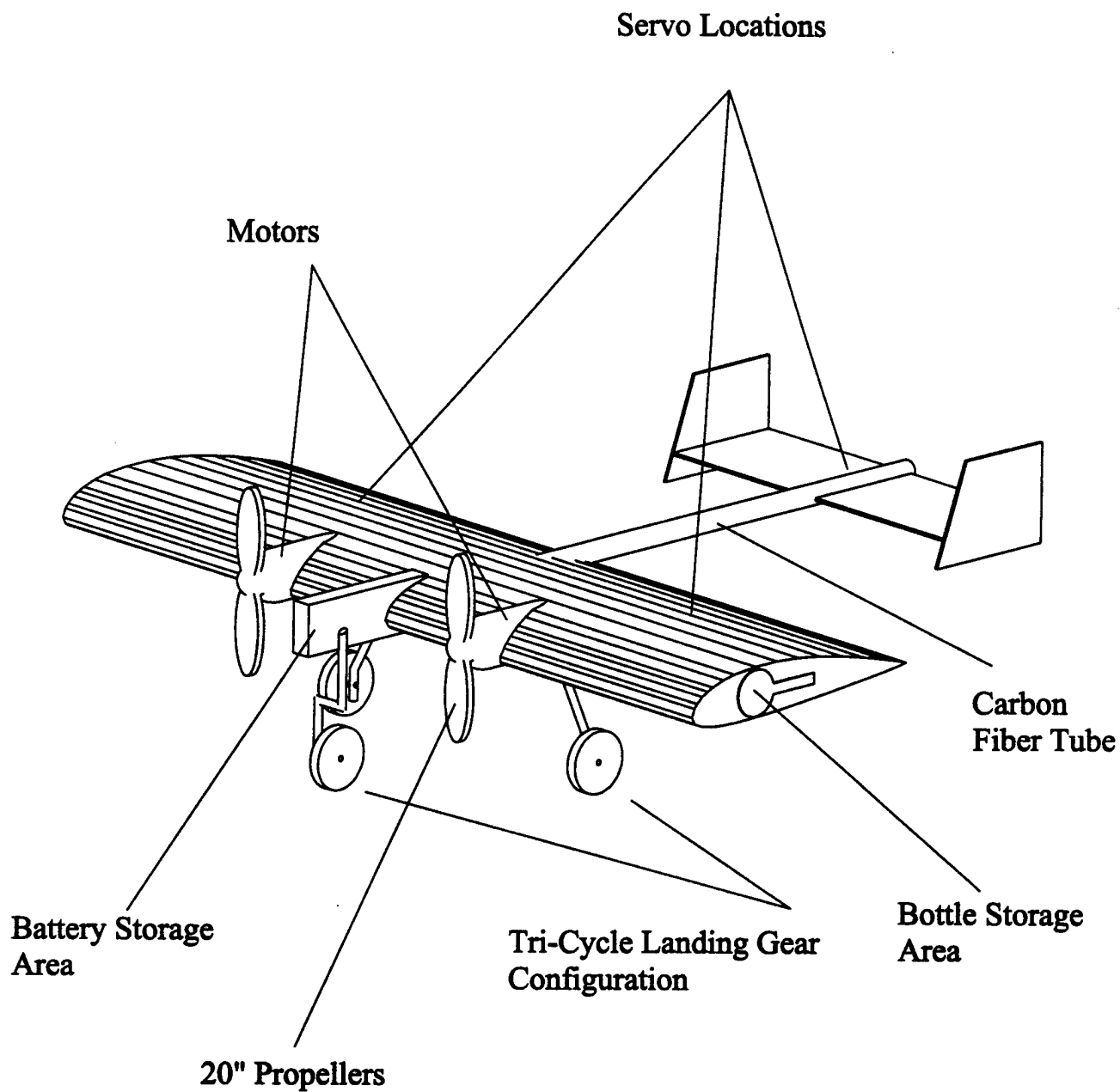
AIAA Cessna/ONR Design Build and Fly Competition

Scale: 1:15

Drawing No.

Sheet 1 of 1

4



Miami University

Aeronautics & Manufacturing Engineering Depts.

Oxford Ohio 45056

Title
Span Loader Pictorial

The Miami University Aircraft Design Team

AIAA Cessna/ONR Design Build and Fly Competition

Scale: 1:15

Drawing No.

Sheet 1 of 1

5

6. Manufacturing Plan

One of the keys to our design was to make the aircraft rather simple to construct. Given our relative lack of experience with model aircraft construction, we wanted to simplify this task as much as possible. We also hoped that this would help to keep the cost of our aircraft down as well. As part of this simplification process, we designed the components of our aircraft to enable us to construct many of the parts concurrently with each other, thus saving valuable time. Additionally, we designed the parts so that they could be easily modified in order to enhance the performance and handling of the aircraft.

Since our wing essentially functions as both the wing and the fuselage, its construction involved the most time and effort. Because all of the other components interface with the wing, we knew that it would eventually be a bottleneck, and focused a lot of effort into completing it. The first step in constructing the wing was preparing a foam cutter which could be utilized to form the wing shape from a block of high density Styrofoam. Because of the size of our wing, we needed to custom make a wire cutter. Once this was complete, we fashioned end caps for either side of the wing that served to guide the wire along the wing silhouette. We made these end caps by downloading the correct airfoil coordinates from the Internet and translating these into a language that our CNC mill would understand. Next, we cut the end caps on the mill from a sheet of aluminum. These end caps were then carefully bolted into position on the half wing Styrofoam core using a number of small screws. Once this was done, we used our hot wire cutter to shape the half wing. With this completed, we now had the basic core of our wing, and essentially, the fuselage of our aircraft. Before the two pieces could be joined together, we also needed to finish construction on some other aircraft components.

Concurrently with the cutting of the wing, we were performing work on other components of our aircraft. It was especially important that we complete construction of our nose section, which would fit in between the two wing sections.

The nose section, which holds the main motor batteries, as well as the front gear and steering servo, was constructed out of aircraft grade quarter inch plywood. The nose section begins just in front of the carbon fiber spar, towards the leading edge, and continues out to where the front gear is mounted. Three large holes were drilled into this plate, one where the bottles slide through, and two where the batteries mount. This main plate is capped for structural integrity with half-inch wood on both the top and the bottom of the plate. The top and bottom cap have been epoxied into place. The front firewall is mounted to the end of the nose section, and the front gear mounted to that.

While work was being performed on the wing and the nose section of our aircraft, we were also completing construction of our main landing gear. Our main landing gear consists of a hollow 6061T6 aluminum tube with an outside diameter of .75" and an inside diameter of .68" as well as a 6" x 12" x 3/32" 2024 aluminum sheet. The tube was bent to the predetermined angles and length using a pipe bender, with a full sized plotted schematic serving as a guide. This section was then arc welded to the aluminum

sheet. To finish construction of the main gear, lightening holes were added to the aluminum sheet, as were bolt holes that will be used to anchor the landing gear in place.

At this time, the middle halves of the wing sections were routed out to accommodate the nose section as well as the one-inch carbon fiber rod necessary to mount the empennage. Next, we joined the two wing halves with the rear carbon fiber rod in place. At this time we joined only the rear half of the wing, from the trailing edge towards the position of the main spar.

Once the two wing sections were joined together, we still needed separate the entire wingspan, just behind the quarter chord line in order to insert a carbon fiber spar, which would strengthen the wing. As before, we used the foam cutter to make the cut, and then placed the rear section into the vice that we had created to cradle our wing, with the newly cut face pointing upward, parallel with the floor. Next, we routed out a groove in the rear section of the wing to accommodate the carbon fiber main spar. We then cut three strips of woven carbon fiber slightly longer than the total length of the wing, allowing room to remove the excess carbon fiber at the wing tips. We mixed a quantity of epoxy and applied it to the length of the wing. Once this was done, the first layer of carbon fiber cloth was spanned across the length of the wing, working the glue through the carbon fiber. Over this first cloth, we mixed and poured more epoxy. On top of this went another carbon fiber cloth, and the process was repeated until we had three layers of carbon fiber across the length of the wing. Finally, we applied epoxy to the top of this third layer of cloth and placed the front leading edge section of the wing back into place, and secured it so that it would dry in place.

With the wing glued back into place, we still had much more work to accomplish before the wing would be finished. Our next step was to cut out weight saving pockets into the rear of the wing. Before this was accomplished, however, we needed to mount our main landing gear to the bottom of the wing just behind the aircraft's main spar. In order to do this, we first traced the outline of the mounting plate on the Styrofoam. Before doing this, lightning holes were cut into the mounting plate, and holes were drilled into the plate and foam, all of the way through to two plates position on the top of the wing that help hold the gear in position. Once this was done, we used a propylene torch to heat the mounting plate and gear and pressed it into position in the Styrofoam. Using this method gave us several advantages. First, the lightning holes in the gear left a raised foam section that will help to hold our gear in position. Secondly, the melting of the foam under the gear caused the Styrofoam to stiffen. To perform this, we once again employed the hot wire cutting method. In order to make sure that the holes would be round and well lined up, we milled circles into two separate sheets of PVC, which were used as guides on the top and bottom of the wing for the wire. These were fastened in place on the wing using small drywall screws. In order to get the cutter inside of the molds, we first heated a steel rod using a torch and plunged it through the Styrofoam to create a hole in the center of the future pocket, to slip the wire from the cutter through. From there, it was easy to guide the wire around the inner edge of the PVC to create the weight saving pockets.

With the pockets cut, we only had one task left for our multifunctional wire cutter-cutting the ailerons. To accomplish this task, we used two slender, square sheets of aluminum to serve as guides for the cutter. Two people each held the sheets in position on the top and bottom of the wing as the third person slid the wire cutter along the aluminum guides.

Another very important part of our manufacturing process was the mounting of the motor pods, which are made from aluminum tubing. Because of our motor configuration, it is important that these motors be mounted precisely, while being anchored strongly to the aircraft. The tubes that house the motor were left longer than deemed necessary so that we could slide them backward and forward to accommodate the center of gravity. In order to make an indentation matching the size of the motor pods, another tube of the same size was cut to length, and one end was sharpened using a lathe. The wing was then leveled on the floor, and this tube was twisted along a steel beam into the Styrofoam. The steel beam ensured that the hole was level to the centerline of the wing. The tube was twisted in a set length, and then removed, taking the excess Styrofoam along with it. The finished product was a very smooth home for the motor pods. Once we had the aircraft balanced, the motor pods were inserted into these holes and secured with epoxy.

As work was being completed on the wing, construction of the tail of the aircraft was also being finalized. The tail was very easy to construct, with the most difficult part being the joining of the boom to the stabilizer. The tail was constructed of $\frac{1}{4}$ inch balsa sheeting. The horizontal portion was cut first, with the ends slotted to allow for a good connection to the vertical sections. We also inserted ten lightening holes in the stabilizer using a hole drill. The vertical sections were cut using a razor blade, and were stiffened by applying carbon fiber tape from the top to the bottom of each section. Before the vertical sections were attached, MonoKote was applied to both the vertical and horizontal sections of the tail. Next, a slot was cut into the one-inch diameter carbon fiber boom to accommodate the horizontal section for a solid connection between the tail and boom. The tail boom was then slid into place over the MonoKote, with special care taken to ensure that the tail was perpendicular to the tail arm. Finally, the vertical fins were fastened to the horizontal section using epoxy, ensuring the vertical fins were perpendicular with horizontal section, and parallel with the length of the tail boom. Additionally, an elevator was prepared out of balsa stock, shaped, MonoKoted, and attached using cyanoacrylate (CA) hinges and ZAP CA. Finally, a servo well was made and the servo mounted near the tail boom. The appropriate hardware, control horns, servo horns, and linkages, were installed. The elevator servo lead was threaded into a small hole in the tail boom and run towards the receiver well in the main wing.

Our next task was to mount the aileron servos and to route holes for the receiver, its battery pack, and the accompanying wires that drive all of our electrical systems. We first used a marker to trace out the circuit diagram onto the wing of the aircraft. Once this was completed, we used a router to mill out the wells required for the batteries, receivers, and servos. In order to route canals for our wires, we simply traced along the path for the wires as we had drawn it with a marker using a soldering iron.

Currently, we have to sheet the wings with 3/32" balsa, then MonoKote. After this is completed we will install our electronics, power pods, and undercarriage. Following this, we will balance the aircraft by making the tail boom shorter as needed to make the craft slightly nose heavy. Lastly, we will adjust all control throws, and set up the dual-rates on our transmitter, charge the batteries and go fly!

TABLE 6.1

Manufacturing Milestone Chart

Activity	Week of 1/2/00	Week of 1/9/00	Week of 1/16/00	Week of 1/23/00	Week of 1/30/00	Week of 2/6/00	Week of 2/13/00	Week of 2/20/00	Week of 2/27/00	Week of 3/5/00	Week of 3/12/00	Week of 3/19/00	Week of 3/26/00	Week of 4/2/00	Week of 4/9/00	Week of 4/16/00	Week of 4/23/00	Week of 4/30/00
Build Foam Cutter																		
Cut end caps																		
Cut Wing																		
Build Nose																		
Build Tail																		
Build Landing Gear																		
Motor Pod Construction																		
Wing Modification & Attachments																		
Ailerons/Servos																		
Install Electronics																		
Coat Wing																		
Final Adjustments																		

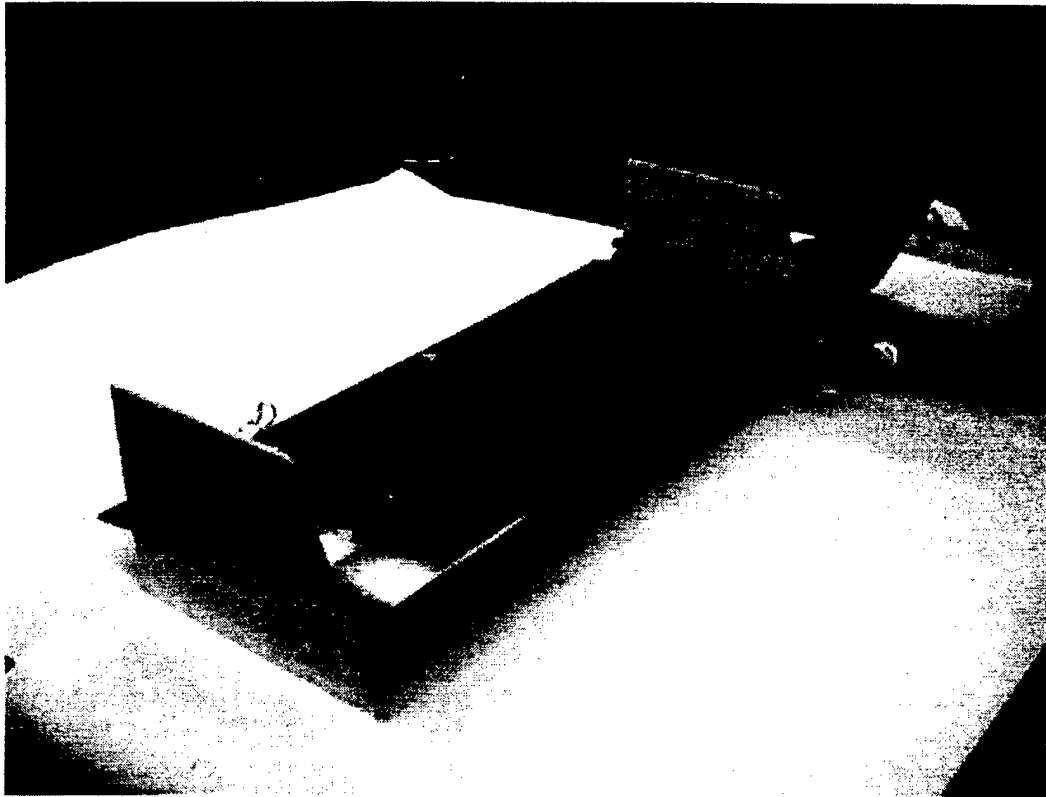


Figure 6.2: Working on the Tail

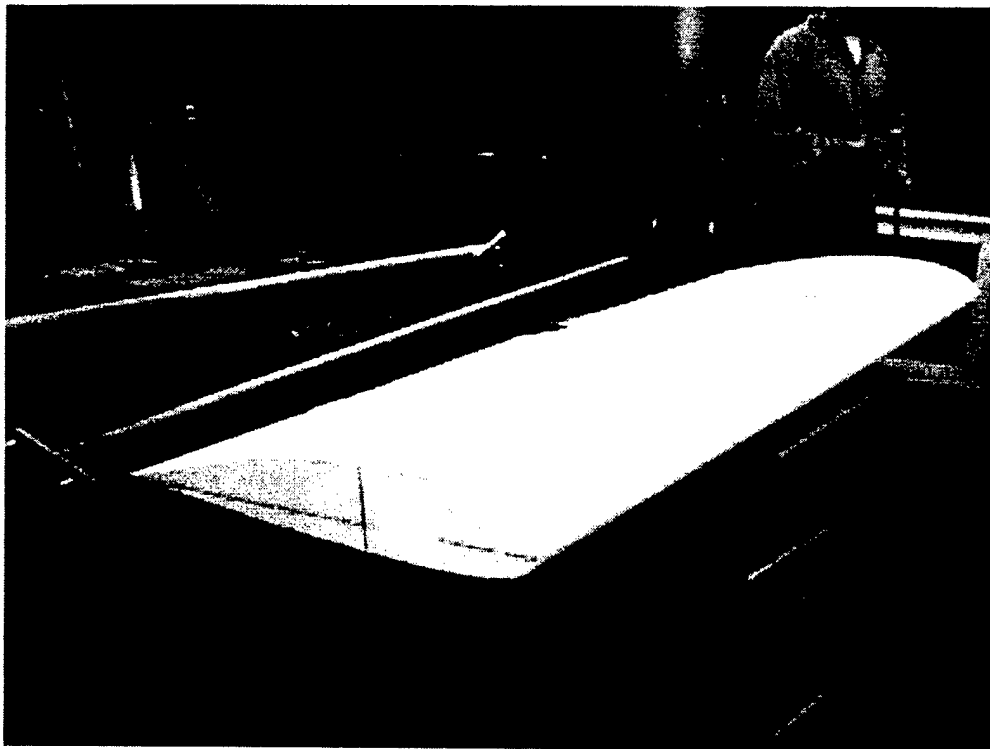


Figure 6.3: A View of the Wing

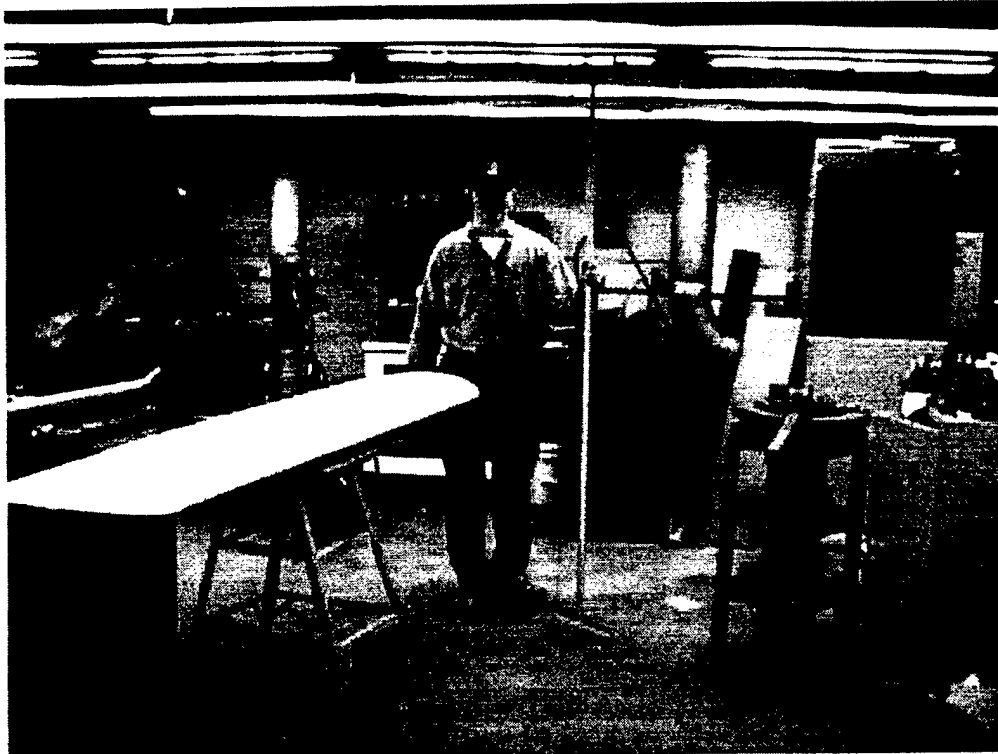


Figure 6.4: The Foam Cutter

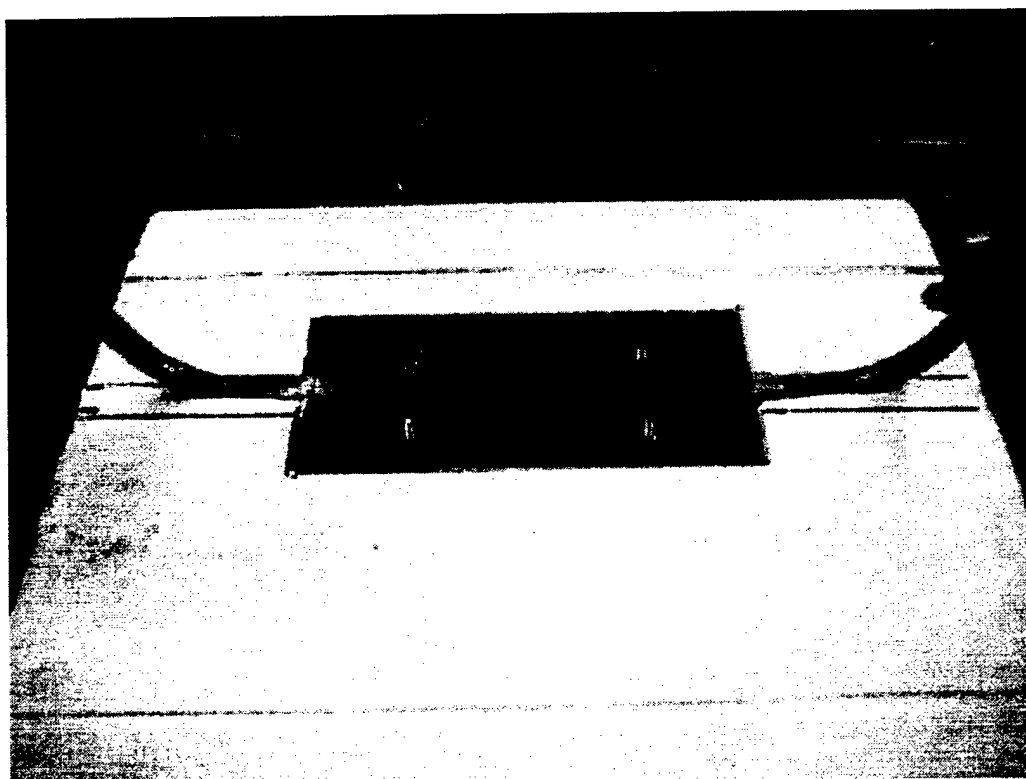


Figure 6.5: Landing Gear Attachment

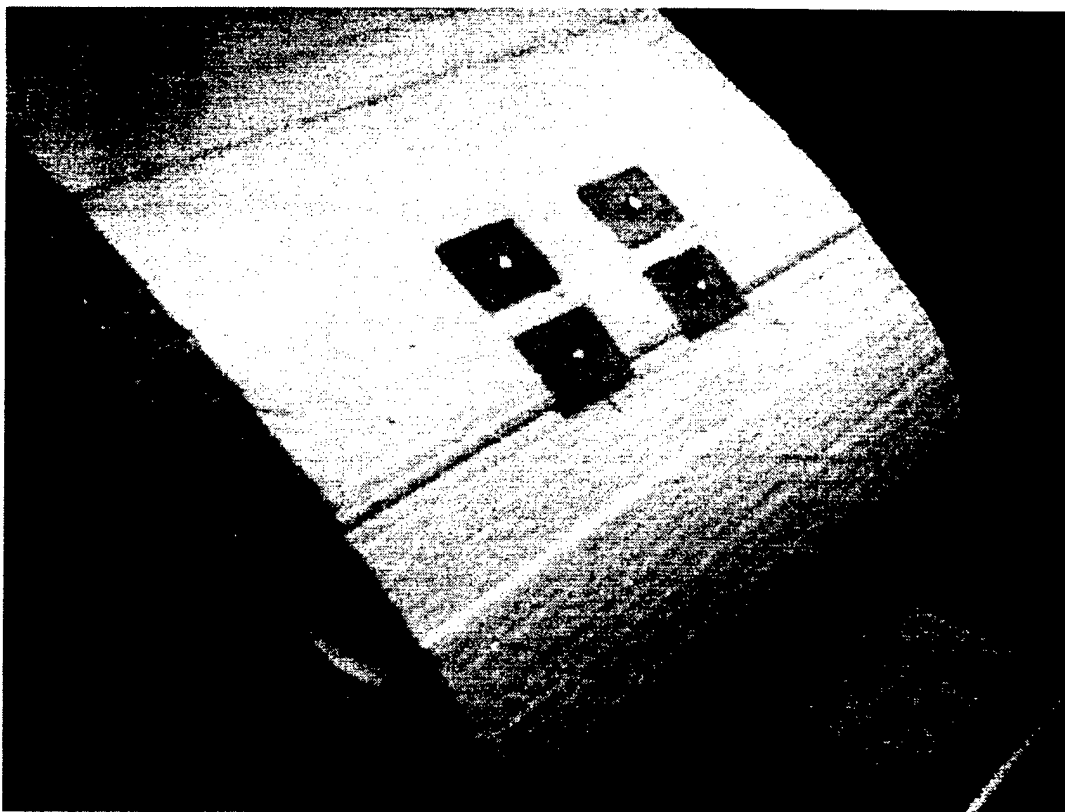


Figure 6.6: Top of Wing

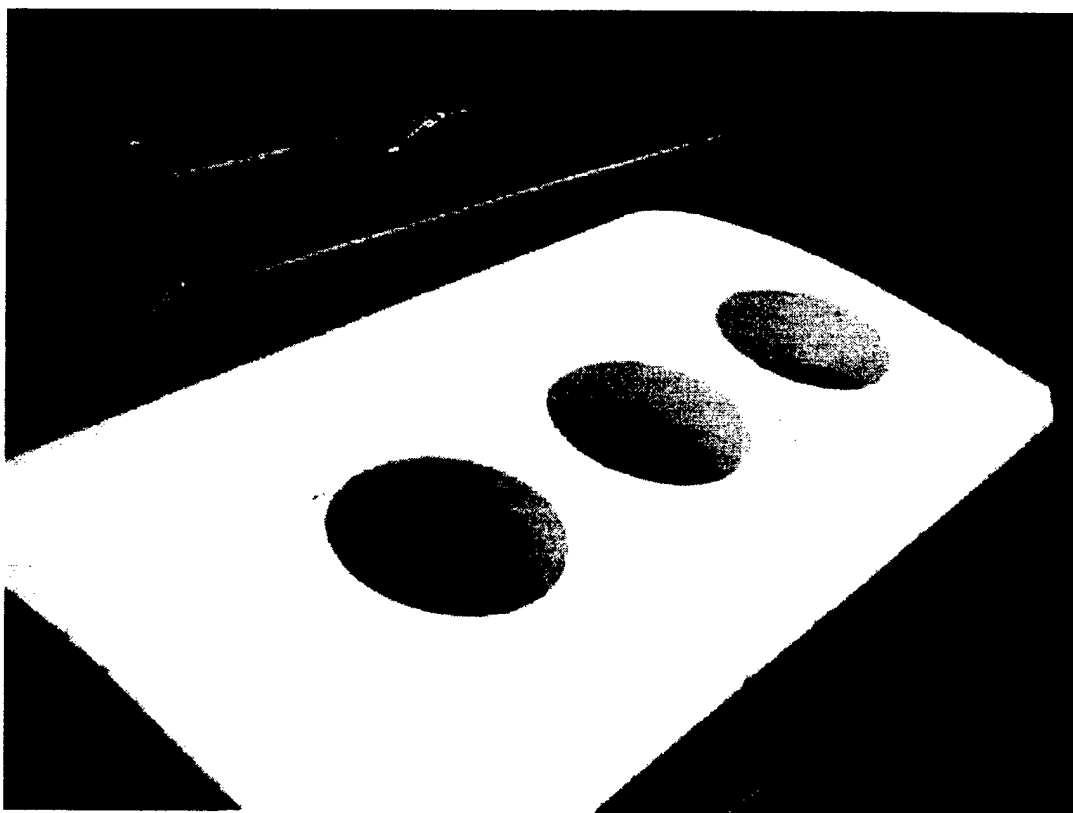


Figure 6.7: Holes Cut in Wing

References

- AIAA. Cessna ONR Student Design/Build/Fly Competition Rules, 1999.
- AIAA Student Design/Build/Fly Competition. College Station: Texas A&M University, 1998.
- Cawthorne, Nigel. Engineers at Work: Airliners. New York: Gloucester Press, 1988.
- Dieter, George. Engineering Design. Ed. Kevin T. Kane. 3rd ed. Boston: McGraw Hill, 1991.
- Hale, Francis. Introduction to Aircraft Performance, Selection, and Design. New York: John Wiley & Sons, 1984.
- Jenkins, M. "Aeronautics." Standard Handbook for Mechanical Engineers. Ed. Eugene A. Avallone. New York: McGraw Hill, 1996. 59-99.
- Lambert, Mark. Aircraft Technology. New York: The Bookwright Press, 1990.
- Lennon, Andy. Basics of R/C Model Aircraft Design. Wilton: Air Age Inc., 1996.
- "Monthly Data for Wichita" National Weather Service. Online. Internet. 15 Oct. 1999. Available: <http://www.erh.noaa.gov/ict/eli.htm>.
- Raymer, Daniel. Aircraft Design: A Conceptual Report. Washington D.C.: American Institute of Aeronautics & Astronautics, 1989.
- Shevell, Richard. Fundamentals of Flight. Ed. Gertrude Szyferblatt. 2nd ed. Englewood Cliffs: Prentice Hall, 1989.
- Smith, Hubert. The Illustrated Guide to Aerodynamics. Blue Ridge Summit: Tab Books Inc., 1985.
- The MUX-1. Oxford: Miami University, 1998.
- Time-Life Books. How Things Work: Flight. Alexandria: St. Remy Press, 1990.
- http://amber.aae.uiuc.edu/~m-selig/ads/coord_database.html#N

"The Hammerhead"

Special Features

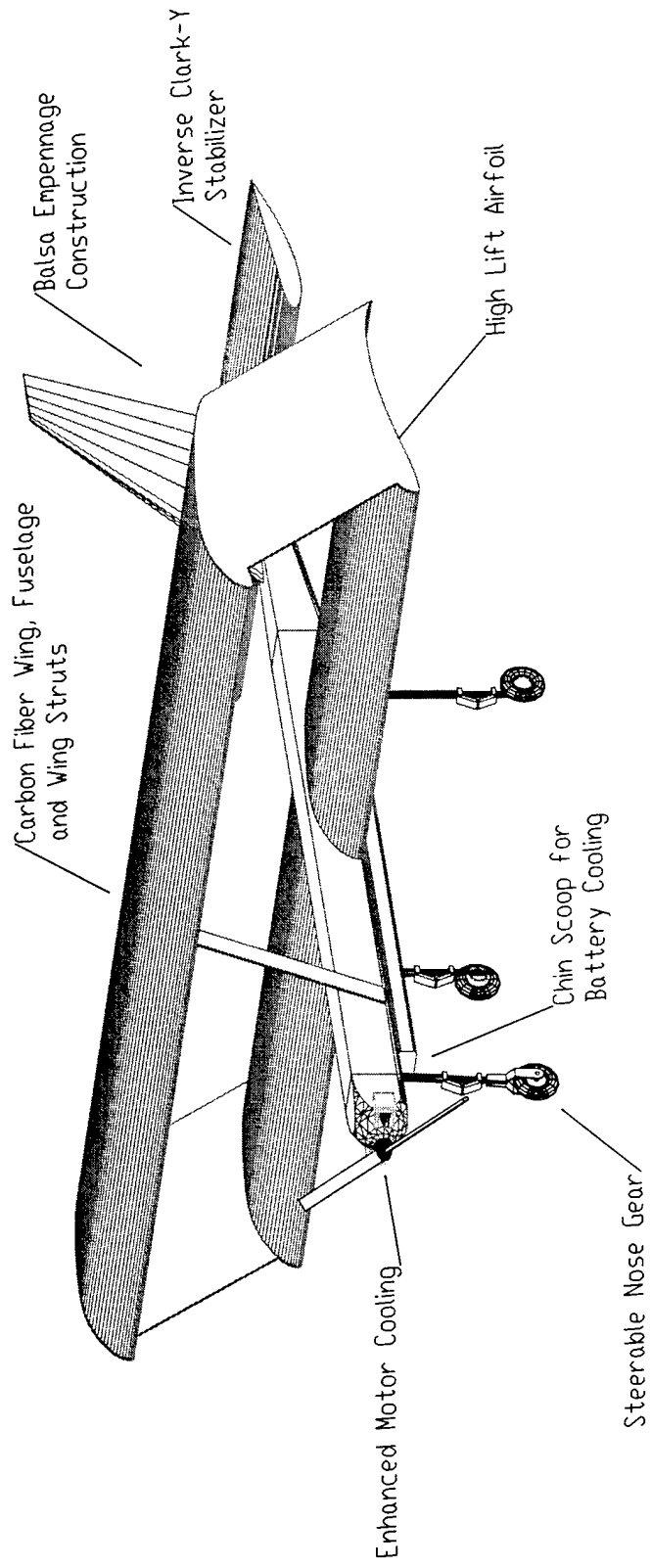


TABLE OF CONTENTS

1	EXECUTIVE SUMMARY	1
1.1	DEVELOPMENT PROCESS	1
1.2	DESIGN TOOLS OVERVIEW	2
1.3	PRELIMINARY BUDGET	4
2	MANAGEMENT SUMMARY	6
2.1	TEAM ARCHITECTURE	6
2.2	MANAGEMENT STRUCTURE	7
3	CONCEPTUAL DESIGN	10
3.1	ALTERNATIVE CONCEPTS INVESTIGATED	10
3.2	DESIGN PARAMETERS INVESTIGATED	11
3.3	FIGURES OF MERIT EMPLOYED	13
3.4	ANALYTICAL METHODS	14
3.5	CONFIGURATION SELECTION	15
4	PRELIMINARY DESIGN	20
4.1	DESIGN PARAMETERS INVESTIGATED	20
4.2	FIGURES OF MERIT DETAILED	21
4.3	ANALYTICAL METHODS DETAILED	23
4.3.1	<i>Wing Surface and Control Sizing</i>	24
4.3.2	<i>Tail Surface and Control Sizing</i>	24
4.3.3	<i>Fuselage Contribution</i>	25
4.3.4	<i>Weight and Balance</i>	25
5	DETAIL DESIGN	32
5.1	PERFORMANCE DATA	32
5.1.1	<i>Take-Off Performance</i>	32
5.1.2	<i>Handling Qualities</i>	32
5.1.3	<i>G-Loading Capability</i>	33
5.1.4	<i>Range and Endurance</i>	33
5.1.5	<i>Payload Fraction</i>	33
5.2	COMPONENT SELECTION AND SYSTEMS ARCHITECTURE	34
5.2.1	<i>Propulsion System</i>	34
5.2.2	<i>Landing Gear and Braking System</i>	35
5.2.3	<i>Aerodynamics</i>	36
5.3	WIND TUNNEL TESTING	36
5.4	SIZING AND CONFIGURATION	37
6	MANUFACTURING PLAN	49
6.1	MANUFACTURING PROCESSES INVESTIGATED	49
6.2	FIGURES OF MERIT	50
6.3	ASSEMBLIES OF THE FINAL DESIGN	51
6.3.1	<i>Wings and Spar</i>	51
6.3.2	<i>Fuselage</i>	51
6.3.3	<i>Motor Mount</i>	51
6.3.4	<i>Landing Gear and Brakes</i>	51
6.3.5	<i>Empennage</i>	52
6.4	MANUFACTURING MILESTONE CHART	52

LIST OF FIGURES

FIGURE 2.1 TEAM ARCHITECTURE DIAGRAM.....	6
FIGURE 2.2 MILESTONE CHART SHOWING PLANNED AND ACTUAL TIMING OF MAJOR ELEMENTS .	9
FIGURE 3.1 AIRCRAFT CONFIGURATION VERSUS FACTORED COST AND ESTIMATED SCORE	16
FIGURE 3.2 SCORE VERSUS NUMBER OF LITERS FOR VARYING WING LOADINGS.	17
FIGURE 3.3 SCORE EVALUATION SPREADSHEET FLOWCHART.....	18
FIGURE 3.4 FIGURES OF MERIT RANKED.....	19
FIGURE 4.1 EXAMPLES OF FUSELAGE CROSS-SECTIONS.....	22
FIGURE 4.2 FUSELAGE CONFIGURATION DECISION MATRIX.....	25
FIGURE 4.3 LANDING GEAR CONFIGURATION DECISION MATRIX	26
FIGURE 4.4 SHOCK ABSORBER DESIGN DECISION MATRIX	26
FIGURE 4.5 BIPLANE INTERFERENCE FACTOR.....	27
FIGURE 4.6 ROLL RATE VERSUS CONTROL POWER	28
FIGURE 4.7 HORIZONTAL TAIL MOMENT ARM VERSUS HORIZONTAL TAIL AREA REQUIRED.....	29
FIGURE 4.8 COMPONENT SIZING	29
FIGURE 4.9 SIZING AND STABILITY CALCULATIONS	30
FIGURE 4.10 WEIGHT AND BALANCE.....	31
FIGURE 5.1 C_L VERSUS α	37
FIGURE 5.2 C_D VERSUS α	38
FIGURE 5.3 C_M VS α	38
FIGURE 5.4 WIND TUNNEL TEST SETUP	39
FIGURE 5.5 WIND TUNNEL TESTING IN PROGRESS	39
FIGURE 5.6 SCORE VS. LITERS WITH DIFFERENT BATTERIES.....	40
FIGURE 5.7 C_P VS. J	41
FIGURE 5.8 C_T VS. J	42
FIGURE 5.9 EFFICIENCY VS. J	43
FIGURE 5.10 THRUST VS. TIME	44
FIGURE 5.11 POWER VS. TIME	45
FIGURE 5.12 NOSE WHEEL 3D VIEW	46
FIGURE 5.13 MAIN WHEEL 3D VIEW.....	47
FIGURE 5.14 MAIN STRUT MOUNTING BLOCK 3D CUT-AWAY VIEW.....	48
FIGURE 6.1 MANUFACTURING MILESTONE CHART	52
FIGURE 6.2 MATERIAL DECISION MATRIX.....	53
FIGURE 6.3 LOWER WING FOAM CORE LAY-UP	53

1 Executive Summary

1.1 Development Process

Oklahoma State University's O.R.A.N.G.E. A.B.I.S.S team adopted an active development process for the Cessna/ONR Design/Build/Fly 2000 Competition. The approach taken to derive the final configuration was systematic, as to expedite an efficient convergence to a competitive aircraft.

Much research was conducted in the field of remotely piloted aircraft in order to advance the learning curve. Propulsion research, as well as aerodynamic wind tunnel testing, was conducted and evaluated. Current periodicals, the Internet, and other publications were consulted in the process. Various material construction techniques were also investigated. Historical data was readily accessible within the Oklahoma State University Mechanical and Aerospace Engineering Department.

During the conceptual design phase, the team brainstormed and generated innovative ideas. The ideas presented were not criticized, but presented freely. This allowed equal and objective design input from every member on the team, regardless of background or academic level. As the design process progressed, the conceptual sketches were further interpreted and analyzed. The team members reviewed the ideas and established figures of merit for each concept configuration including, but not limited to, construction feasibility, cost, performance, and durability. Practical considerations drove the design for this conceptual approach.

As the conceptual process developed, a Score Evaluation Spreadsheet was developed with the design. The spreadsheet developed by the Aerodynamics Group incorporated Rated Aircraft Cost, numerous performance parameters, and strategy from previous years contests. The spreadsheet evolved to be "all encompassing" in the preliminary stage, including general configuration parameters ranging from monoplane versus biplane to efficiency factors. Rated Aircraft Cost was included to determine score based upon a particular configuration. Thus, numerous configurations could be analyzed, and trends for these configurations could be compared in order to optimize for the highest possible score. Theoretically, an aircraft was developed to attain the highest score possible.

In addition to developing the conceptual ideas and the Score Evaluation Spreadsheet in parallel, practical issues were considered as well. Although the conceptual ideas would be easy to construct, the basic ideas might not generate the best possible score. Conversely, the developed Score Evaluation Spreadsheet might generate the optimal score, but might not be feasible with current construction technology. Therefore, a transition between the theoretical and conceptual ideas had to be established.

As the design process transitioned to the preliminary stage, the conceptual drawings were analyzed in further detail. In this stage, basic sizing was completed for various components. A consequential score evaluation and trade study was completed to observe the relation between

score and resultant performance parameters. Wind tunnel modeling was performed in this phase in order to obtain data for the detail design phase.

In the detailed design phase, more in depth work was accomplished as to the actual performance sizing of the aircraft. The sizing of control surfaces, determination of control rates, and center of gravity analysis was addressed in this design phase. The Propulsion Group finalized selection of the motor, prop, and batteries to be used. The Structures Group decided upon appropriate construction methods to be used for the specific aircraft components and materials.

A systematic design process was employed to expedite the system of evolution. The process included **conceptual, preliminary, and detail design** stages. Tasks were chronologically organized into these three groups to efficiently derive a final product.

1.2 Design Tools Overview

The selection of design tools was based upon appropriateness for the task, previous experience, and individual proficiency.

Conceptual Design Tool:

- Microsoft Excel

Microsoft Excel was used as the driving force to create a design for score optimization. The Score Evaluation Spreadsheet was the paramount tool in the design process.

Preliminary Design Tools:

- UIUC Airfoil Database
- Martin Hepperle's Airfoil Analysis Web page
- MotoCalc
- Microsoft Excel
- MathCAD

The UIUC Airfoil Database contains a plethora of airfoil profile sections. The coordinates from this database were inputted into AutoCAD to generate the airfoil sections used in the drawings. Martin Hepperle's Airfoil Analysis Webpage was utilized in conjunction with the UIUC Airfoil Database to attain preliminary design data for performance.

MotoCalc was used primarily by the Propulsion Group as a database to conduct research on motors and battery options. This software was used mainly in the preliminary design phase. Microsoft Excel was used in conjunction with MathCAD to size aircraft components and control surfaces. In addition, excel models of DC motor operations were created.

MathCAD was utilized for more rigorous mathematical modeling and complex equations, such as stability calculations and control sizing. Excel was used to expedite data reduction from wind tunnel testing, and to incorporate the Rated Aircraft Cost within the Score Evaluation Spreadsheet.

Detail Design Tools:

- AutoCAD
- Microsoft Excel

AutoCAD was used to produce basic construction drawings, as well as spawn 3D rendered views of the finished prototype to allow checking of all major interfaces. AutoCAD was used throughout the various phases of the design process.

Microsoft Excel was also used as a detailed design tool for the primary purpose of sizing landing gear for allowable stresses. The spreadsheet format allowed for various loads and angles of impact to be accounted for in the sizing of landing gear.

Additional Design Aids:

In addition to the above computational software, other published references were inquired as well. For detail design of the biplane configuration, Aircraft Design: A Conceptual Approach by Daniel P. Raymer served as a useful tool. The Propulsion Group benefited from Astroflight's published Electric Motor Handbook by Robert Boucher.

Technical references also provided useful help and advice. Dr. Andrew S. Arena, Jr. in the Oklahoma State University Mechanical and Aerospace Engineering Department aided with technical advice. Joseph Conner, engineering graduate student, helped in setting up the wind tunnel experiments and provided useful knowledge of electric propulsion and model airplane techniques. Brian Vermillion, president of Advanced Racing Composites, supplied information and background on composite construction, which was very useful in the conceptual phase of design.

1.3 Preliminary Budget

A preliminary budget was constructed to maintain a running balance and to efficiently and effectively remain within budget. The budget is based on historical estimated costs. The projected budget is as follows:

Prototype Preliminary Budget

Consumables

Description	Quantity	Price	Total
2 oz Thin CA	3		\$16.97
2 oz Med CA+	2	\$5.99	\$11.98
Aerosol Activator	1	\$4.99	\$4.99
Epoxy	2	\$7.99	\$15.98
Knives & Blades	5	\$1.50	\$7.50
Dremel Accessories	1	\$10.00	\$10.00
Sandpaper	2	\$4.00	\$8.00
Spirit Glider	1	\$73.97	\$73.97
Plotter Paper	1	\$20.00	\$20.00
Vacuum Bagging	1	\$40.00	\$40.00
Tape	2	\$40.00	\$40.00
Total			\$249.39

Mechanical and Electrical

Description	Quantity	Price	Total
Motor	1	\$225.00	\$225.00
Gear Box	1	\$50.00	\$50.00
Speed Controller	1	\$130.00	\$130.00
Propellers	3	\$40.00	\$120.00
Batteries	35	\$8.00	\$280.00
Wiring and Connectors	1	\$20.00	\$20.00
Servos	8	\$30.00	\$240.00
Solder	1	\$3.00	\$3.00
Piezo Gyros	2	\$130.00	\$260.00
Receiver Batteries	1	\$20.00	\$20.00
Total			\$1,348.00

Construction Materials

Description	Quantity	Price	Total
Balsa	1	\$25.00	\$25.00
Other Wood	1	\$20.00	\$20.00
C/F Prepreg/sq ft	90	\$7.20	\$648.00
Blue Foam	1	\$40.00	\$40.00
Monokote	2	\$12.99	\$25.98
Sullivan Tires	5	\$8.00	\$40.00
Aluminum	1	\$70.00	\$70.00
Misc. Landing Gear	1	\$40.00	\$40.00
Control Horns	10	\$0.50	\$5.00
Hinges	5	\$1.50	\$7.50
Push Rods	6	\$0.50	\$3.00
Total			\$924.48

Total Cost

Initial Prototype \$2,522

Final Design Projected Budget

Consumables

Description	Quantity	Price	Total
2 oz Thin CA	3		\$16.97
2 oz Med CA+	2	\$5.99	\$11.98
Aerosol Activator	1	\$4.99	\$4.99
Sandpaper	2	\$4.00	\$8.00
Vacuum Bagging	1	\$40.00	\$40.00
Tape	2	\$40.00	\$40.00
Total			\$121.94

Mechanical and Electrical

Description	Quantity	Price	Total
Motor	1	\$225.00	\$225.00
Gear Box	1	\$50.00	\$50.00
Speed Controller	1	\$130.00	\$130.00
Propellers	2	\$40.00	\$80.00
Batteries	35	\$8.00	\$280.00
Wiring and Connectors	1	\$20.00	\$20.00
Servos	8	\$30.00	\$240.00
Total			\$1,025.00

Construction Materials

Description	Quantity	Price	Total
Balsa	1	\$25.00	\$25.00
Other Wood	1	\$20.00	\$20.00
C/F Prepreg/sq ft	90	\$7.20	\$648.00
Blue Foam	1	\$40.00	\$40.00
Monokote	1	\$12.99	\$12.99
Sullivan Tires	5	\$8.00	\$40.00
Aluminum	1	\$60.00	\$60.00
Misc. Landing Gear	1	\$15.00	\$15.00
Control Horns	10	\$0.50	\$5.00
Hinges	5	\$1.50	\$7.50
Push Rods	6	\$0.50	\$3.00
Total			\$876.49

Total Cost

Final Prototype \$2,023

Estimated Travel Expenses

Description	Quantity	Price	Total
Van Rental	1.5	\$225.00	\$225.00
Motel	4.5	\$55.00	\$495.00
Total			\$720.00

Total	
Cost	\$5,265

2 Management Summary

2.1 Team Architecture

The team consists of students ranging from freshman to graduate students, and is divided into three groups: Aerodynamics, Propulsion, and Structures. A Marketing group was also established to support funding. A chief engineer was selected for the team to facilitate organization and communication. Team members were surveyed by Dr. Arena, the team advisor, and were then allocated into the three subgroups based upon technical background and personal interests. These three subgroups are guided by a respective group lead. The three subgroups were further subdivided into smaller sections, depending upon anticipated complexity of tasks. The team structure is outlined in the following diagram:

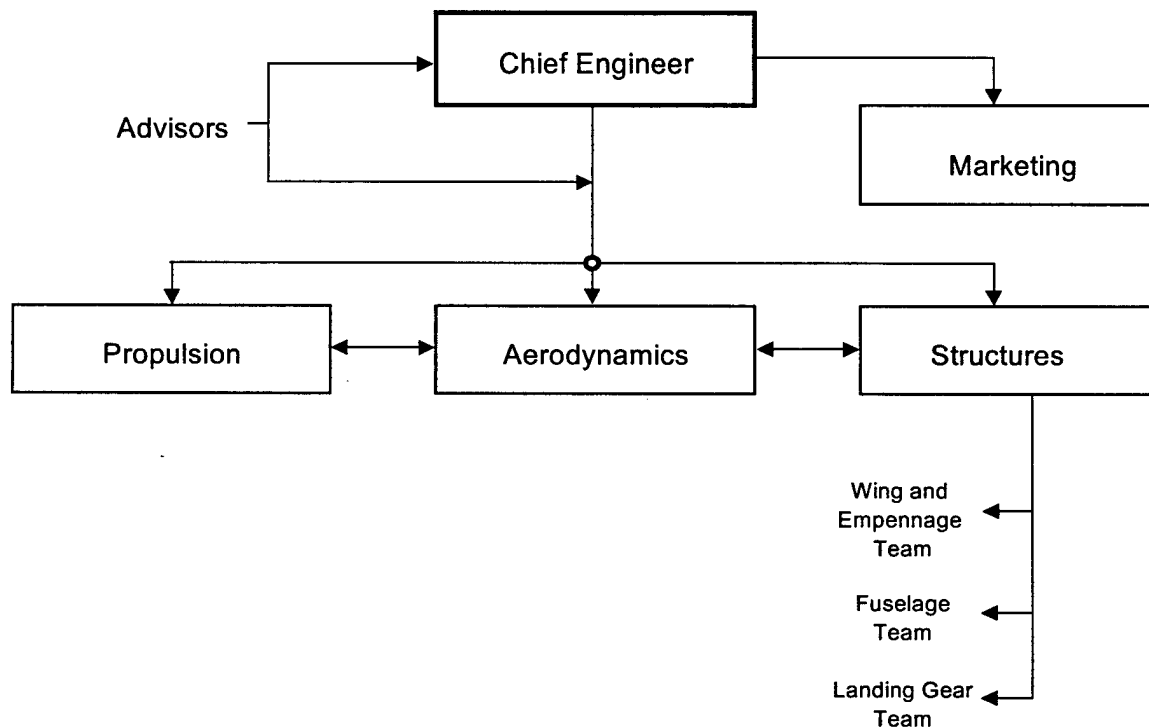


Figure 2.1 Team Architecture Diagram

An active managerial approach was implemented to expedite communication between each technical group. Although each member is appointed to a specific group, the member is not confined to that specific group, and interdisciplinary activity is encouraged. For instance, the Aerodynamics Group is highly encouraged to be adequately involved with the Structures and Propulsion Groups. This approach expedites communication on the overall project, and results in a more refined final product.

2.2 Management Structure

With the architecture of the team clearly defined, the management structure of the team can be further outlined. Each team member, as stated above, was appointed to their respective task based on experience and personal preference.

The Aerodynamics Group made up approximately one-fourth of the team. This group is primarily responsible for configuration design, performance calculations, weight and balance, and stability and control. They have accomplished detailed wind tunnel testing on various configurations and have also been very instrumental in structural development, primarily with the construction of the wings.

The Propulsion Group also consists of approximately one-fourth of the team. This group is responsible for battery, motor, and propeller selection and testing, and the interfacing between each component. The Propulsion Group is actively involved with the Aerodynamics Group in correlating performance requirements and limitations. This group is also involved with the Structures Group to facilitate an agreement on motor-fuselage interfacing, battery arrangement, and battery placement.

The Structures Group comprises the remaining members of the team. This group has been conducting research on design and construction methods, including component matching, interfacing, and composite lay-up techniques. Connection points and interfacing was of primary concern of this group. Due to the large spectrum of the Structures Group, it is further subdivided into Landing Gear and Brakes, Wing and Empennage, and Fuselage subgroups.

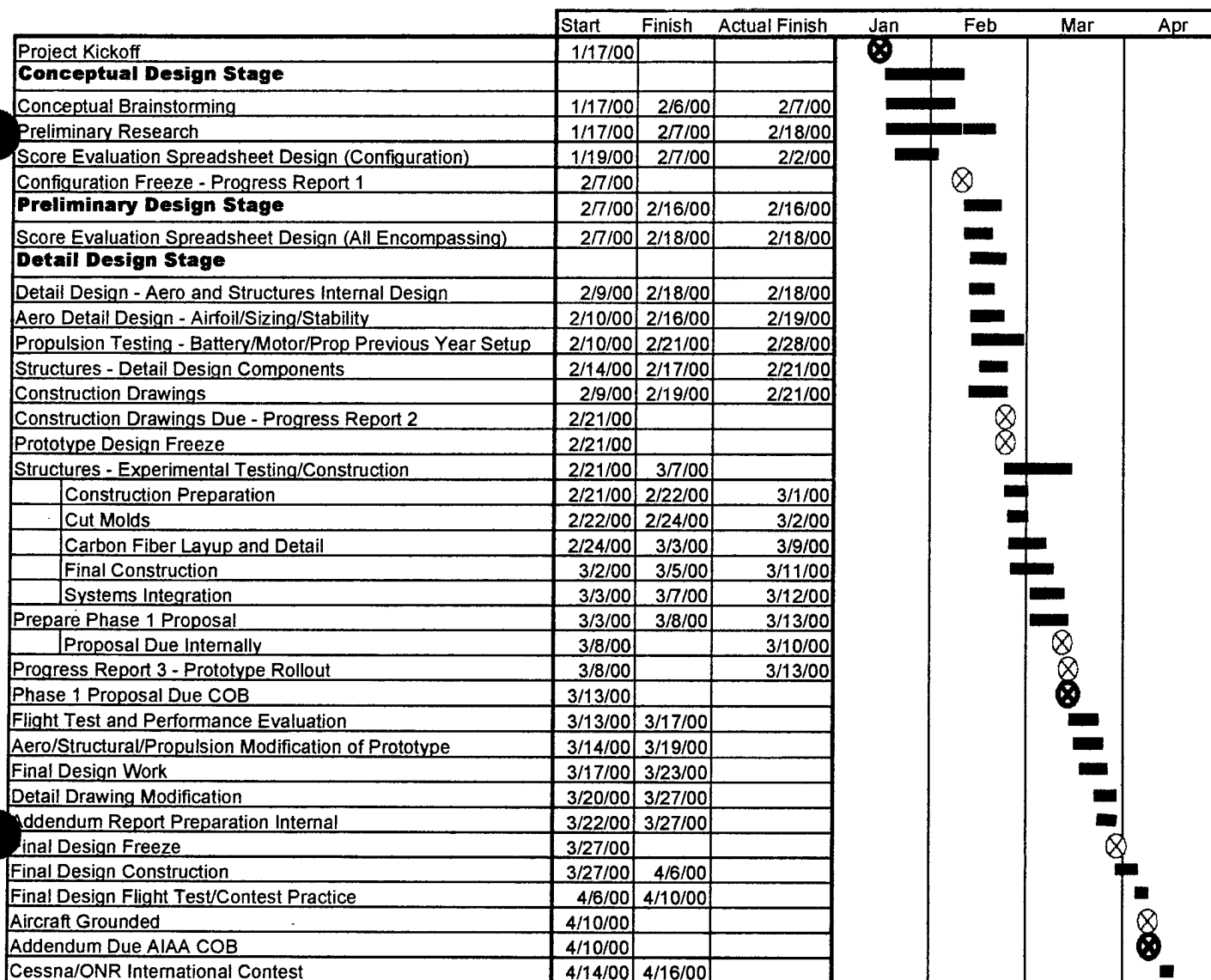
The Landing Gear and Brakes Subgroup is primarily concerned with the design and construction of the ground handling systems. Therefore, members with the most efficient machining skills were appointed to this subgroup. The Wing and Empennage Subgroup is responsible for the construction of their respective components and is instrumental in determining the layout of the internal configuration and the controls system. The Fuselage Subgroup held the responsibility of fuselage layout, along with propulsion and wing integration. Initially, these team members constructed a "practice plane" model to acquire the necessary proficiency.

Each of the above groups is led by an assigned Group Lead. The Group Leads are responsible for facilitating communication between the groups and establishing efficient and paralleled tasks for each group member. These tasks are assigned through the Milestone Chart in Figure 2.2. The Milestone Chart helped to facilitate schedule control among the groups so that each group member knew the major elements and at what time these elements were to be completed. The group leads could then plan their group work accordingly.

The Chief Engineer leads the project as a whole. This person is involved in coordinating, scheduling, ordering, and maintaining communication between the groups. Not only does the Chief Engineer coordinate the team, but also holds involvement in every aspect of the design, including, but not limited to, Aerodynamics, Propulsion, and Structures.

The Chief Engineer plays an intricate part in all the groups by maintaining configuration control. As all team members design and construct the airplane in parallel, communication is essential in configuration control. E-mail, FTP, phone lists, and regular team meetings are the primary forms of communication.

Figure 2.2 details the anticipated progress of the design stages. Major contest deadlines are depicted, as are internal deadlines.



Scheduled Time ■
 Actual Time ■
 Internal Deadline ⊗
 Contest Deadline ⊗

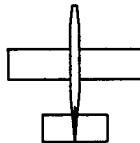
Figure 2.2 Milestone Chart Showing Planned and Actual Timing of Major Elements

3 Conceptual Design

3.1 Alternative Concepts Investigated

To achieve the design most suited for the established mission, it was necessary to review and critique multiple aircraft configurations. These alternatives were considered and narrowed down by a variety of factors that will be discussed. The aircraft configurations considered were as follows:

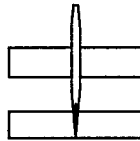
- Standard Monoplane



- Biplane



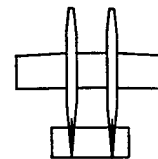
- Tandem Wing



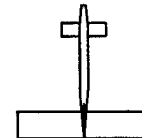
- Flying Wing



- Dual Fuselage Monoplane



- Canard Configuration



The standard monoplane configuration of a single fuselage, single wing, standard tail aircraft is simple and has been proven historically to be safe and stable.

The biplane configuration of a standard fuselage with two wings, one above the other, allows for increased lift with lower drag due to a higher aspect ratio for each wing.

The tandem wing configuration consists of a standard fuselage and two wings, one located substantially forward of the other. In this configuration, one wing can act as the stabilizing airfoil, allowing removal of the horizontal tail surface.

The flying wing configuration, the lifting airfoil acts as the fuselage and horizontal-stabilizing surface. This design eliminates the need for vertical and horizontal tail surfaces and streamlines the aircraft, increasing the overall drag characteristics.

The dual fuselage configuration incorporates a standard wing design with two fuselages mounted side by side. This configuration is most often used with two engines, one at the

nose of each fuselage, and with two vertical surfaces mounted independently on each fuselage.

The canard configuration can be used with multiple fuselage and wing designs. The canard replaces the horizontal tail surface with a similar controlling surface mount forward of the main lifting wing. This design is primarily used where the elimination of wing stall is desired.

For an overview of the cost and score performance of each configuration, see Figure 3.1 at the end of Section 3.

3.2 Design Parameters Investigated

Primary design parameters were investigated during the conceptual design phase to determine which had the most significant impact on the Figures of Merit (FOM). These design parameters are as follows:

- Amount of water to be carried
- Payload configuration and access
- Wing loading
- Airfoil selection
- Power loading
- Aspect ratio
- Wing geometry
- Number of wings
- Number of fuselages
- Number and location of motors
- Number and location of batteries
- Landing gear configuration
- Braking and steering
- Component cooling
- Material selection
- Fuselage length

The amount of water to be carried was affected directly by the selected wing and power loading and the aspect ratio of the wing. Proper matching of these components is essential to assure takeoff in 100 feet and to maximize flight score.

Payload access had to consider such things as wing configuration and fuselage shape. Rapid access to payload for loading and unloading was necessary to maximize the number of sorties in a mission during the competition. Different options considered were a detachable nose and tail to pull out the water bottles, a top hinged hatch with and without the bottles attached to the hatch, and replaceable pods attached to the fuselage. Different configurations for the bottles included laying the bottles on their side and

upright in the fuselage. Different bottle sizes were investigated for the two different configuration possibilities.

Airfoil selection was one of the most important considerations in the design phase. The right airfoil was required to optimize the lift needed for the intended mission. For the competition, an airfoil with a high lift to drag ratio throughout the angle of attack range was desired due to the takeoff requirement. The higher this ratio, the more weight the aircraft can lift with no penalty in drag or power.

Wing geometry plays an important role in the aerodynamic performance. A tapered wing effectively approaches the ideal lift distribution of an elliptical wing without the added difficulty of constructing the elliptical shape. This, however, produces unfavorable stall characteristics compared to that of a constant-chord wing. A rectangular wing stalls at the root first leaving some aileron effectiveness. This, along with the ease of construction of a constant-chord wing, led to the use of a straight, rectangular geometry.

Multiple wing designs must be considered due to span limitations placed on the design. Aspect ratios less than three can have very poor drag qualities, which can lead to a variety of limitations. To counter this, multiple wings can be used. This results in larger wing area for limited spans, retains high aspect ratio, and preserves efficiency and drag qualities.

Multiple fuselages must be considered to blend the placement of multiple engines and tail surfaces if necessary. More than one fuselage may be desired if loading requirements require a long fuselage. A dual fuselage design would allow more cargo room while maintaining a reasonable fuselage length.

The number of motors required is primarily determined by the availability of a motor that can provide sufficient power and also by the efficiency of the configuration. Multiple motors may be desired for smaller prop usage or location restrictions. The motor location is critical due to the effects of prop-wash and motor-out handling qualities of the aircraft. Restrictions in motor placement must be considered such as ground clearance and structural attachment.

The number of batteries required depended upon the power required from the battery pack. Since the battery pack weight is limited to five pounds, it was decided that the power density of the batteries was an important parameter to consider when selecting the type of battery to use. Battery incorporation into the design was critical to assure that the aircraft fell into the CG limitations and that adequate cooling could be accomplished. Payload locations had to be decided in conjunction with battery location and the effect of heat generated from the battery packs on surrounding components.

During a mission, several takeoffs and landings must be executed. Therefore, it was decided that the landing gear configuration, which directly affects the ground handling of the aircraft, was an important parameter to consider. Tricycle, bicycle, and tail dragger configurations were all considered in the conceptual design. Shock absorbers such as oleo

strut, spring or torsion bar, cantilevered gear, and rubber were investigated to minimize the landing impact on the airframe.

The competition missions are limited to ten minutes with a starting point for each takeoff. With this time restraint, brakes would allow the aircraft to stop faster during landing rollout. Also, it will allow the plane to stop before the takeoff starting point, saving precious time and possibly preventing the need to return to the starting point after landing. Commercial brakes were considered as well as a self-manufactured design. Steering was determined to be an important factor because it would allow a faster return to the starting line if the line was passed. Nose gear steering, differential braking, and pure rudder were all ideas investigated.

Component cooling was necessary in two major places, the motor and the batteries. The cooling air must come from either the prop-wash or the in-flight airflow. Using the prop wash for cooling will supply cooling air proportional to the loads being drawn while the in-flight airflow will not suffice while operating in ground conditions.

Material selection was an important design consideration due to limitations of certain materials. While balsa and Monokote construction are lightweight and easy to construct, they limit the use of complex airfoils and fuselage designs. The use of lightweight metals provides strong structures but increase weight significantly. Composite construction using fiberglass or carbon fiber are expensive and difficult to work with, but allow very complex and rigid designs.

3.3 Figures of Merit Employed

The following are the Figures of Merit that were used in the consideration of different design configurations:

- Flight score
- True aircraft cost
- Ease of construction
- Payload access
- Propulsion capabilities
- Handling qualities

The primary Figure of Merit was flight score. However, all the above Figures of Merit were considered in achieving a reliable and safe design while maximizing score.

The Rated Aircraft Cost was used to eliminate designs that would incur large penalties in cost due to multiple fuselages, multiple vertical and horizontal tail surfaces, excessive wing area, and number of motors.

The true aircraft cost was used in a similar manner to the rated aircraft cost. The true aircraft cost reflected actual budget requirements of the design.

Ease of construction was used to ensure that the final design would be within the manufacturing abilities of the team and to ensure that a time consuming, complex design was avoided due to time constraints.

Payload access was also a major concern due to the high turn around time desired. The final design must have easy access to the payload to ensure that complications do not arise in the payload removal or addition to the airplane between sorties.

Propulsion capabilities were evaluated for the conceptual designs to ensure that the potential for multiple motor configurations existed if deemed necessary by the propulsion team.

Handling qualities are of the most important considerations in the design phase. Ground handling is included among these qualities. If the aircraft is uncontrollable, the design mission cannot be accomplished. While certain designs may be extremely efficient, if handling qualities are marginal, the risk of aircraft loss is high. Aircraft handling is a safety issue and should be treated as such.

3.4 Analytical Methods

In conjunction with the conceptual design stage, analytical design had to be performed to find the optimum configuration that would maximize the final flight score. This entailed the overall optimization of the aircraft by varying certain parameters, which included such things as wing loading, maximum power required, endurance, and cost factor. The entire spreadsheet was set up to show the results for aircraft carrying two to eight liters of water.

First, basic dimensioning equations were derived to size different parts based on a varying design payload. Power requirements were then derived based on the predetermined component sizes, the gross takeoff weight of the aircraft, and maximum takeoff distance. Efficiencies for the propulsion system were then determined from historical sources and assisted in determining the required battery power for required system performance. The power required for the desired cruise speed was then calculated, and by estimating course length, the predicted number of laps possible for minimum endurance was determined. Set limits for current flow removed any configurations that exceeded a 50 Amp current flow to prevent system damage and to preserve safety.

The aircraft cost factor was determined from the given equations supplied in the contest rules. The estimated sizing, weight, and component number along with the battery, motor, and propeller requirements to arrive at the final, factored cost for the aircraft. The predicted score was then calculated based on the endurance, range, number of liters carried, and the aircraft cost factor and was varied with wing loading for optimization. A graph showing the optimal score versus liters of water based on wing loading can be

found in Figure 3.2. The predicted score is derived independently of the report score and is only used as a comparison tool to aid in the selection of the overall aircraft configuration.

A flowchart located in Figure 3.3 shows a simplified logic tree of the score evaluation spreadsheet. Inputs include such things as the number of components installed, wing loading, coefficient of lift and drag, weight (gross takeoff and empty), take off distance, lap time, battery cell type and number of cells, maximum allowable current, and aircraft efficiency factors. Once these inputs are identified, a Visual Basic macro was used to vary and plot wing loading to find the maximum score versus number of liters. The optimal wing loading can then be loaded into the spreadsheet along with other parameters to accurately determine the final approximation.

The calculations were tested for accuracy by using the aircraft configuration data from previous years and comparing the theoretical performance data to actual recorded information. Adjustments were made accordingly in areas where error was excessive.

3.5 Configuration Selection

The final configuration was made with the use of Figure 3.4 and the score evaluation calculations. The final configuration consisted of the following characteristics:

- Biplane wing design
- Single, slender fuselage
- Single vertical and horizontal tail surfaces
- Tricycle landing gear
- Single motor
- Lower cowling battery arrangement

The primary reason the biplane design was decided upon was to maximize wing area while maintaining a reasonable aspect ratio along with the optimized wing loading.

The single, slender fuselage was selected to minimize drag, have easy and fast accessibility to the payload, and to increase the longitudinal and lateral moments of inertia to assist in oscillation damping.

The tail configuration of one vertical and one horizontal surface provided the required trim while minimizing the cost factor and drag.

The tricycle landing gear was preferred to a tail-dragger configuration for stability in ground handling. The gear location was determined to prevent tipping in taxiing and gusty wind conditions.

The single motor configuration was chosen based on the availability of a motor that provided the required power and minimization of score loss due to the cost factor. It also

blended well with the single fuselage selection and provided thrust along the centerline of the aircraft.

The battery pack was arranged with the cells laid side-by-side in series. This configuration was necessary for the cells to be stored in the battery cowling located beneath the fuselage. The purpose for storing the cells beneath the fuselage was threefold. First, removing the batteries from within the fuselage allowed for more compact bottle spacing and a more compact fuselage. Second, storing the batteries outside the fuselage kept heat generated by the batteries away from the rest of the system. Third, storing the cells in the battery cowling meant the center of gravity of the plane could be fine-tuned easily by shifting the battery pack within the battery cowling.

Overall, it is felt that this is an efficient and competitive design that will be within the capabilities of the team to design and construct while meeting the basic mission requirements.

Aircraft Configuration	Factored Cost (Dollars)	Estimated Score
Standard Monoplane	5404.29	21.26
Biplane	6181.50	24.26
Tandem Wing	6308.42	23.78
Flying Wing	5037.50	20.35
Dual Fuselage Monoplane	7223.41	15.59
Canard Monoplane	5404.29	21.26

Figure 3.1 Aircraft configuration versus factored cost and estimated score

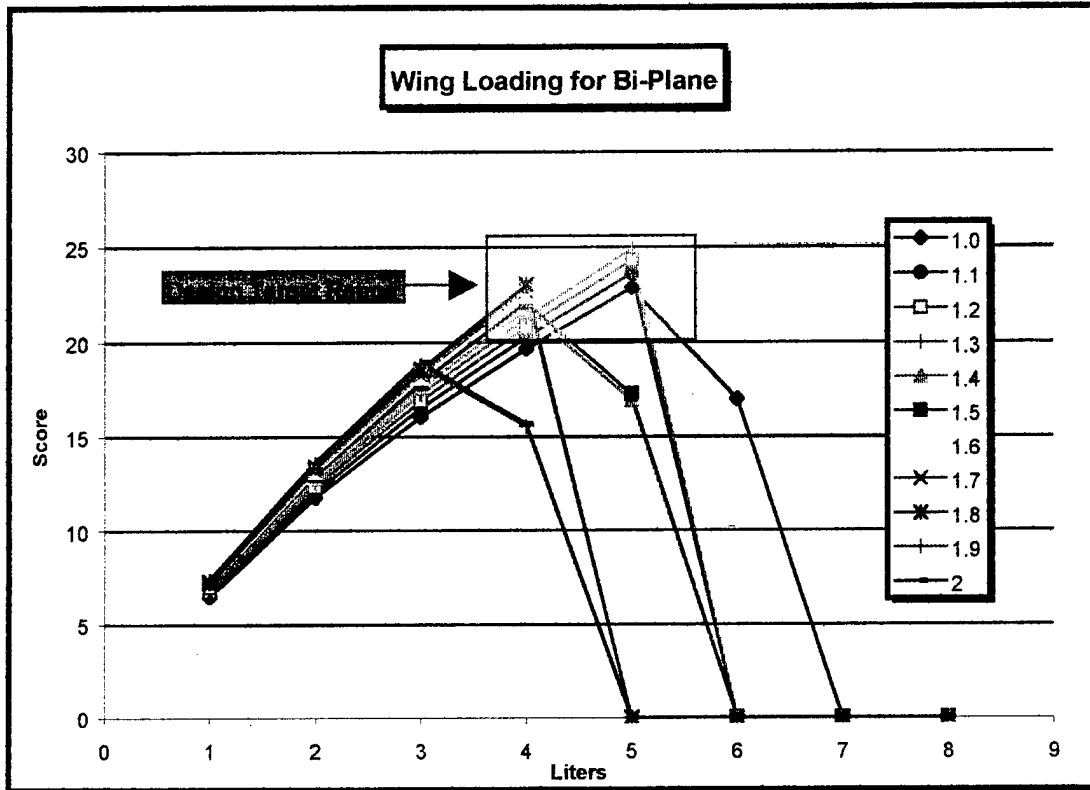


Figure 3.2 Score versus number of liters for varying wing loadings.

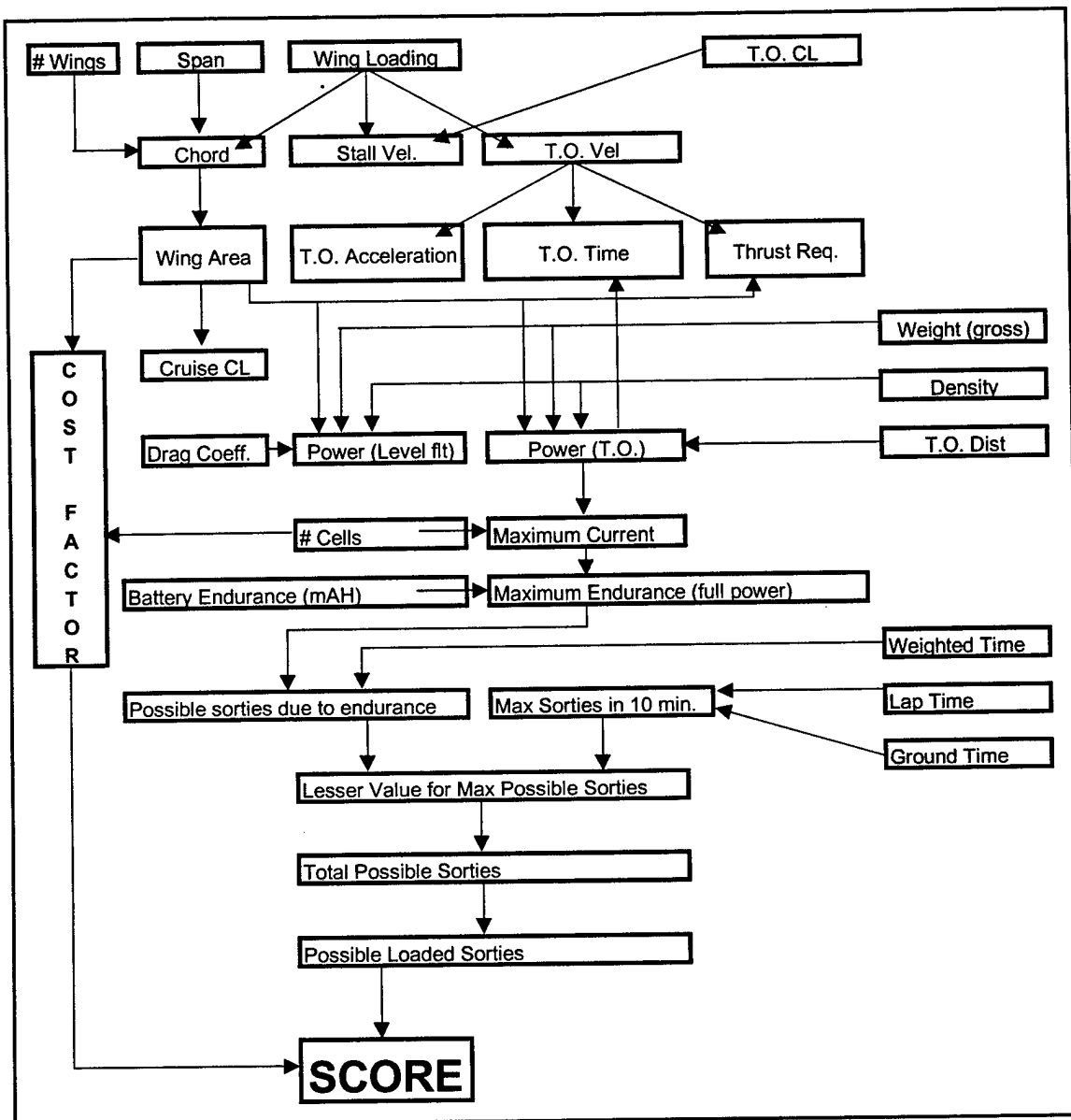


Figure 3.3 Score evaluation spreadsheet flowchart

Figures of Merit	Weight Factor	Standard Monoplane	Biplane	Tandem Wing	Flying Wing	Dual Fuselage	Canard
Rated Aircraft Cost	0.3	4	3	4	5	2	4
True Aircraft Cost	0.1	4	3	2	1	1	4
Ease of Construction	0.05	5	3	3	4	1	5
Payload Access	0.1	5	4	4	2	3	4
Propulsion Capabilities	0.05	4	5	4	3	3	3
Aerodynamic Stability	0.2	4	5	3	1	4	5
Efficiency w/ Span limitations	0.1	3	5	5	3	3	4
Take Off Limitations	0.1	3	5	4	3	4	2
Totals	1	3.050	3.150	3.050	2.650	2.050	2.950

Figure 3.4 Figures of Merit Ranked

4 Preliminary Design

During the preliminary design phase, the aerodynamic shape, structural layout, and power characteristics were better outlined and sized to be suitable for the competition objectives. Preliminary layout drawings of the plane were presented in this stage.

4.1 Design Parameters Investigated

Design parameters were investigated during the preliminary design phase. These design parameters are as follows:

- Aspect ratio
- Wing loading
- Number of Wings
- Power loading
- Volumes of tail
- Fuselage configuration
- Payload configuration
- Landing gear configuration

The aspect ratio of a monoplane design was insufficient for the wing area needed. A reasonable aspect ratio was obtained by adding another wing. By taking advantage of the full wing span allowed (seven feet), and using the chord of 20 inches determined by the score optimization spreadsheet, the resulting aspect ratio for each wing was 4.19.

Wing loading was chosen to optimize the score. The score optimization spreadsheet was utilized again to plot different wing loadings versus number of liters carried. Given the wing area chosen above, the best wing loading was 1.3.

Fuselage configuration is directly related to the payload amount to be carried. The payload is one-liter cylindrical bottles of any dimension, which must be accessible for easy removal and replacement. However, fuselage length needed to be minimized to maximize score. In addition to payload arrangement being a primary concern, aircraft stability and drag due to cross sectional area were vital concerns in the fuselage arrangement.

Landing gear type and wheel size was determined through ground handling characteristics and impact absorption characteristics. In designing the landing gear, weight, impact load, and drag had to be considered. The predicted weight for the team's aircraft ranged from 25 to 35 pounds loaded. The goal was to design the gear to be as light as possible while maintaining sufficient strength to withstand the loads. Several different types of shock absorbers were investigated including oleo, spring shocks, and rubber shocks. The figures of merit in the design of the shock absorbers were ease of manufacture, reliability, and weight required.

Various landing gear configurations were researched and trade studies conducted to find the optimal configuration to accommodate our design needs. The designs considered were tail-dragger, tricycle, and bicycle configurations. The Aerodynamics Group was consulted as to the possible impact of varying designs on the handling qualities during landing. These considerations were incorporated into the figures of merit. The method of steering for the aircraft is specific to each landing gear configuration, therefore, it will be determined by the configuration selected.

4.2 Figures of Merit Detailed

The Aerodynamics Group performed trade-off studies to obtain simultaneous optimization of component spacing.

The recommended separation between the two wings of a biplane is one chord length, but analysis showed the gap could be reduced to 14 inches without significantly decreasing the efficiency. Numerically, the efficiency dropped from .67 to .6. See Figure 4.5. The top wing was placed as close to the bottom wing as possible in order to decrease the moment of inertia and profile area.

While historical research indicated that stagger in biplane wings was only for increased pilot visibility, the Aerodynamics Group found several reasons to include a positive stagger in the design. First, when the top wing is staggered forward it is at a slightly larger relative angle of attack due to decalage and stalls before the bottom wing. This produces a nose down pitching moment because the aft wing is still generating lift, and the plane will naturally recover from the stall. Second, the stagger allows favorable center of gravity location. A trade-off between decalage effects and moving the landing gear as far aft as possible resulted in a stagger of 10 inches. With the CG three inches in front of the lower wing spar, the odd number of liters can be centered on the CG. In the zero-stagger configuration, the middle bottle would have to be placed on top of the lower wing spar. The tight fuselage sizing would not allow for this without the addition of a structurally and aerodynamically undesirable "bubble" for the bottle. The bubble would complicate payload removal hatches, and it would form an unnecessary protrusion in the case that four liters was deemed optimal.

From the Score Evaluation Spreadsheet, it was determined that the five liters of water would be the optimum payload with possibilities of increasing that number after testing. It was determined that the smallest frontal area possible was the most desirable trait because it would minimize form drag. Laying the bottles lengthwise in the fuselage could attain a small frontal area. The decision between oblate and prolate fuselage depended upon the dimensions of the one-liter bottles. A trade study in optimizing the drag versus fuselage length was performed and it was determined that 3.5" X 7" bottles, which were readily available, were optimal for transporting the cargo. This bottle size led to a prolate shaped fuselage of approximately seven feet.

The shape of the fuselage was determined from concepts such as a round balsa stringer, round carbon fiber, and square carbon fiber or wood (see Figure 4.1). The square carbon fiber shape was chosen for the team's configuration because of ease of manufacturing, durability, and ease of loading and unloading (see Figure 4.2). Carbon fiber was chosen over wood because of greater strength and stability

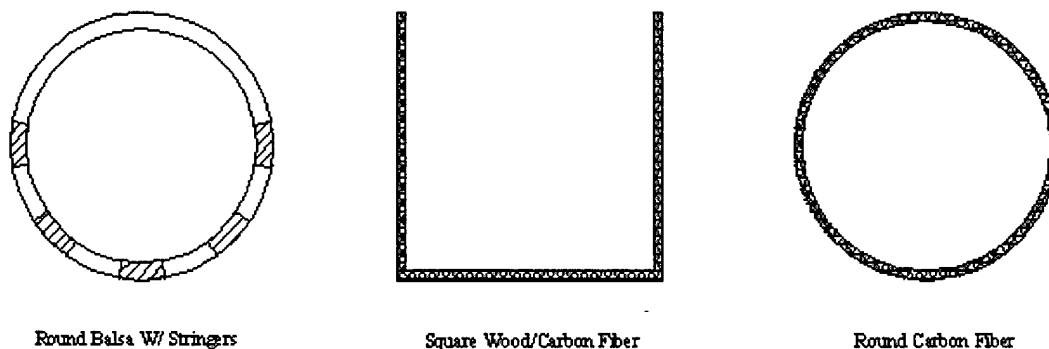


Figure 4.1 Examples of fuselage cross-sections

As this year's competition requires a series of loaded and unloaded sorties, quick removal and insertion of the payload are critical factors that affect the shape of the fuselage. Film from last year's competition was analyzed to find the fastest way to load and unload payload. The top hatch that flipped up giving access to the payload inside the fuselage and the removable nose cone or tail cone proved to be among the slowest of the methods observed. The fastest way incorporated a removable hatch on top of the fuselage connected to the payload that could be replaced with an identical hatch containing no bottles for the unloaded sorties.

After an extensive research, literature, historical data review, and consultation with the Aerodynamics Group, the landing gear configuration chosen was the tricycle configuration for its ground stability, takeoff performance, and landing stability. Tail dragging was primarily eliminated as a configuration possibility due to the tendency to ground loop as a result of the center of gravity being located behind the main struts. The bicycle configuration was not chosen because of the reduced handling qualities while on ground. Figure 4.3 is a decision matrix summarizing the results.

The height of the landing gear was dependent upon the size and mounting of the propeller and the amount of clearance desired for the propeller. A clearance of one inch below the propeller when the nose gear was fully compressed and the main gear was fully uncompressed was chosen as the minimum clearance to protect the motor and prop. Also, the spacing of the gear was considered to prevent tipping of airplane in cross winds. From references and historical data, a distance of one-third the wing span was found to be the ideal spacing of the gear to prevent tipping in high winds while on the ground. This distance correlated to fourteen inches from centerline of the fuselage to the main strut of the landing gear.

Three primary configurations for the shock absorbers were considered and analyzed for use in the landing gear. These configurations were oleo, rubber, and springs. Oleo shocks were investigated and found too complicated to manufacture, hard to repair, and their reliability was highly dependent on the quality of manufacturing. Given the limited machining ability of the Structures Group members, it was determined that oleo shocks carried a high risk of incorrect manufacturing. The Rubber shock absorber was heavily weighed against the spring shock but eliminated due to the potential for increased size and drag due to the large volume required for expansion of the rubber. The spring shock was chosen because of its simple design and reliability. It was also believed that this design would prove simple and fast to manufacture. (Figure 4.4)

Preliminary loads for landing were calculated from design specifications provided by the Aerodynamic Group and used in conjunction with a 1.5-g factor of safety. A spreadsheet was made by inputting different diameters of rod and tubing and calculating the stresses incurred by the worst case side loading. From the diameter and stress spreadsheet, materials were chosen based on their yield strength and density. Aircraft grade aluminum 6061-T651 was chosen for the strut material due to the high strength and lower density versus other aircraft grade aluminum and steels.

Nose gear steering was chosen as the best method of steering because of reliability, time savings, and ease of use for pilot. Differential braking of the main gear was not incorporated for steering to simplify ground controls. Instead, the main gear brakes will actuate simultaneously while utilizing the nose wheel for steering.

The brake design chosen was designed by students at OSU and manufactured by the Structures Group. The decision for in-house manufacturing of the braking system was driven largely by the lack of availability of small scale hydraulic braking and/or the prohibitive cost of such a system. The brake design incorporates a hydraulically actuated internal drum brake. The hydraulics will be controlled through servos and master cylinders located within each wing on easy-access panels.

4.3 Analytical Methods Detailed

The Aerodynamics Group created a series of MathCad programs to assist in the iteration of sizing calculations. The program began with wing analysis and worked through to the tail calculations. A 10% factor of safety was incorporated into the resulting dimensions of the surface controls.

Mounting the landing gear on the wings instead of the fuselage was a limiting factor. For a tricycle setup, the recommended placement of the gear is 15° aft of the CG to eliminate a tipping tendency during ground handling. The gear was mounted on the lower wing spar located at the quarter chord with the CG two inches behind the leading edge of the lower wing.

4.3.1 Wing Surface and Control Sizing

The ailerons were sized by setting an initial span and control power. The desired deflection was set at 15° . Robert C. Nelson's Flight Stability and Automatic Control provided a curve showing the relation between the flap effectiveness parameter, τ , and the ratio of control surface area to lifting surface area. This curve was regenerated in Microsoft Excel to obtain a specific equation. This equation was then input into the MathCad Sizing program. The effectiveness was calculated and then the ratio could be solved. Now the required area was known and divided by the initial span to get the corresponding aileron chord length. If the chord was unreasonable, the initial span was changed and the process was repeated. With the addition of velocity and estimated moment of inertia about the roll axis, the corresponding lift and torque were solved, which ultimately gave a roll rate. This process was repeated until a desirable roll rate was achieved. Figure 4.6 shows the roll rate versus control power.

4.3.2 Tail Surface and Control Sizing

With the center of gravity positioned at 3 inches forward of the main gear, the wing moments were found. An initial tail volume was estimated and the neutral point and static margin located. The Cm_{cg} of the tail needed to counter the wing was determined. Then the tail area was found. See Figure 4.7. A wing angle of attack giving a favorable cruise lift coefficient was input. Then, the tail incidence angle was set at to trim the plane with 0° of elevator deflection. Because of the tail sizing needed for trim, the static margin increased to 30%. This value is higher than for typical planes, but was necessary and acceptable for the design. Again, 10% was added to the elevator size for a margin of safety.

An inverted Clark-Y airfoil gave desirable lift coefficients and decreased drag for the incidence angle used. The vertical tail area was calculated using a historical tail volume coefficient found in the AIAA text by Raymer. For the rudder, the maximum deflection was set and the effectiveness was given a value. Then the ratio and $C_n\beta$ were found which determined size. The effectiveness was adjusted to get a $C_n\beta$ value comparable to ones found for existing aircraft. The final rudder dimensions fell into the recommended value of 30-35% of the vertical tail. Aerodynamic balancing of the rudder was based on the recommended 25% value found in textbooks and existing aircraft.

An NACA 0009 airfoil was chosen for the vertical tail because of its symmetry and thin profile. The surface was swept back for aesthetics and to attain a longer moment arm for the aerodynamic center.

4.3.3 Fuselage Contribution

The pitching moment caused by the fuselage was calculated by hand and found to be insignificant. This arises because the area of the fuselage is small compared to that of the wings. Although fuselage effects were found to be negligible, the Structures Group was continuously consulted regarding the interfacing of components and the feasibility of construction. Connecting points will be smoothly flared to reduce drag.

4.3.4 Weight and Balance

The batteries were used to fine-tune the CG. A weight and balance spreadsheet, Figure 4.10, calculated the necessary location of the battery pack.

Figure 4.8 and Figure 4.9 show the results of the surface and control sizing.

The analytical methods employed by the Structures Group varied from the basic physics of force analysis to spreadsheets used to calculate approximate stresses in bodies. Basic force analyses were performed on the action of landing and decelerating to find the relative landing forces. These forces were placed into the spreadsheet with dimensional approximations to size and select the materials for construction. The landing forces were also used to size the springs required for the shock absorbers.

Figures of Merit	Weight Factor	Round Balsa Stringers	Round Carbon Fiber	Square Wood/Carbon Fiber
Ease of Strength Analysis	0.05	2	4	4
Weight	0.25	3	4	3
Ease of Manufacture	0.3	2	2	4
Aerodynamic Shape	0.15	4	5	3
Real Cost	0.05	2	2	3
Ease of Loading/Unloading	0.2	1	3	4
Totals	1	2.35	3.25	3.55

Figure 4.2 Fuselage configuration decision matrix

Figures of Merit	Weight Factor	Tricycle	Tail Dragger	Bicycle
Weight	0.15	1	3	2
Ground Stability	0.15	5	1	3
Drag	0.1	2	3	4
Take off Performance	0.2	4	2	1
Ease of Construction	0.1	3	4	1
Landing Stability	0.3	5	3	1
Totals	1	3.7	2.6	1.75

Figure 4.3 Landing gear configuration decision matrix

Figures of Merit	Weight Factor	Oleo/Pneumatic	Spring	Rubber
Ease of Manufacture	0.4	2	5	4
Reliability	0.35	2	4	5
Expected Weight	0.25	3	4	3
Totals	1	2.25	4.4	4.1

Figure 4.4 Shock absorber design decision matrix

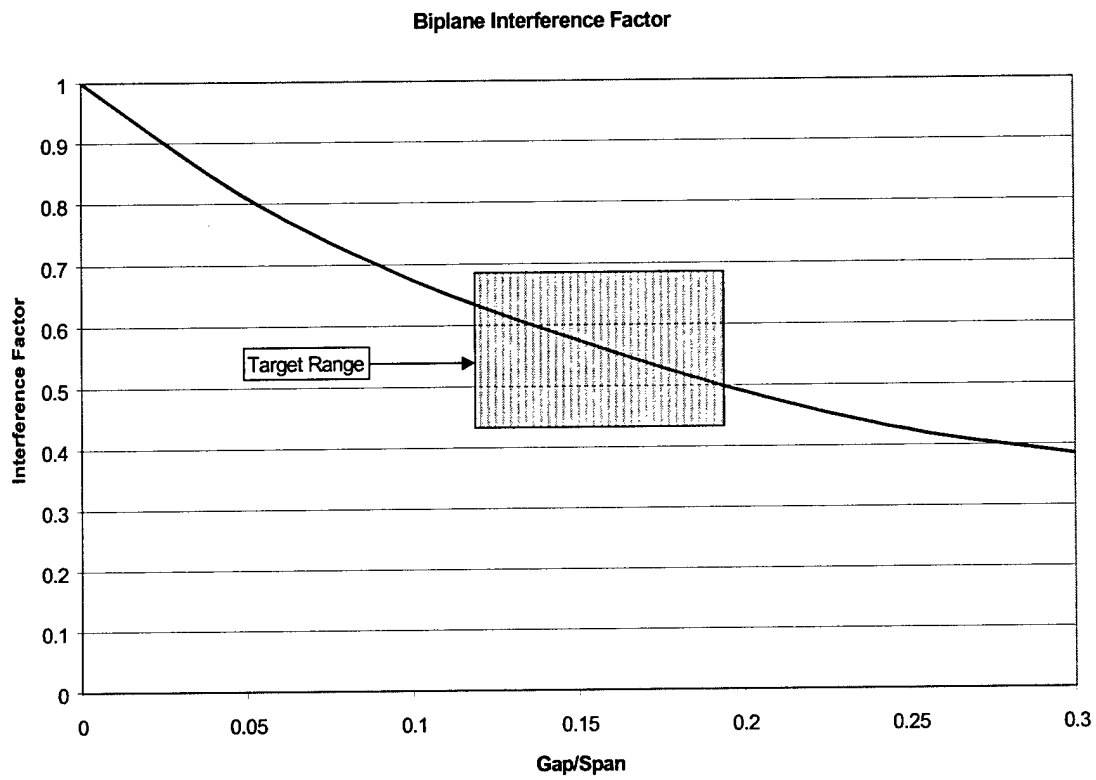


Figure 4.5 Biplane Interference Factor

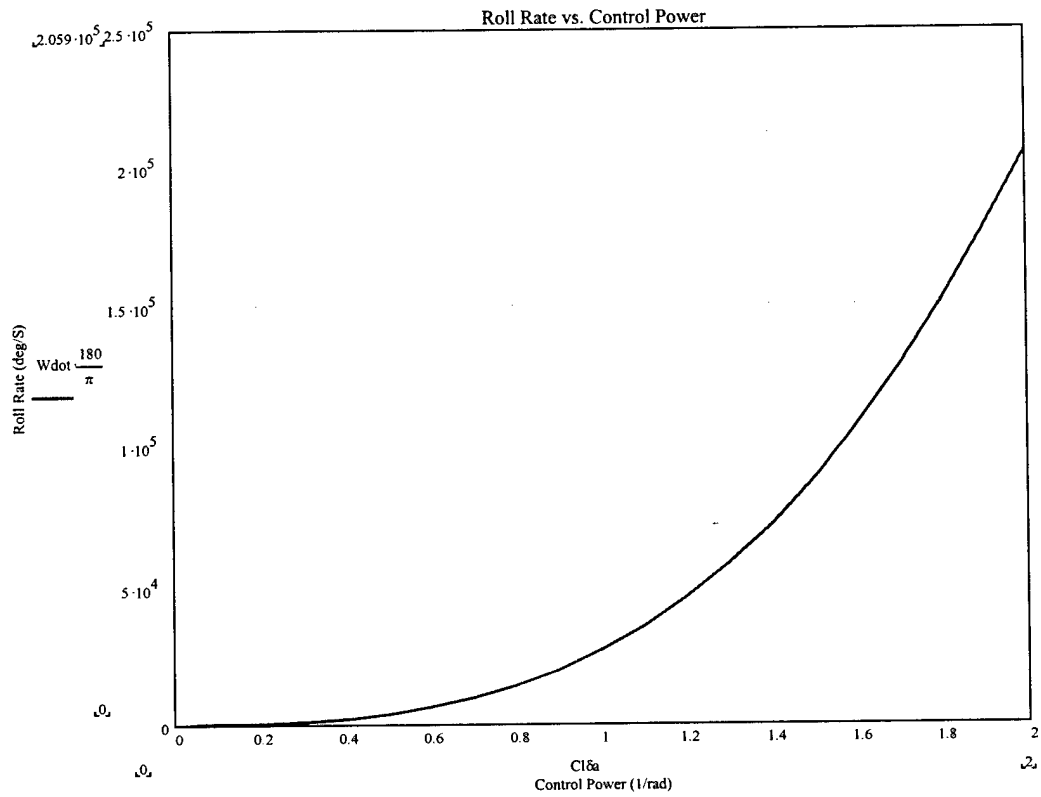


Figure 4.6 Roll Rate versus Control Power

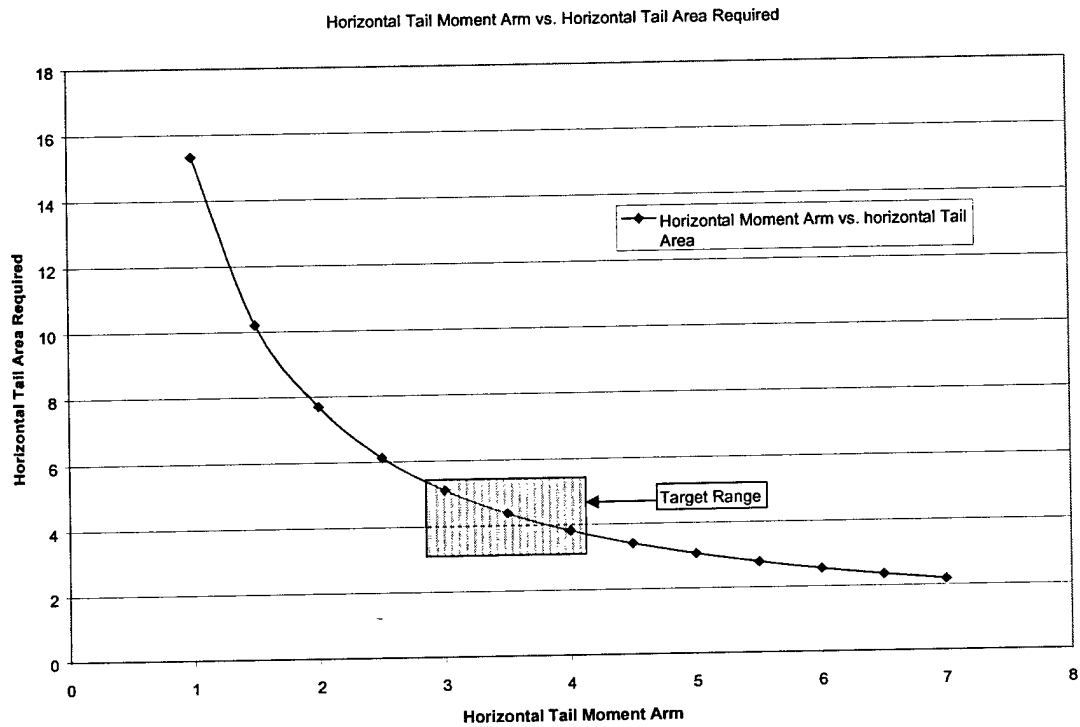


Figure 4.7 Horizontal Tail Moment Arm versus Horizontal Tail Area Required

	Horizontal	Elevator	Wing	Aileron	Vertical	Rudder
Chord (in.)	13.83	2.51	20.00	4.42	12.00	-----
Span (in.)	41.48	41.48	84.00	1.50	14.40	14.40
Area (sq. ft.)	4.38	0.72	11.67	0.55		
Flap effectiveness		0.308		0.136		
Servo deflection (degrees)		20.0		39.8		32.0
Servo force (lbs.)		0.848		0.848		0.848
Force (lbs.)		0.434		0.757		6.606

Figure 4.8 Component Sizing

Neutral Point	8.054
Static Margin	0.303
Tail Volume	0.8
Roll Rate (deg./sec)	53.465
Outer Edge Aileron Position (ft.)	3.5
Inner Edge Aileron Position (ft.)	2.0
Rudder Deflection (deg.)	15.0
Cn	0.030
CnB	0.187
Cnr	0.019

Figure 4.9 Sizing and Stability Calculations

Component		oz.	moment arm	Datum Dist.	moment
motor/gear box	1	12.5	-32.5	7.5	5.86
controler	1	3	-28	12	2.25
mount	1	7	-31	9	3.94
prop	1	3	-34	6	1.13
batteries	1	80	-3.4	36.6	183.00
front fuselage	1	4.64	-17	23	6.67
Aft fuselage	1	4.16	25	65	16.90
Horz tail	1	16	42	82	82.00
Vert tail	1	8	45	85	42.50
Spar	1	2.5	3	43	6.72
Bottle 1	1	38.2	-3	37	88.34
Bottle 2	1	38.2	-11	29	69.24
Bottle 3	1	38.2	-19	21	50.14
Bottle 4	1	38.2	12.5	52.5	125.34
Bottle 5	1	38.2	20.5	60.5	144.44
Upper Wing	1	32.08	-7	33	66.17
Lower Wing	1	3.2	3	43	8.60
End Plate	2	1	-2	38	2.38
Reciever	1	1.13	26	66	4.66
Gyro	2	1	26	66	4.13
Batteries	1	3.17	28	68	13.47
Elevator Servo	2	1.58	42	82	8.10
Rudder Servo	1	2	42	82	10.25
L. Aileron Servo	1	1.58	3	43	4.25
R. Aileron Servo	1	1.58	3	43	4.25
NWS Servo	1	2	-28	12	1.50
Nose Landing Gear	1	0.65	-27	13	0.53
Main Landing Gear	2	1.25	3	43	3.36
Brakes Assy	2	4	2	42	10.50

Weight-->	384.0 oz.	Moment Sum	960.09
	24.0 lbs.	Datum Sum	960.05

Payload Fraction
Wb/Wa--> 0.49737

- 1) Moment sum is a sum of all individual moments
 - 2) Datum sum is the distance from the datum to the CG multiplied by the total weight
 - 3) When the 2 match, the aircraft is centered about the CG location
- Note: Datum is located 40 inches forward of CG location which is 2 inches aft of the lower wing leading edge.

Figure 4.10 Weight and Balance

5 Detail Design

5.1 Performance Data

5.1.1 Take-Off Performance

Take off performance was directly related to the power provided by the Propulsion Group. For the gross take off weight of the aircraft, enough power had to be provided for the aircraft to lift off within 75% of the maximum take off distance of one hundred feet. This limit was predetermined to ensure that a take off with less than maximum power could be accomplished. Based on a power of approximately eight hundred watts, it was determined that the aircraft could meet or exceed this limitation.

5.1.2 Handling Qualities

Considering the competition location, it was determined that the aircraft must be designed to handle gusty wind conditions. This required that the ailerons and rudder deflect quickly and sufficiently to counter unstable wind conditions, and the control sizing to be such that roll and yaw performance were good but controllable with standard servo actuators.

The stall characteristics of the aircraft were also of primary concern. Handling at high angles of attack under loaded conditions require that the wings have stall characteristics that would help prevent a spin in the event that the aircraft entered a stalled condition. Several steps were taken to eliminate bad stall characteristics:

First, the wing shape was considered. A tapered wing could be used to provide a more elliptical lift and increase aircraft efficiency but would cause the wing to stall very uniformly, giving the pilot very little reaction time before spin entry. A rectangular wing decreases the overall lift and efficiency of the aircraft but when entering a stall, the root of the wing stalls first and spreads outboard over the wing, reducing the rate of stall and giving the pilot more control in the preliminary stages of the stall. Therefore, the rectangular wing was selected from a safety standpoint.

Next, to assist in stall recovery, the decalage angle, or the difference in incidence angle of the wings relative to each other was researched. Using analytical and wind tunnel test data discussed in Section 5.3, it was found that a decalage angle of negative one degree (the top wing at one degree lower incidence angle than the bottom wing) would allow the top wing to stall approximately five degrees before the bottom wing. The top wing was staggered ten inches forward of the bottom wing with the CG located three inches forward of the bottom wing's quarter chord. When the top wing stalls, the lift of the bottom wing is located aft of the CG and caused a forward pitching moment about the CG forcing the nose down and assisting in the stall recovery.

As each mission requires a series of loaded and unloaded sorties, a significant amount of the gross weight will be removed during parts of each mission. This could cause the CG to shift due to the weight change. However, the payload will be loaded symmetrically around the CG to negate a CG shift during loading and unloading.

5.1.3 G-Loading Capability

As gusty wind conditions were expected due to the competition location, the accelerations that the aircraft could encounter in gusty wind conditions could easily exceed 2.5G's. Therefore, a reasonable G-loading limitation of 4G's was placed on the aircraft for safety of flight. This was determined to be reasonable based on the construction methods and materials selected for construction. All structural elements were sized according to the 4G maximum load.

A single piece spar assembly was designed into the lower wing and fuselage in which the main landing gear is mounted. This provides a structure to absorb excessive G-load that could be experienced during rough landings. With the high G factor of safety designed into the spar, the landing gear was designed with a 1.5G load capacity. This ensures that in the event of a structural failure in the landing gear, the wing will not collapse and cause further damage. The length of the spar was dependent upon the historical data and research conducted for the optimal landing gear placement. As previously stated, the length from the centerline of the fuselage to main gear strut is fourteen inches.

5.1.4 Range and Endurance

In reviewing the mission requirements it was determined that since range was constant endurance should be the primary focus. Based on loading conditions, power requirements, power efficiencies and battery limitations, various calculations were performed to maximize endurance through battery selection. For the design range of five liters of water, a full power endurance of 6.5 minutes was predicted. This decreases approximately 20% for each additional bottle carried.

5.1.5 Payload Fraction

To keep the payload fraction high, several measures were taken to reduce structural weight:

- 1) Landing gear was manufactured from scratch to save weight over prefabricated landing gear.
- 2) For greater strength, foam cores would be left in some carbon fiber sections of the aircraft. Beaded white polystyrene was selected over blue extruded

polystyrene as form material for the carbon fiber, as white is half the density of the blue.

- 3) Carbon fiber was selected as the main construction material for its high strength to weight ratio.
- 4) Since the vertical and horizontal tails do not see large forces they will be constructed of a balsa structure and Monokote covering. This provides an adequate structure with a very light weight.

The final payload fraction was determined to be 41%.

5.2 Component Selection and Systems Architecture

5.2.1 Propulsion System

The propulsion system required optimizing the overall system performance through component matching. If these components are not properly matched and overall efficiency is not optimized, then the overall performance of the system suffers. The components of the propulsion system include the batteries, the motor, and the propeller. Each of the propulsion system components was commercially available as required by contest rules.

In developing the battery pack, a spreadsheet was used to maximize power density given the five-pound limit per pack. Types of batteries considered were Sanyo 2800, Sanyo 3000, and SR 2500. The battery that provided the maximum overall score possible was the Sanyo 3000 mAh cell. Figure 5.6 compares the score versus liters carried of the various types of batteries tested. The Sanyo 3000 mAh cell satisfied the power requirements, held to the current limit, and provided the flexibility to increase the number of liters carried by the aircraft. Using the Sanyo 3000mAh battery resulted in a 25-cell battery pack.

The motor was chosen based on the maximum power required as determined by the Aero-Controls group. Only a few companies manufacture electric motors suitable for the requirements of the system. Motor manufacturers considered were Aveox and Astroflight. Ultimately, the motor with the best efficiency that could meet our needs was chosen. Brushless motors were considered, however, it was discovered that the inefficiency introduced into the system by the controller for brushless motors negates the efficiency gained by choosing brushless over brush motors.

Commercially available custom windings were also considered, but they were deemed unnecessary for anticipated operating conditions. The motor best suited for the desired performance was the Astro Cobalt 40 8T#20 motor with a 3.1:1 gearbox. The gearbox was used to reduce the number of revolutions per minute of the propeller, hence, producing the desired thrust.

An analysis was performed to match a propeller to the system based on experimental data. The propeller that provided the highest takeoff thrust and best efficiency was selected for use. Using equations that described the performance of several different propellers in terms of C_T , C_P , thrust, and efficiency, a spreadsheet was developed to aid in selecting the propeller that helps optimize overall performance. Figure 5.7 through Figure 5.9 show the resulting data. Takeoff thrust requirements were considered first, then cruise thrust, and then efficiency. The propeller with 0.7 pitch-to-diameter ratio best suited our needs. The takeoff thrust provided by this propeller was 8.7 pounds. The cruise velocity attainable with this propeller was 57 feet per second.

Maintaining maximum possible overall efficiency in the propulsion system was critical. In an attempt to reduce losses in the system, tests were conducted on last year's system using a dynamometer to determine the impact of cooling schemes. Cooling the batteries had no impact on the overall performance of the propulsion system. However, cooling the motor had a significant impact on the overall efficiency of the motor. With this in mind, fins were developed to help dissipate heat away from the motor, thereby helping maintain higher efficiency during operation. As seen in Figure 5.10 and Figure 5.11, the thrust and power increased by approximately seven percent. The endurance also increased by approximately 15 seconds.

The propulsion system consisted of an Astro Cobalt 40 8T#20 motor with a set of cooling fins attached directly to the motor to expedite cooling. The motor used a 3.1:1 gearbox to drive an APC propeller with a 0.7 pitch-to-diameter ratio. One battery pack consisting of 25 Sanyo 3000mAh cells and weighing less than five pounds served as the power source of the system.

5.2.2 Landing Gear and Braking System

The landing gear was manufactured in-house and consisted of a tricycle design with a hydraulic braking system located on each of the main gear hubs. The nose landing gear is steerable which alleviates the need for differential braking. The steerable nose wheel is supported within a yoke and centered on the nose wheel strut (see Figure 5.12). The main wheels consist of the braking device in the center of the wheel that is attached to the main strut (see Figure 5.13). The landing gear struts consist of spring shock absorbers pinned into a wooden block mounted at the end of the wing spar (see Figure 5.14). The insertion of the strut through the wing and into the spar also acts a securing device for holding the wings in place.

The drum style braking system uses water as the working fluid and consists of a master cylinder, pressure hose, wheel cylinder, brake shoe and hub. The master cylinder for each wheel hub brake is located on an access panel behind each main strut in the wing. This panel also provides access to the aileron control servo. The brake hydraulic lines are connected together through a pressure line running through the fuselage to ensure that the brakes will have equal pressure actuation regardless of any discrepancies in the control servos or master cylinders.

5.2.3 Aerodynamics

As discussed before, the Selig 1223 airfoil was selected primarily on its high lift to drag ratio. It was the primary reason for the use of composite materials due to its complex design. The 1223 demonstrated excellent qualities from wind tunnel tests that have confirmed published data of the airfoil.

Wing area was determined through the score evaluation and was sized to maximize score. This led to a wing loading of 1.3 and a total wing area between the two wings of 22.6 square feet.

Tail volume was designed by summing the moments of the wing, fuselage and tail. Due to the high forward pitching characteristics of the wings, an inverted Clark Y airfoil was used for the horizontal tail to decrease drag at the incidence angle of negative six degrees required to stabilize the aircraft at cruise. Refer to Figure 5.3 for the C_M versus α plot.

The vertical tail was sized to achieve the C_{nB} of 0.187, approximately that used by larger general aviation aircraft. The rudder was sized in the same manner to give a C_{nr} of 0.019. This was deemed adequate to control the aircraft in yaw in gusty wind conditions.

5.3 Wind Tunnel Testing

In order to validate performance data for the Selig 1223 airfoil, and to study the effects of the airfoil in the biplane wing configuration, it was decided to construct a one third scale wing set in order to perform flow visualization and determine lift and drag with the use of a force balance. The wings were mounted so the decalage angle between the wings could be varied and the assembly could be varied from an angle of attack of negative thirteen to positive thirty. This allowed a study of the stall characteristics of the airfoil when in the monoplane and biplane configurations and the effects of the wings on each other. This also allowed flow visualization to determine the proper decalage angle in which the top wing would stall at a slightly lower angle of attack to increase stall recovery and stability.

Tests were performed at a Reynolds number of 400,000 and a velocity of 85 ft/s. Resulting data for lift and drag from the force balance used during the study can be found in Figure 5.1 and Figure 5.2. Some flow visualizations were accomplished at slower velocities and Reynolds numbers to study variances in the stall characteristics at lower Reynolds numbers. This data proved to be invaluable in the flow visualization alone and showed that with the wings spaced 75% of a chord length apart, very little lift was lost due to interference. It also showed that, at 30 degrees angle of attack, the effects of the top wing prolonged the full stall of the lower wing to a Reynolds number of half that of the test number. Evaluation of this data determined the decalage angle of the top wing to be set at negative one degree. A slight loss in the maximum coefficient of lift was suffered but was deemed to be a necessary trade off for improved stall safety. Pictures

showing wind tunnel setup and operation can be found in Figure 5.4 and Figure 5.5 respectively.

5.4 Sizing and Configuration

Basic empty weight	17.5 lbs.
Payload weight	11.5 lbs.
Gross TO weight	29 lbs.
Payload fraction	0.40
Gross TO weight wing loading	1.3
Aspect ratio for each wing	4.19
Total Wing area	22.6 ft ²
Wing span	7 ft
Mean aerodynamic chord length	1.67 ft
Wing stagger	10 inches
Wing Separation	14 inches
Number of Servos	8 Servos
Final Configuration RAC	\$6181.50
Final Configuration Estimated Score	24.26

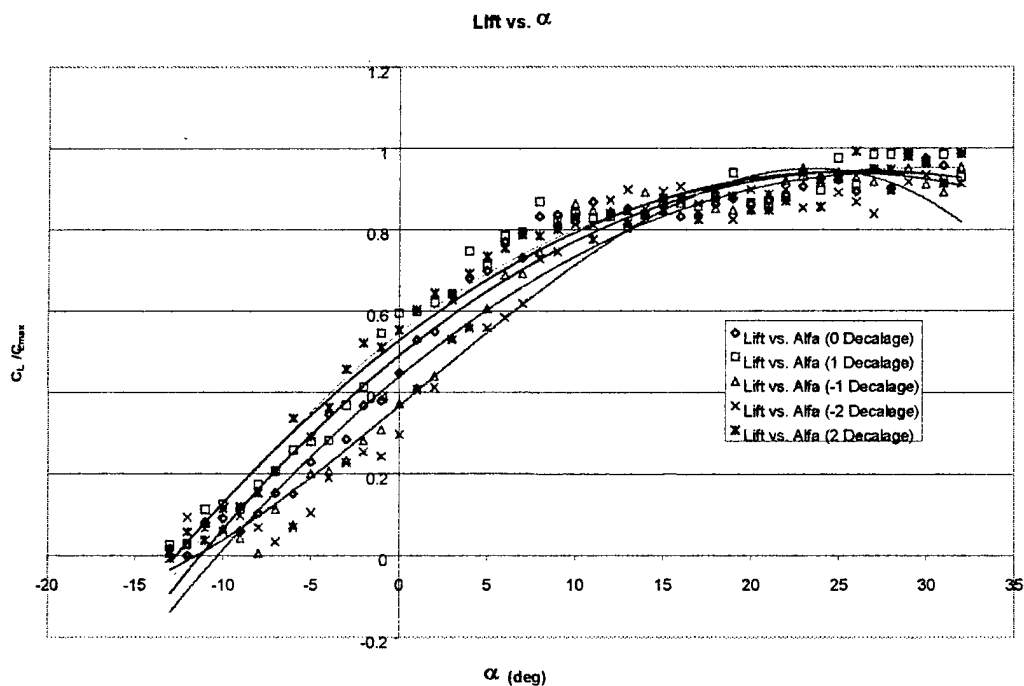


Figure 5.1 C_L versus α

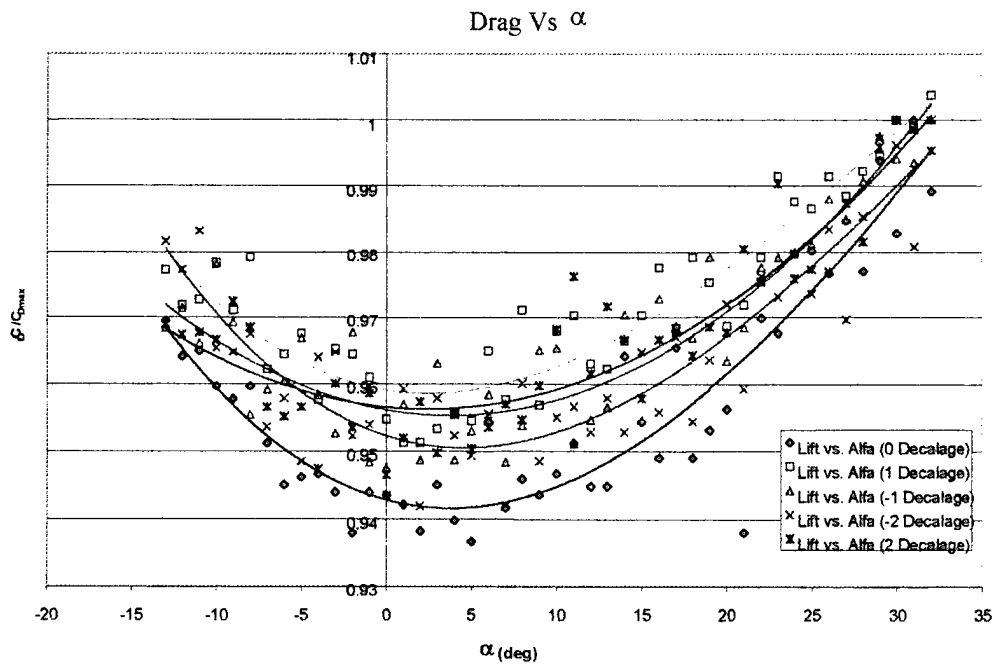


Figure 5.2 C_D versus α

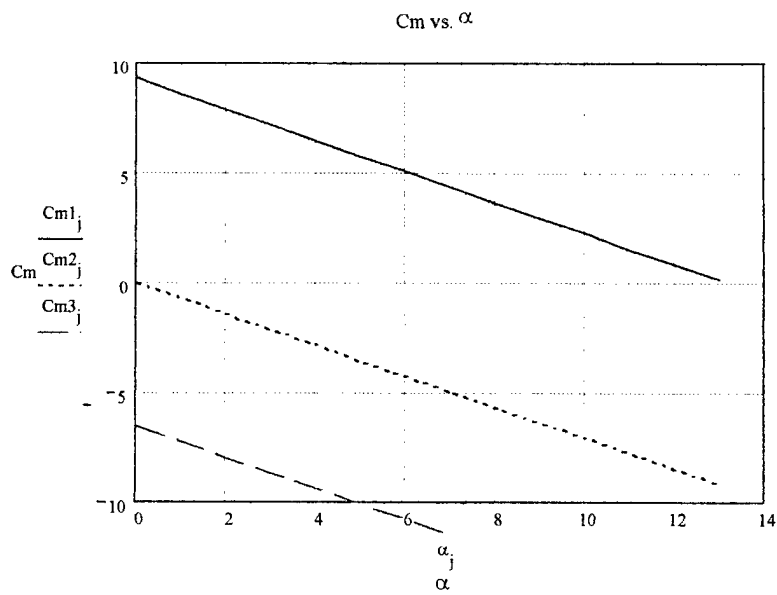


Figure 5.3 C_m Vs α

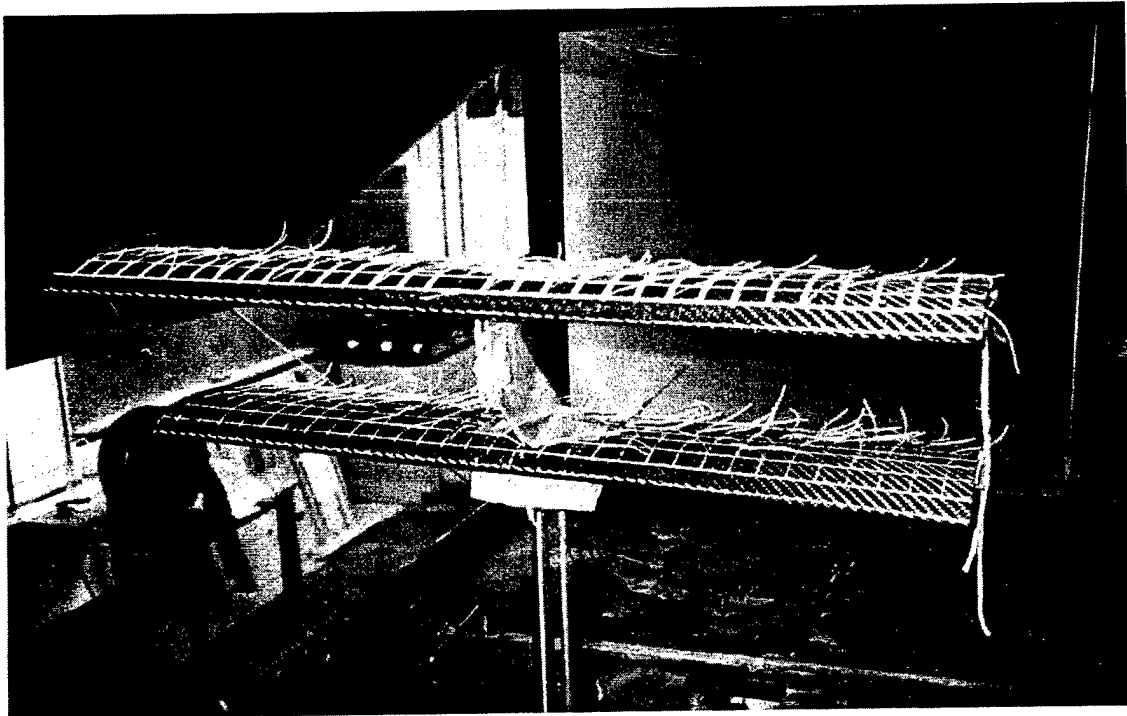


Figure 5.4 Wind tunnel test setup

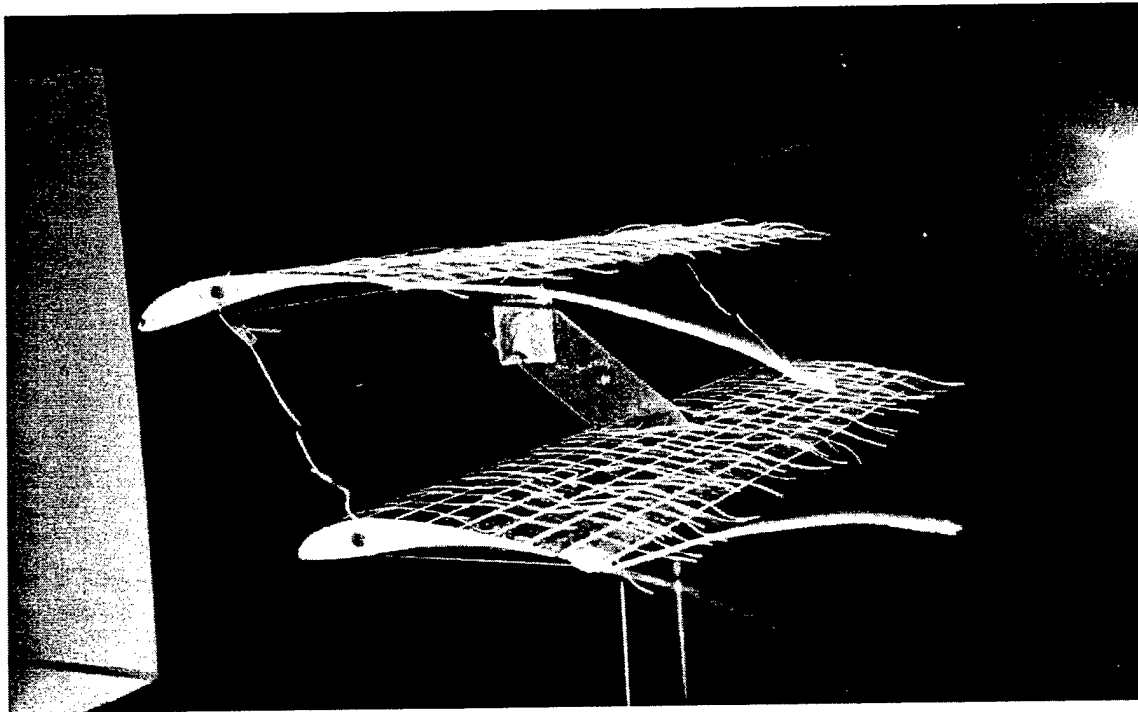


Figure 5.5 Wind-tunnel testing in progress

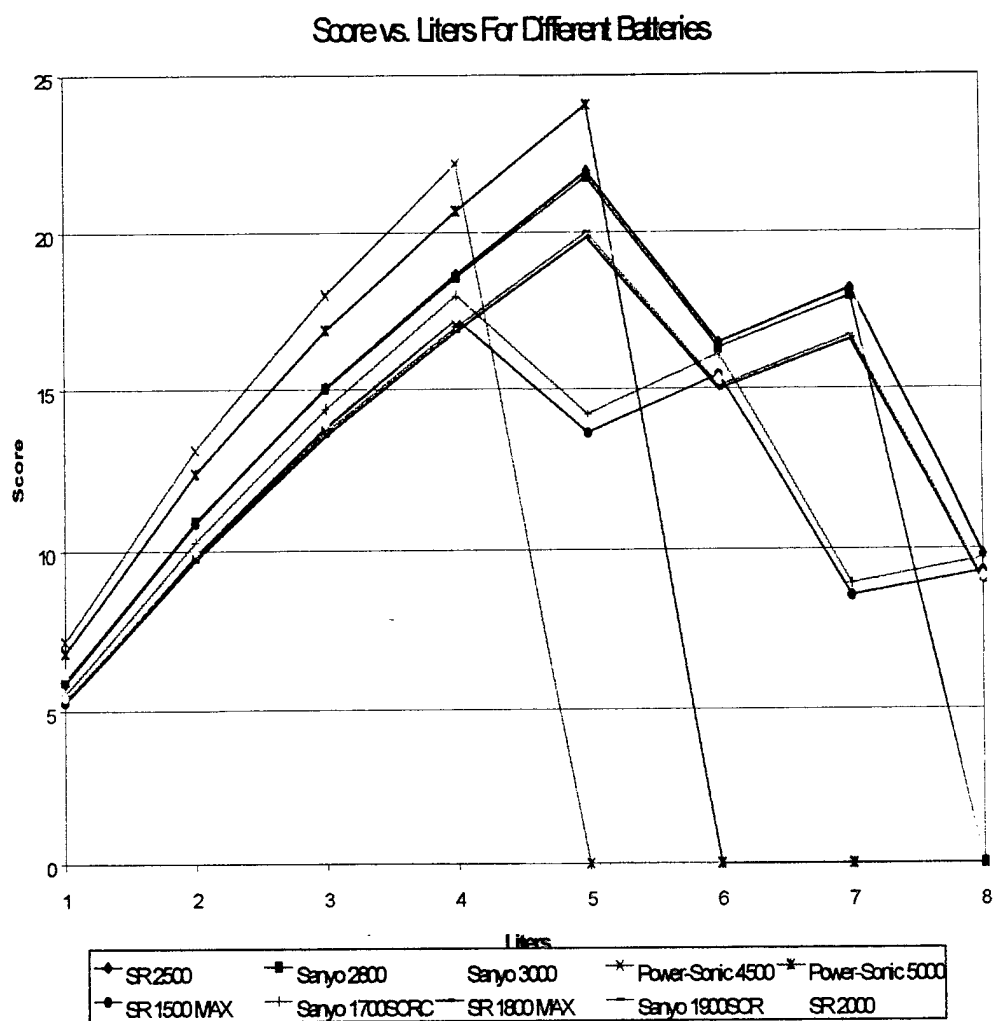


Figure 5.6 Score vs. Liters with Different Batteries

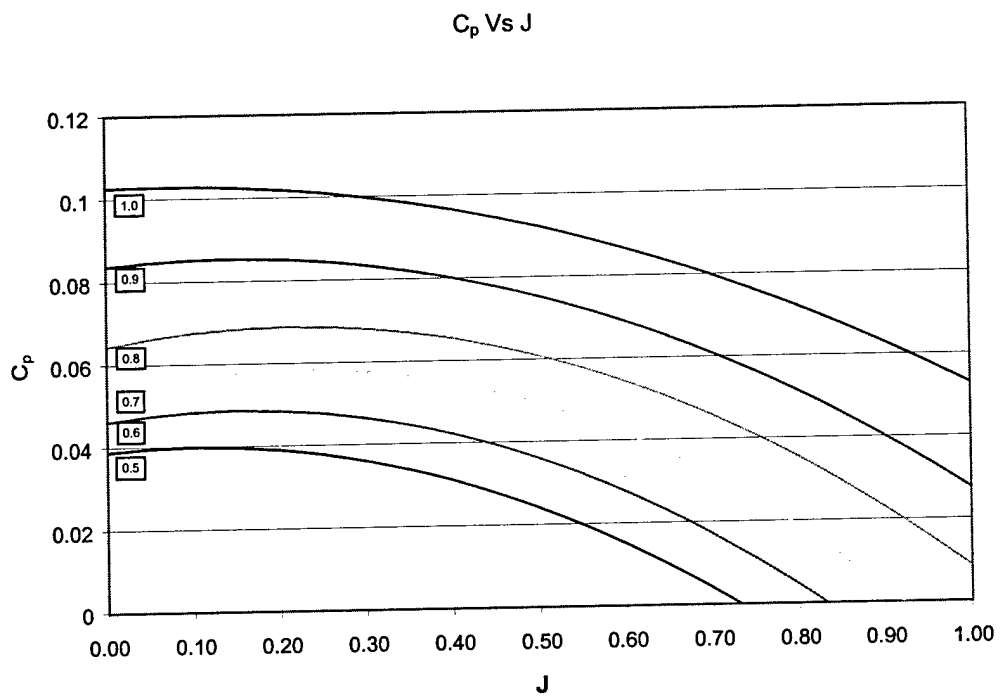


Figure 5.7 C_p vs. J

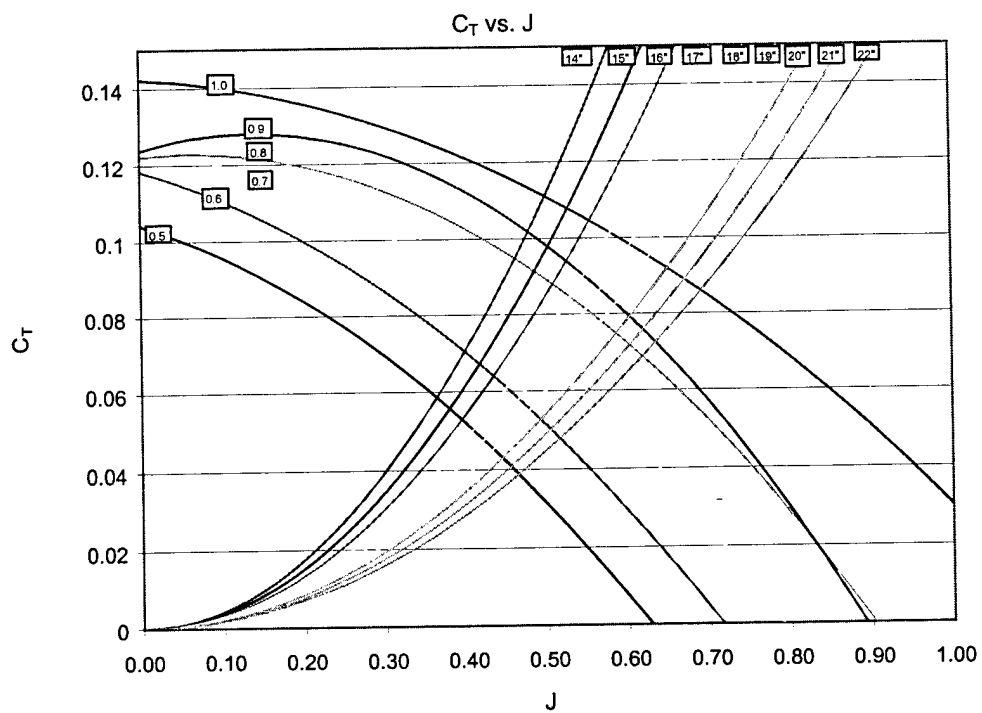


Figure 5.8 C_T vs. J

Efficiency vs. J

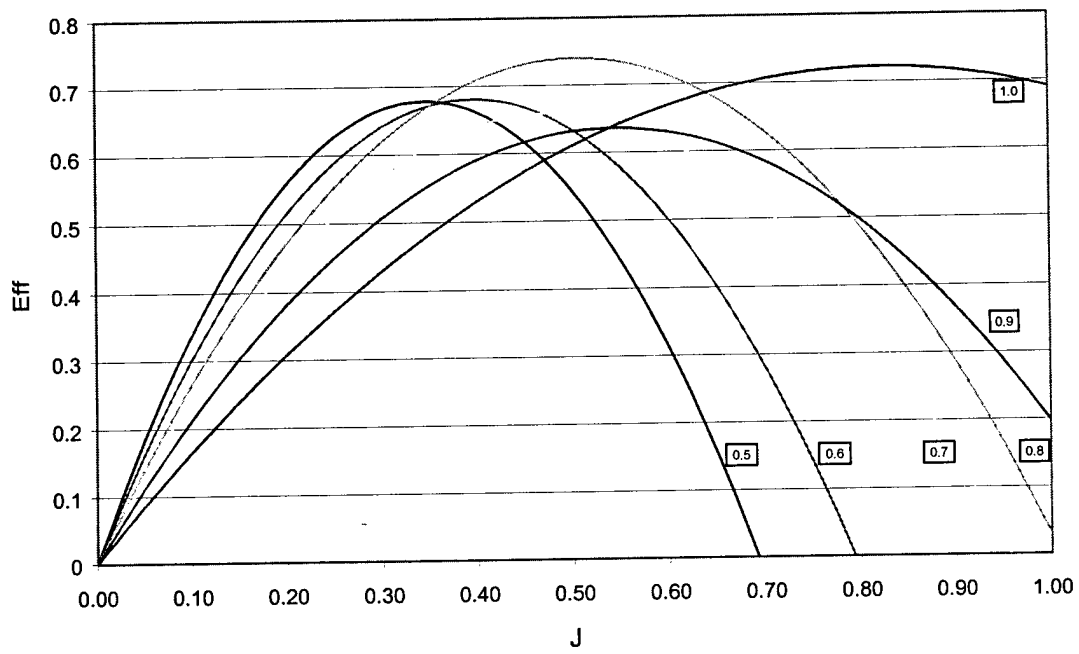


Figure 5.9 Efficiency vs. J.

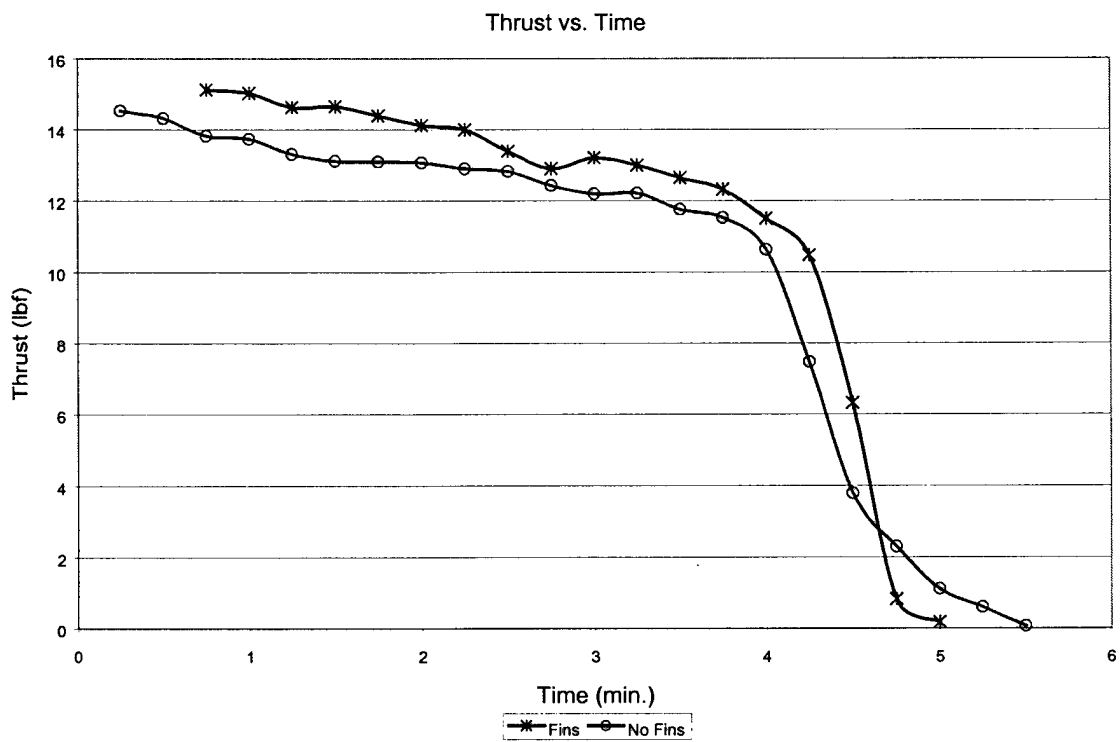


Figure 5.10 Thrust vs. Time

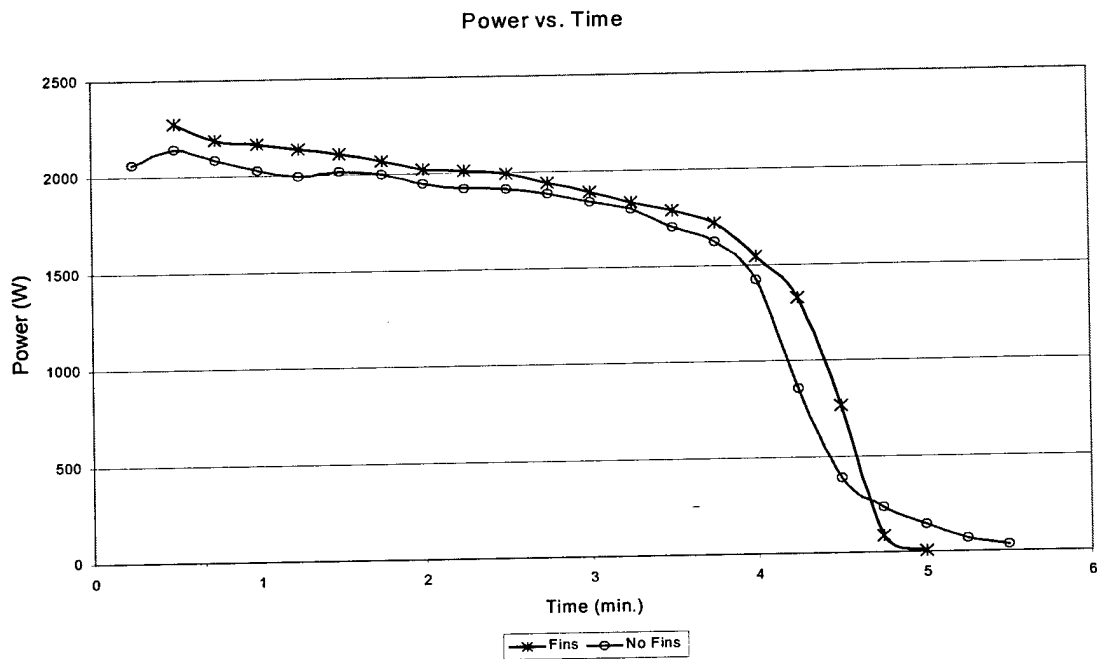


Figure 5.11 Power vs. Time

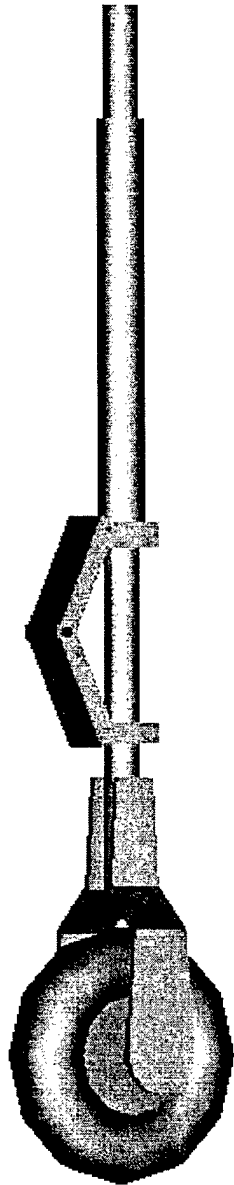


Figure 5.12 Nose Wheel 3D View

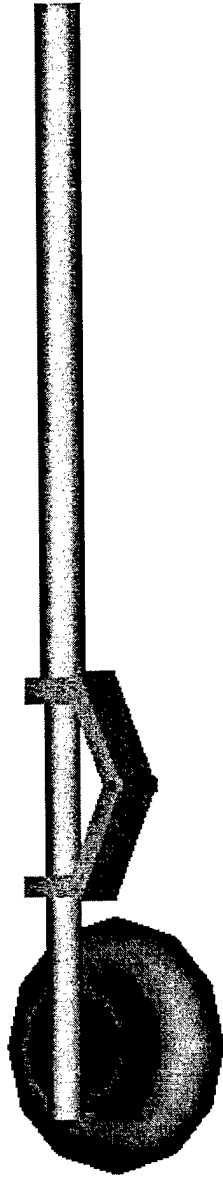


Figure 5.13 Main Wheel 3D View

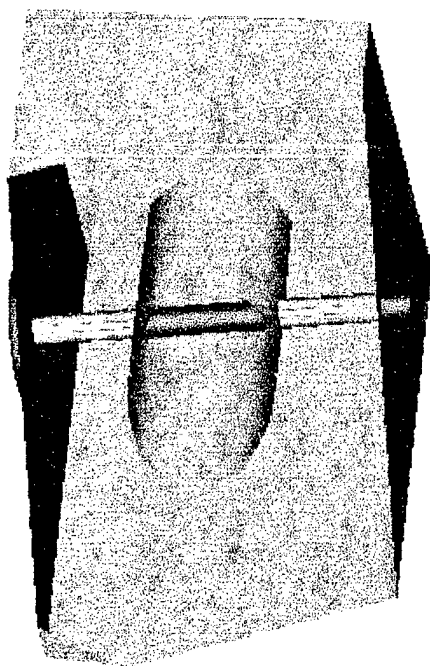


Figure 5.14 Main Strut Mounting Block 3D Cut-Away View

6 Manufacturing Plan

6.1 Manufacturing Processes Investigated

The processes considered for the manufacture of the aircraft centered on the following materials:

- Balsa wood and Monokote™
- Carbon fiber and Kevlar™
- Aluminum

The first process considered, which involved primarily balsa wood and Monokote, was thought to be the most common method of constructing small-scale aircraft. The wings of the aircraft would be formed by cutting thin ribs from sheets of balsa, gluing the ribs to a central spar (or to multiple spars if extra support were needed) and coating the structure with Monokote. The horizontal and vertical stabilizers would be constructed in the same manner as the wings. The fuselage would consist of thin balsa sheets forming a box structure, with several balsa longerons running the length of the fuselage for support. Small pieces of plywood or pine would be used for high-stress components such as the motor mount, landing gear blocks, and fuselage doublers. Thus, an aircraft constructed using this process would consist primarily of a balsa wood frame covered with Monokote, with plywood or pine adding extra strength to critical areas.

The second process, which involved primarily carbon fiber and Kevlar, was considered as a means to produce a much more durable and streamlined aircraft. This method would consist of laying up pre-preg carbon fiber over foam molds for the fuselage, wings, and stabilizers. Kevlar would be used to reinforce high-stress areas such as the motor mount and component attachment locations.

The third process, which involved only aluminum, was known to be common in larger aircraft. Fabrication using aluminum would involve careful machining of individual parts, followed by riveting the parts together. The strength provided by aluminum would allow this aircraft to be essentially a hollow shell.

Finally, a combination of the above three options was considered as a fourth potential manufacturing process. This process would consider each component of the plane (i.e., wings, fuselage, and stabilizers) individually, and the best material for each component would be selected.

6.2 Figures of Merit

The figures of merit used to screen competing concepts were the following:

- Strength to weight ratio of materials
- Availability of materials
- Cost of materials
- Required skill levels
- Required time of construction
- Ability to produce desired profiles

The composite materials possessed the best strength to weight ratio. An addition of a foam core increased the second moment of inertia, giving even higher strength. White polystyrene foam was found to have approximately half the density of blue insulation foam.

Although the availability of materials was essential, it did not restrict the team's choice of manufacturing processes since all of the materials under consideration were readily available. Monokote and large sheets of balsa could be easily ordered from hobby shops. Carbon fiber and Kevlar were available from nearby composite manufacturers. Aluminum sheets could be purchased at local hardware stores.

Cost of materials was an important consideration, but it did not completely restrict use of the more expensive materials (carbon fiber and Kevlar) since funding was available in the form of sponsorship from local businesses. Also, one manufacturer of composite products was willing to sell materials to the team at no profit, which made composite materials much more affordable.

The necessary skill levels associated with each manufacturing process limited the feasibility of some processes. For example, all members on the team had some experience with machining aluminum, but few possessed the expertise to machine all parts of the aircraft from aluminum.

Required time of construction was a concern because less than three weeks were available for constructing the prototype after construction drawings were complete, and even less time was available for constructing the final aircraft after flight testing the prototype.

The ability to produce desired profiles had the highest impact on the manufacturing processes selected. The only material that would allow the production of sophisticated high camber airfoils and a streamlined fuselage was carbon fiber. In contrast, balsa wood would permit few curved surfaces on the aircraft, and aluminum would be difficult to machine to an exact profile. Achieving desired component profiles was extremely important to the team due to the impact this would have on the aircraft's overall performance in flight.

The figures of merit were incorporated into a decision matrix as seen in Figure 6.2. This provides a general view of the individual characteristics of each material considered. The most suitable material for each aircraft component was then selected while maintaining an acceptable balance for interfacing materials.

6.3 Assemblies of the Final Design

After carefully considering each figure of merit described above, it was decided to produce the aircraft using a combination of different materials and manufacturing processes.

6.3.1 Wings and Spar

A carbon fiber skin with a white polystyrene beaded foam core was used for the wings. A template of the Selig 1223 airfoil was constructed and used in conjunction with a commercially available foam cutter to ensure precise shaping of the foam wing cores. The ailerons were attached to the lower wing using a gapless hinge to prevent airflow disruption. A carbon fiber wing spar was rigidly attached to the fuselage. The lower wing simply slides onto the wing spar and is held in place by the landing gear, as described below. A carbon arrow shaft is inserted aft of the main carbon fiber spar in the lower wing, through the fuselage, to act as a torsional secondary spar. The upper wing is attached to the aircraft by end struts and a center strut, made of a carbon fiber foam carbon fiber sandwich. The end struts are bolted in place with nylon bolts. The center strut is epoxied to the upper wing and bolted to the fuselage for easy removal.

6.3.2 Fuselage

The fuselage was constructed out of carbon fiber, with Kevlar and wood inserted to reinforce high-stress areas. Foam was used to obtain the desired fuselage profile. After the carbon fiber had cured over the foam molds, the foam was extracted to allow for the placement of the payload. Wooden bulkheads were then added to the fuselage for both torsional and bending strength.

6.3.3 Motor Mount

An aluminum motor mount was constructed and bolted to a Kevlar firewall in the fuselage. It was formed from a single piece of aluminum sheet that was cut and bent in place. It was then secured together with rivets.

6.3.4 Landing Gear and Brakes

The landing gear and brakes were constructed of aluminum. The main gear was supported by a small block of pine embedded at the endpoints of the spar. This block of wood was also utilized in the attachment of the lower wing. A quick release pin secures the gear and wing into the spar while allowing easy removal of the lower wing for

shipping purposes. Kevlar reinforcements were added to the nose gear and fuselage junction.

6.3.5 Empennage

The vertical and horizontal stabilizers were constructed of balsa wood and Monokote. As described above, these were formed by cutting thin ribs from sheets of balsa, gluing the ribs to a central spar, and coating the structure with Monokote. This significantly reduced the weight and resultant moment of the stabilizers, as compared with a carbon fiber and foam core buildup. The spars of the vertical stabilizer extend into the rear of the tail and then are epoxied in place. The horizontal tail has a carbon arrow shaft spar that extends through the rear of the fuselage. It is then epoxied to the rear of the fuselage.

6.4 Manufacturing Milestone Chart

The construction of the prototype began on February 22 and was completed on March 13. The following milestone chart illustrates the construction process graphically.

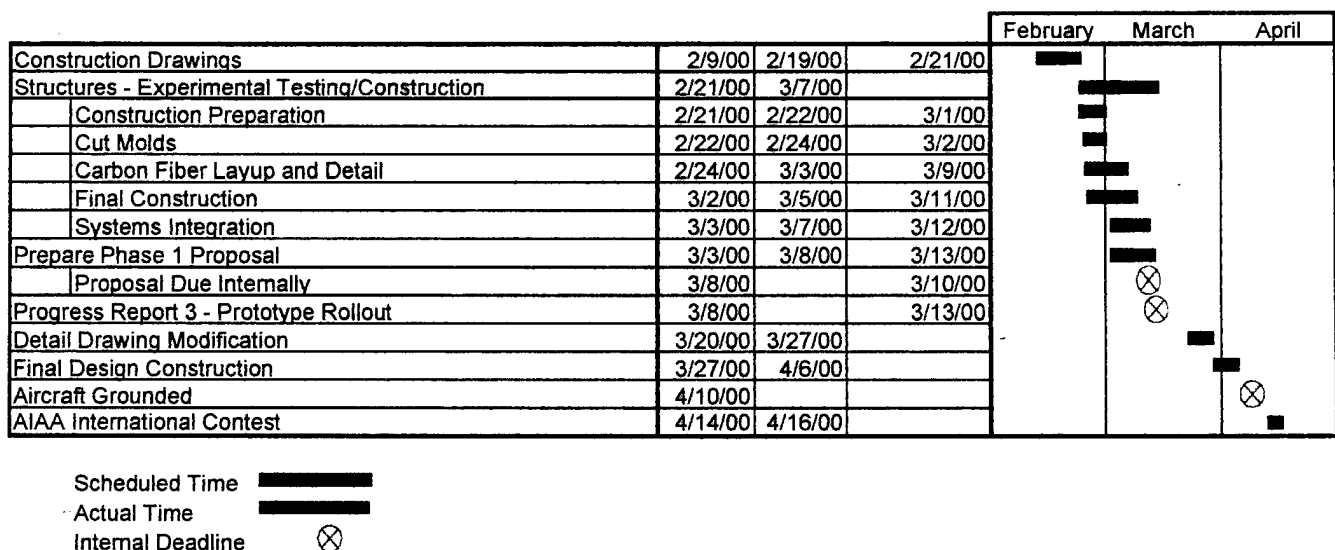


Figure 6.1 Manufacturing Milestone Chart

Figures of Merit	Weight Factor	Balsa Wood and Monokote	Carbon Fiber and Kevlar	Aluminum
Strength to Weight Ratio	0.2	4	5	3
Availability of Materials	0.05	5	3	4
Cost of Materials	0.05	5	2	3
Required Skill Levels	0.15	5	2	2
Required Time of Construction	0.2	4	5	2
Ability to Produce Desired Profiles	0.35	2	5	3
Totals	1	3.55	4.3	2.7

Figure 6.2 Material Decision Matrix

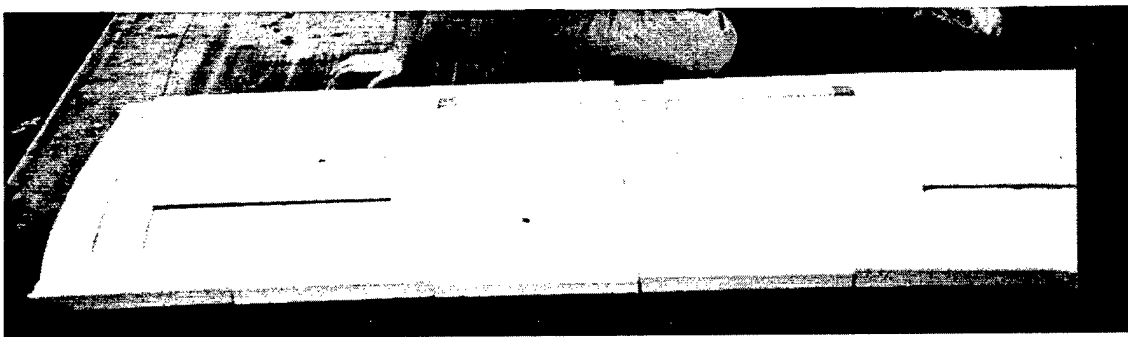
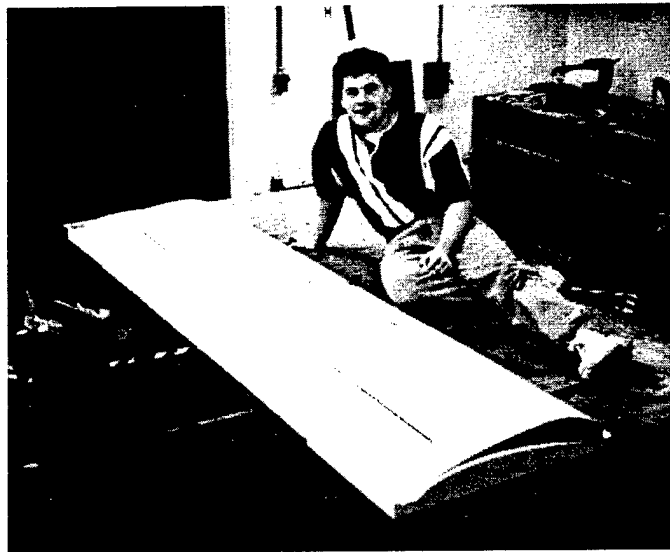
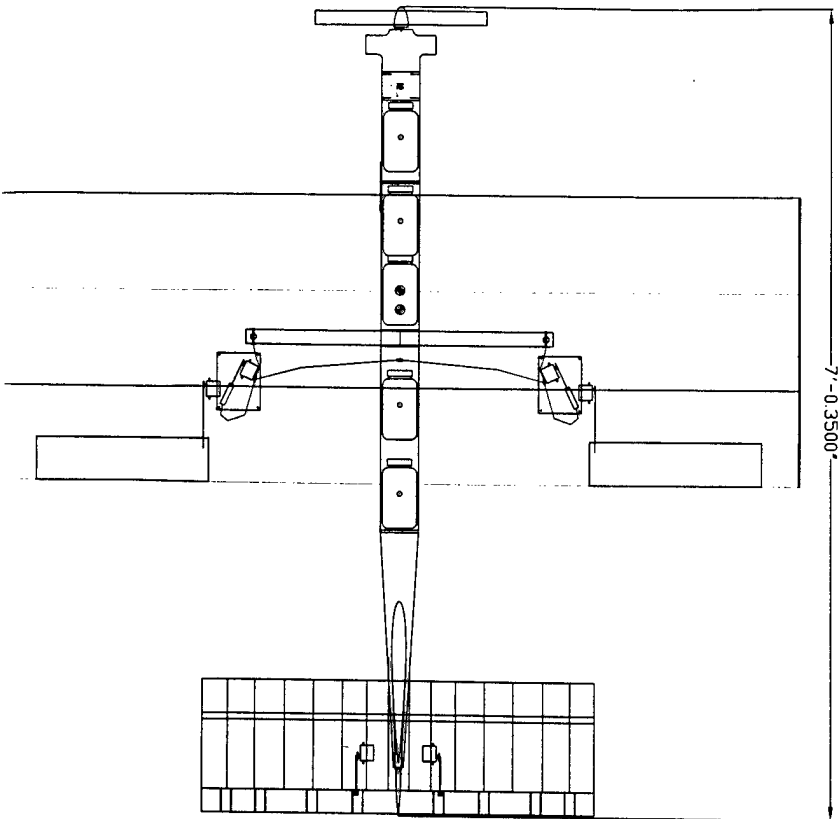
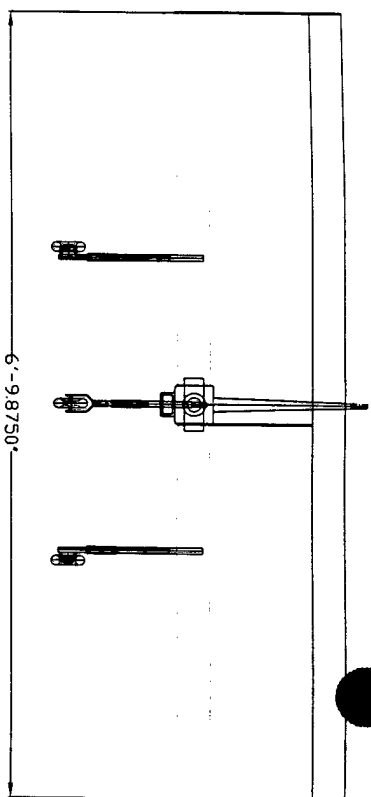
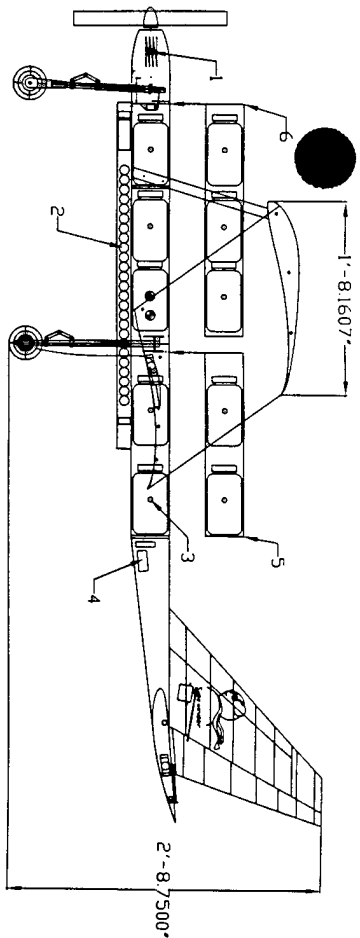
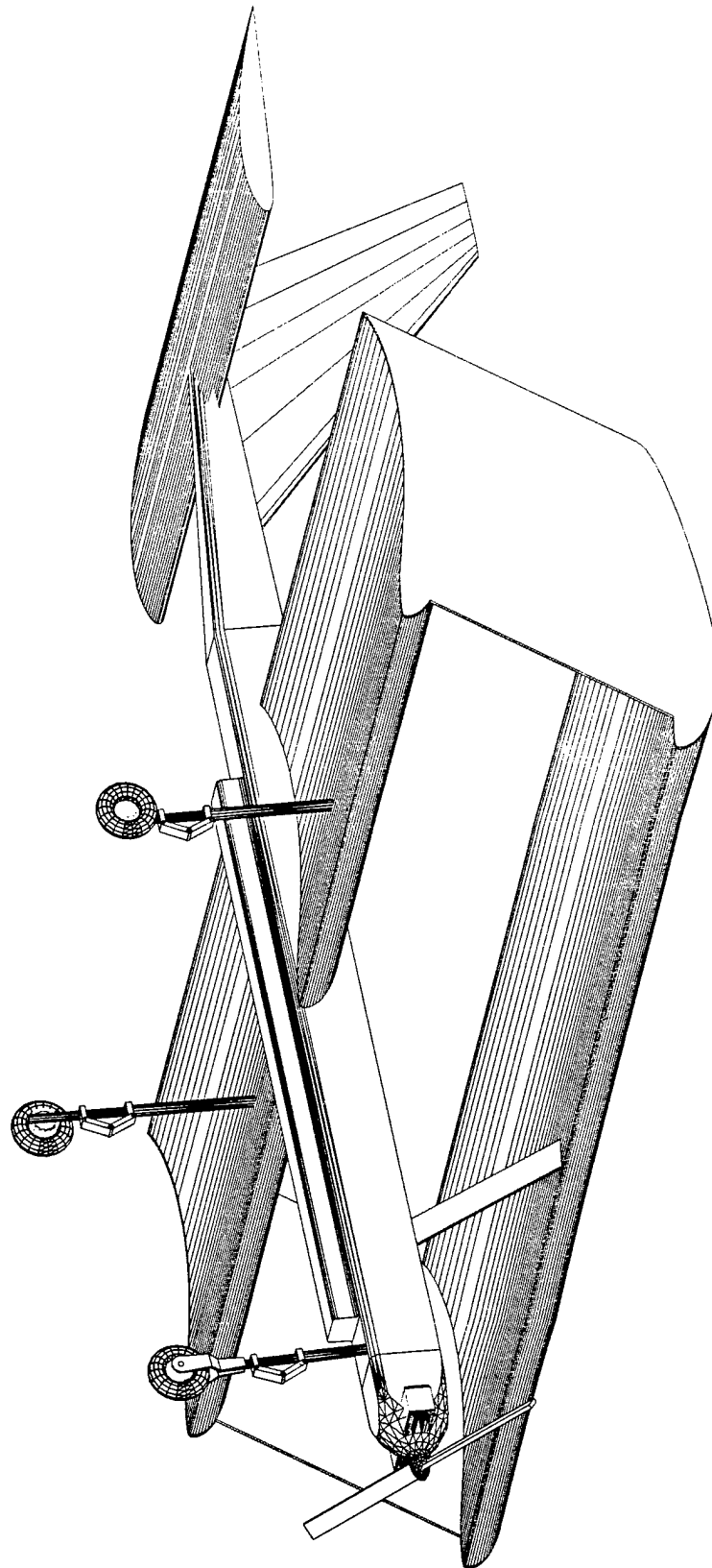


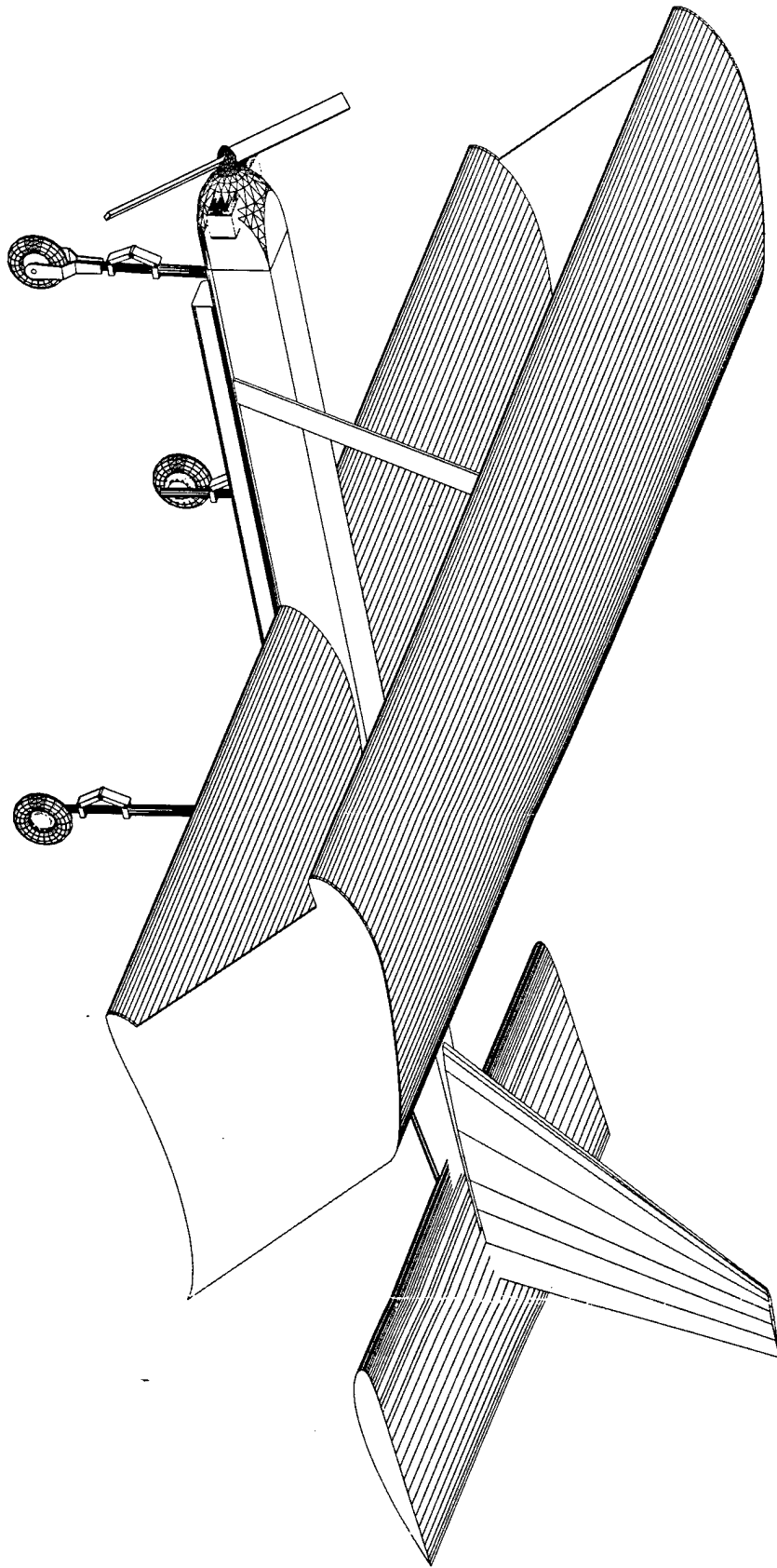
Figure 6.3 Lower Wing Foam Core Lay-up



1. Cooling Fins attached to Motor
2. Battery Pack
3. Water Bottle
4. Receiver and Systems Batteries
5. Aft Hatch
6. Forward Hatch

OKLAHOMA STATE
AEROSPACE
 ENGINEERING





2000 Cessna/ONR Student Design/Build/Fly Competition

Addendum Phase

TABLE OF CONTENTS

7	Lessons Learned	3
7.1	AERODYNAMICS GROUP.....	3
7.1.1	<i>First Flight</i>	3
7.1.2	<i>Second Flight</i>	3
7.1.3	<i>Lessons Learned</i>	3
7.1.4	<i>Changes Made</i>	4
7.2	PROPULSION GROUP.....	4
7.2.1	<i>First Flight</i>	4
7.2.2	<i>Second Flight</i>	4
7.2.3	<i>Changes Made</i>	4
7.3	STRUCTURES GROUP.....	5
7.3.1	<i>Fuselage</i>	5
7.3.2	<i>Wings and Tail</i>	5
7.3.3	<i>Landing Gear and Brakes</i>	6
7.4	IMPACT OF DESIGN CHANGES.....	7
7.4.1	<i>Manufacturing Techniques and Time Factors</i>	7
7.4.2	<i>Budget</i>	7
8	Aircraft Cost	11
8.1	MANUFACTURER'S EMPTY WEIGHT.....	11
8.2	RATED ENGINE POWER.....	11
8.3	MANUFACTURER'S COST.....	11
8.4	WING(S).....	11
8.5	FUSELAGE AND/OR PODS.....	12
8.6	EMPENNAGE.....	12
8.7	FLIGHT SYSTEMS.....	12
8.8	PROPULSION SYSTEM.....	12

LIST OF FIGURES / TABLES

FIGURE 7.1 POWER REQUIRED VERSUS CHORD LENGTH FOR VARYING VELOCITIES.....	8
FIGURE 7.2 CHORD LENGTH EFFECT ON WEIGHT AND LIFT	8
FIGURE 7.3 BUDGET DISTRIBUTION CHART	9
FIGURE 7.4 PROTOTYPE AIRCRAFT DURING FIRST TAKE-OFF.....	10
FIGURE 7.5 COMPETITION AIRCRAFT DURING FIRST FLIGHT	10
FIGURE 7.6 COMPETITION AIRCRAFT CLIMBING DURING FIRST FLIGHT	10
FIGURE 8.1 RATED AIRCRAFT COST PERCENTAGE PER SECTION	14
TABLE 7.1 PROJECTED AND ACTUAL COSTS OF COMPETITION AIRCRAFT.....	9
TABLE 8.1 RATED AIRCRAFT COST	13

7 Lessons Learned

After completion of prototype construction, the team took the opportunity to perform extensive flight tests. This testing allowed any arising problems to be solved and modifications to be made to the aircraft before construction of the final aircraft.

7.1 Aerodynamics Group

7.1.1 First Flight

The first flight occurred on the afternoon of March the twenty-fourth. The aircraft, along with ballast to correct the center of gravity, was approximately seven pounds overweight, forcing the first flight to take place with the equivalent of three liters of water on board. The aircraft lifted off smoothly into a 15-knot quartering crosswind and climbed slowly to altitude. After completion of one lap around the pattern, the flight was brought to an end by landing the aircraft into the wind. During final approach, the aircraft came close to hovering and touched down with an approximate 10-foot landing roll.

Observations made during this flight highlighted two things. First, the Selig 1223 airfoil performed better in the bi-wing design than initially determined. This was determined by calculating the coefficient of lift from the stall speed and known weight of the aircraft during the flight. Since the aircraft came close to hovering during approach, the approximate wind speed could be used as the stall speed. Second, the parasite drag of the aircraft was much higher than predicted. The known power of the flight was used along with the approximate cruise speed and weight to estimate the parasite drag of the aircraft. This allowed the aircraft to fly at very low airspeeds but prohibited the aircraft from attaining adequate cruise velocities.

7.1.2 Second Flight

The second flight of the day was performed with a larger propeller producing an increase in performance while validating data from the previous flight. In this flight, various turns along with straight and level flight were accomplished. On the base leg to landing, propulsive power was lost and an engine-out landing was performed short of the runway. No damage was done to the aircraft, to the amazement of the cows sharing the field.

7.1.3 Lessons Learned

Aside from the drag and propulsion discoveries, data from both flights showed the stability and control of the aircraft was as predicted with one exception. Slight pitching difficulties were initially encountered, which were corrected by trimming the elevator and shifting the angle of the thrust line by two degrees. The vertical center of gravity

was higher than the thrust line and resulted in a pitching up moment. Angling the motor down slightly placed the thrust line through the center of gravity, correcting the pitching problem and reducing the amount of nose-down trim needed. Roll and yaw response was reported to be excellent with rudder and aileron controls coordinated and provided excellent handling in turbulent conditions.

7.1.4 Changes Made

Based on the data gathered from the test flights, further analysis was performed to minimize drag and weight while maximizing lift and score (See Figure 7.1 and Figure 7.2). This information led to two major changes and a few minor ones. First, the wing area was reduced by 25 percent. In doing this, the overall volume, thus the weight, of the wings was decreased exponentially while lift was decreased linearly (See Figure 7.2). This also decreased the drag created by the wings due to surface area. Second, much effort was focused on devising a lay-up method for the carbon fiber that would produce a smooth finish. The surface finish on the prototype aircraft's wings was very rough, and combined with the area of the wing, created higher than acceptable drag. Other minor changes included decreasing the horizontal tail sizing proportionally with the wing. Also, a thinner, symmetrical airfoil was used in place of the inverted Clark Y airfoil originally selected, as the pitching moment of the Selig 1223 airfoil was not as great as expected.

7.2 Propulsion Group

7.2.1 First Flight

From previous unsuccessful take-off attempts, it was determined that a higher propulsion power was required. A larger propeller was mounted to the motor for the second flight. With the larger propeller the plane was able to take off and climb successfully, but power was still insufficient to produce adequate flight speeds.

7.2.2 Second Flight

During the second flight the same propulsion configuration was successfully used although the motor was damaged from the increased current drawn required from the larger propeller. Additional test flights were terminated since enough information had been collected to refine the prototype aircraft.

7.2.3 Changes Made

In order to increase power capacity, the AstroFlight Cobalt 640 motor has been replaced with an AstroFlight FAI 660 motor for the final plane. The FAI 660 motor is rated to 60 Amperes, where the Cobalt 640 can only handle 30 Amperes. The Cobalt 661, 662, 690 and Cobalt 691 were also considered as replacements for the Cobalt 640, but these motors could not handle current in excess of 35 Amperes. The FAI 660 was also the

most efficient option with a 25-cell battery pack. Only AstroFlight motors were considered because speed controllers and connections had already been purchased to match their motors.

Propeller size was increased from the original design for the reasons discussed above. The propeller diameter was increased by 13 percent. This increased the static thrust of the propulsion system by 40 percent. The increase in thrust along with the reduction of wing area will result in an increase of the flight velocity of the aircraft.

The number of cells in the battery pack was not changed, but the battery pack configuration was modified from the original design. Instead of placing the batteries side-by-side in one long row, the batteries were placed side-by-side in two rows and then stacked, one row on top of the other. This allows the batteries to be shifted from the front or the back of the aircraft in order to adjust the aircraft's center of gravity. The revised battery configuration also reduces the amount of support that has to be used on the pack, therefore reducing the overall pack weight.

7.3 Structures Group

After the flight testing of the prototype, several modifications were made to the aircraft structure to improve the physical characteristics. Final AutoCAD drawings of the items that differ from the preliminary designs have been made and are included at the end of this report.

7.3.1 Fuselage

The design of the final fuselage was similar to that of the prototype with the major modifications being a decrease in the overall length and an increase in the depth of the battery cowling.

Changes in construction procedures were aimed towards making the exterior surfaces as smooth as possible. This was accomplished by placing Plexiglas against the fuselage surfaces during the curing process of the carbon fiber. The decrease in fuselage length paired with the refined construction resulted in a weight savings of approximately one pound.

As designed, the fuselage can hold five bottles lying horizontally or eight bottles standing vertically with a different hatch cover. Separate fairings were constructed to enclose the bottles in the horizontal and vertical positions.

7.3.2 Wings and Tail

As mentioned above, changes to the wing and tail included a wing and tail area reduction of 25 percent and the use of a symmetrical horizontal stabilizer. A smoother surface was accomplished on the wings by creating a hard female mold from foam and

diluted spackle. The spackle prevented the structure of the foam from being translated into the finish of the carbon fiber and reduced the surface roughness significantly. The elevator hinge was replaced by a piano-style gapless hinge, like that of the ailerons, to help reduce drag.

7.3.3 Landing Gear and Brakes

Taxi tests performed by the aircraft showed that the purchased main gear springs were less stiff than advertised by the manufacturer. New, stiffer, smaller diameter springs replaced the initial springs before flight-testing.

During flight testing, the torque arms for the landing gear used on the prototype were found to have too much torsional play. In addition, after hard landings, the torque arm attachments that were press fit onto the struts were prone to twisting. A new design to keep the strut assembly aligned was created for the final aircraft. Using a key in the inner strut that slides within a slot in the outer strut, alignment was retained without the use of torque arms (See refined AutoCAD drawings). The new design reduced weight and drag associated with the torque arms and simplified the manufacturing process.

With the new smaller diameter spring installed into the main gear, a smaller diameter strut could be machined to encase the spring. This smaller main gear, as well as the new design for strut alignment, reduced the weight of each strut by approximately 1/4 pound.

The nose strut assembly worked well, but it was determined that the spring-loaded gear was not needed. This enabled a wire design to be used which provides a smaller frontal area, simplifies steering, and has the ability to deflect back on ground rolling impacts (i.e. potholes).

The landing gear worked as designed in taking the loads encountered during landing and taxiing. The lower nose strut bent under an excessive load during an off-field landing, showing that the lower struts would give prior to wing and fuselage damage occurring.

Overall, the design of the landing gear and brakes worked very well. The main gear spring struts took all of the impact on landing as anticipated and the main gear brakes worked well in stopping the aircraft within a limited area. The final aircraft will keep the brakes as an option, with installation dependent on the required strategy.

7.4 Impact of Design Changes

7.4.1 Manufacturing Techniques and Time Factors

Building and flying a prototype aircraft proved to be invaluable in all aspects of the design phase. A summary of the design changes made are as follows:

- Wing area reduced by 25%
- Horizontal tail area reduced and changed to symmetrical airfoil
- Fuselage and wing finished refined
- Torque arms replaced by key/slot design
- Nose strut replaced with wire spring gear
- Thrust line shifted 2 degrees
- Astroflight FAI 660 series motor replaced 640 series motor
- Battery cowling size increased
- Battery pack changed from single row to double row
- 9.5 lb. weight reduction from prototype to final design

As the final aircraft was built, the processes used in manufacturing were refined based on lessons learned while building the prototype aircraft. Modifications made to various subsystems within the aircraft, as described above, saved on materials and time, while the experience of building the prototype enabled the final aircraft to be built to a higher standard of quality and reduce construction time from one month to one week.

7.4.2 Budget

The true cost of the final aircraft is illustrated in Table 7.1. As seen, the difference between the projected and actual costs is quite significant. This is mostly due to insufficient experience with carbon fiber handling and construction techniques. Experimentation with the carbon fiber and associated techniques led to increases in the budget of the final design.

Throughout the semester, the team has taken an active marketing approach, successfully recruiting the required sponsorship. In addition to the 1200 dollars allocated by the University, the team has raised approximately 4000 dollars in sponsorship. Although the actual budget expanded significantly, the costs were offset by surpassing the original funding goal. This not only allowed the team to complete the final aircraft, but also to purchase spare parts for the Competition.

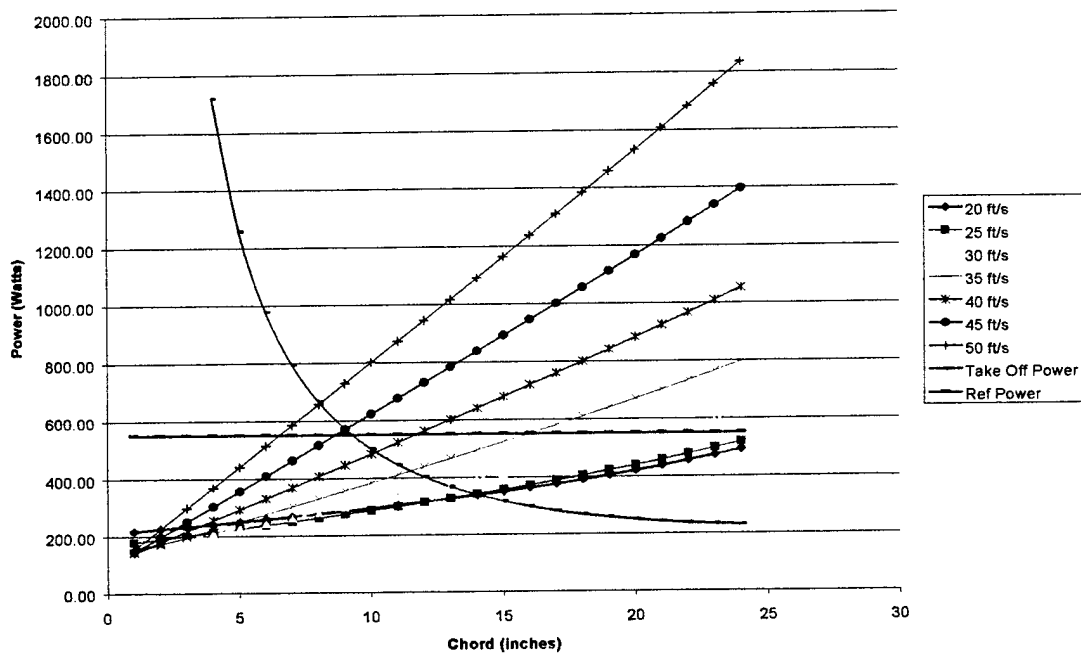


Figure 7.1 Power Required versus Chord Length for Varying Velocities

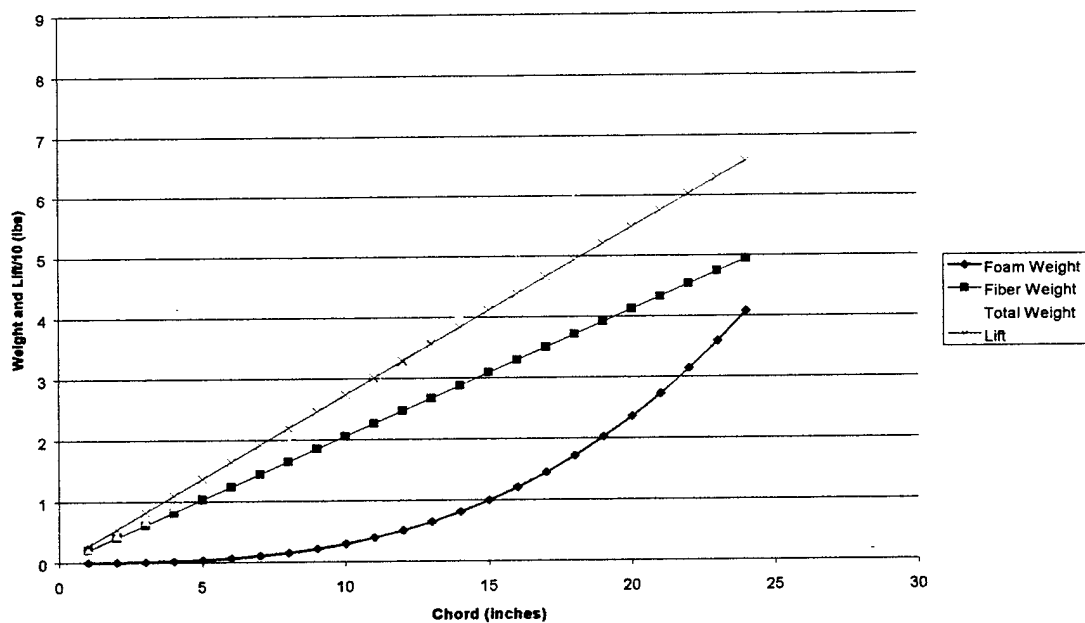


Figure 7.2 Chord Length Effect on Weight and Lift

Table 7.1 Projected and Actual Costs of Competition Aircraft

Consumables

Description	Quantity	Price	Projected Cost	Actual Cost
CA glue	3	\$4.90	\$14.70	\$8.49
Epoxy	5	\$1.97	\$9.85	\$3.94
Sandpaper	2	\$4.00	\$8.00	\$5.53
Bagging Film	19 yd	\$1.75	\$33.25	\$45.50
Breather	8 yd	\$3.13	\$25.04	\$37.50
Perf Release	5 yd	\$3.50	\$17.50	\$24.50
Non Perf Release	11 yd	\$5.25	\$57.75	\$73.50
Chromate Sealant	3 roll	\$4.50	\$13.50	\$22.50
Miscellaneous	1	\$20.00	\$20.00	\$45.00
Total			\$199.59	\$266.46

Mechanical and Electrical

	Quantity	Price	Projected Cost	Actual Cost
Motor	1	\$275.00	\$225.00	\$550.00
Speed Controller	1	\$130.00	\$130.00	\$180.00
Propellers	2	\$40.00	\$80.00	\$125.00
Batteries	35	\$8.00	\$280.00	\$262.50
Wiring and Connectors	1	\$20.00	\$20.00	\$57.99
Servos	8	\$30.00	\$240.00	\$112.94
Total			\$975.00	\$1,288.43

Construction Material

	Quantity	Price	Projected Cost	Actual Cost
Wood	1	\$25.00	\$25.00	\$17.00
C/F Preprg Twill	90 sq ft	\$7.20	\$648.00	\$900.00
C/F Preprg Uni Tape	17	\$3.00	\$51.00	\$90.00
Kevlar	3 sq ft	\$11.97	\$35.91	\$119.70
Foam	1	\$40.00	\$40.00	\$30.72
Arrow Shafts	4	\$5.00	\$20.00	\$35.00
Monokote	1	\$12.99	\$12.99	\$25.98
Sullivan Tires	5	\$8.00	\$40.00	\$24.00
Roller Blade Wheels	2	\$5.00	\$10.00	\$10.00
Bearings	9	\$2.00	\$18.00	\$24.99
Springs	7	\$1.25	\$8.75	\$10.52
Aluminum	1	\$60.00	\$60.00	\$43.00
Nose Landing Gear	1	\$22.95	\$22.95	\$22.95
Push Rods	6	\$0.50	\$3.00	\$8.00
Miscellaneous	1	\$15.00	\$15.00	\$29.71
Total			\$1,010.60	\$1,391.57

Total Cost by Category

	Projected	Actual
Consumables	\$199.59	\$266.46
Mechanical and Electrical	\$975.00	\$1,288.43
Construction Material	\$1,010.60	\$1,391.57
Total	\$2,185.19	\$2,946.46

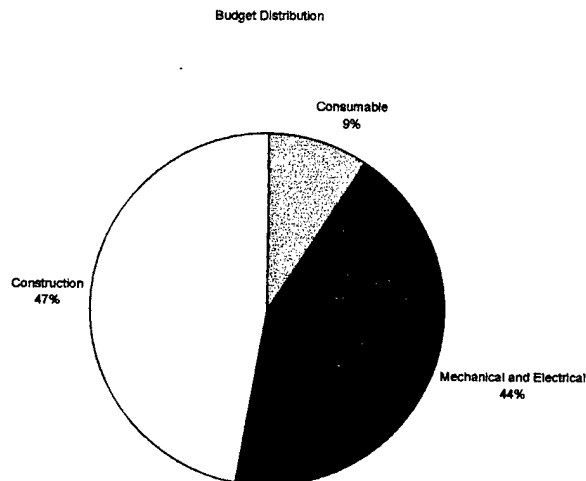


Figure 7.3 Budget Distribution Chart

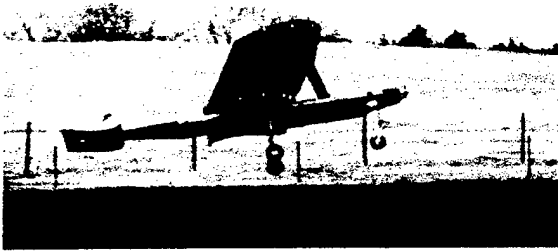


Figure 7.4 Prototype Aircraft During First Take-Off

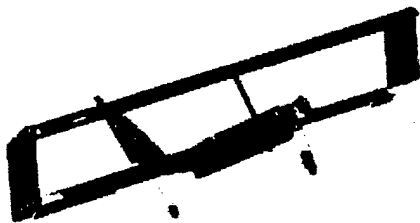


Figure 7.5 Competition Aircraft During First Flight



Figure 7.6 Competition Aircraft Climbing During First Flight

8 Aircraft Cost

The total Rated Aircraft Cost for the ORANGE ABISS aircraft is \$6,016. The break down of this cost is shown in Table 8.1. See Figure 8.1 for a percentage breakdown of the cost per section.

8.1 Manufacturer's Empty Weight

The total Manufacturer's Empty Weight for the competition aircraft is 15.2 pounds. This amounted to \$1,520 or 25.3 percent of the total Rated Aircraft Cost. A slight increase in weight was obtained from the use of carbon fiber construction over balsa wood construction, but was necessary to achieve the durability and complex wing structure desired. A slight increase in weight was obtained from the addition of a custom made landing gear that was both rugged and tuned to the performance of the aircraft. Weight was minimized in the area of the tail by utilizing balsa wood and Monokote construction. Wing weight was minimized by using polystyrene foam as a wing core. This foam is half the density of the typically used blue foam.

8.2 Rated Engine Power

In this design, one motor was determined capable of providing the power required for all phases of flight. This minimized the rated cost of this section to \$1,500, or 24.9 percent of the overall RAC. Twenty-five of the batteries that gave the optimum propulsion configuration could be used within the five-pound limit, helping to maintain a low cost factor. Both of these factors were considered and played a part in the decision of the final configuration to maximize score.

8.3 Manufacturer's Cost

This section was determined to be the most important and weighed very heavily in final design considerations. The final RAC of this section totaled to \$2,996 and 49.8 percent of the total cost. It is broken into the following five sections:

- 1) Wing(s)
- 2) Fuselage and/or Pods
- 3) Empennage
- 4) Flight Systems
- 5) Propulsion Systems

8.4 Wing(s)

This section was broken into the number of wings and the total wing area. This was found to be the most expensive part of the Manufacturer's Cost and was a major consideration during the design phase. The wing area was matched to the power available deemed necessary and the ability to meet the short field take-off requirements. The wing area was also optimized to allow versatility and minimize the cost while

maintaining high lift capabilities. Due to the wing area required to achieve the mission, it was decided that the performance increase associated with the bi-wing design offset the increased cost. This was done for two reasons. First, the aspect ratio could be much higher with a bi-wing design, increasing overall wing efficiency; and second, it allowed the volume of the foam core to be lessened, reducing the total wing weight considerably.

8.5 Fuselage and/or Pods

The goal of the fuselage design was to minimize frontal area and create a streamline structure. To meet these goals, the bottles were placed longitudinally into the fuselage. While this increased the payload bay length from other designs considered, the fuselage was kept short by strategic placement of such things as the battery pack, servos and controllers.

8.6 Empennage

In this category, sizing was not an issue in the cost factor, only the number of components. With the engine and fuselage configuration, there were no stipulations that required a non-standard tail design. Therefore, single vertical and horizontal tail surfaces of the appropriate sizing were designed to accomplish the stability required.

8.7 Flight Systems

This section consisted only of the number of servos used. For the competition aircraft's configuration, seven servos were required, with two of those being optional. One servo was used on each individual aileron to allow differential operation and trimming. With the use of aerodynamic balancing, only one servo was selected for rudder control with a separate servo for nose wheel steering. This allowed the steering rates to be changed using the control radio without affecting rudder control or deflection. One high torque servo was selected to control the elevator. The two remaining servos are high torque servos that operate the braking system, one for each master cylinder.

8.8 Propulsion System

The two focal areas of this section were the number of motors and the number of battery cells to be used. After determining the power requirements, research showed that a single motor could provide the required power. Based on the motor performance, power requirements and strategy, the optimum battery cell was selected. The optimization of the batteries was based on its performance, real world cost and weight. Once selected, the maximum number of cells was determined by the maximum five-pound battery pack weight. For the competition aircraft, 25 cells of the 3000 maH batteries were used.

Table 8.1 Rated Aircraft Cost

Coef.	Description	Value
A	Manufacturers Empty Weight Multiplier	\$100 / lb.
B	Rated Engine Power Multiplier	\$1 / Watt
C	Manufacturing Cost Multiplier	\$20 / hour
MEW \$MEW	Manufacturers Empty Weight (A * MEW) / 1000	15.2 lb. \$1.520 (thousands)
REP \$REP	Rated Engine Power # engines # cells (# engines * 50A * 1.2V/cell * # cells) (B * REP) / 1000	1 25 1500 Watts \$1.500 (thousands)
MFHR WBS WBS #1 WBS #2 WBS #3 WBS #4 WBS #5 MFHR \$MFHR	Manufacturing Man Hours Work Breakdown Structure Wing # wings projected area (5 hr./wing + 4 hr./ft ² projected area) Fuselage # bodies length (5 hr./body + 4 hr./ft length) Empennage # vertical surfaces # horizontal surfaces (5 hr. + 5 hr./vert.surf. + 10 hr./horiz.surf.) Flight Systems # servos (5 hr. + 1 hr./servo) Propulsion Systems # engines # propellers (5 hr./engine + 5 hr./propeller) Σ WBS hours (C * MFHR) / 1000	 2 17.5 ft ² 80 hr. 1 5.7 ft 27.8 hr. 1 1 20 hr. 7 12 hr. 1 1 10 hr. 149.8 hrs. \$2.996 (thousands)
RAC	Rated Aircraft Cost (A*MEW + B*REP + C*MFHR) / 1000	\$6.016 (thousands)

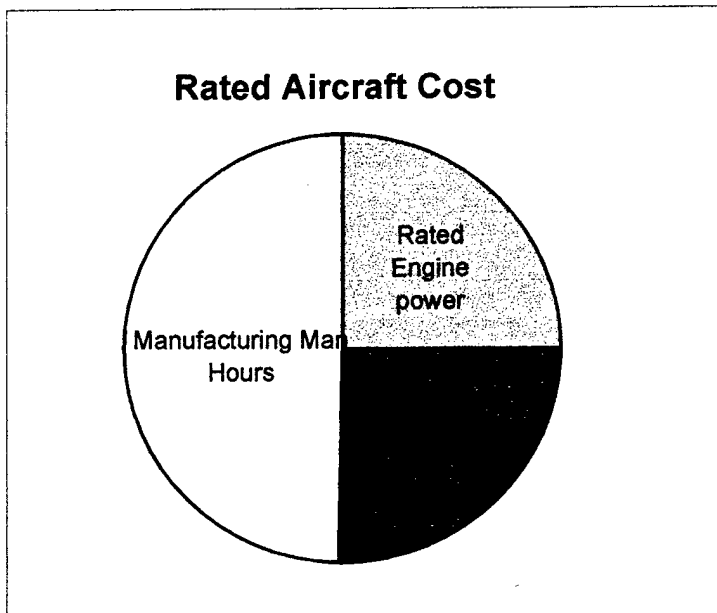
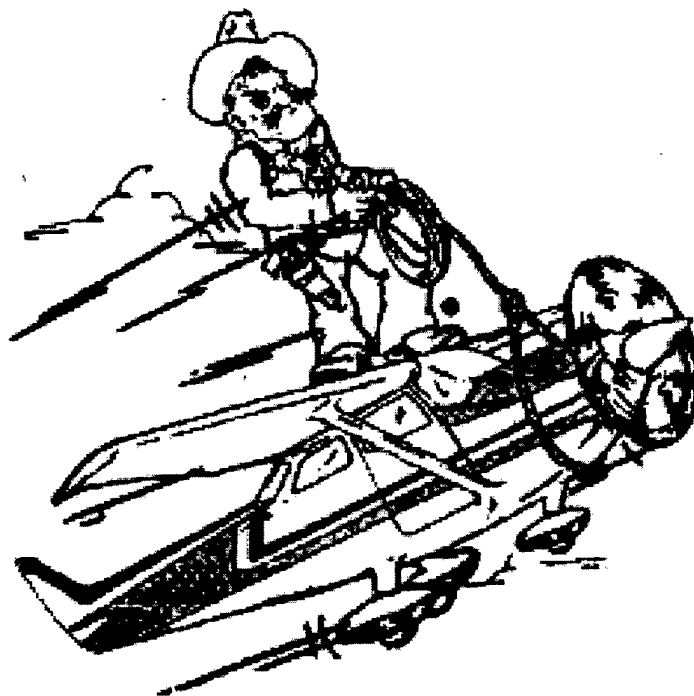


Figure 8.1 Rated Aircraft Cost Percentage Per Section

Cessna/ONR Student Design/Build/Fly
Competition

OSU Team #2
Flight Factory



Design Report – Proposal Phase

Oklahoma State University
March 13, 2000

Table of Contents

1. Executive Summary	1
1.1 Major Areas of Development.....	1
1.2 Overview of Design Tools	2
1.2.1 Conceptual Design Tools.....	2
1.2.2 Preliminary Design Tools	2
1.2.3 Detailed Design Tools.....	3
2. Management Summary	4
2.1 Architecture of the Design team	4
Chart 2.1 – Team Organizational Chart.....	6
Chart 2.2 – Management Milestone Chart.....	7
3. Conceptual Design	8
3.1 Alternative Concepts Investigated.....	8
3.2 Design Parameters Investigated.....	8
3.2.1 Wing Construction.....	8
3.2.2 Wing Attachment.....	9
3.2.3 Payload Arrangement.....	10
3.2.4 Landing Gear	10
3.2.5 Fuselage	11
3.2.6 Propulsion	12
3.3 Figures of Merit	12
3.4 Final Ranking of Figures of Merit	13
3.5 RAC for Each of the Concepts	14
3.6 Analytic Methods.....	14
3.7 Configuration Selection	14
Table 3.1 – RAC for Conceptual Designs	16
Table 3.2 – Decision Matrix for Figures of Merit	16
Figure 3.1 – Monoplane Score Analysis.....	17
Figure 3.2 – Biplane Score Analysis.....	18
4. Preliminary Design	19
4.1 Design Parameters Considered	19
4.2 Figures of Merit	20
4.3 Aerodynamic Analytic Methods	21
4.4 Propulsion Analytic Methods	22
4.4.1 Excel	22

4.4.2 Dynamometer and Wind Tunnel Testing.....	22
4.5 Preliminary Sizing and Key Features	22
4.5.1 Wing Configurations.....	22
4.5.2 Tail Configurations and Sizing.....	23
4.5.3 Battery Sizing.....	23
4.5.4 Motor Sizing	23
5. Detail Design.....	24
5.1 Final Design Performance.....	24
5.1.1 Wing Performance	24
5.1.2 Take Off Performance.....	25
5.1.3 Cruise Performance and Range.....	25
5.1.4 Structural g-load Capability.....	25
5.1.5 Selection Based on Score.....	26
5.1.6 Stability Analysis and Handling Qualities.....	26
5.2 Component Selection and Systems Architecture.....	27
5.2.1 Battery Pack.....	27
5.2.2 Motor.....	28
5.2.3 Propeller/Gearing.....	29
5.2.4 Radio and Servos	29
5.3 Structures	29
Table 5.1 – Initial Calculations from Spreadsheet.....	31
Table 5.2 - Airfoil Data.....	31
Table 5.3 - Spreadsheet Calculation Result	31
Table 5.4 - Stability and Control Results.....	32
Figure 5.1 – Initial Design Range.....	33
Figure 5.2 – Specific Design Range	34
Figure 5.3 – Battery Selection	35
Figure 5.4 – Cm versus Alpha with Elevator Influence.....	36
Figure 5.5 – Aileron Deflection Effect on Roll Moment.....	36
Figure 5.6 – Cm versus Alpha	37
Figure 5.7 – Cn versus Beta with Rudder Influence	37
5.5 Drawing Package	38
6. Manufacturing Plan.....	39
6.1 Processes investigated.....	39
6.2 Figures of Merit	39
6.3 Manufacturing Process.....	40
6.3.1 Fuselage	40
6.3.2 Wing.....	41
6.3.3 Landing Gear	42
6.3.4 Final Assembly	42

Chart 6.1 – Manufacturing Milestone Chart	44
Figure 6.1 – Kevlar Landing Gear and Servo Insert	45
Figure 6.2 – Making the Cowling Mold	45
Figure 6.3 – Applying Carbon Fiber to Lower Wing	46
Figure 6.4 – Inserting the Bottom Wing for the First Time	46
Figure 6.5 – Front View of First Assembly	47
Figure 6.6 – Rear View of First Assembly	47

1. Executive Summary

1.1 Major Areas of Development

The OSU Flight Factory (FF) began preparing for the 1999/00 Design/Build/Fly (DBF) contest by reviewing rules and mission requirements. Scoring this year includes a Rated Aircraft Cost (RAC) which heavily influences the configuration. It became apparent that lifting the maximum amount of water would not necessarily result in the highest score due to the penalties incurred from the RAC. The wing span limit of 7 feet and battery pack weight limit of 5 pounds also made the design of this year's aircraft challenging.

To aid in the process of conceptual development, each member of the team submitted a couple of conceptual sketches. From this brainstorming many different ideas were compiled and evaluated. The FF considered a monoplane, biplane, canard, flying wing, three-surface, and tandem wing. Other ideas that were a result of these brainstorming sessions were specific components and systems. These ranged from payload location to the number of orientation of the motors. The sketches were taken by the configuration team and used as a starting point for the initial configuration.

The designs considered were evaluated based on a number of parameters. The primary consideration was flight score. Other parameters included ease of construction, building skill level, availability of materials, and time constraints. The pool of concepts was narrowed down to a monoplane or a biplane with a single fuselage. A twin boom or twin fuselage design was ruled out because of the RAC penalty incurred.

A monoplane was appealing for a number of different reasons. Payload access with a single wing is easier since there is unrestricted access to the payload doors. Also, manufacturing time and cost are reduced with only one wing to build. Finally, the RAC for a single wing suffers no additional penalty.

A biplane was considered because of the wing span limit of 7 feet. A biplane will provide enough wing area at a reasonable aspect ratio to achieve the desired performance characteristics. The RAC for a biplane is worse than a monoplane, but the aerodynamic tradeoffs may be worth the RAC.

Since many aerodynamic properties, such as wing area, number of wings and fuselage length, were given a penalty by the RAC, it could not be intuitively determined whether a monoplane or a biplane should be chosen. This required an aerodynamic analysis that was optimized for score. This analysis was a spreadsheet that iterated through many different component sizes for both monoplane and a biplane, calculated the RAC for each, and ultimately the score. From this analysis it was determined what the overall configuration should be and how many liters of water should be carried to give the OSU Flight Factory the best score.

The results of this analysis were carefully considered to find the final configuration with the highest score potential. With the aerodynamic analysis complete and the RAC considered for each design our team concluded that a biplane carrying 5 liters of water would result in the highest attainable score. Our analysis showed that a biplane was clearly the most efficient method of getting the necessary wing area. With the limited wing span a monoplane suffered with a low aspect ratio that precipitated throughout the design.

1.2 Overview of Design Tools

The design tools for the individual phases were chosen based on recommendation from previous design teams and the expertise of the members of our team. Information and data was collected from magazines, published texts, personal interview, and historical data from previous AIAA DBF teams. Computational methods were also used to aid in the optimization of the design.

1.2.1 Conceptual Design Tools

Design tools used during the conceptual phase were:

- Aircraft Design: A Conceptual Approach
- Aircraft Design Literature
- Microsoft Excel
- Historical Data

Aircraft Design: A Conceptual Approach is a aircraft design reference by Daniel P. Raymer. This book has extensive general information for each of the conceptual designs our team was considering. We learned the positive and negative aspects of the monoplane, biplane, tandem wing, canard, flying wing, and three surface. This information gave the FF a conceptual baseline from which we could proceed. Other aircraft design literature was also investigated. The FF obtained as many books and magazines as possible that provided ideas for our configuration.

Microsoft Excel was used to setup a RAC spreadsheet. This spreadsheet calculated the RAC for any combination of variables that it was given. This proved to be very useful in determining the RAC difference between the different conceptual designs developed by the FF. RAC calculations were very important at this stage, because RAC ultimately effects the final score.

Historical data played a major role in the conceptual design phase. Since the FF was starting from scratch it was very beneficial to reference previous AIAA DBF airplanes and data. The airplane and team members from the OSU Aggie Aquanauts proved to be a valuable conceptual design tool. Other existing airplane, whether scale or full size, were examined to find desirable characteristics for our design.

1.2.2 Preliminary Design Tools

Design tools used during the preliminary phase were:

- Aircraft Design: A Conceptual Approach
- Flight Stability and Automatic Control
- Microsoft Excel
- Dynamometer and Propulsion Wind Tunnel Tests

Aircraft Design: A Conceptual Approach by Daniel P. Raymer was consulted for the preliminary design phase. As the FF moved into a phase where more quantitative results were necessary, the Raymer text provided equations to estimate wing stagger and decalage for a biplane and interference factors. Flight Stability and Automatic Control by Robert C. Nelson was used in the sizing and location of all control surfaces to achieve a stable aircraft.

Microsoft Excel was used extensively in the preliminary design phase for aerodynamic and propulsion system calculations. A spreadsheet was generated that would allow the FF to find the optimum combination of aerodynamic properties and propulsion components to give the best overall design.

A dynamometer was used by the propulsion team to collect experimental data from propulsion systems that would aid in the selection of the optimum motor and battery combination for our application. This allowed the propulsion team to examine the effects of different cowling shapes, motor locations and propeller selections on thrust and battery endurance.

1.2.3 Detailed Design Tools

Design tools used during the preliminary phase were:

- MathCAD
- Microsoft Excel
- Dynamometer
- AutoCAD

MathCAD was used in conjunction with Microsoft Excel to perform the stability and control analysis of the aircraft. A MathCAD provided a interface to setup the necessary equations and easily change the parameters in order to get the desired stability.

The dynamometer was used to test the final propulsion system and aid with propeller selection. This dynamometer was invaluable in confirming the performance of the propulsion system.

AutoCAD was used to develop detailed drawings of each individual component of the final design. This allowed the FF to find any spacing problems with the design layout as well as generated full size construction drawings to aid in the manufacturing of the aircraft.

2. Management Summary

2.1 Architecture of the Design Team

The OSU Flight Factory (FF) decided that the best organizational scheme would be to divide the team into three groups. Since the FF was composed of students ranging from freshman to graduate students, organization would be critical. These three groups were the Aerodynamics and Configuration group, Propulsion group, and Structures group. A leader was chosen for each of these groups and a chief engineer was placed in charge of the entire team. The structures group was then broken down into sub-groups that were specifically in charge of the wing, fuselage, and landing gear. A leader was then established for each sub-group. A break down of the FF organization can be found in Chart 2.1.

The FF was broken down into these smaller groups to aid in communication and individual task expertise. The range of knowledge needed to effectively design and build this airplane was too broad for each person in the FF to have a hand in every task. The group leaders made sure that each group member was assigned a specific task and that all members understood the group's overall goals. This specialization allowed the individual members of each group to research their specific area and become an expert, thus giving the FF a detailed understanding of each design and construction component.

The Aerodynamics and Configuration group was responsible for optimizing the score of the aircraft. This optimal configuration also included the airplane's complete aerodynamic analysis. The Aerodynamics and Configuration group worked closely with the Propulsion group to find the best motor and batteries for this optimum design. It was necessary for the motor, batteries, and aerodynamics to be optimized simultaneously in order for the RAC analysis to be correct.

For this organizational scheme to be effective it was absolutely necessary for the three group leaders and the chief engineer to be in constant communication. Weekly meetings were scheduled in which the chief engineer and group leaders discussed current progress and future goals. The chief engineer's main responsibility was to understand each area of the overall project and keep everything on schedule. Without this organizational structure each group's components may not match up and work properly.

The chief engineer organized the purchasing and material selection. Placing orders through the university is a fairly complicated process, so the chief engineer acted as the liaison between the university purchasing department and the FF. A treasurer was also established to keep the FF budget in check.

With three different groups working on a number of different tasks simultaneously it was necessary to develop a schedule. This schedule outlined the beginning and completion dates of every major event in the design process. This

would ensure that all prerequisite tasks were completed on time to meet the necessary deadlines. This chart is shown in Chart 2.2.

Team Organizational Chart

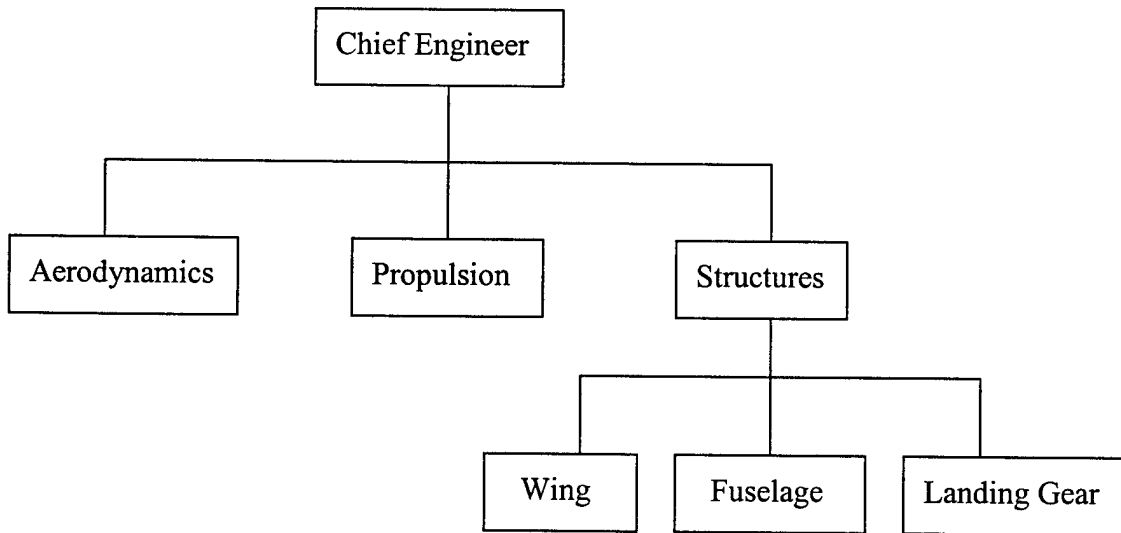


Chart 2.1

Management Milestone Chart

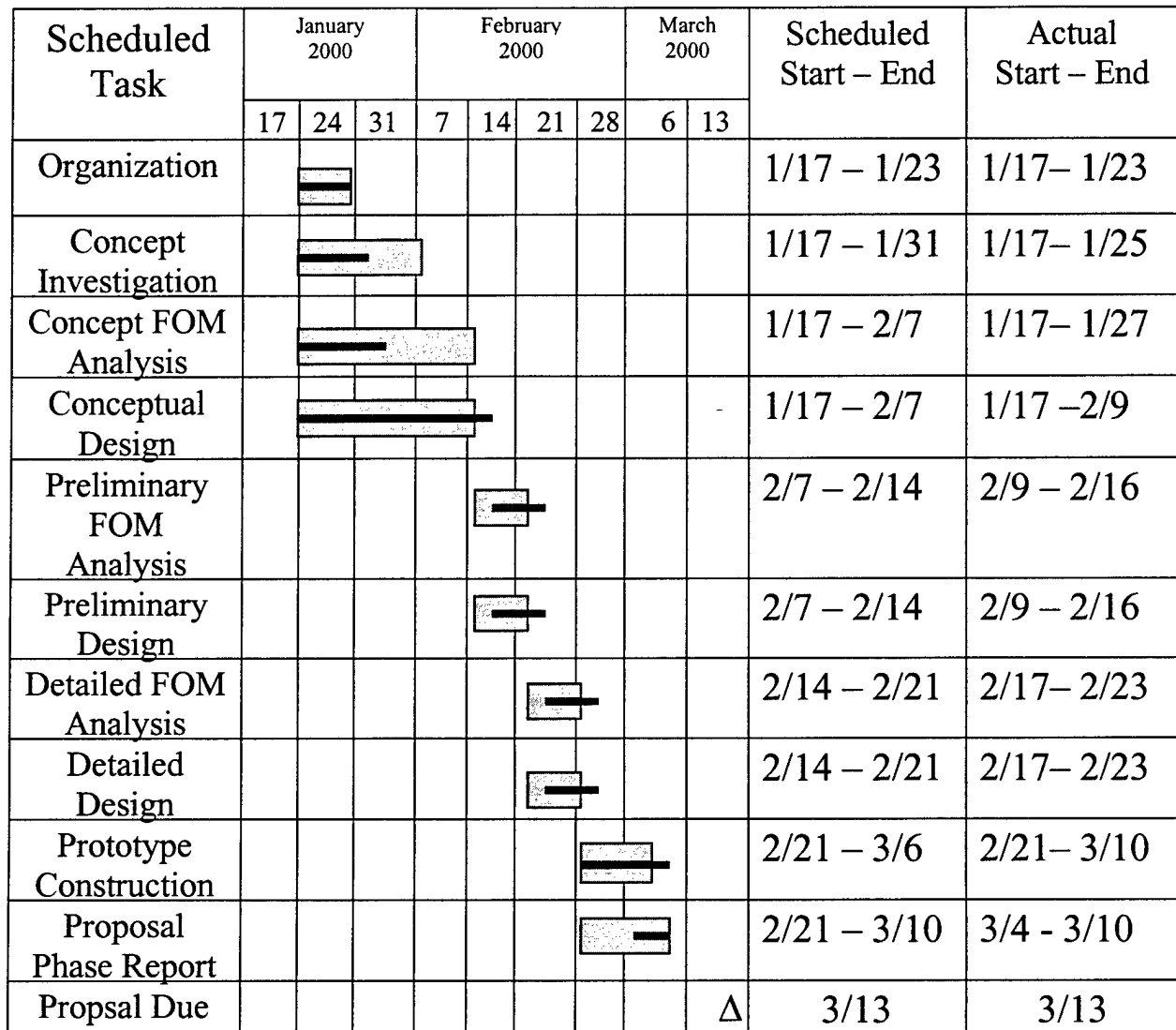
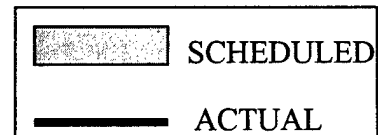


Chart 2.2



3. Conceptual Design

3.1 Alternative Concepts Investigated

There were a variety of concepts that were carefully examined throughout the conceptual design stage. Our idea was the more concepts would give more choices in the process of determining the most efficient configuration for this particular competition.

The first concept the team considered was the conventional design. The conventional design consisted of one wing and one fuselage. Multiple fuselage design was considered but had been rejected since the number of fuselage would directly affect the Rated Aircraft Cost (RAC).

Next, the biplane design was evaluated. The biplane would have the same basic configuration as the conventional design but with two wings either parallel or stagger for design purposes. Also, the team investigated canard design. Two different canard configurations were considered: control-canard and lifting canard.

Similarly, the flying wing was studied. There would be no horizontal stabilizers on the single wing airplane for this configuration. Another alternative conceptual design being investigated was three-surface airplane. However, RAC was the biggest concern in this design.

No less important was the tandem wing design. This design had two identical wing placed in line together with only one vertical surface for directional stability. Again, RAC was the major concern here.

3.2 Design Parameters Investigated

3.2.1 Wing Construction

One of the first things considered was possible wing construction methods. The following are the design parameters for the wing:

- Number of Spars
- Type of Wing Skin
- Wing Core Material

After obtaining information on airplane construction from library searches, the Internet, and personal contacts, our team reviewed the various wing construction methods and characteristics. Popular construction methods include single spar, double spar, foam core and structural skin.

A single spar wing could be constructed using a traditional balsa wood buildup. This would consist of ribs used to space the wing components apart and give the wing the proper shape. The spar would be placed at the quarter chord and designed to

carry the wing load. A lightweight skin would then be placed over the entire wing surface to achieve the desired contours.

A double spar would be constructed in a similar fashion to the single spar. In this case the second spar would be near the three-quarter chord. The second spar will help reduce twisting in the wing and aid in the joining of a two-piece wing.

A foam core wing would replace the wooden ribs with a solid piece of foam. This foam would then be wrapped with a skin such as carbon fiber or fiberglass. Construction of a complex airfoil shape would be easier with a foam wing, since the shape could be cut with a hot-wire foam cutter.

Finally, a structural skin could be used for the wing. This would consist of carbon fiber or fiberglass shell without an internal structure. This method reduces weight, but would be prone to buckling.

3.2.2 Wing Attachment

The following are the design parameters for wing attachment:

- Number of Wing Sections
- Type of Struts

During the conceptual design phase a number of different wing to fuselage attachments were considered. These were wing profile cutout, notch and plug, and, two-piece with interlocking spars. The wing needed to be removable for transportation, but still be strong enough to support the lift loads.

The complete profile of the wing could be passed through an airfoil shaped hole in the fuselage and attached with bolts. However, if this is done, the space required in the fuselage must be at least as large as the chord and maximum thickness of the wing.

In an effort to shorten the length needed to attach a one-piece wing into the fuselage, the top or bottom of the fuselage could have a notched out recess shorter in length than the wing cord. The wing could be modified in the central portion to plug into the notch in the fuselage. The wing box plugging into the fuselage could be attached with pins or bolts. However, it should be noted that this method of construction could severely weaken the fuselage and create drag due to breaks along the fuselage at the attachment point.

Finally, a two-piece wing could have tubular or hollow rectangular spars that plug into the fuselage with a joiner inside and outside of the two spars. The spars would then be pinned in place with the joiners and sleeves. The problem with this design is that the joiners would have to support all bending moment of the wings. This suggests that the spar setup would be heavier than it really needs to be. Another

possibility would be to have a removable spar that slides into both wings. The spar would slide through the fuselage and pinned or bolted in place.

In the case of a biplane, the upper wing could be attached in three different ways. A center strut could extend upward from the fuselage to hold the top wing. This method is fairly simple, but may require extra struts between the upper and lower wings throughout the span to adequately attach the upper wing. Second, an end strut could be placed toward the tip of each wing, joining them together. Lastly, a combination of a center strut and end struts could be used if needed for strength.

3.2.3 Payload Arrangement

Once the size of the bottles was known, bottle placement needed to be determined. The following are the design parameters for payload arrangement:

- Frontal Area and Length of Fuselage
- Number of Payload Packages
- Payload Door Configuration
- Constant Center of Gravity

The payload needed to be arranged to reduce frontal area and fuselage length. The two arrangements considered were laying the bottles lengthwise end-to-end and standing them upright. In either case the bottles needed to be placed symmetrically about the center of gravity.

Laying the bottles lengthwise will result in a longer fuselage, but will reduce frontal area and overall fuselage weight. This configuration will reduce drag, but will also receive a penalty in RAC for the fuselage length. Standing the bottles upright would reduce the fuselage length, but greatly increase the frontal area. This design would pay a drag penalty, but help lower the RAC.

Due to the ten-minute time limit per mission, the ground time needs to be minimal. Since the majority of ground-time is taken up in loading, the payload must be easily removed. Removing the bottles as one or two units would be much faster than taking them out individually. The payload access doors should be secure during flight, but easy to open and provide unrestricted access to the payload.

Regardless of the number of bottles, they must be arranged in a fashion that will balance about the center of gravity. This is necessary to maintain the same flight characteristics whether the airplane is loaded or empty. Since each mission contains a loaded and unloaded sortie, this bottle-loading scheme is vital.

3.2.4 Landing Gear

The following are the design parameters for the landing gear:

- Location
- Shock Absorbency
- Braking
- Steering

The two basic types of landing gear configuration are tricycle and tail-dragger. A tricycle gear configuration has a single nose gear with two main gear toward the middle of the aircraft. A tail-dragger configuration has two main gear toward the front of the aircraft and a small wheel on the tail. The landing gear must provide shock absorbency during hard landings to protect the airframe from damage and increase the durability of the airplane. Braking is very important for minimizing ground time between sorties. Good steering is easier to achieve with tricycle gear through a steerable nose gear. The main gear spacing is key to the steering of the aircraft. The closer together the mains are, the tighter the plane will turn, but will also be more unstable on the ground.

3.2.5 Fuselage

The following are the design parameters for the fuselage:

- Construction Material
- Type of Buildup
- Payload Access

There were several options that were considered for the fuselage construction. One option explored was to make the fuselage from balsa with longerons to support the bending moments in the fuselage. The sides could then be covered with thin balsa sheeting or with Monokote. A second option considered was to build the fuselage with longerons, but cover the plane with carbon fiber to supply additional rigidity. The last alternative considered was to leave the longerons out of the fuselage and use sandwich construction employing a core bonded between layers of carbon fiber to obtain the required structural integrity.

In regards to ease of construction, the balsa build-up with longerons, the carbon fiber with longerons, or the carbon fiber sandwich methods are all about the same. While the balsa fuselage requires extensive assembly time, the carbon fiber preparation is time intensive.

The payload could be accessed through the top or the back of the fuselage. If the bottles are laid horizontally, then they would be loaded from the back of the fuselage in a single line. However, if oriented upright, the bottles could be loaded from the top. Inserting the payload from the top would allow the flight control systems to be accessed easily.

Weight will be an important design parameter in the fuselage since the Manufacturers Empty Weight (MEW) affects the score and constructing a lightweight airplane will increase the amount of water our airplane can carry. Carbon fiber is

very strong for a given weight and may prove to be a good choice for this reason.

3.2.6 Propulsion

The following are the design parameters for the propulsion system:

- Battery Pack Weight
- Number/Type/Brand of Cells in Battery
- Number of Motors
- Type/Brand of Motor

In order to lift the maximum amount of payload, the battery pack needed to utilize the full five-pound limitation. Oklahoma State's battery pack used in last year's competition was over eight pounds and helped to lift eight liters of water. Therefore, it was reasoned that a five-pound pack would not be able to generate enough power to take off with an eight-liter payload multiple times. This ruled out a pack that weighed any less than five pounds since there was so little power to spare.

The main concern for the five-pound battery pack was to maximize its power to weight ratio by investigating the many possible types of NiCad cells available. The cells considered would have varying weights, therefore dictating the number of cells that could be placed into the pack. However, these cells would also have varying rated capacities. In addition, each brand of cell would have small variances when compared to its counterpart of a different brand name. Most importantly, the number of cells affected overall score. Close attention was paid to high capacity and quick charge types.

Due to the fact that there was limited power available, it was understood that only one motor would be needed to convert the electrical energy into its desired form. This ruled out utilizing multiple motors to power the aircraft.

The final motor choice would be based on finding a motor that would run at its maximum efficiency given the finalized battery pack voltage and desired amperage. Both brush-less and standard motors were considered, but even though the brush-less motors have higher efficiencies and weigh less, the controllers used in conjunction with them tend to be much more inefficient than the standard controllers. Therefore, the brush-less motors were counted out due to these cumulative inefficiencies.

3.3 Figures of Merit

The figures of merit carefully studied throughout the conceptual design stage were as follows:

- Flight Score
- Flying Qualities
- Ground Handling
- Safety

- Construction Difficulty

The first goal of the conceptual design phase was maximizing score. A good final design would be an airplane that would be able to win the contest no matter what the configuration was. Analysis should be done to figure out the best configuration for the contest. RAC was the major effect on the score.

Our secondary concern was the flying qualities of the design. The final design's stability will determine the pilot's ability to efficiently navigate the flight course. The nature of this mission is not a high performance aircraft, but a reliable cargo plane. Multiple missions on two days must be completed and this drives our design to trade some performance for stability.

Another figure of merit was the ground handling. It was considered to support the completion of the mission. Since a number of take-off and landings are preformed during each mission it is critical for the pilot to have complete control of the aircraft while on the ground. If the airplane is not easily maneuverable on the ground, our team will pay a time penalty during the payload exchange. This makes braking an issue since the plane must be on the start line before team members may approach the aircraft.

Fourth, safety of the airplane became one of the figures of merit. Since members of the ground crew will be in constant interaction with the airplane, the flight systems should have safety devices to disarm the motor while the flight crew is near the airplane. The airplane will be flying multiple missions over the two-day contest and must be safe in flight and on the ground.

Construction difficulty was chosen as a figure of merit due to the inexperience most members of our team had in constructing airplanes. Our team has a limited amount of time to build this airplane and must be able to learn the necessary skills within that time. Attempting to build an airplane over our skill level would result in an unreliable craft that may not perform to our design specifications.

3.4 Final Ranking of Figures of Merit

After reanalyzed all the figures of merit, the final ranking of figures of merit, from the most important, were as follows:

- Flight Score
- Construction Difficulty
- Safety
- Flying Qualities
- Ground Handling

3.5 RAC for Each of the Concepts

The RAC directly influences the overall score of our aircraft. The RAC of each overall configuration was initially analyzed. Without the exact specifications of the final aircraft, the RAC can not be explicitly calculated. However, a good representation can be made of the advantages and penalties incurred for each configuration. The lowest RAC does not necessarily reflect the highest overall score, since the number of sorties and liters of water may be different for various configurations. The RAC for each conceptual design is found in **Table 3.1**. According to these results the flying wing would be the cheapest design, but not necessarily the best in terms of score and construction. Since the many of the RAC variables are not known during this conceptual design stage, these values were chosen as constant for each design and are as follows:

- Single engine with 38 cells and one propeller
- One fuselage with 5-feet long
- Manufacturing Empty Weight 12.95 pounds
- 6 servos

3.6 Analytic Methods

A spreadsheet was chosen to be the main tool in analysis during the conceptual design phase. A RAC calculation was setup to easily calculated RAC for each concept by simply entering the RAC variables. This made our initial calculations quick and accurate.

For the conceptual phase our team gathered as much historical data as possible. Since the FF was designing from scratch we needed a frame of reference to being. First, we looked to previous Oklahoma State University DBF teams. Last year the Aggie Aquanauts had good design which we were able use as a starting point. Thought the mission requirements for the Aquanauts were different than ours, their performance data was used as a baseline for our conceptual design.

3.7 Configuration Selection

Selection of the final configuration was aided the decision matrix shown in Table 3.2. The table showed the comparison of the performance for each of the conceptual design for each figure of merit. The importance of the figures of merit was determined by the weight factor.

The score was given a weight of 5 since this was the main objective of our aircraft. If our configuration did not have the ability to give a high score, than we could not possible win the contest. Construction difficulty was behind score with a weight factor of 2. The best possible design would be useless if it could not be built correctly. Third was safety, which was given a weight factor of 1. Our team needed to interact constantly with the plane on the ground and spectators must be safe during the flight. Stability was fourth with a weight factor of 1. We knew that stability during flight was necessary for our plane to properly navigate the course. If the plane was uncontrollable, then we would risk damaging the plane as well as jeopardizing

safety. Finally was ground handling with a weight factor of 1. Navigation of the aircraft on the ground is essential for maximizing the plane's time in the air for each mission.

An initial score analysis including the RAC was done between the monoplane and biplane to determine which would result in the best score capability. These trends can be seen in Figure 3.1 (Monoplane) and Figure 3.2 (Biplane). After inspection of these plots it can be seen that although the RAC for a biplane is penalized for an extra wing, the overall score is better than the monoplane. This was taken into consideration as the final configuration decision was made.

The decision matrix shows that the biplane was the best plane to compete in this particular contest. Thus, the team decided to go for the biplane with score being the most dominating factor. From the analysis, the final configuration would be including the features as follows:

- A single fuselage
- Conventional tail (one horizontal and vertical surfaces)
- A tricycle landing gear
- Symmetric design (constant center of gravity location)

A single fuselage was chosen to avoid direct penalty on score since it would increase the RAC. Also, single fuselage would reduce drag. Conventional tail was chosen to attain easy construction and to provide the directional stability to the airplane.

By consolidating the handling quality, the team decided that the tricycle landing gear would best fit the job. Finally, we designed a symmetric airplane simply because the course direction would only be known on the day of contest. Additionally, it would reduce the difficulty of stability control analysis on an asymmetric airplane.

Conceptual Designs	RAC (\$Thousands)
1. Conventional	6.02
2. Biplane	6.12
3. Canard	6.02
4. Flying Wing	5.72
5. Three-Surface	6.22
6. Tandem	6.02

Table 3.1 RAC for Conceptual Designs

Weight Factor	Figures of Merit	C	B	CN	FW	TS	TW
5	Fight Score	3.0	4.0	3.0	2.0	2.0	3.0
2	Construction Difficulty	4.0	3.5	2.5	1.5	1.0	1.0
1	Safety	4.0	4.0	4.0	2.0	1.0	1.0
1	Flying Qualities	4.0	3.5	2.0	0.5	1.0	1.5
1	Ground Handling	4.0	3.5	2.0	1.0	1.0	1.0
10	Total	35.0	38.0	28.0	16.5	15.0	20.5

Table 3.2 Decision Matrix for Figures of Merit

Definition of Symbols:

C = Conventional

B = Biplane

CN = Canard

FW = Flying Wing

TS = Three-Surface

TW = Tandem Wing

Wing Loading Variation (Monoplane)

Design Report – Proposal Phase

OSU Flight Factory

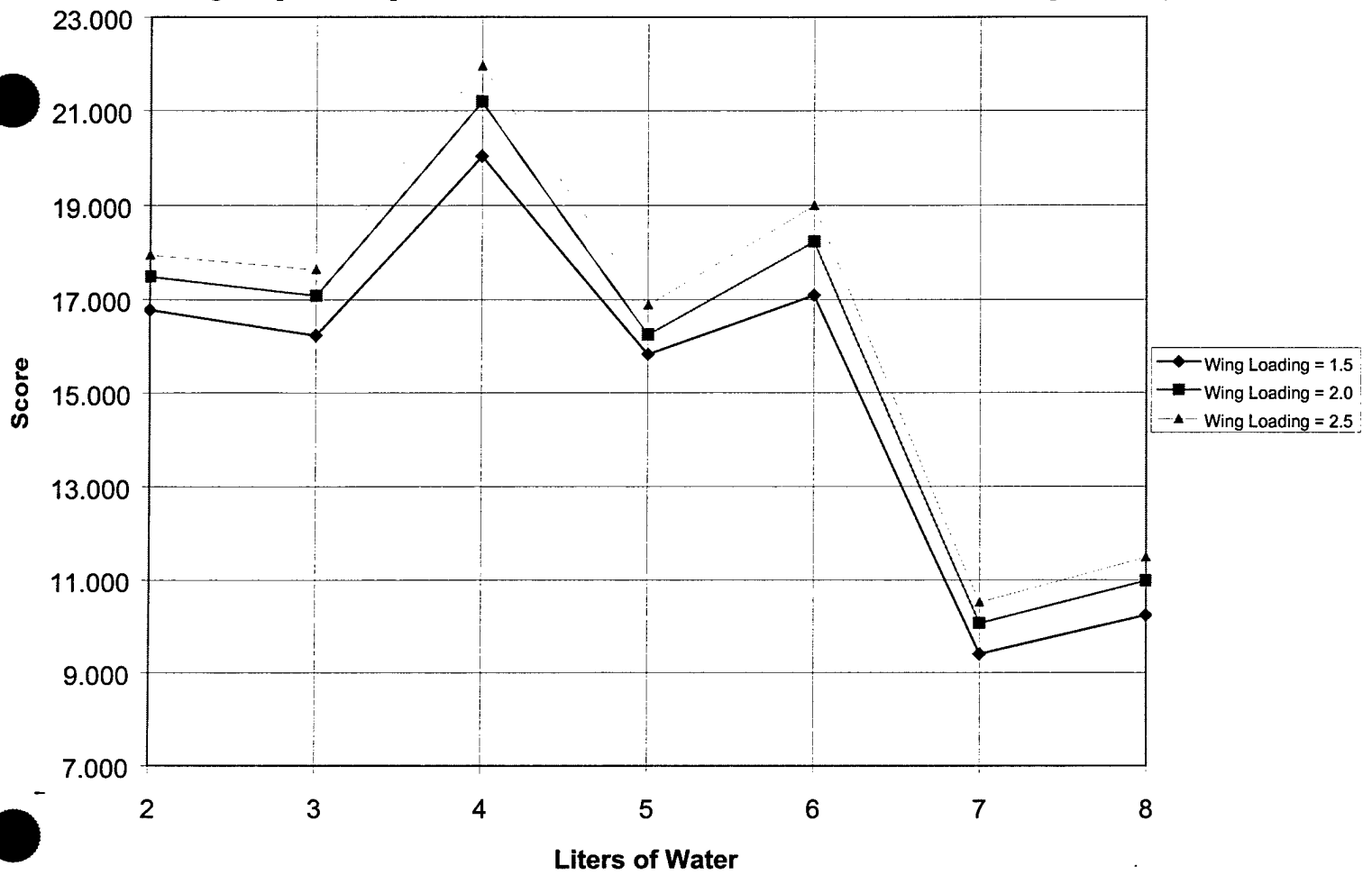


Figure 3.1 Monoplane Score Analysis

Wing Loading Variation (Biplane)

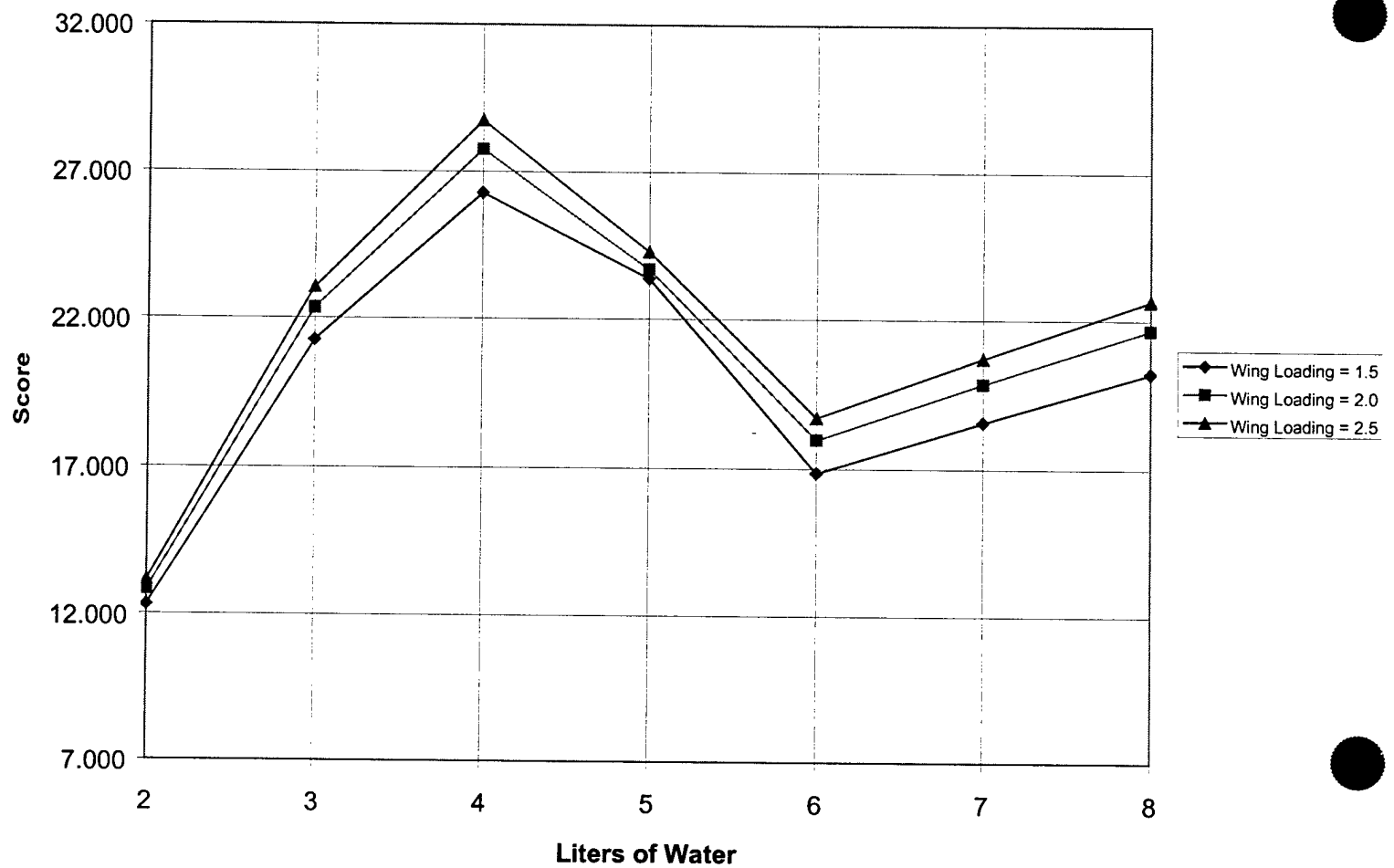


Figure 3.2 Biplane Score Analysis

4. Preliminary Design

4.1 Design Parameters Considered

In the preliminary design phase, we investigated some key design parameters that would optimize the score. These are design parameters that we considered for our biplane.

- Liters of water to carry
- Wing loading
- Power loading
- Payload fraction
- Aspect ratio
- Maximum lift coefficient of airfoil (C_{lmax})
- Amount of stagger
- Gap between two wings
- Decalage
- Fuselage shape
- Tail volumes
- Landing gear location
- Static margin

The best design has maximum score. Carrying more water per sortie does not necessarily mean more score. You might get penalized on wing area, fuselage length, power required and others. Thus, we need to figure out how much water we want to carry so that we can maximize the score. The shape of the fuselage actually depends on how many liters water the aircraft is going to carry. We do not want to extend the length of the fuselage because this would increase the cost.

We know the payload weight and then we assumed a payload fraction based on historical data to estimate the aircraft empty weight for score estimation. By knowing the total gross weight of the aircraft, we assumed a wing loading to get the wing area required. Given that the wingspan is fixed to seven feet, we decided to go for rectangular wings without any taper for stall prevention and the ease of manufacturing.

The section lift coefficient (CL) of an airfoil can determine the aircraft performance significantly. However, the aspect ratio would affect the lift coefficient of the wing. So, we have to make sure the aspect ratio would be appropriate to give a required CL.

The power loading or power-to-weight ratio is an important parameter for propulsion system design. We want to make sure we have enough power for takeoff and do other operations. The power loading also determined the climb rate of the aircraft. We want high power loading so that we can get airborne quickly and cruise at low drag to maximize the speed. Time is one of the factors to win. The 100 foot

runway limit is the factor that drives the required power for our airplane. The power needed for other operations is not near as high as for the take-off situation.

We want the landing gear that would create minimum drag during cruising and yet strong enough for most critical operation, which is landing. We decided to attach the main landing gear at the quarter chord of the lower wing. Although it is hard in terms of construction, it provides good ground handling characteristics. To make sure the nose gear take care some of the load when the aircraft is moving on the ground, we made sure the center of gravity (CG) was located far enough in front of the main landing gear to prevent all the weight from resting on the main gear. This would also give an easier rotation during takeoff. To make this possible, the wings had to be staggered to achieve the correct CG location for aerodynamic stability and landing gear configuration. The gap between the wings is to be set so that it would maximize the performance and providing room for payload bay access. The decalage or the relative angle between the two wings is to be set so that they would operate at approximate the same lift coefficients (CL) to maximize performance.

The last design parameter that we considered is the tail volume for both horizontal and vertical. The tail volume needed was based on the desired static margin. The static margin was to be around 10 to 20 percent for the prototype. This will provide plenty of stability and seems conservative. We may reduce the static margin for the final aircraft to increase maneuverability.

4.2 Figures of Merit

The figures of merit for the preliminary design phase are as follows:

- Score
- Ease of Construction
- Durability
- Weight

Once again, score is the overriding figure of merit. If maximum score is not considered as the most important factor in the design, then we will limit our chances of winning the contest. The RAC is one of the controllable factors in the score calculation and in this design phase the fuselage length and wing area come to the forefront of our consideration.

The ease of construction must be a consideration in the preliminary design phase. Developing a preliminary configuration that achieves a very high score is meaningless if it can not be built with the expertise and knowledge our team possesses. Our team is also faced with time constraints in terms of construction. Only a limited amount of time is available for learning new construction techniques and implementing them.

Due to the nature of the contest, our design will need to be very durable. Multiple missions will be flown within a two-day span. Being able to fly more missions than

other teams will give the FF the best opportunity to put together 3 high scoring missions.

Since the battery pack is limited to five pounds, the amount of power available is also limited. It should be noted that every pound taken out of the Manufactures Empty Weight (MEW) not only reduces RAC, but increases the payload potential of the airplane by one pound.

4.3 Aerodynamic Analytic Methods

During the preliminary design phase we found out that the section lift coefficient of an airfoil can give affect the performance significantly. This was most critical for the take-off phase. Therefore, the airfoil has to be picked carefully. We visited the UIUC airfoil data site to see the performance of variety of airfoils. And then we picked eight airfoils for further investigation. We download the airfoil data from UIUC airfoil data site, and then we plot the section lift coefficient for a range of angle of attack. Since our aircraft is cruising at relatively low speed, we are looking for low Reynolds number airfoil, which is approximately 400000. We look for the maximum section lift coefficient and the correspond angle of attack. This is the angle of attack which stall would occur. Other than that, we studied the lift characteristics at the stall region. We want to pick an airfoil that has good stall characteristics. The main concern with stall was to avoid a sharp stall curve that could result in a crash if the wings were to stall. We are interested in at the lift curves that drop gradually after stall. We also investigated the drag characteristics of the airfoils. In this case we are maximizing lift-to-drag ratio. Among the airfoils that we investigated are:

- CH10-48-13
- Fx74-CL5-140
- S1210
- S1223
- S7037
- E423
- SD7062
- USNPS-4

After performing a detailed comparison, we selected our airfoil to be Selig 1223. It has outstanding lift performance and good stall characteristics with acceptable drag. The analysis was done using equations derived from the texts *Aircraft Design: A Conceptual Approach*, by Daniel P. Raymer and *Flight Stability and Automatic Control*, by Robert C. Nelson. -The deriving of equations was necessary due to the fact to analyze a biplane configuration as well as conventional aircraft design. So, after deriving equations we used Excel to do preliminary calculations to give the size of the wing and the coefficients of lift for take off and cruise. We also found the velocities and the coefficient of drag for the aircraft.

4.4 Propulsion Analytic Methods

Once all of the design parameters for the propulsion system were established, the performance of the battery pack, motor and other components needed to be in harmony. Furthermore, they needed to be maximized while keeping overall score at a maximum. This was to be accomplished by investigating extensive lists of batteries and motors that were commercially available to us. Excel was the main tool used to help organize and calculate the massive amounts of data. Then once the entire propulsion system was procured and assembled, multiple test runs were conducted through the use of a dynamometer.

4.4.1 Excel

A “virtual” propulsion system was created in multiple Excel spreadsheets that matched all possible combinations of battery packs and motors, bearing in mind the overall score that would result. First, a list consisting of hundreds of NiCad cells from several different manufacturers was entered into a spreadsheet, noting each cell’s rated capacity, weight, and internal resistance. A resulting five-pound pack was “created”. Its resulting voltage and internal resistance was noted, from which its maximum power output for the eight-minute time interval was determined.

The next step was to match each candidate motor to each possible battery pack, bearing in mind maximization of the overall score. Once again, detailed lists of motors from several different manufacturers were compiled. Each motor’s specific qualities, such as the voltage and torque constants, were entered into the spreadsheet, and the motor’s efficiency was calculated that corresponded to the battery pack voltage and the desired discharge current. These spreadsheets clearly showed which battery-motor combinations offered the highest overall score.

4.4.2 Dynamometer and Propulsion Wind Tunnel Testing

Once the final battery-motor combination was established and the necessary propellers chosen, extensive testing was performed on the entire propulsion system. This involved both static and a wind tunnel simulation with the systems outputs being measured. A dynamometer was used to measure thrust and torque produced throughout the duration of all simulations, as well as propeller RPM. Battery pack performance was also recorded in the form of voltage, current, power, and temperature outputs for all simulations. Multiple mock-up contest scenarios were tested for the propulsion system, such as simulating takeoff and cruise wind conditions in a wind tunnel. This data was also very useful in supplementing the propeller analysis conducted for the aircraft.

4.5 Preliminary Sizing and Key Features

4.5.1 Wing Configurations

Like we mentioned before, we have to stagger the wing by some amount. To put center of gravity between the main and nose gear and yet have easy rotation during

takeoff, we determined that, the top wing has to be staggered six inches forward and the top and bottom wing are sixteen inches apart. The center of gravity is set to be on the leading edge of the bottom wing. We performed decalage analysis of two wings to make sure both wings are operating at approximately the same lift coefficients. It turned out the bottom wing has to have a higher incidence angle relative to the top wing. This is due to the down wash created by the top wing. Given the wing loading we figure out the wing area to be 12.86 ft^2 . Divide the number by two, we got the wing area for each wing.

4.5.2 Tail Configurations and Sizing

We constrained our fuselage length to be five feet. This would be enough room for our payload of five liters of water. We would get penalized for long fuselage length. We ran the stability and control analysis to get the size of the tail, both horizontal and vertical. And then, we made adjustments to achieve a static margin within ten to twenty percent of the mean aerodynamic chord. It turned out that the horizontal and vertical stabilizer larger than expected due to the short fuselage. A NACA 0009 airfoil was chosen for the vertical and horizontal tails. This symmetric airfoil is fairly standard for this type of an application.

4.5.3 Battery Sizing

In order to maximize the liters of water lifted, it was necessary to maximize the power output of the batteries. Therefore, the battery pack needed to utilize the full five-pound limit. The weight of each different type of cell considered was used to determine how many could fit into a five-pound pack. This allowed us to calculate resulting theoretical values of voltage, power and internal resistance.

4.5.4 Motor Sizing

Selection of the motor consisted of matching each candidate motor's properties to each possible battery pack. The best combination according to highest overall score and maximum power output for the eight minute time interval was then chosen, resulting in the best motor for the purposes intended (as well as a corresponding best cell).

From there, all the variables such as Take Off Gross Weight (TOGW), MEW, wing area, aspect ratio, takeoff lift coefficient, takeoff velocity, power required to takeoff, cruise lift coefficient, and cruise velocity were figured out respectively. Providing the information on battery and number of cells from the propulsion group, the airplane endurance was determined.

5. Detail Design

5.1 Final Design Performance

The aerodynamic group calculated all the important performance parameters of the final aircraft. Each of these parameters were found using the Excel optimization spreadsheet. To achieve the maximum score all of these factors were calculated simultaneously at fine increments throughout the design range. This allowed the score trends to be graphed and the maximum achievable score was found. By sweeping through a wide range of wing loadings we determined the optimum payload capacity was 5 liters of water. The final design performance calculations for the design are as follows.

5.1.1 Wing Performance

Since the major variable in our calculations was wing loading, finding the optimum wing area for maximum score was fairly simple. The analysis shows that 5 liters of water per scoring sortie will result in the highest score, since the wing area can be fairly small. A payload fraction of 38% was assumed based on historical data and structures calculations. Knowing the battery endurance the wings were sized for maximum score. This design wing area was just enough area to achieve the flight endurance necessary to complete 3 scoring sorties. Any extra wing area would prove to be detrimental since the RAC would increase and the five pound battery limit as well as 10 minute mission limit would not allow for a fourth scoring sortie. The final wing area is 12.95 ft^2 and the chord of each wing is 11.02 inches. This small wing area resulted in a fairly high aspect ratio. Each wing has an aspect ratio of 7.62. Higher aspect ratios increase the lift and drag characteristics of the airfoil. This is another benefit of choosing a smaller wing area and ultimately increases the score. We used a Selig 1223 airfoil for our wings with a maximum coefficient of lift of 2.27. This is the two dimensional coefficient of lift for this airfoil. We then corrected the lift coefficient for aspect ratio.

The stagger and gap of the wings was the next consideration undertaken. The gap of the wings is 16 inches from centerline to centerline. This was due to the fact that the further the wings were apart, the less interference between the wings. This interference factor was calculated according to the method described by Raymer in Aircraft Design: A Conceptual Approach. The stagger was introduced into the design to compensate for center of gravity location. This resulted in the center of gravity being at the leading edge of the front wing, and the stagger being positive 6 inches. The positive number indicates that the upper wing is located in front of the lower wing. The wings were staggered to locate the CG in an aerodynamically desirable location while leaving the main gear behind the CG enough to put some weight on the nose gear.

To achieve the desired take-off and cruise performance, the wings must be mounted at the correct angle of incidence. For this biplane there will be decalage,

which refers to the difference in incidence angle between the top and bottom wings. The decalage of the staggered wings had to be calculated. The difference in incidence angles comes from the down wash of the upper wing affecting the effective angle of attack of the lower wing due to positive stagger. And conversely, up wash of the lower wing affects the effective angle of attack of the upper wing due to positive stagger. So the incidence angles of each wing were adjusted accordingly, resulting in a -3 degree incidence angle of the upper wing and a -2 degree incidence angle of the lower wing. The negative incidence angle on both wings stems from using a highly cambered airfoil. The critical wing data is found in Table 5.3

5.1.2 Take Off Performance

We knew the airplane must be able to take-off within the 100 foot runway limit. To meet this requirement the aircraft needs to attain take off velocity within 100 feet. The take-off velocity was determined by the lift coefficient and take-off gross weight. The take-off distance was found knowing the wing loading, power loading, and lift coefficient. The design take-off distance was 78.3 feet to account for error in calculations. Since the aircraft will need to rotate about the main gear in order for the wings to be at the correct angle of attack, the tail section had to be designed in a manner that it would not scrape the runway during take-off. This take-off data is found in Table 5.3.

5.1.3 Cruise Performance and Range

The cruise characteristics of the airplane were designed for maximum speed and low drag. The faster our airplane could navigate the course, the more scoring sorties could be flown. For this reason the cruise velocity, cruise lift coefficient, and cruise drag were calculated and are found in Table 5.3. Knowing the cruise velocity, the time needed to fly each sortie was calculated. Including ground time for payload exchange, it was estimated that one set of sorties would take 2.86 minutes. A set of sorties was defined as one scoring sortie and two empty sorties. Using this information in conjunction with the battery endurance of 8 minutes our calculations estimate our plane can complete 2.85 scoring sorties. This would give us a range of approximately 7.6 miles if the aircraft were cruising the entire time in a straight line, without taking off and landing. The design endurance and range are assuming that the aircraft is carrying 5 liters of water for the duration of the flight. We assumed that 3 scoring sorties could be attained since the final sortie will be counted if we are on the making the downwind turn.

5.1.4 Structural g-load Capability

To meet the contest rules the aircraft must at least pass a 2.5 g-load test. This test is performed by lifting the aircraft by the wing tips. A biplane may be lifted equally by each of the wing tips. Since a 360 degree turn must be performed during the contest it is important that the structure be able to handle at least 2.5 g-loads. A 60 degree bank turn maintaining altitude is a 2-g turn. To facilitate in lap speed it is essential to have the capability to perform tight turns. Our biplane is designed to pass

the wing tip lift test while being suspended by only the bottom wing. This will ensure that our aircraft will not break during a hard turn.

5.1.5 Selection Based on Score

By inspecting Figure 5.1 and Figure 5.2 it can be seen how the OSU Flight Factory chose the final design. Figure 5.1 shows the score versus liters of water for a wide range of wing loadings. Once the correct design was found Figure 5.2 was generated to more exactly select the optimum configuration. Though a number of the 4 liter designs show a higher score than our final design, they were thrown out due to manufacturing. We determined that it was not feasible to build an airplane structure lightweight enough to achieve the performance shown by the 4 liter designs. Our final design MEW with 5 liters of water is 12.95 pounds. The 4 liter designs require a 10 pound MEW which was determined too difficult to build by the structures team. Thus, considering the Rated Aircraft Cost for our airplane completing 3 scoring sorties with 5 liters payload in each sortie, we calculate our score multiplier to be 24.863. The score multiplier is the Total Flight score divided by Rated Aircraft Cost. The final score will be based on the report score which will be multiplied by the score multiplier.

5.1.6. Stability Analysis and Handling Qualities

The static stability of the aircraft could now be analyzed to give the size of the horizontal and vertical stabilizers. We set the total length of the aircraft to be 60 inches long. This length was decided upon to minimize score, accommodate payload, and decrease the possibility of the tail dragging during take-off. The purpose of this stability analysis was to size the tail section in such a manner to trim the aircraft at a positive angle of attack. Sizing the horizontal tail and setting it at the correct incidence angle would be the most important. If the horizontal stabilizer is set at the wrong angle, then the elevator must be deflected to trim the airplane. Elevator deflection results in unwanted drag. The ideal setup is for all control surfaces to have zero deflection during straight and level flight.

This stability analysis was performed using MathCAD. The moment balance equations could be easily setup to generate the moment coefficient versus angle of attack curves needed to find the correct tail sizes. The completed longitudinal analysis then gives us the size of the horizontal stabilizer, elevator and ailerons. The distance from horizontal stabilizer quarter chord to the center of gravity was 33 inches. The results were that our horizontal stabilizer needed an area of 3.5 square feet. This was broken into 1 ft chord and having a span of 3.5 feet. The aspect ratio of the horizontal stabilizer is 3.5. Figure 5.6 shows that this tail configuration will trim the aircraft at a positive angle of attack while being stable and balanced.

The elevator could now be sized. The size of the elevator was dependant on the pitching moment capability desired for our aircraft. The effect of elevator deflection angle on pitching moment is shown in Figure 5.4. The result was a 40.32 square inch elevator with a chord of 1.43 inches. The span of the elevator is equal to the span of

the horizontal stabilizer. This is best described by saying the elevator is 12% of the horizontal stabilizer area.

The ailerons were then sized using certain assumptions. These were that the bottom wing would be the only wing that would have ailerons. This was due to the fact that having both wings have ailerons would either require a strut between the bottom and top wing and added servos. Neither of these options were promising. Since the ailerons must provide adequate roll control it was necessary to determine the aileron area needed. Figure 5.5 shows the effect of the final aileron size on roll moment. The resulting area of one aileron is 64.82 square inches. This means that the ailerons are 9% of the total wing area.

The directional stability of this aircraft could now be calculated. This analysis gave us the size of the vertical stabilizer and the size of the rudder. We used a length from the center of gravity of the aircraft to the quarter chord of the vertical stabilizer of 33.6 inches. The vertical tail must counteract the destabilizing effect of the fuselage ahead of the CG. The result was that the vertical stabilizer had an area of 170 square inches. This was broken into a 12.6 -inch chord and a 13.5-inch span for the vertical stabilizer. This gave an aspect ratio of 1.1.

The rudder could now be sized. A plot of yaw moment versus sideslip angle was developed to aid in the sizing of the rudder (Figure 5.7). The size of the rudder ended up being 51 square inches and the chord of the rudder being 3.0 inches on the trailing edge of the vertical stabilizer. An aerodynamic horn was put on the rudder to reduce the moment about the hinges. By placing a portion of the rudder area ahead of the hinge line, the air flow will actually help turn the rudder. This will reduce the torque required by the rudder servo and prevent a more expensive servo from needing to be used. The rudder area resulting is 30% of the total vertical stabilizer area.

The overall handling qualities of this aircraft would best be described by giving the static margin of this airplane. The static margin of this aircraft is 10%. Which will give us a responsive airplane for a prototype.

5.2 Component Selection and Systems Architecture

5.2.1 Battery Pack

The final battery pack selection was based on the analysis of many different battery types. The more cells used in the battery pack increased the RAC and penalized the overall score of our airplane. This was taken into consideration, but the lowest RAC was not necessarily the best battery pack choice. As shown in Figure 5.3, the battery pack of choice was composed of 36 Sanyo KR-2300SCE cells. The other top scoring packs were good strictly based on score, but had other undesirable properties that could potentially damage the motor. Battery packs 3 and 4 in the figure derived their power from a very high number of cells which resulted in a low score and a voltage too high for the motor to handle. Battery packs 1 and 2 were very high capacity cells and derived their power from current instead of voltage. While

this significantly reduced the number of cells and increased the score, this high current level would be damaging to the motor. Thus, pack number five was chosen for this competition.

The Sayno KR-2300SCE cells assembled in a pack of 36 have an internal resistance of 209 mΩ, resulting in a voltage of 42 Volts. For a full throttle flight time of eight minutes, the available current was 17 Amps. This provided a net power of 724 Watts into the motor. All of these specifications fell within the desired performance range for our propulsion system. The current and the voltage were both low enough to safely drive the motor and the internal losses due to resistance were reasonable.

With the correct battery type selected the final battery pack was ready to be assembled. Over 90 batteries were tested to find the 72 batteries with the highest capacity and performance. These 72 batteries would then be assembled into two battery packs to be used for the competition. Each battery was initially fully charged and labeled. Then each cell was discharged over a 15 to 20 minute period. Two digital multimeters were connected to the cell monitoring the voltage and current. Voltage and current readings were taken every 30 seconds during the discharge period. Once the cell was full spent, the voltage and current data versus time was entered into an Excel spreadsheet. After compiling the data for all 90 batteries the 72 with the highest capacity and endurance were chosen for the competition battery packs. Even one bad cell in a pack of 36 can ruin the overall pack performance. The capacity of the entire pack is determined by the worst cell. Thus, the OSU Flight Factory assembled two battery packs that would be worthy for competition.

5.2.2 Motor

Over the past couple of DBF competitions Oklahoma State University has discovered that AstroFlight motors are one of the best choices for the airplane's powerplant. After searching through the specifications of other manufacturers and considering the performance needed for this contest, AstroFlight was chosen again. An Astroflight 640G Cobalt motor was chosen to drive the aircraft. This motor was chosen specifically for our battery pack's voltage and current capabilities. The ideal operating current for the 640G was in line with the KR-2300SCE battery pack for maximum efficiency. Matching the battery pack current with the ideal motor current is absolutely essential for attaining the maximum efficiency. After losses the AstroFlight 640G supplied approximately 600 Watts to the propeller.

The motor speed is regulated by a speed controller. The experts at AstroFlight were consulted in the selection of a low-loss speed controller. Knowing the battery pack characteristics and the motor being used, the ideal AstroFlight speed controller was selected for maximum efficiency.

5.2.3 Propeller/Gearing

Analysis shows we need 9.5 pounds of thrust to get our fully loaded airplane off the ground in 100 feet. An APC propeller with a diameter of 20 inches and a pitch of 14 was used to gain a static thrust of 9.5 pounds. To accomplish this required thrust, a gearing ratio of 3.1:1 was needed. This propeller provided a good compromise between takeoff thrust desired cruise velocity. In the future, multiple propellers will be chosen for different wind and take-off conditions. This APC 20X14 is a general purpose propeller assuming zero wind, which is the worst case for take-off at full payload.

5.2.4 Radio and Servos

The radio chosen for our aircraft is an eight channel Futaba PCM transmitter and receiver. This radio has enough functions to control each task needed in the airplane as well as the reliability and quality of a PCM signal. The servos were selected based on the torque needed for each application. To increase the torque for a given servo a 6-Volt receiver battery was used instead of a standard 4.8-Volt battery. This voltage increase gives approximately a 20% increase in torque to each servo. This 6 Volt receiver pack also has a higher capacity than its 4.8 volt counterpart. This extra battery life will be beneficial during the contest if running back to back missions. The hinge moments of each control surface were determined during the aerodynamic analysis, thus the correct servo was selected for the job. The control surface hinge moments were found to be as follows:

- Elevator ---- 65.1 oz-in
- Rudder ----- 41 oz-in
- Ailerons ----- 63 oz-in

From this data the control surface servos were selected. For the elevator and ailerons Tower Hobbies TS-59 servos were chosen. These are high torque servos that are not much larger in size or weight than a standard servo. They deliver 72 oz-in o torque at 6 Volts. The rudder, nose gear steering, and braking are powered by Futaba 3001 servos. These are standard servos that are inexpensive. At 6 Volts they each deliver 53 oz-in of torque.

5.3 Structures

The detailed design phase for the structures team involved laying out the entire aircraft. AutoCAD was used extensively during this stage to help visualize the integration of the individual components. The most critical areas were payload location, wing attachment, tail attachment, landing gear location, and servo location.

Since the design payload was 5 liters of water, there were two options for balancing the payload about the center of gravity to maintain correct flight characteristics. First, was to put two pairs of the bottles equal distances from the

center of gravity while placing the fifth bottle directly on the CG. The second option was to put the bottles in one group of three and another group of two. The set of two bottles would need to be placed further from the CG than the set of three to achieve a moment balance. Since the battery pack was very heavy with respect to the rest of the airplane structure we knew the batteries needed to be located near or on the CG. This drove us to choosing the second bottle configuration to keep the CG area of the fuselage free for the battery pack. The 1 liter polyethylene bottles chosen are 7.75 inches tall and 3.5 inches in diameter. Thus, to stand the bottles vertically the fuselage was chosen to be 8 inches tall and 4 inches wide.

The bottom wing would be slid through the fuselage and attached to the top wing with two end struts. These end struts will need to be strong since they are the only component holding the top wing to the rest of the structure. The top wing is to be 16 inches above the bottom wing and eight inches above the top of the fuselage. These end struts would be permanently attached to both wings with epoxy. Bolting the end struts on was considered, but was thought to induce too much 'play' in the wing connection system.

The tail would be connected in the same fashion as the wing. The horizontal stabilizer would be inserted through a slot in the correct location of the tail and glued into place. The vertical stabilizer would be affixed permanently with epoxy to the top of the tail section.

The main landing gear were to be mounted in the wing. This was the best location to provide a wide enough wheel base for the desired ground handling. They would be attached into the thickest part of the wing to provide the best rigidity. The nose gear would be mounted on a front bulkhead. The nose gear would provide both the steering and braking for the airplane. A hydraulic drum brake would be contained within the wheel hub to maintain a low profile and not increase drag.

The servos for actuating the control surfaces need to be mounted as close to the moving surface as possible. This would eliminate the need for long control rods and sloppy linkages. The aileron servos were placed on the underside of the wings just behind the main gear. This location allowed the servos to be shielded from the airflow by the main gear and have very short control rods. Servo wires were run out each side of the wing to the aileron servos. The rudder and elevator servos were placed inside the tail of the fuselage. Neither the horizontal or vertical stabilizers are large enough to house the servos, so control rods were run out the tail of the fuselage to the control surfaces.

Table 5.1 Initial Calculations from Spreadsheet

Wing Loading	=	2.251	lb/ft ²
Payload fraction	=	38	%
Payload	=	5	Liters of Water
Endurance	=	8.15	minutes
Range	=	7.6	miles
Fuselage Length	=	60	in
Number of Scoring Sorites	=	3	

Table 5.2 Airfoil Data

Airfoil of Wing	=	Selig 1223
Maximum Coefficient of Lift of Airfoil	=	2.27
Maximum CL of Wing (corrected)	=	2.082
Airfoil for both Stabilizers	=	NACA 0009

Table 5.3 Spreadsheet Calculation Results

Area of both wings	=	1852	in ²
chord of the wing	=	11.02	in
AR of the wings	=	7.62	
Stagger of the wings	=	6	in
gap between the wings	=	16	in
incidence angle of upper wing	=	-3	degrees
incidence angle of lower wing	=	-2	degrees
total fuselage length	=	60	in
take off gross weight (with batteries)	=	27.50	lbs
MEW	=	12.95	lbs
Velocity To stall	=	43.55	ft/s

Take off Data

Take off Distance	=	78.3	ft
Velocity Take Off	=	52.77	ft/s
CLTO	=	0.98	

Cruise Data

Velocity	=	82.93	ft/s
Coefficient of Lift	=	0.28	
Coefficient of Drag	=	0.035	

Table 5.4 Stability and Control Results

c.g. location	=	leading edge of bottom wing
static margin	=	10.5 %

Horizontal Stabilizer Data

length from c.g to the quarter chord	=	33	inches
area	=	3.5	ft ²
span	=	3.5	ft
chord	=	1	ft
AR	=	3.5	
elevator area	=	60	in ²
elevator chord	=	1.43	in
percent area of the horizontal stabilizer	=	12	%

Aileron Data (for both ailerons)

area	=	108	in ²
percent area of the wing	=	9	%

Vertical Stabilizer Data

Area	=	170	in ²
chord	=	12.6	in
span	=	13.5	in
AR	=	1.1	
rudder area	=	51	in ²
rudder chord	=	3	in
rudder span	=	13.5	in
percent area of the vertical stabilizer	=	30	%

Wing Loading Variation

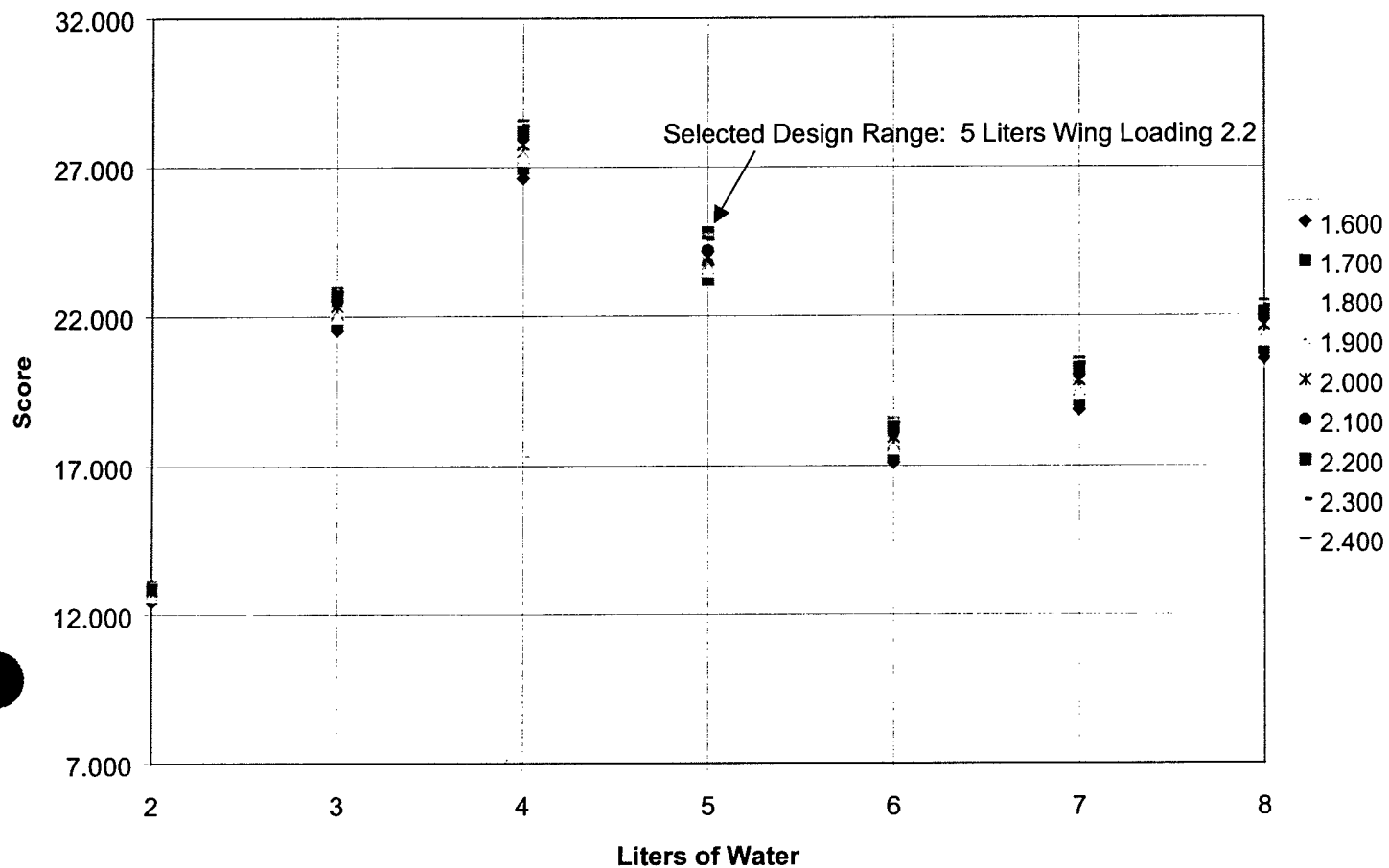


Figure 5.1 Initial Design Range

Wing Loading Variation

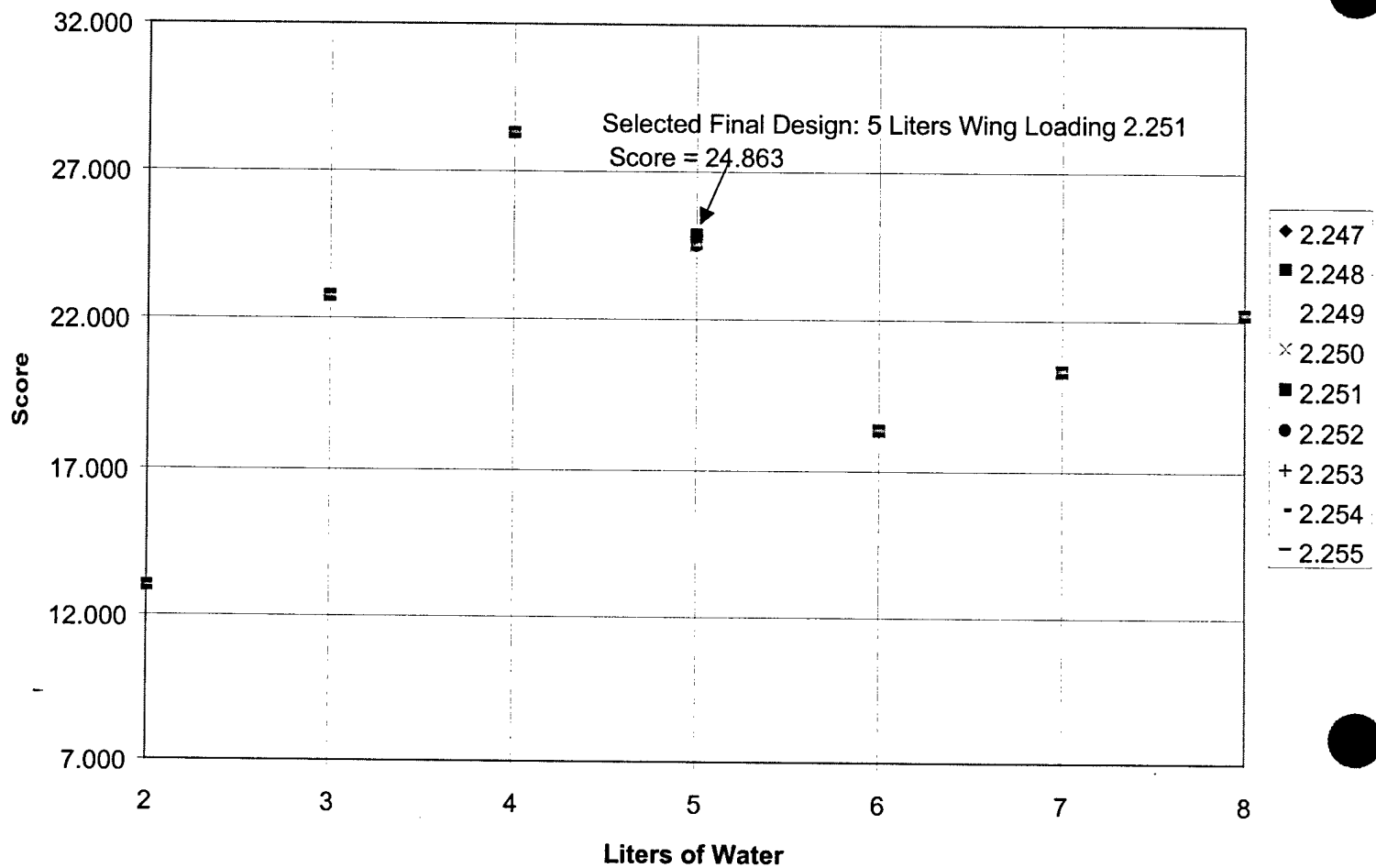


Figure 5.2 Specific Design Selection

Battery Selection

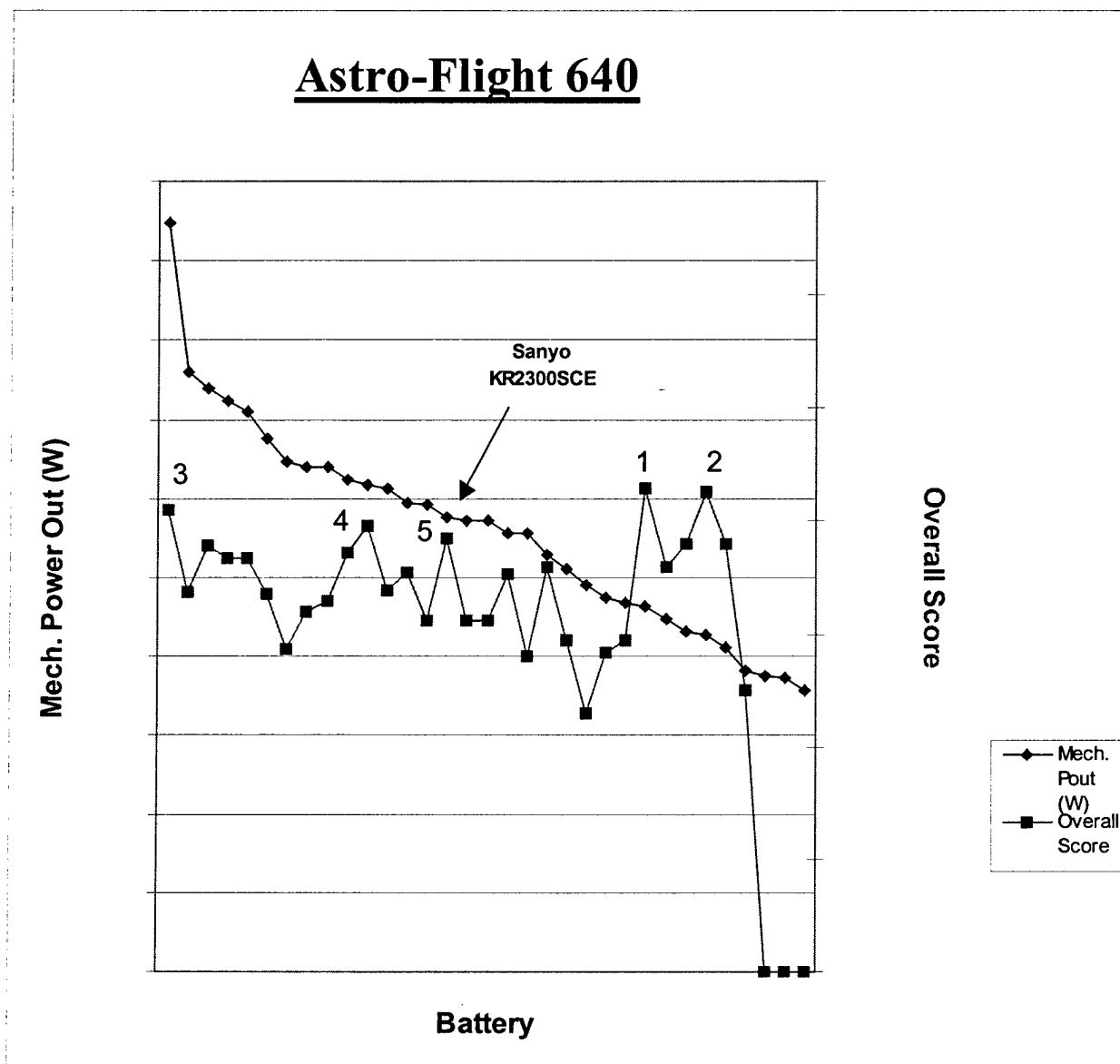


Figure 5.3 Battery Selection

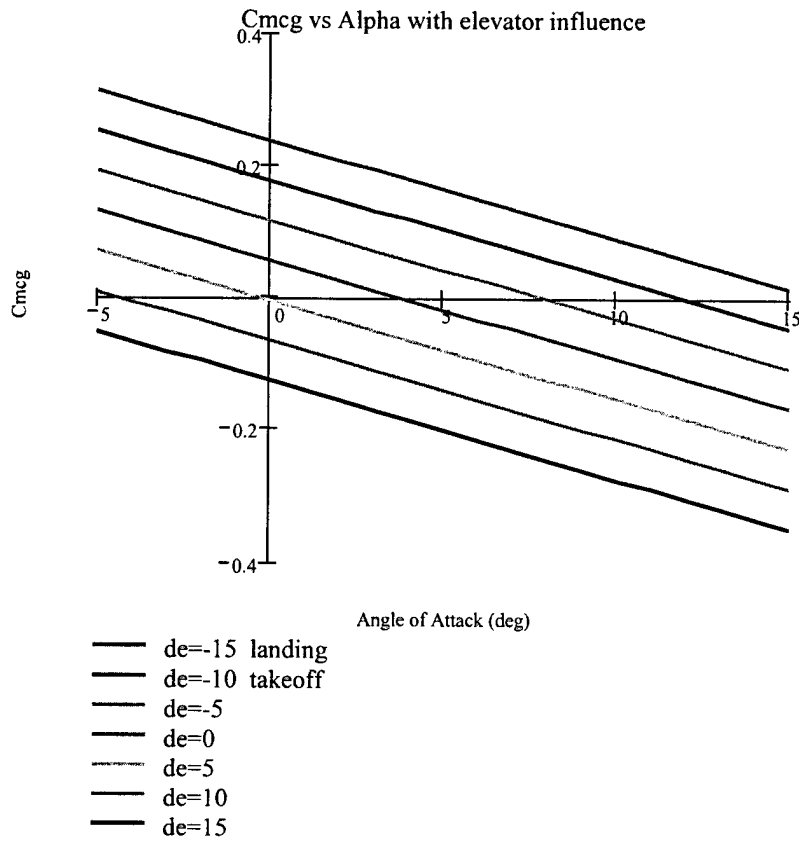


Figure 5.4 Cm versus Alpha with Elevator Influence

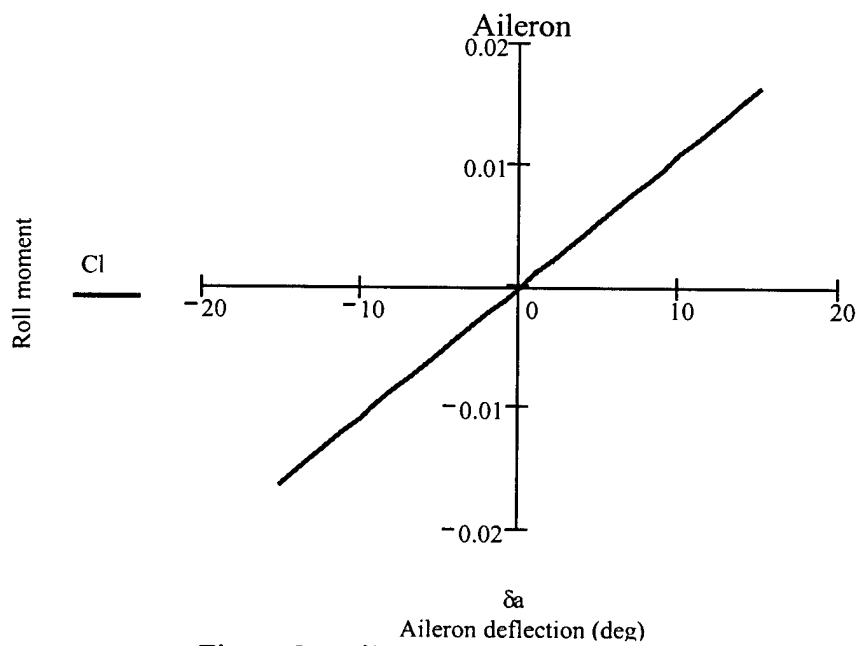
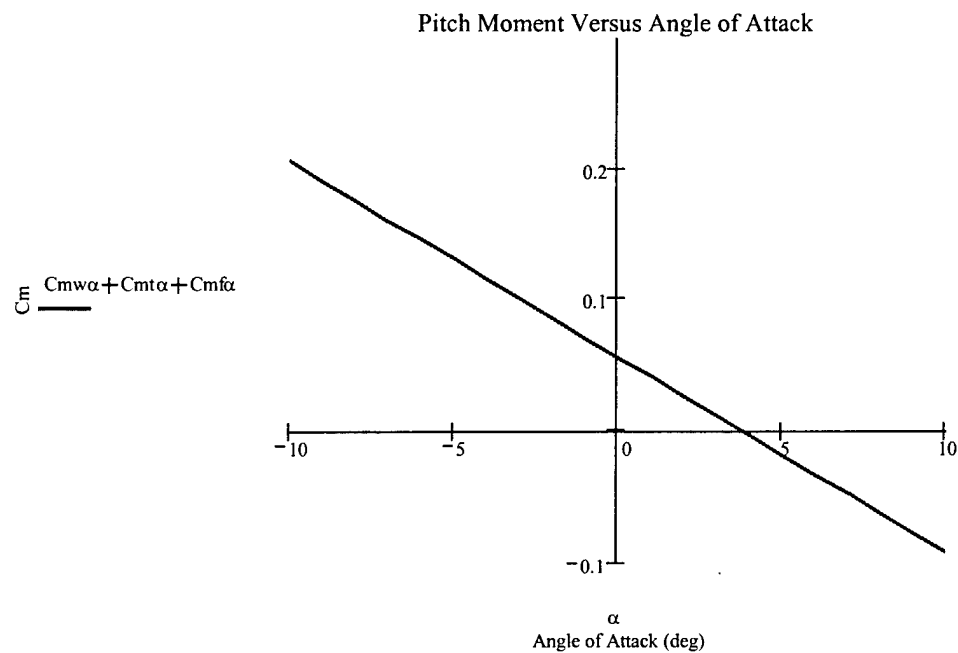
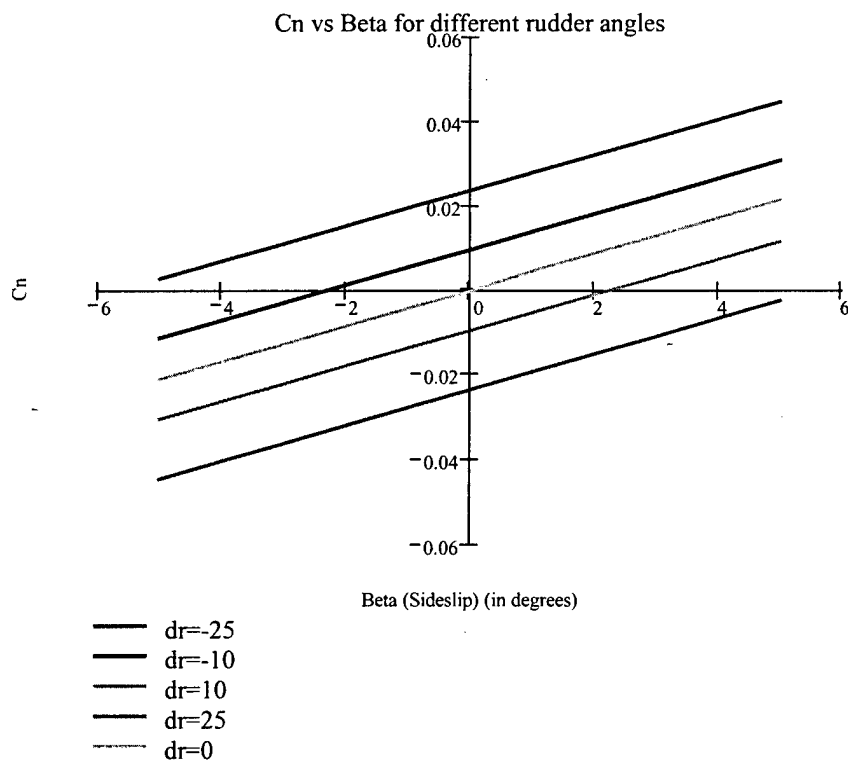


Figure 5.5 Aileron Deflection Effect on Roll Moment

Figure 5.6 C_m versus AlphaFigure 5.7 C_n versus Beta with Rudder Influence

5.5 Flight Factory Drawing Package

Figure 5.5.1 – Component Layout A

Figure 5.5.2 – Component Layout B

Figure 5.5.3 – Side View

Figure 5.5.4 – Top View

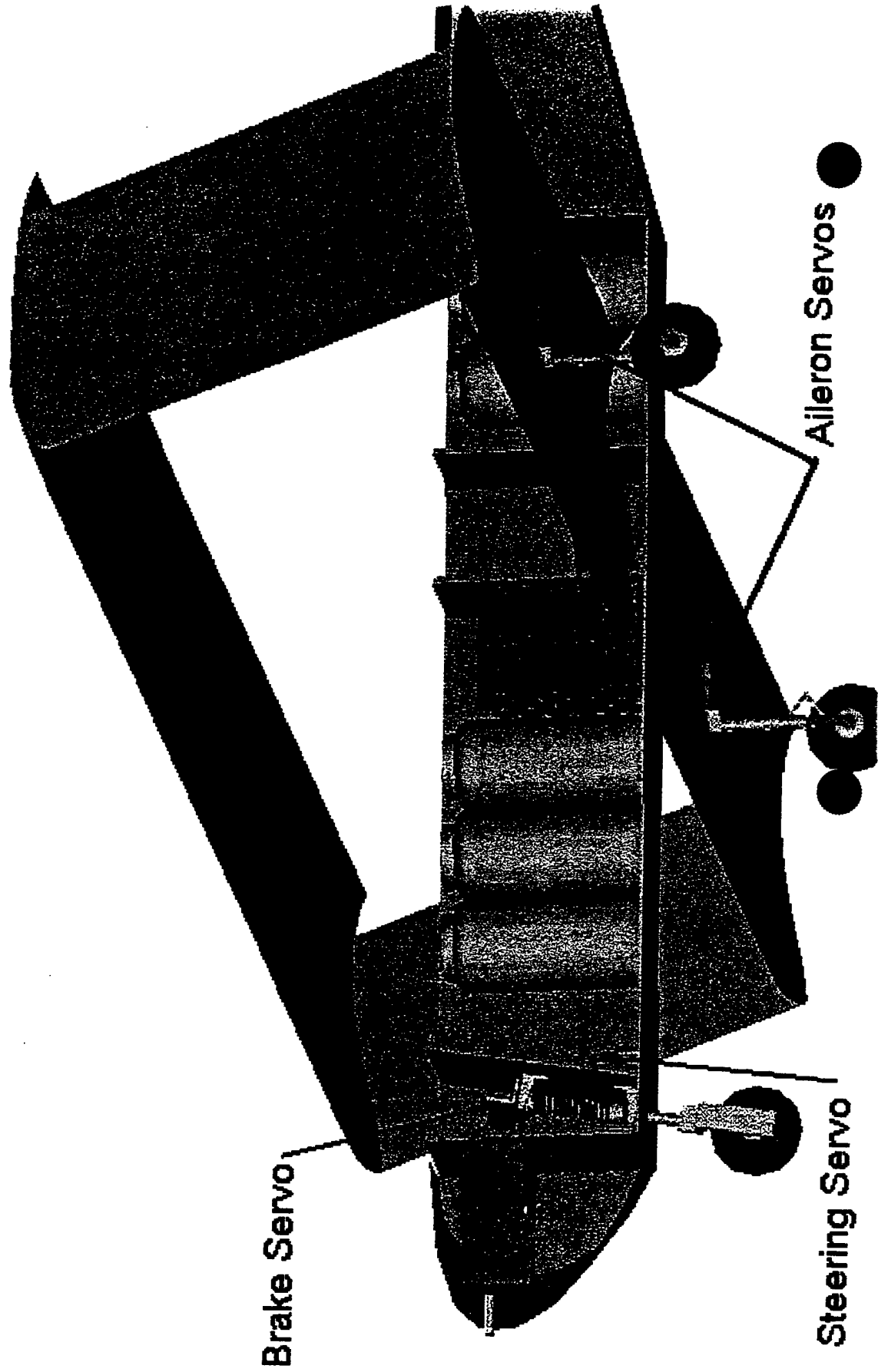
Figure 5.5.5 – Front View

Figure 5.5.6 – Payload Access

Figure 5.5.7 – Nose Gear

Note: All dimensions are in inches

Flight Factory

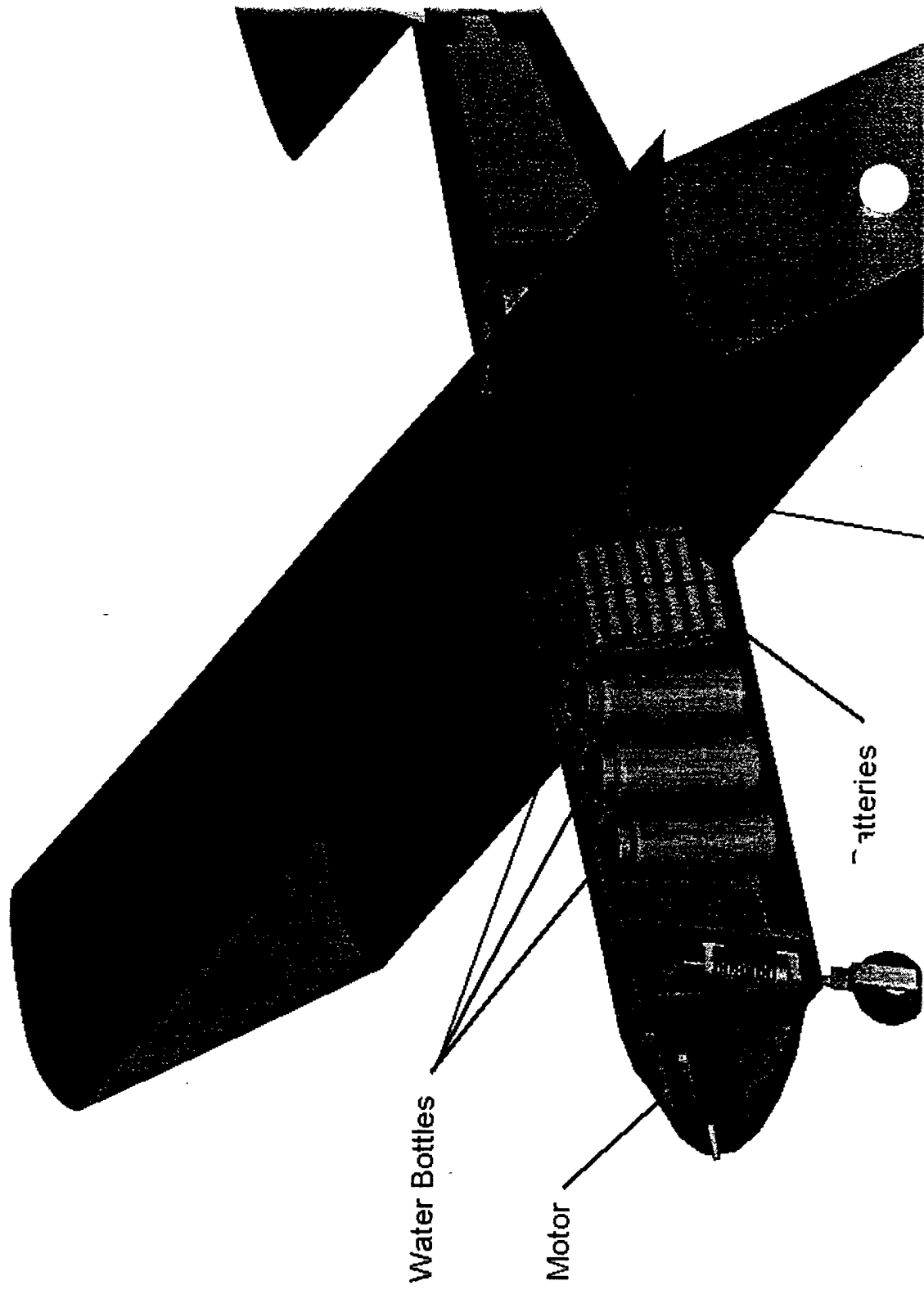


Brake Servo

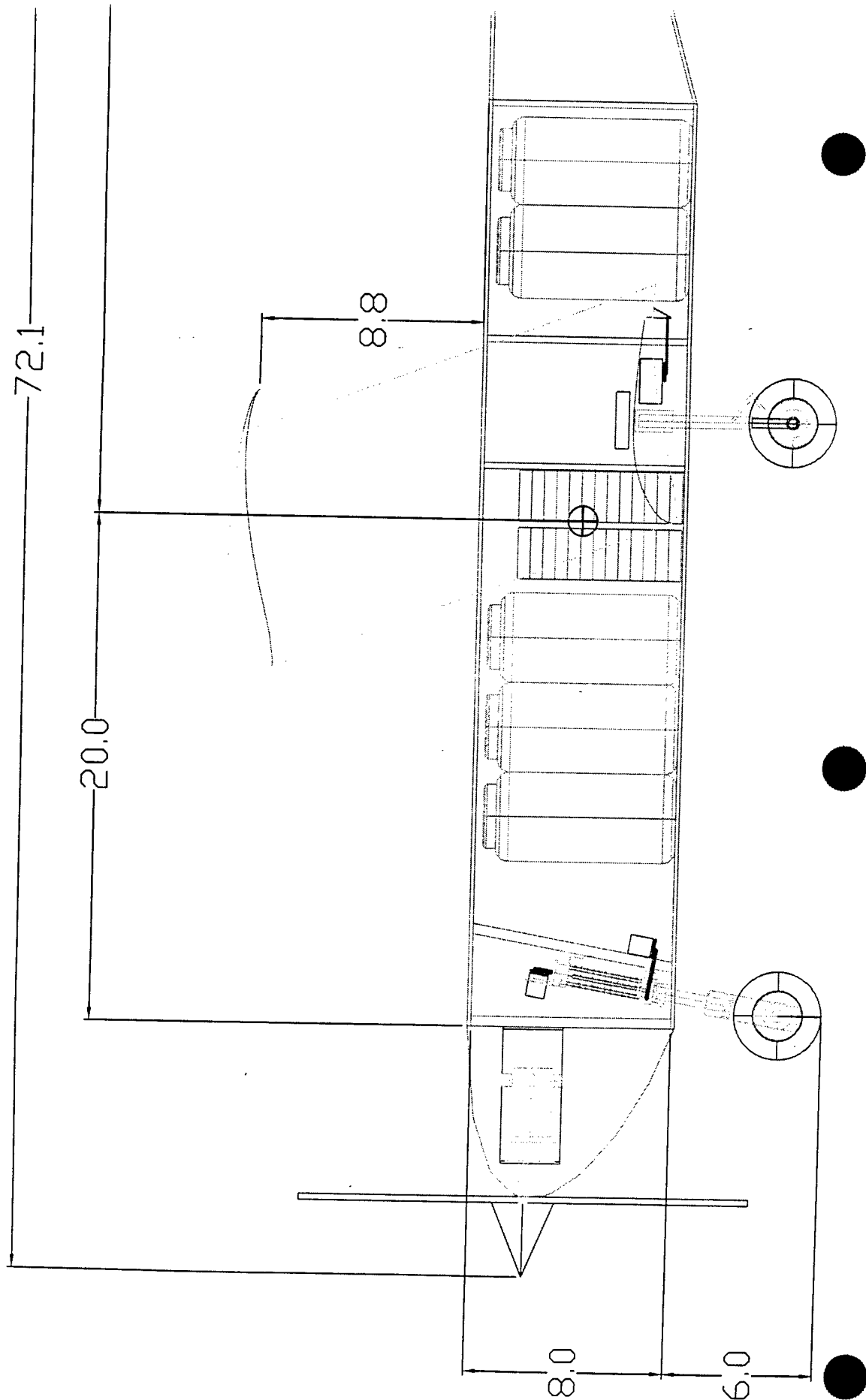
Steering Servo

Aileron Servos

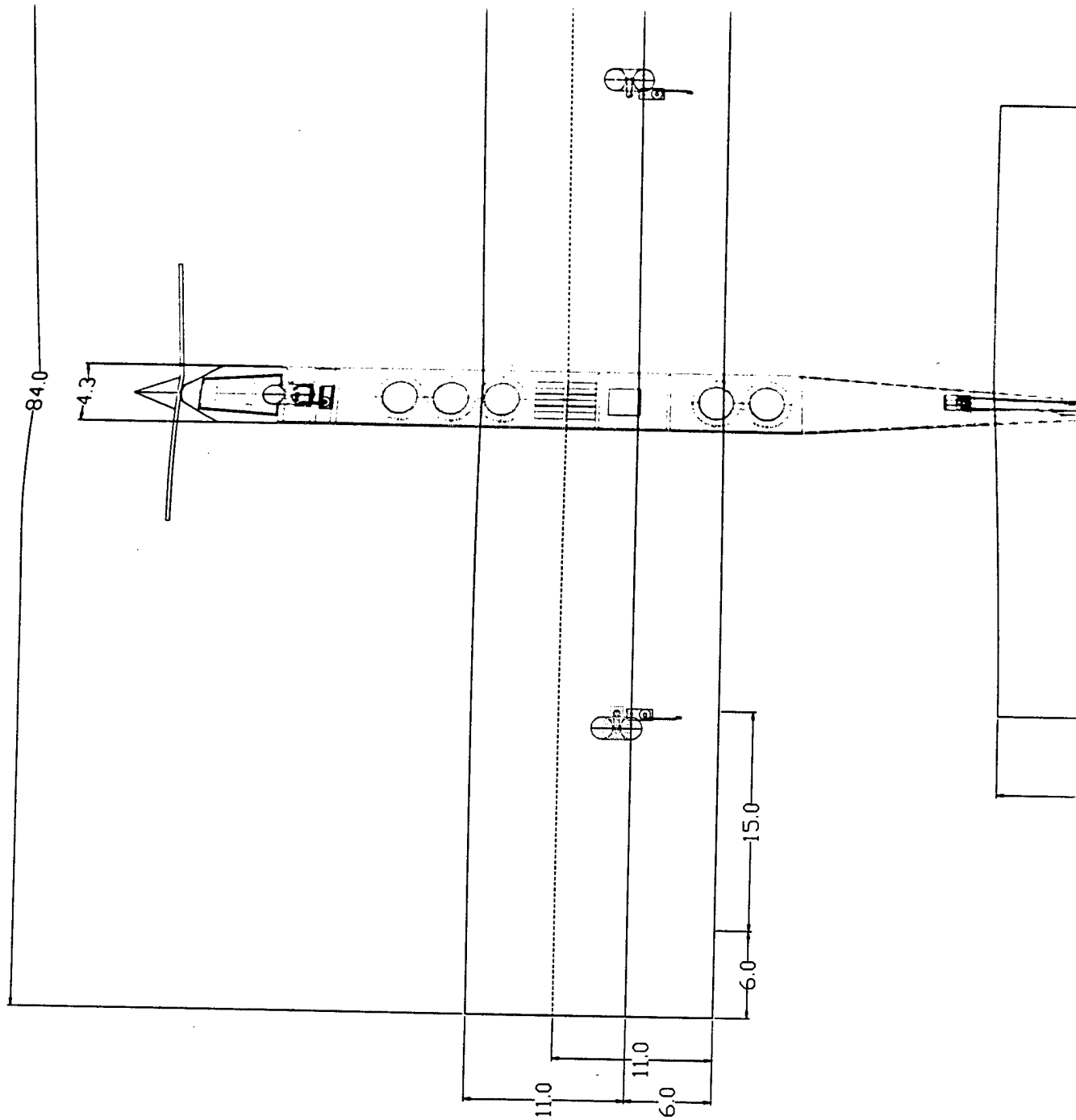
Flight Factory



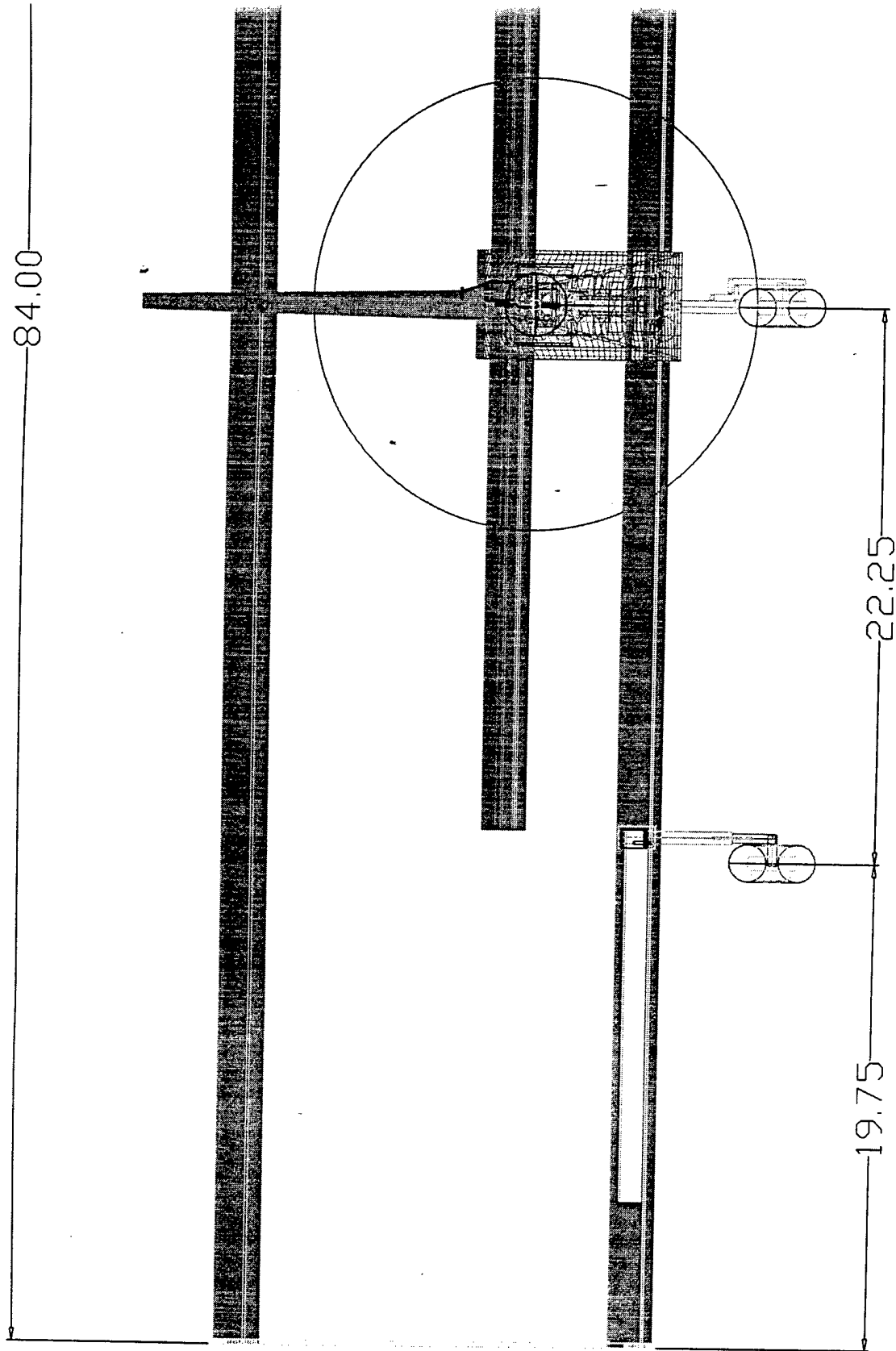
Flight Factory



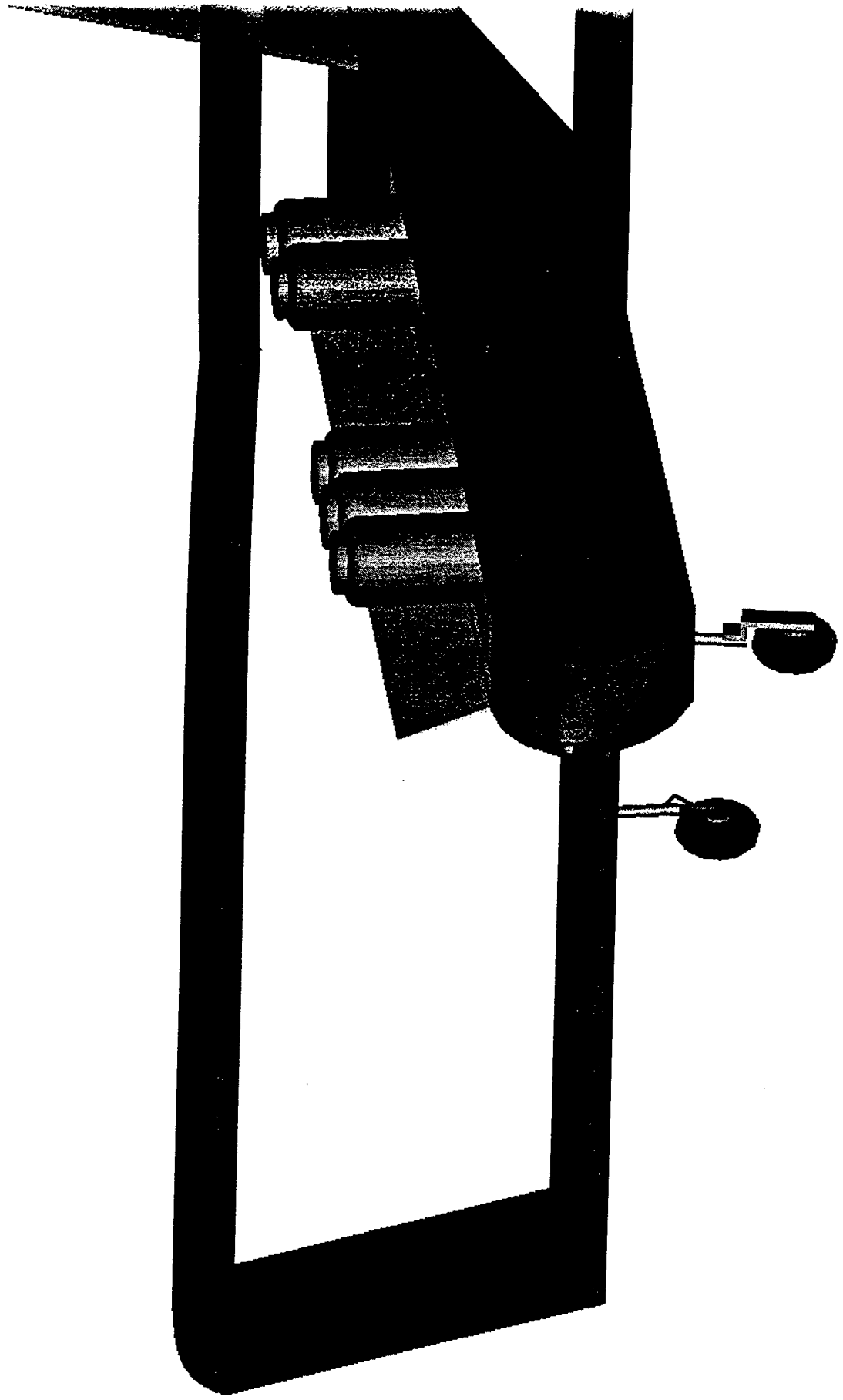
Flight Factory



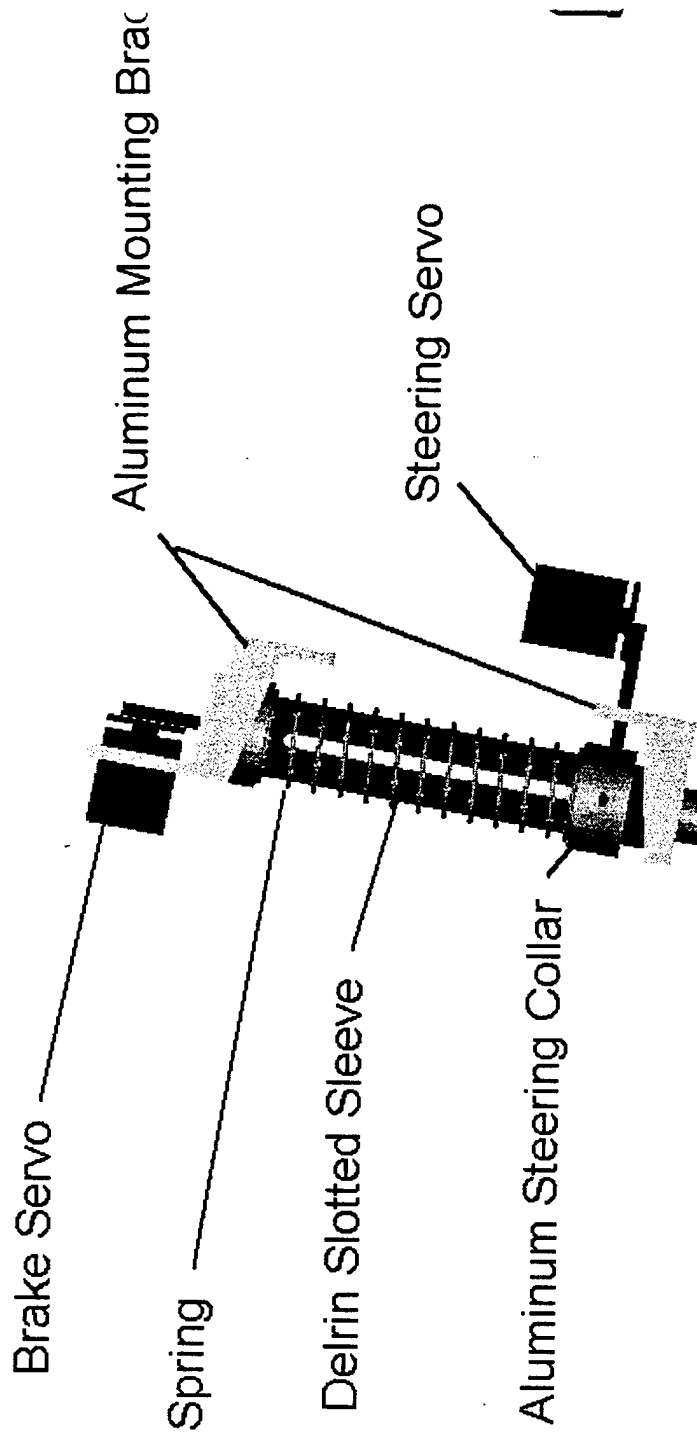
Flight Factory



Flight Factory



Flight Factory



Hydraulic Brake

6. Manufacturing Plan

6.1 Processes investigated

The standard method for construction of small scale planes generally the use of softwood/balsa/monokote. Lighter, lower strength materials such as balsa are used in low stress areas such as for fuselage skin. High strength materials such as aircraft grade plywood, birch, spruce, and carbon fiber are used in areas of high stress. Elements including the motor mounts and spar caps can easily be strengthened with carbon fiber or kevlar for high toughness. Alternately, skin elements on the wing and sections of the fuselage could be covered with monokote. In order for the Structures team to gain experience in conventional construction techniques using softwood, the group constructed a standard model trainer plane. This method of construction would be inexpensive, modify and repair easily, and materials were readily available.

Additionally, modern methods of construction employing materials such as carbon fiber, fiberglass, and kevlar as structural skin elements and the main materials were investigated. Experts in the field were also consulted. Wet lays up as well as the use of pre-preg fabrics were investigated. Methods of plaster, foam, and polyester resin positive and negative molds were also investigated. It was determined that the simplest and most common method of generating the necessary molds was to use foam as both to add structural strength (wing shear webbing as well as providing the exact shape) and serve as both the positive and negative molds. Following this section, the FOM's for each of the methods are given and the chosen construction methods are presented.

6.2 Figures of Merit

FOM's Used to Screen Competing Construction Concepts:

- Availability
- Required skill levels
- Cost
- Weight/Strength Ratio
- Complex Geometry Capability

First, the materials we select to construct the final airplane must be readily available. During the construction process we will most likely need to by additional materials above and beyond an initial supply. In our case, all these materials including carbon fiber, kevlar, fiberglass, balsa wood and the necessary accessories are available from a local supplier.

Second, the members of the structures, or construction, team must have the necessary skill to complete the construction. If they do not already have the ability, it must be easily learned. A balsa wood kit plane was constructed by the structures team to ensure that all team members were familiar with these traditional construction methods. A carbon fiber expert was brought in and gave a seminar and demonstration on the use of carbon fiber and other composite materials. After this

seminar all the team members were adequately trained to use these composite materials

The third consideration for construction technique was the cost of materials. We had to work with the funds at our disposal when choosing the construction method. A wooden or traditional build up is considerably cheaper than carbon fiber construction.

Keeping the aircraft weight as low as possible was absolutely essential. Every pound saved on structure weight is a pound of water that could be added as payload. While balsa wood is a good choice for small remote controlled airplanes, to achieve the strength demanded by the mission of our plane a large amount of balsa would be needed. In this case carbon fiber has desirable properties. If implemented correctly, the strength to weight ratio of carbon fiber is much higher than that of balsa wood.

Finally was the complex geometry capability. The Selig 1223 airfoil that was chosen is highly cambered and must be precisely manufactured. Getting the covering on a balsa wood wing to follow the curves would be very difficult. However, carbon fiber would work very well. The exact shape of the airfoil could be cut with a hot wire out of foam and then the carbon fiber would be laid over the foam mold. This would achieve the exact airfoil shape desired.

After considering all the figures of merit for construction methods it was determined that carbon fiber was the material of choice. Carbon fiber is available, easy to construct, very strong, and moldable to complex shapes. Though it does cost more than a traditional buildup, it was determined that the advantages of the carbon fiber out-weighed the extra cost.

6.3 Manufacturing Process

6.3.1 Fuselage

Since carbon fiber was the obvious choice for a fuselage material, the next step was to develop a specific fuselage construction plan. First a male mold that fit the inside of the fuselage was cut from a high density blue foam with a wire foam cutter. On this mold there would be a layer of 1/8 in honeycomb sandwiched by two layers of carbon fiber twill. On the inside of the fuselage at the bulkhead locations, a woven material called "peel-ply" was placed to give the necessary surface texture for bonding the bulkheads to the fuselage with epoxy. It is important to note, that a film adhesive was applied anywhere there was a honeycomb to carbon fiber interface prior to baking to prevent delaminating and to maintain strength. A release film was also placed between the male fuselage mold and the carbon fiber so that the foam could be separated from the baked carbon fiber. A small piece of Kevlar was placed on the bottom of tail to protect the structure during improper landings. This was then placed in a vacuum bag and the layers of carbon fiber and honeycomb were compressed by a vacuum pump against the mold. The entire piece was then placed in a curing oven while still under vacuum and baked until the resin in the carbon fiber set up. This resulted in carbon fiber fuselage that exactly matched the shape of the mold.

The main bulkheads were made by sandwiching 1/8" honeycomb with a layer of carbon fiber twill on each side. The front bulkhead was constructed by gluing two main bulkheads together. This front bulkhead also doubled as the motor mount. The second bulkhead from the front was made of plywood and held the nose gear. All bulkheads were then mounted to the internal surface of the fuselage using epoxy. A motor cowling was manufactured by sanding a block of foam until it was small enough to fit the front of the fuselage, yet big enough to house the motor and motor mount. This produced a tapered shape that could then be wrapped in carbon fiber, vacuumed, and baked to maintain an aerodynamic shape (Figure 6.2). Hatch covers were made from 1/8 inch balsa wood that was reinforced by square 3/16 in balsa wood. Also, the hatch covers were fitted with a lip that would slide just to the inside of the fuselage to provide stability.

6.3.2 Wing

Since the airfoil selected by the Aerodynamics group was a very high-performance and high-camber airfoil, it was absolutely critical that the shape be exact and kept to high tolerances for proper performance. For this reason a carbon fiber construction technique was chosen.

To begin construction of the wing, Formica templates of the exact airfoil shape were created and then used to cut the wing out of foam. The templates were designed so that a two part foam female negative could be obtained from the same cuts made to obtain the foam male positive. From initial experiments, closer tolerances on the wing could be maintained when using a shorter length wire. Therefore, the wings would be made from several foam mold sections bonded together to the length of the entire wing (Figure 6.3).

The next step was to wrap the positive male mold in carbon fiber. Once the airfoil shaped male mold was covered in carbon it was then wrapped in a film release and placed into the female cradle. The film release was to prevent the wing from sticking to the cradle during the cure period. Finally, the entire wing was inserted in a vacuum bag and placed under a 20 inches of mercury vacuum. According to the carbon fiber supplier's specifications, wing was cured at 180 degrees Fahrenheit for 5 hours.

The total weight for both wings constructed under this method would result in a total wing weight of both wings of approximately 3.4lb. This weight does not include the end struts or landing gear connections in the lower wing. Assuming an increase in weight of the lower wing of approximately fifty- percent due to internal hard points at the wing ends and at the landing gear, the total estimated wing weight of both wings is approximately 4lb.

To provide support for the landing gear, a complete reinforced wing section of 6 inches in width was constructed from the foam core, balsa ribs, pony spars, and reinforced with kevlar (Figure 6.1). Four ribs made from 1/4 inch balsa were sandwiched the aluminum landing gear mount. Then two inches of foam on both sides of the mounting ribs were further sandwiched by balsa ribs. Pony spars made

from $\frac{1}{4}$ inch basswood were then notched through the foam and ribs on both sides top and bottom of the mount. All these elements were then bonded together with pre-preg kevlar. A space was created just behind the landing gear to accept the aileron servo. Both of these landing gear support sections were then baked and then laid up with the complete wing and covered in carbon fiber. The recess for the aileron servo was cut out of the wing skin after fabrication.

6.3.3 Landing Gear

Robart RoboStruts were chosen for our main gear. These RoboStruts proved to be good performers in terms of weight and shock absorbancy. The RoboStruts are constructed of 4130 chromoly steel tubing and utilize an internal spring to absorb landing impact. For our aircraft, we modified the length of the RoboStruts to better fulfil our needs; as well as using a custom spring that is more suited to our aircraft than the standard spring.

The nose gear used on our aircraft was designed and constructed by members of the design team. This proved to be quite a challenge because the nose gear must provide both steering and braking, while remaining lightweight and aerodynamically clean. The final design fulfils all of these requirements. The assembly is mounted to the aircraft by two brackets on a bulkhead. These bracket were constructed of 1.5 in. aluminum angle and provide support for a steering block made of 1 in. Teflon impregnated Delrin rod. The steering block is slotted to allow the strut to float vertically, while still providing directional control and has a 0.5 in. hole reamed through its center. A spring collar is mounted to the strut by 8-32 machine screws, which pass through the slots in the steering block, and compresses a spring against the upper bracket to absorb impact. An aluminum rod serves as the strut, its outer diameter is 0.5 in. and its length is 9.75 in. This strut also serves as the master cylinder for the braking system. Using the strut as the master cylinder significantly decreases weight because an existing structure is used for braking control instead of using an otherwise unneeded piece. The braking system used was previously designed and built as a design project by a team of students specifically for this aircraft. The brake is hydraulically actuated drum brake that is mounted inside the nose wheel hub. A servo mounted on the top of the strut operates the cylinder to activate the brake. When mounted in the aircraft the nose gear will have a 10-degree castor angle. This gives more steering control during taxi as well as allowing a smaller, lighter strut to be used. A smaller strut can be used because the moment generated by braking or a frontal impact is slightly offset by the weight of the aircraft.

6.3.4 Final Assembly

Once each of the individual components was built, they needed to be assembled into the final aircraft. The fuselage was a one-piece carbon fiber and honeycomb sandwich. A slot of the lower wing (Figure 6.4) and horizontal tail was cut in the side of the fuselage to accept these two components. A full size drawing of the fuselage side encompassing the wing was pasted on the side of the fuselage in the correct wing location. The drawing included the wing mounted at the correct incidence angle.

Once one of these pictures was pasted on each side of the fuselage a Dremel tool was used to cut out the airfoil shape.

The inside of the fuselage was reinforced with 1 inch wide balsa wood. This provided a larger contact surface for the bottom wing when it was slid into place. Now that the proper lower wing installment was established it was fastened into place using epoxy. Using epoxy reduces the need for heavy bolts and will result in a tight fit between the fuselage and the lower wing. The horizontal and vertical tails were glued into place and prepared to be attached to the flight control systems.

Next the servos and flight control systems were put into place. The tail servos were mounted on balsa wood stilts near the most aft bulkhead. From here the control linkages were attached to the rudder and elevator. The aileron servos were set in place directly behind the main landing gear where their control rods were attached to directly to the ailerons. The receiver and battery were wrapped in foam rubber to prevent vibration from damaging them.

Once all critical elements were in the fuselage the end struts and top wing were glued into place with epoxy. The final step was to attach the landing gear and bolt on the motor. The airplane was now ready to accept the payload and propulsion batteries. Figures 6.5 and 6.6 show our airplane after the first assembly of the fuselage, tail and wings.

Manufacturing Milestone Chart

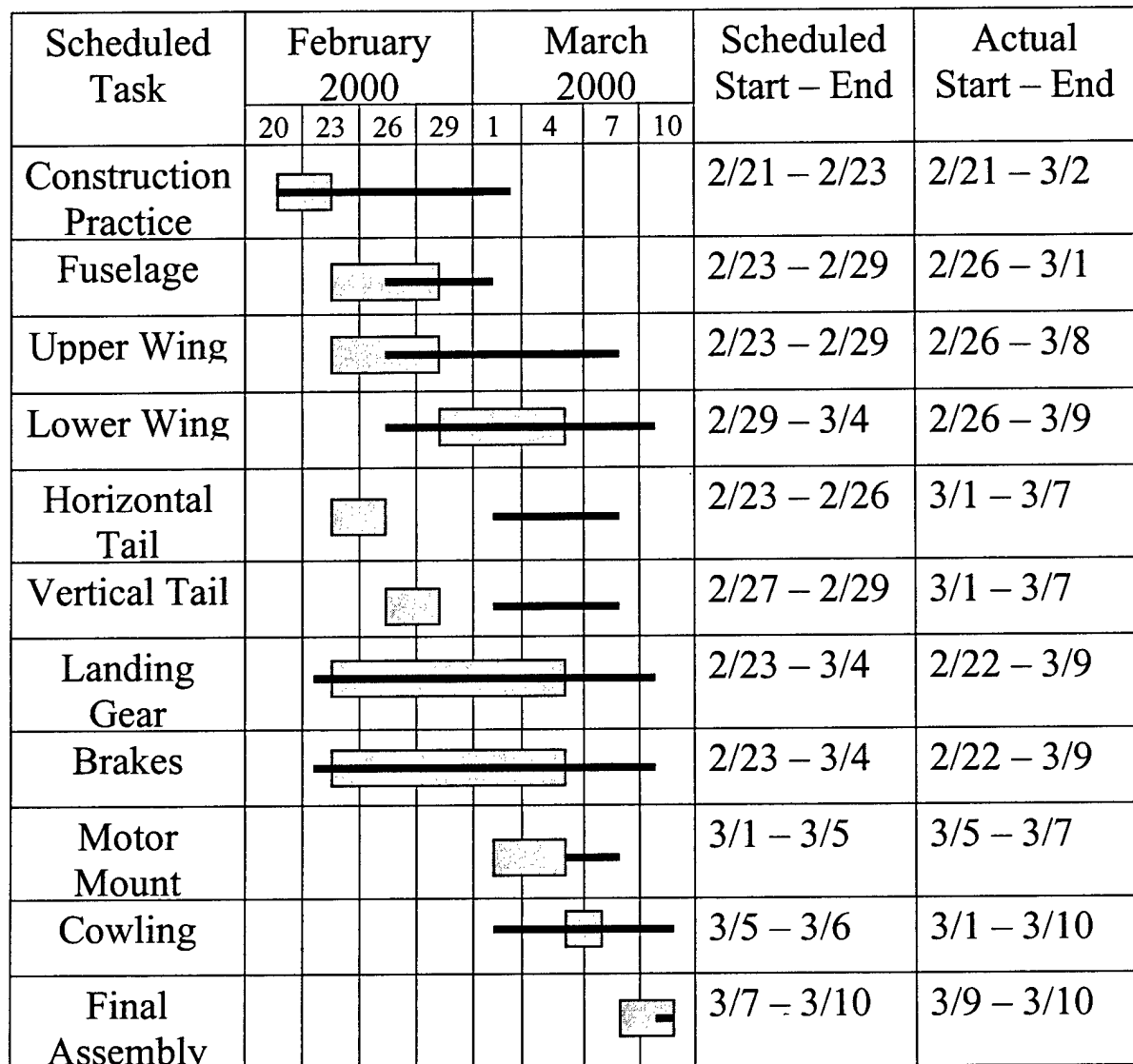
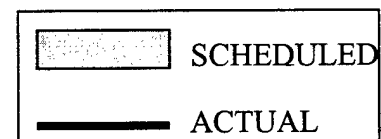


Chart 6.1



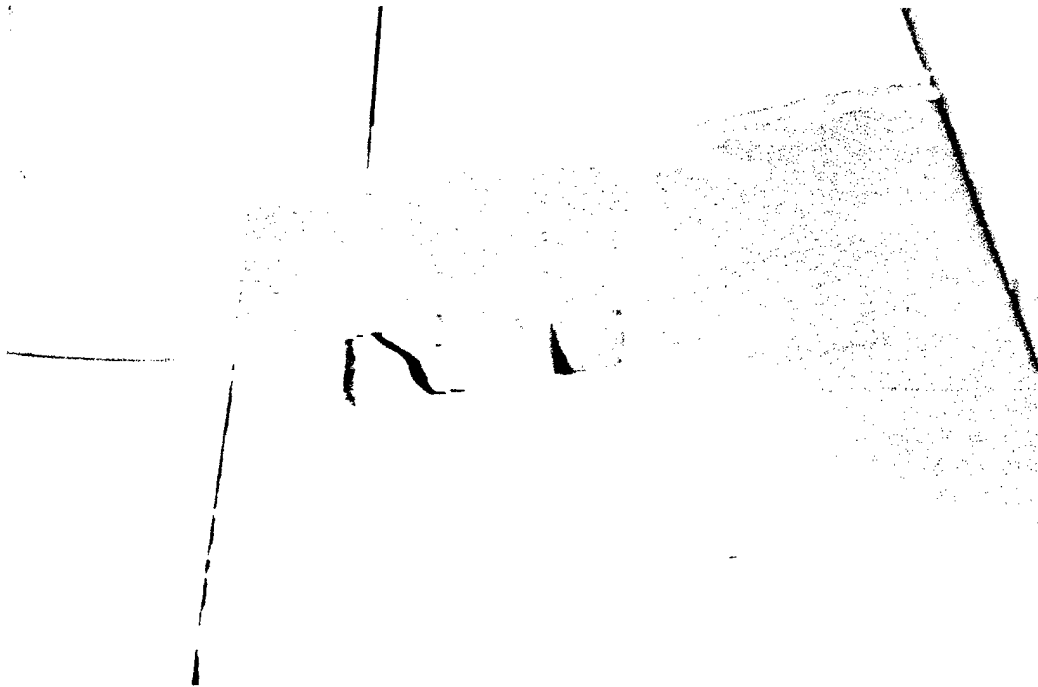


Figure 6.1 Kevlar Insert in Bottom Wing



Figure 6.2 Making the Cowling Mold



Figure 6.3 Applying Carbon Fiber to Lower Wing



Figure 6.4 Inserting Bottom Wing for the First Time

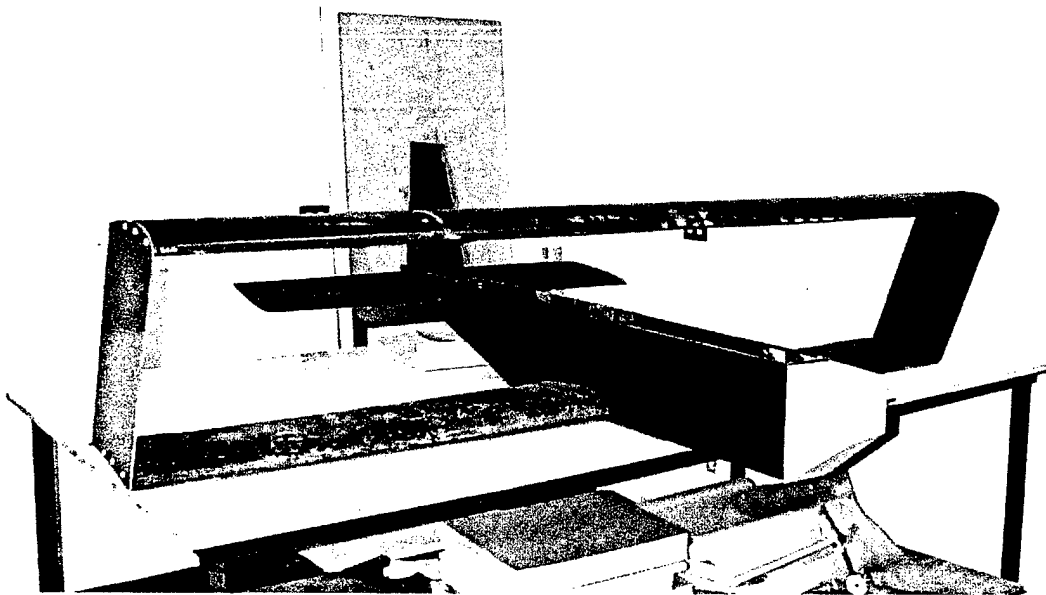
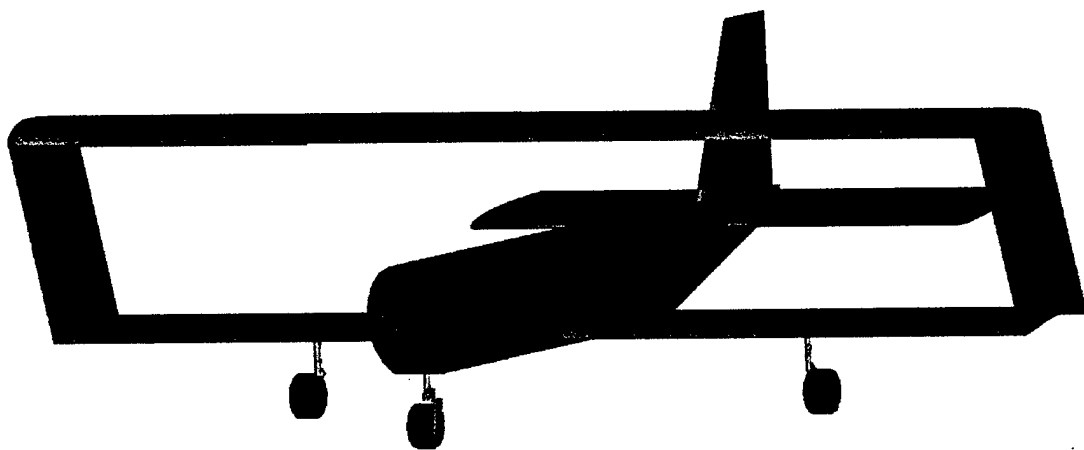


Figure 6.5 Front View of First Assembly



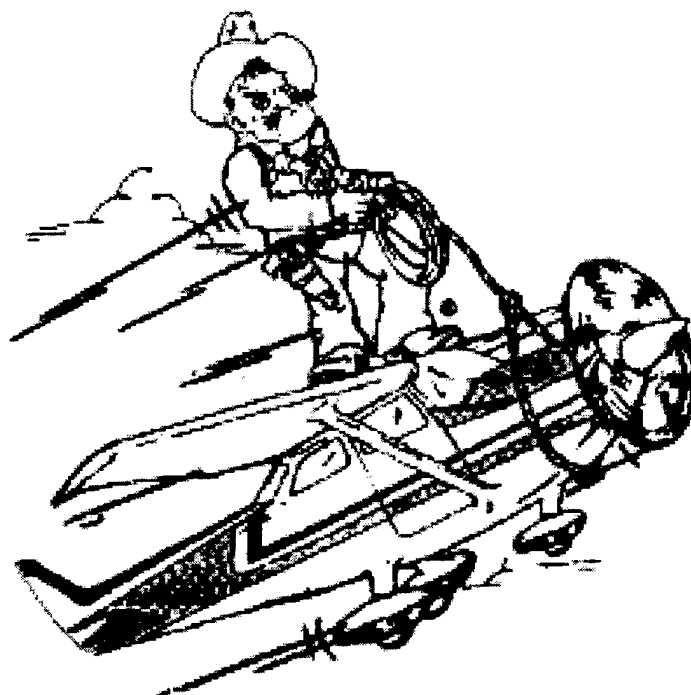
Figure 6.6 Rear View of First Assembly

Flight Factory



Cessna/ONR Student Design/Build/Fly
Competition

OSU Team #2
Flight Factory



Design Report – Addendum Phase

Oklahoma State University
April 10, 2000

Table of Contents

1. Lessons Learned	1
1.1 Prototype Testing.....	1
1.1.1 Taxi Test	1
1.1.2 First Test Flight.....	1
1.1.3 Second Test Flight	1
1.1.4 Third Test Flight	2
1.2 Final Contest Aircraft versus Proposal Design.....	2
1.2.1 Aerodynamics and Configuration Group.....	2
1.2.2 Propulsion Group.....	3
1.2.3 Structures Group	3
Figure 1.1 – Prototype First Successful Flight	6
Table 1.1 – Summary of Lessons Learned from Prototype aircraft.....	7
Figure 1.2 – Side View Final Aircraft	8
2. Aircraft Cost	9
2.1 Rated Aircraft Cost	9
Table 2.1 – Final Competition Aircraft’s Rated Aircraft Cost	11
Figure 2.1 – Distribution of Rated Aircraft Cost	12

1. Lessons Learned

1.1 Prototype Testing

Over the past few weeks since the proposal phase the OSU Flight Factory was able to test fly our prototype aircraft. This proved to be highly beneficial for verifying the performance characteristics of our design and providing the data needed to modify our design to be as competitive as possible for the contest.

1.1.1 Taxi Test

Our first test was a taxi test in a large parking lot. This was done to check the propulsion system while in the aircraft as well as the ground handling characteristics. This taxi test showed that the steering worked extremely well, but pulled a little to the left. The aircraft's wide main gear spacing allowed it to be turned at high speeds without any worry of tipping the plane. The nose wheel brake did not work as well as expected. While the stopping power of the brake was excellent, the hydraulic system was not setup correctly to give both free spinning and full stopping modes.

1.1.2 First Test Flight

Our first test flight was conducted on Friday March 24th at the Ditch Witch facility in Perry, Oklahoma. The runway at Ditch Witch is paved and will most likely simulate the contest site. We began by conducting a complete pre-flight inspection of the aircraft. Once all controls and components were checked, the motor was run up to verify the correct installation and operation of the propulsion systems. The first test flight was performed without payload and a take-off weight of 25.5 pounds. The test pilot, pointed the aircraft into the wind and accelerated to take-off speed. The aircraft accelerated slower than expected and took off in over 100 feet. The aircraft slowly climbed for about 5 seconds at full power and then began to sink. Since it was apparent that the aircraft would not fly, the pilot set the plane down in a nearby field. Due to the lack of climbing ability the plane came down rather hard and broke the bottom wing loose from the fuselage.

After studying the flight video and noticing the nose high characteristics of the airplane, additional wing calculations were performed to determine that the wing incidence angles were about 6 degrees too low. From the acceleration characteristics of the first test flight the Flight Factory also chose to increase the thrust for the next test flight by increasing the propeller diameter.

1.1.3 Second Test Flight

After the repairs and corrections were made the OSU Flight Factory was ready to fly again. This second test flight was much more successful than the first. With the corrected incidence angle and increased power the aircraft took off in 72 feet and climbed very well. The pilot spent the remainder of this flight trimming the control surfaces to achieve straight and level flight. The pilot found that once the aircraft was properly trimmed it was a little sluggish in the roll mode, but otherwise flew very well. A picture from this flight is seen in Figure 1.1.

1.1.4 Third Test Flight

The third test flight was used to simulate contest missions, check battery endurance, and determine sortie times for the loaded and unloaded configurations. The Flight Factory placed 2 liters of water in the aircraft and setup the contest flight course. Due to the increase in power, it was expected that the endurance would drop well below the endurance needed to complete 3 scoring sorties. The aircraft took off with 2 liters, take-off weight of 29.9 pounds, in 85 feet. The pilot had no problem turning around the pylons or performing the 360 degree turn. The flight time for this sortie was 75 seconds, which is very close to what the Flight Factory had predicted. Then the payload was removed from the aircraft and 2 empty laps were flown without incident in a time of 134 seconds. During the second scoring sortie it became apparent that the battery power was dwindling and the pilot chose to make the final turn a few hundred feet short in order to get the plane back to the runway before batteries gave out. The total flight time for this mission was 3 minutes 35 seconds.

Next, a fully charged battery pack was placed in the plane and a payload of 3 liters was added. Since a 2 liter payload was unable to make 2 scoring sorties, only 1 scoring sortie and 1 empty sortie was attempted. The airplane took-off within 100 feet and flew as expected. A summary of Lessons Learned from the prototype aircraft is found in Table 1.1.

1.2 Final Contest Aircraft versus Proposal Design

1.2.1 Aerodynamics and Configuration Group

Knowing the flight characteristics of the prototype aircraft the aerodynamics group was able to make a few minor corrections final contest aircraft. The results of the first test flight caused an inspection of the airfoil characteristics due to the lack of climbing ability and nose high flight pattern. The bottom wing for the first test flight was mounted at negative 3 degrees. After additional research it was discovered that the current wing incidence was creating a large amount of drag during take-off and causing the plane to cruise nose up. Setting the bottom wing incidence at plus 3 degrees would significantly reduce drag and allow the aircraft to take-off more readily.

Additional analysis of the decalage also revealed the top wing's incidence should be one degree less than the bottom instead of one degree more. The prototype had a decalage of plus 1 degree to the bottom wing and was causing uneven lift distribution between the top and bottom wing. Since the top wing's angle of attack was too high with respect to the bottom wing, the top wing was carrying more than half the lifting load. This uneven-distribution causes inefficient wing operation. This problem was corrected by having a decalage of negative 1 on the final contest aircraft.

The Flight Factory discovered that to achieve proper CG location the fuselage needed to be slightly longer since the prototype was tail heavy. This increase in fuselage area in front of the CG would create instability in yaw direction. Thus, the vertical tail area was increased by making it 2.5 inches taller. The prototype was not unstable in yaw, but the slight increase in drag of a larger tail was worth the risk of instability.

The flight test showed that the aircraft had no problem pitching up or down, but needed full elevator deflection to do so. The aerodynamics team was worried that in a dive there would be a lack of tail volume, so the elevator chord was increased from 1.5 inches to 2.5 inches.

1.2.2 Propulsion Group

The actual performance data of the propulsion system came exceptionally close to the estimated values of the various desired propulsion parameters. The *Excel* spreadsheet and *MathCad* documents used to calculate such outputs as thrust, RPM and endurance were remarkably accurate at estimating such values given a specific battery pack, motor and propeller. However, even though the initial propulsion system performed in the manner that was it was designed, the selected Astro-Flight Cobalt 640 motor was unable to handle the increased power output needed at a lowered endurance level. The Astro-Flight Cobalt 640 was simply inadequate to handle the load. Consequently, the Astro-Flight Cobalt 661 motor was chosen to take the 640's place on the contest plane. This modification suitably matched the power requirements needed for our efficiency and load handling.

As a consequence of using another motor, a different propeller that matched these changing parameters was needed to power the plane. The chosen propeller was a 20 x 12 prop with hollow blades fabricated from unidirectional and bi-directional carbon fiber and epoxy. This preference was selected due to its high performance in addition to its lightweight and strength.

1.2.3 Structures Group

After the flight tests, the structures group determined that the aircraft was extremely strong and durable because of the carbon fiber construction methods. This was proven by the easy repair of the aircraft after the crash during the first test flight. Knowing that every pound taken out of the airplane structure would increase our payload capacity as well as decrease Rated Aircraft Cost (RAC), the structures group made number of construction method changes to reduce the empty weight of the aircraft. In addition to weight savings, there were a couple of configuration changes to various parts of the aircraft to optimize overall performance.

Wing:

The carbon fiber used on the prototype airplane had a 'wet' side and a 'dry' side. The dry side needed an additional layer of adhesive to prevent the carbon fiber from becoming starved for resin. A new type of carbon fiber was found that does not require this layer of adhesive and will save a significant amount of weight on the wings of the final contest aircraft.

Fuselage:

The honeycomb used between the layers of carbon fiber in the prototype fuselage was replaced with a foam core for the final aircraft. Due to the nature of honeycomb, a layer of adhesive must be used between the honeycomb and carbon fiber regardless of the type of carbon fiber used. Once again, this was additional weight in the fuselage that could be taken out by changing to a different material. While the honeycomb was stronger, the foam core

should be sufficiently strong to do the job. The sides of the fuselage and the bulkheads contained a foam core, while the bottom of the fuselage was 2 layers of carbon fiber. This method proved easier than attempting to bend the foam core from the sides to the bottom of the fuselage since the blue foam tends to break when bent around a sharp corner.

The fuselage for the final contest aircraft was initially made about 1 foot longer than necessary. Since center of gravity (CG) needed to be properly located within the fuselage, this gave the Flight Factory the flexibility of assembling all critical components of the aircraft and then cutting the fuselage to length for correct CG and payload location. Calculations for this length were performed for the prototype, but the lack of exact manufacturing techniques prevented the aircraft balance from being perfect. This new method will allow the exact fuselage length to be found.

Since the new contest strategy was to perform only two scoring sorties, this meant the availability of more power over a shorter period of time that could be delivered by the motor. This increase in power would allow the aircraft to carry more weight than the prototype. Taking this into consideration, the fuselage was designed to carry 6 liters of water, with the capability of adding a 7th liter in case the aircraft was able. The sixth bottle would lay horizontally atop the bottom wing. The seventh bottle would lay atop the sixth bottle, but would stick out above the top of the fuselage. Another set of fuselage lids was manufactured to force the seventh bottle inside the fuselage, and would be placed on the plane in a time of need.

Stabilizers:

Since white foam is approximately half the density of blue foam, the horizontal and vertical stabilizers were made from white foam instead of blue foam on the final contest aircraft. The prototype tail section proved to be over designed on strength and was also tail heavy. Switching to white foam not only reduced the overall weight of the aircraft, but helped correct the tail heavy tendencies of the prototype.

End Struts:

The end struts were modified to fit the new incidence angles of the wings. Since the end struts are the supporting members for the top wing, the angle at which they attach to the wings determines the decalage. Also, the kevlar on the outside of the end struts was trimmed from covering the entire outside, to just a strip matching up with the top and bottom wings. These strips of kevlar provide a very durable surface for the wing bolts to attach through the end struts to the wings.

Center Strut:

While performing a wing lift load of our prototype aircraft at full weight, it was determined that the top wing may not be strong enough under a high g-loading. Thus, a center strut made from a single steel wire was added to the center of the top wing. This wire was very lightweight and would transfer the force of the lifting load on the top wing into the bottom of the fuselage, where the wire was attached.

Motor Mount:

The overall size and shape of the motor mount performed in a desirable fashion. However, we found that the motor produced more vibration than expected so the motor was

attached to the aluminum mount through a piece of rubber on each side. The prototype had the motor mount attached with rubber to the fuselage, but not the motor to the mount.

Landing Gear:

The rubber wheels used on the prototype aircraft proved to have too much rolling resistance. For this reason roller blade wheels were chosen for the main gear of the final aircraft. The harder roller blade wheels will reduce ground friction and decrease take-off distance.

The shoe in the nose wheel brake was given 2 O-Rings instead of one, which helped seal the hydraulic fluid inside the brake system and increased braking power. A bleed screw was added to the brake system to aid in the removal of unwanted air from the hydraulic line. Additionally, the prototype nose gear was prone to bend during a hard landing. In order to strengthen the nose gear, the diameter of the aluminum shaft was increased. A side view of the final aircraft can be found in Figure 1.2.

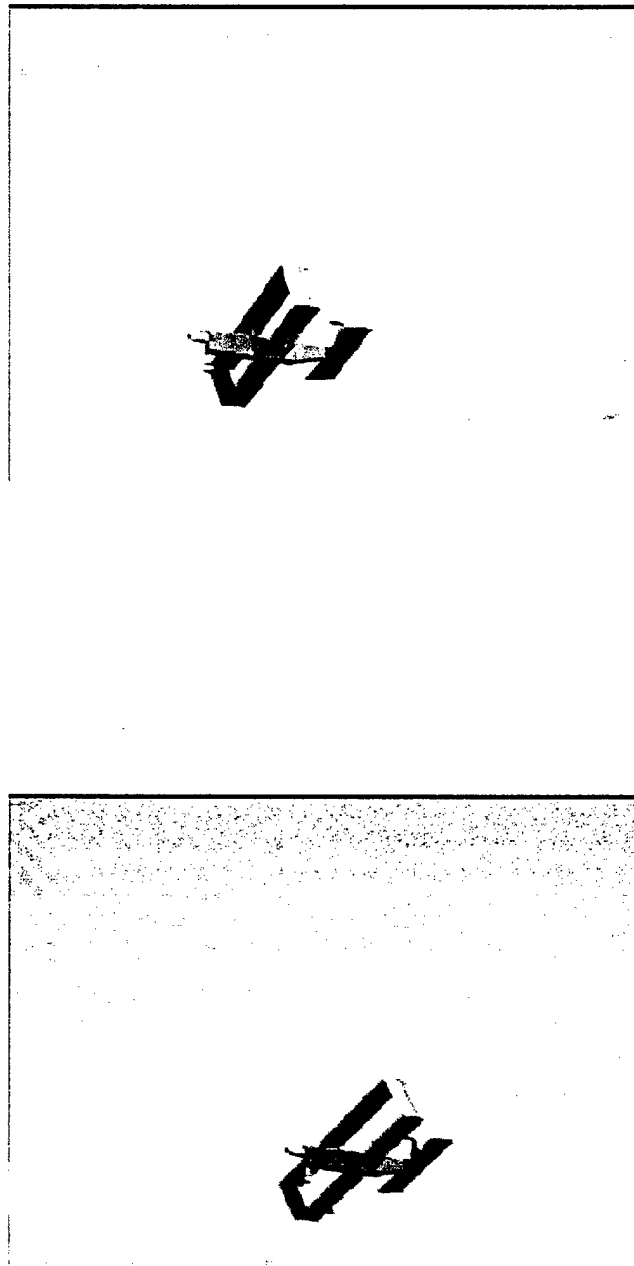


Figure 1.1: Prototype First Successful Flight

LESSONS LEARNED

	Prototype Test	Rating	Problem Description	Proposed Solution
Taxi :	Steering	Very Good	None	None
	Braking	Fair	Insufficient stopping power	Fix brake shoe
Flight 1:	Take-Off	Poor	Over 100 feet	Adjust Wing Incidence & Increase Power
	Climb	Poor	Did not climb	Increase Power
	Turn Left	-	-	-
	Turn Right	-	-	-
	Straight & Level Flight	-	-	-
	Descent	-	-	-
	Landing	-	-	-
	Sortie Flight Time	-	-	-
	Power	Poor	Insufficient Power	Increase Propeller diameter
Flight 2:	Take-Off	Very Good	None	None
	Climb	Very Good	None	None
	Turn Left	Fair	Insufficient Roll Power	Increase Aileron size
	Turn Right	Fair	Insufficient Roll Power	Increase Aileron size
	Straight & Level Flight	Good	None	None
	Descent	Good	None	None
	Landing	Good	None	None
	Sortie Flight Time	-	-	-
	Power	Very Good	None	None
Flight 3:	Take-Off	Very Good	None	None
	Climb	Very Good	None	None
	Turn Left	Fair	Insufficient Roll Power	Increase Aileron size
	Turn Right	Fair	Insufficient Roll Power	Increase Aileron size
	Straight & Level Flight	Very Good	None	None
	Descent	Good	None	None
	Landing	Good	None	None
	Sortie Flight Time	Very Good	None	None
	Power	Very Good	None	None

Table 1.1 - Summary of Lessons Learned from Prototype aircraft

2. Aircraft Cost

2.1 Final Competition Rated Aircraft Cost

The rated aircraft cost for the final competition aircraft is very important since it directly affects the score. To achieve the highest overall score the Flight Factory attempted to reduce RAC while reaping a high flight score.

Initially the Flight Factory planned on three, five liter scoring sorties within each ten minute mission. After flight testing it became apparent that our design needed too much power to achieve the endurance needed for three scoring sorties. At this point the strategy was to perform 2 scoring sorties with as much payload as possible. The wing area was left the same since increasing it would penalize our RAC. Instead more power was added to lift the extra weight without any more wing area. This power was delivered by increasing the propeller diameter since this did not hurt the RAC.

The final competition aircraft has two wings, each with a chord of .92 feet and a span of 6.98 feet. This results in a total wing area of 12.84 square feet. Since this area is distributed over 2 wings, the RAC receives a penalty of \$100 dollars. Including both wings at \$200 and the wing area at \$1027.2, the total RAC for the wings is \$1227.20.

The single fuselage is 5.83 feet long with one horizontal and one vertical stabilizer. With a cost penalty of \$100 per fuselage and \$80 per foot, the final RAC for the fuselage is 566.40. The vertical stabilizer cost \$100 and the horizontal costs \$200. There is also a basic charge of \$100 for the tail section. This results in a combined RAC for the fuselage and tail section of \$966.40

The propulsion system consists of 1 motor, 1 propeller and 36 battery cells. The motor and the propeller each cost \$100 dollars for a propulsion system RAC of \$200. The cells have an RAC of \$60 a each, for a total battery pack RAC of \$2160. The propulsion battery pack is by far the most expensive component of our aircraft in terms of RAC.

The aircraft control system uses 6 servos to control all operations of the airplane. There is a servo for each aileron, one for the elevator, one for the rudder, one for brakes, and another for steering. Each servo has a RAC of \$20 and the flight systems have basic charge of \$100. This results in a total flight systems RAC of \$220.

All components together, excluding the payload and propulsion batteries, weigh 15.1 pounds. At \$100 per pound, the cost for the aircraft empty weight is \$1510. When these parameters are applied to the Rated Aircraft Cost calculation, the OSU Flight Factory's final competition aircraft RAC is \$6.2836(thousands).

A complete breakdown and calculation of the final competition aircraft's RAC is found in Table 2.1. A breakdown of Rated Aircraft Cost for each of the airframe dependant parameters is found in Figure 2.1. As seen in the figure, the number of cells, aircraft empty weight, and the wing area make of 77% of the total RAC. Keeping the wing area low decreased the cost in 2 ways. There is a direct penalty for wing area, and the smaller wings have less weight.

The Flight Factory feels that this is a competitive RAC for the amount of payload the airplane is capable of ferrying during a 10 minute mission.

RATED AIRCRAFT COST

Airframe Dependent Parameters

# cells= 36	Projected Wing Area (sq. ft.)= 12.84
# engines= 1	Length of fuselage (ft)= 5.83
# propellers= 1	# Vertical Surfaces= 1
# Wings= 2	# Horizontal Surfaces= 1
#servos= 6	Empty Aircraft Weight (lbs)= 15.1
# fuselages= 1	

Coefficient	Description	Supplied Cost Model	Value
A	Manufacturers Empty Weight Multiplier	\$100/lb	\$100 /lb
B	Rated Engine Power Multiplier	\$1/watt	\$1 /watt
C	Manufacturing Cost Multiplier	\$20/hour	\$20 /hour
MEW	Manufacturers Empty Weight	Actual airframe weight, lb., without payload or batteries	15.1 (lbs)
REP	Rated Engine Power	# engines*50A*1.2V/cell*#cells	2160 (Watts)
MFHR	Manufacturing Man Hours	MFHR = SWBS hours	130.7 (hrs)
		WBS 1.0 Wing(s):	
		5 hr/wing	10.0 (hrs)
		+4 hr/sq ft Projected Area	51.4 (hrs)
		WBS 2.0 Fuselage and/ or pods:	
		5 hr/body	5.0 (hrs)
		+4 hr/ft of length	23.3 (hrs)
		WBS 3.0 Empenage:	
		5 hr (basic)	5.0 (hrs)
		+5 hr/Vertical Surface	5.0 (hrs)
		+10 hr/Horizontal Surface	10.0 (hrs)
		WBS 4.0 Flight Systems:	
		5 hr (basic)	5.0 (hrs)
		+1 hr/servo	6.0 (hrs)
		WBS 5.0 Propulsion Systems:	
		5 hr/engine	5.0 (hrs)
		+5 hr/propeller or fan	5.0 (hrs)

$$\text{Rated Aircraft Cost, \$ (Thousands)} = (A * MEW + B * REP + C * MFHR) / 1000$$

$$\text{Rated Aircraft Cost, \$ (Thousands)} = \$6.2836$$

Table 2.1 - Final Competition Aircraft's Rated Aircraft Cost

Distribution of Rated Aircraft Cost

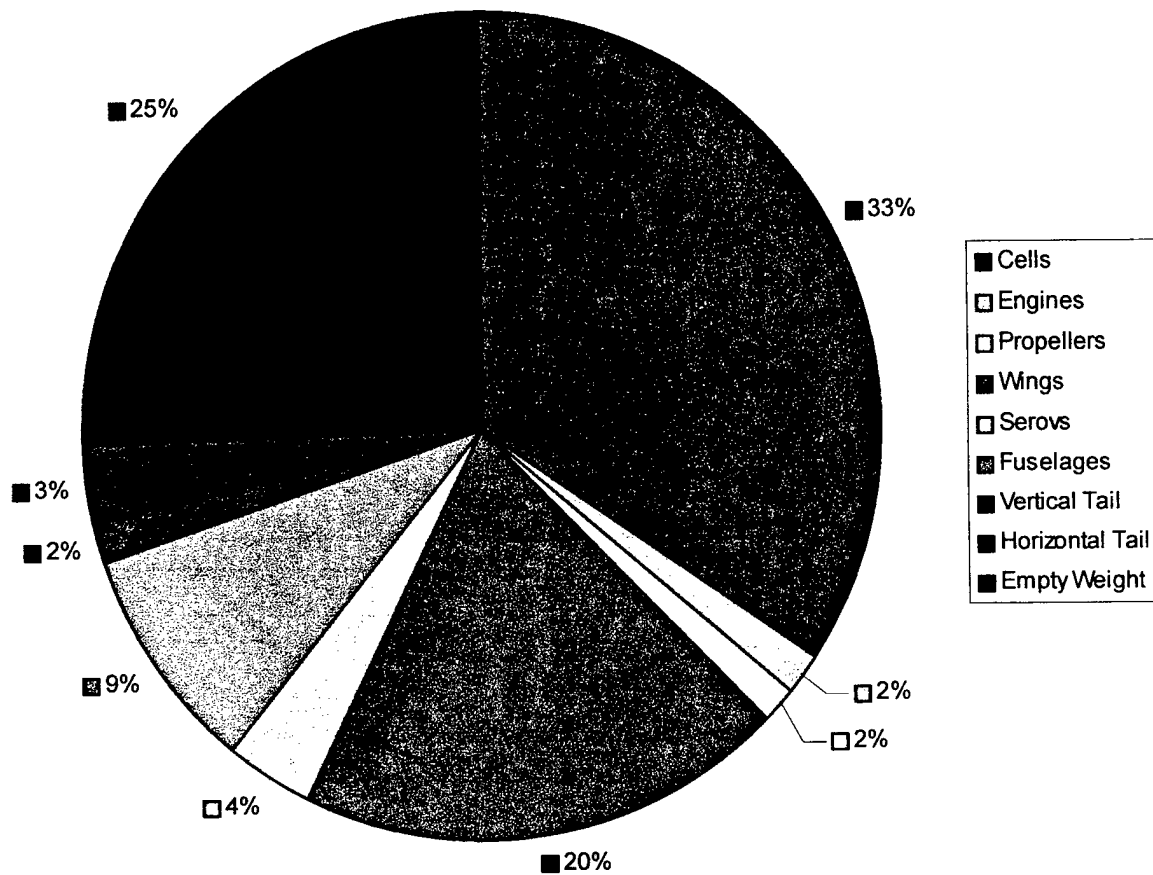
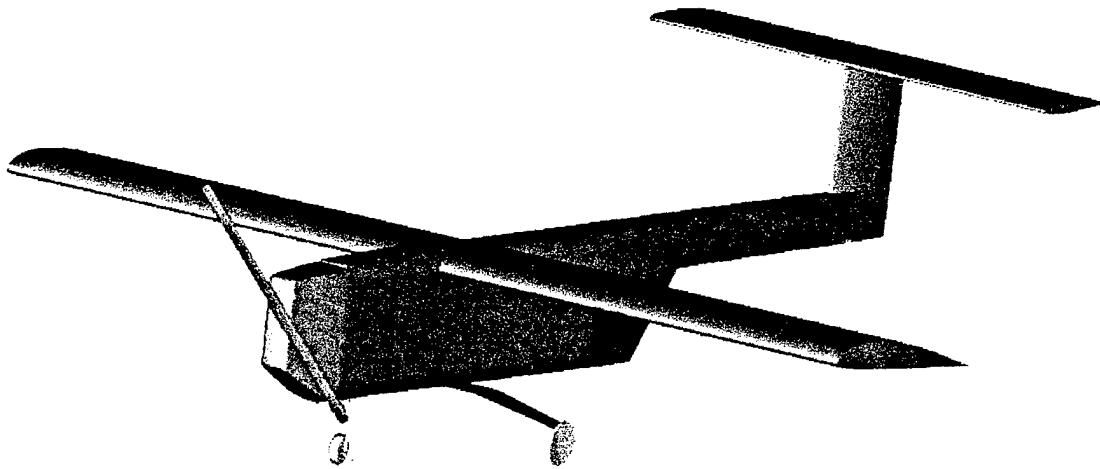


Figure 2.1: Distribution of Rated Aircraft Cost

2000 AIAA DBF Competition Design Report

——— *Proposal Phase* ———



Queen's University at Kingston

Team #1 – “Obsidian”

Department of Mechanical Engineering

Department of Engineering Physics

March 13, 2000

Table of Contents

Nomenclature	3
1.0 Executive Summary.....	5
1.1 Major Development Areas.....	5
1.2 Design Tool Overview.....	6
1.1.1 Conceptual Design	6
1.1.2 Preliminary Design	6
1.1.3 Detail Design.....	7
2.0 Management Summary	8
2.1 Personnel and Configuration	8
2.2 Schedule.....	9
3.0 Conceptual Design	10
3.1 Design Parameters	10
3.1.1 Power Train.....	10
3.1.2 Motor Placement	11
3.1.3 Wing Placement	11
3.1.4 Wing Design	13
3.1.5 Fuselage Design	15
3.1.6 Undercarriage.....	16
3.1.7 Tail Design	18
3.2 Figures of Merit.....	18
Drag Penalty.....	19
Weight Penalty	19
Performance	19
Ease of Manufacture	19
3.3 Concept Evaluation	19
3.3.1 Analytical Method.....	19
4.0 Preliminary Design	26
4.1 Take-off Gross Weight (TOGW) Estimation	26
4.2 Propulsion Systems Selection.....	26
4.3 Wing Area and Airfoil Selection.....	27
4.3.1 C_L at the Best Lift to Drag (L/D) Angle of Attack.....	27
4.3.2 Maximum C_L	27
4.3.3 Stall Characteristics	27
4.3.4 C_D at Expected Cruise AOA	27
4.4 Aspect Ratio.....	28
4.5 Tail Sizing.....	29
4.6 Airframe and Fuselage Sizing.....	30
5.0 Detail Design.....	32
5.1 Weight.....	32
5.2 Payload Fraction.....	32
5.3 Wing Performance.....	32
5.4 Tail Sizing.....	34
5.5 Fuselage Sizing.....	35
5.6 Drag.....	35
5.7 Total Drag.....	36
5.8 Power System.....	36

5.9 Control Systems	37
5.10 G-Loading.....	37
5.11 Structural Loading	37
5.12 Take-off Performance	38
5.12.1 Ground Roll.....	38
5.12.2 Climb out Distance	39
5.13 Turning Radius.....	40
5.14 Endurance and Range	40
5.14.1 Endurance	40
5.14.2 Range.....	40
5.15 Stability.....	41
5.15.1 Longitudinal Stability	41
5.15.2 Lateral-Directional Stability	41
5.15.3 Roll Stability	41
Manufacturing Plan.....	43
6.1 Wing Construction	43
6.1.1 Foam and Fiberglass	43
6.1.2 Built-up Construction	43
6.1.3 Carbon Fiber Monocoque	43
6.2 Fuselage Construction.....	44
6.2.1 Balsa Stringer.....	44
6.2.2 Corrugated Plastic	44
6.2.3 Molded Carbon Fiber.....	44
6.2.4 Fiberglass.....	44
6.3 Tail Construction	45
6.3.1 Foam and Fiberglass	45
6.3.2 Sheet Balsa.....	45
6.3.3 Built-up Construction	45
6.4 Undercarriage Construction.....	45
6.4.1 Aluminum	45
6.4.2 Tool Steel.....	45
6.4.3 Amarid, Carbon Fiber, and Structural Honeycomb	46
6.5 Figures of Merit	46
6.5.1 Weight.....	46
6.5.2 Structure	46
6.5.3 Skill	46
6.5.4 Expense.....	47
6.5.5 Time.....	47
6.6 Evaluation and Selection.....	47
6.6.1 Analytical Method	47
6.6.2 Construction Method Selection.....	47
Appendix A: Calculation Spreadsheets.....	50
Appendix B: References.....	51
Appendix C: Belt Drive detail.....	75
Appendix D: Drawing Package.....	78

Nomenclature

A	Parasite drag coefficient
A_{wetted}	Wetted area
AOA	Angle of attack
AR	Aspect ratio
a_m	Average acceleration on ground roll
Ac	Aerodynamic centre
B	Induced drag coefficient
C	Chord
C_D	Coefficient of drag
$C_{D\text{para}}$	Coefficient of parasite drag
$C_{D\text{induced}}$	Coefficient of induced drag
C_f	Skin friction drag coefficient
CG	Center of gravity
C_L	Coefficient of lift of wing
C_{Lh}	Coefficient of lift of stabilator
$C_{L\alpha}$	Derivative of C_L with respect to AOA
$C_{L\text{max}}$	Maximum coefficient of lift
C_M	Coefficient of pitching moment
c_p	Power coefficient
c_t	Thrust coefficient
D	Propeller diameter
D	Drag
d_c	Climb-out distance
d_r	Ground roll distance
d_{TO}	Take-off distance
E	Wing efficiency factor
G	Acceleration due to gravity
FOM	Figure of merit
H	Altitude
I	Mass moment of inertia
K	Form factor
L	Lift
M	Mass
M	Pitching moment
R	Turning radius
Re	Reynold's number
S_h	Stabilator planform area

S_w	Wing planform area
T	Thrust
$TOGW$	Takeoff gross weight
T	Maximum airfoil thickness
V	Velocity
V_{max}	Maximum cruise speed
V_{min}	Minimum cruise speed (stall speed)
V_{mean}	Mean velocity on takeoff roll
V_{stall}	Stall speed
V_{TO}	Takeoff speed
W	Fuselage Width
W	Weight
X_{CG}	Position of CG
X_{ACW}	Position of wing aerodynamic center
X_{ACH}	Position of stabilator aerodynamic center
X_{NP}	Position of stability neutral point
α	Angle of attack
β	Angle of bank
ρ	Air mass density
σ	Maximum stress
ε	Downwash angle
η	Efficiency
θ	Pitch Angle
μ	Dynamic viscosity
γ	Kinematic viscosity

1.0 Executive Summary

This year's entry to the Design/Build/Fly (DBF) marks a radical change from Queen's previous entries. For the first time since 1992, Queen's will be fielding two aircraft in a competition. The reuse of several major components (wing, motors) led to two teams being possible, with half of the club designing one aircraft and the other half of the club designing the second entry. It should be noted that although the teams did operate individually at times, as can be seen by the different design philosophies of the two aircraft, the majority of the time was spent working together to pool our resources. Such developments as the carbon fiber fuselages, the composite undercarriages, and the belt drives would not have been possible without the cooperation of both teams. The reports have been written by this coalition of students, with the individual report being tailored to the specific aircraft as required.

1.1 Major Development Areas

Queen's first entry, named "Obsidian" due to the fuselage matching the rich color of the mineral, exhibits several new and innovative design features and construction techniques in an attempt to produce the lightest and most efficient aircraft possible. The size of the aircraft is significantly larger than anything developed by Queen's in the past, and as such it required the design of a strengthened landing gear arrangement, a new method of producing fuselages, and a method of obtaining more thrust from the existing electric motor.

In the early days of conceptual design, Obsidian's layout was very similar to Queen's '98-'99 DBF entry. Limited by the motor system to a 3 liter design with approximately 800 square inches of wing area, it was felt that this was a good, solid design that could be successful. This design would expand on the experience gained by many years of building similar planes for the various Society of American Engineers' (SAE) and American Institute for Aeronautics and Astronautics (AIAA) model aircraft competitions. As similar aircraft had been built for several years, the design was well developed with many of the unknowns of designing an unmanned aerial vehicle (UAV) already have been solved.

Further examination of the *rated aircraft cost* penalty system led to the conclusion that the initial design would not be competitive. The final score could be radically improved by increasing the size of the aircraft to the point where it could carry the maximum 8 liters of payload around the course. As the motor system we possessed, a MaxCim N32-13Y with a 3.53 gearbox, would not provide the thrust necessary to lift such a craft, research and fundraising started for a larger brushless motor such as the MaxCim MegaMAX series.

It was at this point that a team member began spending time inputting different cell and motor combinations into the analysis program ElectriCalc, in an attempt to find the optimum motor to purchase. Through the course of this optimization, it was found that a smaller motor operating near its maximum RPM and current could produce as much if not more thrust than the larger motors once it had been mated to a very high ratio gearbox.

Further research indicated that an 11:1 reduction was necessary to allow our current motor to spin a 24X16 propeller. This design would produce approximately 11 lbs. of thrust with a 60 mph pitch speed, thus providing sufficient power to fly the 8 liter aircraft. Performance when loaded would be marginal, so work began to develop the lightest structure possible, and to develop techniques to ensure the craft would be able to takeoff within the allotted 100'.

Attention was turned to the wing's design. It was decided that Obsidian had to be a monoplane as it would be difficult to build the structure to separate the wings by a semispan

(for greater wing efficiency) without adding more weight than we could budget towards it. With the decision to construct a monoplane, research was started into high lift devices. The wing area could be reduced if the coefficient of lift could be increased temporarily for the critical takeoff run. Once airborne, the high lift devices could be retracted, thus reducing the effective area of the wing and decreasing the drag.

True Fowler flaps were discarded due to their complicated linkages, which could be unreliable and heavy. Regular camber flaps were discarded because they would not produce enough of an increase in the coefficient of lift. The design eventually chosen was a single slot flap with elongated pivots. The placement of the pivots would allow the flap to increase the wing area during partial deployment, similar to a Fowler flap, but would greatly simplify the mechanical set-up required.

With a primary design for the wing already established, work began on the fuselage. Upon examining the variety of construction options available, we chose to attempt a carbon fiber U-channel design. Working closely with Queen's solar vehicle team, the recognized composites experts on campus, a male mould was designed and built and composite fuselages were laid up and baked. The use of their facilities was invaluable to the success of Obsidian, producing a light, yet rigid fuselage, strong composite landing gear, and robust flap pivots.

Through the rest of the design process, the belt drive, high lift devices, and new fuselage construction technique were refined and combined with established theory and experience to produce Obsidian, Queen's most ambitious airplane to date.

1.2 Design Tool Overview

1.1.1 Conceptual Design

Throughout the conceptual design phase of Obsidian's development, a variety of tools were used to develop and evaluate different aspects of the aircraft's design. These range from reading model airplane oriented books and magazines, to research done on the internet, to making use of a spreadsheet detailing the *rated aircraft cost* penalty for the various designs.

This research exposed the team to a variety of successful aircraft configurations, which were then entered into the spreadsheet to analytically compare them with other designs. The same sources helped to educate the team on the design and characteristics of electrically powered airplanes, a relatively new and fluid field in model aeronautics.

1.1.2 Preliminary Design

Once the team entered this portion of the design process, the techniques used became more analytical than the quantitative methods used in the conceptual design. The *rated aircraft cost* spreadsheet was still used, but to screen slight variations of Obsidian's design rather than the large structural variations examined in the previous section. Component weight was measured, estimated, or obtained from manufacturing specification sheets to allow for some first iteration values to be generated. Simple aerodynamic formulae were used to determine such things as the coefficient of lift and tail sizing, and to determine areas that needed further development.

Computer software in the form of ElectriCalc and MotoCalc were used to obtain an estimation of the power system's performance once the belt drive had been built. The

information provided by these programs was used in conjunction with drive pulley formulae to design a belt drive reduction system able to withstand the loading required.

1.1.3 Detail Design

The final stage of the design process meant a transition to purely analytical methods. Classical aeronautical theory was used to determine such things as drag, stall speeds, takeoff rolls, and turning radii. These formulas were inputted into a master spreadsheet, so that slight changes in the plane's design would result in updated performance figures without hours of number crunching, which had been the case in previous years.

The final values obtained from this spreadsheet were used to produce the drawing package. Obsidian was drafted into AutoCAD 14 and later Mechanical Desktop 3.0 to obtain the required construction blueprints and to ensure that the components mated correctly.

2.0 Management Summary

2.1 Personnel and Configuration

Name	Year and Faculty	Responsibilities
David McCracken (Project Manager)	Junior- Mechanical Engineering	-Conceptual, Preliminary, and Detail Design -Drawing Package -Construction Supervisor
Eric Morrow	Senior- Engineering Physics	-Conceptual Design -Drawing Package -Stability Analysis -Undercarriage Preparation
Clement Lo	Sophomore- Computer Engineering	-Conceptual Design -Wing Construction -Graphics Design
Mat "Bruce" Easton	Junior- Mechanical Engineering	-Conceptual Design -Wing Construction -Composite Components
Laleah Carscallen	Sophomore- Applied Math	-Conceptual Design -Business Manager -Fuselage Construction
Shawn Ruff	Sophomore- Engineering Physics	-Conceptual Design -Fuselage Construction

The management structure chosen for this year's aero design team was very fluid, with team members changing tasks as required to meet deadlines. David McCracken was chosen to replace the departing Bruce Haycock (graduated May 1999) as project manager. His position on the team meant that he was responsible for calling meetings, ordering material, and ensuring that the rest of the team worked diligently on the different sections of the project.

Initially, the team remained as one entity so that the returning members could teach some of the basics of design and theory to the newer members. This period began with the team's first meeting in early October and continued until the conceptual design section was completed in mid-December. This slow start proved to be beneficial, as the team was able to take our '98-'99 Design/Build/Fly (DBF) aircraft on several test flights to give new members some first hand experience of what is expected from a competition aircraft.

With the real world experiences fresh in everyone's mind, the conceptual design stage began. David is an experienced modeler, and the group was able to brainstorm new and feasible alternatives with his guidance until the design was gelled as an eight-liter monoplane with a heavily geared MaxCim N32-13Y as the power plant.

With a design agreed upon, David and Eric began work on the preliminary and detail design, including the drawing package. Laleah began fundraising with Nicole Doucet (a member of Queen's second team) to raise funds to finance the construction of Obsidian and Minnow and to finance the trip to the actual competition in April. It should be noted that throughout the project, both Queen's teams worked very closely to ensure that maximum result could be obtained through our limited resources. This can be seen in the similarities of

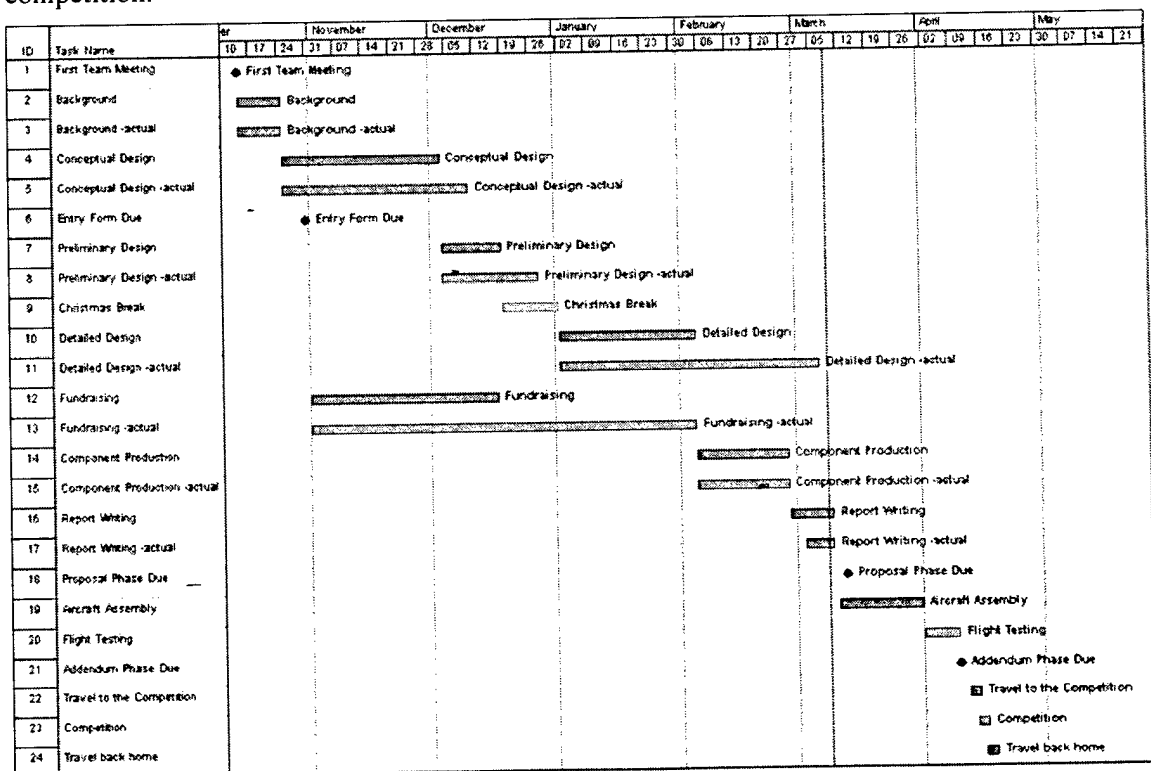
the two designs, although the different design philosophies of the two managers, David McCracken and Dave Young, are apparent when considering the payload capacities of the two aircraft. Both teams met with each other on a weekly basis during the conceptual design phase, and many composite components were pulled from the same mould to conserve resources. Similarly, the reports were written as a group to ensure that everyone who worked on the design and analysis of various components would be able to describe their contribution to both teams.

While Obsidian was being designed and drawn in AutoCAD 14 and Mechanical Desktop 3.0, the remainder of the team worked on an individual basis to investigate battery technology, speed control progress, working with composites, high lift devices, and wheel design. Weekly meetings continued through to the beginning of February, when it became time to start construction.

At this time, the team regrouped and then split up again to form the wing, fuselage, and tail teams. Each team was responsible for the construction of their section of the aircraft, with David helping and overseeing each group to ensure the assemblies would mate correctly. Work was paused for a two-week period to write the report, and then will be restarted to complete assembly and to perform test flying.

2.2 Schedule

The scheduling and timing of the team was the sole responsibility of David. Weekly meetings were announced via email, and the appropriate room bookings were always made to allow either the Obsidian team or both the Obsidian and Minnow teams to meet in a suitable conference room on campus. The actual timing of various events such as the deadline for having a design, and the deadline for having materials ordered were set by careful consideration of what needed to be done by the time of the competition, and of how long each would take. David's experience with model planes and with the DBF competition led to reasonable timeline, which was followed as closely as possible. Several unforeseen events did cause delays, but we still anticipate ample time for flight testing before the competition.



3.0 Conceptual Design

This year's DBF marks a radical change from the '98-'99 contest. Instead of brute force dominating the field, aircraft designers must now optimize their craft for the greatest efficiency possible within the payload, wingspan, and cost penalty systems applied. In the initial iterations, Obsidian resembled Queen's previous entry, a high winged, three liter design using a MaxCim N32-13Y brushless DC motor. Throughout this conceptual phase, the design expanded to a six liter biplane, then up to the final design chosen, an eight liter monoplane. Throughout the process, figures of merit (FOMs) were used in conjunction with a spreadsheet detailing the *rated aircraft cost* to refine the original concept into a competitive design.

3.1 Design Parameters

3.1.1 Power Train

Due to financial limitations, a MaxCim N32-13Y brushless DC motor was reused for this competition (having competed in the '98-'99 DBF). This motor has a maximum output of 1200 watts (1.59 hp), thus limiting the overall dimensions and weight of the airplane. However, there is a large variance in the actual performance of that can be obtained from this motor with different battery cell, gearing and propeller configurations. Based on basic design guidelines of radio controlled electric modelers, 88 watts per kilogram of plane (0.053 hp/lb.) is recommended for rise off ground (ROG) flight. Thus, the MaxCim should provide adequate power for a plane upwards of 13.6 kgs (30 lbs.), providing a large variety for design options. The use of more than one motor has a significant point penalty and does not offer an increase in efficiency or run time with the set battery pack weight.

With the battery pack weight limit set at 2.27 kg (5lbs), a tradeoff must be made between number of cells and capacity per individual cell. With a penalty for the number of cells used, fewer cells of a larger capacity would be more beneficial than a larger number of lower capacity cells, even if the total power of the pack is the same. Upon examining the power density of each individual cell, the Sanyo 3000CR was found to have a value of 1246 mAh/oz, which is significantly higher than the other high capacity cells like the Sanyo KR-2800CE (1165 mAh/oz) and the KR-5000DEL (1021 mAh/oz). Thus we decided to use the 3000CR cell for its superior power density, which would increase the available power for the flight.

Gearboxes are commonly used in radio controlled modeling to allow a motor to spin a larger diameter propeller at a lower rpm. The advantage gained through its use is a higher static thrust and better take-off run performance to the detriment of a reduced top speed. With the nature of this competition requiring multiple takeoffs within the sortie

and short cruising flight times between take-off and landing, a gearbox which allows quick takeoffs has the distinct advantage over an airplane geared for speed.

3.1.2 Motor Placement

Several different power-plant configurations were evaluated for use in this competition. Ducted fans were examined as a potential propulsion method, but due to their notoriously poor acceleration characteristics they were quickly rejected. Propellers are needed to provide the low speed thrust needed to perform a 30.48 m (100ft) take-off.

Propellers are generally used in either a tractor or pusher configuration. A pusher propeller allows the plane to fly in undisturbed air, reducing drag. However, this configuration has several drawbacks. It reduces the ground clearance of the propeller during takeoff rotation, and may require a longer, heavier landing gear. The push prop design lacks the inherent stability of the tractor configuration due to the location of the thrust vector behind the center of gravity, towards the tail. Finally, while the push-prop may allow the aircraft body to fly in undisturbed air, it places the propeller itself in the turbulent wake of the fuselage, reducing its aerodynamic efficiency. A tractor prop has the advantage of placing its prop wash over the tail surfaces, increasing their effectiveness at low speeds during taxiing and ground roll.

This prop wash can also be advantageous if the propeller is placed directly in front of the wing, providing a blown surface effect that increases the air velocity and lift over a portion of the wing. This technique would require a dual motor configuration or an asymmetrical thrust configuration. Dual motors were previously ruled out due to the incurred penalty. However, asymmetrical thrust provides an interesting alternative that has showed promise in some full scale developments, but would require further investigation than time permits during this project year.

3.1.3 Wing Placement

A wide variety of wing designs were considered throughout the design portion of this year's competition. Aside from the traditional high, mid, and low-wing designs, we also investigated bi- and multi-plane layouts, a parasol design, canard and tandem configurations, and also a three surface design.

A high wing design offers good lateral stability and reasonable wingtip clearance on take-off and landing. The wing can be faired into the fuselage to reduce interference drag, as well as allowing the load to be easily transmitted through the structure to the spar. Unfortunately, the positioning of the wing above the cargo compartment results in a difficult to access compartment, resulting in longer loading/unloading times.

A mid-wing design results in an aerodynamically stable model. Unlike the high wing, which will tend to right itself to level flight, a mid-wing will remain in a bank

indefinitely until pilot input is added to right the aircraft. The main disadvantage of this design in this competition is that the wing spar would have to pass right through the cargo compartment, leading to a more complex cargo hold and hatch design.

A low-wing design places the center of gravity above the wing spar. This produces an aircraft which is unstable and requires constant pilot input to control. Although the design does offer superior cargo access, the undesirable flight characteristics would be a serious problem in a contest that requires a large percentage of flight time be spent where precise and careful flying is essential: during landing and taking off.

A biplane design stacks two approximately equal sized airfoils one above the other. The main disadvantage of this design is that for the wings to operate at maximum efficiency, a minimum distance of one semi-span must separate the wings. The structure required to keep the wings this far apart would result in prohibitively high induced drag and weight.

A multi-plane design adds at least another wing to the biplane design. While this would increase the total lifting capability of the structure (increased wing area), it also adds a great deal of structural weight and drag to the airplane through the necessity of keeping each wing separated by a semi-span.

A parasol design was given consideration due to its inherent stability, which exceeds that of even a high wing aircraft due to the increased distance between the center of lift and the center of gravity giving a strong pendulum effect. This design is also attractive with a limited wingspan design criterion as the act of raising the wing above the fuselage increases the wing's effective span by adding the lift that is generated where the fuselage was formerly located. Unfortunately, this design involves a complicated bracing system to adequately transmit the payload weight to the wing spar. As the wing is elevated above the fuselage, this bracing system must be located in the slipstream, resulting in a high drag penalty.

A canard configuration was considered as a method of increasing wing area (a main wing and a smaller front wing), while reducing the aircraft cost rating by being able to omit the horizontal stabilizer. Unfortunately, canard equipped aircraft are known for their inherently long take-off rolls.

The front wing of a canard is given a higher wing loading than the rear main wing to ensure that the front wing will stall first. When the aircraft enters a low speed, nose high attitude, the front wing must stall first so that the nose of the aircraft drops and normal flight speed and attitude can be recovered. Unfortunately, the higher wing loading on the front wing is detrimental to the take-off performance because the plane cannot rotate as quickly as a conventional aircraft.

A tandem wing was evaluated for reasons similar to the canard design mentioned above. A tandem wing is an aircraft with a similarly sized wing located at the nose and tail of the fuselage. While this design does increase the wing area with little increase in frontal area and drag, the design suffers from the same take-off problems that the canard configuration does.

A three surface design was considered as a good alternative to the canard and tandem wing configurations. This design uses a conventional horizontal tail behind the two main lifting surfaces, positioning the elevator with enough of a moment arm to rotate the aircraft and permit short takeoffs. However, the necessity of having three wing spars passing through the fuselage limits the available cargo space and ease of loading.

3.1.4 Wing Design

The wing itself requires at least as much thought as the fuselage or propulsion system. The shape (airfoil, taper, aspect ratio) must be considered as well as any high lift devices or wing tip designs to ensure that the final structure will be able to provide enough lift to permit the plane to fly. Wing loading must be taken into consideration, but a general guideline is 25 oz/ft², with anything above 45 oz/ft² to be very difficult to fly.

The airfoil was the first wing characteristic to consider. There are four main choices in airfoil design and shape: fully symmetrical, semi-symmetrical, flat-bottomed, and undercambered.

The fully symmetrical airfoil does not produce any lift when the angle of attack is zero. Relying only on angle of attack for its lift, the wing is ideal for inverted flight and for use on lightly loaded aircraft. Unfortunately, the maximum coefficient of lift is around 0.9.

The semi-symmetrical airfoil produces moderate lift at a zero angle of attack (a coefficient of lift around 0.2). This airfoil is an excellent choice for most semi-aerobatic aircraft and is able to carry moderate wing loading. At the maximum angle of attack, C_L is around 1.1.

The flat-bottomed airfoil is thicker than either the semi or fully symmetrical wings and thus has higher lift at the penalty of increased drag. A typical coefficient of lift at a zero angle of attack is 0.4 and this can increase with the angle of attack to around 1.4. Performance is usually very stable and such wings are used on most docile aircraft and trainers.

The undercambered airfoil has the highest lifting capability of the four. Coefficient of lift begins around 0.5 at a zero angle of attack and it can increase to 1.6 at maximum. Unfortunately, this comes at a high price. These high performance airfoils require razor thin trailing edges, which are delicate and difficult to build, and they often exhibit undesirable flight characteristics such as wingtip stalling.

High lift devices allow the coefficient of lift of the wing to be changed for varying flight situations. Consisting of such things as camber flaps, slotted flaps, Fowler flaps, and leading edge slats, they are moveable flight surfaces, which can be deployed to

increase drag and lift on landings and takeoffs, and yet can be retracted to a streamlined shape for increased efficiency at cruise.

The problem with flaps is that deploying them can change the pitching moment of the wing, which can result in the plane nosing down into a dive, or up into a stall. To remedy this, the flaps can be built so that they only slightly affect the pitching moment. By building the flaps so that they measure 30% of the wing's chord, the geometry results in a very smoothly operating flap, which upon deployment keeps the plane's attitude constant but still slows the craft down due to the extra drag.

Camber flaps are the most common used on model aircraft. Consisting of a web hinge similar to an aileron, they can increase the maximum lift by 50%. They are very simple to construct, using a simple linkage, and result in a very light device.

Slotted flaps are rare on model aircraft, but they are common on full-sized planes. The channeled airflow over the flap results in an increase of maximum lift of 65%. While the linkages are more complex than the camber flaps, they are still within the grasp of most modelers.

Fowler flaps are rare on both model aircraft and full-sized planes. Their complicated linkages can move a flap out to increase the maximum lift by 90%, but the actual mechanics are heavy and difficult to construct.

Leading edge slats can increase the maximum lift by 60% but they have a serious problem. By being on the leading edge, the joint between the retracted flap and the rest of the wing must be perfect or else airflow separation may occur. This would destroy the lifting efficiency of the wing and may endanger the aircraft.

Wing tips are considered by many to be a "black art". They are still under heavy development and the aeronautical community has not agreed on the "ideal" wingtip at this time. The goal of any wing tip is to reduce or redirect the wingtip vortices, thus increasing the effective efficiency of the wing. This can be accomplished by tip plates, Horner wingtips, or by winglets.

Tip plates are thin pieces of wood or plastic cut slightly larger than the airfoil and glued to the end of the wing. The theory is to simulate the "infinite span" wing seen in a wind tunnel situation. As the test wing stretches from one wind tunnel wall to the other, there is no opportunity for wing tip vortices to form. By gluing on the tip plates, it is effectively gluing on a portion of the "wall", and the vortices, while not completely gone, are reduced.

Horner wingtips are sculpted in such a way to channel the tip vortices out and down from the wing. This prevents them from disturbing the air flowing over the wing, and may also impart some lift. Unfortunately, while the wingtips are often used on full-sized aircraft, they are prone to damage on models, where scraping a wing tip on landings is not totally uncommon.

Winglets are the most complicated of wing tip devices. Consisting of a separate airfoil mounted vertically (or inclined) from the main wing's tip, they disrupt the tip vortices so that they do not disturb the airflow across the wing. Winglets are application specific and require hours of computational fluid dynamics with the specific main wing to ensure that they will perform as expected.

3.1.5 Fuselage Design

Once the wing has been designed, the next step is to examine the fuselage. There are a wide variety of possible fuselage designs, each with their own advantages and disadvantages. The general designs considered were conventional, double, blended, and a flying wing.

The conventional fuselage is exactly as implied by its name – conventional. It consists of a long structure, square, round, or oval cross-sectioned, with the wing(s) mounted at approximately at third of its length, and the tail appendage mounted at the rear. Cargo is held in a tubular bay centered under the wing's spar and can be loaded from either the top, the bottom, or either end, depending on the configuration of the final design.

This type of fuselage is easy to build and provides a solid base to mount the landing gear while still providing enough clearance for the propeller. The design is not the most streamlined choice, but with drag reduction techniques, the drag penalty can be reduced to an acceptable value.

The double fuselage consists of two parallel conventional fuselages separated by a section of the wing. This design is utilized when extra cargo space is required and twin engines are to be used. The fuselages provide storage for the power train, and the remainder of the volume can be used for cargo in a fashion similar to the conventional fuselage mentioned above.

This design offers a solid mounting surface for the undercarriage and, so long as the fuselage spacing is adequate, it provides sufficient propeller clearance. Unfortunately, this is the least streamlined design that we considered. The fuselages provide a huge surface area for their volumes, and the interference drag between the assorted wing, horizontal tail, and fuselages becomes prohibitive.

The blended fuselage is a compromise between a flying wing and a conventional fuselage. It is made up of a large, flat fuselage in an approximate airfoil shape. This fuselage is then faired into the wing to produce a low-drag surface. The fuselage then continues as either a single or twin boom design to support the tail structure.

Cargo is held in rectangular bays between the wing structure and access is usually obtained through the top, though care should be taken to ensure that the hatches are

perfectly flush with the top surface of the fuselage to prevent a flow separation bubble from forming. The fuselage does produce some lift, and thus must be treated as an airfoil to prevent unnecessary drag and thus destroying the streamlining advantage of such a design.

This configuration does not allow a very large propeller to be used, as there is very little, if any, fuselage under-hang beneath the wing to mount the undercarriage. The undercarriage is often affixed to the wing spar further out along the wing to provide a wide wheel track and to provide good ground handling, but this does not raise the wing/fuselage to the height enjoyed by the other designs examined above.

The tail of this design must be designed with extreme care to ensure that it will not be blanketed by the wing/fuselage during flight maneuvers. The boom(s) should be inclined upwards to remove the tail surfaces from the turbulent air behind the main structure, so they can enjoy clean undisturbed air to operate in.

The flying wing is the final extreme of blending the fuselage into the wing to reduce drag. In this configuration, the fuselage does not exist like it does on a conventional airplane or even like on the blended fuselage design. There is no bulge beyond the typical airfoil section of the wing other than for the propeller mounting. The cargo compartment is totally enclosed between the structure of the wing, and is usually unloaded from the top. Care must be taken with the hatch covers to ensure that they fit well, in a similar fashion to the blended fuselage design mentioned above. This configuration results in the absolute minimum drag that is practical with propeller driven model aircraft. It should be noted that a flying wing does not exhibit the stability common to most conventional aircraft. The flying wing must be very carefully designed with this in mind.

The flying wing's undercarriage is fastened to the wing spar, but it cannot raise the wing very high off the ground because the loads on the landing gear attachment points would require prohibitively heavy reinforcing. As such, the flying wing cannot utilize a propeller with a very large diameter when compared to a conventional design.

3.1.6 Undercarriage

The undercarriage is the most abused portion of the aircraft, yet its safe and consistent operation is essential. Although there are a wide variety of landing gear configurations, they can be subdivided into three main categories: tricycle gear, tail dragger gear, and bicycle gear. The two first choices are very common among, and the bicycle gear configuration appears only occasionally among specialty aircraft.

The tricycle gear configuration places two main wheels slightly behind the aircraft's center of gravity in a parallel arrangement, with one wheel on each side of the fuselage. A third, medium-sized wheel is then placed at the nose of the aircraft, resulting in a gear

configuration that resembles a child's tricycle. The advantages of this design is that the plane remains at close to a zero angle of attack while on the ground, reducing drag and improving ground handling, while still permitting the pilot to see what is in front of the aircraft. While visibility is not an issue with model aircraft, ground handling and drag reduction are. A tricycle gear equipped plane will often have a shorter take-off run and greater resistance to nosing over on landings than the other common design, the tail-dragger.

Unfortunately, this type of undercarriage suffers from the highest drag of the three designs. As all three wheels are relatively large, the air resistance encountered can be substantial and should be evaluated against the benefits of this design.

A tail-dragger design uses parallel main wheels similar to the tricycle gear configuration, with the main difference being their positioning relative to the aircraft's center of gravity. The main gear is located ahead of this center of gravity, thus giving the plane a distinct tail down attitude (thus it "drags its tail"). To ensure control, a very small wheel is attached to the rear of the fuselage to provide some directional control at low speeds.

In a take-off run, the plane rolls on all three wheels until it reaches a velocity that permits the elevator to produce a force great enough to raise the tail off the ground. Because of the severe nose-up attitude, the wing and fuselage's angle of attack produces a great deal of drag, thus slowing the aircraft's acceleration and lengthening the take-off run. When the tail lifts off the ground, the fuselage rotates so that it is parallel with the airflow, reducing drag. The aircraft then accelerates quickly and takes off.

In flight, the tail-dragger exhibits less drag than a tricycle gear configuration. This is due to the replacement of one medium sized wheel at the front of the fuselage with a very small wheel at the rear. The disadvantages of the tail-dragger design are apparent on landings. Because there isn't a wheel situated at the front of the aircraft, they are prone to nosing over on landings, resulting in propeller and perhaps structural damage. In a competition where a great deal of time is spent on the ground, the undesirable ground handling characteristics of this configuration must be considered versus the reduced drag in flight.

A bicycle gear configuration is seen where drag considerations are paramount over ground handling characteristics. It is often seen on glider aircraft, or occasionally on high performance military aircraft and may be used in conjunction with small stabilizing wheels on the wing tips. The design consists of two narrow wheels mounted in series along the centerline of the fuselage. This technique lends itself to smooth fairing, which can reduce drag even further. Unfortunately, their ground handling characteristics are poor at best. With both wheels mounted along the centerline, there is little to no lateral stability at low speeds before the ailerons become effective.

3.1.7 Tail Design

The careful design and configuration of the tail is essential to ensure good flight characteristics of the final aircraft. Tail efficiency can be greatly improved if the elevator is removed from the wing's downwash (50% efficiency of a conventional tail versus 90% efficiency of a high T-tail), but more exotic configurations may require greater care in building to ensure that weight does not increase by a large margin. The typical tails seen on model aircraft are the conventional tail, the T-tail, and the V-tail.

The conventional tail uses a vertical fin and rudder mounted along the fuselage's centerline. There is a horizontal stabilizer and elevator then mounted along the fuselage at the base of the fin. This design is the most common, robust, and simple tail appendage, but it places the horizontal surfaces in the wing's downwash, thus reducing their effectiveness. To compensate for this, the tail's planform area must be increased to permit an acceptable force to be created by the elevator.

The T-tail is occasionally seen where high efficiency is required. The vertical surfaces are identical to those of a conventional tail, but they must be built slightly heavier to provide enough strength. This strength is required because the horizontal flight surfaces are mounted to the top of the fin, thus removing them from the wing's downwash and allowing them to operate in undisturbed air. The increased efficiency can be translated into a surface with a smaller planform area, thus partially compensating for the increased structural weight of the fin. This design's chief advantage is that the smaller horizontal surfaces and the removal of wing tip vortices from the end of the fin (the stabilizer acts as a large tip plate), reducing the drag of the tail.

The V-tail configuration is rarely seen except where drag reduction is the chief concern. The design uses two flight surfaces mounted at an angle at the rear of the fuselage. By combining the vertical and horizontal surfaces, the total tail surface area is reduced, thus reducing the weight and drag. Unfortunately, the design requires complicated control linkages (or a computerized radio), and has been known to be unable to recover from stalls and spins due to a blanketing effect of one control surface on the other.

3.2 Figures of Merit

Each configuration was analysed based on its advantages, disadvantages, and *rated aircraft cost penalty*. A summary of the FOM for each design is given along with the relative weighting factor.

Drag Penalty

This is a measure of the relative drag penalty of the design. A higher drag structure would negatively affect the final aircraft's range, takeoff performance, and maximum speed and should be avoided if possible. This FOM was assigned a weighting factor of 4

Weight Penalty

This is a measure of the relative weight of the given design. Due to the minimal reserve power budget, extra weight should be avoided at all cost to ensure adequate flight performance of the aircraft. This FOM was assigned a weighting factor of 5

Performance

This is a measure of how efficient the design is. A large, heavy component would receive a lower score than a small, well-designed alternative. This FOM was assigned a weighting factor of 4

Ease of Manufacture

This is a measure of how easily it is to incorporate the configuration into the final design. More exotic and complicated technologies demand more resources, thus this FOM was given a weighing factor of 4

3.1 Concept Evaluation

3.3.1 Analytical Method

An evaluation of competing concepts under each design parameter was conducted by rating each concept on a scale of 0 to 5, with 5 being the best choice based on the qualitative considerations described above. The rating were then multiplied by the weighing factor of each FOM, summed, and then the score was divided by the relative aircraft cost penalty to produce a final score for each concept. (Table 3.1)

It should be noted that the flying wing was found to be superior to the conventional fuselage in the FOM. This is not surprising, flying wings have been sought after for years for their superior drag characteristics. Unfortunately the absence of a tail appendage results in unpredictable flight performance without a large amount of development. For this reason, the second place entry, the conventional fuselage, was chosen for its good established flight characteristics on the basis that a stable, trouble-free airframe would be superior to a delicate one in this type of rigorous competition.

Figure 3.1 Conceptual design evaluation

	Drag (4)	Weight (5)	Performance (4)	Ease of manufacture (4)	Rated aircraft cost	Total
Motor						
Tractor	3	5	4	4	1	69
Pusher	3	5	3	3	1	61
Twin	2	3	5	2	2	25.5
Asymmetrical	3	4	4	2	1	56

Wing Placement						
High	4	4	4	4	1	68
mid	5	4	3	3	1	64
Low	4	4	3	4	1	64
Biplane	3	3	3	3	2	25.5
Multiplane	2	3	2	3	3	14.3
Parasol	3	2	4	2	1	46
Canard	4	3	3	2	1	51
Tandem	4	3	3	2	1	51
Three surface	4	2	4	2	2	25

Wing Design						
Fully symmetrical	5	5	2	4	1	69
Semi-symmetrical	4	5	3	4	1	69
flat-bottomed	4	5	4	5	1	77
Undercambered	3	4	3	3	1	56

High Lift Devices						
Camber flaps	4	5	1	5	1	65
Slotted flaps	4	4	4	4	1	68
Fowler flaps	4	2	5	1	1	50
Leading edge slats	3	2	3	1	1	38

Wing Tips						
tip plates	3	4	3	5	1	64
Horner wing tips	4	3	4	4	1	63
Winglets	3	3	4	2	1	51

Fuselage						
Conventional	3	4	4	4	2	32
Double	2	2	3	3	4	10.5
Blended	4	3	4	3	2	29.5
Flying wing	5	3	3	1	1	51

Undercarriage						
Tricycle	3	3	5	4	1	63
tail dragger	4	4	3	3	1	60
Bicycle	5	5	1	2	1	57

Tail						
Conventional	3	4	4	5	1	68
T-tail	4	3	5	4	1	67
V-tail	5	4	3	3	1	64

Cessna / ONR Student Design / Build / Fly Competition

Description	Coefficient	Variables	Description	Values
-------------	-------------	-----------	-------------	--------

large chord
monoplane
conventional tail
single fuselage
single motor

FLIGHT SCORE

Liters of Water Carried Multiplier	Water Load	$10 * n$	Water Load =	80
Liters of Water	n	number of liters	n =	

RATED AIRCRAFT COST

Manufactures Empty Weight Multiplier	A	$\$100 * MEW$	A = \$	1,400.00
Manufactures Empty Weight	MEW (pounds)	airframe weight	MEW =	

Rated motor Power Multiplier	B	$\$1 * REP$	B = \$	1,620.00
Rated motor Power	REP (watts)	$\# \text{ motors} * 50A * 1.2V/cell * \# \text{ cells}$	REP =	1620
			# motors =	
			# cells =	20

Manufacturing Cost Multiplier	C	$\$20 * MFHR$	C = \$	2,460.00
Manufacturing Man Hours	MFHR (hours)	Prescribed assembly Hours by WBS	MFHR =	123
		MFHR = the sum of WBS		
		Wings WBS = 5hrs/wing + 4 hrs / sq foot	Wing WBS =	53
			# wings =	
			area (sq.ft) =	

Fuselage WBS = 5hrs/body + 4hrs / foot	Fuselage WBS =	33
	# bodys/pods =	
	length (ft) =	

Empenage WBS = 5 hrs + 5 hrs/vert surf	mpenage WBS =	15
	# vert. surfaces =	
	# horz. surfaces =	

Flight Systems WBS = 5 hrs + 1 hr/ serv	light Sys. WBS =	12
	# servos =	

Propulsion Systems WBS = 5 hrs / motor	ropulsion WBS =	10
	# motors =	
	# props =	

Single Flight Score	SFS	Flights * Water Loads	SFS =	240
	Flights	Is the number of water caring flight within	# flights =	

Written Report Score	WRS	Score on written report as assigned by ju	WRS =	
		note -a written score of 87 was used as a constant		

Total Flight Score	TFS	3*single flight	TFS =	720
--------------------	-----	-----------------	-------	-----

Rated Aircraft Cost	RAC (\$1000)	$(MEW + REP + MFHR) / 1000$	RAC =	5.48
---------------------	--------------	-----------------------------	-------	------

FINAL SCORE	Final Score	Written Report Score * Total Flight Score	FINAL SCORE	11430.65693
-------------	-------------	---	-------------	-------------

Description	Values
large chord	
monoplane	
conventional tail	
single fuselage	
twin motor	
Water Load =	80
n =	

A = \$	1,500.00
MEW =	

B = \$	4,800.00
REP =	4800
# motors =	
# cells =	

C = \$	2,660.00
MFHR =	133

Wing WBS =	53
# wings =	
area (sq.ft) =	

Fuselage WBS =	33
# bodys/pods =	
length (ft) =	

Empenage WBS =	15
# vert. surfaces =	
# horz. surfaces =	

Flight Sys. WBS =	12
# servos =	

Propulsion WBS =	20
# motors =	
# props =	

SFS =	240
# flights =	

WRS =	
-------	--

TFS =	720
-------	-----

RAC =	8.96
-------	------

FINAL SCORE	6991.071429
-------------	-------------

Description	Values
small chord	
biplane	
conventional tail	
single fuselage	
single motor	
Water Load =	80
n =	

A = \$	1,500.00
MEW =	

B = \$	1,620.00
REP =	1620
# motors =	
# cells =	

C = \$	2,640.00
MFHR =	132

Wing WBS =	58
# wings =	
area (sq.ft) =	

Fuselage WBS =	33
# bodys/pods =	
length (ft) =	

Empenage WBS =	15
# vert. surfaces =	
# horz. surfaces =	

Flight Sys. WBS =	16
# servos =	

Propulsion WBS =	10
# motors =	
# props =	

SFS =	240
# flights =	

WRS =	
-------	--

TFS =	720
-------	-----

RAC =	5.76
-------	------

FINAL SCORE	10875
-------------	-------

Description	Values
big chord	
monoplane	
V tail	
single fuselage	
single motor	
Water Load =	80
n =	1

A = \$	1,400.00
MEW =	12

B = \$	1,620.00
REP =	1620
# motors =	2
# cells =	2

C = \$	2,460.00
MFHR =	123

Wing WBS =	53
# wings =	1
area (sq.ft) =	12

Fuselage WBS =	33
# bodys/pods =	1
length (ft) =	1

Empenage WBS =	15
# vert. surfaces =	1
# horz. surfaces =	1

Flight Sys. WBS =	12
# servos =	1

Propulsion WBS =	10
# motors =	1
# props =	1

SFS =	240
# flights =	1

WRS =	1
-------	---

TFS =	720
-------	-----

RAC =	5.48
-------	------

FINAL SCORE	11430.65693
-------------	-------------

Description	Values
large chord	
flying wing	
vertical fin	
no fuselage	
single motor	
Water Load =	80
n =	1

A = \$	1,000.00
MEW =	10

B = \$	1,620.00
REP =	1620
# motors =	2
# cells =	2

C = \$	1,840.00
MFHR =	92

Wing WBS =	61
# wings =	1
area (sq.ft) =	14

Fuselage WBS =	0
# bodys/pods =	0
length (ft) =	0

Empenage WBS =	10
# vert. surfaces =	1
# horz. surfaces =	0

Flight Sys. WBS =	11
# servos =	0

Propulsion WBS =	10
# motors =	1
# props =	1

SFS =	240
# flights =	1

WRS =	1
-------	---

TFS =	720
-------	-----

RAC =	4.46
-------	------

FINAL SCORE	14044.84305
-------------	-------------

Description	Values
large chord	
flying wing	
vertical fin	
podded fuselage	
single motor	
Water Load =	80
n =	

A = \$	1,000.00
MEW =	

B = \$	1,620.00
REP =	1620
# motors =	
# cells =	

C = \$	2,260.00
MFHR =	113

Wing WBS =	61
# wings =	
area (sq.ft) =	

Fuselage WBS =	21
# bodys/pods =	
length (ft) =	

Empenage WBS =	10
# vert. surfaces =	
# horz. surfaces =	

Flight Sys. WBS =	11
# servos =	

Propulsion WBS =	10
# motors =	
# props =	

SFS =	240
# flights =	

WRS =	
-------	--

TFS =	720
-------	-----

RAC =	4.88
-------	------

FINAL SCORE	12836.06557
-------------	-------------

4.0 Preliminary Design

4.1 Take-off Gross Weight (TOGW) Estimation

The first step in the preliminary design phase was estimating the gross weight of the aircraft, as this parameter is crucial in determining its size and performance. To determine the TOGW, it was necessary to compile the individual weights of known components needed for the aircraft and estimating various airframe structures.

With a designed cargo capacity of 8 liters, this yielded a cargo weight of 8.8 kg (each bottle weights 0.1 kg) or 19.4 lbs. A large plane would be needed to carry this load and research was done into commercial model airplanes of this size to check if our weight estimates were close. Typical sport models with a wingspan close to 7 ft were found to weight between 5kg and 10 kg (11 to 22 lbs.). With carefully weight management and engineering, an empty airframe weight of 4 kg was expected. Along with a 2.3 kg battery pack (5lbs) and the payload, a TOGW of 15 kg (33lbs) seemed reasonable.

4.2 Propulsion Systems Selection

The propulsion system was selected so as to provide the maximum possible thrust and efficiency in order to make the best use of available battery power. MaxCim, Aveox, and Astroflight motors were compared based on their published efficiencies, predicted performance, cost, and their performance in past competitions. MotoCalc and ElectricCalc, commercial software packages, were used to compare the various possible configurations of motor, controller, gearbox, propeller, and batteries for their efficiency, thrust, and estimated run-time.

With a MaxCim MaxNEO 13Y and a MaxCim N32-13Y motor on hand, both providing powerful and efficient thrust, and our team suffering from an unsure budget, the decision was made early in the design phase to use these motors. Unfortunately, commercially available gearboxes would not allow us to maximize the potential of these motors, and thus a reduction drive needed to be produced. Using ElectricCalc and Motocalc, many gearbox configurations were examined and a final configuration of an 11:1 reduction unit and 26 3000mAh cells would produced a maximum of 12lbs of thrust in cruise 15lbs of static thrust.

The batteries were selected by comparing weight, capacity, internal resistance and power density. Sanyo N-3000 CR mAh cells were found to the highest power density between the different size cells of batteries. With the 2.3 kg (5 lbs.) battery pack limit, the maximum number of these cells that could be used is 26. This configuration provided the correct voltage and amperage needed for maximum thrust and efficiency.

The design of a custom motor reduction drive became of prime importance. A light, efficient and strong drive would be needed to transmit the power from the motor to propeller with minimal losses. An 11:1 reduction was not feasible with a gear drive without multiple steps, lowering efficiency. The other option was a belt drive, although a V-belt was quickly

ruled out due to the necessary tension and loss in this method. Thus a toothed belt drive was selected in order to drive the propeller with minimal resistance.

4.3 *Wing Area and Airfoil Selection*

The wing area and airfoil were chosen based on the lift requirements at the expected cruise speed, as well as take-off performance, stall characteristics, and induced drag estimates. The FOMs used in the selection are as follows.

4.3.1 C_L at the Best Lift to Drag (L/D) Angle of Attack

The C_L at best L/D was used to gain insight into the amount of lift the wing would produce while operating at peak efficiency. This was considered important since the more lift the airfoil generates, the smaller the wing area can be, thus reducing drag.

4.3.2 Maximum C_L

The maximum C_L was considered to be important as this determines the stall speed, take-off speed, and maximum g-loading for a fixed wing area. Due to the requirement for take-off within a limited distance and the energy advantage obtained by minimizing the amount of time in climb, a high C_L was considered advantageous. In addition, this also allows for high-g maneuvers without the onset of an accelerated stall, giving the aircraft the ability to use a minimal turning radius and effectively shortening each lap.

4.3.3 Stall Characteristics

Like many other parameters, this FOM arises from past experience. An airfoil with a more docile stall is considered to be significantly advantageous in the event of an unplanned circumstance, particularly just after rotation. A gentler stall will increase the time available to react and increase the likelihood of recovery. The stalling characteristics were compared based on published lift and drag data, and on previous experience in observing the in-flight stall characteristics of most of the airfoils considered.

4.3.4 C_D at Expected Cruise AOA

Due to the restrictions on available battery power, once a maximum thrust is achieved through careful selection of a motor and electronics, the top speed can only be increased through drag reduction. The airfoils were compared at the expected cruise C_L , where the drag will have the most influence on performance.

The airfoil was selected based on these criteria, along with initial calculations for the estimated gross weight and airspeed. The gross weight was taken as 15kg (33 lbs.), as estimated in section 4.1. The cruise speed was estimated based on data from ElectriCalc using an airplane with worst case $C_d=0.06$, and adjusting the weight and wing area. Initially, the wing surface area was taken as 1.084 m^2 (11.67 ft^2). This gives a rough estimate of top speed of 25.5 m/s (83.7 ft/s or 57 mph). From this, the C_L at cruise was determined from the standard lift equation. Three-dimensional effects reducing the overall lift of the wing will be more thoroughly examined in the detailed design when the final wing configuration has been selected.

$$C_{L \min} = \frac{2L}{\eta \rho S_w V_{\max}^2}$$

Where η is the efficiency of the wing, assumed to be 0.75, and L is the total lift required (equal to the gross weight).

This gives a required C_L of 0.46 ± 0.1 . Take-off speed, stall speed, and maximum g-loading were examined next to define the required limits on the C_L . ElectriCalc also provided minimum speeds and cruise speeds and these values were used to estimate the maximum C_L required. Using the same C_L formula as above, replacing V_{\max} with V_{Stall} gives a required maximum C_L of 2.3 ± 0.1 . This value is quite high and not obtainable from most airfoils. Not wanting to reduce the aspect ratio any further, which would dramatically increase the drag, it was decided to employ high lift devices in the wing to achieve the higher C_L needed only for takeoff and landing. Fowler flaps, although difficult to construct would increase the C_L by about 90% when deployed to 40 degrees. Although only 20 degrees would be used at takeoff, this, combined with a slightly higher takeoff speed than predicted from ElectriCalc would produce the necessary lift. Thus an airfoil with a C_L in the vicinity of 1.4 ± 0.1 would prove adequate. It was also desired to have an aircraft capable of manoeuvring with a g loading of 2, which gives a required maximum C_L of 0.92 ± 0.1 . As such, the airfoil was required to have a $C_{L\min}$ of 0.46 and a $C_{L\max}$ of 1.4. Airfoil lift and drag data were obtained from the UIUC Low-Speed Airfoil Test program. The airfoil could then be chosen from the extremely wide number available, using the FOMs listed above and the desired values calculated. The final selection made was the **Clark-Y**, with a C_L of 0.337 and a C_D of 0.0074 at its minimum drag angle of 0° , and a maximum C_L of 1.32 as the angle of attack approaches the critical angle of approximately 12° . An angle of incidence of approximately 4 degrees would be needed to provide the lift at cruise velocity. In addition, the Clark Y has relatively good stall characteristics, with a gentle approach and fall from the $C_{L\max}$.

4.4 Aspect Ratio

A higher aspect ratio will reduce the induced drag of the aircraft, thus allowing for a faster cruise speed. However, with a set wingspan of 2.13m (7ft) maximum, and a large wing area

required, even using the full span created a low aspect ratio. The wing area had been previously selected as 1.087 m^2 (11.67 ft^2) and thus with a 2.13 m (7 ft) span, an average chord of 0.53 m (1.75 ft) was required. A common practice to reduce induced drag is to use a tapered wing to provide an approximation to an elliptical wing. However, any taper that would provide a near elliptical lift distribution would cause a significant increase in the root chord if the same wing area were kept. This would increase drag beyond the point where a taper would provide any significant benefit. Thus a constant chord wing was chosen with a chord of 0.53 m (1.75 ft). This produced an aspect ratio of four. This is a very low aspect ratio and three-dimensional effects will produce a large induced drag. This was deemed unavoidable with the single wing configuration selected and the wing area needed to support the payload. Tip plates will be employed in an attempt to reduce these effects and increase lift.

4.5 Tail Sizing

The design considerations used to determine the required tail surface dimensions are stability and control authority. The airfoil is capable of approximately $1.5g$ before stalling (see section 5.4.2), and has a coefficient of moment of approximately -0.08 for a cruise angle of 4° . The stabilizer must be capable of overcoming both the pitching moment of the wing and the moment caused by a finite separation between the center of gravity and the center of pressure (assumed for now to be within 0.0127 m or 0.5 in. of each other). The tail must then still provide enough torque for control. This leads to the inequality:

$$X_{ach} \frac{1}{2} C_{Lh} \rho S_h V^2 \geq \frac{1}{2} C_{M} \rho S_w V^2 c + 2.4 X_{acw} W + I \ddot{\theta}$$

From this, the product of stabilizer maximum coefficient of lift, surface area, and distance from the center of gravity ($X_{ach} C_{Lh} S_h$) can be found. It is common practice to use a stabilizer that is approximately 20 to 22% percent of the wing area and an elevator that is 40% of the stabilizer area. The mission profile warranted a 22% surface. Analysis found that a 0.25 m^2 (2.7 ft^2) stabilizer located 1.27 m (50 in.) from the CG, with a NACA0009 airfoil (C_{Lmax} of 1.3) (ref. 7), provides the desired qualities. These will be further quantified in detailed design.

It was decided that a T-tail design would be used. Construction of this design is only marginally heavier than a conventional tail, yet is upwards of 30% more efficient. Raising the horizontal stabilizer into clean air greatly increases its effectiveness while reducing interference drag by reducing the joints between rudder, tail and fuselage.

The vertical stabilizer supports the horizontal tail and must be quite stiff, so a slightly thicker airfoil, a NACA 0012 was used. The chord of the vertical fin was set to the same as the horizontal stabilizer to minimize interference drag. Its height was then set to effectively raise the horizontal tail out of the downwash from the wing, and to provide enough yaw stability. For an airplane to be stable in yaw, the Center of Lateral Area should be about 25% back from the center of gravity. In the preliminary AutoCAD design, quick area moment calculations were done to show that the area selected was adequate for yaw control. Also, common model design practice states that a vertical tail area should be approximately 50% of the horizontal

tail area should be used. Thus a vertical fin area of 0.12 m^2 (1.3 ft^2) should be employed. Further analysis of vertical fin height is done in the detail design section.

4.6 Airframe and Fuselage Sizing

During the preliminary design stage, several design parameter and sizing trades were considered. While innovative design and construction methods were investigated, they were weighed against ease of manufacture and functionality. The decision of airframe design depended upon trades between simplicity of construction, strength, weight and reduction of drag.

All features of the preliminary design of the fuselage were weighed against the following Figures of Merit (FOMs):

Efficiency – The layout chosen for the fuselage should optimize the space required for the airframe structure while also limiting the fuselage's overall size. The placement of the bottles and the bottle size and shape were the main factors contributing to the preliminary design of the most efficient airframe possible.

Manufacturing Ease – The preliminary design of the airframe should limit the cost and time required for its construction. Also, shop tools and facilities must be considered.

Functionality – The fuselage must function properly as a cargo-carrying aircraft that requires repeated removal and loading of the bottles. The design feature used for access to the bottles must be both quick and rugged due to the rushed nature of cargo insertion/removal.

Structural Rigidity – The airframe structure must be sufficiently strong and stiff to account for the substantial payload and the repeated landings that the aircraft will encounter. The type of materials used and the thickness chosen for the primary structural components of the aircraft depended on their ability to withstand its loading.

Drag Penalty – The design of the airframe should minimize the amount of parasitic and induced drag created by the fuselage. The overall shape of the airframe, whether streamlined or square, dictates the increased drag possibilities of the fuselage. An aerodynamic shape and the reduction of parasite drag were important in order to reduce the flight time of the non-cargo ferry mission part of the flight profile.

The preliminary design utilizes a main "U" channel where the two tubes of four water bottles sit one on top of each other, centered under the aircraft's center of gravity. A second section on top of the water bottles houses the battery packs and wing mounts. A streamlined tailboom will extend from the top rear of the "U" channel and a removable fairing from the bottom rear will provide access to the water bottles.

Figure 4.1 Summary of Physical Properties

Feature	Description
Propulsion	Motor: MaxN32-13Y Brushless DC Speed Controller: Maxu 35-36 Cells: 26 Sanyo 3000 CR Gear Box: Custom 11:1 Propeller: 24-16 Zinger
Wing	Span: 2.13 m (84.00 in) Aspect Ratio: 4 Airfoil: Clark-Y Differential Ailerons: 0.41 m (16.00 in) x 25% chord Flaps: 0.61 m (24.00 in) x 30% chord
Stabilizer	Span: 1.00 m (39.40 in) Chord: 0.25m (9.85 in) Airfoil: NACA0009
Rudder	Height: 0.38 m (15.00 in) Chord: 0.10 m (4.00 in) Plane Fin
Main Landing Gear	Wheel Base: 0.37 m (14.44 in) Thickness: 0.01 m (0.50 in) Height: 0.15 m (5.81 in)

5.0 Detail Design

Drawings of the final aircraft design are attached in Appendix D. These drawings include detailed two-dimensional drawings and templates used for construction, and three-dimensional models for visual presentation.

The design of any airplane is a highly iterative process, involving many changes to the initial preliminary design before arriving at the final configuration. As reviewed in the preliminary design, many approximations involving aircraft weight, speed and sizing were made, and as these factors change they affect every other aspect of the design.

5.1 Weight

The estimated weight of the airplane and the required wing area to support this weight were calculated. An estimate of the components, structure and payload to be carried was tabulated. Care was taken not to underestimate the weight of the aircraft, as all primary design features require an accurate approximation of this weight in their calculations. The TOGW was calculated to be 15.5 kg (34.25 lbs). This is broken down into 8.8 kg (19.4 lbs) of water payload (including the weight of the bottles), 2.3 kg (5lbs) of batteries and an airframe weight of 4.2 kg (9.25 lbs).

5.2 Payload Fraction

Payload fraction is a measure of the payload's contribution to the take-off gross weight of the aircraft. It is given by:

$$\text{PayloadFraction} = \frac{W_{\text{Payload}}}{\text{TOGW}} = \frac{8.782\text{kg} \times 9.81\text{kg} \cdot \text{m} / \text{s}}{15.529\text{kg} \times 9.81\text{kg} \cdot \text{m} / \text{s}} = 0.566$$

The payload fraction of this aircraft is therefore predicted to be 0.566

5.3 Wing Performance

The wing platform was designed to optimize efficiency under the given design constraints. A high wing design incorporating 60% span flaps, 40% span ailerons and zero dihedral was used. A low aspect ratio of 4 was needed in order to achieve a reasonable wing loading and sufficient lift. This yields a chord of 0.553 m (1.75 ft) and an effective wing area (fuselage interrupts wing) of 1.084 m² (11.67 ft²). The resulting wing loading of 143.3 g/dec² (47.0 oz/ft²) is quite large, but has been shown to be possible in successful competitive airplanes. With the partial Fowler Flaps used, the wing area increases 9% to 1.18 m² (12.7 ft²) and the resulting wing loading is reduced to 131.4 g/dec² (43.1 oz/ft²). The ability to retract this wing area allows for lower drag in cruising and unloaded flights, while allowing quicker takeoffs and slower approaches.

With the selected Clark Y airfoil and platform area, C_{LMAX} , C_{LMIN} , $C_{LCRUISE}$ were calculated. Here, an efficiency of 90% was used as the wing construction efficiency – that is, the ability to reproduce the true airfoil in model form.

$$V_{STALL} = \sqrt{\frac{2Mg}{C_{Lmax} \rho S_w}}$$

Using the maximum C_L obtainable from the Clark Y airfoil and taking into account the increase in lift the flap provides allows stall speeds to be determined for 0°, 20° and 40° flap settings.

The coefficient of lift when the flaps are deployed effects only 60% of the wingspan, resulting in the following C_L 's.

Table 5.1. Flap Position C_L , Wing loading, V_{STALL}

Flap Position	C_L	Wing Loading	Wing Loading	V_{STALL}	V_{STALL}	Condition
0°	1.32	143.3 g/dec ²	47.0 oz/ft ²	13.18 m/s	28.02 mph	Level Flight
20°	1.87	137.1 g/dec ²	44.9 oz/ft ²	11.06 m/s	23.52 mph	Takeoff
40°	2.03	134.4 g/dec ²	43.1 oz/ft ²	10.62 m/s	22.58 mph	Landing

Initial Velocity approximations provided in ElectriCalc were for cruising and maximum velocities, as its calculations account for both propeller efficiencies, drag and thrust.

$$V_{Max} = \sqrt{\frac{2T_{max}}{\rho C_D S_w}}$$

Table 5.2. Max and Cruise Velocities

	Velocity	Velocity	Cl
V_{CRUISE}	25.5 m/s	57 mph	0.46
V_{MAX}	23.4 m/s	52 mph	0.39

With the known cruising velocity, the angle of incidence for the wing was determined. This angle provides the model with the correct lift for level flight at the cruise velocity and takes into account the aspect ratio.

$$a = \frac{a_0 + 18.24 \times C_{Lcruise} \times (1.0 + T)}{AR} = 3.3^\circ$$

T = platform adjustment factor for aspect ratio (Fig 4., pg 6, Lennon, Andy; "Basics of Model Aircraft Design")

The pitching moment of the wing at the cruise velocity was calculated to be -30.65 N/m (-2171 oz/in). The pitching moment usually significantly increases with the use of flaps. However, using flaps which are 30% of the wing chord minimize this increase in pitching moment when deployed.

5.4 Tail Sizing

The T-tail configuration used allows the stabilizer to operate at near 90% efficiency as opposed to 40% for horizontal tails located low on the fuselage. It also reduces interference drag because there is only junction between the vertical fin and stabilizer, as opposed to two when the stabilizer is on the fuselage.

The NACA 0009 symmetrical airfoil was chosen for use in the stabilizer due to its low drag characteristics.

The horizontal tail has an area of 0.25 m^2 (388 in^2), which is 22% of the wing area. An aspect ratio of 4 gives a 0.25m (0.82 ft) chord and a 1.00m (3.82 ft) span. The elevator area was set at 40% of the stabilizer area providing 0.1 m^2 (1.08ft^2) of area.

Basic model airplane guild lines suggest that the horizontal tail be placed approximately 2.5 times the wing chord from the neutral point of the wing to the neutral point of the stabilizer. Thus a tail moment arm of 1.27m (4.17ft) is used.

With a pitching moment of -30.65 N/m (-2171 oz/in) and a tail moment arm of 1.27m (4.17ft) the horizontal tail must provide a down force of 43.3 N (48.3 oz) assuming 90% stabilizer efficiency. This down force is provided by the negative lift from the stabilizer airfoil, requiring a $C_{L\text{stab}} = -0.159$.

The angle of incidence to provide this C_L was taken from published airfoil data and was shown to be -1.75° for two-dimensional flow. Using the same equation as the wing to account for the effects of an aspect ratio of 4, the tail incidence becomes -2.56° .

The down wash from the wing and its effect on the stabilizer must be taken into account. The horizontal moment arm and the height of the stabilizer from the wing were calculated and their values were used with charts (Figure 2, pg 40, Lennon, Andy; "Basics of RC Model Aircraft Design") to provide the correct tail incidence required. A final incidence of -0.80° is used.

The rudder uses a NACA 0012 airfoil in order to provide a slightly thicker spar for supporting the horizontal tail. The chord of the vertical fin was set to be the same as the stabilizer in order to reduce the interference drag when the two are bolted together. Basic RC airplane design guidelines show that a vertical tail area of 8% of the wing area would provide adequate control. A study of the vertical area on this model indicates the center of lateral area will be close to 25% of tail moment arm. Thus a vertical stabilizer chord of 0.25m (0.82 ft) and a height of 0.265m

(0.875 ft) was chosen. The rudder area was set at 40% of the vertical tail chord and extends downwards to taper into the fuselage.

5.5 Fuselage Sizing

As the design being used has many uncertainties in power plant efficiency and empty airframe weight, a need to be able adjust the payload is required without changing the center of gravity. The two tubes of 4 water bottles were staggered so that any number of water bottles could be used. This feature requires the main fuselage "U" channel to be 0.90 meters long (3.25 ft) and the height of the "U" channel to be 0.22 meters (0.729 ft). The tail boom length was set by the tail moment arm needed and is 0.86m (2.83 ft) long. A fuselage width just wide enough to surround the bottles was selected to be 0.1m (3.33 ft) wide. This width provides ample volume for all other control and mounting components except for the reduction drive, which will require blisters around the larger diameter pulley (0.11 m (0.375 ft) in diameter).

Access to the cargo area is via a side swinging tail fairing. This fairing is aerodynamically tapered to the tail boom and "U" channel. Hinges on one side and a pin and latch fastener on the other keep the water bottles securely in the airplane.

5.6 Drag

In order to make accurate predictions of the flight speed and acceleration, the drag on the airplane must be calculated. In this basic estimation, the total drag is taken to be the sum of parasitic drag and the induced drag from the wing, given by the equation:

$$C_{DTotal} = A + B \times C_L^2$$

This approximation does not take into account interference drag caused by the junction of various parts. This form of drag can be reduced considerably if proper drag reduction techniques are incorporated.

Parasite drag was estimated using the "component build-up" method. A flat-plate skin friction drag coefficient (C_f) is calculated for each major component of the aircraft and then multiplied by a "form factor" (k) that estimates losses due to form drag:

$$C_{dPara} = \sum \left[\frac{k \times C_f \times A_{wetted}}{S_w} \right]_{component}$$

where

$$C_f = \frac{0.455}{(\log_{10} Re)^{2.56}}$$

for turbulent flow over a smooth plate, and

$$Re = \frac{V \times L}{\gamma}$$

Table 5.3. Parasite drag estimation using "component build-up" method.

	$A_{\text{wetted}} \text{ (m}^2\text{)}$	$Re \text{ (}\rho VL/\mu\text{)}$	C_f	Form factor, k	$C_{D\text{para}}$
Wing	2.17	9.30×10^5	4.68×10^{-3}	1.21 ($t/c = 0.1$)	1.13×10^{-2}
Fuselage	1.64	3.46×10^6	3.71×10^{-3}	1.17 ($L/D = 7.5$)	6.57×10^{-3}
Wheels	2.46×10^{-2}	1.33×10^5	6.90×10^{-3}	1.32 ($t/d = 0.08$)	2.07×10^{-4}
Gear Struts	8.54×10^{-2}	1.33×10^5	6.90×10^{-3}	1.18 ($t/w = 0.08$)	6.42×10^{-4}
Stabilizer	5.01×10^{-1}	1.75×10^6	4.17×10^{-3}	1.10 ($t/c = 0.02$)	2.12×10^{-3}
Vertical Fin	2.11×10^{-1}	6.15×10^5	5.06×10^{-3}	1.07 ($t/c = 0.05$)	1.05×10^{-3}
Total					0.0219

Induced drag is estimated using the "wing efficiency" method. The induced drag coefficient is given by:

$$C_{d\text{induced}} = \frac{C_L^2}{\pi \times AR \times e} \quad \text{where,} \quad e = 1.78(1 - 0.045 \times AR^{0.68}) - 0.64$$

This resulted in a value of $e=0.934$

$C_{d\text{Induced}}$ was calculated at max, cruise and stall speeds.

$C_{d\text{InducedMAX}}$	0.013	Maxium Velocity
$C_{d\text{InducedCRUISE}}$	0.018	Cruise Velocity
$C_{d\text{InducedSTALL}}$	0.148	Stall – 0° Flaps
$C_{d\text{InducedSTALL}}$	0.294	Stall – 20° Flaps
$C_{d\text{InducedSTALL}}$	0.352	Stall – 40° Flaps

Table 5.4 Drag at Max, Min and Stall Velocities

5.7 Total Drag

The total drag coefficient is the sum of the of the surface drag and the induced drag of the aircraft in cruise and is therefore given by:

$$C_{D\text{Total}} = 0.0219 + 0.018 = \mathbf{0.0226}.$$

5.8 Power System

Initial calculations predicted that the MaxCim N32-13Y would be capable of producing upwards of 53 N (12 lbf) of thrust. This thrust is achieved using a 24×16 prop, 26 Sanyo N-3000CR mAh cells and an 11:1 reduction unit.

As stated in the preliminary design a toothed belt drive unit was needed in order to maximize the efficiency of the reduction. A properly constructed and tensioned belt drive is capable of efficiencies close to 95% if a toothed timing belt system is used. Obsidian's belt drive was constructed of commercially available 120 and 11 groove sprockets mated to appropriate shafting.

5.9 Control Systems

Control of the aircraft is provided by a Futaba 8 channel PCM transmitter and receiver with its failsafe programmed as per competition rules. A four cell 600mAh battery pack is used to power the receiver and servos. This pack size is large enough to complete several missions, but will be peak charged again after each ten-minute flight.

All servos must provide quick, accurate and strong control authority to the flight surfaces. Any slop in the control set-up could lead to flutter, and possible departure of that control surface. To reduce this risk, all servos are ball bearing supported and their torque output is matched to the operation they must perform. Control linkages between the servo and flight surface were kept as short as possible to reduce flex.

Table 5.5 Servos Used

Surface	Name	Torque	Speed	BB	Gears	Weight	# Used
Ailerons	Hitec HS-225BB	3.9 kg/cm	0.14s/60°	Y	Nylon	27 g	2
Flaps	Hitec HS-815	19.94 kg/cm	0.38s/140°	Y	Metal	153g	2
Elevator	JR NES-4721	8.6 kg/cm	0.22s/60°	Y	Metal	49 g	1
Rudder	Hitec HS-225BB	3.9 kg/cm	0.14s/60°	Y	Nylon	27 g	1
Nose Gear	Hitec HS-205MG	3.1 kg/cm	0.20s/60°	Y	Metal	32 g	1
Brake	Hitec HS-225BB	3.9 kg/cm	0.14s/60°	Y	Nylon	27 g	1

Mini servos are used in place of standard servos, as they are light and provide more torque. Metal gears were selected for the servo used for nose gear steering as nylon gears at this location are easily stripped from the sudden impact. An elevator failure would be catastrophic, hence the larger precision servo used at this location. The area of the flaps dictates a powerful servo must be used for their operation. As having one servo fail would result in an uncontrollable spin, the strongest servo available was used for this application.

5.10 G-Loading

In predicting the maximum g-load the aircraft is capable of handling, two major parameters were investigated. Firstly, the aircraft's structural capabilities were estimated with a calculation of the spar's maximum allowable bending stress. Predictions were then made on the accelerated stall properties of the wing, using published lift data for the selected airfoil.

5.11 Structural Loading

A g-load rating of 4 was assigned as a prediction of the maximum loading the airplane would experience under normal flying condition and while at the maximum TOGW. From here the size and strength of the wing could be determined.

For initial calculations, the assumption was made that the wing spar carried all wing loads and would experience heavier loads than any other aircraft part. Thus, the maximum bending stresses the spar can handle will determine the g-load capability of the plane.

The wing's manufacturing plan calls an "I" beam spar to be used, with a carbon laminate for each flange and a vertical grain balsa shear web. Thus, the maximum bending stresses these elements can handle will determine the g-load capability of the plane. As nearly all g-loadings placed on the airframe would be positive, this puts the upper spar into compression and the lower into tension. Thus a carbon fiber laminate over balsa was used for the lower spar and a carbon fiber laminate over Douglas fir as the upper spar. It was also assumed that the carbon fiber on the lower spar handled all the tension loads and the fir in the upper spar handled all compression loads. From these assumptions, the cross sectional area of these respective materials could be calculated.

The maximum bending moment experience by the wing was calculated using basic force and moment analysis and found to be 480 kN/m (2740 lbf/ft). The second moment of inertia (I_y) was calculated for the area of the carbon fiber and the fir. With the known distance to the neutral plane (z), the bending stress could be calculated using the equation:

$$\sigma_x = \frac{M \times z}{I_y}$$

The dimensions of the upper spars (stock sizes) were then iterated to achieve a safety factor of 1 with positive 4-g loading. It was found that 2 layers of carbon fiber on a 1.25 in by 0.25 in piece of balsa was required for the bottom spar. An additional 2 layers of carbon fiber were added to increase strength with only a marginal weight penalty, increasing its rated g-loading to approximately 13 g's. The fir upper spar's dimensions were also set to 1.25 in by 0.25 in, resulting in a g loading of 3.6. While this is below the rated aircraft g-loading, the heavy weight of this material was of greater concern. Three layers of carbon fiber were laminated to this spar, and along with the wing sheeting, a 4-g rating is easily obtained from these dimensions.

5.12 Take-off Performance

Take-off distance is broken into three components: ground roll, rotation distance, and climb-out distance. Rotation distance is assumed to be negligible for this calculation.

5.12.1 Ground Roll

The ground roll distance (d_g) of the aircraft is given by:

$$d_g = \frac{V_{TO}^2}{2 \times a_{mean}}$$

where,

$$M \cdot a_{mean} = \left[T_{mean} - \left(A + B \cdot C_{Lg}^2 \right) \frac{1}{4} \rho V_{TO}^2 S_w - \mu \left(W - C_{Lg} \frac{1}{4} \rho V_{TO}^2 S_w \right) \right]$$

Take-off speed (V_{TO}) is taken as 15% above stall speed:

$$V_{TO} = 1.15 \times V_{stall}$$

The C_L and C_D used in this equation are the values at cruise speed, as the plane can be considered in level flight while on the ground with its wing angle of incidence relative to the runway. Static thrust is estimated from the available motor data from ElectriCalc. This yielded a ground roll acceleration of 3.26 m/s^2 (10.5 ft/s^2).

The ground roll was then calculated at the take off velocities when no flaps are deployed and when 20° flaps are deployed.

Table 5.6 Takeoff distance

	V_{TO}	V_{TO}	d_g	d_g
0° Flaps	15.2 m/s	34.0 mph	35.3 m	115.8 ft
20° Flaps	12.7 m/s	28.4 mph	24.8 m	81.5 ft

This ground roll distance exceeds the competition's maximum value of 100 ft when flaps are not used at takeoff. However, flaps were built into the model to reduce this takeoff distance. With a 20° flap setting, the model begins to rotate at 81.5 ft. These distances are given under a no wind condition.

5.12.2 Climb out Distance

The climb out angle for the airplane is given by the equation:

$$\tan \theta = \frac{T}{W} - \frac{D}{L}$$

A climb angle of only 5.9° is achieved. If this rate of climb was held constant so that there is no gain in velocity after lift off, a distance of 97 m (319 ft) would be needed to reach an altitude of 10 m (32.8 ft). The performance under these assumptions is quite poor, as expected for an under-powered airplane. Therefore the flight profile dictates that after rotation, a constant altitude quite low above the ground is needed for some distance in order to build up velocity of the airplane and increase the climb angle.

5.13 Turning Radius

The minimum controlled level turning radius for an airplane is determined by the maximum radial acceleration the wing can sustain before an accelerated stall. The maximum g-load that can be produced by the aircraft is given by the ratio of the maximum lift available from the airfoil to the lift generated in steady level flight. The angle of bank at which the wing can still provide the necessary lift for the airplane is given by:

$$\cos\beta = \frac{C_{L_{cruise}}}{C_{L_{max}}}$$

Thus the maximum angle of bank is 69° . The maximum radial acceleration before the onset of an accelerated stall is calculated using the equation:

$$\tan\beta = \frac{a_{stall}}{1 \times g}$$

This gives a loading of 2.66g's. Thus, if the aircraft more than 2.66g lateral acceleration, the maximum lift available from the wing will be exceeded and a accelerated stall will occur. From this data the minimum radius of turn with no altitude loss is 21m (69 ft) as given by the equation:

$$R = \frac{V_{cruise}^2}{a_{stall}}$$

5.14 Endurance and Range

5.14.1 Endurance

The aircraft achieves maximum endurance when flying at its minimum throttle setting, which provides sufficient thrust for the plane to achieve a velocity just above its stall speed ($V_{endurance}$). Thus, endurance is highly dependant on the motor and electrical system used.

The ElectriCalc commercial software package is used to estimate the endurance of the aircraft with the selected motor and battery arrangement. It was found that an airspeed of 13.2m/s (32mph) could be achieved with a minimum throttle setting of 52%. At this setting, ElectriCalc estimated a run-time of 23.3minutes. This endurance estimate neglects power needed for take-off, climb-out, and landing.

5.14.2 Range

The maximum range characteristics of an electrically powered aircraft differ from those of a gas-powered plane, as motor efficiency drops at increased throttle settings. The maximum range of

the aircraft is achieved not at the best lift-to-drag velocity, but at the lowest possible throttle setting—at the endurance throttle setting. To calculate the range, the endurance prediction of 23.3 minutes is multiplied by the endurance velocity of 13.2 m/s (32 mph). This method produces a maximum range value of 21.2 km (13.2 mph). This range is assuming zero wind conditions and neglects the power needed for takeoff and climb, landing and energy loss maneuvers (turning).

5.15 Stability

5.15.1 Longitudinal Stability

The maximum allowable distance between the center of gravity of the plane and the location of the $\frac{1}{4}$ chord of the wing was determined using the following stability criterion:

$$\frac{dC_{M(CoG)}}{dL} = \frac{x}{c} - \eta_H \left(\frac{S_H}{S_W} \right) \left(\frac{l_H}{c} \right) \left(\frac{a_H}{a} \right) \left(1 - \frac{d\epsilon}{d\alpha} \right) + \frac{dC_{Mf}}{dC_L} \leq 0$$

The marginally stable case value of x , the distance from the $\frac{1}{4}$ chord, was found by setting the above inequality to zero and evaluating. This yielded a value of 52%, which means that for the aircraft to be longitudinally stable, the center of gravity can be no more than 52% of the wing chord.

5.15.2 Lateral-Directional Stability

Yaw stability is based on the position of the center of lateral area of the airplane as discussed in section 5.4. Vertical tail sizing was used to position the center of lateral area at approximately 25% of the tail moment arm from the neutral point of the wing, about 0.32 m (1.0 ft) from the 25% chord.

As a determination of the directional stability of the aircraft, the following inequality was evaluated using the physical properties of the aircraft.

$$a_f \left(\frac{l_f}{c} \right) \left(\frac{S_f}{S_w} \right) \geq \frac{dC_{mf}}{d\phi}$$

The evaluated derivative was found to be 3.2, which is greater than zero indicating that the aircraft was directionally stable.

5.15.3 Roll Stability

Roll stability is assumed adequate due to the large pendulum effect from the payload. With no dihedral in the wing (to ease manufacturing capabilities), the pendulum effect of the cargo provides all self-leveling stability. Large ailerons, each 0.054 m^2 (0.58 ft^2) in area, allows proper control authority.

Cessna / ONR Student Design / Build / Fly Competition

Description	Coefficient	Variables	Description	Values
-------------	-------------	-----------	-------------	--------

large chord
monoplane
conventional tail
single fuselage
single motor

FLIGHT SCORE

Liters of Water Carried Multiplier	Water Load	$10 * n$	Water Load =	80
Liters of Water	n	number of liters	n =	

RATED AIRCRAFT COST

Manufactures Empty Weight Multiplier	A	$\$100 * MEW$	A =	\$ 1,400.00
Manufactures Empty Weight	MEW (pounds)	airframe weight	MEW =	

Rated motor Power Multiplier	B	$\$1 * REP$	B =	\$ 1,620.00
Rated motor Power	REP (watts)	$\# \text{ motors} * 50A * 1.2V/cell * \# \text{ cells}$	REP =	1620
			# motors =	
			# cells =	

Manufacturing Cost Multiplier	C	$\$20 * MFHR$	C =	\$ 2,460.00
Manufacturing Man Hours	MFHR (hours)	Prescribed assembly Hours by WBS	MFHR =	123
		MFHR = the sum of WBS		
		Wings WBS = $5\text{hrs/wing} + 4\text{ hrs / sq foot}$	Wing WBS =	53
			# wings =	
			area (sq.ft) =	

Fuselage WBS = $5\text{hrs/body} + 4\text{hrs / foot}$	Fuselage WBS =	33
	# bodys/pods =	
	length (ft) =	

Empenage WBS = $5\text{ hrs} + 5\text{ hrs/vert surf}$	mpenage WBS =	15
	# vert. surfaces =	
	# horz. surfaces =	

Flight Systems WBS = $5\text{ hrs} + 1\text{ hr/ serv}$	light Sys. WBS =	12
	# servos =	

Propulsion Systems WBS = 5 hrs / motor	ropulsion WBS =	10
	# motors =	
	# props =	

Single Flight Score	SFS	Flights * Water Loads	SFS =	240
	Flights	Is the number of water caring flight within	# flights =	

Written Report Score	WRS	Score on written report as assigned by ju	WRS =	
		note -a written score of 87 was used as a constant		

Total Flight Score	TFS	3*single flight	TFS =	720
--------------------	-----	-----------------	-------	-----

Rated Aircraft Cost	RAC (\$1000)	$(MEW + REP + MFHR) / 1000$	RAC =	5.48
---------------------	--------------	-----------------------------	-------	------

FINAL SCORE	Final Score	Written Report Score * Total Flight Score	FINAL SCORE	11430.65693
-------------	-------------	---	-------------	-------------

6.0 Manufacturing Plan

Obsidian's design can be broken down into four separate components, each of which employs a different construction technique. Different methods of building the wing, fuselage, tail appendage, and landing gear were analyzed and the best choices were determined with a figure of merit matrix.

6.1 Wing Construction

6.1.1 Foam and Fiberglass

This technique involves cutting a wing from low density foam using a hot-wire cutting apparatus. The wing cores are then strengthened by adding balsa or carbon fiber spars along the top and bottom surfaces. Provision is then made for flap and aileron actuation installation, and then the entire surface is coated with one or two layers of fiberglass. This results in a structurally strong wing without too much effort. The chief disadvantage of this technique is that the weight can become prohibitive.

6.1.2 Built-up Construction

Built-up construction is the oldest and most traditional form of building a wing; unfortunately, it is also the most time consuming. Ribs are cut in an airfoil shape from thin balsa or aircraft plywood and are then positioned on a jig so that there are 4 to 6 inches between each one. The spars, made of balsa, spruce, carbon fiber, or of some combination, are glued in and a shear web of cross-grained balsa is positioned to form the web of the I-beam structure. Leading and trailing edges are formed by gluing balsa to the front and back of the ribs, and the whole structure is then sanded to ensure a streamlined shape. Thin balsa sheeting is applied from the leading edge back to the spar on both the top and bottom of the wing, forming a strong D-tube structure, which is good in torsion. The whole structure is then covered with a thin plastic film to form an airfoil. This technique forms a light, rigid structure.

6.1.3 Carbon Fiber Monocoque

This technique is the most technically demanding of the three choices presented here. An airfoil is drawn up in a 3-D modeling computer program and is transmitted to a computer controlled milling machine. The machine must mill two female molds, one for the top of the wing, the other for the bottom of the wing, from a temperature stable material. The molds are then prepared and pre-impregnated carbon fiber is laid up into the cavity. The mold is then placed under vacuum in an autoclave and baked at approximately 120 degrees Celsius for three hours. Once cooled, the wing halves are released from their molds and are carefully sanded and glued together. This technique requires very complex and expensive facilities, materials, and expertise; however, it results in a very light, strong wing.

6.2 Fuselage Construction

6.2.1 Balsa Stringer

This form of construction stretches back to the first days of both full-sized and model aircraft flight. Many thin strips of wood (balsa on model planes) connect several wooden formers to produce the fuselage frame. This frame is then covered by doped paper or silk, or in more recent times, by shrinkable plastic.

6.2.2 Corrugated Plastic

While not in common use, the Queen's Aero Design team made use of this material in last year's AIAA entry. The plastic consists of two thin plates, separated by many thin plastic pieces, similar to corrugated cardboard. A fuselage can be made very rapidly by scoring the plastic and then folding it to form a 90-degree corner. Triangular bracing is then glued to the inside of the joint to ensure that it remains in place. This results in a very crash resistant structure (determined experimentally through several high speed encounters with the ground), which evenly supports the cargo. Unfortunately, this method of construction is heavy and forming joints of an angle other than 90-degrees is difficult.

6.2.3 Molded Carbon Fiber

This technique makes use of expensive composite materials to produce a very strong and lightweight fuselage. A mold of the required fuselage shape is made up of a heat resistant material. Several layers of pre-impregnated carbon fiber are laid up onto the mold, a sheet of thin structural honeycomb (which acts as a shear web for the carbon) is placed into the lay-up, and then more carbon fiber is laid up on top. The assembly is vacuum bagged and then heated until the epoxy cures. This technique requires access to expensive materials, equipment, and expertise, but can produce excellent results.

6.2.4 Fiberglass

The use of fiberglass and a "lost foam" mandrel has been used by high performance model aircraft for several years. The technique involves the production of a fuselage from medium density foam. This mandrel is then coated with several layers of fiberglass in a wet lay-up, and then the foam is dissolved with a strong solvent. The remaining fiberglass is then internally braced with wing mounting blocks, bulkheads, and other required structure, resulting in a lightweight stressed-skin fuselage. While not as strong as the carbon fiber/structural honeycomb, fiberglass does not require expensive heat resistant molds, expensive materials, or a great deal of technical experience.

6.3 Tail Construction

6.3.1 Foam and Fiberglass

A strong and smooth airfoil can quickly be made by cutting the required shape from medium density foam and then adding a single layer of fiberglass. The fibreglassed surface is then covered by a sheet of thin plastic and the whole assembly is placed in a vacuum until the epoxy has hardened. The plastic sheets can then be peeled away, leaving a perfect tail surface. While this method of construction can result in a perfectly sculpted complex airfoil, it tends to be heavier than the other options available.

6.3.2 Sheet Balsa

By far the easiest way to construct a tail, thick sheet balsa can be cut in the required planform shape and then the edges can be rounded with a sanding block. Although the tail does not take a proper streamlined shape, the extra drag is usually accepted for the ease of construction. This method of construction is heavy, durable, and is prone to warping with changes in temperature in humidity.

6.3.3 Built-up Construction

A built-up tail is the lightest, but most fragile option under consideration. Construction is very similar to a built-up wing, with a set of evenly spaced ribs joined by a double spar and shear web, and the leading and trailing edges. Sheeting is sometimes extended right to the trailing edge to give a slight increase in torsional stiffness. The chief disadvantage of this design is that it is very time consuming to construct. Also worth considering is that the tiny balsa structure that makes up a built-up surface is vulnerable to damage, especially on a portion of the plane that is often accidentally banged and knocked during storage and transportation.

6.4 Undercarriage Construction

6.4.1 Aluminum

Aluminum landing gear is very common on model aircraft. An approximately 1/8" aluminum plate (thickness varies with the load requirements) is trimmed and then bent to form an arch shape. Holes are drilled for mounting the axles and for mounting the assembly to the aircraft. These undercarriages are commercially available, reliable, and cheap. Their chief disadvantage is that they tend to bend with rough landings, necessitating emergency repairs in situations where multiple flights are to be made within a certain time.

6.4.2 Tool Steel

Tool Steel (music wire, piano wire) is often used for model aircraft landing gear. Although it is a very brittle form of steel, landing gear made from it can flex and give with

impact a great deal before catastrophic failure occurs. Music wire is obtained in the right size for the application then is carefully bent to fit the mounts built into the fuselage. If necessary, two wires can be soldered into a truss arrangement to give the assembly extra stiffness. This form of undercarriage is rigid and is not prone to bending on heavy landings. Its weakness is heavy weight and the difficulty of mounting the wires to ensure that they do not break loose under landing loads.

6.4.3 Amarid, Carbon Fiber, and Structural Honeycomb

Composite undercarriages are starting to replace the more traditional aluminum and music wire arrangements. Made up of either pre-impregnated carbon fiber or amarid, and formed around a structural honeycomb core, they combine lightweight with a very structurally stiff package. Construction involves building a mold of a temperature resistant material and then laying up the composite materials on top of it. The assembly is put under vacuum in an autoclave and then baked for three hours to cure the epoxy. The final landing gear is removed from the mold, trimmed, and is then put into service. While this landing gear is ideal for situations involving heavy loads, it also requires the expensive materials and equipment common to all composite components.

6.5 *Figures of Merit*

To choose the best combination of manufacturing processes for Obsidian, a qualitative figure of merit was conceived to evaluate each technique's merits and weaknesses in a simple to interpret chart. Five criteria were selected, weight, structure, time, skill, and expense, and each construction method will be given a qualitative score that illustrates its performance in each category. The separate categories are described in detail below.

6.5.1 Weight

In a high performance competition aircraft, flight performance dictates who will win, and who will be defeated or worse, who will crash. If the aircraft design is effective and well planned out, then building weight is the one element that can seriously affect every aspect of the flight envelope. Where it is reasonable, a builder should always strive to make the components as light and efficient as possible. Thus, this was selected as the first criterion in the FOM.

6.5.2 Structure

Structural failure is expensive and can be dangerous under the wrong conditions. To ensure that the aircraft will be able to withstand the flight loads experienced throughout the mission, structural integrity was chosen as the second criterion in the FOM.

6.5.3 Skill

To produce the required components of the aircraft, the selected construction technique must either be known to the team or it must be easy to learn. Also worth considering, more experience with the specified building technique produces a more accurate final product and

less waste, thus it is desirable to choose methods that are familiar to a larger number of team members. Skill was selected as the third criterion in the FOM.

6.5.4 Expense

Among the various construction techniques discussed, there is a huge difference in cost. This is due to some techniques using exotic materials or machining, while the more mundane and traditional techniques make use of the builder's individual skill rather than a complex mould or machine. As Obsidian was built with our meager budget in mind, the cheaper option is often worth pursuing due to fiscal necessity. As such, the expense of the construction technique was chosen as the fourth entry into the FOM.

6.5.5 Time

The final item worth considering when evaluating the construction choices is the length of time that the method requires. Obsidian was designed and built on a 100% volunteer basis because Queen's does not offer course credit towards participation in a design competition., so all design and construction must be made around the demands of a full engineering course load. Time is precious and was given a place in the FOM

6.6 Evaluation and Selection

6.6.1 Analytical Method

Each construction technique was evaluated in terms of each of the five criteria listed above. The weight of the method was estimated in ounces. The structural integrity of the method was given a rating on a scale from 0 to 10, with 10 being the strongest choice. The required skill of the choices was ranked on a scale from 0 to 5, with 5 being the easiest construction method. The cost of the method was estimated using a Canadian dollar value with American funds also indicated. The final entry, time, was given a value of the estimated construction hours required for each method.

Total scores were tabulated with the following equation, which weights the relative importance of each of the criterion.

$$\text{Total} = 100/\text{weight} + \text{structure}/3 + 3/\text{skill} + 10/\text{expense} + 1/\text{time}$$

6.6.2 Construction Method Selection

The figure of merit indicates that a carbon fiber monocoque would be the optimized construction method for the wing. Upon investigating the resources required for this type of construction, it was found that the campus autoclave would not be able to bake any composite component that would not fit in a 1m cube. The 7-foot span dictated by the design does not meet this criterion, thus we were not able to utilize this method at this time. For this year's competition, the FOM's second choice of a built-up wing was used.

The autoclave's size did not affect the FOM's choice of composite construction for the fuselage and the undercarriage; thus these techniques were used on both components. The final component, the tail, used a built-up construction as chosen by the FOM.

Figure 6.1 Manufacturing Process Evaluation

	Weight (oz)	Structure	Skill	Expense		Time	Total
				Can\$	US\$		
Wing							
Foam and Fiberglass	72	7	3	120	80	28	4.84
Built-up Construction	44	6	4	150	101	20	5.14
Carbon Fiber Monocoque	32	8	5	2000	1340	100	6.41
Fuselage							
Balsa Stringer	45	2	5	100	67	80	3.60
Corrugated Plastic	80	5	2	30	20	20	4.80
Molded Carbon Fiber	50	9	5	1000	670	30	5.64
Fiberglass	80	4	4	400	268	30	3.39
Tail							
Foam and Fiberglass	12	6	3	10	7	10	12.43
Sheet Balsa	18	7	1	6	4	4	12.81
Built-up Construction	10	5	4	10	7	8	13.54
Undercarriage							
Aluminum	20	4	2	30	20	2	8.67
Tool Steel	24	7	4	15	10	5	8.12
Amarid, Carbon Fiber, And Structural Honeycomb	9	9	5	100	67	12	14.89

Figure 6.2 Manufacturing Milestones

Milestone	Proposed Date (m/wk)	Actual Date (m/wk)
1.0 Wing		
1.1 Spars built	2/1	2/2
1.2 Ribs cut and sanded	2/3	2/3
1.3 Initial wing construction	2/3	2/3
1.4 Flap and aileron construction	2/3	
1.5 Wing sheeting applied	2/3	
1.6 Control surfaces mounted	3/2	
1.7 Wing covered	3/2	
2.0 Fuselage		
2.1 Mould made	1/1	1/1
2.2 Composites laid up and baked	2/1	2/3
2.3 Tail boom cut from foam	2/1	2/1
2.4 Bulkheads installed	2/2	2/4
2.5 Fairings cut from foam	2/2	2/2
2.6 Fiberglassing	3/2	
2.7 Assembly	3/3	
3.0 Undercarriage		
3.1 Mould made	1/1	1/2
3.2 Composites laid up and baked	2/1	2/2
3.3 Trimmed and sanded	2/1	2/3
3.4 Mounted	3/3	
4.0 Tail		
4.1 Spars built	2/1	2/3
4.2 Ribs cut out	2/2	
4.3 Initial assembly	2/3	
4.4 Sheeting	2/3	
4.5 Servo installation	3/2	
4.6 Mounting	3/2	

Appendix A: Calculation Spreadsheets

Weight Estimation					
Description	Weight (lbs)	Weight (kgs)	Number	Subtotal (lbs)	Subtotal (kgs)
1 Liter of Water	2.420	1.098	8	19.360	8.782
Battery Pack	5.000	2.268	1	5.000	2.268
Receiver	0.125	0.057	1	0.125	0.057
Micro Servos	0.063	0.028	5	0.313	0.142
Standard Servos	0.125	0.057	1	0.125	0.057
Flap Servos	0.313	0.142	2	0.625	0.283
Landing gear	0.500	0.227	1	0.500	0.227
Wheels	0.125	0.057	3	0.375	0.170
Wing	2.750	1.247	1	2.750	1.247
Tail	0.500	0.227	1	0.500	0.227
Fuselage	3.000	1.361	1	3.000	1.361
Motor	0.500	0.227	1	0.500	0.227
Speed Control	0.188	0.085	1	0.188	0.085
Gear Box	0.500	0.227	1	0.500	0.227
Prop	0.375	0.170	1	0.375	0.170
TOGW				34.235	15.529
Empty Flying Weight				14.250	6.464
Airframe Weight				9.250	4.196

Payload Fraction

Payload Fraction = $W_{\text{payload}} / \text{TOGW}$

Payload Fraction = 0.56550314

DRAG ESTIMATION							
Summary of Equations Used							
Re = (Density Air / Viscosity Air)*Velocity*Length (metric)				Reynolds number			
Cdf = 0.455/((log10(Re))^2.55)				Coefficient of frictional drag			
CdPara = (k*Cf*Awetted)/Swing				Coefficient of parasitic drag			
Cdinduced = CI^2/(Pi()*AR*e)				Coefficient of induced drag			
De = 2*(H+W)/Pi				Equivalent fuselage diameter			
e = 1.78*(1-0.045*(AR^0.68))- .64				efficiency value			
Constants							
Density of Air (p) =		1.225 kg/m^3	1.00000				
Viscosity of Air (u) =		0.000017894 kg/m/sec	373.718 slug/ft/ sec				
Cruise Velocity		25.48 m/s	assumed from motocalc				
Parasite drag estimation using "component build-up" method						*Form Factors from Mech 480	
	Awetted (m^2)	Re (pVL/u)	Cf	Thickness Ratio		Form Factor (k)	CdPara
Wing	2.168	930446	0.004676	0.0952 (t/c)		1.21	0.011316
Fuselage	1.642	3455941	0.003706	7.5109 (L/De)		1.17	0.006568
Wheels	0.025	132921	0.006902	0.0833 (t/d)		1.32	0.000207
Gear Struts	0.085	132921	0.006902	0.0833 (t/w)		1.18	0.000642
Stabilator	0.501	436423	0.005403	0.0190 (t/c)		1.10	0.002746
Rudder	0.211	614759	0.005056	0.0495 (t/c)		1.07	0.001054

Total							0.022531
Equivalent diameter of fuselage							
<i>Converts fuselage perimeter to a equivalent circular cross section diameter</i>							
De = $2*(H+W)/\pi$							
De = 0.263775445							
Induced Drag							
Cdinduced = $Cl^2/(\pi \cdot AR \cdot e)$							
AR = aspect ration							
Cl = coefficient of lift							
e = $1.78 \cdot (1 - 0.045 \cdot (AR^{0.68})) - .64$							
e = 0.934							
Cdinducedmaxve							
l = 0.013							
using max Cl							
Cdinducedcruise							
= 0.018							
using cruise CL							
Cdinducedstall = 0.148							
CL at 0 degree flaps							
Cdinducedstall = 0.299							
CL at 20 degree flaps							
Cdinducedstall = 0.352							
CL at 40 degree flaps							
Total Coefficient of drag at cruise velocity							
Cd Total at Cruise = 0.041							

LONGITUDINAL STABILITY

Summary of Equations Used

$$\frac{dC_{m_{cg}}/dL}{dC_{m_f}/dCl} = x/c - \eta_H(S_H/S_W)(l_H/c)((dCl_H/d\alpha)/(dCl/d\alpha)) +$$

longitudinal stability (Oothuseizen)

$$dC_{m_f}/dCl = k_f W_f^2 L_f / (CS_W)$$

Calculation of Rear Most CG

$l_H = 50$	in	tail moment arm
$C = 21$	in	mean aerodynamic chord
$S_H = 388$	in ²	horizontal tail area
$S_W = 1680$	in ²	wing area
$\eta_H = 0.9$		horizontal tail efficiency
$dCl_H/d\alpha = 5.73$	radians ⁻¹	slope of stabilizer Cl vs AOA
$=$		
$dCl/d\alpha = 5.2$	radians ⁻¹	slope of wing Cl vs AOA
$k_f = 0.6$		empirical pitching factor from Raymer
$W_f = 4$	in	width of fuselage
$L_f = 78$	in	length of fuselage

CG = 52.4 % of chord

LATERAL-DIRECTIONAL STABILITY

Summary of Equations Used

$$dC_{m_F}/d\phi = (dCl_f/d\alpha)(S_f/S_W)(l_H/c)$$

lateral-directional stability criterion (Oothuseizen)

Calculation of Rear Most CG

$l_H = 50$	in	tail moment arm
$C = 21$	in	mean aerodynamic chord
$S_H = 388$	in ²	fin area
$S_W = 1680$	in ²	wing area
$dC_{l_f}/d\alpha = 5.73$	radians ⁻¹	slope of fin C_l vs AOA
$dC_{m_f}/d\phi$	3.2	< 0

Horizontal Tail Design

Summary of Equations Used

HTA =	horizontal tail area	(pg 33, Basics of RC Model Aircraft Design)
$(2.5 \cdot \text{MAC} \cdot 22\% \cdot \text{WA}) / \text{TMA}$	elevator area	
EA = 40% * HTA	horizontal lift force	
Horizontal Lift = Pitching Moment * Moment Arm		
Cl _t =	tail coefficient of lift	
$(\text{HL} \cdot 3519) / (\rho \cdot V_{\text{cruise}}^2 \cdot \text{Stail})$		
$\alpha = \alpha_0 + ((18.24 \cdot \text{Cl}) \cdot (1 + T)) / \text{AR}$	angle of incidence account for aspect ratio effects	

Horizontal Tail Area

based on a comparison to an airplane of AR = 6 and a 22% area at a distance of 2.5 times the chord

HTA = $(2.5 \cdot \text{MAC} \cdot 22\% \cdot \text{WA}) / \text{TMA}$ (pg 33, Basics of RC Model Aircraft Design)

HTA = horizontal tail area

TMA = tail moment arm in inches

WA = wing area

MAC = mean aerodynamic chord

TMA = 50 in variable based on design

TMA = 1.27 m

HTA = 388 in² stab area for given tail moment arm

HTA = 0.25 m²

Elevator Area

For a flapped model, an elevator area of 40% should be used

EA = 40% * HTA

$EA = 155 \text{ in}^2$
$EA = 0.100 \text{ m}^2$

Estimated Tail Efficiency

estimated between 40 and 90% based on vertical position of tail relative to wing

THE = 0.9	predicted efficiency value for a T tail
-----------	---

Lift of Horizontal Tail Needed

Wing Pitching Moment

PM = -2171 oz/in pitching moment of wing at cruise

PM = -30.7 N/m pitching moment of wing at cruise

Horizontal Lift = Pitching Moment * Moment Arm

HL = -43.4 oz

HL = -38.9 N

Tail lift accounting for tail efficiency

HL = -48.3 oz negative pitching moment requires downforce

HL = -43.3 N

Coefficient of Lift for Tail

$C_{lt} = (HL * 3519) / (\rho * V_{cruise}^2 * S_{tail})$

$C_{lt} = -0.16$ coefficient of lift need for tail airfoil

Angle of Incidence of Tail

Interpolation of alpha at given coefficient of lift
Values Taken at $Re = 399900$

	Alpha	Cl	Cd
	1.67	0.151	0.0074
	2.11	0.198	0.0079
Difference	0.44	0.047	0.0005
alpha =	-1.75 degrees		

$$a = a_o + ((18.24 * Cl) * (1 + T)) / AR$$

$a_o = -1.75$ angle of attack at coefficient of lift needed from airfoil properties

$Cl = -0.159$ Cl_{cruise}

$T = 0.12$ platform adjustment for aspect ratio (figure 4, pg 6 of Basics of Model Aircraft Design)

$AR = 4$ aspect ratio of wing

$a' = -2.56$ degree tailplane incidence neglecting downwash
es from wing

Downwash Angle Estimation

$SS = 42.00$ in	wing semi-span
$X = 50.00$ in	distance from wing 1/4MAC to tail 1/4MAC (TMA)
$X / SS = 119.05 \%$	distance from wing 1/4MAC to tail 1/4MAC as a percent of semispan
$H' = 10.00 \%$	vertical wake displacement in percent of semispan for a $Cl_{cruise} = 1$ (fig 2, pg of Basics of RC Model Aircraft Design, column b)
$H = 4.64 \%$	vertical wake displacement in percent of semispan for a $Cl_{cruise} = 396$
$HTE = 15$ in	horizontal tail elevation above wing
$M = 35.714 \%$	horizontal tail elevation above wing as a percent of semispan
$M + H = 40.35 \%$	vertical location of horizontal tail relative to the wake Cl as a percent of semispan
$DWA' = 3.8$ deg	downwash angle at $Cl = 1$ (fig 2, pg 40, The Basics of RC

Model Aircraft Design, column c)	
DWA = 1.7630 deg	downwash 0.46396
	angle at CI = 2742
a = -0.80 degrees	tailplane incidence

Spar Sizing

Summary of Equations Used

$DI = SS \cdot z$	force on wing from distributed load
$I = A \cdot y^2$	Second moment of inertia of area
$\text{stress} = M \cdot y / I$	bending stress

Dimensions and Material Properties

B =	84 in	spar span
SS =	40	semi span minus fuselage width
H =	2.44 in	height from carbon fiber endcap to endcap
y =	1.22 in	neutral plane (1/2 H)
m =	34.2 lbs	mass of plane
g =	4	g loading due to circumferential forces
F =	136.9 lbf	force wing must support
z =	1.71 lbf/in	distributed lift load
w =	1.25 in	spar width
t carbon =	0.0087 in	thickness of each layer of unidirection preimpregnated carbon fiber
n =	4	number of layers of carbon fiber in the lamination
tc =	0.0348 in	thickness of carbon fiber lamination on each end
tf =	0.25 in	thickness of Douglas Fir Compressive spar
E(C) =	21000000 lbf/in ²	Youngs Modulus of carbon fiber
T.S. C	175000 psi	Tensile Strength of carbon fiber
T.S. Fir	12400 psi	Tensile Strength of Douglas Fir
C.S. Fir	7240 psi	Compressive Strength of Douglas Fir

E(Fir) = 1950000 psi	Youngs Modulus of Douglas Fir		
SS*z = 68.47	lbf		
M = 2738.8	lbf/in	M = 479635 N/m	force moment

Carbon Fiber

$$I = A \cdot y^2$$

$$\text{stress} = M \cdot y / I$$

Second moment of area for the carbon fiber

$$I = \frac{0.0627810 \text{ in}^4}{2}$$

stress = 52408 psi max tensile bending stress on bottom carbon fiber spar

S.F. = 3.34 safety factor of the spar against carbon fiber failure under a 4 G loading

Douglas Fir

$$I = A \cdot y^2$$

$$\text{stress} = M \cdot y / I$$

$$I = 0.3738403 \text{ in}^4$$

stress = 8013 psi compressive bending stress on top spruce spar

S.F. = 0.904 safety factor of the spar against Douglas Fir-fiber failure under 4 G loading ignoring compressional strength of carbon fiber

Coefficient of Lift

Summary of Equations Used	
$Cl_{max} = \frac{2 \cdot L}{\text{efficiency} \cdot p \cdot S_w \cdot V_{min}^2}$	maximum coefficient of lift needed at minimum velocity
$Cl_{min} = \frac{2 \cdot L}{\text{efficiency} \cdot p \cdot S_w \cdot V_{max}^2}$	minimum coefficient of lift needed at maximum velocity
$Cl_{cruise} = \frac{2 \cdot L}{\text{efficiency} \cdot p \cdot S_w \cdot V_{cruise}^2}$	cruise coefficient of lift needed at cruise velocity
$a = a_o + ((18.24 \cdot Cl) \cdot (1+T))/AR$	angle of incidence accounting for aspect ratio effects
$\text{Pitching Moment (oz/in)} = \frac{(C_m \cdot p \cdot V_{cruise}^2 \cdot S_{wing} \cdot \text{Chord})}{35}$	pitching moment of wing
$Cl = \text{Clairfoil} \cdot (((1 + \text{Flaplift}) \cdot \text{Flaplength}) + (1 - \text{Flaplength}))$	coefficient of lift account for flap efficiencies and length
$Cl_{climb} = \frac{2 \cdot L}{\text{efficiency} \cdot p \cdot S_w \cdot V_{min}^2}$	coefficient of lift during climb
$V_{stall} = ((2 \cdot M \cdot g) / (Cl_{max} \cdot p \cdot S_w))^{.5}$	velocity at stall

Constants

Gravit	9.81 m/s ²
y =	
Efficiency	0.9 = 90% wing construction accuracy
ncy =	efficiency

Coefficients of Lift using ElectriCalc Velocities

$Cl_{max} = \frac{2 \cdot L}{\text{efficiency} \cdot p \cdot S_w \cdot V_{min}^2}$
$Cl_{ma} = 2.41$
x =
$Cl_{min} = \frac{2 \cdot L}{\text{efficiency} \cdot p \cdot S_w \cdot V_{max}^2}$

Cl _{min} 0.39
=
Cl _{cruise} = $2 * L / (\text{efficiency} * \rho * S_w * V_{\text{cruise}}^2)$
Cl _{cruise} 0.46
se =

Maximum Cl obtainable from Wing Platform

Max Cl of Airfoil	1.32	maximum lift selected airfoil produces
Flap 20	0.7	Predicted additional lift provided by flaps
Lift deg.		
Flap 40	0.9	based on flap design and extension
Lift deg.		
Flap Length	0.6	Length of flaps in percent of wingspan

$$Cl = Cl_{\text{airfoil}} * (((1 + \text{Flap lift}) * \text{Flap length}) + (1 - \text{Flap length}))$$

CL ₂₀	1.87	Maximum Cl wing produced when flaps are deployed
=	20 degrees	

CL ₄₀	2.03	Maximum Cl wing produced when flaps are deployed
=	40 degrees	

$$V_{\text{stall}} = ((2 * M * g) / (Cl_{\text{max}} * \rho * S_w))^{.5}$$

V _{stall}	13.2 m/s	Calculated stall speed with 0 degree flaps
=		

V _{stall}	28.0 mph
=	

V _{stall}	11.1 m/s	Calculated stall speeds with 20 degree flaps
=		

V _{stall}	23.5 mph
=	

V _{stall}	10.6 m/s	Calculated stall speed with 40 degree flaps
=		

V _{stall}	22.6 mph
=	

Thus the maximum using 20 degree flap

coefficient of lift at takeoff = 1.87 extension
44

The takeoff velocity is taken at 1.15 times the stall velocity at 20 degree flaps, corresponding to C_l of

$C_{lclimb} =$

$$2 * L / (\text{efficiency} * p * S_w * (V_{min} * K)^2)$$

$C_{lclimb} = 1.57$ C_l needed during climbout a 1.15 times
 $b =$ V_{stall}

Total of Section and Induced Angle of Attack (AOA)

Interpolation of alpha at given coefficient of lift

Values Taken at $Re = 399900$

	Alpha	C_l	C_d
	0.1	0.377	0.0074
	1.69	0.55	0.0079
Difference	1.59	0.173	0.0005
alpha	0.90		
=			

$$a = a_o + ((18.24 * C_l) * (1 + T)) / AR$$

$a_o = 0.899$ angle of attack at coefficient of lift needed from airfoil properties

$C_l = 0.463$ $C_{lcruise}$

$T = 0.12$ platform adjustment for aspect ratio (figure 4, pg 6 of Basics of Model Aircraft Design)

$AR = 4$ aspect ratio of wing

$a = 3.27$ angle of incidence of wing on model

Pitching Moment

Pitching Moment (oz/in) =

$$(C_m * p * V_{cruise}^2 * S_{wing} * Chord) / 3519$$

Interpolating for C_m		
Using Data for $Re = 401900$		
alpha	Cl	Cm
0.63	0.406	-
		0.0771
1.87	0.56	-
		0.0815
Differ	1.24	0.154
ence		0.0044
$C_m =$ - pitching coefficient of wing at cruise 0.078 8		
PM = -2171 oz/in pitching moment		
PM = -30.7 N/m pitching moment		

Range

Summary of Equations Used

$V_{min} = 1.15 * V_{stall}$	minimum flying velocity
$Range = Velocity * Time$	distance plane covers over ground under now wind conditions

Minium Velocity

$V_{stall} = 13.18 \text{ m/s}$	stall speed at 0 degree flaps
$V_{stall} = 28.03 \text{ mph}$	
$V_{min} = 1.15 * V_{stall}$	
$V_{min} = 15.2 \text{ m/s}$	minimum speed at which the airplane can fly without stalling
$V_{min} = 32.2 \text{ mph}$	

Endurance of Motor System

Endurance =	23.3 min	at throttle setting to produce V_{min} , values taken from electricalc
Endurance =	1398 seconds	
Throttle =	52 %	throttle setting at minium velocity, from electricalc

Range

$Range = Velocity * Time$	
$Range = 21197 \text{ m}$	
$Range = 21.2 \text{ km}$	distance plane covers over ground under no wind conditions
$Range = 13.2 \text{ miles}$	neglecting takeoff, landing and energy loss maneuvers

Turning Radius

Summary of Equations Used

$\cos B =$	bank angle which the plane can still horizontal level
Cl_{cruise}/Cl_{max}	flight
$\tan B =$	g-loading before accelerated stall
$a/1 \cdot g$	
$R = (V_{cruise}^2)/a$	radius of turn with no altitude loss

$Cl_{cruise} = 0.46$	minimum lift needed during cruise
$Cl_{max} = 1.32$	maximum lift airfoil can produce without use of flaps (from tables)
$V_{cruise} = 23.4$	cruise velocity of airplane

Bank Angle	
$\cos B =$	
Cl_{cruise}/Cl_{max}	
$\cos B =$	0.351
$\beta = 1.2$	radians
$\beta = 69.4$	degrees degrees of bank that the wing can still provide the necessary lift

G-Loading Before Accelerated Stall

$\tan B =$	
$a/1 \cdot g$	
$a =$	2.66 g maximum radial acceleration before the onset of an accelerated stall
$a =$	26.1 m/s ²

Radius of Level Turn

$R = (V_{cruise}^2)/a$	
$R =$	21.0 m
$R =$	69.0 ft minimum radius of turn before accelerated stall

TAKEOFF PERFORMANCE

Summary of Equations Used

$V_{\text{takeoff}} = k \cdot V_{\text{stall}}$	safe takeoff velocity
$a = (T - (A + B \cdot C_{l_g}^2) \cdot \frac{1}{4} \cdot \rho \cdot V_m^2 \cdot S_w - u \cdot (W - C_{l_g} \cdot \frac{1}{4} \cdot \rho \cdot V_m^2 \cdot S_w)) / M$	ground run acceleration
$d_g = (V_{to}^2) / (2 \cdot a)$	ground roll distance
$d_c =$ $h / \tan \theta$	horizontal distance to climb to height h
$d_c = h / (T/M - ((A + B \cdot C_{l_{to}}^2 / k^4) / (C_{l_{to}} / k^2)))$	
$\tan \theta = T/W - D/L$	climb out angle

Values Used in calculations

$V_{\text{stall}20}$	11.1 m/s	Calculated stall speed	With 20 degree flaps
V_{stall}	13.2	Calculated stall speed	With 0 degree flaps
k	1.15	is 15% above stall speed	usually equals 1.1 to 1.2
V_{to20}	12.7 m/s	takeoff velocity	With 20 degree flaps
V_{to0}	15.2 m/s	takeoff velocity	With 0 degree flaps
V_{mean}	9.0 m/s	mean takeoff velocity	
T	53.4 N	takeoff thrust	
u	0.015	rolling resistance (estimate)	
A	0.023	Parasite Drag Coefficient	
B	0.148	Induced drag Coefficient	C_d cruise used based on C_L cruise being used
M	15.5 kg	mass	
W	152.3 N	weight	
ρ	1.225 kg/m ³	density of air	
S_w	1.084 m ²	wing platform	
C_l	0.464	coefficient of lift on takeoff run	C_l cruise used because AOA is fixed at cruise while on ground
C_l'	1.575	coefficient of lift during	

H =	10.000 m	climbout climbout altitude
-----	----------	-------------------------------

**Ground Run
Acceleration**

$$a = (T - (A + B \cdot Clg^2) \cdot \frac{1}{4} \cdot p \cdot Vm^2 \cdot Sw - u \cdot (W - Clg \cdot \frac{1}{4} \cdot p \cdot Vm^2 \cdot Sw)) / M$$

$$a = 3.21 \text{ m/s}^2$$

$$a = 10.53 \text{ ft/s}^2$$

**Ground Run
Distance**

$$dg = (Vto^2) / (2 \cdot a) = \text{ground roll}$$

$$dg = 25.23 \text{ m} \quad \text{ground roll with 20 degree flaps}$$

$$dg = 82.78 \text{ ft}$$

$$dg = 35.83 \text{ m} \quad \text{ground roll with 0 degree flaps}$$

$$dg = 117.55 \text{ ft}$$

**Climb Out Distance to an Altitude of "h"
meters**

$$dc =$$

$$h / \tan \theta$$

$$dc = h / (T/M - ((A + B \cdot Clto^2 / k^4) / (Clto / k^2)))$$

$$\tan \theta = T/W - D/L$$

$$\tan \theta = 0.1024217$$

$$82$$

$$\text{Climb Angle} = 0.10 \text{ rad}$$

$$\text{Angle} =$$

$$\text{Climb Angle} = 5.85 \text{ degrees}$$

$$\text{Angle} =$$

$$dc = 97.64 \text{ m} \quad \text{distance to climb to height h}$$

$$dc = 320.32 \text{ ft}$$

WING LOADING

Summary of Equations Used

Wingloading = Weight/Wing
Area

Values used in Calculations

	Imperial	Metric
Wingspan	84.0 in	2.13 m
Root Chord	21.0 in	0.53 m
Tip Chord	21.0 in	0.53 m
Fuselage Width	4.0 in	0.10 m
Weight	34.2 lbs 548 oz	15.5 kg 15529 g
Average Chord	21.0 in	0.53
Wing Area	1680 in ² 11.7 ft ²	1.08 m ² 108.4 dec ²

Wing Loading With No Flaps

Wing Loading	0.02 lbs/in ²	14.3 kg/m ²
no flaps	2.93 lbs/ft ²	0.14 kg/dec ²
	47.0 oz/ft ²	143 g/dec ²

Flap Extension Area

Individual Flap Area	151.2 in ²	0.098 m ²	
Total Flap Area	302.4 in ²	0.195 m ²	
Flap Extension Area	151.2 in ²	0.098 m ²	
Total Wing Area	1831 in ²	1.181 m ²	at 40 degree flaps
	1756 in ²	1.133 m ²	at 20 degree flaps
	12.72 ft ²	118.1 dec ²	at 40 degree

	12.19 ft ²	113.3 dec ²	flaps
--	-----------------------	------------------------	-------

Wing Loading With Extended Flaps			
Wing Loading	43.1 oz/ft ²	131.4 g/dec ² at 40 degree	flaps
Flaps Extended	44.9 oz/ft ²	137.1 g/dec ² at 20 degree	flaps

KEY DIMENSIONS AND FEATURES			
Feature	Item	Imperial Units	Metric Units
Propulsion			
	Motor	MaxN32-13Y Brushless DC	MaxN32-13Y Brushless DC
	Speed Controller	Maxu 35-36 Brushless	Maxu 35-36 Brushless
	Cells	26cells by 3000mah each	26cells by 3000mah each
	Reduction	11 to 1	11 to 1
	Propeller	24 by 16	24 by 16
	Static Thrust on Takeoff	12 lbf	53.3808 N
	Static Thrust	12 lbf	53.3808 N
	Run Time Full Throttle	4 min	4 min
	Motor Efficiency	90 %	90 %
	Energy Efficiency	70 %	70 %
Wing			
	Span	84.000 in	2.134 m
	Root Chord	21.000 in	0.533 m
	Tip Chord	21.000 in	0.533 m
	Average Chord	21.000 in	0.533 m
	Wing Thickness	2.000 in	0.051 m
	Aspect Ratio	4.000	4.000
	Wing Area	1680.000 in ²	1.084 m ²
	Taper	none	none
	Sweep	none	none
	Airfoil	Clark Y	Clark Y
	Aileron Length	16.000 in	0.406 m
	Aileron Width	5.250 in	0.133 m
	Aileron Area (each)	84.000 in ²	0.054 m
	Flaps Length	24.000 in	0.610 m
	Flaps Width	6.300 in	0.160 m
	Flap Area (each)	151.200 in ²	0.098 m ²
Horizontal Stabilizer			
	Tail Aspect Ratio	4.000	4.000 m
	Target Stab Area	388.080 in ²	0.250 m ²
	Chord	9.850 in	0.250 m

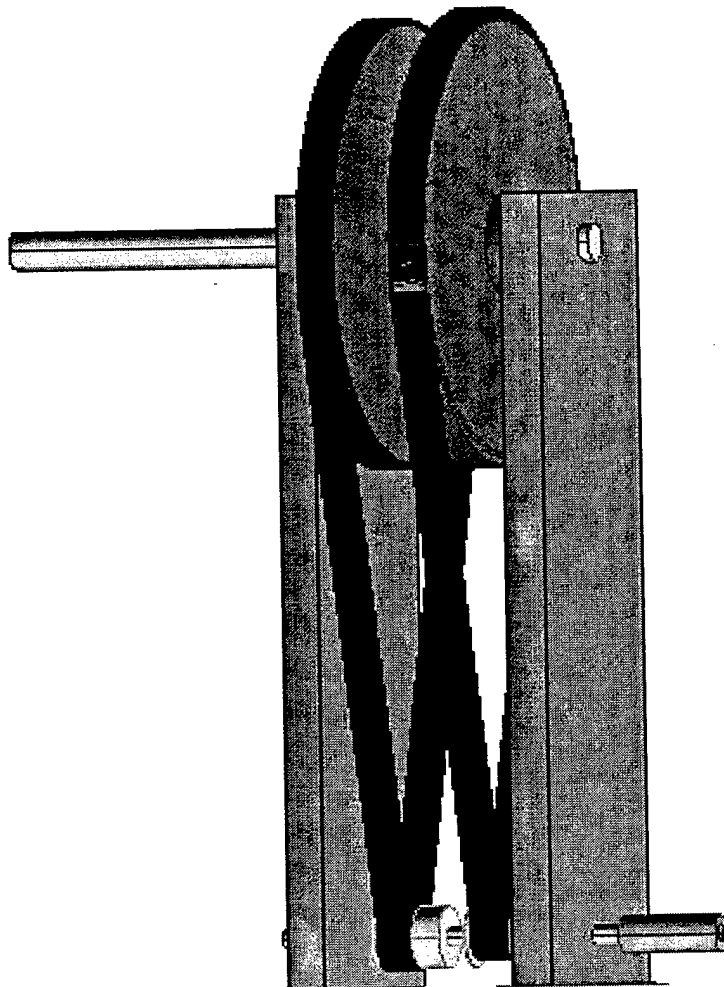
	Span	39.400 in	1.001 m
	Iterated Area	388.090 in ²	0.250 m ²
	Tail Moment Arm	50.000 in	1.270 m
	Tail Thickness	0.750 in	0.019 m
	Airfoil	NACA 0009	NACA 0009
	Taper	single taper	single taper
	Sweep	none	none
	Target Elevator Area	155.232 in ²	0.100 m ²
	Elevator Span	39.400 in	1.001 m
	Elevator Chord	3.940 in	0.100 m ²
Vertical Fin/Rudder			
	Vert Fin Height	10.500 in	0.267 m
	Tip Chord	9.875 in	0.251 m
	Root Chord	9.875 in	0.251 m
	Average Chord	9.875 in	0.251 m
	Vert. Fin Area	103.688 in ²	0.067 m ²
	Rudder Tip Chord	4.000 in	0.102 m
	Rudder Root Chord	4.000 in	0.102 m
	Average Rudder Chord	4.000 in	0.102 m
	Rudder Height	15.000 in	0.381 m
	Rudder Area	60.000 in ²	0.039 m ²
	Rudder/Fin Thickness	0.688 in	0.017 m
	Airfoil	NACA 0009	NACA 0009
	Taper	none	none
	Sweep	none	none
Fuselage			
	Length	78.000 in	1.981 m
	Height	12.313 in	0.313 m
	Width	4.000 in	0.102 m
Main Landing Gear			
	Wheel Diameter	3.000 in	0.076 m
	Wheel Base	14.438 in	0.367 m
	Thickness	0.250 in	0.006 m
	Avg Width	3.000 in	0.076 m
	Height	5.813 in	0.148 m
	Brakes	none	none
Nose Gear			
	Wheel Diameter	2.500 in	0.064 m
	Thickness	0.500 in	0.013 m
	Height	5.813 in	0.148 m

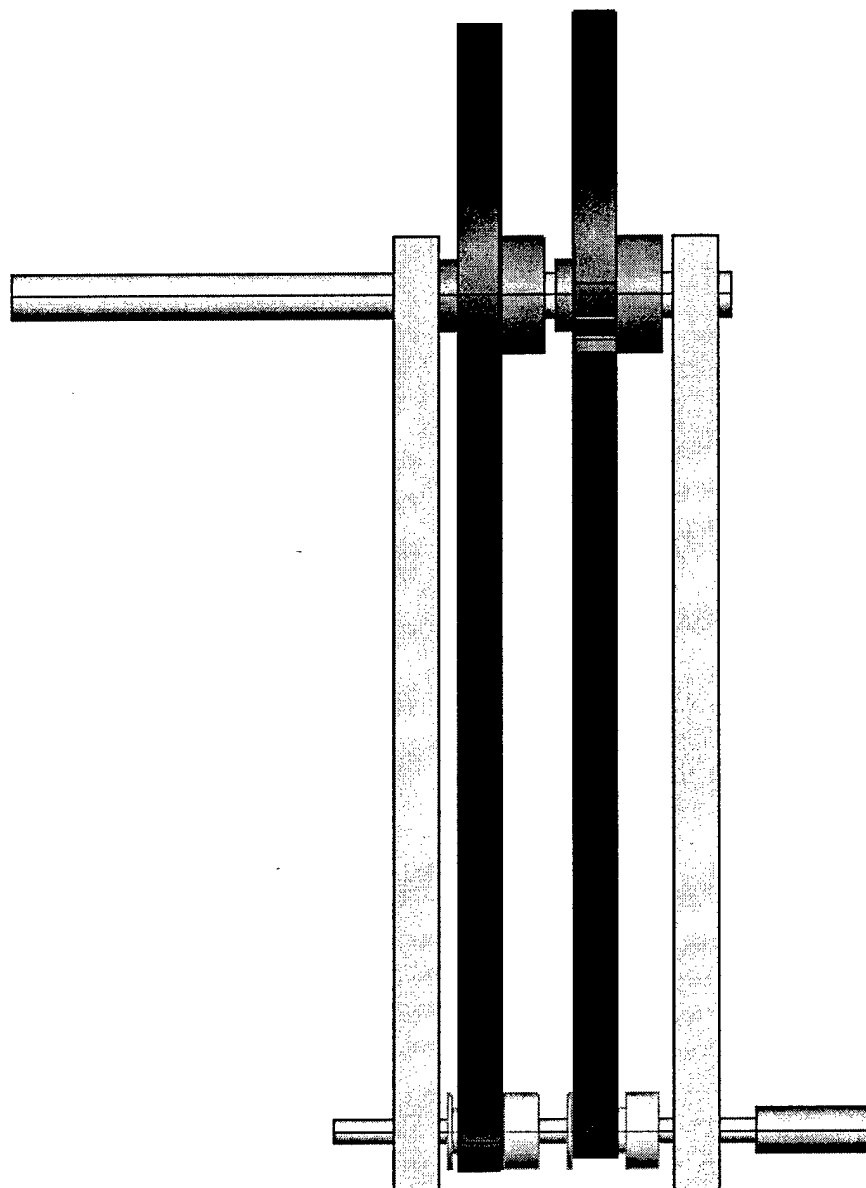
	Wire Diameter	0.250 in	0.006 m
	Brakes	yes	yes
From Electrocalc			
	Vmax	57 mph	25.5 m/s
	Vcruise	52 mph	23.4 m/s
	Vmin	23 mph	10.3 m/s

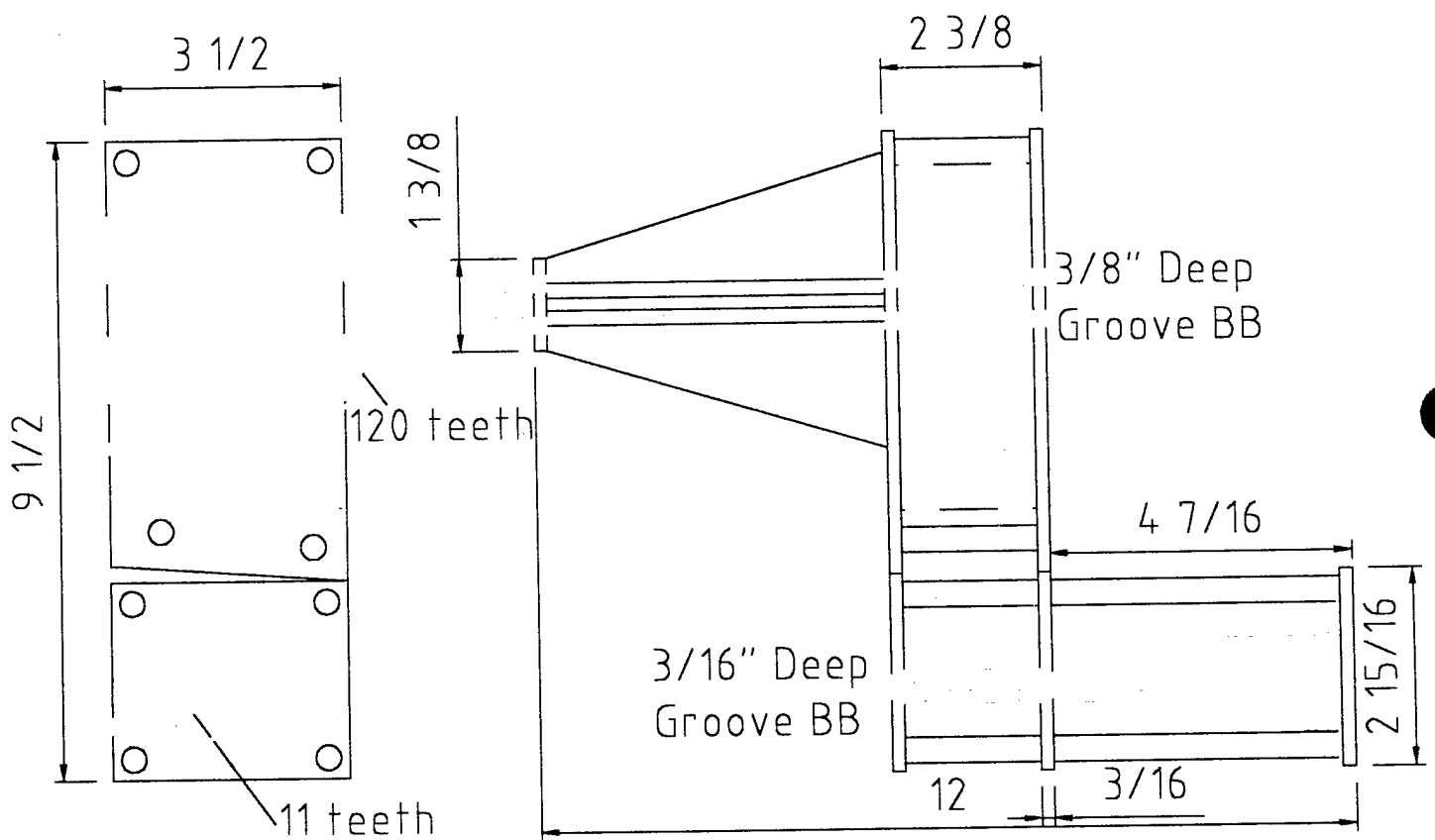
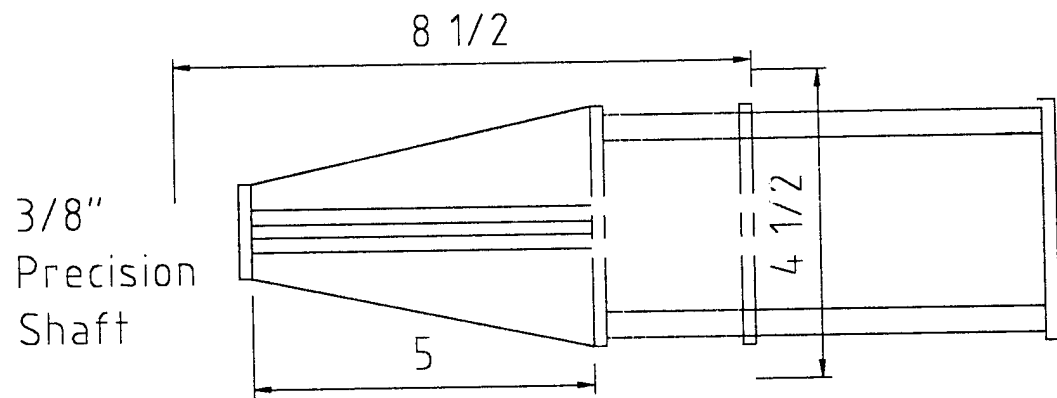
Appendix B: References

1. Eppler, Richard. Airfoil Design and Data. Springer-Verlag: Germany. 1990.
2. Foster, Steve. "*Undercarriage Design for Queen's Cargo Aircraft*." Undergraduate Thesis Project, Department of Mechanical Engineering. March, 1994.
3. Horton, Johanna Lisa. "*Cargo Aircraft Stability Analysis*." Undergraduate Thesis Project, Department of Mathematics and Engineering. April, 1993.
4. McCormick, Barnes. Aerodynamics, Aeronautics, and Flight Mechanics, second edition. John Wiley & Sons, Inc.: New York. 1995.
5. Munson, Young, and Okiishi. Fundamentals of Fluid Mechanics, second edition. John Wiley & Sons, Inc.: New York. 1994.
6. Raymer, Daniel. Aircraft Design: A Conceptual Approach. AIAA Education Series. American Institute of Aeronautics and Astronautics, Inc.: Washington, D.C. 1989.
7. Abbott, Ira. Theory of Wing Sections. McGraw-Hill Book Company Inc.: Toronto. 1949.
8. White, Frank M. Fluid Mechanics, 4th Edition. McGraw-Hill Book Company Inc.: Toronto. 1999.
9. Lennon, Andy. Basics of R/C Model Aircraft Design. Y. DeFrancesco: Ridgefield, CT. 1999.

Appendix C: Belt Drive detail



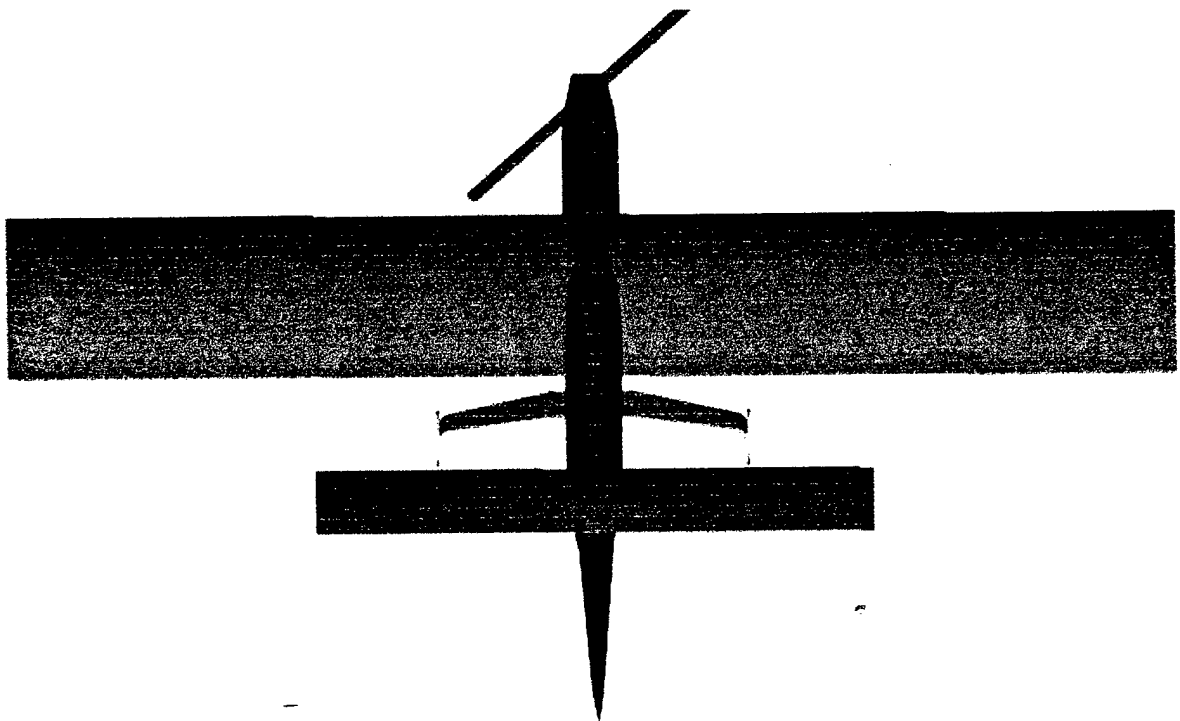
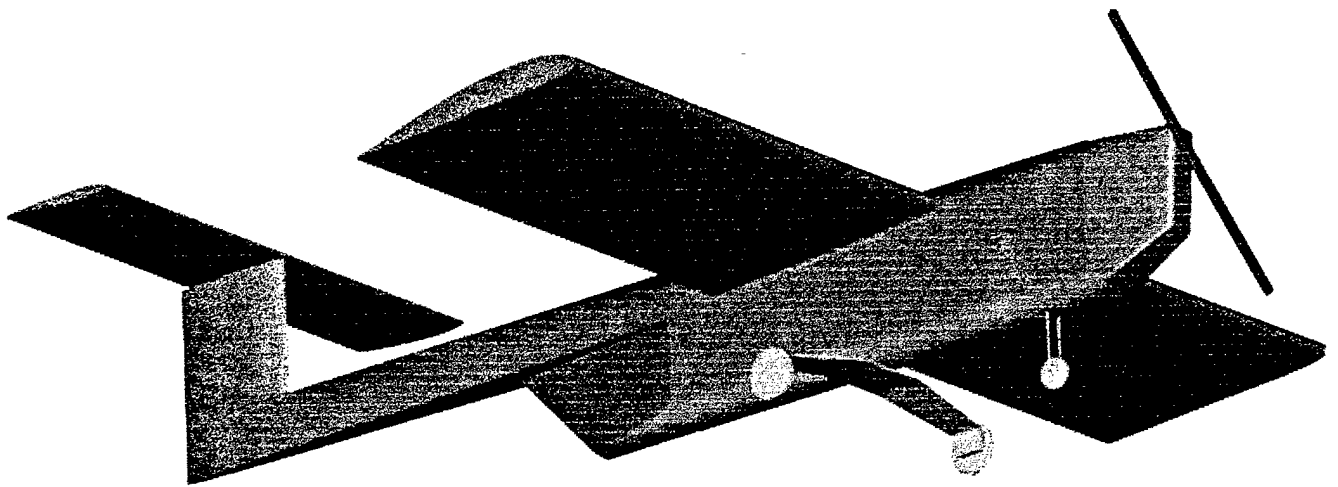
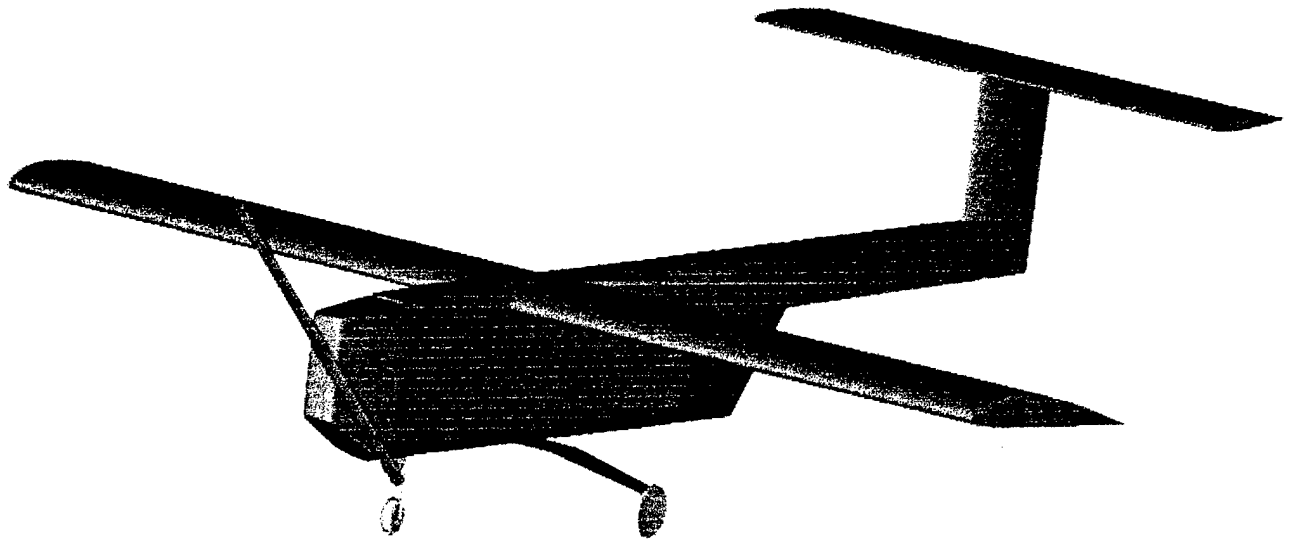




Front Plate
Removed for
Clarity

Queen's Aero Design Team
Obsidian Reduction Drive

Appendix D: Drawing Package



Payload

Payload

Flight Systems

Elevator Servo

Rudder Servo

Receiver

Speed Control

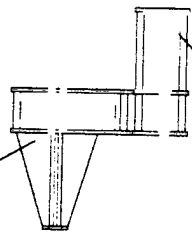
Steering Servo

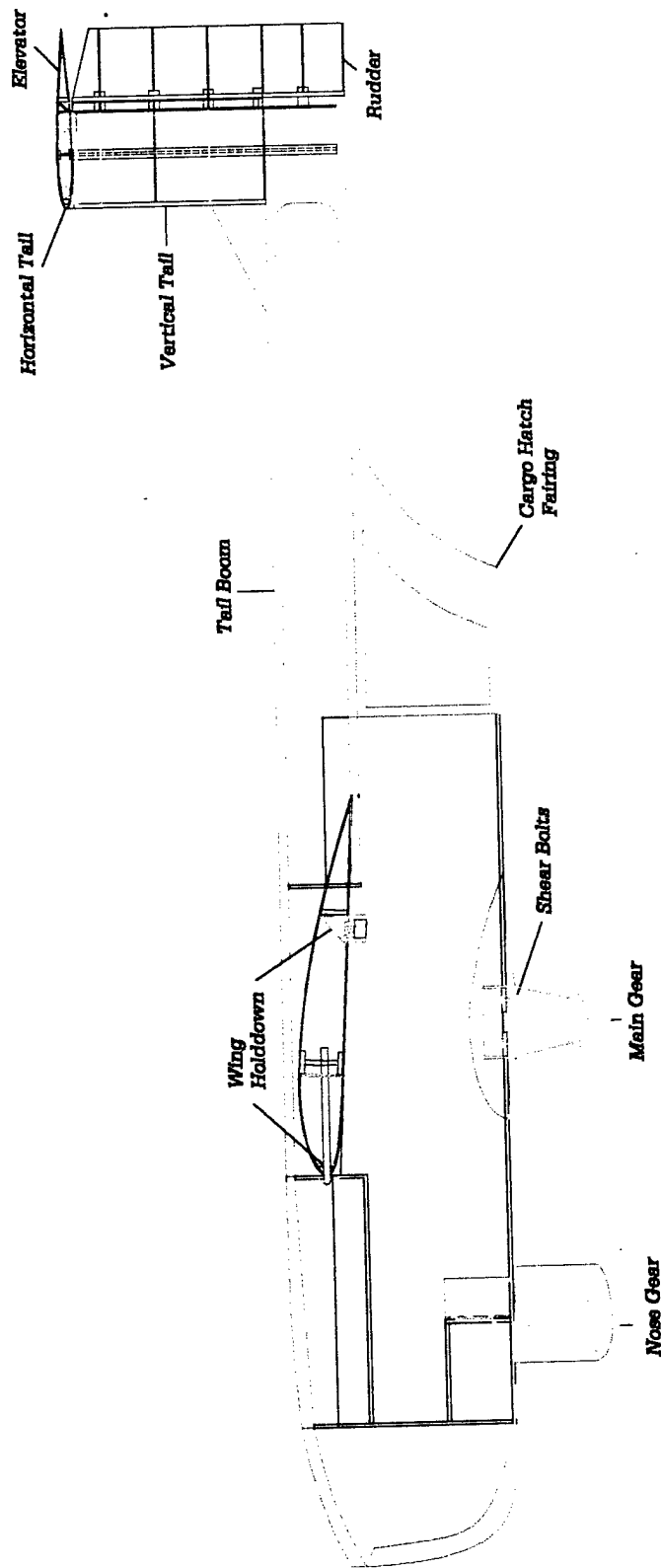
Batteries

Belt Drive

Motor

Propeller





Materials By Color *Airframe*

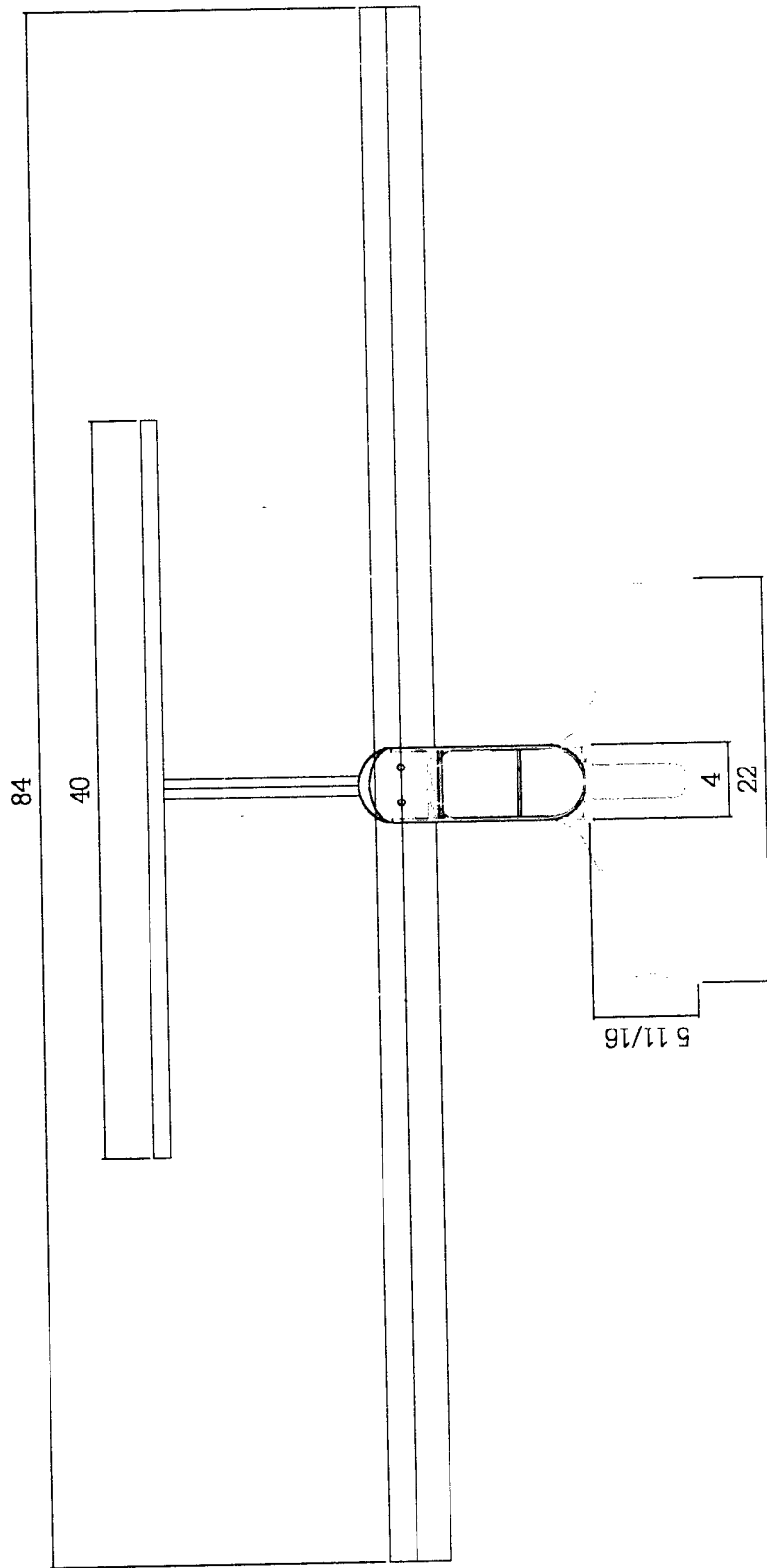
Balsa Wood

Carbon Fiber/Nomex

Spruce

Plastic

OBSIDIAN

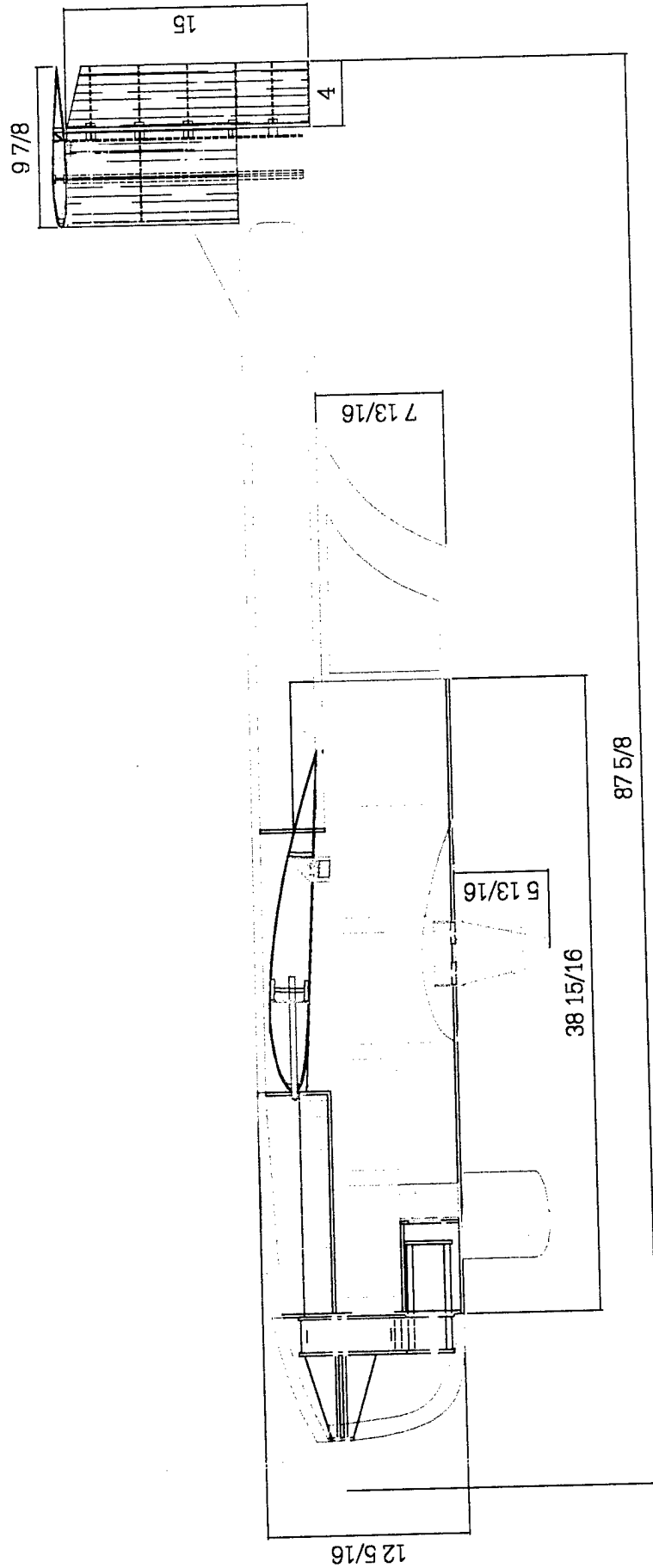


OBSIDIAN

Queen's Aero Design Team

Dimensioned Front View

All Dimensions in Inches

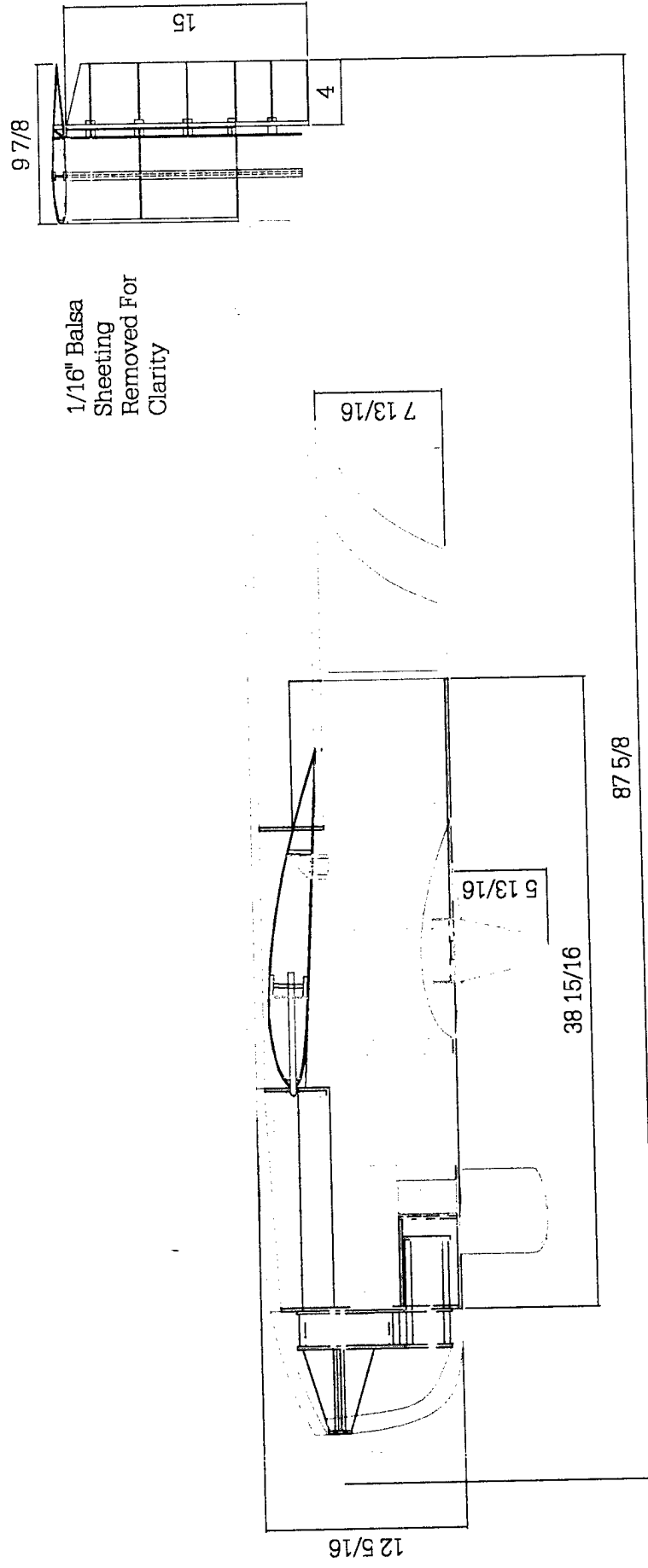


OBSIDIAN

Queen's Aero Design Team

Dimensioned Side View

All Dimensions in Inches

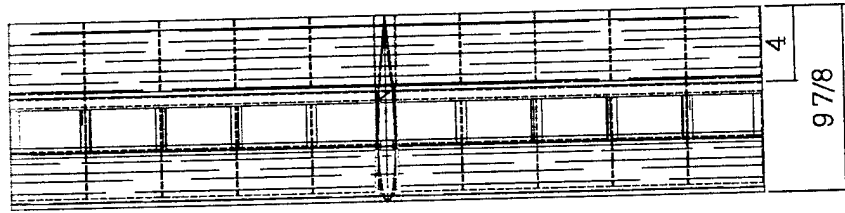


OBSIDIAN

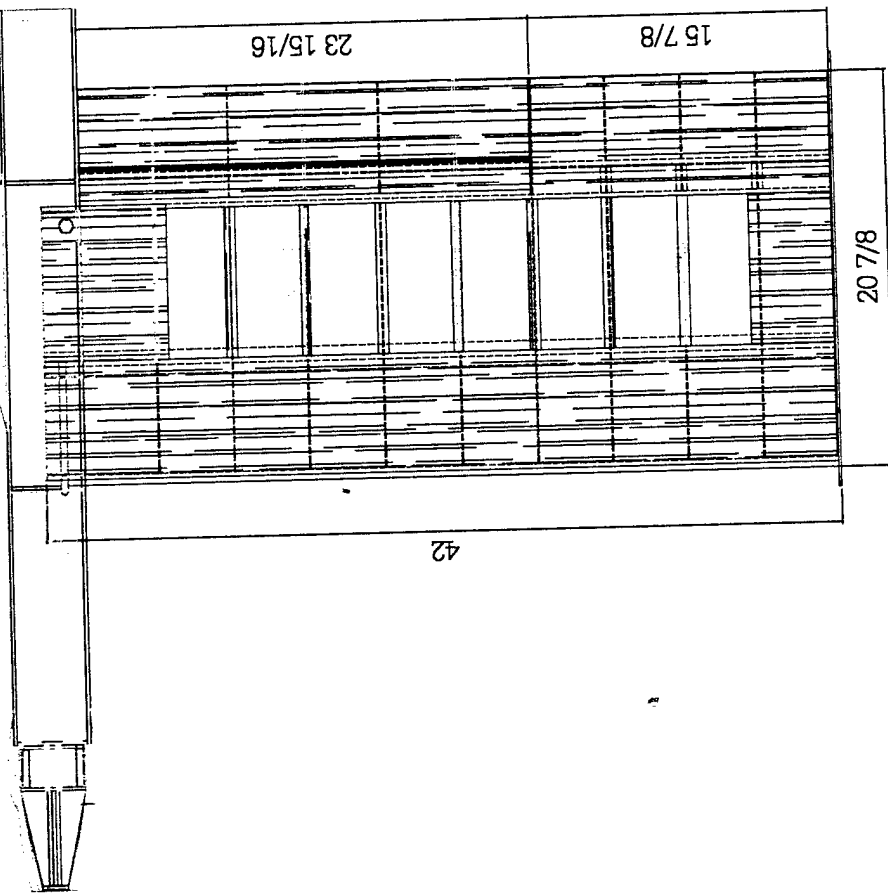
Queen's Aero Design Team

Dimensioned Side View

All Dimensions in Inches



Swing
Cargo Door

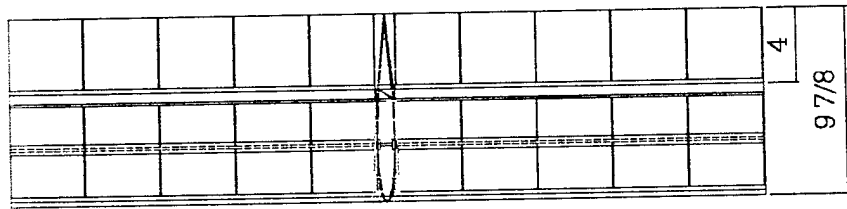


OBSIDIAN

Queen's Aero Design Team

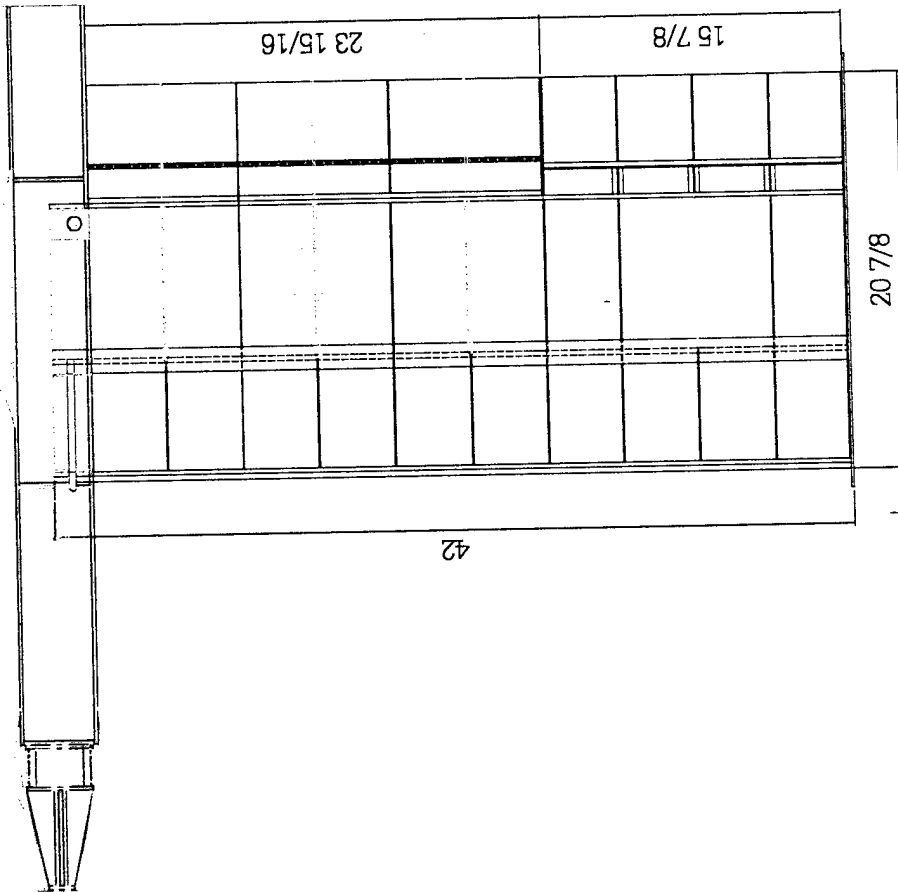
Dimensioned Top View

All Dimensions in Inches



Swing
Cargo Door

1/16" Balsa
Sheeting
Removed For
Clarity

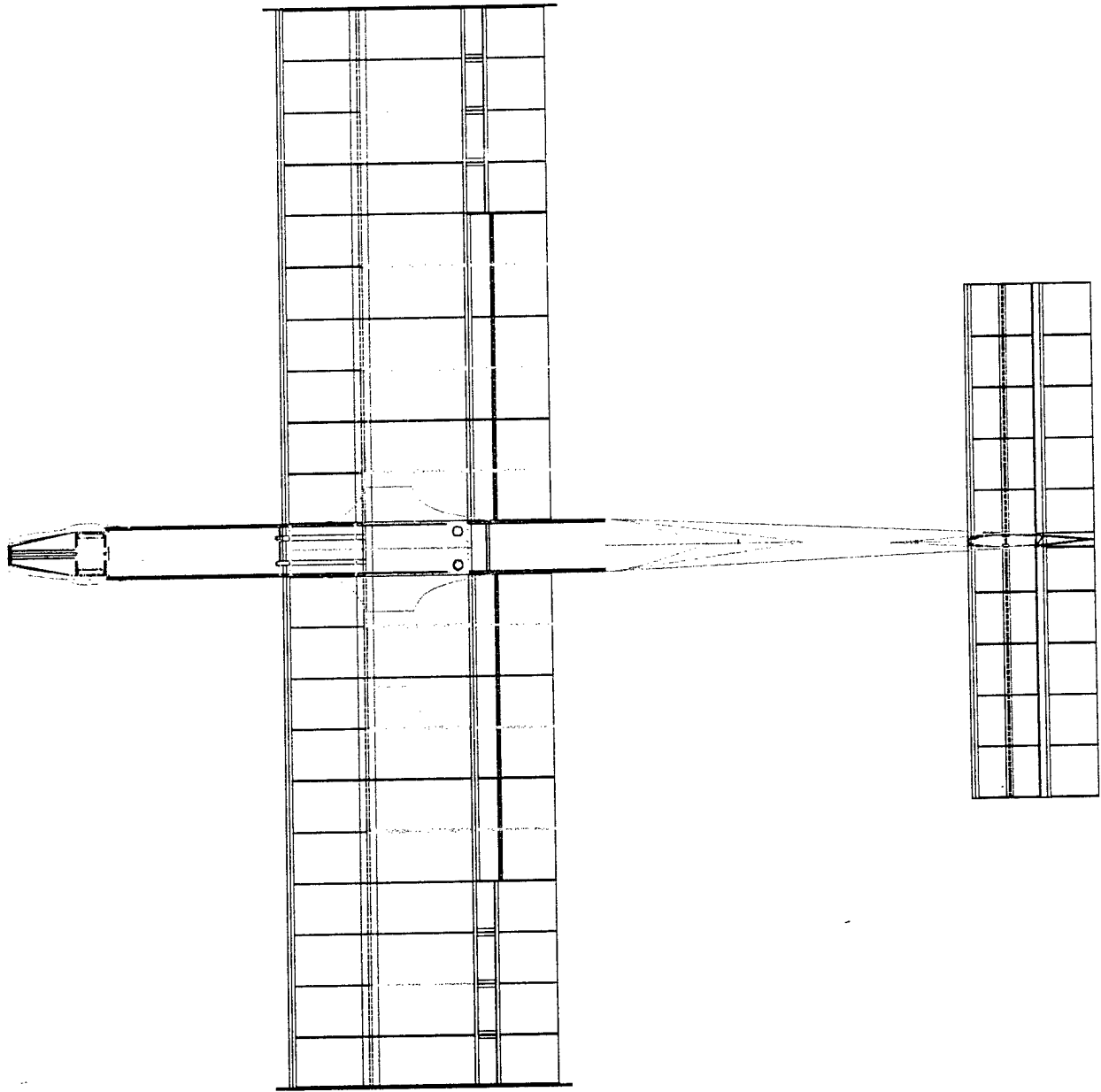


OBSIDIAN

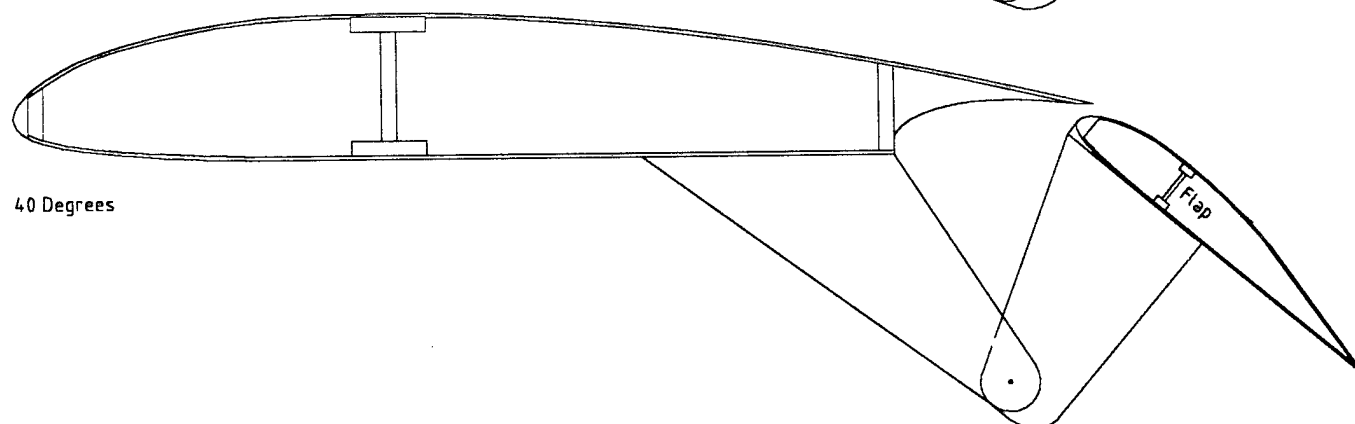
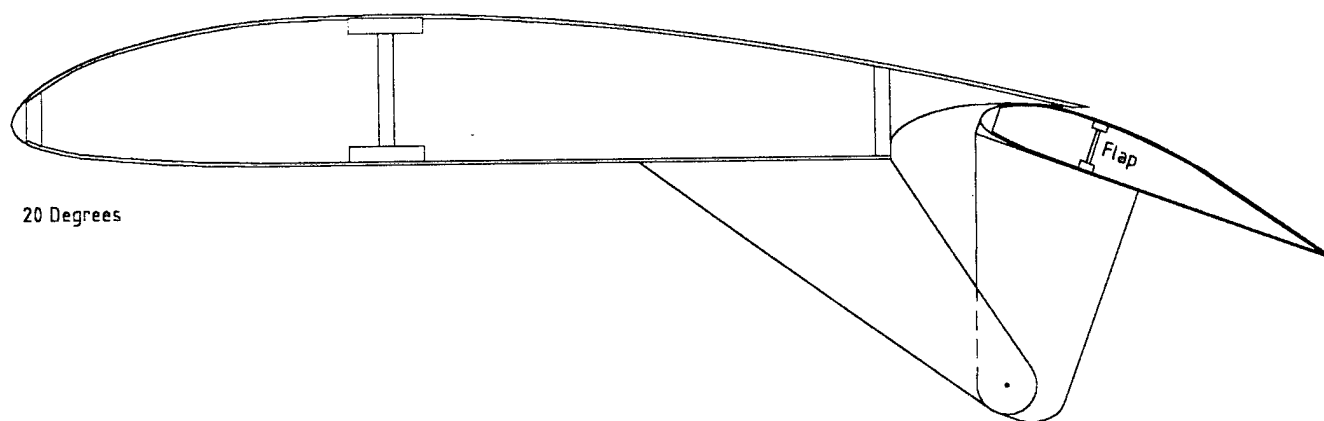
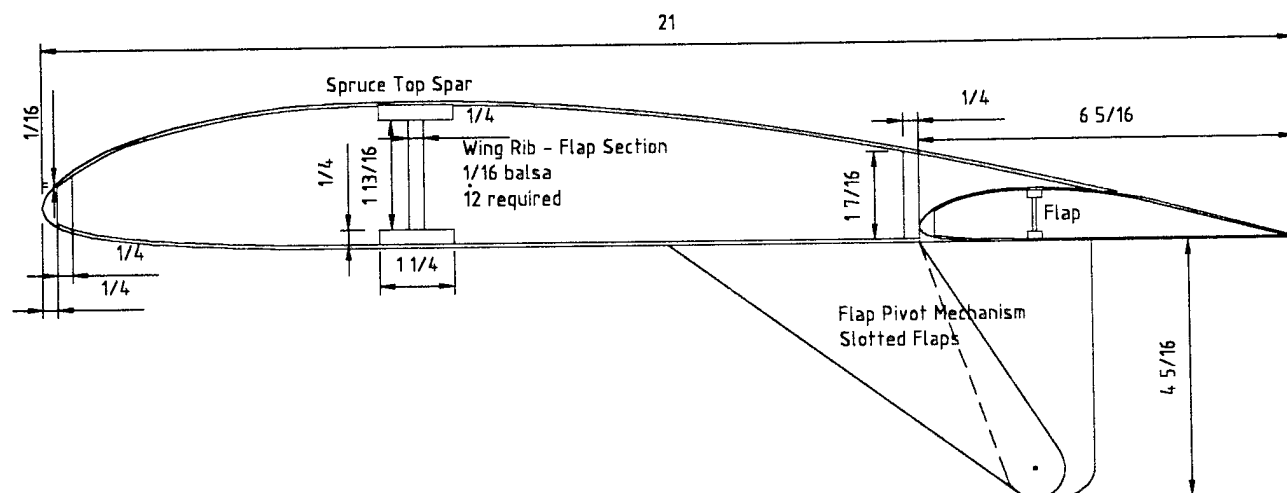
Queen's Aero Design Team

Dimensioned Top View

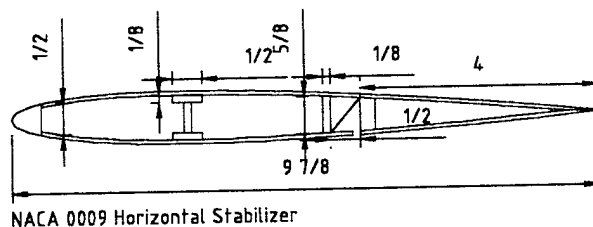
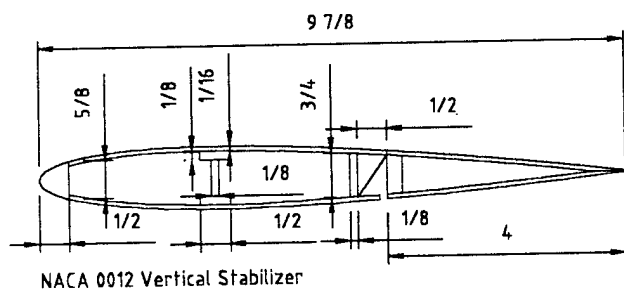
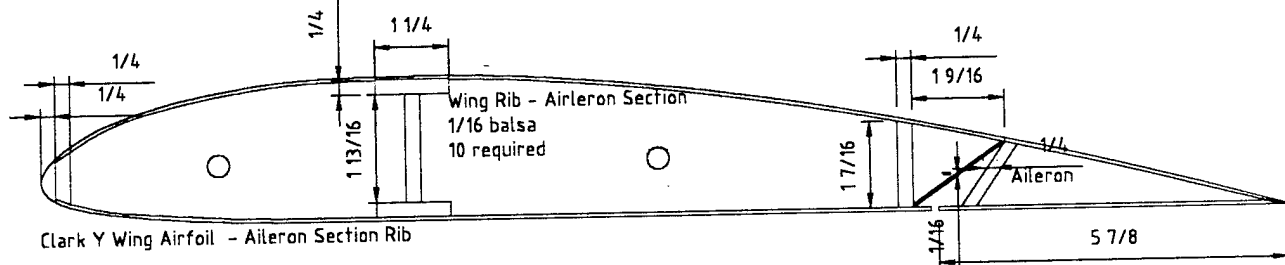
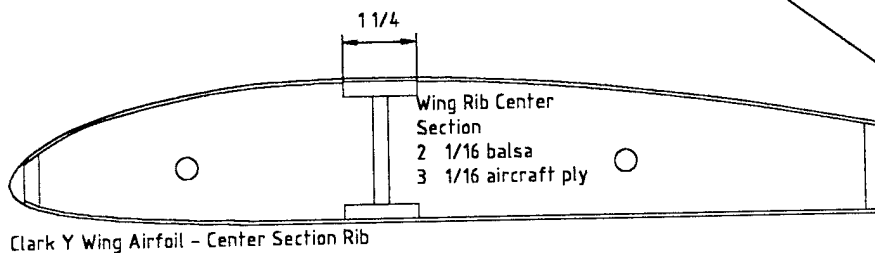
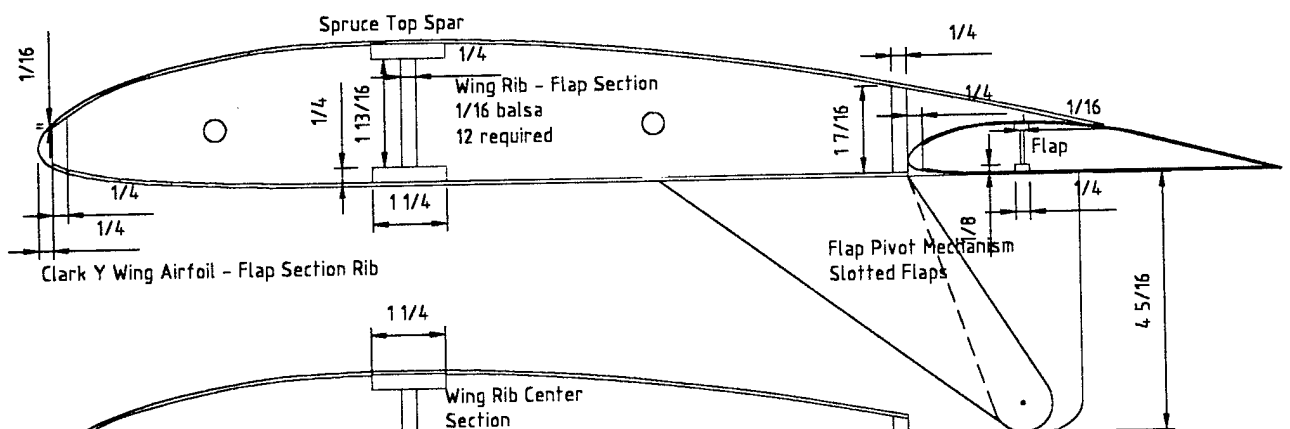
All Dimensions in Inches



● **OBSIDIAN** *Queen's Aero Design Team*



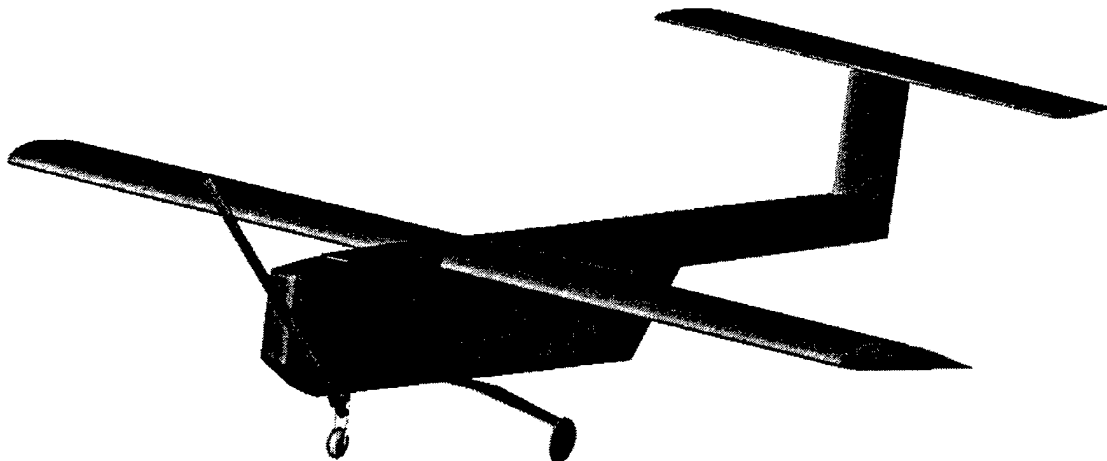
Queen's Aero Design Team
Obsidian Flap Design



Queen's Aero Design Team
Airfoil Templates

2000 AIAA DBF Competition Design Report

——— *Addendum Phase* ———



Queen's University at Kingston

Team #1 – “Obsidian”

Department of Mechanical Engineering

Department of Engineering Physics

April 10, 2000



Table of Contents

7.0: Lessons Learned	91
7.1: Changes from the Proposal	91
7.2: Improvements for 2 nd -Generation Design	93
7.3: Cost Estimate	94
8.0: Aircraft Cost.....	97

7.0 Lessons Learned

7.1 Changes from the Proposal

Unlike last year's radical redesign, Obsidian does not vary greatly from the report submitted during the proposal phase. The greatest change has been to the propulsion system, particularly the belt drive reduction unit. Initially, the belt drive used a double belt design, but testing with the prototype indicated that a single belt system would provide sufficient power transmission for this application. The initial design also utilized a composite made up of a layer of honeycomb sandwiched between two layers of pre-impregnated unidirectional carbon fiber. Unfortunately, this material was found to be unsuitable for the construction of the reduction unit for two reasons: poor crush resistance, and de-lamination.

The design requires carbon tubes to be affixed to the composite plates with Robertson wood screws. This allows the belt drive to be disassembled quickly to replace components or to perform minor adjustment to the drive components. However, it was found that the concentrated stress applied by these screws caused the honeycomb to crush slightly, making the precise alignment required by this application to be very difficult.

The de-lamination problem encountered with the composites was a result of the age of the pre-impregnated carbon-fiber. The material consists of carbon fibers in a semi-cured epoxy matrix, and it must be stored at sub-zero temperatures to prevent the epoxy from curing before it can be used. However, as the roll ages, a greater percentage of the epoxy solidifies, weakening the resulting bond strength when the material is actually used. The expense of this material creates a dependence on donations from industry, thus student projects must utilize what is available.

As the carbon fiber and honeycomb material did not withstand the stresses inherent in the belt-drives, the team made up replacement plates of 3/16" solid carbon fiber. Although heavier, the plates result in a very rigid reduction system that lends itself to precise alignment of the rotating components.

Further testing with the improved reduction system indicated that the system was more efficient than expected. Current draw was 35% lower than forecasted by ElectriCalc and MotoCalc, so the belt drive ratio was reduced to 10:1 for more thrust. It was in this form that Obsidian's power system was deemed acceptable for the D/B/F competition.

The most visible change to Obsidian is the omission of both the cowl and the landing gear fairings. The new reduction system is slightly larger than the original design, the increase in size a result of a desire to obtain a more rigid structure.

Unfortunately, this increase in size makes the fitting of a cowl very difficult. It was felt that any attempt to streamline the structure would not result in a noticeable gain in aerodynamic efficiency. The belt-drive's frontal area and short propeller shaft prevents the long taper required for better aerodynamics. An advantage of not having a cowl is the increased airflow through the motor compartment aids in the cooling of the MaxCim motor.

The landing gear fairing was omitted from the final design due to time and material constraints. Upon the realization that the belt-drive would have to be replaced with one constructed of more robust material, it was decided that all components that were not essential to the flight of the UAV be put on hold until the new power system was in place and tested. By the time that this criteria was satisfied, the team's finishing epoxy supply had been exhausted on other more important fairings and hatches. It was decided that the budget could not support the purchase of new epoxy in this contest year, thus the fairing could not be made.

7.2

7.3 Improvements for 2nd-Generation Design

There are several areas in Obsidian's design that might be improved for a second-generation design, but they are only details. It is felt that Obsidian's design is very close to the optimum solution for this year's AIAA D/B/F contest in that it is built light, yet strong. If it were to be built again, the first thing to be changed would be to build a lighter belt-drive with CNC milled aluminum making up the bulk of the unit. This construction technique would increase the thermal heat transfer from the motor, leading to a cooler and more efficient motor system.

Streamlining would also be examined further with additional time and resources. The belt-drive would be fully enclosed, with custom ducting to ensure that the speed control and the motor remain cool. All component joints would be considered and fairings would be added to reduce interference drag. Work could also be done in a wind tunnel using simple flow visualization techniques to help identify problem areas and to fit fairings that reduce the disturbances.

A second-generation design would feature a less obtrusive flap design. The current slot-lip flaps require six large pivots that extend from the bottom surface of the wing. These pivots are a large source of parasitic drag, but were used on Obsidian to produce a simple and reliable flap mechanism. Future designs would investigate other forms of high lift devices and methods to utilize internal linkages. If carefully designed, their inherent complexity could be simplified into a robust mechanism with better aerodynamic properties without a large weight penalty.

Another portion of Obsidian that would be examined for a second-generation design would be the wing tips. The very low aspect ratio wing used in this competition produces large vortices at the wing tips, which disturb the air over the outer portion of the wing, reducing the efficiency of the surface. Although Obsidian employs tip plates in an attempt to reduce these vortices, Horner wing tips or some method of active control would reduce the vortices further. This testing would again require access to a large wind tunnel, but the benefits of a more efficient wing are substantial.

The last point that would be improved in a second-generation design is based on construction techniques rather than actual airframe design. Obsidian currently uses Philips head, hex head, flat head, and Robertson head fasteners in the various assemblies. If it were to be built again, a large stock of hex head screws and bolts would be purchased and used exclusively. Although Robertson head fasteners are very good, Philips head and flat head screws tend to strip, or do not hold a screwdriver

securely. There is nothing more frustrating than having to remove a component, only to find that it cannot be easily removed due to damaged fasteners.

7.4 Cost Estimate

Costs are broken down for each section of the aircraft. For comparison, both manufacturer's list price and actual procurement cost (which includes donations, discounts, taxes, shipping, and customs charges) are provided. Costs marked with an asterisk (*) are estimated. All figures have been converted to US dollars at an assumed exchange rate of \$1 US = \$1.40 Canadian. It should be noted that without the donation of the carbon fiber by Queen's Solar Vehicle Team, Obsidian would not have been financially possible.

Many costs from the estimate below were not included in the Proposal Phase as they were not relevant considerations in selecting one design or process over another (ie: paint, propeller, battery pack). This year the actual procurement cost was much less the manufactures suggested price due to the generous sponsorship obtained from several companies and Queen's organizations.

In many instances, actual procurement costs varied significantly from manufacturer's list prices. This is due to several factors. The team has long-standing relationship with local hobby shops and receives a discount on most standard materials. Many materials cannot be bought in the small quantities required for this aircraft, and thus leftovers from previous years are always available. Also, the weak Canadian dollar, in combination with foreign shipping and customs charges, heavily affected the actual price of any item purchased outside Canada. This surcharge was especially seen while obtaining material for the belt drive.

Table 7.1. Cost Estimate.

	<i>Manufacturer's List Price</i>	<i>Actual Procurement Cost</i>
<u>Wing</u>		
Uni-directional carbon fiber	50	0 (leftovers)
Monokote	50	38
<u>Tail</u>		
Uni-directional carbon fiber	10*	0 (donation)
MonoKote	5	4
<u>Fuselage</u>		
Uni-directional carbon fiber	3000*	0 (leftovers)
Honeycomb	200	250 (customs)
Pink Foam	15	15
Fiberglass	15	12
<u>Landing Gear</u>		
Uni-directional carbon fiber	5000*	0 (donated)
Main wheels	11	0 (leftovers)
Bearings	15	15
Nose wheel assembly	6	5
Axles	5	4
<u>Motor and Electronics</u>		
MaxN32-13Y Motor	220	220
Motor controller	300	0 (donated)
Motor mount	13	13
Motor Battery pack	350	0 (donated)
Radio Receiver	120*	0 (borrowed)
Servos (8)	360	145 (donation)
Servo battery pack	18	15
Wiring	5	4

<u>Belt drive</u>		
Running gear (belts, pulleys, etc)	250	350 (customs)
Bearings	75	75
Uni-directional carbon fiber	1500*	0 (donated)
Carbon fiber tube	22	20
<u>Other</u>		
Epoxy	100	0 (leftovers)
Balsa wood	100*	75*
Aircraft plywood	40*	30*
Paint	4	4
Propeller	130	100
Miscellaneous nuts and bolts	50*	38*
TOTAL	\$ 12036	\$ 1432

8.0 Aircraft Cost

To document Obsidian's *Rated Aircraft Cost*, first examine the weight of the aircraft. Without the five-pound battery pack on board, the plane tips the scales at 12 pounds. The *Manufactures Empty Weight (MEW)* multiplier is 100 dollars per pound of airframe; thus the cost of Obsidian's weight is \$1200.

Next examine the propulsion system. Obsidian is powered by a single MaxCim N32-13Y brushless DC motor and 26 3000mAh Ni-Cad cells. The supplied *Rated Engine Power (REP)* formula is $REP = \#engines * 50 \text{ amps} * 1.2 \text{ volts/cell} * \# \text{ cells}$. Obsidian's propulsion system thus has a REP of 1560 watts. When the *Rated Engine Power Multiplier* (\$1/watt) is applied, Obsidian's cost is \$1560

The final cost section is *Manufacturing Man Hours (MFHR)* and it is a sum of the assembly time required for the wing, the fuselage, the empenage, the flight system, and the propulsion system.

The wing is given a rating of 5 hours per wing plus 4 hours per square foot of projected area. Obsidian has a single wing with an area of 11.67 square feet; so the time required to build it would be 51.68 hours.

The fuselage is given a rating of 5 hours per body plus 4 hours per foot of length. Obsidian possess a single 6.25' fuselage without any extra pods or nacelles, thus the time required is 30 hours.

The empenage is given a rating of 5 hours plus 5 hours for each vertical surface and 10 hours for each horizontal surface. Obsidian has been designed with a conventional tail (one vertical surface and one horizontal surface), so the total time required to build them is calculated to be 20 hours.

Flight systems are calculated to take 5 hours plus 1 hour for each additional servo. Obsidian has two servos operating the flaps, two servos operating the ailerons, a servo to steer the nose wheel, a servo to operate the wheel brake, a servo to operate the rudder and a servo to operate the elevator. A total of 8 servos results in a build time of 13 hours.

The propulsion system is calculated to take 5 hours per motor plus another five hours for each propeller or ducted fan. Obsidian has been designed with a conventional single motor driving a single propeller, thus the system should take 10 hours to build.

The MFHR is the sum of the systems described above, thus MFHR is equal to 124.68 hours. When multiplied by the supplied *Manufacturing Cost Multiplier* (\$20/hour), the total construction cost of Obsidian is \$2,493.68.

Obsidian's *Rated Aircraft Cost* is the sum of the empty weight cost, the engine power cost, and the man hours cost. Thus, Obsidian's total cost is 5.2536 thousand dollars.

Figure 8.1: Airframe Dependent Parameters

Manufactures Empty Weight Multiplier	A	\$100 * MEW	A =	\$ 1,200.00
Manufactures Empty Weight	MEW (pounds)	airframe weight	MEW =	12

Rated motor Power Multiplier	B	\$1 * REP	B =	\$ 1,560.00
Rated motor Power	REP (watts)	# motors * 50A * 1.2V/cell * # cells	REP =	1560
			# motors =	1
			# cells =	26

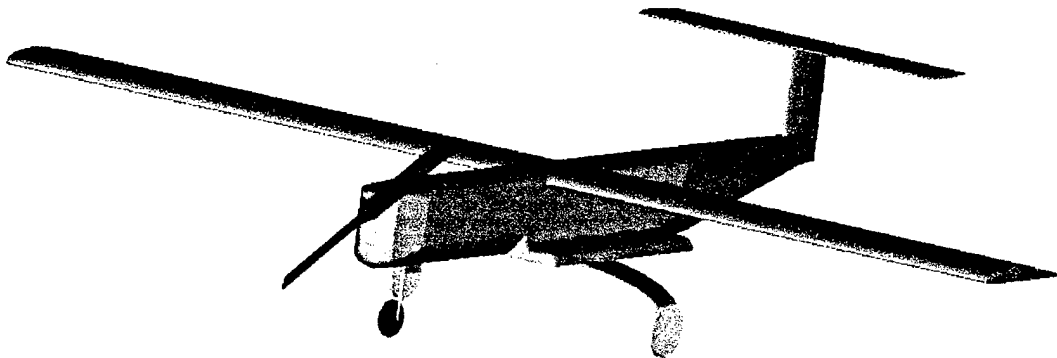
Figure 8.2: Manufacturing Hours

Manufacturing Cost Multiplier	C	\$20 * MFHR	C =	\$ 2,493.60
Manufacturing Man Hours	MFHR (hours)	Prescribed assembly Hours by WBS	MFHR =	124.68
		MFHR = the sum of WBS		
		Wings WBS = 5hrs/wing + 4 hrs / sq foot projected area	Wing WBS =	51.68
			# wings =	1
			area (sq.ft) =	11.67
		Fuselage WBS = 5hrs/body + 4hrs / foot or length	Fuselage WBS =	30
			# bodys/pods =	1
			length (ft) =	6.25
		Empenage WBS = 5 hrs + 5 hrs/vert surf. + 10 hrs/ horz surf.	Empenage WBS =	20
			# vert. surfaces =	1
			# horz. surfaces =	1
		Flight Systems WBS = 5 hrs + 1 hr/ servo	Flight Sys. WBS =	13
			# servos =	7
		Propulsion Systems WBS = 5 hrs / motor + 5 hrs / prop	Propulsion WBS =	10
			# motors =	1
			# props =	1

$$1200 + 2473.6 + 1560 = 5173.6 = 5.17$$

2000 AIAA DBF Competition Design Report

————— *Proposal Phase* —————



Queen's University at Kingston

Team #2 – “Minnow”

Department of Mechanical Engineering

Department of Engineering Physics

March 13, 2000

Table of Contents

Nomenclature	3
1.0 Executive Summary	5
1.1 Major Development Areas.....	5
1.2 Design Tool Overview.....	6
1.1.1 Conceptual Design	6
1.1.2 Preliminary Design.....	6
1.1.2 Detail Design.....	6
2.0 Management Summary	8
2.1 Personnel and Configuration	8
2.2 Schedule.....	9
3.0 Conceptual Design	10
3.1 Design Parameters	10
3.1.1 Power Train.....	10
3.1.2 Motor Placement	11
3.1.3 Wing Placement	11
3.1.4 Wing Design.....	13
3.1.5 Fuselage Design	13
3.1.6 Undercarriage	14
3.1.7 Tail Design	16
3.2 Figures of Merit.....	16
3.2.1 Drag Penalty.....	17
3.2.2 Weight Penalty	17
3.2.3 Performance	17
3.2.4 Ease of Manufacture.....	17
3.3 Concept Evaluation	17
3.3.1 Analytical Method.....	17
4.0 Preliminary Design	23
4.1 Take-off Gross Weight (TOGW) Estimation.....	23
4.2 Propulsion Systems Selection.....	23
4.3 Wing Area and Airfoil Selection.....	24
4.3.1 C_L at the Best Lift to Drag (L/D) Angle of Attack.....	24
4.3.2 Maximum C_L	24
4.3.4 Stall Characteristics.....	24
4.3.5 C_D at Expected Cruise AOA	24
4.4 Aspect Ratio.....	25
4.5 Tail Sizing.....	26
4.6 Airframe and Fuselage Sizing	26
5.0 Detail Design.....	29
5.1 Weight.....	29
5.2 Payload Fraction.....	29
5.3 Wing Performance.....	29
5.4 Tail Sizing.....	31
5.5 Fuselage Sizing.....	32
5.6 Drag.....	32

5.7 Total Drag	33
5.8 Power System.....	34
5.9 Control Systems	34
5.10 G-Loading.....	34
5.11 Structural Loading.....	35
5.12 Take-off Performance	36
5.12.1 Ground Roll.....	36
5.12.2 Climb out Distance.....	36
5.13 Turning Radius	37
5.14 Endurance and Range	37
5.14.1 Endurance.....	37
5.14.2 Range.....	37
5.15 Stability.....	38
5.15.1 Longitudinal Stability.....	38
5.15.2 Lateral-Directional Stability.....	38
5.15.3 Roll Stability	38
6.0 Manufacturing Plan.....	40
6.1 Fuselage Construction.....	40
6.1.1 Balsa Stringer	40
6.1.2 Corrugated Plastic	40
6.1.3 Molded Carbon Fiber	40
6.1.4 Fiberglass	40
6.2 Tail Construction.....	41
6.2.1 Foam and Fiberglass.....	41
6.2.2 Sheet Balsa	41
6.2.3 Built-up Construction.....	41
6.3 Undercarriage Construction	41
6.3.1 Aluminum	41
6.3.2 Tool Steel	41
6.3.3 Amarid, Carbon Fiber, and Structural Honeycomb	42
6.4 Figures of Merit.....	42
6.4.1 Weight	42
6.4.2 Structure	42
6.4.3 Skill	42
6.4.4 Expense	43
6.4.5 Time	43
6.5 Evaluation and Selection.....	43
6.5.1 Analytical Method.....	43
6.5.2 Construction Method Selection.....	43
Appendix A: Calculation Spreadsheets	46
Appendix B: References	62
Appendix C: Belt Drive Detail.....	63
Appendix D: Drawing Package.....	65

Nomenclature

A	Parasite drag coefficient
A_{wetted}	Wetted area
AOA	Angle of attack
AR	Aspect ratio
a_m	Average acceleration on ground roll
Ac	Aerodynamic center
B	Induced drag coefficient
C	Chord
C_D	Coefficient of drag
$C_{D\text{para}}$	Coefficient of parasite drag
$C_{D\text{induced}}$	Coefficient of induced drag
C_f	Skin friction drag coefficient
CG	Center of gravity
C_L	Coefficient of lift of wing
C_{Lh}	Coefficient of lift of stabilator
$C_{L\alpha}$	Derivative of C_L with respect to AOA
$C_{L\text{max}}$	Maximum coefficient of lift
C_M	Coefficient of pitching moment
c_p	Power coefficient
c_t	Thrust coefficient
D	Propeller diameter
D	Drag
d_c	Climb-out distance
d_r	Ground roll distance
d_{TO}	Take-off distance
E	Wing efficiency factor
G	Acceleration due to gravity
FOM	Figure of merit
H	Altitude
I	Mass moment of inertia
K	Form factor
L	Lift
M	Mass
M	Pitching moment
R	Turning radius
Re	Reynold's number
S_h	Stabilator planform area
S_w	Wing planform area
T	Thrust
TOGW	Takeoff gross weight

T	Maximum airfoil thickness
V	Velocity
V_{\max}	Maximum cruise speed
V_{\min}	Minimum cruise speed (stall speed)
V_{mean}	Mean velocity on takeoff roll
V_{stall}	Stall speed
V_{TO}	Takeoff speed
W	Fuselage Width
W	Weight
X_{CG}	Position of CG
X_{ACW}	Position of wing aerodynamic center
X_{ACH}	Position of stabilator aerodynamic center
X_{NP}	Position of stability neutral point
α	Angle of attack
β	Angle of bank
ρ	Air mass density
σ	Maximum stress
ε	Downwash angle
η	Efficiency
θ	Pitch Angle
μ	Dynamic viscosity
γ	Kinematic viscosity

1.0 Executive Summary

This year's entry to the Design/Build/Fly (DBF) marks a radical change from Queen's previous entries. For the first time since 1992, Queen's will be fielding two aircraft in a competition. The reuse of several major components (wing, motors) led to two teams being possible, with half of the club designing one aircraft and the other half of the club designing the second entry. It should be noted that although the teams did operate individually at times, as can be seen by the different design philosophies of the two aircraft, the majority of the time was spent working together to pool our resources. Such developments as the carbon fiber fuselages, the composite undercarriages, and the belt drives would not have been possible without the cooperation of both teams. The reports have been written by this coalition of students, with the individual report being tailored to the specific aircraft as required.

1.1 Major Development Areas

Queen's second entry, named "Minnow" due to its small stature, exhibits several new and innovative design features and construction techniques in an attempt to produce the lightest and most efficient aircraft possible. The general layout is very similar to Queen's aircraft from the past, but it utilizes composite construction for increased rigidity with reduced weight. Minnow also features a custom designed belt drive as a means of obtaining a large amount of thrust from a small electric motor, saving weight and resources as it allows the reuse of Queen's MaxCim MaxNEO-13Y brushless electric motor.

Minnow's design was based loosely on last year's aircraft. The '98-'99 entry was found to possess excellent flight characteristics and its 3 liter payload was considered a good compromise between load and speed. Unfortunately, last year's entry suffered from a lack of refinement in the fuselage, thus its performance was lower than expected. Minnow's goal was to change this through a light, streamlined fuselage and a more powerful motor and belt drive system.

Upon beginning the conceptual phase of the design, time was spent evaluating the *rated aircraft cost* penalty system that was new to this year's competition. It was found that the use of multiple motors was strongly discouraged, thus a smaller single motored plane would be more competitive than at last year's competition. Further research indicated that if the aircraft carried 3 liters through 4 sorties, it would be competitive with very large aircraft carrying 8 liters through 3 sorties. Extra incentive for producing a small fast plane were the weather conditions in Kansas during the spring. If the weather were windy during the competition, as all signs pointed to, then very large under powered aircraft would not be able to fly. The winner of the contest would be the smaller, faster airplanes with a better thrust to weight ratio, who would be able to fly against the prevailing wind.

Research was begun in the conceptual design stage to examine different propeller/belt drive/battery combinations in an effort to produce the fastest drive system with enough static thrust to permit takeoffs in the required 100 feet. To conserve costs, every effort was made to be able to use the existing 25 cell speed control. Research indicated that a 5 lb. battery pack could be made with 26 Sanyo 3000CR cells, thus it was decided to reduce this number by one so that the speed control could be used. With a 25 cell pack, a 6.85:1 ratio belt drive was selected to give a thrust to weight ratio when empty of greater than one. It was felt that this performance would be beneficial given the uncertainty of the weather.

With a tentative power system and payload weight decided upon, attention was turned towards the rest of the aircraft. The wing used during the '98-'99 Design/Build/Fly competition was still in good repair and had been designed for a plane of this size. The

decision was made to reuse this structure, after first overhauling it and clipping 6 inches from each wing tip so that it would fall within the new wingspan restriction of 7 feet.

The fuselage was the next item to be designed. As the flight profile called for a fast aircraft, extra attention was warranted to reduce parasitic drag on the airframe. This was achieved by using rounded fairings wherever possible to reduce interference drag, and the tail-boom was designed to transition slowly back from the bulk of the fuselage to a slender oval at the rudder. Further streamlining was calculated with the addition of a fairing around the nose wheel and another around the battery packs mounted at the landing gear/fuselage junction on each side of the aircraft.

These improvements were all calculated to rejuvenate the '98-'99 entry into a small, fast plane that would be very competitive in Kansas. While not as ambitious as the other Queen's team, Obsidian, it was felt that refining an existing design would result in a very reliable and well-designed aircraft.

1.2 Design Tool Overview

1.1.1 Conceptual Design

Throughout the conceptual design phase of Minnow's development, a variety of tools were used to develop and evaluate different aspects of the aircraft's design. These range from reading model airplane oriented books and magazines, to research done on the internet, to making use of a spreadsheet detailing the *rated aircraft cost* penalty for the various designs.

This research revealed that a small monoplane of modest payload and wing area would be competitive against larger and more complex aircraft configurations. The research helped the team reach decisions of which aspects of the prior design needed refining, and which aspects could be reused. The same sources helped to educate the team on the design and characteristics of electrically powered airplanes, a relatively new and fluid field in model aeronautics.

1.1.2 Preliminary Design

Once the team entered this portion of the design process, the techniques used became more analytical than the quantitative methods used in the conceptual design. The *rated aircraft cost* spreadsheet was still used, again compare slight variations of Minnow's design as various ideas were generated and tested. Component weight was measured, estimated, or obtained from manufacturing specification sheets to allow for some first iteration values to be generated. Simple aerodynamic formulae were used to determine such things as the wing loading and tail sizing, to ensure that the reuse of the wing would indeed be feasible.

Computer software in the form of ElectriCalc and MotoCalc were used to obtain an estimation of the power system's performance once the belt drive had been built. The information provided by these programs was used in conjunction with drive pulley formulae to design a belt drive reduction system able to withstand the loading required.

1.1.2 Detail Design

The final stage of the design process meant a transition to purely analytical methods. Classical aeronautical theory was used to determine such things as drag, stall speeds, takeoff rolls, and turning radii of the new aircraft. These formulas were inputted into a

master spreadsheet, so that slight changes in the plane's design would result in updated performance figures without hours of number crunching, which had been the case in previous years.

The final values obtained from this spreadsheet were used to produce the drawing package. Minnow was drafted into AutoCAD 14 and later Mechanical Desktop 3.0 to obtain the required construction blueprints and to ensure that the components mated correctly.

2.0 Management Summary

2.1 Personnel and Configuration

Name	Year and Faculty	Responsibilities
Dave Young (Project Manager)	Junior- Mechanical Engineering	-Conceptual, Preliminary, and Detail Design -Propulsion -Drawing Package -Construction Supervisor
Nicole Doucet (Business Manager)	Sophomore- Applied Math	-Conceptual Design -Public Relations -Finances -Wing Overhaul -Composite Component Manufacturing
Phil Lavoie	Masters Student- Fluid Dynamics	-Conceptual Design -Drawing Package -Fuselage Construction
Jennifer Breckon	Sophomore- Mechanical Engineering	-Conceptual Design -Fuselage Construction
Andrew Dodds	Sophomore- Mechanical Engineering	-Conceptual Design -Fuselage Construction -Tail Construction

The management structure chosen for this year's aero design team was very fluid, with team members changing tasks as required to meet deadlines. Dave Young was chosen as project manager for the second Queen's entry. His position on the team meant that he was responsible for calling meetings, ordering material, and ensuring that the rest of the team worked diligently on the different sections of the project.

Initially, the team remained as one entity so that the returning members could teach some of the basics of design and theory to the less experienced members. This period began with the team's first meeting in early October and continued until the conceptual design section was completed in mid-December. This slow start proved to be beneficial, as the team was able to take our '98-'99 Design/Build/Fly (DBF) aircraft on several test flights to give new members some first hand experience of what is expected from a competition aircraft.

With the real world experiences fresh in everyone's mind, the conceptual design stage began. Dave is an experienced modeler, and the group was able to brainstorm new and feasible alternatives with his guidance until the design was gelled as a three-liter monoplane of similar layout as Queen's '98-'99 entry.

With a design agreed upon, Dave and Phil began work on the preliminary and detail design, including the drawing package. Nicole began fundraising with Laleah Carscallen (a member of Queen's Obsidian team) to raise funds to finance the construction of Obsidian and Minnow and to finance the trip to the actual competition in April. It should be again noted that throughout the project, both Queen's teams worked very closely to ensure that maximum result could be obtained through our limited resources. This can be seen in the similarities of the two designs, although the different design philosophies of the two managers, David McCracken and Dave Young, are apparent when considering the payload capacities of the two aircraft. Both teams met with each other on a weekly basis during the conceptual design

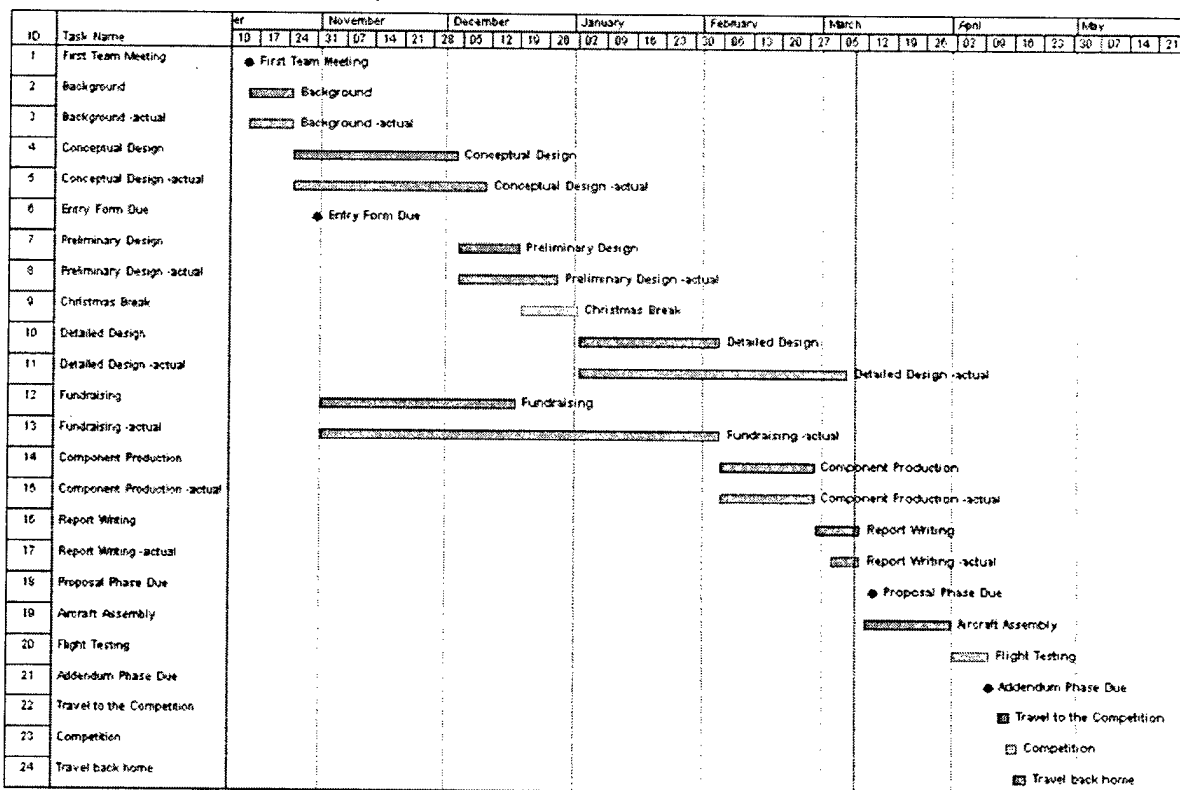
phase, and many composite components were pulled from the same mould to conserve resources. Similarly, the reports were written as a group to ensure that everyone who worked on the design and analysis of various components would be able to describe their contribution to both teams.

While Minnow was being designed and drawn in AutoCAD 14 and Mechanical Desktop 3.0, the remainder of the team worked on an individual basis to investigate battery technology, working with composites, and undercarriage and wheel design. Weekly meetings continued through to the beginning of February, when it became time to start construction.

At this time, the team regrouped and then split up again to form the wing, fuselage, and tail teams. Each team was responsible for the construction (or in the case of the wing, the renovation and modification) of their section of the aircraft, with Dave helping and overseeing each group to ensure the assemblies would mate correctly. Work was paused for a two-week period to write the report, and then will be restarted to complete assembly and to perform test flying.

2.2 Schedule

The scheduling and timing of the team was the sole responsibility of Dave. Weekly meetings were announced via email, and the appropriate room bookings were always made to allow either the Minnow team or both the Minnow and Obsidian teams to meet in a suitable conference room on campus. The actual timing of various events such as the deadline for having a design, and the deadline for having materials ordered were set by careful consideration of what needed to be done by the time of the competition, and of how long each would take. Dave's experience with model planes and with the DBF competition led to reasonable timeline, which was followed as closely as possible. Several unforeseen events did cause delays, but we still anticipate ample time for flight testing before the competition.



3.0 Conceptual Design

This year's DBF marks a radical change from the '98-'99 contest. Instead of brute force dominating the field, aircraft designers must now optimize their craft for the greatest efficiency possible within the payload, wingspan, and cost penalty systems applied. Minnow's design philosophy is that a small, light aircraft with a powerful motor would fare better in the windy weather conditions expected in Kansas. As such, a variety of designs were evaluated in an analytic FOM taking the *rated aircraft cost* and merits of the various designs into consideration.

3.1 Design Parameters

3.1.1 Power Train

Due to financial limitations, a MaxCim MaxNEO-13Y brushless DC motor was reused for this competition (having competed in two prior DBF competitions). This motor has a maximum output of 1200 watts (1.59 hp), thus limiting the overall dimensions and weight of the airplane. However, there is a large variance in the actual performance that can be obtained from this motor with different battery cells, gearing, and propeller configurations. Based on basic design guidelines of radio controlled electric modelers, 88 watts per kilogram of plane (0.053 hp/lb.) is recommended for rise off ground (ROG) flight. Thus, the MaxCim should provide adequate power for a plane upwards of 13.6 kgs (30 lbs.), providing a large variety of design options. The use of more than one motor has a significant point penalty and does not offer an increase in efficiency or run time with the set battery pack weight.

With the battery pack weight limit set at 2.27 kg (5lbs), a tradeoff must be made between number of cells and capacity per individual cell. With a penalty for the number of cells used, fewer cells of a larger capacity would be more beneficial than a larger number of lower capacity cells, even if the total power of the pack is the same. Upon examining the power density of each individual cell, the Sanyo 3000CR was found to have a value of 1246 mAh/oz, which is significantly higher than the other high capacity cells, the Sanyo KR-2800CE (1165 mAh/oz) or the KR-5000DEL (1021 mAh/oz), for example. Thus we decided to use the 3000CR cell for its superior power density, which would increase the available power for the flight.

Gearboxes are commonly used in radio controlled modeling to allow a motor to spin a larger diameter propeller at a lower rpm. The advantage gained through its use is a higher static thrust and better take-off run performance to the detriment of a reduced top speed. With the nature of this competition requiring multiple takeoffs within the sortie and short cruising flight times between take-off and landing, a gearbox which allows quick takeoffs while still allowing good flight speeds is the idea combination.

3.1.2 Motor Placement

Several different power-plant configurations were evaluated for use in this competition. Ducted fans were examined as a potential propulsion method, but due to their notoriously poor acceleration characteristics they were quickly rejected. Propellers are needed to provide the low speed thrust needed to perform a 30.48 m (100ft) take-off.

Propellers are generally used in either a tractor or pusher configuration. A pusher propeller allows the plane to fly in undisturbed air, reducing drag. However, this configuration has several drawbacks. It reduces the ground clearance of the propeller during takeoff rotation, and may require a longer, heavier landing gear. The push prop design lacks the inherent stability of the tractor configuration due to the location of the thrust vector behind the center of gravity, towards the tail. Finally, while the push-prop may allow the aircraft body to fly in undisturbed air, it places the propeller itself in the turbulent wake of the fuselage, reducing its aerodynamic efficiency. A tractor prop has the advantage of placing its prop wash over the tail surfaces, increasing their effectiveness at low speeds during taxiing and ground roll.

This prop wash can also be advantageous if the propeller is placed directly in front of the wing, providing a blown surface effect that increases the air velocity and lift over a portion of the wing. This technique would require a dual motor configuration or an asymmetrical thrust configuration. Dual motors were previously ruled out due to the incurred penalty. However, asymmetrical thrust provides an interesting alternative that has showed promise in some full scale developments, but would require further investigation than time permits during this project year.

3.1.3 Wing Placement

A wide variety of wing designs were considered throughout the design portion of this year's competition. Aside from the traditional high, mid, and low-wing designs, we also investigated bi- and multi-plane layouts, a parasol design, canard and tandem configurations, and also a three surface design. Every effort was made to reuse the '98-'99 DBF wing as it is still airworthy and frees up resources for other avenues of design and construction.

A high wing design offers good lateral stability and reasonable wingtip clearance on take-off and landing. The wing can be faired into the fuselage to reduce interference drag, as well as allowing the load to be easily transmitted through the structure to the spar. Unfortunately, the positioning of the wing above the cargo compartment results in a difficult to access compartment, resulting in longer loading/unloading times.

A mid-wing design results in an aerodynamically stable model. Unlike the high wing, which will tend to right itself to level flight, a mid-wing will remain in a bank indefinitely until pilot input is added to right the aircraft. The main disadvantage of this design in this competition is that the wing spar would have to pass right through the cargo compartment, leading to a more complex cargo hold and hatch design.

A low-wing design places the center of gravity above the wing spar. This produces an aircraft which is unstable and requires constant pilot input to control. Although the design does offer superior cargo access, the undesirable flight characteristics would be a serious problem in a contest that requires a large percentage of flight time be spent where precise and careful flying is essential: during landing and taking off.

A biplane design stacks two approximately equal sized airfoils one above the other. The main disadvantage of this design is that for the wings to operate at maximum efficiency, a minimum distance of one semi-span must separate the wings. The structure required to keep the wings this far apart would result in prohibitively high induced drag and weight.

A multi-plane design adds at least another wing to the biplane design. While this would increase the total lifting capability of the structure (increased wing area), it also adds a great deal of structural weight and drag to the airplane through the necessity of keeping each wing separated by a semi-span.

A parasol design was given consideration due to its inherent stability, which exceeds that of even a high wing aircraft due to the increased distance between the center of lift and the center of gravity giving a strong pendulum effect. This design is also attractive with a limited wingspan design criterion as the act of raising the wing above the fuselage increases the wing's effective span by adding the lift that is generated where the fuselage was formerly located. Unfortunately, this design involves a complicated bracing system to adequately transmit the payload weight to the wing spar. As the wing is elevated above the fuselage, this bracing system must be located in the slipstream, resulting in a high drag penalty.

A canard configuration was considered as a method of increasing wing area (a main wing and a smaller front wing), while reducing the aircraft cost rating by being able to omit the horizontal stabilizer. Unfortunately, canard equipped aircraft are known for their inherently long take-off rolls.

The front wing of a canard is given a higher wing loading than the rear main wing to ensure that the front wing will stall first. When the aircraft enters a low speed, nose high attitude, the front wing must stall first so that the nose of the aircraft drops and normal flight speed and attitude can be recovered. Unfortunately, the higher wing loading on the front wing is detrimental to the take-off performance because the plane cannot rotate as quickly as a conventional aircraft.

A tandem wing was evaluated for reasons similar to the canard design mentioned above. A tandem wing is an aircraft with a similarly sized wing located at the nose and tail of the fuselage. While this design does increase the wing area with little increase in frontal area and drag, the design suffers from the same take-off problems that the canard configuration does.

A three surface design was considered as a good alternative to the canard and tandem wing configurations. This design uses a conventional horizontal tail behind the two main lifting surfaces, positioning the elevator with enough of a moment arm to rotate the

aircraft and permit short takeoffs. However, the necessity of having three wing spars passing through the fuselage limits the available cargo space and ease of loading.

3.1.4 Wing Design

Wing tips are considered by many to be a "black art". They are still under heavy development and the aeronautical community has not agreed on the "ideal" wingtip at this time. The goal of any wing tip is to reduce or redirect the wingtip vortices, thus increasing the effective efficiency of the wing. This can be accomplished by tip plates, Horner wingtips, or by winglets.

Tip plates are thin pieces of wood or plastic cut slightly larger than the airfoil and glued to the end of the wing. The theory is to simulate the "infinite span" wing seen in a wind tunnel situation. As the test wing stretches from one wind tunnel wall to the other, there is no opportunity for wing tip vortices to form. By gluing on the tip plates, it is effectively gluing on a portion of the "wall", and the vortices, while not completely gone, are reduced.

Horner wingtips are sculpted in such a way to channel the tip vortices out and down from the wing. This prevents them from disturbing the air flowing over the wing, and may also impart some lift. Unfortunately, while the wingtips are often used on full-sized aircraft, they are prone to damage on models, where scraping a wing tip on landings is not totally uncommon.

Winglets are the most complicated of wing tip devices. Consisting of a separate airfoil mounted vertically (or inclined) from the main wing's tip, they disrupt the tip vortices so that they do not disturb the airflow across the wing. Winglets are application specific and require hours of computational fluid dynamics with the specific main wing to ensure that they will perform as expected.

3.1.5 Fuselage Design

Once the wing has been designed, the next step is to examine the fuselage. There are a wide variety of possible fuselage designs, each with their own advantages and disadvantages. The general designs considered were conventional, double, blended, and a flying wing.

The conventional fuselage is exactly as implied by its name – conventional. It consists of a long structure, with a square, round, or oval cross-section, with the wing(s) mounted at approximately at third of its length, and the tail appendage mounted at the rear. Cargo is held in a tubular bay centered under the wing's spar and can be loaded from either the top, the bottom, or either end, depending on the configuration of the final design.

This type of fuselage is easy to build and provides a solid base to mount the landing gear while still providing enough clearance for the propeller. The design is not the most

streamlined choice, but with drag reduction techniques, the drag penalty can be reduced to an acceptable value.

The double fuselage consists of two parallel conventional fuselages separated by a section of the wing. This design is utilized when extra cargo space is required and twin engines are to be used. The fuselages provide storage for the power train, and the remainder of the volume can be used for cargo in a fashion similar to the conventional fuselage mentioned above.

This design offers a solid mounting surface for the undercarriage and, so long as the fuselage spacing is adequate, it provides sufficient propeller clearance. Unfortunately, this is the least streamlined design that we considered. The fuselages provide a huge surface area for their volumes, and the interference drag between the assorted wing, horizontal tail, and fuselages becomes prohibitive.

The blended fuselage is a compromise between a flying wing and a conventional fuselage. It is made up of a large, flat fuselage in an approximate airfoil shape. This fuselage is then faired into the wing to produce a low-drag surface. The fuselage then continues as either a single or twin boom design to support the tail structure.

Cargo is held in rectangular bays between the wing structure and access is usually obtained through the top, though care should be taken to ensure that the hatches are perfectly flush with the top surface of the fuselage to prevent a flow separation bubble from forming. The fuselage does produce some lift, and thus must be treated as an airfoil to prevent unnecessary drag and thus destroying the streamlining advantage of such a design.

This configuration does not allow a very large propeller to be used, as there is very little, if any, fuselage under-hang beneath the wing to mount the undercarriage. The undercarriage is often affixed to the wing spar further out along the wing to provide a wide wheel track and to provide good ground handling, but this does not raise the wing/fuselage to the height enjoyed by the other designs examined above.

The tail of this design must be designed with extreme care to ensure that it will not be blanketed by the wing/fuselage during flight maneuvers. The boom(s) should be inclined upwards to remove the tail surfaces from the turbulent air behind the main structure, so they can enjoy clean, undisturbed air to operate in.

3.1.6 Undercarriage

The undercarriage is the most abused portion of the aircraft, yet its safe and consistent operation is essential. Although there are a wide variety of landing gear configurations, they can be subdivided into three main categories: tricycle gear, tail dragger gear, and bicycle gear. The two first choices are very common, but the bicycle gear configuration appears only occasionally among specialty aircraft.

The tricycle gear configuration places two main wheels slightly behind the aircraft's center of gravity in a parallel arrangement, with one wheel on each side of the fuselage. A third, medium-sized wheel is then placed at the nose of the aircraft, resulting in a gear configuration that resembles a child's tricycle. The advantages of this design is that the plane remains at close to a zero angle of attack while on the ground, reducing drag and improving ground handling, while still permitting the pilot to see what is in front of the aircraft. While visibility is not an issue with model aircraft, ground handling and drag reduction are. A tricycle gear equipped plane will often have a shorter take-off run and greater resistance to nosing over on landings than the other common design, the tail-dragger.

Unfortunately, this type of undercarriage suffers from the highest drag of the three designs. As all three wheels are relatively large, the air resistance encountered can be substantial and should be evaluated against the benefits of this design.

A tail-dragger design uses parallel main wheels similar to the tricycle gear configuration, with the main difference being their positioning relative to the aircraft's center of gravity. The main gear is located ahead of this center of gravity, thus giving the plane a distinct tail down attitude (it "drags its tail"). To ensure control, a very small wheel is attached to the rear of the fuselage to provide some directional control at low speeds.

In a take-off run, the plane rolls on all three wheels until it reaches a velocity that permits the elevator to produce a force great enough to raise the tail off the ground. Because of the severe nose-up attitude, the wing and fuselage's angle of attack produces a great deal of drag, thus slowing the aircraft's acceleration and lengthening the take-off run. When the tail lifts off the ground, the fuselage rotates so that it is parallel with the airflow, reducing drag. The aircraft then accelerates quickly and takes off.

In flight, the tail-dragger exhibits less drag than a tricycle gear configuration. This is due to the replacement of one medium sized wheel at the front of the fuselage with a very small wheel at the rear. The disadvantages of the tail-dragger design are apparent on landings. Because there isn't a wheel situated at the front of the aircraft, they are prone to nosing over on landings, resulting in propeller and perhaps structural damage. In a competition where a great deal of time is spent on the ground, the undesirable ground handling characteristics of this configuration must be considered versus the reduced drag in flight.

A bicycle gear configuration is seen where drag considerations are paramount over ground handling characteristics. It is often seen on glider aircraft, or occasionally on high performance military aircraft and may be used in conjunction with small stabilizing wheels on the wing tips. The design consists of two narrow wheels mounted in series along the centerline of the fuselage. This technique lends itself to smooth fairing, which can reduce drag even further. Unfortunately, their ground handling characteristics are

poor at best. With both wheels mounted along the centerline, there is little to no lateral stability at low speeds before the ailerons become effective.

3.1.7 Tail Design

The careful design and configuration of the tail is essential to ensure good flight characteristics of the final aircraft. Tail efficiency can be greatly improved if the elevator is removed from the wing's downwash (50% efficiency of a conventional tail versus 90% efficiency of a high T-tail), but more exotic configurations may require greater care in building to ensure that weight does not increase by a large margin. The typical tails seen on model aircraft are the conventional tail, the T-tail, and the V-tail.

The conventional tail uses a vertical fin and rudder mounted along the fuselage's centerline. There is a horizontal stabilizer and elevator then mounted along the fuselage at the base of the fin. This design is the most common, robust, and simple tail appendage, but it places the horizontal surfaces in the wing's downwash, thus reducing their effectiveness. To compensate for this, the tail's planform area must be increased to permit an acceptable force to be created by the elevator.

The T-tail is occasionally seen where high efficiency is required. The vertical surfaces are identical to those of a conventional tail, but they must be built slightly heavier to provide enough strength. This strength is required because the horizontal flight surfaces are mounted to the top of the fin, thus removing them from the wing's downwash and allowing them to operate in undisturbed air. The increased efficiency can be translated into a surface with a smaller planform area, thus partially compensating for the increased structural weight of the fin. This design's chief advantage is that the smaller horizontal surfaces and the removal of wing tip vortices from the end of the fin (the stabilizer acts as a large tip plate), reducing the drag of the tail.

The V-tail configuration is rarely seen except where drag reduction is the chief concern. The design uses two flight surfaces mounted at an angle at the rear of the fuselage. By combining the vertical and horizontal surfaces, the total tail surface area is reduced, thus reducing the weight and drag. Unfortunately, the design requires complicated control linkages (or a computerized radio), and has been known to be unable to recover from stalls and spins due to a blanketing effect of one control surface on the other.

3.2 Figures of Merit

Each configuration was analyzed based on its advantages, disadvantages, and *rated aircraft cost penalty*. A summary of the FOM for each design is given along with the relative weighting factor.

3.2.1 Drag Penalty

This is a measure of the relative drag penalty of the design. A higher drag structure would negatively affect the final aircraft's range, takeoff performance, and maximum speed and should be avoided if possible. This FOM was assigned a weighting factor of 4.

3.2.2 Weight Penalty

This is a measure of the relative weight of the given design. Due to the minimal reserve power budget, extra weight should be avoided at all cost to ensure adequate flight performance of the aircraft. This FOM was assigned a weighting factor of 5.

3.2.3 Performance

This is a measure of how efficient the design is. A large, heavy component would receive a lower score than a small, well-designed alternative. This FOM was assigned a weighting factor of 4.

3.2.4 Ease of Manufacture

This is a measure of how easily it is to incorporate the configuration into the final design. More exotic and complicated technologies demand more resources, so this FOM was given a weighing factor of 4.

3.3 *Concept Evaluation*

3.3.1 Analytical Method

An evaluation of competing concepts under each design parameter was conducted by rating each concept on a scale of 0 to 5, with 5 being the best choice based on the qualitative considerations described above. The rating were then multiplied by the weighing factor of each FOM, summed, and then the score was divided by the relative aircraft cost penalty to produce a final score for each concept. (Table 3.1)

Figure 3.1 Conceptual design evaluation

	Drag (4)	Weight (5)	Performance (4)	Ease of manufacture (4)	Rated aircraft cost	Total
Motor						
Tractor	3	5	4	4	1	69
Pusher	3	5	3	3	1	61
Twin	2	3	5	2	2	25.5
Asymmetrical	3	4	4	2	1	56

Wing Placement						
High	4	4	4	4	1	68
Mid	5	4	3	3	1	64
Low	4	4	3	4	1	64
Biplane	3	3	3	3	2	25.5
Multiplane	2	3	2	3	3	14.3
Parasol	3	2	4	2	1	46
Canard	4	3	3	2	1	51
Tandem	4	3	3	2	1	51
Three Surface	4	2	4	2	2	25

Wing Tips						
Tip Plates	3	4	3	5	1	64
Horner Wing Tips	4	3	4	4	1	63
Winglets	3	3	4	2	1	51

Fuselage						
Conventional	3	4	4	4	2	32
Double	2	2	3	3	4	10.5
Blended	4	3	4	3	2	29.5

Undercarriage						
Tricycle	3	3	5	4	1	63
Tail Dragger	4	4	3	3	1	60
Bicycle	5	5	1	2	1	57

Tail						
Conventional	3	4	4	5	1	68
T-tail	4	3	5	4	1	67
V-tail	5	4	3	3	1	64

Description	Coefficient	Variables	Description	Values
			large chord monoplane conventional tail single fuselage single motor	
FLIGHT SCORE				
Liters of Water Carried Multiplier	Water Load	10 * n	Water Load =	30
Liters of Water	n	number of liters	n =	
RATED AIRCRAFT COST				
Manufactures Empty Weight Multiplier	A	\$100 * MEW	A = \$	900.00
Manufactures Empty Weight	MEW (pounds)	airframe weight	MEW =	
Rated motor Power Multiplier	B	\$1 * REP	B = \$	1,500.00
Rated motor Power	REP (watts)	# motors * 50A * 1.2V/cell * # cells	REP =	1500
			# motors =	
			# cells =	
Manufacturing Cost Multiplier	C	\$20 * MFHR	C = \$	1,820.00
Manufacturing Man Hours	MFHR (hours)	Prescribed assembly Hours by WBS	MFHR =	91
		MFHR = the sum of WBS		
		Wings WBS = 5hrs/wing + 4 hrs / sq foot pro	Wing WBS =	33
			# wings =	
			area (sq.ft) =	
		Fuselage WBS = 5hrs/body + 4hrs / foot or l	Fuselage WBS =	21
			# bodys/pods =	
			length (ft) =	
		Empenage WBS = 5 hrs + 5 hrs/vert surf. +	Empenage WBS =	15
			# vert. surfaces =	
			# horz. surfaces =	
		Flight Systems WBS = 5 hrs + 1 hr/ servo	Flight Sys. WBS =	12
			# servos =	
		Propulsion Systems WBS = 5 hrs / motor +	Propulsion WBS =	10
			# motors =	
			# props =	
Single Flight Score	SFS	Flights * Water Loads	SFS =	120
	Flights	Is the number of water caring flight within tim	# flights =	
Written Report Score	WRS	Score on written report as assigned by judg	WRS =	
Total Flight Score	TFS	3*single flight	TFS =	360
Rated Aircraft Cost	RAC (\$1000)	(MEW + REP + MFHR) / 1000	RAC =	4.22
FINAL SCORE	Final Score	Written Report Score * Total Flight Score / R	FINAL SCORE	7421.800948

Description	Values
large chord	
monoplane	
conventional tail	
single fuselage	
twin motor	
Water Load =	30
n =	

A =	\$ 1,000.00
MEW =	

B =	\$ 4,320.00
REP =	4320
# motors =	
# cells =	

C =	\$ 2,020.00
MFHR =	101

Wing WBS =	33
# wings =	
area (sq.ft) =	

Fuselage WBS =	21
# bodys/pods =	
length (ft) =	

Empenage WBS =	15
# vert. surfaces =	
# horz. surfaces =	

Flight Sys. WBS =	12
# servos =	

Propulsion WBS =	20
# motors =	
# props =	

SFS =	120
# flights =	

WRS =	
-------	--

TFS =	360
-------	-----

RAC =	7.34
-------	------

FINAL SCORE	4267.029973
-------------	-------------

Description	Values
small chord	
biplane	
conventional tail	
single fuselage	
single motor	
Water Load =	30
n =	

A =	\$ 1,000.00
MEW =	

B =	\$ 1,500.00
REP =	1500
# motors =	
# cells =	

C =	\$ 2,000.00
MFHR =	100

Wing WBS =	38
# wings =	
area (sq.ft) =	

Fuselage WBS =	21
# bodys/pods =	
length (ft) =	

Empenage WBS =	15
# vert. surfaces =	
# horz. surfaces =	

Flight Sys. WBS =	16
# servos =	

Propulsion WBS =	10
# motors =	
# props =	

SFS =	120
# flights =	

WRS =	
-------	--

TFS =	360
-------	-----

RAC =	4.5
-------	-----

FINAL SCORE	6960
-------------	------

Description	Values
big chord	
monoplane	
V tail	
single fuselage	
single motor	
Water Load =	30
n =	

A = \$	900.00
MEW =	

B = \$	1,500.00
REP =	1500
# motors =	
# cells =	

C = \$	1,820.00
MFHR =	91

Wing WBS =	33
# wings =	
area (sq.ft) =	

Fuselage WBS =	21
# bodys/pods =	
length (ft) =	

Empenage WBS =	15
# vert. surfaces =	
# horz. surfaces =	

Flight Sys. WBS =	12
# servos =	

Propulsion WBS =	10
# motors =	
# props =	

SFS =	120
# flights =	

WRS =	
-------	--

TFS =	360
-------	-----

RAC =	4.22
-------	------

FINAL SCORE	7421.800948
-------------	-------------

Description	Values
large chord	
flying wing	
vertical fin	
no fuselage	
single motor	
Water Load =	30
n =	

A = \$	800.00
MEW =	

B = \$	1,500.00
REP =	1500
# motors =	
# cells =	

C = \$	1,440.00
MFHR =	72

Wing WBS =	41
# wings =	
area (sq.ft) =	

Fuselage WBS =	0
# bodys/pods =	
length (ft) =	

Empenage WBS =	10
# vert. surfaces =	
# horz. surfaces =	

Flight Sys. WBS =	11
# servos =	

Propulsion WBS =	10
# motors =	
# props =	

SFS =	120
# flights =	

WRS =	
-------	--

TFS =	360
-------	-----

RAC =	3.74
-------	------

FINAL SCORE	8374.331551
-------------	-------------

Description	Values
large chord	
flying wing	
vertical fin	
podded fuselage	
single motor	
Water Load =	30
n =	1

A = \$	800.00
MEW =	4

B = \$	1,500.00
REP =	1500
# motors =	1
# cells =	1

C = \$	1,780.00
MFHR =	89

Wing WBS =	41
# wings =	1
area (sq.ft) =	1

Fuselage WBS =	17
# bodys/pods =	1
length (ft) =	1

Empenage WBS =	10
# vert. surfaces =	1
# horz. surfaces =	1

Flight Sys. WBS =	11
# servos =	1

Propulsion WBS =	10
# motors =	1
# props =	1

SFS =	120
# flights =	1

WRS =	1
-------	---

TFS =	360
-------	-----

RAC =	4.08
-------	------

FINAL SCORE	7676.470588
-------------	-------------

4.0 Preliminary Design

4.1 Take-off Gross Weight (TOGW) Estimation

The first step in the preliminary design phase was estimating the gross weight of the aircraft, as this parameter is crucial in determining its size and performance. To determine the TOGW, it was necessary to compile the individual weights of known components needed for the aircraft, and estimating various airframe structures.

With a designed cargo capacity of 3 liters, this yielded a cargo weight of 3.3 kg (each bottle weights 0.1 kg) or 7.3 lbs. As this was the cargo carried by the Queen's 1999 DBF entry, which weighted 2.7 kg (6 lbs) empty, this airplane provided a starting point for weight estimations. With careful weight management and engineering, the empty airframe weight could be reduced to a predicted 2.4 kg (5.1 lbs). Along with a 2.2 kg (4.8 lbs) battery pack and the payload, a TOGW of 7.9 kg (17.4lbs) seemed reasonable.

4.2 Propulsion Systems Selection

The propulsion system was selected so as to provide the maximum possible thrust and efficiency in order to make the best use of available battery power. MaxCim, Aveox, and Astroflight motors were compared based on their published efficiencies, predicted performance, cost, and their performance in past competitions. MotoCalc and ElectriCalc, commercial software packages, were used to compare the various possible configurations of motor, controller, gearbox, propeller, and batteries for their efficiency, thrust, and estimated run-time.

With a MaxCim MaxNEO 13Y and a MaxCim N32-13Y motor on hand, both providing powerful and efficient thrust, and our team suffering from an unsure budget, the decision was made early in the design phase to use these motors. Unfortunately, commercially available gearboxes would not allow us to maximize the potential of these motors, so a reduction drive needed to be produced. Using Electricalc and Motocalc, many gearbox configurations were examined and a final configuration of a 6.5:1 reduction unit and 25 3000mAh cells would produced a maximum of 8.7lbs of thrust in cruise flight and 11lbs of static thrust. The speed controller to be reused from the previous year (Maxu35B-25NB) was rated to a maximum of 25 cells, setting the limit for the number of cells to use. Batteries were selected by comparing weight, capacity, internal resistance and power density. Sanyo N-3000 CR mAh cells were found to have the highest power density between the different size cells of batteries.

The design of a custom motor reduction drive became of prime importance. A light, efficient, and strong drive would be needed to transmit the power from the motor to propeller with minimal losses. A 6.5:1 reduction was to be built using similar toothed belt drive principles as Queen's other entry, Obsidian. By both using the same method of reduction, resources could be pooled for their development. A toothed belt drive was determined to be the only method of reduction feasible for Obsidian - providing minimal resistance loses, and Minnow was to follow suit.

4.3 Wing Area and Airfoil Selection

One of the main features of the Minnow was to reuse the wing from last years Queen's 1999 DBF entry. With only slight modification, the 2.4 m (8 ft) span wing could be clipped to 2.1 m (7ft) and still provide sufficient lift for Minnow so long as the airframe weight could be reduced slightly over last years. The following FOM were examined on this wing to check the feasibility of reusing it.

4.3.1 C_L at the Best Lift to Drag (L/D) Angle of Attack

The C_L at best L/D was used to gain insight into the amount of lift that the wing would produce while operating at peak efficiency. This was considered important since the more lift the airfoil generates, the smaller the wing area can be, reducing drag.

4.3.2 Maximum C_L

The maximum C_L was considered to be important as this determines the stall speed, take-off speed, and maximum g-loading for a fixed wing area. Due to the requirement for take-off within a limited distance and the energy advantage obtained by minimizing the amount of time in climb, a high C_L was considered advantageous. In addition, this also allows for high-g maneuvers without the onset of an accelerated stall, giving the aircraft the ability to use a minimal turning radius and effectively shortening each lap.

4.3.4 Stall Characteristics

Like many other parameters, this FOM arises from past experience. An airfoil with a more docile stall is considered to be significantly advantageous in the event of an unplanned circumstance, particularly just after rotation. A gentler stall will increase the time available to react and increase the likelihood of recovery. The stalling characteristics were compared based on published lift and drag data, and on previous experience in observing the in-flight stall characteristics of most of the airfoils considered.

4.3.5 C_D at Expected Cruise AOA

Due to the restrictions on available battery power, once a maximum thrust is achieved through careful selection of a motor and electronics, the top speed can only be increased through drag reduction. The airfoils were compared at the expected cruise C_L , where the drag will have the most influence on performance.

The cruise speed was estimated based on data from ElectriCalc using an airplane with worst-case $C_d=0.06$, and adjusting the weight and wing area (wing area already set). This

gives a rough estimate of top speed of 26.8 m/s (60 mph). From this, the C_L at cruise was determined from the standard lift equation. Three-dimensional effects reducing the overall lift of the wing will be more thoroughly examined in the detailed design when wing incidence is being determined.

$$C_{L_{min}} = \frac{2L}{\eta \rho S_w V_{max}^2}$$

Where η is the efficiency of the wing, assumed to be 0.90%, and L is the total lift required (equal to the gross weight).

This gives a required C_L of 0.5 ± 0.1 . Take-off speed, stall speed, and maximum g-loading were examined next to define the required limits on the C_L . ElectriCalc also provided minimum speeds and cruise speeds and these values were used to estimate the maximum C_L required. Using the same C_L formula as above, replacing V_{Max} with V_{Stall} gives a required maximum C_L of 2.8 ± 0.1 . This value is quite high and not obtainable from the Clark Y airfoil in the wing. This meant a higher ground speed would be necessary in order to reduce the C_L needed. Also, the wing is equipped with plain flaps in order to achieve the higher C_L needed only for takeoff and landing. Plain flaps would increase the C_L by about 55% when deployed to 40 degrees. Although only 20 degrees would be used at takeoff, this, combined with a higher takeoff speed than predicted from ElectriCalc would produce the necessary lift. It was also desired to have an aircraft capable of maneuvering with a g-loading of 2, which gives a required maximum C_L of 0.98 ± 0.1 . As such, the airfoil was required to have a $C_{L_{Min}}$ of 0.42 and a $C_{L_{Max}}$ of 1.4. Airfoil lift and drag data were obtained from the UIUC Low-Speed Airfoil Test program. The Clark-Y was used in last years wing, with a C_L of 0.337 and a C_D of 0.0074 at its minimum drag angle of 0° , and a maximum C_L of 1.32 as the angle of attack approaches the critical angle of approximately 12° , filled this requirement. An angle of incidence of approximately 2 degrees would be needed to provide the lift at cruise velocity. In addition, the Clark Y has relatively good stall characteristics, with a gentle approach and fall from the $C_{L_{Max}}$.

4.4 Aspect Ratio

The original Queen's 1999 DBF entry's wing had an aspect ratio 10.7. This was reduced to 9.2 after the wings were clipped. This high aspect ratio will reduce the induced drag of the aircraft, thus allowing for a faster cruise speed. However, maneuverability is compromised due to an increased moment of inertia about the longitudinal axis. As well, a longer wing experiences higher bending moments and is more likely to flex under loading. This makes construction more difficult and structurally heavier than a shorter wing. These problems do not outweigh the advantages of the increase in wing efficiency, however. As demonstrated by last year's entry, maneuverability and structural rigidity were non-issues. A double taper was used in order to provide a more evenly distributed lift to reduce induced drag further. Tip plates will also be employed in an attempt to control vortices and increase lift.

4.5 Tail Sizing

The design considerations used to determine the required tail surface dimensions are stability and control authority. The stabilizer must be capable of overcoming both the pitching moment of the wing and the moment caused by a finite separation between the center of gravity and the center of pressure. The tail must then still provide enough torque for control. In order to minimize its size and reduce drag, the tail is placed as far aft as feasible to give it a large moment arm on which to act. It is common practice to use a stabilizer that is approximately 20 to 22% percent of the wing area, and an elevator that is 40% of the stabilizer area. With the slow speeds and multiple takeoffs and landing in this competition, pitch authority was deemed very important. With no penalty for stabilizer area, an area that is 22% of the wing was preferred. It has been found that a 0.081 m^2 (0.87 ft^2) stabilizer located 0.76m (2.5 ft.) from the wing quarter chord, with a NACA0009 airfoil ($C_{L_{\max}}$ of 1.3) (ref. 7), provides the desired qualities. These will be further quantified in detailed design.

It was decided that a T-tail design would be used. Construction of this design is only marginally heavier than a conventional tail, yet is upwards of 50% more efficient. Raising the horizontal stabilizer into clean air greatly increases its effectiveness, while reducing interference drag by reducing the joints between rudder, tail, and fuselage.

The vertical stabilizer supports the horizontal stabilizer and must thus be quite stiff. In order to increase its rigidity, a slightly thicker airfoil, a NACA 0012 was used. This airfoil would also prove thick enough to mount control servos in the vertical tail. The chord of the vertical fin was set to the same as the horizontal stabilizer to minimize interference drag. Its height was then set to effectively raise the horizontal tail out of the downwash from the wing, and to provide enough yaw stability. For an airplane to be stable in yaw, the Center of Lateral Area should be about 25% back from the center of gravity. In the preliminary AutoCAD design, quick area moment calculations were done to show that the area selected was adequate for yaw control. Also, common model design practice states that a vertical tail area should be approximately 50% of the horizontal tail area should be used. Therefore, a vertical fin area of 0.032 m^2 ($.35 \text{ ft}^2$) should be employed.

4.6 Airframe and Fuselage Sizing

During the preliminary design stage, several design parameters and sizing trades were considered. While innovative design and construction methods were investigated, they were weighed against ease of manufacture and functionality. The decision of airframe design depended upon trades between simplicity of construction, strength, weight, and reduction of drag.

All features of the preliminary design of the fuselage were weighed against the following Figures of Merit (FOMs):

Efficiency – The layout chosen for the fuselage should optimize the space required for the airframe structure while also limiting the fuselage's overall size. The placement of the bottles and the bottle size and shape were the main factors contributing to the preliminary design of the most efficient airframe possible.

Manufacturing Ease – The preliminary design of the airframe should limit the cost and time required for its construction. Also, shop tools and facilities must be considered.

Functionality – The fuselage must function properly as a cargo-carrying aircraft that requires repeated removal and loading of the bottles. The design feature used for access to the bottles must be both quick and rugged due to the rushed nature of cargo insertion/removal.

Structural Rigidity – The airframe structure must be sufficiently strong and stiff to account for the substantial payload and the repeated landings that the aircraft will encounter. The type of materials used and the thickness chosen for the primary structural components of the aircraft depended on their ability to withstand its loading.

Drag Penalty – The design of the airframe should minimize the amount of parasitic and induced drag created by the fuselage. The overall shape of the airframe, whether streamlined or square, dictates the increased drag possibilities of the fuselage. An aerodynamic shape and the reduction of parasite drag were important in order to reduce the flight time of the non-cargo ferry mission part of the flight profile.

The preliminary design utilizes a main "U" channel where three water bottle sit. The water bottles must be centered under the center of gravity of the airplane so that no balance problems are encountered from payload changes. A removable streamlined hatch on top of the fuselage allows access to the water bottles for insertion and removal. The wing is also mounted to the top of the "U" channel and a streamlined tail boom will extend from the rear of the fuselage to the tail. The batteries are placed in the landing gear fairings in order to reduce fuselage cross sectional area, provide cooling and take advantage of the strong landing gear structure. The belt drive and motor are cowled into the front of the "U" channel.

Figure 4.1 Summary of Physical Properties

Feature	Description
Propulsion	Motor: MaxNEO 13Y Brushless DC Speed Controller: Max 35A-25NB Cells: 25 Sanyo 3000 CR Gear Box: Custom 6.85:1 Propeller: 18-12 Zinger
Wing	Span: 2.13 m (84.00 in) Aspect Ratio: 9.2 Airfoil: Clark-Y Differential Ailerons: 0.41 m (16.00 in) x 25% chord Flaps: 0.61 m (24.00 in) x 30% chord
Stabilizer	Span: 0.64 m (25.00 in) Chord: 0.13m (5.00 in) Airfoil: NACA0009
Rudder	Height: 0.22 m (8.50 in) Chord: 0.05 m (2.00 in) Airfoil: NACA0012
Fuselage	Cross-section: 0.10 m x 0.15 m (4.00 in x 6.00 in) Length: 1.32 m (52.00 in)
Main Landing Gear	Wheel Base: 0.37 m (14.44 in) Thickness: 0.005 m (0.25 in) Height: 0.15 m (5.81 in)

5.0 Detail Design

Drawings of the final aircraft design are attached in Appendix D. These drawings include detailed two-dimensional drawings and templates used for construction, and three-dimensional models for visual presentation.

The design of any airplane is a highly iterative process, involving many changes to the initial preliminary design before arriving at the final configuration. As reviewed in the preliminary design, many approximations involving aircraft weight, speed and sizing were made. This year, the use of spreadsheets for nearly all calculations allowed for easy changes to design parameters while instantly updating all other calculations.

5.1 Weight

The estimated weight of the airplane and the required wing area to support this weight were calculated. An estimate of the components, structure and payload to be carried was tabulated. Care was taken not to underestimate the weight of the aircraft, as all primary design features require an accurate approximation of this weight in their calculations. The TOGW was calculated to be 7.9 kg (17.4 lbs). This is broken down into 3.3 kg (7.3 lbs) of water payload (including the weight of the bottles), 2.2 kg (4.8 lbs) of batteries, and an airframe weight of 2.4 kg (5.3 lbs). When flying without cargo, the takeoff weight is 4.5 kg (10.1 lbs). Care was taken to reduce weight wherever possible throughout the structure and to weigh each component as it was being built to check for excessive mass.

5.2 Payload Fraction

Payload fraction is a measure of the payload's contribution to the take-off gross weight of the aircraft. The payload fraction for this airplane is predicted to be 0.418.

$$\text{PayloadFraction} = \frac{W_{\text{Payload}}}{\text{TOGW}} = \frac{3.3\text{kg} \times 9.81\text{kg} \cdot \text{m/s}}{7.9\text{kg} \times 9.81\text{kg} \cdot \text{m/s}} = 0.418$$

5.3 Wing Performance

As previously stated in the preliminary design, the Minnow was designed around the Queen's Aero Design 99 DBF entry's wing. This wing was designed for last year's entry carrying a 3 water bottle payload, the same payload to be used in the Minnow. The original wing platform was designed with a 2.4 m (8ft) span and a 0.25 m (0.83 ft) root chord tapering to a 0.2 m (0.67 ft) tip chord. With the addition of a 7 ft wing span limit, this wing was clipped to 2.1 m (7ft), changing the tip chord to 0.21 m (0.68 ft). Originally designed with 50% span flaps and 50% span ailerons, the clipped wings changes the spans to 60% and 40% respectively. These flaps are plain flaps and do not provide any additional wing area. The clipped wing resulted in an aspect ratio of 9.2 and an effective wing area (fuselage interrupts wing) of 0.47 m² (5.1 ft²). The resulting wing loading of 167.3 g/dec² (54.0 oz/ft²) is quite large, but has been shown to be

possible in successful competitive airplanes with lower power to weight ratios than Minnow. A tapered wing was used in order to provide a more even lift distribution.

With the selected Clark Y airfoil and platform area, C_{LMAX} , C_{LMIN} , $C_{LCRUISE}$ were calculated. Here, an efficiency of 90% was used as the wing construction efficiency – that is, the ability to reproduce the true airfoil in model form. A platform adjustment for aspect ratio was used in the calculation of the wing incidence angle that takes into account three-dimensional effects.

$$V_{STALL} = \sqrt{\frac{2Mg}{C_{Lmax} \rho S}}$$

Using the maximum C_L obtainable from the Clark Y airfoil and taking into account the increase in lift the flap provides allows stall speeds to be determined for 0°, 20° and 40° flap settings.

The coefficient of lift when the flaps are deployed effects only 60% of the wingspan (although with the computer radio used, ailerons can also act as flaps if so required) resulting in the following overall C_L 's.

Table 5.1. Flap Position C_L , Wing loading, V_{STALL}

Flap Position	C_L	Wing Loading	Wing Loading	V_{STALL}	V_{STALL}	Condition
0°	1.32	167.3 g/dec ²	54.8 oz/ft ²	14.2 m/s	30.3 mph	Level Flight
20°	1.57	167.3 g/dec ²	54.8 oz/ft ²	13.1 m/s	27.7 mph	Takeoff
40°	1.75	167.3 g/dec ²	54.8 oz/ft ²	12.4 m/s	26.3 mph	Landing

Initial Velocity approximations provided in ElectriCalc were for cruising and maximum velocities, as its calculations account for propeller efficiencies, drag, and thrust.

$$V_{Max} = \sqrt{\frac{2T_{max}}{\rho C_D S_W}}$$

	Velocity	Velocity	C_L
V_{CRUISE}	24.6 m/s	60 mph	0.41
V_{MAX}	26.8 m/s	55 mph	0.49

Table 5.2. Max and Cruise Velocities

With the known cruising velocity, the angle of incidence for the wing was determined. This angle provides the model with the correct lift for level flight at the cruise velocity and takes into account the aspect ratio.

$$\alpha = \frac{a_0 + 18.24 \times C_{Lcruise} \times (1.0 + T)}{AR} = 2.2^\circ$$

T = platform adjustment factor for aspect ratio (Fig 4., pg 6, Lennon, Andy, "Basics of Model Aircraft Design")

α_0 = angle of incidence for required C_L under two dimensional flow.

The pitching moment of the wing at the cruise velocity was calculated to be -6.47 N/m (-458 oz/in). Hence the forward pitching moment requires the horizontal tail to provide the necessary force to keep from doing so. The pitching moment usually significantly increases with the use of flaps that are only 25% the wing chord, as utilised on the Minnow. Using the programming functions of the computer radio, elevator up trim can be set to automatically move as the flaps are lowered.

5.4 Tail Sizing

The T-tail configuration used allows the stabilizer to operate at near 90% efficiency as opposed to 40% for horizontal tails located low on the fuselage. It also reduces interference drag with only one junction between the vertical fin and stabilizer, as opposed to two.

The NACA 0009 symmetrical airfoil was chosen for use in the stabilizer, due to its low drag characteristics.

The horizontal tail has an area of 0.081 m^2 (0.87 ft^2), which is 22% of the wing area. An aspect ratio of 5 gives a 0.13m (0.42 ft) chord and a 0.64m (2.1 ft) span. The elevator area was set at 40% of the stabilizer area, providing 0.032 m^2 (0.34ft^2) of area. These dimensions are quite generous, as with the slow speed flight common in this competition, authoritative control is necessary.

Basic model airplane guidelines suggest that the horizontal tail be placed approximately 2.5 times the wing chord, from the neutral point of the wing to the neutral point of the stabilizer. However, the tail was placed at 3 times the wing chord from the neutral point, based on the experience of the 1999 DBF entry, and the large fuselage area ahead of the CG. Consequently, a tail moment arm of 0.76m (2.5ft) is used. The longer the tail moment arm, the smaller the horizontal tail needed, as tail volume remains constant.

With a pitching moment of -6.47 N/m (-458 oz/in) and a tail moment arm of 0.76m (2.5ft), the horizontal tail must provide a down force of 5.48 N (17.0 oz) assuming 90% stabilizer efficiency. This down force is provided by the negative lift from the stabilizer airfoil, requiring a $C_{L_{\text{stab}}} = -0.161$.

The angle of incidence to provide this C_L is -1.76° for two-dimensional flow. Using the same equation as the wing to account for the effects of an aspect ratio of 5, the tail incidence becomes -2.43° .

The down wash from the wing and its effect on the stabilizer must be taken into account. As air flows past the wing, the wake from the wing follows a slightly downward path, thus altering the direction of the oncoming air on the stabilizer. The horizontal moment arm and the height of the stabilizer from the wing are taken into account and their values, given as a percent of the semispan, were used with charts, (Figure 2, pg 40, Lennon, Andy; "Basics of RC Model Aircraft Design"), to provide the correct tail incidence required. A final angle of incidence of 0.06° is used.

The rudder uses a NACA 0012 airfoil in order to provide a slightly thicker spar for supporting the horizontal tail. This airfoil also exhibits low drag characteristics and zero pitching moment as required for a vertical stabilizer. The chord of the vertical fin was set to be the same as the stabilizer in order to reduce the interference drag when the two are joined together. Basic RC airplane design guidelines show that a vertical tail area of 8% of the wing area would provide adequate control. A study of the vertical area on this model indicates the center of lateral area will be close to 25% of the tail moment arm behind the CG. The height of the vertical fin must provide this area. A vertical stabilizer chord of 0.127m (0.42 ft) and a height of 0.22m (0.71 ft) was chosen. The rudder area was set at 40% of the vertical tail chord and extends downwards to taper into the fuselage.

A benefit of the T-tail design is that the horizontal stabilizer acts as a winglet on the top of the vertical stabilizer, allowing the vertical fin to behave as if it had a larger aspect ratio. A dorsal fin of about 10% of the vertical fin area will be employed in order to strengthen the vertical fin to fuselage joint, and to further increase directional stability.

5.5 Fuselage Sizing

The fuselage in the design selected must carry all the water, batteries and the propulsion system internally. It also provides a mounting location for the wings, tail, and landing gear. These requirements set the overall dimensions of the fuselage.

As the design being used has many uncertainties in power plant efficiency and empty airframe weight, the need to be able adjust the payload size is apparent. However, the CG must remain constant regardless of the number of water bottles on board. Thus the three bottles were centered at the center of gravity, so that any number of water bottles could be used (empty bottles needed as spacers still). This feature requires the main fuselage "U" channel to be 0.81 meters long (2.7 ft). The height of the "U" channel is 0.127 meters (0.42 ft), as dictated by the height of the water bottles and wing hold down supports. The tail boom length was set by the tail moment arm needed and is 0.86m (2.83 ft) long. A fuselage width just wide enough to surround the bottles was selected to be 0.1m (3.33 ft) wide. This width provides ample volume for all other control and mounting components. The batteries were placed in fairings on the landing gear to take advantage of the strength of this structure and to provide cooling.

The cargo area is accessed via a removable top hatch, pulling the water bottles out one at a time (connected by string). This allows a smaller and more aerodynamic tail structure than a rear door access design, but slower. However, with only 3 bottles too remove, this method should only result in a marginal increase in time changing cargo, easily made up for in flight performance.

5.6 Drag

In order to make accurate predictions of the flight speed and acceleration, the drag on the airplane must be calculated. In this basic estimation, the total drag is taken to be the sum of parasitic drag and the induced drag from the wing, given by the equation:

$$C_{DTotal} = A + B \times C_L^2$$

This approximation does not take into account interference drag caused by the junction of various parts. This form of drag can be considerable if proper drag reduction techniques are not incorporated. Fairings will be used on this airplane in order to reduce drag wherever possible.

It was noted that a cylinder has the same amount of drag as an aerodynamic profile 10 times its diameter. An aerodynamic fairing over the dual-strut nose gear will help reduce the drag of these components.

Parasite drag was estimated using the "component build-up" method. A flat-plate skin friction drag coefficient (C_f) is calculated for each major component of the aircraft and then multiplied by a "form factor" (k) that estimates losses due to form drag:

$$C_{dPara} = \sum \left[\frac{k \times C_f \times A_{wetted}}{S_w} \right]_{component} \quad \text{Where, } C_f = \frac{0.455}{(\log_{10} Re)^{2.56}} \quad \text{and} \quad Re = \frac{V \times L}{\gamma}$$

C_f is given for turbulent flow over a smooth plate.

Table 5.3 Parasite drag estimation using "component build-up" method.

	$A_{wetted} (m^2)$	$Re (\rho V L / \mu)$	C_f	Form factor, k	C_{DPara}
Wing	9.42×10^{-1}	4.26×10^5	5.43×10^{-3}	1.21 ($t/c = 0.1$)	1.31×10^{-2}
Fuselage	6.71×10^{-1}	2.43×10^5	3.94×10^{-3}	1.17 ($L/D = 7.5$)	6.56×10^{-3}
Wheels	2.46×10^{-2}	1.4×10^5	6.83×10^{-3}	1.32 ($t/d = 0.08$)	4.70×10^{-4}
Gear Struts	8.54×10^{-2}	1.4×10^5	6.83×10^{-3}	1.18 ($t/w = 0.08$)	1.46×10^{-3}
Stabilizer	1.61×10^{-1}	2.33×10^5	6.13×10^{-3}	1.10 ($t/c = 0.02$)	2.31×10^{-3}
Vertical Fin	8.60×10^{-2}	3.26×10^5	5.72×10^{-3}	1.07 ($t/c = 0.05$)	1.12×10^{-3}
Total					0.0251

Induced drag is estimated using the "wing efficiency" method. The induced drag coefficient is given by:

$$C_{dInduced} = \frac{C_L^2}{\pi \times AR \times e} \quad \text{where,} \quad e = 1.78(1 - 0.045 \times AR^{0.68}) - 0.64$$

This resulted in a value of $e = 0.778$

$C_{dInduced}$ was calculated at max, cruise and stall speeds.

$C_{dInducedMAXVEL}$	0.008	Maximum Velocity
$C_{dInducedCRUISE}$	0.011	Cruise Velocity
$C_{dInducedSTALL}$	0.077	Stall – 0° Flaps
$C_{dInducedSTALL}$	0.110	Stall – 20° Flaps
$C_{dInducedSTALL}$	0.136	Stall – 40° Flaps

Table 5.4 Drag at Max, Min and Stall Velocities

5.7 Total Drag

The total drag coefficient is the sum of the of the surface drag and the induced drag of the aircraft in cruise and is therefore given by:

$$C_{DTotal} = 0.025 + 0.011 = \mathbf{0.036}.$$

5.8 Power System

Initial calculations predicted that the MaxCim N32-13Y would be capable of producing upwards of 53 N (12 lbf) of thrust. This amount of thrust was not required on the Minnow, and it was thus decided to use a more conservative gear reduction in order to achieve a higher top speed. A final configuration using a 18×10 prop, 25 Sanyo N-3000CR mAh cells and an 6.54:1 reduction unit provides 38.7 N (8.7 lbf) of thrust. This provides adequate power for the Minnow at a higher top speed than a larger reduction unit.

As stated in the preliminary design a toothed belt drive unit was needed in order too maximize the efficiency of the reduction. A properly constructed and tensioned belt drive is capable of efficiencies close to 95% if a toothed timing belt system is used. Minnow's belt drive was constructed of commercially available 72 and 11 groove sprockets. A flexible coupling connects the motor to the input shaft, and a double timing belt connects the 11 groove sprockets to the 72 groove sprockets mounted on the output shaft.

5.9 Control Systems

Control of the aircraft is provided by a Futaba 8 channel PCM transmitter and receiver with its failsafe programmed as per competition rules. A four cell 600mAh battery pack is used to power the receiver and servos. This pack size is large enough to complete several missions, but will be peak charged again after each ten-minute flight.

All servos must provide quick, accurate, and strong control authority to the flight surfaces. Any slop in the control set-up could lead to flutter, and possible departure of that control surface. To reduce this risk, all servos are ball bearing supported and their torque output is matched to the operation they must perform. Control linkages between the servo and flight surface were kept as short as possible to reduce flex.

Hitec HS-225BB mini servos (3.9 kg/cm, 0.14s/60°, 27 g, nylon gears) are used in place of standard servos, as they are lighter and provide more torque. The mini servos in an airplane of this size are able to handle all flight loads incurred and are used on all flight surfaces. A Hitec HS-205MG metal geared mini servo (3.1 kg/cm, 0.20s/60°, 32 g) was selected for the nose gear steering servo, as previous one-point landings have shown that nylon gears at this location are easily stripped from the sudden impact.

5.10 G-Loading

With Minnow reusing Queen's 1999 DBF entry wing, the structural integrity of it has already been proven in many successful flights. The procedure for determining the spar sizing in last

year's plane was the basis for the spar design techniques used this year in the other Queen's entry, and are highlighted here.

In predicting the maximum g-load the aircraft is capable of handling, two major parameters were investigated. First, the aircraft's structural capabilities were estimated with a calculation of the spar's maximum allowable bending stress. Predictions were then made on the accelerated stall properties of the wing, using published lift data for the selected airfoil.

5.11 Structural Loading

A g-load rating of 4 was assigned as a prediction of the maximum loading the airplane would experience under normal flying condition and while at the maximum TOGW. From here the size and strength of the wing could be determined. For initial calculations, the assumption was made that the wing spar carried all wing loads and would experience heavier loads than any other aircraft part. Thus, the maximum bending stresses the spar can handle will determine the g-load capability of the plane.

The wing's manufacturing plan calls an "I" beam spar to be used, with a carbon laminate for each flange and a vertical grain balsa shear web. Thus, the maximum bending stresses these elements can handle will determine the g-load capability of the plane. As nearly all g-loadings placed on the airframe would be positive, this puts the upper spar into compression and the lower into tension. A carbon fiber laminate over balsa was used for the lower spar and a carbon fiber laminate over Douglas fir as the upper spar. It was also assumed that the carbon fiber on the lower spar handled all the tension loads and the fir in the upper spar handled all compression loads. From these assumptions, the cross sectional area of these respective materials could be calculated.

The maximum bending moment experience by the wing was calculated using basic force and moment analysis and found to be 480 kN/m (2740 lbf/ft). The second moment of inertia (I_y) was calculated for the area of the carbon fiber and the fir. As the distance to the neutral plane (z) is known, the bending stress could be calculated using the equation:

$$\sigma_x = \frac{M \times z}{I_y}$$

The dimensions of the upper spars (stock sizes) were then iterated to achieve a safety factor of 1 with positive 4 g loading. It was found that 2 layers of carbon fiber on a 1.0 in by 0.25 in piece of balsa was required for the bottom spar. An additional 2 layers of carbon fiber was added to increase strength with only a the marginal weight penalty, increasing its rated g-loading to approximately 10g's. The fir upper spar's dimensions were also set to 1.0 in by 0.25 in, resulting in a g-loading of 2.6. While this is below the rated aircraft g-loading, the heavy weight of this material was decidedly of more concern. Four layers of carbon fiber were laminated to this spar, and along with the wing sheeting, a 4 g rating is easily obtained from these dimensions, as proven

by the execution of several maneuvers outside of the envelop usually expected of a heavy lift aircraft.

5.12 Take-off Performance

Take-off distance is broken into three components: ground roll, rotation distance, and climb-out distance. Rotation distance is assumed to be negligible for this calculation.

5.12.1 Ground Roll

The ground roll distance (d_g) of the aircraft is given by:

$$d_g = \frac{V_{TO}^2}{2 \times a} \quad \text{Where,} \quad M \cdot a_{mean} = \left[T_{mean} - \left(A + B \cdot C_{Lg}^2 \right) \frac{1}{4} \rho V_{TO}^2 S_w - \mu \left(W - C_{Lg} \frac{1}{4} \rho V_{TO}^2 S_w \right) \right]$$

Take-off speed (V_{TO}) is taken as 15% above stall speed:

$$V_{TO} = 1.15 \times V_{stall}$$

The C_L and C_D used in this equation are the values at cruise speed, as the plane can be considered in level flight while on the ground with its wing angle of incidence relative to the runway. Static thrust is estimated from the available motor data from ElectriCalc. This yielded a ground roll acceleration of 4.67 m/s^2 (15.4 ft/s^2). The ground roll was then calculated at the take off velocities when no flaps are deployed and when 20° flaps are deployed.

Table 5.5 Takeoff distance

	V_{TO}	V_{TO}	d_g	d_g
0° Flaps	16.4 m/s	36.7 mph	28.6 m	93.9 ft
20° Flaps	15.0 m/s	28.4 mph	33.6 m	78.8 ft

Both ground runs are within the 100 ft takeoff limit, but with no flaps deployed there is very little room to play with. These distances are given under a no wind condition, which is unlikely. Gentle wind will reduce the take off run and air density values must also be considered. Hot or humid days will decrease the efficiency of both the wing and propeller, increasing ground roll distance. Thus the extra feet available with a flap take off is felt to be an adequate safety margin.

5.12.2 Climb out Distance

The climb out angle for the airplane is given by the equation:

$$\tan \theta = \frac{T}{W} - \frac{D}{L}$$

A climb angle of only 21° is achieved. If this rate of climb is held constant so that there is no gain in velocity after lift off, a distance of 26.4 m (86.5 ft) would be needed to reach an altitude of 10 m (32.8 ft). This is a very reasonable climb angle for a cargo aircraft.

5.13 Turning Radius

The minimum controlled level turning radius for an airplane is determined by the maximum radial acceleration the wing can sustain before an accelerated stall. The maximum g-load that can be produced by the aircraft is given by the ratio of the maximum lift available from the airfoil to the lift generated in steady level flight. The angle of bank at which the wing can still provide the necessary lift for the airplane is given by:

$$\cos\beta = \frac{C_{L\text{cruise}}}{C_{L\text{max}}}$$

Thus the maximum angle of bank is 68°. The maximum radial acceleration before the onset of an accelerated stall is calculated using the equation:

$$\tan\beta = \frac{a_{\text{stall}}}{1 \times g}$$

This gives a loading of 2.5 g's. Thus, if the aircraft is turned any harder than 2.5 g's, the maximum lift available from the wing will be exceeded and an accelerated stall will occur.

From this data the minimum radius of turn with no altitude loss is 25m (81 ft) as given by the equation:

$$R = \frac{V_{\text{cruise}}^2}{a_{\text{stall}}}$$

5.14 Endurance and Range

5.14.1 Endurance

The aircraft achieves maximum endurance when flying at its minimum throttle setting, which provides sufficient thrust for the plane to achieve a velocity just above its stall speed ($V_{\text{endurance}}$). This shows that endurance is highly dependant on the motor and electrical system used.

The ElectriCalc commercial software package is used to estimate the endurance of the aircraft with the selected motor and battery arrangement. Electrical specifications for both the MaxCim N32-13Y motor and the Sanyo N-3000CR cell pack are used as ElectriCalc's input. ElectriCalc then calculates the operating characteristics of the propulsion system as a function of throttle setting. Included among the output parameters are current draw, motor power and efficiency, and run-time at the calculated RPM and velocity (estimated by ElectriCalc from wing loading and $C_{D\text{Parasite}}$). It was found that an airspeed of 16.4m/s (34.8mph) could be achieved with a minimum throttle setting of 54%. At this setting, ElectriCalc estimated a run-time of 26.2 minutes. This endurance estimate neglects power needed for take-off, climb-out, and landing.

3.14.2 Range

The maximum range characteristics of an electrically powered aircraft differ from those of a gas-powered plane, as motor efficiency drops at increased throttle settings. Losses caused by higher current draw reduce the effective range of the aircraft as throttle setting is increased. Thus, the maximum range of the aircraft is achieved not at the best lift-to-drag velocity, but at the lowest

possible throttle setting—at the endurance throttle setting. To calculate the range, the endurance prediction of 26.2 minutes is multiplied by the endurance velocity of 16.4 m/s (34.8 mph). This method produces a maximum range value of 25.8 km (16.0 mph). This range is assuming zero wind conditions and neglects the power needed for takeoff and climb, landing and energy loss maneuvers (turning).

5.15 Stability

5.15.1 Longitudinal Stability

The maximum allowable distance between the center of gravity of the plane and the location of the $\frac{1}{4}$ chord of the wing was determined using the following stability criterion:

$$\frac{dC_{M(CoG)}}{dL} = \frac{x}{c} - \eta_H \left(\frac{S_H}{S_W} \right) \left(\frac{l_H}{c} \right) \left(\frac{a_H}{a} \right) \left(1 - \frac{d\epsilon}{d\alpha} \right) + \frac{dC_{Mf}}{dC_L} \leq 0$$

The marginally stable case value of x , the distance from the $\frac{1}{4}$ chord, was found by setting the above inequality to zero and evaluating. This yielded a value of 47%, which means that for the aircraft to be longitudinally stable, the center of gravity can be no more than 47% of the wing chord.

5.15.2 Lateral-Directional Stability

Yaw stability is based on the position of the center of lateral area of the airplane as discussed in section 5.4. Vertical tail sizing was used to position the center of lateral area at approximately 25% of the tail moment arm from the neutral point of the wing, about 0.32 m (1.0 ft) from the 25% chord.

As a determination of the directional stability of the aircraft, the following inequality was evaluated using the physical properties of the aircraft.

$$a_f \left(\frac{l_f}{c} \right) \left(\frac{S_f}{S_w} \right) \geq \frac{dC_{mf}}{d\phi}$$

The evaluated derivative was found to be 3.1, which is greater than zero indicating that the aircraft was directionally stable.

5.15.3 Roll Stability

Roll stability is assumed adequate due to the large pendulum effect from the payload. With no dihedral in the wing (to ease manufacturing capabilities), the pendulum effect of the cargo provides all self-leveling stability. When empty, the weight of the landing gear suspended from the bottom of the fuselage provides this effect. Large ailerons, each 0.054 m^2 (0.58 ft^2) in area, allows proper control authority.

Description	Coefficient	Variables	Description	Values
			large chord monoplane conventional tail single fuselage single motor	
FLIGHT SCORE				
Liters of Water Carried Multiplier	Water Load	$10 * n$	Water Load =	30
Liters of Water	n	number of liters	n =	
RATED AIRCRAFT COST				
Manufactures Empty Weight Multiplier	A	$\$100 * MEW$	A = \$	900.00
Manufactures Empty Weight	MEW (pounds)	airframe weight	MEW =	
Rated motor Power Multiplier	B	$\$1 * REP$	B = \$	1,500.00
Rated motor Power	REP (watts)	# motors * 50A * 1.2V/cell * # cells	REP =	1500
			# motors =	
			# cells =	
Manufacturing Cost Multiplier	C	$\$20 * MFHR$	C = \$	1,820.00
Manufacturing Man Hours	MFHR (hours)	Prescribed assembly Hours by WBS	MFHR =	91
MFHR = the sum of WBS				
Wings WBS = 5hrs/wing + 4 hrs / sq foot pro			Wing WBS =	33
			# wings =	
			area (sq.ft) =	
Fuselage WBS = 5hrs/body + 4hrs / foot or			Fuselage WBS =	21
			# bodys/pods =	
			length (ft) =	
Empenage WBS = 5 hrs + 5 hrs/vert surf. +			Empenage WBS =	15
			# vert. surfaces =	
			# horz. surfaces =	
Flight Systems WBS = 5 hrs + 1 hr/ servo			Flight Sys. WBS =	12
			# servos =	
Propulsion Systems WBS = 5 hrs / motor +			Propulsion WBS =	10
			# motors =	
			# props =	
Single Flight Score	SFS	Flights * Water Loads	SFS =	120
	Flights	Is the number of water caring flight within tim	# flights =	
Written Report Score	WRS	Score on written report as assigned by judg	WRS =	
Total Flight Score	TFS	3*single flight	TFS =	360
Rated Aircraft Cost	RAC (\$1000)	$(MEW + REP + MFHR) / 1000$	RAC =	4.22
FINAL SCORE	Final Score	Written Report Score * Total Flight Score / R	FINAL SCORE	7421.800948

6.0 Manufacturing Plan

Minnow's design can be broken down into four separate components, each of which employs a different construction technique. The wing from the '98-'99 DBF competition was reused, so this eliminated a significant portion of the manufacturing. The other main structures, the fuselage, tail appendage, and landing gear, were analyzed and the best construction choices were determined with a figure of merit matrix.

6.1 Fuselage Construction

6.1.1 Balsa Stringer

This form of construction stretches back to the first days of both full-sized and model aircraft flight. Many thin strips of wood (balsa on model planes) connect several wooden formers to produce the fuselage frame. This frame is then covered by doped paper or silk, or in more recent times, by shrinkable plastic.

6.1.2 Corrugated Plastic

While not in common use, the Queen's Aero Design team made use of this material in last year's AIAA entry. The plastic consists of two thin plates, separated by many thin plastic pieces, similar to corrugated cardboard. A fuselage can be made very rapidly by scoring the plastic and then folding it to form a 90-degree corner. Triangular bracing is then glued to the inside of the joint to ensure that it remains in place. This results in a very crash resistant structure (determined experimentally through several high speed encounters with the ground), which evenly supports the cargo. Unfortunately, this method of construction is heavy and forming joints of an angle other than 90-degrees is difficult.

6.1.3 Molded Carbon Fiber

This technique makes use of expensive composite materials to produce a very strong and lightweight fuselage. A mold of the required fuselage shape is made up of a heat resistant material. Several layers of pre-impregnated carbon fiber are laid up onto the mold, a sheet of thin structural honeycomb (which acts as a shear web for the carbon) is placed into the lay-up, and then more carbon fiber is laid up on top. The assembly is vacuum bagged and then heated until the epoxy cures. This technique requires access to expensive materials, equipment, and expertise, but can produce excellent results.

6.1.4 Fiberglass

High performance model aircraft has used the use of fiberglass and a "lost foam" mandrel for several years. The technique involves the production of a fuselage from medium density foam. This mandrel is then coated with several layers of fiberglass in a wet lay-up, and then the foam is dissolved with a strong solvent. The remaining fiberglass is then internally braced with wing mounting blocks, bulkheads, and other required structure, resulting in a lightweight stressed-skin fuselage. While not as strong as the carbon fiber/structural honeycomb, fiberglass does not require expensive heat resistant molds, expensive materials, or a great deal of technical experience.

6.2 Tail Construction

6.2.1 Foam and Fiberglass

Cutting the required shape from medium density foam and then adding a single layer of fiberglass can quickly make a strong and smooth airfoil. A sheet of thin plastic then covers the fibreglassed surface and the whole assembly is placed in a vacuum until the epoxy has hardened. The plastic sheets can then be peeled away, leaving a perfect tail surface. While this method of construction can result in a perfectly sculpted complex airfoil, it tends to be heavier than the other options available.

6.2.2 Sheet Balsa

By far the easiest way to construct a tail, thick sheet balsa can be cut in the required planform shape and then the edges can be rounded with a sanding block. Although the tail does not take a proper streamlined shape, the extra drag is usually accepted for the ease of construction. This method of construction is heavy, durable, and is prone to warping with changes in temperature in humidity.

6.2.3 Built-up Construction

A built-up tail is the lightest, but most fragile option under consideration. Construction is very similar to a built-up wing, with a set of evenly spaced ribs joined by a double spar and shear web, and the leading and trailing edges. Sheeting is sometimes extended right to the trailing edge to give a slight increase in torsional stiffness. The chief disadvantage of this design is that it is very time consuming to construct. Also worth considering is that the tiny balsa structure that makes up a built-up surface is vulnerable to damage, especially on a portion of the plane that is often accidentally banged and knocked during storage and transportation.

6.3 Undercarriage Construction

6.3.1 Aluminum

Aluminum landing gear is very common on model aircraft. An approximately 1/8" aluminum plate (thickness varies with the load requirements) is trimmed and then bent to form an arch shape. Holes are drilled for mounting the axles and for mounting the assembly to the aircraft. These undercarriages are commercially available, reliable, and cheap. Their chief disadvantage is that they tend to bend with rough landings, necessitating emergency repairs in situations where multiple flights are to be made within a certain time.

6.3.2 Tool Steel

Tool Steel (music wire, piano wire) is often used for model aircraft landing gear. Although it is a very brittle form of steel, landing gear made from it can flex and give with impact a great deal before catastrophic failure occurs. Music wire is obtained in the right size for the application then is carefully bent to fit the mounts built into the fuselage. If necessary, two wires can be soldered into a truss arrangement to give the assembly extra stiffness. This form of undercarriage is rigid and is not prone to bending on heavy landings. Its weakness is

heavy weight and the difficulty of mounting the wires to ensure that they do not break loose under landing loads.

6.3.3 Amarid, Carbon Fiber, and Structural Honeycomb

Composite undercarriages are starting to replace the more traditional aluminum and music wire arrangements. Made up of either pre-impregnated carbon fiber or amarid, and formed around a structural honeycomb core, they combine lightweight with a very structurally stiff package. Construction involves building a mold of a temperature resistant material and then laying up the composite materials on top of it. The assembly is put under vacuum in an autoclave and then baked for three hours to cure the epoxy. The final landing gear is removed from the mold, trimmed, and is then put into service. While this landing gear is ideal for situations involving heavy loads, it also requires the expensive materials and equipment common to all composite components.

6.4 *Figures of Merit*

To choose the best combination of manufacturing processes for Obsidian, a qualitative figure of merit was conceived to evaluate each technique's merits and weaknesses in a simple to interpret chart. Five criteria were selected, weight, structure, time, skill, and expense, and each construction method will be given a qualitative score that illustrates its performance in each category. The separate categories are described in detail below.

6.4.1 Weight

In a high performance competition aircraft, flight performance dictates who will win, and who will be defeated or worse, who will crash. If the aircraft design is effective and well planned out, then building weight is the one element that can seriously affect every aspect of the flight envelope. Where it is reasonable, a builder should always strive to make the components as light and efficient as possible. Thus, this was selected as the first criterion in the FOM.

6.4.2 Structure

The individual components of Obsidian operate on a weak link arrangement. It does not matter how strong the undercarriage is if the wing spars snap in flight. To ensure that the aircraft will be able to withstand the flight loads experienced throughout the mission, structural integrity was chosen as the second criterion in the FOM.

6.4.3 Skill

To produce the required components of the aircraft, the selected construction technique must either be known to the team or it must be easy to learn. Some methods require the use of specialized solvents, glues, fibers, and equipment, all of which must be introduced to a beginner in the field. Also, more experience with the specified building technique produces a more accurate final product and less waste, thus it is desirable to choose methods that are familiar to a larger number of team members. Skill was selected as the third criterion in the FOM.

6.4.4 Expense

Among the various construction techniques discussed, there is a huge difference in cost. This is due to some techniques using exotic materials or machining, while the more mundane and traditional techniques make use of the builder's individual skill rather than a complex mould or machine. As Obsidian was built with our meager budget in mind, the cheaper option is often worth pursuing due to fiscal necessity. As such, the expense of the construction technique was chosen as the fourth entry into the FOM.

6.4.5 Time

The final item worth considering when evaluating the construction choices is the length of time that the method requires. Obsidian was designed and built on a 100% volunteer basis because Queen's does not offer course credit towards participation in a design competition. Thus every calculation, every order, every glue joint must be juggled around the demands of a full engineering course load. Needless to say, a construction technique that saves a few hours of time is potentially valuable as it frees up resources that can be used for further work on other assignments.

6.5 *Evaluation and Selection*

6.5.1 Analytical Method

Each construction technique was evaluated in terms of each of the five criteria listed above. The weight of the method was estimated in ounces. The structural integrity of the method was given a rating on a scale from 0 to 10, with 10 being the strongest choice. The required skill of the choices was ranked on a scale from 0 to 5, with 5 being the easiest construction method. The cost of the method was estimated using a Canadian dollar value with American funds also indicated. The final entry, time, was given a value of the estimated construction hours required for each method.

Total scores were tabulated with the following equation, which weights the relative importance of each of the criteria.

$$\text{Total} = 100 * (1/\text{weight}) + (\text{structure}/3) + 3 * (1/\text{skill}) + 10(1/\text{expense}) + (1/\text{time})$$

6.5.2 Construction Method Selection

Upon examination of the FOM, it was determined that composites would be the best choice for building the fuselage and the landing gear. Build-up construction was chosen for the tail, it being a simple and light method that did not require the structural strength of the other choices.

Figure 6.1 Manufacturing Process Evaluation

	Weight (oz)	Structure	Skill	Expense		Time	Total
				Can\$	US\$		
Fuselage							
Balsa Stringer	30	2	5	80	54	65	4.74
Corrugated Plastic	45	5	2	25	17	15	5.86
Molded Carbon Fiber	30	9	5	800	536	25	6.99
Fiberglass	38	4	4	300	201	25	4.79
Tail							
Foam and Fiberglass	7	6	3	10	7	10	18.39
Sheet Balsa	10	7	1	6	4	4	17.25
Built-up Construction	4	5	4	10	7	8	28.54
Undercarriage							
Aluminum	16	4	2	22	15	2	10.04
Tool Steel	20	7	4	10	7	5	9.28
Amarid, Carbon Fiber, and Structural Honeycomb	9	9	5	100	67	12	14.89

Figure 6.2 Manufacturing Milestones

<u>Milestone</u>	<u>Proposed Date (m/wk)</u>	<u>Actual Date (m/wk)</u>
1.0 Fuselage		
1.1 Mould made	1/1	1/1
1.2 Composites laid up and baked	2/1	2/3
1.3 Tail boom cut from foam	2/1	2/1
1.4 Bulkheads installed	2/2	2/4
1.5 Fairings cut from foam	2/2	2/2
1.6 Fiberglassing	3/2	
1.7 Assembly	3/3	
2.0 Undercarriage		
2.1 Mould made	1/1	1/2
2.2 Composites laid up and baked	2/1	2/2
2.3 Trimmed and sanded	2/1	2/3
3.4 Mounted	3/3	
3.0 Tail		
3.1 Spars built	2/1	2/3
3.2 Ribs cut out	2/2	2/4
3.3 Initial assembly	2/3	2/4
3.4 Sheeting	2/3	2/4
3.5 Servo installation	3/2	
3.6 Mounting	3/2	

Appendix A: Calculation Spreadsheets**Weight Estimation**

Description	Weight (lbs)	Weight (kgs)	Number	Subtotal (lbs)	Subtotal (kgs)
1 Liter of Water	2.420	1.098	3	7.260	3.293
Battery Pack	4.800	2.177	1	4.800	2.177
Receiver	0.125	0.057	1	0.125	0.057
Micro Servos	0.063	0.028	6	0.375	0.170
Standard Servos	0.125	0.057	0	0.000	0.000
Flap Servos	0.313	0.142	0	0.000	0.000
Landing gear	0.500	0.227	1	0.500	0.227
Wheels	0.125	0.057	3	0.375	0.170
Wing	1.500	0.680	1	1.500	0.680
Tail	0.125	0.057	1	0.125	0.057
Fuselage	1.000	0.454	1	1.000	0.454
Motor	0.500	0.227	1	0.500	0.227
Speed Control	0.188	0.085	1	0.188	0.085
Gear Box	0.375	0.170	1	0.375	0.170
Prop	0.250	0.113	1	0.250	0.113
TOGW				17.4	7.88
Empty Flying Weight				10.1	4.59
Airframe Weight				5.31	2.41

Payload Fraction

Payload Fraction = $W_{\text{payload}} / \text{TOGW}$

Payload Fraction = 0.417901856

DRAG ESTIMATION						
Summary of Equations Used						
$Re = (\text{Density Air} / \text{Viscosity Air}) * \text{Velocity} * \text{Length (metric)}$				Reynolds number		
$Cdf = 0.455 / ((\log_{10}(Re))^2 * 5.5)$				Coefficient of frictional drag		
$CdPara = (k * Cf * Awetted) / Swing$				Coefficient of parasitic drag		
$Cdinduced = Cl^2 / (Pi() * AR * e)$				Coefficient of induced drag		
$De = 2 * (H+W) / Pi$				Equivalent fuselage diameter		
$e = 1.78 * (1 - 0.045 * (AR^{0.68})) - .64$				efficiency value		
Constants						
Density of Air (p) =		1.225	kg/m ³	1.00000		
Viscosity of Air (u) =		0.000017894	kg/m/sec	373.718	slug/ft/sec	
Cruise Velocity		26.82	m/s	assumed from motocalc		
Parasite drag estimation using "component build-up" method				<i>*Form Factors from Mech 480 notes</i>		
	Awetted (m²)	Re (pVL/u)	Cf	Thickness Ratio	Form Factor (k)	CdPara
Wing	0.942	425580	0.005430	0.1096 (t/c)	1.21	0.013140
Fuselage	0.671	242522	0.003938	8.1681 (L/De)	1.17	0.006564
Wheels	0.025	139917	0.006826	0.0833 (t/d)	1.32	0.000470
Gear Struts	0.085	139917	0.006826	0.0833 (t/w)	1.18	0.001470
Stabilator	0.161	233194	0.006129	0.0150 (t/c)	1.10	0.002309
Rudder	0.086	326472	0.005723	0.0714 (t/c)	1.07	0.001124
Total						0.025067
Equivalent diameter of fuselage						
<i>Converts fuselage perimeter to a equivalent circular cross section diameter</i>						
$De = 2 * (H+W) / Pi$						
De = 0.162						
Induced Drag						
$Cdinduced = Cl^2 / (Pi() * AR * e)$						
AR = aspect ration						
Cl = coefficient of lift						
$e = 1.78 * (1 - 0.045 * (AR^{0.68})) - .64$						
e = 0.778						
Cdinducedmaxvel = 0.008		using max Cl				
Cdinducedcruise = 0.011		using cruise CL				
Cdinducedstall = 0.077		CL at 0 degree flaps				
Cdinducedstall = 0.110		CL at 20 degree flaps				
Cdinducedstall = 0.136		CL at 40 degree flaps				
Total Coefficient of drag at cruise velocity						
Cd Total at Cruise =		0.0357				

LONGITUDINAL STABILITY

Summary of Equations Used

$$dCm_{cg}/dL = x/c - \eta_H(S_H/S_W)(l_H/c)((dC_{l_H}/d\alpha)/(dC_l/d\alpha)) + dCm_f/dC_l$$

longitudinal stability criterion
(Oothuseizen)

$$dCm_f/dC_l = k_f W_f^2 L_f / (C S_W)$$

Calculation of Rear Most CG

$l_H = 30$	in	tail moment arm
$C = 9.125$	in	mean aerodynamic chord
$S_H = 122$	in ²	horizontal tail area
$S_W = 730$	in ²	wing area
$\eta_H = 0.9$		horizontal tail efficiency
$dC_{l_H}/d\alpha = 5.73$	radians ⁻¹	slope of stabilizer C_l vs AOA
$dC_l/d\alpha = 5.2$	radians ⁻¹	slope of wing C_l vs AOA
$k_f = 0.6$		empirical pitching factor from Raymer
$W_f = 4$	in	width of fuselage
$L_f = 52$	in	length of fuselage

CG = 47.1 % of chord

LATERAL-DIRECTIONAL STABILITY

Summary of Equations Used

$$dCm_f/d\phi = (dC_{l_f}/d\alpha)(S_f/S_W)(l_H/c)$$

lateral stability criterion
(Oothuseizen)

Calculation of Rear Most CG

$l_H = 30$	in	tail moment arm
$C = 9.125$	in	mean aerodynamic chord
$S_H = 122$	in ²	fin area
$S_W = 730$	in ²	wing area
$dC_{l_f}/d\alpha = 5.73$	radians ⁻¹	slope of fin C_l vs AOA

$dCm_f/d\phi = 3.1 < 0$

Horizontal Tail Design

Summary of Equations Used

$HTA = (2.5 \cdot MAC \cdot 22\% \cdot WA) / TMA$	horizontal tail area (pg 33, Basics of RC Model Aircraft Design)
$EA = 40\% \cdot HTA$	elevator area
Horizontal Lift = Pitching Moment * Moment Arm	horizontal lift force
$Cl_t = (HL \cdot 3519) / (p \cdot V_{cruise}^2 \cdot Stail)$	tail coefficient of lift
$a = a_o + ((18.24 \cdot Cl) \cdot (1+T)) / AR$	angle of incidence account for aspect ratio effects

Horizontal Tail Area

based on a comparison to an airplane of $AR = 6$ and a 22% area at a distance of 2.5 times the chord

$$HTA = (2.5 \cdot MAC \cdot 22\% \cdot WA) / TMA \quad (\text{pg 33, Basics of RC Model Aircraft Design})$$

HTA = horizontal tail area

TMA = tail moment arm in inches

WA = wing area

MAC = mean aerodynamic chord

TMA = 30 in variable based on design

TMA = 0.76 m

HTA = 122 in² stab area for given tail moment arm

HTA = 0.079 m²

Elevator Area

For a flapped model, an elevator area of 40% should be used

EA =

$40\% \cdot HTA$

EA = 48.8 in²

EA = 0.032 m²

Estimated Tail Efficiency

estimated between 40 and 90% based on vertical position of tail relative to wing

THE = 0.9 predicted efficiency value for a T tail

Lift of Horizontal Tail Needed

Wing Pitching Moment

PM = -458 oz/in pitching moment of wing at cruise

PM = -6.47 N/m pitching moment of wing at cruise

Horizontal Lift = Pitching Moment * Moment Arm

HL = -15.3 oz

HL = -4.93 N

Tail lift accounting for tail efficiency

HL = -17.0 oz negative pitching moment requires downforce**HL = -5.48 N****Coefficient of Lift for Tail** $Cl_t = (HL * 3519) / (\rho * V_{cruise}^2 * S_{tail})$ **$Cl_t = -0.161$ coefficient of lift need for tail airfoil****Angle of Incidence of Tail**Interpolation of alpha at given coefficient of lift
Values Taken at $Re = 399900$

Alpha	Cl	Cd
1.67	0.15	0.00
	1	74
2.11	0.19	0.00
	8	79
Difference	0.44	0.04
	7	05
alpha = -1.76 degrees		

$$a = a_o + ((18.24 * Cl) * (1 + T)) / AR$$

$a_o =$ - angle of attack at coefficient of lift needed from airfoil properties

1.759

3886

$Cl =$ - Cl_{cruise}

0.160

5483

$T =$ 0.15 platform adjustment for aspect ratio (figure 4, pg 6 of Basics of Model Aircraft Design)

$AR =$ 5 aspect ratio of wing

$a' = -2.43$ degr tailplane incidence neglecting downwash from wing
ees

Downwash Angle Estimation	
SS = 42.00 in	wing semi-span
X = 30.00 in	distance from wing 1/4MAC to tail 1/4MAC (TMA)
X / SS = 71.43 %	distance from wing 1/4MAC to tail 1/4MAC as a percent of semispan
H' = 4.00 %	vertical wake displacement in percent of semispan for a Clcruise =1 (fig 2, pg of Basics of RC Model Aircraft Design, column b)
H = 1.96 %	vertical wake displacement in percent of 0.48 semispan for a Clcruise = 9
HTE = 8 in	horizontal tail elevation above wing
M = 19.04 %	horizontal tail elevation above wing as a perecent of semispan
7619	
M+H = 21.00 %	vertical location of horizontal tail relative to the wake Cl as a percent of semispan
DWA' = 5.1 degr	downwash angle at Cl =1(fig 2, pg 40, The Basics of RC Model
ees	Aircraft Design, column c)
DWA = 2.493 degr	downwash angle 0.48899
8992 ees	at Cl = 9851
a = 0.061 degr	tailplane incidence
ees	

Spar Sizing

Summary of Equations Used

$DI = SS \cdot z$	force on wing from distributed load
$I = A \cdot y^2$	Second moment of inertia of area
$\text{stress} = M \cdot y / I$	bending stress

Dimensions and Material Properties

B =	84 in	spar span
SS =	40	semi span minus fuselage width
H =	1.25 in	height from carbon fiber endcap to endcap
y =	0.625 in	neutral plane (1/2 H)
m =	17.3725 lbs	mass of plane
g =	4	g loading due to circumferential forces
F =	69.49 lbf	force wing must support
z =	0.868625 lbf/in	distributed lift load
w =	1 in	spar width
t carbon =	0.0087 in	thickness of each layer of unidirection preimpregnated carbon fiber
n =	4	number of layers of carbon fiber in the lamination
tc =	0.0348 in	thickness of carbon fiber lamination on each end
tf =	0.25 in	thickness of Douglas Fir Compressive spar
E(C) =	21000000 lbf/in ²	Youngs Modulus of carbon fiber
T.S. C	175000 psi	Tensile Strength of carbon fiber
T.S. Fir	12400 psi	Tensile Strength of Douglas Fir
C.S. Fir	7240 psi	Compressive Strength of Douglas Fir
E(Fir) =	1950000 psi	Youngs Modulus of Douglas Fir
SS ² z =	34.745 lbf	
M =	1389.8 lbf/in	M = 243390.1 N/m force moment

Carbon Fiber

$I = A \cdot y^2$		Second moment of area for the carbon fiber
stress = $M \cdot y / I$		
$I = 0.01284739 \text{ in}^4$		
stress =	65729 psi	max tensile bending stress on bottom carbon fiber spar
S.F. =	2.66	safety factor of the spar against carbon fiber failure under a 4 G loading

Douglas Fir

$I = A \cdot y^2$			
$\text{stress} = M \cdot y / I$			
	$I = 0.0625$	in^4	
stress =	11118	psi	compressive bending stress on top spruce spar
S.F. =	0.651		safety factor of the spar against Douglas Fir fiber failure under 4 G loading ignoring compressional strength of carbon fiber

Coefficient of Lift

Summary of Equations Used

$Cl_{max} = 2 \cdot L / (\text{efficiency} \cdot p \cdot Sw \cdot V_{min}^2)$	maximum coefficient of lift needed at minimum velocity
$Cl_{min} = 2 \cdot L / (\text{efficiency} \cdot p \cdot Sw \cdot V_{max}^2)$	minimum coefficient of lift needed at maximum velocity
$Cl_{cruise} = 2 \cdot L / (\text{efficiency} \cdot p \cdot Sw \cdot V_{cruise}^2)$	cruise coefficient of lift needed at cruise velocity
$\alpha = \alpha_0 + ((18.24 \cdot Cl) \cdot (1 + T)) / AR$	angle of incidence accounting for aspect ratio effects
Pitching Moment (oz/in) = $(Cm \cdot p \cdot V_{cruise}^2 \cdot S_{wing} \cdot Chord) / 3519$	pitching moment of wing
$Cl = Cl_{airfoil} \cdot (((1 + Flaplift) \cdot Flaplength) + (1 - Flaplength))$	coefficient of lift account for flap efficiencies and length
$Cl_{climb} = 2 \cdot L / (\text{efficiency} \cdot p \cdot Sw \cdot V_{min}^2)$	coefficient of lift during climb
$V_{stall} = ((2 \cdot M \cdot g) / (Cl_{max} \cdot p \cdot Sw))^{\frac{1}{2}}$	velocity at stall

Constants

Gravity =	9.81 m/s ²
Efficiency =	0.9 = 90% wing construction accuracy efficiency

Coefficients of Lift using ElectriCalc Velocities

$$Cl_{max} = 2 \cdot L / (\text{efficiency} \cdot p \cdot Sw \cdot V_{min}^2)$$

$$Cl_{max} = 2.817$$

$$Cl_{min} = 2 \cdot L / (\text{efficiency} \cdot p \cdot Sw \cdot V_{max}^2)$$

$$Cl_{min} = 0.414$$

$$Cl_{cruise} = 2 \cdot L / (\text{efficiency} \cdot p \cdot Sw \cdot V_{cruise}^2)$$

$$Cl_{cruise} = 0.489$$

Maximum Cl obtainable from Wing Platform

Max Cl of Airfoil	1.32	maximum lift selected airfoil produces
Flap Lift 20 degrees	0.32	Predicted additional lift provided by flaps
Flap Lift 40 degrees	0.54	based on flap design and extension
Flap Length	0.6	Length of flaps in percent of wingspan

$$Cl = Cl_{airfoil} \cdot (((1 + Flaplift) \cdot Flaplength) + (1 - Flaplength))$$

$$CL_{20} = 1.57 \text{ Maximum Cl wing produced when flaps are deployed 20 degrees}$$

$$CL_{40} = 1.75 \text{ Maximum Cl wing produced when flaps are deployed 40 degrees}$$

$$V_{stall} = ((2 \cdot M \cdot g) / (Cl_{max} \cdot p \cdot Sw))^{\frac{1}{2}}$$

$$V_{stall} = 14.2 \text{ m/s} \quad \text{Calculated stall speed with 0 degree flaps}$$

$$V_{stall} = 30.3 \text{ mph}$$

Vstall =	13.1 m/s	Calculated stall speeds with 20 degree flaps
Vstall =	27.7 mph	
Vstall =	12.4 m/s	Calculated stall speed with 40 degree flaps
Vstall =	26.3 mph	
Thus the maxium coefficient of lift at 1.5734 using 20 degree flap extension		
takeoff =	4	
The takeoff velocity is taken at 1.15 times the stall velocity at 20 degree flaps, corresponding to Cl of		
Clclimb =	$2 * L / (\text{efficiency} * p * S_w * (V_{min} * K)^2)$	
Clclimb = 1.32	Cl needed during climout a 1.15 times Vstall	

Total of Section and Induced Angle of Attack (AOA)

Interpolation of alpha at given coefficient of lift
Values Taken at Re = 399900

Alpha	Cl	Cd
0.1	0.377	0.0074
1.69	0.55	0.0079
Differenc e	1.59	0.173
alpha =	1.13	

$$a = a_o + ((18.24 * Cl) * (1 + T)) / AR$$

ao = 1.13 angle of attack at coefficient of lift needed from airfoil properties

Cl = 0.49 Clcruise

T = 0.14 platform adjustment for aspect ratio (figure 4, pg 6 of Basics of Model Aircraft Design)

AR = 9.21 aspect ratio of wing

a = 2.23 angle of incidence of wing on model

Pitching Moment

$$\text{Pitching Moment (oz/in)} = (C_m * p * V_{cruise}^2 * S_{wing} * \text{Chord}) / 3519$$

Interpolating for
Cm

Using Data for Re = 401900

alpha	Cl	Cm
0.63	0.406	-0.0771
1.87	0.56	-0.0815
Differenc e	1.24	0.154

Cm = -0.0795 pitching coefficient of wing at cruise

PM = -458 oz/in pitching moment

PM = -6.47 N/m pitching moment

Range

Summary of Equations Used		
$V_{min} = 1.15 * V_{stall}$		minimum flying velocity
$Range = Velocity * Time$		distance plane covers over ground under now wind conditions

Minium Velocity		
$V_{stall} =$	14.24827 m/s	stall speed at 0 degree flaps
$V_{stall} =$	30.2897 mph	
$V_{min} = 1.15 * V_{stall}$		
$V_{min} =$	16.4 m/s	minimum speed at which the airplane can fly without stalling
$V_{min} =$	34.8 mph	=Vendurance

Endurance of Motor System		
Enduranc e =	26.2 min	at throttle setting to produce V_{min} , values taken from electricalc
Enduranc e =	1572 seconds	
Throttle =	52 %	throttle setting at minium velocity, from electricalc

Range		
$Range = Velocity * Time$		
Range =	25758 m	
Range =	25.8 km	distance plane covers over ground under no wind conditions
Range =	16.0 miles	neglecting takeoff, landing and energy loss maneuvers

Turning Radius

Summary of Equations Used

$\text{CosB} = \text{Cl}_{\text{cruise}}/\text{Cl}_{\text{max}}$	bank angle which the plane can still horizontal level flight
$\text{TanB} = a/1*g$	g-loading before accelerated stall
$R = (\text{V}_{\text{cruise}}^2)/a$	radius of turn with no altitude loss

$\text{Cl}_{\text{cruise}} = 0.489$	minimum lift needed during cruise
$\text{Cl}_{\text{max}} = 1.320$	maximum lift airfoil can produce without use of flaps (from tables)
$\text{V}_{\text{cruise}} = 24.676$	cruise velocity of airplane

Bank Angle

$\text{CosB} = \text{Cl}_{\text{cruise}}/\text{Cl}_{\text{max}}$	
$\text{CosB} = 0.3704544$	
$\beta = 1.2$	radians
$\beta = 68.3$	degrees degrees of bank that the wing can still provide the necessary lift

G-Loading Before Accelerated Stall

$\text{TanB} = a/1*g$	
$a = 2.51 \text{ g}$	maximum radial acceleration before the onset of an accelerated stall
$a = 24.6 \text{ m/s}^2$	

Radius of Level Turn

$R = (\text{V}_{\text{cruise}}^2)/a$	
$R = 24.8 \text{ m}$	
$R = 81.2 \text{ ft}$	minimum radius of turn before accelerated stall

TAKEOFF PERFORMANCE

Summary of Equations Used

$V_{\text{takeoff}} = k \cdot V_{\text{stall}}$	safe takeoff velocity
$a = (T - (A + B \cdot C_{lg}^2) \cdot \frac{1}{4} \cdot \rho \cdot V_m^2 \cdot S_w - u \cdot (W - C_{lg} \cdot \frac{1}{4} \cdot \rho \cdot V_m^2 \cdot S_w)) / M$	ground run acceleration
$d_g = (V_{to}^2) / (2 \cdot a)$	ground roll distance
$d_c = h / \tan \theta$	horizontal distance to climb to height h
$d_c = h / (T/M - ((A + B \cdot C_{lto}^2 / k^4) / (C_{lto} / k^2)))$	
$\tan \theta = T/W - D/L$	climb out angle

Values Used in calculations

$V_{\text{stall}20} =$	13.1 m/s	Calculated stall speed	With 20 degree flaps
$V_{\text{stall}} =$	14.2	Calculated stall speed	With 0 degree flaps
$k =$	1.15	is 15% above stall speed	usually equals 1.1 to 1.2
$V_{to20} =$	15.0 m/s	takeoff velocity	With 20 degree flaps
$V_{to0} =$	16.4 m/s	takeoff velocity	With 0 degree flaps
$V_{\text{mean}} =$	10.6 m/s	mean takeoff velocity	
$T =$	38.701 N	takeoff thrust	
$u =$	0.015	rolling resistance (estimate)	
$A =$	0.025	Parasite Drag Coefficient	
$B =$	0.077	Induced drag Coefficient	C_d cruise used based on C_L cruise being used
$M =$	7.880 kg	mass	
$W =$	77.303 N	weight	
$\rho =$	1.225 kg/m ³	density of air	
$S_w =$	0.471 m ²	wing platform	
$C_l =$	0.489	coefficient of lift on takeoff run	C_l cruise used because AOA is fixed at cruise while on ground
$C_{l'} =$	1.322	coefficient of lift during climbout	
$H =$	10.000 m	climbout altitude	

Ground Run Acceleration

$$a = (T - (A + B \cdot C_{lg}^2) \cdot \frac{1}{4} \cdot \rho \cdot V_m^2 \cdot S_w - u \cdot (W - C_{lg} \cdot \frac{1}{4} \cdot \rho \cdot V_m^2 \cdot S_w)) / M$$

$$a = 4.69 \text{ m/s}^2$$

$$a = 15.4 \text{ ft/s}^2$$

Ground Run Distance

$$d_g = (V_{to}^2) / (2 \cdot a) = \text{ground roll}$$

$$d_g = 24.0 \text{ m} \quad \text{ground roll with 20 degree flaps}$$

$$d_g = 78.8 \text{ ft}$$

$$d_g = 28.6 \text{ m} \quad \text{ground roll with 0 degree flaps}$$

$$d_g = 93.9 \text{ ft}$$

Climb Out Distance to an Altitude of "h" meters

$$dc = h/\tan\theta$$

$$dc = h/(T/M - ((A+B \cdot Clto^2/k^4)/(Clto/k^2)))$$

$$\tan\theta = T/W - D/L$$

$$\tan\theta = 0.379256205$$

$$\text{Climb} = 0.362 \text{ rad}$$

$$\text{Angle} =$$

$$\text{Climb} = 20.8 \text{ degree}$$

$$\text{Angle} = s$$

$$dc = 26.4 \text{ m} \quad \text{distance to climb to height h}$$

$$dc = 86.5 \text{ ft}$$

WING LOADING

Summary of Equations Used

Wingloading = Weight/Wing Area

Values used in Calculations

	Imperial	Metric
Wingspan	84.000 in	2.134 m
Root Chord	10.000 in	0.254 m
Tip Chord	8.250 in	0.210 m
Fuselage Width	4.000 in	0.102 m
Weight	17.373 lbs 277.960 oz	7.880 kg 7879.992 g
Average Chord	9.125 in	0.232
Wing Area	730.000 in ² 5.069 ft ²	0.471 m ² 47.097 dec ²

Wing Loading With No Flaps

Wing Loading	0.024 lbs/in ²	16.7 kg/m ²
no flaps	3.43 lbs/ft ²	0.167 kg/dec ²
	54.8 oz/ft ²	167 g/dec ²

Flap Extension Area

Individual Flap Area	65.7 in ²	0.042387 m ²	
Total Flap Area	131.4 in ²	0.084774 m ²	
Flap Extension Area	0 in ²	0 m ²	
Total Wing Area	730.000 in ²	0.471 m ²	at 40 degree flaps
	730.000 in ²	0.471 m ²	at 20 degree flaps
	5.069 ft ²	47.097 dec ²	at 40 degree flaps
	5.069 ft ²	47.097 dec ²	

Wing Loading With Extended Flaps

Wing Loading	54.8 oz/ft ²	167.3 g/dec ²	at 40 degree flaps
Flaps Extended	54.8 oz/ft ²	167.3 g/dec ²	at 20 degree flaps

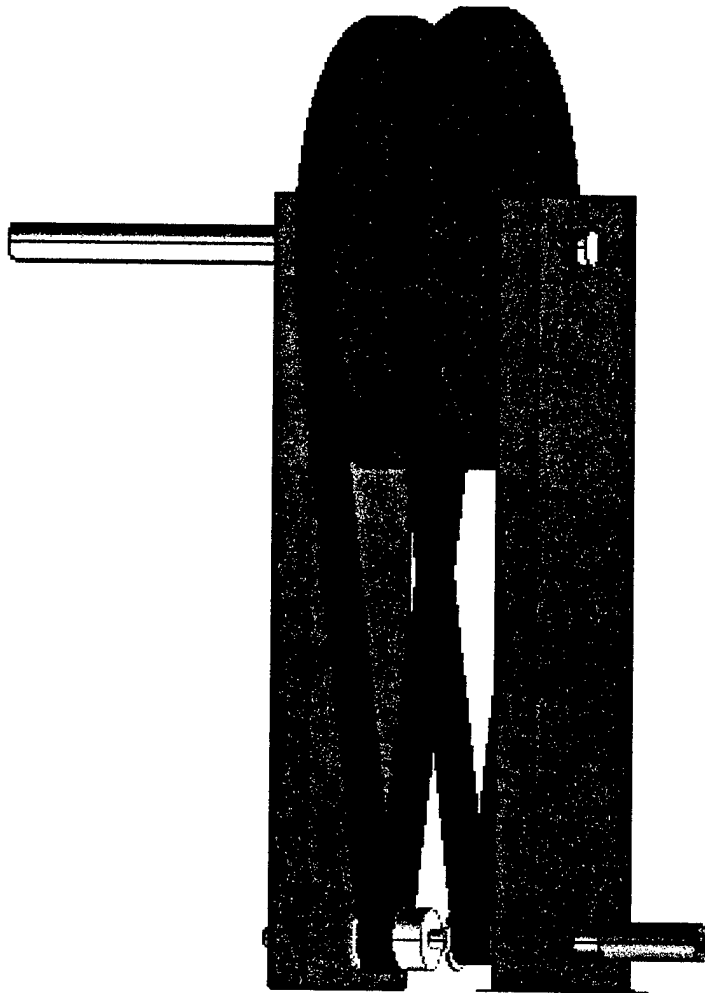
KEY DIMENSIONS AND FEATURES			
Feature	Item	Imperial Units	Metric Units
Propulsion			
	Motor	MaxNeo 13Y Brushless DC	MaxNeo 13Y Brushless DC
	Speed Controller		
	Cells	25cells by 3000mah each	25cells by 3000mah each
	Reduction	6.85 to 1	6 to 1
	Propeller	18 by 12	18 by 12
	Static Thrust on Takeoff	8.7 lbf	38.70108 N
	Static Thrust	8.7 lbf	38.70108 N
	Run Time Full Throttle	4 min	4 min
	Motor Efficiency	90 %	90 %
	Energy Efficiency	70 %	70 %
Wing			
	Span	84.000 in	2.134 m
	Root Chord	10.000 in	0.254 m
	Tip Chord	8.250 in	0.210 m
	Average Chord	9.125 in	0.232 m
	Wing Thickness	1.000 in	0.025 m
	Aspect Ratio	9.205	9.205
	Wing Area	730.000 in ²	0.471 m ²
	Taper	double taper	double taper
	Sweep	none	none
	Airfoil	Clark Y	Clark Y
	Aileron Length	16.000 in	0.406 m
	Aileron Width	2.281 in	0.058 m
	Aileron Area (each)	36.500 in ²	0.024 m ²
	Flaps Length	24.000 in	0.610 m
	Flaps Width	2.738 in	0.070 m
	Flap Area (each)	65.700 in ²	0.042 m ²
Horizontal Stabilizer			
	Tail Aspect Ratio	5.000	5.000 m
	Target Stab Area	122.123 in ²	0.079 m ²
	Chord	5.000 in	0.127 m
	Span	25.000 in	0.635 m
	Iterated Area	125.000 in ²	0.081 m ²
	Tail Moment Arm	30.000 in	0.762 m
	Tail Thickness	0.375 in	0.010 m
	Airfoil	NACA 0009	NACA 0009

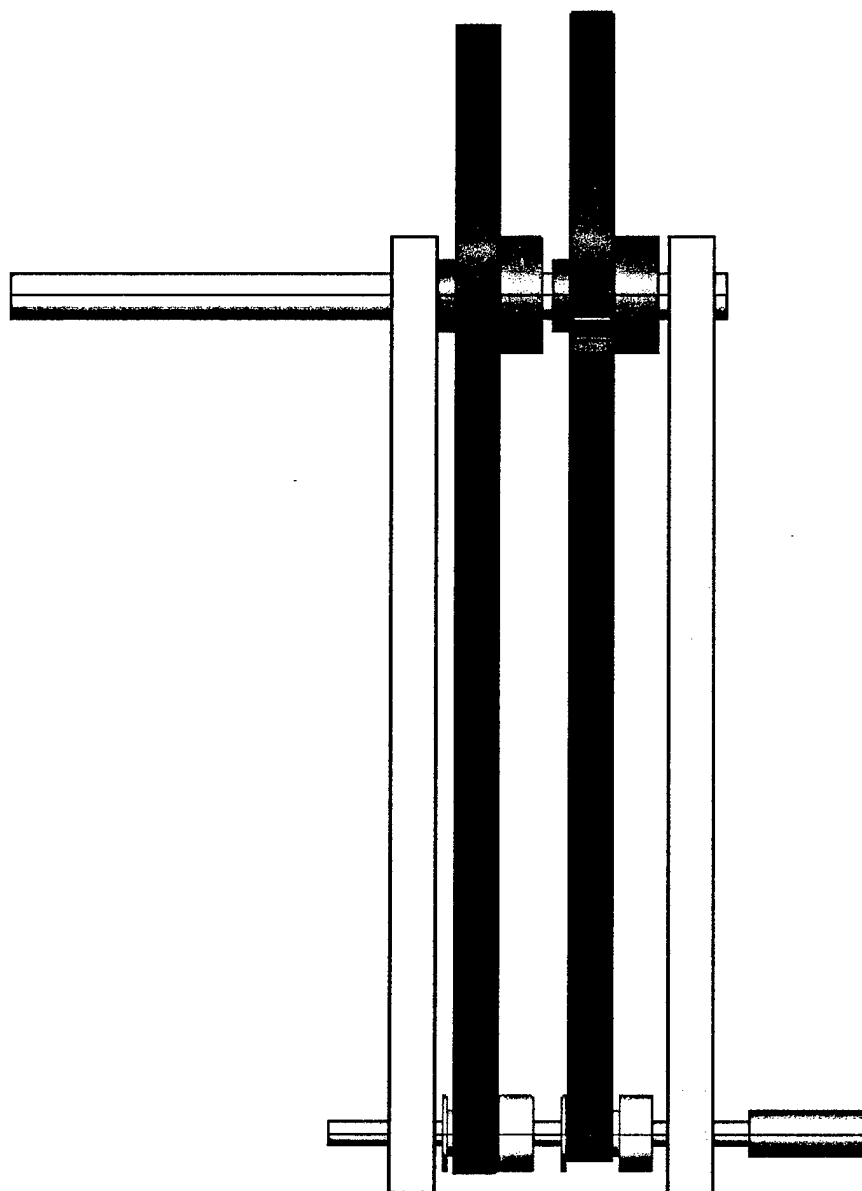
	Taper	single taper		single taper	
	Sweep	none		none	
	Target Elevator Area	48.849 in ²		0.032 m ²	
	Elevator Span	25.000 in		0.635 m	
	Elevator Chord	1.954 in		0.050 m ²	
Vertical Fin/Rudder					
	Vert Fin Height	10.000 in		0.254 m	
	Tip Chord	5.000 in		0.127 m	
	Root Chord	5.000 in		0.127 m	
	Average Chord	5.000 in		0.127 m	
	Vert. Fin Area	50.000 in ²		0.032 m ²	
	Rudder Tip Chord	2.000 in		0.051 m	
	Rudder Root Chord	2.000 in		0.051 m	
	Average Rudder Chord	2.000 in		0.051 m	
	Rudder Height	8.500 in		0.216 m	
	Rudder Area	17.000 in ²		0.011 m ²	
	Rudder/Fin Thickness	0.500 in		0.013 m	
	Airfoil	NACA 0012		NACA 0012	
	Taper	none		none	
	Sweep	none		none	
Fuselage					
	Length	52.000 in		1.321 m	
	Height	6.000 in		0.152 m	
	Width	4.000 in		0.102 m	
Main Landing Gear					
	Wheel Diameter	3.000 in		0.076 m	
	Wheel Base	14.438 in		0.367 m	
	Thickness	0.250 in		0.006 m	
	Avg Width	3.000 in		0.076 m	
	Height	5.813 in		0.148 m	
	Brakes	none		none	
Nose Gear					
	Wheel Diameter	2.500 in		0.064 m	
	Thickness	0.500 in		0.013 m	
	Height	5.813 in		0.148 m	
	Wire Diameter	0.250 in		0.006 m	
	Brakes	yes		yes	
From Electrocalc					
	Vmax	60 mp/h		26.8 m/s	
	Vcruise	55 mp/h		24.7 m/s	
	Vmin	23 mp/h		10.3 m/s	

Appendix B: References

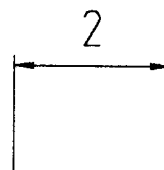
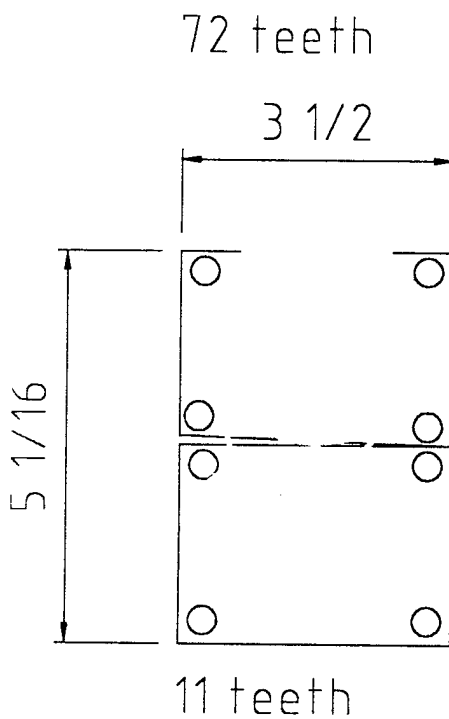
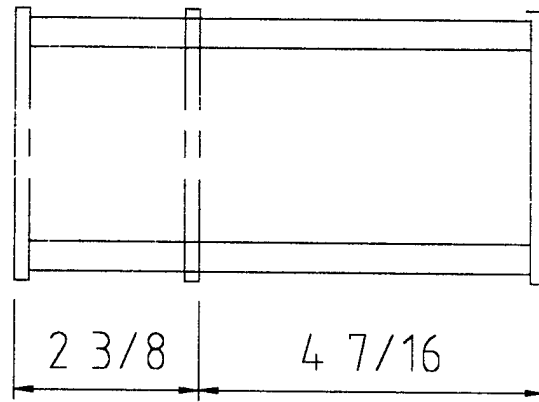
1. Eppler, Richard. Airfoil Design and Data. Springer-Verlag: Germany. 1990.
2. Foster, Steve. "*Undercarriage Design for Queen's Cargo Aircraft*." Undergraduate Thesis Project, Department of Mechanical Engineering. March, 1994.
3. Horton, Johanna Lisa. "*Cargo Aircraft Stability Analysis*." Undergraduate Thesis Project, Department of Mathematics and Engineering. April, 1993.
4. McCormick, Barnes. Aerodynamics, Aeronautics, and Flight Mechanics, second edition. John Wiley & Sons, Inc.: New York. 1995.
5. Munson, Young, and Okiishi. Fundamentals of Fluid Mechanics, second edition. John Wiley & Sons, Inc.: New York. 1994.
6. Raymer, Daniel. Aircraft Design: A Conceptual Approach. AIAA Education Series. American Institute of Aeronautics and Astronautics, Inc.: Washington, D.C. 1989.
7. Abbott, Ira. Theory of Wing Sections. McGraw-Hill Book Company Inc.: Toronto. 1949.
8. White, Frank M. Fluid Mechanics, 4th Edition. McGraw-Hill Book Company Inc.: Toronto. 1999.
9. Lennon, Andy. Basics of R/C Model Aircraft Design. Y. DeFrancesco: Ridgefield, CT. 1999.

Appendix C: Belt Drive detail



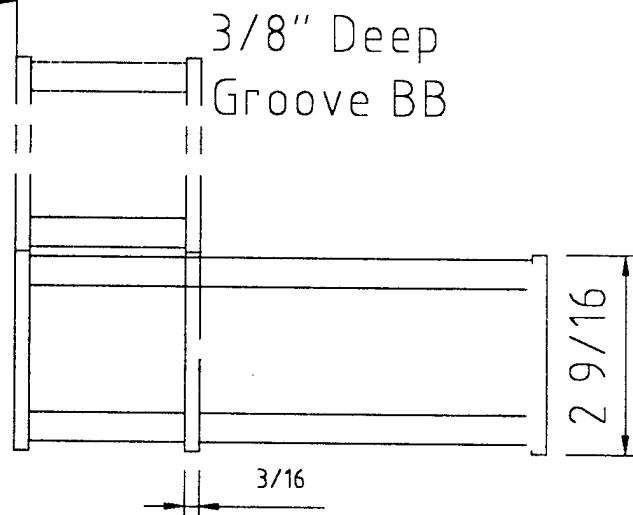


3/8"
Precision
Shaft



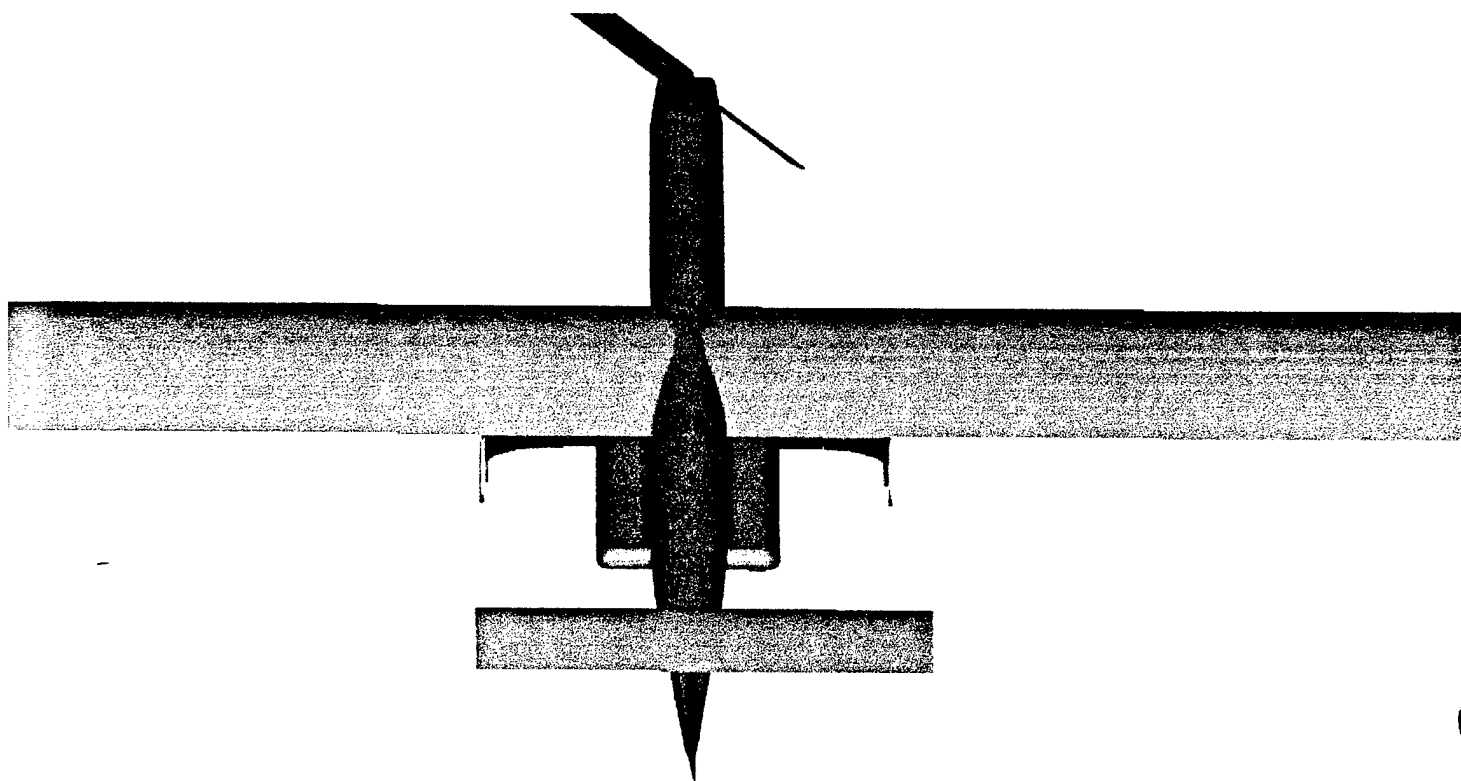
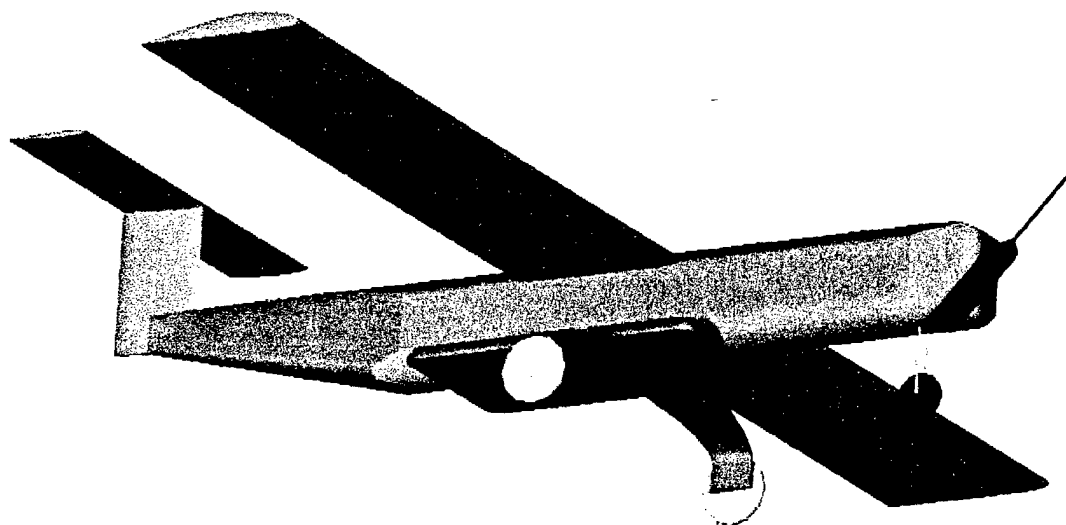
3/8" Deep
Groove BB

3/16" Deep
Groove BB



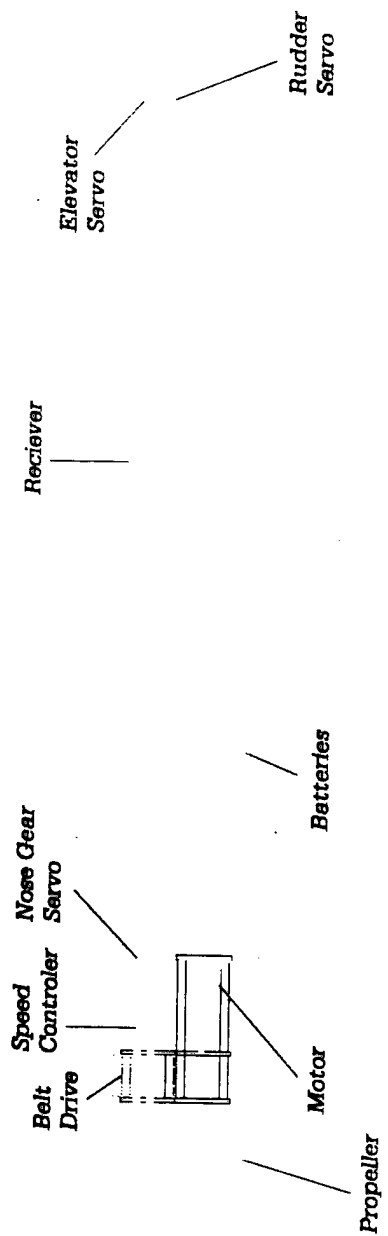
Queen's Aero Design Team
Minnow Belt Drive

Appendix D: Drawing Package

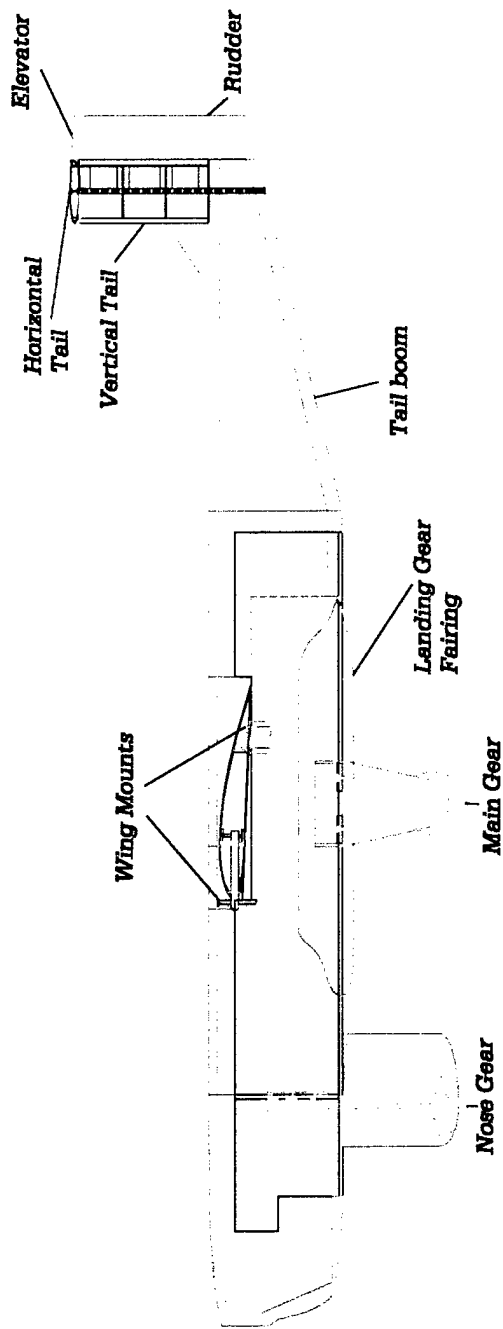


Payload

Payload



Flight Systems



Materials By Color

Balsa Wood

Acrylic Paint

Carbon Fiber/Nomex

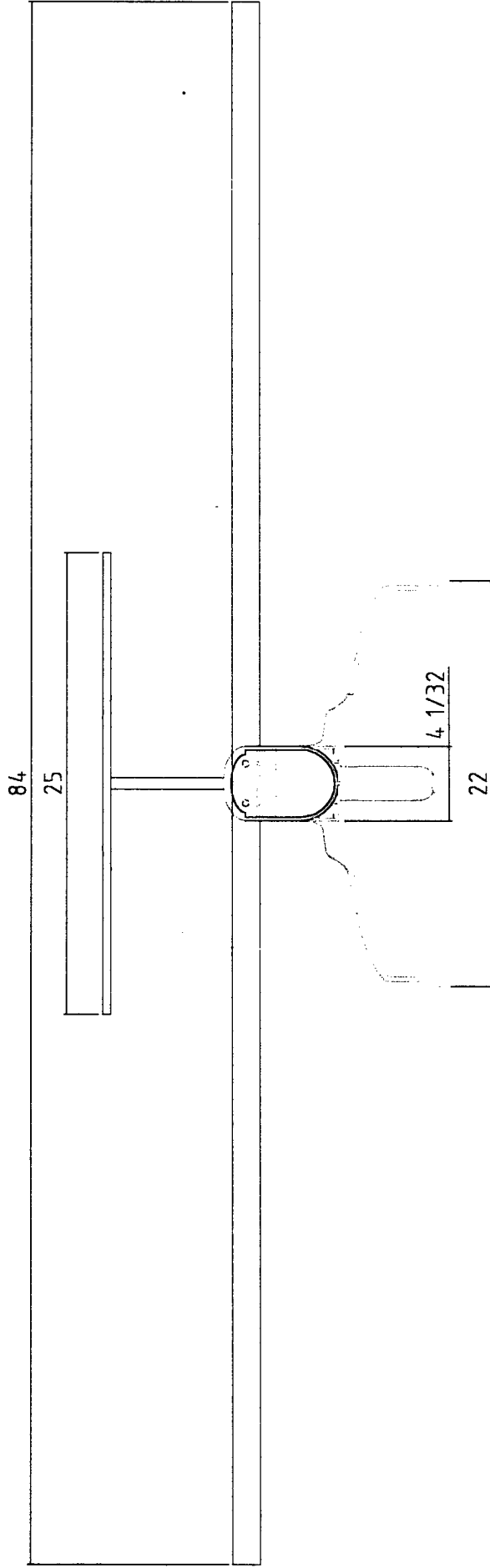
Aircraft Plywood

Spruce

Foam

Airframe

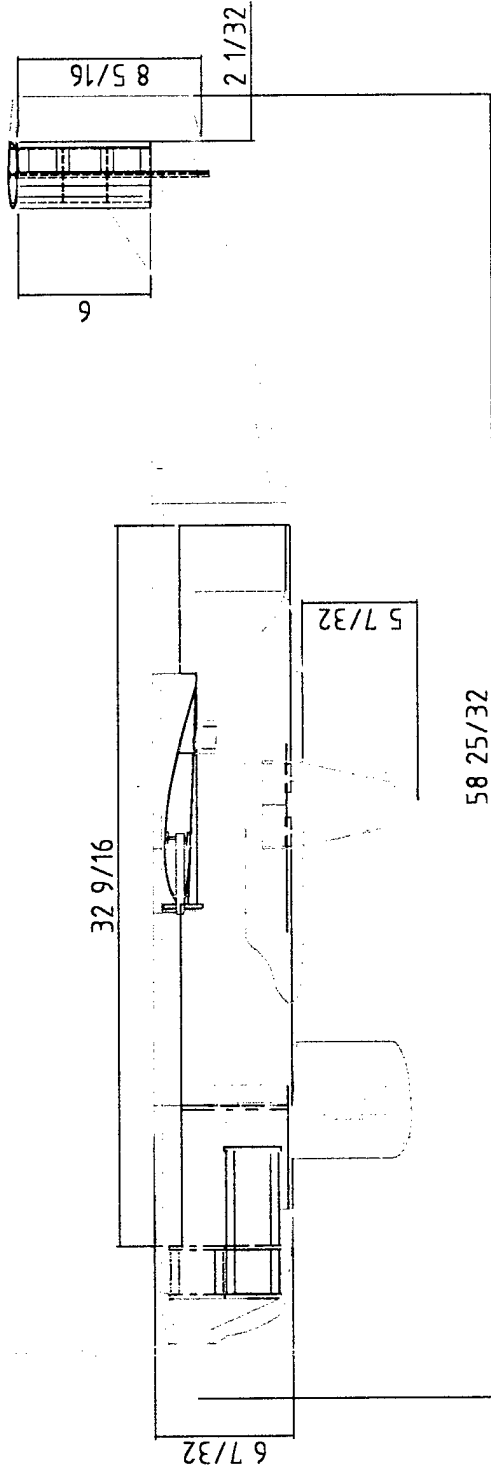
MINNOW



MINNOW Queen's Aero Design Team

Dimensioned Front View

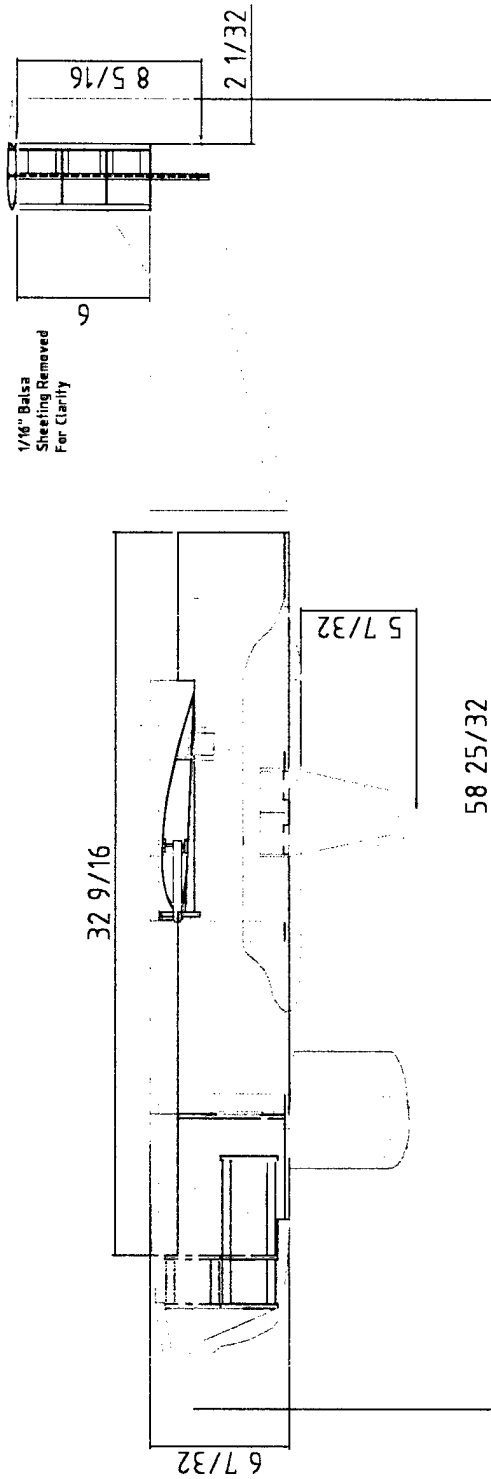
All Dimensions in Inches



MINNOW Queen's Aero Design Team

Dimensioned Side View

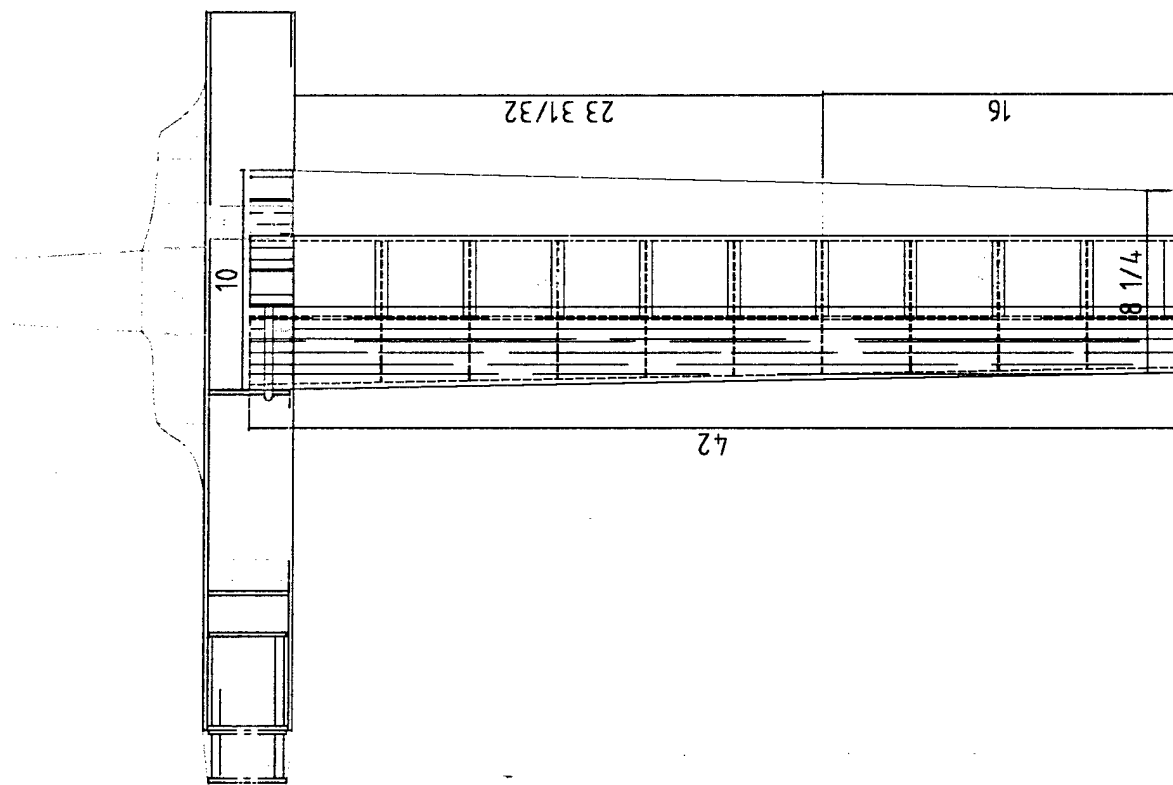
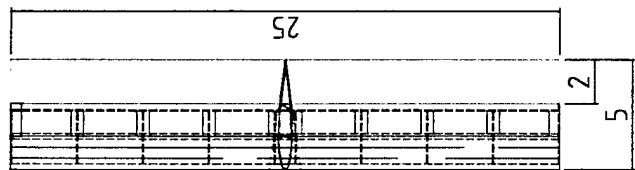
All Dimensions in Inches



MINNOW Queen's Aero Design Team

Dimensioned Side View

All Dimensions in Inches



MINNOW

Queen's Aero Design Team

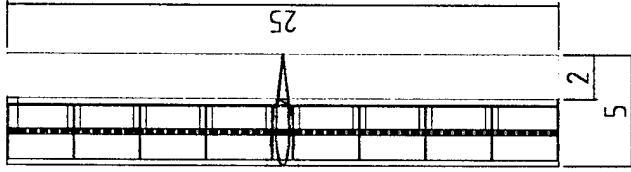
Dimensioned Top View

All Dimensions in Inches

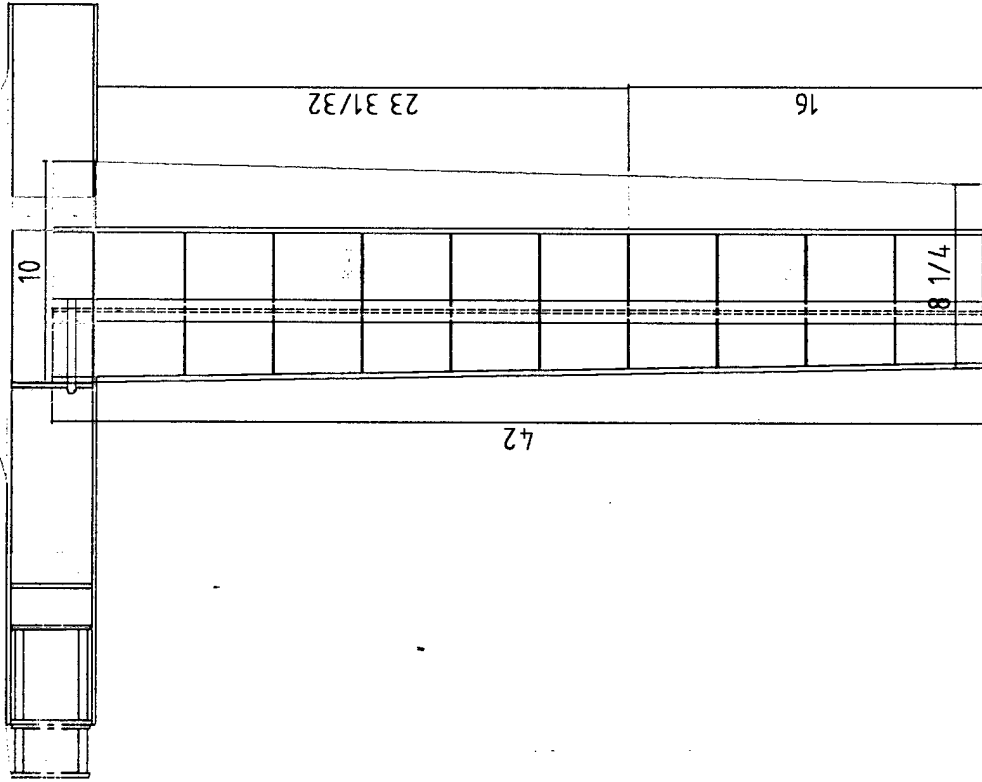
MINNOW Queen's Aero Design Team

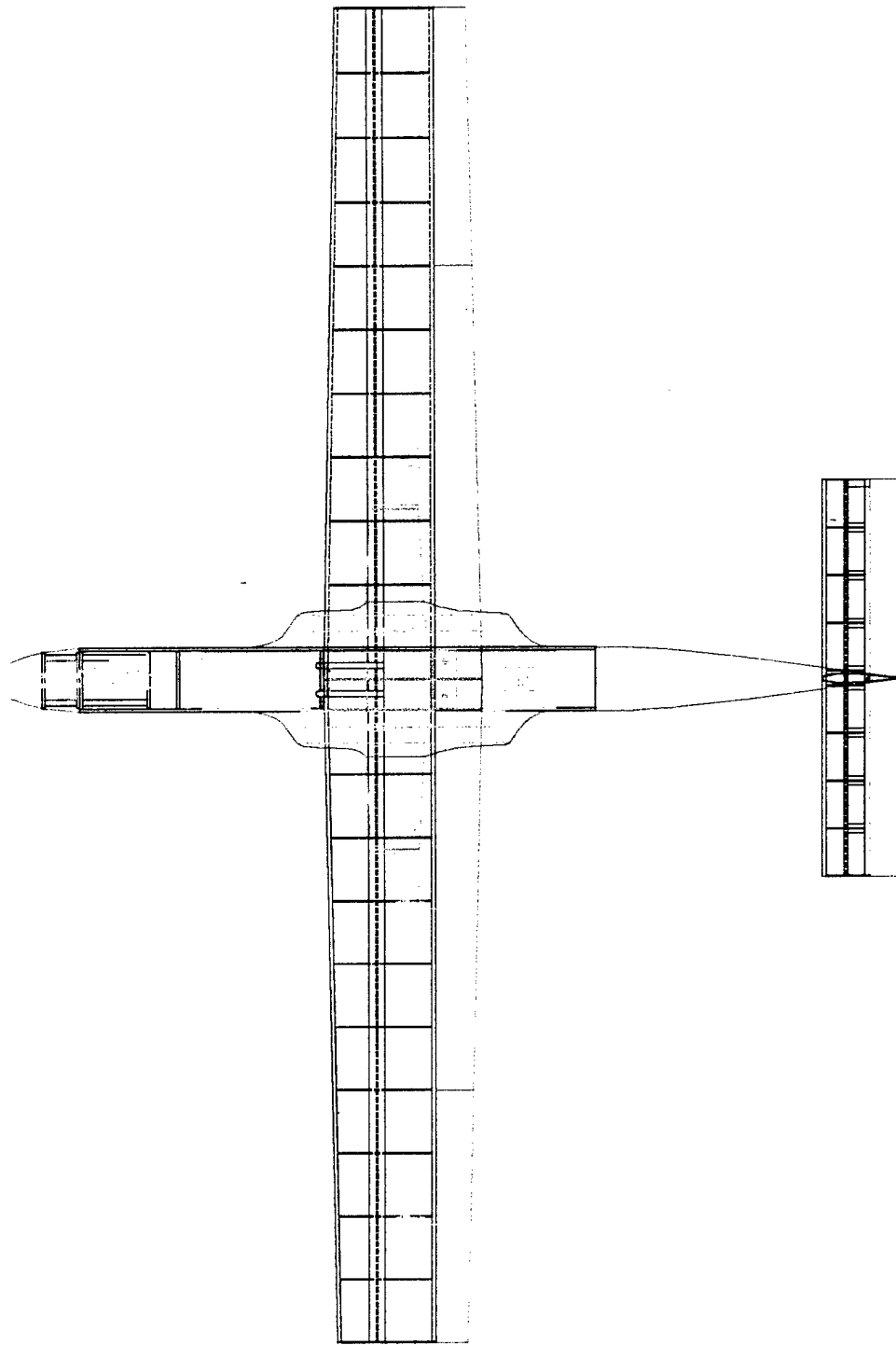
Dimensioned Top View

All Dimensions in Inches



1/16" Balsa
Sheeting Removed
For Clarity





MINNOW Queen's Aero Design Team

2000 AIAA DBF Competition Design Report

——— *Addendum Phase* ———



Queen's University at Kingston

Team #2 – “Minnow”

Department of Mechanical Engineering

Department of Engineering Physics

April 10, 2000

Table of Contents

7.0: Lessons Learned	79
7.1: Changes from the Proposal	79
7.2: Improvements for 2 nd -Generation Design	81
7.3: Cost Estimate	82
8.0: Aircraft Cost.....	85

7.0 Lessons Learned

7.1 Changes from the Proposal

The constructed Minnow aircraft does not vary greatly from the aircraft described in the proposal report. Only two significant modifications were made to the original design; they include a redesign of the belt drive reduction system and the elimination of aerodynamic fairings covering the wheels.

Preliminary calculations used for the belt drive suggested that a double belt was required for the reduction, but testing with a prototype indicated that a single belt system would provide sufficient power transmission. The initial design also utilized a composite made up of a layer of honeycomb sandwiched between two layers of pre-impregnated unidirectional carbon fiber. The composite design was chosen for strength to weight considerations. Unfortunately, the composite was found to be unsuitable for the construction of the reduction unit due to a poor crush resistance, and chronic delamination between the honeycomb and the carbon fiber.

The design connects the opposing composite plates with Robertson wood screws, separated by tubes carbon fiber. This configuration was to allow the belt drive to be disassembled quickly to replace components or to perform minor adjustment to the drive components. However, it was found that the concentrated stress applied by the screws caused the honeycomb to deform, making the necessary precision in the alignment of the rotating components unattainable.

The composite plates also experienced significant delamination between the honeycomb and the pre-impregnated carbon fiber. This issue was a result of the age of the pre-impregnated carbon fiber. The material consists of carbon fibers in a semi-cured epoxy matrix, and it must be stored at sub-zero temperatures to prevent the epoxy from curing before it can be used. However, as the roll ages, the epoxy slowly solidifies, weakening the resulting bond strength when the material is finally utilized. Due to the relatively high expense of this material, the team relied on industry donations of older or slightly imperfect rolls in which the curing reactions had begun.

To address these issues, replacement plates of 3/16” solid carbon fiber were constructed. Although heavier, the plates resulted in a very rigid reduction system that lended itself to the precise alignment of the rotating components.

Further testing with the improved reduction system indicated that the system had a higher than expected efficiency. Current draw was 15% lower than forecasted by ElectriCalc and MotoCalc, leading to the mounting of a larger propeller (18 x 12 versus 18 x 10).

7.2

7.3 Improvements for 2nd-Generation Design

There are several areas in the Minnow design that might be improved for a second-generation design.

The belt reduction structure should be CNC milled of aluminum. This would serve to save weight over the carbon fiber design, while providing the required strength. The high heat transfer coefficient of the aluminum would increase thermal conduction away from the motor, leading to a cooler and more efficient propulsion system.

Streamlining should also be examined further given additional time and resources. All component joints should be evaluated and fairings should be added to reduce interference drag. Work could also be done in a wind tunnel using simple flow visualization techniques to help identify high turbulence areas and to fit fairings that reduce the disturbances.

To facilitate ease of construction and repair, the fasteners used in the aircraft should be standardized as much as possible, so that the minimum number of tools are required. Minnow currently uses Philips head, hex head, flat head, and Robertson head fasteners in the various assemblies. In future designs, hex head fasteners will be used exclusively throughout the aircraft.

7.4 Cost Estimate

Costs are broken down for each section of the aircraft. For comparison, both manufacturer's list price and actual procurement cost (which includes donations, discounts, taxes, shipping, and customs charges) are provided. Costs marked with an asterisk (*) are estimated. All figures have been converted to US dollars at an assumed exchange rate of \$1 US = \$1.40 Canadian. It should be noted that without the donation of the carbon fiber by Queen's Solar Vehicle Team, Minnow would not have been financially possible.

Many costs from the estimate below were not included in the Proposal Phase as they were not relevant considerations in selecting one design or process over another (ie: paint, propeller, battery pack). This year the actual procurement cost was much less the manufactures suggested price due to the generous sponsorship obtained from several companies and Queen's organizations.

In many instances, actual procurement costs varied significantly from manufacturer's list prices. This is due to several factors. The team has long-standing relationship with local hobby shops and receives a discount on most standard materials. Many materials cannot be bought in the small quantities required for this aircraft, and thus leftover stock from previous year's entries were available. Also, the weak Canadian dollar, in combination with foreign shipping and customs charges, heavily affected the actual price of any item purchased outside Canada. This surcharge was especially seen while obtaining material for the belt drive.

Table 7.1. Cost Estimate.

	Manufacturer's List Price	Actual Procurement Cost
<u>Wing</u>		
Uni-directional carbon fiber	50	0 (reused wing structure)
Monokote	20	14
<u>Tail</u>		
Uni-directional carbon fiber	8*	0 (donated)
MonoKote	2	1
<u>Fuselage</u>		
Uni-directional carbon fiber	1500*	0 (donated)
Honeycomb	100	0 (donated)
Pink Foam	10	10
Fiberglass	10	8
<u>Landing Gear</u>		
Uni-directional carbon fiber	4000*	0 (donated)
Main wheels	11	0 (donated)
Bearings	15	15
Nose wheel assembly	6	5
Axles	5	4
<u>Motor and Electronics</u>		
MaxN32-13Y Motor	220	0 (reused)
Motor controller	190	0 (reused)
Motor mount	13	13
Motor Battery pack	350	0 (reused)
Radio Receiver	120*	0 (borrowed)
Servos (7)	140	0 (donated)
Servo battery pack	18	15
Wiring	5	4

<u>Belt drive</u>		
Running gear (belts, pulleys, etc)	250	350
Bearings	75	75
Uni-directional carbon fiber	1200*	0 (donated)
Carbon fiber tube	22	20
<u>Other</u>		
Epoxy	100	0 (stock)
Balsa wood	40*	30*
Aircraft plywood	40*	30*
Paint	4	4
Propeller	130	100
Miscellaneous nuts and bolts	50*	38*
TOTAL	\$ 8704	\$ 736

8.0 Aircraft Cost

To document Minnow's *Rated Aircraft Cost*, first examine the weight of the aircraft. Without the five-pound battery pack on board, the plane weighs 8 pounds. The *Manufactures Empty Weight (MEW)* multiplier is 100 dollars per pound of airframe; thus the cost of Minnow's weight is \$800.

Next examine the propulsion system. Minnow is powered by a single MaxCim NEO-13Y brushless DC motor and 25 3000mAh Ni-Cad cells. The supplied *Rated Engine Power (REP)* formula is $REP = \#engines * 50 \text{ amps} * 1.2 \text{ volts/cell} * \# \text{ cells}$. Minnow's propulsion system thus has a REP of 1500 watts. When the *Rated Engine Power Multiplier* (\$1/watt) is applied, Minnow's cost is \$1500

The final cost section is *Manufacturing Man Hours (MFHR)* and it is a sum of the assembly time required for the wing, the fuselage, the empennage, the flight system, and the propulsion system.

The wing is given a rating of 5 hours per wing plus 4 hours per square foot of projected area. Minnow has a single wing with an area of 5.07 square feet; so the construction time required was 25.28 hours.

The fuselage is given a rating of 5 hours per body plus 4 hours per foot of length. Minnow possesses a single 4.73-foot long fuselage without any extra pods or nacelles, thus the time required is 23.92 hours.

The empennage is given a rating of 5 hours plus 5 hours for each vertical surface and 10 hours for each horizontal surface. Minnow has been designed with a conventional tail (one vertical surface and one horizontal surface), so the total construction time required was calculated to be 20 hours.

Flight systems are calculated to take 5 hours plus 1 hour for each additional servo. Minnow has two servos operating the flaps, two servos operating the ailerons, a servo to steer the nose wheel, a servo to operate the rudder and a servo to operate the elevator. A total of 7 servos resulted in a build time of 12 hours.

The propulsion system is calculated to take 5 hours per motor plus another five hours for each propeller or ducted fan. Minnow has been designed with a conventional single motor driving a single propeller, thus the system should take 10 hours to build.

The MFHR is the sum of the systems described above, thus MFHR is equal to 91.20 hours. When multiplied by the supplied *Manufacturing Cost Multiplier* (\$20/hour), the total construction cost of Minnow is \$1,824.00.

Minnow's *Rated Aircraft Cost* is the sum of the empty weight cost, the engine power cost, and the man hours cost. Therefore, Minnow's total cost is \$4124.

Figure 8.1: Airframe Dependent Parameters

Manufactures Empty Weight Multiplier	A	\$100 * MEW	A = \$	800.00
Manufactures Empty Weight	MEW (pounds)	airframe weight	MEW =	8

9.5

Rated motor Power Multiplier	B	\$1 * REP	B = \$	1,500.00
Rated motor Power	REP (watts)	# motors * 50A * 1.2V/cell * # cells	REP =	1500
		# motors =		1
		# cells =		25

Figure 8.2: Manufacturing Hours

Manufacturing Cost Multiplier	C	\$20 * MFHR	C = \$	1,824.00
Manufacturing Man Hours	MFHR (hours)	Prescribed assembly Hours by WBS	MFHR =	91.2

2165.0

108.3

MFHR = the sum of WBS

Wings WBS = 5hrs/wing + 4 hrs / sq foot projected area	Wing WBS =	25.28
	# wings =	1
	area (sq.ft) =	5.07

42.33

9.33

Fuselage WBS = 5hrs/body + 4hrs / foot or length	Fuselage WBS =	23.92
	# bodies/pods =	1
	length (ft) =	4.73

11.83

Empennage WBS = 5 hrs + 5 hrs/vert surf. + 5 hrs/ horz surf.	Empennage WBS =	20
	# vert. surfaces =	1
	# horz. surfaces =	1

15.20

Flight Systems WBS = 5 hrs + 1 hr/ servo	Flight Sys. WBS =	12
	# servos =	7

Propulsion Systems WBS = 5 hrs / motor + 5 hrs / prop	Propulsion WBS =	10
	# motors =	1
	# props =	1

$$\text{Rated Aircraft Cost} = 9.5 \times 100 + 1500 \times 1 + 2165.0 = 3774.5$$

~~3774~~

4.614

1999/2000 AIAA Foundation/Cessna/ONR Design/Build/Fly Competition

PROPOSAL FOR THE DESIGN OF AN UNMANNED AIR VEHICLE

Prepared for Dr. D. W. Levy, Cessna Aircraft Company

By Syracuse University

Nick Borer, Project Leader

Jessica Lux

Reid Thomas

Jason Farkas

Eliza Honey

Tori Garnier

Renea LaRock

Keith Fuhrhop

Alex Ansah-Arkorful

Hezkhel Teferra

Dr. V. R. Murthy, Faculty Advisor

ACKNOWLEDGEMENTS

The Syracuse University 1999/2000 Design/Build/Fly team would to extend special thanks to:

Dr. Vadrevu R. Murthy
Professor, Syracuse University

Dr. Barry D. Davidson
Associate Professor, Syracuse University

Garvin F. T. Forrester
Lockheed Martin Corporation

Arun D. Chawan

Anthony J. Vinciguerra

Syracuse University
L. C. Smith College of Engineering and Computer Science
Department of Mechanical, Aerospace, and Manufacturing Engineering

Syracuse University Composite Materials Laboratory

Syracuse University Student Chapter of the American Institute of Aeronautics and Astronautics

Anyone we missed

The design and fabrication of the SF1 would not have been possible without the contributions of these individuals and organizations. Thank you all for your support.

TABLE OF CONTENTS

ACKNOWLEDGEMENTS	i
TABLE OF CONTENTS	ii
1. EXECUTIVE SUMMARY	1
1.1. Design Development	1
1.2. Design Tools Utilized	1
2. MANAGEMENT SUMMARY	3
2.1. Design Team Architecture	3
2.2. Design Deadlines	3
3. CONCEPTUAL DESIGN	5
3.1. Figures of Merit	5
3.2. Alternative Concepts Investigated	5
3.2.1. Conventional Configuration	5
3.2.2. Conventional Twin Boom	5
3.2.3. Control Canard	6
3.2.4. Flying Wing	6
3.2.5. Blended Wing	6
3.3. Design Parameters Investigated	6
3.3.1. Wing Placement	7
3.3.2. Propulsion	7
3.3.3. Landing Gear Arrangement	7
3.4. Final Ranking of Figures of Merit	7
3.5. Configuration Selection	7
4. PRELIMINARY DESIGN	9
4.1. Sizing Trade Studies	9
4.1.1. Figures of Merit	9
4.1.2. Sizing Analysis	9
4.2. Propulsion Trade Studies	10
4.2.1. Figures of Merit	10
4.2.2. Propellers Versus Ducted Fans	10
4.2.3. Propulsion Studies	11
4.3. Airfoil Selection	13
4.3.1. Figures of Merit	13
4.3.2. Airfoil Studies	13
5. DETAIL DESIGN	17
5.1. Final Sizing	17
5.1.1. Wing	17
5.1.2. Canard	17
5.1.3. Fuselage	18
5.1.4. Fin	18
5.2. Weights and Balance	19
5.2.1. Final Weight Estimation	19
5.2.2. Center of Gravity	19
5.3. Performance Estimation	19
5.3.1. Drag Polar	19
5.3.2. Cruise Performance	20
5.3.3. Take-Off Performance	21
5.3.4. Turning Performance	21
5.3.5. Estimated Mission Performance	21

5.4. Stability and Control	22
5.4.1. Stability Derivatives	22
5.4.2. Control Surface Sizing	22
5.5. Structural Analysis	22
5.5.1. Load Factor	22
5.5.2. Wing Analysis	23
5.5.3. Fuselage Analysis	24
5.6. Subsystems	24
5.6.1. Landing Gear	24
5.6.2. Radio Control Devices	24
5.6.3. Cooling Provisions	25
5.6.4. Boundary Layer Diverter	25
5.7. Drawing Package	25
 6. MANUFACTURING PLAN	 29
6.1. Figures of Merit	29
6.2. Wing Construction	29
6.3. Fuselage Construction	30
6.4. Tail Fin and Canard	30
6.5. Systems Integration	31
 REFERENCES	 33
APPENDIX A: Motocalc Output	A-1
APPENDIX B: CG Calculations	B-1
 TABLES	
2-1. Milestone Chart	4
3-1. Figures of merit for each configuration considered	8
4-1. Initial sizing estimates	15
4-2. Propeller vs. ducted fan setup	15
5-1. Performance estimates	26
5-2. Static stability derivatives	27
5-3. Structural load limits	27
6-1. Figures of merit comparison	32
6-2. Wing task schedule	32
6-3. Fuselage task schedule	32
6-4. Bulkhead placement	33
 FIGURES	
3.1. Conventional configuration	8
3.2. Conventional twin boom	8
3.3. Control canard	8
3.4. Flying wing	8
3.5. Blended wing	8
4.1. Single flight score vs. number of liters carried for various wing loadings	14
4.2. Section lift coefficient vs. angle of attack for a NASA LS(1)-0417 airfoil	15
4.3. Section drag coefficient vs. angle of attack for a NASA LS(1)-0417 airfoil	15
4.4. Section moment coefficient vs. angle of attack for a NASA LS(1)-0417 airfoil	16
5.1. SF1 drag polar	26
5.2. Final exterior dimensions of the SF1	27
5.3. Inboard profile	28

1. EXECUTIVE SUMMARY

1.1. OVERVIEW

This document presents the analysis, design, and manufacturing of Syracuse University's 1999-2000 entry in the Cessna/ONR student Design/Build/Fly competition. The conceptual, preliminary, and detailed design phases of Team Syracuse's entry, termed the SF1, are outlined, as well as a manufacturing plan and discussion of team management.

1.2. DESIGN DEVELOPMENT

Initially, the design team considered five configurations for the SF1 – a conventional design, conventional with twin boom, a canard configuration, a flying wing configuration, and a blended wing fuselage. Of these, a canard with low wing configuration was selected. This design had several advantages over the baseline conventional configuration and the three other options considered. It offered better balance because the center of gravity was moved closer to the center of the aircraft. No Rated Aircraft Cost increases were incurred over the baseline configuration. The team also considered it a safer design because the canard would stall before the wing, causing the aircraft to pitch downward and thus recover from the stall. Finally, this configuration allowed for the inclusion of either ducted fans or propellers, both of which were considered by the team.

After selecting a configuration, the design was optimized with respect to important parameters such as wing loading, payload capacity, and thrust loading. In propulsive trade studies, both propellers and ducted fans were investigated. After extensive study, ducted fans were selected for their superior crashworthiness and lower required ground clearance, among other advantages.

With the propulsive setup finalized, the team finalized sizing, performed load and balance calculations, and performed a static stability analysis. A structural analysis, limited to the study of bending loads, was conducted for the wing and the fuselage. It was also necessary at this point to refine the design of the SF1 to meet the short take off requirement of the competition. Flaps were included in the design to decrease the calculated take off distance.

At this stage, with the design of the SF1 finalized, the team turned to the development of a manufacturing plan. After comparing both composite material and wood as possible materials for the construction of the fuselage, wood was selected for its cost effectiveness and the ease with which this section could be manufactured. This would be through a conventional skin-stringer approach, often seen in full-scale subsonic aircraft. The wing, however, would be manufactured from a foam core wrapped in fiberglass. The use of a foam core would enable the team to manufacture the composite skin without the use of a mold, which would result in a more time- and cost-effective design.

1.3. DESIGN TOOLS UTILIZED

Tools employed in the design of the SF1 include AutoCAD, Aveox's Virtual Test Stand, Calcfoil, Microsoft Excel, MotoCalc, Profili, Promal, SolidWorks 99, and the World Wide Web.

The World Wide Web proved to be an excellent research tool during the conceptual and preliminary design phases. The team utilized searching capabilities to find empirical data on similar designs, research commercially available landing gear, research electric ducted fan manufacturers, explore the possibility of having foam core wings commercially cut, and locate other component retailers. Two of the above listed design tools—Aveox's Virtual Test Stand and Calcfoil—are only available over the Internet.

Calcfoil [<http://beadec1.ea.bs.dlr.de/Airfoils/calcfoil.htm>] utilizes the conformal mapping method to determine the aerodynamic coefficients of various airfoils. The team used Calcfoil to compare the lift, drag, and pitching moments of the various airfoils considered.

The Virtual Test Stand, available at the Aveox web site [<http://www.aveox.com/hobby.htm>], provides static thrust and current draw data for Aveox motors. This tool was employed when the team compared propellers to ducted fans during the propulsive setup.

Italian airfoil plotting program Profili was used to print scale diagrams of the airfoils selected for the wing, canard, and fin. Profili provides a scale drawing of any airfoil in its database based on a user-specified chord length. These printed drawings were then used in the manufacturing of the wing, canard, and fin.

SolidWorks 99, a solid modeling and rendering program, was used to generate the 3-view and isometric schematics of the SF1 for the drawing package. It was also used for determining the structural layout of the fuselage. AutoCAD R14, a computer-aided design program, was used to create conceptual sketches of the various configurations considered in the conceptual design phase.

Promal was used to analyze the global material properties of the fiberglass wing skins. It also was used to predict first-ply-failure of the said wing skins by determining the strength ratios in each ply and choosing the lowest value. This software was provided with Reference 9.

Microsoft Excel proved especially useful during preliminary and detailed design. A number of spreadsheets were created to analyze several of the key aspects of the SF1's final design, such as sizing, stability, and performance data. This program could also be used to iterate values using the Solver function.

2. MANAGEMENT SUMMARY

2.1. DESIGN TEAM ARCHITECTURE

Team Syracuse consists of senior aerospace engineering majors Alex Ansah-Arkorful, Nick Borer, Jason Farkas, and Hezkhel Teferra, senior engineering physics major Keith Fuhrhop, sophomore aerospace engineering majors Jessica Lux and Reid Thomas, and freshman aerospace engineering majors Victoria Garnier, Eliza Honey, and Renea LaRock. This ten-member team was lead by Borer, who has two previous years of design team experience and acted in this capacity last year. Assignments were handed out to team members at weekly meetings and via email, and progress was monitored through the use of a posted milestone chart and task list.

As the team leader, Borer administered tasks to other team members and performed the bulk of the conceptual, preliminary, and detailed design work on the SF1, with the help of other team members. Borer also created the solid model of the design. By calling team meetings weekly from September 1999, Borer kept the team on task and monitored the progress of the design.

Thomas, who has an extensive model aircraft background and one year of design team experience, was designated pilot of the SF1. He investigated the purchase of commercial landing gear and manufactured the wind tunnel model. Thomas also worked on a materials cost analysis, managed the team's budget, and created CAD drawings of the design.

With one year of design team experience, team member Lux worked on the propulsive setup with Borer and Fuhrhop. She also weighed components and performed CG calculations during the preliminary design phase. Lux and Thomas worked on a materials cost analysis, and Lux investigated the transportation of the plane to the contest site.

Various team members assisted throughout the preliminary and detailed design phases. Engineering physics major Fuhrhop used his background to work with Borer and Lux on the propulsive setup. Teferra and Borer developed a payload retrieval system for the SF1. Farkas performed a fiberglass cost analysis and fuselage stress analysis.

Freshman team members Garnier, Honey, and LaRock performed valuable general research on similar configurations, materials, and airfoils. In addition, LaRock investigated the battery configuration and created CAD drawings of the design. They attended all team meetings and were exposed to the process so that they will be able to continue to work on the project next year.

2.2. DESIGN DEADLINES

As mentioned before, a milestone chart was employed to keep the design team on target and aware of upcoming deadlines, both self-imposed and contest-mandated. This milestone chart, with team goals and actual completion dates, is reproduced in Table 2-1.

The dates listed in this milestone chart represent a marked departure from years past. Team Syracuse began the conceptual design phase in early September, rather than late October as in past competitions. The team also adhered to this schedule in real time by posting it in their design room and updating progress continually.

In early February, the team presented a progress update and budget request to the engineering faculty. This presentation kept the design team to a fixed deadline for finishing detailed design and the solid model of the SF1. Prior to the mid-project briefing, the design team budget allowed only for the construction of the SF1, not for air travel of team members to the contest site. Lux, Borer, Honey, and Garnier prepared the presentation, and all members of the team assisted in the presentation.

Task	Projected Date	Completed Date
Baseline configuration selection	10/07/00	10/07/99
Entry form due	10/31/99	10/31/99
Final propulsion setup	11/04/99	11/04/99
Systems placement	12/02/99	12/29/99
Initial sizing and performance	01/18/00	1/24/00
Final sizing and performance	02/02/00	02/06/00
Complete manufacturing plan	02/02/00	02/14/00
Mid-project briefing and budget proposal to faculty	02/09/00	02/09/00
Begin drafting report	02/09/00	02/14/00
Order parts	02/14/00	02/22/00
Begin manufacturing	02/20/00	02/25/00
Hand report to faculty	03/06/00	03/06/00
Report due	03/13/00	03/13/00
Finish manufacturing	03/31/00	TBD
Flight testing	04/01/00	TBD
Addendum completed	04/01/00	TBD
Final modifications	04/09/00	TBD
Plane shipped	04/10/00	TBD
Addendum due	04/10/00	TBD
Fly-off	04/15/00	TBD

Table 2-1. Milestone Chart

3. CONCEPTUAL DESIGN

The conceptual design phase began with brainstorming of different configurations that would best meet the mission requirements. A baseline conventional configuration was selected, to which all other configurations would be compared. The team used a ranking system of specific figures of merit (FOM) to compare various design parameters to the baseline configuration. The FOMs included Rated Aircraft Cost (RAC), design, manufacturability, and stability. Each configuration was assessed with a point total from the ranking and the configuration with the most points was selected as the final configuration.

3.1. FIGURES OF MERIT

The figures of merit considered during the conceptual design phase were:

- Rated Aircraft Cost
- Design Issues
- Stability
- Manufacturing Issues

The team's primary figure of merit was rated aircraft cost. Since overall scoring is divided by the RAC, it is ideal to have this as low as possible. This can be accomplished by reducing the number of surfaces, motors, bodies, and pods and by keeping the fuselage as short as possible. At this stage of the design phase, it was possible to qualitatively compare the number of bodies and sizes of each configuration.

Availability of design data was another FOM used to assess each configuration. Each candidate configuration was qualitatively inspected to determine if the design possessed a large enough empirical database which the team could reference. Finally, original designs were also given merit as challenging new opportunities to learn from.

Stability was another important FOM examined during the conceptual design phase. Any aircraft must be statically stable with good handling qualities in all flight conditions and be easily controllable. This has been an issue in the past, so this year's team devoted considerable time to stability and handling qualities.

Additionally, each configuration was assessed for ease and cost of manufacturing. A smaller, simpler aircraft reduces the cost and manufacturing time, allowing for more test flight time and modifications. Cost was a consideration because the team operates under a very limited budget. Any design that was extravagant with components or materials would likely have pushed the team over budget.

3.2. ALTERNATIVE CONCEPTS INVESTIGATED

3.2.1. Conventional Configuration

A conventional design (the baseline configuration to which all other candidate configurations are compared) is known from previous team experience to have passable handling qualities and design simplicity. A graphic representation of this configuration is provided in Figure 3.1. Extensive databases with detailed design procedures are available for conventional aircraft, making performance and stability analysis more reliable and easier. This configuration lends itself to a single motor, thereby reducing the RAC. Also, manufacturing would be relatively straightforward due to past experience. However, this configuration places the CG too much forward, which could lead to stability problems.

3.2.2. Conventional Twin Boom

Next, a conventional twin boom was considered. This configuration, represented in Figure 3.2, allows the payload to be accessed from the back instead of the top, and has better handling qualities compared to the baseline. Manufacturing processes are also similar to the baseline. Twin booms also provide additional space for the placement of motors, batteries, and speed controllers, freeing the fuselage

to house more payload. Additionally, this design has not been used previously by team Syracuse and would add to the overall learning experience. The fuselage is shorter than the baseline, but this design lends itself to multiple motors and tail surfaces, which increases the overall RAC.

3.2.3. Control Canard

Subsequently, a control canard was looked at, similar to the Beech Starship. This layout, which is illustrated by Figure 3.3, offered several advantages. In previous years, there had been a problem with the center of gravity (CG) being located behind the neutral point, creating longitudinal stability problems. For the airplane to be statically stable, it is desirable to have the CG ahead of the neutral point. When the wing is moved further aft, as is the case in a canard configuration, the neutral point travels aft as well. This places the CG ahead of the neutral point and closer to the center of the airplane, making it easier to balance the placement of the control and propulsion systems.

Another advantage of a control canard is that they are designed to stall before the wing, avoiding adverse pitch-up and deep stall. Since the canard stalls before the wing, the nose of the plane will drop, enabling the pilot to correct the problem before any accidental ground contact occurs. Control canards also add extra lift during rotation by adding lift to the front of the aircraft as opposed to the baseline, tail-aft design, which creates negative lift at the rear of the plane. This advantage would be ideal for the short field take-off requirement. A control canard configuration would have a similar RAC as the baseline because both involve the same relative size of surfaces. Manufacturability would also be roughly equivalent. Finally, this would be another new experience for the team.

The only concerns to selecting a control canard configuration were that the canard wake might cause interference over the wing if both were placed in the same plane. However, trade studies have shown that these effects are insignificant when the canard and wing are placed in different planes. Other concerns were that less design data available for canards than a conventional design, but dedicated research produced sufficient information for comparisons. Finally, the team's designated pilot would need more test flights to familiarize himself with this configuration.

3.2.4. Flying Wing

The flying wing configuration considered had a substantially lower RAC due to the lack of a fuselage and empennage. This configuration would be a tremendous learning experience, adding to the design FOM. However, it was found that stability and control requirements would have been extremely difficult to satisfy, and would likely have handling problems in the windy conditions that are likely at the competition site. Due to the complex, three-dimensional wing geometry and reflex camber at the rear of the airfoils, manufacturing of a flying wing is extremely difficult. Also, there are few aircraft with this configuration so there are limited references available for comparison. Refer to Figure 3.4 for a graphical representation of this configuration.

3.2.5. Blended Wing

Finally, a blended wing consisting of one large wing and an empennage was considered. This design, much like Syracuse's entry in last year's competition, would have added to the RAC because of the larger wing area and the addition of an empennage. Also, like the flying wing, there could be stability problems, manufacturing would be more challenging, and there are no references available. Figure 3.5 illustrates this configuration.

3.3. DESIGN PARAMETERS INVESTIGATED

The following design parameters were investigated during the conceptual design stage:

- Wing Placement
- Propulsion
- Landing Gear Type

3.3.1. Wing Placement

When making the decision between low wing versus high wing placement, payload accessibility was the primary factor. A high wing would allow wing mounted propellers to be used without worrying about ground clearance. However, the carry-through for the wing would interfere with the payload compartment, making access difficult. A low wing would enhance accessibility, as the carry-through would be placed below the payload. Additionally, since a control canard configuration was being considered, it was decided that a low wing with high canard would be ideal to avoid wake interference on the wing.

3.3.2. Propulsion

The team considered both propellers and electric ducted fans for the propulsion system. Propellers are the standard propulsive system in most radio-controlled aircraft. The advent of brushless motor technology, however, has enabled motors to spin at higher rpm, making it possible to efficiently run ducted fans. Ducted fans are smaller in diameter than propellers, making it easier for the ground crew to load and unload the payload without hindrance from large diameter propellers. They also allow shorter landing gear, which reduces weight and parasite drag. Ducted fans also produce a larger static thrust for a given power at takeoff. These preliminary findings warranted further consideration in the preliminary design phase.

3.3.3. Landing Gear Arrangement

Tricycle landing gear proved to be the best configuration with the aft wing of a control canard. The drawback to fixed landing gear is that it adds to the parasite drag of the airplane. Because of this, retractable landing gear (retracts) were investigated in an effort to reduce the drag. The only advantages gained from retracts, however, was the reduction in drag. Retracts proved to be a disadvantage as they would increase aircraft weight, and manufacturing complexity, as well as increasing the volume to accommodate the pneumatic tank. Adding volume to the aircraft adversely affects the RAC. Also, the pneumatic tanks have a capacity for only four or five cycles, and the team's initial design required seven. Finally, retracts are a great deal more expensive than standard landing gear.

3.4. FINAL RANKING OF FIGURES OF MERIT

The analytical methods described helped determine the final ranking of the figures of merit. The final ranking of the figures of merit, in order of importance are:

- Rated aircraft cost
- Design issues
- Stability
- Manufacturing issues

These FOMs were then ranked on a scale of -3 to +3. Each candidate configuration's ranked FOMs were added up and a total assessed for each.

3.5. CONFIGURATION SELECTION

Once all of the configurations were assessed with the ranking scheme mentioned, a final configuration was selected. The ranking process involved assessing each configuration's FOM's with a number between negative three and positive three. These points were summed for each configuration and compared. As shown in Table 3-1, the control canard configuration is the best design choice.

The control canard layout lends itself nicely to short take-offs and it allows the CG to be placed ahead of the neutral point. This could solve the recurring problem of stability and allowed the CG to be placed in a location that produced the same handling qualities in cargo and ferry sorties. It also allows for the usage of either propellers or ducted fans for propulsion.

	Stability	Manufacturability	RAC	New Design	Total
Conventional	0	0	0	0	0
Twin boom	1	-1	-2	1	-1
Canard	2	0	0	2	4
Flying wing	-3	1	1	2	1
Blended wing	-2	1	0	1	0

Table 3-1. *Figures of Merit for each configuration considered*

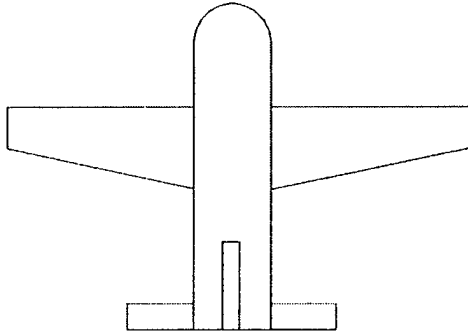


Figure 3.1 *Conventional configuration*

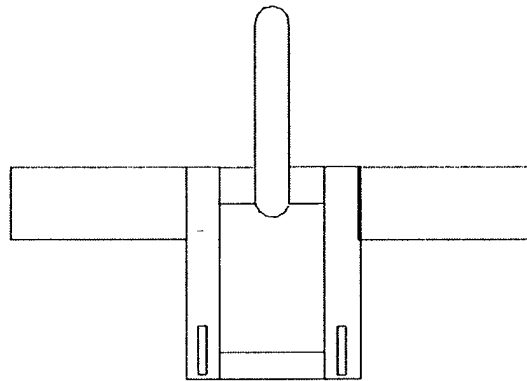


Figure 3.2 *Conventional twin-boom*

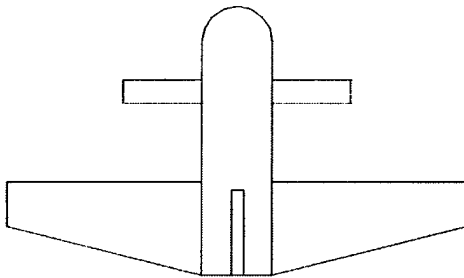


Figure 3.3 *Control canard*



Figure 3.4 *Flying wing*

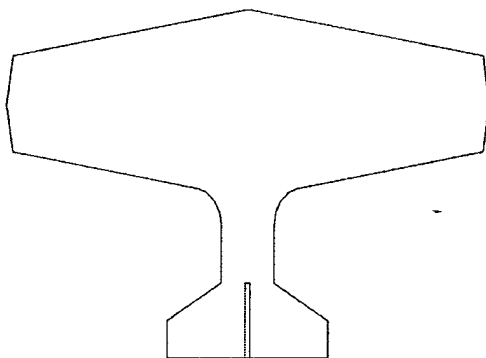


Figure 3.5 *Blended wing*

4. PRELIMINARY DESIGN

The next step in the design process was to determine the thrust loading, wing loading, and weight. A number of trade studies determined these primary and other secondary parameters for the SF1. These critical values were necessary for the detailed design analysis.

4.1. SIZING TRADE STUDIES

4.1.1. Figures of Merit

Four Figures of Merit (FOMs) were defined to facilitate the initial sizing of the SF1. These were:

- Rated Aircraft Cost
- Wing Loading
- Payload Capacity/Fraction
- Aspect Ratio

Rated Aircraft Cost (RAC) represents a divisor in the team's final score at the fly-off. Therefore, it was necessary to minimize this value within the design constraints. It is based on a number of individual aircraft parameters, including but not limited to the empty weight, projected wing area, fuselage and pod length, and motor power. The complete formulation of the RAC was given in the competition rules.

The wing loading contributes to handling qualities, take-off weight, and field length. A higher value for wing loading is generally better for handling, especially in the windy conditions that will likely prevail at the contest site. Higher wing loading also yields less weight, since less wing area is used to generate the same lift force. Short take-off characteristics, however, favor a lower wing loading.

The payload capacity of the aircraft was the third FOM, as the team's final score is directly proportional to the number of liters carried during each mission. A secondary consideration is the payload fraction, because it is necessary for the aircraft to handle satisfactorily both with and without payload. This parameter has a significant effect on the wing loading for non-payload (ferry) missions. If the payload fraction were too high, the aircraft may not exhibit desirable handling on the ferry sorties, especially in windy situations.

Finally, the wing aspect ratio, which has a significant impact on induced drag, was considered as the fourth FOM. Since the span was limited to seven feet per the current rules, the larger values of wing area that may seem so desirable for greater lift may not be as attractive due to larger induced drag and manufacturing complexity that arise from a smaller aspect ratio.

4.1.2. Sizing Analysis

Two independent variables, wing loading and payload capacity, were sufficient for analysis of the basic sizing parameters. All of the other variables were either partially or entirely dependent on these two values and as such were inherently justified.

First, the relations of the dependent variables was established. The parameters calculated were fuselage length, number and weight of motors, radio systems weight, number and weight of batteries, total aircraft weight, wing area, aspect ratio, payload fraction, RAC, estimated number of payload sorties completed, and single flight score. Some of these relations were educated guesses based on experience, while others were based on specified formulae (such as the aspect ratio). These relations were then embedded into a spreadsheet and values calculated, based only on the dependent and independent variables. The payload capacity was varied from two to eight liters in increments of one liter. The values for wing loading were varied from two to three pounds per square foot in increments of 0.25. Any wing loading value over three pounds per square foot would have difficulty meeting the short take-off requirement due to the lower values of thrust loading found in this class of model aircraft, so higher values were not considered. Figure 4.1 shows the results of this analysis. Inspection of this table indicates that each of

these "mini-designs" were compared via a Single Flight Score (SFS), computed by taking the product of the estimated number of payload sorties and the payload capacity, divided by the estimated RAC.

By this method, the optimum design would carry six liters of water and have a wing loading of three pounds per square foot. The accuracy of this trade study was in question, however, because it was based on a number of estimates and assumptions. The six liter, three pound per square foot design had a few fundamental qualities of which team members were wary. First, it had a lower aspect ratio, so its induced drag would be higher. This would result in poorer cruise performance. Next, its payload fraction was relatively high, which could translate into handling problems during the ferry sorties if adverse wind conditions were present. Finally, predictions based on past experience indicated this design could complete only two payload sorties due to the battery pack weight limit imposed by the rules. Therefore, this particular design would be run-time limited, meaning that the aircraft could not fully utilize the ten-minute competition period.

Further inspection of Figure 4.1 shows that a relative maximum in the SFS exists for the design with four liters capacity and a wing loading of three pounds per square foot. This design was desirable because of its moderately high aspect ratio and lower payload fraction. As such, it would perform better than the previously mentioned design. It was also just outside of the estimated realm of run-time limited performance, so it would likely be able to fly for the entire ten-minute competition period.

Other factors were also taken into consideration. The team was entertaining ideas of constructing a foam core wing with a composite skin, so the total wing area was scrutinized. A heavier design necessitates a larger wing area, which would incur higher costs in terms of material. Finally, past experience with foam core wings has shown that it is easier to cut the cores if the root sections are smaller.

With these new considerations, the four liter capacity design with a wing loading of three pounds per square foot was chosen. The target weight for this design, initially estimated at 21.3 pounds, was reduced to 21 pounds after more in-depth analysis of the component weights. The other parameters discussed earlier were then recalculated based on this new target weight. Table 4-1 lists the final estimates of the SF1 sizing parameters. Note that this configuration calls for two motors, which leads to the next discussion.

4.2. PROPULSION TRADE STUDIES

Prior experience showed that the team would most likely need two motors to propel the aircraft. This observation was mostly based on the thrust loading of the aircraft, and a general knowledge of the ranges of the thrust that could be achieved with the current technology.

4.2.1. Figures of Merit

Propulsion study FOMs were defined as thrust-to-weight ratio (thrust loading), run-time, and RAC. The critical thrust loading condition would occur at maximum take-off weight, so ferry sorties were neglected in choosing a minimum value for the thrust loading. A critical value had to be chosen both to meet the short take-off requirement and to give adequate thrust at cruise speeds for satisfactory handling qualities. This was found to be about 0.35, based on the thrust loadings of successful aircraft with similar missions.

The design resulting from the sizing trade studies indicated that the aircraft would need to fly the entire competition period. As such, the run-time of the propulsion system would have to be high enough for the aircraft to compete for ten minutes with little reduction in performance. The run-time would depend on the battery setup and propulsive device.

The Rated Engine Power (REP) contributed greatly to the aircraft's total RAC. This was a factor in choosing of the number of motors and cells used. Also, any units installed in pods not affixed to the fuselage would add to the RAC, so the propulsion setup was scrutinized accordingly.

4.2.2. Propellers Versus Ducted Fans

Competition rules specify that an unmodified, over-the-counter electric motor must be used in conjunction with a commercially available propulsive device for thrust. This device could be either a propeller or ducted fan unit with direct drive, gear, or belt reduction. Teams have traditionally used propellers, which have a number of advantages, namely lower cost and complexity. There is a smaller empirical database for ducted fan designs, especially with electric powered model aircraft. However, electric ducted fans (EDFs) are becoming increasingly popular with hobbyists, so sufficient information is available if one is patient enough to dig a little deeper.

This is the first year that the team members have seriously considered using EDFs over propellers. Therefore, it was necessary to compare the two to see which would be better suited for the SF1. This comparison identified several critical areas, as outlined below.

Battery setup

The load on a motor is a function of its torque and shaft speed. The torque output is directly proportional to the incoming current, while the shaft speed is directly proportional to the incoming voltage. The total power of the motor is found from the product of the incoming voltage and current.

Generally, motors that swing large diameter propellers need a large amount of torque. In this case, torque becomes more important than shaft speed. Quite often, electrically powered models with propellers utilize some sort of gear reduction, which reduces the shaft speed while increasing the torque. Many sources on electric-propeller model aircraft urge the builder to scrutinize the torque of the motor and not the power output. Therefore, many electric-propeller aircraft have a very large current input into the motor. Electric ducted fans, however, are generally very small in diameter, and turn at much higher speeds than propellers. As such, torque becomes less important while shaft speed becomes more important. This indicates that more voltage is needed to the motor than before.

The battery setup must be tailored to the operating point of the motors. If larger current draw is expected, as is the case with propellers, more batteries need to be connected in series to increase the run-time of the motors. However, EDFs operate at less current and higher voltage, so more batteries can be placed in series. An estimated 40 sub-C size cells could be used for the maximum battery pack weight of five pounds, with each cell capable of 1.2 volts and 2000 mAh. Once the propulsive device and motor were chosen, the optimum battery setup could be found to give adequate power and run-time.

Ground clearance

Ground clearance is an important quality when choosing landing gear setup. Therefore, the clearance necessary for the propeller configuration was estimated based on the diameter of the propeller and the take-off attitude of the aircraft. Ground clearance would not be an issue for ducted fans, since they would be fully enclosed in a duct close to the fuselage centerline.

Crashworthiness

Radio-controlled aircraft, due to the added complexity of having the pilot attempt to fly the plane from a fixed point on the ground, can and do crash. A good design should be able to endure a moderate crash with minimal damage. This feature is especially desirable for this competition, as damaged aircraft that are repaired within 20 minutes after the crash are credited with their full single flight score.

All of Syracuse University's previous entries in this competition have suffered some form of damage due to a crash landing, so it was reasonable to assume this might again be the case. Last year, during a particularly challenging landing, the team's entry suffered broken motor mounts when the propellers struck the ground. However, the motor mount can be difficult and time-consuming to repair – all but the slightest damage to this critical structure would take far more than 20 minutes to mend.

The advantages of using an electric ducted fan become readily apparent in this consideration. The entire propulsive assembly is contained within a duct system, which further protects both the motor and fan

unit in the event of adverse airframe contact with the ground. It would take a very hard crash to dislodge the motor and fan unit from their housing, so EDFs shine in this category.

Other considerations

There are a few other factors to consider when comparing a ducted fan setup to a propeller setup. Engine-out performance for aircraft with multiple motors is related to how closely the motors are located to the aircraft centerline. Ducted fans, having a smaller diameter than propellers, could be placed closer to the aircraft centerline. This could result in better engine-out handling qualities.

The use of multiple motors brings about the question of how to mount them. Large diameter propellers would most likely need to be placed in wing pods, which would raise the RAC. The only way around this would be to set up the motors in a tractor-pusher configuration along the fuselage centerline. However, this would require more ground clearance and thus larger landing gear due to propeller strike concerns for the pusher propeller during rotation. Ducted fans could be placed in nacelles that are an integral part of the fuselage, eliminating the need for extra pods and thus keeping the RAC lower. Since these nacelles would be built as part of the fuselage, they would also be easier to integrate into the final aircraft than wing-mounted engine pods would.

Propellers do have an advantage over ducted fans during cruise. The added wetted area of the ducts contributes to higher drag at cruise speeds, which makes them slightly less efficient. However, this could be offset by the larger ground clearance requirement of the propellers – larger fixed landing gear lead to increased drag. Finally, experiments with ducted fans has shown that these units have a slightly higher take-off thrust than propellers (Reference 1), which could be very helpful in meeting the short take-off requirement.

4.2.3. Propulsion Studies

Consideration of the qualities listed above seemed to favor using ducted fans, but both external propeller and ducted fan setups were examined further before the final propulsive device was determined. Either configuration would use brushless motors. While expensive, these motors offer an efficiency that is absolutely necessary to remain competitive. Due to positive past experience with Aveox motors speed controllers, the decision was made to compare only Aveox brushless motors.

One group of team members optimized a propeller setup, while another optimized a ducted fan setup. Both were optimized to a thrust of approximately 58 ounces and a total run time of at least six minutes. This thrust came from the minimum value assigned for thrust loading, and the run time was an estimate based on time in the air. Both were to use up to 20 sub-C size cells as mentioned earlier. The analyses were carried out using Motocalc, a computer program for estimating various values of electrically powered aircraft. Table 4-2 summarizes the results of this comparison.

The propeller setup offered a much lower cost than the fan. This was due to the large price difference between the fan and propeller unit and because the propeller setup utilized motors purchased for last year's entry. The ducted fan setup required a different motor because of a difference in efficiency.

The Motocalc output seemed to slightly favor a propeller setup. However, this came at a cost of large diameter propellers (~17 inches), which introduced clearance problems. In light of the favorable qualities of ducted fans outlined previously, as well as the similarity between the calculated values of the two setups, the decision was made to adopt direct drive ducted fans as the propulsion system. It was felt that the advantages of these units outweighed the price concerns, and after a careful budget analysis it was deemed that the team could afford to buy the extra equipment necessary for ducted fans. It was not of trivial importance that such a setup would be a new experience for the team, which would increase the experience base of the team members when considering a setup for next year. The Motocalc output for the final propulsion configuration can be found in Appendix A.

4.3. AIRFOIL SELECTION

The final step in the preliminary design of the SF1 was the airfoil selection for the wing. This involved much consideration, as an improperly chosen airfoil section would result in poor performance.

4.3.1. Figures of Merit

The primary FOMs considered during airfoil selection included the maximum lift coefficient, drag, and the stall angle of attack. Of lesser importance was satisfactory performance at the lower Reynolds numbers that the wing was anticipated to encounter.

The maximum lift coefficient, $C_{l_{max}}$, is a parameter in take-off performance related to the stall speed of the aircraft. Higher values of $C_{l_{max}}$ indicate that lower stall speeds are attainable, translating into a shorter take-off field length.

It is necessary for the aircraft to be controllable in a comfortable range for the pilot. If the aircraft stalls at a low angle of attack, the pilot may have difficulty keeping the aircraft flying. Therefore, an airfoil with a higher stalling angle of attack was desired.

Finally, low drag is always a goal when designing an aircraft. Several airfoils exist that maintain laminar flow over a significant portion of their surface, and thus have a low "drag bucket" near their design lift coefficient. This would be an important quality in airfoil selection.

4.3.2. Airfoil Studies

Several families of airfoils were studied for use in the wing of the SF1. First inspected were the venerable NACA six-series airfoils as published in Reference 2. These airfoils have very low drag coefficients near their design lift coefficient, which is highly desirable. However, they generally have a lower stalling angle of attack and lower maximum lift coefficient than airfoils designed for turbulent flow regimes. Finally, the drag reduction is not realized for off-design conditions. Since the aircraft would be experience a variety of attitude changes, this family of airfoils may not be ideal for the SF1.

Another family of interest was the NASA Low-Speed (LS) series of airfoils, also known as the General Aviation (Whitcomb) or GA(W) series. These airfoils were designed to operate at lower Reynolds numbers and can attain large values of $C_{l_{max}}$. They are characterized by a large leading edge radius, blunt trailing edge, and highly cambered rear surface. They are designed to operate with a turbulent boundary layer, which slightly increases the drag. However, the high maximum lift coefficients and larger stalling angles of attack made these airfoils very attractive.

Data was compiled for the NACA 6-series and NASA LS-series airfoils from a web-based program called Calcfoil. This program utilizes conformal mapping to calculate the velocity distribution over the airfoil, from which the various aerodynamic coefficients can be found (lift, drag, and pitching moment). The necessary inputs are airfoil ordinates in percentage of chord and Reynolds number. Data for published airfoils from Reference 2 was tested against the results of the Calcfoil model, and found to be acceptable. The airfoil ordinates for the LS series were then acquired from Reference 3 and computed for Reynolds numbers of 200,000, 600,000, and 1,000,000, based on various flight conditions.

Based on these studies, the NASA LS(1)-0417 (also known as the GA(W)-1) appeared to be the ideal airfoil for this design. It has a $C_{l_{max}}$ value of approximately 1.8, a thickness to chord ratio of 17%, and a stalling angle of attack of approximately 16 degrees. The high $C_{l_{max}}$ value would be beneficial for the short take-off requirement, while the higher stalling angle indicated better controllability over a wide range of attitudes. Finally, the relatively large thickness ratio meant a thicker wing was possible, which would result in a lighter structure due to the increase in the geometric moment of inertia of the wing. The Calcfoil output for the lift, drag, and pitching moment coefficients of the LS(1)-0417 airfoil can be found in Figures 4.2 through 4.4.

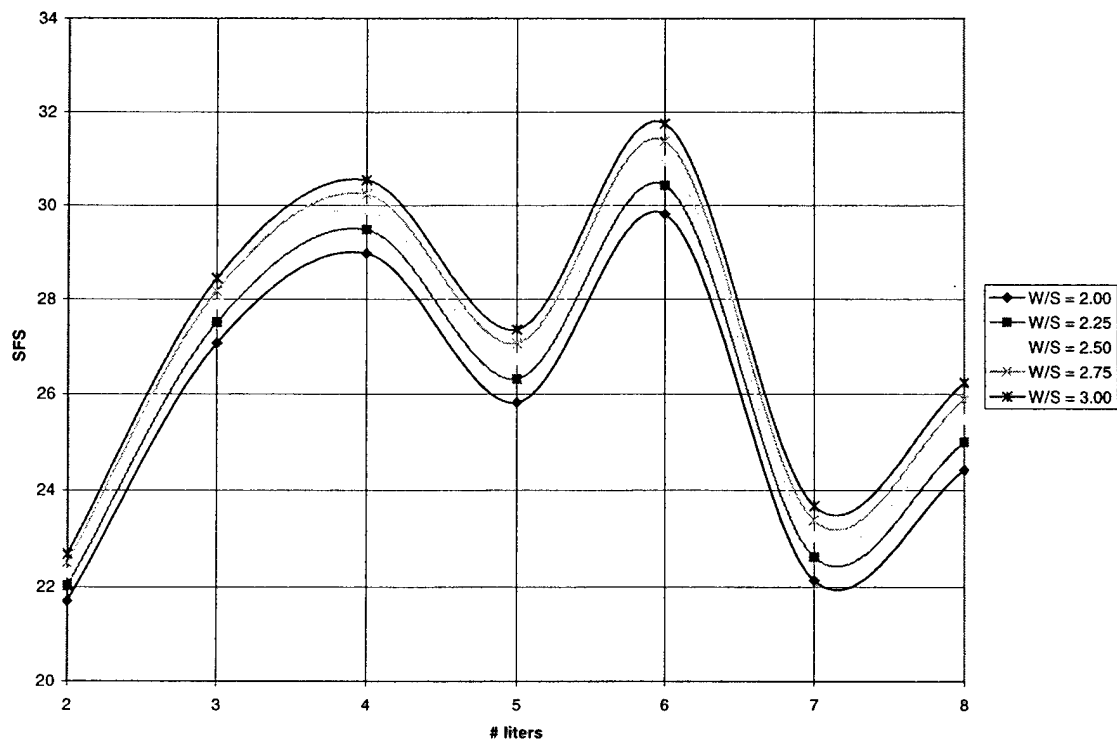


Figure 4.1. Single flight score vs. number of liters carried for various wing loadings

wing loading	3.00 psf
payload capacity	4.00 liters
weight	21.0 lbf
gross wing area	7.00 ft ²
aspect ratio	7.00
payload fraction	0.42
RAC	5.23

Table 4-1. Initial sizing estimates

parameter	prop setup	EDF setup
motor	Aveox 1412/2Y	Aveox 1412/5Y
prop/fan diameter (in)	18	4.13
prop/fan pitch	8	8.43
gear ratio	3.7:1	1:1
battery pack(s)	2 x 10 cell	1 x 20 cell
amps to motor	29.9	28.9
volts to motor	10.6	21.5
output (W)	273.8	524
efficiency (%)	86.4	84.4
prop/fan RPM	3940	10798
thrust (oz)	57.9	58.9

Table 4-2. Propeller vs. ducted fan setup

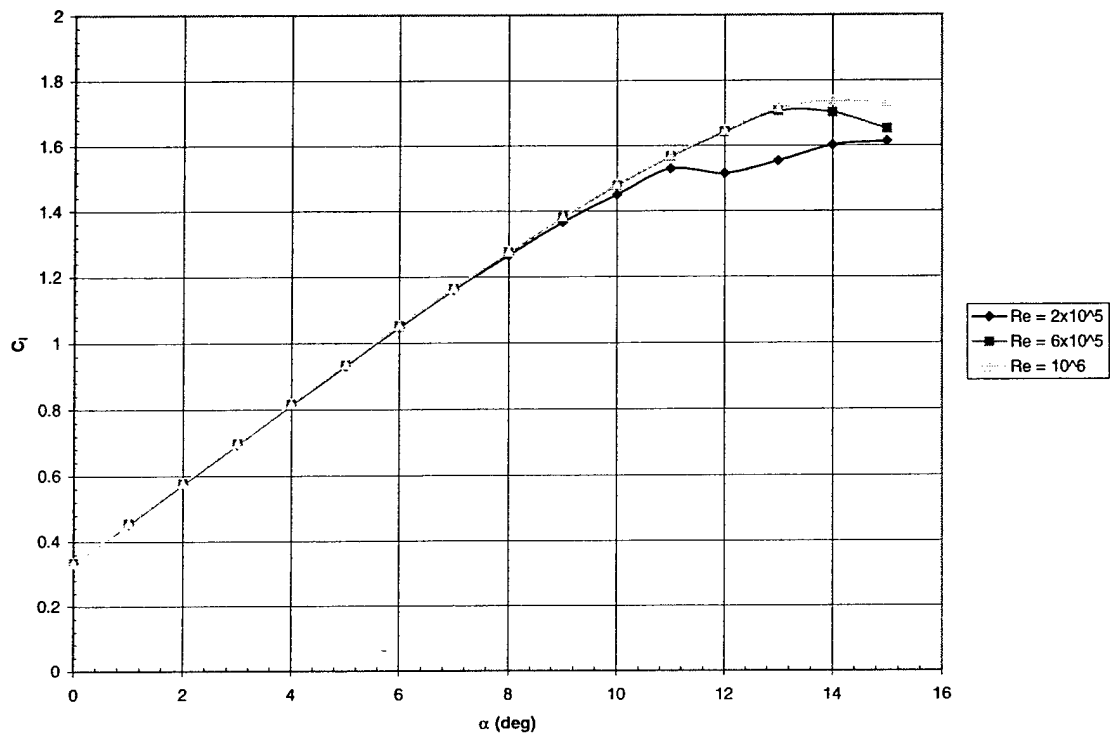


Figure 4.2. Section lift coefficient vs. angle of attack for a NASA LS(1)-0417 airfoil

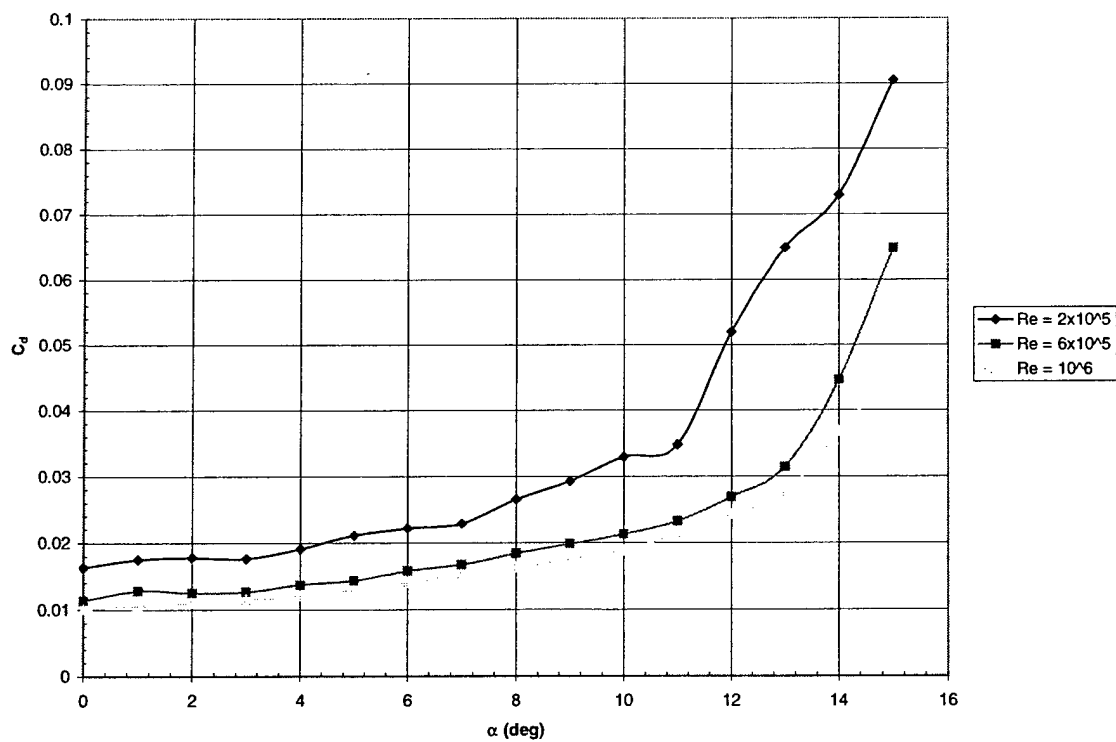


Figure 4.3. Section drag coefficient vs. angle of attack for a NASA LS(1)-0417 airfoil

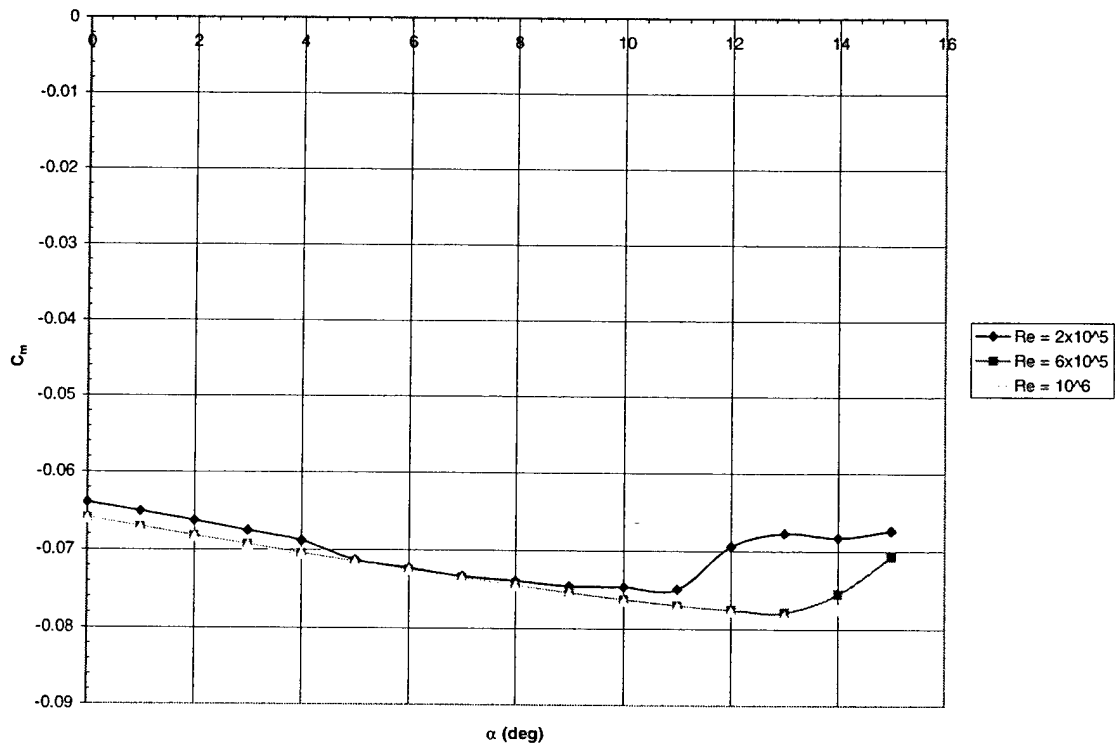


Figure 4.4. Section moment coefficient vs. angle of attack for a NASA LS(1)-0417 airfoil

5. DETAIL DESIGN

With the initial sizing parameters identified, it was possible to proceed with the final sizing and performance analysis of the SF1. This involved several intermediate steps, and was the most time-consuming and difficult tasks of the project.

5.1. FINAL SIZING

The final aircraft sizing parameters needed to be determined so the wing, canard, fuselage, and fin geometry would be fully defined. These sizing parameters were also important in the stability and performance estimations.

5.1.1. Wing

Much of the wing sizing was determined in the preliminary design phase. With the span limited to seven feet and the wing area determined from the previous phase, the aspect ratio was found to be 7.0. This also determined the span and mean geometric chord of the wing.

The SF1 was not expected to perform at Mach numbers greater than 0.1, so wing sweep was not necessary to combat compressibility effects. It was believed that the aircraft would be well-balanced about the wing root, so no sweep was necessary to move the wing mean aerodynamic chord (MAC) forward or aft. Adding sweep would only add structural weight. Therefore, the quarter chord of the wing was left unswept, and would remain so as long as aircraft balance did not demand otherwise.

Following this, the taper ratio was considered. Taper is introduced to a wing to approximate an elliptic lift distribution, thereby increasing the efficiency of the span loading. Reference 4 provides a table that relates quarter chord sweep to taper ratio for efficient operation, and gives the taper ratio for a straight wing to be approximately 0.5.

Finally, the dihedral angle of the wing was chosen to be five degrees. This value was determined from a table in Reference 4 that suggested a dihedral angle from five to seven degrees for aircraft with unswept, low wing configurations. The dihedral would only be changed if the lateral stability analysis, performed later, indicated that the aircraft was unstable in roll or sideslip.

5.1.2. Canard

The canard of the SF1 needed to be designed so that the aircraft was statically stable in pitch. This occurs when the following conditions are met:

- $C_{m0} > 0$
- $C_{m\alpha} < 0$
- $|h - h_n| \geq 0.1$

where C_{m0} is the zero-lift pitching moment coefficient of the total airplane, $C_{m\alpha}$ is the pitching moment derivative with respect to the angle of attack, and $|h - h_n|$ is the static margin, in percent of the wing MAC. A spreadsheet was created that listed the relations of these parameters to wing geometric properties, such as the wing area, span, and aspect ratio. The procedure to find the above parameters were found from Reference 5, with slight modifications for canard aircraft. The canard wake was assumed to have little effect on the aerodynamic characteristics of the main wing, since it was known that the canard would be well above the plane of the wing. The canard is the forward lifting surface on the SF1, so the downwash effects from the wing on the canard needed not be taken into account.

Next, the canard moment arm from the wing aerodynamic center was estimated. This was necessary in order to determine the volume coefficient of the canard to determine h_n , the stick-fixed neutral point location from the leading edge of the wing MAC in percent MAC. This estimation was made by assuming the aircraft center of gravity was at the wing quarter chord, and adding the lengths of half of the

payload compartment (as this would be centered at the aircraft CG), battery compartment, systems compartment, and aerodynamic fairing together. This resulted in a quarter-chord to quarter-chord moment arm of 28 inches.

The aircraft CG, canard volume coefficient, and canard incidence angle were determined such that all of the static longitudinal stability criteria were met. The canard area resulted from this analysis, which was used to determine its final geometry. It is necessary for the canard to stall first to prevent adverse pitch-up. As such, it was placed at a higher incidence and has a larger aspect ratio than the wing. A good rule of thumb to determine the canard aspect ratio is to divide the wing aspect ratio by a number ranging from 0.75 to 0.9. The final canard aspect ratio of 8.0 fell within this range.

With the aspect ratio and area known, the mean geometric chord and span of the canard could be determined. The taper ratio was selected to be 1.0. While this results in a less efficient planform, it is easier to manufacture. Since the canard is not a primary lifting surface, it does not need to reach its full lift potential for most flight modes. As such, aerodynamic efficiency played a lesser role to manufacturing ease.

The final geometric property chosen for the canard was the quarter chord sweep angle. As with the wing, any canard sweep would only add structural weight. Therefore, the canard was given no sweep at the quarter chord.

5.1.3. Fuselage

Sizing the fuselage was a straightforward process. The length needed to be minimized to keep the RAC and total surface area down (the latter for less parasite drag). This length was initially estimated in the previous design phase, but needed further study to finalize the dimensions.

In an effort to keep the dimensions of the fuselage down, a basic inboard profile was considered. The fuselage was defined in six compartments: forward aerodynamic fairing, systems compartment, battery compartment #1, payload compartment, battery compartment #2, and aft aerodynamic fairing. The lengths of all but the aerodynamic fairings could be related to the actual component lengths. The height and width of the other compartments would dictate the dimensions of each fairing.

The fuselage profile has a major influence on total drag, so an airfoil was considered for this body. The peculiarities of the inboard profile of this fuselage indicated that the airfoil should have a relatively uniform thickness distribution, and should have its maximum thickness located at about half of the fuselage length. Laminar flow characteristics would be highly desirable for further drag reduction. Finally, all of the analyses carried out assumed the body contributed very little to the lift of the aircraft, since no advantages were seen for cambered airfoils. Therefore, only symmetrical airfoils were considered.

The NACA 66-012 airfoil was chosen for the profile of the fuselage. This airfoil has a maximum thickness of 12% at 0.45c, which met the requirements for the component arrangement. The height requirements of the internal components of the fuselage then dictated a fuselage length of 56 inches. This value was very close to the value found for fuselage length during preliminary design.

5.1.4. Fin

The final step in the sizing process was to choose the vertical fin geometry. A fin volume coefficient of 0.07 met the necessary design criteria for aircraft of similar configurations as found in Reference 4. Fin volume coefficients are a function of the fin moment arm, fin area, gross (planform) wing area, and wing MAC. Both wing values were known, and the location of the tail was fixed from the fuselage sizing. Specifying a fin volume coefficient thus determined the fin area.

A smaller fin was desirable, since this would reduce its weight and wetted area. Sweeping the fin back would increase the fin moment arm and thus yaw authority because the MAC would be moved further aft. Therefore, the same yaw authority could be maintained from a smaller tail. Studies from Reference 4

indicated that this advantage was apparent for up to approximately 30 degrees, while sweep beyond this angle would increase the fin weight. As such, the quarter chord fin sweep was set to 30 degrees.

The selection of the fin aspect ratio was limited to a study of existing aircraft. The general trend for most aircraft is a fin that is roughly one-third the aspect ratio of the wing. This method led to the final selection of the SF1's fin aspect ratio of 2.0.

Selection of the fin taper ratio was similar to that of the wing, as it was related to the wing sweep. The selected value of 0.33 was slightly larger than the empirical predictions. However, any value lower than this would have resulted in a very small fin tip chord, which would make it difficult to integrate the rudder properly. The fin dimensions could now be determined from the area, sweep angle, taper ratio, and aspect ratio.

5.2. WEIGHTS AND BALANCE

5.2.1. Final Weight Estimation

The final weight of the aircraft was estimated from individual component weights. The aircraft structures, now sized, could be re-evaluated for the final weight calculation. This value was important as it determined the aircraft performance and handling qualities. The final weight of the SF1 was estimated to be 21.2 pounds, 44.9% of which would be payload. This value will be re-evaluated following construction.

5.2.2. Center of Gravity

All entries are expected to demonstrate adequate handling qualities for both maximum and ferry loading conditions. Therefore, the CG of the payload was to be located as close as possible to the CG of the entire aircraft. This would result in little change in the static margin for either load case. The ideal CG location of the SF1 was known from the longitudinal stability calculations carried out during canard sizing. The actual CG location needed to be as close to this as possible. As such, the components locations were estimated and iterated until these two values for CG location converged.

The CG calculations involved a simple static analysis. The weight estimation carried out previously indicated each component's weight. The location of each component's centroid was then found from the nose of the aircraft. The moments about the nose of the aircraft due to each component were then summed, and this sum was subsequently divided by the total weight of the aircraft. This indicated the aircraft CG location from the nose. Some components, such as the battery packs and payload, were considered fixed within the aircraft, while others, such as the radio control equipment, could be moved within their compartments.

The values for the necessary and actual CG locations of both the ferry and maximum load cases converged to within one hundredth of an inch after iteration of the component locations. These CG calculations can be found in Appendix B. The locations after construction will likely vary from this range, so the actual locations of the components may differ slightly after the aircraft is built.

5.3. PERFORMANCE ESTIMATION

With final sizing completed, it was possible to estimate the performance of the SF1 in various flight modes. The take-off performance was crucial as a maximum ground roll distance was specified by the competition rules. All of the performance parameters considered ambient conditions of a standard day at 2000 feet above sea level, slightly more than the 1400 foot elevation of the contest site.

5.3.1. Drag Polar

It was first necessary to estimate the drag of the aircraft, as this plays a critical role in aircraft performance. Level one estimation was used to find the drag polar of the SF1, which historically provides a very good fit to the actual drag polar. If anything, level one estimation slightly overpredicts drag.

There are three main contributions to airplane drag. These are induced, compressibility, and skin friction drag. These latter two contributions are often known as the zero-lift drag of the aircraft. Therefore, the drag polar can be represented by

$$C_D = C_{D_0} + KC_L^2 \quad (1)$$

where C_D is the total drag, C_{D_0} is the zero-lift drag, K is the induced drag coefficient, and C_L is the aircraft lift coefficient. The SF1 is not expected to attain Mach numbers greater than 0.1, so compressibility drag was neglected during estimation. This left parasite drag as the only contribution to the zero-lift component of the aircraft drag polar.

In level one estimation, the skin friction drag coefficient is first considered for each body. The drag coefficients are found by approximating the skin friction coefficient of the body, assuming a worst-case turbulent boundary layer. The skin friction coefficients are then found from

$$C_f = \frac{0.455}{[\log(Re)]^{2.58}} \quad (2)$$

where C_f is the skin friction coefficient and Re is the Reynolds number based on the length of the body. The SF1 required C_f values of the wing, canard, fin, fuselage, and ducts. The parasite (and thus zero-lift) drag of the aircraft could then be found from

$$C_{D_0} = \frac{1.2(\sum C_{f_{body}} S_{wet_{body}})}{S} \quad (3)$$

where $C_{f_{body}}$ is the skin friction coefficient of a specified body, $S_{wet_{body}}$ is the approximate wetted area of that body, and S is the reference (planform) wing area.

It can be seen from equation (2) larger values of Reynolds numbers will decrease the skin friction coefficient. As such, the Reynolds number of each body was estimated for the approximate stall speed of 35 ft/s.

The estimation of the induced drag was much less work-intensive. The induced drag coefficient K is given by

$$K = \frac{1}{\pi A e} \quad (4)$$

where A is wing aspect ratio and e is Oswald's span efficiency factor. For unswept wings, this value can be estimated from

$$e = 1.78(1 - 0.045A^{.68}) - 0.64 \quad (5)$$

Figure 5.1 shows the level one drag polar found for the SF1.

5.3.2. Cruise Performance

During cruise, lift is equal to the weight of the aircraft and drag is equal to the thrust of the propulsive system. Optimum long-range cruise occurs at the best lift-to-drag (L/D) ratio. This, however,

would not be the case for the SF1 due to the time limit imposed by the competition rules. It was reasoned that the aircraft needed to cruise at or near its maximum velocity to attain as many sorties as possible.

The gross thrust of the aircraft was found by specifying the motors, number of cells, and fan units (chosen during the preliminary design phase) in Motocalc and listing the results at speeds from zero to 80 miles per hour. The level flight lift and drag coefficients were then calculated for this range of speeds and tabulated with the thrust data. The net thrust was calculated by subtracting the gross thrust from the level drag coefficient. The aircraft's maximum level flight velocity occurred when the net thrust was equal to zero. Due to the large number of estimations involved, this maximum speed found was only accurate to the nearest five miles per hour.

The above calculations yielded the level cruise flight velocity and airspeed for the SF1. Interestingly enough, the lift coefficient at this speed was very close to the design lift coefficient of the airfoil selected. Therefore, no wing incidence was necessary for the payload sorties. This did not hold for the ferry sorties, so the SF1 will either need to fly at a slightly negative attitude or be allowed to climb during the cruise portion of these sorties. Table 5-1 lists the maximum level cruise velocity of the aircraft for both maximum and ferry loading conditions.

5.3.3. Take-Off Performance

The competition rules specified that the SF1 needed to take off within 100 feet while operating at its maximum gross take-off weight. This represented the total ground roll distance only.

Ground roll distance calculations were made from a method discussed in Reference 4. The thrust found at 70% of the liftoff velocity as used to calculate the thrust-to-weight ratio for this particular formulation, as recommended by the author. The wind speed was assumed to be zero. The initial output of these calculations indicated that the SF1 would exhibit a ground roll of more than 100 feet for take-off. In order to take off within the specified distance, the aircraft would need a maximum lift coefficient of approximately 2.2. This was only attainable through the use of high-lift devices.

Control synergy was highly desired to reduce the complexity of the SF1's control system, so plain flaperons were considered as opposed to independent flaps and ailerons. Also, the lift and drag of the aircraft in ground effect were determined via Reference 6. The resulting configuration employed a flaperon spanning 70% of the wing and 20% of the wing chord. This gave a maximum airplane lift coefficient of approximately 2.22 in ground effect, which enabled the SF1 to take off within 100 feet in the worst-case scenario. Table 5-1 gives a summary of the take-off ground roll for both loading conditions.

5.3.4. Turning Performance

Both the instantaneous and sustained turning performance of the SF1 needed to be determined to estimate the total mission time. Reference 4 provided methods for estimating the best turn rate for both modes. The fastest instantaneous turn rate of the aircraft was computed at the maximum lift coefficient and flight velocity, which dictated the limit load factor of the SF1. The best instantaneous and sustained turn rates of the SF1 are presented in Table 5-1.

5.3.5. Estimated Mission Performance

The payload sorties are to be a single lap with a 360-degree turn on the post take-off cruise leg of the course. The aircraft will then land, change out its payload, and return to the air for a ferry sortie. Next, the aircraft is to take off for a ferry sortie, which is marked by two laps without any 360-degree turns. The entire cycle is repeated through the useful run-time of the aircraft or ten minutes, whichever is less. The performance estimations above predicted a payload sortie time of 66 seconds and a ferry sortie time of 78 seconds. This indicates that the SF1 can accomplish four payload and three ferry sorties in the ten-minute competition period if the pit crew can change the payload in under 17 seconds.

5.4. STABILITY AND CONTROL

Stability was a major concern in the design of the SF1. Longitudinal static stability criteria drove the sizing of the canard, as mentioned earlier. The entire design was evaluated to see if it met the requirements for static stability.

5.4.1. Stability Derivatives

Aircraft stability is often demonstrated through the use of dimensionless stability derivatives. Reference 7 states that the following must be true to demonstrate basic static stability:

- $C_{L\alpha} > 0$ – aircraft lift-curve slope
- $C_{m\alpha} < 0$ – pitching moment curve slope
- $C_{mq} < 0$ – variation of pitching moment coefficient with pitch rate
- $C_{Du} > 0$ – variation of drag coefficient with speed
- $C_{mu} > 0$ – variation of moment coefficient with speed
- $C_{y\beta} < 0$ – variation of side force coefficient with sideslip angle
- $C_{l\beta} < 0$ – variation of rolling moment coefficient with sideslip angle
- $C_{n\beta} > 0$ – variation of yawing moment coefficient with sideslip angle
- $C_{lp} < 0$ – variation of rolling moment coefficient with roll rate
- $C_{np} < 0$ – variation of yawing moment coefficient with roll rate

Each of these stability derivatives was estimated for cruise per the methods of Reference 5, ignoring compressibility effects and assuming small angles of attack. These values were then compared to aircraft with similar missions as found in Reference 8. The final static stability derivatives of the SF1 were found to satisfy all of the requirements listed above, and correlated well with the empirical data. These derivatives can be found in Table 5-2.

5.4.2. Control Surface Sizing

The primary control surfaces of the SF1 are flaperons for roll, elevators for pitch, and a rudder for yaw. All are plain flap devices with hinge lines at the same taper ratio as their parent body (wing, canard, and fin). The flaperon geometry was given above in section 5.3.3. The elevators and rudder were sized according to the approximate methods found in Reference 4. This resulted in an elevator spans 75% of the canard and a rudder that occupies 90% of the rudder span. Both the rudder and elevators have a chord length that is 30% of the fin and canard, respectively. Flight testing will indicate the sensitivity level necessary for the control system so the aircraft will be controllable for maximum pilot comfort.

5.5. STRUCTURAL ANALYSIS

5.5.1. Load Factor

The limit load factor of the SF1 was determined from the worst case zero-gust flight condition of an instantaneous turn at the maximum lift coefficient and maximum velocity. This resulted in a limit load factor of approximately 7.0. This was multiplied by 1.5, the standard factor of safety for aerospace vehicles as specified by the Federal Aviation Regulations, resulting in an ultimate load factor of 10.5.

Initially, this value may seem needlessly high for anything other than a high-performance fighter aircraft. However, it provided a nice cushion in the event of a hard landing or even for a moderate crash. Crashworthiness was an important consideration as outlined earlier in section 4.2.2. Furthermore, most aerospace structures are both strength and stiffness critical. An ultimate load factor of 10.5 would ensure that only small deflections would be apparent for virtually every loading condition. Therefore, this ultimate load factor was considered in the structural analysis of both the wing and fuselage.

5.5.2. Wing Analysis

The team wished to assemble the wing from a foam core wrapped in fiberglass cloth. This would result in a wing structure that would be stronger and lighter than one made of wood built for the same loads. The design was considered a bending-critical application.

The wing was approximated as a cantilever beam for structural analysis. The lift was approximated as a trapezoidal distributed load, and was calculated for 10.5 times the 1-g flight load. The resulting bending moment was greatest at the wing root.

Since the foam cores would carry substantially less load than the fiberglass, they were neglected entirely for bending analysis. As the wing skin would be much thinner than the thickness of the wing, the loads in the upper skin were treated as pure axial compression, while the lower skin was assumed to be under axial tension. Each of these loads was approximated to act at the center of each skin. As both forces acted in opposite directions, this resulted in a couple equal to the distance between the two axial forces times the magnitude of this force. The magnitude of this couple would equal the magnitude of the root bending moment. Since the root bending moment and distance between wing skins were known, the magnitude of the axial forces in the wing skins was found by dividing the root bending moment by the distance between the skins. These forces were found for skins with two to nine plies of fiberglass. The resulting average ply stresses could be found by dividing this force by the cross-sectional area of the skins.

The fiberglass cloth that was to be used had fibers running at right angles to each other. As such, each ply of material would effectively behave like two plies of unidirectional material at right angles to each other, with the only major difference being the Poisson ratio of the material (due to the weave of the fabric). Therefore, the qualities for a single unidirectional ply of fiberglass could be used in the calculation of the material properties of the upper and lower wing skins. These properties (longitudinal Young's modulus, ultimate tensile strength, and ultimate compressive strength) were estimated from Reference 9.

It is desirable to construct laminates that are balanced and symmetric; that is, laminates have the same number of plies running at an angle $+\theta$ as at an angle of $-\theta$, and that are symmetric about their thickness centerline. It has been shown that laminates that are especially resistant to impact damage have plies at a ± 45 degree orientation on the outermost layer. Therefore, the ply orientation of the wing was chosen such that the outer layer of cloth would be at a ± 45 degree orientation. These plies would also provide the best torsional rigidity. The fabric in the middle layers would need to have a 0/90 degree orientation to carry the bending loads of the wing.

Layups of two and three layers of fabric were chosen for further analysis. The first had an orientation of $[\pm 45/0/90]$, and the second $[\pm 45/0/90/\pm 45]$ (note that each layer of fabric consisted of two plies of material). These layups were entered into Promal, a composite material analysis program supplied with Reference 9. Each was analyzed for a unit load of one pound in the longitudinal direction. The strength ratios and global strains were found for each ply, and the lowest values taken for first-ply-failure (FPF). These values, when multiplied together, gave the strain-to-failure of each laminate. This strain was compared with the strain in each wing skin under the seven-g load and the factors of safety determined. It was found that two layers of fabric exhibited failure at a factor of safety of approximately 1.39, which was not acceptable. The three-layer laminate exhibited a factor of safety of approximately 1.88, giving it the capability to withstand over 13 g's. Again, while this may seem excessive, the benefits of increased crashworthiness and lack of considerable deflection were of prime importance.

Finally, the entire wing structure underwent a deflection analysis. The wing was assumed to be a cantilever beam with a force acting at half of its length, and the deflection found from Reference 10. Since the actual wing is tapered, the moment of inertia of the beam was taken to be at a cross-section halfway through the span. All of these approximations most likely result in very large errors. However, this deflection analysis was just a check to ensure that the order of magnitude of the deflection was not very large. The result of this analysis was a 4.3 inch tip deflection during the 10.5-g ultimate loading condition. This was deemed acceptable for the SF1.

5.5.3. Fuselage Analysis

The fuselage also underwent a simple bending structural analysis. It differed from the wing analysis in that the fuselage was modeled as a beam supported at its CG. Each component was represented by a point mass located at their respective centroid locations, as specified in section 5.2.2. The moments of each of these point masses times the limit load factor was taken about the aircraft CG. Since the aircraft was balanced about this point, the moment ahead and behind the CG were equal and opposite. Therefore, only one side was considered, so the fuselage could be analyzed as a cantilever beam.

The fuselage of the SF1 is characterized by eight rectangular plywood and balsa bulkheads connected at the corners by four balsa longerons. The bulkheads merely provide control and reinforcement points, while the longerons carry the fuselage bending loads. The longerons at the center of gravity will be fashioned from standard 0.25 x 0.5 inch balsa stock. These are separated by a distance of approximately 4.25 inches at the CG, which is much larger than the longerons themselves. As such, the upper and lower longeron pairs were assumed to undergo axial tension and compression (in this case, the upper surface would be in tension and the lower surface in compression). The stress in the upper skin was then found utilizing the same method described for the stress in the wing skins. This stress was compared to the ultimate tensile strength (equal to the ultimate compressive strength in this case) for balsa wood as found in Reference 11.

The ultimate tensile strength was divided by the actual stress in the longerons to determine the factor of safety. This, like the wing, was found to be higher than necessary at approximately 3.68, giving a maximum load capability of 25.7 g's.

The conclusion of both of these analyses indicated that the structure of the SF1 would be able to withstand any flight loads the aircraft might experience, as well as moderate crash loads. Table 5-3 summarizes the results of the wing and fuselage structural analyses.

5.6. SUBSYSTEMS

5.6.1. Landing Gear

The placement of the landing gear was determined by the methods of Reference 4 for tricycle configurations. The main gear, estimated at a length of eight inches, was set at a tipback angle 15 degrees from the aircraft CG. The nose gear location was found from a simple static analysis, setting the force on this member at 10% of the total aircraft weight and summing the forces and moments to find the location. The minimum lateral distance of the main gear from the CG was found from the landing gear length and the maximum overturn angle (angle from the CG to the main wheel seen from a location where the nose gear and main gear appear aligned) of 63 degrees. The lateral distance was then set at 10 inches for structural convenience, resulting in a lower overturn angle. This would make the SF1 less likely to scrape a wing on the tarmac when taxiing around a sharp corner.

5.6.2. Radio Control Devices

Team Syracuse again elected to use its Futaba six-channel 6XA radio with a six-channel pulse-code modulation (PCM) receiver as the control system for the SF1. The PCM receiver was essential to meet the radio fail-safe requirements as described in the contest rules. These settings could be directly programmed into the radio unit.

This radio has a host of other functions. It is capable of flaperon mixing, which is essential for this year's aircraft as described earlier. Also, it offers dual-rate aileron/flaperon control. This could be useful is the large flaperons are found to over-control the aircraft at higher speeds. The dual-rate feature allows the pilot to limit the throw of the aileron/flaperon in flight with a switch on the radio transmitter. The limit is specified by the user in terms of percent throw, and is again programmed directly into the radio unit. This value will be specified during the test flights of the SF1.

Control surface movement is provided through the use of Futaba S3003 Standard Precision servos. These provide 42 ounce-inches of torque and can travel 60 degrees in 0.22 seconds. These are attached to the various control surfaces via long pushrods. Four of these servos are necessary for control of the SF1 – one for the elevator, one for the rudder and nose gear, and two for the flaperons. The motors are controlled by dual Aveox M160 speed controllers, each connected via a y-harness to the throttle channel on the receiver.

5.6.3. Cooling Provisions

The SF1 has two NACA flush inlets well forward of the wing to provide cooling air to the various electrical systems. This air is ducted past the forward batteries, speed controllers, and rear batteries, and finally exits via an aperture in the back of the fuselage.

5.6.4. Boundary Layer Diverter

The inlets for the twin ducted fans of the SF1 are nestled close to the fuselage to reduce the yawing moment that would result from an engine-out condition. The inlets could not be placed flush with the fuselage, however, because the fans would ingest the low-energy boundary layer of the fuselage. Therefore, it was necessary to design a boundary layer diverter if the form a simple two-dimensional duct. The necessary width of the diverter was found by assuming the worst-case laminar boundary layer. The boundary layer thickness was found from the Blasius solution to laminar boundary layers as discussed in Reference 12. This resulted in a diverter width of 0.25 inches.

5.7. DRAWING PACKAGE

Solid models for the SF1 were created using SolidWorks 99. Figure 5.2 shows the external 3-view and isometric layout of the final configuration. Figure 5.3 is an isometric view of the inboard profile.

<i>identifier</i>	<i>symbol</i>	<i>cargo</i>	<i>ferry</i>	<i>unit</i>
max. level speed	V_{\max}	60	65	mph
take-off ground roll	S_G	98.2	52.2	ft
max. sustained turn rate	$d\psi/dt$	48.6	68.6	deg/s
max. instantaneous turn rate	$d\psi/dt_i$	134.4	134.4	deg/s

Table 5-1. *Performance estimates*

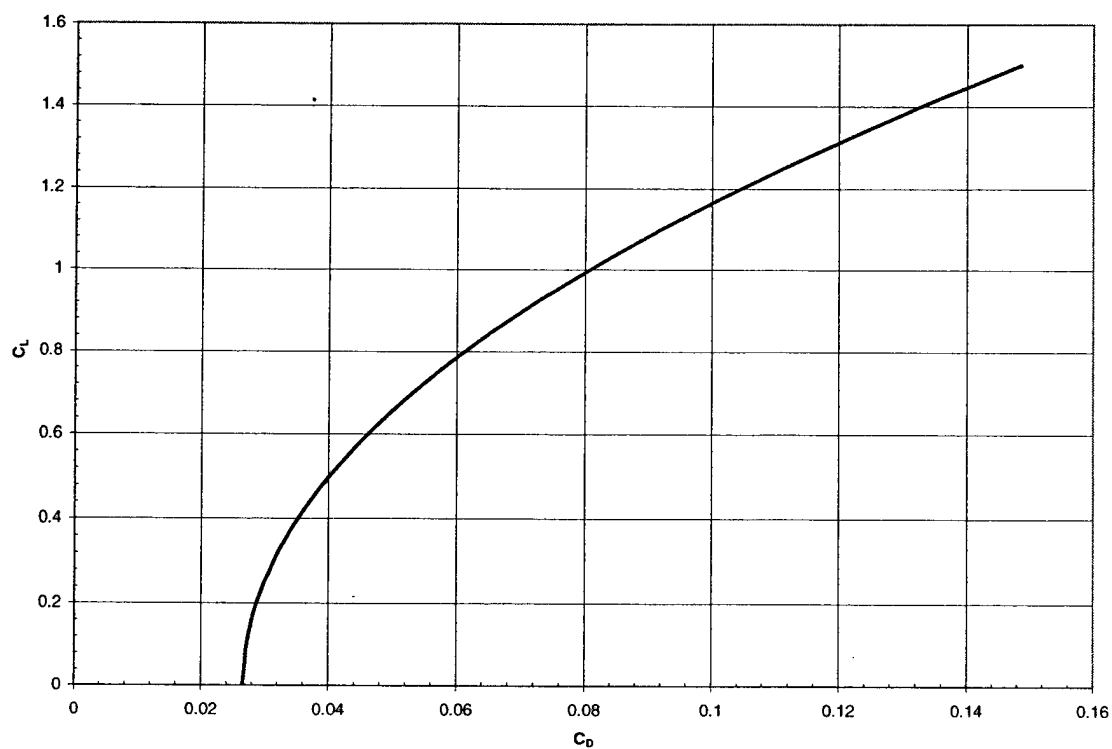


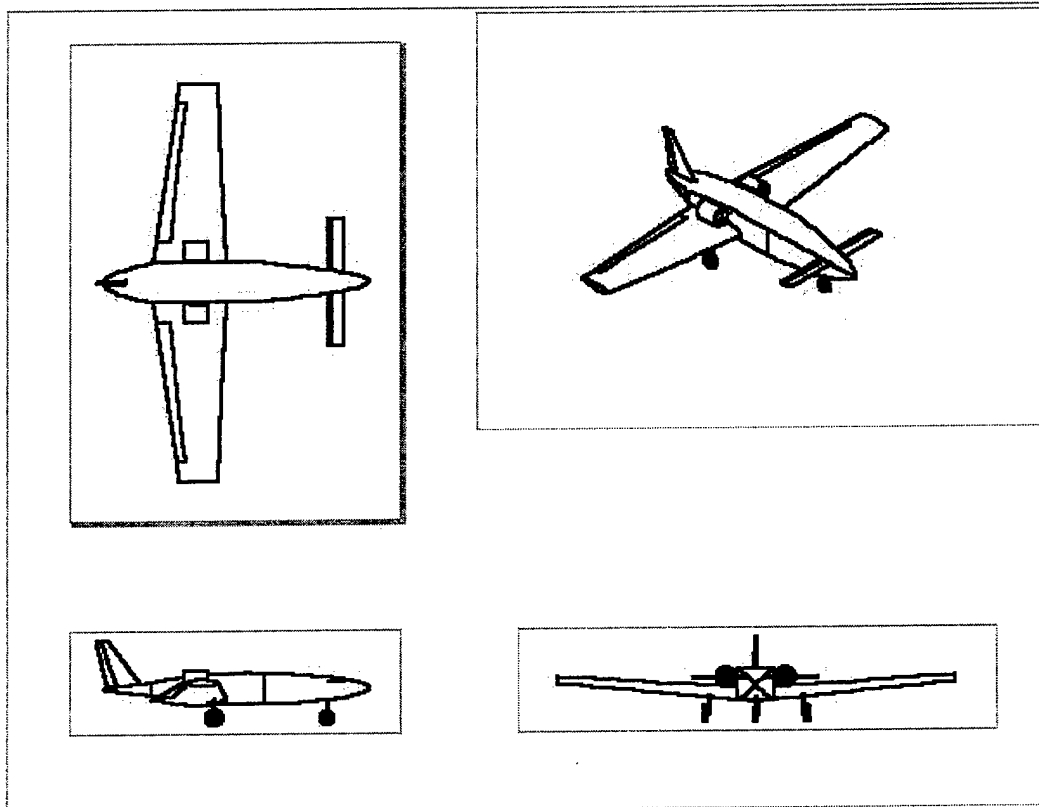
Figure 5.1. SFI drag polar

$C_{L\alpha}$	5.367 rad^{-1}	$C_{y\beta}$	-0.224 rad^{-1}
$C_{m\alpha}$	-0.537 rad^{-1}	$C_{l\beta}$	-0.024 rad^{-1}
C_{mq}	-1.464 rad^{-1}	$C_{n\beta}$	0.014 rad^{-1}
C_{Du}	0.000	C_{lp}	-0.455 rad^{-1}
C_{mu}	0.000	C_{np}	-0.029 rad^{-1}

Table 5-2. Static stability derivatives

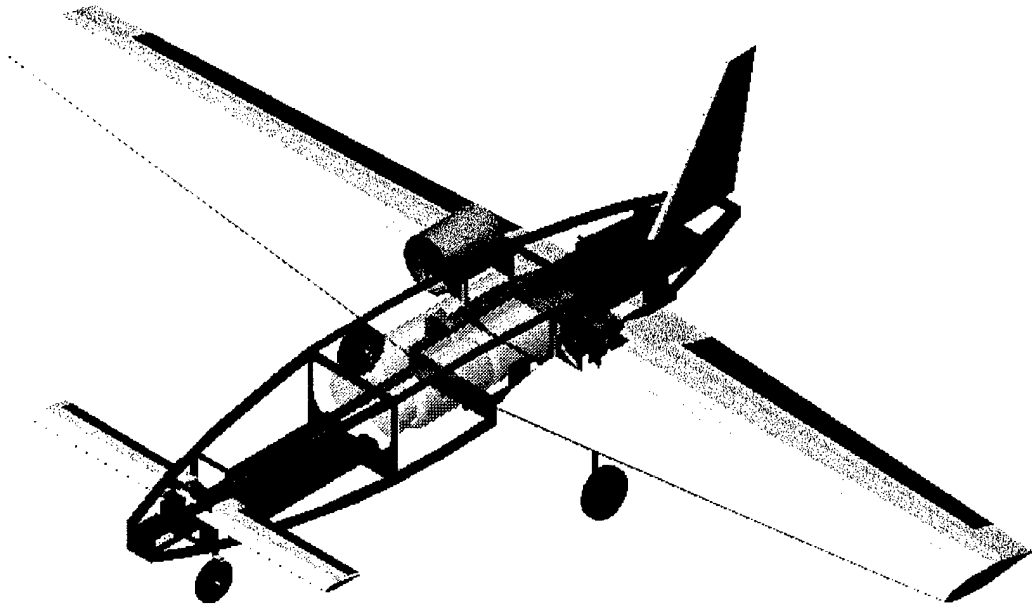
body	max g-load	factor of safety
wing	13.17	1.88
fuselage	25.7	3.68

Table 5-3. Structural load limits



<i>Location of critical areas from nose</i>			
<i>Item</i>	<i>Distance</i>		
Front fairing	0.00 in	Wing span	84.00 in
Systems compartment	2.00 in	Wing root chord	16.00 in
LE of canard MAC	5.16 in	Wing tip chord	8.00 in
Nose gear	9.00 in	Wing MAC	12.44 in
Battery compartment #1	10.50 in	Canard span	26.77 in
Payload compartment	21.00 in	Canard root chord	3.35 in
Center of gravity (both)	30.48 in	Canard tip chord	3.35 in
LE of wing MAC	30.89 in	Canard MAC	3.35 in
Neutral point	31.72 in	Fin span	10.24 in
Main gear	32.62 in	Fin root chord	7.68 in
Battery compartment #2	39.00 in	Fin tip chord	2.56 in
LE of fin MAC	48.11 in	Fin MAC	5.55 in
End fairing	56.00 in	Fuselage length	56.00 in
		Max fuselage width	8.00 in
		Max fuselage height	6.72 in

Figure 5.2. Final exterior dimensions of the SF1



<i>Component</i>	<i>Location</i>	<i>Component</i>	<i>Location</i>
Receiver	3.00 in	1-liter bottles (2)	34.48 in
Receiver battery	3.00 in	AP-2 fan unit	36.00 in
Rudder servo	5.00 in	AP-2 stator unit	38.00 in
Elevator servo	5.00 in	1412/5Y motor	38.00 in
Battery packs (2)	15.75 in	Battery packs (2)	44.25 in
1-liter bottles (2)	26.48 in	Left flaperon servo	45.00 in
Speed controllers (2)	32.25 in	Right flaperon servo	45.00 in

Figure 5.3. Inboard profile

6. MANUFACTURING PLAN

The manufacturing plan for the SF1 was designed to minimize cost and time while maintaining reasonable skill requirements. All material selections were made in accordance with chosen figures of merit and required skills. The construction of the model utilized the modeling skills of individual members and the dedication of the entire team.

6.1. FIGURES OF MERIT

To aid in all manufacturing decisions the team used six figures of merit (FOM) when considering materials. These were:

- Availability
- Reparability
- Strength/Weight Ratio
- Skill Matrix
- Time
- Cost

The details of the team's considerations are presented in Table 6-1. Based upon past experiences the team decided to place heavy consideration upon the Skill Matrix category – for example, in the 1998-99 competition, the construction of foam cores proved extremely difficult and time consuming. With this consideration, the team decided to manufacture the fuselage with wood, using mainly balsa and light ply. Wood was also considered for the wing, but was too heavy for the design parameters. Other considerations for the wing, such as carbon fiber, all required a high skill level. Because of these considerations, the team decided to purchase custom foam core wings and wrap them in fiberglass. Doing so also removed the need for the high skill level needed to cut the foam cores and construct a mold for a pure fiberglass wing.

6.2. WING CONSTRUCTION

Based on the team's skills and Table 6-1, wood appeared to be the most favorable material for wing construction. As described above, however, the team did not choose wood construction. Based on past experience and the advice of model enthusiasts on the team, the team decided an all-wood wing, if built to adequately withstand the design loads, would be too heavy. Rather, it was determined that a fiberglass wrapped foam core wing would be preferable. An Internet search produced a company, RPV Industries, which produces custom foam cores. This proved ideal, as less work was required for the precision manufacture of the wing.

RPV Industries' method for manufacture satisfied the team's requirements for accuracy. They manufacture thin metal templates, which are placed on either side of blocks of expanded polypropylene foam. Then the company uses the "hot wire" approach to cut the foam. A thin stainless steel wire is stretched to the desired length and a current is run through the wire, which then follows the templates to create a smooth, precise semi-span. A quarter-inch round section was cut from the quarter chord of each semi span. Upon receiving the wing cores, the team cut dihedral into each semi-span. Graphite rods joined at the center were added to the cut grooves at the quarter chord, and the two halves were epoxied together with 30-minute epoxy.

Typical foam core wings for model aircraft are sheeted in some thickness of balsa, but the team again required more structural rigidity than balsa provides. The team then looked at covering the wing in a composite material, and selected fiberglass as the best material for this section due to its cost, which is significantly less than carbon fiber. With pre-formed wing cores, the complex and laborious task of constructing a mold was eliminated and senior members of the team were confident that wrapping the wing cores in fiberglass was within the teams' skill range. With materials selected, the team set target dates for wing manufacturing. These are presented in Table 6-2.

The team met with a structures and composite materials specialist to finalize the procedure for curing the fiberglass. For the wing he stressed the importance for accurate ply orientations, in order to ensure strength, stiffness, and damage tolerance. The first ply layer will be added starting from the trailing edge, continuing around the leading edge and back under to the trailing edge. Excess fabric will be allowed to extend beyond the trailing edge and trimmed off after the fiberglass had cured. The first ply layer will be saturated in epoxy resin and the excess removed. The second ply will then be added and again resin will be added and the excess removed. This process is to be repeated for all three layers of fiberglass. The cloth will then be covered in polyester release peel ply and bleeder/breather material. The wing will be vacuum bagged, and a tight seal will be ensured by plugging leaks with putty. The team plans to manufacture a curing oven from store-bought insulation board (such as Ultra-R®) and heat it with portable heating lamps. The heat will be applied in order to better allow the resin to flow and fill any voids created, and to allow excess resin to escape to the bleeder/breather material. All wrinkles in the vacuum bag will be worked to the back of the wing, and the apparatus placed in the curing oven overnight. When the wing is removed from the oven, the bleeder/breather and release cloth will be peeled off. After trimming the edges, the entire wing will be lightly sanded and covered in paint and lacquer to create a smooth finish.

The team plans to cut flaperons from the foam core and cover them in fiberglass via this method. Two ¼" balsa sheets will then be added to the foam at the joint to allow for the use of CA hinges to minimize the hinge gap created. The flaperon mixing of the team's Futaba 6XA transmitter will be activated, and one standard Futaba servo will be connected to each flaperon.

The center section of the wing will be trimmed in a shallow parabola to allow for the engine nacelles. The team will trim the wing in sections and sand to the correct dimensions. Light ply formers will be epoxied to this region for additional strength and support. Two ¼" dowels will be inserted in the front of the wing to mount the wing to the fuselage and two ¼" holes will be drilled in the aft section to allow for nylon wing bolts to secure the wing to the fuselage.

6.3. FUSELAGE CONSTRUCTION

Despite the many benefits of composite materials, the team felt that the accurate construction of a mold was too difficult and too expensive to be beneficial. There were also concerns about the integrity of the joint created between the two halves that would be formed. Wood was selected because it incorporated the lowest cost and skill level with the shortest construction time. After material selection the team established target dates for fuselage construction. These are presented in Table 6-3.

For construction, the fuselage was broken into key compartments and locations; bulkheads of ¼" balsa or 1/8" light ply were placed at these locations of the fuselage. These are presented in Table 6-4. The bulkheads will be hollowed out when possible to reduce weight. To install the bulkheads at the correct locations, a jig will be created. Spare balsa will be used to raise the bulkheads to the necessary height, where they will be pinned perpendicular to the construction table.

To build up the frame, longerons will be epoxied to the bulkheads along the sides and bottom of the fuselage; large spaces between bulkheads will be filled with structural pieces where necessary and the rest were filled with stringers. The wing attachment point on the fuselage will be reinforced with balsa and padded with foam rubber. The fuselage will be sheeted in 1/16" balsa, and a solid block of balsa will be added for the nose cone. After sanding the fuselage to final shape, lightweight balsa filler will be added and the fuselage covered in Top Flight Monokote™, a plastic shrink-wrap material.

6.4. TAIL FIN AND CANARD

Wood was also selected for both tail sections since it allowed for manufacturing to proceed rapidly and accurately without sacrificing strength. The team will manufacture the vertical fin and canard sections simultaneously, and will join them to the fuselage (refer to Table 6-4), before the finishing materials were added.

The team plans to assemble the vertical tail section as a traditional wood wing. Ribs will be cut from 3/32" balsa and joined to an upper and lower spar at the quarter-chord. This will be reinforced with vertical grain sheeting and sheeting of the front and rear sections of the tail. A half-inch gap will be cut at the hinge line and 1/4" balsa stock will be added to each section. The rudder will then be joined to the tail with CA hinges and a control horn added; both sections will be covered in Monokote™.

The canard surface will likewise be manufactured as a wood wing. Ribs will be added to upper and lower spars on a jig, which will allow the team to offset the spars. Doing this will ensure that epoxying the spars to a forward bulkhead attaches the canard at the proper incidence angle. The canard will be sheeted at the front and back with 3/32" balsa with a half-inch gap cut at the hinge line to allow for 1/4" stock. The elevators will be attached with CA hinges and aileron torque rods.

6.5 SYSTEMS INTEGRATION

All servos will be mounted on hardwood rails located in the forward compartment and in the wing for the flaperons. Flexible pushrods will be used to connect the rudder and nose gear to the appropriate servo. After being wrapped in foam to reduce vibrations, the receiver and battery will be placed in the forward compartment. The receiver wire will run through the plane and kept inside to reduce drag. The wire will run inside of fuel tubing around the NiCd batteries to help protect it from the heat generated. The elevators will operate with aileron torque rods connected inside of the fuselage. Landing gear, purchased from Robart, will be installed in the wing with the hardware provided. The nose gear will be attached to bulkhead #2 with 6-32 screws and locknuts.

<i>Material</i>	<i>Availability</i>	<i>Reparability</i>	<i>Strength/Weight</i>	<i>Skill Matrix</i>	<i>Time</i>	<i>Cost</i>
Wood	Excellent	Excellent	Fair	Low	Low	Low
Fiberglass	Excellent	Poor	High	High	Fair	Fair
Carbon Fiber	Good	Poor	Very High	High	Fair	High
Foam Core	Fair	Fair	Fair	High	Low	Low

Table 6-1. *Figures of Merit comparison*

<i>Task</i>	<i>Target Date</i>	<i>Date Completed</i>
Foam cores ordered	2/21	2/22
Fiberglass ordered	2/23	2/23
Lay up wing	3/3	TBD

Table 6-2. *Wing task schedule*

<i>Task</i>	<i>Target Date</i>	<i>Date Completed</i>
Structural design	2/25	2/24
Purchase materials	2/26	2/26
Components shaped	3/3	TBD
Frame completed	3/10	TBD
Sheeting and sanding	3/24	TBD
Finished	3/31	TBD

Table 6-3. *Fuselage task schedule*

<i>Bulkhead Number</i>	<i>Material</i>	<i>X from nose (in.)</i>	<i>Reason</i>
1	Balsa	2	Shape/Front of systems compartment
2	Ply	6.25	Canard attachment
3	Ply	9	Nose gear attachment
4	Ply	21	Control point/Front of payload compartment
5	Ply	35	Nacelle attachment
6	Ply	39	Back of nacelle/ Back of payload compartment
7	Balsa	49.5	End of battery compartment/Fin attachment
8	Balsa	54	End cap fairing/Fin attachment

Table 6-4. Bulkhead placement

REFERENCES

1. McCormick, B. W. Jr.; Aerodynamics of V/STOL Flight; Academic Press; New York, 1967
2. Abbot, I. H. and Von Doenhoff, A. E.; Theory of Wing Sections; Dover Publications, Inc.; New York, 1959
3. Selig, M.; UIUC Airfoil Coordinates Database; http://amber.aae.uiuc.edu/~m-selig/ads/coord_database.html; University of Illinois; Urbana, 1995
4. Raymer, D. P.; Aircraft Design: A Conceptual Approach; American Institute of Aeronautics and Astronautics; Reston, 1999
5. Roskam, J.; Methods for Estimating Stability and Control Derivatives of Conventional Subsonic Airplanes; published by the author; Lawrence, 1971
6. Roskam, J., and Lan, C. E.; Airplane Aerodynamics and Performance; DARcorporation; Lawrence, 1997
7. Roskam, J.; Flight Dynamics of Rigid and Elastic Airplanes; published by the author; Lawrence, 1972
8. Hoak, D. E.; Ellison, D. E. et al; USAF Stability and Control Datcom; Flight Control Division, Air Force Flight Dynamics Laboratory, Wright-Patterson Air Force Base, 1960
9. Kaw, A. K.; Mechanics of Composite Materials; CRC Press; Boca Raton, 1997
10. Hibbeler, R. C.; Mechanics of Materials; Prentice Hall; Upper Saddle River, 1997
11. Dietenberger, M. A., Green, D. W. et al; Wood Handbook; Forest Products Laboratory, USDA Forest Service, Madison, 1999
12. Anderson, J. D. Jr.; Fundamentals of Aerodynamics; McGraw-Hill, Inc.; New York, 1991

APPENDIX A

Motocalc Output

In-Flight Analysis - SF1
Sea Level

Motor: Aveox 1412/5Y Pattern 40; 585 RPM/V; 0.105 Ohms; 0.5A idle.

Battery: Sanyo 2000SCR; 20 cells; 2000mAh; 0.004 Ohms/cell.

Speed Control: Aveox M160; 0.007 Ohms; High rate.

Drive System: Kress AP-2 4.13"; 4.13x8.43 (1.75in hub).

Ducting: 4.13in D x 0in L (0° taper) intake; 4.13in D x 0in L (0° taper) exhaust.

AirSpd (MPH)	EPitch (in)	Batt Amps	Motor Amps	Motor Volts	Input (W)	Output (W)	Loss (W)	Effic (%)	SysEf (%)	Fan RPM	Thrust (oz)	Efflx (MPH)	Time (m:s)
0	8.43	28.9	28.9	21.5	620.9	524	96.9	84.4	75.6	10794	59.7	70.7	4:09
1	8.33	28.3	28.3	21.5	609.2	515.9	93.3	84.7	76	10863	59.1	70.3	4:15
2	8.24	27.7	27.7	21.6	597.5	507.8	89.7	85	76.5	10932	58.5	70	4:20
3	8.14	27.1	27.1	21.6	585.9	499.6	86.3	85.3	76.9	11000	57.9	69.6	4:26
4	8.05	26.5	26.5	21.7	574.4	491.4	83.1	85.5	77.3	11066	57.2	69.2	4:32
5	7.96	25.9	25.9	21.7	563	483.1	79.9	85.8	77.8	11132	56.6	68.8	4:38
6	7.86	25.3	25.3	21.8	551.7	474.9	76.8	86.1	78.2	11197	55.9	68.4	4:44
7	7.77	24.7	24.7	21.8	540.5	466.6	73.9	86.3	78.6	11261	55.3	68	4:51
8	7.68	24.2	24.2	21.9	529.3	458.3	71	86.6	79	11325	54.6	67.6	4:58
9	7.6	23.6	23.6	21.9	518.3	450	68.3	86.8	79.4	11387	54	67.2	5:05
10	7.51	23.1	23.1	22	507.3	441.7	65.7	87.1	79.8	11449	53.3	66.8	5:12
11	7.42	22.5	22.5	22	496.5	433.4	63.1	87.3	80.2	11510	52.6	66.4	5:20
12	7.33	22	22	22.1	485.7	425.1	60.7	87.5	80.5	11570	51.9	65.9	5:27
13	7.25	21.5	21.5	22.1	475.1	416.7	58.3	87.7	80.9	11629	51.3	65.5	5:35
14	7.17	20.9	20.9	22.2	464.5	408.4	56	87.9	81.3	11688	50.6	65.1	5:44
15	7.08	20.4	20.4	22.2	454	400.2	53.9	88.1	81.6	11745	49.9	64.6	5:52
16	7	19.9	19.9	22.3	443.7	391.9	51.8	88.3	82	11802	49.2	64.2	6:01
17	6.92	19.4	19.4	22.3	433.4	383.6	49.8	88.5	82.3	11858	48.5	63.7	6:11
18	6.83	18.9	18.9	22.4	423.2	375.4	47.8	88.7	82.6	11913	47.8	63.3	6:20
19	6.75	18.4	18.4	22.4	413.2	367.2	46	88.9	82.9	11968	47.1	62.8	6:30
20	6.67	18	18	22.4	403.2	359	44.2	89	83.2	12021	46.4	62.3	6:41
21	6.59	17.5	17.5	22.5	393.4	350.9	42.5	89.2	83.5	12074	45.7	61.9	6:51
22	6.51	17	17	22.5	383.7	342.8	40.8	89.4	83.8	12126	45	61.4	7:03
23	6.44	16.6	16.6	22.6	374	334.8	39.3	89.5	84.1	12178	44.3	60.9	7:14
24	6.36	16.1	16.1	22.6	364.5	326.7	37.8	89.6	84.4	12228	43.6	60.4	7:26
25	6.28	15.7	15.7	22.6	355.1	318.8	36.3	89.8	84.7	12278	42.9	59.9	7:39
26	6.2	15.3	15.3	22.7	345.8	310.9	35	89.9	84.9	12327	42.2	59.4	7:52
27	6.13	14.8	14.8	22.7	336.7	303	33.7	90	85.2	12375	41.5	58.9	8:06
28	6.05	14.4	14.4	22.7	327.6	295.2	32.4	90.1	85.4	12422	40.7	58.4	8:20
29	5.97	14	14	22.8	318.7	287.5	31.2	90.2	85.6	12469	40	57.9	8:35
30	5.9	13.6	13.6	22.8	309.8	279.8	30.1	90.3	85.9	12515	39.3	57.4	8:50
31	5.82	13.2	13.2	22.9	301.1	272.2	29	90.4	86.1	12560	38.6	56.8	9:06
32	5.75	12.8	12.8	22.9	292.6	264.6	27.9	90.5	86.3	12604	37.9	56.3	9:23
33	5.67	12.4	12.4	22.9	284.1	257.2	26.9	90.5	86.5	12648	37.2	55.8	9:41
34	5.6	12	12	23	275.8	249.8	26	90.6	86.6	12691	36.4	55.2	9:59
35	5.53	11.6	11.6	23	267.5	242.4	25.1	90.6	86.8	12733	35.7	54.7	10:19
36	5.45	11.3	11.3	23	259.5	235.2	24.3	90.7	86.9	12774	35	54.1	10:39
37	5.38	10.9	10.9	23.1	251.5	228	23.5	90.7	87.1	12815	34.3	53.6	11:00
38	5.31	10.6	10.6	23.1	243.7	221	22.7	90.7	87.2	12854	33.6	53	11:22
39	5.24	10.2	10.2	23.1	235.9	214	22	90.7	87.3	12893	32.9	52.5	11:45
40	5.16	9.9	9.9	23.1	228.4	207.1	21.3	90.7	87.4	12932	32.2	51.9	12:10

APPENDIX A

Motocalc Output

AirSpd (MPH)	EPitch (in)	Batt Amps	Motor Amps	Motor Volts	Input (W)	Output (W)	Loss (W)	Effic (%)	SysEf (%)	Fan RPM	Thrust (oz)	Efflx (MPH)	Time (m:s)
41	5.09	9.5	9.5	23.2	220.9	200.3	20.6	90.7	87.5	12969	31.5	51.3	12:35
42	5.02	9.2	9.2	23.2	213.6	193.6	20	90.6	87.6	13006	30.7	50.7	13:02
43	4.95	8.9	8.9	23.2	206.4	186.9	19.4	90.6	87.7	13042	30	50.1	13:30
44	4.88	8.6	8.6	23.3	199.3	180.4	18.9	90.5	87.7	13077	29.3	49.6	14:00
45	4.81	8.3	8.3	23.3	192.4	174	18.4	90.4	87.7	13112	28.6	49	14:31
46	4.73	8	8	23.3	185.6	167.7	17.9	90.4	87.8	13146	27.9	48.4	15:04
47	4.66	7.7	7.7	23.3	178.9	161.5	17.4	90.3	87.7	13179	27.2	47.8	15:39
48	4.59	7.4	7.4	23.4	172.4	155.4	17	90.1	87.7	13211	26.6	47.1	16:15
49	4.52	7.1	7.1	23.4	166	149.4	16.6	90	87.7	13242	25.9	46.5	16:54
50	4.45	6.8	6.8	23.4	159.8	143.5	16.2	89.8	87.6	13273	25.2	45.9	17:35
51	4.38	6.6	6.6	23.4	153.7	137.8	15.9	89.7	87.5	13303	24.5	45.3	18:18
52	4.31	6.3	6.3	23.5	147.7	132.1	15.6	89.5	87.4	13333	23.8	44.7	19:03
53	4.24	6	6	23.5	141.8	126.6	15.3	89.2	87.3	13361	23.2	44	19:52
54	4.17	5.8	5.8	23.5	136.1	121.2	15	89	87.1	13389	22.5	43.4	20:43
55	4.1	5.6	5.6	23.5	130.6	115.9	14.7	88.7	87	13416	21.8	42.8	21:37
56	4.03	5.3	5.3	23.5	125.1	110.7	14.5	88.4	86.7	13443	21.2	42.1	22:34
57	3.96	5.1	5.1	23.6	119.8	105.6	14.2	88.1	86.5	13469	20.5	41.5	23:35
58	3.89	4.9	4.9	23.6	114.7	100.7	14	87.8	86.2	13494	19.9	40.8	24:40
59	3.82	4.6	4.6	23.6	109.7	95.9	13.8	87.4	85.9	13518	19.2	40.1	25:49
60	3.75	4.4	4.4	23.6	104.8	91.2	13.6	87	85.6	13542	18.6	39.5	27:02
61	3.68	4.2	4.2	23.6	100.1	86.6	13.5	86.5	85.2	13564	18	38.8	28:20
62	3.61	4	4	23.6	95.5	82.1	13.3	86	84.8	13587	17.4	38.1	29:43
63	3.54	3.8	3.8	23.7	91	77.8	13.2	85.5	84.3	13608	16.7	37.4	31:12
64	3.47	3.7	3.7	23.7	86.7	73.6	13.1	84.9	83.8	13629	16.1	36.8	32:47
65	3.4	3.5	3.5	23.7	82.5	69.6	12.9	84.3	83.3	13649	15.5	36.1	34:28
66	3.33	3.3	3.3	23.7	78.5	65.6	12.8	83.6	82.6	13668	15	35.4	36:16
67	3.26	3.1	3.1	23.7	74.6	61.8	12.7	82.9	82	13687	14.4	34.7	38:11
68	3.19	3	3	23.7	70.8	58.2	12.6	82.1	81.2	13705	13.8	34	40:14
69	3.12	2.8	2.8	23.8	67.2	54.6	12.6	81.3	80.5	13722	13.2	33.3	42:26
70	3.05	2.7	2.7	23.8	63.7	51.2	12.5	80.4	79.6	13739	12.7	32.6	44:48
71	2.98	2.5	2.5	23.8	60.3	47.9	12.4	79.4	78.7	13755	12.1	31.8	47:19
72	2.91	2.4	2.4	23.8	57.1	44.7	12.4	78.3	77.6	13771	11.6	31.1	50:01
73	2.84	2.3	2.3	23.8	54	41.7	12.3	77.2	76.5	13785	11	30.4	52:55
74	2.77	2.1	2.1	23.8	51	38.7	12.3	75.9	75.3	13799	10.5	29.7	56:01
75	2.7	2	2	23.8	48.2	35.9	12.2	74.6	74.1	13813	10	28.9	59:21
76	2.63	1.9	1.9	23.8	45.5	33.3	12.2	73.2	72.7	13826	9.5	28.2	1:02:55
77	2.55	1.8	1.8	23.8	42.9	30.7	12.2	71.6	71.2	13838	9	27.5	1:06:44
78	2.48	1.7	1.7	23.9	40.4	28.3	12.1	70	69.5	13850	8.5	26.7	1:10:49
79	2.41	1.6	1.6	23.9	38.1	26	12.1	68.2	67.8	13861	8.1	26	1:15:11
80	2.34	1.5	1.5	23.9	35.9	23.8	12.1	66.3	65.9	13871	7.6	25.2	1:19:51
81	2.27	1.4	1.4	23.9	33.8	21.7	12.1	64.3	63.9	13881	7.1	24.5	1:24:49
82	2.2	1.3	1.3	23.9	31.8	19.7	12.1	62.1	61.8	13890	6.7	23.7	1:30:07
83	2.12	1.3	1.3	23.9	29.9	17.9	12	59.8	59.5	13899	6.3	22.9	1:35:44
84	2.05	1.2	1.2	23.9	28.2	16.2	12	57.3	57.1	13907	5.9	22.2	1:41:42
85	1.98	1.1	1.1	23.9	26.6	14.5	12	54.7	54.5	13915	5.5	21.4	1:47:59
86	1.91	1	1	23.9	25	13	12	52	51.8	13922	5.1	20.6	1:54:36
87	1.83	1	1	23.9	23.6	11.6	12	49.1	49	13929	4.7	19.9	2:01:32
88	1.76	0.9	0.9	23.9	22.3	10.3	12	46.2	46	13935	4.3	19.1	2:08:45
89	1.69	0.9	0.9	23.9	21.1	9.1	12	43.1	42.9	13941	4	18.3	2:16:14
90	1.62	0.8	0.8	23.9	19.9	8	12	39.9	39.8	13946	3.7	17.5	2:23:56

APPENDIX B **CG Calculations**

Component	x_i (in.)	quantity	unit weight (oz)	total weight (oz)	Moment (oz-in)
receiver	3.00	1	0.96	0.96	2.9
receiver battery	3.00	1	3.52	3.52	10.6
rudder servo	5.00	1	1.60	1.60	8.0
canard servo	5.00	1	1.60	1.60	8.0
aileron servo	45.00	1	1.60	1.60	72.0
battery packs	15.75	2	20.00	40.00	630.0
battery packs	44.25	2	20.00	40.00	1770.0
speed controller	32.25	2	2.00	4.00	129.0
1412/5Y motor	38.00	2	10.25	20.50	779.0
fan	36.00	2	4.00	8.00	288.0
canard	6.56	1	3.00	3.00	19.7
wing	36.26	1	30.00	30.00	1087.8
fin	52.27	1	3.00	3.00	156.8
nose gear	9.04	1	5.00	5.00	45.2
main gear	32.62	2	4.00	8.00	261.0
fuselage	26.60	1	16.00	16.00	425.6
payload	30.48	4	38.10	152.40	4645.2
<i>total</i>				<i>339.18</i>	<i>10338.6</i>

	max	ferry	
weight	21.20	11.67	lbf
CG	30.48	30.48	in

payload fraction 0.449

1999/2000 AIAA Foundation/Cessna/ONR Design/Build/Fly Competition

PROPOSAL FOR THE DESIGN OF AN UNMANNED AIR VEHICLE PART II: ADDENDUM PHASE

Submitted 7 April 2000

Prepared for Dr. D. W. Levy, Cessna Aircraft Company

By Syracuse University

Nick Borer, Project Leader

Jessica Lux

Reid Thomas

Jason Farkas

Eliza Honey

Tori Garnier

Renea LaRock

Keith Fuhrhop

Alex Ansah-Arkorful

Hezkhel Teferra

Dr. V. R. Murthy, Faculty Advisor

TABLE OF CONTENTS

TABLE OF CONTENTS	i
7. LESSONS LEARNED	1
7.1. Design Changes Implemented	1
7.1.1. Wing	1
7.1.2. Flaperon Sizing	2
7.1.3. Landing Gear Placement	2
7.2. Lessons from This Year	2
7.3. Future Considerations	3
8. AIRCRAFT COST	5
8.1. Rated Aircraft Cost	5
8.2. Rated Aircraft Cost Comparisons	5

TABLES

8-1. <i>Rated Aircraft Cost</i>	6
8-2. <i>Rated Engine Power Calculation</i>	6
8-3. <i>Work Breakdown Structure for Calculation of Manufacturing Man Hours</i>	6

7. LESSONS LEARNED

The SF1 incorporates a number of design features that are unique when compared to previous entries, both by Syracuse University and other competing schools. Over the course of the design and construction of the actual airframe, several changes have been made and many suggestions noted for future reference.

7.1. DESIGN CHANGES IMPLEMENTED

The final configuration of the SF1 as described in the proposal phase is virtually identical to the configuration of the completed aircraft. However, some subtle changes were made either to ease construction or as a result of further analyses.

7.1.1. Wing

The wing was the most heavily modified structure of the aircraft. While cosmetically and aerodynamically similar, the wing on the actual SF1 was manufactured from wood, as opposed to the foam core with fiberglass skin originally proposed.

A foam core wing was constructed and draped with fiberglass as outlined in the proposal phase during mid-March. However, the resulting structure, while strong, emerged deformed and with a grievous amount of surface wrinkles. Both of these aspects would have adverse effects on the aerodynamic characteristics of the wing, and it did not seem that these poor surface and shape qualities could be fixed with any amount of sanding and filling. Therefore, the team had to construct another wing.

The team lacked funds and time to procure another foam-core wing, so an alternative design was presented for the structure of the new wing. Some team members had experience building wing structures from wood, as two Syracuse University's previous entries utilized such a structure. Typical wood-wing design involves a number of ribs cut in the shape of the airfoil attached via a central spar to counter bending loads. Smaller, non-structural members are placed at the leading and trailing edges of the ribs to help maintain a three-dimensional shape. Thin wood sheeting is attached from the leading edge to the spar to provide torsional rigidity. The entire wing is then wrapped in a thin, lightweight heat-shrink plastic to form a smooth aerodynamic surface.

The new wing structure was analyzed for bending loads only, as these would be the primary flight loads the wing would encounter and most likely the driver of the design. The structural analysis was carried out much in the same fashion as described for the wing in the proposal phase, except that the skin was neglected and two spars were considered instead as the primary load bearing members. These spars were initially guessed to have a cross-section of $\frac{1}{2}$ -inch by $\frac{1}{2}$ -inch, as this represents a common dimension available for most aircraft-grade hardwoods. Spruce was the material of choice due to its strength, lower cost, and relatively light weight.

It was important to place the spars at the farthest vertical distance possible within to wing in order to maximize its moment of inertia. This was accomplished by placing the spars at 40% of the chord of the wing, as this was where the airfoil reached its maximum thickness.

The bending loads were then calculated at the root of the wing per the methods of the proposal phase. The first iteration of the wing design proved to be sufficient, so the wing spars as described were utilized. When neglecting the stiffness contribution of all other structural members, the new wing was predicted to withstand approximately 8.9 g's. This was deemed sufficient in light of the maximum expected flight loads of seven g's, resulting in a factor of safety of 1.27. While this was not very high, it was the best that could be done to keep the wing as light as possible. Furthermore, the wood wing received a boost in crashworthiness, as it is far easier to repair in the field if it were to break due to a bad landing or crash.

Other wing materials and dimensions were determined from experience and rules of thumb. The ribs were set at a spacing was set at a maximum of four inches, with some smaller regions to accommodate the flaperons. The 24 ribs 3/32-inch balsa sheet, as was the leading edge sheeting. The leading edge piece was manufactured from 3/8-inch balsa stock, while the two trailing edge supports were each cut from 1/4-inch balsa stock. Each of the rib bays where the main landing gear was to be attached was reinforced with 1/8-inch plywood sheets. The main gear itself was set into a large, heavy block of basswood attached to these sheets.

This resulted in a wing structure that was approximately 42 ounces, 12 ounces heavier than that predicted for the fiberglass/foam core structure. The entire wing structure was designed and built in just seven days due to the time crunch that the failed fiberglass wing imposed.

7.1.2. FLAPERON SIZING

The change in the wing structure resulted in a small change in the flaperon sizing. Previously, the flaperons had a chord length of 20% of the local wing chord and spanned from 20% to 90% of the wing semi-span. The spanwise length and location of the flaperon was changed to better accommodate the wood wing structure such that it would extend between the third and eleventh rib in each wing half. This resulted in a flaperon spanning from eight inches to 38 inches from the wing axis of symmetry, an increase of six-tenths of an inch. This would have little effect on the overall aircraft performance, and resulted in a structure that was easier to fabricate.

7.1.3. LANDING GEAR PLACEMENT

A minor change was made in the placement of the main landing gear. As originally proposed, centerline of the aircraft was located eight inches from the ground. The tipback angle of the main gear, as described in Reference 4, should be about 15 degrees. With the previous dimensions, this indicated locating the main gear 2.14 inches back from the center of gravity of the SF1. The minimum overturn angle of 63 degrees indicated that each main gear strut should have a lateral distance from the center of gravity of at least 8.72 inches.

The arrival of the landing gear struts from the manufacturer resulted in a change of the landing gear placement. The strut for the nose gear could not be cut or placed higher than a given point in the fuselage for structural reasons. This, combined with the required 3.5-inch wheel, resulted in a centerline-to-ground distance of approximately 10 inches.

This new height was considered in locating the main landing gear. In order to maintain the 15-degree tipback angle, the main gear was relocated to a point 2.68 inches back from the center of gravity. The minimum lateral distance of the main gear from the center of gravity was then revised to be 10.90 inches. This value was pushed up to 11 inches for ease of record keeping and manufacture.

7.2. LESSONS FROM THIS YEAR

Perhaps the single biggest lesson from the fabrication of this year's entry came in the form of a failure. This is the mishap with the foam core wing, which, when considering the combined costs of the material and hardware required, set the team back \$400, a substantial fraction of the team's budget.

The failure was the result of poor planning more than anything else. In order to try to stay ahead of schedule and save precious material (and thus money), the fiberglass for the wing was laid up without testing a piece in the proposed set-up. This set-up was characterized by laying up the plies on the foam wing one at a time while wetting out the fibers with resin, smoothing out the plies, and then placing the entire assembly in a vacuum bag to rid the wing of excess resin and thus weight. The vacuum-bagged wing was placed inside a curing oven fashioned from aluminum-sided insulation with two heat lamps and circulating fans placed inside.

This process was believed to be the most efficient way to manufacture the wing. There was some concern for the vacuum bagging process, as it might lead to some surface wrinkling. The team predicted that these wrinkles would be small, however, and could be kneaded out of the bag to the excess at the trailing edge (to be trimmed later) before it was placed in the oven to cure.

The vacuum bagging proved to be the wing's undoing, but not because of the wrinkles. The team, working on the assurances of the foam-core manufacturer, believed that the foam would not react to the resin, which was true. The foam, however, was porous, which was not considered at any phase of the design. As such, the vacuum removed any excess air from small pockets within the wing, which caused it to deform. Also, some of the resin seeped into these small pockets in the foam core instead of the bleeder/breather material. This caused local changes in the material properties of the foam, resulting in increased deformation and wrinkling of the plies. The final product was a relatively strong structure with a poor shape and surface finish – completely unsatisfactory for the wing of any aircraft.

The lesson here was simple – a small piece of the foam, shipped as packing material with the original foam core wing, should have been tested prior to full-scale fabrication of the wing. The resulting structure would likely be deformed, which would lead the team to the same conclusions found above. Since a smooth surface finish without deformation was possible without the vacuum, the procedure outlined previously would be modified to exclude the vacuum-bagging portion. This would have resulted in a slightly heavier structure than planned for due to the excess resin in the fiberglass, but still would have been quite satisfactory.

Other lessons came from fabricating the wing. The fiberglass, as first cut, fit the wing well, with some overlap. The ply angles were carefully calculated when considering the cut of the fabric, and all seemed well. However, this particular fiberglass, being very fine, stretched and shrank very easily when pulled at approximately 45 degrees (a direction in which there were no fibers). When draped over the wing, the ± 45 degree plies stretched very easily. At first, the team members "painted" the resin on with chordwise strokes and dabs, which stretched the fibers downward and resulted in voids in the spanwise direction. As such, several patches had to be cut to fill these voids. The middle 0/90 degree ply went on much more smoothly, and it was discovered that the team members should "paint" in the same direction as the fibers as to not stretch or pull the fabric. The third ply, again at a ± 45 degree orientation, was wet out using this technique, and thus the number of patches necessary reduced.

This sort of "on-the-job" training, if nothing else, was certainly valuable to the underclassmen associated with the team. This provided an excellent learning experience in the peculiarities of the construction of a composite component. Too often, it seems, one hears "make that part from a composite material." While this is often the wisest decision from a design engineering standpoint (in terms of weight or strength benefits), it may not be the best from a manufacturing standpoint, especially for what amounts to a prototype.

The biggest lesson for everyone involved was the merging of theory and reality. Students are asked to design a real aircraft for a real-life application. Too often, it seems, students get bogged down with theory and do not perceive how it relates to reality. As always, the biggest, and perhaps hardest lesson is that nothing in life is isentropic.

7.3. FUTURE CONSIDERATIONS

The design presented for the proposal phase of this competition represented the cumulative work and knowledge of all of the team members and the suggestions of various advisors. It was as complete and thorough as the team believed necessary at the time. However, some further analysis may have resulted in a slightly more optimized design.

As mentioned in the original proposal, stability was considered an area that needed greater scrutiny than in years past. This was accomplished by investigating the basic static stability derivatives of the aircraft, and by establishing criteria for longitudinal static stability. While this is sufficient, future teams may find it useful and rewarding to investigate the dynamic stability of the aircraft.

Further structural analyses may also be necessary as weights rise or dramatic configurations are considered. All of the structural analyses of the SF1 were carried out for simple bending only, and the members designed for the worst case loading condition and location (e.g. bending stress only at the wing root). In the case of the wing, a tapered spar could be considered to reduce weight.

Furthermore, the wing lift distribution used in these calculations was a crude approximation based in part on two-dimensional airfoil theory. Following the submission of the design report, senior team members became aware of a method that resulted in spanwise lift distributions that were accurate within a few percent. This, combined with an in-depth study of the drag distribution (based on surface area and section lift), could have resulted in a wing structure better tailored to the loads it is expected to experience. Ultimately, this would most likely have led to a lighter weight design.

Graduate student assistance could be a great help as well. Many graduate students at Syracuse University take courses in computational fluid dynamics, which could be of great help to eliminate areas of increased drag and flow separation. Also, some critical areas could be identified that may not otherwise be found without additional flight tests.

Suggestions for manufacturing are mostly for the fabrication of composite parts. Teams from Syracuse University have worked with wood structures for all four entries now, so more exposure to composite materials and methods of manufacture would be a plus. Certainly, team members know now not to vacuum-bag over a part manufactured from EPP foam. Other, non-primary flight structures could be tried as composites first, such that a failure would not set the team reeling, financially or otherwise.

As hoped, the progress of this year's entry was accelerated when compared to previous years. However, setbacks (such as that with the wing) made a tight schedule even tighter, and as such the team will only have two days to subject the design to flight tests before sending it to the competition site. Better communication and planning could have resulted in fewer problems and earlier progress, creating less havoc near critical contest deadlines. Also, more flight tests mean better pilot familiarity with the aircraft, which is always a plus when the contest arrives.

The SF1 represents the hard work and dedication of all team members for eight months or more. The experience of designing and building this aircraft will remain with them all for the rest of their lives, professional or otherwise, and has left its mark as a positive learning experience for those involved. Some team members will continue on with the knowledge they have for future teams, but all will apply it to their future classes and careers.

8. AIRCRAFT COST

The rated aircraft cost is calculated via a contest supplied model, based on the airframe weight, rated engine power, and the manufacturing man hours for the aircraft.

8.1. RATED AIRCRAFT COST

The aircraft cost equation, as supplied in the contest rules, is given by

$$\text{Rated Aircraft Cost, \$ (Thousands)} = (A * \text{MEW} + B * \text{REP} + C * \text{MFHR}) / 1000 \quad (1)$$

where A is the Manufacturer's Empty Weight Multiplier, B is the Rated Engine Power Multiplier, and C is the Manufacturing Cost Multiplier. MEW is the Manufacturer's Empty Weight, REP is the Rated Engine Power, and MFHR refers to the Manufacturing Man Hours for the aircraft.

Parameters A, B, and C are contest-supplied figures. The values of these multipliers are provided in Table 8-1. The Manufacturer's Empty Weight refers to the weight of the airframe, in pounds, without payload or batteries. Rated Engine Power is the product of the number of motors, 50 Amps (a standardized current draw), 1.2 volts per cell, and the number of cells. The calculation for the SF1's REP is provided in Table 8-2. The Manufacturing Man Hours can be calculated through the work breakdown structure detailed in Table 8-3. Team Syracuse's calculated values for MEW, REP, and MFHR, and the final Rated Aircraft Cost (RAC), are provided in Table 8-1.

By using the values from Table 8-1 in the Rated Aircraft Cost equation provided above, Team Syracuse arrived at a RAC of 5.40. This number is slightly higher than the team's predicted RAC, as discussed below.

8.2. RATED AIRCRAFT COST COMPARISONS

The expected RAC for the SF1, based on the final design parameters, was 5.21. Changes in materials and construction techniques led to the difference observed between the theoretical and actual values for the RAC.

Only one aspect of the RAC calculation—the Manufacturer's Empty Weight—could reasonably be altered during construction. The Rated Engine Power remained constant, as the team did not change the number of motors or batteries used. The Manufacturing Man Hours also remained constant, because no design changes which added or reduced the number of components occurred. Only the value of the MEW, based solely on the airframe weight, changed during construction.

The team predicted a MEW of 7 pounds, but the actual value, as seen in Table 8-1 was almost two pounds heavier. The wood wing, as discussed in section 7.1.1., added another 12 ounces to this weight. The ducts added another six ounces on top of the five calculated for the fan weight, contributing a total of 12 more ounces to the airframe weight. The remaining six ounces likely came from other sources – control rods, balsa reinforcements, and wiring. These were thought to be accounted for with a "fudge factor" in the initial weight estimation, but it appears the value arrived at was not enough.

Parameter	Value
A	100
B	1
C	20
MEW	8.9
REP	2400
MFMH	105.68
Rated Aircraft Cost (Thousands of dollars)	5.40

Table 8-1. Rated Aircraft Cost

Parameter	Value
No. of Motors	2
No. of cells	20
Rated Engine Power	2400

Table 8-2. Rated Engine Power Calculation

Component	Value	Multiplier	Manufacturing Hours
Wing	15 hr./wing		5
Sq. ft. of area	74 hr./sq. ft. area		28
Fuselage	15 hr./body		5
Ft. of length	4.674 hr./ft. of length		18.68
Empenage	15 hr.		5
vertical surface	15 hr./vertical surface		5
horizontal surface	110 hr./horizontal surface		10
Flight systems	15 hr.		5
servos	41 hr./servo		4
Propulsion Systems			
motors	25 hr./engine		10
fans	25 hr./propeller or fan		10
Total MFMH			105.68

Table 8-3. Work Breakdown Structure for Calculation of Manufacturing Man Hours



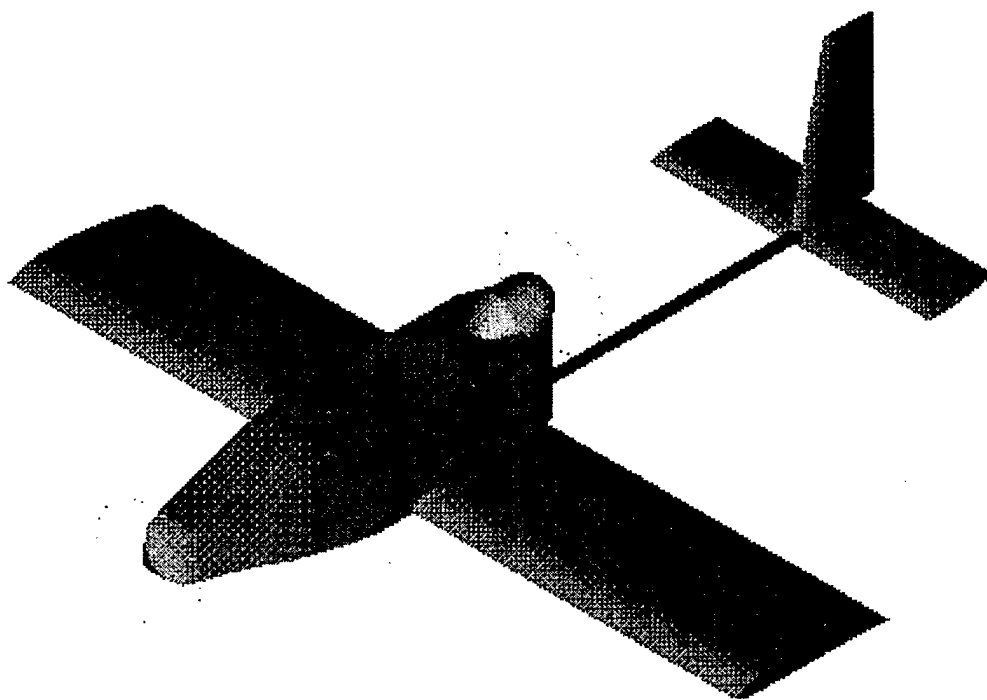
Università degli Studi di Roma "La Sapienza"
Facoltà di Ingegneria / Dipartimento Meccanica e Aeronautica



AIAA Student Design/Build/Fly Competition 1999/00

DESIGN REPORT

PROPOSAL PHASE



GALILEO

CONTENTS

1. EXECUTIVE SUMMARY
2. MANAGEMENT SUMMARY
3. CONCEPTUAL DESIGN
4. PRELIMINARY DESIGN
5. DETAIL DESIGN
6. MANUFACTURING PLAN

Section 1: *Executive summary*

The process leading the RPV realization can be divided into the following phases:

- Design development (conceptual, preliminary and detail)
- Knowledge acquisition
- Team management
- Sponsorship and external support
- Model building
- In-flight test

It is easily understandable how strictly these steps are linked, so that, during the design and building process, we often have to change our minds and the decisions we had already made. However, here we will try to summarize the leading line we followed.

On the base of D/B/F 1999/2000 rules we considered several possible concepts, answering the requirements, and among them the preliminary development process selected the one would had become "Galileo".

In this first choice we tried to carry out a model which would satisfy take-off performances' ties and would totalize a good competition's score.

At the beginning, we had to chose our design strategy between two possible main configurations:

- *fast and light*
- *slow and heavy*

we spent some time in trying to answer this question, and we opted for the possibility of carrying a lot of pay-load, for lower number of sorties. Once this first decision had been made, we determined the development's main areas that the project needed to be investigated:

- Flight mechanics
- Aerodynamics
- Structures
- Propulsion

At this time a specific development area and a defined task in team's management has been assigned to each member. Better, the team was divided into four groups, working independently but always in touch, to develop the detail design.

So we underlined the problems directly connected with the model's realization:

- Low Reynolds number flow
- Electric engine
- Electric power
- Materials
- Servo-controls

The tools we used in this phase are:

- MILS8 : a potential flow simulator designed by eng. Luca Cistriani to study interacting lifting surfaces.
- MOTOR1 : a software for evaluating the performances of the propulsive system, by L. Cistriani.
- TAKE-OFF : another s/w by L. Cistriani, for evaluating take-off performances.
- AUTO CAD : Computer aided design.
- Microsoft Word and Excel.

At the same time, we realized we needed some collaboration from outside our team.. Actually, a lot of time has been spent in trying to find a sponsorship (in fact, from such point of view we have not had any help from University, even though the efforts of our advisor). Unfortunately searching in the world of modelers, model shops, UAV industries, only a few subjects appeared interested. But at last someone was sensitive to

our need. In fact we would not be able to carry on our work without the fundamental help from "Istituto Tecnico Industriale Statale Galileo Galilei" of Rome, our main sponsor : a high school which gave us the material and the laboratories to build our model. This collaboration school-university, which has been possible thanks to the interest of the head of the I.T.I.S. Galilei, and to prof. Giorgio Sforza (who believed since the beginning in our capabilities), has been important for us, but also for the school-students, who had the opportunity to follow each phase of the development process. It is to thank the kind people we met there we gave to our project the name "GALILEO".

We do not neglect the help we received from AIDAA (Italian Association of Aeronautics and Astronautics) thanks to the concern of prof. Mario Marchetti, and from a few modelers who were enthusiast to help us with their precious suggestions. In particular we are glad to thank Mr. Tommaso Gabrielli, whose experience in models' building helped us to solve the manufacturing's problems, and Mr. Angelo Silvagni, for his suggestions about power plant's use and management. We would like also to thank our advisor, prof. Guido De Matteis, for his support.

And we can not end this presentation chart without thanking eng. Luca Cistriani, whose the advice and inciting have been a continuous stimulus for our work.

Section 2: Management Summary

Team's members are students in Aerospace Engineering at "la Sapienza" University of Rome. On the base of last year's experience, when only three students took a part in the D/B/F contest, this year the number of sharing has increased. A few students offered some help or effectively entered in the team, but also this year three of them abandoned us during the conceptual design's phase, when our difficulties seemed to be really enormous. However seven students have taken part in Galileo's project until now. So, it has been possible to assign to each of us a basic development's area, according to the specific interest of each one, so that the team this year could have a more organized architecture, as it follows:

student	basic assignement area
Argentini Enrico	Flight Mechanics and Computer Design
Fabiani Fabrizio	Aerodynamics
Giovannini Andrea	Flight Mechanics, on board systems
Greco Paolo	Structures
Puccica Filiberto	Structures
Sbaraglia Luca	Propulsion and preliminary designer
Tromboni Pier Domenico	Structures

Better, this was our first idea, trying to give the team a well defined architecture. Actually, during the development's process, we felt the need to coordinate the work of each of us. So, being absent a system's chief architect, each one had to take a part in the work of each other. This trend has been accentuated in the building process, a phase in which nobody of us had an his own experience. However, we thought to individuate some different areas, as in the following scheme but we have to said this was only a general direction:

• building work director	Filiberto
• builders	all of us
• configuration controller	Enrico, Pier Domenico
• sponsor relationship curators	Luca, Andrea, Paolo
• materials suppliers	Luca, Andrea, Paolo
• report preparation director	Enrico, Luca, Paolo
• report writers	all of us
• computer designer	Enrico

It has to be said that very important has been for us the collaboration of Andrea Giovannini, who took in our team the experience of last year D/B/F.

A plan has been made to fix the timings of the whole development process; it is shown in the following table. We have to say that it gives an indication of the actual timings (especially for the beginning, when all of us were busy in studying for University exams):

- 1 Oct-1 Nov: preliminaries
- forming the design team
 - acquiring know-how
 - looking for sponsorship

1 Nov-1 Dec: conceptual design

- analyses of possible different solutions
- selecting the target concept

1 Dec-1 Jan: preliminary design

- development methods
- defining all the parameters of the target concept
- selecting sponsors
- assigning the design areas

1 Jan-15 Jan: detail design

- sizing the various components
- check up performances
- supplying materials

15 Jan-20 Mar: fabrication process

13 Mar: presentation of proposal phase written report

20 Mar-10 Apr: (not only) flight tests

- mounting and dismounting
- aircraft performances
- competition's crew's training
- performing a competition's simulation

10 Apr: transfer to the contest site: Wichita, Kansas, USA

15 Apr: fly-off

We would like to underline here we have realized that the aspects of financing and sponsor relationship are much more important to the project's success than we thought before. However, the improvement in such aspects we had this year with respect to last year D/B/F, the kindness and the interest of the people we met, the contacts we got, the practical realization of the model leave us hoping that the students who follow us will find less troubles in their work, and we are sure their number will increase.

Section 3: *CONCEPTUAL DESIGN*

Introduction

The main target of this section of design was to find a concept which optimised the function:

$$SI = SFS/RAC$$

Here: SI = Score Indication
SFS = Single Flight Score
RAC = Rated Aircraft Cost

So we produced a parallel study either for the design parameters and for the FOMs

3.1 Design parameters

The design parameters considered are :

free

independent

TOW= Take Off Weight
Number of cells

statistic

WPL= Pay Load Weight
Number of motors
WE= Empty Weight
Wing Surface
Length of aircraft

fixed

Wing Span
Thrust Weight ratio
Time of each phase of flight
Take Off Watt per Kg of TOW
Cruise Watt per Kg of TOW
Mean motor thrust
Mean motor Weight

The free-independent parameters are those we increase, while the free-statistic parameters are those jointed to independent parameters with statistic correlations deduced from studies about UAVs.

The fixed parameters are those imposed from fundamental requirements which must be satisfied (thrust-weight ratio), regulations of competition, rules of thumb, requirements of commercial products.

FRN = Flight Rounds Number (1 flight round = 1 full lap with payload + 2 full laps with no payload)

These design parameters have seemed to be important because they give an estimation of the RAC and of the SFS and more they lead to a specific shape of the concept able to optimise the SI.

3.2 Alternative concepts

The design parameters draw at point 3.1 must have the following characteristics:

- The highest thrust, therefore more than one motor.
- The highest wing surface, therefore tandem-wing or canard configuration

This involves a choice which goes towards a configuration "Slow and heavy" rather than one "fast and light" as is sketched in **Fig 3.2.1**

This consideration has limited the choice to following four configurations (**Fig. 3.2 A-D**) :

- A) The most important element is the presence of the canard wings, which offer the advantage of a lighter landing gear and a vertical thrust component to help take-off. Tandem wing or canard wings advantage are: greater total wing surface if wing span is fixed, with acceptable aspect ratio; low induced drag; lift subdivided into more than one wing surface, therefore less loaded structures. Over against, in order to limit the effect of interference, like downwash that is the deviation of flow, down towards, wings should be placed as far as possible either longitudinally or vertically. (This aspect would have been investigated in detail in a following phase, preliminary design, with the help of a specific software MILS8). Another problem is the location of neutral point (NP), particularly critical because of mass concentrated on the rear wing.
- B) The latter can be solved with this configuration where the advancing of wings and of motors causes a consequent advancing of center of gravity (CG) position, at the cost of adding control longitudinal surfaces.
- C) This configuration shows a lot of advantages thanks a very good distribution of mass, to the presence of two fins and a good controllability, due to two rudders and a wide horizontal tail. Nevertheless the redundancy of surfaces and the presence of two booms penalizes RAC and the total weight.
- D) The fourth configuration reduces as much as possible the weight eliminating the redundant structures, like twin tail booms. Wing undergo an uniform flow like motors propellers. This configuration is going to be studied with some attention, as it promises good performances. In fact it is the one which maximizes the FOMs (Figures Of Merit), as is sketched in the following table (**tab. 3.2.1**).

3.3 Figure Of Merit

Now we analyze the FOMs that we considered more important:

PAYLOAD CAPACITY : This is a very important parameter , because the more payload we carry, the higher is the score. On the other side the water has a great volume and then require a great cargo bay (and then heavy structures).

WETTED AREA : Is the total area exposed at the flow, the greater is this area the higher will be the friction drag, considering that the most of this area is non-lifting surfaces.

DEGREE OF CONFIDENCE : means the possibility of beginning the design from well knows problems.

MASS DISTRIBUTION : means the possibility of positioning the system masses easily, so to make easier the balance of aircraft with and without the payload.

PAYLOAD HANDLING : It is very important may access to payload, so to minimize the time of loading and unloading during the race.

BUILDING EASE : Is equivalent to less cost for material and manufacturing.

DISASSEMBLY : It is important because of the need to send the airplane through the ocean. The expedition cost increase with the package dimensions.

RAC : No need for further explanations.

These FOM are explained in **tab. 3.2.1**

3.4 Analytic method

The method used to optimize the SI function is a graphic method; better it we built the FI function , we studied its trend and its maximum. The values of design parameters in coincidence of this maximum supplied the requirements that the final concept should have to respect.

The design parameters are jointed by statistic correlations obtained from studies about UAVs and commercial electric models.

The accuracy of the method used we do not expect to be absolute, but for this section of design it's enough because with short time and simple means it allows obtain correct indications for the final concept.

The first step was to determine the power necessary to complete a flight round in function of TOW.

The trend of this parameters is determined from a rule of thumb of electric modelers. This establish for electric aerobatics models how many Watts are necessary per one Kg of TOW per one second of flight, both in Take Off and in cruise. These values have explained in **tab 3.4.1** Note that the power necessary for the climb it's the same than the are necessary for Take Off.

The values of flight's stages (take off, climb, cruise) are those estimated for Caesar I.

The principal design parameters is the TOW and Power Available (nr. of cells): for each their variation we obtain others design parameters.

In primis the number of flight round is a function of TOW, WPL and PA.

WPL is correlated to TOW according to **fig 3.2.1** and $WE = TOW - WPL$.

The wing surface is correlated to TOW according to **fig 3.4.1**

The number of wings on increases of one when Aspect Ratio is minor of 4.

The cell weight depend of Power Available because weight of each cell is 60 g .

The length of airframe is correlated to wing surface according to **fig 3.4.2** and powerplant weight is correlated according to **fig 3.4.3**

The number of motors descend from the value of Thrust Weight ratio (T/W) necessary for take off and from the value of mean motor static thrust, to each variation of TOW.

The airframe weight = $WE - \text{powerplant weight}$.

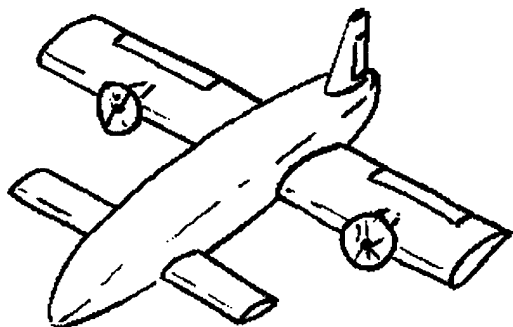
For each value of design parameters on compute the values of SFS and RAC so SI.

We have the maximum value of SI for the maximum value of Power Available and its trend is explained in **figure 3.4.6**

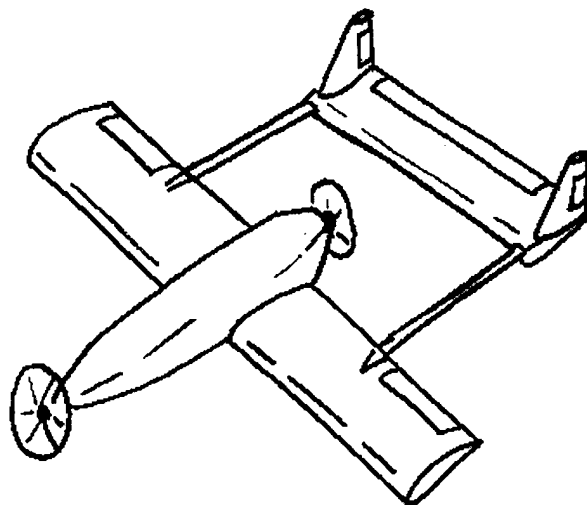
We have decided for a concept with a TOW around 12/13 Kg because from the study of FI function descend than for this value of TOW parameter we have better margin for increase the number of litre of water charged.

Fig 3.2

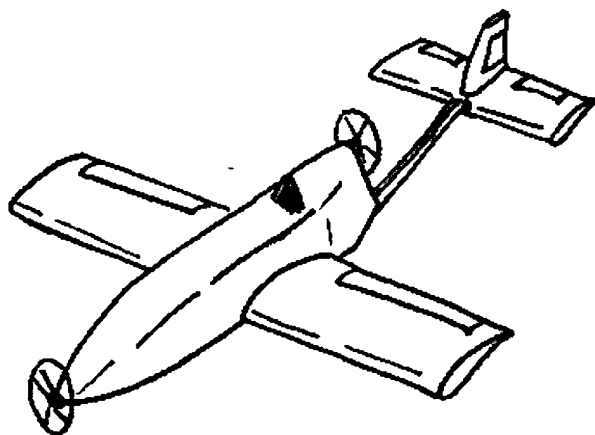
A



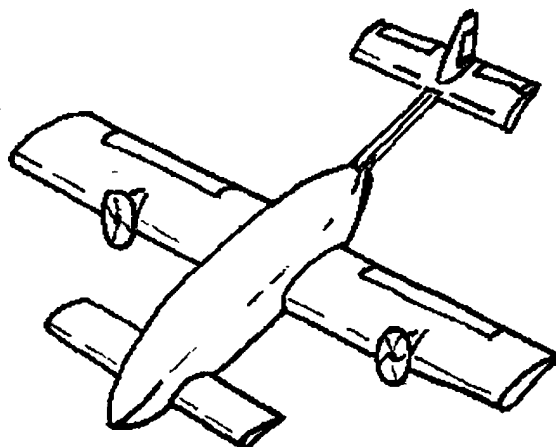
B



D



C



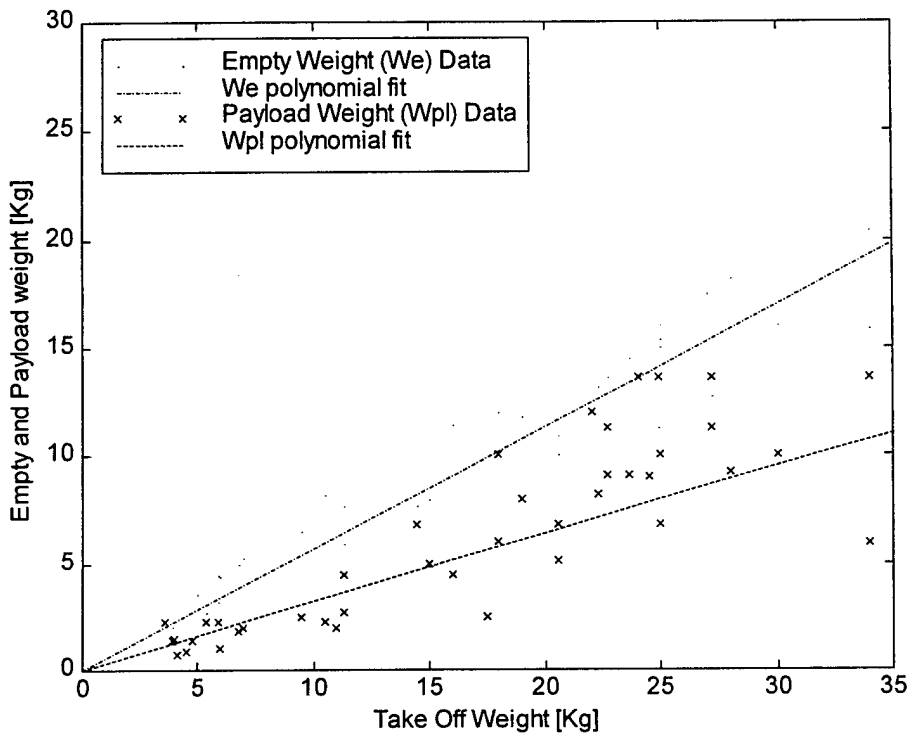


Fig. 3.2.1

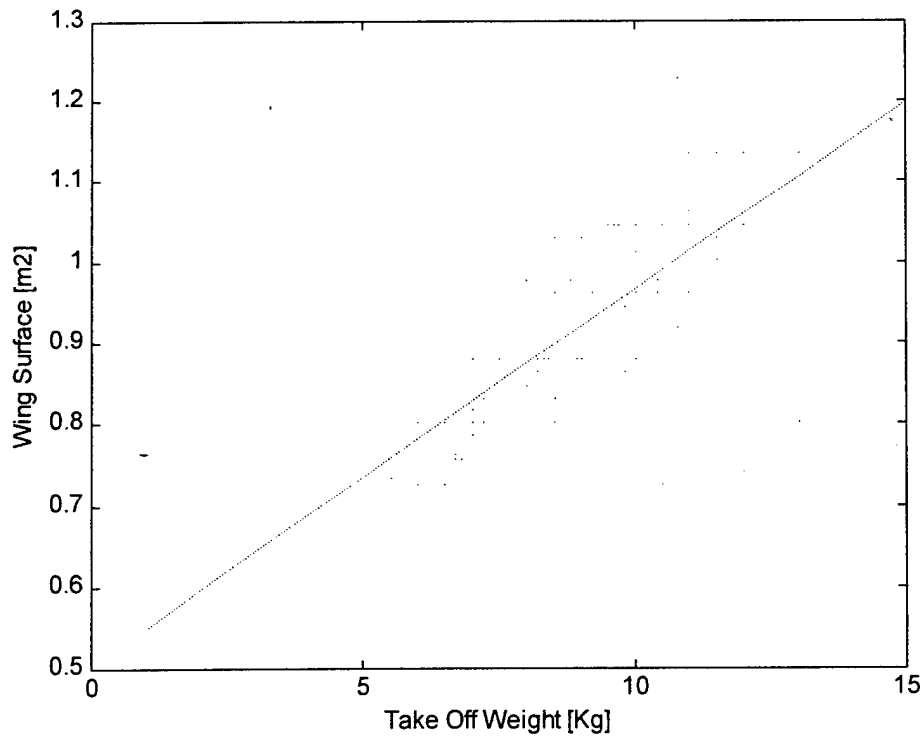


Fig 3.4.1

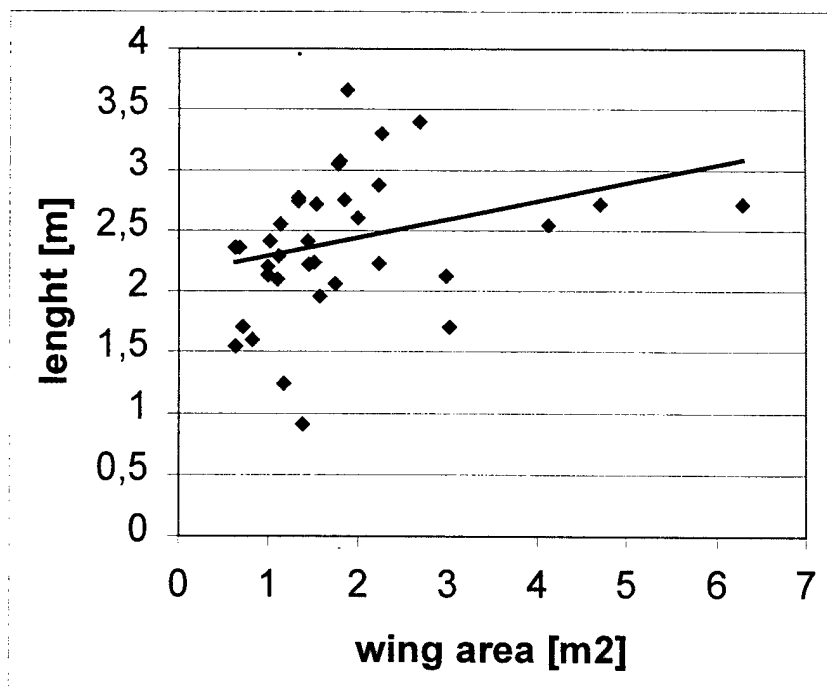


Fig. 3.4.2

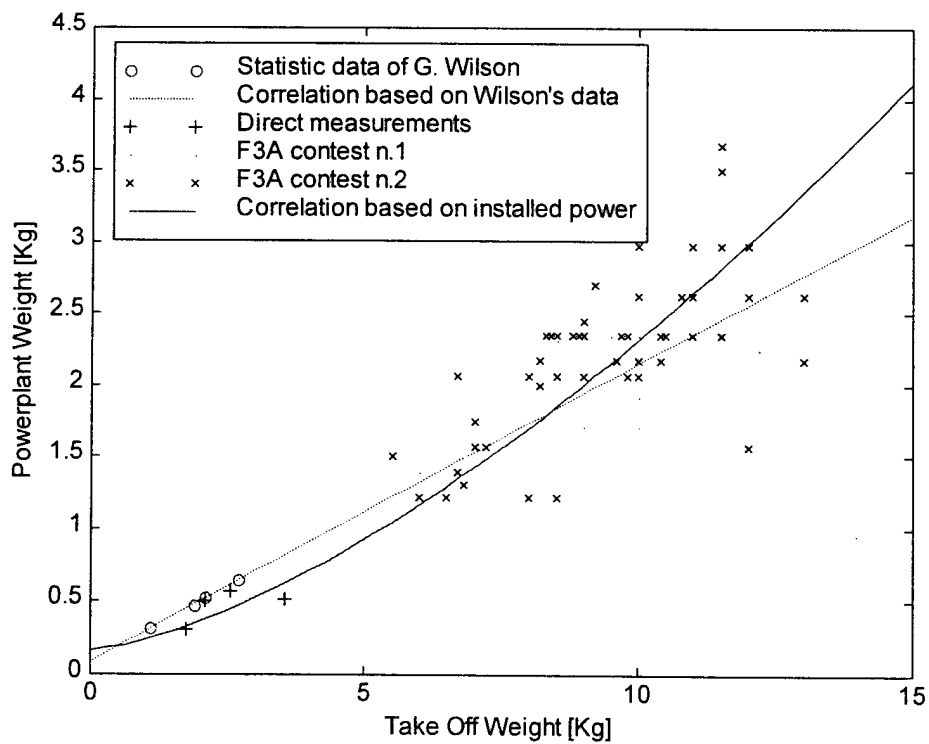


Fig. 3.4.3

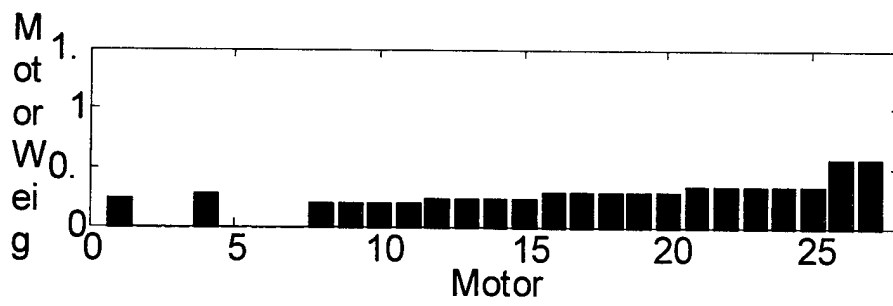


Fig 3.4.4

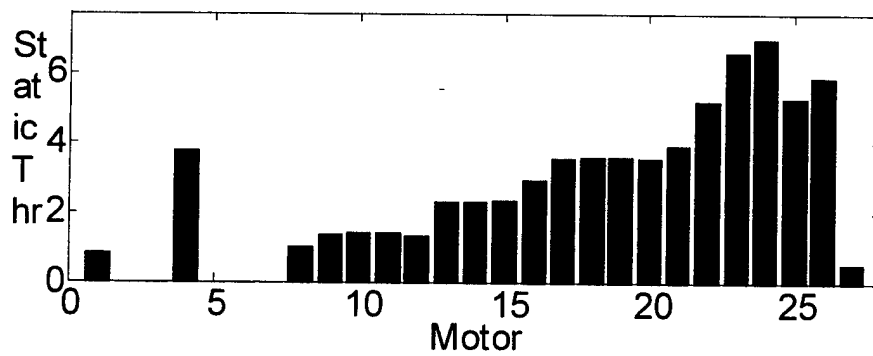


Fig. 3.4.5

LEGEND

+ =
sufficient
++ = good
+++ = top

- = nearly
suff.
-- = insufficient

	(A)	(B)	(C)	(D)
PAYLOAD CAPACITY	+	+	+	++
WETTED AREA	++	++	+++	+
DEGREE OF CONFIDENCE	-	-	--	-
MASS DISTRIBUTION	--	+	++	++
MOTOR PERFORMANCE	--	-	++	++
PAYLOAD HANDLING	+	+	+	+++
BUILDING EASE	-	-	-	+
DISASSEMBLY	-	-	+	++
RAC	+	-	-	++

Tab 3.2.1

free parameters

TOW

WPL

WE

n° tom

n° cell

Wing Surface

n° wing

length

n° motors

fixed parameters

Take off: Watt x 198,5

Kg

Cruise: Watt x 124,063

Kg

t1 [s] 4

t2 [s] 6

t3 [s] 40

t4 [s] 3

t5 [s] 5

t6 [s] 73

Wing span [m] 2,1

mean motor thrust [Kg] 4

TAW 0,45

mean motor Weight [kg] 0,317

max n° celles and max power weight 37 - 2,2 kg

control parameters

Aspect ratio - AR

n° cell	37	10,217	13,8833	18,55	23,05	22,76667	27,433	33,6	37	37	37	37	37	37	37	37	37
Power available [Watt s]	319680	88272	119952	160272	199152	196704	237024	290304	319680	319680	319680	3E+05	319680	319680	319680	319680	319680
TOW [Kg]		5	6	7	8	9	10	11	12	13	14	15	16	17	18	19	
WE [Kg]		3,3498	4,0198	4,68977	5,35974	6,029703	6,6997	7,3696	8,0396	8,7096	9,3795	10,05	10,719	11,389	12,059	12,7294	
WPL [Kg]		1,6502	1,9802	2,31023	2,64026	2,970297	3,3003	3,6304	3,9604	4,2904	4,6205	4,95	5,2805	5,6106	5,9406	6,27063	
n° tom		1,254	1,41999	1,62625	1,76816	1,552382	1,6835	1,8745	1,8922	1,7466	1,6219	1,514	1,4191	1,3357	1,2615	1,19506	
Wing Surface [m2]		0,7287	0,77378	0,81891	0,86404	0,90917	0,9543	0,9994	1,0446	1,0897	1,1348	1,18	1,2251	1,2702	1,3153	1,36047	
AR		6,0523	5,69929	5,38521	5,10393	4,850578	4,6212	4,4125	4,2219	4,047	3,8861	3,737	3,5998	3,4719	3,3527	3,24153	
n° wing		1	1	1	1	1	1	1	1	1	2	2	2	2	2	2	2
cell weight [Kg]	2,22	0,613	0,833	1,113	1,383	1,366	1,646	2,016	2,2	2,2	2,2	2,2	2,2	2,2	2,2	2,2	2,2
length [m]		2,2166	2,2238	2,23103	2,23825	2,245467	2,2527	2,2599	2,2671	2,2744	2,2816	2,289	2,296	2,3032	2,3105	2,31768	
n° motors		0,5625	0,675	0,7875	0,9	1,0125	1,125	1,2375	1,35	1,4625	1,575	1,688	1,8	1,9125	2,025	2,1375	
		1	1	1	1	2	2	2	2	2	2	2	2	3	3	3	3
powerplant weight [Kg]		0,93	1,15	1,43	1,7	2	2,28	2,65	2,9	3,35	3,75	4,11	4,5	4,9	5,35	5,68	
airframe weight [Kg]		2,4198	2,8698	3,25977	3,65974	4,029703	4,4197	4,7196	5,1396	5,5396	5,9295	6,3195	6,7094	7,0994	7,4894	7,8794	
S_FL_SCORE		20,692	28,1185	37,5702	46,6842	46,11037	55,562	68,052	74,938	74,938	74,938	74,94	74,938	74,938	74,938	74,9378	
SCORE		4,7432	6,53546	8,48241	10,242	6,682245	7,9068	9,539	10,312	10,186	9,9165	9,775	9,6464	7,4279	7,3627	7,27998	
A	100																
B	1																
C	20																
MEW [Lb]		5,3348	6,32677	7,18649	8,06825	8,883883	9,7436	10,405	11,331	11,816	12,411	13,09	13,711	14,307	14,792	15,541	
REP		2220	2220	2220	2220	4440	4440	4440	4440	4440	4440	4440	4440	6660	6660	6660	
MFHR		80,451	72,4891	74,5268	76,5644	78,60212	80,64	82,677	84,715	86,753	93,79	95,83	97,866	99,904	101,94	103,979	
RAC		4,3625	4,30246	4,42918	4,55811	6,900431	7,0272	7,134	7,2674	7,3566	7,5569	7,666	7,7685	10,089	10,178	10,2937	
WBS 1,0		36,37	38,3128	40,2557	42,1987	44,14159	46,085	48,027	49,97	51,913	58,856	60,8	62,742	64,685	66,628	68,571	
WBS 2,0		34,082	34,1763	34,2711	34,3658	34,46053	34,555	34,65	34,745	34,839	34,934	35,03	35,124	35,218	35,313	35,4079	
WBS 5,0		10	10	10	10	20	20	20	20	20	20	20	20	30	30	30	

Tab 3.4.1

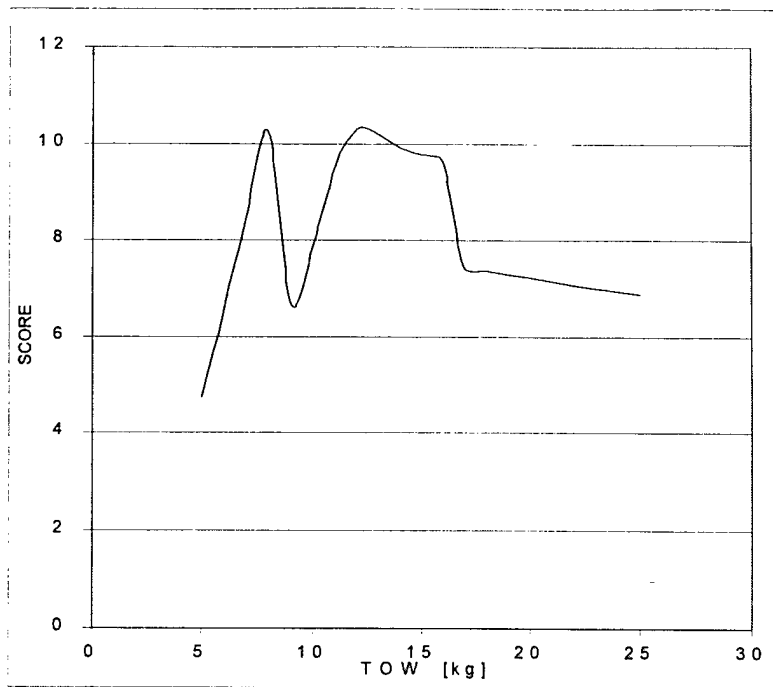


Fig. 3.4.6

Fig. 3.7

Section 4 : Preliminary Design

Once the final configuration has been selected, we began to refine the sizing, already begun in the conceptual design. In fact from the previous step we know the following aircraft's data:

- weight at take-off ~ 13-15 kg
- payload ~ 4-6 kg
- maximum static thrust ~ 6-7 kg.

The most important items of this section are:

- Wing surface determination and airfoil selection
- Cruise speed selection
- Tail surfaces positioning and sizing
- Center of gravity and payload positioning
- Structural design
- Propulsion definition

The first two items are heavily interconnected. In fact, in each stage of flight, speed V , wing surface S and total lift coefficient C_L must fit the equation

$$(1) \quad nW = \frac{1}{2} \rho V^2 S C_L$$

where ρ is the air density, n the load factor and W the total weight of the aircraft.

Wing and airfoil geometry and Cruise speed

The most critical conditions for this item are the take-off and the high load factor maneuver when the wing must perform the higher lift.

From the maximum field length and the maximum thrust we have estimate the take-off speed in about 15 m/s. Considering that FAR rules on the take-off say that the take-off speed should be ~1.2 times the stall speed in the take-off configuration, we consider as take-off speed ~13 m/s. Considering that at lift-off $n=1$, $W=13$ kg, $\rho \sim 1.224$ kg/m³, the (1) say that

$$C_L S \sim 1.233 \text{ m}^2$$

if we consider, as example, $C_L=1$ we have a wing area of 1.233 m², considering the maximum wing span of 7 feet (~2.1 m) we obtain a mean chord of ~0.59 m and an aspect ratio near 3.5 (!). So we see that we need an airfoil that gives us a higher C_L , and then a shorter chord and a better aspect ratio (and then a higher efficiency in the cruise !).

To find the better wing geometry (that means the chord, and then the aspect ratio) we tried to optimize the cruise speed to maximize the endurance with the energy of the cells.

We tried, as first attempt, with an area of 1 m^2 and, to estimate the drag, we use the parabolic expression $C_D = C_{D0} + K C_L^2$ (with characteristic value for C_{D0} and K). Then we calculate the energy and the time requested for the cruise as functions of speed. We took in account also the dependence of the thrust from the speed. We repeated the calculation for several values of S . The results show that the best speed is $\sim 20\text{-}25 \text{ m/s}$, $C_L \sim 0.44$ (quite independent from S !) and a time of $\sim 17\text{-}21 \text{ s}$ per lap.

Considering the range of speed (with a Reynolds' number $\sim 500'000\text{-}700'000$) we decided to use a laminar airfoil, the Selig SD7032, a low moment airfoil design for RC sailplanes. This airfoil can perform a maximum $C_L \sim 1.4$ and has the minimum of C_D when $C_L \sim 0.5$.

To minimize the drag in cruise we decided to have little geometric incidence both in cargo and unloaded laps. So we arrived to a wing area of 0.9 m^2 that gives $C_L \sim 0.58$ in cargo and $C_L \sim 0.4$ for unloaded. This give a mean chord of about 0.45 m (aspect ratio ~ 4.6) and a cruise speed $\sim 20 \text{ m/s}$.

The wing's shape is rectangular for simplicity's sake (we have no experience in manufacturing!). It is also to notice that a taper (for example $C_t/C_r = 0.5$) would bring a root chord nearly 0.6 , that can have interference with the fuselage, and a tip chord ~ 0.3 , that can cause stall for the low Reynolds' number.

The wing is low for several structural reason: this way the fuselage's structure leans on the wing's one that lifts it; it is easier to reach the payload; the wing's lower surface gives more strength in event of rough landing.

To compensate the negative contributes to the lateral-directional stability due to low and unswept wing, there is a dihedral ($\sim 3^\circ$) that improve the lateral static stability without causing the dutch-roll.

We thought to add winglets at the wing tips, to reduce the induced drag, cause by the low aspect ratio, but the numerical results of the analysis of the potential flow show us that the improve in the induced drag does not compensate the increase of friction drag on the winglets, due to low Reynolds number, and the higher RAC.

Tail surfaces, Center of gravity and Payload

These two problems are strictly correlated, in fact the aim of the tail horizontal surfaces is to produce the moment around the center of gravity, that can balance the moment produced by the wing, the fuselage and the propulsion system.

There is also, in this case, the problem of having moment balance in two load condition. We have solve this problem by putting the center of the cargo bay as near as possible to the empty center of gravity.

The cargo bay can hold up to six bottles, in a length of $\sim 0.45 \text{ m}$ and a section of 0.19×0.17 . About the horizontal surface we started by putting the center of gravity in the aerodynamic center of the wing and fixing the static margin of stability, that is fixing the position of the neutral point. To fix the position of the neutral point we had to chose the area of the horizontal tail and the distance between wing and tail.

We choose the aspect ratio of the tail = 4 and his chord at least of 0.2 m (to have a Reynolds high enough to prevent the stall). Then the horizontal surface has a span = 0.8 m, an area = 0.16 m² and an arm (distance between the aerodynamic centers of the wing and the one of the tail) ~ 1.2 m.

The position of the center of gravity is set moving the other masses in the fuselage (motors, cells, fuselage itself ...), but not the payload.

This analysis lead to a fuselage of ~ 1.1 m, with after end coincident with the trailing edge of the wing. Fore the cargo bay there is a large room that can hold all the electric and electronic components (receiver, servos, their cells, ...).

The vertical tail has been sized from a typical value of the tail volume coefficient (~0.054) and reasonable ones for the aspect ratio (~4.5) and the taper ratio (~0.6); we decided to have tapered vertical surface and a rectangular horizontal one because we wanted to have the possibility to define later if the configuration is mono or twin boom.

Then we over-sized a little the vertical tail, so we have positive rigidity in roll and yaw (static stability) but more directional than lateral stability, to be sure to have not dutch-roll, also at the cost to have an instable spiral, easy to compensate in flight.

For both horizontal and vertical surfaces we chose a NACA 0009, a thin and symmetric airfoil that will work at little angles of incidence (no more the 3-5°), giving so little induced drag. The other components of drag will be quite little because of the reduced total wetted area.

Structural design

Although the structural design usually follows the aerodynamic one, and moves up from a shape of the external surface of the aircraft which is already defined; that was not exactly the situation we were in when we began to study the dimensioning of CaesarII's structures. In fact, because of the very short time we had to complete our work (if we wanted to have enough time to build our RPV), we had to start structural dimensioning much before the external shape had been completely known.

That involved two problems we had to resolve. The first one: to produce a scheme of the aircraft's structures which could be easily adapted if some configuration's parameter had been changed (what happened several times !). The second and more penalizing one: we did not know exactly the loading system on the various parts of the vehicle. That is the reason which could not permit to us to use typical procedures of modern structural engineering, based on FEM simulations. Neither we could use a fully experimental approach (we did not have so much time).

So we turned our sights to the old simple methods for structure calculation based on the classic rules of the Science of Buildings.

To remedy the possible under dimensioning the approximations of such theories could involve, we had to consider large insurance coefficients, doing so we gave up obtaining the optimum result. So, we opted for a structure stronger but heavier then necessary. (This is a point which could be improved in an eventual evolution of our vehicle, moving up from our results -we are thinking to next year's DBF. for example-, but for us it was a compulsory choice).

More over, this kind of approach was suggested by the materials we thought to use to build CaesarII. In fact. considering our limits (again the short time. our ability in manufacturing, the laboratories we had, the costs of materials), we opted for a pretty all wooden structure, where structural properties of wood cannot be known with a high degree of confidence. So, we organized our work in different steps, as it follows:

S.D.1- a **global static analysis of the RPV** has been done to individuate all the loads acting on the structural elements of the plain. At this point we considered to be known only the global loads. such as lift, drag, thrust, aerodynamic moments, weight of pay load, batteries and motors. The structure weight was obviously unknown, except for the estimation showed in the previous sections;

S.D.2- then we split the plain lino single "elementary cells" we could study Mt the simple theories mentioned before:

- 1: horizontal tail,
- 2: vertical tail,
- 3: tail boom(s) (in fact, originally two booms were expected),
- 4: wing,
- 5: fuselage.

We estimated the load's distributions on each cell, and we passed to the **static analysis and first dimensioning of each single cell**;

S.D.3- in performing step 2 we singled out some critical points (such as the points of junction) in which dimensioning we should pay more attention; so the **analysis and synthesis of such critical points** has been made at the end, when the most part of the structure had already been dimensioned and the building work had already began.

Section 5 : Detail Design

Table of Contents :

- 5.1: Flight Mechanics
- 5.2: Propulsion System
- 5.3: The Structural Design
- 5.4: The Aerodynamic Design
- 5.5: Landing Gear
- 5.6: Component Selection's Summary
- 5.7 Take off performances' check

5.1 Flight mechanics

5.1.1 Longitudinal Stability

In order to have longitudinal static stability, the center of gravity, cg, must be forward the neutral point, NP, (the point about which the total aerodynamic moment does not depend from the angle of attack). The position of NP depends mainly from the positions of all the aerodynamic surfaces, their area, their lift gradient and their relative position (downwash !). Lesser contributions come from fuselage and propellers.

We decided to have cg on the aerodynamic center of the wing, at 25 % of chord, like in the most airplane, and to fix the static margin (the distance between cg and NP) at 20 % of the chord (~0.1 m).

Thanks a potential flow simulator (MILS8, written by Eng. Luca Cistriani) we defined the position and the area of the horizontal tail surface, also taking in account the consideration about the drag and the stall, as described in the previous section . The area is ~ 0.16 m² and the arm (distance between the aerodynamic centers of wing and tail) is ~ 1.2 m, so we have a tail volume coefficient ~ 0.5, like most aircraft of the same class.

5.1.2 Cruise and turn flight

To select the optimum flight speed, we used an Excel electronic sheet to calculate the energy and the time spent in each stage of the mission (cruise and turnings). From the previous sections we have the aircraft parameter:

- Total weight 13 kg
- Wing span 2.1 m and airfoil chord 0.45 m
- Number of motors and propeller model (Graupner Super Extra 0.4x0.2 m , 3-bladed)

In the cruise, for several value of cruise speed we found the value of C_L , the Drag (from an estimated $C_D = C_{D0} + K C_L^2$, with typical value of C_{D0} and K), the thrust (= Drag !), the time, propeller parameters for that speed (from the Renard's formulas), propeller RPM and the total cells' energy spent for the cruise (considering for the motor an efficiency of 0.8, a very low one !) (**table. 5.1.I** and **figure 5.1.I**).

Then we considered the flight in turning, repeating the same calculates for several values of speed (V) and load factor (n). For each couple of values we calculated the turning radium (and the length), the

time, the propulsion parameters and the energy spent. In **table 5.1.II** we show an example for load factor = 1.7. In **table 5.1.III** and **figure 5.1.II** there is the energy as a function of V and n.

We decided to turn at the same cruise speed, so we summed the "consume" in cruise and the one in turn. We found a global optimum for the energy spent, and so for the number of lap that is possible to run. The best speed for cruise and turn is ~ 20 m/s, an optimal n ~ 1.3 (**table 5.1.IV**) and a total time per lap ~ 40 s. this may allow the aircraft to run two cargo sortie at the full load and one cargo sortie with a reduced load. More or less a Single Flight Score of 80-100 for a total flight time of ~ 4'40".

5.2 : Propulsion System

Established the final concept of Galileo, the right motor for us must give a static thrust of about 7-8 Kg, i.e. a static thrust for each motor of about 3.5-4 Kg. So to have a thrust to weight ratio of about 0.5. Actually it is the coupling of motor with the propeller that must produce this value and because we don't choose the propeller, because only for the Graupner super Extra 3 blades we know the C_T and C_Q coefficients, we have studied only the various commercial motors with the program Motor1.0 developed from Eng. Luca Cistriani.

We have choose the Aveox 1412/2Y and its performances are explained in **figure 5.2.I**

5.3 : The Structural Design

As we said in the previous section, because of the need to begin the building work as soon as possible, a highly optimized structural design was sacrificed in favor of a simpler and faster solution which could produce a structure stronger but heavier than necessary. We have already illustrated the planning of the structural design, shared in different steps. It is necessary to repeat here that, however early we might begin this work, we should have to wait for the loading distributions on the various cells were estimated, considering the different conditions Galileo would have found during its life. Unfortunately, these data were not known in due time. So we thought to consider a basic condition in which each cell is subject to the most critical load it could ever meet in its operative life. A critical condition is the take off with all the pay load, when the wing gives the maximum lift, the tail the maximum negative lift, the power is maximum as well. A critical condition for the tail's structure is a pull up at an high load factor (e.g.: $n_z = 3$). Another critical load for structural dimensioning is the one the landing gear gives in a rough landing. So, we took the take off as our basic condition, considering the tail working as in a sudden pull up and adding to the loading system a concentrated load able to simulate a sudden landing (in so doing we opted once again for an over-dimensioned structure which could be designed in a short time and which could give a certain degree of insurance even if some parameter of the configuration or of the typical mission had been changed).

Then we passed to the analysis of the stresses on the various cells with the methods specified in the previous section. That is, at this stage each cell has been seen from a far point of view, in order it could be approximated with an engineering beam to study its flexion, and with a De Saint Venant's cylinder to study its torsion. Before passing to this study we had to decide the value of the "load factor" n_z the RPV would have to support. Flight Mechanics' studies showed the maximum value of n_z during the target mission would have been equals to 1.5 (in the turnings). A stricter requirement it seemed to be the static exam the aeromodel would have to pass, that is to be hung for the wing tips. A brief study of primary approximation allowed us to evaluate the value of n_z that makes an elliptical distribution of lift along the wing span (which was the target of the aerodynamic work) equivalent to the critical condition mentioned before. Considering the hole mass of the vehicle concentrated in the middle of the wing, we

could deduce the value of n_z we had to consider in the structures' dimensioning to have the same maximum internal loads as in the hinging test: $n_z = \frac{3}{4} \pi$, that is $n_z = 2.536$.

We took $n_z = 3$ to remedy the possible mistakes involved by the drastic approximation adopted.

At this point we could pass to the static analysis and first dimensioning of each single cell, following the scheme illustrated in section 4. We will spend later a few words to explain how we proceeded in each case. Now, we matter to make clear the design philosophy we adopted.

In the contest of a linear analysis, we decoupled the static problem in few independent sub-problems (such as bending, twisting, compression,...) and we determined the fields of inner stresses and strains involved by the outer loading systems. Passing to dimension the structural elements, the first step was to decide *the kind of structure* we should have to consider. Once the class of materials had been chosen (as we said in the previous section, many reasons had driven us towards a pretty all wooden structure), it was a consequence to think to the classical scheme of semi-monocoque structure to mould its resisting components. That is, we individuated three classes of structural elements:

- longitudinal elements: spars, stiffeners;
- transversal elements: ribs, fuselage's frames;
- external skins;

each one carrying out a specific task (from a structural point of view) as it will be clearer in the following. In particular, for wing's and tail's spars we chose a box solution, which is common between wooden aeromodels. In fact, it is simple to build and it guarantees a good resistance to normal stresses due to bending moments and to tangential stresses due to shear forces (without considering it has an its own twisting rigidity).

Now, let us consider briefly the solutions adopted in dimensioning each single cell.

5.3.1 : Wing

A lot of studies have been done for the structural synthesis of the wing. In fact, this was the first structural cell we began investigating and the last one which saw a definitive dimensioning. Galileo is situated on the border line between the littler aero-models and the bigger light aircrafts of general aviation, so it was not so simple to find the optimal wing structure. For this reason, at the beginning of our work we considered a few different solutions and dimensioned each one to resist to the loads previously illustrated. Then we compared the values of the masses of such solutions and chose the lighter one. This winner configuration is shown in **figure 5.3.I**: a D-box with twin boxed spars which takes from the leading edge until the 55% of the chord, to guarantee the airfoil not to deform at least before this point, in order to exploit its laminar flow in design conditions. Once known the geometry of the airfoil, the spars have been located in positions that answer two contrasting questions:

- not to be too far from the point where the airfoil's thickness is maximum, in order to have a sufficient bending rigidity;
- not to be the one next to the other, in order to have enough twisting rigidity and, as we said, to locate the end of the D-box at 55% of the chord.

A good compromise it seemed to be the solution shown in **figure 5.3.I**. A "false" spar has been located just before the flaperon's leading edge, to transfer the hinge's stresses to the resisting structure.

Although inner stresses have a decreasing distribution along the wing span (from root towards tips), we assumed a resisting section constant along the span. Actually, we wondered if it was worth to give the section's thickness a taper from root to tips. To be able to answer this question, we calculated the saving in mass a tapered section would have involved, and we judged it to be negligible if compared with the bigger difficulty in manufacturing it (we estimated this saving in the order of about 20-30 g). So, we dimensioned the section's thicknesses in order to resist the maximum stresses which happen at the root section. **Figures 5.3.II, III, IV, V** show the expected rates of bending moments and shear forces in two different planes along the wing span (x axis). Now we are going to produce an example

about how the thicknesses have been dimensioned. We considered the section of the whole D-box able to resist to normal stresses due to bending moments. Calculations of primary approximation had shown the thickness of spars' cores and of skin could reduce to very little values (1 or 2 mm), but the dimensions of spars' caps had to be bigger (a few mm). So, helped by electronic sheets, we carried out a parametric study which evaluated the value of the maximum normal stress and the value of wing's mass as functions of the caps' dimensions. Plotting these functions we could choose opportune values for that dimensions, watching out that the maximum stress, multiplied for an insurance coefficient of 2, was littler than the maximum permissible load (which was known, once the materials had been chosen). **Figures 5.3.VI, VII** show that sort of diagrams; in both cases, k_0 is the thickness of spars' caps in a direction normal to the airfoil's chord (the "caps' chord" is considered to be fixed at 5mm; in general, one of these two dimensions has been considered as a parameter).

The little space we have in this report does not allow to us to produce a detailed illustration of the dimensioning of each structural element. We matter to say that parametric studies like the one described have been conducted to determine all the thicknesses were in the game, and to determine the distance between the ribs that avoid spars' and skin's buckling phenomena. Skin and spars' cores have been dimensioned to resist to tangential stresses due to shear forces and twisting moment (on the base of the theory of Jourowskji, considering the wing's structure as a multi-cell box with a variable thickness). Instead, the thickness of the ribs has been determined on the base of a statistic approach, that is comparing this value for a class of wooden aeromodels (parameters in such studies were the wing loading and the wing span). The flaperon has been designed as a simply connected beam, with a stressed skin.

5.3.2 : Tail

The arguments described in 5.3.1 are valid for the horizontal and vertical tails, as well. We only would like to add that for such cells we opted for a solution mono-boxed-spar with stressed skin (actually the part of the skin we trust on is the one connecting the leading edge with the spar's caps). The spar has been located at the point of maximum thickness of the airfoil, **figure 5.3.VIII**. To dimension the resisting elements of such cells we adopted the classical theory of semi-monocoque structure in which we added further approximations. In fact, we thought the loads on the tail were not so critical. More over, the full tail would have been so light that a more detailed analysis taking to save a little percentage of weight was practically useless. So, our hypotheses:

- only the spars' caps resist to the normal stresses involved by bending moments;
- only the spars' cores resist to tangential stresses due to shear forces;
- only the considered part of the skin resist to tangential stresses due to the twisting moment.

5.3.3 : Fuselage

Similar arguments are valid for the resisting elements of the fuselage, which are represented in **figure 5.3.IX**. We matter only to specify that we chose a basic structure formed by four main stiffeners located as far as possible from the axis of symmetry, a series of eleven frames and a stressed skin. Other four littler stiffeners have been designed to carry the pay load and to supply as a guide for it. Other special stiffeners make up the "castles" for the two motors. Each element has been accurately dimensioned (in so doing taking an insurance coefficient of 3, considering our bigger difficulty in moulding such a composite structure), but the little space we have in this report does not allow us to be more exhaustive. We only will add that for the four main stiffeners we decided it was worth to consider a step rate. That is, their section is constant (section 1) along the fuselage's main axis in the hole part corresponding to the pay load's location, then it is steeply reduced to a littler value (section 2) which is again constant until the nose of the vehicle.

5.3.4 : Tail Boom

A special attention has been paid in the design of this component. Its only task is to carry the tail at a certain distance from the vehicle's center of gravity in order to trim it. So, it is wished to have the littler section as possible, in order to reduce its wet surface and so its aerodynamic drag. This requirement, together with the demand of a little weight, fight against the need of strength and stiffness (considering its tip's maximum permissible deflection was estimated in the order of 1 cm). For these reasons, we became soon aware the tail boom could not be built in any kind of wood. Actually, at the moment, a final decision about it has not been made yet. In fact, we have dimensioned a conical boom made of aluminum (avional 2024, total weight equals 2.5 hg), but it seems that using a carbon fiber composite its weight could be even halved! Unfortunately, we met a huge difficulty in finding commercial beams in carbon fiber with the dimensions we need; and more, it seems to be impossible knowing exactly the mechanic characteristics of such commercial carbon tubes. At the moment of scribing this report, we are carrying out a series of static test on commercial carbon pipes. If we gain the results we are expecting for, we will adopt such sort of solution; if we do not, we will mount the conical boom made of aluminum we have already built.

5.3.5 : Junction's Points

We thought to make such junctions using nylon made screws which link special stiffening stuck with glue to the part to connect. The screws are necessary in order to make easily the assembly and the removal. **Figure 5.3.X** shows the linking we thought to for the junction wing-fuselage. Something similar we have to design for the junction boom-fuselage and boom-tail, but we will be able to make that sort of decision only when we are sure about the material the boom is made of.

5.4 : The Aerodynamic Design

In performing the aerodynamic design we moved up from the results of previous analyses (about competition's strategy and preliminary design) which did not leave to us a high degree of freedom. In fact, the main parameters in an aerodynamic shaping, such as wing's and tail's surfaces and spans, had already been fixed; and more we were asked for values of global c_L , c_D and c_M very strictly determined. Without considering that our lean ability and experience in manufacturing advised us against adopting too brave solutions. So, the choices we made to shape Galileo are the best compromises we could think to between aerodynamic performances and manufacturing's simplicity, as it will be described in the following.

5.4.1 : Wing

How it is easily imaginable, the first part we paid attention to was the wing: its shape and, even though before, its position with respect the fuselage. That is, at first we wondered: **high wing or low wing?**

The configuration with a low wing has been preferred because, even if it involve a little penalty in terms of lateral-directional stability and an increasing in form drag (Oswald's factor) due to the interaction between fuselage's and wing's upper side's boundary layers, it offers a remarkable simplicity in the loading and unloading operations (whose a successful outcome during the competition could be so much important) and a bigger structural stiffness (fuselage's lower side), which is important in possible (even if not wished!) sudden landings.

Then, we passed to consider **the wing plan form**. A rectangular plan has been selected most of all for practical reasons: the extreme simplicity in building rewards of the penalty connected with a lift distribution (along the span) which sends away (not so much, after all!) from an elliptical one (the last being able to minimize the induced drag, as it is well known). Actually, we thought firstly to a tapered

wing; but the ties about the wing's span and surface (the first imposed by the competitions' rules, the second by the lift that was necessary once our strategy of design had been made) would have led to a root chord too long, involving structural (the junction wing-fuselage) and aerodynamic (interference, tip stall) problems.

Once made these decisions, we wondered if it was worth to give the wing a *depth of camber* (ϕ). It is true that it would have carried the benefits of a higher lateral-directional stability, but it would have involved an increasing in induced drag as well (as a function of $1/\cos \phi$, that is an increasing of 1.5% for a depth of 10°). And this was a disadvantage we could not permit, considering the rectangular not tapered wing and its very low aspect ratio.

It is true that all the decisions made since this point had penalized the lateral-directional stability of the vehicle. To remedy this matter, we thought to adopt a *dihedral angle*, that was fixed by our studies at the little value of $+3^\circ$ to keep a certain margin of dynamic lateral stability. Actually, the values of roll's and yaw's rigidities we got are able to guarantee a good margin of spiral's and dutch-roll's stability.

In order to limit the effects on the induced drag due to the low aspect ratio we thought to mount two couples of *winglets* at wing's tips which could give both a better effective aspect ratio and Oswald's efficiency factor. To evaluate the possible benefits this solution could produce, a detailed survey of the overall performance decay due to potential flow interference effects has been conducted. Then, we came back to the idea of improving wing's performances by adding two high-span winglets. Since down-wash is probably over-estimated by the potential flow method we used and this countermeasure provides penalties like

- skin friction drag due to extended wing surface and low Reynolds number on winglets;
- greater structural weight due to the winglets themselves and the increasing in bending moments they produce;

we decide not to add the winglets.

To select the opportune *airfoil* we turned our sights to the class seemed to give the best performances working in the condition Galileo would have found in its missions. The ones seemed to answer better our demands were the Selig airfoils, which have been specially designed for low Reynolds numbers and whose experimental drag polars were known. These airfoils are dedicated most of all to R.P. gliders whose Reynolds numbers' range is $[100, 600] E+03$. The one we have chosen is the Selig 7032, a laminar airfoil offering the performances we were looking for, whose diagram c_l vs α (deg) is represented in **figure 5.4.V**. It has a maximum thickness equals the 10% of the chord (so 4.5 cm, being our wing chord equals 45 cm) located at 30% of the chord (13.5 cm after the leading edge); its critical Re (Reynolds number yielding boundary layer's separation) equals $100 E+03$. In its various flying conditions Galileo will be always in the super-critical state (take-off Re is already higher than $300 E+03$). More over, flying the most at angles of attack lying in the polar's "laminar pack", it will able to exploit the lowest viscous and form drag coefficients of such laminar airfoils.

The choice of the 7032 is also due to its low moment coefficient; in fact, being $c_{mo} = -0.1$, it gives a little contribution to the *nose down* moment, which can be contrasted just considering a tail's setting equals -4° only. This last one, together with the setting of the wing ($=+3.5^\circ$) and of the pushing (rear) propeller's axis (which should be sloping down to reduce the nose down moment due to the thrust) have been determined in order to give a suitable pitch rigidity and to trim the vehicle without penalizing too much the total drag and the value of c_{Lmax} .

5.4.2 : Tail

The leading idea in designing this component was a T-tail, with a fin fixed on the top of the stabilizer. The elevator had to be hinged on the upper side of the horizontal tail, with its hinge line in correspondence of the one of the rudder, in order to be able to make a sufficient deflection thanks to the tapered form of the ruder itself. (We thought even to the possibility to eliminate the rudder -to save the weight of a servo-, because we thought we would be able to perform turnings by using only ailerons and elevator. However, when this decision had to be made, we were not sure yet about the person would have been our pilot; so we opted for a more conventional solution.)

To realize the horizontal stabilizer we thought to assume a symmetric airfoil -in order not to have further noseheavy moments at an angle of attack equals zero-, with a little thickness. The one we have chosen is the NACA 0009, which, having a maximum thickness equals 9% of the chord (at 30% of the chord), gives a critical Re enough low to allow the vehicle to fly in super-critical state also during take off (low Reynolds numbers). The stabilizer has been located 20 cm above the wing's plane to exploit the benefits of the slipstream (rear propeller). In fact, in so doing tail's efficiency should increase of nearly the 20%. To dimension the fin, we trusted on statistic data.

5.4.3 : Results

The software we used to perform the aerodynamic study is MILS8, by eng. Luca Cistriani. **Table 5.4.I** is an example of the output of such software, showing the aerodynamic data inherent the two horizontal surfaces: wing and tail. These data are referred to a cruise condition with no pay load, and show the values of c_L and c_D of the two surfaces and the value of total drag (considering both the induced drag and the addendum due to the interference between the various parts of the vehicle). **Figures 5.4.I, II, III, IV** show the slopes along the wing semi-span of c_L , lift, induced drag (due to the finite aspect ratio) and induced incidence (Schrenk's approximation).

5.5 : Landing Gear

There are two kinds of undercarriage:

- **REAR TRICYCLE**: is composed by two main wheels placed in front of center of gravity (CG), which support almost all the weight, and small rear wheel, which sometimes moves.

The high incidence, increases the drag making easier landing, but the landing run is subject to the directional instability. In fact, the centrifuge force creates a couple which as the transversal reactions of the main wheels. This couple aims at amplifying involuntary bending of the trajectory.

- **FRONT TRICYCLE**: is composed by two main wheels, which weighs W_p , placed behind the center of gravity (CG) at a distance x_2 and one front wheel which weighs W_a , placed at distance x_1 to satisfy the following relation:

$$x_1 \cdot W_a = x_2 \cdot W_p$$

DESIGN ANALYSIS: carriage must be so much high to permit that the aircraft assumes a pull-up trim close to stall in order to obtain the least speed at landing. Besides, propeller must be to determined distance from ground. Stall angle α_{st} is influenced by various factors, such as:

- Ground effect: begins at a distance equivalent to half wing span from ground and α_{st} decreases as the wing lengthening.
- Flaps: when they are wide reduce α_{st} of 2° - 4° .

We decided to incline the rear carriage of an angle: $\gamma_p = \alpha_{st} - \alpha_c + 3^\circ$

where: α_c = wing setting angle

In order to solve the above enumerated problems, we inclined the front carriage of an angle $\gamma_a = 10^\circ$ in order to avoid the upsettigs because of high decelerations.

STRUCTURAL ANALYSIS: the energy that carriage must absorb in the impact with ground is:

$$E = \frac{1}{2} \frac{W_{TOT}}{g} \cdot V_z^2$$

where: W_{TOT} = total weight
 g = gravity acceleration
 v_z = vertical velocity

Structures whose section is rectangular, undergoes a strain:

$$\sigma = \frac{M \cdot y}{I \cdot 2}$$

where : I = moment of inertia
 y = thickness
 M = momentum

In our case $M = -\frac{F}{2} l (\sin \vartheta - \cos \vartheta + 1)$

where $F = m a_z + W_{TOT}$

The maximum value is $M = -F l$

At the moment of scribing this report we are evaluating more realistic values for V_z , that will condition the final sizing of the landing gear.

Figure 5.5.I represents the landing gear's height h_1 as a function of the distance h_2 between the bottom of the rear propeller and the ground level. **Figure 5.5.II** represents the radius of the wheel (spoke) as a function of h_1 .

5.6 : Components Selection's Summary

The choices we made in selection building's targets, components and materials are discussed in the previous paragraphs. We think it can be useful to summarize in an opportune table the most important of them, also underlining the system's architecture: this is the task of **Table 5.6.I**. The views of the plane are presented in **Figure 5.6.I**.

5.7 : Take off performances' check

After having produced a more detailed design of Galileo, we worried to check its take off performances were the ones we expected, that is if it would be able to take off with the hole expected pay load. To make us sure on that, we produced the following brief study.

Vehicle's behavior during take off is strongly linked to the run distance, which is an input in the problem, being probably the strictest design's tie. So, at first we fixed the value of this distance equals the maximum value allowed:

$$S_g = 100 \text{ ft} = 30 \text{ m}$$

Other input in the problem are (SI units):

μ = friction coefficient = 0.05

ρ = air density = 1.22

k = aerodynamic induction coefficient = 0.07572

The parameters we thought were important to evaluate take off performance are:

$$\frac{T}{W} = \mu + (1.2)^2 \frac{Ka \frac{2W/S^2}{\rho Cl}}{[\exp(2gKaSg) - 1]} \quad Kt = \frac{T}{W} - \mu$$

$$Vf = 1.2 \sqrt{\frac{2W/S}{\rho Cl}} \quad Ka = \frac{\rho}{2W/S} [\mu Cl - Cdo - KCl^2]$$

This study has been conducted by assuming the wing load W/S as an independent variable and calculating the values of the other parameters as functions of W/S , with the help of an electronic sheet. The range for the wing load we considered is:

$W/S \in [8, 16] \text{ Kg/m}^2$

Table 5.7.I shows an example of such analysis. It is to be noticed that at this point Galileo's configuration was known, so the following constant were also input in the problem:

$C_{Lmax} = 1.4$

$C_{Do} = 0.08$

AR = aspect ratio = 4.6

e = Oswald's factor = 0.913896

So, we could know the value of the stall velocity :

$vs = 12.1 \text{ m/s}$

We assumed a take off velocity: ~

$vf = 14.52 \text{ m/s}$

and, by using the mentioned electronic sheet, we could determine:

$T/W = 0.5$

$W/S = 127 \text{ N/m}^2$

So, we were able to estimate the necessary thrust at take off, equals 6.5 Kg. This value is less than the one of the available thrust, and that comforted our hope to be able to carry a pay load higher than the one we had firstly planned (3/4 Kg) without changing the structural parameters of the vehicle, which are linked with the RAC.

So, it seemed our design worked as we wanted, at least from the point of view of take off performances.

V	Cl	Cd	T	t	Ct	Cp	giri elica	Energia
10	2,32	0,804	44,29	45,60	0,14	0,08700	100,48	62842,2039
11	1,91	0,550	36,68	41,45	0,14	0,08700	91,44	43056,4032
12	1,61	0,391	31,00	38,00	0,13	0,08600	87,24	33887,7606
13	1,37	0,287	26,71	35,08	0,13	0,08600	80,97	25006,3476
14	1,18	0,217	23,41	32,57	0,13	0,08500	76,70	19509,4785
15	1,03	0,168	20,87	30,40	0,11	0,08000	77,82	17897,1663
16	0,90	0,134	18,91	28,50	0,11	0,08000	74,08	14472,4991
17	0,80	0,109	17,41	26,82	0,09	0,07300	77,71	14350,5115
18	0,71	0,091	16,27	25,33	0,09	0,07300	75,12	12243,5949
19	0,64	0,078	15,42	24,00	0,08	0,06200	78,44	11215,6023
20	0,58	0,067	14,82	22,80	0,08	0,06200	76,90	10039,4959
21	0,53	0,059	14,43	21,71	0,07	0,06200	79,98	10754,5341
22	0,48	0,053	14,21	20,73	0,07	0,06200	79,36	10032,0429

Tab 5.1I

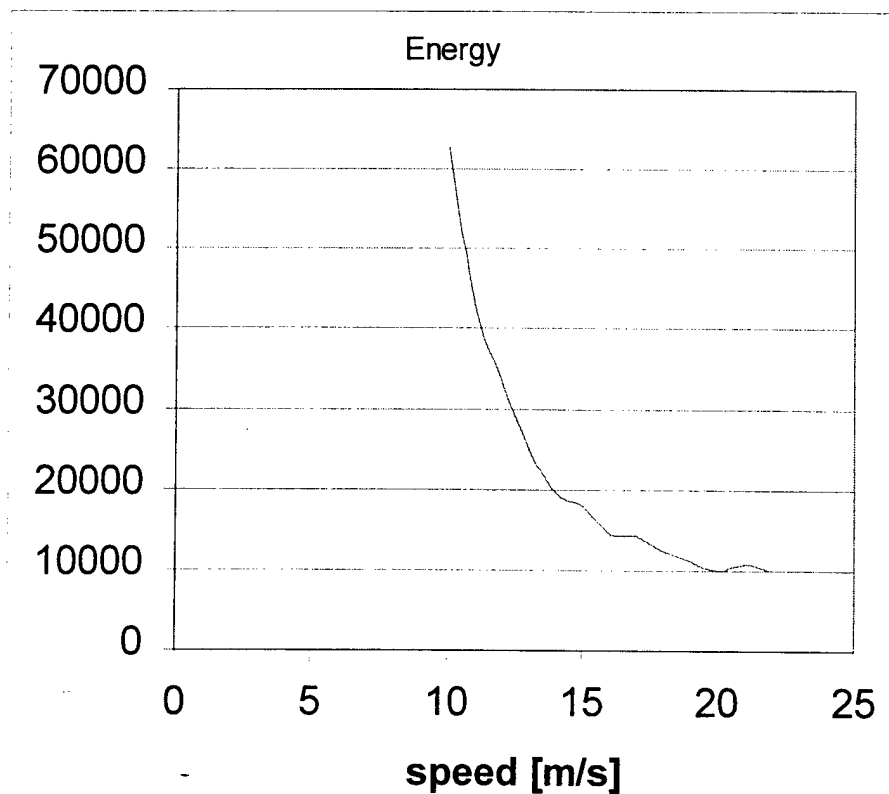


Fig. 5.1.I – Energy spent in cruise.

W	78,48	phi °								
n	1,74338	55								
V	R	I	t°	CL	Cd	T	Ct	Cp	RPsec	En
12	10,28	129,16	10,76	1,73	0,45	35,58	0,130	0,08600	114,9	21929,883
13	12,06	151,59	11,66	1,47	0,33	30,57	0,130	0,08600	106,5	18920,657
14	13,99	175,81	12,56	1,27	0,25	26,71	0,127	0,08500	100,1	16740,89
15	16,06	201,82	13,45	1,10	0,19	23,72	0,127	0,08400	94,9	15095,958
16	18,27	229,63	14,35	0,97	0,15	21,39	0,110	0,08000	92,4	14127,577
17	20,63	259,23	15,25	0,86	0,12	19,57	0,110	0,08000	88,4	13142,855
18	23,13	290,62	16,15	0,77	0,10	18,17	0,092	0,07300	89,1	13034,153
19	25,77	323,81	17,04	0,69	0,09	17,11	0,092	0,07000	88,3	12835,137
20	28,55	358,79	17,94	0,62	0,07	16,32	0,092	0,07300	84,5	12328,347
21	31,48	395,57	18,84	0,56	0,06	15,77	0,072	0,06200	90,1	13335,647
22	34,55	434,14	19,73	0,51	0,06	15,41	0,072	0,06200	89,1	13496,022
23	37,76	474,50	20,63	0,47	0,05	15,22	0,07	0,06200	88,5	13848,064
24	41,12	516,66	21,53	0,43	0,05	15,17	0,07	0,06200	88,4	14386,461

Tab. 5.1.II

Energy W=127									
vel / n	1,15	1,22	1,305	1,4142	1,5557	1,7434	2	2,3662	
12	67402,1081	65553,7585	66790,51	71197,921	79529,338	93502,6062	116655,7746	156617,9	
13	57960,8541	56251,0059	57186,01	60827,419	67807,342	79578,6155	99140,75065	132969,1	
14	51059,0171	49411,0074	50082,38	53112,531	59038,532	69108,9732	85910,32369	115034,57	
15	45787,1918	44147,1881	44574,43	47086,808	52142,374	60823,1711	75380,6968	100691,85	
16	42561,3519	40852,0635	41049,65	43150,507	47552,874	55218,2529	68159,05938	90744,508	
17	39281,0808	37501,5073	37465,76	39148,179	42885,777	49516,5768	60807,84373	80607,606	
18	38604,5979	36627,8849	36347,15	37711,929	41018,773	47035,0783	57394,82889	75668,439	
19	37635,5805	35461,1177	34921,34	35939,697	38767,67	44092,2752	53394,32212	69923,499	
20	35761,1128	33440,2644	32654,30	33302,482	35585,293	40092,9194	48117,285	62508,444	
21	38247,061	35477,2695	34329,52	34664,764	36654,492	40859,9792	48534,13578	62458,55	
22	38260,3325	35193,0343	33729,62	33699,15	35229,631	38811,5842	45567,47856	58008,526	
23	38804,5289	35390,4212	33585,45	33184,224	34272,964	37278,1355	43206,98587	54333,988	
24	39855,6449	36041,4653	33863,86	33080,023	33735,314	36197,4788	41371,14119	51322,126	

Tab 5.1.III

	1,15	1,22	1,305	1,4142	1,5557	1,7434	2	2,3662
12	101289,9	99441,5	100678,3	105085,7	113417,1	127390,4	150543,5	190505,7
13	82967,2	81257,4	82192,4	85833,8	92813,7	104585,0	124147,1	157975,4
14	70568,5	68920,5	69591,9	72622,0	78548,0	88618,5	105419,8	134544,0
15	63684,4	62044,4	62471,6	64984,0	70039,5	78720,3	93277,9	118589,0
16	57033,9	55324,6	55522,1	57623,0	62025,4	69690,8	82631,6	105217,0
17	53631,6	51852,0	51816,3	53498,7	57236,3	63867,1	75158,4	94958,1
18	50848,2	48871,5	48590,7	49955,5	53262,4	59278,7	69638,4	87912,0
19	48851,2	46676,7	46136,9	47155,3	49983,3	55307,9	64609,9	81139,1
20	45800,6	43479,8	42693,8	43342,0	45624,8	50132,4	58156,8	72547,9
21	49001,6	46231,8	45084,1	45419,3	47409,0	51614,5	59288,7	73213,1
22	48292,4	45225,1	43761,7	43731,2	45261,7	48843,6	55599,5	68040,6
23	48330,3	44916,2	43111,2	42710,0	43798,7	46803,9	52732,7	63859,8
24	49044,6	45230,4	43052,8	42269,0	42924,3	45386,4	50560,1	60511,1

Tab 5.1.IV – Total energy spent for cruise and turning versus speed and load factor.

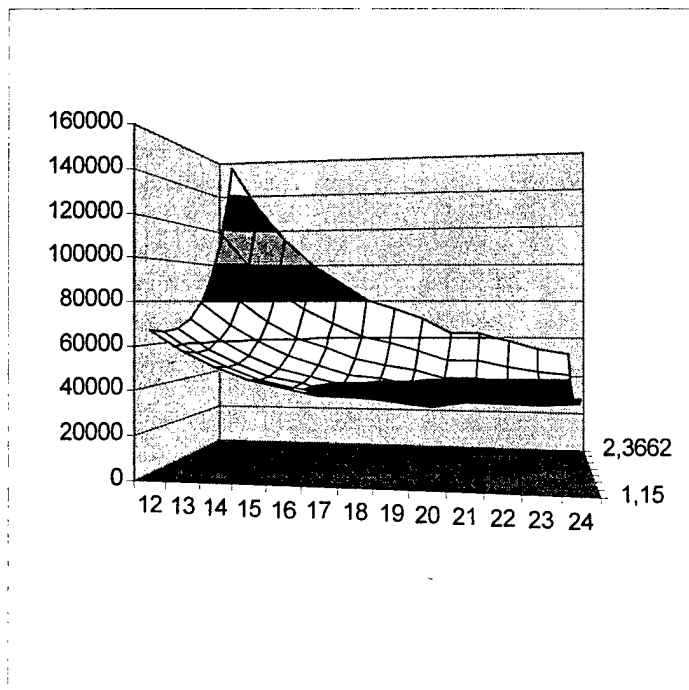


Fig. 5.1.II

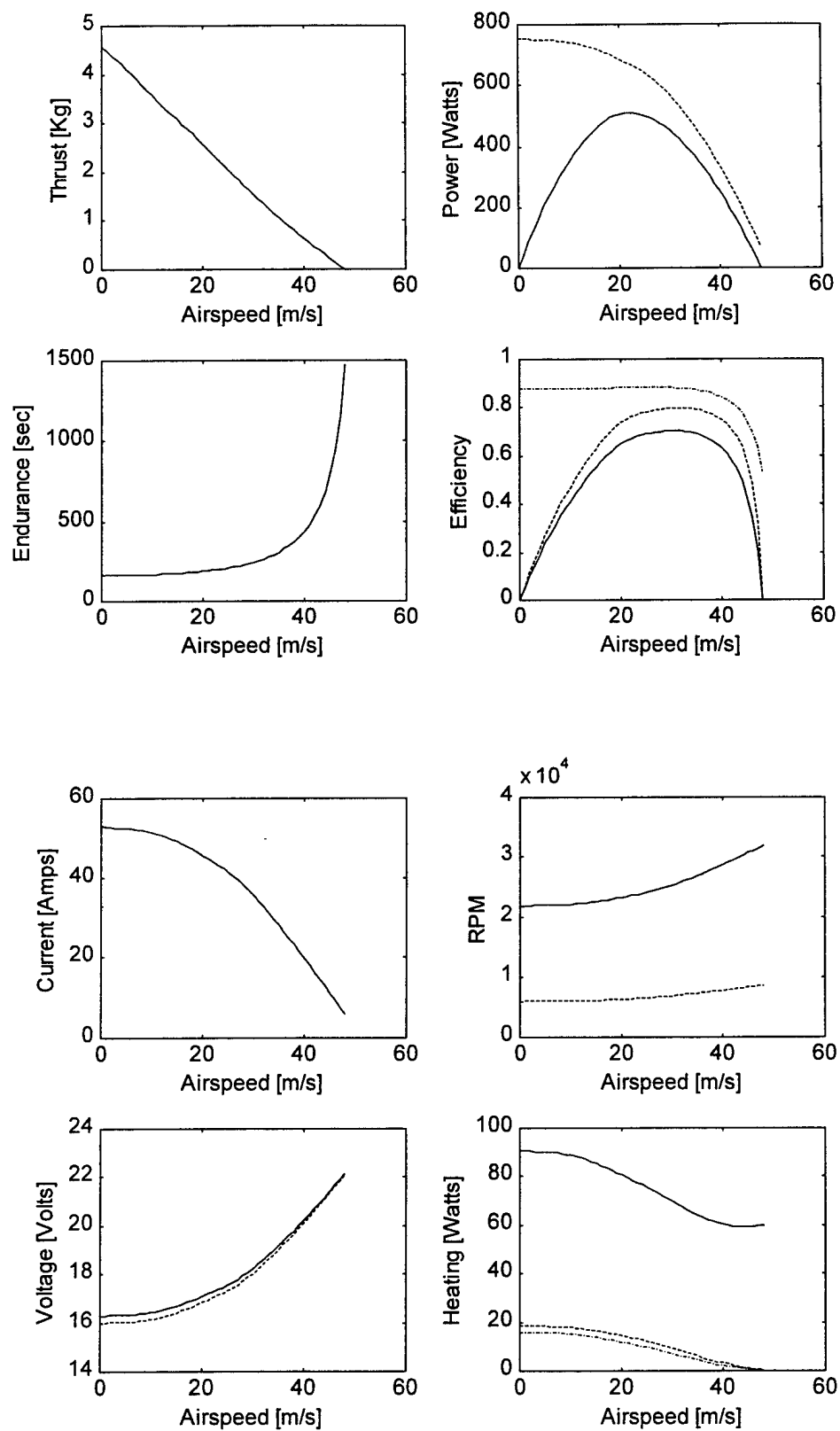


Fig. 5.2.I motor performance

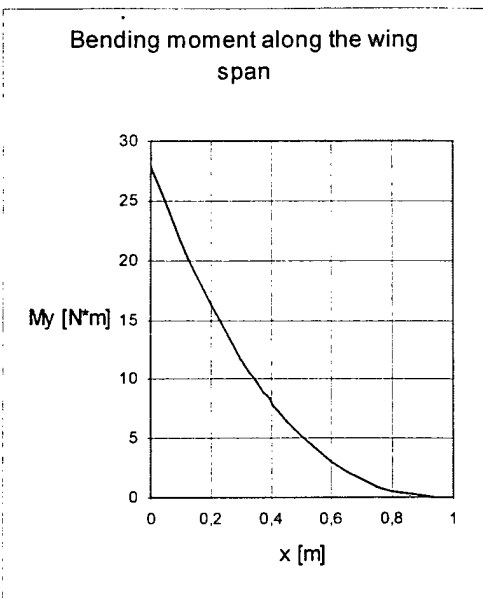


Fig 5.3.II

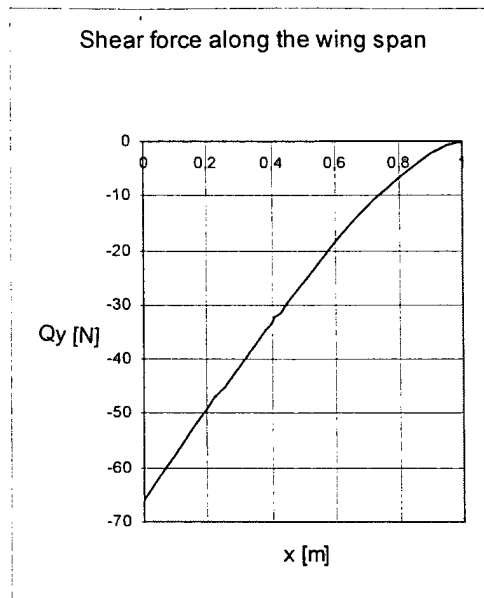


Fig 5.3.III

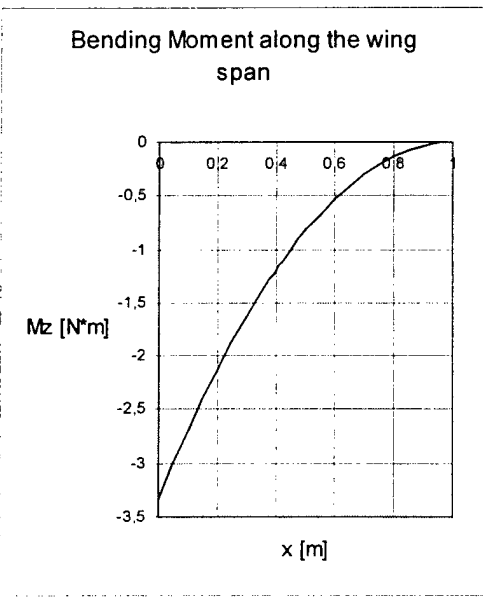


Fig 5.3.IV

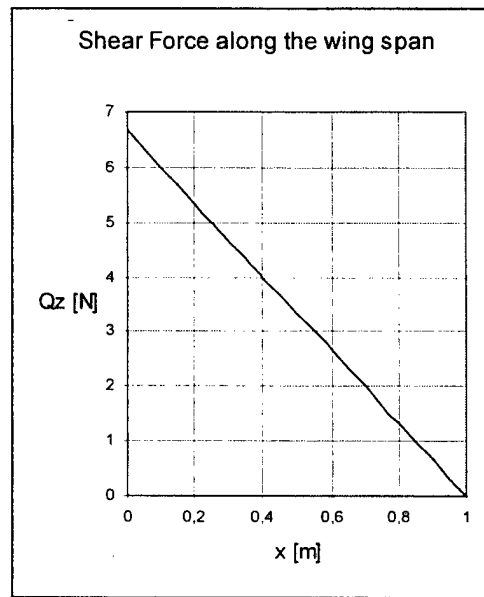


Fig 5.3.V

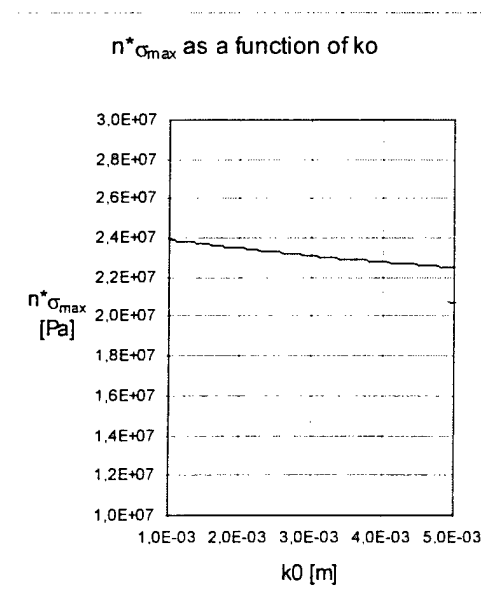


Fig 5.3.VI

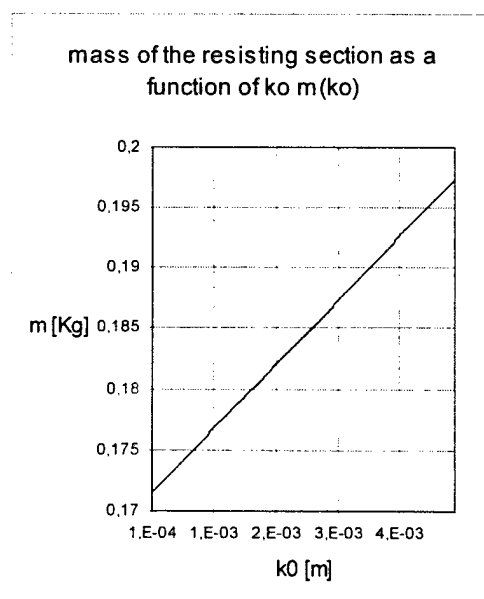


Fig 5.3.VII

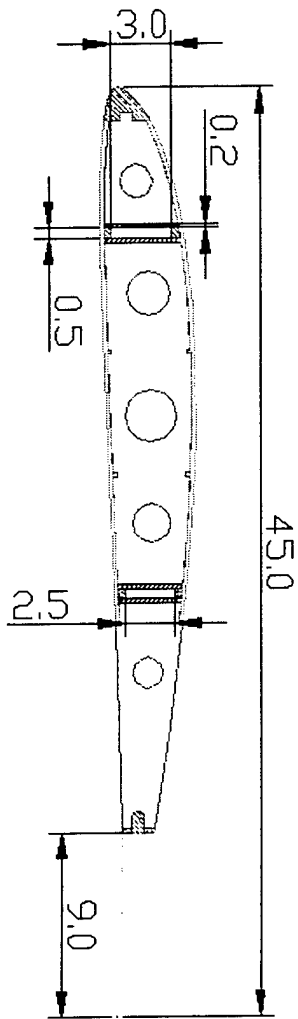


Fig 5.3.Ia

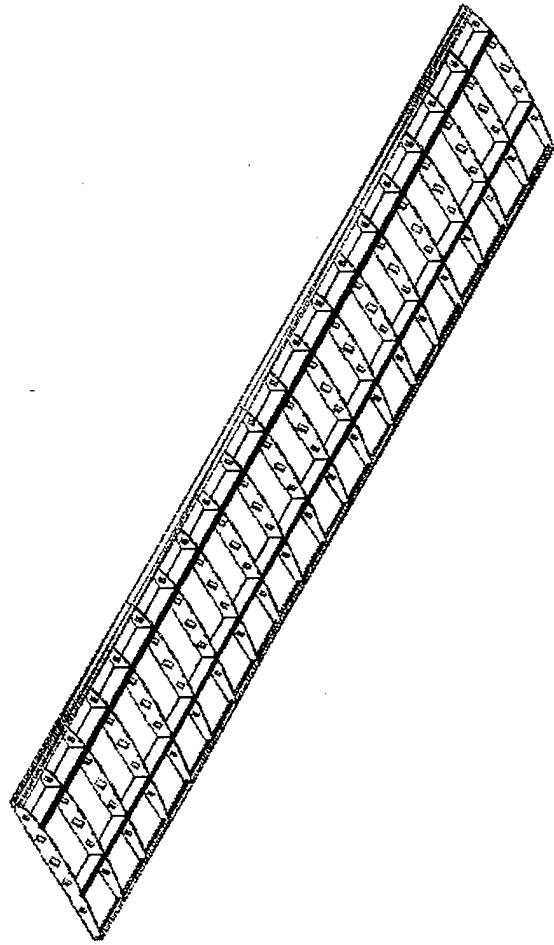


Fig 5.3.Ib

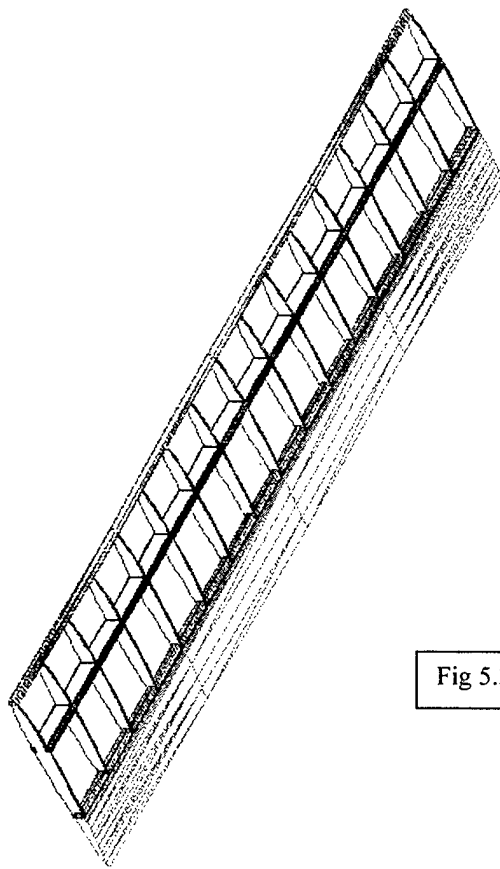
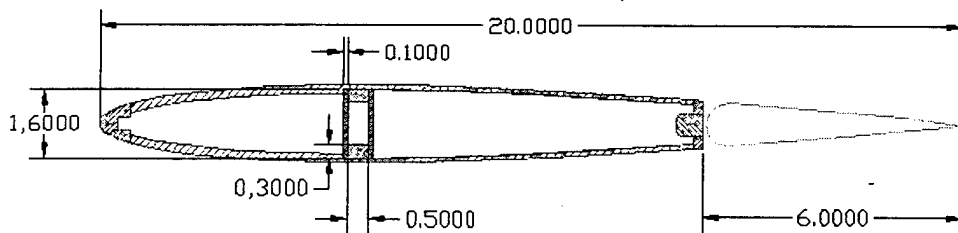
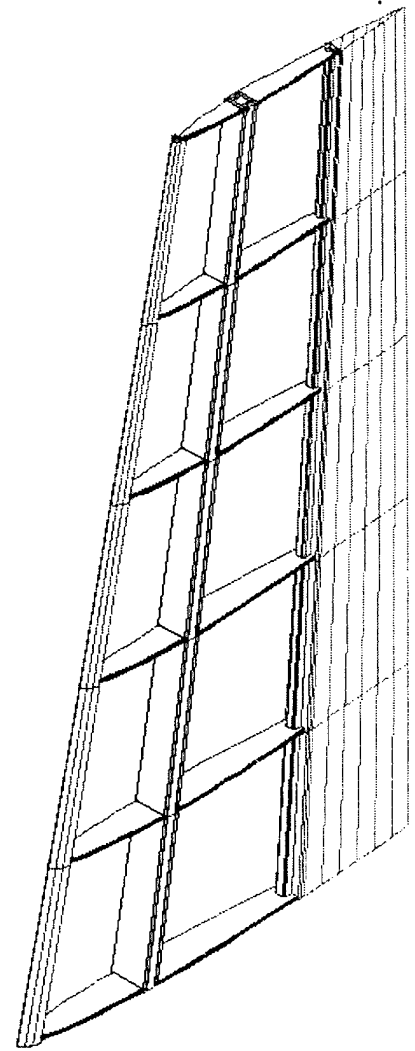
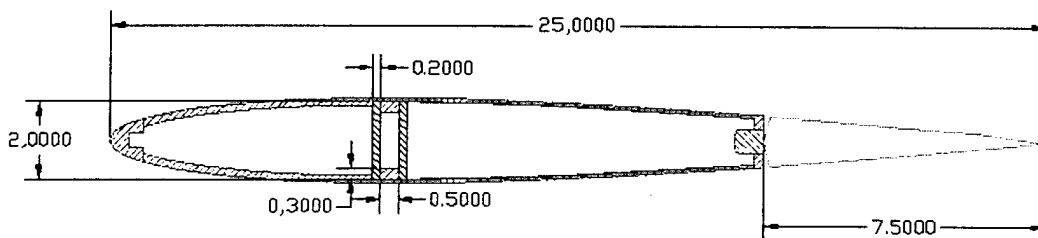


Fig 5.3.VIII



horizontal



vertical

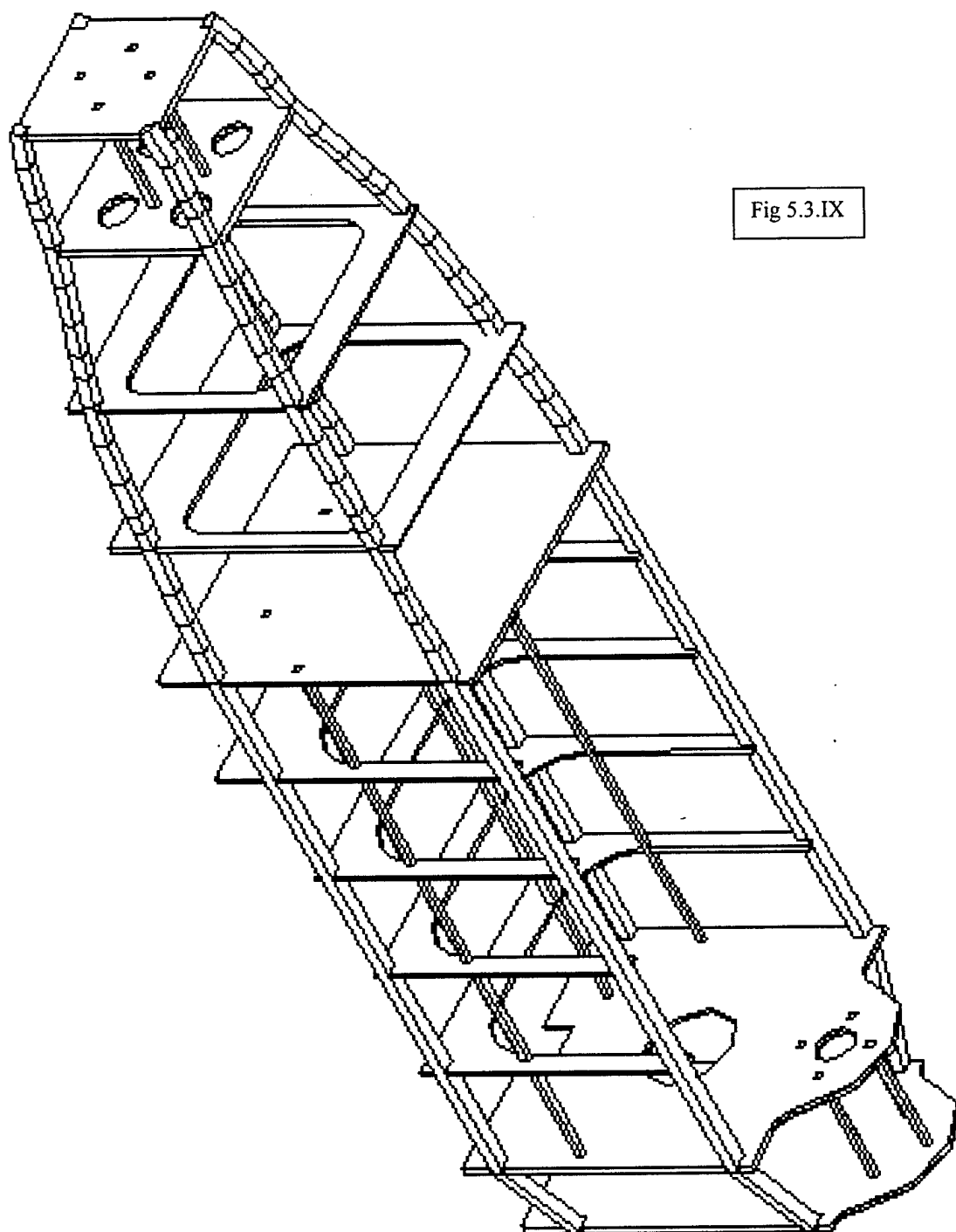


Fig 5.3.IX

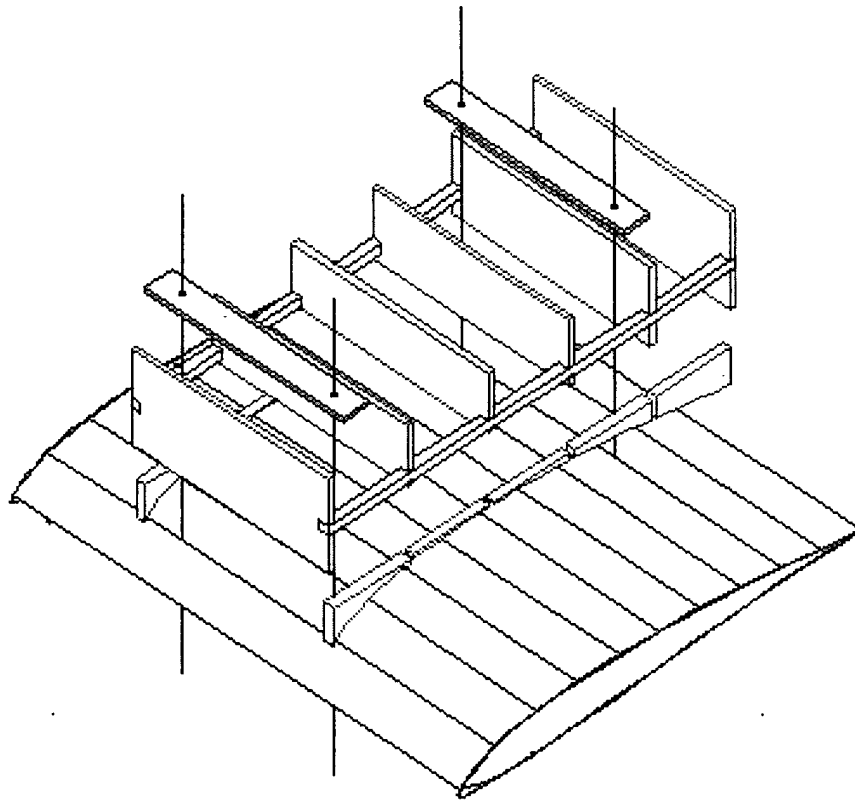


Fig 5.3.X

Tab. 5.4.I

Fuselage Angle of Attack:.....	0.000	[deg]
Surf. n. 1 Lift Coefficient:	0.494	
Surf. n. 2 Lift Coefficient:	-0.480	
Surf. n. 1 Ind. Drag Coefficient:	0.026	
Surf. n. 2 Ind. Drag Coefficient:	0.002	
Surf. n. 1 Moment Coefficient:	-0.096	
Surf. n. 2 Moment Coefficient:	2.878	
Maximum Profile Lift Coefficient :.....	0.592	
Maximum Profile Lift Coefficient :.....	0.067	
V [m/s], Flying Speed at Calculated Total Lift Coefficient :.....	18.659	
FRONT WING Total Lift Coefficient:.....	0.494	
REAR WING Total Lift Coefficient:.....	-0.480	
Total Lift Coefficient:.....	0.409	
Total Induced Drag Coefficient:.....	0.026	
Cd0:.....	0.035	
Total Parasite Drag [kg]:.....	0.685	
Total Induced Drag [kg]:.....	0.516	
Total Drag [kg]:.....	1.200	
Parasite Drag / Total Drag [nil]:.....	0.570	
Input Thrust [kg]:.....	0.000	
Va (Input Thrust / 2) [nil]:.....	0.000	
Total Aero Moment Coefficient about Xcg:.....	0.131	
Total Moment Coefficient about Xcg:.....	0.131	

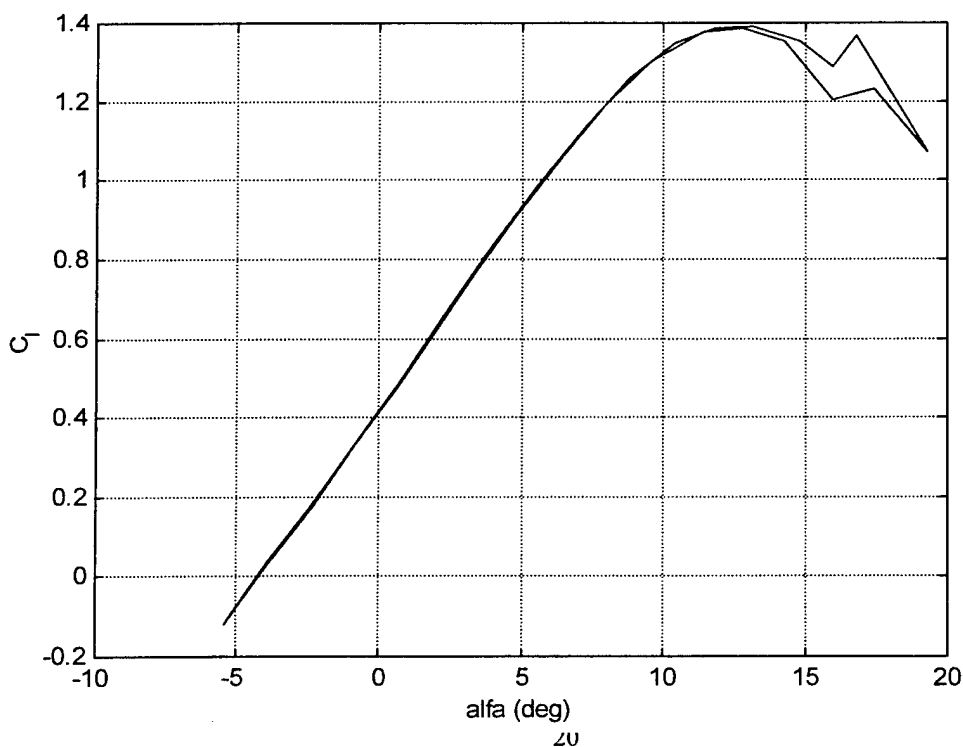


Fig 5.4.V

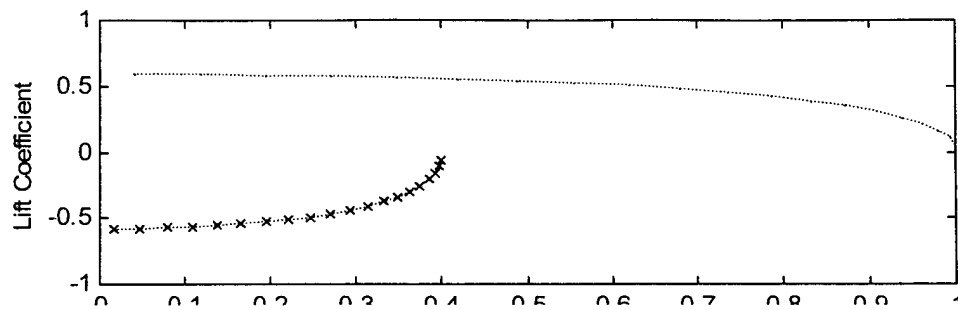


Fig 5.4.I

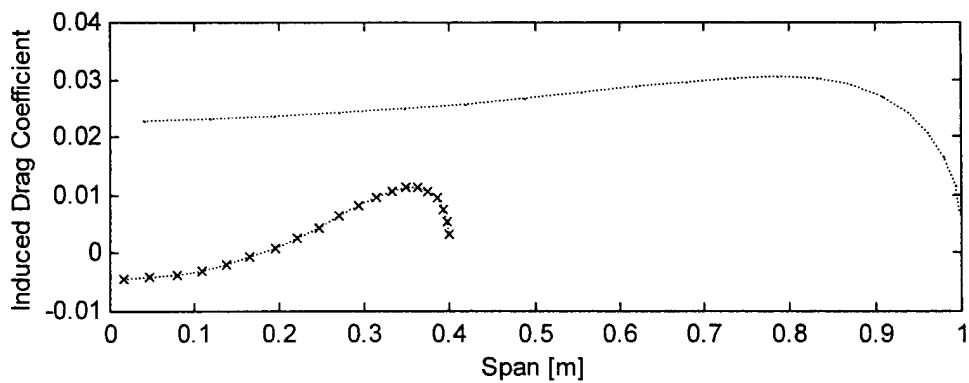


Fig 5.4.II

Fig 5.5.II

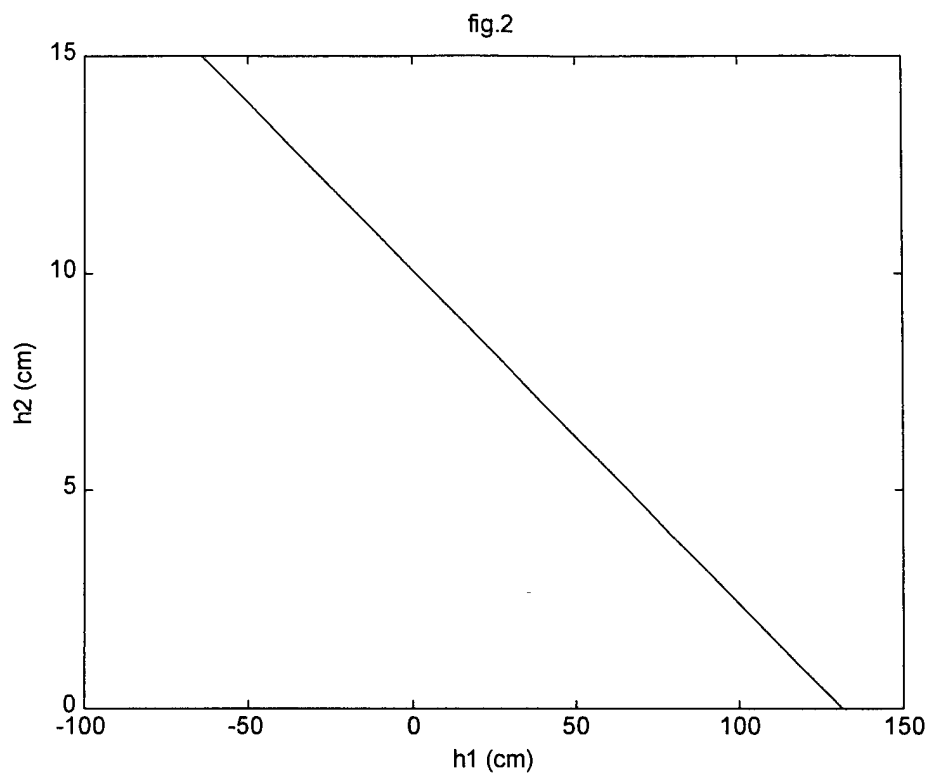
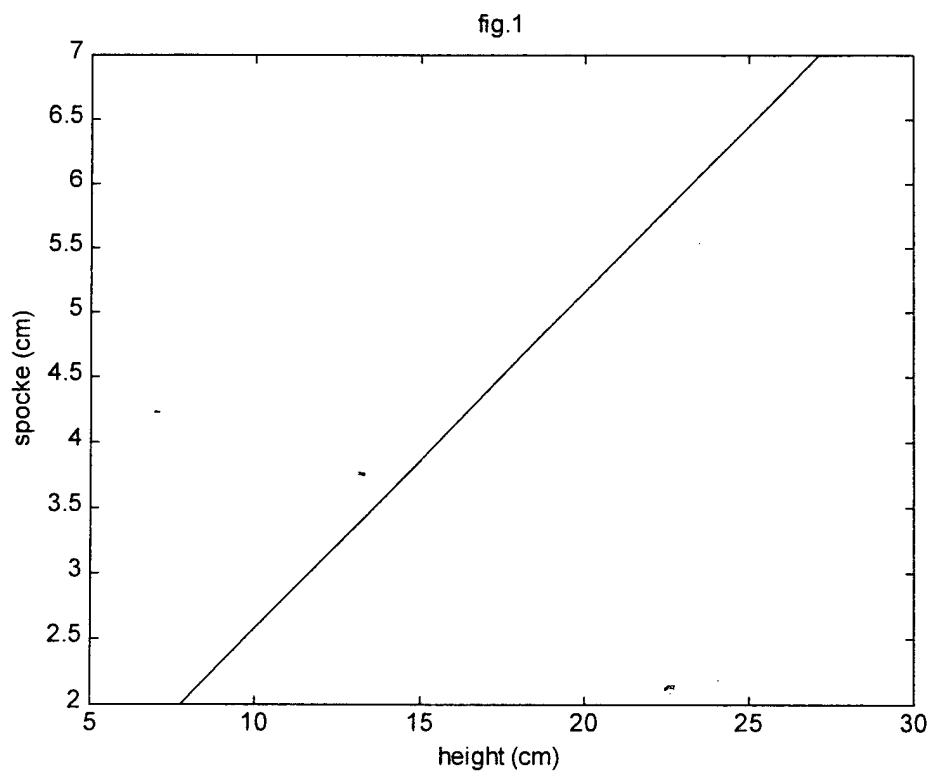


Fig 5.5.I



Galileo

(SI units)

pay load	6 round bottles of water											
	concept	geom. characteristics	span	root chord	taper ratio	depth	asppt ratio	lenght	height	width	airfoil	
		1 wing	2	0.45	1	0	4.6				SELIG 7032	
		2 flaperons	1.8	0.1	1	0						
		1 horizontal tail	0.8	0.2	1	0	4				NACA 0009	
		1 elelavor	0.7	0.07	1	0						
		1 vertical tail	0.45	0.25	0.6						NACA 0009	
		1 rudder										
		1 fuselage						1.18	0.27	0.23		
	1 tail boom						1					
bus	propulsion	2 motors		Aveox1 1412/2Y								
		2 controllers		plettenberg								
		2 red. gears		Robbe	planeta	3.7.;1						
		2 propellers		3 blade	Graupner	Super extra	0.4x0.18					
	rem. control	radio										
		receiver										
	sevos											
	materials	characteristics	r	E	tension	compr.	bending	shear				
		balsa wood	170	3,50E+09	2,40E+06	1,0E+06	2,40E+06	1,20E+06				
		lime wood	530	7,00E+09	8,30E+06	4,50E+06	8,80E+06	4,40E+06				
		aluminium2024	2600	7,38E+10	3,10E+08	2,55E+08	2,55E+08	2,55E+08				

Tab 5.6.I

μ	0,05			AR	8
ρ	1,22			e	0,913896
Cl max	1,4			Sg [m]	30
Cdo	0,08				
K	0,07572				

W/S [N/m2]	Ka	T/W	Vf [m/s]	Kt
156,8	-0,00062	0,585573	16,26018	0,535573
147	-0,00066	0,557825	15,74385	0,507825
137,2	-0,0007	0,530123	15,21001	0,480123
127,4	-0,00076	0,502477	14,65673	0,452477
117,6	-0,00082	0,474902	14,08173	0,424902
107,8	-0,0009	0,447417	13,48223	0,397417
98	-0,00099	0,420049	12,8548	0,370049
88,2	-0,0011	0,392834	12,19513	0,342834
78,48	-0,00123	0,366048	11,50355	0,316048

Tab 5.7.I

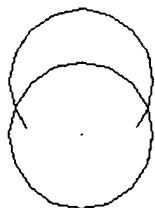
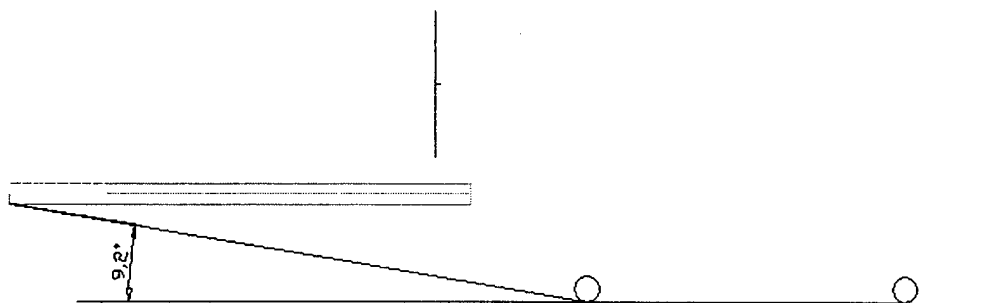


Fig. 5.6.I

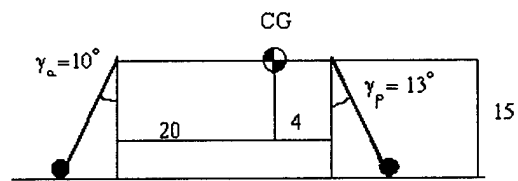


Fig. 5.5.III

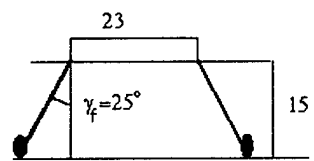


Fig. 5.5.IV

Section 6 : *Manufacturing plan*

Manufacturing Processes and material selection are two stages that in parallel and integrate each other. The most used material in our project has been wood, specially balsa, for skins, and lime for the structural elements. We choose these materials for their law cost and because they are easy to be mould.

The structures of wing's and tail's surfaces has been beaded to have a lower weight and because that kind of structure is very well known and easy to be studied. The fuselage has been realized with frames and stiffeners for the same reason.

Because the wood is easy to deal, we could employ easy-to-use tools like electric saws, drills, and files. Also the assembly required quite simple processes and techniques, no specific glue or soldering, but modelers glue like the epoxy twin-components or the vinilic one.

To tackle the cost to buy the primary need goods, we used the found given to us from AIDAA, even if the Galilei itself took a part in our expenses.

Where the structural need did not allow to employ the wood, we had to choice alternative materials, such as aluminum and carbon fiber composites, always considering as a primary target the law cost and the high performances. The hardest thing was to find the materials in the right format.

To design some critical points as the junctions boom-fuselage, the wing attachment, the landing gear connection and the motors' castles we applied our inventiveness, considering that the real world's aircraft's solutions can not be used for the models.

Table 6.I show a manufacturing milestone chart displaying scheduled event timings. It is certainly more truthful than the table reported in section 2: the day of the competition was so near at this time that we mattered to follow the plan with high fidelity.

team A2	team B2	MANUFACTURE ACTIVITY	date	team A1	team B1
Enrico and Fabrizio	Andrea and Paolo			Luca and Pier Domenico	Filiberto
FUSELAGE					
ribs	spars		14/01/00 frames		stiffeners
ribs	spars		18/01/00 frames		stiffeners
ribs	spars		21/01/00 frames		stiffeners
ribs	leading and trailing edge		25/01/00 frames		stiffeners
reinforced ribs	leading and trailing edge		28/01/00 assembly		assembly
reinforced ribs	wing support		01/02/00 assembly		assembly
assembly	assembly		04/02/00 weight control		weight control
assembly	assembly		07/02/00 partial cover		partial cover
TAIL					
assembly	assembly		11/02/00 ribs		spars
weight control	weight control		14/02/00 ribs		spars
connector boom-wing-fuselage			18/02/00 ribs		spars
connector boom-wing-fuselage			22/02/00 ribs		lead / trail edge
connector boom-wing-fuselage			25/02/00 connector tail planes		
partial cover	partial cover		29/02/00 connector		tail planes
assembly	assembly		03/03/00 assembly		assembly
assembly	assembly		07/03/00 assembly		assembly
report	editing	and writing			
MOTORS					
installation	installation		14/03/00 installation		installation
installation	installation		17/03/00 installation		installation

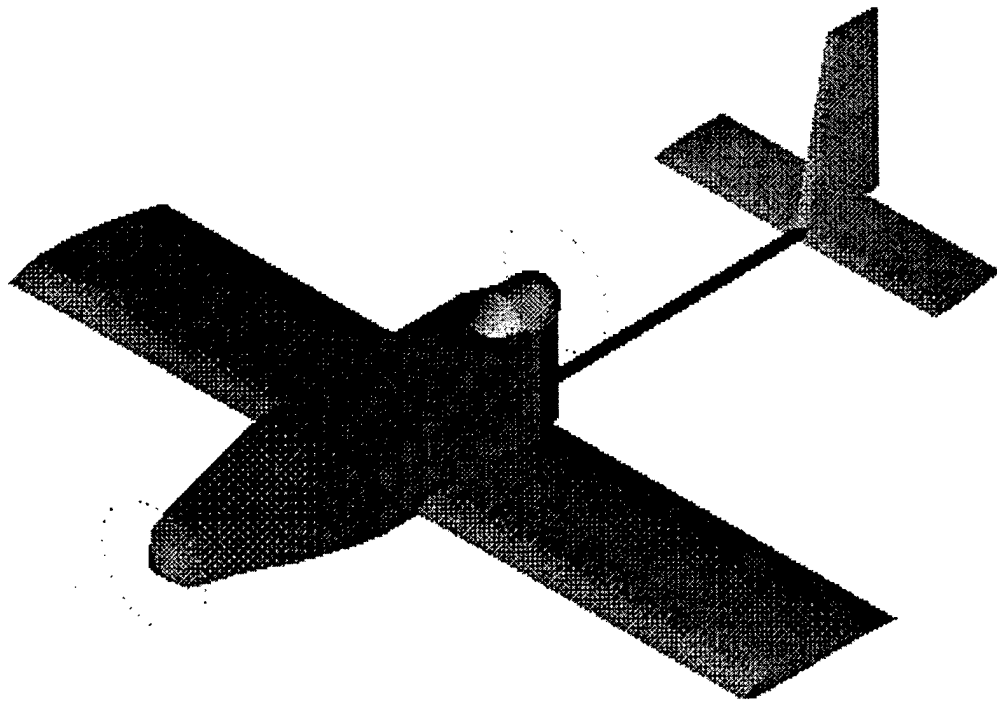
Tab 6.I

Università degli Studi di Roma "La Sapienza"
Facoltà di Ingegneria / Dipartimento Meccanica e Aeronautica

AIAA Student Design/Build/Fly Competition 1999/00

DESIGN REPORT

ADDENDUM PHASE



GALILEO

CONTENTS

- 7. LESSONS LEARNED
- 8. AIRCRAFT COST
- 9. ACKNOWLEDGEMENT

We would like to remember prof. Enzo De Angelis, who leaved us a few days ago.

Although we have known him only for a short time, we could appreciate his kindness and his courtesy. His interest and his enthusiasm have been fundamental to help us to carry on our project.

Section 7-Lessons learned

Index

7.1 Introduction

7.2 Structures

7.3 Propulsion System

7.1 Intro: lessons learned and improvements suggested for an eventual next design

In the proposal phase design report we underlined that the aspect of the research of external contacts and aids for supplying funds, materials and tools was actually much more important than we had thought at the beginning of our work. It is just because of difficulties linked with this aspect that we had to produce some changes in the concept described in the previous report (see 7.3).

But now we have to admit another area of knowledge has been too much disregarded, for our fault.

We are thinking of the technical knowledge, result of the practice and the experiences, whose "those in the knowledge" are the only owners (actually, each one in his own manner!). A kind of knowledge which unfortunately our university studies, with their character so much theoretical, had never taught us to appreciate the value.

The participation in the D/B/F competition, and the getting deeply in the problems of the construction and experimentation, has given us the chance to wonder seriously about the comparison-collision between the theoretical, academic science and the technical, practical one. And in the attempt to find an equilibrium between both of them, this year our project assumed an aspect less elegant and sophisticated (from a theoretical point of view) than last year, but we can be proud having carried in flight our "Galileo".

The world of the technical knowledge we are referring to is, in our case, the one of the aero-models, and of the people who stroll about it. If it is true that since the beginning we looked for contacts in such world, it is also true that our research was for someone who was able to "implement" our design, employing himself in solving only the building problems. Only in the last period, in order to prepare the flight tests of our model, we frequented aero-models clubs, spoke to people expert in models' building and piloting this sort of vehicles, tried to get their secrets out of them.

Just in so doing we realized we had to produce other changes in our concept. In particular, it has been very important in this phase the contribution of our pilot, Luca Friggeri, and of Mr Richard Borg, people who we are glad to thank with enthusiasm for their advices and suggestions about stability and manoeuvrability of the vehicle; only we sorrow not to have asked for such suggestions much earlier!

In the following we are going to illustrate the changes (not so many, after all!) we produced in the "real thing" with respect to the proposal design. In the section about structures we also will present the results of a smart theoretical study of the wing box performed by the finite element method to evaluate the stresses, and so the sizing, of the main structural elements of the wing. The all to confirm once again that, to improve our work, we should have to link better and more deeply the contributes of the theory and of the experimentation. And so, we should have to anticipate much the manufacturing process with respect to the day of the competition, in order to make a real series of tests to optimise the configuration. And this is what we are proposing to do next year!

In conclusion of this introduction we will add that, regarding the manufacturing process implementation, we learned one thing would have made the work surely much faster was to elect a

system architect who could assume the responsibility to make decisions and to coordinate the different teams of work. Nevertheless in our condition of students, it is very difficult to delegate to one person this heavy task. More over, the lack of such figure forced us to participate each one in the work of each other, and, after all, this has been important for our knowledge's growth.

7.2 Structures

7.2.1 Tail boom

The structural aspect which was still unsolved at the time of writing the proposal phase report regards the tail boom. Actually, the tests we have produced on the tubes made of carbon fiber we could find in the market did not give us trustable results, because of the shortage of the time (we did not perform a significant number of tests) and because however we could not find commercial carbon tubes having the dimensions we needed.

Every way, the boom made of aluminium we had already built was too penalizing for its high weight. So, we decided to adopt an "intermediate" solution: we have taken a boom made of glass fiber (used for fishing) strenghten by collars of carbon fiber in the more critical points (fuselage junction).

7.2.2 Motor castles

For these elements we leaved the wooden solution firstly considered in favour of two little domes, made of a composite material (carbon fiber and epoxy-resins) that we built our self. This solutions gives us the advantage of a resistant structure with a low weight and an aerodynamic shape.

7.2.3 Undercarriage

As a consequence of the aerodynamics considerations, we thought it right to consider an acceleration at landing equals to 3g. The resulting strength $F=382.2 \text{ N}$ will act on both the legs of the undercarriage. Because of the intensity of strength is opportune to use an aluminum ($\sigma=2.55 \cdot 10^8 \text{ Pa}$) rectangular section. The formula of Navier in the critical section, that is the joint with the fuselage, gives us:

thickness	$b=5 \text{ mm}$
width	$a=24 \text{ mm}$
momentum of inertia	$I=2.5 \text{ E } -10 \text{ m}^4$
safety factor	$n=2$

The angle γ_p , mentioned at the detail phase, has been reduced to the value $\gamma_p = 10^\circ$, because of the changes of the aerodynamics behaviour and the centre of gravity position due to structural changes (boom, tail). As a consequence, it results:

distance between joint and CG :	$l_1 = 4.67 \text{ cm}$
height undercarriage :	$h = 26.5 \text{ cm}$

Owing to these considerations we have bought the following undercarriage:

JOHNATHAN EXTRA 300	
width :	$l = 54 \text{ cm}$

height :	$h = 22.5 \text{ cm}$
thickness	$s = 5 \text{ mm}$
dihedral angle	$\gamma_p = 10.3^\circ$
price :	$\text{£ } 35000 \text{ (\$ } 17.50 \text{)}$
weight :	$w_p = 0.5 \text{ Kg}$

It answers, in matter of safety, to detailed notes wished. For fore undercarriage are not asked high performance; we have chose the following :

EUROKIT

width :	$l = 3 \text{ cm}$
height :	$h = 17 \text{ cm}$
thickness :	$s = 3.5 \text{ mm}$
dihedral angle :	$\gamma_a = 0^\circ$
price :	$\text{£ } 12500 \text{ (\$ } 6.25 \text{)}$
weight :	$w_a = 0.1 \text{ Kg}$

7.2.4 Study of the wing box with the Finite Elements Method

In order to value the validity of the choices done about the thickness of the proof structures of wings, we have done a FEM (finite elements method) simulation. The tool used is NASTRAN TM.

In order to analyse the not uniform bending stress, we have assumed as input the following parameters (root section):

- shearing stress : $Q = 80 \text{ N}$
- center of shear position : $X_{ca} = X_{ct} =$
- values characteristic of balsa : $E = 3.5 \text{ Gpa}$
 $\rho = 170 \text{ Kg/m}^3$
 $\sigma_c = 10 \text{ Mpa}$
 $\sigma_f = 24 \text{ Mpa}$
 $\sigma_t = 12 \text{ Mpa}$

We have choice the thickness of spars' cores equals to double of thickness of skin covering ($t = 2s$).

In fact, thanks o the study of twisting stress done in the detail phase, we have arrived to conclusion that, in the most critical condition (square box, $m = 1$)the stress is minimum if $t = 2s$.

Using a curvilinear abscissa origineted in leading edge, we have valued the strain of Von-Mises ($\sigma' = \sqrt{\sigma^2 + 4\tau^2}$) which acts on them.

According to numeration of fig.7.I, we got for the stresses on the various elements the values shown in Table 7.I.

Figure 7.II represents the diagram of the stresses along the elements of the wing box.

7.2.5 Wing

By frequenting aero-models clubs, we realized that the acceleration these vehicle are subject can be greater than 3g. More over, an acceleration of 5g is well probable! So, we had to come back to our calculations about the structure of the wing, which was sized considering a load factor equals to 3. The

new solution sees a wing with three spars: we added a central spar in the old wing box. It section is a "double T".

7.3 Propulsion System

In the proposal design we had chosen a couple of motors Aveox 1412/2Y with 3 blades propellers. Actually, this solution has been impossible to realize.

In fact, we have to say that finding such motors has been very difficult because of problems of a commercial nature, most of all about -it looks strange but it's true!- the ways of money transfer from a state institute (the I.T.I.S: Galilei, our supplier) and the seller (Aveox).

So, we had hurry to think to a different choice of the motors, trying to answer new figures of merit as the availability in very short time and a flexible way of payment.

The result has been a couple of Graupner 220/30-3 p4, with reducer 5:1, with no sensors. These motors, brushless as the Aveox ones, seemed to guarantee good performances, perhaps the best between European brushless motors.

Strictly linked to the motor it is its controller. More over, this coupling should be compatible with the propeller.

To gain the optimum configuration of the propulsion system, we used the program MOTOR 1 (mentioned in the proposal phase design report), inputting the data about the motors and the controller Graupner 451s, and analysing the performances of several propellers.

Once selected a few propellers which seemed to answer best our needs, we produced some experiments at the test-bench on them, to verify the outputs of the computer simulation (MOTOR 1), regarding current, voltage and power absorbed by the motor, agreed with the experimental results.

Table 7.II, and its plot figure 7.III, show the results of the tests on the APC 16 X 13 two blades propeller; table 7.III shows the output of the numerical simulation.

We could see the results about the three mentioned parameters are well corresponding and so we could think it would be the same for the values of thrust and rounds per minute.

We thought the propellers able to exploit all the potential of the Graupner motors (with a number of 16 cells) without reaching dangerous conditions (>45 ampere) would be the APC 15 X13 for the pusher motor (rear) and the 16 X 9 for the puller one (front).

When this decision had been made, Mr Angelo Silvagni lent us a motor Aveox 1412/2Y with a reducer box 3:1, whose bench-tests with a series of propellers were known (table 7.IV).

So, the final choice for the propulsion system, considering the results of bench-tests, the computer estimations about performances and the easy availability (in the market) of the right propellers, is:

front motor
Aveox 1412/2Y
with propeller Menz 16 X 10
powered by 20 cells;

rear motor
Graupner 220/30-3 p4 g5
with propeller APC 15 X 11 for a "safer" choice,
with propeller APC 16 X 13 for a "braver" choice,

powered by 16 cells.

Number of
element σ_{VM}

(10E5 Pa)

1	4,13
2	4,01
3	3,78
4	3,47
5	3,02
6	2,51
7	1,93
8	1,36
9	1,96
10	2,63
11	1,99
12	1,90
13	1,91
14	1,96
15	2,02
16	2,07
17	2,11
18	2,15
19	2,18
20	2,20
21	2,22
22	2,23
23	2,23
24	2,24
25	2,22
26	2,28
27	2,36
28	2,57
29	3,42
30	2,68

Number of
element σ_{VM}

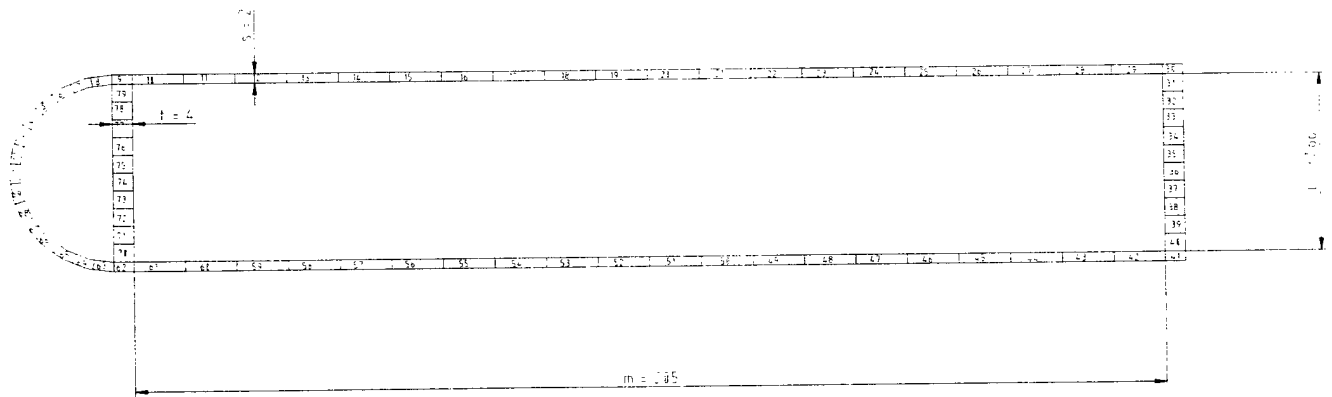
(10E5 Pa)

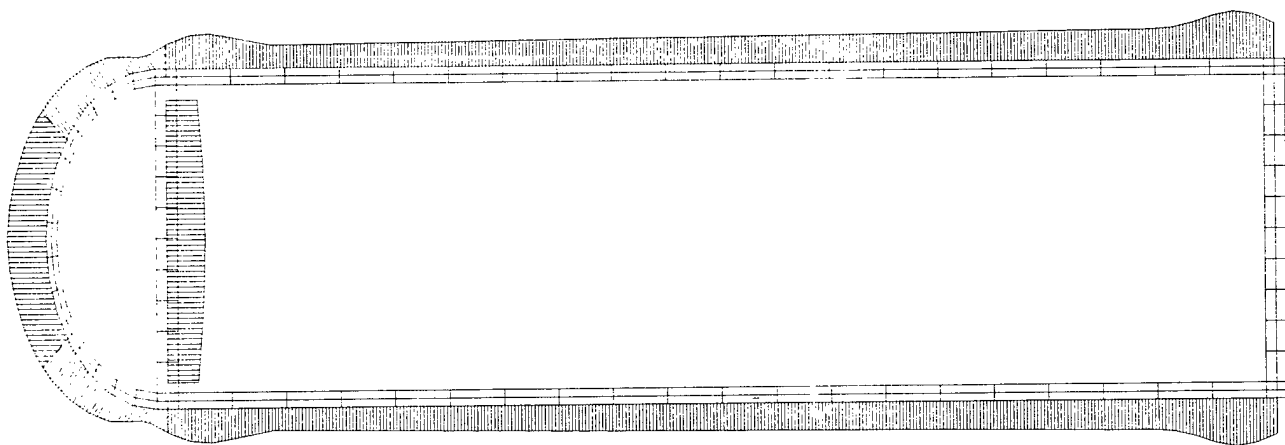
31	3,638
32	3,862
33	4,084
34	4,218
35	4,284
36	4,284
37	4,218
38	4,084
39	3,862
40	3,638
41	2,687
42	3,423
43	2,576
44	2,369
45	2,283
46	2,254
47	2,243
48	2,238
49	2,232
50	2,222
51	2,207
52	2,184
53	2,154
54	2,117
55	2,073
56	2,021
57	1,968
58	1,919
59	1,909
60	1,995

Number of
element σ_{VM}

(10E5 Pa)

61	2,635
62	1,965
63	1,367
64	1,935
65	2,515
66	3,028
67	3,471
68	3,788
69	4,011
70	2,926
71	3,187
72	3,415
73	3,548
74	3,614
75	3,614
76	3,548
77	3,415
78	3,187
79	2,923



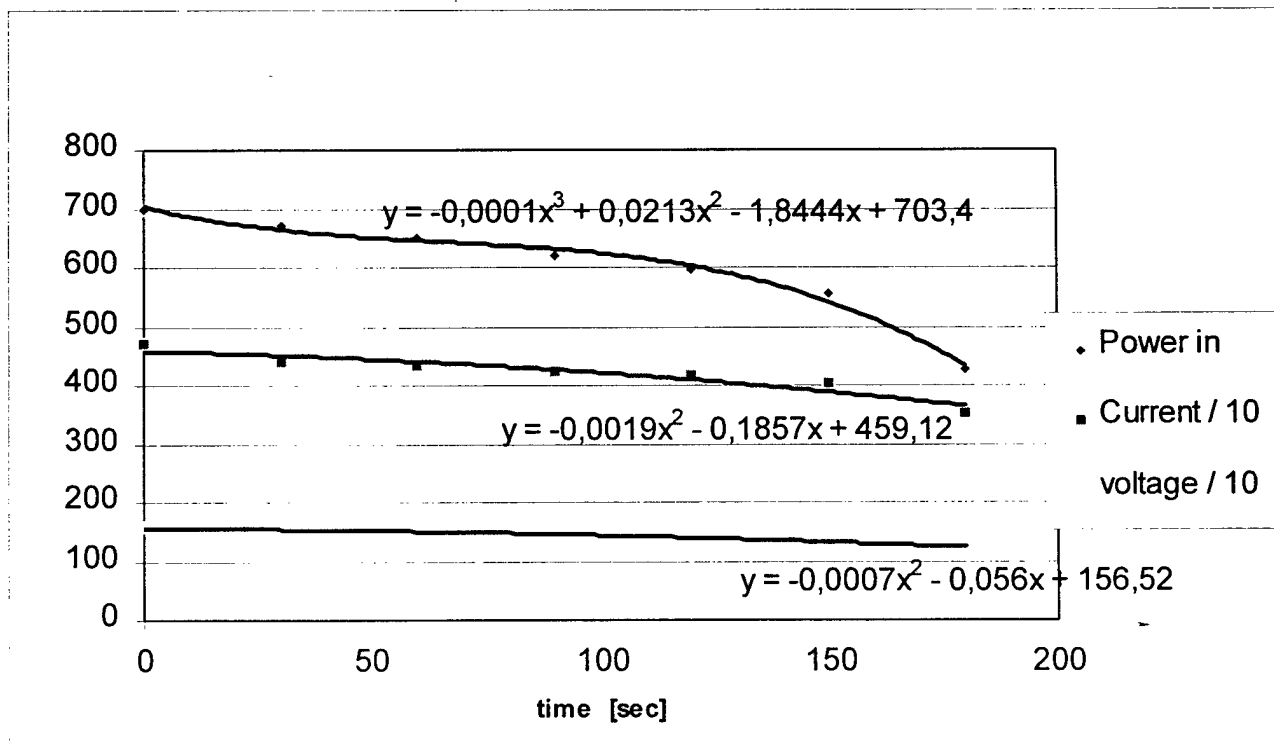


scale s=10E5 Pa/m

propeller 16x13 APC
 motor Graupner 220/30-3 p4 gear 5
 controller Graupner SL 45
 cells Sanyo RC2400

time [sec]	V	A	Watt (in)
0	16.0	47	700
30	15.0	44	670
60	14.9	43	652
90	14.5	42	620
120	14.2	41.8	597
150	13.7	40.5	557
180	12.0	35.2	427
210			
240	stop	stop	stop

270



Tab. 7.III

APC 16x13 and Graupner 220/30 3 p4 g5 from Motor1

STATIC PERFORMANCES (time 0")

Thrust (T):..... 3.95 [Kg]
 Torque (Q):..... 1.06 [Nm]
 Motor RPM:..... 5476 [RPM]
 Current (Ii):..... 47.92 [Amps]
 Battery Output Voltage (Vi):..... 16.817 [Volts]
 Motor Input Power:..... 792.7 [Watts]
 Motor Efficiency:..... 0.77
 Endurance:..... 180.3 [Secs]

MAXIMUM USEFUL POWER PERFORMANCES

Airspeed(V):..... 20 [m/s]
 Thrust (T):..... 2.07 [Kg]
 Torque (Q):..... 0.87 [Nm]
 Motor RPM:..... 5878 [RPM]
 Current (Ii):..... 39.91 [Amps]
 Battery Output Voltage (Vi):..... 17.722 [Volts]
 Motor Input Power:..... 698.2 [Watts]
 Useful Power:..... 405.6 [Watts]
 Motor Efficiency:..... 0.77
 Propeller Efficiency:..... 0.76
 Global Efficiency:..... 0.57
 Endurance:..... 216.5 [Secs]

MAXIMUM GLOBAL EFFICIENCY PERFORMANCES

Airspeed(V):..... 28 [m/s]
 Thrust (T):..... 1.29 [Kg]
 Torque (Q):..... 0.67 [Nm]
 Motor RPM:..... 6320 [RPM]
 Current (Ii):..... 31.47 [Amps]
 Battery Output Voltage (Vi):..... 18.727 [Volts]
 Motor Input Power:..... 583.7 [Watts]
 Useful Power:..... 354.6 [Watts]
 Motor Efficiency:..... 0.76
 Propeller Efficiency:..... 0.80
 Global Efficiency:..... 0.60
 Endurance:..... 274.5 [Secs]

Tab. 7.IV

Aveox 1412/2y and APC 16x10 from Silvagni A.
 Static performance

Tens	Current	Torque	Rpm	P. in	P. out	Thrust			
[V]	[A]	[Nm]		[Watt]	[Watt]	[N]			

22.35	44.9	1.083	6768	990	767	36.8			
-------	------	-------	------	-----	-----	------	--	--	--

Section 8 : Aircraft Cost

As we have said in the previous section, the flight tests show us some problems. After the changes made considering the problems about the longitudinal trim that arose during the flight tests, the final configuration of the model is :

Wing span	:	2.10	m	
Wing chord	:	0.47	m	
Wing area	:	0.987	m ²	→ 0.624 ft ²
Total length	:	2.08	m	→ 6.824 ft
Total weight (w/o cells)	:	6.310	kg	→ 13.911 lb

From these data we can calculate the Rated Aircraft Cost, as described in the model supplied by the contest (**Tab. 8.I**). Its value is about 8.347, this means that every liter of water brought during the contest will give us 1.19 points. With the mission we expected to realize (with a Single Flight Score of 80-100) and hoping that there will not be accident, we should reach the score of 9.5-12.

We have also calculated, for obvious reasons, the real cost and time spent for the building of the airplane as shown in **Tab. 8.II**, in which we used the value suggested by the RAC model to estimate the cost of our work.

We can see that the actual cost of the airplane is lower than the RAC. In fact the RAC is a weight function that penalize the bigger airplane, this way is possible to put into evidence the efficiency of the plane. The materials used for GALILEO (wood, aluminum profiles, plastic cover) are very cheap, so its real cost has been low, but it is a quite large model (is it too large? only the fly-off and the comparison with the other model will show us), so it has an high RAC.

MEW [kg]	6,31	A * Mew	\$1.391,117
MEW [lb.]	.13,91		
# motors		REP	4320,000W
# cells	3	B * REP	\$4.320,000
# wings			
Wing Surf. [m^2]	0,98	WBS Wing	47,496hr.
Wing Surf [sq ft]	10,62		
# Fuselages			
Length [m]	2,08	WBS Fuselage	32,297hr.
Length [ft]	6,82		
# Vertical Surfaces		WBS Empennage	20,000hr.
# Horizontal Surfaces			
# Servos		WBS Flight Systems	12,000hr.
# Propeller		WBS Propulsion Systems	20,000hr.
		MFHR	131,793hr.
		C * MFHR	\$2.635,850
		RAC	8,34

Tab. 8.I

Woods	L. 700.000	\$350
Glues	L. 200.000	\$100
Motors	L. 1.300.000	\$650
Controllers	L. 700.000	\$350
Propellers	L. 60.000	\$30
Cells	L. 500.000	\$250
Servos	L. 700.000	\$350
Receiver	L. 100.000	\$50
other	L. 300.000	\$150
Manufacturing	150	\$3.000
Man Hours		
Total	L. 4.360.000	\$5.280

Tab. 8.II

Section 9. Acknowledgement

We wish to thank all the people who have been on our side in this enterprise and without whom we would have not been able to reach the results that we set. In particular we want to remember:

Prof. Guido De Matteis, our advisor;
Prof. Giorgio Sforza, who has always trusted us, for his aid and his incitement;
the Head prof. Franca De Zardo and all the teachers and the administrative staff of Galilei;
Mr. Tommaso Gabrielli, who taught us how to build an aero-model;
Eng. Luca Cistriani, for his fundamental suggestions;
Prof. Mario Marchetti and all the people of AIDAA;
Mr. Richard Borg, whose experience in piloting and setting models has been at our disposal;
Mr. Angelo Silvani, for his advices about the power plant;
Stud. Gianluca Fais, for his support;
Col. G. Soci, for his attention;

and all the students of the class VA of Galilei, whose interest and enthusiasm have given us the incentive and the pleasure of carrying on our work:

Emanuela Amato,
Cristian Battistini,
Alessio Ceccarelli,
Michele Cinquepalmi,
Emanuele Dottori,
Simone Martini,
Daniele Minicucci,
Simone Papa,
Alessandro Petrini,
Romano Valenzisi,
Enrico Vertecchi.

*Opening our eyes,
Thinking to what we couldn't say;
Watching in the sky
The clouds going away.
Watching in the blue,
Imaging what we can not see:
Galileo you can do
Our dreams to be really free!*

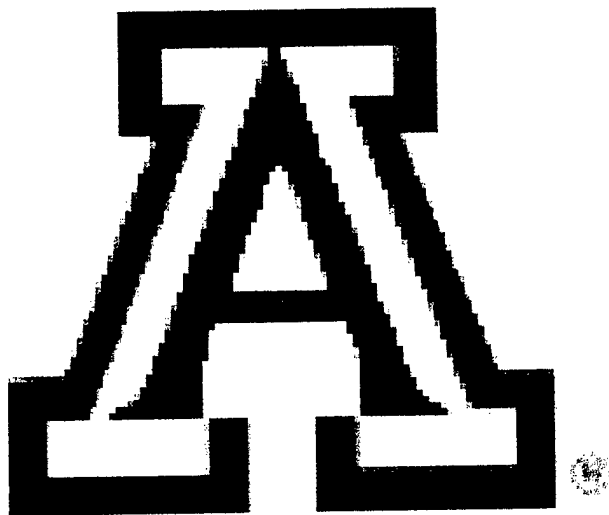
AIAA DBF/Cessna ONR

2000 Competition Report

Submitted by:

Team AirCat 2000

**University of Arizona, AIAA Student Chapter
Tucson, Arizona**



THE UNIVERSITY OF ARIZONA.

March 10th 2000

Table of Contents

1. Executive Summary.....	1
1.1 Project Overview.....	1
1.2 Conceptual Design Phase Overview.....	1
1.3 Preliminary Design Phase Overview.....	2
1.4 Detailed Design Phase and Goals.....	3
2. Management Summary.....	4
2.1 Management Overview.....	4
2.2 Team Members.....	4
2.3 Deadline Dates.....	5
3. Conceptual Design Phase.....	7
3.1 Objective.....	7
3.2 Weight Sizing.....	7
3.3 Comparative Study.....	8
3.4 Figures Of Merit.....	9
3.5 Devolopment of Aircraft Configuration.....	10
3.6 Preliminary Layout.....	10
3.7 Dealing With the Rated Aircraft Cost.....	13
3.8 Meeting Goals Set during the Conceptual Design..	14
3.9 Conclusion.....	14
4. Preliminary Design Stage.....	20
4.1 Overview.....	20
4.2 Propulsion System Selection.....	20
4.3 Takeoff Sizing.....	22
4.4 Power Available and Power Required.....	23
4.5 Empennage Sizing.....	24
4.6 Landing Gear Sizing.....	24
4.7 Conclusions.....	24

5.	Detailed Design.....	29
5.1	Objective.....	29
5.2	Servo Selection.....	29
5.3	Detailed Fuselage Design.....	29
5.4	Detailed Wing Design.....	30
5.5	Landing Gear.....	32
5.6	Payload Compartment.....	32
5.7	Final Performance Predictions.....	33
5.8	Stability.....	34
5.9	Conclusion.....	35
6.	Manufacturing Plan.....	40
6.1	Objective.....	40
6.2	Figures of Merit.....	40
6.3	Manufacturing Plan.....	41
6.4	Manufacturing Timing.....	43
	Drawing Package.....	44

To be submitted later

7.	Addendum Phase.....	?
8.	Cost.....	?

Executive Summary

1.1 Project Overview

Faced with the need for a completely new design and returning no members from the 1998-1999 design team, the 1999-2000 University of Arizona team attempted to turn its inexperience in the competition into an advantage rather than a disadvantage. Throughout the design, the team was focused on the goal of brining the lightest aircraft capable of lifting all eight liters. As well, the team set to achieve at a minimum 10 full sorties comprising of 4 payload sorties.

1.2 Conceptual Design Phase Overview

1.2.1 Mission Requirements

The teams' first task during the conceptual design was to familiarize the members with the mission requirements and changes from the prior years competition. Having a good knowledge of the mission profile and rules helped the teams' design tremendously.

1.2.2 Weight Sizing and 30 lb. Weight Goal

Rather than hastily continuing from the mission requirements into a discussion of the configuration of the aircraft, the team decided to make some initial estimates of the take off weight and set a goal for the weight of the aircraft. Weight is expected to play a dominant role in the design and this step resulted in initial parameters on the weight of the aircraft. At this point in the design, the teams decided to set its sights towards carrying all eight liters while keeping the design takeoff weight under 30 pounds. Considering that eight liters of water weighs approximately 18 pounds, only 12 pounds are left for engines, servos, batteries, and the structure. Assuming that the engines, batteries, and flight control systems weigh approximately seven pounds, five pounds are left for the structure. Therefore, the team set a goal of designing a five-pound structure. Wanting to meet the five-pound empty weight goal, the team constantly concerned itself with the weight of all components used in the structure during the design process.

1.2.3 Preliminary configuration Layout

Having found an initial estimation of the weight of the aircraft and set goals towards the final weight of the aircraft, discussion took place to set a preliminary configuration for the aircraft. A wide variety of ideas arose from the teams brainstorming meetings and the team found it necessary to use an organized method of eliminating competing designs. Developing a comparative study of the configurations of past designs entered into the competition proved effective. Past designs gave the team an indication of what concepts worked well in the competition and what concepts failed. Following the history, the teams' focus shifted towards what its three AMA registered pilots preferred

to fly. Pilot preference ultimately decided much of the configuration. At this point the team was ready to determine an initial configuration for the aircraft.

Many ideas arose for the initial configuration of the aircraft. Included in the discussions was the possibility of using an electric jet design, a flying wing layout, a conventional aircraft, and other configurations. The electric jet was later ruled out due to the poor takeoff capabilities of ducted fan engines, the manufacturing difficulties involved, and the poor duration of flight associated with ducted fan units. The flying wing configuration was not recommended by the pilots and ruled out due to issues of stability and the pilots' experience with flying such aircraft. Having ruled out these and many other possibilities, the final configuration during the conceptual design phase developed into a one engine, high wing, and trainer type of aircraft capable of lifting up to eight liters of water. The payload would be stored in a single fuselage and loaded and unloaded from the rear of the plane. Methods of obtaining the desired goals on performance and weight were discussed.

1.2.4 Design Tools Used During Conceptual Design Phase

Texts used:

"Model Aircraft Aerodynamics" by Martin Simmons

"Airplane Design: Part I: Preliminary Sizing of Airplanes" by Dr. Jan Roskam

"Airplane Design: Part II: Preliminary Configuration Design and Propulsion Selection" by Dr. Jan Roskam

Software:

Microsoft Excel (used for weight sizing calculations)

1.3 Preliminary Design Phase Overview

1.3.1 Performance Sizing

Following the conceptual design phase, the team entered the preliminary design phase of the aircraft. During this phase, the feasibility of the initial configuration was investigated and the plane was sized for takeoff, climb, turns, and landing. The plane was sized assuming a headwind was available to aid during the takeoff stage of the flight.

1.3.2 Changes in Aircraft Configuration

Calculated during the preliminary design stage, the power developed using only one engine could propel the aircraft; however, taking advantage of the rules and using two engines on separate battery packs results in the same rated aircraft cost and much more power for takeoff. Also, the propeller diameter required to develop the power needed to take off was calculated to be approximately 28 inches, requiring an amazing amount of clearance from the ground. Thus, the design changed to a twin-engine configuration, with two motors mounted on the wings. A positive aspect of the twin-engine design was the payload could now be loaded and unloaded from the front of the plane through a removable nose. While the rated aircraft cost rose considerably, the aircraft could

perform much more sorties and payload could be loaded much more efficiently.

1.3.3 Design Tools Used During Conceptual Design Phase

Texts:

“Model Aircraft Aerodynamics” by Martin Simmons

“Airplane Design: Part I: Preliminary Sizing of Airplanes” by Dr. Jan Roskam

“Airplane Design: Part II: Preliminary Configuration Design and Propulsion Selection” by Dr. Jan Roskam

“Introduction to Flight” by John D. Anderson, Jr.

“Aerodynamics, Aeronautics, and Flight Mechanics” by Barnes W. McCormick

Software:

Motocalc (used to evaluate the performance of propulsion system combinations)

Mathcad (used for performance sizing calculations)

Microsoft Excel (used for performance sizing calculations)

Other:

Aveox virtual test stand (used to evaluate the performance of propulsion system)

UIUC online low speed wind tunnel test results (used to compare airfoil candidates)

1.4 Detailed Design Phase and Goals

1.4.1 Detailed Design Overview

The detailed design is the area where the team feels the plane developed most of its unique features. While the chosen configuration is ordinary, the team believes that the aircraft's unique hybrid structure and ability to carry a large payload while retaining a relatively high flight speed will place the University of Arizona in the winners' circle. The primary focus of the team during the detailed design stage was to meet the specific performance and weight goals placed on the aircraft.

1.4.2 Detailed Design Tools

Texts:

“Airplane Design: Part III: Layout Design of Cockpit, Fuselage, Wing and Empennage: Cutaways and Inboard Profiles” by Dr. Jan Roskam

“Model Aircraft Aerodynamics” by Martin Simmons

Software:

Autocad

Airfoil Analysis (used for performance Calculations)

Mathcad (used for performance calculations)

Microsoft Excel

Matlab (used for stability analysis)

Management Summary

2.1 Management Overview

The 1999-2000 University of Arizona team returned no members from the previous years design team. 11 members make up the University of Arizona team. Leaders were assigned in different areas of the project. The team meetings were lead by junior, Chris Miller, who has considerable experience with radio-controlled aircraft. While Chris Miller lead the team meetings, seniors Faizal Riza Abd Rahman, James Harader, and Lokson Woo primarily led the conceptual, preliminary, and detailed design stages. Junior, Matt Anguilo, assumed the role of treasurer and took up the task of raising funds for the project. Having the most experience with radio controlled aircraft construction, freshmen Keith Brock and Patrick Haley helped lead the manufacturing stage of the aircraft.

2.2 Team Members

Chris Miller, a junior in mechanical engineering, was given the task of leading team meetings and voted team leader during the prior year's election. He has 12 years of experience with radio controlled aircraft including experience with balsa, foam, and fiberglass. Chris is also a current AMA registered pilot.

Faizal Riza Abd Rahman, a senior in both aerospace and mechanical engineering, was assigned with the stability calculations and to design a control scheme for the aircraft. He has no experience with the construction of RC aircraft specifically, but helped greatly with the manufacturing plan for the aircraft.

James Harader, a senior in aerospace engineering, took on the duty of aerodynamics and performance calculations for the aircraft. His prior experience with RC aircraft construction was limited to foam and balsa construction.

Lokson Woo, a senior in aerospace engineering, worked on the fuselage design, performance, and stability and control calculations. Again, Lokson Woo has no previous experience with RC aircraft.

Matt Anguilo, a junior in aerospace engineering, assumed the role of treasurer and fundraiser for the project. Matt performed many of the administrative tasks of the project and has experience with sailplane construction.

Keith Brock, a freshman in mechanical engineering, became one of the leaders during the manufacturing stage of the project. Having constructed over fifty radio-controlled aircraft, Keith brought a considerable amount of building experience to the team. He is currently a club instructor for Southern Arizona Modelers and has been designated as an

alternate pilot for this year's competition. Keith has experience with monokote, econokote, coverite, fiberglass, balsa, foam, plywood, basswood, plastics, and carbon graphite, ducted fan assembly, electric jet assembly.

Patrick Haley, a freshman in mechanical engineering, was designated as pilot for this year's competition.

Geoff Hill, a junior in aerospace engineering, has no experience with radio-controlled aircraft and helped primarily in the construction phase.

Micheal Rodgers, a junior in aerospace engineering, has no prior experience in construction of radio controlled aircraft and helped primarily during the construction phase of the project.

Motoyuki Aki, a freshman in aerospace engineering, worked primarily during the construction phase of the project.

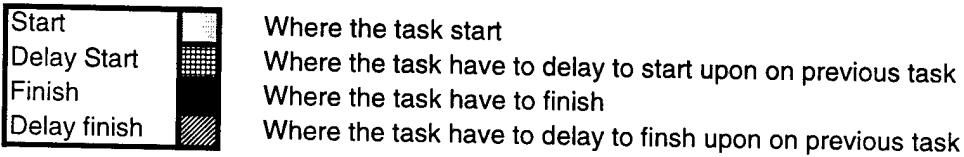
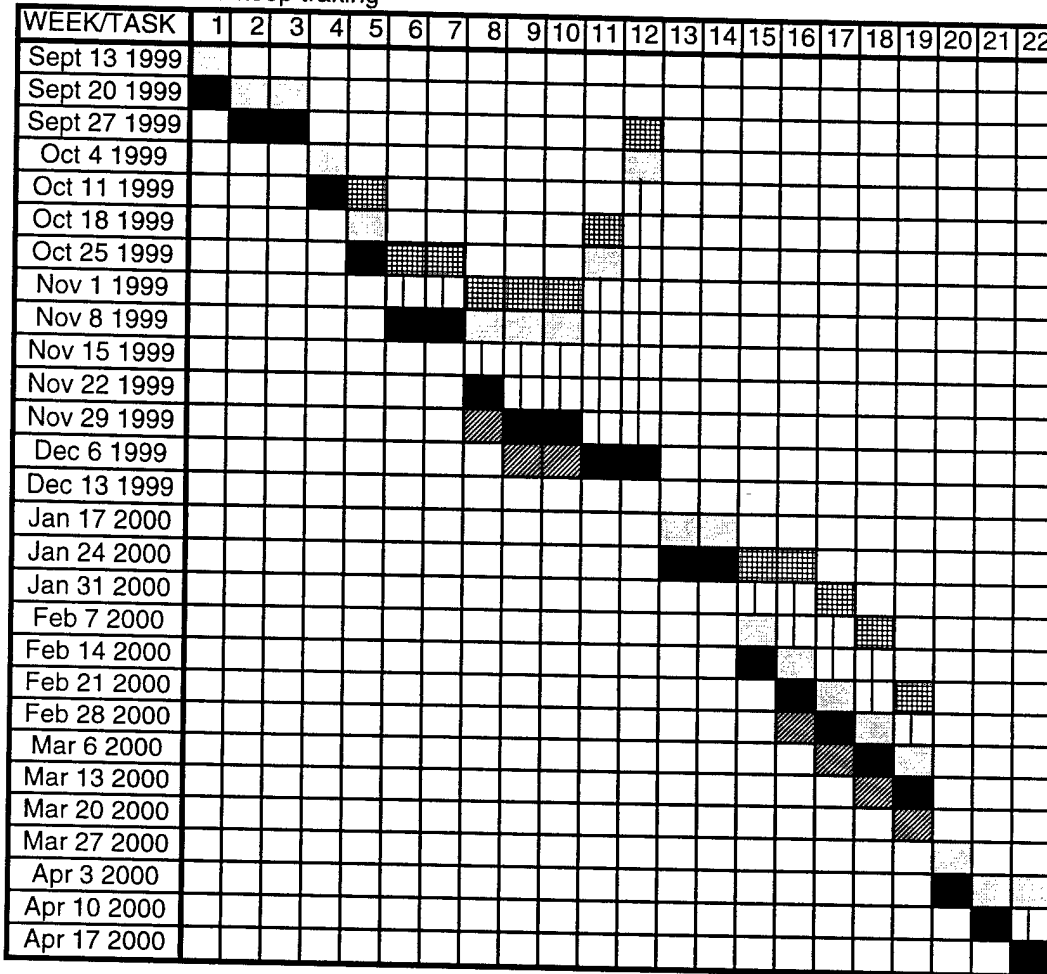
2.3 Deadline Selection

The team selected deadlines such that adequate time existed to flight test the aircraft. The beginning of winter vacation, December 14th, was selected as the deadline for the completion of the detailed design. March 13 was selected as the deadline for manufacturing the aircraft, leaving a month for flight testing.

Schedule for Fall 1999 and Spring 2000

Task #	Date (week)	Task Objective to complete	Important Date
1	Sept 12 1999	Proposal due/Goal statement	Oct 31 1999 Completed entry form
2	Sept 20 1999	Identification of need/background research	
3	Sept 27 1999	Weight sizing determination	
4	Oct 4 1999	Performance sizing	
4	Oct 11 1999	Performance sizing	
5	Oct 18 1999	Outline of configuration possibilities	Dec 1-3 1999 Presentation Dec 17 1999 End of Classes Jan 12 2000 Classes begin
6	Oct 25 1999	Design of fuselage	
7	Nov 1 1999	Design of wing	
8	Nov 8 1999	Design of empennage	
9	Nov 15 1999	Strength analysis	
10	Nov 22 1999	Choosing the best configuration	Mar 13 2000 Written report due (proposal phase)
11	Nov 29 1999	Budget calculation	
12	Dec 6 1999	Final report	
	Dec 13 1999	FINAL EXAM WEEK	
	Jan 17 2000	SPRING SEMESTER	
13	Jan 24 2000	Start dividing work	Apr 10 2000 Written report due (addendum phase)
14	Jan 31 2000	Collect/buy material	
15	Feb 7 2000	Wing construction	
16	Feb 14 2000	Wing testing/empennage construction	
17	Feb 21 2000	Empennage testing/fuselage construction	
18	Feb 28 2000	Landing gear construction	Apr 22-23 2000 Competition date
19	Mar 6 2000	Assembling the construction	
	Mar 13 2000	SPRING BREAK	
19	Mar 20 2000	Assembling the construction	
20	Mar 27 2000	Finishing the design	
21	Apr 3 2000	Testing/reassembling	
21	Apr 10 2000	Testing/reassembling	
22	Apr 17 2000	Final testing	

Milestone chart to keep tracking



Note: the line in the middle of the box show the prograss of the week
the TASKS refering to schedule

Conceptual Design Phase

3.1 Objective

The objective of the teams conceptual design phase was to arrive at a reasonable preliminary configuration, which could best accomplish the mission as specified in the mission requirements. At the same time, the team wanted to use proven design concepts. To familiarize itself with what other teams had accomplished in the past, the team added a comparative study into the conceptual design stage. Near the end of the conceptual design stage the team set goals for the performance and weight of the aircraft.

3.2 Weight Sizing

3.2.1 Method

Weight sizing was performed using the method described by Part I of the series "Airplane Design", authored by Jon Roskam. This method requires the existence of data from aircraft that closely resemble the aircraft proposed by the mission specifications. Weight sizing is not generally a step used in RC design because the designers usually lack data or the need for detailed calculations; however, the team found the data from the 1998/1999 competition provided a good starting point for the design. Because it was thought that the results of the weight studies might be a deciding factor in several of the competing concepts, weight sizing was performed before the preliminary configuration was set.

3.2.2 Results

The data was nearly linear on a log-log plot with the exception of two teams who fell off of the trend. Those teams' data were Excluded from the analysis. Thought to have loaded up with as many batteries as the team could fit, the Utah State entry fell far off of the norm and was not included. As well, the East Stroudsburg entry was very heavy for its design payload weight and not included in the study. The average payload fraction for the 1998-1999 competition was .37, although one team managed a payload fraction of .52. At a full payload value of 18 lbs, the takeoff weight was estimated to be approximately 36 pounds; however, this is a very high estimate of the takeoff weight because many teams filled their planes with battery cells last year. Based on the data and on the members with RC experience, the team set 30 pounds as a maximum weight if the plane was designed to lift all eight liters of payload

3.2.3 Errors in Weight Estimate

Sources of error exist in the estimate of the takeoff weight including the two teams whose data points changed the slopes of the lines considerably on the plots. As well, typical

weight sizing studies compare the takeoff weight against empty weight. In the case of this study, the operating empty weight was used, as the battery weight of last year's entries was not readily available. Including the battery weight in the study could introduce error into the estimate of the empty weight and takeoff weight

3.3 Comparative Study

3.3.1 Objective

With little experience in the design/build/fly competition, the team studied the history of past competitions to familiarize itself with the work done by other teams and the competition it could expect. Topics studied included: The overall configurations, the propulsion systems used, and the prior performance by teams in Wichita.

3.3.2 Results

While a few teams chose unusual configurations such as Syracuse Universities choice of a flying wing configuration, the majority of teams in the past chose conventional configurations. Furthermore, those who chose unusual configurations generally placed near last in the final standings. At the same time, planes with conventional configurations generally placed well; however, with most of the aircraft entered in the competition having conventional configurations what separates the top finishers from the rest of the entries?

Several explanations are believed to explain why certain teams finished well, while others did not. First, access to and selection of quality propulsion systems divided the lower half of standings with conventional configurations from the upper half with similar configurations. A quality propulsion system is necessary to compete for a high standing in the competition. Still, some planes had nearly the same configuration and propulsion system and yet one team outperformed the other by a considerable margin. Aerodynamic advantages and experience of the pilots are two areas that could separate two teams with nearly identical aircraft.

Finally the team studied the performance of aircraft in Wichita by studying the aircraft entered in the 1997/1998 competition. While the mission profile was much different, the performance expected by a plane carrying a 7.5 payload was estimated to be at most 5 payload sorties. Using the statistics from the 1997/1998 USC entry, the equivalent rated aircraft cost was estimated to be approximately 1397 and with the ability to accomplish 5 payload sorties and a report score of approximately 100 a final score of 5000 could be obtained. A design capable of competing in the contest would at the very least need the capability of scoring at least 4000 points.

3.4 Figures of Merit

3.4.1 Pilot Experience and Preference

Wanting to design around the pilot, the preference of the pilot was highly weighed into the design. Designing a configuration with which the pilot is not accustomed to flying requires the pilot spend more time during the flight testing phase of the project. The more comfortable the pilot feels with the control and design of the aircraft the better he will perform during the contest.

3.4.2 Rated Aircraft Cost

Included in the figures of merit is the rated aircraft cost, which affects the final score of the aircraft. The configuration of the aircraft mildly affects the rated aircraft cost. Choosing a configuration which best limits the rated aircraft cost is still desired, especially if the plane carries a small payload.

3.4.3 Weight

To maintain competitiveness, the aircraft must be very light. Ultimately though, the weight is not a large factor in deciding the configuration but was included as a means of comparing competing concepts whose final ranking is very close.

3.4.4 Stability

Stability of the aircraft is a necessity. While some configurations offer good stability characteristics, others offer very poor stability. An aircraft with good stability will maneuver around the course much quicker than one with poor stability. Stability was considered a major factor in the configuration selection.

3.4.5 Safety

Safety was included in the figures of merit, but not weighed heavily. Having two pilots with experience flying nearly every configuration possible, the team felt confident that the pilots could safely maneuver any aircraft around the course. Moreover, the experienced builders on the team were convinced they could build any type of aircraft and maintain nearly the same level of safety.

3.4.6 Comparative Study Results

Wanting to use a proven configuration in the contest, the result of the comparative study was not taken lightly during the choice of the preliminary configuration. The team wanted to avoid making the mistakes other teams made in the past.

3.4.7 Payload Access

Easy loading and unloading of the payload increases the amount of time the plane can spend in the air and the amount of sorties

3.4.8 Ground Handling

Requirements such as the takeoff field length and the ability to land and taxi quickly require the aircraft have excellent ground handling capabilities. Rather than worry about the plane tipping over during takeoff, the team would much rather the pilot concentrates on his position on the runway and distance from the 100 ft takeoff requirement. Therefore, ground handling is included as a figure of merit.

3.5 Development of Aircraft Configuration

3.5.1 Ranking Procedure

To decide between competing configurations, the team developed a ranking system similar to that used by Texas A&M the previous year. Each having its own weight; the figures of merit were analyzed for each possible configuration. Chosen to have the largest maximum value in the ranking system, pilot preference was assigned 4 points. Following the pilot preference at 3 points each were stability and comparative study figures of merit. The other 5 figures of merits were each assigned 2 points. Table 3.5-1 depicts the results of the ranking process.

3.5.2 Choice of General Configuration

Although the team desired to bring new concepts into the competition, the configuration of the aircraft was chosen to be conventional. Conventional aircraft have outperformed non-conventional aircraft throughout the competition history. Furthermore, most of the pilots' experience is flying aircraft with conventional configurations.

3.6 Preliminary Layout

3.6.1 Design Parameters Investigated

While a general configuration was set, the details of the configuration were still unknown. As a result, the teams' focus shifted towards the layout of the aircraft. Investigated during the preliminary layout were such things as how many engines are required, what characteristics the wing will have, and what type of landing gear the aircraft to design. During this portion of the design much more tradeoffs arose, as many of the decisions have no clear solutions.

3.6.2 Preliminary Propulsion Configuration

3.6.2.1 Engine Type

As a starting point in the preliminary design, the team discussed the type of engines to be used in the propulsion system. Two types of electric engines exist on the market, the conventional electric engine and the electric ducted fan motor. Table 3.6-1 shows the tradeoffs between the two types of engines. While a ducted fan motor allows for much faster flight speeds, the poor duration, poor takeoff capability, and very difficult manufacturing process required for ducted fan engines negated them as a consideration for the design. The team chose to use conventional electric engines.

3.6.2.2 Number of Engines

Having determined the engine type, the team discussed the number of engines to be used on the aircraft. The team decided that either a single engine design with one large battery pack or two engines running off of two separate battery packs would work best with the rated aircraft cost model. At this stage of the design the number of engines was set at one. Two engines running off of separate battery packs were determined to have the same rated engine power, thus the same rated aircraft cost for that section; however, the number of propellers and number of engines are increased by 1, leading to an increase of 200 in the rated aircraft cost.

3.6.2.3 Engine Location

With only one engine powering the aircraft the engine location could either be forward or aft of the fuselage. Choosing to use the most common design, the team positioned the engine at the front of the fuselage. The rated aircraft cost does not take the engine location into account, thus the decision was solely based on the experience of the team.

3.6.3 Wing Configuration

3.6.3.1 Low, Mid, or High Wing?

Next on the agenda, the position of the wing was debated. A mid wing was immediately thrown out, as the carry through structure would interfere with the ability to store payload. Figure 3.6-2 tabulates the tradeoffs involved in choosing between a high, mid, and low placement of the wing. A high wing was chosen as it provides better stability to the aircraft. As well, the pilots have flown many high wing trainer aircraft and feel comfortable with this type of configuration. Both a high or low placement of the wing gives very similar characteristics. In the event that a small payload is to be carried the team might reconsider a mid wing placement. The decision of wing placement has no bearing on the rated aircraft cost.

3.6.3.2 Sweep, Dihedral, and Taper Ratio

The sweep, dihedral angle, and taper ratio have large effects on how the aircraft flies. Including a forward or aft sweep in the wing design can significantly add difficulty in the manufacturing process and unnecessary extra weight. The team decided to keep the sweep angle at zero because the negative effects of having sweep in the wing highly outweighed the positive. A small dihedral, possibly two degrees, will be used to add stability during straight level flight of the aircraft. Finally, the effect of having a taper ratio was discussed in great detail. Having several tradeoffs, table 3.6-3 shows the effect of adding a taper to the wing. A rectangular wing configuration was chosen due to the difficulties involved in manufacturing a tapered wing. While a tapered wing in theory outperforms a rectangular wing, small manufacturing defects may arise due to the difficulty of manufacturing a taper and cancel any performance benefits gained by tapering the wing.

3.6.4 Empennage Configuration

The team discussed which type of empennage should be used for the flight. The team chose a standard tail configuration based on the rated aircraft cost. A T-tail was discussed, but the team felt that the T-tail would be difficult to manufacture and more weight. Also, use of a V-tail was considered, but the team felt most comfortable with manufacturing a standard tail unit.

3.6.5 Fuselage Configuration

Little was known about the size of the bottles at this point in the design so much of the fuselage configuration was saved for later discussion. The team did however decide on a single fuselage design over a multiple fuselage design. A single fuselage design weighs less, is easier to manufacture, and creates less drag than a multiple fuselage design. Also decided, the payload would be stored in the fuselage rather than pods. The length and number of bodies is included in the rated aircraft cost model, but the team's decision of using a single fuselage fit the rated aircraft cost rather nicely.

3.6.6 Landing Gear Type

The landing gear stirred many debates amongst the group. Tricycle, Tail, and Bicycle configurations were considered for the aircraft, with the results of the discussion on tradeoffs displayed in table 3.6-4. The nose gear configuration was chosen due to its superior ground handling capabilities in high winds and the pilots' ability to manage the aircraft. The pilot recommended heavily against use of a tail wheel. The landing gear type has little effect on the total aircraft cost. The team also considered retractable gear, but the weight increase and difficulty of manufacturing retractable gear heavily outweigh any aerodynamic advantages that can be attained.

3.7 Dealing with the Rated Aircraft Cost

3.7.1 Objective

Wanting to maximize the final score of the aircraft, much time was spent evaluating the effect of the rated aircraft cost and the number of liters of water to be lifted. Using performance estimates derived from past competitions and estimates of the rated aircraft cost for the corresponding designs, the effects of carrying medium and large payloads was investigated. Although the team used rather crude approximations, the effects of carrying a small amount of payload versus a large amount of payload can be found in this simple manner. A small aircraft was not evaluated for potential use in the competition because the number of laps the plane would have to fly to acquire a decent score is considerable. Realistically, the rated aircraft cost contribution from setting the configuration alone would place a small aircraft out of contention.

3.7.2 Rated Aircraft Cost Breakdown

Having already set the configuration of the aircraft, the rated aircraft cost was broken down into two segments. Parameters of the rated aircraft cost, which were determined solely by the preliminary configuration of the aircraft, were grouped in a category named configuration rated aircraft cost. The tabulated result for different configurations was shown in section 3.5.2. All other sections of the rated aircraft cost were grouped in a second category, later named sizing rated aircraft cost. The configuration rated aircraft cost included the rated aircraft cost induced by the number of wings, number of bodies, number of empennages, number of vertical surfaces, number of horizontal surfaces, number of engines, and number of propellers. As well, the number of servos might fit well in the configuration rated aircraft cost but the number of servos was thought to depend on the size of the plane. The larger the plane the more control surfaces are needed, such as flaps to help the large plane lift off. Accordingly, the number of servos was grouped with the sizing rated aircraft cost variables.

3.7.3 Estimated Scoring for a Medium Sized Aircraft

Using the data from the 1997/1998 competitions, an estimate of the score for a competitive aircraft carrying 4 liters of water was performed. The University of Southern California's entry into the 1998 contest flew 12 sorties in less than seven minutes. The team estimated that the aircraft could accomplish 5 payload sorties in 10 minutes, or 13 sorties overall. A take off weight of 16 pounds was assumed, with 2.5 pounds for the batteries, 8.8 pounds for the payload and the remaining weight by the engines, structure, and flight control systems. Table 3.7-1 shows an estimation of the score capable by a potential medium sized aircraft. A 650 square inch wing area and the use of 15 battery cells were assumed for the calculation. A final maximum score of 5658 was assumed for a medium sized aircraft. A score of 90, approximately the average score of past years winners, on the report score is assumed for both the medium and full size aircraft

estimates. The ratio of configuration aircraft cost to total aircraft cost was found to be .28. In other words, the configuration contributed as 28 percent of the total rated aircraft cost.

3.7.4 Estimated Scoring for a Large Sized Aircraft

The estimation of the performance of a large aircraft was conducted in much the same manner. The team used its experience to derive the performance of the aircraft. A 30 lb aircraft is achievable and 4 payload sorties (10 total sorties) are thought to be the maximum possible. The wing area was assumed to be 1100 square inches and the number of cells was assumed to be 26 (the amount of 3000 mah batteries which weighs approximately 5 pounds). The final scoring potential of the aircraft is a maximum of 6328 points with the configuration contributing 20 percent of the rated aircraft cost.

3.7.5 Comparison of the Results

As can be seen through the estimates, the estimated scores for both a large and medium sized aircraft are very similar. Choosing the amount of payload could not be based on the score the aircraft could achieve. The team decided on an aircraft capable of carrying 8 liters for the following reasons. First, the number of takeoffs and landings is decreased, limiting the chances for pilot error during these stages. Also, the number of times the payload must be loaded and unloaded decreases. Finally, in a very high wind the number of sorties the planes can achieve might be comparable for both cases leaving the larger plane with a definite advantage. Limiting the chances for pilot error and mistakes during loading and unloading dictated the choice of attempting to carry 8 liters in the aircraft.

3.8 Meeting the Goals Set during the Conceptual Design

Although many of the details of the aircraft were known following the study of the rated aircraft cost, the aircraft was not necessarily guaranteed to perform well unless the specific design goals could be met. Exactly what goals have been placed on the aircraft? First, the aircraft was selected to carry the full payload weight and yet weigh 30 lbs. In order to keep tight tabs on the weight, the team developed tables estimating weight of each component of the aircraft as they were added during the design. This kept the team up to date with the current status regarding the weight of the aircraft. As well, the team set a goal of accomplishing four payload sorties during each run. This requires the team to fly at an average speed of approximately 50 feet per second (34 mph). The team concerned itself with the speed of the aircraft accordingly throughout the preliminary and detailed design stages.

3.9 Conclusion

During the conceptual design stage, the aircraft developed into a conventional, single fuselage, high wing design. A single engine will be mounted at the front of the fuselage

and have the capability of propelling a 30 pound aircraft. A quick examination of the rated aircraft cost derived from the results of previous competitions showed that the potential score of an aircraft is not necessarily determined by the amount of payload it carries. A large aircraft has the advantage of limiting the number of times the payload must be loaded and unloaded, and the number of times the team must land and thus was chosen for the design. Limiting the number of sorties to be completed during the competition limits the number of opportunities for mistakes during the competition. Finally, the team set clear goals for the weight and speed of the aircraft. Having accomplished a conceptual design, the team closed the conceptual design stage of the project and continued into the preliminary design.

Table 3.5-1: Overall Configuration Ranking Results

	Conventional	Biplane	Tandem Wing	Canard	Flying Wing	Three Surface
Figure of Merit/max value						
Pilot Experience/4	4	3.5	2	2.5	1.5	1.5
Rated Aircraft Cost/2	1.5	1	1	1.5	1.75	.5
Weight/2	1.5	1	1	1.5	1.5	1
Stability/3	2.5	2	1.5	2.5	1	1.5
Safety/2	2	2	1.5	2	1.5	1.5
Comparative Study/3	3	2.5	1	2	1	1
Ground Handling/2	2	2	1.5	1.5	1	1.5
Payload Access/2	2	2	1.5	1.5	1	1.5
Total/20	18.5	16	11	15	10.75	9.5

Table 3.6-1: Design Tradeoffs between Conventional Electric Motors and Ducted Fan Motors

Design Parameter	Conventional Electric Motor	Ducted Fan Motor
Maximum Flight Speed	Average	High
Manufacturing Difficulty	Easy	Very Difficult
Takeoff Performance	Average	Below Average
Duration	High	Low
Weight	Average	Average

Table 3.6-2: Design Tradeoffs between Wing Configurations

Design Parameter	High Wing	Mid Wing	Low Wing
Weight	Good	Average	Poor
Interference Drag	Good	Good	Poor
Dihedral Effect	Negative	Neutral	Positive
Payload Storage	Good	Poor	Good
Effect on Stability	Good	Average	Poor

Table 3.6-3: Effect of Adding a Taper to the Wing

Design Parameter	Rectangular Wing	Tapered Wing
Weight	High	Low
Tip Stall	Good	Poor
Manufacturing Difficulty	Easy	Difficult

Table 3.6-4: Effect of Landing Gear Configuration

Design Parameter	Nose Wheel	Tail Wheel	Bicycle Gear
Weight	Medium	Low	High
Steering	Good	Poor	Poor
Pilot Preference	High	Low	Low
Takeoff Rotation	Good	Good	Poor

Table 3.7-1: Scoring Potential of a Medium Size Aircraft

Item	Estimated Value	MEW	REP	MFHR	RAC
No. of Laps	5	-	-	-	-
No. of Liters	4	-	-	-	-
Empty Weight (lbs)	5	5	0	0	500
Engine 1					
No. of Cells	15		900		900
Engine 2					
Number of Cells	0		0		0
No. of Wings	1			5	100
Wing Area (sq in)	650			18	361
No. of Body	1			5	100
Total length bodies (ft)	5			20	400
Empennage	1			5	100
No. of Vertical surface	1			5	100
No. of Horizontal surface	1			10	200
Basic flight system	1			5	100
No. of Servos	5			6	120
No. of Engines	1			5	100
No. of Props	1			5	100
SUM		5	900	89	3181
Estimated Score	5658				

Table 3.7-2: Scoring Potential of a Large Aircraft

Item	Estimated Value	MEW	REP	MFHR	RAC
No. of Laps	5	-	-	-	-
No. of Liters	4	-	-	-	-
Empty Weight (lbs)	8	8	0	0	800
Engine 1					
No. of Cells	26		1560		1560
Engine 2					
Number of Cells			0		0
No. of Wings	1			5	100
Wing Area (sq in)	1100			31	611
No. of Body	1			5	100
Total length bodies (ft)	7			28	560
Empennage	1			5	100
No. of Vertical surface	1			5	100
No. of Horizontal surface	1			10	200
Basic flight system	1			5	100
No. of Servos	7			6	120
No. of Engines	1			5	100
No. of Props	1			5	100
SUM		8	1560	110	4551
	6328				
Estimated Score					

Preliminary Design

4.1 Overview

Having decided on a configuration to be used for the competition, the team set its sights towards the preliminary design. Many methods exist for conducting the preliminary design; however most require access to extensive data from similar aircraft. The team decided a practical method was needed to size and design the plane in such a short time frame. In order to reduce the number of unknown variables the team studied the availability of electric engines on the market, and selected a propulsion system for which the plane would be designed around. Following the selection of the propulsion system, the team began sizing the aircraft to meet mission specifications. While not a true preliminary design as used in full size aircraft, the team found this method very effective in designing the aircraft.

4.2 Propulsion System Selection

4.2.1 Battery Selection

Having no batteries that would be effective in the contest, the team became determined to select batteries that would allow the propulsion system to be competitive. The Battery Figure of Merit (BatFOM), an index created to compare battery combinations, is calculated from the maximum potential energy storage capacity of the batteries, the voltage available, and the rated aircraft cost model assuming a one engine design. The team chose the Battery FOM to be

$$\text{BatFOM} = \frac{(\text{PE})(\text{Voltage})}{(\text{RAC})}$$

Potential energy and voltage are placed in the numerator as the energy stored in the battery is very important and the voltage input determines the continuous power output of the motor. The rated aircraft cost is placed in the denominator such that the higher the rated aircraft cost becomes the less the rating becomes for the battery combination. As seen in table 4.2-1, twelve battery combinations were investigated. While the 5000 mah cells are commonly associated with a very low rated aircraft cost, the amount of voltage available from the cells limits the amount of power that can be created by the engine. The 2000 mah cells create a great deal of power and potential energy, but the rated aircraft cost drives the battery index down. Although the Sanyo 3000 CR batteries did not possess the highest battery index, they were chosen as the batteries to be used for the aircraft because of their reputation of good performance in competition.

4.2.2 Motor Candidates

After choosing the batteries, the team compiled a list of motor candidates. Motors that were believed powerful enough to propel the aircraft were the Aveox 1400 series, Aveox 1800 series, Astroflight 60, and Astroflight 90. The Aveox 1800 series motors were eliminated because of their extreme cost.

4.2.3 Propeller and Gear Selection

Knowing that the engine must be geared and a propeller chosen, the team researched what gear ratios were available and what sizes of propellers were on the market. The team found that Model Electronics Corp. in Seattle had the best selection of gear ratios with 70 ratios between 2 and 6. As well, the team discovered a ¼ scale aircraft engine distributor in Tucson that carried high performance composite propellers with diameter as high as 30 inches and pitch up to 15 inches. Carrying Mejzlik, Menz, and Bolly propellers, the local distributor carried a wide enough selection of propellers for the team to end its search. As well, the team was able to work out a deal with the distributor and flight test propellers at no cost.

4.2.4 Matching of the Propulsion System

Using the software packages, Motocalc and the Aveox virtual test stand, the team analyzed the performance of different propulsion combinations. Very early in the analysis it became clear that a single engine design would not be sufficient for an aircraft carrying 8 liters of water. The team reconfigured the aircraft such that two engines running on separate battery packs would propel the aircraft. The engines would be located on the wings allowing the team to load and unload payload through a removable nose section. Although the rated aircraft cost increased slightly (200+ points), the payload could now be loaded and unloaded at a much quicker rate.

After careful analysis, the team chose to use two Aveox 1415 2Y motors in conjunction with two Aveox M-260C speed controllers, two Model Electronics Corp. 2.85:1 gearboxes, and two 20x12 propellers. The exact propeller diameter and pitch used on the aircraft will be determined during flight-testing, however 20 x 12 was thought to be the starting place when selecting the propeller and used in the design analysis. Following the Motocalc and Aveox virtual test stand analysis of the propulsion system the team discovered "Model Aircraft Aerodynamics", a book with a section on propeller performance. Using the method in the book for sizing propellers to determine the best propeller diameter and pitch, calculations gave a 20.7-inch propeller with 12 inches of pitch confirming the choice to use 20x12 propellers. Table 4.2-2 gives the propulsion systems final characteristics.

4.3 Takeoff Sizing

4.3.1 Method

Using the method described in “Aerodynamics, Aeronautics, and Flight Mechanics”, the wing was sized for takeoff with wind taken into consideration. During this section of the preliminary design the airfoil was chosen and wing geometry set such that the aircraft could perform the 100-ft takeoff distance requirement.

4.3.2 Wichita Climate

In order to have a more accurate estimate of the takeoff distance, the effect of the wind was considered in the takeoff estimates. Wind data for Wichita was gathered from online data provided by the Federal Climate Complex in Asheville. After examining the data, the team found that the average wind speed for april in Wichita is 14 knots from the south. The team decided to design the plane, expecting a minimum wind speed equal to 75 percent of 14 knots, or 10.5 knots. Wind speed can have a large effect on the stability of the control near the ground. On a very windy day, which is common in Wichita, the air near the ground tends to be more turbulent. With little time to recover, the plane must have a relatively high airspeed when near the ground. At higher elevations the wind has much less effect and the pilot has time to recover from gusts. Thus, the team kept the ground speed during takeoff in consideration.

4.3.3 Airfoil Selection

Next, the team decided to study airfoils for potential use on the aircraft. The “Model Aerodynamics” appendix provided a lengthy list of airfoil candidates, nearly all of which are designed for low speed flight. Certain characteristics are desired when selecting an airfoil for low speed flight. A bad choice for an airfoil could result in the inability of the aircraft to perform certain functions. In some airfoil cases, the flow will separate along the top surface of the airfoil creating what is called a laminar separation bubble. Several airfoils have been designed to combat the effect of the flow separating while it is still laminar.

The team chose to use the Selig-Donavan 7037 over competing airfoils, mainly the Eppler series airfoils, because the SD7037 could accomplish all of the tasks required of it rather well. The maximum lift coefficient for the SD7037, as published from UIUC wind tunnel data available online, confirm the airfoils multi task capability. The airfoil is capable of a maximum lift coefficient of approximately 1.3 with a drag coefficient of .04, while at low angles of attack the drag coefficient drops to .007 with a lift coefficient of approximately .466. In other words, the airfoil has the capability of creating a high lift when high lift is needed and the ability to create suitable lift coefficients for the cruise segments while maintaining a very low drag. The L/D characteristics of the airfoil are similar to that of the NACA 23012, commonly found on full size aircraft.

4.3.4 Results

Having enough data, the team performed a takeoff sizing routine to estimate the wing area needed for take off. Table 4.3 gives the results of the takeoff sizing. Assumptions made during the takeoff sizing include the values of ground coefficients, the efficiency of the wing during takeoff, and the wind conditions in Wichita. Resulting from the takeoff sizing calculations, flaps are needed to takeoff in the required distance. A wing area of 1092 inches was calculated for the wing such that takeoff is achievable in 87 feet with the aid of a 10.5 knot headwind and takeoff flaps. The average power required from the engines to achieve takeoff is estimated to be 1114 watts using Motocalc software. Using this average power and an estimated time of 2.8 seconds for the ground roll, the energy consumption from the battery packs for each takeoff is approximately .86 watt-hours. Wanting to design the aircraft such that it is capable of four payload sorties, the total estimated energy loss is 3.4 Watt-Hours for takeoff portion at full payload.

Next, the takeoff power needed for the aircraft without payload was investigated. The flaps will not be used for takeoff with no payload. As well, the thrust level will be reduced to 70 percent to conserve energy. Liftoff with no payload is possible at just over 32 feet at 70 percent power. An average of 360 watts is required from the batteries during this segment of the flight, with a lift off speed of approximately 50 ft/sec. The Estimated energy loss for 3 liftoffs at the empty weight is approximately .3 Watt-Hours. The takeoff portions for ten sorties are then estimated to require approximately 4.1 Watt-Hours of the 50 Watt-Hours available for flight. Table 4.3-1 summarizes the results of the takeoff sizing calculations with no payload.

4.4 Power Available and Power Required

The power available and power required curves are useful in determining how the aircraft will perform. Trying to accomplish the goal of approximately a 55 feet per second average airspeed, the team needed to confirm that the aircraft could fly faster than the average speed. Using the methods in "Aerodynamics, Aeronautics, and Flight Mechanics", the team developed the power curves shown in figures 4.4-1 and 4.4-2. Figure 4.4-1 shows the power curves for a thrust level of 70 percent. As can be seen by finding the intersection of the power available and power required curves, the maximum speed of a fully filled aircraft at 70 percent thrust is approximately 65 ft/s. While empty, the aircraft is capable of reaching speeds as high as 70 ft/s. As shown in figure 4.4-2, the maximum flight speed is near five to ten ft/s higher when the plane is placed at 100 percent thrust. Interestingly, the plane increases its flight speed from 65 to 75 ft/s by using more thrust, but the power input into the motor changes from 172 watts to 363 watts. During full throttle flight with no payload, the number of watts required is nearly identical to that with full payload; however, at 70 percent throttle the number of watts is only 100 watts to achieve a speed of approximately 71 ft/s. The team decided to conserve energy through both runs, as the required power increased significantly, while the flight speed would only increase by five to ten ft/s.

4.5 Empennage Sizing

The horizontal and vertical tail was sized using comparisons to $\frac{1}{4}$ scale aircraft near the same weight range. Based on the results of the research of $\frac{1}{4}$ scale aircraft, the team decided on a horizontal tail area of approximately 240 square inches. While small compared to many of the tails seen in last year's competition, the pilot has experience flying tailless aircraft. As well, the tail has receives added airflow from the twin propeller arrangement allowing the area to be small. The team decided to use a symmetrical airfoil for the design with a 10 inch chord length and 2 foot span, with 25 percent of the chord acting as an elevator. The vertical tail was sized in a similar manner at 150 square inches. The team later analyzed the stability of the aircraft to confirm the empennage sizes obtained from similar aircraft.

4.6 Landing Gear Sizing

The landing gear is designed as an arc shape with the height and length of the landing gear measuring 5 inches and 12 inches respectively. The landing gear will be approximately 3 inches wide and the nose gear will be approximately $\frac{1}{8}$ inch in diameter and 5 inches in height. This sizing of the landing gear was based on clearance and stability criteria. The main landing gear is located approximately 2.5 inches behind the center of gravity of the airplane. Knowing the location with respect to the center of gravity of the airplane, four angles determine the stability of a landing gear configuration. Measured at 20.72 degrees, the longitudinal tip-over angle is much larger than the required 15 degrees for longitudinal stability. The second considered is the lateral tip over angle, which was sized at the 55 degrees required for stability. The longitudinal clearance was measured at 33 degrees, well within the requirements for stability of the landing gear. Finally, the lateral ground clearance, which is 20.86 degrees, is larger than required.

4.7 Conclusions

The teams chose to take a practical approach to the preliminary sizing of the aircraft. Rather than deal with many unknowns, research was put into a competitive propulsion system to design the aircraft around. Following the selection of the propulsion system, the wing was sized around the takeoff of the aircraft, later to be revised if turns and landing could not be accomplished. As a result of the large headwinds available in Wichita, the wing was sized such that takeoff could not be achieved without the aid of the wind. This allows the wing area to be smaller, decreasing the weight of the aircraft. The result of finding the maximum speed during level flight is over 15 ft/s larger than the average speed needed to complete 4 payload sorties allowed the team to continue it's efforts towards carrying the full amount of payload.

Table 4.2-1: Comparison of Battery Cells

Manuf.	Model Number	Capacity	Weight	#cells	Max volts	Equivalent PE	RAC	PE/RAC	Battery Index
-	-	mah	Oz/cell		V	(watt-hours)	-	-	-
SR	2000	2000	1.86	43	54	107.5	2581	0.0417	2.24
SR	2800	2800	2.47	32	40	113.4	1943	0.0583	2.36
SR	5000	5000	5.3	15	19	94.3	906	0.1042	1.97
Pan.	P-230SCS	2300	2.01	40	50	114.4	2388	0.0479	2.38
Pan.	P-280CR	2800	2.79	29	36	100.4	1720	0.0583	2.09
Pan.	P-500DR	5000	5.1	16	20	98.0	941	0.1042	2.04
Sanyo	N-1C	2200	3.35	24	30	65.7	1433	0.0458	1.37
Sanyo	N-4000DL	4000	5.64	14	18	70.9	851	0.0833	1.48
Sanyo	N-2500CR	2500	2.85	28	35	87.5	1680	0.0521	1.82
Sanyo	N-3000CR	3000	2.96	27	34	101.3	1620	0.0625	2.11
Sanyo	N-4000DRL	4000	5.64	14	18	70.9	851	0.0833	1.48
Sanyo	KR-5000DEL	5000	5.29	15	19	94.5	907	0.1042	1.97

Table 4.2-2: Final Propulsion System Characteristics (one engine)

Engine	Aveox 1415 2Y
Gear Ratio	2.85
Propeller Diameter	20 in
Propeller Pitch	12 in
Propeller RPM (static)	4273
Motor RPM (static)	12179
Thrust (static)	140.2 oz
Power Input (static)	787.4 Watts
Power Output (static)	676.7 Watts
Motor Efficiency (static)	85.9 %
System Efficiency (static)	63.9 %
Battery Amps (static)	67.9 amps
Max Motor Efficiency	90.0 %
Speed at Max Motor Efficiency	45 MPH
Current at Max Motor Efficiency	31.7 amps
Max System Efficiency	81.8 %
Speed at Max System Efficiency	57 MPH
Current at Max System Efficiency	19.8 amps
Rated Aircraft Cost/Engine	780\$

Table 4.2-3: Propulsion System Weight Breakdown

Component	Estimated Weight (oz)
2 Aveox 1415 2Y Engines	20.8
2 Model Electronics Gearboxes	5
2 Aveox M260C Speed Controllers	4
2 Propellers	5
Mounting Hardware	3
Total Estimated Weight	37.8

Table 4.3-1: Takeoff Performance With Payload

Takeoff Weight	W_{to}	30 lb
Density of Air	ρ	.00249 slug/ft ³
Ground Friction Coefficient	μ_g	.06
Skin Friction Coefficient	C_F	.01
Takeoff Lift Coefficient	C_{lto}	1.75
Headwind Velocity	V_w	17.4 ft/s
Headwind Factor	k	.791
Ground Effect Correction Factor	Φ	.839
Takeoff Velocity	V_{to}	53 ft/s
Average Takeoff Velocity (with wind factor)	V_{toave}	48 ft/s
Average Ground Speed	V_{gave}	30 ft/s
Liftoff Ground Speed	V_g	36 ft/s
Average Takeoff Lift	L	21.6 lb
Average Takeoff Drag	D	3.148 lb
Average Takeoff Thrust	T	10.8 lb
Average Takeoff Acceleration	a	7.9 ft/s
Average Takeoff Power	P	1115 W
Takeoff Distance	S_{lo}	85.7 feet
Takeoff Time	t	2.804 seconds
Energy Consumed During Ground Roll (1 takeoff)	E_{to}	.86 W-Hours

Table 4.3-2: Takeoff Performance without Payload

Takeoff Weight	W_{to}	12 lb
Density of Air	ρ	.00249 slug/ft ³
Ground Friction Coefficient	μ_g	.06
Skin Friction Coefficient	C_F	.01
Takeoff Lift Coefficient	C_{lto}	.9
Headwind Velocity	V_w	17.4 ft/s
Headwind Factor	k	.767
Ground Effect Correction Factor	Φ	.839
Takeoff Velocity	V_{to}	50 ft/s
Average Takeoff Velocity (with wind factor)	V_{toave}	47 ft/s
Average Ground Speed	V_{gave}	34 ft/s
Liftoff Ground Speed	V_g	38 ft/s
Average Takeoff Lift	L	8.64 lb
Average Takeoff Drag	D	1.02 lb
Average Takeoff Thrust	T	9.75 lb
Average Takeoff Acceleration	a	20 ft/s
Average Takeoff Power	P	360 W
Takeoff Distance	S_{lo}	30 feet
Takeoff Time	t	1 seconds
Energy Consumed During Ground Roll (1 takeoff)	E_{to}	.1 W-Hours

Figure 4.4-1: Power Available & Required Curves at 70 Percent Thrust

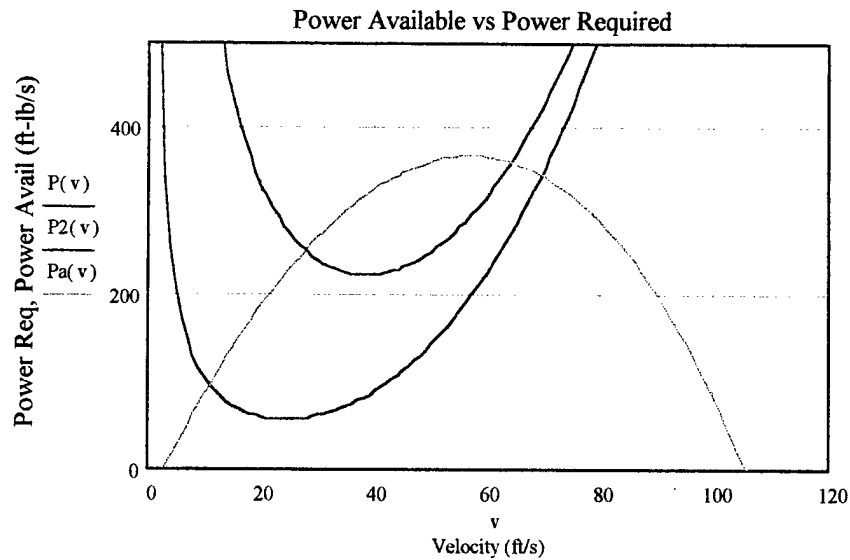
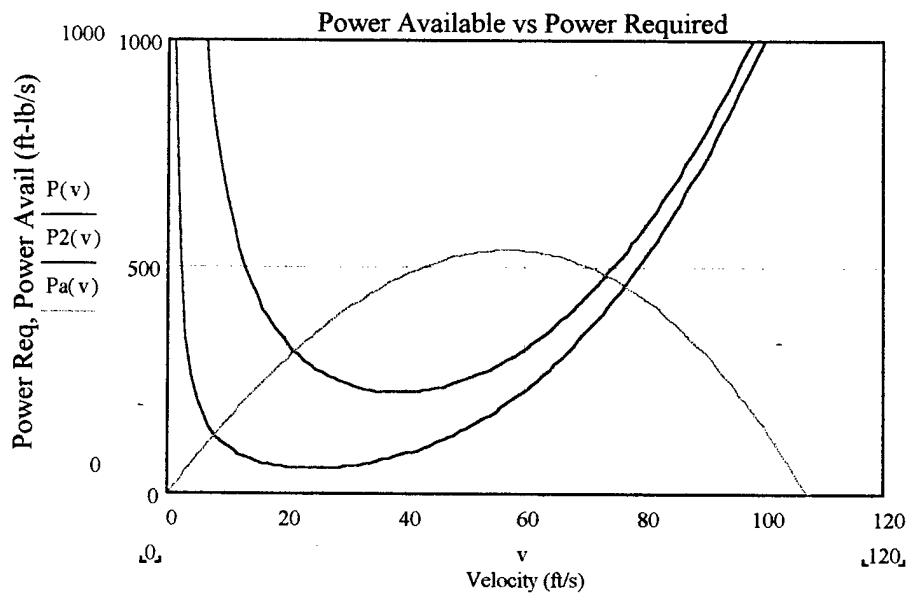


Figure 4.4-2: Power Available and Required Curves at 100 Percent Thrust



Note: Red line indicates the power required at full payload, blue the power required with no payload, and tan the power available at the given thrust

Detailed Design

5.1 Objective

The detailed design stage is the area where the team could explore its versatility. With members on the team experienced with all methods of construction, the team was free to explore materials options which other teams can not. The final structure designed is quite unique, consisting of balsa wood, carbon fibers, and fiberglass. What could be thought of as the teams figure of merits, the final objective during the detailed design stage was to design the structure such that it met the 30 pound weight requirement and at the same time could meet the 55 ft/s average flight speed requirement. The weight was only roughly estimated during the detailed design due to the difficulty in estimating the amount of epoxy actually needed for the structure. These rough estimates are realistic as long as the amount of epoxy used on the aircraft is controlled.

5.2 Servo Selection

Relying on the experience of the members with years of RC experience, lightweight micro servos were selected for use on the aircraft. The micro servos are capable of producing 22 in-oz of torque and weigh approximately .32 ounces. With two servos needed for the ailerons, two for the flaps, one for the rudder, one for the nose gear, and one for the elevator, seven servos in all will be used on the aircraft. Although the rated aircraft cost includes the number of servos, the penalty for using servos is nearly negligible. The control system was designed with the maximum number of control surfaces available so that the pilot would have excellent control of the aircraft.

5.3 Detailed Fuselage Design

5.3.1 Fuselage Sizing

Highly dependent on the size of the bottles, the fuselage was estimated at just over 5 feet long. The fuselage has 3 sections, a nose, a payload compartment, and the tapered portion extending out to the empennage. The team decided to use a 2x4 arrangement (two bottles wide and four long) for the bottles in the fuselage. This arrangement led to an elliptical fuselage of height of 7.5 inches and width of 7 inches. The bottle compartment measures 80 cm long allowing just enough room for the payload. Tapering to a thickness of approximately 2 inches at the rear of the plane, the fuselage also contains a taper that decreases the width to 4 inches at the rear of the plane. At a value of nine the fineness ratio, an important factor in the drag of the fuselage, is comparable to most aircraft flying at low speeds.

5.3.2 Materials Selection

Materials considered for the fuselage structure included carbon fiber, fiberglass, and balsa. Too brittle to act as a fuselage skin, carbon graphite was quickly eliminated as a potential material for the structure. Wood is the most common fuselage structure; however the team chose to use fiberglass for the fuselage skin. Fiberglass is very easy to work with, has the ability to form any shape, and is very light weight. Also, several members of the team had more than enough experience with fiberglass to warrant its use in the structure.

5.3.3 Fuselage Structure

With a fiberglass skin, the aircraft fuselage uses longerons, and formers to provide strength to the structure. Providing excellent strength, six uni-directional carbon fiber rods were chosen to act as longerons in the fuselage. The formers will be constructed out of foam and fiberglass and placed every 6 inches apart in the payload section and 10 inches apart in the tapered section of the fuselage. The fiberglass skin will be four layers of 2-ounce bi-directional fiberglass. The structure is expected to give excellent strength while remaining considerably light.

5.3.4 Fuselage Weight

Wanting to keep have the weight of the fuselage in check, the team made some rough estimates. Approximating the fuselage as a cylinder of radius 7.5 inches and length 5.5 feet, the surface area of the fuselage is roughly 21.5 square feet (2.4 square yards). At 2-oz/ square yard, 4 layers of fiberglass weigh approximately 1 pound. Added to this weight is the weight of the epoxy estimated to be equal to the weight of the fabric, about 1 pound. Miscellaneous hardware, longerons, formers, and reinforcement in high stress areas was estimated to be only $\frac{1}{4}$ of a pound, giving a final estimate of 2 $\frac{1}{4}$ pounds for the complete fuselage.

5.4 Detailed Wing Design

5.4.1 Wing Structure Options

Although the wing was sized during the conceptual design stage many details still remained open. What type of structure would the wing have and what materials would be used? The team investigated both a semi-monocoque structure and a composite structure with a foam core. A semi-monocoque structure, usually made out of balsa wood with a spruce spar, is the most common structure used in model aircraft. The team decided to use a hybrid structure, consisting of a foam core, spar, and skin.

5.4.2 Wing Construction Details

Having decided on a hybrid structure the team first researched what material should be used for the core. The candidates for the core material were Styrofoam (white foam), spyder foam, and high-density urethane foam (blue foam). Considering that the wing volume is approximately .5 cubic feet and the density of white foam is .8 lbs less per cubic feet than the density of spyder or urethane foam, white foam was chosen for the core material. This led to a weight saving of approximately .4 pounds.

Four materials were examined for use as the skin material. Balsa provides a lightweight structure, but requires strong spars or blue foam be used to strengthen the wing against bending. Secondly, Kevlar was evaluated for potential use in the structure; however, Kevlar is very difficult to work with. Fiberglass and Carbon fiber were the remaining structures considered. The team built a test wing out of carbon graphite, which failed miserably under compression excluding it from use as a wing material. After discussing the options with some local 1/4 aircraft hobbyists, the team chose to sheet the foam with balsa. Needing sturdy reinforcement against bending, the spar is designed from 1/4 inch balsa, sheeted on each side with 2.9 oz carbon graphite. This makes for a sturdy lightweight spar and is commonly used in 1/4 in scale aircraft. The skin of the aircraft will be formed from .32 inch thick balsa, vacuumed to the skin to give excellent strength characteristics.

5.4.3 Integration of Engine into the Wing

Changing the design from a single engine aircraft to a two engine aircraft complicated the design of the wing. Needing a surface to mount the engine on the wing, the team decided glue a thin plate of wood into the wing at the section where the engines were to be located, as described in a model aircraft magazine article. The team constructed a model to test the construction method and effectiveness of this design and concluded that the design would be able to withstand the loads placed by the engines. The only other issue was to decide on the location of the engines such that the propellers would have adequate clearance from the fuselage. The team sized the center location of the engine at 29 inches from the center of the fuselage, such that there would be five inches of clearance for the propeller.

5.4.4 Ailerons

The ailerons were sized to be 20.5 inches spanwise, and 2.75 inches chordwise (25 percent of the wing chord). Blue foam is to be used as the core material in the ailerons since white foam is difficult to hotwire for thin parts. Carbon graphite will be used as the skin for the ailerons and the ailerons will be hinged to the wing at the top surface.

5.4.5 Flaps

Much like the ailerons, flaps are to be made using blue foam rather than white foam. Occupying the remaining space available along the wing, the spanwise length of the flaps was designed to be 18.5 inches. The flaps will undergo the same mounting procedure as the ailerons.

5.4.6 Estimated Weight for the wing structure

Again, a very rough estimate is made to give a rough idea of the weight of the wing. The balsa skin carbon graphite, plywood, and epoxy used in the structure were estimated to weigh 1 1/8 pounds. Adding to that, the spar and foam bring the final weight of the wing at approximately two pounds. Two pounds is a reasonable weight for the wing of an aircraft in the thirty to forty pound range.

5.5 Landing Gear

Choosing to build its own landing gear, the team decided to use left over bi-directional carbon graphite from the test wing and fiberglass as the material. 40 layers of fabric will be used in the construction of the landing gear. The estimated weight of the landing gear is 10 ounces, with the ability to withstand the landing stress of up to a 50 pound aircraft.

5.6 Payload Compartment

The ability to quickly load and unload payload gives an advantage in the competition. As well, the payload compartment must be lightweight to keep the weight at a minimum. To give the payload a resting surface, one inside layer of fiberglass will create a smooth surface for the landing gear to rest on. A removable wood dowel will hold down the bottles. At the end of the dowel is a small plate. When the dowel is pulled out from the aircraft the small plate puts pressure on the bottles and forces the bottles out of the aircraft. The dowel is then quickly shoved back in and the nose put back in place. The nose will be hinged at the top surface and held at the bottom surface by a cotter pin. This allows the nose to be opened and closed quickly for quick payload access. During sorties in which the payload must be loaded, the team member whose task it is will place the bottles in two at a time into the structure. The estimated time of unloading and loading is between 15 and 20 seconds. Needing to load or unload the payload 6 times, the estimated total time spent changing the payload is approximately 1 1/2 to 2 minutes leaving only 8 minutes for actual flight of the aircraft.

5.7 Final Performance Predictions

5.7.1 Segment 1: Takeoff

The detailed takeoff calculations were obtained during the preliminary sizing portion of the design. To recap, for a full payload sortie the takeoff time is 2.8 seconds and the energy used during a single takeoff is .86 Watt-Hours. Takeoff is achieved in 87 feet assuming a headwind of 10.5 knots. During the sorties in which no payload is carried the takeoff distance decreases to approximately 30 feet with .1 Watt-Hours used to achieve liftoff in one second.

5.7.2 Segment 2: Climb

Table 5.8-1 and figures 5.8-1 and 5.8-2 show the estimated performance for the climb segment of flight. As can be seen, the rate altitude the aircraft can fly at is considerably less than the 200 feet as described in the mission statement. The aircraft does have the ability of flying higher than 90 feet if needed. Figures 5.8-1 and 5.8-2 show the rate of climb versus velocity for both the payload and non-payload climb segments. The energy used during the climb segment is quite high. This is explained by the low ground speed caused by the headwind. The segments on the downwind leg of the sorties should be very fast and use very little power.

5.7.3 Segment 3: Turn 1 (180 degrees)

Figures 5.8-2 and 5.8-3 summarize the planes turning capability. During the time the aircraft is carrying payload, only turns with large radii can be managed. The turns are negotiated with 100 percent thrust and 70 percent thrust during the payload and non-payload flights respectively.

5.7.4 Segment 4: Cruise 1

As discovered during the preliminary design phase, the team can conserve energy and maintain a reasonable airspeed at 70 percent thrust levels for both payload and non-payload sorties. Table 5.8-4 shows the details of flight at the cruise speed. The cruise segment of flight on the downwind leg takes the least energy during the flight.

5.7.5 Segment 5: Turn 2 (360 degrees) (With Payload Sorties Only)

The pilot will perform the 360-degree turn at any time on the downwind leg that he feels comfortable performing the maneuver. The 360-degree turn is expected to be similar to the 180-degree turns, only the maneuver will last twice as long.

5.7.6 Segment 6: Cruise 2

Refer to 5.8.4

5.7.7 Segment 7: Turn 3 (180 degrees)

Refer to the Segment 3 turn.

5.7.8 Segment 9: Land and Taxi

Landing is assumed to take no more than the power required cruising 500 feet in the headwind. The landing distance for the payload carrying case was estimated to be 140 feet as shown in table 5.7-6

5.7.9 Final Performance Predictions

The aircraft was found to exceed expectations regarding the time the aircraft took to complete sorties. 8 minutes was the allowable time for completion and the estimates for the aircraft show that only 7.6 are needed. However, errors in the estimates such as not including the time to accelerate to cruise speed could very well take more than .4 minutes. The energy required for 10 sorties is just under 50 Watt-Hours. Having changed to a two-engine design with two battery packs the batteries can only manage 51 Watt-hours of energy used. The team decided to take a risk and begin production of the aircraft and inform the pilot to take the cruise speed section of the course very easy to conserve power.

5.8 Stability

A minimum of stability analysis was performed on the aircraft. The team found the derivative of the coefficient of moment with respect to the angle of attack is $- .6$, slightly negative. This leads the team to believe that the aircraft is statically stable in the longitudinal direction. Feeling that the stability and control could be found better during flight testing and knowing that the ailerons were sized appropriately through the comparison to other aircraft the team skipped much of the stability analysis on the aircraft as it was nearing manufacturing time at this stage.

5.10 Conclusion

At the end of the detailed design stage the team concluded that its design was feasible and that a 30 pound aircraft which can fly 8 liters around the course four times is possible. As the weight of the aircraft depends more on the manufacturing method and how much epoxy was used, the team shifted its focus to the manufacturing methods that would be required to build the aircraft.

Table 5.7-1: Estimated Climb Performance of the Aircraft

Parameter	Performance W/O	Performance W/ Payload
Thrust Level	70 %	100 %
Power Input	350 Watts	950 Watts
R/C	7.8	7.8 ft/s
Distance Traveled	370 feet	317 feet
Airspeed	48 ft/s	60 ft/s
Ground Speed	31 ft/s	43 ft/s
Final Altitude	92 feet	60 feet
Climb Angle	14 degrees	10.7 degrees
Time to Climb	11.9 seconds	7.4 seconds
Energy Consumed	1.16 Watt-Hours	1.95 Watt-Hours

Figure 5.7-1: Rate of Climb at 100 Percent Thrust and Full Payload

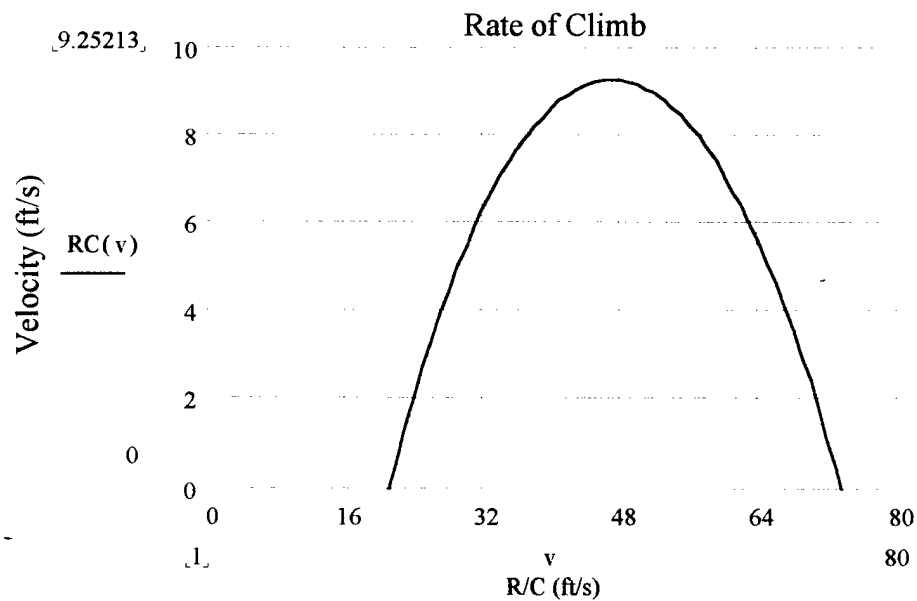


Figure 5.7-2: Rate of climb at 70 Percent Thrust Without Payload

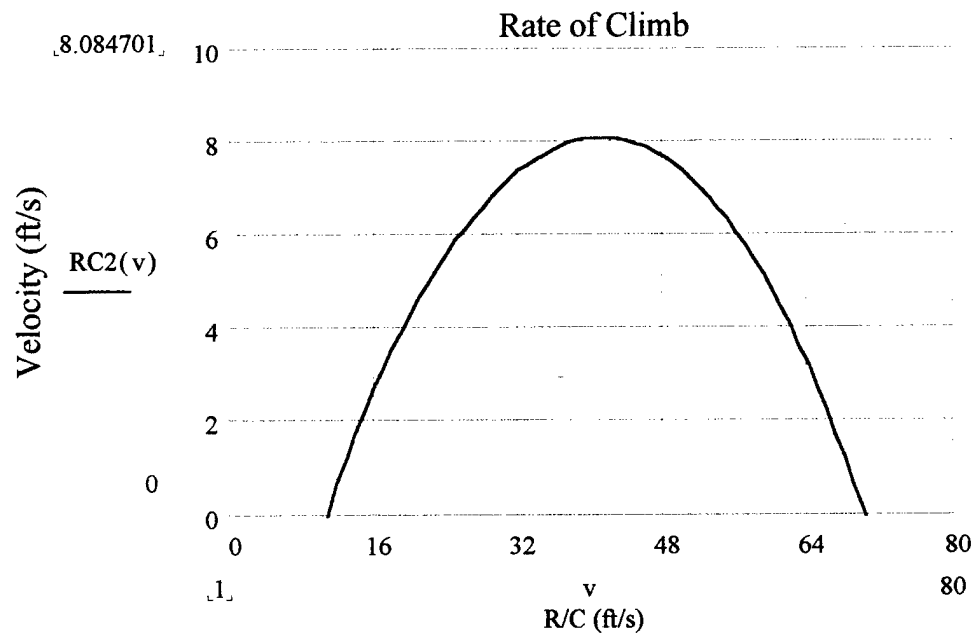


Table 5.7-2 Performance of the Aircraft in Turns with Payload

Parameter	180 degree turn	360 Degree Turn
Thrust Level	100 %	100 %
Input Watts	1100 Watts	1100 Watts
Load Factor	2.5	2.5
Distance Traveled	213 feet	416 feet
Airspeed	50 ft/s	50 ft/s
Angular Velocity	1.47 rad/s	1.47 rad/s
Time	4.2 seconds	8.4 seconds
Energy Consumed	1.3 Watt-Hours	2.6 Watt-Hours

Table 5.7-3 Performance of the Aircraft in Turns without Payload

Parameter	180 degree turn
Thrust Level	70 percent
Input Watts	1100 Watts
Load Factor	2.5
Distance Traveled	100 feet
Airspeed	50 ft/s
Angular Velocity	3 rad/s
Time	2 seconds
Energy Consumed	.19 Watt-Hours

Table 5.7-4: Estimated Cruise Performance of the Aircraft (downwind)

Parameter	Performance W/O	Performance W/ Payload
Thrust Level	70 %	70 %
Power Input	100 Watts	172 Watts
Distance Traveled	1000 feet	1000 feet
Airspeed	70 ft/s	65 ft/s
Ground Speed	87 ft/s	82 ft/s
Time	11.5 seconds	12.2 seconds
Energy Consumed	.32 Watt-Hours	.58 Watt-Hours

Table 5.7-5: Estimated Cruise Performance of the Aircraft (upwind)

Parameter	Performance W/O	Upwind For Landing
Thrust Level	70 %	70 %
Power Input	100 Watts	362 Watts
Distance Traveled	1000 feet	500 feet
Airspeed	70 ft/s	65 ft/s
Ground Speed	53 ft/s	47 ft/s
Time to Climb	18.9 seconds	10 seconds
Energy Consumed	.525 Watt-Hours	1 Watt-Hour

Table 5.7-6: Estimated Landing Performance

Parameter	Performance W/O	Upwind For Landing
Landing Distance	40 feet	140 ft
Time	2 seconds	4.2 seconds

Manufacturing Plan

6.1 Objective

After completing the design of the aircraft the team moved towards the manufacturing stage of the project. Although the design weight matched closely with the weight estimate of 30 pounds, the manufacturing methods used ultimately decide the final weight of the structure when using composite materials. Choosing the correct manufacturing methods can lead to a very lightweight and sturdy structure. Knowing this, the team decided that the objective of the manufacturing plan should be to choose the correct methods of construction for the project. As well, the manufacturing plan should be constructed such that the actual construction phase of the project is organized in written form allowing team members to prepare beforehand for each task.

6.2 Figures of merit

6.2.1 Required Skill Levels

The team considered the skill level to build certain components of the aircraft when choosing the manufacturing method and assigning specific tasks. Although only three teammates had experience using composites, the team was confident that manufacturing methods could be found which allow the inexperienced members to work effectively on the aircraft.

6.2.3 Required time of construction

The required time of construction plays a key role in the choice of manufacturing process. Having spent a great deal of time in the design phase of the project, the team required that many of the manufacturing processes be chosen to minimize the time spent in building the aircraft. As well, the team took into consideration the time spent if a part were damaged or built poorly.

6.2.3 Finishing Time

A great proportion of the time spent on composite structures is spent on finishing the components. Thus, the finishing time required by each method is included as a separate figure of merit from the required time of construction.

6.2.4 Reliability of the Construction Method

Trying to avoid costly errors and delays, the team required that the methods of construction be reliable. For example, consider the case of constructing the wing. A

method that is unreliable, yielding poor results a large percentage of the time, will be unsuitable for large components. Construction methods for large components need to be reliable and simple such that the parts made are satisfactory for use in the competition

6.3 Manufacturing plan

6.3.1 Available Construction Methods

Two types of molds, male and female, exist for use in the construction of composite parts. A male mold requires less work and less time to construct the actual mold; however, the finishing time for the part can be expected to be much higher than a female mold. A female mold requires an extraordinary amount of time to construct but yields an excellent finish. Wanting to keep the finishing time at a minimum the team researched techniques that would minimize the finishing time. The team chose to vacuum bag the components, as it has the positive effect of reducing the finishing time, reduces the weight of the final part, and increases the strength of the component. As well, on parts using a male mold technique sheets of mylar will be used to help reduce the finishing time. Using mylar with a male mold is very effective, giving a nearly perfect part when removed from the vacuum bag.

6.3.2 Wing construction

Based on the experience of the members, the team chose a male mold technique for the wing. Although the wing requires a very smooth surface to perform well, the geometry of the wing is such that a male mold can be very effective.

The actual construction of the wing is quite simple and has been estimated to require approximately 70 man-hours. Acting as the male mold for the wing, two foam cores will be cut using templates and a hot-wire. Each foam core, later to be joined in an assembly stage, acts as half of the wing. The foam core will then be sanded to ensure that the mold is of proper shape. Next, the engine compartments will be cut out of the mold and a plywood sheet glued into the foam to act as a mounting point for the engines. All of the preparation for the vacuum bagging process is now completed.

After spending approximately 12 hours in the vacuum bag, the wing may be removed and inspected for defects. The entire process will then be repeated for the lower surface of the wing. To obtain a quality leading edge shape, a balsa leading edge will be installed. As well, the team will perform circular cutouts on the lower half of the wing such that the wing may enclose the servos. Circular cutouts are chosen rather than square cutouts to avoid stress concentrations caused by sharp corners.

6.3.3 Ailerons, Flaps, Rudder and Elevator construction

The flaps and ailerons are constructed using blue foam. The templates used during the wing construction will also be used during the construction of the flaps and ailerons. Both the flaps and ailerons will be covered in carbon graphite. The rudder and elevator will be made from balsa wood because of the difficulty involved in constructing such thin parts out of composite materials. Covering the balsa wood, a monokote layer is used to give the balsa a smoother surface and added appearance.

6.3.4 Fuselage construction

Although the wing will be made using a male mold type of construction, the fuselage will be constructed from a female mold. The choice of using a female mold was based on the experience of freshman Keith Brock in constructing fuselages from both types of molds. A female mold can be expected to give a much better finish for a fuselage than a male mold. The estimated time required to construct the complete fuselage is approximately 250 man-hours.

Choosing to use a female mold rather than a male mold for the fuselage, the process of hot-wiring the foam will be used to obtain a foam core for the fuselage. The nose and rear section must be shaped by hand due to the inability of the hot-wire to shape such complicated curves. Following the construction of the foam into the shape of the fuselage, plaster will be spread over the mold to provide a sanding surface. The plaster will then be sanded and the process repeated until a relatively smooth surface is obtained. Although the surface has been sanded many times at this point, small imperfections will still be visible throughout the mold. To remove the small imperfections still present in the mold, the same process will be repeated; however, primer coats will be used instead of plaster. Next, the fuselage mold is painted with spray paint, leaving a glossy smooth finish, completing the male mold.

After completing the male mold, a female mold needs to be constructed. A fiberglass female mold can be constructed using the male mold and a splitter plate. The splitter plate, made out of plywood, splits the structure in two such that two female molds are created. Fiberglass cloth is used to create a female mold from the male mold. The mold is then sanded down and any imperfections from the process are fixed using plaster and sanding coats.

After the above process obtains the female mold, the four layers of fiberglass will be placed into the mold to form the actual fuselage. Although a female mold gives very smooth skin, a sanding layer using microballoons and epoxy will be used to nullify any imperfections still remaining after removal from the mold. The process is then repeated for the other half of the fuselage and the two halves joined.

6.3.4 Landing gear construction

The landing gear is made from combination of fiberglass and carbon fiber. It will be shape of arc since an arc shape avoids stress concentrations. Acting as the mold for the landing gear, a block of wood is cut to the shape of the landing gear. The wood is then sanded to a smooth surface and release agent is applied. One layer of fiberglass is placed on the mold then two layers of carbon graphite and the pattern repeated until 42 layers of fabric have been placed down. After each layer of fabric is placed, epoxy is spread over the fabric. After the final layer of fabric has been soaked in epoxy, a sheet of mylar is placed over the entire structure. Mylar has the effect of giving the composite underneath a near glass like finish, creating less finishing work after the part is removed. The nose gear will be purchased, as it can be quite difficult and time consuming of a part to manufacture. The estimated time to construct the landing gear is 6 hours.

6.3.3 Bottle compartment, Battery compartment, Engine, Servos and control parts installation

The fuselage will be joined via the formers and an overlapping layer of fiberglass. After joining the fuselage, plywood is inserted to strengthen the landing gear and wing joining sections. Next, the landing gear and wing will be attached to the fuselage. Beneath the wing, foam tape is used to set the angle of incidence and protect the wing from impact damage during landing.

Following the attachment of the wing and landing gear, the engines will be mounted to the wing. The engines are mounted using twist ties and by four screws, screwing into the gearboxes previously mounted to the engine for static testing. The final steps of the engine installation are to run the wires to the engine and to attach the cowling to the wing.

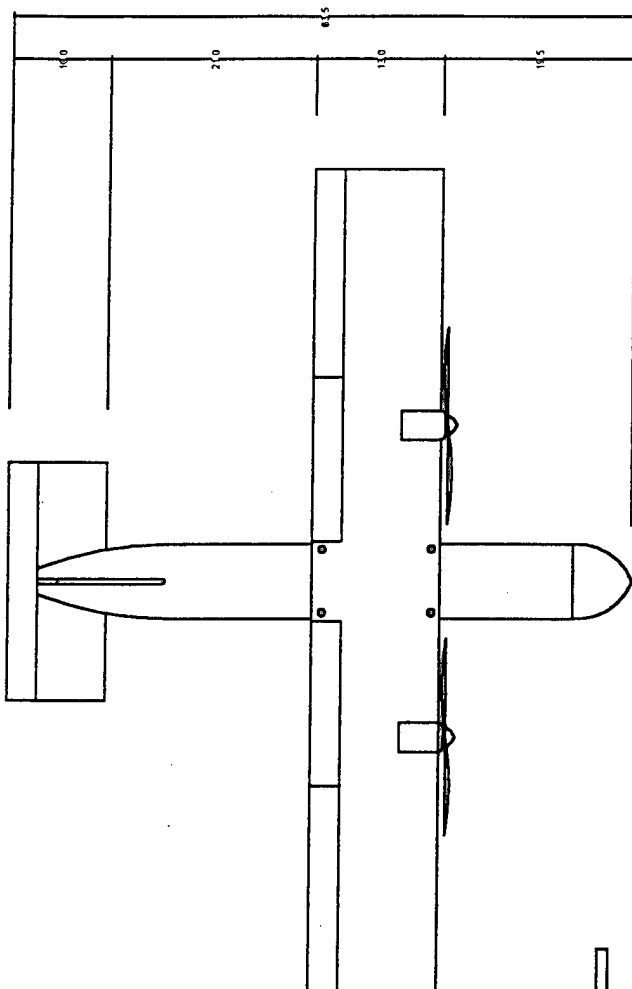
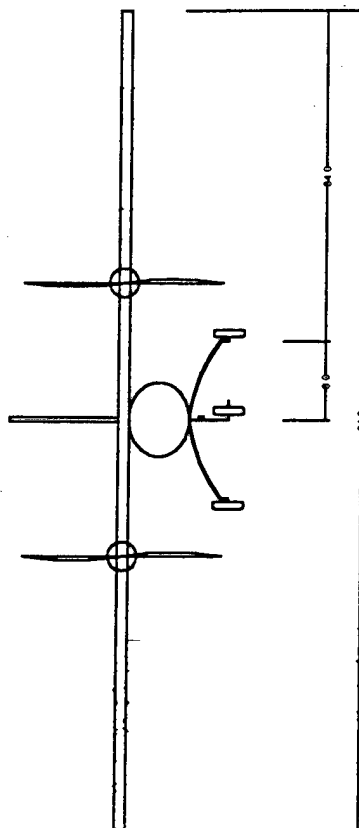
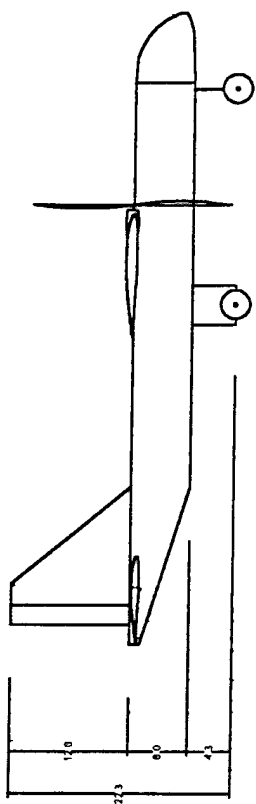
The control surface such as ailerons, flaps, rudder and elevator will be attached using hinge. The pin connector for the rudder however will be attached at the bottom part near the horizontal wing. When installing the vertical tail, the clearance between the vertical and horizontal tail surfaces must be checked. The pin connector will be attached with push rod, which will place inside the wing. And finally, the servos are hooked up to the push rods.

6.4 Manufacturing timing

The whole manufacturing process is estimated to require 450 total hours of time. Although composite materials normally take an abundance of time finishing, the team used a female mold and mylar to reduce the finishing time. Most of the time spent on the project will be towards the construction of the fuselage. The tools required for the process is given below. Used to monitor the progress the manufacturing process, a milestone chart is shown in figure 6.4.

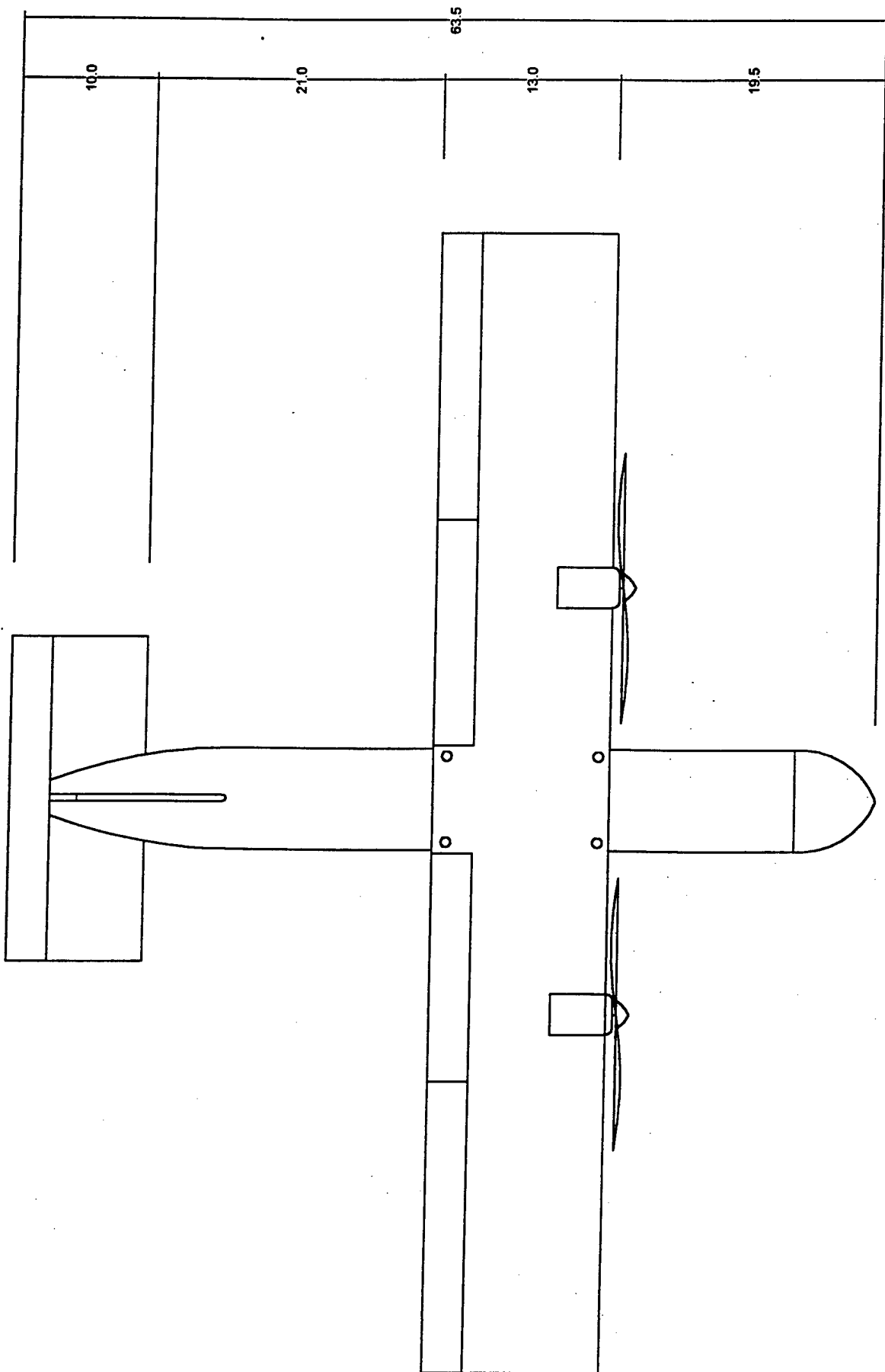
1. Vacuum pump system
2. Vacuum process tools (tacky tape sealant strip, breather, Mylar, Vacuum bag)
3. Carbon fiber
4. Hazardous protections (masks, gloves, safety glasses and etc.)
5. Measurement devices (ruler, measuring cup and etc.)
6. Molding devices (foams, woods, scissors, saw, hot wire, primer, release agent, plaster, and etc.)
7. Epoxy and hardener
8. Fiber glass
9. Control devices (servos, tube for wire, hinge, push road, pin connector and etc.)
10. Woods (Balsa, plywood and etc.)
11. Miscellaneous tools (glue, masking tape, scissors, paper, spatula, sandpaper and etc.)

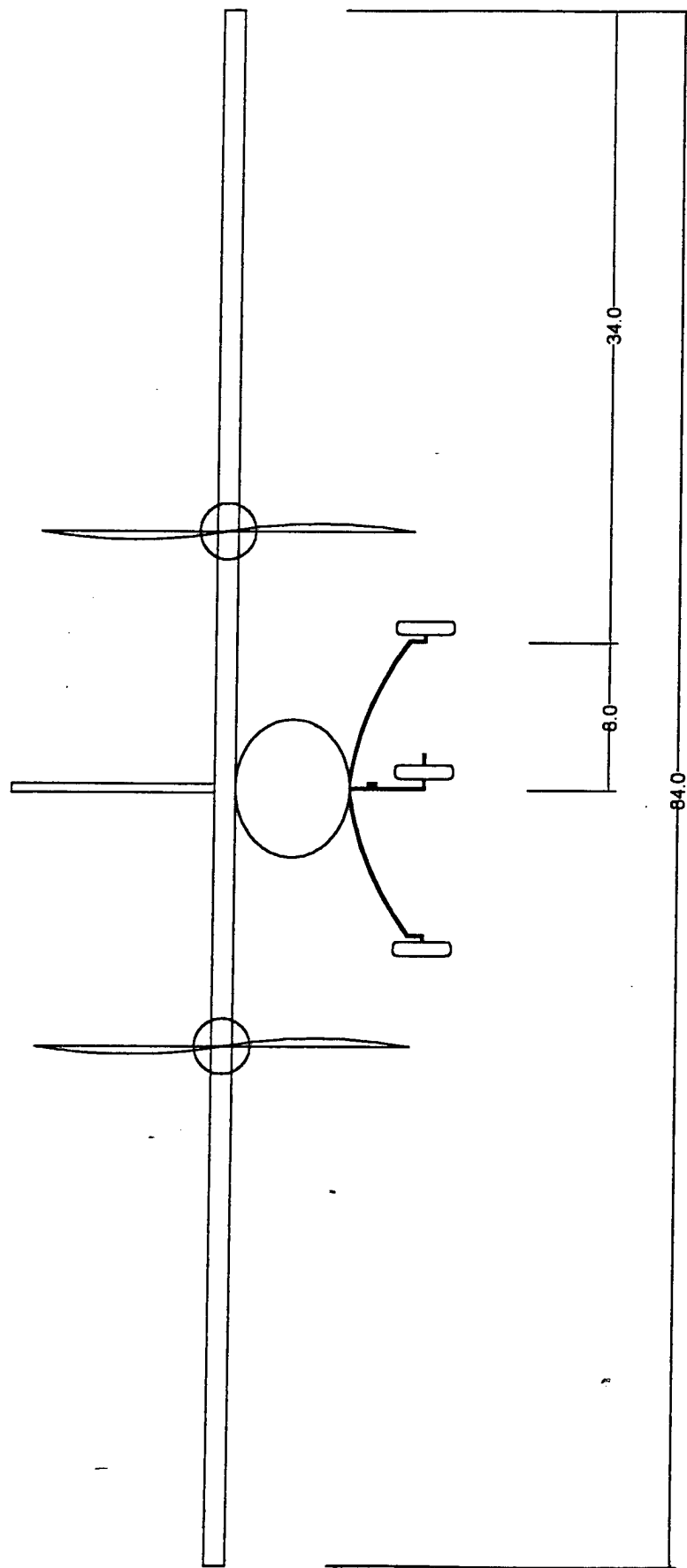
Task	Jan 30 2000	Feb 6 2000	Feb 13 2000	Feb 20 2000	Feb 27 2000	Mar 5 2000	Mar 12 2000	Mar 19 2000
Preparation to laminate wing	Δ	Δ						
Laminate the wing wing pieces	Δ	Δ	Δ					
Joining the wing		Δ	Δ					
Engine installation		Δ		Δ				
Servos installation		Δ		Δ				
Ailerons and flaps		Δ		Δ				
Construction of fuselage mold	Δ		Δ					
Preparation of laminate fuselage			Δ	Δ				
Laminate of fuselage				Δ	Δ			
Installation of bottle slot					Δ-Δ			
Bottle compartment					Δ-Δ			
Installation of nose					Δ-Δ			
Preparation of landing gear		Δ		Δ				
Landing gear construction			Δ	Δ				
Preparation of empennage const.				Δ-Δ				
Empennage construction				Δ	Δ			
Joining the wing to fuselage					Δ-Δ			
Joining the empennage to fuselage						Δ	Δ	Δ
Finishing							Δ	Δ
Test Flight								Δ-Δ

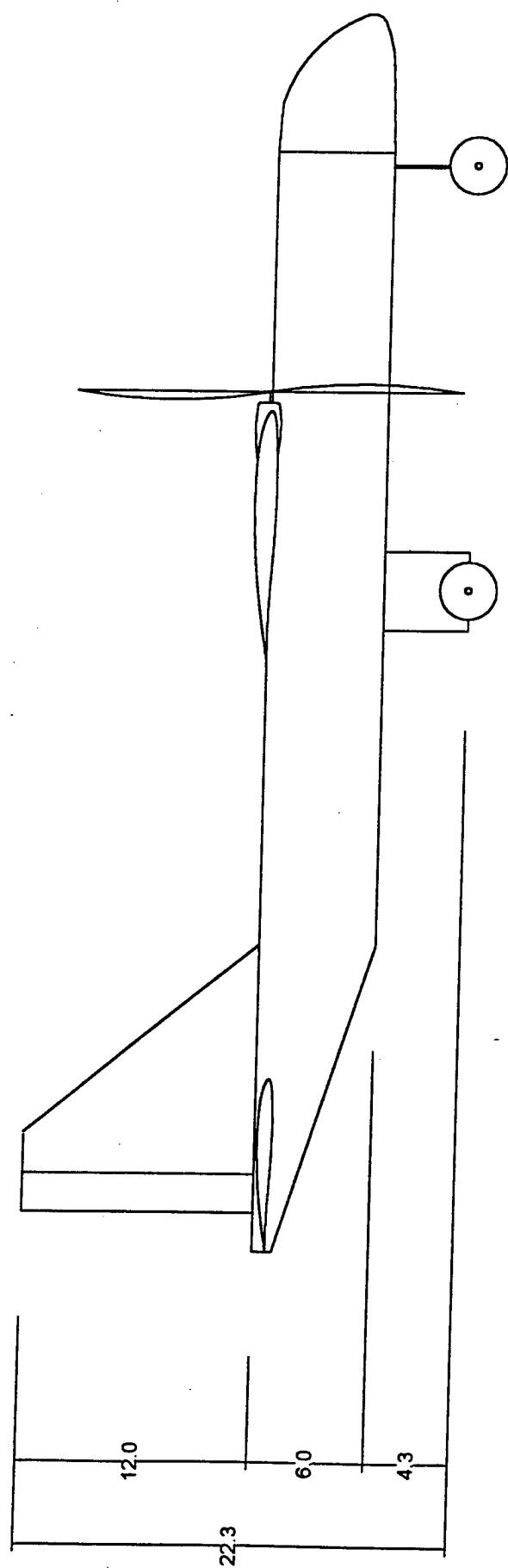


THE UNIVERSITY OF ARIZONA
 AMERICAN INSTITUTE OF AERONAUTICS & ASTRONAUTS
 AIRCAT 2000

DECEMBER 5, 1999
 SHEET 1 OF 1







AIAA DBF/Cessna ONR

2000 Competition Report

Addendum Phase

Submitted by:

Team AirCat 2000

University of Arizona, AIAA Student Chapter
Tucson, Arizona



THE UNIVERSITY OF ARIZONA.

March 10th 2000

Addendum Table of Contents

8.1 Changes Made to the Aircraft.....	57
8.2 Changes Planned for 2000/2001 DBF.....	57
9.1 Rated Aircraft Cost Model.....	58
9.2 Actual Manufacturing Time Breakdown.....	58

Lessons Learned

8.1 Changes made to the Aircraft

8.1.1 Changes in Propulsion System

The propulsion system underwent several changes after the proposal phase. Initially located internally, the speed controllers were moved externally on the wings to meet cooling requirements for the controllers. As well, bench tests concluded that approximately a 16x8 or 18x8 propeller provided more rpm's and thrust than the originally specified 20 x 10 propellers. The battery pack underwent changes as well. Originally the system was made to include 13 cells in each battery pack. While the team was able to produce the 13 cell battery packs and meet the five pound weight requirement, the batteries did not fit well in the fuselage and made the plane nose heavy. The team opted to split each 13-cell pack into two packs. The first consists of eight cells and the second of four cells. This allowed the team to run 12 cells on each motor and balance the weight of the aircraft more effectively.

8.1.2 Changes in the Aircraft Structure

The aircraft structure underwent several changes as well during the building phase. The quick quick payload removal device was left out of the structure as the team determined that the payload could be removed just as quickly by hand. While this saved some weight, the weight of the structure was considerably higher than the design weight. The fuselage was the primary contributor to the extra weight. As well, the wing structure changed some. Rather than have the engine wires run through the interior of the wing, the team changed the design during the building phase because the cut outs in the foam were thought to possibly reduce the structural integrity of the wing. The maximum payload capacity was changed from eight liters of water to six liters of water to accommodate the extra weight of the structure. While the scoring decreases somewhat, the plane is still thought to be competitive.

8.2 Changes Planned for 2000/2001 DBF

Lack of experience in the competition proved very costly during this years development of the aircraft. The team had high goals and expectations which may not all be met; however, the team also had specific goals which were definitely met during the stages of this years competition. Most notable, the team is bringing a plane to the competition and expects to improve on its prior performance in the Design/Build/Fly contest.

The team expects to make changes in several areas for next years competition. The management and leadership of the team was not apparent during the beginning stages of the design. Next years team will have gained valuable experience in planning and preperation of the design. The experience of this years competition will certainly show during the early stages next year. As well, the team needs to get the aircraft flying much earlier next year such that changes can be made if needed. The ideal case would be to have the aircraft flying near the end of winter break.

The team learned through this years competition about the importance of the structure of the wing of the aircraft. While the structure of the fuselage proved effective, the fuselage is a little too heavy and strong for it's application this year. Next years fuselage will most likely be a little lighter with maybe one less layer of fiberglass. As well the wing is likely to undergo minor structural changes. The structural rigidity of the wing came under question as the wing could have possibly used a stronger spar. To strengthen the wing for next year, the team would add a second spar which would only extend out near the root section of the aircraft. This would give the wing a significantly more strength at very little added weight to the aircraft.

The overall impression of this year's team and aircraft is good. The team did manage to make a significant improvement over past year's design and expects to have a much higher finish. Although the team has no experience in the competition, the teams enthusiasm and hard work has allowed it to still produce a competitive aircraft. The team feels it has met its overall goal of elevating its performance in the competition. The future of the team in further competitions is bright with two freshmen having the most building experience on the team and the now added experience of competing in the 1999/2000 competition.

Final Rated Aircraft Cost and Work Breakdown

9.1 Rated Aircraft Cost Model

Table 9.1 shows the breakdown of the final rated aircraft cost for the aircraft. The final aircraft empty weight is 11.75 pounds giving a manufacturer empty weight rated aircraft cost contribution of 1175. The rated engine power is found using the model in the FAQ located on the contest web site. With 24 cells, 12 for each engine, the rated engine power contribution to the rated aircraft cost is 1440. The manufacturing rated aircraft cost is 2507. Adding the three contributions to the rated aircraft cost gives a final value of 5122 for the rated aircraft cost.

9.2 Actual Manufacturing Time Breakdown

Table 9.2 shows the manufacturing breakdown for the aircraft. The final amount of hours spent on the aircraft was approximately 550 man-hours, 300 hours spent on the fuselage, 200 hours on the wing, and 200 hours in assembly, landing gear, and integration other aspects. Table 9.2 gives the breakdown of the manufacturing time spent on each major subsection of the aircraft. The manufacturing time was very near the time allocated in the proposal stage.

Table 9.1: Rated Aircraft Cost Table

Item	Value	MEW	REP	MFHR	RAC
We(lbs)	11.75	12	0	0	1175
Engine 1					
#cells	12		720		720
Engine 2					
#cells	12		720		720
#wings	1			5	100
Wing Area(sq in)	1092			30	607
#body	3			15	300
total length bodies(ft)	6			24	480
Empennage	1			5	100
#vertical surface	1			5	100
#horizontal surface	1			10	200
basic flight system	1			5	100
#servos	6			6	120
#engines	2			10	200
#props	2			10	200
SUM		12	1440	125	5122

Table 9.2: Actual Manufacturing Time Breakdown

Item	Manufacturing Hours
Ailerons	2
Flaps	2
Wing	190
Fuselage	300
Landing Gear	3
Servo installation	2
Engine Installation	4
assembly	10
Empennage	8
Finishing	30
Sum	551

University at Buffalo



Design, Build, Fly Competition

Buffalo Wing 2

Proposal Phase

Prepared By:
Yi Shen
Joe Scaglione
Gilbert Romanowski
Nicholas Leone

Table of Contents

Part I – Executive Summary	1
Part II – Management Summary	3
Part III – Conceptual Design	5
Part IV – Preliminary Design	7
Part V – Detail Design	10
Part VI – Manufacturing Plan	11
Appendix	13

Part I

Executive Summary

The development process for the design of the plane consisted of debates, research, consideration of designs and choosing the most practical design for the plane.

In the early development stage debates were held to come up with ideas for designs of the plane. From these debates three basic designs were established: a flying wing, a twin boom configuration, and a bi-plane design. From there research was done to establish the most suitable for the competition.

The second stage of development was the research of the different designs concepts. After all the research was done it was found that all the designs had their own pros and cons. The flying wing design was the most aerodynamic of all the design concepts. And because this, the flying wing was the first consideration of the DBF team for the competition. But because the instability of the design and cumbersome manufacture established from last years' tried and failed design the team changed its mind. The twin boom configuration had many desirable qualities, for the example the result from the placement of the engines. The placement of the engines put the control surfaces of the vertical and horizontal stabilizer in the wake of the engines, giving the plane great stability in flight. However, the most important consideration of the team was cargo capacity, which both the flying wing and twin boom configurations lacked. This consideration was one of the deciding factors for the final design consideration. The bi-plane design was brought up in one of the last debate meetings and was a late contender for consideration for the design of the plane, but because of research done by one of the

members it was found the Bi-plane was quite a desirable design. Its two wing configuration gave it a better lift characteristic than the single wing configuration, it also provided more stability compared to the flying wing, and also provided a large cargo capacity that none of the other designs could match. It did have its drawbacks though, because its large cargo capacity and the nature of the wing configuration the bi-plane produces a fair amount of drag. But it was decided by the team despite the lack of aerodynamics that the bi-plane configuration would be design of the plane that would be taken to the competition.

Part II

Management Summary

The team leaders, Yi Shen and Joe Scaglione, handled management of the team. They broke the team in to sub-teams, consisting of aerodynamics, structures and propulsion; they also made a schedule to follow and also gave set of milestones to achieve.

The sub-teams were responsible for the research into the design considerations for the plane and gave the pros and cons of each consideration. Aerodynamics specialized in the flight characteristics of the design concepts. They introduced to the team's debate meetings the lift capabilities, consequences of drag, and stability factors of the each design concept. The structures sub-team specialized in manufacturing processes of the designs, they were the ones who told the team if a design concept would be feasible to build with the team's very little experience in construction of model aircraft. Propulsion sub-team had one of the easier jobs to do considering that requirements of the DBF competition limited the amount of engines because of the 5-pound battery limit. At the team's debate meetings they would report their findings, shared their opinions on the design concepts, and made sure that they were not left out of the development stage of the competition.

The schedule laid out by the team leaders was at best general but it did give the correct steps for the team to function in an orderly fashion. First would come research, then design, then development of the design, then construction and finally testing of the plane.

The research phase is used to determine the best design concept for the competition. This phase consists of debates, considerations of the design of the plane and research into the feasibility of the design concepts. The next phase is the design of the chosen concept. This entails a basic design to gain some perspective on where the plane is headed. The development phase is where the plane really started to take shape (on paper at least). Development consists of the basic structure of the plane and placement of the motors, cargo, and other components. The construction phase consists of the actual building of the plane and ironing out of any rough edges that are missed in the development phase. The testing of plane is the last phase. This consists of flight tests that provide flight data necessary to make final adjustments to the flight control systems.

The milestones or goals set by the team leaders are made up of sections and subsections of categories. The first of these is simply getting started. This consists of group discussion of the rules of the competition, and organization into sub-teams. The next goal is to decide on a design for the aircraft. The construction goal is made up of sub goals that include construction of the wings; which included the manufacture of the ribs, spars, leading edges, and trailing edges; construction of the tail and the control surfaces; construction of the body of the plane; and final assembly. The last milestone is the testing phase.

Part III

Conceptual Design

The new rules and scoring for the DBF competition was the guideline for designing the buffalo wing. Due to the limited wingspan and relatively large payload, it was decided that a high lift design was needed. Three different high lift configurations were examined: a flying wing, twin boom biplane, and single fuselage biplane. Research into each concept included aerodynamics texts, wind tunnel data, and 1/7-scale models. The design parameters used for the evaluation are: lift required, wing area required, weight, cargo volume, drag, stability, aerodynamics, engine power, battery capacity.

The Figures of Merit (FOM) used to evaluate each design parameter are:

- Manufacturing ease and time
- Aerodynamic lift and drag
- Structural strength and weight
- Speed, stability, and maneuverability
- Cost

The FOM chart is included in the appendix. Each FOM is given a score weight, on a 1 to 10 scale, which determines its importance to the entire design. Then each design parameter was given a score on a 1 to 10 scale, 10 being the most desirable. Although some of the design parameters are mutually exclusive, the chart gives a fairly accurate portrayal of the different designs that were discussed. Note that for the motor selection, thrust was substituted for lift in order to portray the benefits of having multiple motors.

From the FOM chart, the best general configuration was decided to be the following:

- Bi-plane
- Single fuselage
- Straight wing
- Low horizontal stabilizer
- Tail dragger gear
- Twin motors

A preliminary configuration was drawn up that included all of these design aspects. This drawing is included in the appendix.

Part IV

Preliminary Design

Once the biplane configuration was chosen, the team had to work on the next design stage. The fuselage, motor(s), tail size, payload location, and the radio control system details all had to be worked out.

The first thing the team worked on was the wing area and loading. For the approximate Reynolds's number used to design our plane, the maximum wing loading should not exceed 35 oz./sq.-ft and should stay at or under 30 oz/sq.-ft for good flight characteristics. To find the wing area they took the maximum weight of the payload, and added the estimated weight of the airframe, motors, radio and batteries.

Component	Weight (Lb.)
Payload	17.6
Batteries	5
Radio	2
Motors	2
Airframe	6
Total	32.6

To figure out the wing area, they used the targeted weight and a wing loading of 35oz/sq.-ft. The wing area needed came out to be 14.6 sq.-ft. For a biplane with a seven foot wing span, this worked out to making a 7'x1' wing to make 14 sq.-ft of wing area.

Research by one of the members indicated that performances of the wings are highly dependent on their location with respect to each other. The vertical separation between two wings should be equal to the length of the wing cord. For better performance, the horizontal location of the bottom wing needs to be staggered behind the top wing. The stagger distance was determined to be 50%. The choice came as a compromise. It would be easier to build the wings if they were closer to each other horizontally. However, setting the wings too far apart will make the fuselage too long and weaken the cargo area. It was decided to set the lower wing back by 50% of the cord for improved performance without elongating the fuselage too much.

Next on the list was the tail surfaces. The team was faced with deciding on whether or not to use an airfoiled tail or to leave it flat, and decide on the surface areas, and construction method. The team decided to leave the fin and stabilizer flat rather than using an airfoil for them. The decision came about mainly because flat surfaces was much easier to build and significantly less time consuming. The construction for both the fin and stabilizer is a basic balsa frame covered with thin balsa on both sides. They were built up using $\frac{1}{4}$ " x $\frac{3}{4}$ " strips of balsa and covered with $\frac{1}{16}$ " thick balsa sheets. The tail surface areas came next. To calculate them, the team decided to put stabilizer area to be 20% of the wing area and fin to be 15%. This worked out to 1.6875 sq.-ft. for the fin and 3.000 sq.-ft. for the stabilizer area.

Once the wing and tail areas are worked out, the team concentrated on the dimensions for the fuselage. The main concern for sizing the fuselage was the payload volume and spacing between the top and bottom wings. The team decided to carry the maximum amount of the allowed cargo, eight of the 1 Liter bottles. The cargo space

needed was an 8-1/4" x 7" x 17", and the vertical wing separation needed to be 12". The team decided to put the cargo on top of the center of gravity (CG) so that the CG of the plane and the CG of the cargo coincide longitudinally. The advantage of this cargo placement is that the plane's CG will not change whether or not the cargo is inside the plane. The fuselage was then sized around the cargo area and the wing placement. It's box design proved to be easy to build and practical.

The twin wing mounted motors proposed the next challenge. The team decided to mount it on the top wing due to the better propeller clearance it provides. It is mounted in the wing via two reinforced ribs that protrude forward of the leading edge and are separated 4 inches apart to accommodate the motors. The ribs are reinforced with 5 layers of carbon fiber, a firewall is mounted on to the front of the ribs and the motor and gearbox is attached to the firewall via screws.

Relatively easy to make was the landing gear. The team decided on a two foot track width to get good ground handling and resistance to tipping over from cross winds. The landing gear was made by cutting a foam block out to the shape of it and laminating 3 layers of 1/16" balsa and 18 layers of carbon fiber. A 5/16" axle is inserted into the lower part of the landing gear and the wheel is then mounted to it.

After all the major parts of the aircraft was build, the team installed the radio control components and aligned the motor, wing, fuselage, fin and horizontal stabilizer, and then assembled it. After assembly, the entire plane's outer surfaces were given a final light sanding. When it was ready to be covered, it was wiped with a tack cloth to get all the balsa dust off and covered with monocoat. That concludes the construction of the aircraft.

Part V

Detail Design

The detail design section includes final performance data and component selection and placement. The aircraft has not been finished as of this writing. Since the detailed design part of the report requires the aircraft to be completed, we cannot supply the data necessary to make this report meaningful. Please refer to the appendix to see the drawing package.

Part VI

Manufacturing Process

The main process discussed involved constructing the plane mainly from balsa wood. Other wood, such as spruce, would only be used in high stress areas of the planes. These areas would be the two main spars in each wing, the landing gear mounts, and the engine mounts.

For other areas, such as the fuselage, where overall weight is a concern, balsa would be used in combination with carbon fiber. The four main structural members of the fuselage would be layered with carbon fiber and epoxy, creating a rigid structure that could withstand the stresses of the cargo. Carbon fiber and balsa would also be layered on selected ribs in the wings, where the engines would be mounted.

Lightweight metals, such as aluminum and titanium, were also considered. However, their weight and expense would not justify their use in the plane. Composites and balsa wood prove most economical in construction of the airplane.

Figures of Merit

Availability of Materials:

The majority of the balsa wood used for construction could be obtained at local hobby stores. This would not be a major problem. However, the large rolls of carbon fiber would have to be ordered from a composite manufacturer from outside the area.

Cost:

The all balsa wood design proposed would be the least expensive. Total projected cost of balsa wood is around \$300. This is less expensive than fiberglass or aluminum, which would be in the range of \$1200 to \$1600. The amount of carbon fiber needed is minimal. This would only be used for layering, so a thirty (30) foot roll would be sufficient. Cost estimate for this amount is \$80.

Skill Level:

With only a couple team members who have experience building aircraft, skill level is a heavy consideration. However, the choice of balsa as the core material should make it easier for less experienced builders to get involved. The ease with which the material can be cut and shaped should not prove to be a great challenge. Novices in airplane design can also do the layering of the carbon fiber. This only involves spreading epoxy evenly over the surface of the fabric.

Manufacturing Timetable

Start Date-End Date	Item constructed	Total time (hours)
11/1/99-12/18/99	Ribs constructed for wings, fuselage parts cut	30
12/21/99-1/16/00	Critical parts layered with carbon fiber	20
1/16/00-2/1/00	Horizontal and vertical stabilizers completed	20
2/1/00-2/22/00	Construction of wings completed	40
2/22/00-3/2/00	Construction of fuselage complete	20
3/2/00-3/8/00	Engines mounted on wings	10

Complete Aircraft

Start Date – End Date	Total Manufacturing Time
11/1/99 – 3/8/00	140 hours

Appendix

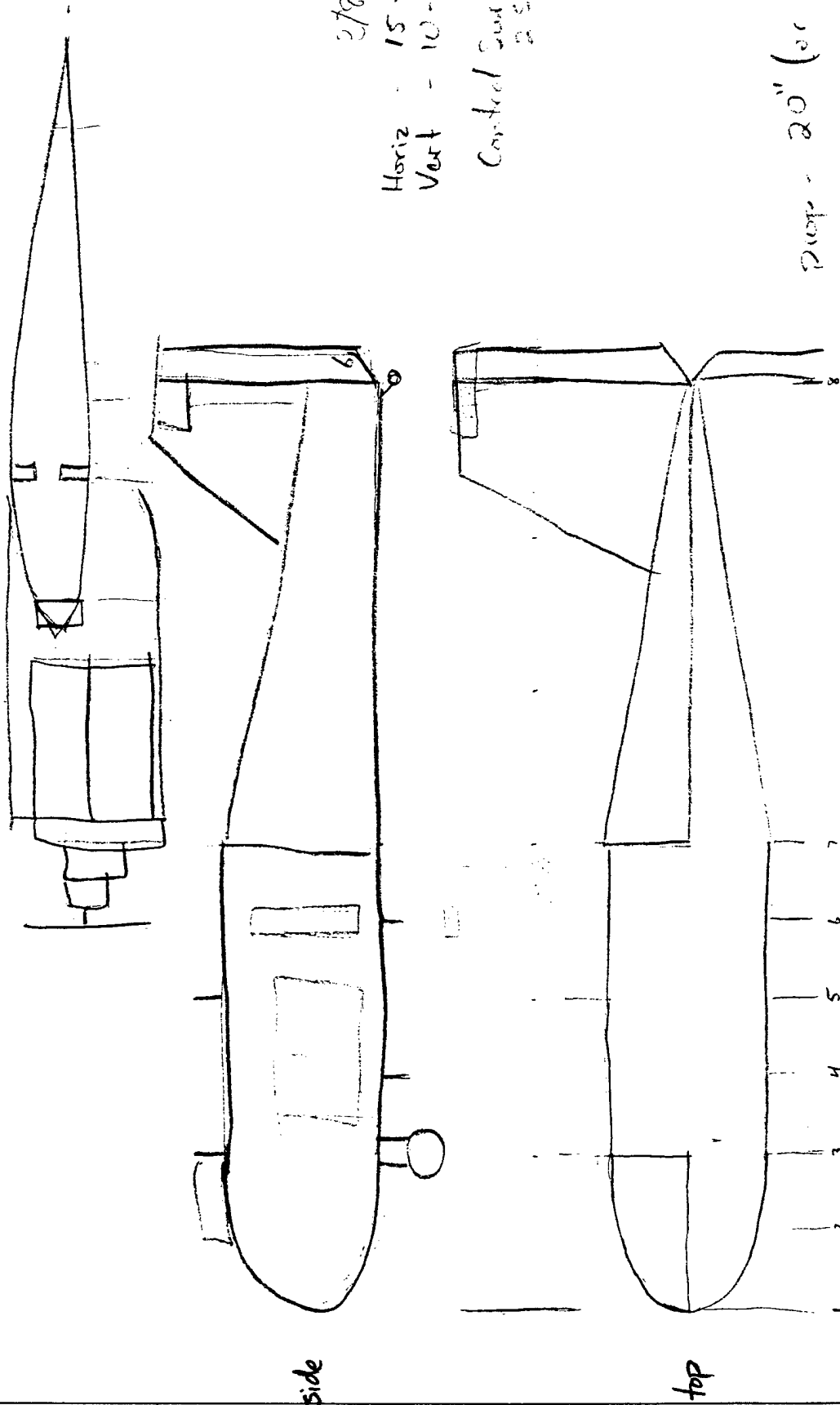
Figures of Merit Chart	1
Drawing Package	
Preliminary Side and Top View and Motor Mount Configuration -Shows rough depiction of preliminary ideas	2
Scaled 3-view and Rear View -Shows top, side, front, and rear views	3
Isometric Wireframe	4
Side View of Forward Fuselage -Shows layout of payload, battery pack, and radio components	5
Pictures	
Forward fuselage framing and close-up of framing construction	6
Wing construction and close-up of wing construction	7

FOM CHART

	Manufacturing		Aerodynamics		Structure			Performance			Cost	Total
	Ease	Time	Lift	Drag	Strength	Weight	Volume	Speed	Stability	Maneuver.		
score weight	9	8	9	3	7	7	9	3	5	4	5	
General Config.												
	Bi-plane	6	7	5	6	5	7	5	7	5	6	420
	Mono-plane	6	7	5	6	6	5	5	6	7	5	398
Flying wing	5	7	8	8	7	6	4	8	3	5	5	408
Aft-fuselage												
	Single	8	N/A	6	7	5	7	6	5	5	7	399
Twin Boom	3	3	N/A	4	6	5	4	4	5	5	4	253
Stabilizer												
	V-tail	5	N/A	5	4	6	N/A	5	4	4	4	241
	T-tail	3	N/A	6	3	4	N/A	6	5	5	6	211
Low Horizontal	8	8	N/A	5	5	5	N/A	5	5	5	6	311
Wing Config.												
	Straight	7	7	4	7	6	N/A	4	5	5	7	377
	Swept	3	7	5	4	4	N/A	6	5	5	4	268
	Dihedral	4	4	N/A	N/A	5	4	N/A	N/A	6	5	202
Taper	3	3	5	5	6	4	N/A	6	5	6	4	268
Landing Gear												
	Tail-dragger	7	N/A	6	5	7	N/A	6	4	5	6	309
Tricycle	5	5	N/A	4	5	5	N/A	5	7	5	5	262
Motor Selection			(Thrust)									
	Single	6	3	5	N/A	6	N/A	5	5	5	6	276
Double	4	4	9	5	N/A	5	N/A	5	5	5	5	284

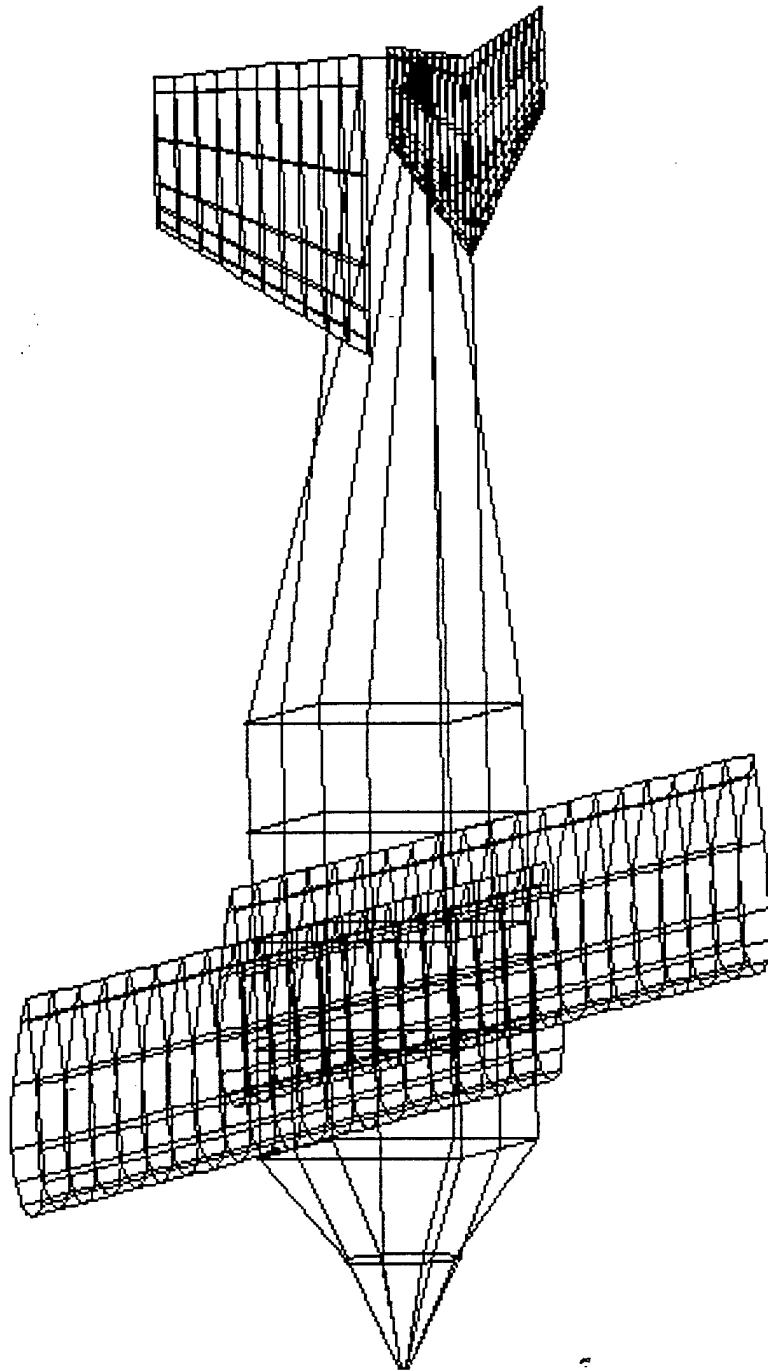
Best Configuration:

Biplane	420
Single Fuse	399
Low Horizontal Stab	311
Straight Wing	377
Tail-dragger	309
Double Motor	284



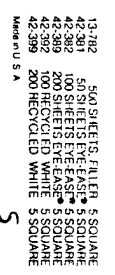
278 + hk
 Horiz - 15 - 20%
 Vert - 10 - 15%
 Control Surface:
 25%

Prop - 20" (or less)

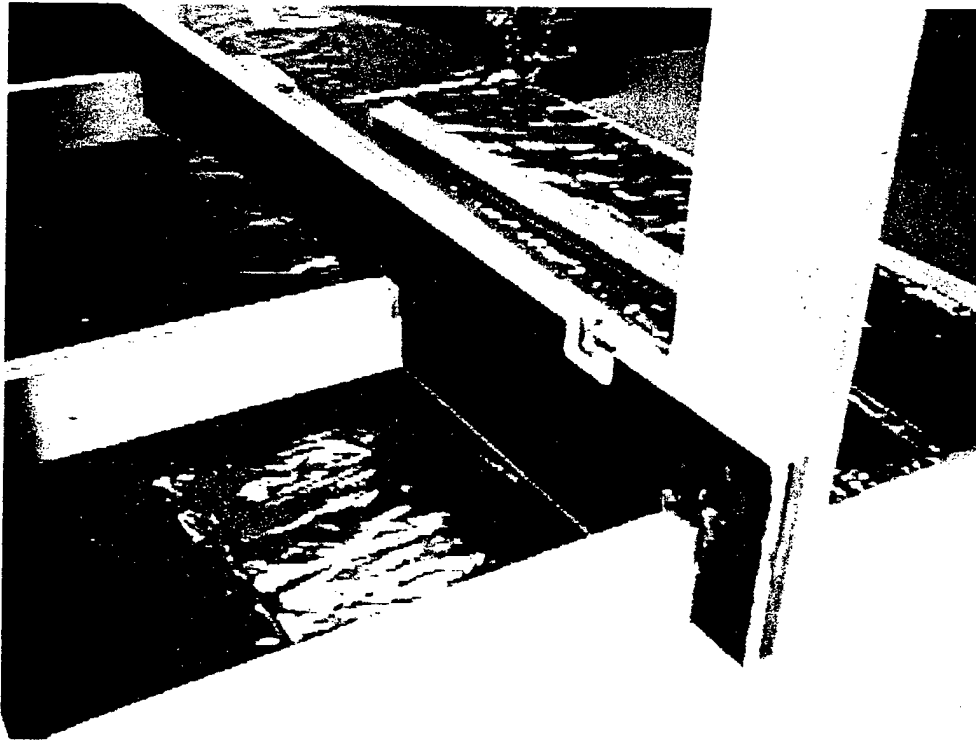
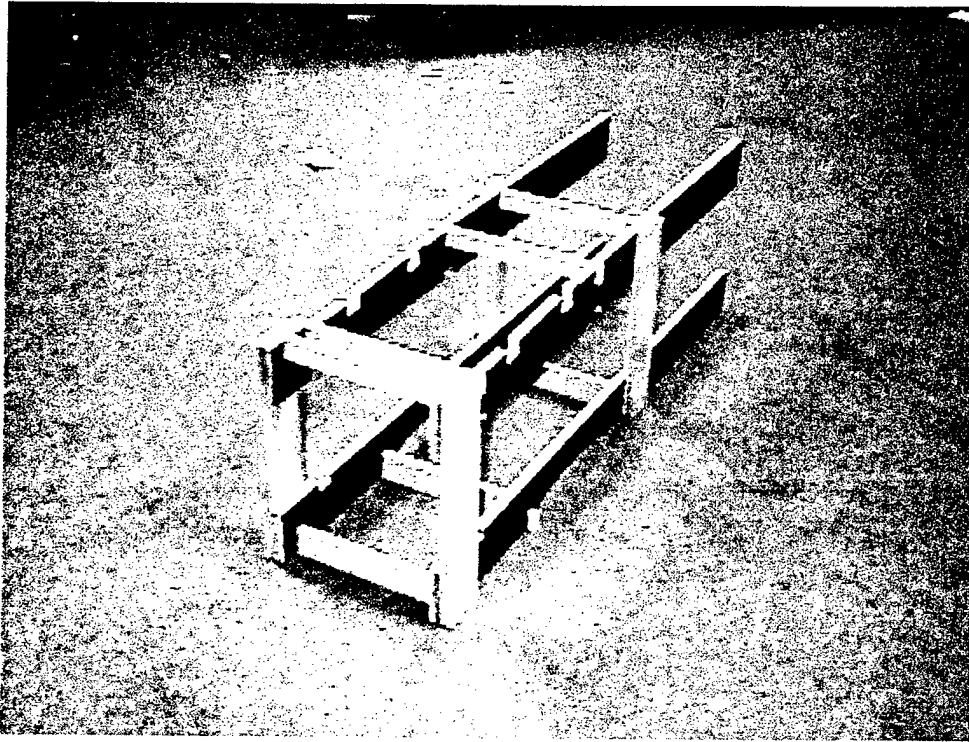


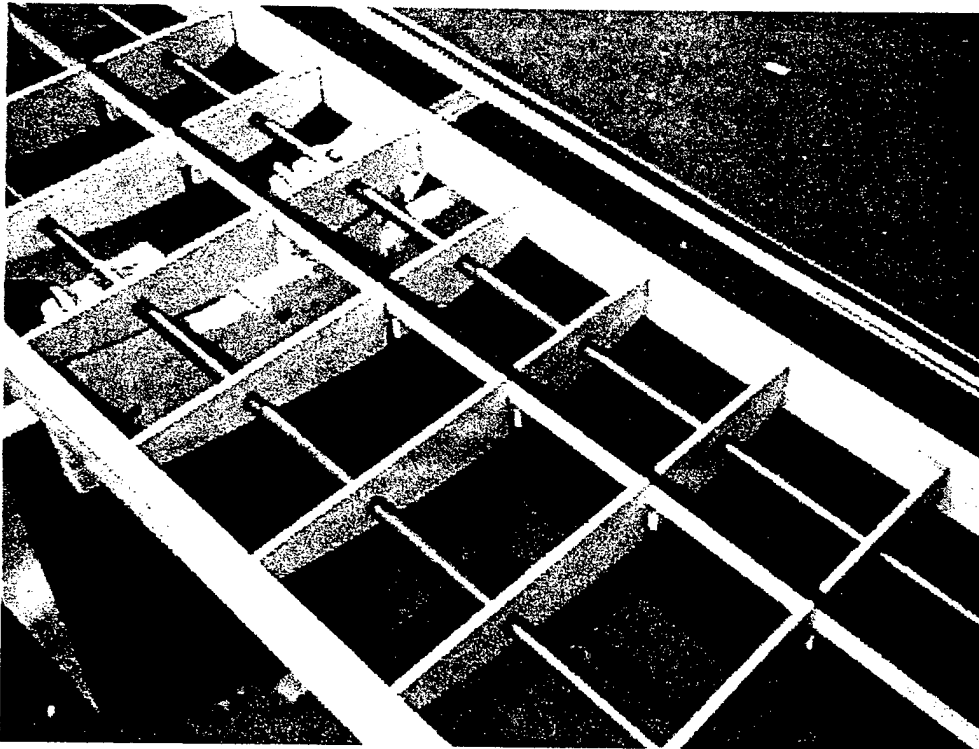
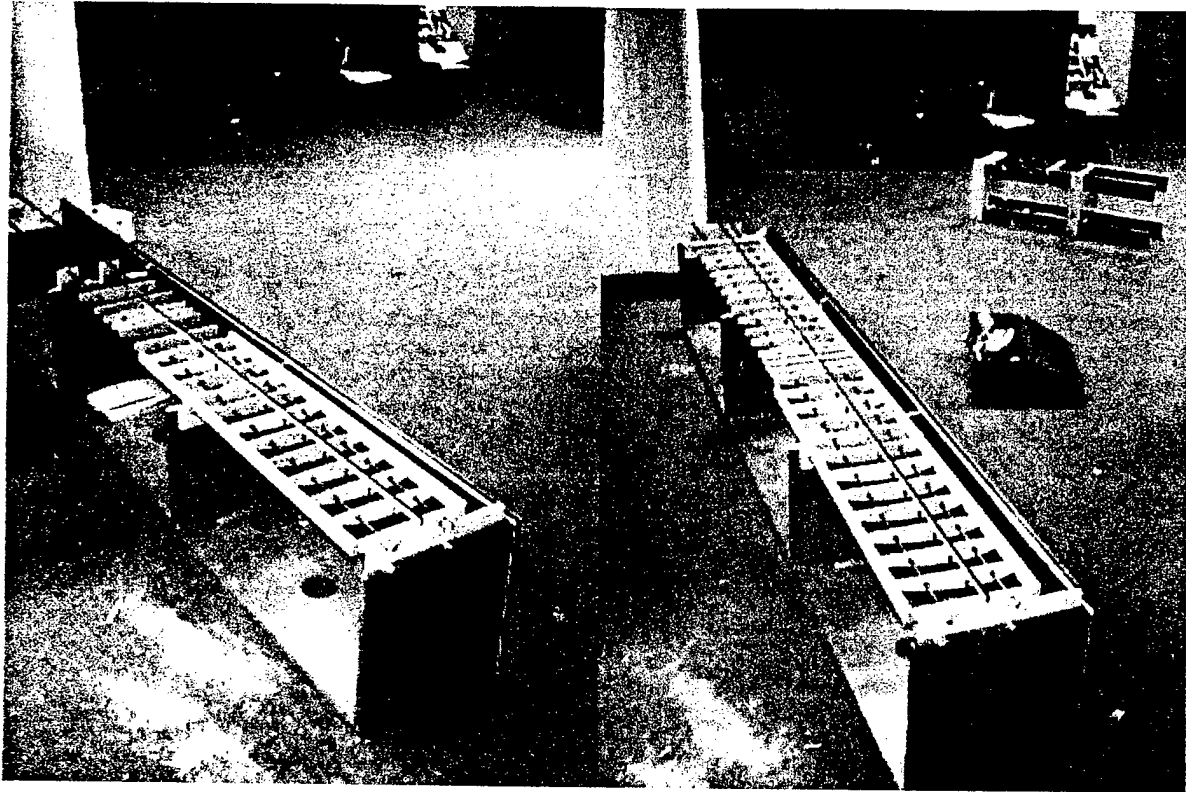
6

9



5





University at Buffalo



Design, Build, Fly Competition

Buffalo Wing 2

Addendum Phase

Prepared By:
Yi Shen
Joe Scaglione
Gilbert Romanowski
Nicholas Leone

Table of Contents

Part I - Lessons Learned	2
---------------------------------	----------

Part II – Rated Aircraft Cost	4
--------------------------------------	----------

Lessons Learned

The University at Buffalo DBF airplane, Buffalo Wing 2, underwent only minor changes to the design from the proposal phase. These modifications were used only to ensure to structural integrity of the aircraft. The four improvements made were doubling the size of the spars in the top wing and putting reinforcements in the bottom wing, connecting both wings with support wires, and placing a spring between the two wheels of the landing gear.

The reason behind doubling the spars for the top wing comes from testing the strength of the bottom wing. Before construction had begun on the top wing, the bottom wing was found to have too much flex near the edge. When the wing was placed between two chairs and a force was applied at the center, the amount of flex was approximately two inches. The solution to this problem was to place two birch wood, 5/16" dowels through holes that were drilled in the ribs earlier. One dowel was placed 1 1/2 " from the leading edge and the other was placed 1 1/2 " from the trailing edge. These reinforcements significantly improved the rigidity of the bottom wing.

For the top wing, it was decided by the design team to double the spars. This would be a faster method than the dowels because the wing was not built yet. The construction team prepared four separate spars and used epoxy to fuse them into two spars, thereby doubling the strength of the top wing. When this method was tested, the top wing was found to have more than enough strength to keep the plane in the air.

There was also a concern about how the wings would share the load. The end panels originally proposed were found, through scale model use, not to be exceptionally supportive of both wings. The design team then proposed using wires placed in a x-

pattern to connect both wings. When this idea was tested on a scale model of the plane, the results were very encouraging. With tension in the wires, both wings were not subjected to a significant amount of flex.

The next area of Buffalo Wing 2 that had an uncertain amount of structural integrity was the landing gear. This was of great concern because the gear must be able to handle the stresses of a four-G landing. Considering the plane has a final weight of around 30 pounds, a landing like this would put 120 pound of force on the landing gear legs. The solution to this was a method that has been used on Radio Controlled aircraft in the past. Two 1/16" steel wires, connected in the middle by a stiff spring, would be used to absorb the shock when the plane hits the ground. These would also keep the legs from spreading apart from each other.

The amount of strength added to Buffalo Wing 2 from these modifications is truly significant. The landing gear and the wings are more rigid than ever and the fuselage could probably hold twice the weight that is required in competition. This all comes with only minor additions to the total weight. Buffalo Wing 2 is made to haul cargo and it does so in a structurally safe and efficient way.

Aircraft Cost

Manufacturer's Empty Weight	35lb
Number of battery cells	28
Number of Wings	2
Wing Area	13.85 sq. ft.
Fuselage Length	6 1/3 ft.
Number of Servos	4
Number of engines	2

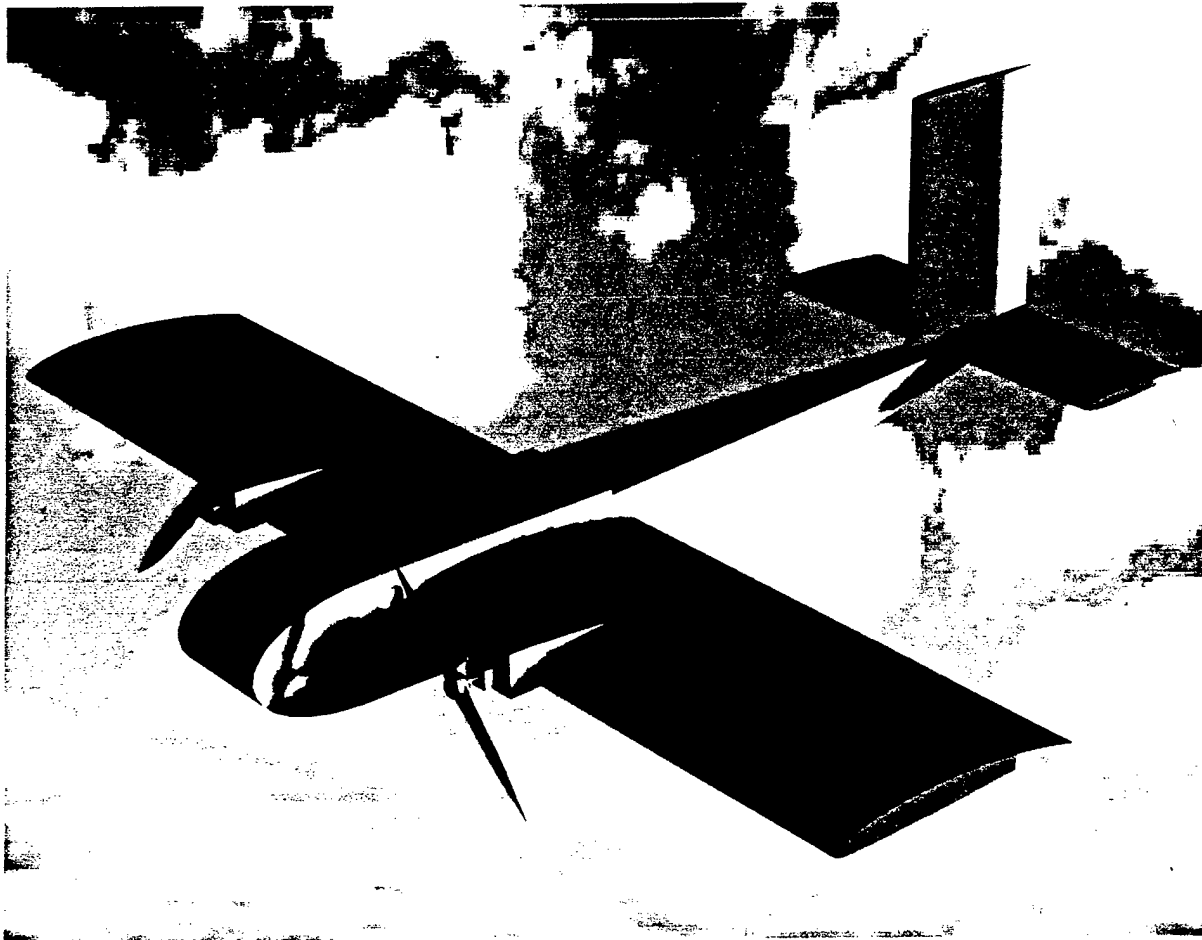
$$\text{Rated Aircraft Cost, \$ (Thousands)} = (A * \text{MEW} + B * \text{REP} + C * \text{MFHR}) / 1000$$

Coef.	Description	Value
A	Manufacturers Empty Weight Multiplier	\$100 / lb.
B	Rated Engine Power Multiplier	\$1 / watt
C	Manufacturing Cost Multiplier	\$20 / hour
MEW	Manufacturers Empty Weight	13 lb.
REP	Rated Engine Power	2 engines * 50A * 1.2 V/cell * 24 cells = 2880
MFHR	Manufacturing Man Hours	WBS 1.0 Wing(s): 5 hr. * 2 wings + 4 hr * 13.85sq. ft. = 65.4
		WBS 2.0 Fuselage and/or pods 5 hr * 1 body + 4 hr * 6 1/3 ft = 30.33
		WBS 3.0 Empenage 5 hr. + 5 hr. * 1 Vertical Surface + 10 hr. * 1 Horizontal Surface = 20
		WBS 4.0 Flight Systems 5 hr. + 1 hr. * 4 servos = 9
		WBS 5.0 Propulsion Systems 5 hr * 2 engines + 5 hr * 2 propellers = 20

$$\text{Rated Aircraft Cost} = (100 * 13 + 1 * 2880 + 20 * (65.4 + 30.33 + 20 + 9 + 20)) / 1000 = \$7.07 \text{ (thousands)}$$



RPP-2 Hobbes
Final Design Report



AIAA Student Design/Build/Fly Competition

Wichita, Kansas

**Department of Aeronautical and Astronautical Engineering
University of Illinois at Urbana-Champaign**

April 14, 2000

RPP-2 Hobbes
Final Design Report

AIAA Student Design/Build/Fly Competition


Wichita, Kansas

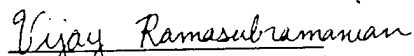
Department of Aeronautical and Astronautical Engineering
University of Illinois at Urbana-Champaign

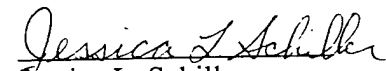
April 14, 2000

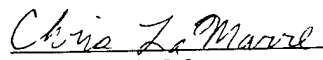
RPP-2 Project Team



Jason M. Merret

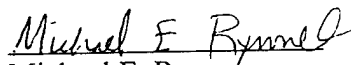

Eunice Y. Lee


Vijay N. Ramasubramanian


Jessica L. Schiller

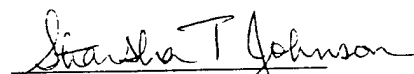

Chris M. LaMarre


Robert R. Quirk

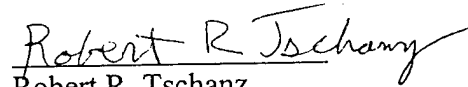

Michael E. Rynne

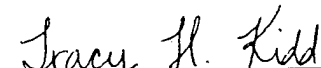

Carey A. Lunsford



Karl R. Klingbeil

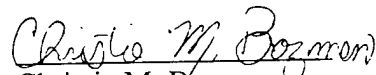

Starsha T. Johnson



Michael S. Sexauer

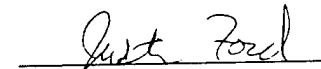

Robert R. Tschanz

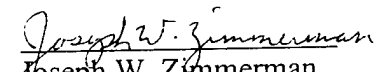

Tracy H. Kidd

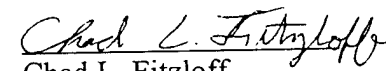

Shalin H. Mody



Christie M. Bozman

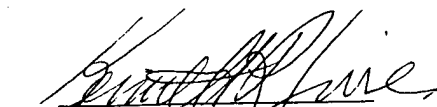

Leah C. Stefanos



Justin K. Ford



Joseph W. Zimmerman


Chad L. Fitzloff


Andrew D. Young


Dr. Kenneth R. Sivier
Faculty Advisor


Mike Cross
Pilot


AnnMarie Cross
Hobbico Advisor

Acknowledgements

This year's project owes its success to many sources, and we would like to take this opportunity to acknowledge their help. We thank Jim Schmidt and Hobbico for their continued and unparalleled support through donations of building materials, tools, and this year, employees. Their continued dedication to the team has surpassed all our expectations and has been a constant motivation for the team. Special thanks goes to Mike and AnnMarie Cross for their hard work, dedication, and sacrifices for the team. Their guidance and compassion has truly inspired this year's team. We thank the Department of Aeronautical and Astronautical Engineering for providing the necessary space for a workshop as well as needed monetary support, and the use of a low-speed wind tunnel for propulsion testing. There were also several sources of monetary support. We thank the College of Engineering at UIUC, the Illinois section of the AIAA, and Region III. Thanks also goes to our corporate sponsors, Motorola and Pratt & Whitney. We especially thank James Kessler, a UIUC alumnus for his continued support of the team. Finally, Professor Kenneth Sivier has continued to advise and encourage the team. Our deepest gratitude goes to him for his endless encouragement and continued guidance.

Table of Contents

1.0 Executive Summary	1
2.0 Management Summary	2
3.0 Conceptual Design	5
3.1 System Requirements	5
3.2 Figures of Merit	6
3.3 Conceptual Design Analysis Tools	6
3.4 Configuration Studies	7
3.4.1 Prototype Aircraft	7
3.4.1.1 Configurations Considered	7
3.4.1.2 Conceptual Design Analysis Results	8
3.4.1.3 Figures of Merit Results	8
3.4.1.4 Payload Sizing	9
3.4.1.5 Prototype Conclusions	10
3.4.2 Competition Aircraft	10
3.4.2.1 Configurations Considered	10
3.4.2.2 Conceptual Design Analysis Results	11
3.4.2.3 Figures of Merit Results	11
3.4.2.4 Conclusion	11
4.0 Preliminary Design	20
4.1 Design Parameters Investigation	20
4.2 Aerodynamics	20
4.3 Propulsion System Selection	21
4.4 Structures	22
4.5 Aircraft Weight Build Up	22
4.6 Performance Analyses	22
4.6.1 Takeoff Analysis	22
4.6.2 Energy and Time Analyses	23
4.7 Stability Analyses	24
4.8 Prototype Design Summary	24
5.0 Detailed Design	33
5.1 Introduction	33
5.2 Prototype Aircraft Flight Testing	33
5.2.1 Objectives	33
5.2.2 Test Site and Instrumentation	33
5.2.3 Procedure	33
5.2.4 Results	34
5.3 Aerodynamics	36
5.4 Propulsion	36
5.5 Structures	38
5.5.1 Major Changes From Prototype	38

5.5.2 Structural Modeling and Results	39
5.5.4 Final Structure	39
5.5.6 g-Load Capability	39
5.6 Ground Operations	40
5.7 Final Weights and Balance	40
5.8 Performance Analyses	41
5.8.1 Takeoff Analysis	41
5.8.2 Energy and Time Analyses	41
5.9 Stability and Control Analysis	41
5.10 Final Design Summary	42
6.0 Manufacturing Plan	58
6.1 Component Requirements	58
6.2 Manufacturing Processes Investigated	58
6.2.1 Wing	58
6.2.2 Fuselage	58
6.2.3 Empennage	59
6.3 Figures of Merit	59
6.4 Evaluation	59
6.5 Results: Manufacturing Processes for Prototype	60
6.5.1 Fuselage	60
6.5.2 Wing	60
6.5.3 Tail	61
6.6 Lessons Learned and Improvements to be made to the Competition Aircraft.	61
6.7 Results: Manufacturing Processes for Final Design	61
6.7.1 Fuselage	61
6.7.2 Wing	62
6.7.3 Tail	62
6.8 Construction Details	62
6.9 Cost Reduction Methods	62
7.0 Lessons Learned (To be submitted a later date)	
8.0 Aircraft Cost (To be submitted at a later date)	
9.0 References	65

1.0 Executive Summary

This report presents the design process and results for the University of Illinois' entry into the fourth annual AIAA Student Design/Build/Fly Competition. The final design, RPP-2 *Hobbes*, is the product of detailed aerodynamic and structural modeling as well as performance analyses. The design processes discussed in this report rely on both experimental data, acquired through construction and testing of a prototype, YRPP-2 *Sam*, and analytical modeling. The aircraft is designed to satisfy all of the competition requirements and maximize the amount of payload during the allotted time.

The design process began with a consideration of several different configurations. Figures of Merit used include: rated cost per final score, complexity, innovation, robustness, and ground operations. The two primary tools evaluating the conceptual design were the aircraft rated cost model and the takeoff model.

The preliminary design stage produced many experimental and analytic studies of aircraft performance. Some of the design tools developed at this stage were: takeoff analysis, as well as time and energy analyses. Some of the experimental tools used were: structural testing of wingtip loadings, propulsion system testing, and flight testing of a prototype, YRPP-2 *Sam*. The flight tests of the prototype aided in gathering the needed data for improving the analytical models and revealed areas where more design work was required. Such areas included the rudder and elevator.

The prototype easily completed the 100 ft. takeoff limit. The rudder and elevator were increased to give the pilot more control. A major conclusion from flight test data was an addition of a second motor for the competition aircraft. The construction and testing of the prototype provided valuable data for designing and building the final competition aircraft.

The final design, RPP-2 *Hobbes*, satisfies all of the requirements described in the 1999-2000 Rules and Vehicle Design Specifications and was also designed for maximum payload sorties in the allotted time. The predicted empty weight, including batteries is 12.5 lbs. With 8 liters of payload, weighing 20 lbs., the total estimated gross weight is 32.5 lbs. The team can expect to complete 3 or 4 scoring sorties for an 8 liter payload with a cruise velocity around 80 ft/s.

The University of Illinois at Urbana-Champaign is proud to submit this design to the sponsors of the AIAA Design/Build/Fly Competition.

2.0 Management Summary

The organization of the design team was strongly influenced by the beginning of the design activities in the summer of 1999. The team leader, chosen at the end of last year, contacted and organized a core group. This allowed this group to begin the preliminary design and be ready to delegate tasks once school started. This core group was made up of students of previous year's teams who were in the area during June, July, and August. The team had semi-weekly meetings.

Once school started, the core group members became department heads and tasks were divided accordingly. Summer progress was reviewed for returning and new members. This quickly incorporated them into team. The team continued semi-weekly meetings that were organized by the team leader. The first meeting of the week was a general meeting to update all team members on team progress. The second meeting was primarily for the team leader and department heads to discuss activities and maintain the progress of the departments. Following this meeting, each department had its own meeting or work session. When the prototype design was set and was construction complete, a third weekly meeting for flight testing was added. Flight testing, was done primarily on the weekends.

A summary of the departments and their respective members is given in Fig. 2.1. Note that many team members participated in more than one department. This was especially helpful for effective communication and efficient functioning within the team.

A milestone chart was created to help keep the departments on schedule. This was developed at the beginning of the academic year and efficiently utilized seasonal changes. The milestone chart is shown in Fig. 2.2. Due to the multiple weekly meetings, delays in the schedule were minimized and team communication was maintained. Adhering to deadlines reduced deviances from the schedule, with the largest time lag being only one week.

TEAM MANAGEMENT

Jason Merret*
 Eunice Lee
 Jessica Schiller

DATA AERODYNAMICS

Christie Bozman*

PERFORMANCE & ENERGY ANALYSIS

Eunice Lee*
 Rob Quirk
 Leah Stefanos

PROPULSION

Vijay Ramasubramanian*
 Andrew Young
 Tracy Fritz
 Nathaniel Sutton

STABILITY & CONTROL

Mike Sexauer*
 Tracy Kidd

MANUFACTURING

Chris Lamarre*
 Carey Lundsford
 Joseph Zimmerman
 Michael Anderson
 Karl Klingebiel
 Chad Vetter
 Michael Rynne
 Justin Ford

STRUCUTRE

Robert Tschanz*
 Starsha Johnson

FLIGHT TESTING & COLLECTION

Tracy Kidd*
 Chris Lamarre
 Carey Lundsford
 Joseph Zimmerman
 Michael Anderson

FUNDRAISING & DOCUMENTATION

Jessica Schiller*
 Shalin Mody
 Leah Stefanos

ADVISING

Professor Kenneth Sivier*
 Mike Cross, pilot
 AnnMarie Cross

* denotes department head

Figure 2.1: Team Architecture

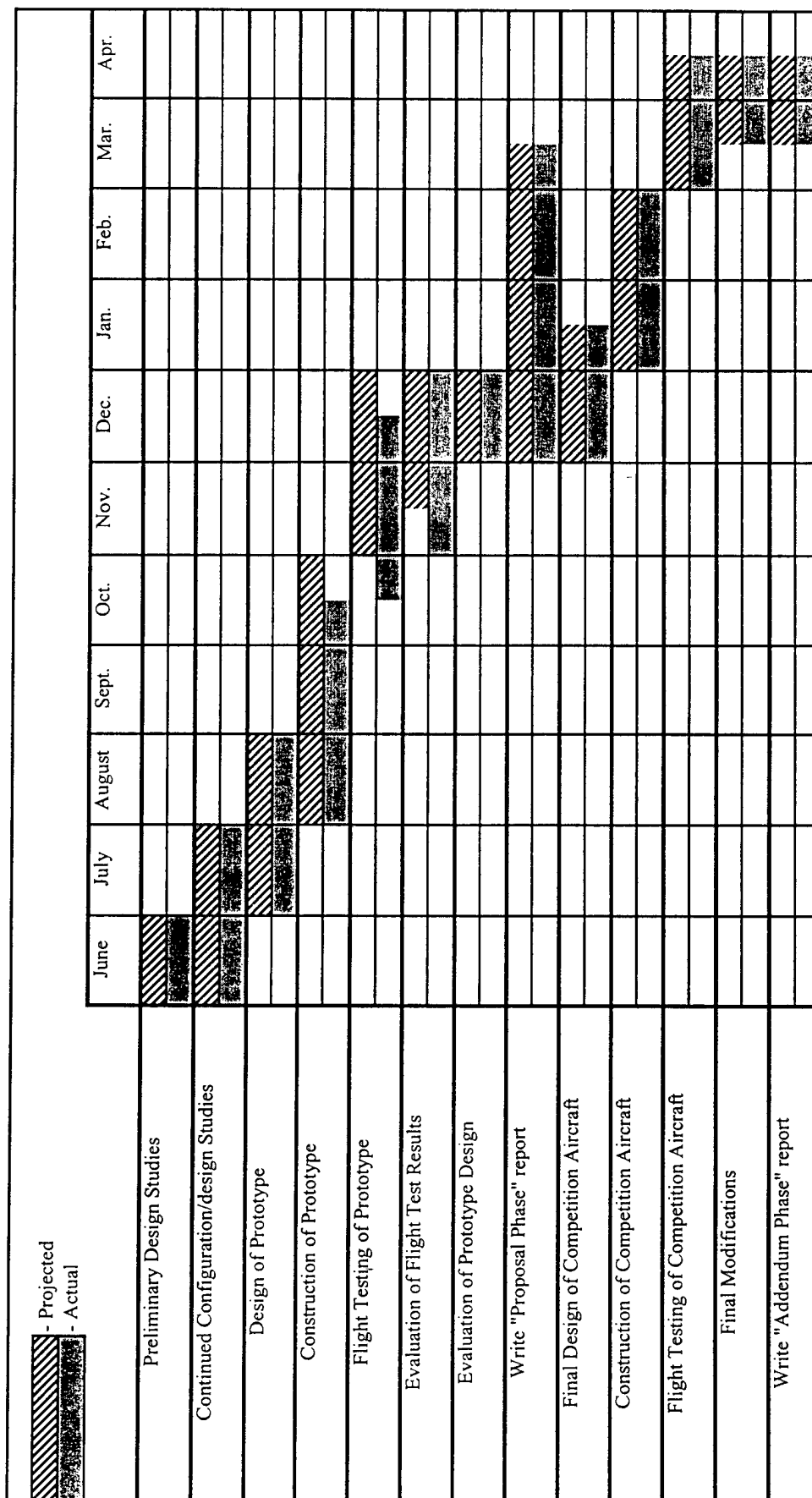


Figure 2.2 Project Timeline

3.0 Conceptual Design

3.1 System Requirements

The aircraft system requirements are specified in the 1999-2000 Rules and Vehicle Design. After receiving the rules, the following major design requirements, influencing the conceptual design, were selected:

- The system design objective is to achieve the highest score possible by optimizing the payload-to-sortie ratio using a maximum of 5 lbs. of batteries
- The aircraft must carry a payload of between 2 and 8 liters, satisfy the 100 feet takeoff limit, and fly both the unloaded and loaded sorties within a 10 minute flight period
- The design must have good flying qualities, be very robust, and use practical and affordable manufacturing processes

Using these requirements the following design drivers were determined:

- High final score by optimizing the payload-to-sortie ratio
- Limited energy, a maximum battery weight of 5 lbs.
- 100 ft takeoff requirement
- Good flying qualities both unloaded and loaded
- Quick payload exchanges
- Durability to withstand the numerous landings
- Low cost and ease of manufacture

The final cost and the takeoff requirement were determined to be the principal objectives of the conceptual design. Due to the cost model, larger aircraft that will carry more payload will also cost more. As a result of the battery limitation, larger aircraft may not complete as many sorties as a smaller aircraft. Therefore a smaller aircraft could achieve a higher final score by completing more sorties than a large aircraft even though it carries a smaller payload. In order to maximize the final score, the optimum ratio of payload to number of sorties had to be determined. Using the aircraft cost model, approximate costs were calculated for the prototype configurations as discussed in the next few sections of the report. In addition, each of the configurations was analyzed using a simple takeoff model to ensure that it could fulfill the 100 ft. takeoff requirement. Once the costs of the conceptual designs were determined, the single flight and total

flight scores were estimated. The other requirements were not considered in this analysis, since they were considered of minor importance in terms of the payload-to-sortie ratio and the takeoff requirement.

3.2 Figures of Merit

The complexity of this year's competition required many Figures of Merit (FOMs) to evaluate the configurations. The FOMs were all given numerical ratings based on the definitions below and are presented in Table 3.1.

- **Rated Cost/Final Score:** this represents the rated cost of the configuration. A lower cost means a higher total flight score.
- **Complexity:** the level of difficulty in designing and building this aircraft. A more complex aircraft is more susceptible to errors in design and construction.
- **Innovation:** the level of ingenuity and creativeness used in designing the aircraft. A more innovative aircraft is looked more favorably upon for its use of unique design concepts.
- **Robustness:** the good flying qualities and durability to withstand the numerous landings. The design must be able to fly in all types of weather and environmental conditions.
- **Ground Operations:** the time required to change the bottles between sorties and the batteries between flights. It also includes the time required to repair and maintain the aircraft on the ground
- **Monetary Cost:** the capital required to build the aircraft.

3.3 Conceptual Design Analysis Tools

The two tools used to evaluate the conceptual designs were the aircraft rated cost model included in the 1999/2000 contest rules and the takeoff model, discussed in section 4.6. In order to compute the rated cost and takeoff distance, a few aircraft parameters such as drag, weight, and aircraft geometry had to be estimated. The aircraft drag estimates were determined from technical data and past experience. Using the payload fractions from all of last year's aircraft, the average payload weight fraction was computed to be 36.9% of the takeoff weight. From this fraction, the final takeoff weights of the aircraft were estimated based on the payload weight. The weights were then

adjusted slightly for each of the different concepts such as additional weight for a second wing. All other factors, such as the number of servos, fuselage length, and tail areas were adjusted for each aircraft according to size of the payload and type of configuration.

Since both the cost estimates and the takeoff model depend on the wing area, it was determined first. Using the takeoff model, graphs of thrust required vs. aircraft weight, for different wing areas, were developed for 0 and 10 mph headwinds. These graphs are presented in Figures 3.1 and 3.2. Then for each concept, the wing area required for a takeoff distance of 100 ft. was determined using Figures 3.1 and 3.2. For the prototype design, the thrust available was assumed to be approximately 7 lbs. This was based on last year's experience. Since larger aircraft require more energy, the size of the battery pack was increased from 2.5 lbs. for the smaller aircraft to 5 lbs. for the larger aircraft.

Once all of these factors were estimated, the rated cost of each aircraft was calculated. Then using the cost of each aircraft, the single and total flight scores were computed. In order to compare all of the different concepts, the number of sorties was varied for each single flight. Using last year as a basis, the number of sorties was estimated to range from 3 to 5 total sorties. This corresponds to 2 or 3 loaded sorties. The number of sorties was varied, from flight to flight, to account for weather changes between flights, missed takeoff requirements, and any other factors that could cause a non-ideal flight. Since the report score is only a constant multiplier, a value of 90 was assumed.

3.4 Configuration Studies

The configuration studies for this report covers both the prototype aircraft and the competition aircraft. Therefore this section of the report does not exactly follow timeline of the project. Although the conceptual design of the competition aircraft actually occurred after the prototype flight-testing, it was convenient to include it in this section.

3.4.1 Prototype Aircraft

3.4.1.1 Configurations Considered

The configurations that were considered for this study are shown in Figure 3.3 through Figure 3.7. Even though all of these ideas were applicable to the competition,

some of them were more promising. The vectored thrust concept was very good idea, but was the most complex and would require additional time to design and manufacture. Since time and complexity were important considerations for the prototype aircraft, this concept was not evaluated. The canard concept was assumed to be very similar to the conventional aircraft in respect to the cost and takeoff analyses. Therefore, it was not considered as a separate concept. The remaining concepts were traditional, biplane and flying wing. Each of these concepts could have additional variations such as the number of motors and size of the payload. In order to simplify comparisons in this study, the same payload (4 liters) and number of motors (1) were used for each of the concepts.

3.4.1.2 Conceptual Design Analysis Results

Using the cost model and wing areas determined from the takeoff analysis, the rated cost and total flight score of the three concepts were determined and compared. The results are shown Table 3.2 and Table 3.3. Due to the absence of the tail, the cost of the flying wing concept was lower than either the traditional concept or the biplane concept. The biplane had the highest cost as a result of the extra wing and the associated additional weight. Since the total flight score is determined by dividing by the cost, the lower cost of the flying wing showed the highest total flight score. The number of loaded sorties per flight does play a large role in the total flight score. As seen in Table 3.3, the traditional concept would score higher than the flying wing by completing one more sortie in any of its three flights, increasing the total number of sorties by one. This could be a very large factor, taking into consideration the weather patterns of Wichita, Kansas and the performance of the flying wings two years ago.

3.4.1.3 Figures of Merit Results

The results of the FOM analysis are presented Table 3.4. As discussed above, the rated cost/total flight score FOM rating for the flying wing concept was a 5 since it had the highest total flight score. The biplane had an FOM rating of 1 since it had the lowest total flight score. The traditional concept rated a 5 on the complexity and robustness FOMs while it rated 1 on the innovation FOM. Conversely, the flying wing rated 1 on

the complexity and 2 on robustness FOMs and 5 on the innovation FOM. The ground operations FOM was difficult to rate since it involves many factors. Since the traditional concept is very simple, it would be very easy to change water bottles and batteries, transport, and assemble. Therefore it received the highest rating of 5. The added complexity of assembly and transport of the biplane concept lowered its rating to 3. The flying wing concept received a rating of 1 because of the limited space in a flying wing causing the most complexity in changing batteries and water. In addition, transport would be very difficult since the plane would have to remain in one piece. The monetary cost of the prototype was also quite important due to the limited budget of the team. Since the traditional concept was the simplest of the three concepts, it should be the least expensive and received a rating of 4. The additional material required for the biplane would cost more and therefore it received a rating of 3. The flying wing would require special materials and parts such as fiberglass and carbon fiber, which drive up costs. Consequently, it also received a rating of 3. At this point it was evident that the traditional concept was the best choice for the prototype with its total FOM score of 23.

3.4.1.4 Payload Sizing

Once the concept was determined from the FOM analysis, the payload of the aircraft was determined. The payload sizing was approached in the same manner as the conceptual analysis. Table 3.5 presents the cost of a traditional aircraft as the payload is increased from three to eight liters while Table 3.6 presents the corresponding total flight scores. It can be seen that, as the payload increases for a constant number of loaded sorties/flight, the total flight score also increases. It is important to consider that all of the flights might not be ideal and that the number of loaded sorties/flight might vary. With this in consideration, a four liter plane that completes seven total loaded sorties in the three flights will score almost as high as an eight liter plane that completes 6 total loaded sorties. In addition, a 4 liter plane that completes 8 total loaded sorties will score higher than an eight liter plane that completes six total loaded sorties. With this in mind and that a smaller aircraft will be easier to build and maintain, a payload of 4 liter was chosen for the prototype.

3.4.1.5 Prototype Conclusions

Due the advantages of a very simple configuration, the traditional concept was selected for the prototype design. This configuration is very simple, robust, and easy to work with on the ground. Although the total flight score of this aircraft is not the highest of the concepts, other factors proved to be just as important. A major factor in the design of the prototype was monetary cost. The project budget was limited and existing components had to be used in order to save money. The previous year's MaxCim motor and 19 (2.5 lbs) and 23 (3 lbs) cell battery packs were used as the propulsion system. In addition, some of the structural components such as the carbon fiber rod were reused from previous years.

3.4.2 Competition Aircraft

3.4.2.1 Configurations Considered

As will be discussed Section 5 below, much useful and important information was gathered from building and flying the prototype. The traditional concept worked extremely well for the prototype aircraft. Therefore this basic concept was chosen for the competition aircraft. One major result of the flight-testing was that it appears possible to complete the same number of sorties with a larger aircraft because the limiting factor was found to be time, not energy. As seen in the prototype payload sizing results, a payload of eight liters would produce the highest score for a constant number of sorties per flight. The flight testing indicated that by increasing the size of the prototype, and using two motors and five lbs. of batteries, it could to lift eight liters of water within the 100 ft. takeoff distance. Therefore, a payload of eight liters was chosen for the competition aircraft and the configuration concepts varied around the placement of the payload.

Since the conceptual designs for the competition aircraft were based mainly payload and motor location, only two concepts were developed. These concepts are shown in Figures 3.8 and 3.9. Figure 3.8 shows the traditional concept based directly on the prototype. Figure 3.9 shows a variation of the traditional concept using a lifting-body design. By placing the bottles horizontally, it was possible to use the fuselage area as a lifting surface. In addition, this concept provided placement for motors without using wing pods.

3.4.2.2 Conceptual Design Analysis Results

Since the concepts are of similar size and shape the empty weight of each aircraft was assumed to be 9 lbs. The cost estimates for the two concepts are presented in Table 3.7 and the total flight scores are presented in Table 3.8. The initial estimated cost for the traditional concept is 6.04 while the cost for the lifting body is 5.76. The difference between these two costs is only 5%. The reason for this difference in cost and score was the wing pods on the traditional concept.

3.4.2.3 Figures of Merit Results

The FOMs discussed in Section 3.2 were again used to rate the concepts for the competition aircraft. The results of this analysis are presented in Table 3.9. Since the cost of the lifting body concept was slightly lower, it was given a rating of 5 while the traditional concept was given a rating of 4. The complexity of the lifting-body would be much greater than that of the traditional concept and therefore it was rated a 3. Again the traditional concept was not very innovative and given a rating of 1 for that FOM. Since the lifting body was only a variation of the traditional concept was given a rating of only 3. Due to the traditional concept's simplicity, it would be very robust and therefore rated a 5. The lifting body's added complexity and structure would cause it to be less robust and it rated a 4. The shape of the lifting body would make it considerably more difficult to change batteries and operate payload hatches. In addition, transport and repair of the lifting body would be difficult. Therefore, it was given a rating of 3 for ground operations. It was assumed that monetary cost of the competition aircraft was not a factor so this FOM was not considered for the competition aircraft. The results of the FOM analysis were quite close, but the traditional concept had the higher total FOM score of 20. Therefore this concept was chosen for the competition aircraft.

3.4.2.4 Conclusion

Again the major advantages of the simple traditional concept prevailed. This concept was proven during the prototype flight-testing and would make an excellent

competition aircraft. Using the same concept again would make designing the competition aircraft easier than designing an entirely new concept. Most of the analysis done for the prototype could be reused with only minor changes and modifications. Therefore, the competition aircraft could be designed quickly and efficiently leaving a considerable amount of time to flight test the final aircraft before the competition. Although this concept did not have the lowest cost, it had the best overall characteristics required for this competition.

Table 3.1: Figures of Merit for Conceptual Design

Figure of Merit	Ranking		
	5	3	1
Rated Cost/Total Flight Score	Low Cost/High Score	Average Cost/Average Score	High Cost/Low Score
Complexity	Simple	Average	Complex
Innovation	Innovative		Traditional
Robustness	High	Average	Low
Ground Operations	Good/Fast/Easy	Average	Poor/Slow/Difficult
Monetary Cost	Cheap	Reasonable	Expensive

Table 3.2: Prototype Conceptual Final Concept Costs

Component	Concept		
	Traditional	Bi-Plane	Flying Wing
Payload (L)	4	4	4
Payload (lbs)	10	10	10
Battery Weight (lbs)	2.95	2.95	2.95
Empty Weight (lbs)	13.8	15.2	13.8
Full Weight (lbs)	26.7	28.1	26.7
# of wings	1	2	1
b (ft)	7	5.5	7
c (ft)	1.25	1	1.5
Total Wing Area (ft ²)	8.75	11	10.5
AR	5.6	2.8	4.7
# of Pods	1	1	1
Fuse Length (ft)	5	5	3
# of Engines	1	1	1
# of Cells/Engine	23	23	23
# of Propellers	1	1	1
# of servos	7	7	7
Cost	4.90	5.32	4.88

Table 3.3: Prototype Conceptual Final Concept Total Flight Scores

Report Score	90				Traditional	Bi-Plane	Flying Wing			
					Cost					
					4.90	5.32	4.88			
Payload (L)	Loaded Sorties Flight 1	Loaded Sorties Flight 2	Loaded Sorties Flight 3	Total Number of Loaded Sorties in Three Flights	Total Flight Score					
4	2	2	2	6	4409	4062	4427			
4	3	2	2	7	5143	4739	5164			
4	3	3	2	8	5878	5416	5902			
4	3	3	3	9	6613	6093	6640			

Table 3.4: Final Figure of Merit Ranking of Prototype Conceptual Designs

Figure of Merit	Concept		
	Traditional	Biplane	Flying Wing
Rated Cost/Final Score	3	1	5
Complexity	5	4	1
Innovation	1	3	5
Robustness	5	4	2
Ground Operations	5	5	3
Monetary Cost	4	3	3
Totals	23	20	19

Table 3.5: Prototype Payload Sizing Costs

Component						
Payload (L)	3	4	5	6	7	8
Payload (lbs)	7.5	10	12.5	15	17.5	20
Battery Weight (lbs)	2.44	2.95	3.47	3.85	4.49	4.88
Empty Weight (lbs)	10.1	13.8	17.5	21.3	24.8	28.6
Full Weight (lbs)	20.1	26.7	33.4	40.1	46.8	53.5
# of wings	1	1	1	1	1	1
b (ft)	7	7	7	7	7	7
c (ft)	1	1.25	1.5	1.75	2	2.25
Total Wing Area (ft ²)	7	8.75	10.5	12.25	14	15.75
AR	7.0	5.6	4.7	4.0	3.5	3.1
# of Pods	1	1	1	1	1	1
Fuse Length (ft)	5	5	6	6	7	7
# of Engines	1	1	1	1	1	1
# of Cells/Engine	19	23	27	30	35	38
# of Propellers	1	1	1	1	1	1
# of servos	7	7	7	8	8	8
Cost	4.15	4.90	5.73	6.45	7.32	8.02

Table 3.6: Prototype Payload Sizing Total Flight Scores

Report Score		90		Cost						
				4.15	4.90	5.73	6.45	7.32	8.02	
				Payload (L)						
				3	4	5	6	7	8	
Loaded Sorties Flight 1	Loaded Sorties Flight 2	Loaded Sorties Flight 3	Total Number of Loaded Sorties in Three Flights	Total Score						
2	2	2	6	3902	4409	4715	5025	5163	5385	
3	2	2	7	4552	5143	5500	5863	6023	6283	
3	3	2	8	5202	5878	6286	6701	6884	7180	
3	3	3	9	5852	6613	7072	7538	7744	8078	

Table 3.7: Competition Aircraft Concepts Preliminary Costs

Component	Concept	
	Traditional	Lifting Body
Payload (L)	8	8
Payload (lbs)	20	20
Battery Weight (lbs)	4.88	4.88
Empty Weight (lbs)	9.0	9.0
Full Weight (lbs)	33.9	33.9
# of wings	1	1
b (ft)	7	7
c (ft)	1.5	1.5
Total Wing Area (ft ²)	10.5	10.5
AR	4.7	4.7
# of Pods	3	1
Fuse Length (ft)	6.25	6.25
Pod 1 Length (ft)	0.5	0
Pod 2 Length (ft)	0.5	0
# of Engines	2	2
# of Battery Packs	2	2
# of Cells/Engine	19	19
# of Propellers	2	2
# of servos	7	7
Cost	6.04	5.76

Table 3.8: Competition Aircraft Concepts Preliminary Total Flight Scores

Report Score 90					Traditional	Lifting body
					6.04	5.76
Payload (L)	Loaded Sorties Flight 1	Loaded Sorties Flight 2	Loaded Sorties Flight 3	Total Number of Loaded Sorties in Three Flights		
8	2	2	2	6	7152	7500
8	3	2	2	7	8344	8750
8	3	3	2	8	9536	10000
8	3	3	3	9	10728	11250

Table 3.9: Competition Aircraft Concepts Figures of Merit Results

Figure of Merit	Concept	
	Traditional	Lifting Body
Rated Cost/Final Score	4	5
Complexity	5	3
Innovation	1	3
Robustness	5	4
Ground Operations	5	3
Totals	20	18

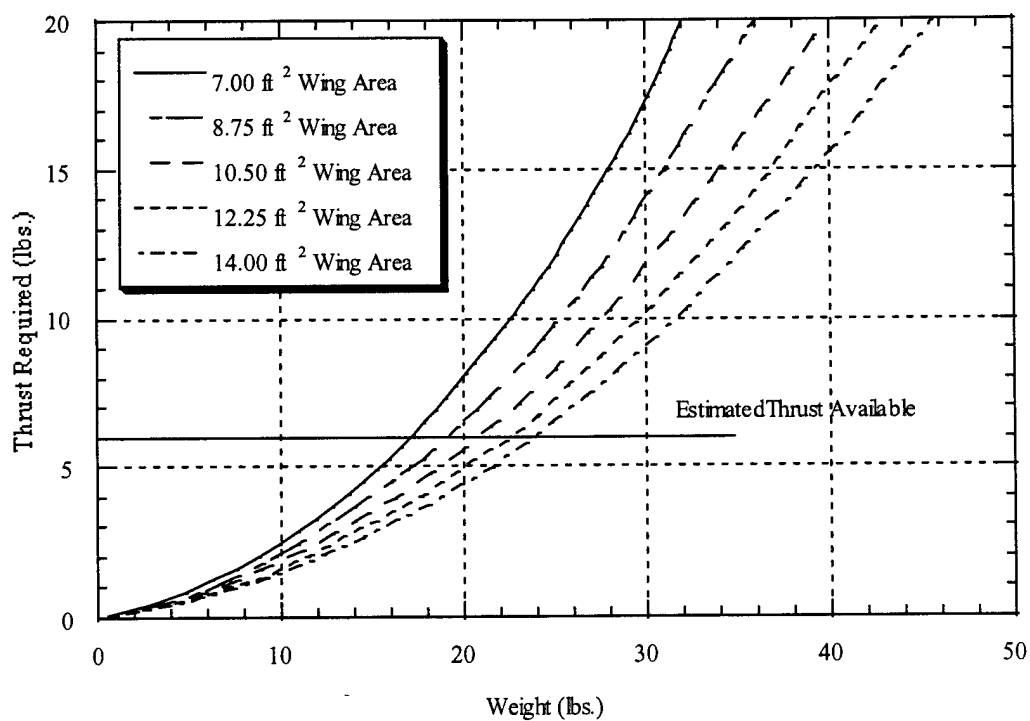


Figure 3.1: Thrust Required for 100 ft Takeoff vs. Total Aircraft Weight (with 0 mph headwind)

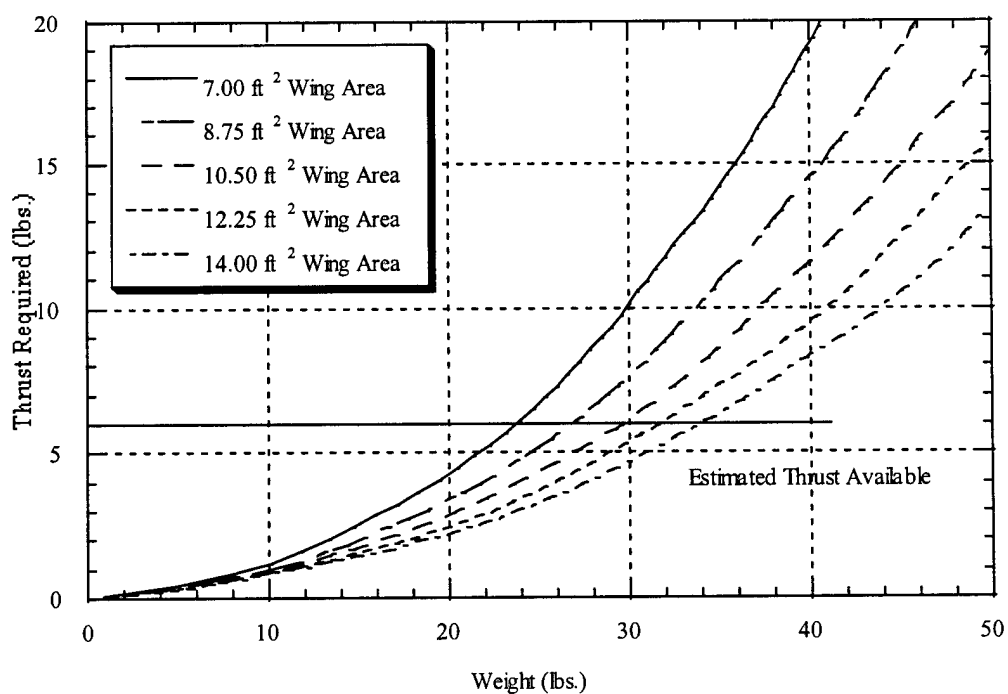


Figure 3.2: Thrust Required for 100 ft Takeoff vs. Total Aircraft Weight (with 10 mph headwind)

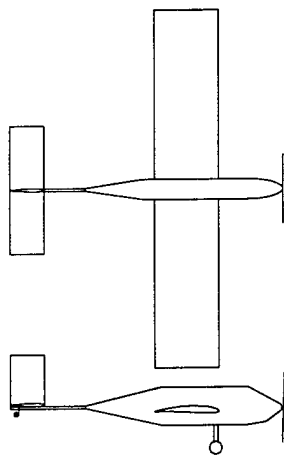


Figure 3.3: Traditional Concept

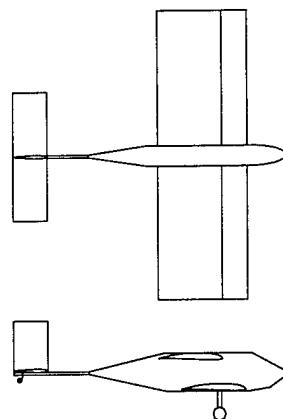


Figure 3.4: Biplane Concept

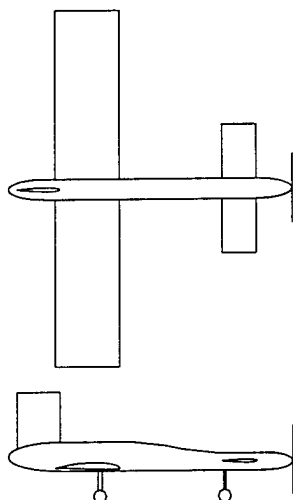


Figure 3.5: Canard Concept

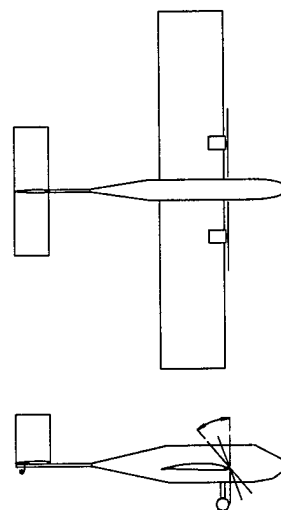


Figure 3.6: Thrust Vectoring Concept

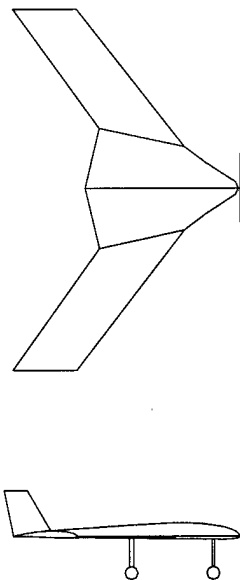


Figure 3.7: Flying Wing Concept

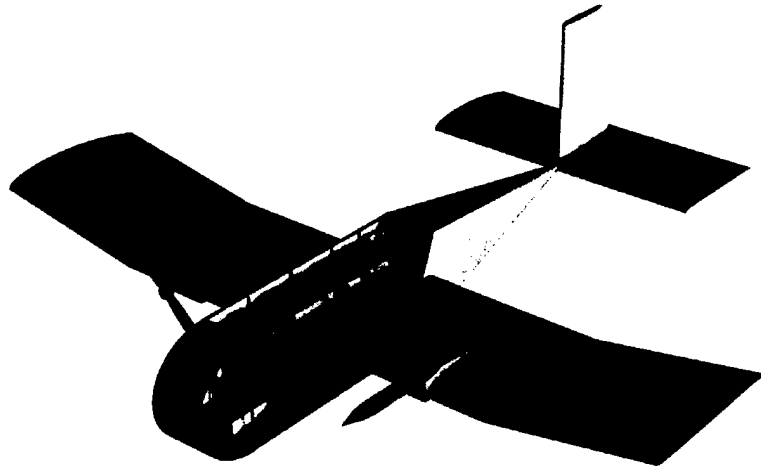


Figure 3.8: Competition Aircraft Traditional Concept

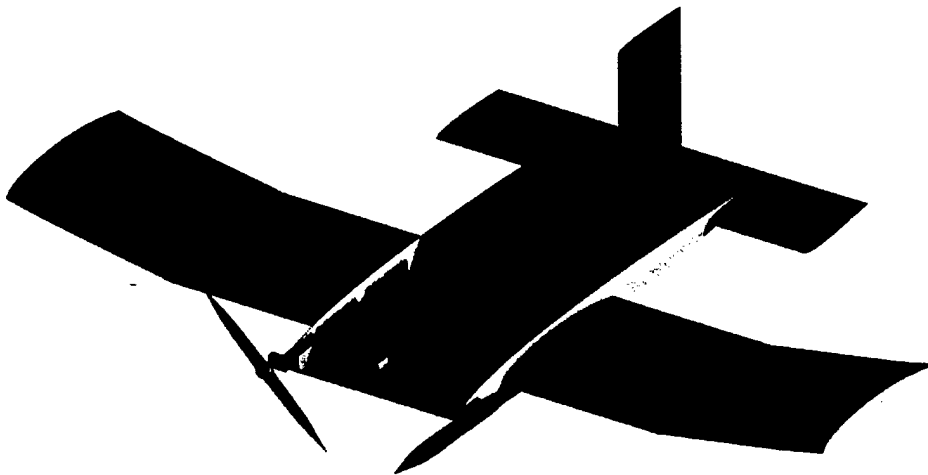


Figure 3.9: Competition Aircraft Lifting Body Concept

4.0 Preliminary Design

4.1 Design Parameters Investigation

The conceptual design work revealed a number of important parameters, affecting the vehicle sizing and performance, that were addressed in the preliminary design. These were:

- Gross weight of the aircraft
- Flight Reynolds numbers
- Payload size for the maximum final score
- Takeoff and lap performance of the aircraft
- Wing and tail size for minimum takeoff distance and stability

Other aspects of design were reserved for the final design.

4.2 Aerodynamics

The wing airfoil selection was largely governed by three major factors: high lift, low parasite drag, and ease of construction. Airfoils were compared at the aircraft's approximate cruise Reynolds number of 640,000. The high maximum lift permits taking off with the most payload in the allowed 100 feet takeoff distance. The low drag aspect provides lower energy usage during cruise and favors a short takeoff distance. The ease of construction factor provides a relatively short building time and lower actual cost. The ease of construction factor eliminated many high-cambered airfoils and those with sharp trailing edges and also led to a search for a simple flat-bottomed profile. This combination of factors reduced the airfoils to the following; Clark-Y, SD7062, SG6042, SG6042, and USNPS-4. The SG6042 was finally chosen because it had a high $C_{l\max}$, a low drag, and would be very easy to build. Figure 4.1 presents the SG6042 profile and aerodynamic performance data taken from Lyon¹.

The governing factors of tail airfoil selection were zero-lift drag, no C_{m_0} , and a moderate thickness required for structural strength and ease of construction. These factors led to selection of the NACA 0009 airfoil for the tail airfoil shape. Figure 4.2 presents the NACA 0009 profile and the aerodynamic performance data taken from Selig².

The coefficient of parasite drag, C_{D_0} , was calculated by summing the approximate the drag coefficients for the fuselage, wing, the horizontal tail, and the vertical tail found using the method in Roskam³, see Table 4.1 for drag breakdown of prototype.

Using the lift-curve for the SG6042 the lift curve for the wing was computed using a team-written lifting line computer program. Using this lift curve the $C_{L\max}$ of the wing is 1.38. The effect of flaps was approximated using the method in Raymer⁴ and resulted in a $C_{L\max}$ of 1.71. Next, the effects of the fuselage on $C_{L\max}$ were calculated using the method in Roskam³ resulting in a $C_{L\max\text{ plane}}$ of 1.3.

4.3 Propulsion System Selection

A brushless MaxCim MaxNEO-13Y DC motor coupled with a MaxCim Max- 35A-25NB speed controller was chosen for multiple reasons. Several comparative studies undertaken in previous years have shown the MaxCim units to be well-suited to the team's needs. As a result, the team already possessed three sets of these units, making them very attractive for use in the prototype. The MaxNEO motor has also proven to be an efficient unit capable of producing the shaft power required. When used with a gearbox, its most efficient operating range can be shifted to meet the speed and power requirements of the aircraft and propeller combination. The gearbox chosen was a SuperBox by Model Electronics Corporation since it is recommended by the motor manufacturer and since the team has successfully used this gearbox in the past.

In the interest of expediency and cost effectiveness, battery packs from previous years were used for the prototype. Thus the battery was a 23 series-cell pack comprised of Sanyo RC2000 cells with approximately 2000 mAh charge capacity. The total energy capacity was approximately 165.6 kJ assuming a constant loaded output voltage of 1 V/cell.

For the selected motor and battery combination, ElectriCalc⁵, was used to provide thrust and power consumption estimates for various propellers. The propeller brand, APC, was chosen due to the success the team has had with these propellers. The ElectriCalc-based propeller diameter/propeller pitch/gear ratio study showed that an APC 14" x 10" propeller in conjunction with a 4.0:1 gear ratio would provide the required 5 lb. of takeoff thrust for the prototype aircraft. In addition, the study showed that the 4.0:1 gear ratio would be flexible enough to provide high efficiency for propeller sizes up to 19" in diameter. This provided the option of studying the performance of various propellers during the prototype aircraft's flight test program.

4.4 Structures

Since it was decided to test a prototype aircraft before building a competition craft, time was a primary consideration. As a result, little structural analysis was carried out on the

prototype design. The prototype's structure was based on team members' experience. The wing, fuselage and tail sections were constructed in classical model airplane fashion to simplify construction and ensure adequate strength. The fuselage consisted of 3/16" sidewalls and 3/16" plywood bulkheads for mounting the motor, wing, landing gear, and tail boom. The tail, with the attached carbon fiber boom, was removable from the fuselage section for ease of transportation.

4.5 Aircraft Weight Build Up

A detailed weight buildup spreadsheet was developed for the prototype aircraft. This was done because of the importance of controlling the aircraft weight and the center-of-gravity location. Weights for some components such as the batteries, motors, and servos, were measured, while other component weights were calculated using densities and volumes of the material. The densities for basswood, balsa wood, and carbon fiber were obtained from MatWeb⁶. Component locations were measured from AutoCAD drawings. The prototype weight buildup and results are presented in Table 4.2. The final empty weight of the aircraft was estimated to be 10.3 lbs with a center of gravity at 26.5% MAC.

4.6 Performance Analyses

The objectives of the performance analyses were to create valid models to accurately predict takeoff performance and energy usage during the flights and time elapsed during the flights. Then, the minimum required thrust and optimal flight plans could be predicted.

4.6.1 Takeoff Analysis

The Mission Profile requires that the aircraft must takeoff within 100 feet. Therefore, a takeoff analysis was carried out to predict the takeoff distance for various combinations of weight, lift, drag, available thrust, and headwind.

A program was written to calculate the takeoff distance, time to takeoff, and velocities during the takeoff roll. A fourth-order Runge-Kutta method was used to solve the equations of motion, taken from Raymer⁴. Experimental and computational analyses provided the models for the thrust as a function of airspeed. Different models for rolling friction were also compared. The parameters used in the preliminary design takeoff analysis are summarized in Table 4.3.

Takeoff distance and time predictions were based on weight, wing area and headwind. Figures 3.1 and 3.2 illustrate the effects of these factors on the required thrust. Table 4.4 shows the predicted takeoff performance for a wing chord of 15 inches. For each headwind and static thrust combination, the maximum weight capable of being lifted off in no more than 100 feet, the actual distance required, the stall velocity, and the time to lift off are calculated for different combinations of $C_{L_{max}}$, static thrust and headwind. Figure 4.3 illustrates the predicted velocities during takeoff for an unloaded plane with $C_{L_{max}}$ of 1.1 in no-wind conditions. The result will be used in the analysis of the flight test data, see section 5.2.4.

To maximize the total score, these results were incorporated with the rated cost analysis. For an assumed available thrust of 5 lb., an initial design point of 15 in. chord, gross takeoff weight of 25 lb. and 10 mph headwind was chosen.

4.6.2 Energy and Time Analyses

Because of the complex interactions between speed, turn characteristics, climb characteristics, weight, energy usage, battery capacity, and time, maximizing the total number of liters carried while reducing cost is not a trivial task. So to maximize the contest score, predictions of the energy usage and time for scoring-type (one lap with a 360^0 turn) and non-scoring-type (two laps with no 360^0 turns) sorties at varying combinations of speed, turn rate, climb rate, thrust and weight were needed.

Because the analysis was completed after the selection of the initial design point for the prototype, it did not influence the design of the prototype. Instead, it was to be used for comparison with the flight testing data to validate the analysis methods. This would facilitate the use of the analysis in the design of the competition aircraft.

The laps were divided into three flight segments: steady-level flight, turning, and climbing. The equations used for the analyses were obtained from Raymer⁴. Analysis programs were written to predict time and energy usage for each of these flight segments for different combinations of thrust, weight, load factors (for turns), and airspeeds. The conditions for minimum energy usage and time for each flight segment and their energy usage and time values were identified. These data were combined to create tables of minimum energy required for scoring and non-scoring sorties with various payload weights and propulsion system thrusts.

For an empty weight of 14 lb., Tables 4.5 & 4.6 show the predicted performance of the prototype when flown at minimum energy usage conditions and minimum time elapsed conditions. However, these analyses did not include the takeoff and the short straight-away segments right after climbing to cruise altitude and right before descent. Including estimated energy usage and time for these segments and the crew time between sorties (see Table 4.7), the estimated flight performance of the prototype is shown in Tables 4.8 & 4.9. With 10 minutes allowed per flight and 166 kJ of energy, flights with 3 or 4 scoring sorties were expected.

4.7 Stability Analyses

Both horizontal and vertical surfaces were sized using volume coefficients and historical data in Raymer⁴. The horizontal and vertical tail sizes resulting from this analysis have been included in Table 4.10. Sizing of the control surfaces was also based on historical data Raymer⁴. A simple longitudinal stability analysis, using Roskam⁷, was performed for the prototype aircraft. The static margin for this aircraft was computed to be 12%, provided that the center of gravity was at 26.5% mean aerodynamic chord.

4.8 Prototype Design Summary

After extensive conceptual design analysis and discussion, the following design parameters' values were found. At a cruise Reynold's number of about 640,000, the SG6042 airfoil was chosen for the wing, while a NACA 0009 airfoil was chosen for the tail. These airfoils produce a $C_{L \max \text{ plane}}$ of 1.3. A MaxCim Max NEO-13Y, brushless DC motor, driving an APC 14" x 10" propellor through a SuperBox gear box with a 4.0:1 ratio was the chosen propulsion system. The motor was coupled with a MaxCim Max-35A-25NB speed controller and attached to a battery pack of 23 series-cells, giving an total energy capacity of 166 kJ and 5 lb of takeoff thrust.

With an expected empty weight of 10.3 lb (which provides a gross takeoff weight of 25 lb) 5 lb of thrust, a 15" cord, and a 10 mph headwind, the prototype can takeoff within the 100 ft requirement. Three or four scoring flight sorties can be expected for the given parameters. With the center of gravity at 26.5% MAC, the prototype has a static margin of 12%.

For the conventional, one motor prototype configuration, the wing, fuselage, and tail were constructed using classical model airplane method. This was to provide adequate structural strength without spending extra time on analysis. For easier travel, a removable carbon fiber tail boom was incorporated. See Fig. 4.4 for prototype aircraft external configuration.

Table 4.1: Prototype Aircraft Parasite Drag Buildup

Component	C_{D0}
Wing	0.0129
Fuselage	0.0100
Horizontal Tail	0.0032
Vertical Tail	0.0019
Total C_{D0}	0.0280

Table 4.2: Prototype Weight Buildup

Component	Weight (lbs)	Distance from Wing LE (in)	Wt. * Dist. (in-lb)
Fuselage			
Spinner	0.15	13.7	2.055
Propeller	0.17	12.58	2.139
Motor	0.59	9.21	5.434
motor mount	0.33	9.2	3.036
Bulkhead #1	0.1157	6.81	0.788
Speed Control	0.206	9	1.854
Battery	3.025	4.47	13.522
Bulkhead #2	0.1157	3.75	0.434
Spar bulkhead	0.14	-4.07	-0.570
Bulkhead #3	0.1157	-12.97	-1.501
Servo battery	0.231	5.35	1.236
Bulkhead #4	0.115	-16.94	-1.948
Bulkhead #5	0.115	-17.34	-1.994
Tail boom	0.284	-29.28	-8.316
Hatch	0.209	-5	-1.045
Tail gear	0.1	-46.625	-4.663
Side panels	0.37935	-6.75	-2.561
Landing gear	0.5	0	0.000
Rails	0.1604	-5.125	-0.822
Wing			
Ribs	0.17553	-4.5	-0.790
Main Spar	0.2808	-4.5	-1.264
Lower Spar	0.1403	-4.5	-0.631
Rear Spars	0.1403	-8.96	-1.257
Edge	0.15	-4.5	-0.675
Trailing Edge	0.15	-10.99	-1.649
Shear Webs	0.0303	-4.9	-0.148
fwd. Sheeting	0.45	-2.25	-1.013
Rear Sheeting	0.3122	-2.08	-0.649
Wing Servos	0.63	-6.25	-3.938
Tail			
Ribs	0.0232	-43.55	-1.010
Main Spar	0.0501	-43.548	-2.182
Rear Spars	0.0125	-45.4325	-0.568
Edge	0.0213	-43.548	-0.928
Trailing Edge	0.0213	-46.9375	-1.000
Sheeting	0.1383	-44.5	-6.154
Vert. Spar	0.0195	-43.548	-0.849
Rear Vert. Spar	0.0049	-45.4325	-0.223
Vert. Edge	0.0083	-43.548	-0.361
Vert. Trailing Edge	0.0083	-46.9375	-0.390
Vert. Sheeting	0.0537	-44.5	-2.390
Boom Rib	0.0459	-43.55	-1.999
Tail Servos (4)	0.425	-43.88	-18.649
Weight (lbs.)			
Payload Weight (lbs.)			10
Weight With Payload (lbs.)			20.34
Payload Fraction			0.492
CG (inches From Wing LE)			3.97
% MGC			26.50

Table 4.3: Prototype Design Takeoff Parameters

Parasitic Drag Coefficient	0.028
Oswald's Efficiency Factor	$1.78 * (1 - 0.045 * AR^{0.68}) - 0.64$
Rolling Drag Coefficient	0.05
Lift Coefficient During Roll	0.75
Span	7 ft
Thrust	$5 * (1 - 0.007 * \text{Airspeed}) \text{ lb}$

Table 4.4: Prototype Takeoff Performance

CLmax	Wind (mph)	Thrust (lb)	W (lb)	Dist (ft)	Vstall (ft/s)	Time (s)
1.2	0	4	14	93	33.5	5.2
		5	16	97	35.9	5.1
		6	17	89	37.0	4.5
		7	19	96	39.1	4.6
	10	4	20	98	40.1	7.3
		5	22	96	42.1	6.6
		6	24	97	43.9	6.2
		7	25	89	44.8	5.5
1.3	0	4	14	85	32.2	5.0
		5	16	88	34.4	4.8
		6	18	93	36.6	4.8
		7	20	99	38.6	4.8
	10	4	21	99	39.4	7.5
		5	23	96	41.4	6.8
		6	25	96	43.1	6.4
		7	27	98	44.7	6.1
1.4	0	4	15	93	32.2	5.4
		5	17	94	34.3	5.2
		6	19	97	36.2	5.0
		7	20	91	37.2	4.6
	10	4	21	87	38.1	7.0
		5	24	96	40.6	7.0
		6	26	95	42.3	6.5
		7	28	97	44.0	6.2

Table 4.5: Prototype Minimum Energy Usage

1 Scoring Sortie Type, Avg. Airspeed 50 ft/s					
Payload (L)	Total Energy (J)	Total Time (s)	%Energy in Climb	%Energy in Cruise	%Energy in Turns
0	5882	55.1	23.1	34.6	42.3
1	7261	50.3	23.9	33.3	42.7
2	8733	51.5	24.8	31.5	43.7
3	10585	48.1	25.5	29.5	45.0
4	12472	45.1	27.1	28.2	44.8
1 Non-Scoring Sortie Type, Avg. Airspeed 50 ft/s					
Payload (L)	Total Energy (J)	Total Time (s)	%Energy in Climb	%Energy in Cruise	%Energy in Turns
0	9956	105.1	13.6	61.4	25.0
1	12099	90.3	14.4	60.0	25.6
2	14229	91.5	15.2	57.9	26.8
3	16831	88.1	16.1	55.7	28.3
4	19496	78.4	17.3	54.0	28.6

Table 4.6: Prototype Minimum Time Elapsed

1 Scoring Sortie Type, Avg. Airspeed 80 ft/s					
Payload (L)	Total Energy (J)	Total Time (s)	%Energy in Climb	%Energy in Cruise	%Energy in Turns
0	11334	28.8	15.6	34.3	50.1
1	12641	29.6	17.1	31.7	51.2
2	14148	30.6	18.5	29.2	52.3
3	15875	31.7	19.8	26.9	53.2
4	17852	33.0	21.1	24.9	54.0
1 Non-Scoring Sortie Type, Avg. Airspeed 80 ft/s					
Payload (L)	Total Energy (J)	Total Time (s)	%Energy in Climb	%Energy in Cruise	%Energy in Turns
0	19120	53.8	9.2	61.1	29.7
1	20647	54.6	10.5	58.2	31.3
2	22412	55.6	11.7	55.3	33.0
3	24431	56.7	12.9	52.5	34.6
4	26738	58.0	14.1	49.9	36.1

Table 4.7: Energy and Time Estimates for Takeoff, Landing and Ground Operations

Takeoff energy (J)	1000
Takeoff + Landing Time (s)	15
Crew Time (s)	30

Table 4.8: Prototype Minimum Energy per Flight

Payload (L)	3 Scoring Sorties		4 Scoring Sorties		5 Scoring Sorties	
	Total Energy(kJ)	Total Time (min)	Total Energy(kJ)	Total Time (min)	Total Energy(kJ)	Total Time (min)
0	42.56	9.5	60.40	13.7	78.23	17.9
1	50.98	8.8	72.34	12.6	93.70	16.5
2	59.66	8.9	84.62	12.8	109.58	16.6
3	70.42	8.6	99.83	12.4	129.25	16.1
4	81.41	8.1	115.38	11.7	149.34	15.2

Table 4.9: Prototype Minimum Time per Flight

Payload (L)	3 Scoring Sorties		4 Scoring Sorties		5 Scoring Sorties	
	Total Energy(kJ)	Total Time (min)	Total Energy(kJ)	Total Time (min)	Total Energy(kJ)	Total Time (min)
0	77.24	6.5	109.70	9.4	142.15	12.2
1	84.22	6.6	119.51	9.5	154.79	12.4
2	92.27	6.6	130.83	9.6	169.39	12.5
3	101.49	6.7	143.79	9.7	186.10	12.7
4	112.03	6.8	158.62	9.9	205.21	12.9

Table 4.10: Prototype Tail Geometry

Tail Attributes	Horizontal	Vertical
Area	240 in ²	96 in ²
Aspect Ratio	3.75	1.5
Taper Ratio	1	1
Airfoil	NACA 00009	
Elevator	25% chord, 40%span	
Rudder	25% chord	
Ailerons	25% chord, 40%span	
Wing MAC	15 in.	
Wing Dihedral	5° on outboard panels	
Veritical Tail MAC	10 in.	
Horizontal Tail MAC	8 in.	
C.G (Measured from L.E.)	5.625 in.	
Neutral Point (Measured from L.E).	7.55 in.	
Static Margin (%)	12%	

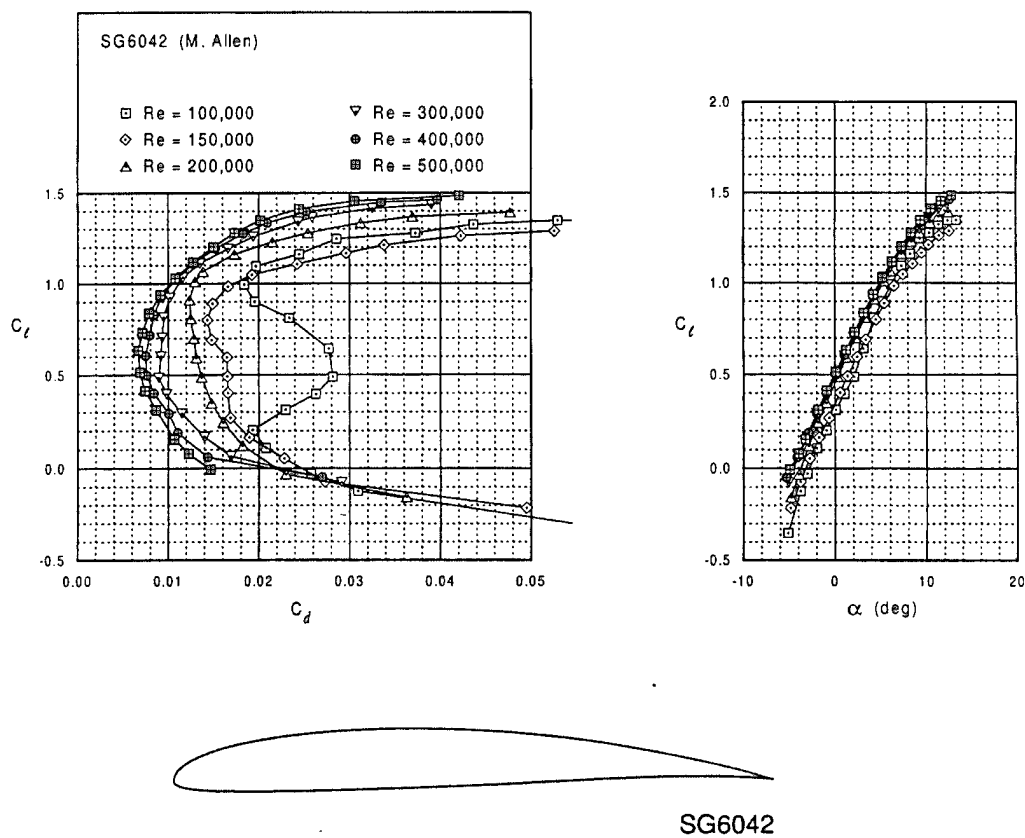


Figure 4.1: Airfoil profile, drag polar and lift and moment curves for SG6042 Ref X (Lyon¹)

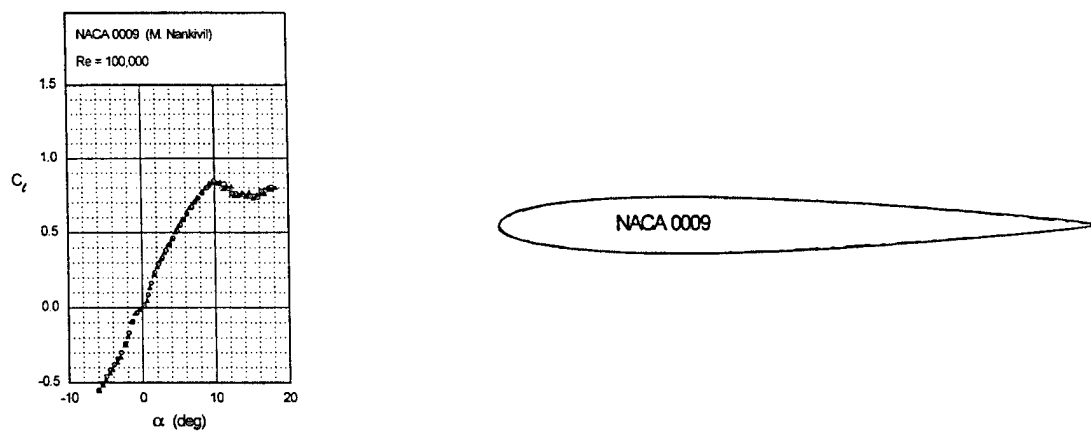


Figure 4.2 Airfoil profile and lift curve for NACA 0009 (Selig²)

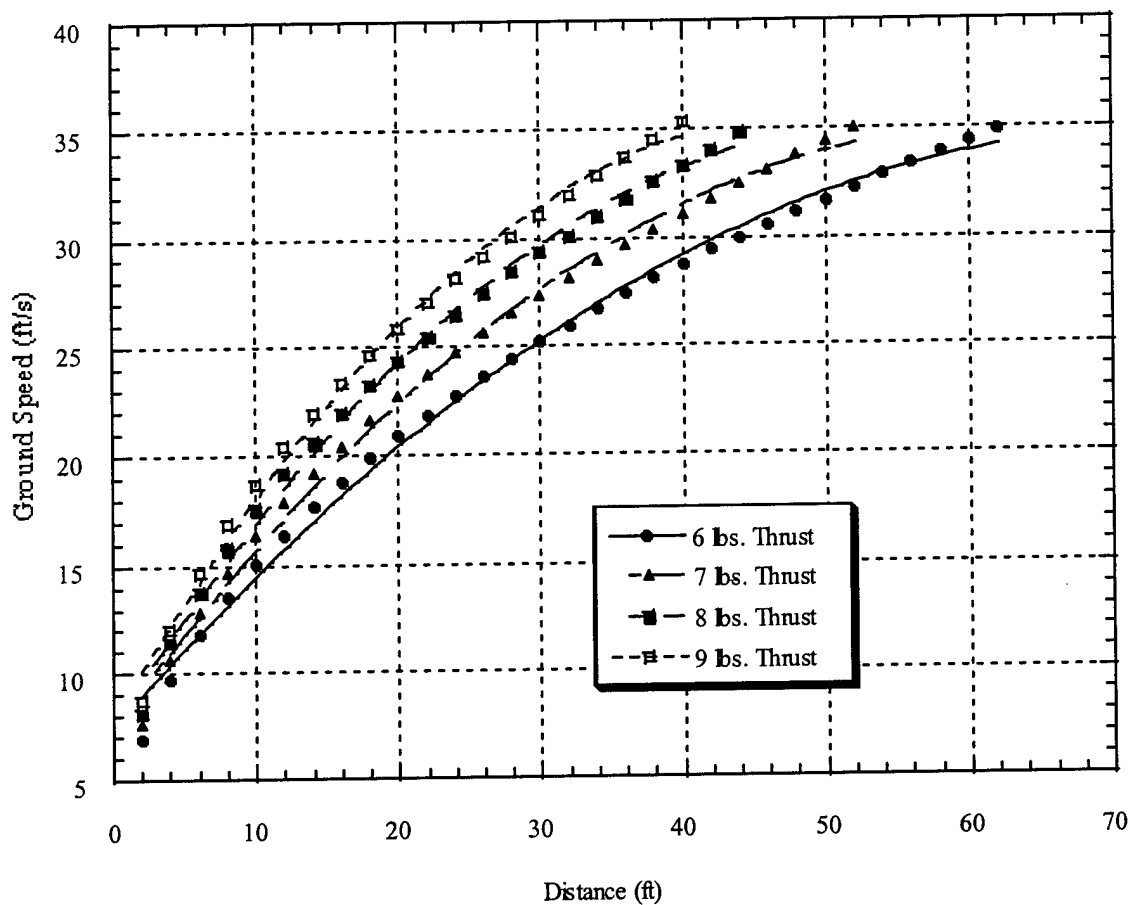
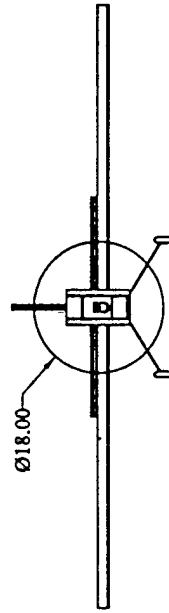
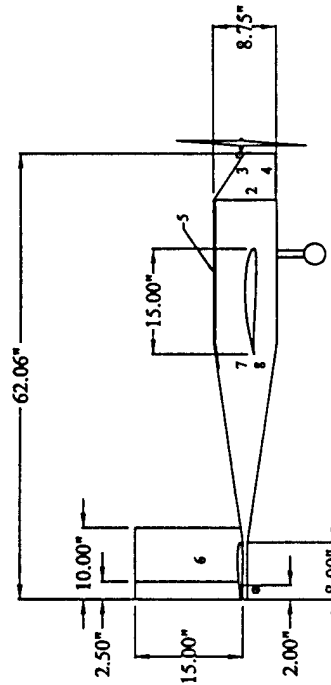
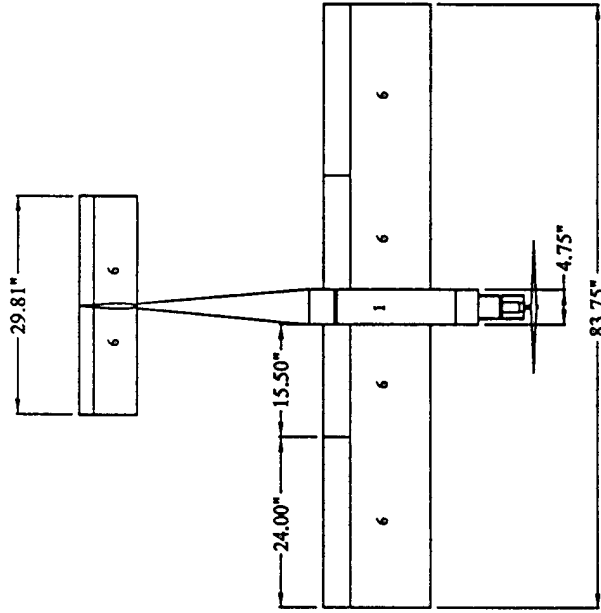


Figure 4.3: Prototype Takeoff Velocities and Liftoff with $C_{L\max} = 1.1$ and 0 mph Headwind

- 1 PAYLOAD
- 2 SPEED CONTROLLER
- 3 BATTERY PACK
- 4 MOTOR
- 5 PAYLOAD HATCH
- 6 SERVO
- 7 RECEIVER
- 8 SERVO BATTERY



5.0 Detailed Design

5.1 Introduction

This section includes all the data collected during flight tests followed by the detailed analyses for the final design, RPP-2, *Hobbes*. Tables and figures of the data collected, calculated, and analyzed can be found at the end of this section along with the drawing package.

5.2 Prototype Aircraft Flight Testing

5.2.1 Objectives

There were four key objectives of flight testing: collect performance data on takeoff performance, sortie time, and energy usage; evaluate stability and control characteristics; familiarize pilot with aircraft flying and handling characteristics and with contest mission profile and flight requirements; and familiarize ground operations team with aircraft servicing and maintenance. The performance data would be used to validate and calibrate the analytical methods used for takeoff and energy studies. Less important objectives included C_{Lmax} determination through stall testing.

5.2.2 Test Site and Instrumentation

Flight tests were conducted on a 1100-ft by 300-ft section of taxiway at the Chanute Air Force Base in Rantoul, Illinois. One hundred forty feet of the taxiway was marked at 10 foot intervals with spray paint. An Astro Flight Super Whatt Meter was installed on the aircraft to measure current (amps), voltage (volts), power (watts), and capacity (milliamp-hours). A Flytec 3005 variometer was used to record maximum rate of climb and maximum altitude. A Hall Windmeter was used to measure wind speed. Two video cameras were used to videotape the flights. On the final day of testing, an additional mini-camera was installed in the aircraft to transmit the Whatt Meter readings in real-time. The transmission was recorded with a VCR.

5.2.3 Procedure

The flight testing crew consisted of: pilot, pilot recorder, turn judges, spotter, timer, recorder, camera operators. The pilot flew the plane while the pilot recorder stood by the pilot to

record verbal reports from the pilot and to notify the pilot of when to turn. Two turn judges were placed 500 feet each way from the starting line to signal passing the upwind and downwind pylons. The spotter, timer, and recorder worked together to identify, time, and record maneuvers (i.e., takeoff, turns, touchdown). The camera operators recorded the flight, with particular attention paid to the takeoff. In addition to maneuver time data, for each flight, time of day, aircraft configuration, flight conditions and test objectives were recorded. Aircraft configuration data included: battery pack, payload, receiver/transmitter voltage, control surface throws, flap settings, throttle setting, propeller, and gear ratio. Figure 5.1 shows a sample data collection sheet.

Stall tests were conducted by flying slowly over the marked runway and watching for stall. This was videotaped.

5.2.4 Results

The pilot became acquainted with the aircraft and skillful at anticipating the aircraft roll and landing the aircraft near the required take off line. Slight roll instability due to a high center of gravity location and landing gear fatigue were problems YRPP-2 had in the first few test flights. These problems were corrected early in the flight testing program.

The time the aircraft reached each 10-foot runway marker was determined from the video tapes. The time between markers was divided by the distance, which yielded an average velocity for that segment. The calculated average speed over each 10-foot segment of runway was averaged for no-wind, unloaded flights at full throttle and 60% throttle. Curve-fits to the takeoff velocities are illustrated in Figure 5.2. Differentiating the curve-fit equations yielded an acceleration curve. By comparing the acceleration and lift-off points to the predicted takeoff performance for different characteristics, it was concluded that the prototype had about 8 pounds of thrust and a $C_{L_{max}}$ of about 1.1 (see Figure 4.3 for predicted performance).

The static motor thrust was also measured. Using two different scales, one test yielded a thrust of 7 pounds and the other yielded about 9 pounds. Although 8 pounds of thrust, as determined above, is higher than originally expected, it agrees with the independent thrust test results of 7 and 9 lbs. A $C_{L_{max}}$ of 1.1 is significantly lower than expected. The stall tests were analyzed to determine stall speed. The average speed was calculated with a procedure similar to the takeoff velocities' analysis. After calculating the stall speed, $C_{L_{max}}$ was calculated to be

about 1.2. These C_{Lmax} values are very similar. Table 5.2 summarizes the prototype's characteristics.

According to the takeoff data, the aircraft took off in about 0.5 seconds less time than predicted for its configuration. This discrepancy is most likely due to the delay in starting the stopwatch when the motor started. So, in fact, the time-to-takeoff predictions are very close. The distance to takeoff tended to be 5 to 10 feet longer than predicted. This is to be expected, however, because the takeoff program calculates the distance to the point where the aircraft reaches its stall speed. In the field, however, the pilot does not know exactly when the aircraft reaches stall speed, nor for safety reasons, does he want the aircraft to lift off at its stall speed. Since the aircraft lifted off typically 5 to 10 feet after its predicted stall speed, it is likely that the distance to stall speed prediction is fairly good. So, in general, the takeoff code was shown to be fairly accurate in its modeling of the takeoff. Therefore, no modifications were made to the program for the analysis of the competition aircraft.

No-wind flight testing data indicated that the aircraft typically flew most of the course at a speed around 80 ft/s, slowing down to about 70 ft/s in the 180-degree turns. The 360-degree turns typically had a radius of 65 ft.

In no-wind conditions, one unloaded, scoring-type sortie used about 32.9 kJ and one unloaded, non-scoring-type sortie used about 47.8 kJ. The lap energy usage in no-wind conditions was two to three times greater than predicted for an average flight speed of 80 ft/s. By comparing flights with 360-deg. turns to flights without them, it was calculated that the 360 deg. turn used an average of 4.0 kJ. This value is almost double the predicted energy use for a 65-ft radius turn at 80 ft/s. To calculate the average energy used in the 1000-ft cruise, energy usage of single and double laps were compared while subtracting out the contribution of the extra turns. The cruise used an average of 7.6 kJ. This is also about twice the expected energy usage to cruise 1000 ft at 80 ft/s. At this point it is unknown how much the takeoff and climb energies differed from the expected values. The energy data are categorized by lap type in Table 5.3.

Although it has not yet been determined why energy analysis predictions are so much less than indicated by the flight data, the predictions can be scaled to predict the performance of the competition aircraft. Flight testing of the competition aircraft may shed light on the discrepancy in energy usage.

In no-wind conditions, one unloaded, scoring sortie type took about 50 seconds from starting up the motor to coming to a stop. One unloaded, non-scoring sortie type took about 90 seconds (see Table 5.1). These times are about 15 seconds greater than predicted. However, this is easily understood. The takeoff time was originally estimated to be about 5 seconds. Takeoff times, in fact, varied from about 4.5 - 6.5 seconds. The landing time was predicted to be about 10 seconds. The final approach is about that long, but including the rollout, the landing time is about 17 seconds. In addition, the analysis did not take into account the reduction in power during the last turn onto final approach necessary in order to stop at the starting line. Therefore, the last turn takes much longer than expected. This last turn usually takes about 10 seconds (as opposed to the estimated 3 seconds). Taking these corrections into account, the analytical time predictions are fairly close for an average flight speed of 80 ft/s.

The 23-cell battery packs produced about 160 kJ of energy during the flight testing. Although the packs were not exhausted after this point, there was too little energy to continue flying. This agrees well with the initial prediction of 166 kJ of available energy.

5.3 Aerodynamics

Since the competition plane configuration was changed from the prototype design to include two engines, as well as other components, the drag breakdown and maximum lift coefficient changed. During the testing of the prototype, the airfoils selected for the wing and the tail proved to be more than adequate to meet the requirements for the competition. Therefore, the same airfoils will be used on the competition plane. The C_{D_0} for the competition plane is 0.035 an increase of 20.09% from the prototype and seen in Table 5.4. The new $C_{L \text{ max plane}}$ of 1.25 was computed using the same method as described in section 4.2.

5.4 Propulsion

The flight-testing validated the efficiency and high performance of the prototype's motor and speed controller pair. Therefore, the MaxNEO - 13Y and MaxCim 35A - 25NB were chosen for the twin-motored competition aircraft as well. Flight testing had revealed the APC 18" x 8" propeller in conjunction with a 4.0:1 gear ratio to have good takeoff and partial-throttle cruise thrust. To maintain this performance, each motor needed sufficient voltage to produce the required thrust. Simulation with MotoCalc⁸ indicated that 19 cells for each motor provided sufficient takeoff thrust. Results from these MotoCalc studies, which varied propeller size and

throttle level, are included as Figs. 5.3 – 5.5. Figure 5.5 shows that the 18" x 8" propeller configuration has a maximum thrust of approximately 7.5 lb per motor.

Commonly available cells with the highest charge capacity-to-weight ratio were sought to minimize battery weight. Of the Ni-Cd cell types immediately available, the Sanyo RC2000 models featured the highest capacity-to-weight ratio at 1075.3 mAh/oz with a cell capacity of 2000 mAh. As of this writing, a new 2400 mAh cell model with the same dimensions and only 0.04 oz heavier than the RC2000 cell had been announced by Sanyo and other Ni-Cd cell manufacturers. These parameters lead to a superior charge capacity-to-weight ratio for the 2400 mAh cell. However, the new cells are not expected to be generally available by the time flight testing begins for the competition aircraft. Each battery pack will therefore consist of 19 Sanyo RC2000 cells in series so that the overall pack charge capacity is 2000 mAh with the combined voltage of 19 cells. The energy capacity of each pack will be 136.8 kJ, for a total energy capacity of 273.6 kJ between both packs. Each motor will be connected to its own independent 19-cell battery pack to avoid the destructive interference of a parallel pack configuration during discharge.

In order to ensure that 2000 mAh was sufficient capacity, MotoCalc⁸ was also used to find steady-state run duration figures for various throttle settings for airspeeds from 20 to 50 ft/s. These results are presented as Fig. 5.6. Based on the results, partial throttle run-times of greater than 15 min. for steady flight can be observed for cruise thrusts greater than 1.5 lb. These trends suggest that with the use of a partial-throttle strategy, the dual motor design will be able to efficiently cruise while providing acceptable runtime with RC2000 cells.

The propulsion system configuration for the competition aircraft is not frozen. Experience has taught the team that the best way to select a final propulsion configuration is from flight-testing data. Consequently, the competition twin-motor aircraft will be flight tested to determine such parameters as: excess thrust at takeoff, partial-throttle sortie energy consumption, and partial-throttle sortie time. As a result of the testing, the battery and propeller selections may change. MotoCalc studies show that a reduced cell count results in less thrust (see Figs. 5.3 – 5.5). However, it is desirable to eliminate cells from the battery packs in order to reduce rated cost. Thus the final objectives in optimizing the propulsion system will be to determine the fewest number of cells with which the aircraft can still operate efficiently and in compliance with the contest performance requirements.

5.5 Structures

5.5.1 Major Changes From Prototype

As a result of the decision to design for eight liters of water, the competition plane is significantly different than the prototype. First, two motors will be used; one will be mounted on each wing rather than one centrally located motor. For transportation purposes, the tail boom on the prototype was removable. For the competition plane, the wings are detachable. In addition, there are significant structural differences between the two planes.

Although the prototype was designed and constructed without close attention to the airframe strength, flight testing and static loading proved that the structure was stronger than needed. Removing excess structural weight became a priority for the competition aircraft. In addition, the increase in payload for the competition plane made reducing structural weight even more important.

In order to lighten the structure, a new spar configuration utilizing high strength carbon fiber bars and a lightweight balsa shear web, was introduced. The resulting wing was estimated to weight 1.51 lb. without the motors and their associated structure, a 38% decrease from the 2.46 lb. prototype wing. Additional changes to the structure included using 1/8" plywood rather than 3/16" balsa fuselage sides. The plywood supplied increased strength for the larger payload and, with large lightening holes, weighed 0.52 lbs., as compared to 0.38 lbs. for the balsa used on the prototype. The load paths were studied in order to decrease the number of heavy bulkheads required. While the prototype had six bulkheads in the main fuselage section, the design for the competition plane reduced that number to three. In addition the bulkheads were made of 1/8" instead of 3/16" plywood. The resulting fuselage weighs, without batteries, 2.6 lbs., which is much less than the prototype body's weight of 4.0 lbs.

The structural design of the aft fuselage was also modified. Replacing the prototype's carbon fiber boom with a truss structure served a threefold purpose. First, the truss eliminated the need for multiple boom mounting bulkheads in the fuselage thus saving weight. Secondly, it provided a rigid structure to prevent torsion in the tail. Finally, it saved money by utilizing cheaper building materials. The truss structure weighs 0.39 lbs., while the carbon fiber boom method weighed at least 0.51 lbs., largely because of the associated extra bulkheads and aluminum tube. The tail itself was modified to decrease its weight by eliminating the spars and

increasing the size of the leading and trailing edges. The overall weight saving in the tail is estimated to be approximately 0.34 lbs.

5.5.2 Structural Modeling and Results

With the decrease in structural weight, much analysis was performed to ensure the airframe could withstand worst case flying conditions. To accommodate the heavier payload planned for the competition plane, the wing is required to hold a minimum of 61.25 ft-lb moment at the wing root simulating the structural verification as stated in the contest rules. The analysis of the I-beam spar showed that the wing was strong enough to support a 130-lb. total aircraft weight holding the aircraft by the wing tips. Table 5.5 shows that the balsa shear web is the limiting factor, failure in shearing the balsa would occur before the carbon fiber fractured. The tail boom truss was analyzed using ANSYS FEA⁹ software to verify that the maximum allowable tail load of 15 lbs. Simple calculations for the tail strength were also made to verify that the changes from the prototype do not jeopardize strength.

5.5.4 Final Structure

The structure of the competition aircraft meets the key design parameters: strength, light weight, ease of construct, and readily available materials. Although various materials were investigated early in the project, the results indicated a combination of balsa, basswood, and plywood would provide the optimum strength/weight characteristics. Foam and fiberglass would have been more difficult to use. Although, in many instances, they would be stronger, careful design with balsa, bass and plywood provided sufficient strength and less weight.

5.5.6 g-Load Capability

A V-n diagram for the competition plane is presented in Fig. 5.7. Under maximum load conditions and based on the wing strength, the positive limit load factor is 3.7, while the plane is capable of a negative limit load factor of -2.0. The stall speed is calculated to be 46 ft/s, the maneuver or cruise speed is 80 ft/s, and the dive speed is 112 ft/s.

5.6 Ground Operations

As a result of the test flights of the prototype aircraft, it became apparent that ground-handling time would be significant portion of the flight time. The payload placement and hatches have been designed to be quickly accessible to the ground crew. Therefore the bottles are attached directly to the top of the hatches and are removed as one piece. In addition, the hatches have been designed to allow a variation in payload from two to eight liters. This allows the plane to fly with payload less than the maximum.

5.7 Final Weights and Balance

One of the intended purposes of the prototype was to learn more about the structure and the accuracy of weight estimates. After weighing the completed prototype, it was disappointing to learn that the weight estimate was several pounds under the actual weight, and the CG was several inches behind the calculated point. Investigation of the discrepancies revealed that several changes made during construction had not been accounted for on the drawings or in the weight spreadsheet. In addition, the actual weights of the materials used, i.e., balsa, basswood, and plywood, were heavier than the values found in MatWeb⁶. The prototype highlighted the importance of detailed drawings and communication among the individual groups involved in design and building.

The final predictions for the competition plane's weight and balancing point were carried out with particular attention to details and accuracy. In particular, the densities of the construction materials were measured. Because many of the parts were laser cut, the estimates should be much more accurate and fewer changes should occur during construction. The weights determined from the analysis indicate a significant success in reducing weight. The wing weighs almost a full pound less than the prototype. The total weight of the plane, including batteries and motors, is expected to be approximately 12.5 lbs., less than the prototype even though it has two motors and twice the battery power. The weight buildup can be seen in Table 5.6.

5.8 Performance Analyses

5.8.1 Takeoff Analysis

The competition aircraft will have an estimated thrust of 16 pounds, a wing area of 10.5 ft², a $C_{L_{max}}$ of 1.1 and an empty weight of 12.5 lb. Using the maximum available thrust, at the design point of 10 mph headwind, the aircraft should be able to lift 10 L in 100 feet. In no-wind conditions, the aircraft should be able to lift 7 liters. The expected takeoff performance is tabulated in Table 5.7 for a range of thrusts and headwinds.

5.8.2 Energy and Time Analyses

The energy usage and time predictions for the competition aircraft are presented in Tables 5.8 – 5.10. This includes the corrections to the time and a scaling of the energy usage by two, as suggested by the flight tests of the prototype. It also includes an estimated crew time between flights of 30 seconds. Based on these predictions and 273.6 kJ of available energy, four scoring sorties can be expected for payloads up to 7 liters. With 8 liters, only 3 sorties can be expected. One important thing to note, however, is that the energy analysis is done for a no-wind case. With no wind, the aircraft cannot takeoff with 8 liters. No analysis has been done to estimate the effects of wind on energy usage.

5.9 Stability and Control Analysis

Stability analysis of the RPP-2 was completed using methods found in Raymer⁴ and Roskom⁷. Unlike the prototype's tail sizing, which was based on historical data, the competition aircraft was sized based on stability and control analyses. Final stability values of $C_{m\alpha}$, $C_{n\beta}$, and $C_{l\beta}$ are -0.517 rad^{-1} , 0.633 rad^{-1} , and -0.132 rad^{-1} respectively, indicating a stable aircraft. RPP-2 has a static margin of 12.94%. Table 5.11 list final design values for RPP-2 along with stabilizer and control surface sizing. Control surface percentages were kept unchanged except for the rudder, which was increased to 30 percent. Pilot ratings of YPP-2 and OEI concerns prescribed the substantial increased in the rudder and vertical stabilizer area.

Analyses of trim conditions for longitudinal and lateral are summarized in Figs. 5.9 and 5.10 respectively. Because this is a twin motor design, OEI conditions were of particular interest and are satisfied for side slip angles up to 6° (full rudder and throttle).

Dynamic flying quality results are inconclusive. Quantitative analyses of cargo configurations were completed with the use of Unigraphics. Figure 5.11 summarizes the effects on the moments of inertia for five proposed cargo configurations. Driving factors such as minimizing I_{yy} and frontal area dictated configuration three.

5.10 Final Design Summary

Flight-testing gave not only qualitative, but also quantitative results. After evaluating the differences to the theory and their causes, the final performance predictions could be more accurately estimated. After extensive flight testing, the handling qualities of the aircraft have been optimized for the competition specifications as well as the pilot specifications.

The payload fraction for the competition plane is 20/35. The biggest change from the prototype to the competition plane is the addition of another motor. Now, there will be wing-mounted motors. The wings will be removable, instead of the tail. Also, the rudder was increased to 30% MAC of the vertical tail.

The competition plane will have two large compartments for the bottles. The bottles will be directly attached to the top fuselage hatches for quick payload exchange. Figures 5.12 and 5.13 show external and internal configurations of the competition aircraft.

The structural weight of the competition plane was estimated to be 1.5 lbs. lighter than the prototype. Balsa shear web and carbon fiber are the main building materials. While the prototype had six bulkheads, the new design has three. The new design also uses 1/8" plywood instead of 3/16". The tail boom was changed from a carbon fiber rod to an truss structure.

The wing was thoroughly analyzed to prove it could withstand a 61.25 ft-lb bending moment. The tail boom can support at least 15 lbs. The limiting structural factor of the aircraft is the wing's balsa shear web. The final structure meets the key design parameters of strength, light weight, easy construction, available materials, and low cost. Figures 5.14 and 5.15 show isometric views of the shaded aircraft and the aircraft structures.

Performance analyses for takeoff and energy showed the aircraft could lift a 7 Liter payload with zero headwind and more than the 8 Liter payload maximum payload with 10 mph headwind. Also, with a 7 Liter payload or less, the team can expect to complete 4 scoring sorties and 3 scoring sorties for an 8 Liter payload.

Stability and control analysis shows a stable aircraft with a static margin of 12.9% MAC.

Table 5.1: Flight Test Data

Sortie #	Date	Battery pack	#of cells	Payload	Prop.	Flight Time (s)	Voltage (V)	Charge Used (amp-hrs)	Takeoff Throttle settings	Objectives/Notes
1	13-Nov	Y-1	23	0	16-12	49.30	38.60	0.381	100%	check stability
2	13-Nov	Y-1	23	0	16-12	47.10		0.711	100%	check flap to elevator mix
3	13-Nov	Y-1	23	0	16-12	61.10	29.40	0.958	100%	check flap to elevator mix
4	13-Nov	Y-1	23	0	16-12	50.00	28.90	1.238	100%	check flap to elevator mix
5	13-Nov	Y-1	23	5 lbs lead	16-12	80.00	28.40	1.570	100%	try loaded flaps at 60
6	13-Nov	Y-2	23	0	16-12	XXX	32.50	0.213	100%	try to TO fully loaded >100ft
7	13-Nov	Y-2	23	7.5	16-12	65.00	30.10	0.684	100%	try 7.5 lb payload
8	13-Nov	Y-2	23	7.5	16-12	51.50	29.60	1.050	100%	try 7.5 lb payload TO difficult <100
9	13-Nov	Y-2	23	0	16-12	XXX	29.10	1.709	100%	unloaded stall speed testing
10	13-Nov	Y-2	23	0	16-12	XXX	28.20	1.894	100%	unloaded stall speed testing
11	13-Nov	Y-1	23	0	16-12	50.00	31.50	0.350	100%	Varenometer reading
12	13-Nov	Y-1	23	0	16-12	47.30	29.90	0.714	100%	lap w/ circle to determine diameter
13	13-Nov	Y-1	23	0	16-12	50.00	29.50	1.094	100%	lap w/ circle to determine diameter
14	13-Nov	Y-1	23	0	16-12	64.00	29.20	1.706	100%	2 laps
15	13-Nov	Y-1	23	0	16-12	XXX	28.1	2.053	100%	2 laps planned ran low on energy abort flight
16	13-Nov	blue	19	0	16-12	42.27	26.8	0.275	100%	try 19 cell 1 lap w/o circle
17	13-Nov	blue	19	0	16-12	52.96	24.5	0.596	100%	lap w/ circle to determine diameter
18	13-Nov	blue	19	0	16-12	53.58	24.4	0.929	100%	lap w/ circle to determine diameter
19	13-Nov	blue	19	0	16-10	85.88	24.2	1.484	100%	1 lap planned turbulence caused abort flight
1	20-Nov	Y-2	23	0	18-8	XXX	32.5	0.311		TO 1 lap stall speed. Land unflapped TO flapped land
2	20-Nov	Y-2	23	0	18-8	47.91	29.4	0.579		will power down 50% downleg
3	20-Nov	Y-2	23	0	18-8	XXX	23.9	0.843		will power down 40% downleg
4	20-Nov	Y-2	23	0	18-8	58.61	29.3	1.084		will power down 40% downleg
5	20-Nov	Y-2	23	0	18-8	58.43	29	1.308		will power down 40% downleg
6	20-Nov	Y-2	23	0	18-8	101.52	28.9	1.683		will power down 50% downleg 2nd turn 70%
7	20-Nov	Y-1	23	0	18-8	85.05	32.4	0.433		unloaded 2 circuits 60% upwind 50% downwind power out in last turn
***	***	***	***	***	***	***	***	***	***	TO energy analysis
8	20-Nov	Y-1	23	0	18-8	5.46	29.6	0.500		TO analysis full
9	20-Nov	Y-1	23	0	18-8	5.82	29.7	0.555	60%	60% throttle
10	20-Nov	Y-1	23	0	18-8	6.71	29.6	0.609	60%	60% throttle
11	20-Nov	Y-1	23	0	18-8	6.79	29.6	0.675	60%	60% throttle
12	20-Nov	Y-1	23	0	18-8	6.21	29.6	0.728	60%	60% throttle
13	20-Nov	Y-1	23	0	18-8	5.85	29.6	0.784	60%	60% throttle
14	20-Nov	Y-1	23	0	18-8		29.6	1.166		test tip stall
15	20-Nov	Y-1	23	0	18-8		29.2	1.228		TO analysis 60% throttle couldn't flair broke prop
16	20-Nov	Y-2	23	5	18-8 W	62.66	31.7	0.505		gear box slid on run up thru prop
17	20-Nov	Y-2	23	0	18-8	6.55	29.7	0.642		1 lap loaded
18	20-Nov	Y-2	23	0	18-8	7.14	29.7	0.740		loaded couldn't flair on landing bent shaft
1	21-Nov	Y-1	23	0	18-8	89.62	32.5	0.401		2 circuits 60% power
2	21-Nov	Y-1	23	0	18-8	193.82	29.5	1.482		low passes for tape
3	21-Nov	Y-1	23	0	18-8	63.28	28.5	1.791	60%	60% TO with lap full throttle
4-abort	21-Nov	Y-1	23	0	18-5	0		0		sheered off gear box and prop
4	21-Nov	Y-2	23	5lb steel	18-8	62.02	30	0.492		less power after 360
5	21-Nov	Y-2	23	5lb steel	18-8	65.8	29.6	0.831		less power after 360
6	21-Nov	Y-2	23	5lb steel	18-8	69.05	29	1.181		80% on downwind
7	21-Nov	Y-2	23	5lb steel	18-8	57.81	28.5	1.46		80% on downwind
8	21-Nov	Y-2	23	5lb steel	18-8	5.05	25.6	1.578		ran out of power abort flight bent shaft on landing
9	21-Nov	Y-1	23	10lb water	18-8	70.34	32.2	0.515		full power in turns 80% first down wind 60% 2nd down wind 90% in 360
10	21-Nov	Y-1	23	10lb water	18-8	73.23	29.7	1.012		full power in turns 80% first down wind 60% 2nd down wind 90% in 360 50% after last turn
11	21-Nov	Y-1	23	0	18-8	96	29.2	1.384	60%	2 laps no 360 60% TO 50% upwind 40% down wind
12	21-Nov	Y-1	23	0	18-8	102.85	28.9	1.761	60%	2 laps no 360 60% TO 50% upwind downwind and up wind and out of turn 100% throttle to ground
13	21-Nov	Y-2	23	10lb water	18-8	55.5	32.5	0.353		full throttle 60% down wind
14	21-Nov	Y-2	23	10lb water	18-8	51.75	29.8	0.682		full throttle 60% down wind
15	21-Nov	Y-2	23	10lb water	18-8	50.37	29.4	1.047		full throttle 60% down wind
1	4-Dec	Y-2	23	1lb camera	18-8	65.03		0.559	60%	60% TO 2 laps no circle
2	4-Dec	Y-2	23	1lb camera	18-8	98.47		0.97	60%	60% TO 2 laps no circle
3	4-Dec	Y-2	23	1lb camera	18-8	125.57		1.471	60%	60% TO 2 laps no circle
4	4-Dec	Y-1	23	5lb lead 1 lb camera	18-8	66.14	31.9	0.546		1 lap 1 circle full throttle
5	4-Dec	Y-1	23	5lb lead 1 lb camera	18-8	68	29.5	0.74		less power on TO 1 lap 1 circle full throttle
6	4-Dec	Y-1	23	5lb lead 1 lb camera	18-8	65.7	28.6	1.122		less power on TO 1 lap 1 circle full throttle
7	4-Dec	Y-1	23	5lb lead 1 lb camera	18-8	51.23	28.8	1.392		less power on TO 1 lap 1 circle full throttle
8	4-Dec	Y-2	23	10lb lead 1 lb camera	18-8	71	32.5	0.486		less power on TO 1 lap 1 circle full throttle
9	4-Dec	Y-2	23	10lb lead 1 lb camera	18-8	65.03	29.8	0.991		radio hard hit
10	4-Dec	Y-2	23	10lb lead 1 lb camera	18-8	76.03	29.5	1.547		radio hard hit
11	4-Dec	blue	19	5lb lead 1 lb camera	18-8	XXX		XXX		camera doesn't work didn't take off

Table 5.2: Prototype Characteristics

Empty Weight (lb)	14
Thrust (lb)	8 +/- 1
CLmax	1.1 +/- 0.1
CLroll	0.75
CD0	0.028 +/- 0.005
CDroll	0.05

Table 5.3: Prototype Energy Usage Summary

Wind (mph)	Payload (lb)	AVERAGE ENERGY USAGE (kJ)					
		1 Lap - No Turn	1 Lap - 360° Turn	Difference	2 Laps - No Turn	2 Laps - 360° Turn	Difference
0	0	28.6	32.9	4.3	47.8		
	5	31.1	36.1	5.0			
10	0				38.5		
	1				43.1	49.9	6.8
	10		52.6				
15	6		39.7				
	11		55.3				

Table 5.4: RPP-2 Parasite Drag Buildup

Component	C _{D0}
Wing	0.0117
Fuselage	0.0160
Horizontal Tail	0.0036
Vertical Tail	0.0024
Landing Gear	0.0014
Total	0.0352

Table 5.5: Wing Maximum Load Capability

Material	Failure Mechanism (Total aircraft weight when lifting aircraft by the wing tips)	
	Bending (lbs)	Shear (lbs)
Carbon Fiber	304.0	14259.22
Balsa	400.0	131.20

Table 5.6: RPP-2 Weight Buildup

ITEM	Unit Wt. (lbs)	Qty.	Total Wt. (lbs)	Dist From Ref Point (in)	WT * DIST (lbs-in)
Fuselage					
Bulkhead #1	0.07344	1	0.0734	30	2.2031
Bulkhead #2	0.08415	2	0.1683	40	6.7319
Bulkhead #3	0.04903	1	0.0490	50	2.4516
Bulkhead #4	0.03223	1	0.0322	58	1.8692
Bulkhead #5	0.02437	1	0.0244	66	1.6082
Bulkhead #6	0.01681	1	0.0168	74	1.2441
Bulkhead #7	0.00837	1	0.0084	81.75	0.6840
Battery	0.1315	38	4.9970	29.25	146.1623
Receiver	0.14	1	0.1400	51.25	7.1750
Servo battery	0.231	1	0.2310	51.25	11.8388
Top Tail stringers	0.06610	2	0.1322	73.5716	9.7260
Bottom Tail stringers	0.03350	2	0.0670	73.5716	4.9291
Truss-- Top/Bot. Section 1	0.00277	4	0.0111	53.8125	0.5957
Truss-- Top/Bot. Section 2	0.00254	4	0.0102	61.75	0.6278
Truss-- Top/Bot. Section 3	0.00230	4	0.0092	69.875	0.6427
Truss-- Top/Bot. Section 4	0.00206	4	0.0082	77.75	0.6396
Truss-- Side Section 1	0.00275	4	0.0110	53.8125	0.5915
Truss-- Side Section 2	0.00268	4	0.0107	61.75	0.6628
Truss-- Side Section 3	0.00241	4	0.0097	69.875	0.6748
Truss-- Side Section 4	0.00211	4	0.0085	77.75	0.6570
Balsa Vertical	0.00028	50.75	0.0140	60.75	0.8531
Last Balsa Section	0.00809	2	0.0162	84.6	1.3696
Servo-- Tail Gear	0.159	1	0.1590	70.625	11.2294
Servo-- Rudder	0.159	1	0.1590	70.625	11.2294
Servo-- Elevator	0.159	1	0.1590	70.625	11.2294
Side Panels	0.259	2	0.5179	41.9537	21.7259
Landing gear	0.3	1	0.3000	35	10.5000
Top Rails	0.05769	2	0.1154	34.4818	3.9783
Bottom Rails	0.02909	2	0.0582	34.6251	2.0148
8" CF for Wing Junction	0.02836	2	0.0567	34.6251	1.9639
Basswood 7" strip	0.01225	2	0.0245	34.6251	0.8483
Fuselage Total Weight (lbs)			7.5981		
Wing					
Motor	0.59	2	1.1800	31.54	37.2172
Speed Control	0.206	2	0.4120	38	15.6560
Spinner	0.0625	2	0.1250	29.25	3.6563
Propeller	0.13	2	0.2600	29.25	7.6050
Ribs	0.00558	16	0.0893	40	3.5740
CF Spar	0.04254	14	0.5956	40	23.8224
Balsa Shear Web	0.00926	7	0.0648	40	2.5924
Motor Mount Side A	0.01956	2	0.0391	35.9787	1.4077
Motor Mount Side B	0.01420	2	0.0284	36.1992	1.0279
Motor Mount Side C	0.01958	2	0.0392	35.9796	1.4091
Motor Mount Side D	0.01418	2	0.0284	36.205	1.0267
Motor Mount Side E	0.02014	4	0.0805	32.6067	2.6263
Servos	0.159	4	0.6360	45	28.6200
Sheeting	0.00830	7	0.0581	34.8302	2.0238
Trailing edge	0.00498	14	0.0697	48.1	3.3539
Wing Total Weight			3.7061		
Tail					
Vertical Rib	0.00201	6	0.0121	85.7	1.0349
Vertical Leading Edge	0.00024	15.9375	0.0039	80.8	0.3122
Vertical Trailing Edge	0.00147	15	0.0221	90	1.9848
Horizontal Rib	0.00134	12	0.0161	86.2026	1.3840
Horizontal Leading Edge	0.00022	30	0.0066	82.1	0.5422
Horizontal Trailing Edge	0.00125	30	0.0375	89.0134	3.3398
Extra Weight Added	0	1	0.0000	81	0.0000
Sheeting	0.084	1	0.0840	86.2026	7.2410
Tail Mounting Piece	0.20093	2	0.4019	84.8737	34.1072
Tail Gear	0.1	1	0.1000	89.6	8.9600
Tail Total Weight (lbs)			0.6840		
Weight Without Payload (lbs)					11.99
Payload Weight (lbs)					20.00
Weight With Payload (lbs)					31.99
Payload Fraction					0.625
CG (in From LE of Wing)					4.870
%MGC					27.06

Table 5.7: RPP-2 Predicted Takeoff Performance

Wind (mph)	Thrust (lb)	payload (L)	Dist (ft)	Vstall (ft/s)	Time (s)
0	14	6.2	95	45.2	3.9
	15	6.6	95	46.0	3.8
	16	7	96	46.9	3.8
	17	7.4	96	47.6	3.7
	18	7.8	97	48.4	3.7
	19	8.2	98	49.1	3.7
	20	8.6	99	49.8	3.6
5	14	7.8	97	48.5	4.4
	15	8.2	96	49.1	4.2
	16	8.6	96	49.9	4.2
	17	9	96	50.5	4.1
	18	9.4	97	51.4	4.1
	19	9.8	97	52.0	4.0
	20	10.2	98	52.7	4.0
10	14	9.4	94	51.3	4.7
	15	9.8	93	52.0	4.6
	16	10.2	93	52.8	4.5
	17	11	99	54.0	4.6
	18	11.4	99	54.7	4.6
	19	11.4	93	54.7	4.3
	20	11.8	94	55.5	4.2
15	14	11.4	94	54.7	5.3
	15	11.8	93	55.4	5.1
	16	12.6	99	56.6	5.3
	17	13	99	57.4	5.2
	18	13.4	98	57.9	5.0
	19	13.8	98	58.6	4.9
	20	14.2	98	59.2	4.8

Table 5.8: Energy and Time Estimates for Takeoff , Landing, Ground Operations, and Energy Correction Factor

Takeoff energy (J)	1000
Takeoff + Landing Time (s)	21
Crew Time (s)	30
Energy Correction Factor	2

Table 5.9: RPP-2 Energy Usage and Time Predictions

1 Scoring Sortie Type, Avg. Airspeed 70 ft/s					
Payload (L)	Total Energy (J)	Total Time (s)	%Energy in Climb	%Energy in Cruise	%Energy in Turns
0	7691	23.2	12.5	35.8	51.7
1	8828	23.3	13.1	32.3	54.6
2	10064	25.0	13.5	29.5	57.0
3	11373	26.7	13.8	27.3	58.9
4	12756	28.4	13.9	25.5	60.5
5	14246	28.5	14.0	24.1	61.9
6	15877	28.6	13.9	22.8	63.3
7	17648	28.7	13.8	21.7	64.5
8	25093	25.9	10.7	16.2	73.2
1 Non-Scoring Sortie Type, Avg. Airspeed 70 ft/s					
Payload (L)	Total Energy (J)	Total Time (s)	%Energy in Climb	%Energy in Cruise	%Energy in Turns
0	13197	48.2	7.3	62.6	30.1

Table 5.10: RPP-2 Energy Usage and Time Predictions per Flight

Payload (L)	2 Scoring Sorties		3 Scoring Sorties		4 Scoring Sorties	
	Total Energy (kJ)	Total Time (min)	Total Energy (kJ)	Total Time (min)	Total Energy (kJ)	Total Time (min)
0	63.2	3.6	108.9	6.5	154.7	9.4
1	67.7	3.6	115.8	6.5	163.8	9.4
2	72.6	3.7	123.2	6.6	173.7	9.5
3	77.9	3.7	131.0	6.7	184.2	9.6
4	83.4	3.8	139.3	6.8	195.2	9.8
5	89.4	3.8	148.3	6.8	207.1	9.8
6	95.9	3.8	158.0	6.8	220.2	9.8
7	103.0	3.8	168.7	6.8	234.4	9.8
8	132.8	3.7	213.3	6.7	293.9	9.6

Table 5.11: RPP-2 Tail Geometry

Tail Attributes	Horizontal	Vertical
Area	300 in ²	216 in ²
Aspect Ratio	3	1.5
Taper Ratio	1	1
Airfoil	NACA 00009	
Elevator	25% chord	
Rudder	30% chord	
Ailerons	25% chord, 40%span	
Wing MAC	18 in.	
Wing Dihedral	0°	
Vertical Tail MAC	12 in.	
Horizontal Tail MAC	10 in.	
C.G. (Measured from L.E.)	5.4 in.	
Neutral Point (Measured from L.E.)	6.44 in.	
Static Margin (%)	12.94%	

Sortie # and type: _____ U/L

	units					
Flight #	Date-#					
Time						
Sortie #						
# of bottles						
weight	lbs					
Lap weight						
Battery name						
Battery voltage	V					
Energy	Amp/hrs					
with 360=Y w/o 360=N						
0 start	sec					
1 Take Off	sec					
2 End of Climb	sec					
Lap 1						
3 Beginning of 1st Turn	sec					
4 End of 1st Turn	sec					
5 Beginning of 360 Turn	sec					
6 End of 360 Turn	sec					
7 Beginning of 2nd Turn	sec					
8 power off	sec					
9 End of 2nd Turn	sec					
Lap 2						
Beginning of 1st Turn	sec					
End of 1st Turn	sec					
Beginning of 360 Turn	sec					
End of 360 Turn	sec					
Beginning of 2nd Turn	sec					
power off	sec					
End of 2nd Turn	sec					
10 touchdown	sec					
11 End of roll out	sec					
12 End of sortie	sec					
13 Bottle change	sec					
overall sortie flight time	sec					
Battery voltage	V					
Energy	Amp/hrs					
Max rate of climb	ft/min					
Max altitude	ft					
crew bottle change time	sec					

Figure 5.1: Sample Data Collection Sheet

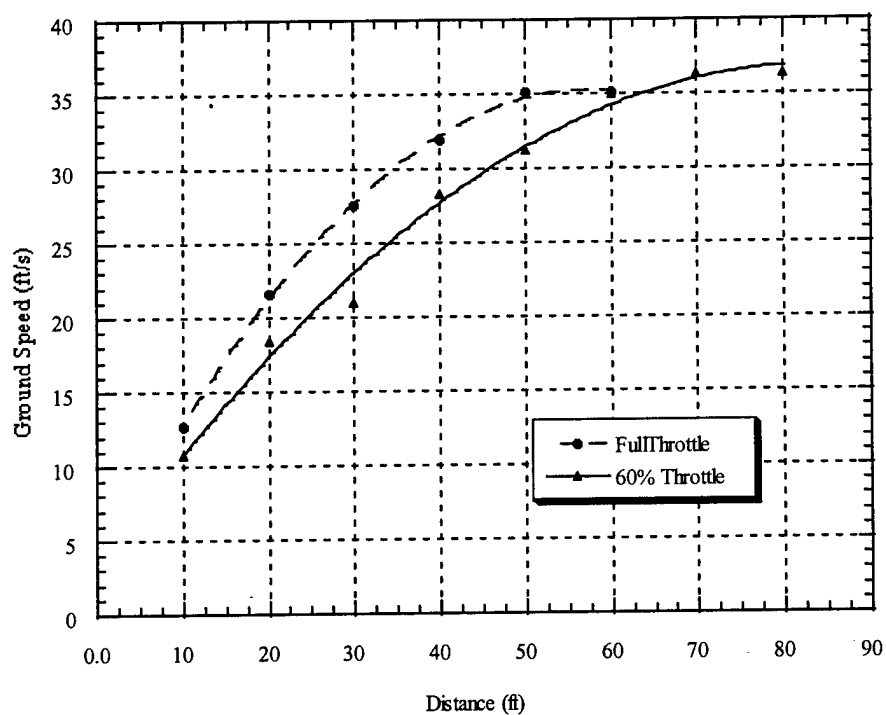


Figure 5.2: Prototype Average Speed During Takeoff

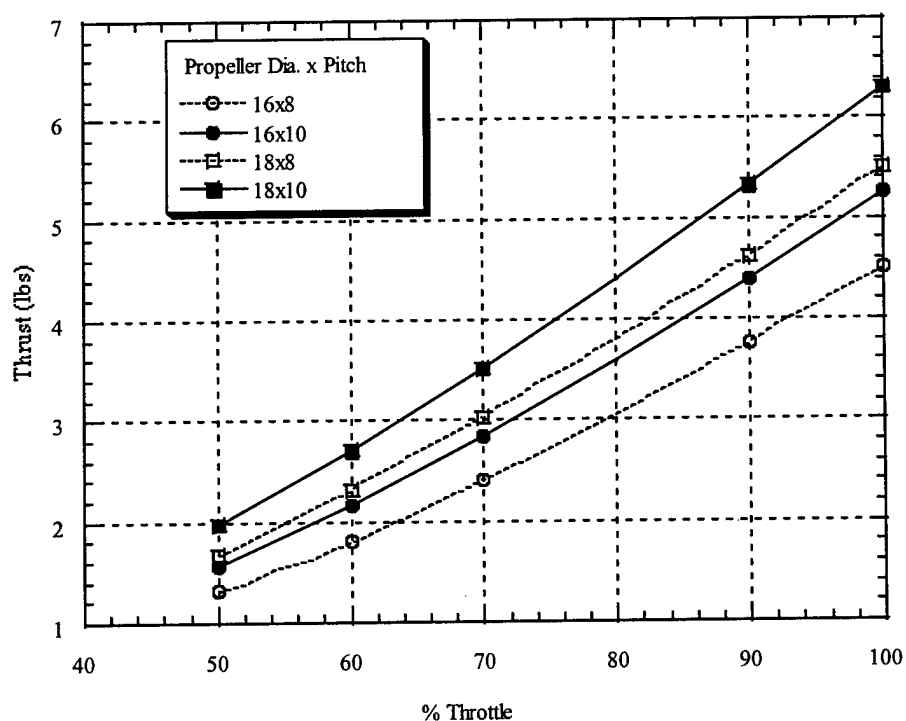


Figure 5.3: Static Thrust vs. % Throttle for a 15 Cell Battery Pack with Varying Propellers (MotoCalc⁸)

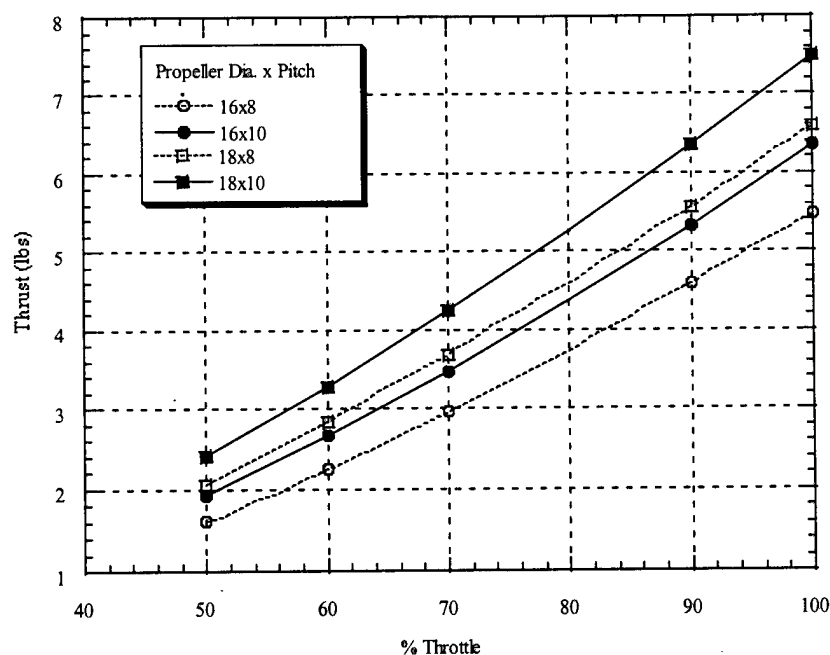


Figure 5.4: Static Thrust vs. % Throttle for a 17 Cell Battery Pack with Varying Propellers Ref X (MotoCalc⁸)

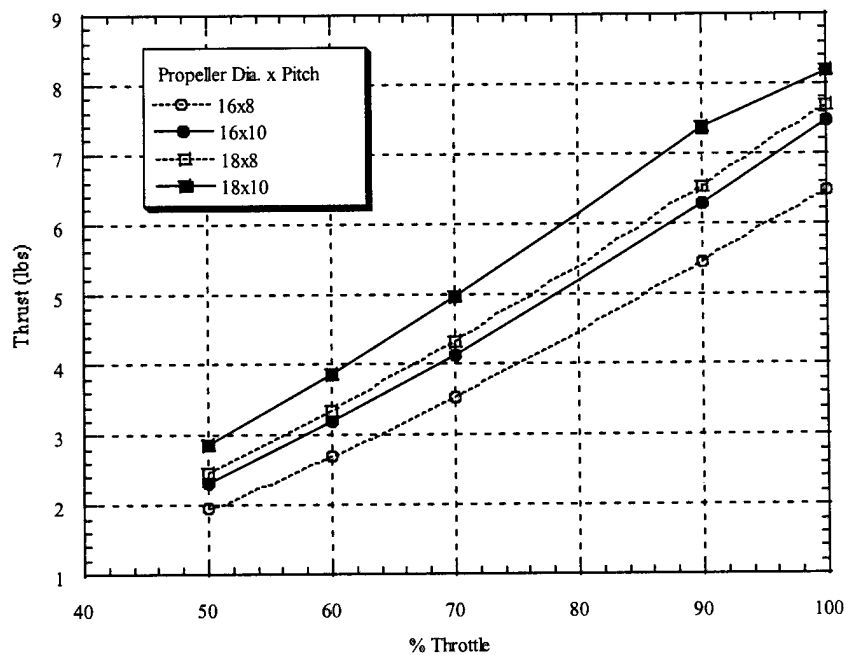


Figure 5.5: Static Thrust vs. % Throttle for a 19 Cell Battery Pack with Varying Propellers (MotoCalc⁸)

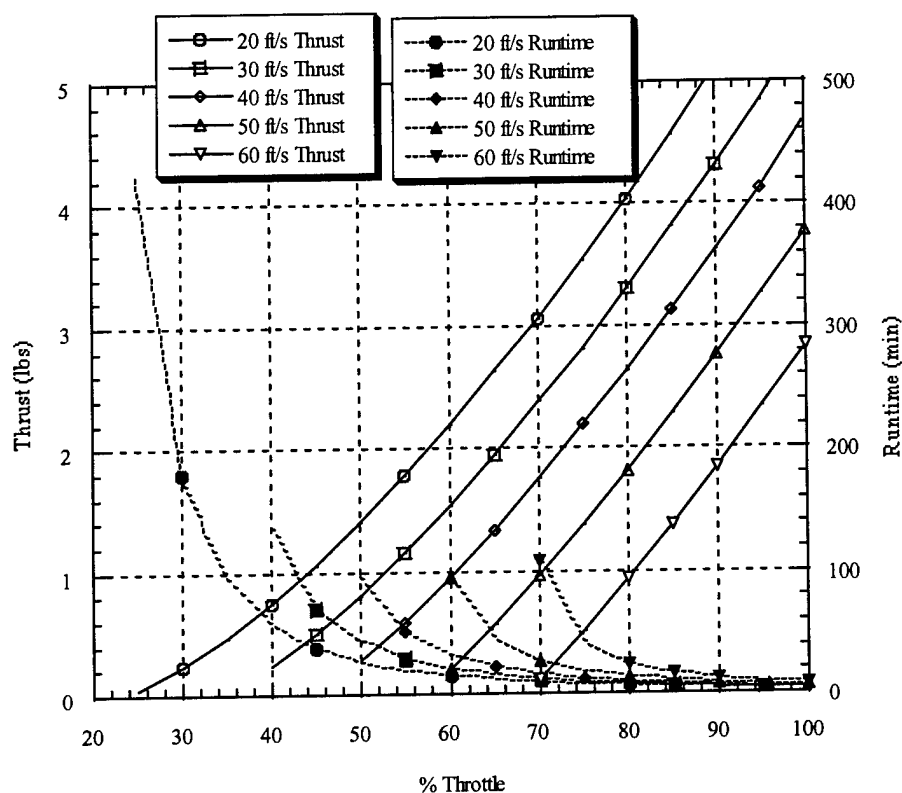


Figure 5.6: Thrust Available and Motor Runtime vs. % Throttle for APC 18x8 Propeller with a 19 Cell Battery Pack (MotoCalc[®])

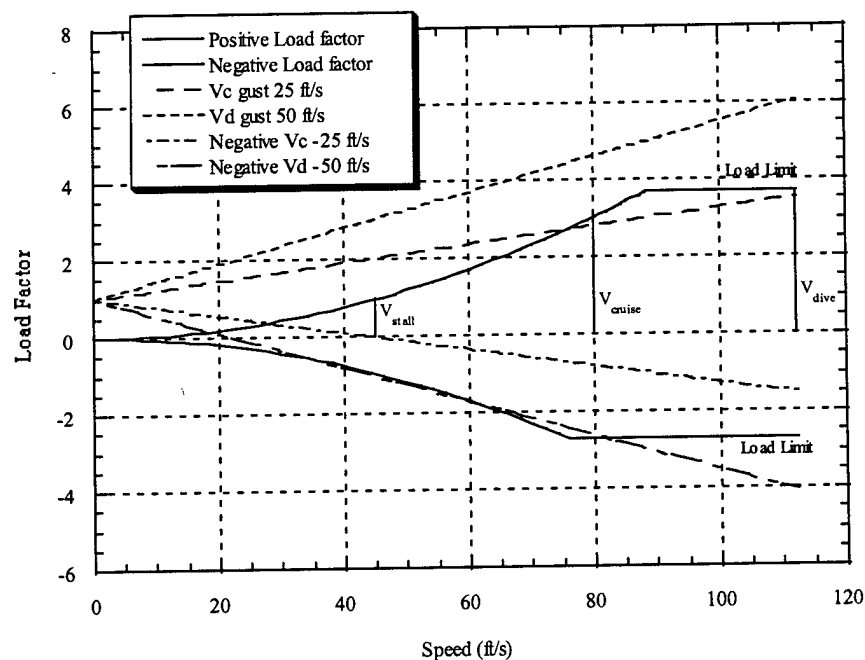


Figure 5.7: V-n Diagram

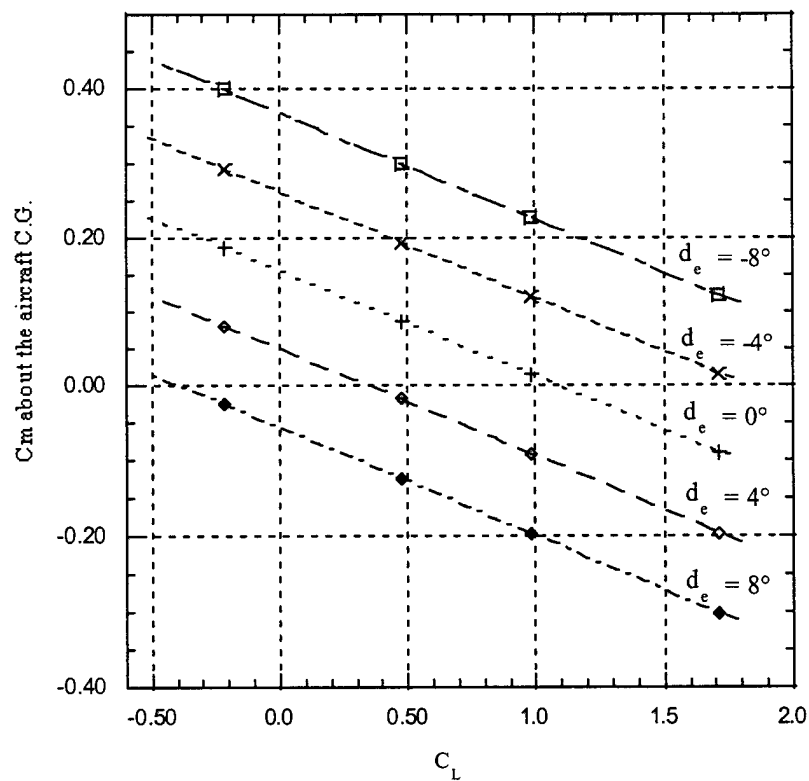


Figure 5.9: Elevator Trim Plot

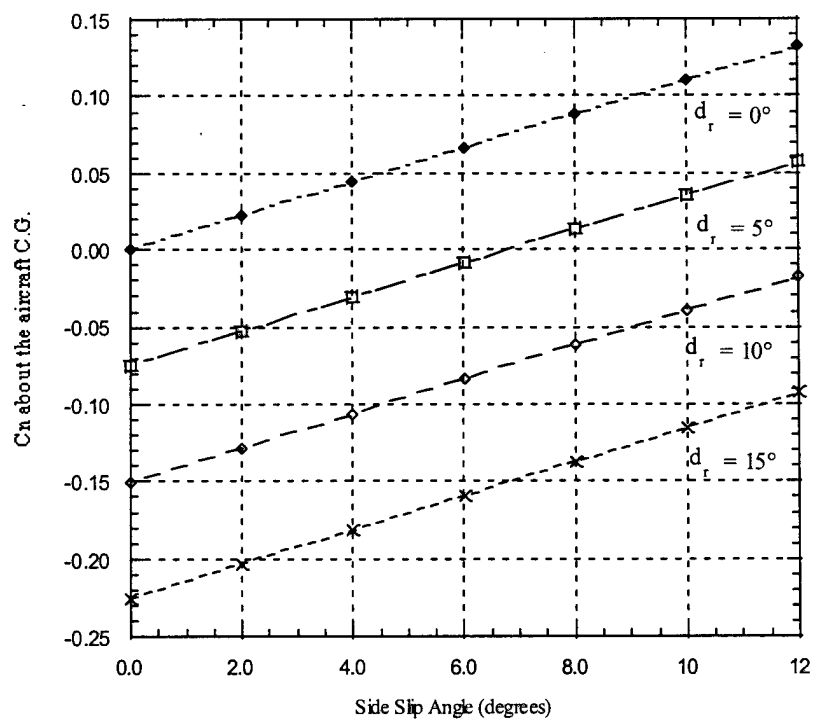


Figure 5.10: Rudder Trim Plot

All units in lb-in²

Concept 1

I_{xx} 83

I_{yy} 1402

I_{zz} 1459



Top View



Side View

Concept 2

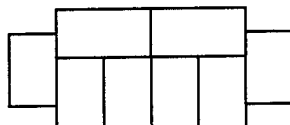
I_{xx} 175

I_{yy} 680

I_{zz} 828



Top View



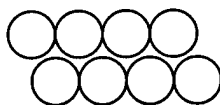
Side View

Concept 3

I_{xx} 124

I_{yy} 408

I_{zz} 423



Top View



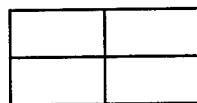
Side View

Concept 4

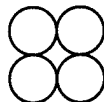
I_{xx} 139

I_{yy} 398

I_{zz} 398



Top View



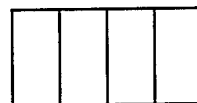
Side View

Concept 5

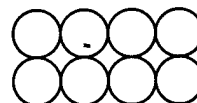
I_{xx} 139

I_{yy} 365

I_{zz} 365

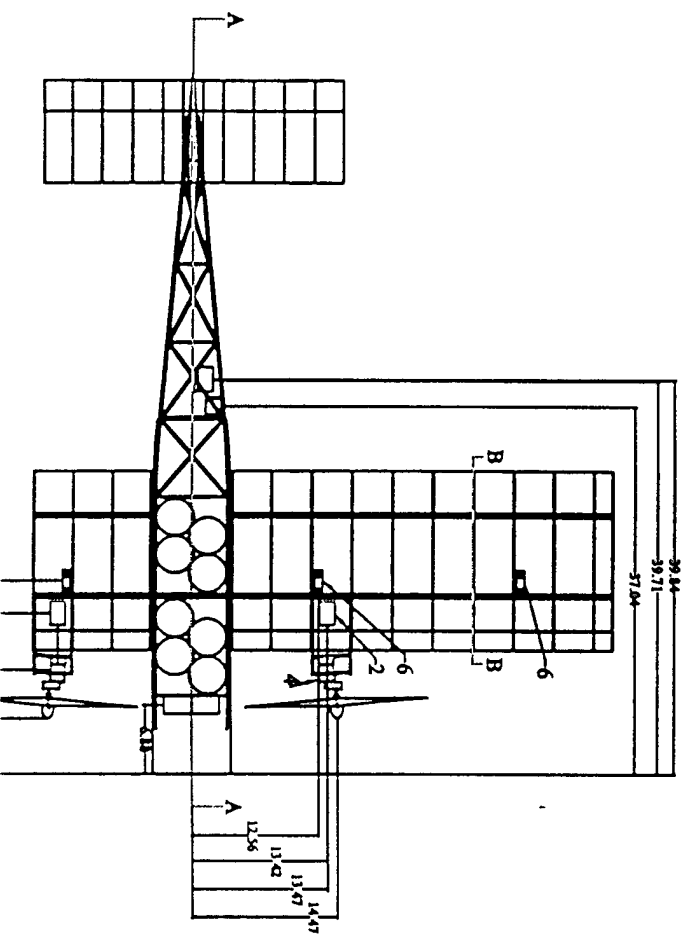
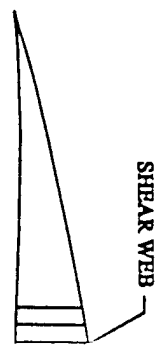
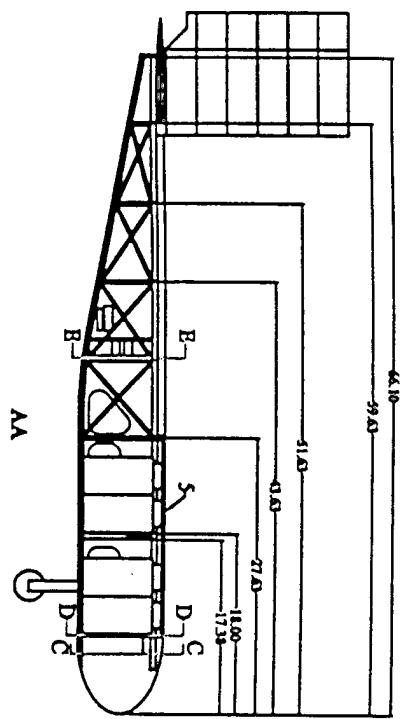


Top View



Side View

Figure 5.11 Payload Configuration Options



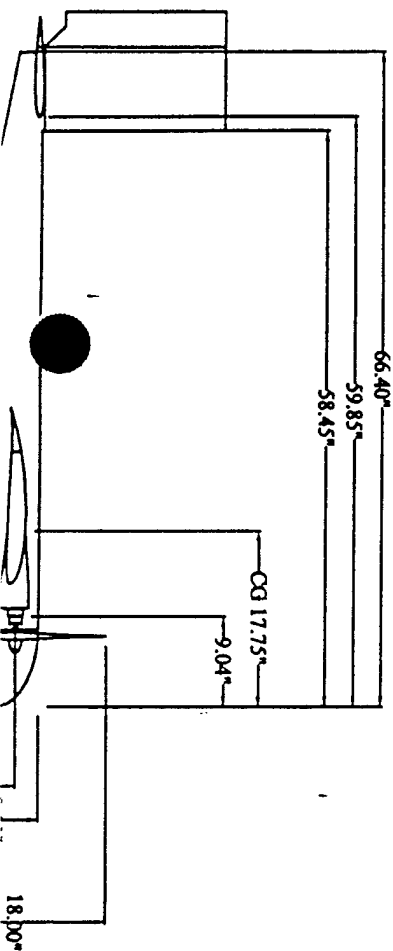
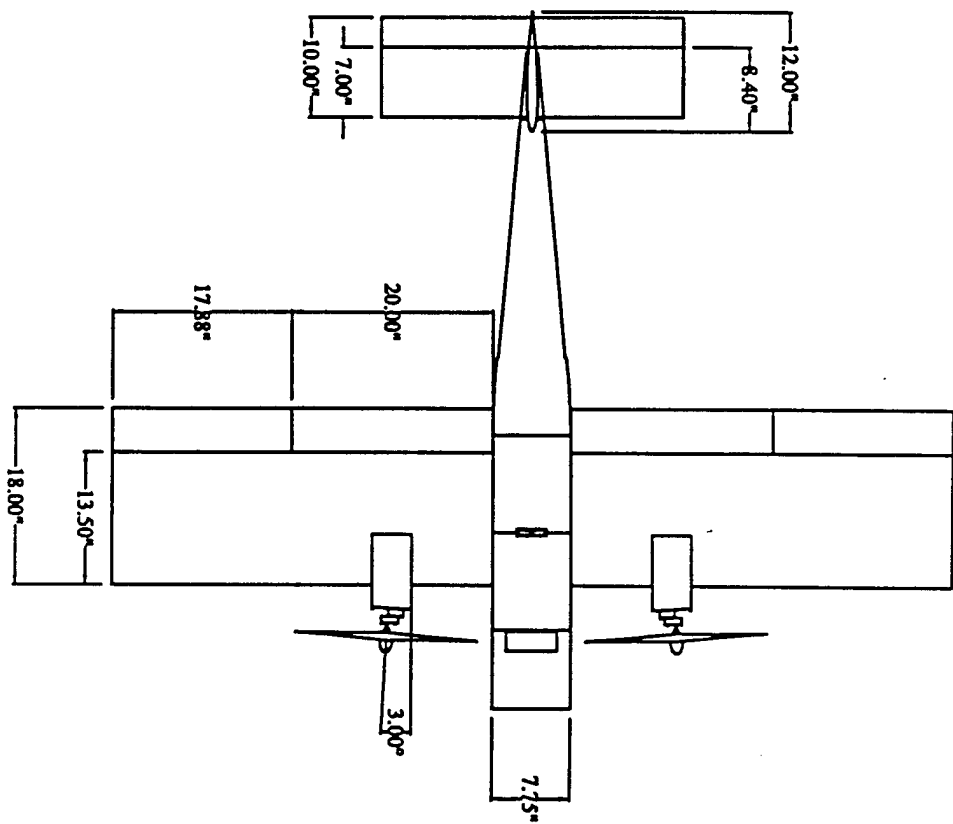




Figure 5.14

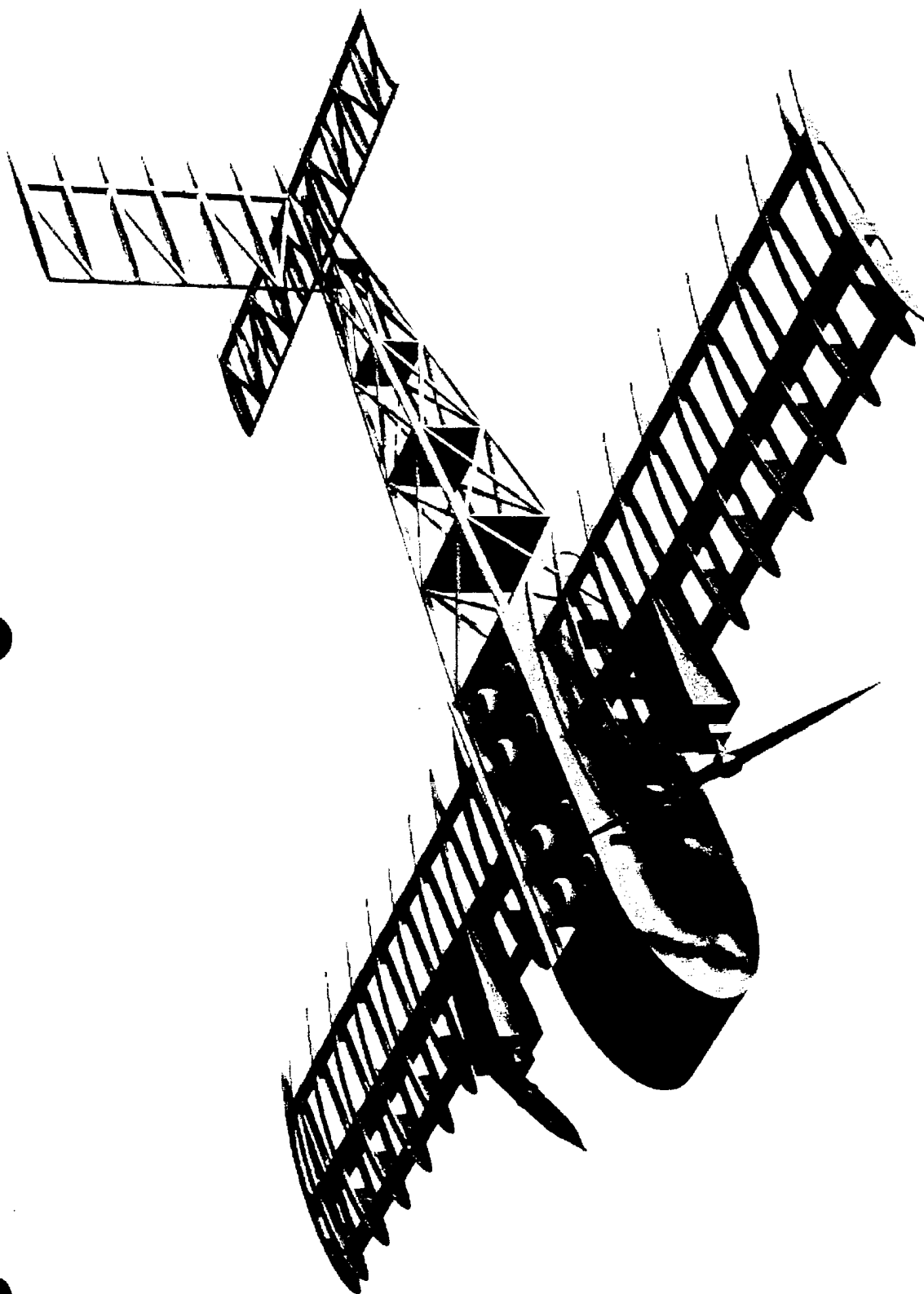


Figure 5.15

6.0 Manufacturing Plan

6.1 Component Requirements

- In order to maximize the score, the aircraft must be able to carry 8 liters of water, the fuselage must be as short as possible, and the structure must be as light as possible.
- In order to meet the takeoff requirement, the aircraft must be as light as possible, employ high-lift flaps, and have little rolling resistance.
- Must be durable enough to withstand the numerous landings and normal handling.
- Payload and batteries must be easily accessible and removable.
- The wing or tail must be removable for travel purposes.
- Construction must use commonly available materials and be able to be completed in the time available.

6.2 Manufacturing Processes Investigated

Several different building techniques were examined, some based on past experience and some from suggestions from the team's pilot.

6.2.1 Wing

The wing assembly needs to be as strong and as light as possible so it can carry the specified load but not increase the rated cost significantly. Two main construction techniques were considered for the wing assembly. The first was to use a foam core covered with fiberglass cloth and resin. The second technique was the traditional built up wing. The spars for built-up of wing could either be made of wood or carbon fiber and employ single or multiple spars. The sheeting would be determined by the torsional strength needed.

6.2.2 Fuselage

The fuselage must be strong enough to carry the weight of the payload and batteries and to handle the loads from the wings, motors, tail, and landing gear. The fuselage also must provide easy access to the electronics, batteries, and payload. The material (either balsa or plywood) used to construct the sides, and the number and type of supporting rails are determined

on the basis of strength-to-weight considerations. Construction of the aft fuselage would either be of a wood, truss framework or use a carbon fiber rod.

6.2.3 Empennage

Like the wing, the empennage could either be of built up or of foam and fiberglass construction. Because the load on the tail is less than that of the wing, a carbon fiber spar was not considered.

6.3 Figures of Merit

- Structural strength: the component must be able to carry the loads experienced in flight.
- Ease of construction: the amount of skill needed and complexity entailed in construction.
- Speed of construction: how fast the desired components could be built.
- Weight: how much the completed parts would weigh.
- Durability: the ability of the aircraft to handle normal operating conditions
- Accuracy: how true to the plans the completed airplane and airfoil would be.
- Material availability: ease of acquiring building materials.
- Material cost: cost of building materials.

The corresponding ranking for the FOMs are included in Table 6.1.

6.4 Evaluation

The different manufacturing processes were evaluated based primarily on past experience. This proved to be a reliable way to estimate the speed, ease of construction, durability, availability, and cost of materials. Structural analysis was used to determine if the components would be able to handle the loads they might be exposed to in flight. For the prototype, speed and ease of construction were given a higher priority due to the fact that the building crew would have little time to complete it or learn new building skills. Decisions for the competition plane, however, were influenced mostly by strength vs. weight concerns.

6.5 Results: Manufacturing Processes for Prototype

The results of FOM analysis are presented in Table 6.2 and 6.3. Despite the slightly lower FOM results, a built up wing and balsa-sided fuselage were chosen due to the importance of ease and speed of construction.

6.5.1 Fuselage

The prototype fuselage sides are constructed out of 3/8" thick balsa. An upper and lower rail on each side of the fuselage gives additional support for the walls. These rails are made of 1/2" by 1/4-in" basswood. Quarter-inch thick plywood bulkheads are used to separate the different compartments, keep fuselage sides square and attach the aft fuselage and wings. Due to cost considerations, the main spar is made of basswood. In order to keep the wing spar continuous and maintain structural integrity and facilitate transportation of the aircraft, the boom and attached tail surfaces are removable. The last two bulkheads in the fuselage hold a length of aluminum tube, which in turn accepts the carbon fiber rod that is used as a tail boom. This gives the tail boom a very strong mount that can stand up to the forces that the tail generates during maneuvers and allows the tail to be easily removable for travel purposes. Stringers were then added around the carbon fiber rod to add torsional stiffness and provide a tapered tail.

6.5.2 Wing

The wing uses built up construction that is similar to last year's design. Familiarity with this technique allowed the prototype to be built in a relatively short time frame. The wing incorporates upper and lower basswood spars. The upper spar, which needs to withstand higher compression loads, is made out of 1/2" by 1/2" basswood. The lower spar is made out of 1/2" by 1/4" basswood. Balsa shear webs were added between the spars to add strength. The wing incorporates a balsa leading edge and by two 1/4" by 1/4" basswood rear spars. The final airfoil shape is created by 3/32" thick balsa ribs sheeted with 1/16" thick balsa and covered with Super Monokote.

6.5.3 Tail

The tail surfaces are of built up construction similar to the wings. They are supported by basswood spars, balsa ribs and full sheeting, and covered in Super Monokote. All servos for the tail surfaces and for the tail wheel are mounted inside the tail surfaces with an access hatch.

6.6 Lessons Learned and Improvements to be made to the Competition Aircraft

Weight-and-balance problems with the prototype showed that the tail servos should be mounted further forward in order to make the design less tail heavy. Problems with engine vibration showed that the engine needed to be secured to the fuselage with multiple clamps and that the balsa sides were not adequate for securing the motor mounts. The motors need to be fastened directly to the fuselage rails or other supporting structures in order to prevent them from shaking loose. A more durable landing gear was also needed to prevent the gear from bending on hard, loaded landings. Several different types of wheels were tested to compare the offsetting effects of rolling resistance. Adherence to the prototype construction timeline (see Fig. 6.1) was very important in the manufacturing of the prototype design. Staying on schedule allowed a large amount of time to be spent flight-testing the aircraft. This policy of adhering to the timeline was continued in the construction of the competition aircraft.

6.7 Results: Manufacturing Processes for Final Design

The lessons learned from previous years and those learned from flight tests with the prototype influenced the construction decisions to be used on the competition aircraft. The main driver for the competition airplane was to make it as strong as possible while keeping it light in order to decrease the rated cost. Access to a laser-cutter allowed the use of slightly more complicated and accurate parts without an associated increase in building time. The results of the FOM analysis for the competition aircraft are included in Table 6.3.

6.7.1 Fuselage

The fuselage retains the basswood rails of the prototype, but the sides are made of 1/8-inch plywood with cutout lightening holes to reduce weight. The bulkheads were scaled down to 1/8-inch plywood with lightening holes. Plywood rails were added along the bottom of the fuselage to withstand the loads that the landing gear imposes on the underside of the fuselage. The carbon fiber boom, used on the prototype, was deemed too heavy, so a considerably lighter truss framework was employed. The servos for the tail surfaces are located in the aft fuselage and use pushrods to deflect the control surfaces.

6.7.2 Wing

The wing for the competition aircraft uses $\frac{1}{2}$ " by $\frac{1}{4}$ " carbon fiber rails for the upper and lower main spars and contains no secondary spars. These carbon fiber spars provide the strength needed, without the bulk or weight of basswood. The balsa shear web is between the carbon fiber spars creating an I-beam structure without adding large amounts of weight. Torsional strength is provided by a leading-edge D-tube which omits the need for sheeting. The D-tube is made of $\frac{1}{64}$ " plywood bent around the front of the ribs. The vertical portion of the "D" is completed with a balsa shear web. This not only provides the strength needed, but is much lighter than the balsa leading edge employed on the prototype. More widely spaced balsa ribs with lightening holes were used to give the wing its shape and reduce weight.

6.7.3 Tail

The tail surfaces were built up using balsa leading and trailing edges. In order to save weight, they are sheeted only out to half span.

6.8 Construction Details

The competition aircraft features removable wings for easy transportation. The carbon fiber spar for each wing extends beyond the first rib and fits into a sleeve in the fuselage. The sleeve is made of $\frac{1}{8}$ " plywood and carbon fiber rails to withstand the bending moments generated by the wing. The wings are secured with bolts passing through the sleeve. A pin on the trailing edge of the wing fits into the fuselage and resists wing twisting. The payload bottles are attached to the upper fuselage hatch, so that multiple bottles can be removed at once. The hatch is secured by pins and one latch, which allows quick access and removal. The motors are located on the wing in mounts that are connected directly to the spar for strength, but pass around the D-tube so as not to compromise the D-tube strength. The timeline for the construction of the competition aircraft is presented in Figure 6.2.

6.9 Cost Reduction Methods

Most of the construction uses balsa and plywood sheets, both of which are readily available and inexpensive. The carbon fiber components were reused from last year's airplane. Last year's battery packs were also reconfigured to the five pound limit.

Table 6.1: Construction Figures of Merit

Figure of Merit	Ranking		
	5	3	1
Strength	Strong	Adequate	Inadequate
Ease of Construction	Easy	Moderate	Difficult
Speed of Construction	Fast	Moderate	Slow
Weight	Light	Moderate	Heavy
Durability	Durable	Moderate	Fragile
Accuracy	Accurate	Moderate	Inaccurate
Material Availability	Readily available	Moderately Available	Obscure
Material Cost	Cheap	Affordable	Expensive

Table 6.2: Wing/Tail Figures of Merit Results

	Built up/balsa leading edge	Built up/D-tube leading edge	Built up/wood spar	Built up/carbonfiber spar	Foam core/fiberglass
Strength	3	4	3	5	5
Ease of Construction	5	3	5	4	1
Speed of Construction	5	4	4	4	2
Weight	3	5	3	5	1
Durability	3	2	3	5	5
Accuracy	3	4	4	4	5
Material Availability	5	5	5	3	3
Material Cost	5	4	5	3	2
Total	32	31	32	33	24

Table 6.3: Fuselage Figures of Merit Results

	Balsa sides	Plywood sides	Fiberglass
Strength	2	4	5
Ease of Construction	5	4	2
Speed of Construction	5	4	2
Weight	4	4	3
Durability	2	4	4
Accuracy	3	4	4
Material Availability	5	5	2
Material Cost	5	4	2
Total	31	33	24

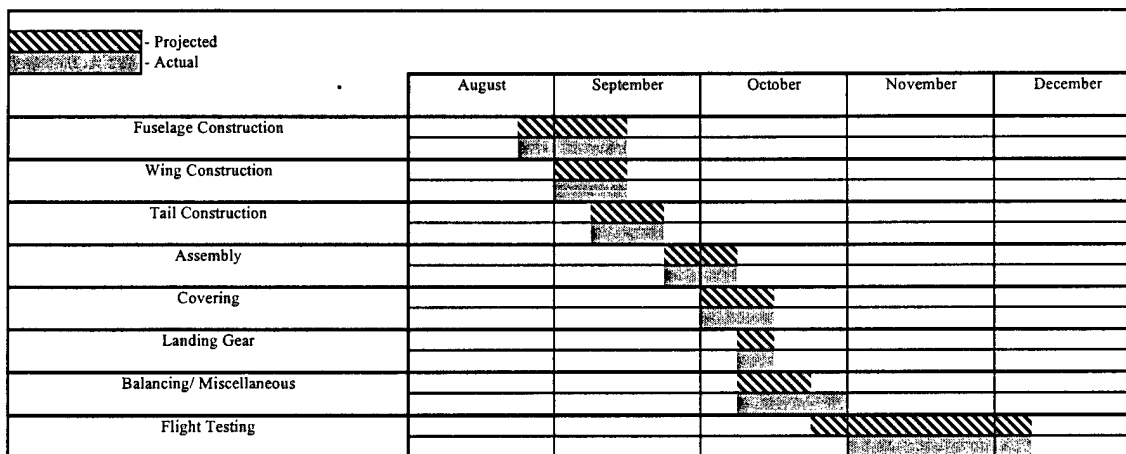


Figure 6.1: Construction Timeline for Prototype YRPP-2

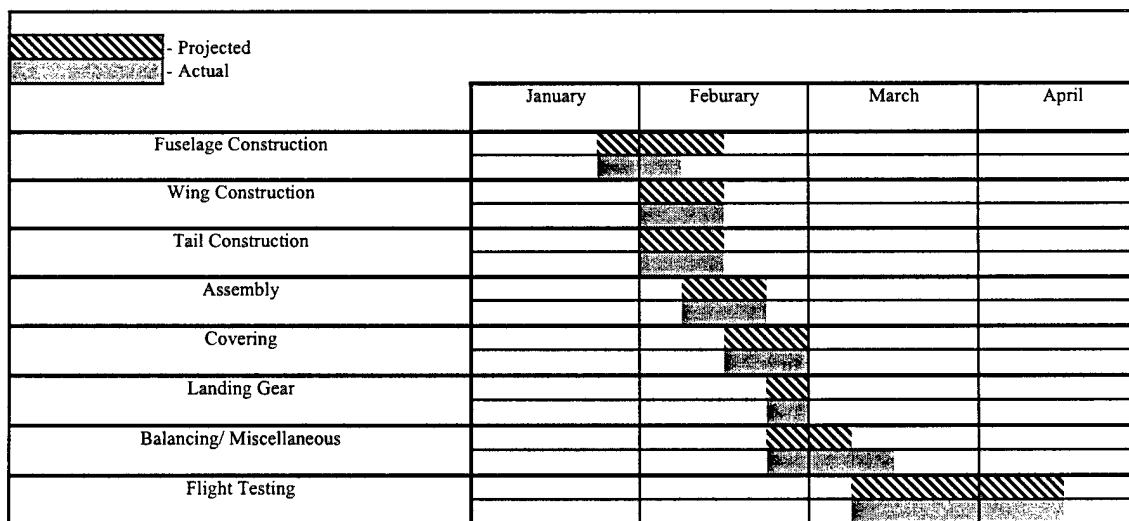
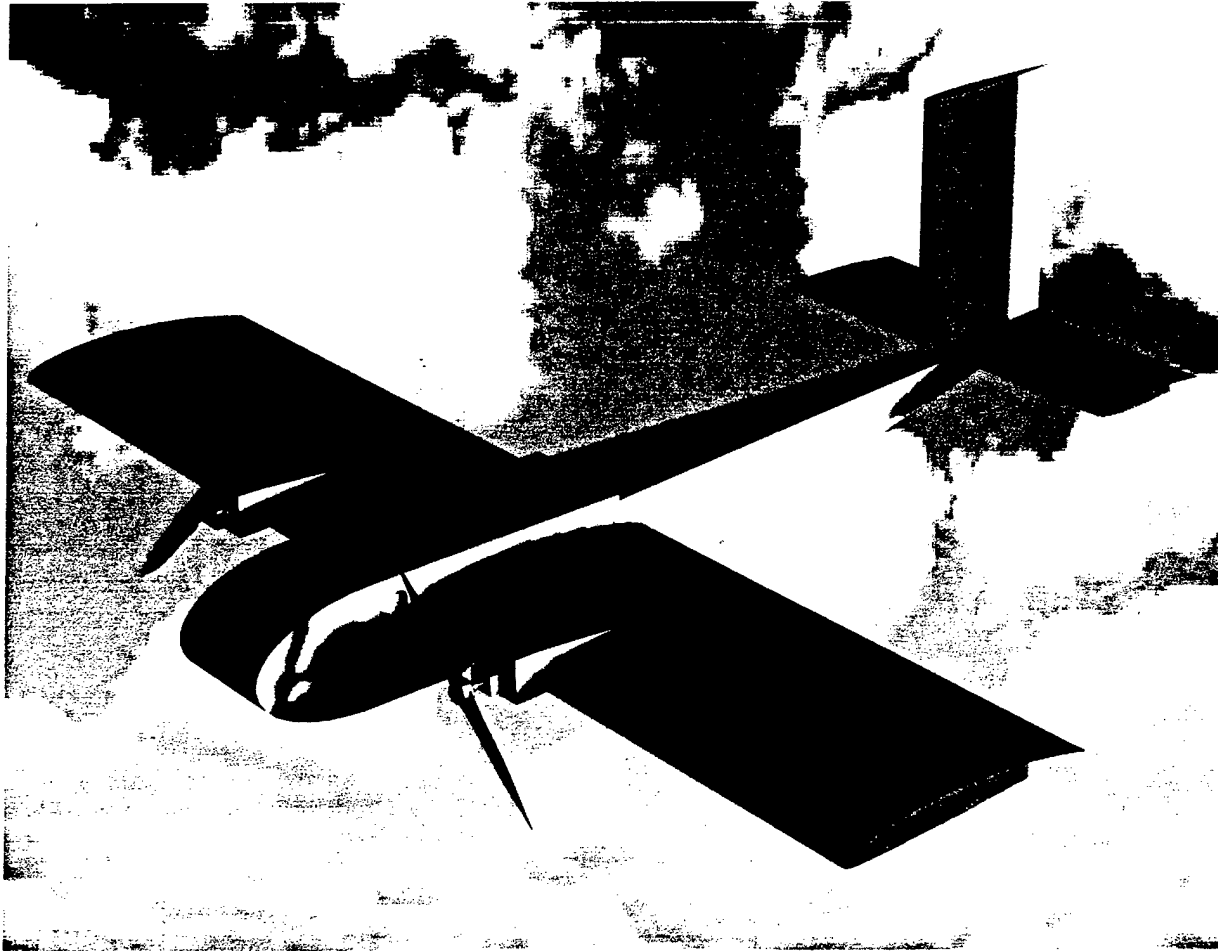


Figure 6.2: Construction Timeline for Competition Aircraft RPP-2

9.0 References

1. Lyon, C.A., Broeren, A.P., Gopalarathnam, A., Giguere, P., and Selig, M.S., *Summary of Low-Speed Airfoil Data – Vol 3*, SoarTech Publications, Virginia Beach, VA. Dec. 1997.
2. Selig, M.S, Guglielmo, J, Broeren, A.P., and Giguere, P., *Summary of Low-Speed Airfoil Data – Vol. 1*, SoarTech Publications, Virginia Beach, VA. June 1995.
3. Roskam, J., *Airplane Design: Part VI: Preliminary Calculation of Aerodynamic, Thrust and Power Characteristics*, Roskam Aviation and Engineering Corporation, Ottawa, KS. 66067, 1987
4. Raymer, D.P., *Aircraft Design: A Conceptual Approach*, 2nd ed., AIAA Education Series, Washington, D.C., 1994.
5. ElectriCalc. Vers.1.0. Computer software. SLK Electronics, 1996. PC.
6. MatWeb, by Automation Creations, Inc. online source www.matweb.com, accessed between 9/99-3/00.
7. Roskam, J., *Airplane Flight Dynamics and Flight Controls*, Roskam Aviation and Engineering Corporation, Ottawa, KS. 66067, 1979.
8. MotoCalc. Vers. 5.01. Computer software. Capable Computing, Inc., 1998.
9. ANSYS. Vers 5.5. Computer software. SAS IP, Inc., 1998

RPP-2 Hobbes
Final Design Report



AIAA Student Design/Build/Fly Competition

Wichita, Kansas

**Department of Aeronautical and Astronautical Engineering
University of Illinois at Urbana-Champaign**

April 14, 2000

RPP-2 Hobbes
Final Design Report

AIAA Student Design/Build/Fly Competition

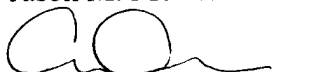
Wichita, Kansas

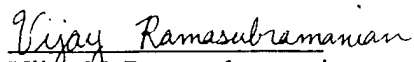
Department of Aeronautical and Astronautical Engineering
University of Illinois at Urbana-Champaign

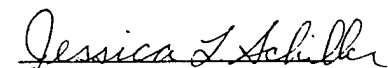
April 14, 2000

RPP-2 Project Team



Jason M. Merret

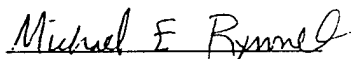

Eunice Y. Lee

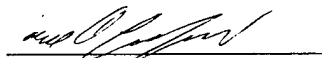

Vijay N. Ramasubramanian


Jessica L. Schiller



Chris M. LaMarre


Robert R. Quirk

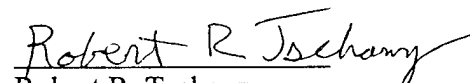

Michael E. Rynne

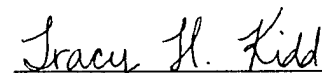

Carey A. Lunsford


Karl R. Klingbeil

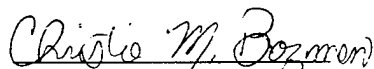

Starsha T. Johnson

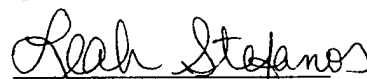

Michael S. Sexauer

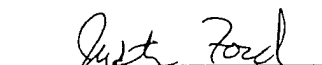

Robert R. Tschanz

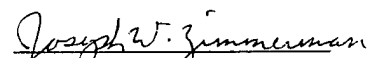

Tracy H. Kidd

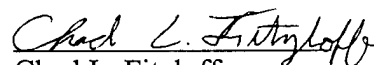

Shalin H. Mody



Christie M. Bozman

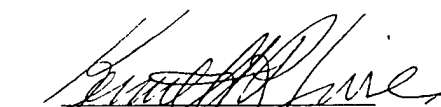

Leah C. Stefanos



Justin K. Ford

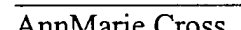

Joseph W. Zimmerman


Chad L. Fitzloff


Andrew D. Young


Dr. Kenneth R. Sivier
Faculty Advisor


Mike Cross
Pilot


AnnMarie Cross
Hobbico Advisor

Acknowledgements

This year's project owes its success to many sources, and we would like to take this opportunity to acknowledge their help. We thank Jim Schmidt and Hobbico for their continued and unparalleled support through donations of building materials, tools, and this year, employees. Their continued dedication to the team has surpassed all our expectations and has been a constant motivation for the team. Special thanks goes to Mike and AnnMarie Cross for their hard work, dedication, and sacrifices for the team. Their guidance and compassion has truly inspired this year's team. We thank the Department of Aeronautical and Astronautical Engineering for providing the necessary space for a workshop as well as needed monetary support, and the use of a low-speed wind tunnel for propulsion testing. There were also several sources of monetary support. We thank the College of Engineering at UIUC, the Illinois section of the AIAA, and Region III. Thanks also goes to our corporate sponsors, Motorola and Pratt & Whitney. We especially thank James Kessler, a UIUC alumnus for his continued support of the team. Finally, Professor Kenneth Sivier has continued to advise and encourage the team. Our deepest gratitude goes to him for his endless encouragement and continued guidance.

Table of Contents

1.0 Executive Summary	1
2.0 Management Summary	2
3.0 Conceptual Design	5
3.1 System Requirements	5
3.2 Figures of Merit	6
3.3 Conceptual Design Analysis Tools	6
3.4 Configuration Studies	7
3.4.1 Prototype Aircraft	7
3.4.1.1 Configurations Considered	7
3.4.1.2 Conceptual Design Analysis Results	8
3.4.1.3 Figures of Merit Results	8
3.4.1.4 Payload Sizing	9
3.4.1.5 Prototype Conclusions	10
3.4.2 Competition Aircraft	10
3.4.2.1 Configurations Considered	10
3.4.2.2 Conceptual Design Analysis Results	11
3.4.2.3 Figures of Merit Results	11
3.4.2.4 Conclusion	11
4.0 Preliminary Design	20
4.1 Design Parameters Investigation	20
4.2 Aerodynamics	20
4.3 Propulsion System Selection	21
4.4 Structures	22
4.5 Aircraft Weight Build Up	22
4.6 Performance Analyses	22
4.6.1 Takeoff Analysis	22
4.6.2 Energy and Time Analyses	23
4.7 Stability Analyses	24
4.8 Prototype Design Summary	24
5.0 Detailed Design	33
5.1 Introduction	33
5.2 Prototype Aircraft Flight Testing	33
5.2.1 Objectives	33
5.2.2 Test Site and Instrumentation	33
5.2.3 Procedure	33
5.2.4 Results	34
5.3 Aerodynamics	36
5.4 Propulsion	36
5.5 Structures	38
5.5.1 Major Changes From Prototype	38

5.5.2 Structural Modeling and Results	39
5.5.4 Final Structure	39
5.5.6 g-Load Capability	39
5.6 Ground Operations	40
5.7 Final Weights and Balance	40
5.8 Performance Analyses	41
5.8.1 Takeoff Analysis	41
5.8.2 Energy and Time Analyses	41
5.9 Stability and Control Analysis	41
5.10 Final Design Summary	42
6.0 Manufacturing Plan	58
6.1 Component Requirements	58
6.2 Manufacturing Processes Investigated	58
6.2.1 Wing	58
6.2.2 Fuselage	58
6.2.3 Empennage	59
6.3 Figures of Merit	59
6.4 Evaluation	59
6.5 Results: Manufacturing Processes for Prototype	60
6.5.1 Fuselage	60
6.5.2 Wing	60
6.5.3 Tail	61
6.6 Lessons Learned and Improvements to be made to the Competition Aircraft	61
6.7 Results: Manufacturing Processes for Final Design	61
6.7.1 Fuselage	61
6.7.2 Wing	62
6.7.3 Tail	62
6.8 Construction Details	62
6.9 Cost Reduction Methods	62
7.0 Lessons Learned	65
7.1 Comparison of the Constructed and Designed Aircraft	65
7.2 Monetary Cost Assessment	65
7.3 Flight Tests	66
7.4 Design Changes after Competition Aircraft Crash	66
7.5 Areas for Improvement	67
7.6 Conclusions	67
8.0 Cost Analysis	70
8.1 Prototype Aircraft	70
8.2 Competition Aircraft	70
9.0 References	74

7.0 Lesson's Learned

7.1 Comparison of the Constructed and Designed Aircraft

Due to time constraints, the final design of the competition aircraft ran concurrent with construction. Many decisions affecting the design were made during construction based on building experience, availability of materials/equipment, and as the result of difficulties that arose. However, the overall design of the aircraft did not change.

Several changes made during production including the strengthening of the airframe. Although calculations for the wing strength indicated material failure would occur at much higher loads than would be experienced during flight, bonding of the carbon fiber and balsa wood used for the spar was inadequate. To increase surface area for bonding and thereby ensure adequate strength, additional balsa strips were added along the seam between the balsa shear web and the carbon fiber spar. In addition, the wing section that was bolted to the fuselage was built-up further ensuring sufficient adhesive strength. The landing gear was also shored up with extra plywood pieces to provide additional strength and surface area.

After completing several successful flights and receiving pilot input (the pilot indicated a substantial downward pitching moment was occurring), the tail incidence was changed to -2.5° to improve aircraft response. Horizontal tail control surface area was also increased in order to give more aircraft pitch control to the pilot. The horizontal tail control surface was increased from 30% to 40%. In addition, 0.25 lbs. was added to the tail in order to move the center of gravity back to approximately 30% of the wing cord. Final propeller selection was decided to be a 16 x 10. This achieved the desired static thrust and energy characteristics based on the prototype and initial flight-testing.

7.2 Monetary Cost Assessment

The cost breakdown of the final aircraft is summarized in Table 7.1. The projected cost of the competition aircraft was \$1645, while the actual cost was \$2035. The increased cost is primarily due to the change in configuration after prototype testing. The largest contributor to the cost change is the addition of a motor.

7.3 Flight Tests

Objectives during final flight-testing were altered to reflect a tighter schedule and changes in priorities. In contrast to the emphasis on energy data collection during the prototype testing, these aircraft flights focused on determining takeoff capabilities and completing the competition flight regime. As calculated, testing confirmed that the aircraft could not take off in 100 ft. with six liters of water in a six mph headwind. With less than a 10 mph headwind, four liters can be lifted in 100 ft.

Each run consisted of a loaded, one-lap sortie with a 360 turn and an unloaded, two-lap sortie without 360 turns. This format allowed the flight crew to practice loading and unloading the plane to simulate competition flights. Unlike the original prediction of 30 seconds, the time from the crew leaving the crew holding box, reloading/unloading, and returning to the holding box was 15 seconds.

Determination of optimal propeller size was another flight-testing objective. Originally, 18 x 8's were chosen, but flight-testing determined 16 x 10's provide better performance.

7.4 Design Changes after Competition Aircraft Crash

Due to the unfortunate crash of the competition aircraft during preliminary flight-testing; the opportunity arose to make several changes in the competition aircraft. However, because of the time constraints, only a few changes were incorporated. First, the wing mounting method was changed to increase the ease of assembly. Rather than having carbon fiber spars and plywood joiners, an aluminum tube now slides into an impregnated cardboard tube located in the fuselage. Although the aluminum tube adds weight to the wing structure, its use has eliminated the massive bulkhead previously used to secure the wing (The tabs on the I-beam design also were constantly broken by handling (crew personal)). Overall, the increase in weight should be minimal; with the ease of assembly justifying the increased weight. A second change involves the placement of the tail control servos closer to the tail. This move was motivated by the opportunity to move the center of gravity back without adding additional weight as in the previous competition aircraft. The incidence of the horizontal tail was also changed during construction to incorporate the modification that had been made to the first competition aircraft. The propeller size has also been changed to a 16x10 in order to increase available static thrust at

takeoff and flight speed. Finally, the appearance of the aircraft was modified by changing the color scheme (in accordance to popular opinion of the construction crew). See Figures 7.1 and 7.2.

7.5 Areas for Improvement

Areas of improvement can always be found in a design. Due to time constraints, building priorities restricted the amount of testing, analysis, and optimization that could be conducted. Given more time for design, improvements in the aircraft structure could result in reduced weight. One way to improve aircraft weight predictions is to design the aircraft using programs such as Unigraphics, which can calculate structure volumes precisely. Detailed calculations of every component could also be used to optimize the aircraft's strength-to-weight ratio. In addition, the overall configuration would benefit from increased streamlining. In particular, the nose of the aircraft (especially the prototype) is non-aerodynamic and would benefit from a redesign (time and building constraints inhibited more efficient aerodynamic designs). A reduction in drag would result in lower energy requirements and reduce sortie times.

7.6 Conclusions

Changes to the competition aircraft include increasing strength of the frame, the incidence of the tail, and the horizontal control surface. The center of gravity was moved back to 30% of the cord. A propeller size of 16 x 10 will be used on the aircraft during the competition. Due to the reconfiguration of the final competition aircraft, the aircraft cost increased to \$2035.

Flight tests provided important information for not only this year's competition, but for years to come. Beginning the design phase early was a key to allowing time for the flight tests. Flight-testing allowed the verification and/or invalidation of theoretical calculations. The team learned that staying on task, maintaining deadlines, and not lagging in production are imperative to being successful. Flight-testing not only provided the critical competition practice needed for the pilot and flight crew, but also allowed the team to develop a strategy for the competition.

One of the largest obstacles with the competition is the time constraint. One way to overcome this obstacle is to improve time management. Other areas for improvement include more flight tests, aggressive weight reduction, and more work on aerodynamics.

Table 7.1 Aircraft Component Costs (rounded to the nearest dollar)

Propulsion System	Cost
batteries	200.00
motors	500.00
speed controllers	200.00
wiring/switches	50.00
gear boxes	115.00
spinners	15.00
propellors	80.00
Propulsion System Sub-total	\$1,160.00
Construction Materials	
wood	200.00
composites	150.00
adhesives	75.00
Construcion Materials Sub-total	\$425.00
Misc.	
servos	250.00
covering	50.00
flight hardware	150.00
Misc. Sub-total	450.00
Total	\$2,035.00

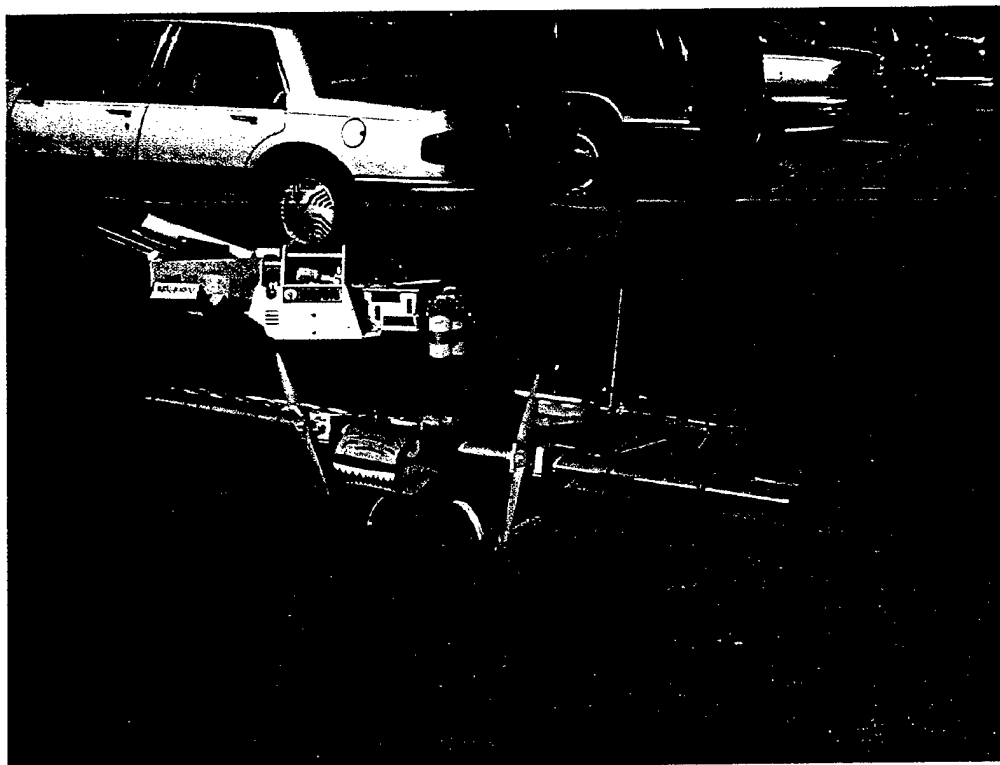


Figure 7.1 RPP-2 "Hobbes"

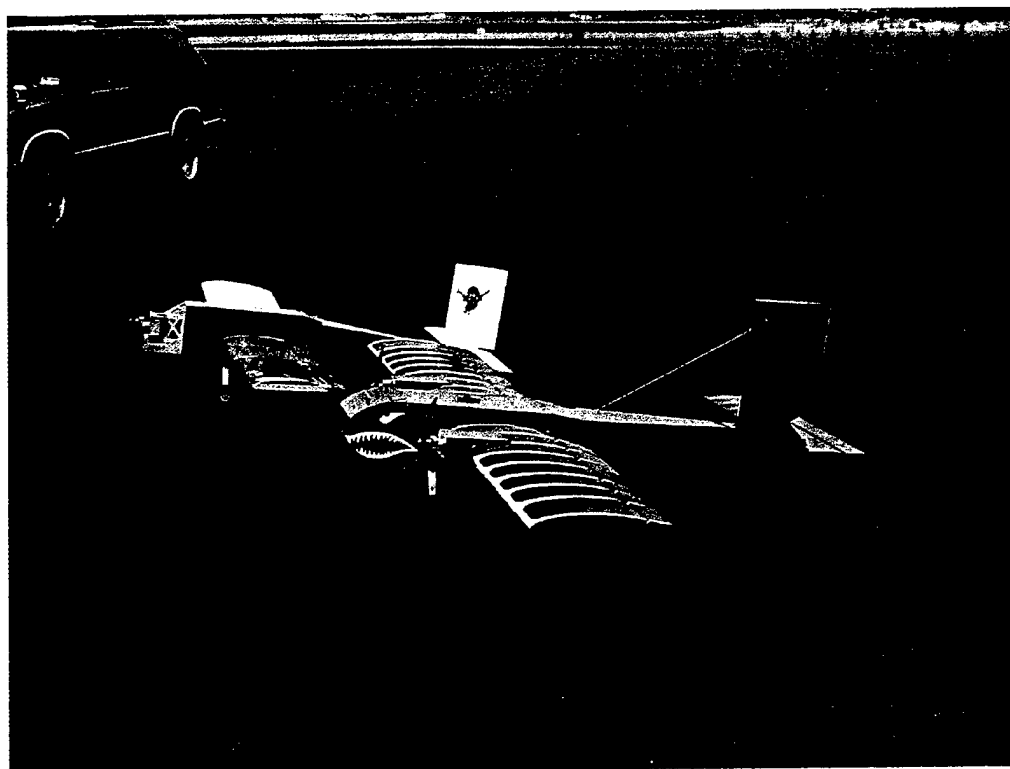


Figure 7.2 YRPP-2 "Sam" and RPP-3 "Phoenix"

8.0 Cost Analysis

8.1 Prototype Aircraft

Tables 8.1-8.3 break down the estimated and actual costs of the prototype YRPP-2. Table 8.1 summarizes the aircraft characteristics of the prototype with the input to the cost model italicized. Table 8.2 summarizes the work breakdown structure and Table 8.3 summarizes the costs of the aircraft. The estimated cost was 4.26 while the actual cost was 4.57. This increase of 7% was mainly due to the increased weight.

8.2 Competition Aircraft

The cost model break down for the competition aircraft, RPP-2 "Hobbes", is shown in Tables 8.4-8.6 using the same format as above. The estimated cost was 6.03 while the actual cost was 6.16. This slight increase of 2.2% in cost was again mainly due to the increase in empty weight of the actual aircraft. The decrease in the number of servos from 7 to 6 had a minimal effect on cost.

RPP-2 "Hobbes" crashed on March 26, 2000 and was destroyed; subsequently, a second competition aircraft was constructed. The cost breakdown for RPP-3 "Phoenix" is presented in Tables 8.7-8.9. Since the aircraft was almost an exact copy of the previous aircraft, the actual cost of RPP-2 was used for the estimated cost of RPP-3. Again, due to an increase in empty weight of 1 lbs, the cost increased to 6.39; a 3.7% increase over RPP- 2 "Hobbes". Therefore, the cost of the final competition aircraft is 6.39, the cost for RPP-3.

Table 8.1 YRPP-2 Aircraft Characteristics (Inputs to Cost Model are *Italicized*)

	Estimated	Actual
Payload (L)	4	4
Payload (lbs)	10	10
Battery Weight (lbs)	2.95	2.95
<i>Empty Weight (lbs)</i>	7.4	10
Total Takeoff Weight with Payload (lbs)	20.4	23.0
Total Takeoff Weight without Payload (lbs)	10.4	13.0
<i># of wings</i>	1	1
b (ft)	7	7
c (ft)	1.25	1.25
<i>Total Wing Area (ft²)</i>	8.75	8.75
<i># of Pods</i>	1	1
<i>Fuse Length (ft)</i>	5	5.583
<i>Pod 1 Length (ft)</i>	0	0
<i>Pod 2 Length (ft)</i>	0	0
<i># of Engines</i>	1	1
<i># of Batteries</i>	1	1
<i># of cells/Engine</i>	23	23
<i># of Propellers</i>	1	1
<i># of servos</i>	7	7

Table 8.2: YRPP-2 Work Breakdown Structure

	Estimated	Actual
Wings (hours)	40.0	40.0
Fuselage (hours)	25.0	27.3
Pods (hours)	0.0	0.0
Empenage (hours)	20.0	20.0
Flight Systems (hours)	12.0	12.0
Engine (hours)	10.0	10.0
MFHR (hours)	107.0	109.3

Table 8.3: YRPP-2 Costs

	Estimated	Actual
A (1/lbs)	100	100
B (1/Watts)	1	1
C (1/hours)	20	20
MEW (lbs)	7.4	10.0
REP (Watts)	1380.0	1380.0
MFHR (hours)	107.0	109.3
Cost	4.26	4.57

Table 8.4: RPP-2 Aircraft Characteristics (Inputs to Cost Model are Italicized)

	Estimated	Actual
Payload (L)	8	8
Payload (lbs)	20	20
Battery Weight (lbs)	5.00	5.00
<i>Empty Weight (lbs)</i>	9.0	10.5
Total Takeoff Weight with Payload (lbs)	34.0	35.5
Total Takeoff Weight without Payload (lbs)	14.0	15.5
<i># of wings</i>	1	1
b (ft)	7	7
c (ft)	1.5	1.5
<i>Total Wing Area (ft²)</i>	10.5	10.5
<i># of Pods</i>	3	3
<i>Fuse Length (ft)</i>	6	6
<i>Pod 1 Length (ft)</i>	0.583	0.583
<i>Pod 2 Length (ft)</i>	0.583	0.583
<i># of Engines</i>	2	2
<i># of Batteries</i>	2	2
<i># of cells/Engine</i>	19	19
<i># of Propellers</i>	2	2
<i># of servos</i>	7	6

Table 8.5: RPP-2 Work Breakdown Structure

	Estimated	Actual
Wings	47.0	47.0
Fuselage	29.0	29.0
Pods	14.7	14.7
Empenage	20.0	20.0
Flight Systems	12.0	11.0
Engine	20.0	20.0
MFHR (hours)	142.7	141.7

Table 8.6: RPP-2 Costs

	Estimated	Actual
A (1/lbs)	100	100
B (1/Watts)	1	1
C (1/hours)	20	20
MEW (lbs)	9.0	10.5
REP (Watts)	2280.0	2280.0
MFHR (hours)	142.7	141.7
Cost	6.03	6.16

Table 8.7: RPP-3 Aircraft Characteristics (Inputs to Cost Model are *Italicized*)

	Estimated	Actual
Payload (L)	8	8
Payload (lbs)	20	20
Battery Weight (lbs)	5.00	5.00
<i>Empty Weight (lbs)</i>	10.5	12.8
Total Takeoff Weight with Payload (lbs)	35.5	37.8
Total Takeoff Weight without Payload (lbs)	15.5	17.8
<i># of wings</i>	1	1
b (ft)	7	7
c (ft)	1.5	1.5
<i>Total Wing Area (ft²)</i>	10.5	10.5
<i># of Pods</i>	3	3
<i>Fuse Length (ft)</i>	6	6
<i>Pod 1 Length (ft)</i>	0.583	0.583
<i>Pod 2 Length (ft)</i>	0.583	0.583
<i># of Engines</i>	2	2
<i># of Batteries</i>	2	2
<i># of cells/Engine</i>	19	19
<i># of Propellers</i>	2	2
<i># of servos</i>	6	6

Table 8.8: RPP-3 Work Breakdown Structure

	Estimated	Actual
Wings	47.0	47.0
Fuselage	29.0	29.0
Pods	14.7	14.7
Empenage	20.0	20.0
Flight Systems	11.0	11.0
Engine	20.0	20.0
MFHR (hours)	141.7	141.7

Table 8.9: RPP-3 Costs

	Estimated	Actual
A (1/lbs)	100	100
B (1/Watts)	1	1
C (1/hours)	20	20
MEW (lbs)	10.5	12.8
REP (Watts)	2280.0	2280.0
MFHR (hours)	141.7	141.7
Cost	6.16	6.39

9.0 References

1. Lyon, C.A., Broeren, A.P., Gopalarathnam, A., Giguere, P., and Selig, M.S., *Summary of Low-Speed Airfoil Data – Vol 3*, SoarTech Publications, Virginia Beach, VA. Dec. 1997.
2. Selig, M.S, Guglielmo, J, Broeren, A.P., and Giguere, P., *Summary of Low-Speed Airfoil Data – Vol. 1*, SoarTech Publications, Virginia Beach, VA. June 1995.
3. Roskam, J., *Airplane Design: Part VI: Preliminary Calculation of Aerodynamic, Thrust and Power Characteristics*, Roskam Aviation and Engineering Corporation, Ottawa, KS. 66067, 1987
4. Raymer, D.P., *Aircraft Design: A Conceptual Approach*, 2nd ed., AIAA Education Series, Washington, D.C., 1994.
5. ElectriCalc. Vers.1.0. Computer software. SLK Electronics, 1996. PC.
6. MatWeb, by Automation Creations, Inc. online source www.matweb.com, accessed between 9/99-3/00.
7. Roskam, J., *Airplane Flight Dynamics and Flight Controls*, Roskam Aviation and Engineering Corporation, Ottawa, KS. 66067, 1979.
8. MotoCalc. Vers. 5.01. Computer software. Capable Computing, Inc., 1998.
9. ANSYS. Vers 5.5. Computer software. SAS IP, Inc., 1998

AIAA Design/Build/Fly Competition

Team: Fly By Knight



University of Central Florida

Team Members:

**Sebastian Echenique
Josh Lobaugh
Benjamin Goff
Art Morse
Jennifer Creelman
Sandra Guerra
Kristina Morace**

**Gary Ballman
Ia Whitney
Mirelis Cotto
Louis Turek
Kevin Chibar
Deyrah Jiminez
Carlos Figueroa**

**Tim Smith
Jennifer Lemanski
Jorge Pagan
Adam Ayala
Jeremy Fernandez
Peter Disusio
Patrick L. Bertiux**

1.0 EXECUTIVE SUMMARY	4
1.1 INTRODUCTION	4
1.2 TOOLS FOR DESIGN	5
2.0 MANAGEMENT SUMMARY	6
2.1 MANAGEMENT TIMING	7
3.0 CONCEPTUAL DESIGN	9
3.1 INTRODUCTION	9
3.2 CONCEPTUAL DESIGN CONSIDERATIONS	10
3.3 FOUR INITIAL PROPOSALS	11
3.4 FIGURES OF MERIT	12
3.5 CONCLUSION	13
4.0 PRELIMINARY DESIGN	14
4.1 DESIGN PARAMETERS	14
4.2 FIGURES OF MERIT	15
4.3 ANALYTIC METHODS USED	15
4.3.1 MOTO CALC	16
4.3.2 VISUAL FOIL	16
4.3.3 IDEAS	16
4.4 PRELIMINARY SIZING AND KEY FEATURES	17
4.4.1 WING SHAPE AND SIZING	17
4.4.2 FUSELAGE SHAPE AND SIZING	17
4.4.3 TAIL SHAPE AND SIZING	17
4.4.5 MOTOR RESEARCH AND TESTING	18
5.0 DETAILED DESIGN	19
5.1 POWER & ELECTRICAL	19
5.1.1 BATTERIES	19
5.1.2 MOTOR	20
5.1.3 WIRING	20
5.1.4 ELECTRICAL SYSTEM PERFORMANCE	20
5.2 AERODYNAMICS, CONTROL AND STABILITY	21
5.2.1 PERFORMANCE	21
5.2.2 STABILITY AND CONTROL	23
5.2.3 POWER CURVES	23
5.3 STRUCTURAL	24
5.3.1 FUSELAGE DESIGN	24

5.3.2 WING STRUCTURE	24
5.3.3 TAIL-BOOM DESIGN	24
5.3.4 LANDING GEAR TESTING AND PERFORMANCE	25
5.4.4 MECHANICAL/ELECTRICAL SYSTEM INTEGRATION	26
<u>6.0 MANUFACTURING PLAN</u>	<u>27</u>
6.1 OVERVIEW	27
6.2 FIGURES OF MERIT	27
6.3 FINAL SELECTION OF MANUFACTURING PROCESS	28
6.4 MANUFACTURING PLAN	28
6.4.1 FUSELAGE CONSTRUCTION	28
6.4.2 TAIL SURFACE CONSTRUCTION	29
6.4.3 WING SURFACE CONSTRUCTION	30
6.4.4 COMPOSITE GEAR CONSTRUCTION	31
6.5 MANUFACTURING TIMING	31
<u>APPENDIX A – MATHCAD CALCULATIONS</u>	<u>32</u>
<u>APPENDIX B – VARIOUS SELIG AIRFOIL CALCULATIONS</u>	<u>33</u>
<u>APPENDIX C – PRELIMINARY AIRFOIL ANALYSIS</u>	<u>36</u>

1.0 Executive Summary

1.1 INTRODUCTION

The University of Central Florida "Fly by Knight" (FbK) entry into the 1999-2000 AIAA Design/Build/Fly (DBF) competition has always been a team effort. Beginning with our very first meeting, everyone's input was noted and considered. These ideas and inputs were considered by an array of education and experience levels, and every comment from the first semester freshman's to the graduating seniors' was taken into account in achieving our final design. The resulting plane was designed over a series of regular team meetings in which all attending members of the group brainstormed. We began those meetings with a simple set of guidelines that stated, "These are our obstacles; how will we overcome them?" The limit on battery pack weight and the minimum amount of water to be lifted created many similar-styled aircraft, but no single idea was rejected until each suggestion was thoroughly analyzed.

In the course of our meetings we came up with several designs that ranged from a flying wing to a more typical double boom aircraft. The flying wing was one of the earliest designs considered. With this configuration the payload is easy to access from either a hatch on the back of the wing or on top of the wing surface. We have learned, however, from previous competitions in Wichita that a flying wing's flight characteristics are less than desirable in high winds. We continued on with this idea, nevertheless, until mounting doubts of building and flying such a plane forced the team to try other designs.

A range of ideas mostly centered on multiple-motored aircraft were considered. The team considered a single boom aircraft with multiple engine configurations. Single, double and triple engine designs were considered. Some tradeoff analyses were completed with each of the engine configurations after which the team decided to pursue a single engine aircraft. The team concluded that multiple engines consumed power excessively and would escalate material cost. With the inability to switch battery packs between sorties this effectively eliminated the multiple engine design.

With our final design pointing towards a single engine, the team started to look at the other characteristics of this typical aircraft design and its drawbacks. The most noticeable problem was the payload. With the standard design and the payload inside the plane, the removal and placement of the payload is not very efficient. It was with that obstacle in mind that the team decided a possible twin boom design should be considered. The ability to remove the payload easily and effectively from a hatch between the booms made the twin boom design well liked. Some of the other benefits were the fact that the structural integrity of bulkheads and other members would not have to be compromised to avoid twisting. Also, the smaller area seen in a side view of the aircraft was beneficial because of the high winds expected in Wichita.

The Student Branch of the UCF AIAA sponsored two design and experiment teams to perform further analyses as a class project. The first was a junior level design-of-experiments group. This group performed motor and prop testing using the low speed wind tunnel at UCF. When the group finished the analysis, an AstroFlight Cobalt 40 motor was selected (The Cobalt 40 is the base motor of the Cobalt 642S, later described). The second design group was a senior level CAD/CAM group, which looked at different

wing configurations using SDRC-IDEAS®. Using IDEAS the group was able to use the finite element analysis tools provided to optimize wing and spar configuration. From the analysis a tubular spar beam was shown to be optimal; however, due to manufacturing difficulties, an I-beam configuration was chosen instead.

1.2 TOOLS FOR DESIGN

The design tools used for the entire process were chosen for their ease of accessibility to all members of the team. From previous years of DBF competitions, the team leader had experience in what techniques and computational methods are best suited for the different steps in design and analysis of the aircraft. Most of the design and analyses were done with the aid of the following:

- SDRC-IDEAS®
- MATHCAD®
- Visualfoil
- Compufoil
- Real Flight
- Microsoft Excel®
- Motocalc
- Aveox's Virtual Test Stand

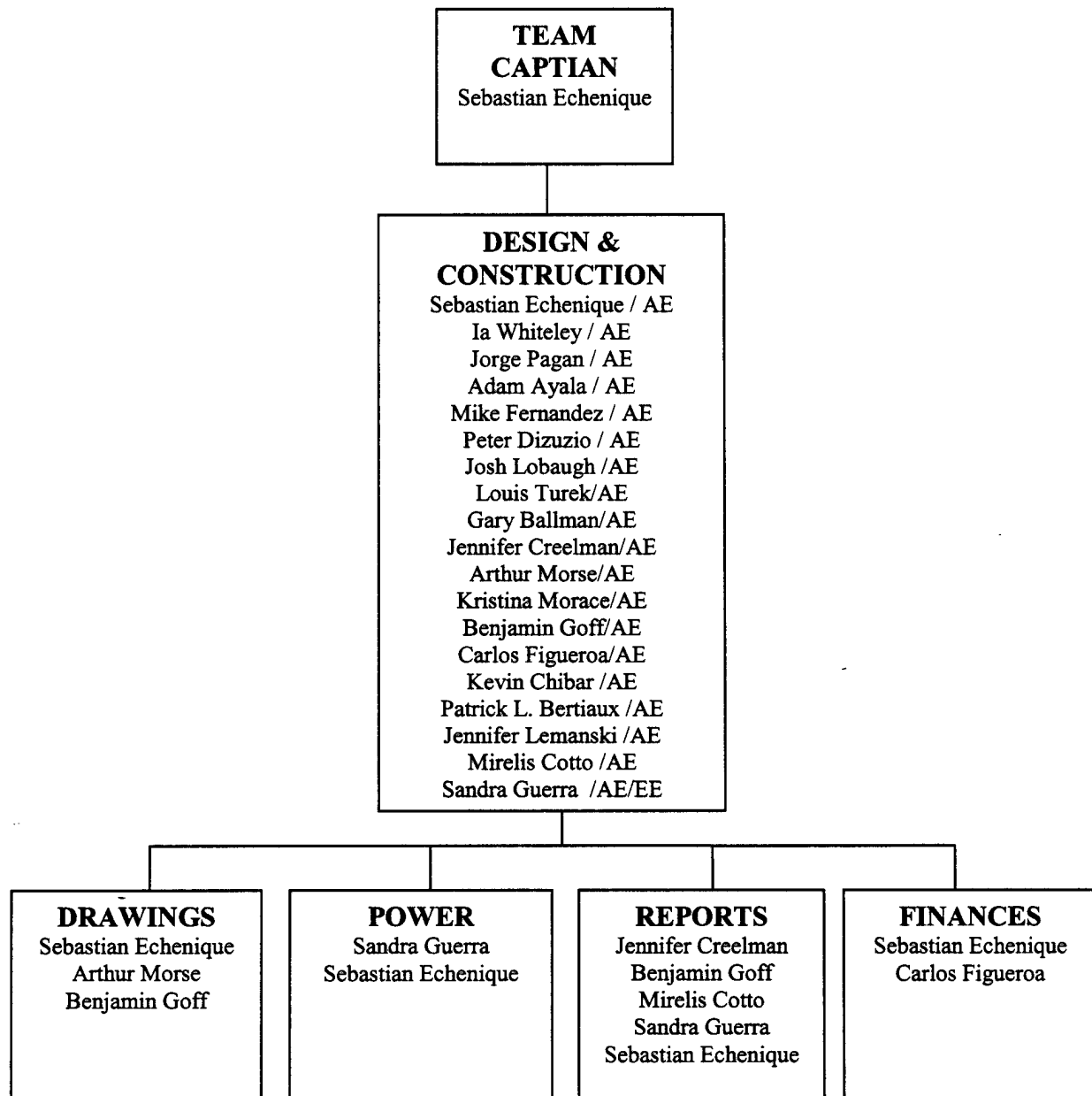
IDEAS and Visualfoil were utilized concurrently in the analysis of the wing. Visualfoil was used to provide the pressure coefficients needed in the IDEAS finite element analysis tools. In addition, Compufoil was used to determine the amount of sweep back in the wings required to produce a straight spar along the quarter chord. Compufoil was also utilized in the production of wing templates for cutting the foam core of the wings.

Motocalc and Aveox's Virtual Test Stand were applied to consider different configurations of the power system. By using both of these tools, the battery, propeller, and motor configuration were optimized to best fit the aircraft and conditions of flight.

Finally, Microsoft Excel® and MATHCAD® were used to mathematically examine ratios and flight characteristics of the aircraft. John D. Anderson's books entitled Introduction to Flight and Fundamentals of Aerodynamics were used extensively to develop the necessary spreadsheets and formulas. The program Real Flight (a commercially available R/C training program by Great Planes®) was used to virtually test the aircraft applying the calculated numbers, thus allowing us to witness the performance of the airplane without ever putting the actual aircraft in danger.

2.0 Management Summary

The design and development of the aircraft was divided among many students ranging from freshmen to seniors. This strategy enables the seniors to pass down their knowledge of design and manufacture to the underclassmen. The following flow chart shows the distribution of tasks as laid out by the team captain, Sebastian Echenique.





Team leader Sebastian Echenique organized team meetings, ordered material, managed the budget and divided the team into its five different sections making sure that everything went according to schedule. Sebastian is a senior Aerospace Engineering student with three years of experience designing, building, and flying remote control airplanes. Previous experience in the AIAA Design/Build/Fly (DBF) competition earned him the position as team leader. Most of his time was spent teaching the underclassmen how to build a radio-controlled airplane, as well as teaching the fundamentals of low speed aerodynamics as to apply to the design of FbK.

The construction as well as the design was definitely achieved through team work. Sebastian made sure that all team members worked on the construction of the plane and also gave input into the design of the plane. Plane meetings were conducted twice a week, where everyone brought ideas to the meeting and discussed them. After an idea was proposed, its pros and cons were listed, helping the team vote on the final design.

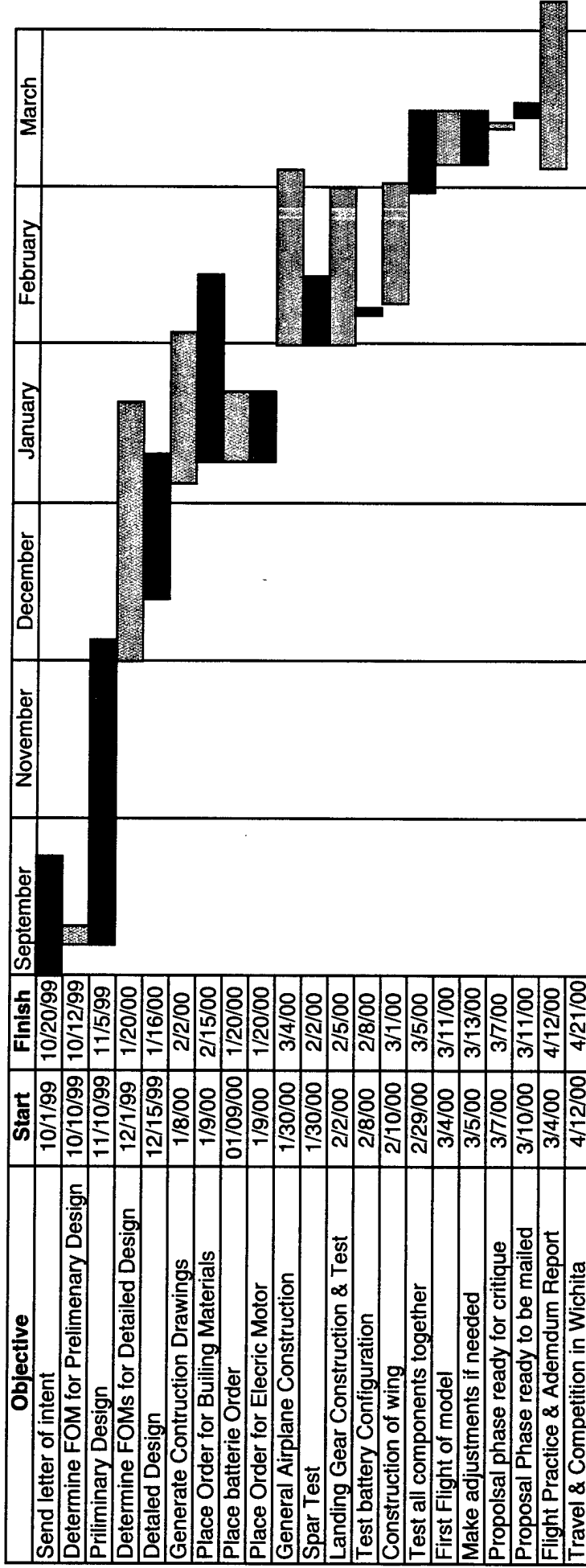
The rest of the work was divided into four sections: Drawings, Power, Reports and Finances. Blue prints were drawn by Sebastian Echenique and Arthur Morse and the detailed drawings were completed by Benjamin Goff in AutoCAD. Sandra Guerra was in charge of power because she is working towards a double major in Aerospace Engineering and Electrical Engineering. Reports were written by Jennifer Creelman, Benjamin Goff, Mirelis Cotto, Arthur Morse and Sebastian Echenique. Finances were handled by Carlos Figueroa (Chair of AIAA) and Sebastian Echenique (Vice Chair).

2.1 Management Timing

In order to complete these tasks on time, the following timeline was created. Limited time was a crucial factor in the design and building of the plane, and therefore the schedule was followed as accurately as possible.

Number	Task	Predicted Schedule Event	Actual Event Completion Date
1	Establish FOM's for conceptual design	9/3/99	9/3/99
2	Conceptual Design	9/30/99	9/30/99
3	Send letter of intent	10/15/99	10/20/99
4	Determine FOM's for Preliminary Design	10/10/99	10/12/99
5	Preliminary Design	11/10/99	11/5/99
6	Determine FOM's for Detailed Design	12/1/99	1/2/00
7	Detailed Design	12/15/99	1/16/00
8	Generate Construction Drawings	1/8/00	1/20/00
9	Place Order for Building Materials	1/9/00	1/12/00
10	Place Battery Order	1/9/00	1/12/00
11	Place Order for Electric Motor	1/9/00	1/12/00
12	Start Building Plane	1/30/00	2/2/00
13	Spar Test	1/30/00	2/2/00
14	Landing Gear Test	2/2/00	2/5/00
15	Test Battery Configuration	2/8/00	2/8/00
16	Start Construction of Wing	2/10/00	2/25/00
17	Test all Components Together	2/30/00	3/5/00
18	First Flight of Model	3/4/00	3/11/00
19	Make Adjustments as Needed	3/5/00	3/13/00
20	Proposal Phase Ready for Critique	3/7/00	3/7/00
21	Proposal Phase Ready to be Mailed	3/10/00	3/11/00

University of Central Florida
Aerospace Engineering



3.0 Conceptual Design

3.1 INTRODUCTION

The conceptual design of the competition aircraft consists of the problem statement (rules), the development of the ideas, feasibility of those ideas, preliminary costs, and timelines. To allow more time for further recruitment, a series of design meetings/open houses were introduced. At these sessions, the rules and design concepts were discussed in detail.

The general rules of the competition are:

Team Requirements

- All team members must be full time students at the university except for the pilot.
- 1/3 off the team members have to be freshmen, sophomores and juniors.
- Pilot need to be AMA certified.

Aircraft Requirements

- The aircraft may be of any configuration except rotary wing or lighter-than air.
- Maximum wing span is 7 feet.
- Must be propeller driven and electric powered with an unmodified, over the counter model-electric motor. May use multiple motors and/or propellers. May be direct drive or with gear or belt reduction. For safety, each aircraft will use a commercially produced propeller. Teams may modify the propeller diameter by clipping the tip.
- Must use over the counter NiCd batteries. For safety, battery packs must have shrink-wrap or other protection over all electrical contact points. The individual cells must be commercially available, and the manufacturers label must be readable (i.e. clear shrink wrap preferred).
- Maximum battery pack weight is 5.0 lb. Battery pack must power propulsion and payload systems. Radio Rx and servos (only) may be on a separate battery pack. Batteries may not be changed between sorties during a flight period.
- Aircraft and pilot must be AMA legal. This means that the aircraft TOGW (take-off gross weight with payload) must be less than 55 lb., and the pilot must be a member of the AMA. Since this is an AMA sanctioned event, the team must submit proof that the aircraft has been flown prior to the contest date (in flight photo or video).

After reading the rules, the team had several problems to solve. A general problem statement was developed and is listed below:

With the given constraints imposed by the AIAA DBF rules, the problem is to design and fly an aircraft capable of lifting the required sortie (and more), while maintaining a low overall cost, a low weight and a strong, safe airframe.

The team considered some innovative ideas in the early design stage. Strong emphasis was placed on four general areas, which all preliminary designs must satisfy.

These four areas of interest were Power, Aerodynamic Concerns, Stability and Control, and Structural Design.

3.2 CONCEPTUAL DESIGN CONSIDERATIONS

The power of our aircraft is of utmost importance. The batteries will be the only source of power on our aircraft. The battery requirements from the AIAA DBF rules are:

- “Off the shelf” Nickel Cadmium (NiCd) batteries
- Cumulatively weighing no more than 5 lb
- Must be shrink-wrapped

This immediately establishes a limit of the maximum power available. Many NiCd battery sizes were researched. The properties of the batteries that we were concerned with included the storage capacity, operating voltage, weight, size, and price. It was determined that a high capacity battery complying with our weight and size restrictions would increase the flight time. A table was compiled that emphasized the power-to-weight ratio of the batteries. This table is located to the right (Table 3.1). In our analysis, the batteries with the highest current to weight ratio were the AAA cells, the A cells and the Sub-C cells. Upon checking for availability, the AAA's were not expected to be in stock until after a crucial deadline of first flight. So, the AAA's were discounted in any further analysis. From our chart, personal experiences, and by reading other Universities reports, two main types of batteries were looked at in detail: Sub-C's and A's.

It is known that, in most cases, as the stability of an aircraft increases the maneuverability of the plane decreases. Designing a plane so that it will have both stability and moderate maneuverability presents the use of a design compromise. The reasoning behind the desire to design a plane to have increased maneuverability is to minimize the turning radius at the edges of the course. This theoretically would allow more time to complete full sorties, the underlying goal of this competition.

Table 3.1 - *Batteries Weight vs Current Chart*

<u>Type</u>	<u>V</u>	<u>I (mAh)</u>	<u>weight (g)</u>	<u>I/W (mAh/g)</u>
<u>AAA</u>	1.2	150	4	37.5
	1.2	250	4	62.5
<u>AA</u>	1.2	110	7	15.714286
	1.2	270	14	19.285714
	1.2	600	24	25
	1.2	800	23	34.782609
<u>A</u>	1.2	500	19	26.315789
	1.2	600	18	33.333333
	1.2	1000	26	38.461538
	1.2	1400	31	45.16129
<u>subC</u>	1.2	1000	39	25.641026
	1.2	1300	50	26
	1.2	1500	47	31.914894
	1.2	1800	47	38.297872
	1.2	1900	56	33.928571
	1.2	2300	58	39.655172
<u>C</u>	1.2	2000	80	25
	1.2	2500	81	30.864198
	1.2	3000	84	35.714286
<u>N</u>	1.2	150	9	16.666667



Stability and control of the any aircraft is determined by the control surfaces, the power of the motor, the placement of components and the velocity of the craft (through all ranges). The control surfaces of the competition aircraft must be strong, strategically placed and properly dimensioned to avoid the inherent penalties of aerodynamics: weight and drag. Such control surfaces considered in the design process were canards, wings, flaps, ailerons, flaperons, rudders, elevators and elevons.

Another important factor in the conceptual design was the ranges of speed endured by the aircraft and the maintainability of those speeds. Through the use of the low speed wind tunnel and a power supply, hours of work were utilized to determine the thrust profiles of many props and different motors.

It is very easy to find information of the latest building trends of modelers. Numerous publications, Internet web sites, local hobby stores and videos carefully explore the various techniques that can be used when building a plane. It is usually a common goal to build a lightweight yet durable aircraft for flight. The most common materials currently used for construction of competition vehicles are balsa wood, foam, and Carbon Fiber. All of these products are lightweight and strong when assembled together properly.

At this stage of the design process, the different conceptual designs were beginning to emerge into their own ideas and concepts. Each of the separate conceptual designs had its own unique structural problems. There was one airframe number that was common to all of the concepts; a seven foot wingspan.

The very fact that our objective is an airplane means Aerodynamic considerations must be taken into account. There were several parameters that every prototype concept in our process must qualify: lift, drag, take-off distance, and general stability.

3.3 FOUR INITIAL PROPOSALS

During the series of open houses and conceptual design meetings, four initial proposals were considered. They were given names by the persons whom initially thought of them. By naming them we are able to effectively describe unique characteristics of the individual concept planes. The concepts were:

- Flying wing (Delta Flyer)
- Double-boom single motor (Fly by Knight – FbK)
- Dual-motor (Dually)
- Tri-motor (Big Mama)

The flying wing idea was an excellently developed concept. The primary reason to use a flying wing is to attain as much lift as possible. Achieving more lift means the craft can carry more payload. There are many advantages to using a flying wing: the previously mentioned high lift, low drag, and large internal volume are just a few. However, to an inexperienced team, a flying wing represents a design and construction nightmare. Also, no member of our team has ever flown a flying wing – nor knows any one who has.

The traditionally styled Fly by Knight (FbK) aircraft was developed to streamline the process of design and construction. A primary concern of the designers of the FbK was the gusty crosswinds in Wichita in Spring. Special attention was paid to the cross section of the fuselage and extra steps were taken to minimize that cross-section. The

FbK has many advantages. A small cross-section, a single motor (to minimize power required), and a simple design are just a few. The drawbacks to this design are the limited payload and poor performance at low speeds (take-off and landing). The FbK was the smallest of the design concepts.

The Dually is a combination of two motors and a single fuselage. This concept was developed to be an option between the powerful Tri-motor and the somewhat questionably powered FbK. The Dually, as the name implies, has two motors (probably mounted on the wings) and has a non-complex fuselage. Some advantages of the Dually are the additional power of the second motor and the additional structure of the wing mounts. Some disadvantages of this concept are the additional weight, price, and complexity.

The Big Mama is a three motor airplane. The Big Mama was a design that came about after concerns of not being able to take-off in the allotted runway space. The Big Mama shares all of the Dually's advantages. As a special note, very interesting airfoil research was done on this concept. The Big Mama's biggest disadvantages are the consumption of power by its three motors. The disadvantages of the third motor are the additional wiring, weight, electronics, re-enforcement's imposed on the team and airframe by that third motor and the fact that the third motor doesn't significantly help the plane get off the ground any faster. The big mama was the largest of the design concepts.

Below is a brief graphical interpretation of the evaluation process:

Table 3.2 - *graphical interpretation*

	FW	FBK	DUALY	TRI
airfoils investigated	NACA 4412 NACA 63213	NACA 2412 NACA 0012	Clark Y FX-60100-126	Selig S1223 NACA 4412
Distance needed for takeoff (max power)	89	133	65	58
Total Lift (est.)	6.8 /NACA 4412 4.0 /NACA 63213	5.8 /NACA 2412 4.8 /NACA 0012	6.2 /Clark Y 4.9 /FX-60	14.37 /Selig S1223 6.8 /NACA 4412
Total Drag (est.) (Fuse drag (0.04) + wing drag)	0.11 /NACA 4412 0.07 /NACA 63213	0.10 /NACA 2412 0.08 /NACA 0012	0.10 /Clark Y 0.08 /FX-60	0.13 /Selig S1223 0.11 /NACA 4412
general stability rating and other comments	Nothing that UCF AIAA has modeled	Similar to other models	Similar to two motor systems	Unknown flight characteristics
ease of construction	N	Y	Y	N

3.4 FIGURES OF MERIT

The potential problems of the designs are numerous. A serious concern displayed by all team members was the landing gear. The landing gear must be strong enough to handle take off and landing forces, while at the same time creating the least amount of drag possible. The team decided that the wheels on the plane should be larger than

normal to handle runway conditions (lower the friction incurred) and add more height to the plane so that the tail wouldn't drag at a 10 degree angle of attack.

The landing gear of an airplane must endure punishing loads. These loads occur mostly on landing. Various types of commercially available landing gear were researched. It was determined that the appropriate landing gear to absorb the loads (encountered by these concept planes) were for large-scale model aircraft. This type of landing gear physically does not fit any of our conceptual designs. Time was invested in the design of a torsion landing gear system and also a composite landing gear system.

Take off performance was another common problem to all airplane designs. Our initial numbers were based on ideas and assumptions (low Reynolds numbers, low ground effect, wing placement, etc...). Therefore, the preliminary numbers are somewhat unreliable.

3.5 CONCLUSION

It was now time to gather the best ideas and start working toward one realistic design. After weighing the pros and cons of each design, no direct decision was able to be made. There were still too many unanswered questions. The team did realize how important it was to start working together. In the spirit of the team, several options of design concept integration were considered. After a brief period of time the team decided to investigate the FbK design in combination with the other three designs. Design Techniques were examined to determine how a conservative or traditional design could be modified and redesigned into an optimum decision. The determination of the actual dimensions of the plane; the wingspan, aspect ratio, weight and size of the fuselage, was beginning to converge into one design.

4.0 Preliminary Design

4.1 DESIGN PARAMETERS

In this phase of the design, specific components are narrowed from the conceptual design phase. The following design parameters were primarily considered during the preliminary design phase:

- Wing loading
- Taper ratio of the wing
- Aspect ratio
- Lift to Drag ratio
- Twin boom configurations
- Power requirements
- Thrust to weight ratio
- Fuselage shape and size
- Payload requirements
- Landing gear requirements

To determine the best wing for the aircraft, various parameters were studied including numerous airfoils, the wing aspect ratio, and the taper ratio of the wing. The choice of an airfoil is very important because it determines the force and moment system distribution acting on the wing. The next determining factor of the wing is the taper ratio. It was found that a wing can be designed with a taper ratio, such that it creates a lift distribution almost identical to the elliptic case in which the induced drag is minimal.

The next area of focus concerning drag as well as stability was the tail. The initial design of the tail boom on the FbK was going to be a high strength Carbon Fiber rod. This was chosen to streamline the process of tail boom and tail surface design construction. The part of the team responsible for financial transactions seriously questioned the spending of money for Carbon Fiber rods of appropriate thickness (to resist bending from the aerodynamic loads of the tail). And yet more questions arose about the ease of the loading and unloading of the payload. Spending several hours "re-optimizing" the FbK, it was determined that a double boom structure would be the quickest way to resolve the questions in conflict. One of the benefits of a twin boom was to avoid torsion of a single boom. The twin boom would also provide more control in windy conditions predicted at the competition site. The team's only concern of the twin boom was that the plane did not become tail heavy. After this decision, a revision was made to our design blueprints and the construction of the tail boom commenced.

Primarily the thrust to weight ratio and the desired power output were studied to achieve efficiency in performance of the plane. The thrust to weight ratio was calculated to ensure that the plane would be able to take off within 100ft.

The shape of the fuselage was predominantly determined by the payload to be carried by the plane. The size of the fuselage was determined by how many water bottles we wanted to carry. Given the weather conditions of Wichita and the fact that the overall score of the competition was flight score * report score/cost of aircraft, the team decided that the most logical approach to winning the competition was to proceed with a small



airplane carrying only two water bottles minimizing the physical size and complexity of the plane and therefore the cost of it.

The landing gear and wheel configuration was the final design parameter determined. The landing gear had to be strong enough to handle take-off and landing forces, while at the same time creating the least amount of drag possible. The team decided that the wheels on the plane should be larger than normal to handle runway conditions and add more height to the plane so that the tail wouldn't drag at a 10 degree angle of attack.

4.2 FIGURES OF MERIT

The constrictions to our design were as follows:

- Ease of construction
- Ease of transportation
- Structural Integrity
- Payload access
- 5 pounds of Batteries

Ease of construction was a major restriction in the design of the aircraft. The majority of the team is underclassman with little or no experience of the construction of a radio controlled airplanes. Also, the time to build the plane was factor. A long construction period would result either in a shorter flight testing period or a withdrawal from competition due to an unfinished airplane.

Ease of transportation was also highly important in the design of the airplane. The airplane had to be able to transported from Florida to Kansas easily. The aircraft also had to be transported to the local flying field (RC World) where we were allowed to use their field for flight-testing. The team made the assumption that it would be easier to design a car faring to transport the airplane.

The next concern of the team was the structural integrity of the wing. The wing would have to under go a spar test conducted at competition. This test would ensure that the wing could hold the weight of the aircraft when lifted by its wing tips. In addition to the spar test, the plane would have to endure rough take off and landing conditions. This was noted from the experience of the previous competition held in the same place in Wichita, Kansas in which the runway conditions were brutal on the plane.

Payload access also had to be considered in the design. The plane would fly two consecutive sorties, one carrying the payload and the other without the payload. Therefore easy access to remove or pack the payload was a must to ensure quick ground time and aircraft handling safety.

4.3 ANALYTIC METHODS USED

Before using analytic methods, the team performed some initial "back of the envelope calculations" to determine the desired lift and power. Obtaining these figures we then turned to analytic tools to determine appropriate wing dimensions and battery configuration.

Table 4.1 – Ideal Characteristics

Ideal Lift	15 lbf
Ideal Drag	.05 lbf
Ideal Power	700 W
Ideal Flight Time	15 min

4.3.1 MotoCalc

The team used MotoCalc optimization software to size the propulsion system. MotoCalc is readily available over the Internet and is quite simple to learn and use. This software uses very basic properties such as motor, batteries, propeller specifications, weight, and airfoil specifications to give estimated powered flight parameters. These parameters include battery amps, power in, power out, motor amps and volts, run times, takeoff speed, thrust and drag.

Using this software, we input several variations of battery sizes, number of cells and motor specifications. Ultimately, we were able to see which power system configuration was going to be most effective. By most effective, the team looked specifically at parameters that most closely matched the mission requirements: namely low speed, high endurance specifications. Therefore, run times, thrust and drag forces were the most crucial elements in the decision-making process of elimination regarding battery size and system configuration.

4.3.2 Visual Foil

Hanley Innovations' VisualFoil 4.0 was used to do virtual testing on a series of airfoils. This software gives you the power to find coefficient of lift, coefficient of drag, pressure distribution, coefficient of lift to coefficient of drag polar, stagnation points, transition points, and separation points. This program lets you work with any Reynolds number and the airfoil can be tested at different angles of attack. The Selig 1223 was the chosen airfoil for testing. Testing was performed at 6 degrees angle of attack (with 15% flaps at 15 degrees deflection) and at Reynolds numbers of 150000. The result provided by the software was a Coefficient of maximum lift is 3.175, coefficient of drag of the wing 0.029 and the center of lift is at 44% of the cord.

4.3.3 Ideas

Using Master Series Ideas, two design groups analyzed the structural integrity of the wing subjected to normal flight conditions. The first group was a senior level Finite Element Modeling (FEM) CAD/CAM team who investigated new foam called syntactic foam. They determined that this foam, although incredibly strong, is too heavy for wing application in Remote Control (R/C) modeling. The second team in the same CAD/CAM class analyzed a wing using

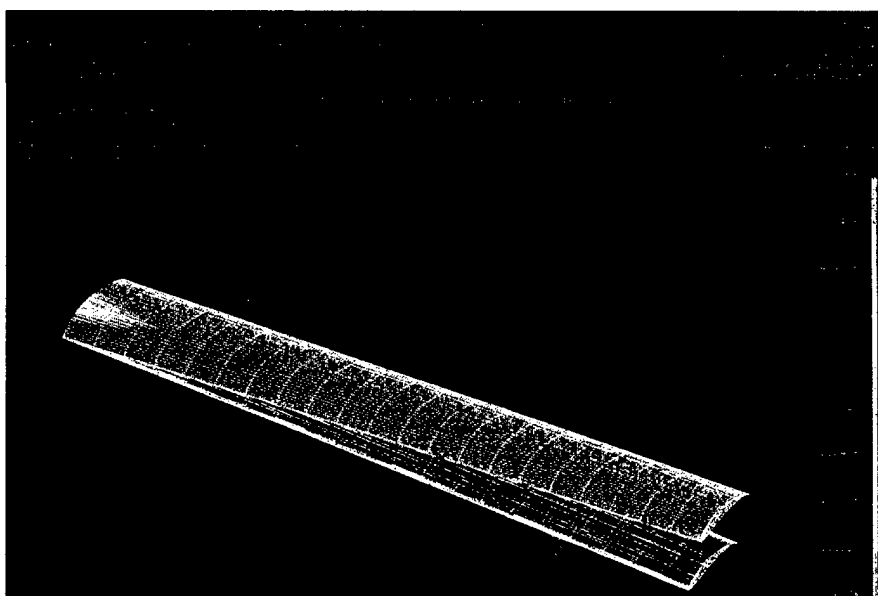


Figure 4.1. CAD/CAM Analysis

standard "off-the-shelf-foam" and Carbon Fiber. The second team determined the structure of several wings with various types of spars that were acceptable in the weight, strength, and cost categories.

4.4 PRELIMINARY SIZING AND KEY FEATURES

4.4.1 Wing Shape and Sizing

The wing of the aircraft is the sole provider of aerodynamic lift on the airplane. It is imperative that the wing be strong and light. The wingspan was limited to seven feet by competition rules. To achieve the greatest lift, the team decided to go with a seven-foot wing and vary the aspect ratio to find the optimum performance of the wing. The designers of the FBK wanted to acquire the highest lift airfoil possible. The reasoning behind the need to find the high lift airfoil was the ability to get off the ground quickly. The Selig 1223 yielded the most efficient results, as shown in Table 3.1. This airfoil is designed for maximum performance at low Reynolds numbers.

In order to take off in the given distance (100 feet), an optimum surface area of the wing was determined to be between 600in^2 and 800in^2 . Using the takeoff distance equation, the most efficient surface area was found to be 756in^2 . Based on easy geometry for construction, an 8in tip chord and a 10in root chord was chosen. These dimensions yield a taper ratio of 0.8. Using this information and the span of the wing (84in) the aspect ratio was calculated to be about 9.33.

4.4.2 Fuselage Shape and Sizing

Several options of the design of the FBK were presented in the conceptual design phase. The main structure of the FBK is the fuselage. The fuselage is the structural part of the aircraft that integrates the wings, tail booms, the payload and the other subsystems used for flight. The critical goal of the fuselage is to accomplish all of the aforementioned integration while maintaining a low weight.

The Structural Design of the FBK is very simple. Two options were discussed about the construction of the fuselage. One of the options was a bulkhead-stringer concept. The second was a traditional box shaped structure. While the traditional box-shaped structure is easier to build and construct, the bulkhead-stringer concept allows more freedom to modify while construction is "in progress." The bulkhead-stringer concept is also lighter and much easier to reinforce (should the need arise). Another positive aspect of the bulkhead-stringer concept is the ability to re-use the standard jigs and tools used in cutting the many parts (production of spare parts and additional airplane components).

4.4.3 Tail Shape and Sizing

A major contribution to stability and control is that of the tail. The horizontal and vertical components of the tail were initially located by comparing the locations of these components on other planes. The decision of a twin boom was primarily to solve the problem of easily loading the payload. In addition to this, the twin tail would also help in the twisting problem of the previous single rod tails have had and the very windy conditions.

4.4.5 Motor Research and Testing

The Research on the motors was done over the Internet, in our wind tunnel, and through programs commercially, and privately developed. The initial research on model aircraft motors yielded two common choices; direct drive or gear driven motors. The gear driven motors are typically for low speed heavy-lift model aircraft while the direct drive motor is for racing.

The Aveox motors offer a lot of power for the money. They have built onto there site a "virtual test stand" that can virtually test any motor that they make. They also offer an excellent customer service line. Previous UCF electric airplane team have used the Aveox 1406-4Y, and the Aveox 1412-5Y. These previous teams have had limited success.

The Cobalt series is much readily available for most hobby stores, hobby catalogs, and Internet hobby sites. The Cobalt motors do not have the high efficiency that the Aveox motors do, however, the are less expensive. UCF AIAA also has access to one Cobalt 40.

Because UCF AIAA has access to these motors, UCF AIAA sponsored a junior design class team to test these motors in a wind tunnel.

The test yielded various results. The Aveox "virtual test stand" is somewhat accurate. We were never able to develop the thrust, RPM or maximum voltage draw. The team was never able to get "ideal" numbers from the manufacturer of the Cobalt motor, however,

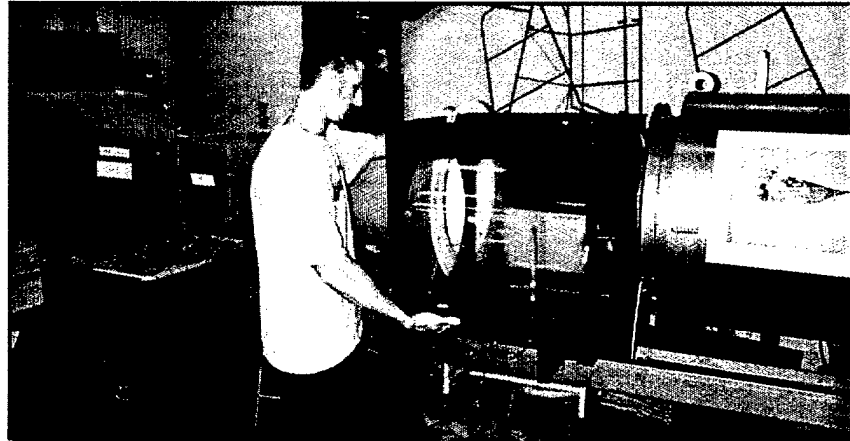


Figure 4.3 - Wind Tunnel Testing

the Cobalt motors did have better overall performance. For a similar prop size the Cobalt motor was able to spin faster and stay cooler versus the Aveox motors.

It was later determined that the Cobalt does offer a better performance with our particular battery. For this reason, the Cobalt 40 was chosen. While in testing, the question of a gearbox arose.

Based on the conclusion of the electrical system modeling, a gear driven motor was selected (based on our calculation program - MotoCalc). After further deliberation a choice was made to purchase a motor pre-configured with the gearbox (It is easier to remove a gearbox rather than add it later). After the appropriate reading was completed, There were only a few motors that qualified for further study. The Cobalt 40 size motors and the Aveox 14 series. The final choice was the Cobalt 642S. The 642S has a pre-configured with a 4.3:1 gearbox.

5.0 Detailed Design

In this phase of the design, specific components are narrowed from the conceptual design phase. The preliminary design consists of two major parts; The team break-down and Vehicle Subsystem design and integration.

The electric airplane team was finalized and broke down into three basic units. The captain chose the members for each subsystem. The captain's choices are based on the individual's request and personal experience.

Subsystems:

- Power & electrical
- Aerodynamics, Control and Stability
- Structural

5.1 Power & Electrical

5.1.1 Batteries

Battery selection was a drawn-out process. Not only was weight an issue, but so were geometric size and the capacitance-to-weight ratio of several A and sub-C batteries considered. There was an imposed limit of five pounds of batteries. Instead of trying to select the largest battery, we decided to choose a smaller battery that had a high capacitance to weight ratio. This would allow us to configure the battery packs to be carried easily within the confines of the fuselage. Because our team had decided to run many missions with two bottles, we felt that the propulsion system should be optimized for low speed endurance, rather than power.

Since we were trying to achieve many sorties with a limited space for batteries, it was agreed upon that weight was a crucial factor in our selection. More than 50 grams was considered the limit that the selected battery would not cross; this eliminated only three batteries from consideration.

The next selection criterion was the battery's milliamp-hour (mAh) rating. This rating is the manufacturer's estimate of the amount of current, measured in millamps, delivered in one hour. We wanted the plane to fly for as long as possible in order to complete many sorties, hence the cut-off line was selected as greater than or equal to 1000 mAh. This effectively eliminated six more battery choices.

The final selection criterion used to choose the battery was the capacitance-to-weight ratio. It was agreed upon that past teams had used the capacitance-to-weight ratio as a starting point for their battery selection and that our inexperienced team would follow suit. The final selection from among the remaining five choices was the Sanyo 1400AE, since it had the highest capacitance-to-weight while still satisfying the other three selection criteria not to mention its lower internal resistance.

5.1.2 Motor

Experience with certain motors and propellers became the key factor in choosing a particular combination for the propulsion system. The motor selection was made from among several choices available from Astroflight and Aveox. Brushless motors are used for racing, and since the mission requirements we specified were for low speed endurance rather than racing, we decided a geared motor would be a better choice. The pilot had extensive experience with Astroflight's products, and since the team already had access to a Cobalt FAI-40 motor, the 642S was the one chosen.

The recommended number of cells for the engine according to the manufacturer, is eighteen wired in series. This would give a total voltage of 21.6V. Allowing for an 80% efficiency, the working voltage was modeled at 17.28V. The electrical energy available is $1.25 \text{ volts per cell} \times 1.4 \text{ amp hours} \times 18 \text{ cells} = 31.5 \text{ watt hours}$. This translates into 83,492 foot pounds of potential energy. Given that our plane weighs 13.5 pounds fully-loaded, this translates into a potential altitude of 5566 feet. Using MotoCalc optimization software, team members were able to select the optimum propeller dimensions, the best number of cells for mission requirements, and anticipate the required takeoff speed and angle of attack to complete the missions as designed.

5.1.3 Wiring

Before we reached the construction phase of our design we wanted to have planned the wiring of the aircraft. The wiring is extremely important because if not properly done can cause serious injury (through fire, shock and heat), and system malfunction. The timely delays in the electric system research caused innumerable problems with the internal wiring. As directed by the captain, a certain electrical bus was placed on the top of the fuselage, in which the electric system must conform. To connect the batteries to the motor a system of six battery packs were chosen. Each battery pack consists of six A batteries wired in series. On each side of the aircraft three packs were placed and put in series with each other through a common connection wire spanning the length of the aircraft. Both battery pack sides were in turn placed in parallel. This effectively gave us 18 batteries in series on either side, and two packs of 18 wired in parallel.

5.1.4 Electrical System Performance

The Pilot Response System (PRS) consists of the radio system and the motor-battery system. The radio system consists of a transmitter, a receiver, a flight system battery, the control servos, and two antennas (one for the receiver and one for the transmitter). The motor-battery system consists of the propulsion batteries, the motor, all the wiring, and the speed controller.

This part of the electrical subsystem is the single most important part of the airplane. If the pilot can not remotely control the aircraft, the airplane is doomed for failure and likely to damage property and injure personnel.

5.2 Aerodynamics, Control and Stability

5.2.1 Performance

Tables were produced of the various data parameters defining the FbK. The data obtained in this table specifies the estimated weight of the plane, the sizing and configuration variables, and the design lift and drag parameters. Carrying the maximum payload desired for FbK (2 one liter bottles), the weight of the aircraft was calculated to be 12.5lbs. Without the payload the weight of the plane was found to be 8.0lbs. Using this information the payload fraction was calculated to be 0.632.

Relating the weight of the airplane with payload to the thrust of the motor, the data indicated a take off distance of 75ft with a lift off velocity of 19.4 mph. This data also relied on the surface area of the wing (756 in^2), that was designed to maximize the lift of the airplane.

The first phase of the mission was designed to take off at full throttle and then cut back to $\frac{3}{4}$ throttle to maximize the life span of the batteries. With the horizontal take off velocity being 19.4 mph, the angle of attack had to be increased to 6 degrees to ensure lift off. With the take off velocity at the given angle of attack, the aircraft was predicted to be taking the first turn of the sortie at an altitude of about 100ft. The turning radius is 46 feet and has a radial speed of 0.183 radians per second.

The second part of the mission was designed to be the gliding phase of the mission. Since the lifetime of the batteries is a crucial factor in the flight characteristics of the plane, gliding would save on power. Three quarters thrust would allow the plane to achieve a 1.2 g's turn with a radius of 46 feet.

The final portion of the mission would be the landing of FbK. Upon landing, flaps would be fully deflected slowing the plane down to a velocity of 21 mph. The landing distance is predicted to be stop within 149 ft. after touchdown.

Table 5.1 Weight Estimates

Payload weight (lbs)	W_p	4.4
Power system weight (batteries, speed control) (lbs)	W_b	2.75
Dry weight of aircraft (lbs)	W_a	4.6
Total payload weight (non-structural) (lbs)	W_{pt}	7.9
Total aircraft weight (lbs)	W_t	12.5
Payload fraction (W_{pt} / W_t)	PF	0.632

Table 5.2 Configuration Variables

Wing loading at takeoff (lb/ft^2)	WL	2.4
Aspect Ratio	AR	9.33
Wing reference area (in^2)	S	756
Wing span (ft)	b	7

Mean aerodynamic chord length (in)

Cbar 9**Table 5.3 Drag and Lift Performance Parameters**

Oswald efficiency factor	e	0.92
Takeoff coefficient of drag	C_{Dto}	0.0431
Takeoff coefficient of lift	C_{Lto}	3.175
Cruise coefficient of drag	C_D	0.01278
Cruise coefficient of lift	C_L	1.574
Landing coefficient of drag	C_{Di}	0.0191
Landing coefficient of lift	C_{Li}	2.01

Table 5.4 Aircraft Takeoff Performance Estimate

Liftoff velocity multiplier	vm	1.2
Density of air (lb*sec ² /ft ⁴)	ρ	0.002377
Takeoff distance (ft)	S_{lo}	75
Wing height above ground (ft)	h	0.8
Rolling friction coefficient	μ_R	0.02
Ground effect	φ	0.77
Average drag (lbs)	D_{avg}	0.433
Average lift (lbs)	L_{avg}	6.693
Takeoff thrust to weight ratio	TtW	0.32
Takeoff velocity (mph)	V_{lo}	19.4
Estimated takeoff thrust (lbs)	T_{lo}	4

Table 5.5 Aircraft Landing Performance Estimate

Landing velocity (mph)	V_{ld}	21
Landing ground roll (ft)	S_{ld}	423
Landing weight (lbs)	W_l	12.5

Table 5.6 Aircraft Turning performance

Turning Velocity (mph)	V_{tu}	30
Turning Radius (ft)	R_{tu}	37

5.2.2 Stability and Control

The ability of an aircraft to resist disturbances during its flight and to process control inputs is vital to its ability to fly successfully under adverse conditions. It is important that the aircraft have sufficient inherent stability to resist wind and other disturbances without seriously reducing maneuverability. In addition, the sensitivity of the aircraft to control inputs cannot be so reduced that the pilot must work harder to perform even minor maneuvers. However, the plane must also not be too sensitive to control inputs, as this would make the plane excessively touchy.

The stability and control calculations performed were based on the geometry of the plane and its control surfaces. The equations were taken from the textbook "Flight Stability and Automatic Control" by Robert C. Nelson. The various geometric values were used to compute the control coefficients. Control coefficients are coefficients, which described the ability of a given control surface to impart a moment (pitching, rolling, and yawing) to the aircraft. Also included in the calculations were the coefficients inherent to the aircraft, such as the pitching moment coefficient of the wing. It was important to take all moment coefficients into account to ensure that the aircraft would maintain wings level low angle of attack flight during cruise, and be resistant to wind disturbances. By calculating the moment coefficients in all three axes of rotation, it was possible to estimate what range of control surface deflection would be required to counteract disruptions to the aircraft. It was also possible to design the aircraft to combat disturbances which the aircraft will likely see, such as cross winds during takeoff and landing.

5.2.3 Power Curves

The maximum lift-to drag ratio (L/D) for the aircraft can be obtained from the power Required (P_R) versus Velocity Relationship, ranging the free stream velocity from 0 ft/s to 80 ft/s. The Thrust required is dependent on the Weight and the Lift to Drag Ratio of the airplane.

The Power available is limited to the motor and the batteries that were selected. The motor that the team picked is the Cobalt 642S with a 4.3:1 gear ratio. The Power Curve for the Selig 1223 and Cobalt 40 with Super-box gear ratio of 4.3:1 is shown above.

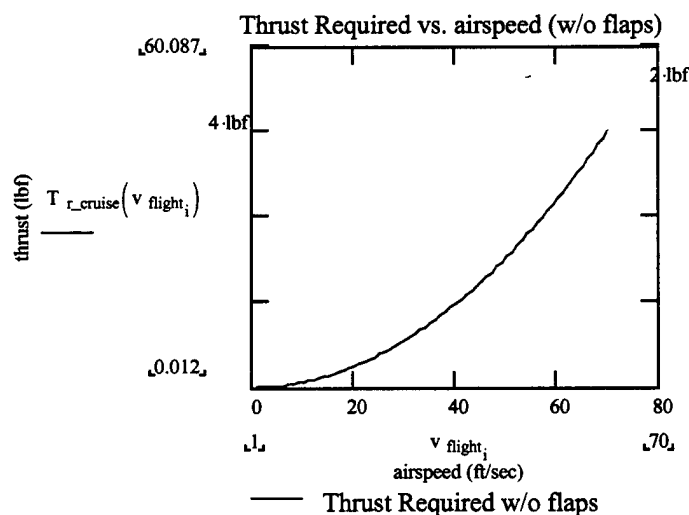


Figure 5.1 – Thrust Required vs. Airspeed

5.3 Structural

5.3.1 Fuselage Design

Several options of the design of the FbK were presented initially in the conceptual design phase and later in the preliminary design phase. The main structure of the FbK is the fuselage. The fuselage is the structural part of the aircraft that integrates the wings, booms, the payload and the other subsystems used for flight. The critical goal of the fuselage is to accomplish all of the aforementioned integration while maintaining a low weight.

The Structural Design of the FbK is very simple. Two options were discussed about the construction of the fuselage. One of the options was a bulkhead stringer concept. The second was a traditional box shaped structure. While the traditional box-shaped structure is easier to build and construct, the bulkhead-stringer concept allows more freedom to modify while construction is "in progress." The bulkhead stringer concept is also lighter and much easier to reinforce (should the need arise). Another positive aspect of the bulkhead stringer concept is the ability to re-use the standard jigs and tools used in cutting the many parts (production of spare parts and additional airplane components).

5.3.2 Wing Structure

The primary structural component of the wing is the spar. The spar is the internal "back-bone" of the wing. The spar must be chosen based on material strength and durability. Several Spars were modeled in the previously discussed CAD/CAM class. The Pahl-Beitz analysis method was used to determine the spar chosen. The results are shown in table 5.1.

RESULTS - TABLE 5.7

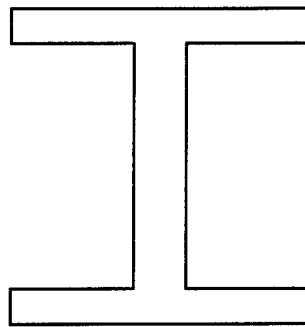
	Weight (lb.)	Deflection (in)	Max Stresses (lbf)	Costs	Mass/Def	Pahl-Bietz
Percentage	0.4	0.15	0.15	0.1	0.2	1
Sparless	10	1	1	10	N/A	N/A
Tubular	7	6	6	7	10	7.3
Box	3	10	7	5	5	5.25
I-Beam	4	9	10	6	6	6.25

Based on the final geometry, given constraints, and our finite element analysis we have chosen the tubular beam for construction of the FbK electric airplane wing.

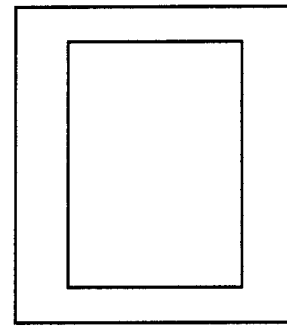
5.3.3 Tail-boom design

The tail boom is designed to take the loading of the horizontal and vertical stabilizers. The booms are designed like beams. Initially two models were built and tested. They were designed to act as an I-beam and a box beam.

The models were built with 1/8th inch sheets of balsa and after our "bench testing," with the simulated aerodynamic loads, the I-beam was slightly stronger and lighter, but much more difficult to construct. Therefore the box beam design was chosen.



I-BEAM



BOX BEAM

FIGURE 5.2

5.3.4 Landing Gear Testing and Performance

Two landing gear systems were initially considered for design and construction. The torsion gear landing system consists of two wheels connected to load arms. These load arms are inter-connected to a non-movable axle braced against the fuselage. When the airplane landing gear experiences a load, the load is transmitted through the arms and into the immobile torsion axle. The axle then tries to rotate. But, because the axle is immobilized the torsion of the bar absorbs the load of impact.

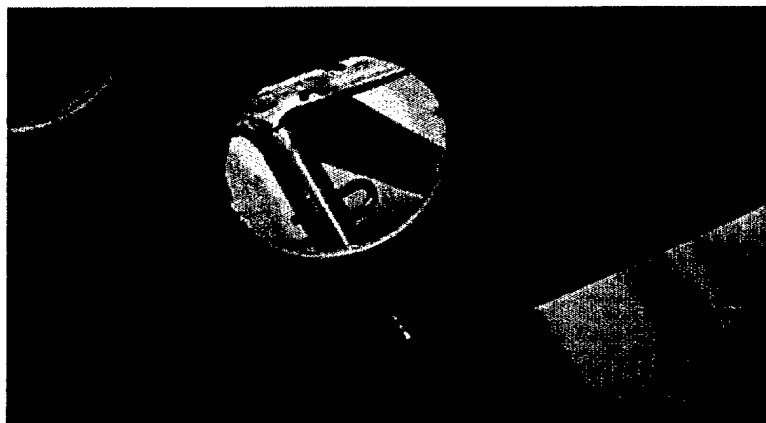


Figure 5.3 – Torsion bar system

The composite landing gear offers a high strength to weight ratio. Some of the members of the team are very experienced with the construction of composite structures.

There were concerns about the weight of the metal components in the torsion system. Also, no persons on the team have experience working with metal, in this manner. The composite landing gear offers a more immediate solution to the problem. Based on current membership and their abilities, the composite landing gear was chosen to be manufactured.

5.4.4 Mechanical/Electrical system integration

The fuselage includes a small gap designed in place for the batteries. After the determination of the actual size of the batteries, this gap was built to tight tolerances to house the specific batteries chosen. Particular attention was paid the cross section of the airplane. This is the reason for the tight tolerances. Various other concerns about the internal wiring caused the team to design an electric power grid inside the fuselage. The determined schematic is below:

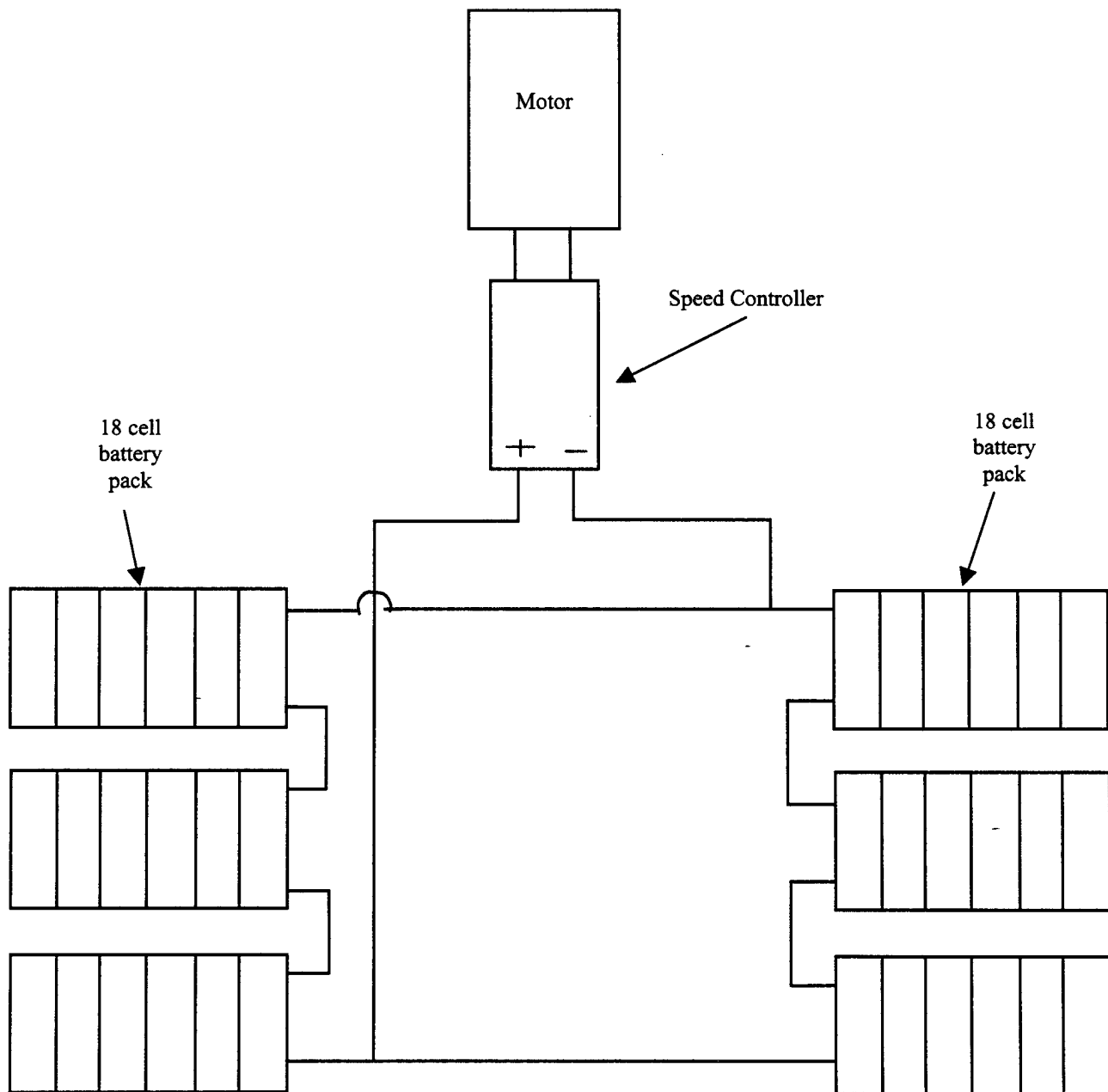


Figure 5.4 – Final Electrical Configuration

6.0 Manufacturing Plan

6.1 OVERVIEW

With the completion of the overall aircraft design, a manufacturing process needed to be decided upon. Three methods for the construction process were chosen. The first method is the most commonly used construction method for an aircraft of this size. It involves using wood for all the structural components of the aircraft. The greater part of the structure would be made of Balsa, whereas the high-stress areas, such as the landing gear plate, and wing attachments would use bass wood, laminate plywood or end-grain balsa. The structure would also require a covering material such as monokote.

The second method considered was a carbon fiber construction. For this construction process the main body of the aircraft would be constructed by wood molds. The wing would be fabricated using fiberglass end molds comparable to those used for the fuselage.

The third method considered was a merging of the previous two, to satisfy the figures of merit for each structural component. A combined structure including wood, carbon fiber, fiberglass and foam for example could be achieved provided the material used for each component was utilized to its highest efficiency.

6.2 FIGURES OF MERIT

The four figures of merit chosen to help in the selection of the competing concepts during the manufacturing plan were:

- Material Availability
- Material Expense
- Required Skill Levels
- Required time of construction

The materials needed for the aircraft had to be readily available. All the materials considered met this figure of merit and could be easily obtained by the team. The wood required such as Balsa and laminate plywood along with fiberglass and foam were always in stock at the hobby store or local craft store. The carbon fiber and large sheets of fiberglass can be ordered from specialty stores or vendors that specialize in composite materials.

Expenses for materials had to be kept to a minimum. A structure completely made of wood would be the least expensive of the considered construction plans. Wood for this aircraft would cost approximately \$50. The Carbon Fiber structure with the fiberglass wings, on the other hand, was discovered to be more expensive than the wood structure.

The required skill level of the team was the most limiting factor in choosing the construction plans. Most of the team members had limited experience with building model airplanes from wood. In contrast some of the team had knowledge on the construction of the aircraft from carbon fiber and fiberglass from previous competition.

The required time for construction of the aircraft was also an important limiting factor since the team could only meet twice a week. Multiple days were scheduled to adhere to the varying schedules of team members. The plane had to be completed as quickly as possible due to the required flight time before the competition. The Carbon

Fiber / Fiberglass construction airframes could be produced quickly, but the molds needed for the structure would take a great deal of time and craftsmanship to create. Wood construction could be done more quickly because it required no molds. By building the wood structure and using the composite as reinforcements, the airframe takes advantage of both styles of construction. This construction was estimated to take approximately a month.

6.3 FINAL SELECTION OF MANUFACTURING PROCESS

Taking into consideration these figures of merit the team determined to use wood for the majority of the structure. The components that would be made of other materials included the wing and the landing gear. The dominant figure of merit that helped govern this decision was the required time for the construction of the aircraft. A dominantly wooden structure could be completed by the middle of the spring semester allowing ample time for flight-testing. Carbon Fiber was chosen rather than aluminum as the material for the landing gear because of the potentiality of making several for replacement of damaged landing gears during testing and competition as well as for its strength. Foam will be the material used for the wings due to its ease and quickness of fabrication. For the landing gear block and the wing-balancing block, end-grain balsa was chosen for its strength.

6.4 MANUFACTURING PLAN

All the sections of the aircraft were constructed simultaneously. Actual size blue prints were drawn for ease of fabrication. The group was divided into teams. Each team was given a section of the aircraft to construct. These sections focused mainly on construction of the fuselage, wings, tail and boom section. The tasks were divided between both upper and lower classmen. Integrating the section with the main assembly and aligning each component followed the completion of each section. For the most part thick CA was used for the construction process for its reliability for good joints and easy application. For the landing gear block and wing-balancing block epoxy was used due to its reliability and strength.

6.4.1 Fuselage Construction

The construction of the fuselage began with 6 bulkheads fabricated from lite-ply with grain positioned in the vertical direction. Each bulkhead was cut to accommodate 16 stringers cut from 3/16" square balsa sticks. The sticks were connected to the bulkheads using thick CA. A large hole was cut (coinciding with the size of the payload bottles), in the center of the bulkheads.

The inside circle has a radius of 3 3/4" and carbon fiber strips were positioned around the circle for reinforcement. The last two bulkheads were notched to accept the tail boom nine inches into the fuselage. The fuselage will be able to contain two

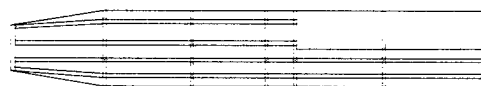


Figure 6.1 – Fuselage Construction

water bottles. End-grain balsa, which is used for the landing gear and wing-balancing blocks, are connected to the bulkheads. The fuselage is covered with 3/32" balsa sheeting.

The payload hatch cover is in the shape of a cone. It will sit between the two tail

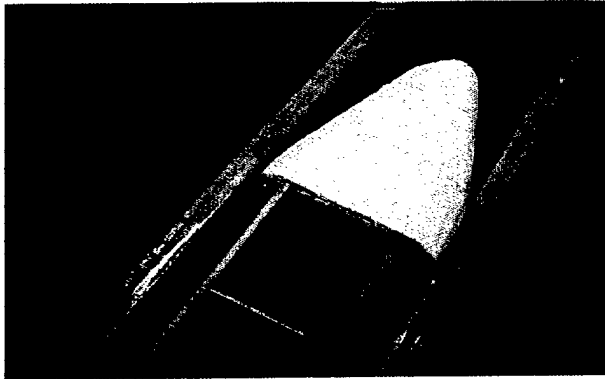


Figure 6.2 – Hatch Integration

booms at the rear of the fuselage. The location is important because of the ease of loading and unloading the payload. The material used to construct the hatch is white foam. The hatch is also shaped to prevent the airflow from separating which increases the drag. The hatch will be pinned to the fuselage from top and bottom.

The nose was shaped around the aircraft's motor. For the cowling 3/32" balsa sheeting was used.

Stringers constructed from 3/16"

square balsa spars were positioned around the motor for support. Two balsa-Carbon Fiber spars were positioned at the top and bottom of the motor for added support and strength. A large plate of balsa was placed on the top of the engine mounts to add torsion strength and also to allow a place to mount other components.

6.4.2 Tail Surface Construction

The tail section was constructed completely of balsa. The horizontal stabilizer is located on the tail section. The distance between the wings and the stabilizers creates a moment arm for the tail to counter the wing moments. Two vertical stabilizers were created for each boom with 1/2" x 3/8" balsa spars. For added support 1/32" balsa strips were used as ribs forming a truss structure in between the forward and back balsa spars. The rudders are connected to the vertical stabilizers with hinges at the top and bottom.

The vertical stabilizers were designed and constructed to aid in the quickness and agility of the aircraft. It also serves its purpose of stabilization. Like the horizontal stabilizers, the vertical stabilizers was constructed with 1/2" x 3/8" balsa spars and 1/32" ribs in a truss formation for added support. The leading edge is rounded off to provide less drag

The elevator used 3/8" square balsa spars for the border. Ribs cut from 3/32" balsa strips used the similar truss formation as the horizontal and vertical stabilizer. The center of the elevator is decreased in width where it will connect with the rudder and horizontal stabilizers.

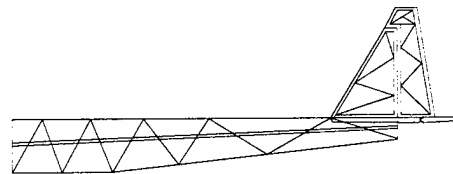


Figure 6.3 – Tail boom and tail surfaces

6.4.3 Wing Surface Construction

The wings are one of the most difficult parts of the aircraft to manufacture. The incorporation of washout, taper, dihedral in generation of a three dimensional wing is very difficult. The wing must be symmetric for the left and right halves to ensure proper lift distribution and good flight characteristics

Wing construction involved many steps and several different techniques. First was the fabrication of templates. Next came the cutting of the foam. Reinforcing the wing with carbon fiber lamination followed, and finally the construction ended with the placement of the control surfaces and servos.

In our research, we found many airfoils that we could use for our wings. We decided on Selig 1223 and printed a template for the of the root and tip sections using compufoil. We then cut the plotted points out and glued them onto a piece of hard wood. Next, we cut the hard wood template out and sanded the template to more closely match the printed plot points. We also marked regular intervals on the template to make the hot wire cutting process as smooth as possible.

The hot wire foam cutting technique used to cut and form wings is a common construction technique. The hot wire system consists of a bow and a voltage source. The bow, is constructed of one wood dow with fiberglass dows mounted in the perpendicular directions. The Fiberglass rods are then stressed, and a NiCr wire is placed in the span between the stressed rods. A voltage is applied to the conductive wires, which allows current to flow, generating heat. This heat is enough to create a very small cut in the foam, effectively slicing the foam.

To construct the wings, we attached the templates for the wing's root and tip to the ends of the white foam. Then two team members cut along the templates on each side. Several sets of wings were cut allowing the involvement of younger team members with more experienced senior members of the team. While cutting, the intervals were called out in unison to ensure the wing's overall surface smoothness. Both the top and bottom surfaces of the wing were cut using this technique. The section of the foam block that is cut away from the actual airfoil section is a perfect protective covering and is referred to as the saddle. When a set of wings have been cut they are stored in the saddle for further use.

In order to prep the wings for carbon fiber process, we used a spray adhesive to glue left and right wings together. After the glue has set, the wing is then cut along the quarter chord and the spar is inserted. Twelve-minute epoxy is used to adhere the two halves of the wing to the spar. The leading and trailing edges of the wing are not always uniform. To alleviate this problem both the leading and trailing edges were removed and replaced them with balsa stock. The leading edge was made from prefabricated balsa and sanded to match the airfoil. The trailing edge was made from a block of balsa sanded to meet the airfoil's shape.

To reinforce the wings we used carbon fiber, and we laminated the surfaces of the wings. Epoxy is brushed onto the CF surface and massaged onto the foam core. After the Carbon Fiber was massaged into the wing we then brushed in a thin second layer of epoxy in order to smooth out any imperfection. The bottom half of the saddle was covered with non-adhesive sheet to prevent the adhering of the wing to the saddle. Next the wing was placed into the bottom half of the saddle and covered with a non-adhesive sheets. The top half of the saddle was then placed on the wing. The wing is then inserted

into a vacuum-sealed bag to apply a uniform force. The saddle and wing assembly is then allowed to cure. After the curing is complete final sanding is done to leading and trailing edges of the wing. To complete the wing, end caps are placed on the ends of the wings, servo holes and ailerons are cut and placed, and then final integration into the fuselage is done. The placement of the wing socket is located at one quarter of the length of the aircraft. This allows excellent flight characteristics as well as a seamless construction.

6.4.4 Composite Gear Construction

For the landing gear, Carbon Fiber was used exclusively for its construction. A foam negative mold was created which layers of CF and epoxy were laid up and cured with the same process as the wings. It was connected to the landing gear plate with four #4 hex bolts, which connected it to the fuselage.



Figure 6.4 – Landing Gear Production

Table 6.1 – Table of composite structure

Layer	Angle of lay-up
1	90°
2	45°
3	90°
4	45°
5	90°
6	45°
7	90°
8	45°
9	90°
10	45°
11	90°
12	45°
13	90°
14	45°
15	90°

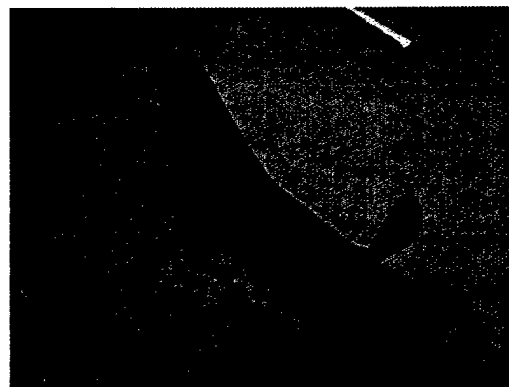


Figure 6.5 – Landing Gear Production

6.5 MANUFACTURING TIMING

The manufacturing of the prototype aircraft commenced on January 7, 2000 and will finish on March 11, 2000. Approximately 300 hours were spent on the fabrication of the model airplane.

Appendix A – MathCAD Calculations

Reynolds number

$$\rho := .002377 \frac{\text{slug}}{\text{ft}^3} \quad v := 30 \frac{\text{ft}}{\text{sec}} \quad c := 9 \cdot \text{in} \quad \mu := 3.7373 \cdot 10^{-7} \frac{\text{slug}}{\text{ft} \cdot \text{sec}}$$

$$\text{Re} := \frac{(\rho \cdot v \cdot c)}{\mu} \quad \text{Re} = 143104.647740347$$

Aircraft Geometry and Properties

Wing geometry

$$S_{\text{wing}} := 756 \cdot \text{in}^2 \quad b := 84 \cdot \text{in} \quad c := \frac{10 \cdot \text{in} + 8 \cdot \text{in}}{2} \quad i_w := 0 \cdot \text{deg} \quad \text{Oswald} := 0.92$$

$$\text{AR} := \frac{b^2}{S_{\text{wing}}} \quad \text{AR} = 9.3$$

$$\frac{S_{\text{wing}}}{c \cdot 2} = 3.5 \text{ ft}$$

Horizontal Stabilizer Geometry

$$\text{horizon_stab_vol} := 22 \cdot \text{in}^3 \quad b_{\text{horz_stab}} := 24 \cdot \text{in} \quad c_{r_horz_stab} := 6 \cdot \text{in} \quad c_{t_horz_stab} := 5 \cdot \text{in}$$

$$S_{\text{horz_stab}} := \frac{c_{r_horz_stab} + c_{t_horz_stab}}{2} \cdot b_{\text{horz_stab}} = 132 \cdot \text{in}^2 - 24.375 \cdot \text{in}^2 = 107.625 \cdot \text{in}^2$$

$$\text{AR}_{\text{horz_stab}} := \frac{b_{\text{horz_stab}}^2}{S_{\text{horz_stab}}} \quad S_{\text{horz_stab}} := 107.625 \cdot \text{in}^2 \quad \text{real total horizontal stab}$$

$$\text{AR}_{\text{horz_stab}} = 4.4$$

$$l_{\text{tail_boom}} := 36 \cdot \text{in}$$

$$\frac{S_{\text{horz_stab}}}{S_{\text{wing}}} = 0.142$$

Stability

Pitching stability:

Wing contribution: $x_{cg_along_chord} := .5$ $x_{ac_along_chord} := .5$

$C_{m_ac_wing} := -.2$ $C_{L_wing} := 1.56$

$C_{m_cg_wing} := C_{m_ac_wing} + C_{L_wing} \cdot (x_{cg_along_chord} - x_{ac_along_chord})$

$C_{m_cg_wing} = -0.2$

Tail contribution:

$C_{L\alpha_flat} := 2 \cdot \pi$ $i_t := 0 \cdot \text{deg}$ $\eta := 1.0$

Tail Efficiency: Tail will be both in propwash and wing wake, thus their effects will be assumed to be cancelled.

$$C_{L\alpha_t} := \frac{C_{L\alpha_flat}}{1 + \frac{C_{L\alpha_flat}}{\pi \cdot AR_{horz_stab}}}$$

Infinite, thin flat plate $C_{L\alpha}$, from Anderson
Fund. of Aero. Page 272
Now corrected for finite length

$\alpha_w := 0 \text{ deg}$

$\tau_{tail} := .2$ From Nelson Flight Control,
Fig 2.21 page 64

$l_{tail} := 36 \text{ in}$

$$V_H := \frac{l_{tail} \cdot S_{horz_stab}}{S_{wing} \cdot c} \quad V_H = 0.569$$

$$\epsilon := \frac{2 \cdot C_{L_wing}}{\pi \cdot AR} \quad \epsilon = 0.106$$

$C_{L_t} := C_{L\alpha_t} \cdot (\alpha_w - i_w - \epsilon + i_t)$ $C_{L_t} = -0.458$

$C_{m_cg_t} := -V_H \cdot \eta \cdot C_{L_t}$ $C_{m_cg_t} = 0.261$

Should be positive to counteract negative pitching of wing.

Due to fuselage top being approximately symmetric to fuselage bottom, pitching moment of fuselage assumed to be zero.

$$C_{m_{cg}} := C_{m_{cg_wing}} + C_{m_{cg_t}} \quad C_{m_{cg}} = 0.061 \quad \text{Should be close to zero.}$$

Directional (side to side) stability:

Vertical stabilizer contribution:

$$\eta_v := 1.0 \quad \text{Vertical stabilizer assumed to be unaffected by wing or prop wash.}$$

$$\text{Vert_Stab_Vol} := 18.9 \cdot \text{in}^3 + 18.9 \cdot \text{in}^3$$

$$\text{Vert_Stab_Vol} = 37.8 \cdot \text{in}^3$$

$$l_v := 36 \text{ in} \quad c_{r_vert_stab} := 9 \text{ in} \quad c_{t_vert_stab} := 2 \text{ in}$$

$$\beta := 0 \text{ deg} \quad h_{vert_stab} := 10.2 \text{ in} \quad S_{vert_stab} := \frac{h_{vert_stab}}{2} \cdot (c_{r_vert_stab} + c_{t_vert_stab})$$

$$S_{vert_stab} = 56.1 \cdot \text{in}^2$$

$$S_{vert_stab} \cdot 2 = 112.2 \cdot \text{in}^2 \quad \text{Total surface area of both vertical stabilizers}$$

$$V_{vert_stab} := \frac{l_v \cdot S_{vert_stab}}{S_{wing} \cdot b}$$

$$AR_{vert_stab} := \frac{h_{vert_stab}^2}{S_{vert_stab}}$$

$$C_{n_beta_flat} := 2 \pi$$

Infinite, thin flat plate $C_{L\alpha}$, from Anderson
Fund. of Aero. Page 272
Now corrected for finite length

$$C_{n_beta_v} := \frac{C_{n_beta_flat}}{1 + \frac{C_{n_beta_flat}}{\pi \cdot AR_{vert_stab}}}$$

$$C_{n_tail} := V_{vert_stab} \cdot \eta_v \cdot C_{n_beta_v} \cdot \beta$$

Fuselage contribution:

$$k_n := .0015 \quad k_{Rl} := 1.0 \quad S_{fs} := 84 \text{ in}^2 \quad l_f := 19 \text{ in}$$

$$C_{n_beta_fuselage} := \frac{-k_n \cdot k_{RI} \cdot S_{fs} \cdot l_f}{S_{wing} \cdot b} \cdot \beta$$

$$C_{n_total} := C_{n_tail} + C_{n_beta_fuselage} \quad C_{n_total} = 0$$

Zero for beta yields zero coefficient.
Remains small for small angle of beta.

Roll Stability:

No parts of plane assumed to have rolling coefficients except for flaperons.

$$C_{L_alpha_wing} := .08 \text{ deg}^{-1} \quad \text{Tabulated from VisualFoil}$$

$$S_{flaperon} := 40 \text{ in}^2$$

$$\text{Flaperon_to_wing_area_ratio} := \frac{S_{flaperon}}{S_{wing}}$$

$$\text{Flaperon_to_wing_area_ratio} = 0.053$$

$$\tau := .175$$

Used to estimate tau from figure 2.21 on page 64 of Nelson Flight Control.

$$C_{l_delta_flaperon} := \frac{2 \cdot C_{L_alpha_wing} \cdot \tau \cdot c \cdot 432 \text{ in}^2}{S_{wing} \cdot b}$$

432 in squared computed from equation 2.96 on page 83 of Nelson Flight Control.

$$C_{l_delta_flaperon} = 0.098$$

Roll control of flaperons: Should be positive

Control Authority

$$C_{l_delta_flaperon} = 0.098 \quad \text{Calculated above}$$

$$C_{n_delta_rudder} := -V_{vert_stab} \cdot \eta_v \cdot \tau \cdot C_{n_beta_v}$$

$$C_{n_delta_rudder} = -0.017 \quad \text{Should be negative}$$

$$C_{m_delta_elevator} := -V_H \cdot \eta_t \cdot \tau_{tail} \cdot C_{L\alpha_t}$$

$$C_{m_delta_elevator} = -0.491 \quad \text{Should be negative}$$

Cruise conditions

cruise without flaps at zero angle of attack

$$\alpha_{\text{trim}} := 0 \quad \rho := 0.002377 \frac{\text{slug}}{\text{ft}^3} \quad C_{D0} := 0.03 \quad C_{Dw} := 0.01278 \quad C_{L_{\text{cruise}}} := 1.574$$

$$S_{\text{wing}} := 756 \cdot \text{in}^2 \quad W := 13 \cdot \text{lbf}$$

$$C_{di} := \frac{C_{L_{\text{cruise}}}^2}{\pi \cdot AR \cdot \text{Oswald}} \quad C_{di} = 0.092 \quad \text{coefficient of drag induced}$$

$$C_{D_{\text{cruise}}} := C_{D0} + C_{Dw} \cdot (\alpha_{\text{trim}} + i_w) + C_{di} \cdot C_{D_{\text{cruise}}} = 0.122$$

$$v_{\text{cruise}} := \sqrt{\frac{W}{0.5 \cdot \rho \cdot S_{\text{wing}} \cdot C_{L_{\text{cruise}}}}} \quad v_{\text{cruise}} = 24.806 \cdot \text{mph} \quad \text{Minimum cruise speed}$$

$$D_{\text{cruise}} := 0.5 \cdot \rho \cdot v_{\text{cruise}}^2 \cdot S_{\text{wing}} \cdot C_{D_{\text{cruise}}} = 1.01 \cdot \text{lbf} = T_r \quad (\text{Thrust required at cruise})$$

$$C_{L_{\text{max.6def_no_flaps}}} := 2.136 \quad \text{deg angle of attack no flaps}$$

$$v_{\text{stall}} := \sqrt{\frac{2 \cdot W}{\rho \cdot S_{\text{wing}} \cdot C_{L_{\text{max.6def_no_flaps}}}}} \quad v_{\text{stall}} = 31 \frac{\text{ft}}{\text{sec}} \quad v_{\text{stall}} = 21 \cdot \text{mph} \quad \text{Cruise stall velocity}$$

$$v_{\text{actual}} := 30 \cdot \text{mph} \quad \text{desired cruise velocity}$$

$$L := \frac{1}{2} \cdot \rho \cdot v_{\text{actual}}^2 \cdot S_{\text{wing}} \cdot C_{L_{\text{cruise}}} = 19.014 \cdot \text{lbf}$$

$$n := \frac{L}{W} \quad n = 1.463$$

$$TR := \frac{v_{\text{cruise}}^2}{g \cdot \sqrt{n^2 - 1}} \quad TR = 38.546 \text{ ft} \quad \text{Turning Radius}$$

Flap conditions

(Cruise condition)

$$C_{D0} := 0.03 \quad C_{L_cruise_flap} := 2.01 \quad C_{Dw_flap} := 0.02945 \quad \alpha_{trim_flap} := 1$$

$$C_{D_cruise_flap} := C_{D0} + C_{Dw_flap} \cdot (\alpha_{trim_flap} + i_w) + \frac{C_{L_cruise_flap}^2}{\pi \cdot e \cdot AR} \quad C_{D_cruise_flap} = 0.11$$

$$v_{cruise_flap} := \sqrt{\frac{W}{.5 \cdot \rho \cdot S_{wing} \cdot C_{L_cruise_flap}}} \quad v_{cruise_flap} = 22 \text{ mph} \quad \text{estimated cruise speed}$$

$$D_{cruise_flap} := .5 \cdot \rho \cdot v_{cruise_flap}^2 \cdot S_{wing} \cdot C_{D_cruise_flap} \quad D_{cruise_flap} = 0.71 \text{ lbf} = T_r \text{ (Thrust required at cruise)}$$

$$C_{L_max_flap} := 3.175 \quad \text{Flapped stall speed at 6 deg angle of attack}$$

$$v_{stall_flap} := \sqrt{\frac{2 \cdot W}{\rho \cdot S_{wing} \cdot C_{L_max_flap}}} \quad v_{stall_flap} = 17 \text{ mph}$$

Takeoff Performance

$$W_{plane} := 8 \text{ lbf} \quad W_{cargo} := 5 \text{ lbf} \quad S := 4.47 \text{ ft}^2 \quad \text{Oswald} := .92$$

$$h := .8 \text{ ft} \quad b := 7 \text{ ft} \quad C_{lmax_no_flaps} := 2.13 \quad C_{D0} := .03 \quad \text{parasite drag from airplane}$$

$$T := 4 \text{ lbf} \quad \text{lbs of thrust} \quad \mu := .02 \quad \rho := .002377 \frac{\text{slug}}{\text{ft}^3}$$

$$W := W_{plane} + W_{cargo} \quad W = 13 \text{ lbf}$$

$$AR := \frac{b^2}{S} \quad AR = 10.962$$

takeoff velocity

$$Cl_{max_with_flaps_6deg} := 3.175$$

$$v := .7 \cdot 1.2 \cdot \sqrt{\frac{2 \cdot W}{\rho \cdot S \cdot Cl_{max_with_flaps_6deg}}} \quad v = 15.9 \text{ mph}$$

ground effect

$$\phi := \frac{\left(16 \frac{h}{b}\right)^2}{1 + \left(16 \frac{h}{b}\right)^2} \quad \phi = 0.77 \quad L := .5 \cdot \rho \cdot v^2 \cdot S \cdot Cl_{max_with_flaps_6deg}$$
$$L = 9.173 \text{ lbf}$$

$$D := \left(C_{Do} + \frac{1.2 \cdot \phi \cdot Cl_{max_with_flaps_6deg}^2}{\pi \cdot Oswald \cdot AR} \right) \cdot .5 \cdot \rho \cdot v^2 \cdot S \quad D = 0.936 \text{ lbf}$$

average drag on take
off
with flaps and at a
6 deg
angle of attack

distance of take off

$$S_{Lo} := \frac{1.44 \cdot W^2}{g \cdot \rho \cdot Cl_{max_with_flaps_6deg} \cdot S \cdot (T - (D + \mu \cdot (W - L)))} \quad S_{Lo} = 75.047 \text{ ft}$$

Landing Performance:

$$Cl_{max_with_flaps_0_deg} := 2.01$$

$$v_{Landing} := .7 \cdot 1.3 \cdot \sqrt{\frac{2 \cdot W}{\rho \cdot S \cdot Cl_{max_with_flaps_0_deg}}} \quad v_{Landing} = 21.649 \text{ mph}$$

$$L_{Landing} := .5 \cdot \rho \cdot v_{Landing}^2 \cdot S \cdot Cl_{max_with_flaps_0_deg} \quad L_{Landing} = 10.765 \text{ lbf}$$

$$D_{Landing} := .5 \cdot \rho \cdot v_{Landing}^2 \cdot S \cdot \left(C_{Do} + \frac{1.2 \cdot \phi \cdot Cl_{max_with_flaps_0_deg}^2}{\pi \cdot Oswald \cdot AR} \right) \quad D_{Landing} = 0.792 \text{ lbf}$$

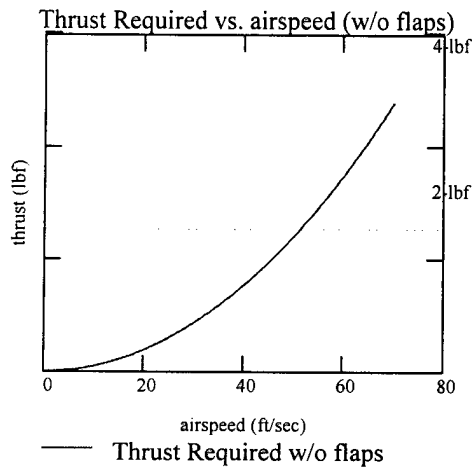
$$S_L := \frac{1.69 \cdot W^2}{g \cdot \rho \cdot Cl_{max_with_flaps_0_deg} \cdot S \cdot [D + \mu \cdot (W - L_{Landing})]} \quad S_L = 423.931 \text{ ft}$$

Thrust Required/Available

$$i := 1..70$$

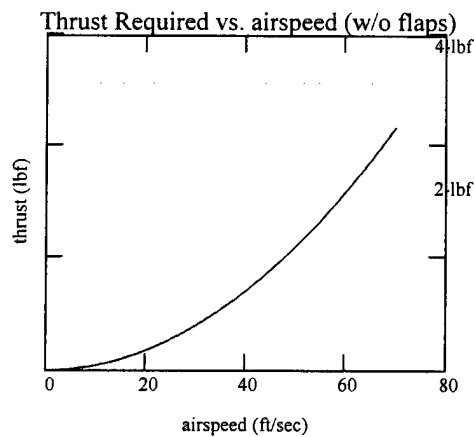
$$v_{\text{flight}_i} := i \cdot \frac{\text{ft}}{\text{sec}}$$

$$T_{r_cruise}(v) := C_{D_cruise} \cdot (.5 \cdot \rho \cdot v^2 \cdot S_{\text{wing}})$$



Thrust Required/Available

$$T_{r_cruise}(v) := C_{D_cruise} \cdot (.5 \cdot \rho \cdot v^2 \cdot S_{\text{wing}}) \quad T_{r_cruise_flap}(v) := C_{D_cruise_flap} \cdot (.5 \cdot \rho \cdot v^2 \cdot S_{\text{wing}})$$



Thrust Required w/o flaps

$$Re = 150000$$

$$C_{L\alpha_flap} := \frac{3.174 - 2.126}{15 \cdot \text{deg}}$$

$$C_{L\alpha_flap} = 0.07 \frac{1}{\text{deg}}$$

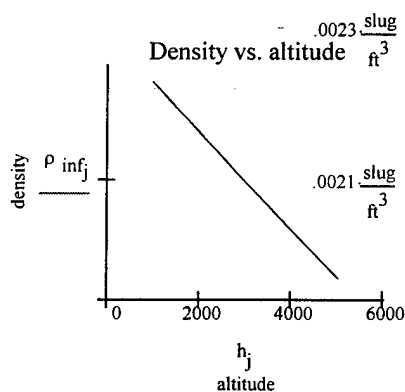
$$C_{m\alpha_flap} := \frac{-0.4165 - -.41}{8 \cdot \text{deg}}$$

$$C_{m\alpha_flap} = -8.125 \cdot 10^{-4} \frac{1}{\text{deg}}$$

$$C_{m0_flap} := -.3986$$

$$\rho_{inf} := \begin{bmatrix} .002377 \\ .002308 \\ .002241 \\ .002175 \\ .002111 \\ .002048 \end{bmatrix} \frac{\text{slug}}{\text{ft}^3} \quad h := \begin{bmatrix} 0 \\ 1 \\ 2 \\ 3 \\ 4 \\ 5 \end{bmatrix} \cdot 1000 \cdot \text{ft}$$

$$j := 1 \dots \text{rows}(h)$$



Power Required:

$$C_{D0} := .03$$

$$C_L := 1.5741$$

$$C_D := \left(C_{D0} + \frac{C_L^2}{\text{Oswald} \cdot \pi \cdot AR} \right) \quad C_D = 0.108$$

$$P_{\text{Required}} := \sqrt{\frac{(32.2) \cdot 2 \cdot W^3 \cdot C_D^2}{\rho \cdot S \cdot C_L^3}}$$

550

power in horse power

$$P_{\text{Required}} = 6.609 \cdot 10^{-4} \text{ hp}$$

$$746 \cdot P_{\text{Required}} = 367.67 \text{ watt}$$

Watts to maintain level flight

Appendix B – Various Selig Airfoil Calculations

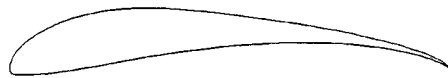


Figure 4.2. Selig 1223

Table 4.1 MotoCalc Computations
Visual Foil Selig 1223 Results

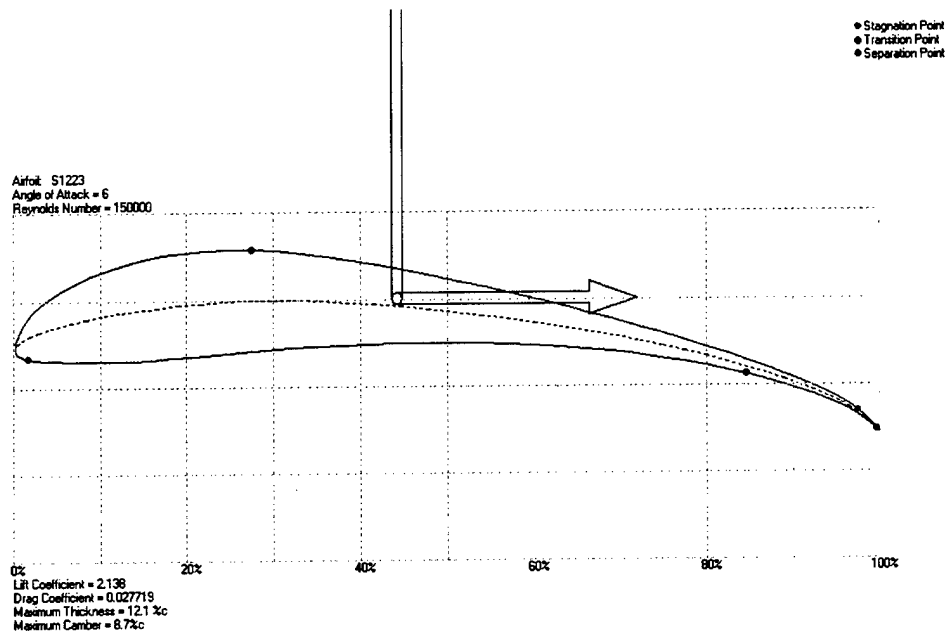


Figure 4.1. Selig 1223 Airfoil

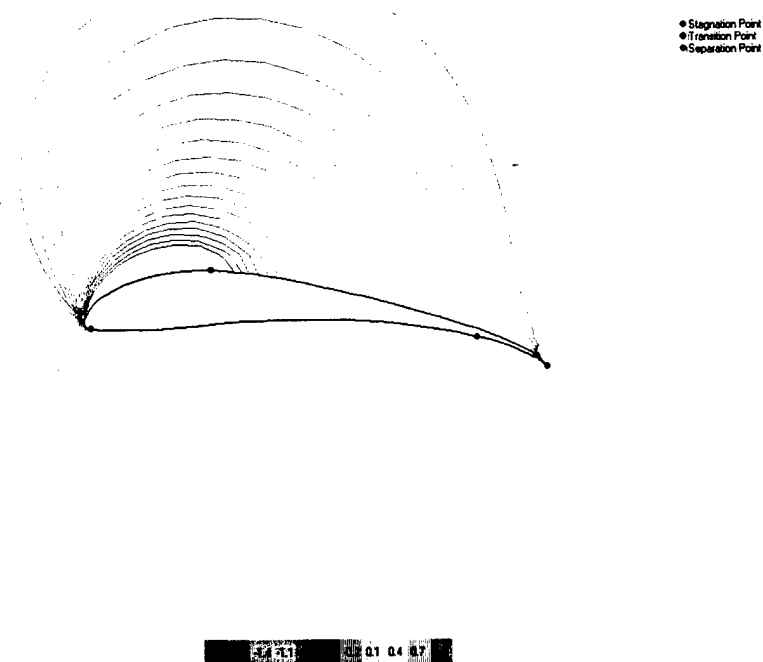


Figure 4.2. Pressure Distribution

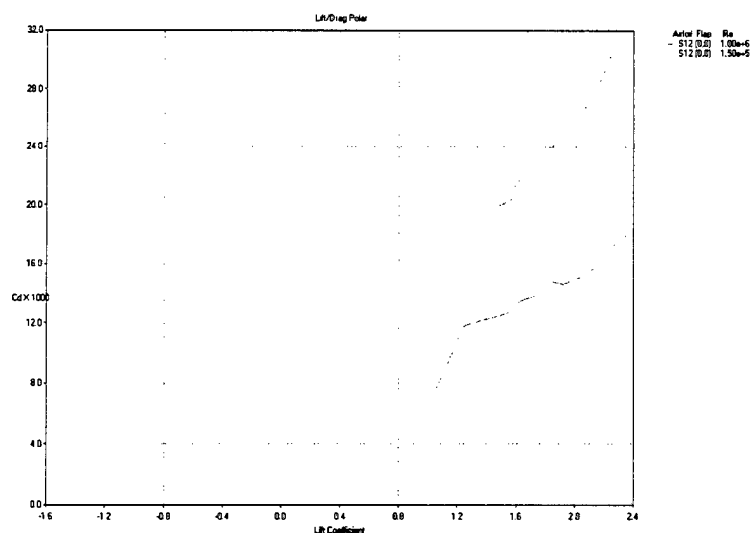


Figure 4.3 Lift vs. Drag

Figure 4.4 Velocity Distribution

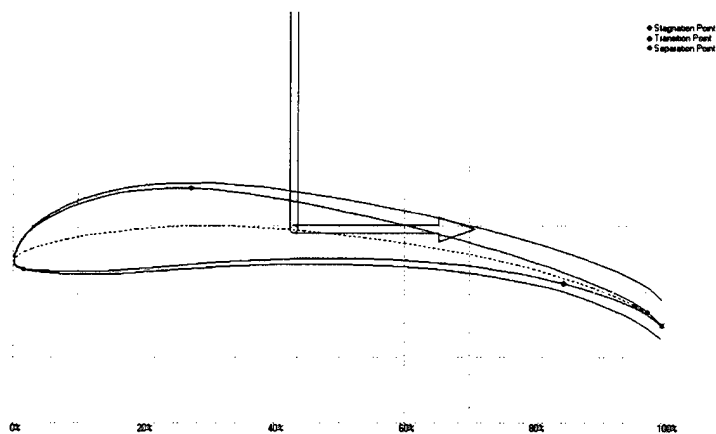
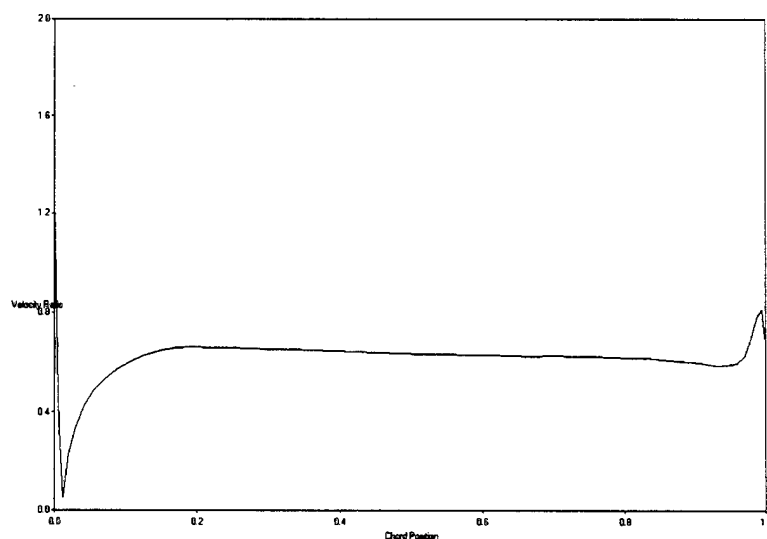


Figure 4.5 Boundary Conditions

Appendix C – Preliminary Airfoil Analysis

Airfoil Designation	Angle of Attack	cl	cd	Ideal SL Lift at 30 ft/s and 756 in ² (lbf)	Ideal SL Drag at 30 ft/s and 756 in ² (lbf)	VLO (W=12.5 lbf)
Re= 150000						
NACA 0012						
	0	0	0.013524	0	0.075627993	
clmax	2	0.206	0.014103	1.151979192	0.078865838	
0.8	4	0.415	0.016141	2.32073478	0.090262603	
	6	0.597	0.019862	3.338502804	0.111070926	
	8	0.775	0.021516	4.3339023	0.120320312	
	10	0.864	0.02765	4.831602048	0.15462245	57.783
NACA 2412						
	0	0.228	0.01176	1.275006096	0.065763472	
clmax	2	0.419	0.012845	2.343103308	0.071830936	
1.14	4	0.624	0.014231	3.489490368	0.07958163	
	6	0.807	0.016918	4.512850524	0.094607689	
	8	0.954	0.022918	5.334893928	0.128160481	
	10	1.04	0.028404	5.81581728	0.158838917	50.304
NACA 4412						
	0	0.455	0.012231	2.54442006	0.068397366	
clmax	2	0.627	0.013886	3.506266764	0.077652345	
1.48	4	0.824	0.015339	4.607916768	0.085777713	
	6	0.995	0.01752	5.56417134	0.097974153	
	8	1.15	0.021365	6.4309518	0.1194759	
	10	1.215	0.030981	6.79444038	0.173249841	44.15
NACA 63213						
	0	0.175	0.01201	0.9786231	0.067161505	
	2	0.392	0.012324	2.192115744	0.068917435	
clmax	4	0.568	0.013437	3.176330976	0.075141478	
0.75	6	0.723	0.018843	4.043111436	0.105372543	
	8	0.254	0.011697	1.420401528	0.065411168	
	10	0.363	0.01577	2.029943916	0.088187922	62.109
Clark Y						
	0	0.37	0.01197	2.06908884	0.06693782	
clmax	2	0.55	0.013082	3.0756726	0.073156271	
1.1	4	0.733	0.06159	4.099032756	0.34441941	
	6	0.9	0.018292	5.0329188	0.102291279	
	8	1.051	0.021713	5.877330732	0.121421962	
	10	1.106	0.028964	6.184897992	0.161970511	51.211



FX 60-100(126)

	0	0.503	0.012551	2.812842396	0.070186849	
	2	0.715	0.013542	3.99837438	0.075728652	
clmax	4	0.874	0.014632	4.887523368	0.081824075	
0.89	6	0.175	0.006085	0.9786231	0.034028123	
	8	0.281	0.008409	1.571389092	0.047024238	
	10	0.388	0.014938	2.169747216	0.083535268	56.933

Selig S1223

	0	1.574	0.020416	8.802015768	0.114168967	
	2	1.706	0.022301	9.540177192	0.124710136	
clmax	4	1.922	0.024766	10.7480777	0.138494741	
2.138	6	2.138	0.027719	11.95597822	0.155008307	
	8	2.354	0.032436	13.16387873	0.181386394	
	10	2.57	0.038999	14.37177924	0.218087556	36.733



AIAA Design/Build/Fly Competition

Team: Fly By Knight

Addendum Phase



University of Central Florida

Team Members:

Sebastian Echenique
Josh Lobaugh
Benjamin Goff
Art Morse
Jennifer Creelman
Sandra Guerra
Kristina Morace

Gary Ballman
Ia Whitney
Mirelis Cotto
Louis Turek
Kevin Chibar
Deyrah Jiminez
Carlos Figueroa

Tim Smith
Jennifer Lemanski
Jorge Pagan
Adam Ayala
Jeremy Fernandez
Peter Disusio
Patrick L. Bertiux

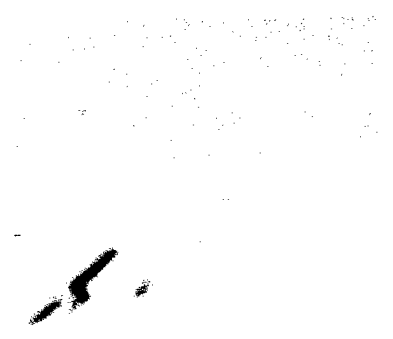


7.0 LESSONS LEARNED	3
7.1 DESIGN MODIFICATIONS	3
7.1.1 FRONT COWLING & MOTOR ATTACHMENT	3
7.1.2 DESIGN REPORT	4
7.2 FURTHER DEVELOPMENT	4
7.2.2 SMALLER SIZE WITH MAINTAINED PAYLOAD CAPACITY	4
7.3 VEHICLE COST SUMMARY	4

7.0 Lessons Learned

As typical UCF luck would have it, the prototype aircraft that was completed on March 11th 2000, crashed after the front wheel hit a rock on take-off, causing the airplane to careen out of control and flip several times. The initial damage was noted as light-to-moderate, and after a brief check out, we recycled the vehicle for the first flight.

The first flight was flawless. The vehicle made two successful laps without the payload included. Upon landing, the vehicle again sustained moderate damage to the front landing gear. After our post flight inspection, structural deficiencies were noted on the forward section of the fuselage.



7.1 DESIGN MODIFICATIONS

7.1.1 Front Cowling & Motor Attachment

The only modifications were those to the front cowling and motor attachment points. The FbK was designed to be (mechanically speaking) maintenance free. In an attempt to streamline production and keep weight low, the front cowling had been permanently glued to the front of the fuselage. This proved to be a costly and time-consuming mistake.

By permanently affixing the cowling to the fuselage, the team was unable to assess the complete damage caused by a) the tumbling incident and b) the hard landing. The original cowling was destroyed while being removed to assess crash damage. Additionally, the motor, front landing gear and the cowling were all attached to the first bulkhead, which was structurally damaged in testing.

The modifications to the forward section of the fuselage are as follows:

- The front bulkhead was strengthened by adding a sheet of cross-grained balsa, and also a strip of scrap Carbon Fiber.
- The cowling was redesigned to be removable and to be attached to the forward stringers, in addition to being attached to the forward bulkhead.
- The motor attach points were hardened and additional screws were added to the cowling to transfer the torsional loads.



After witnessing the first flight, the FbK team feels that the design goals have been met and are awaiting their first competition flight in Wichita.

7.1.2 Design Report

Upon further inspection, the design report has a few corrections. Page 26 is being modified to accept the drawing package. The pages located on the end of this report are to be added to the report (in chronological order) after page 26.

7.2 FURTHER DEVELOPMENT

7.2.2 Smaller Size with Maintained Payload Capacity

Some future developments should include:

- Smaller vehicle designs.
- Addition onboard batteries – Power consumption is a critical area of research that should be explored. More studies need to be done to analyze the power and weight tradeoffs of electric flight.
- More development of the flight control surfaces – More time should be spent developing and researching low Reynolds number airfoils and also the development of other high lift devices (feasible for Remote Control Aircraft or UAV's.)
- Additional Payloads – Serious considerations should be given to the thought of adding telemetry devices (transmitting cameras, audio, pressure readings, etc...) in place of the water payload.

7.3 VEHICLE COST SUMMARY

Table 7.1 – Control System Budget

Control System

<i>Item</i>	<i>Quantity</i>	<i>Unit Price</i>	<i>Item Price</i>
Transmitter	1	\$10.00	\$10.00
Receiver	1	\$129.95	\$129.95
Servos			
S9303	2	\$59.95	\$119.90
S3001	3	\$29.95	\$89.85
Wire Extensions	4	\$4.19	\$16.76
Flight Systems Battery	1	\$19.99	\$19.99

Category Subtotal

\$386.45

Table 7.2 - Structure System Budget

Structure System

<i>Item</i>	<i>Quantity</i>	<i>Unit Price</i>	<i>Item Price</i>
Fuselage			
wood	various	\$50.00	\$50.00
foam	various	\$5.00	\$5.00
Monokote	2	\$13.99	\$27.98
Carbon Fiber	1	\$19.99	\$19.99
wheels	4	\$2.99	\$11.96
posterboard	1	\$0.58	\$0.58
Landing Gear			
Carbon Fiber	1	\$20.00	\$20.00
Structural Epoxy	1	\$29.99	\$29.99
front gear	1	\$3.99	\$3.99
Wing			
Carbon Fiber	1	\$42.99	\$42.99
foam	1	\$8.99	\$8.99
Monokote	2	\$13.99	\$27.98
Structural Epoxy	1	\$29.99	\$29.99
spar wood	1	\$8.99	\$8.99
Payload			
water bottles	4	\$12.99	\$51.96
Miscellaneous Hardware			
nylon screws	4	\$0.59	\$2.36
other screws	various	\$10.00	\$10.00
glue			
CA	3	\$9.99	\$29.97
epoxy	1	\$9.99	\$9.99
Exacto-blades	2	\$2.49	\$4.98

Category Subtotal

\$397.69

Table 7.3 – Propulsion System Budget

Propulsion System

<i>Item</i>	<i>Quantity</i>	<i>Unit Price</i>	<i>Item Price</i>
Sanyo 1400AE	36	\$2.25	\$81.00
wire	14	\$0.80	\$11.20
connectors	24	\$0.49	\$11.76
speed controller	1	\$99.99	\$99.99
motor w/gearbox	1	\$160.00	\$160.00
propellers	6	\$3.99	\$23.94
AC battery charger	1	\$174.95	\$174.95

Category Subtotal

\$562.84

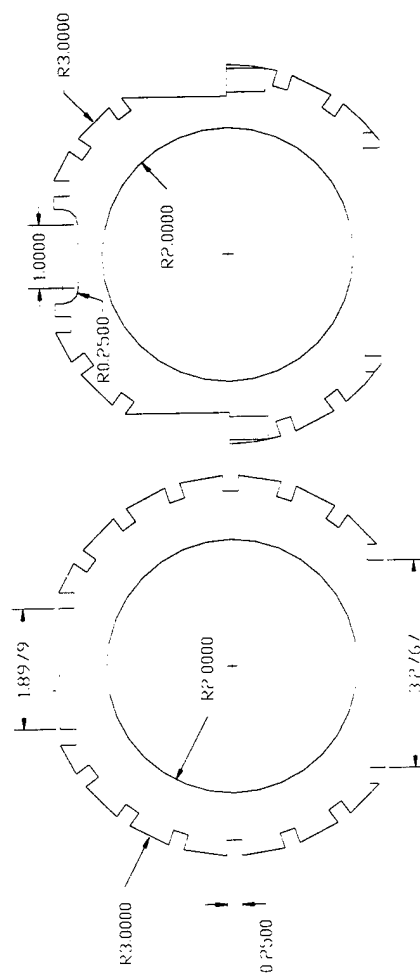
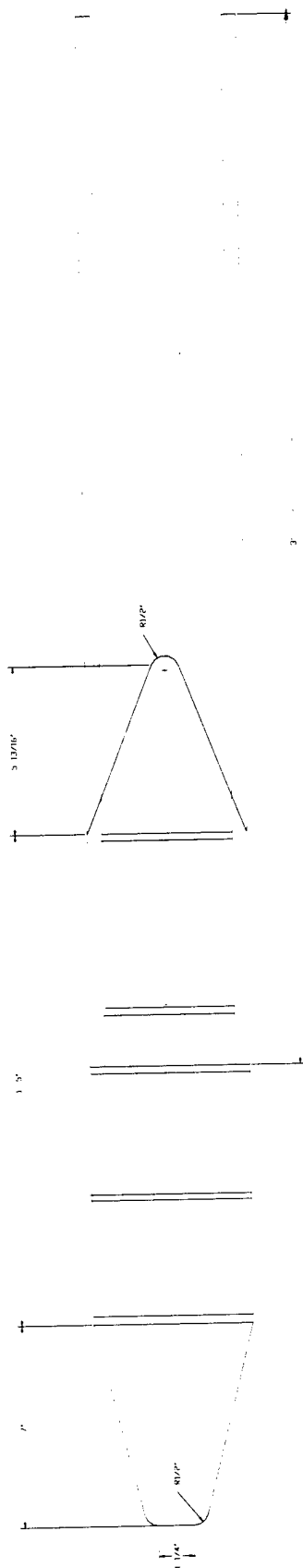
Table 7.4 – System Totals

Control System Subtotal	\$ 386.45
Structure System Subtotal	\$ 397.69
Propulsion System Total	\$ 562.84
Vehicle Total Cost	\$ 1,346.98

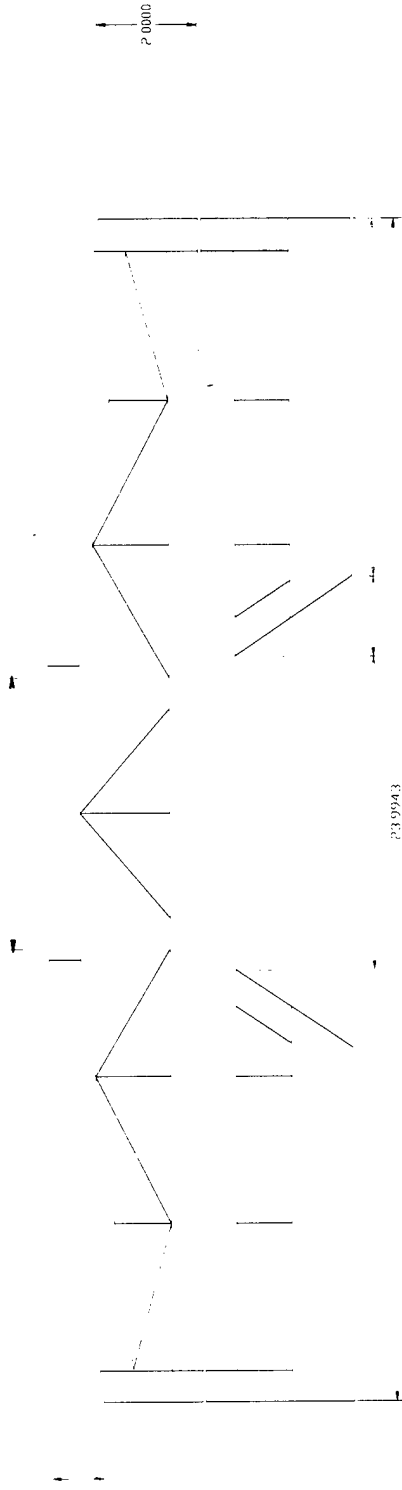
Table 7.5 – Total Workmanship (including modifications)

Task	Man-hours
Airplane	
Fuselage	200
Wing	150
Landing Gear	50
Report	
Detailed drawings	10
Writing	100
Total man-hours	510

Fuselage & Bulkhead Drawings

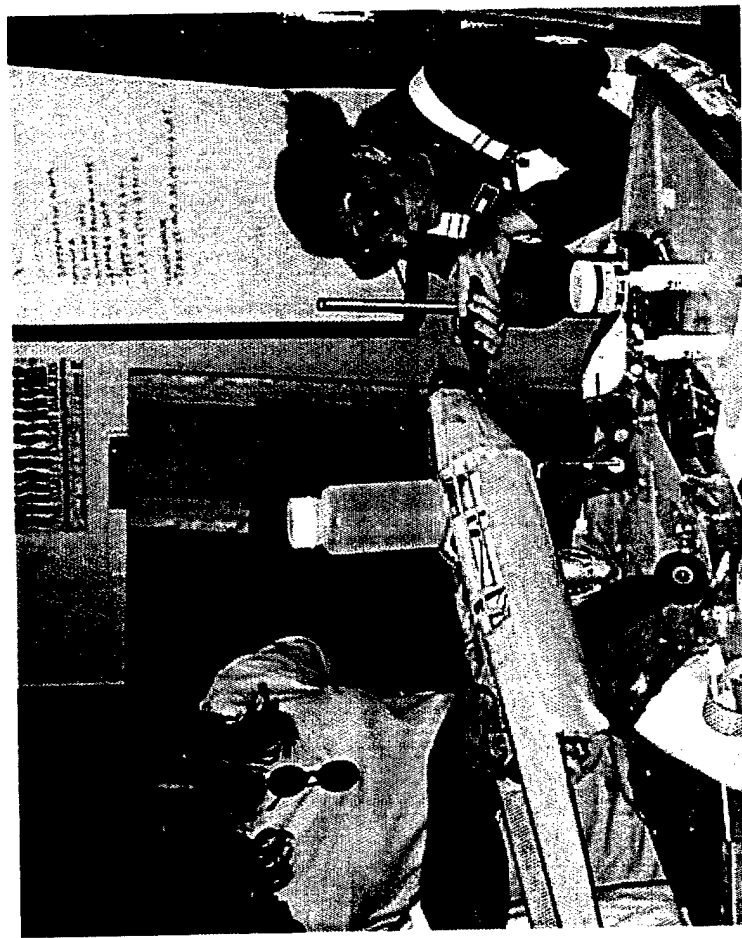


Tail Surface Drawings



P39943

Miscellaneous Pictures and Drawings



AIAA Student Design/Build/Fly Competition

1999-2000



Design Team

David Christensen

Doug Aiken

Eric Gardner

Aaron Stone

Mario Rodrigues

Oscar Quinonez

Cory Tafoya

Richard Medina

University of New Mexico

March 13, 2000

Table of Contents

Pages

Table of Contents	i
1. Executive Summary	
1.1 Development	1
1.2 Design Tools	1
1.3 Method used to Design	1
2. Management Summary	
2.1 Management and assigned areas of the Design team.	2
2.2 Designation of milestone Chart.	3
Table 2.1 - Design time and Development of Milestone Chart	3
3. Conceptual Design	
3.1 Design Constraints	4
3.2 Design Alternatives	4
3.3 Converging on an Idea	4
3.4 Cons of Alternative Designs	5
Figure 3.1 (a) - Sketch of initial aircraft configuration.	5
Figure 3.2 (b) - Side view of initial configuration.	6
3.5 Task Separation, Scheduling, and Cost	6
3.6 Immediate Tasks	6
4. Preliminary Design	
4.1 Direction of the Preliminary Design.	7
Aspect Ratio	7
Taper Ratio	7
Wing Area/Wing Loading	7
Fuselage Volume	7
Thrust Feasibility	8
4.2 Figures of Merit.	8
4.3 Airfoil Selection.	8
4.4 Scoring Benchmark.	8
4.5 Dimensional Design.	9
Figure 4.5(a) - Demonstration of course distance and times of loaded sortie.	9
Figure 4.5(b) - Velocity versus time for the loaded sortie.	10
Figure 4.5(c) V-N Diagram for an airplane at a weight of 37.64 lbs and a wing area of 12 ft ² .	11
Figure 4.5 (d) - V-N Diagram for an airplane at a weight of 37.64 lbs and a wing area of 12 ft ² .	11
5. Detailed Design	12
5.1 Component selection and Systems Architecture	12
5.2 Performance	12
Figure 5.2 (a) - Force diagram of aircraft	12

Table 5.2a: Table of Loaded/Unloaded Sortie Estimates	13
5.3 Component Testing	13
5.4 Structure Analysis	14
Table 5.4 (a) - Aircraft Characteristics	15
Figure 5.4 (b) – Three Dimensional view of the aircraft.	16
Figure 5.4 (c) – Tip View of Aircraft with Dimensions	17
Figure 5.4 (d) – Three dimensional parts of aircraft	18
Figure 5.4 (e) – Nose Cone with dimensions	19
Figure 5.4 (f) – Fuselage Dimensions	20
Table 5.4 (b) –Table of Flight Estimates	21
Table 5.4 (c) - Flight Time	21
6. Manufacturing Plan	
6.1 Manufacturing Processes investigated	22
Table 6.1 (a) Carbon fiber dimensions	22
6.2 Structural Description	22
6.3 Figures of Merit	23
6.4 Fabrication Process	24
<i>Fuselage construction</i>	24
<i>Wing construction</i>	24
<i>Tail section construction</i>	24
<i>Landing gear construction</i>	24
6.5 Manufacturing Timing	25
Table 6.5 (b) - Manufacturing Time	25
Figure 6-1. Pie chart for manufacturing timing.	26

Appendix A

Appendix B

DESIGN LOADS

DISCUSSION

In the design of the aircraft, three sets of loads criteria are employed. Each is related to the other, however, they have distinct effects on the aircraft. These load criteria are explained briefly below. These criteria are: A. Aerodynamic Loads B. Payload Loads and C. Landing Gear Loads.

A. Aerodynamic Loads are the those used in the design to provide adequate strength for the main structural components of the wing, tail, and connections while in flight. At the given loads, the aircraft will see no permanent deformation or operational impairment. An ultimate factor of safety of 2.5 is employed to ensure the aircraft's integrity.

B. Payload Loads are those produced by the water that will be carried during flight. These loads will be used to provide adequate strength for the components of the fuselage while in flight and on the ground. At these loads the aircraft fuselage will see no deformation or structural failure. An ultimate factor of safety of 2.5 is employed to ensure fuselage integrity.

C. Landing Gear Loads are those produced while the aircraft is on the ground in flight and on touch down. These loads will be used to provide adequate strength for the components of the fuselage the gear attaches to and the gear itself. At the given loads the landing gear will suffer no catastrophic failure on landing and will not permanently deform under the weight of the aircraft. An ultimate factor of safety of 2.5 is employed to ensure the overall integrity of every component involved.

1 Executive Summary

1.1 Development:

During the early stages of development, various concepts were considered. First, the team examined last year's airplane. Last year the team had problems with the pull ratio. They calculated the need of 3 motors. Three motors and the batteries made the plane too heavy. This year One motor was to be placed in the nose and the other two in the wings. The team then decided to use one motor in the nose. This year the team was limited by the new regulations from last year.

Next, the team designed the door to the fuselage to open at the top. This allowed easy access from the previous design alternatives from the last year. The fuselage is designed to carry eight bottles, although the analysis was performed using seven bottles. Analysis demonstrated that carrying seven bottles provides optimal performance.

The team then discussed about the structural integrity of the airplane. They designed the airplane using carbon fiber. They first decided on using rectangular pieces but decided that a tubular carbon fiber would be more structurally sound yet weigh less than the rectangular carbon fiber. Using carbon fiber over balsa allowed the airplane to be lighter because fewer pieces would have to be used.

The last item that was covered was reloading the payload. The team wanted something easy to load and unload without difficulty. The team learned from previous years that one removable container holding all the bottles reduced time between sorties.

1.2 Design Tools:

The design tools used to design the airplane were based on previous competition experiences and new software. The team leader was familiar with the procedures that were used in previous years. The team leader explained procedures for each design phase.

1.3 Methods used to design:

For the design, most calculations that were performed were done using "rule of thumb" methods learned from the classroom lectures as well as the required text. Solid Works was the primary tool used for initially analyzing the narrowed design concept from the alternatives.

The preliminary design used Microsoft Excel as the primary analyzing tool. It was used throughout this entire design phase. One of the spreadsheets was used to calculate the performance under different conditions. This spreadsheet integrated aerodynamic formulas and performance data and referred this information back to the scoring analysis.

2 Management summary

2.1 Management and assigned areas of the Design team:

The University of New Mexico doesn't offer an aerospace degree, therefore, all team members are mechanical engineering students. Due to our general lack of knowledge of anything that flies, we had to take a crash course in aeronautic engineering. This is a big draw back for all the students who participated in the contest. Building a plane was a chance to learn something totally new and still apply concepts we had previously learned. The first half of the semester was strictly lectures on learning how to design a aircraft and the second half on building on our design.

For the first semester, our team lead was Brian Macias. Brian had been a part of the spring '99 team and had previous experience building for the AIAA contest. Brian was also the president of the AIAA student section at UNM. Brian's experience proved to be very helpful in the initial design and configuration of our plane. Brian went on Co-op for the spring of '00 and didn't get to have all the fun of putting together another airplane.

For the second semester of our project Eric Gartner took the position of team lead, and also the presidency of the AIAA student section. Eric has an extensive background in aeronautics. Eric has been a pilot for several years and his innate understanding of the subject. He has been crucial in both the design and manufacturing aspects of our aircraft.

Richard Medina tackled the power plant design for this year's contest. Being limited to five pounds of batteries was a new rule for this year's team to contend with, and Rich did an excellent job working closely with the aerodynamics to nail down our cruise speeds and making sure we had plenty of juice to get us around the circuit.

Cory Tafoya chose the job of designing the structure of our aircraft. The general configuration of the aircraft was decided by all of the team members. Cory finalized all the details of the wing body and produced a lightweight and strong structure capable of carrying payload around the circuit.

Aaron Stone designed the aerodynamics for the airplane. Aaron was always interested in fluid dynamics, and a wing body was a new application to the concepts of boundary layers, dynamic pressures, and Reynolds numbers.

The second semester brought several other people on board to help finalize the project. Mario Rodriguez completed the entire drawing package for the plane and was also an excellent craftsman. Oscar Quinones designed the cargo bay and trap door for easy accessibility to our cargo in between sorties. Doug Aitken and David Christensen produced carbon fiber composite materials for the fuselage and wing of the plane. These materials gave us the strength we needed without the expense of adding a large amount of weight to the wing body.

2.2 Designation of Milestone Chart:

Most importantly was the interface among these different subprojects. This agglomeration of subtasks is the reason for a design team. Keeping the big picture in mind and making absolutely sure that all team members were building the same airplane were crucial in getting our project off the ground.

Schedule Milestones	
Initial Meeting	August 24th
Individual Design Concept	October 12th
Conceptual Design Review	October 28th
Preliminary Design Review	November 23rd
Critical Design Review	December 14th
Building Start	December 20th
Report Preparation Start	January 20th
Building Complete	March 9th

Table 2.1 – Design time and Development of Milestone Chart.

This being the second time UNM has participated in the design, build, fly contest; this years team paid close attention to the lessons learned from the team before us. Engineering is an evolutionary process as opposed to revolutionary. This lead us to the initial design configuration of our airplane

3. Conceptual Design

3.1 Design Constraints:

Before anything was designed it was necessary to come up with design constraints, obviously these were provided by the contest rules. All team members studied the rules for the contest and compiled a list of the of design constraints. Our next mission was to take what we had learned and turn it into an airplane.

3.2 Design Alternatives:

On October 12th each team member arrived in class with a solution to our design problem. These solutions consisted of a basic configuration of an aircraft that would meet all of the design constraints. Each configuration proposal was then drawn on the board. A discussion followed. Each member on the team was given a chance to defend his or her configuration. Eight alternatives in all were present. Quickly, we were able to narrow down the number of alternatives to three. This was easy because several of the team members showed up with almost equivalent configurations. One of the design alternatives was a low wing /canard configuration. This particular configuration could easily be made into a puller, a pusher or both. Also, canards produce positive lift as opposed to conventional tails, which produce negative lift. To many team members this positive lift issue seemed like a more efficient way to get bottles of water around a circuit. Next, a bi-plane was a popular configuration. Certainly, last years contest winners had a large influence on this idea. Of course this plane won the contest for a reason, bi-planes produce an enormous amount of lift at the cost of very little drag. In fact, talking to a retired McDonald Douglas/Boeing design engineer, our team was reprimanded for not using the bi-plane design. As a side note, we were able to convince this gentleman later in the semester that our plane configuration was definitely the way to go. The final design idea was probably the most obvious. Since the objective of the contest was essentially to build a cargo plane, several team members showed up with exactly this configuration. Cargo planes in general have a high wing configuration with a large enough fuselage to carry what is needed. Cargo planes also have high lift/ low drag airfoils to assist in the carrying capacity. As this discussion unfolded, the group dynamics of our team began to develop.

3.3 Converging on an Idea:

This class meeting set the stage for rest of the design project. Because we are all budding engineers, it was decided that the best way to measure the features of each of these designs was to come up with a chart and ranking system and see which configuration prevailed. What we learned was that engineer design was an evolutionary process not a revolutionary one. This is our reasoning for choosing the cargo plane configuration over the other two ideas.

This configuration consisted of an airplane with a large fuselage, a high mounted wing, conventional tail, and tricycle landing gear. The fuselage was given a bay door on the top of the plane in order to allow easy access into the fuselage. The wing was mounted high in order to place motors on each wing, this would allow enough clearance for propellers to spin freely. Conventional tails are tried and true, and there is no reason to reinvent the wheel. Finally, the tricycle landing gear is more stable, and doesn't rotate the plane during takeoff and landing. This configuration provided an overall solution to the problem, it was a stable aircraft that could carry bottles around the circuit with minimum work from the pilot.

3.4 Cons of Alternative Designs:

Our reason for not picking the canard design was stability. Canard planes are usually quite agile and "zippy". In the model world these airplanes are thought of as more sportier than anything else. For this reason we steered clear from building the canard plane. This year's contest had new regulations to adhere to which included aircraft cost. Our initial interpretation of this was that it was unfavorable to design a bi-wing airplane. Also, a bi-wing plane meant we had to build two more wings. No one on the team considered themselves craftsman, and we knew that time would have to pay the price due to our lack of skill. Later in doing a detailed cost analysis on the several configurations it was found that having a bi-plane was not the way to go. This is how we were able to convince the gentleman mentioned earlier about our desire to go with a mono-wing configuration. Our next step was complete a drawing of this configuration in order to make sure all team members were on the same page.

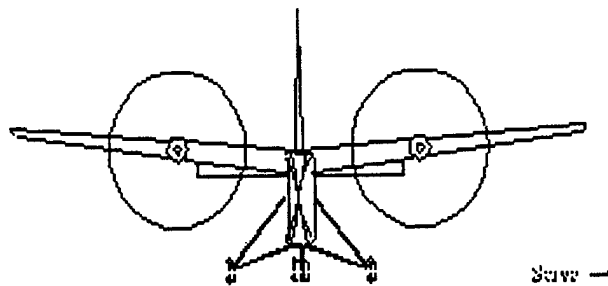


Figure 3.1 (a) – Sketch of initial aircraft configuration.

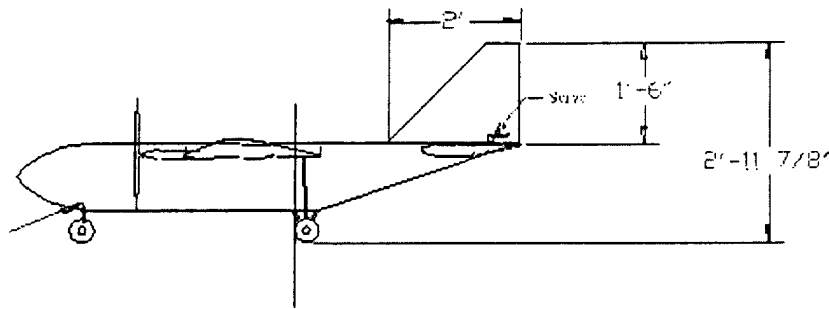


Figure 3.2 (b) – Side view of initial configuration.

3.5 Task Separation, Scheduling, and Cost:

Once we had developed our idea of a feasible solution to the design problem, we split up tasks into manageable sizes amongst all group members. These specific tasks are discussed in the management summary of this report. Next the team leader developed a schedule for the entire term of the project. This schedule consisted of what task would be completed, by whom it would be completed, and most importantly when each task would be completed. The group constantly monitored itself to make sure we were on track. Our biggest concern is that we would have to cut into our test and evaluation phase if we fell behind. Having enough time to test our design could mean the difference between first and last place. Our last issue for the conceptual design was cost. An itemized break down of necessary expenditures was contrived. Now it was time for the real fun to begin. We set out to complete an engineering analysis on our plane.

3.6 Immediate Tasks:

Our first step was to come up with a model of the contest. This model would serve as a guide for all future design changes and iterations. Our goal was to take a cargo plane and make it as fast as the power plant would allow us to fly. This meant reducing drag to its lowest possible value, and being as light weight as possible. This evaluation began with taking a look at aerodynamic loads, cargo loads, and landing gear loads. Our structure would have to withstand all these loads with no plastic deformation. As the preliminary design shows the configuration of our aircraft change considerably.

4. Preliminary Design

4.1 Direction of the Preliminary Design:

Once the basic configuration of the airplane had been determined, the dimensions needed to be established. The dimensions that still needed to be chosen were as follows:

- Aspect Ratio
- Taper Ratio
- Wing Area
- Fuselage Volume
- Airfoil

Factors that affected the above dimensions and needed to be determined are:

- Wing Loading
- Thrust Feasibility

Aspect Ratio

The only dimension that was held constant was the wingspan. The team decided to keep this length and vary the width needed to achieve lift in order to increase the aspect ratio. Keeping the wingspan at 7 feet and solving for wing area, the aspect ratio could be determined.

Taper Ratio

The drag associated with a rectangular wing was great enough that a taper ratio was favored. It was determined, however, that an elliptical wing would be too demanding for a team of inexperienced builders. The aerodynamicist and structure analyst decided that a taper ratio of 0.4 would be optimal in terms of performance and capability. This value is close to John D. Anderson Jr.'s description of a favorable non-elliptical taper ratio of 0.3. Due to structural concerns, the taper ratio was unable to be this low.

Wing Area/Wing Loading

The larger wing area that an airplane has, when using the same airfoil, the slower airspeed the airplane requires to lift off. Also, for a given cargo weight, the wing loading is increased as the wing area is decreased. An increase in wing loading requires more supports in the wings, which further increases the weight, which further increases the wing loading. A larger wing area also raises the cost of the airplane resulting in a lower overall score. The airplane was designed to suspend the estimated weight of the airplane at 2.5 G's. All of these factors were considered during the design.

Fuselage Volume

The fuselage volume designates how many water bottles can be carried for a single sortie. The increase in volume also increases the amount of area that the wind will be striking, either from the front as relative wind or from the side as gusts hit the side of

the fuselage. As wind is predicted to be a concern during the competition, the area on the side of the fuselage became important. An increase in the number of water bottles carried increases the weight. When this is increased, the lift needs to increase to counteract. More thrust is needed to accelerate the airplane to the required velocity to lift the plane within 100 feet. To simplify this portion of the analysis, the size of the fuselage was initially represented only as the number of water bottles and the increase in weight that they supply.

Thrust Feasibility

Due to the way that the cost of the airplane factors into the final score, the team had decided to build an airplane using only one motor. This requirement guided the power plant team to search for a powerful electric motor. The team also determined the power and longevity of the motor using the maximum amount of batteries (5 pound) and a variety of propellers. The maximum amount of time that the batteries could last was estimated at.

4.2 Figures of Merit:

Ease of construction
Feasibility
Final Score

4.3 Airfoil Selection:

First, we needed an airfoil to produce enough lift to get us off the ground. We choose a slightly cambered airfoil, because they produce a larger amount of lift. In order to maintain a simple wing design, and to accommodate our pilot we chose a single slotted flap, as opposed to flaps and ailerons. The flap is one continuous piece that runs along the entire length of the trailing edge of the airfoil. Our pilot doesn't like using flaps, by adding just one larger flap he has the choice to use it as an aileron or as a flap if needed during takeoff. This also allowed us to use fewer servos in the aircraft, which lowered our rated aircraft cost.

The airfoil chosen for the plane was the Eppler 66 airfoil. This is a low Reynolds number airfoil. The boundary layer must be tripped so as to cause a turbulent flow across the wing. A small tripping wire was used at the leading edge of the airfoil.

4.4 Scoring Benchmark:

In order to determine how competitive the University of New Mexico team's design is, an "ultimate" score needed to be determined. Using slightly unrealistic parameters, such as a plane's empty weight equal to 10 lbs, carrying eight water bottles, using one servo, completing five loaded sorties and a score of 100 for the written report resulted in a benchmark score of 16900.

4.5 Dimensional Design:

Since the parameters of the airplane not only affect the performance of the flight but also cost analysis, most of the data was inserted into a spreadsheet. The spreadsheet allowed the team to vary the parameters, each of which changed the cost of the airplane as well as the flight characteristics. Values for weight, wing area, and number of bottles could be inputted and a score for these values can be directly evaluated. Aerodynamic graphs are displayed in Appendix A. An example of the spreadsheet is shown on the next page as Figure 4.5 (a):

	A	B	C	D	E	F	G	H
1	Input							
2	Weight with Bottles	# of Bottles	Weight without Bottles	Wing Area		Score		
3	37.64	7	20	12		12893.3231		
4								
5		Thrust						
6		3.2						
7								
8								
9	Number of bottles flown in 10 minutes * 10	Total Flight Score			Rated Aircraft Cost			
10	280		840		6.515			
11								
12								
13	Velocities Loaded				Unloaded			
14	Velocity	Velocity (L/D max)	Velocity Liftoff	Velocity Climbout	Unloaded Velocity (L/D max)			
15	29.66081632	59.06081632	32.62689796	45.84385714	43.7208762			
16								
17	Wing Loading		Ground Roll		Engine Time			
18	50.18666667		49.77431635		6.236698625			
19								
20								
21	Number of Sorties		Unloaded Necessary		Thrust Necessary to take off in 90 feet			
22	4		45.7		6.913099489			
23								

Figure 4.5 (a) – Microsoft Excel picture showing the use of the spreadsheet.

In order to get an idea for the design of the airplane, a score of 100 was used for the written report. Then estimating the Manufacturers Empty Weight to be at 20 pounds, a wing area of 12 ft², and carrying seven bottles per sortie resulted in a wing loading of 50.19 oz/ft². Is this possible? If yes, check the rest. Velocity at L/D_{max} = 59 MPH. The Ground Roll is 50 feet. The amount of time that the motor is running is 6.24 minutes. The rated aircraft cost is 6.515. The team found that all of these values were feasible. This resulted in an overall score of 12893. The scenario above produced the highest score that our team can feasibly build. This score of 12893 seems competitive with the benchmark score of 16900.

Figure 4.5(b) below illustrates the movement about the loaded course, including times, distances, altitudes, and airspeeds.

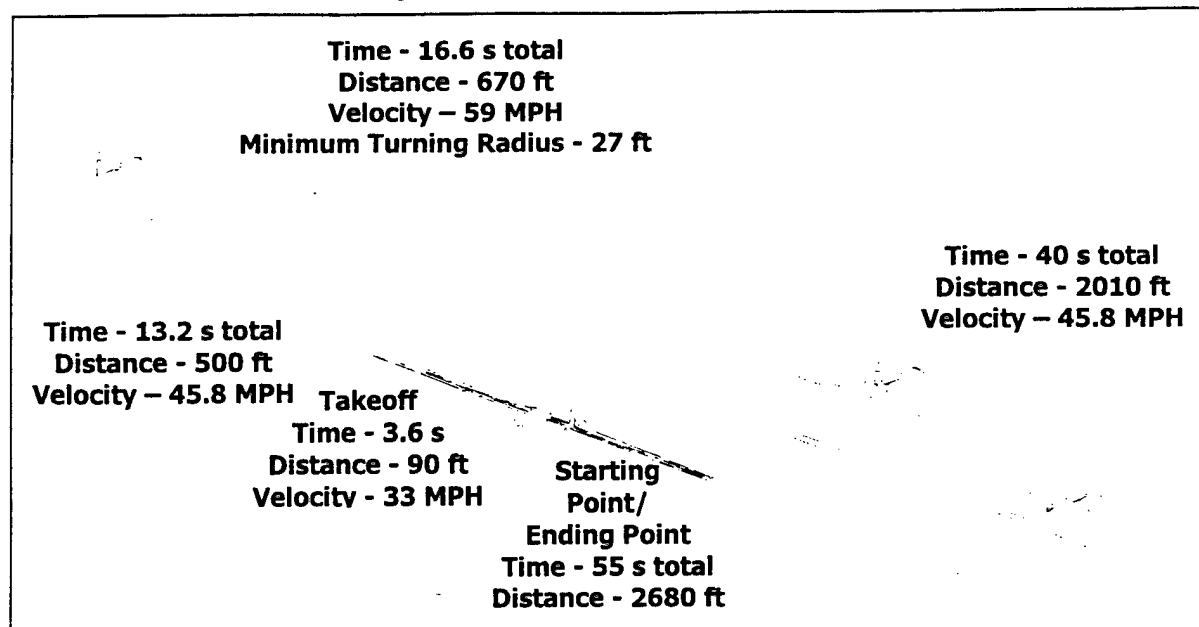


Figure 4.5(b) – Demonstration of course distance and times of loaded sortie.

The airplane rolls down the runway with seven water bottles until it reaches a velocity of 33 MPH. At this point the airplane has developed enough lift to climb. The airplane quickly accelerates to 45.8 MPH and climbs out to 50 ft AGL. The airplane stops the ascent and a right-hand turn is made at 2 G's resulting in a turn radius of 27 ft. The airplane is now traveling at 59 MPH. The downwind straightaway and the 360 are made at 59 MPH. At the end of the 360° turn, the motor is idled and the plane glides at 45.8 MPH around the turn and back down to the runway. The loading and unloading of the cargo is estimated to take at most 20 seconds. The next sortie is unloaded and doesn't require a 360° turn but an extra trip around the traffic pattern before it lands. The cruise velocity of this sortie is actually slower than the cruise velocity of the loaded sortie. This is to increase the efficiency of the power plane. Since the aircraft weighs less, the Velocity at the new L/D is slower. Flying at $V_{(L/D)}$ takes the least amount of work to keep the airplane at a level attitude. Once the airplane lands, the cargo is placed back in the airplane and the circuit starts all over.

Velocity vs Time

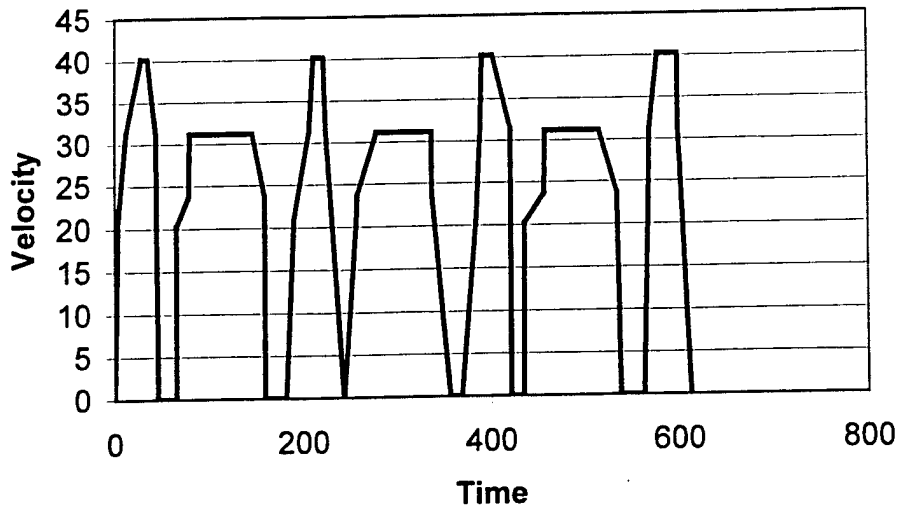


Figure 4.5(c) – V-N Diagram for an airplane at a weight of 37.64 lbs and a wing area of 12 ft².

Using the maximum weight and wing area obtained using the spreadsheets and rule of thumb calculations from William K. Kershner's The Advanced Pilot's Flight Manual, the following V-N Diagram [Figure 4.5(d)] was created.

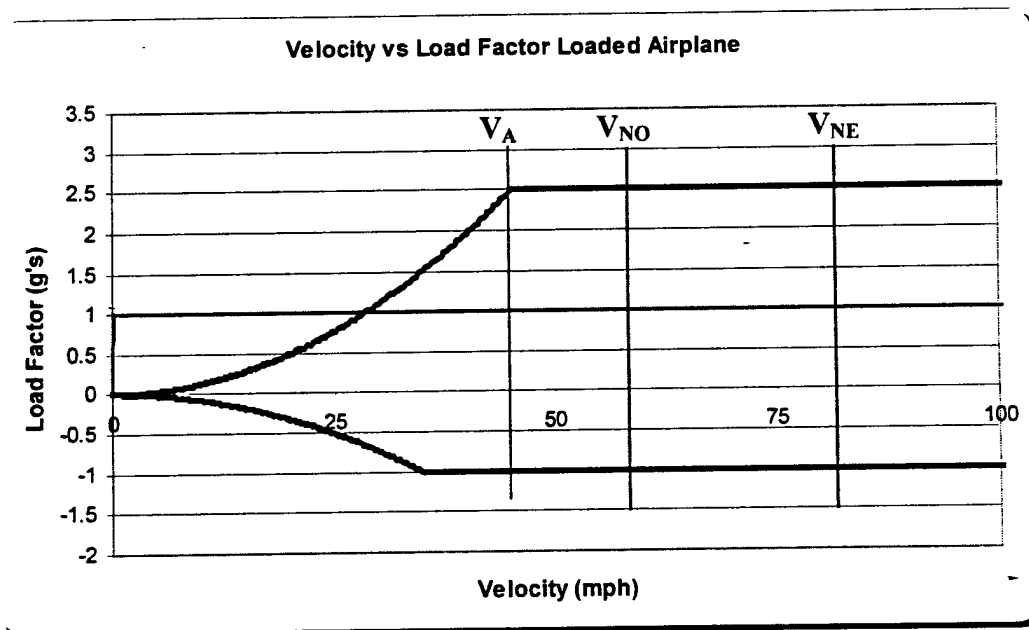


Figure 4.5 (d) – V-N Diagram for an airplane at a weight of 37.64 lbs and a wing area of 12 ft².

5. Detailed Design

5.1 Component selection and Systems Architecture:

The aircraft's selected motor is one Astro 90 motor with a 36 cell power pack. Initial calculations for the power pack were made with Sanyo 2000's. Sermark 1900's were later found and were lighter than the Sanyo's. Both run at 1.2 volts per cell, but the Sanyo's run at 2 amps and the Sermarks run at 1.9 amps. More calculations were made using a spreadsheet of equations from *Aircraft Performance and Design*; by John D. Anderson. The total maximum thrust remained at 15.46 lb. (1.75 hp) with the maximum thrust flight time changing from 3.43 minutes to 3.26 minutes. This battery pack is also 36 cells, and about 4 lb. which is .8 lb. lighter than the pack of Sanyo's. An Astroflight speed control is used for the motor, with an Astro gear box with a ratio of 1.63:1. For the motor a 22 x 10 propeller was selected.

The radio controller and receiver used is the Futaba PCM 1024 at 72 MHz. This six-channel transmitter was used last year and it has the required fail-safe for the contest. The aircraft uses four servos that are all FMA S360M, and both will be powered by a pack of 5 Sermark 1900's. The multi channel receiver also gives us the capability to use a flap based braking system.

The braking system is a combination of flaps and brakes. Upon touchdown the pilot will put the flaps full up. The pilot will also put the ailerons full down. Both will increase drag to slow the plane. The aileron servo does two jobs for the braking system. Not only does it increase drag, but it also has a push/pull cable attached to a small lever break on the nose gear that is only activated in the full down position.

5.2 Performance:

The aircraft is made with carbon fiber and balsa to keep the frame weight down yet strong. Estimated weight calculations were made with the assumption that a maximum load would be 2.5g's which leaves a comfortable factor of safety. The weight of the plane with servos, motor, and cells is 22.4 lb. Maximum weight is 37.6 lb. with 7 bottles of cargo. From these weights, payload fraction is .596. Figure 5.2 (a) shows a diagram of the aircraft with all forces acting on the frame.

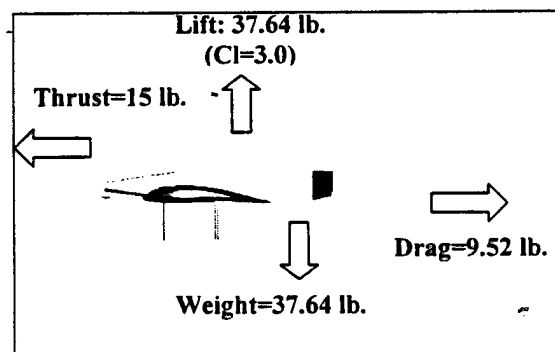


Figure 5.2 (a) – Force diagram of

Estimates were made up on how long each part of the sortie would take for a total of five in the allotted time. From there, velocities were calculated to make each section of the leg. A spreadsheet of calculations of power/thrust/velocity was then modified with the new power pack. However, the new cells did not change this aspect of the previous flight calculations. Table 5.2 (a) depicts the estimated velocities, thrust requirements, and amp draws for each section of the sortie. The only aspects of the sortie that are estimated for are the ones where the motor will be running. To help maximize battery time as well as keeping the motor cooler, the engine will be cut-off or running at absolute minimum during the beginning of the last turn before landing to load/reload. The thrust calculations are based on the fact that the plane will be flying at or near L/D max. A more detailed estimation of the sortie legs along with battery life can be seen on the next page in Table 5.5b.

Loaded					Unloaded			
	Time(sec)	Amps	Vel (ft/s)	Thrust (lb)	Time(sec)	Amps	Vel (ft/s)	Thrust (lb)
Cruise	25.57	6.70	45.7	5.56	72.33	6.36	59.06	4.72
Liftoff	9.82	22.41	23.78	15.2	13.99	21.37	32.63	9.08
Climbout	3.36	23.22	34.74	9.4	1.30	23.35	45.84	6.41

Table 5.2 (a) – Table of Loaded/Unloaded Sortie Estimates

The battery pack provides 3.26 minutes of max thrust flight time. This was used with the calculations of motor maximum amp draw, which ranges from 35-40 amps to find total amp-seconds. From this, amp-seconds were found for each leg of the sortie and this technique simulated battery life. Two sets of calculations were created which best projected the flight of the aircraft leaving the max thrust flight time at 1.54-1.34 minutes. So estimates show that only 60% of the battery power is used up during a five-sortie flight.

5.3 Component Testing:

The wing must withstand a 2.5g loading. To test this the wing was subjected to approximately 2.5 times the weight of the plane, around the center of the wing. Some simulated torsion tests were also performed. One side of the wing was held stationary while the other end was twisted to approximately +/- 5°.

The fuselage was tested before being connected with the wing. Twice the total weight of the batteries and bottles was placed in the fuselage. The nose and rear then suspended it. Placing 8 bottles in the bay and closing it tested the lid. The fuselage was then turned over to be sure lid would not open.

Landing gear will be made of aluminum and carbon fiber. The rear gear was tested by adding weight to generate deflection and then allowing it to spring back once the weight was removed. This weight was increased until a permanent deflection was seen when the weight was removed. A weight of 58 lb. was applied before any

permanent deflection was seen. The front landing gear was subjected to a similar test, but a 30-lb. load was applied.

5.4 Structure Analysis:

Basic statics played a large part in determining the makeup of the airplane. This gave rough estimates as to the size and location of the spars and ribs for the wings, as well as the structure of the fuselage and tail section. The structure designs for both the wing and the tail sections were very similar because the type of loading that each airfoil sees is similar. The wing loading had already been determined by the aerodynamic performance of the aircraft. The job of the structure designer was to design a wing that could withstand these forces. Balsa wood was used for the ribs of the wing. Ribs were placed every six inches along the length of the wing. In between the ribs, a torsion box was built to counter act the force couple placed on the wing by the pressure difference causing lift. Finally, the spars of the plane are made from carbon fiber tubes. Carbon fiber is considerable stiffer than balsa wood for its size. On conventional airplanes, the wing spars are placed directly on top of each other. Due to our tapered wing, the top spars run along the leading edge and the trailing edge of the airfoil. Placing our top spars along these edges allows the spar to carry the bulk of load placed on the wing, as opposed to the ribs having to carry this load. Moving our spars in this manner may cause difficulty in connecting the wing to the fuselage but this insures that the wing can withstand the wing loading. The horizontal stabilizer for the wing was design in a conventional manner. The shape is a Hershey bar airfoil and the spars run parallel, and the ribs are spaced every six inches. The tail has less wing loading than the wings of the airplane, therefore their structure is more than adequate. The fuselage of the airplane is built more like a simple truss bridge. Again, carbon fiber was the material of choice due to its large ultimate strength. A round cross section was employed in order to create a space frame. A round cross section is useful because stress risers are minimized due to the fact that there are no corners on a cylindrical cross section. Once the structure of the plane had been designed, the structures were divided into subsystems to evaluate the stress and feasibility in those sections. The different tasks were divided into a wing section, a fuselage section, a landing gear section and a tail section. Finally, a person was dedicated to making sure that all of the parts interfaced correctly. The stress analysis performed with each of these parts is listed in Appendix B.

The aircraft specs after the Detail Design are shown on the next page in Table 5.4 (a).

Table 5.4 (a) – Aircraft Characteristics	
Aircraft Dimensions	
Wing Span	7 ft
Total Length	71 inches
Wing Mean Chord	1.75 ft
Wing Area	12 ft ²
Wing Airfoil	Eppler 66
Tail Airfoil	NACA 12
Propulsion and Control	
Motor	Astro 90
Battery Pack	36, 1.5V, 1900 mAh, NiCad Cells
Propeller	22 x 10
Bottle Capacity	7 (8 Max)
Servos:	FMA S360M
Number of Servos:	5
Radio Controller	Futaba PCM 1024
Aerodynamics	
Weight	37.64 lb.
Coefficient of Lift	3.29
Lift	37.64 lb
Coefficient of Drag	.81
Drag	9.52 lb.
CG Location	.25 Chord
Neutral Point	.5 Chord

The drawings resulting from all of the engineering analysis performed are attached on the next three pages and are labeled as Figures 5.5(a-e).

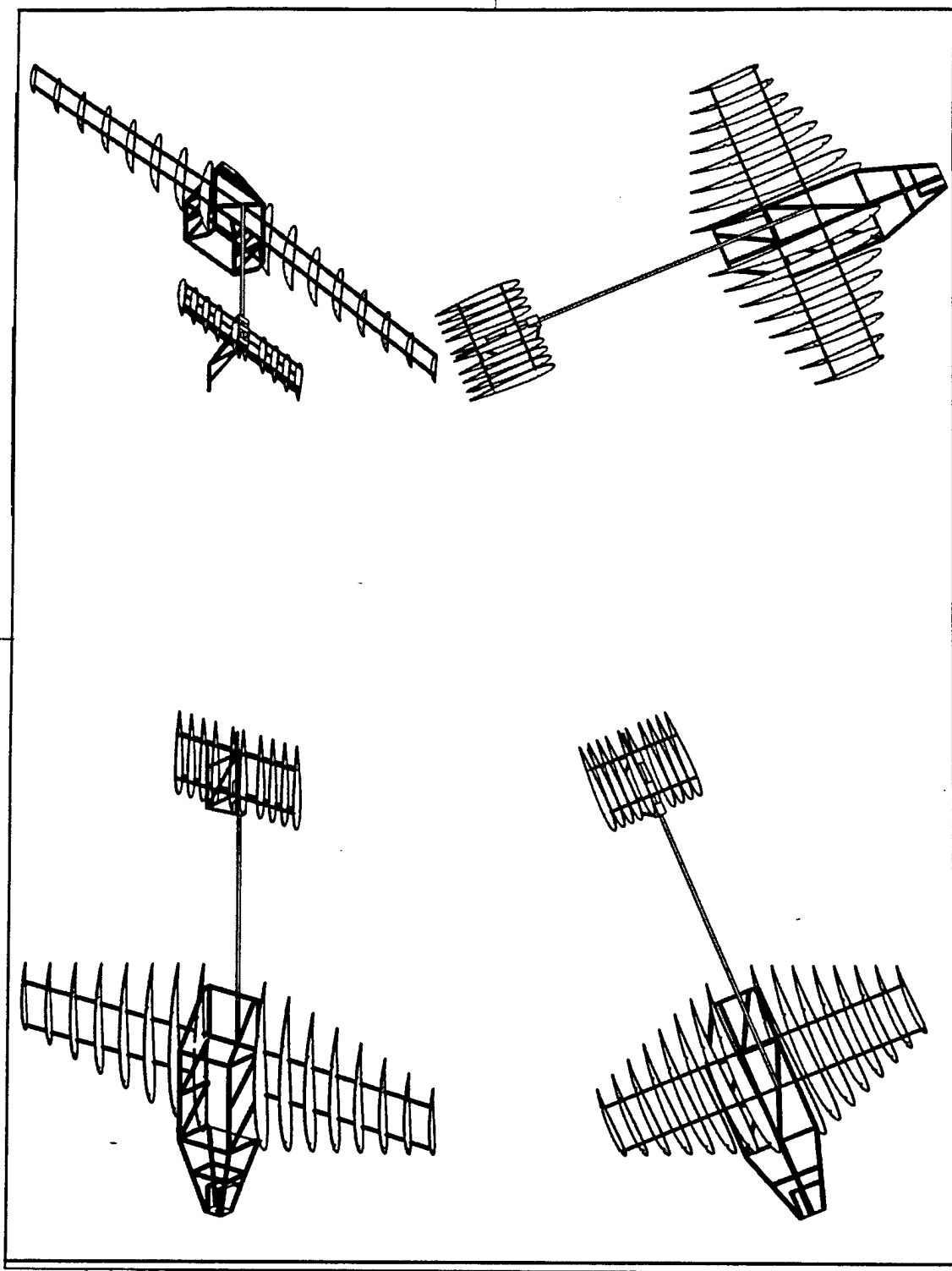


Figure 5.4 (b) – Three Dimensional view of the aircraft.

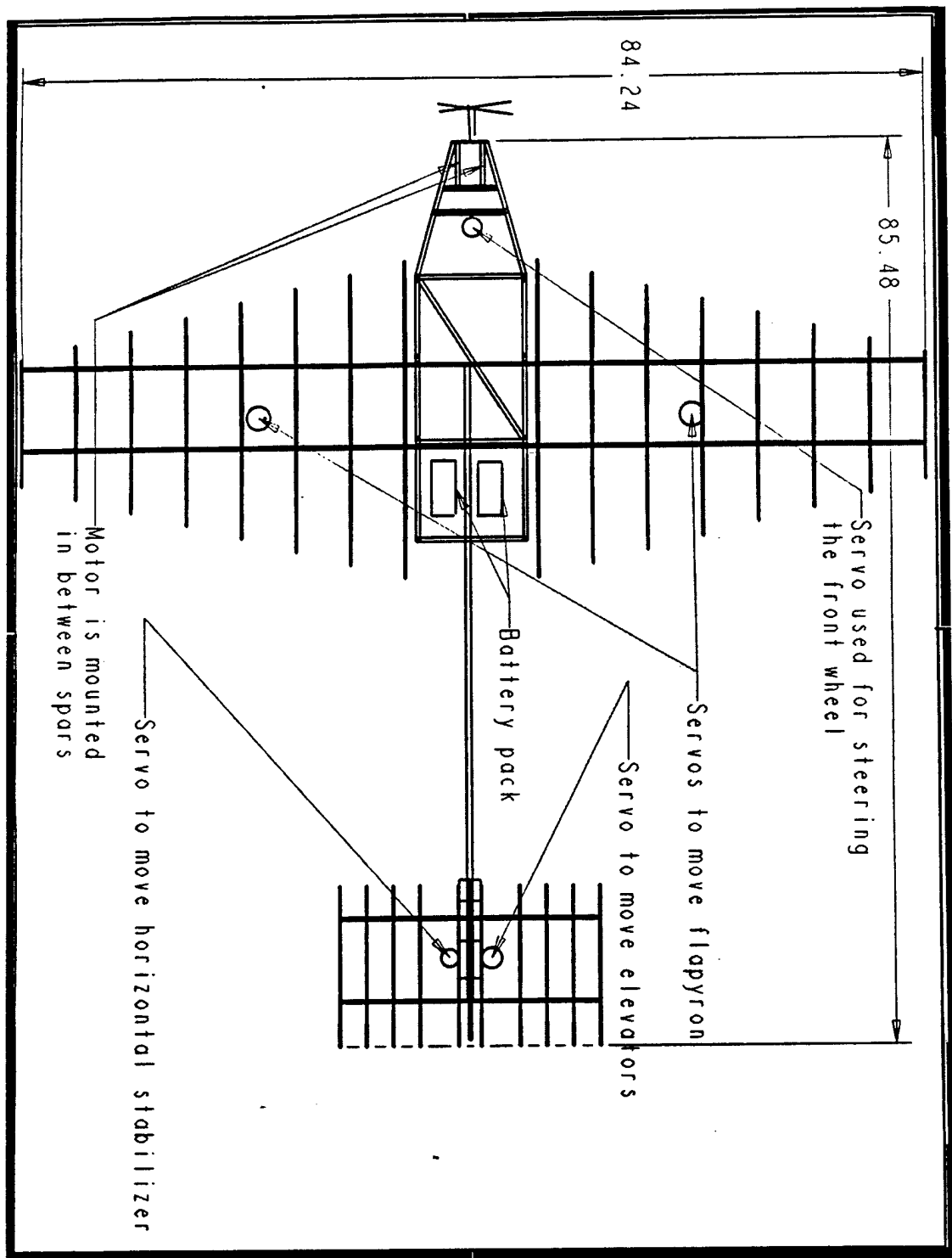


Figure 5.4 (c) – Tip View of Aircraft with Dimensions

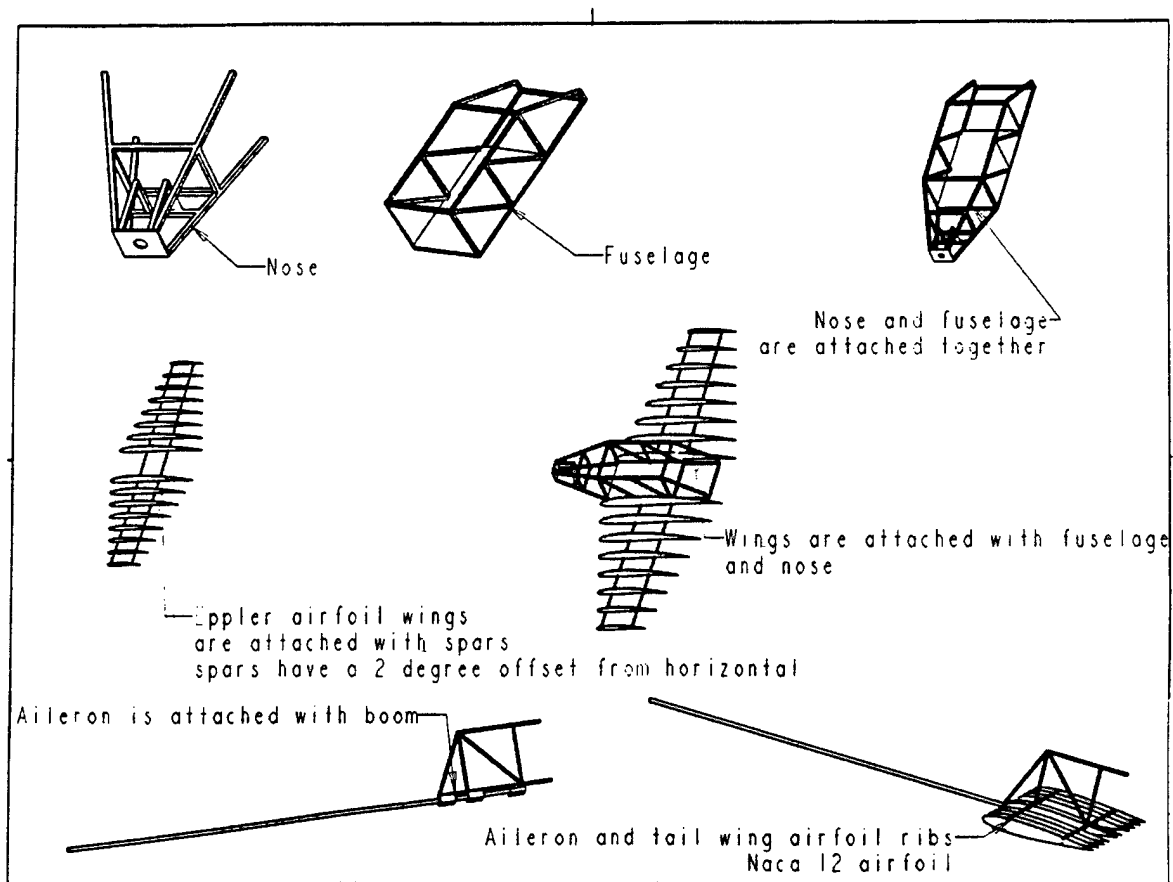
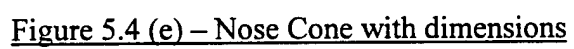


Figure 5.4 (d) – Three dimensional parts of aircraft



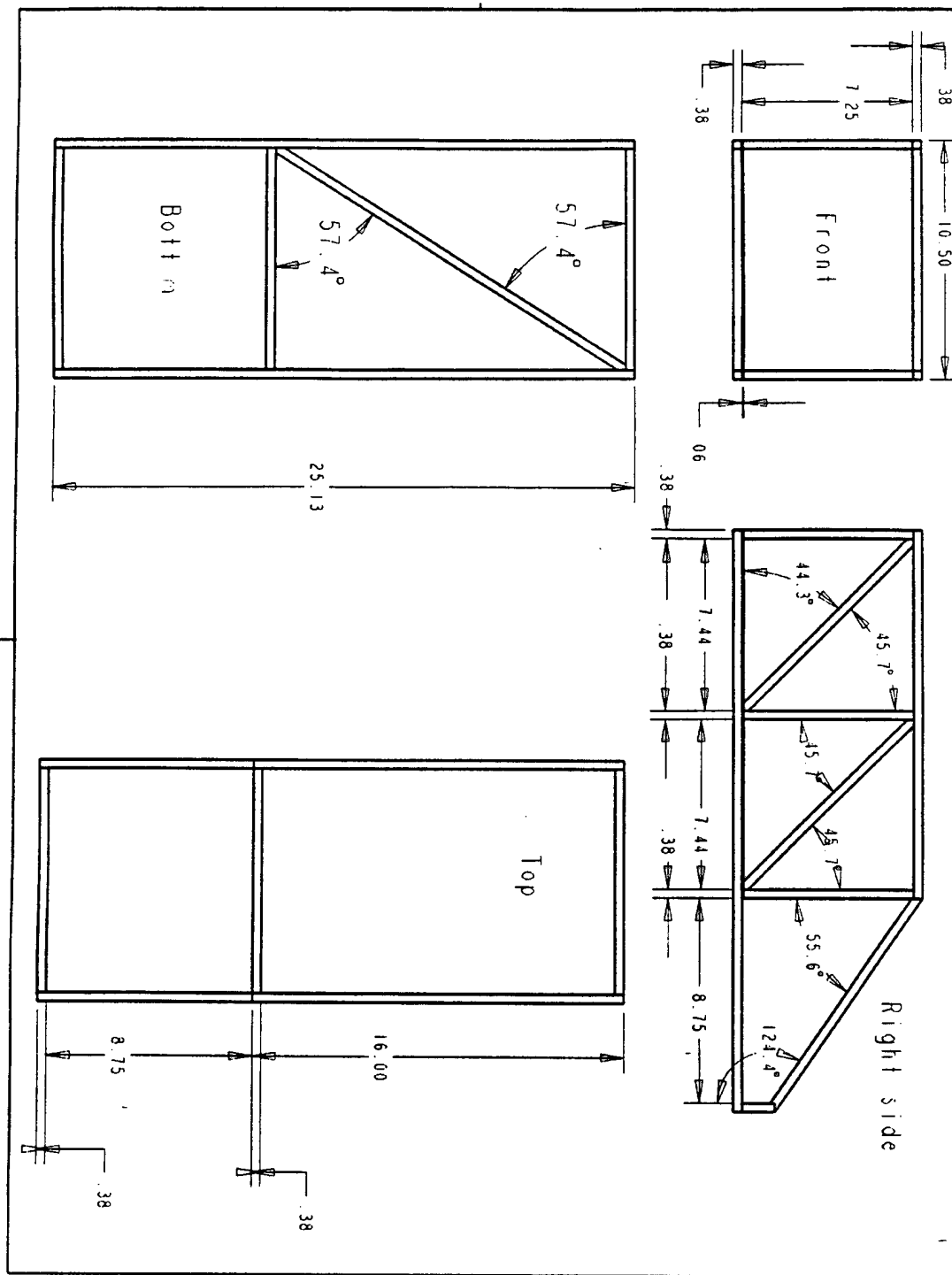


Figure 5.4 (f) – Fuselage Dimensions

Table 5.4b – Table of Flight Estimates

Loaded			
	<u>Cruise</u>	<u>Liftoff</u>	<u>Climb</u>
Velocity (ft/s)	59.06	32.63	45.84
Thrust (lb)	4.72	9.08	6.41
power req (hp)	0.51	0.54	0.47
power req (ft*lb/s)	280.5	297	258.5
current draw (amp)	6.699254	6.893475	6.431174
time (sec)	25.57	9.82	3.36
Unloaded			
	<u>Cruise</u>	<u>Liftoff</u>	<u>Climb</u>
Velocity (ft/s)	45.7	23.78	34.74
Thrust (lb)	5.56	15.2	9.4
power req (hp)	0.46	0.68	0.55
power req (ft*lb/s)	253	374	302.5
current draw (amp)	6.362389	7.735632	6.957011
time (sec)	72.33	13.99	1.30

Table 5.4 (b) – Flight Time

Estimate		Estimate	
1		2	
<u>Sortie</u>	<u>Amp*sec</u>	<u>Sortie</u>	<u>Amp*sec</u>
Battery	6840.05	battery	6840.05
Loaded	260.60	loaded	469.39
Unloaded	577.46	unloaded	789.51
After	3227.208	After	2806.37
flight		flight	
Time Left	1.54 Min	Time	1.34 Min
		Left	

6. Manufacturing Plan

6.1 Manufacturing Processes investigated:

Manufacturing of the aircraft began in early January with the construction of carbon fiber spars and structure members. The pieces were 0.25" x 0.125" and 0.375" x 0.125". These dimensions were chosen for ease of building and strength. The carbon fiber cloth was placed into a polypropylene mold and pressed with resin until the desired dimension was reached. When multiple pieces were complete, two fuselage structures were constructed. The first was constructed with the pieces made by the team and the second constructed with carbon tubes purchased from CST in California. The completed fuselage structures were discussed taking into consideration weight, strength, and construction. The purchased carbon tubing won in all categories. The carbon tubing is produced by wrapping multiple layers of unidirectional carbon prepreg around a mandrel then cured at elevated temperature. The results of the process are a tube that has a greatly desired strength to weight ratio. Three sizes of the carbon tubing were purchased.

Tube diameter	Weight (gr./ft.)	Wall thickness
0.25"	7	0.025"
0.375"	12	0.030"
1.0"	60	0.060"

Table 6.1 (a) – Carbon fiber dimensions.

The team decided that the reason for the failure was the lack of compression during the curing process and the lack of experience with the material. The 0.25" tubing would be used for the entire fuselage structure and, along with the 0.375" pieces, the wing spars. The 1.0-inch tube would be the boom, connecting the fuselage and main wing to the tailpiece. The only pieces of the plane that would not be made of carbon fiber would be the ribs (balsa wood), the base plate of the fuselage (plywood), the mylar skin, the top hatch hinge system (balsa wood), and parts of the landing gear.

6.2 Structural Description:

This aircraft is designed to fly a payload of eight full one liter bottles of water and withstand flight loads two and a half times greater than when at straight and level, unaccelerated flight. The aircraft has one wing and one DC motor with tricycle landing gear.

Each segment of the fuselage and nose will be a simple truss configuration constructed of thin carbon fiber. Each fuselage truss will be attached to another making a three dimensional box to carry the payload. Thin aircraft plywood will provide the floor for the payload. A thin carbon fiber sheet will act as an access door for the payload as well as a cover for the top of the fuselage.

The wing and tail will be composed of carbon fiber spars and balsa wood ribs. The leading and trailing edges of the wing will be constructed with balsa wood as well. Each member of the wing and tail will be joined with epoxy. The connection between the fuselage and tail will be a thin circular boom made from carbon fiber. The boom will

be pinned at the tail and fuselage to allow the aircraft to be separated into two pieces for shipping.

6.3 Figures of Merit:

The figures of merit that were used to decide on the final construction process were:

- Cost for materials
- Availability of materials
- Required skill levels
- Time constraints

The design team for the spring 2000, competition was fortunate to have the materials used by the previous year's team. With donations of carbon fiber cloth and resin from Sandia National Laboratories in Albuquerque, the costs were minimal for the preliminary fuselage. The carbon fiber tubing fit within our budget constraints because money was saved using previously purchased materials and donated materials. The only costs prior to the purchase of the carbon tubing was the polypropylene for the carbon fiber molds, minor machining costs, and tooling that was required for construction. After the tubing was purchased epoxy and insta-cure glue decided on for joint welding.

The availability of materials never became an issue due to the benefits above. The team was already looking for carbon tubing. As stated above, many of the materials were from the 1999 Aero team. This saved time and money for the 2000 team.

The required skill level became an issue when the initial carbon pieces were being constructed. Due to the lack of skill in the production of carbon fiber, the pieces did not meet the level of strength and hardness desired by the team. Other carbon fiber pieces were considered besides rectangular cross sections. Hollow rectangular pieces were considered but not built because of the difficulty of fabrication. Thinner pieces of carbon fiber tape were considered but not built because of difficulty of construction, mainly due to the thin, sharp edges. The team members consisted of multiple people who have had much experience with balsa wood models and one with actual remote control airplane experience. Although most of the members previous experience was with remote control cars this came in handy with the servo to flight control links and concepts. Much of the construction was new territory for many of the group members but being engineers they were all excited to build the plane.

The desired completion date for the airplane was March 15th, which would allow 30 days for test and evaluation. A lot of time was used for the building of the initial carbon fiber pieces. This time was not considered to be a waste of time. By making the carbon fiber we gained knowledge of our project. The estimated time for construction of the fuselage, wings, and tail piece was estimated to be approximately 200 hours and the servo and speed control/motor setup was estimated to be approximately 50 hours. The remaining estimated time was set aside for the test and evaluation. These steps were

predicted to take approximately 50 hours, but this estimation was increased to one month to compensate for unexpected delays.

6.4 Fabrication Process:

Fabrication of the airplane started with the completion of the final fuselage. Then the main wing was completed followed by the entire tail section. The next step was integrating all the pieces, with the tail and fuselage being joined by the 1.0" diameter carbon tubing. The next step was the integration of the flight control parts, the propulsion system, and the landing gear. All the joints were joined using epoxy and insta-glue.

Fuselage construction

The fuselage construction was simple, but time consuming. The team built the entire structure out of 0.25" carbon tubing. A fishmouth type system was decided upon for the joining of the cylindrical pieces. To create the desired fishmouth shape an elementary machine was built using two vices, wood, and a dremel tool with the appropriate adapter.

Wing construction

The wings were constructed with 0.125" balsa wood ribs, two 0.375" diameter spars, and two 0.25" diameter spars. The balsa wood ribs were cut to fit the spars and the wing was constructed according to the design. The difficulty in the wing construction was in the integration of the ribs. Plywood pieces were glued to the four outside spaces between the ribs to add strength because of moments generated by lift. The ailerons and flaps were built by cutting off the tailing ends of each of the ribs and integrating them with a 0.25 diameter carbon tube. Each side of the wing was built separately and then joined together making sure the dihedral specification was met. For each of the aileron and flap one servo was used and a simple linkage system was implemented to control the movement.

Tail section construction

The construction of the tail section was very similar to the main wing. Using both the 0.25" and 0.375" carbon tubes for the spars. The ribs of the horizontal stabilizer were designed all the same time which made the construction much simpler than the main wing. The vertical stabilizer was constructed out of plywood. Two servos were used to control the tail section. One servo was used to control the elevators and the other to control the rudder.

Landing gear construction

The landing gear design from last year's Lobo team proved to be an ongoing obstacle. This year's team wanted to learn from their mistakes. One big problem that the

other team had was the placement of the main gear. The main gear was placed much farther behind the center of gravity than it needed to be. The result of this is that the tail force needs to be large in order to rotate the plane. There are three ways to accomplish this extra force needed. The first two involve either increasing the tail area, increasing the tail length from the center of gravity, or some combination of the two. These two both involve a huge redesign and rebuilding project. The last way is to increase the amount of airflow over the tail. Obviously, the only way to accomplish this is to increase the speed of the airplane. To do this involves a longer takeoff run. The only other portion of the main gear that this year's team thought could be improved on was the wheels. They used a rubber cushion around cutout carbon fiber. Although the wheels from the previous years design were thin for streamlining, they didn't have very good shock absorption and weren't very robust for multiple takeoffs and landings. A design that seemed to work well for a number of other teams last year was a simple in-line skating wheel. The bearing design as well as the material makes these wheels preferred to last year's design. To summarize the main landing gear construction: this year's team calculated the forces needed from the tail to rotate the airplane, and placed the main gear accordingly. This year's team decided to use a castor design for the nose gear as well as a single brake on the nose gear.

6.5 Manufacturing timing:

The construction of the airplane began January 3, 2000 and was completed on March 14, 2000. The approximate time for the entire construction was estimated to be 250 hours and the actual construction time was 300 hours. See the construction time pie chart below.

Component Constructed	Approx Time Required (hrs)
Initial Carbon fiber pieces	40
Fuselage	40
Wings	55
Tail Section	60
Landing Gear	40
Plane pieces Integration	10
Control and Power System	45
Mylar Skin of entire Plane	10

Table 6.5 (b) – Manufacturing Time

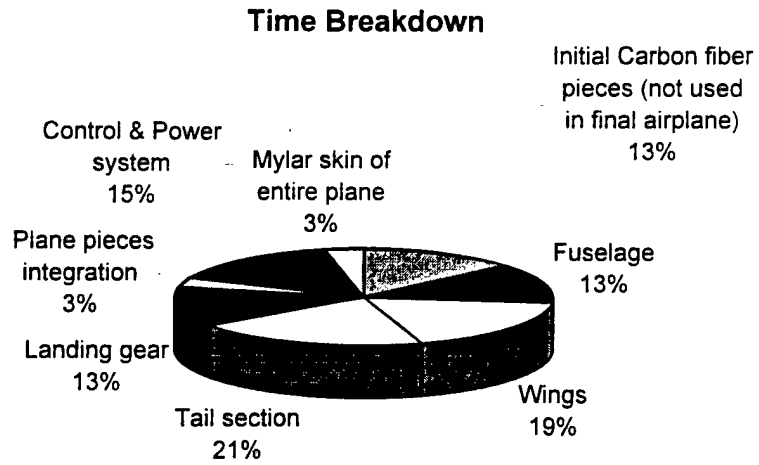
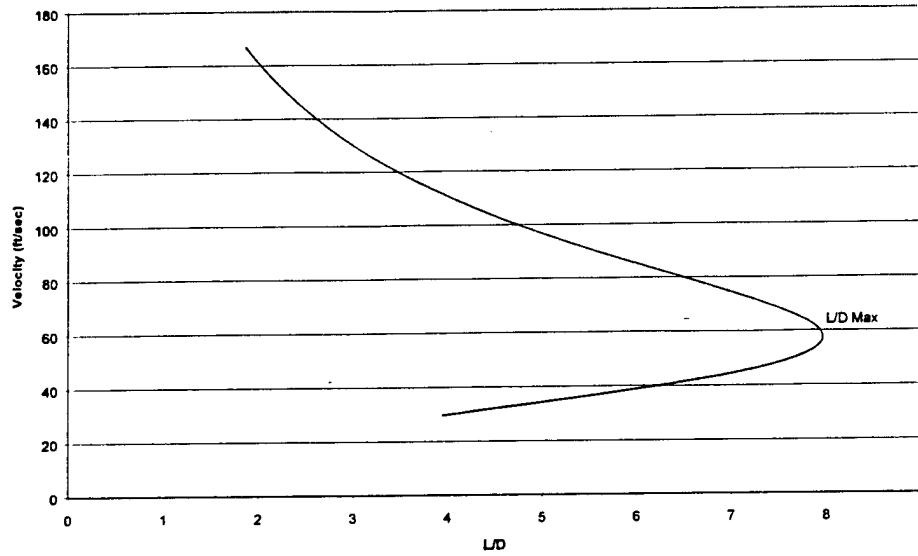


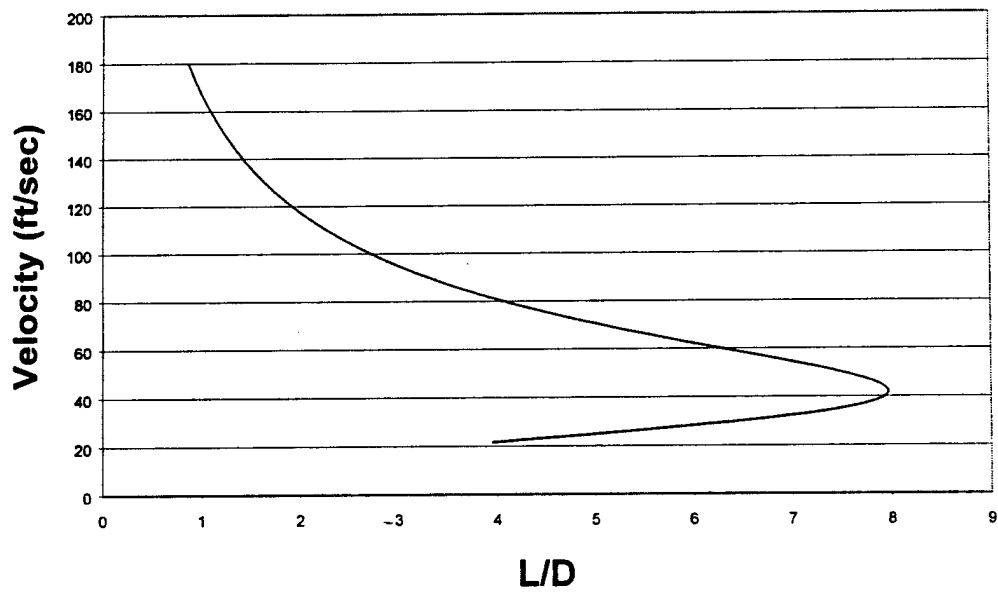
Figure 6.1 – Pie chart for manufacturing timing.

Appendix A - Aerodynamic Graphs

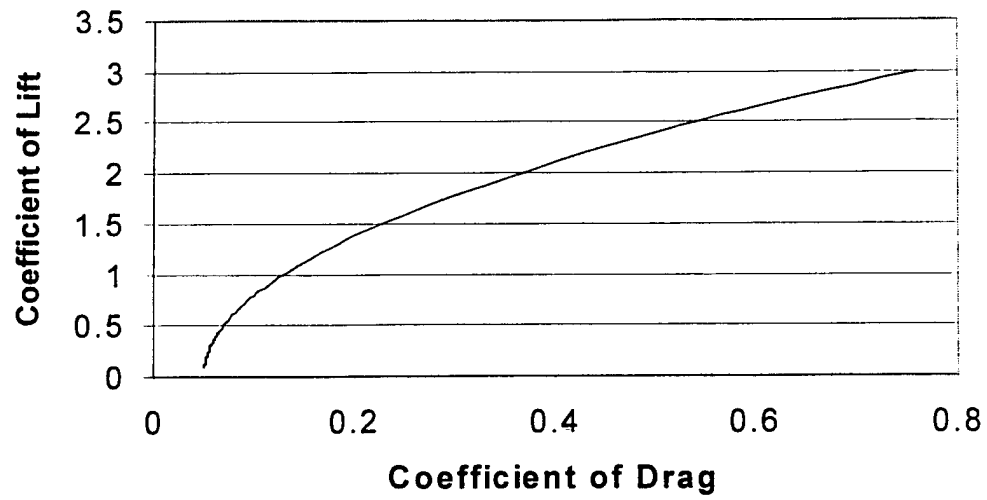
L/D vs. Velocity



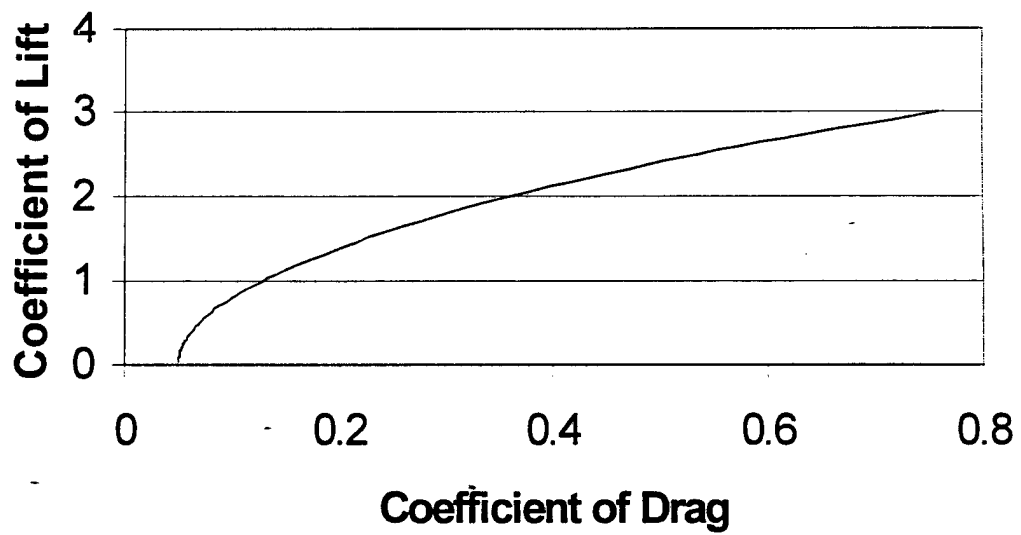
L/D vs. Velocity (Unloaded)



Drag Polar (Loaded)



Drag Polar (unloaded)



Appendix B – Wolfpack Aero Strength Summary

TABLE OF CONTENTS

- i. Table of Contents
- ii. Abstract
- iii. References
- iv. Drawing List
- 1. Airplane Description and Geometry
- 2. Design Loads
- 3. Stress Analysis
 - 3.1 Spars
 - 3.2 Tail Boom
 - 3.3 Fuselage Truss Segment
 - 3.4 Connectors for Wing, and Tail
 - 3.5 Landing Gear
 - 3.6 Motor Mounts

ABSTRACT

This strength summary defines the capability of a radio controlled aircraft to safely fly a payload within the constraints defined by the American Institute of Aeronautics and Astronautics (AIAA) design, build, fly competition, and the loads associated with the payload and flight.

REFERENCES

1. Aircraft Performance and Design, John D. Anderson Jr.
2. Basics of R/C model aircraft design, Andy Lennon
3. Mechanics of Materials, R.C. Hibbeler
4. Rotator 180 Strength Summary, F. Walchak
5. Stress and Analysis of Semimonocoque Structures, J. J. Russell, Ph.D

Pro-Engineer Drawings

Drawing Title No:	Parts include for Fuselage assembly	Description:
Fuselage_assembly.asm	Part1.prt Part2.prt Part3.prt Part4.prt Part5.prt Part6.prt Part7.prt Part8.prt Part9.prt	.375 X .375 inch carbon fiber pieces which vary in length. Pieces are cut in different degree cuts.
Nose.asm	Parts include for Nose assembly Part1ab.prt Plate.prt Part2b.prt Part2b.prt Part4d.prt Part4d.prt	.375 X .375 inch carbon fiber pieces which vary in length. Pieces are cut in different degree cuts.
N_F.asm	Parts include for Nose & Fuselage assembly Nose.Asm Fuselage_Assembly.asm	Nose parts and fuselage parts are integrated together
Wing1.asm	Parts include for Wing 1 assembly Rib1.prt Rib2.prt Rib3.prt Rib4.prt Rib5.prt Rib6.prt Rib7.prt Rib8.prt Spar1_bottom.prt Spar2_bottom.prt	Ribs are modified by using a varying scale factor which produces different sized ribs Spars which hold ribs together
Wing2.asm	Parts include for Wing 2 assembly Rib1.prt Rib2.prt Rib3.prt Rib4.prt Rib5.prt Rib6.prt Rib7.prt Rib8.prt Spar1_bottom.prt Spar2_bottom.prt	Ribs are modified by using a varying scale factor which produces different sized ribs Spars which hold ribs together

Total_wing.asm

Parts include for Total wing assembly

Angle_spar.prt
Wing1.asm
Wing2.asm
Angle_spar.prt

Wing_fuselage.asm

Parts include for Total wing and Fuselage

Total_wing.asm
N_F.asm

Total wing is integrated with
Nose and fuselage.

Tail.asm

Parts include for Tail wing assembly

Spar_1_fourth.prt
Spar_1_fourth.prt
Spar_1_fourth.prt
Spar_1_fourth.prt
Tail_rib1a.prt
Tail_rib1a.prt
Tail_rib1a.prt
Tail_rib1a.prt
Tail_rib1a.prt
Tail_rib1a.prt
Tail_rib1a.prt
Tail_rib1a.prt
Tail_rib1a.prt
Tail_rib1a.prt

.25 X.25 inch spars made of
carbon fiber to hold ribs for the
end of the tail wing.

Ribs are all the same scale
factor.

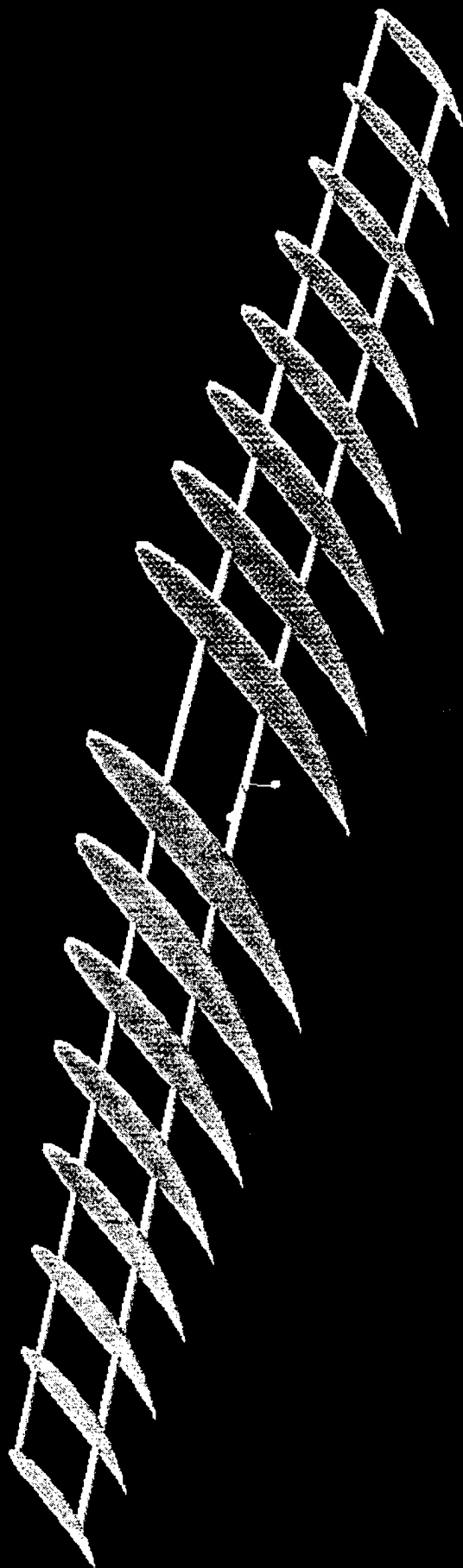
STRUCTURAL DESCRIPTION

This aircraft is designed to fly a payload of eight full one liter bottles of water and withstand flight loads two and a half times greater than normal. The aircraft has one wing and one DC motor with tricycle landing gear. Sketches are shown on following pages in this section.

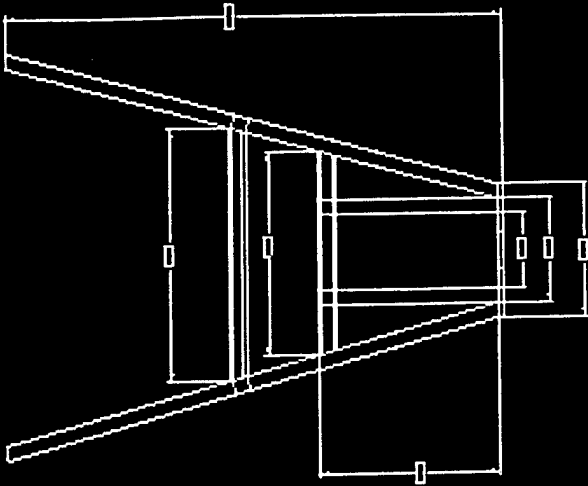
Each segment of the fuselage and nose will be a simple truss configuration constructed of thin carbon fiber. Each fuselage truss will be attached to another making a three dimensional box to carry the payload. Thin aircraft plywood will provide the floor for the payload and a thin carbon fiber sheet will act as an access door for the payload as well as a cover for the top of the fuselage.

The wing and tail will be composed of carbon fiber spars and balsa wood ribs. The leading and trailing edges of the wing will be constructed with balsa wood as well. Each member of the wing and tail will be joined with epoxy. The connection between the fuselage and tail will be a thin circular boom made from carbon fiber. The boom will be pinned at the tail and fuselage to allow the aircraft to be separated into two pieces for shipping.

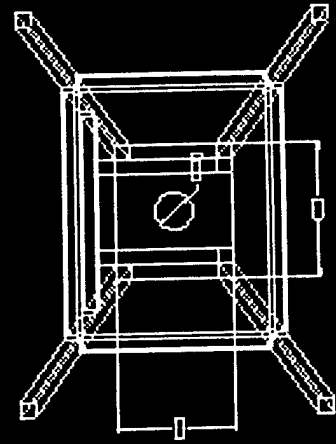
GEOMETRY



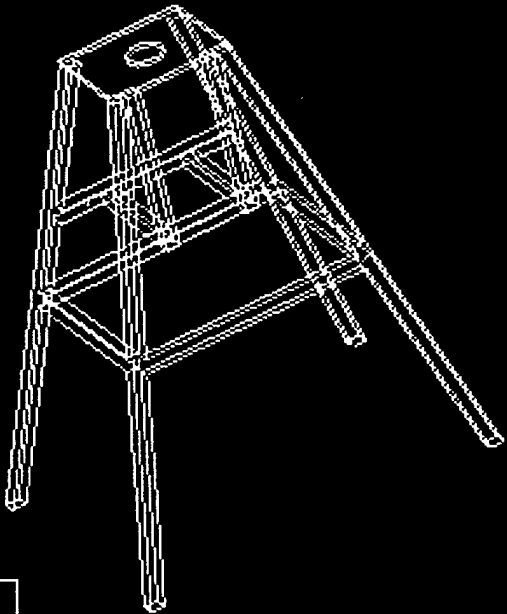
SCALE : 1.000 TYPE : ASSIM NAME : NOSE SIZE : L



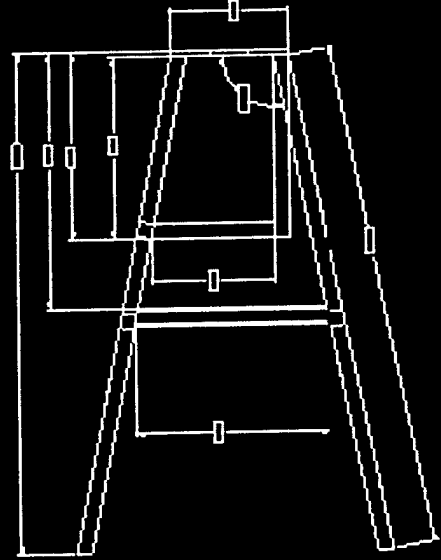
FRONT



BOTTOM



RIGHT SIDE



ASERO DESIGN	
Drawn By :	ASERO DESIGN
Part No :	ASERO DESIGN
Rev :	ASERO DESIGN

FRONT

TOP

RIGHT SIDE

AERO DESIGN	
Drawn by :	
Checked by :	
Scale :	
Date :	

SCALE : 1.000 TYPE : ASSEM NAME : FUSELAGE ASSEMBLY SIZE : E

SCALE : 1.000 TYPE : ASSEM NAME : FUSELAGE-ASSEMBLY SIZE : E

BOTTOM

RIGHT SIDE

AERO DESIGN	
Drawn By :	
Part No :	
Scale :	

2.5 - LAND = 16

Assume

Assumptions

1. Landing on wheel at 100 ft

2. Landing on 1.5 ft

3. Free fall = 1.75

4. Free fall = 37.5



$$37.5 \times 1.5 = 56.25$$

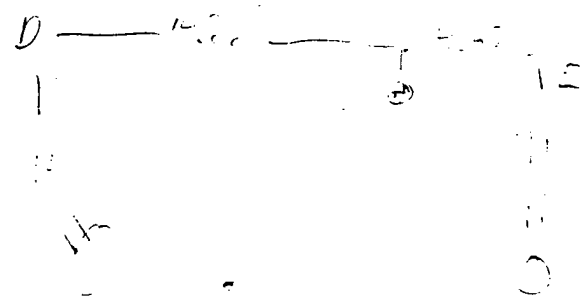
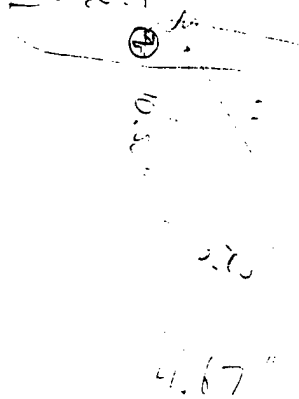
$$56.25 + 1.75 = 58.00$$

Free fall

Free fall

Location of landing on free fall

$$4\% \text{ NAL} = 3.04 (1.75) = 5.32 = 0.17$$



$$\Sigma \text{ } = 0 (1.75) = 5.32 = 0$$

Free fall = 37.5

$$37.5 = 37.5 - 70.00 = 32.5$$

3.4 1/23/00

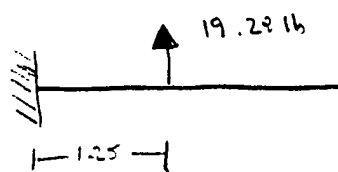
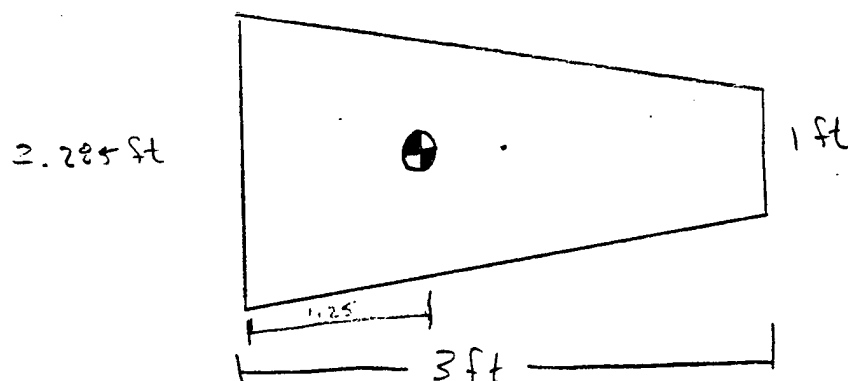
stress analysis on wires/body connection

1st moment caused by lift

lift cause 50.12 oz/ft^2

$$(25.09 \frac{\text{oz}}{\text{ft}^2})(4.9 \text{ ft})(2.5) = (308.61 \text{ oz})(\frac{16}{16.1}) = 19.28 \text{ lb}$$

C_g is approx 1.25 ft from root



moment caused by lift

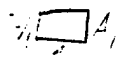
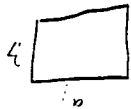
$$\blacktriangleright (19.28)(1.25) = \boxed{24.1 \text{ lb ft}}$$

Mo/ 1000

1.5 = 2500

Cotton Door 16" x 8" x 3/4"

Cotton falls @ 500,000 psi



$$\sigma_0 = \frac{F}{A_0} = \frac{2500}{128} = 19.5 \text{ psi} \quad \checkmark$$

$$A_0 = 128$$

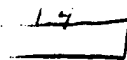
$$A_1 = 32$$

$$\sigma_1 = \frac{F}{A_1} = \frac{2500}{32} = 78.1 \text{ psi} \quad \checkmark$$

Nylon

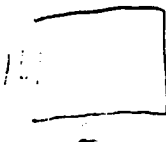
1.5 1 1/2 x 2 x 1/2

Nylon falls @ 300,000 psi



$$1 \cdot 1.46475 \cdot 2$$

$$\sigma_0 = \frac{F}{A_0} = \frac{25}{17.06} = 1.46 \text{ psi} \quad \checkmark$$



$$1 \cdot 2.5$$

$$\sigma_1 = \frac{F}{A_1} = \frac{25}{2.5} = 10 \text{ psi} \quad \checkmark$$

1.5 x 1.5 x 1.5 x 1.5 x 1.5 x 1.5

$$1 = 3/4 \times 1/2$$

$$1.5 \cdot 1.5 = 2.25 \cdot 1.5 = 3.375$$

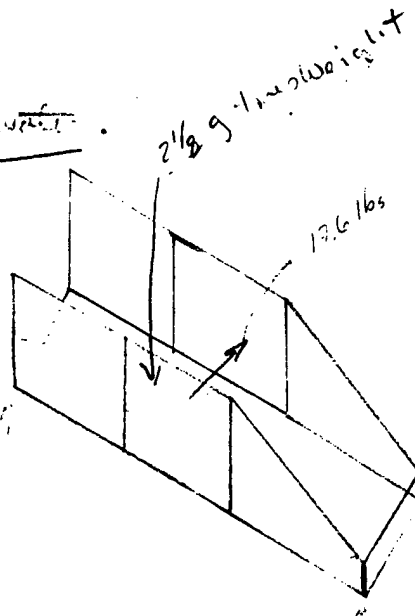
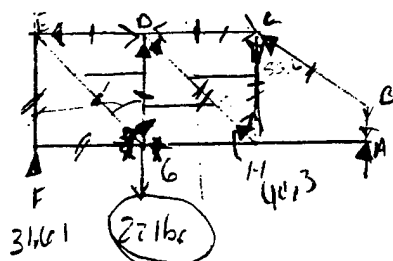
$$\sigma = \frac{F}{A} = \frac{25}{5.906} = 4.25 \text{ psi} \quad \checkmark$$

3.3

Fuselage Analysis

2.2 pounds per bottle.

$$2.2 \times 8 = 17.6 \text{ Pounds distributed}$$



$$2 \frac{1}{2} \times 17.6 \text{ lbs} = 44$$

$$\sum F_{x1F} = 0$$

$$22 \text{ lbs} (\uparrow) = A_y (25.13)$$

$$A_y = 71.6 \text{ lbs}$$

$$\text{Member } AB = A_y$$

$$\sum F_y (B \cos 55.6^\circ - AB) = 0$$

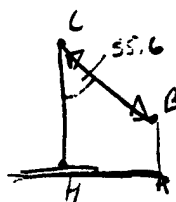
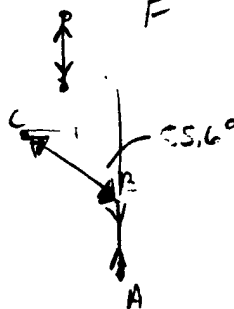
$$AB = 17.39 \text{ lbs } C$$

$$\sum F_y = 0$$

$$16 \cos 55.6 = CH$$

$$CH = 71.6 \text{ lbs } T$$

$$AC = 10.2 \text{ lbs } C$$



$$\frac{71.6}{\cos 45.7^\circ}$$

$$DH = 26.48 \text{ lbs}$$

$$DG = 22 + 16 = 37 \text{ lbs}$$

$$\sum F_x = -10.2 \quad FD = 11.6375 \text{ lbs}$$

$$= FG$$

$$\sum F_y = 0$$

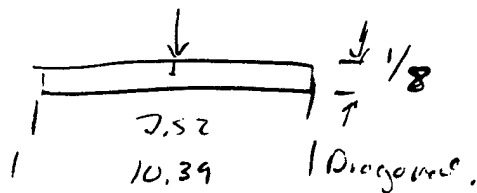
$$FG \cos 45.7^\circ = 26.48$$

$$FG = 20.28 \text{ lbs}$$

$$FF = 15.16 \text{ lbs}$$

-3.3

3.52



$$\sigma = \frac{Mc}{I}$$

$$\sigma = \frac{F}{A}$$

$$AB = .7165$$

$$BC = 26.418 \text{ lbs}$$

$$CP = 10.2 \text{ lbs}$$

$$CH = .7165$$

$$DH = 1 \text{ lbs}$$

$$DG = 1 \text{ lbs}$$

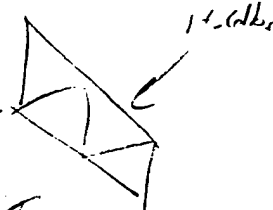
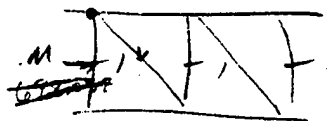
$$FD = 1 \text{ lbs}$$

$$FG = 1 \text{ lbs}$$

$$EF = 1 \text{ lbs}$$

$$I_x = \frac{1}{12} b h^3$$

$$I_x = \frac{1}{12} (7.52) \left(\frac{1}{8}\right)^3 = 1.77 \times 10^{-3}$$



For the Force on the Side of the Body

$$\sigma = \frac{Mc}{I}$$

7.52" length

13.2552" = 11

10.39" length

m = 15.2864

$$\sigma = \frac{13.2552 \left(\frac{1}{16}\right)}{1.77 \times 10^{-3}} = 678.027 \text{ For Vertical Force } = 1$$

$$\sigma = \frac{(15.2864) \left(\frac{1}{16}\right)}{1.77 \times 10^{-3}} = 936.90 \text{ For Diagonal Forces}$$

For tension & compression: This is for individual parts of the truss

$$\sigma = \frac{.7165}{.046875} = 149.333 \text{ psi } AB = CH$$

$$\frac{15}{11} = 320.35 \text{ psi } EF$$

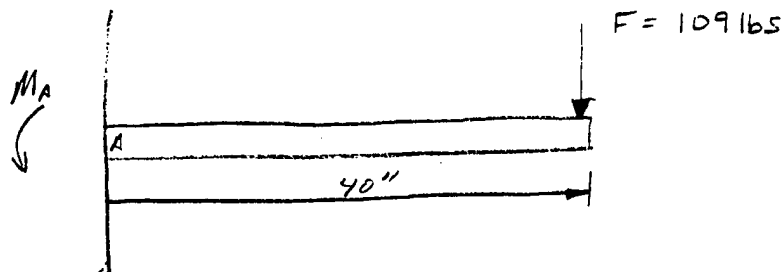
$$\frac{10.2}{.046875} = 217.6 \text{ psi } DC$$

$$\frac{26.418}{.046875} = 564.9 \text{ psi } DH = CB$$

$$\frac{37.164}{.046875} = 789.35 \text{ psi } DG$$

$$\frac{14.6378}{.046875} = 312.17 \text{ psi } FD$$

$$\frac{20.95}{.046875} = 446.93 \text{ psi } FG$$

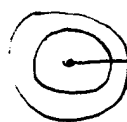


$$\sum M_A = 0$$

$$M_A - 109 \text{ lb} (40 \text{ in}) = 0$$

$$M_A = 4360 \text{ lb} \cdot \text{in}$$

$$\sigma = \frac{M c}{I}$$



$$I = \pi/2 (C_o^4 - C_i^4)$$

$$\sigma (\text{carbon fiber}) = 550,000 \text{ lb/in}^2$$

$$C_o = 1.5 \quad C_i = 1.375$$

$$\sigma = \frac{4360 (0.75)}{\pi/2 (1.5^4 - 1.375^4)} \quad \frac{\text{lb} \cdot \text{in} \cdot \text{in}}{\text{in}^4} = \frac{\text{lb}}{\text{in}^2}$$

$$\sigma = \frac{3270}{2.337} = 1398.99 \text{ lb/in}^2$$

since the tail boom will only need to withstand 1399 lb/in^2 under the max load condition and the tensile strength for Carbon fiber is less than this number, the diameter for the boom is O.K.

$$k_2 = - \left[\frac{d^7 (296.5a^2 + 4133.2)}{d^7 (0.035a^6 + 9.02a^4 + 134.05a^2)} \right]$$

$$J_k = - \left[\frac{1286.5a^2 + 4133.2}{(0.035a^6 + 9.02a^4 + 134.1a^2)} \right] y$$

Yallow (carbon steel) = 550 ksi

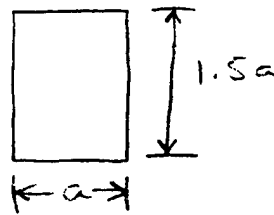
$$\frac{550,000 \text{ psi}}{1.15 \text{ in}} = - \left[\frac{1286.5a^2 + 4133.2}{(0.035a^6 + 9.02a^4 + 134.1a^2)} \right]$$

we solve for a

$$a = 0.00342 \text{ m}$$

$$a = 0.00342 \text{ m}$$

$$h = 0.0123 \text{ m} = \underline{1/64 \text{ in}}$$



we picked $3/8" \times 1/8"$ for wing spars
 $\& \ 1/4" \times 1/8"$ for tail spars

$$M_x = 2292 \text{ lb} \cdot \text{in}$$

$$M_y = 0 \text{ (drag moment)}$$

$$I_{xy \text{ spar}} = 0 \text{ symmetric}$$

$$I_{xx \text{ spar}} = 1.28 a^4$$

$$I_{yy \text{ spar}} = 0.125 a^4$$

$$k_1 = 0$$

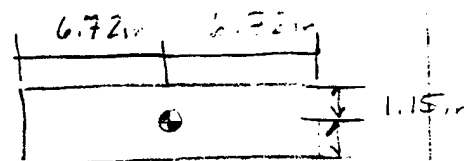
$$k_2 = - \left[\frac{M_x I_{yy} - 0}{I_{xx} I_{yy} - 0} \right]$$

$$\sigma_b = k_1 x^2 + k_2 y$$

$$k_2 = - \left[\frac{M_x I_{yy} - M_y I_{xy}}{I_{xx} I_{yy} - I_{xy}^2} \right]$$

$$I_{yy} = A_1 x_1^2 + I_{yy \text{ spar}}$$

$$I_{xx} = A_1 y_1^2 + I_{xx \text{ spar}}$$



$$\triangleright I_{xx} = (a)(1.5a)(6.72 \text{ in})^2 + 0.28 a^4 = 67.7 a^2 + 0.28 a^4$$

$$\triangleright I_{yy} = (0.125 a^4) + (a)(1.5a)(1.15)^2 = 0.125 a^4 + 1.98 a^2$$

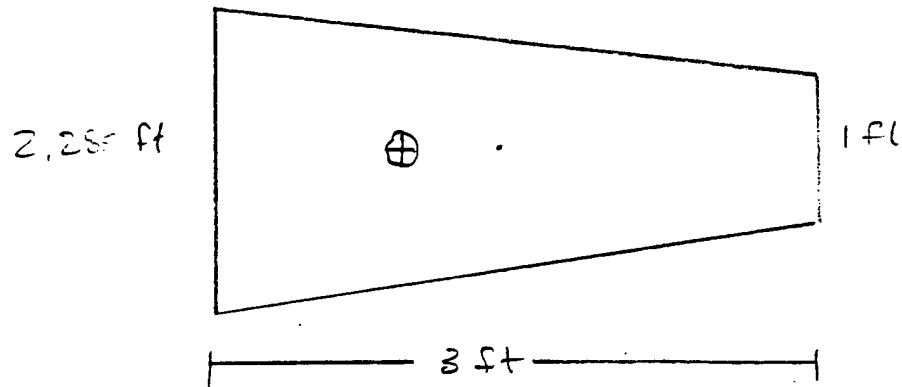
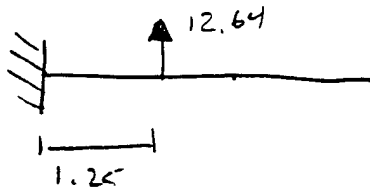
$$k_2 = - \left[\frac{(2292)(0.125 a^4 + 1.98 a^2)}{(67.7 a^2 + 0.28 a^4)(0.125 a^4 + 1.98 a^2)} \right]$$

$$k_2 = - \left[\frac{286.5 a^4 + 4538.16 a^2}{(8.4625 a^6 + 134.05 a^4 + 0.035 a^8 + 0.5544 a^6)} \right]$$

$$k_2 = - \left[\frac{286.5 a^4 + 4538.2 a^2}{(0.035 a^8 + 9.02 a^6 + 134.05 a^4)} \right]$$

3.7

2nd — moment caused by drag



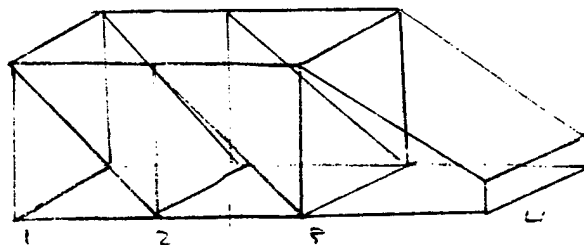
Drag force is 10.11 lb

one wing 5.055 lb

$$15.000 \times 2.5 = 12.64 \text{ lb}$$

$$\blacktriangleright (12.64 \text{ lb} \times 1.25 \text{ ft}) = \boxed{15.79 \text{ ft lb}}$$

Tail connection

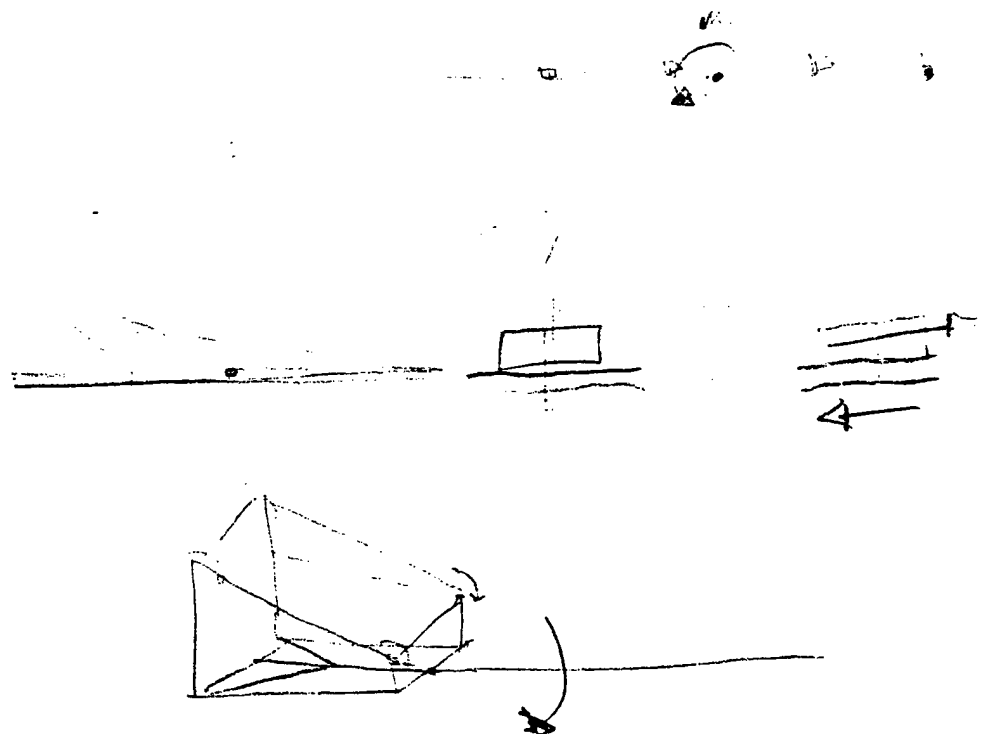


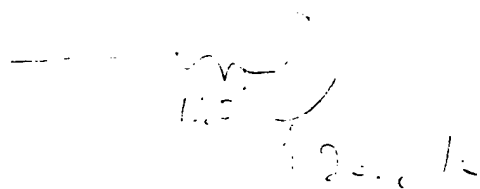
Tail must exert on a moment of 1744 lb in

$$(2.5)(1744 \text{ lb in}) = 4360 \text{ lb in}$$

Tail will run along fuselage and connect at 4 points
members 1, 2, 3, 4 will resist pitching moment from plane.

$$4360/4 = 1090 \text{ lb in per member}$$





$$100.15 \quad A = 20.1(9.5) = 191.95$$

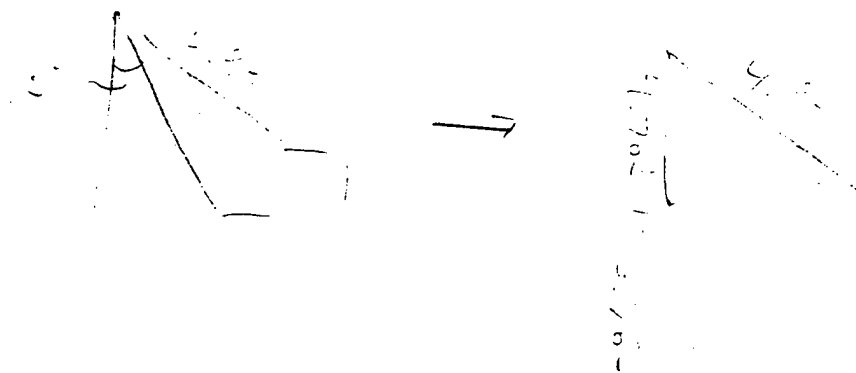
$$C = 191.95$$

$$100.15$$

$$A = 20.1(9.5) = 191.95$$

$$\Sigma A = 0 = 191.95 - 191.95 + 20.1(9.5)$$

$$= 191.95$$



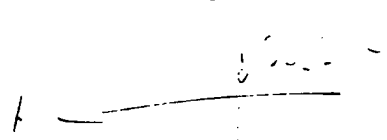
$$\frac{3.0 \times 3.75}{3.75} = 0.50$$

$$\Delta = 40.5^\circ$$

$$\Delta \Delta = 40.5^\circ - 36^\circ = 4.5^\circ \left(\frac{\text{rad}}{180^\circ} \right) = 0.0785 \text{ rad}$$

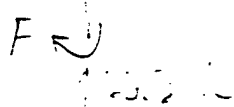
$$\omega = \frac{v}{r} \quad F_c = 45.58 \text{ lb}$$

$$K = 100 \text{ lb/in}$$



$$\sum M_i = 0 = -40.58 + F_H + 36^\circ$$

$$F_H = 4.57 \text{ lb}$$



Main Gear
K = 0.15

$$= \Delta M_i$$

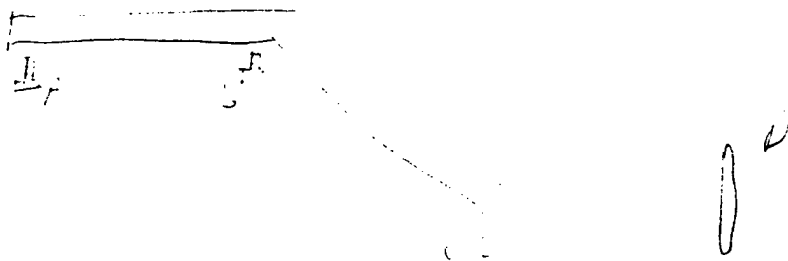
$$= \frac{1}{2} \Delta = 3.75 (0.15) = 1.125$$

$$\sum F_x = 0 \quad \sum F_y = 0$$

$$A = 1.57 \text{ lb}$$

Power for each = 67 lb-in

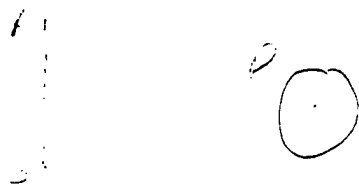
Summary
Main Gear



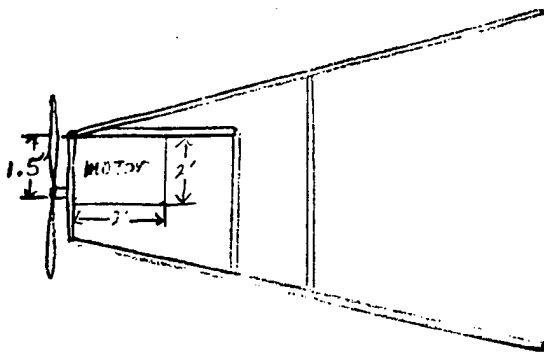
<u>Summary</u>	Age	Shed	Measure
A	50.78		67
S	20.87		55
U	93.75	14.1	
L	93.75	14.1	

Main Gear

Spring Load $\sigma = 5 \times 10^4$ psi



<u>Summary</u>	Age	Shed	Measure
	20.2	9.5712	
	20.6	2.75	45.57
	20.6	2.75	
	20.6	2.75	



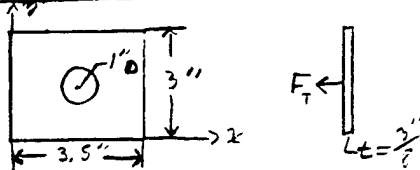
motor max thrust: 15.46 lb.

$\sigma_{max} = T_{max}$ of carbon fiber: 500 ksi

σ = normal

τ = shear

solid plate: $F = T_{max} = 15.46 \text{ lb.}$



assuming solid plate:

$$\sigma = F/A$$

$$\sigma = \frac{15.46 \text{ lb.}}{(3") (3.5")}$$

$$\sigma = 1.47 \text{ psi}$$

$$\tau_y = F/A$$

$$\tau_y = \frac{15.46 \text{ lb.}}{(3") (2/8")}$$

$$\tau_y = 13.74 \text{ psi}$$

$$\tau_x = F/A$$

$$\tau_x = \frac{15.46 \text{ lb.}}{(3.5") (2/8")}$$

$$\tau_x = 11.78 \text{ psi}$$

nose plate with hole:

$$\sigma = F/A$$

$$\sigma = \frac{15.46 \text{ lb.}}{(3") (3.5") - \pi (1")^2}$$

$$\sigma = 2.1 \text{ psi (distributed around hole)}$$

$$\tau_y = F/A$$

$$\tau_y = \frac{15.46 \text{ lb.}}{(3") (2/8") - 1" (2/8")}$$

$$\tau_y = 20.61 \text{ psi}$$

$$\tau_x = F/A$$

$$\tau_x = \frac{15.46 \text{ lb.}}{(3.5") (2/8") - 1" (2/8")}$$

$$\tau_x = 16.49 \text{ psi}$$

solid plate

$$\sigma = 1.47 \text{ psi} < 500 \text{ ksi}$$

$$\tau_y = 13.74 \text{ psi} < 500 \text{ ksi}$$

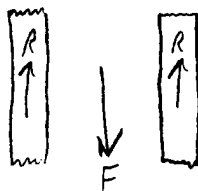
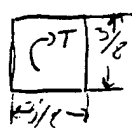
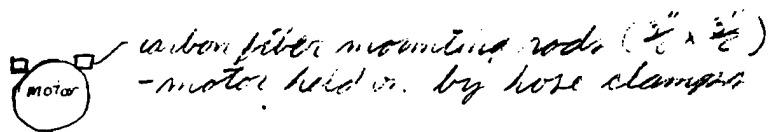
$$\tau_x = 11.78 \text{ psi} < 500 \text{ ksi}$$

plate with hole

$$\sigma = 2.1 \text{ psi} < 500 \text{ ksi}$$

$$\tau_y = 20.61 \text{ psi} < 500 \text{ ksi}$$

$$\tau_x = 16.49 \text{ psi} < 500 \text{ ksi}$$



$$\sum F = 0$$

$$0 = -F + 2R$$

$$R = \frac{F}{2}$$

$$\triangleright T = 19.42 \sin 0.02 = 11.0 \text{ lb-in.}$$

each rod:

$$\sigma = F/A = R/A$$

$$\sigma = \frac{(15.46 \text{ lb.})}{2}$$

$$\frac{(3/8)^2}{\text{in}^2}$$

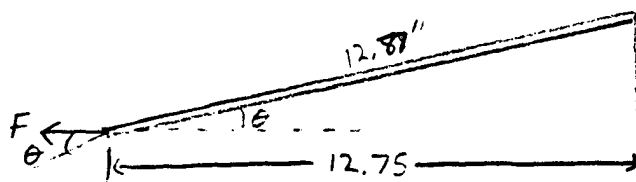
$$\triangleright \sigma = 54.97 \text{ psi} < 500 \text{ ksi}$$

Torsion:

$$\tau = \frac{4.81 T}{a^3}$$

$$\tau = \frac{4.81 (11.96)}{(3/8)^3}$$

$$\triangleright \tau = 545.45 \text{ psi} < 500 \text{ ksi}$$



$$\sigma = F/A$$

$$\sigma = \frac{3.87 (\cos 7.83^\circ) \text{ lb}}{(3/8)^2}$$

$$\triangleright \sigma = 27.26 \text{ psi} < 500 \text{ ksi}$$

$$\tau = \frac{4.81 (T)}{a^3}$$

$$\tau = \frac{4.81 (2.99)}{(3/8)^3}$$

$$\triangleright \tau = 27.22 \text{ psi}$$

$$\theta = \cos^{-1} \left(\frac{12.75}{12.87} \right) = 7.83^\circ$$

$$F = F_T/4 = 3.87 \text{ lb.}$$

↑ assuming thrust is equally distributed

$$\downarrow T = T_T/4 \approx 2.99 \text{ lb-in.}$$

if only top rods receive thrust:

$$\tau = \frac{4.81 (T)}{a^3}$$

$$\tau = \frac{4.81 (5.96)}{(3/8)^3}$$

$$\triangleright \tau = 545.4 \text{ psi}$$

AIAA Student Design/Build/Fly Competition

1999-2000



Design Team

Eric Gartner
David Christensen
Doug Aiken
Aaron Stone
Mario Rodriguez
Oscar Quinonez
Cory Tafoya
Richard Medina

University of New Mexico

April 10, 2000

Table of Contents:

Page

Table of Contents	i
1.0 Lessons Learned	1
1.1 Differences	1 - 3
1.2 Improvements	3 - 5
2.0 Aircraft Cost	6
2.1 Materials	6
2.2 Repair and Redesign	6
2.3 Cost Model	6 - 7
Table 2-1: Aircraft Rated Cost	7
2.4 Manufacturing Hours	8
Table 2-2: WPS hours	8

1.0 Lessons learned

1.1 Differences

During production of the airplane, the team found many things that needed changing. These changes varied from small to large. The modifications made to the plane were designed to improve the structure and the problems that occurred during production.

Carbon Fiber

Carbon fiber was chosen because of its properties. The chassis of the airplane was built out of carbon fiber. The spars for the wings were also built out of carbon fiber. Carbon fiber was used because of its qualities in strength and flexibility. This enabled the body to withstand the forces that are due to the load and the plane itself. The initial carbon fiber was made by two students. These students were currently enrolled in a plastics class. There would be no cost to use the carbon fiber the students made. This decreased the amount of money spent on the whole airplane. The carbon fiber pieces were made into rectangular form. These pieces were used for the entire frame of the plane. Although during construction of the airplane it was discovered that the carbon fiber that was made did not meet the requirements for structural integrity. The team then decided to obtain carbon fiber from another source. The team then bought the carbon fiber commercially. The carbon fiber that was bought differed in dimension than the initial carbon fiber. The original carbon fiber was rectangular shape but the new carbon fiber had a tubular shape. The new carbon fiber changed the size of the fuselage just slightly from the drawings. The dimensions change a little because of the diameter of the carbon fiber. The rest of the plane was sized for the changes in carbon fiber. The carbon fiber was later tested and found to be structurally better than the other carbon fiber. The diameter gave great strength and rigidity to the fuselage.

Batteries

The motor mount and the battery were placed in locations to create equilibrium for the airplane. The motor mount and the battery are the heaviest parts in the plane besides the load. After extensive analysis, it was found that the battery and the motor needed to be repositioned. The batteries were first going to be moved farther forward into the fuselage. The weight from the tail section plus the batteries created an undesirable moment on the plane. By moving the batteries forward it would balance the plane. It was then decided to move the batteries to the front just behind the landing gear. This then gave enough stability for landing and take off. The batteries were also changed for different ones. We changed the original 2000's series nicad batteries for the Sony 1900's. By changing the batteries, we were able to decrease the weight by .8 pounds and increase the power. The only drawback was that we lost 20 sec of max thrust.

Motor Mount

The motor mount initial was held in place by the front edge of the plane. The front end of the plane was made out of carbon fiber. The front end was analyzed and the team discovered that the motor mount could not be mounted to the leading edge of the airplane. It was then decided to securely fasten the motor mount to the bottom of the fuselage. The bottom of the fuselage contained the required strength to withstand the forces created by the motor. This allows the motor mount to securely be held in place by one of the main frames of the fuselage.

Boom

The boom was another item that differed from original design. The airplane was designed with two main parts the fuselage and the tail section. The tail section consisted of the boom and the tail. The boom was to be connected underneath the fuselage. The wings were designed to have a two degree offset from the horizontal axis. With the wings joined at a two degree angle the wing connections would lie just below the bottom of the fuselage. With the boom placed outside it would give ample room for the bottles to be carried. Not only did it make it easier for the bottles but it was easier for the location of the batteries. The area between the wing connections and the fuselage was too small to hold the one inch boom. The team then decided it easier to connect the boom to the inside of the fuselage of the airplane. Mounting the boom to the interior of plane reduced the amount of drag on the plane. It also caused problems for the location of the batteries and the load.

Tail Section

The team designed the tail section to have a negative lift. The team chose the tail design to be a Clark Y. The Clark Y itself has positive lift. To get the negative lift, they invert the wing. Thus the team obtained the empennage to be negative. They found that the design was a little too unstable compared to other empennages. They decided to change the empennage to a NACA0012 foil. This foil then gave them the stability they were looking for. They then angled the foil 2 degrees below the horizontal axis. This then gave them the negative lift they needed for the tail section.

Steering and Rudder Assembly

The steering and the rudder assembly are both operated by individual servos. The team thought it best to use four servos in the airplane. They currently had five at the most in the plane. They decided to combine the steering and the rudder to the same servo. This then decreased the total servos down to four like they wanted. Both the rudder and the steering in applications deal with the same thing; to move the airplane in different directions being on the ground or in the air. The cost and weight would help in the competition. This then increases the chance of having a better cost model. To have the steering and the rudder connected together, they build a lead from the servo to the empennage. There the rudder would be connected. The lead from the servo to the rudder

was encased in plastic tubing due to friction and location. The metal tubing presented caused a frequency that was interfering with the electronics on the plane. Both applications could be used with one servo saving money and resources.

Fuselage

Different bonds were being used to adhere two surfaces together. Some of these bonds work good on different surfaces. The bond used on this plane was called JB weld. It bonded greatly to balsa and other wood. Yet it did not bond well with different types of plastic. When the stress analysis was being analyzed certain connections came apart at the connections. It seems that the type of bond was not strong enough or that the bond was not applied correctly. For this reason the team obtained a stronger adhesive. This glue would then ensure that those locations that separated would hold. The team obtained the glue from a shop class. This glue is heavier and stronger. The weight of the airplane increased slightly. This did not affect much of the calculations since it was distributed throughout the fuselage and the empennage. The fuselage, the tail and the nose were reinforced due to the aerodynamic forces and the load. The reinforcements supported part of the weight that would have separated the bonds between the connections.

1.2 Improvements

There were areas of production and design that the team has decided to improve on. These areas will help strengthen the airplane and improve the overall design for the next year.

Connections

One area of improvement is the connections. The connections are the most important part of the airplane. If the connections fail the airplane also fails. The team has discovered through trial and error, that some types of bonds do not work as well as others do. This is probably due to the differences in materials used. The bond the team was using was called the JB weld. This weld is adequate for planes that are light and have no real cargo. For our case it would be advisable to use another method of joining the pieces together since the two materials are different. It was also found that by increasing the area of contact, the bond was made stronger. Depending on the type of connections, small scores from a razor increased the strength the connections need to keep their bond. We learned that not all types of bonds work for all cases. Thus we would use different bonds that suit the application.

Tools

Another area of improvement that was discussed was tools. Tools are a vital part in putting the plane together correctly. With the right tools, time and money can be saved. Every team in the competition has different tools. For those that have the tools, the airplane can be completed correctly and perfectly the first time. Some tools would be better to cut plastic and others metal. The tools then can aid or destroy a sound design.

There are also tools that would help in the accuracy of the pieces. Although these tools are too expensive for students to buy it would be advisable to have somebody loan tools to the students for future use. With these tools it would help the students make correct pieces for the plane.

Communication

The team members worked together quite efficiently, although there was not enough information on the manufacturing part. Many members found it difficult to exchange information on what was being done on the airplane. This caused much confusion and time. Many mistakes were made because of miscommunication and lack of knowledge. The team found it very important that every member knew what was going on and what to do it. With complete communication the members of the team would know what to do to complete the project without all the mistakes. This is one important part of teamwork that is considered important for future competitions.

Airplane Designs

An important part of the design work is to have accurate drawings. Concerns were voiced that the drawings were made on highly sophisticated software. The drawings took too much time to develop. It is just the same to have drawings made from a 2-d software as it is from a 3d software. Because of the lack of time and the software important parts were excluded from the drawings. The team found that it is easier to include the detail then leave it out. When time comes for the production, the team knows exactly where everything goes. Our team found this the hard way. When you don't it is very hard to change what has been done. Time was wasted as well as material because there was no detailed schematic of the airplane. These details help the production of the plane go smoothly and efficiently.

Commercially available products

As discussed above, a tubular form of carbon fiber was used instead of a rectangular form. The team members wanted a stronger type of carbon fiber than what was made. They realized that carbon made from the students would never be strong enough to hold the basic loads needed for the competition. It was then realized that all the pieces don't need to be made from scratch. The team member could make use of commercial available products. By using outside influence for parts and piece, time and effort can be minimized. Many students get caught up in making all the pieces from scratch. It is not necessary that we make all the pieces from scratch. Some of the pieces can be bought and used. Understanding that time and money can be saved by finding those who have the merchandise can help the overall experience.

Rules of Thumb

There were rules of thumb used in this experiment. The rule of thumb used for the gear placements was called lenning rule. This rule placed the landing gear in a short

distance behind the center of gravity. The only thing a rule of thumb does for the project is calculate a rough answer. The answer is not correct but it is close to the correct answer. When applying any rule it is necessary to prove that this rule will come close to the answer and not lead the answer farther away. Playing it safe will decrease the odds that you are incorrect on your calculations. All rule of thumbs have conditions that make them valid to use. The most important thing one can do is to compare the rule of thumb against the correct method of solution.

2.0 Aircraft Cost

The aircraft was designed to optimize cost. Optimizing cost will bring a better score. The plane was designed after a perfect cost model. This perfect model contained various components that would be subject to testing. The various items for the rated cost of the airplane will be discussed in the following paragraphs.

2.1 Materials

The cost of the materials in past years came from experience from building. The knowledge they have brought back has narrowed the price range. The materials have not change in price over those years but the competition rules have. The price range changes slightly or greatly due to the changing rules. This year more rules have been made to make the competition competitive. Originally the team decided to make there own carbon fiber frames. The decrease in amount of material made the design better. Making carbon fiber correctly is harder and time consuming than buying it. It was decided that it would be better to buy some carbon fiber from commercial vendors. By buying the carbon fiber we increased the structure of the airplane. Although, this increased the amount of money spent on the plane. There was money saved from using last years supply. One of the main concerns the team discovered as they were going through production of the airplane was that materials were being used up insufficiently. Materials cost too much to waste.

2.2 Repair and Redesign

The airplane experienced many problems during production. These problems ranged from assembly to accidents. The mistakes made the project cost more. As the problems continued more materials were needed for completion of the airplane. The team has found that in many cases money has been spent on repeated parts breaking. These parts were probably broken or just misused. Some parts of the design were changed and so more parts would have to be bought. The cost then went up for changes made to the airplane.

2.3 Cost model

The cost model for this aircraft was determined from the contest supplied cost model. It has been determined from this aircraft model that our final rated cost is 6.12. This was based on Empty Weight, Rated Engine Power and Manufacturing Man Hours. These three criterions comprise the whole cost model. These calculations can be found on the next page. Table 2-1

Category	Manufacturer Empty Weight	Rated Engine Power	Manufacturing	
Sub-Category		# of Cells	# of Horizontal	# of Vertical
Quantity	19 pounds	38	1	1
Item Cost	19	2280	15	5
Multiplier	100	1	20	20
Total	1900	2280	300	100

Category	Manufacturing			
Sub-Category	# of Wings	Wing Area	# of Fuselages	Fuselage Length
Quantity	1	12	1	6.5
Item Cost	5	48	5	26
Multiplier	20	20	20	20
Total	100	960	100	520

Category	Manufacturing			
Sub-Category	# of Servos	# of Engines	# of Propellers	
Quantity	4	1	1	
Item Cost	9	5	5	
Multiplier	20	20	20	
Total	180	100	200	

Category	Manufacturer Empty Weight	Rated Engine Power	Manufacturing	Rated Aircraft Cost (Total / 1000)
Total	1900	2280	2460	6.64

Table 2-1: Table of Aircraft's rated cost.

In Table 2-1 it shows the rated value of the airplane for all the items. This value helps rate the team overall score. By changing the values, the cost model will change as well. If the airplane had more servos or any other item it would have increased the score. For this competition, the team is trying to keep this value low. With a lower cost model the overall score is higher. Given a higher score gives the team a better chance to compete with the top teams.

When changing the design during the production phase. It can either increase or decrease the score. For the team to lower the rated cost, the team would have to change the surface area. This could be good or bad. By lowering the wing size they would be lowering the amount of lift. For this competition we want to optimize the airplane. Obtain an equilibrium that best suits our criteria.

2.4 Manufacturing Hours

The manufacturing hours played a great deal of learning experience for the team. The hours that were spent demonstrates the knowledge and ability to manufacture an airplane.

This team is a second year competitor. The team has had little information and experience to go on. The year before was an exceptional source of knowledge. Though the team had only knowledge from last year, they had no real experience in building an airplane. Many hours were spent learning from errors and lack of knowledge. The plane was built in approximately 300 hours. Fifty of which were taken into account for testing and minor modifications. The break down in hours can be seen in Table 2-2.

Items	Hours
Wings	67.5 hrs
Fuselage	50 hrs
Empenage	60 hrs
Flight systems	37.5 hrs
Propulsion Systems	35 hrs

Table 2-2: Manufacturing hours broken down in WPS format.

In the table above all the values are a total representation of time until completion. The table clearly indicates that the wings and tail section required more time than the other sections of the airplane. More time was spent on the wings in order to obtain strength and integrity of the airplane. These areas were more important than the others.

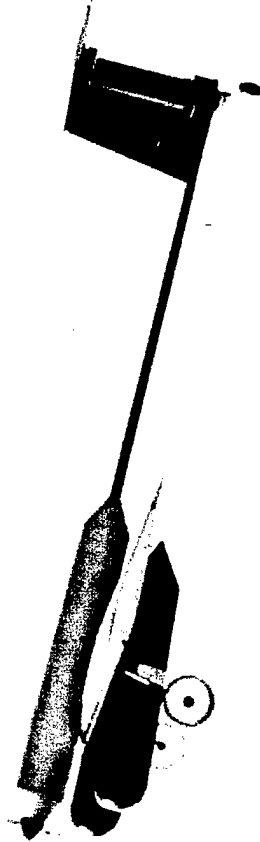


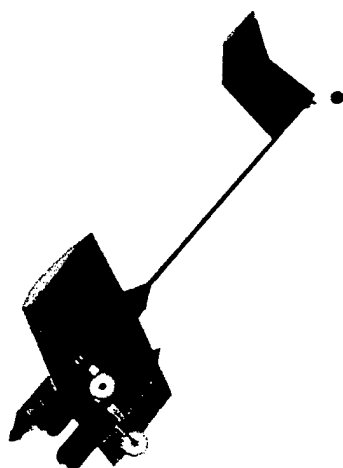
AIAA Cessna/ONR
Student Design/Build/Fly Competition

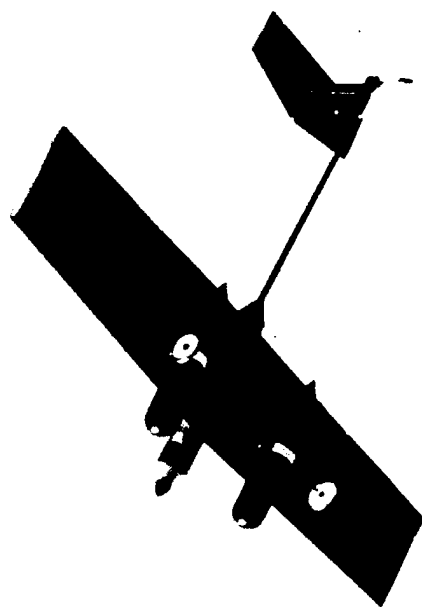
**TEAM T.L.A.R.
FLIGHT PHOTOS**

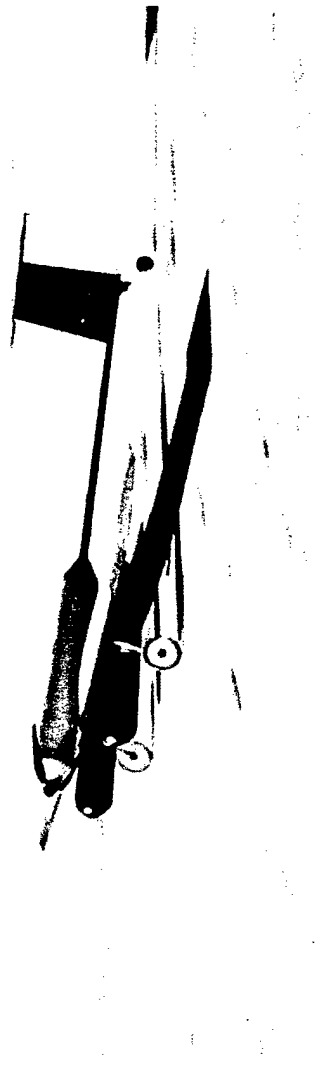
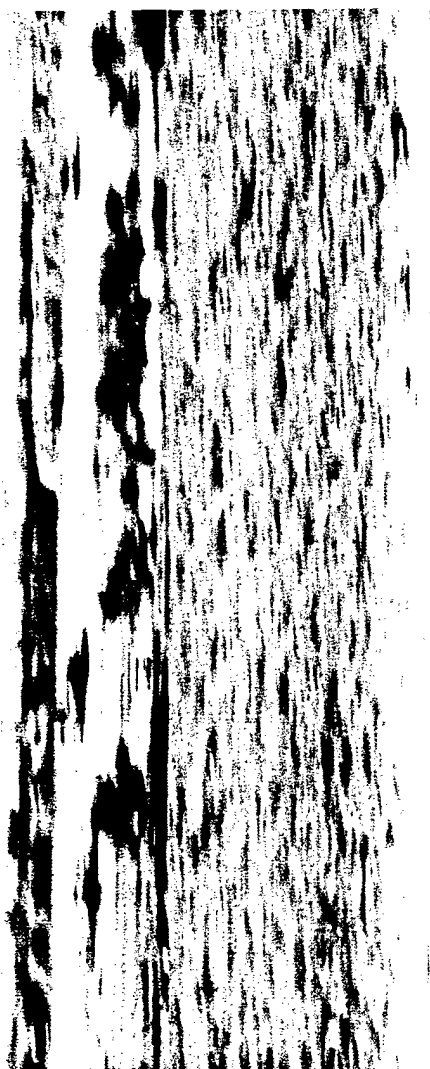
DESIGN AND DEVELOPMENT TEAM:

Andrew Mye
Joshua T. Hu
Annie Powers
Kari Goulard
John Taylor











**American Institute of
Aeronautics and Astronautics**

AIAA Foundation/Cessna Aircraft/ONR
Student Design/Build/Fly Competition

Design Report: Proposal Phase

Submitted By:

**The University of California, San Diego
AIAA Student Chapter Competition Team**

March 13th, 2000



**American Institute of
Aeronautics and Astronautics**

AIAA Foundation/Cessna Aircraft/ONR
Student Design/Build/Fly Competition

Design Report: Proposal Phase

Submitted By:

**The University of California, San Diego
AIAA Student Chapter Competition Team**

March 13th, 2000

i . Table of Contents

<u>Section 1- Executive Summary</u>	<u>Pg. 1</u>
<u>Section 2- Management Summary</u>	<u>Pg. 2</u>
<u>Section 3- Conceptual Design</u>	<u>Pg. 6</u>
<u>Section 4- Preliminary Design</u>	<u>Pg. 9</u>
<u>Section 5- Detail Design</u>	<u>Pg. 12</u>
<u>Section 6- Manufacturing Plan</u>	<u>Pg. 13</u>

1. Executive Summary

1.1 Design process

As this was UCSD's first year entering a competition of this nature, we realized that the first step was to decide on a basic design. We started by looking at last year's designs, visiting hobby shops, as well as a local airfield for model planes. Visiting the airfield turned out to be the most informative, since we were able to view the plane not only on the ground but as well as in flight. As fortune would have it, we viewed a plane that had similar dimensions and thereby had a template from which to spawn our own design. Following careful analysis of the scoring procedure we determined that four liters would be a sufficient payload. This prediction allowed us to proceed with design alternatives, which would promote speed without sacrificing payload capabilities.

The initial design included a biplane configuration with dual motors. We soon realized that this configuration would not suffice due to high drag and difficulty of construction. Following this realization we considered a single wing, dual motor configuration. This design alternative would allow us to utilize the idea of placing the payload into nacelles along with the motors. These pods were located on the wings at a distance that would allow enough clearance for the propellers.

Further alterations to the design occurred when we researched propulsion systems. This research revealed that motors with sufficient thrust capabilities to propel a single engine design exist. With this knowledge we decided to vary the design to a configuration that would accommodate a central pod flanked by two nacelles on the wings.

The fuselage would consist of the central nacelle, while the two outboard nacelles would contain the cargo. This design would permit us to carry the predetermined payload and, thus became our working design. At this point we were free to begin considering possible designs for the other components, such as the nacelles, and horizontal/vertical stabilizers, etc....

1.2 Design Tools

Through extensive research and recommendations from storeowners, several programs and computational tools were discovered. Tools employed during the process included:

- Virtual Motor Test Stand (Aveox):

The ability to vary parameters such as motor model and power input (batteries) aided in determining an effective propulsion system.

- Microsoft Excel:

Excel was found to be extremely useful throughout the entire design process. Spreadsheets for Rated Aircraft Cost, moment, Lift (takeoff and flight), power and plan form (area and wing loading) calculations were generated via Excel.

- VirtualFoil (Hanley Innovations):

This program allowed comparison between various airfoil characteristics. Examples of this include C_d and C_m versus Angle of Attack, Polar plots, velocity and pressure distributions and C_p versus Chord position.

- Macfoil:
Obtained printouts of airfoils with the necessary chord length. These printouts were used as templates for hot wire cutting of blue foam.

2. Management Summary

2.1 Management Architecture

The UCSD project team consisted of 12 undergraduates with diverse backgrounds. Team member profiles are shown below.

Name	Year	Major	Experience
Andrew Mye (Project Manager)	Senior	Mechanical	AutoCad, knowledge of composite materials, machining, programming
Greg Tengan	Senior	Mechanical	AutoCad, programming
Franky Choi (Chapter Vice President)	Senior	Aerospace	Aerospace Structures, Aerodynamics
Brian Faz (Treasurer)	Senior	Mechanical	Fundraising, programming
Kari Goulard	Senior	Mechanical	Pro-Engineering Software
Samantha Infeld	Senior	Aerospace	Aerospace Structures, Aerodynamics, AIAA Chair
Jocelyn Lo	Junior	Mechanical	
Yishai Mendelson	Senior	Aerospace	Aerospace Structures, Aerodynamics
Annie Powers	Freshman	Aerospace	Fundraising, AIAA Secretary
Josephine Sheng	Junior	Electrical	Fundraising, AIAA Council Representative
John Taylor	Junior	Mechanical	Project Coordination, programming
Joshua Hu (Chapter President)	Senior	Aerospace	AUVSI Design Competition, AIAA Chair, fundraising, programming

During one of the initial meetings a decision was made to divide the group into various subgroups, each with it's own chair. These subgroups include wings/stabilizers, cargo pods/boom, landing gear, electrical, and fundraising. Weekly meetings allowed the team to discuss component interfaces, ideas, roadblocks encountered and possible alternatives. This management structure enabled everyone to choose a role that they felt comfortable with and thus ensured quality. In addition, this structure was conducive to timely completion of each subgroup's particular responsibility. These responsibilities are as follows:

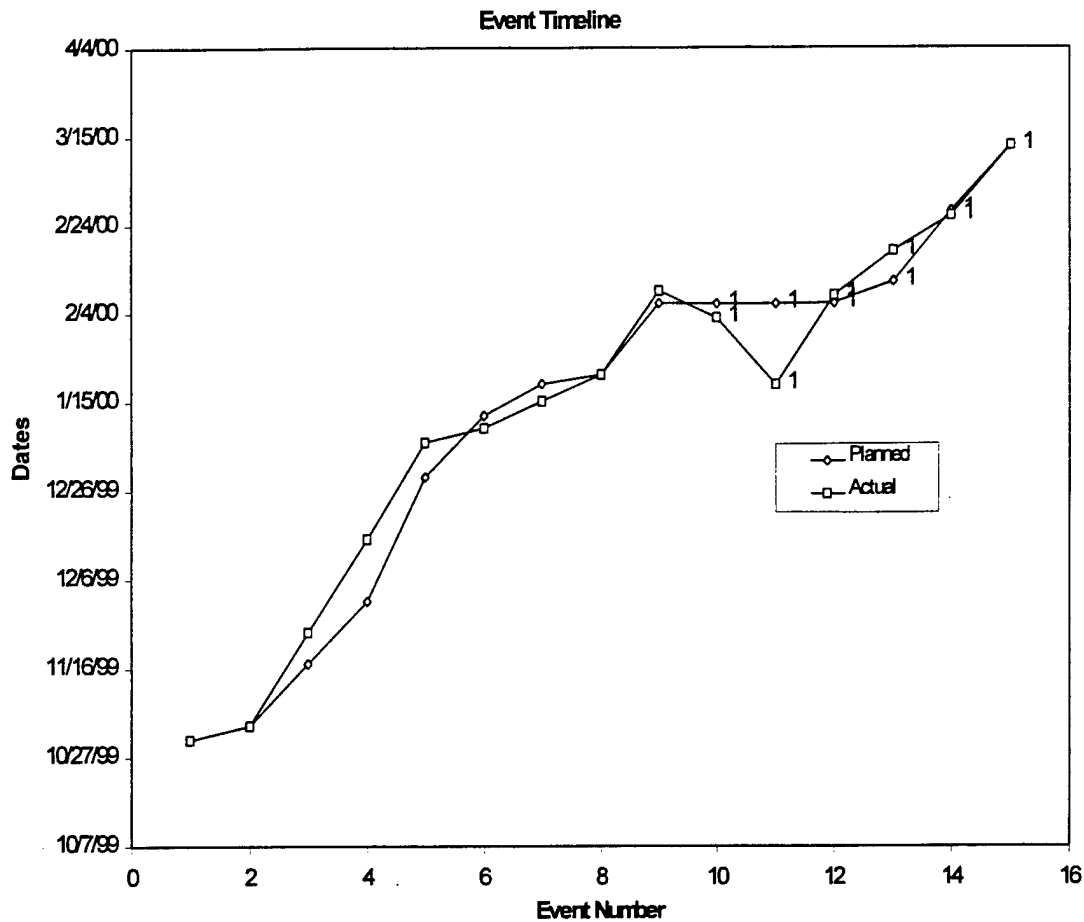
- The wings/stabilizers subgroup began by comparing a range of airfoils. Through use of these comparisons an airfoil was decided upon, an E214, which satisfied the preliminary estimations for necessary lift and drag characteristics. As the specifications of the design (i.e. weight, placement of components, etc...) became available, the necessary calculations, such as the wing loading and pitching moment

about the center of gravity, were completed. The wings/stabilizers subgroup consisted of Josh, Franky, Jocelyn, Yishai, and Greg.

- The cargo pods/boom subgroup focused on designing the cargo/motor pods and the boom. They researched possible designs for the pods and boom and also dealt with the calculations to determine the particular component's strength requirements. In addition, this group also investigated what types of connections to the wings would provide the best stability. This subgroup included Andrew, Kari, and Brian.
- The landing gear subgroup's main responsibility was to develop a landing gear structure. This group worked closely with the pods group to devise a means to attach the structure to the airframe. The landing gear subgroup consisted of Andrew and Brian.
- The electrical subgroup, headed by Josephine, took care of the wiring of the motor, servos, batteries, and onboard radio receiver. In addition, calculations with respect to necessary voltage and amperage were part of this group's responsibilities.
- The fundraising subgroup sought out possible sponsors and acquired both sponsorship and accepted donated components. Those involved in the fundraising aspect of the project included Andrew, Josh, Annie, and Brian.

2.2 Task Scheduling

During the month of October, the group decided upon a schedule of completion dates. Each subgroup was expected to complete tasks by a certain deadline. The following chart (Figure 1) depicts the planned and actual date of completion (D.O.C.) of each major event. Through teamwork and communication we were able to overcome the problems encountered due to inexperience. Andrew, Brian and Josh's leadership skills pulled the team together when things seemed overwhelming and motivated the group to get the tasks accomplished.



<u>Event</u>		<u>Planned D.O.C.</u>	<u>Actual D.O.C.</u>
1.	Submitted Notice of Intent to Compete	10/31/1999	10/31/1999
2.	Conceptual Design FOM's chosen and ranked	11/3/1999	11/3/1999
3.	Conceptual Design finalized	11/17/1999	11/24/1999
4.	Preliminary Design finalized	12/1/1999	12/15/1999
5.	Detailed Design completed	12/29/1999	1/6/2000
6.	Obtained sponsorship for the project	1/12/2000	1/9/2000
7.	Acquired materials and parts for construction	1/10/2000	1/13/2000
8.	Construction started	1/21/2000	1/21/2000
9.	Wings completed	2/6/2000	2/9/2000
10.	Pods completed	2/6/2000	2/3/2000
11.	Boom completed	2/6/2000	1/19/2000
12.	Landing Gear completed	2/6/2000	2/8/2000
13.	Final assembly of aircraft	2/11/2000	2/18/2000
14.	1 st test flight of aircraft	2/27/2000	2/26/2000
15.	Completion of Proposal Phase Report	3/1/2000	3/5/2000

Figure 1: Dates of Completion

3. Conceptual Design

3.1 Design Parameters

In order to ensure safety, stability, structural integrity and quality performance several design parameters were selected. Design parameters that were considered during the design stages included:

- *Undercarriage design:*

The design of the landing gear was considered to be important due to the impact energy encountered during landing. Ground handling is another factor that is affected by the landing gear configuration.

- *Nacelle shape and location:*

The shape of the nacelles, heretofore referred to as Pods, was carefully thought out because of its impact on drag and other flight characteristics. The location of the pods also played a critical role in calculating the center of gravity and, thus had a considerable impact on the overall flight stability. This parameter would be used in determining the location and functional requirements of the undercarriage.

- *Payload access:*

Scores earned during the flight periods are dependent on speed of flight and loading/unloading of cargo. The team realized that optimization of the loading/unloading phases would have allow for a better score. This, therefore, affected the location of the cargo pods.

- *Inter-component attachments:*

The interfaces between components such as the pods and the wings, landing gear and spar and wing section joiners demanded careful consideration. These locations would give rise to stress concentration factors that needed to be neutralized so as to promote structural integrity.

3.2 Figures of Merit

The Figures of Merit, along with ranking, established during the Conceptual Design period are as follows:

- *(1) Lift Characteristics):*

The flight score is determined by the payload capacity of the design, therefore the lift characteristics were of the utmost importance. This criterion was of critical importance while considering the airfoil and shape of external structures.

- (2) *Efficiency of Payload Loading and Unloading:*

Since time is of the essence during the competition, efficiency of payload loading and unloading was a major consideration. This particular FOM had a big impact on the placement and dimensions of many integral components, especially the cargo pods.

- (3) *Durability (structural):*

Taking into consideration the high wind conditions we attempted to construct an airframe that was not only light but also durable. With the understanding that these conditions would lead to bumpy landings and take-offs we made appropriate material choices.

- (4) *Ease of Fabrication:*

Due to limited experience and time in the machine shop we chose structures and components that were easy to construct. The structures/components included the landing gear, spar and boom. This FOM made it very difficult to meet the functional requirements of each of the components.

- (5) *Availability and Cost Efficiency of Materials:*

Establishing connections within the business community was an invaluable step in acquiring advice, monetary and material support. Obtaining financial assistance proved to be more difficult than we thought, therefore we were obligated to make cost and availability a major consideration throughout the entire design process.

3.3 Alternative Designs

- *Wing/Motor Basic Layout:*

Initially, a biplane configuration with dual motors was considered because of the extra lift area it would provide. Although this satisfied FOM 1 it was not in compliance with FOM 4 and FOM 5. We also noted that a biplane configuration increased the drag significantly thereby increasing our power requirements. With this realization we began looking at simpler designs such as a single wing configuration with dual motors.

This configuration required that the plan form area be increased thereby sufficient lift would be attained. This design would satisfy FOM 1 without challenging the requirements of FOM's 4 and 5 would be satisfied. At this point in time we began to gather information on propulsion systems and discovered that single motors existed that could meet the requirements.

This discovery led us to consider a single wing/motor design. This not only met the requirements imposed by the FOM's but also decreased our overall cost and rated aircraft score.

The ranking of these design concepts is as follows:

Figures of Merit:	Lift	Payload	Durability	Fabrication	R.A.C.
Biplane	5	2	-	1	95.29
Single wing dual motors	4	2	-	2	74.78
Single wing single motor	4	2	-	3	68.69

- *Cargo Placement:*

The placement of the cargo pods was dependent on the overall layout of the design. Once we decided on the single wing/motor arrangement, we noticed that the nacelles on the wings could serve as cargo pods. This would allow easy access to the payload and thus was in complete agreement with FOM 2.

- *Spar Design:*

With the basic design of the airplane, and a good estimate of the weight, we could consider a spar design. We began by comparing the mechanical characteristics of tubular, I-beam and rectangular structures. They chose the I-beam structure due to its good strength-to-weight ratio.

- *Landing Gear:*

In designing the landing gear, we searched for a configuration that would be durability, thus satisfying FOM 3. We looked at a torsional configuration, in which the structure's material would absorb the majority of the energy of impact. We immediately recognized the fact that this configuration would reduce the risk of damaging the airframe during landings.

- *Pod Design:*

In considering the design of the pods, low aerodynamic drag was the first priority. We began by researching planes with external fuel tanks. This led us to the conclusion that a cylindrical shape would be best. Cylindrically shaped parts, with the use of a lathe, are easy to fabricate thus satisfying FOM 4.

- *Empennage:*

To avoid the problem of downwash from the wing interfering with performance, a T-type empennage was chosen. This configuration would be easy to construct, consequently FOM 4 would be satisfied.

3.4 Design Selection

Selection of the final configuration was made after careful deliberation. We decided to elect the following design:

- Single wing
- Single motor
- Two cargo pods
- Motor/Battery pod
- Torsional landing gear configuration
- I-beam spar
- T-type empennage

4. Preliminary Design

4.1 Design Parameters Considered

Based on the requirements of the competition, the design parameters considered were:

- Aspect Ratio
- Power Capability
- Airfoil Design
- Tail Shapes
- Thrust-to-Weight Ratio
- Fuselage Shape and Size
- Desired Payload Capacity
- Landing Gear

Aspect ratio was a major consideration as it determines the ability of the plane to glide, affecting the thrust-to-weight ratio. An increased ratio would allow the airplane to require a shorter take-off distance. The airfoil design was extremely important as the purpose was to determine how to achieve the maximum possible lift for the given surface area and weight. The curvature of the airfoil affects both the pressure and velocity distribution, which in turn affects the control of the airplane.

The shape of the tail is another important characteristic in the handling of the airplane. The vertical, horizontal size and locations are key to obtaining the maximum maneuverability of the aircraft.

The desired payload capacity was also another key consideration. The maximum payload allowed would be ideal; however, this adds considerable additional weight, which in turn affects the maneuverability of the airplane, its velocity and lift, along with placing increased strain on the materials.

Power also played an important part in the preliminary design. The motor would need to be light, yet powerful, as it was deemed necessary for the plane to not only have a short take-off ration (less than 100 feet), but to have a rapid climb rate. In order to achieve such stringent requirements, the power capability was carefully determined and a suitable motor selected.

Landing gear required careful consideration; it, more than any other part, would need to be robust, as it would have to absorb the shock of landing again and again. Weak landing gear would result in failure of either the gear or a portion of the plane due to the sudden jolt of ground impact, perhaps even to the point of inability to repair within the allotted time.

4.2 Figures of Merit

- Construction Capability
- Structural Integrity
- Weight

- Payload Access
- Cost

Time and financial aspects were key to the final design. A complicated wing shape would require unreasonable time, not to mention the cost of producing such a design. Furthermore, simplicity allowed for the possibility of mistakes to be corrected in a reasonable amount of time and with minimal additional cost. The last argument in favor of a simple design is its robustness – a simple, solid wing would be able to take the hard jolt of landing and also support more weight than a complicated airfoil construction.

The structural integrity of the airplane and the weight were two considerations that were closely intertwined. It was important for the airplane to be robust, yet be light enough not to require more than a reasonable amount of power to maintain flight. Materials were considered mainly on the basis of their strength-to-weight ratio. The buffeting of winds during flight, possibility of rough landings, and the weight of the payload required that the airplane be able to withstand any and all such events as might occur during the course of the competition.

Finally, payload access was also a consideration. The time constraint of the competition requires quick removal/insertion of the payload. Location of the pods on the airplane and the ability for ground members to access them would increase the amount of time spent in the air by the plane.

4.3 Analytic Methods

4.3.1 VisualFoil

Visual foil was used to compare airfoils and their defining characteristics. This program allowed us to make polar plots, plots of velocity and pressure distributions, moment and pressure coefficients versus angle of attack (AOA), and moment versus AOA. These plots were extremely helpful in choosing an airfoil.

4.3.2 Aveox Virtual Test Stand

We used this program to compare the different battery, motor and propeller dimension combinations. We found this to be helpful when deciding on the propulsion system.

4. Preliminary Determination of Features

Initially, designs were brainstormed and critiqued with consideration of applicability to come later. Immediately, several design considerations to be investigated were separated from the pile: single-wing versus biplane, dual versus single motor, high versus low wing, number of pods, and so on.

4.1 Airfoil

The competition requirements determined the wingspan of the aircraft, leaving only a few design parameters that could be changed by the contestants. Among these were the aspect ratio, the airfoil design, and the decision between a biplane and single-wing. The additional wing of the biplane would provide a great increase in lift. However, the complications involved with the design of such an airplane, as the necessity for an additional non-payload fuselage caused this idea to be rejected.

The next consideration was that of a high wing versus a low wing. A low wing was decided upon as the landing gear could easily be incorporated, and would allow for more support for the pods, as opposed to them being suspended from a high wing. A sweep of zero degrees was chosen because of fabrication difficulty concerns.

4.2 Tail

The empennage of existing RC aircraft was carefully considered when determining the final design. Initially, the horizontal stabilizers were located at the base of the tail, as is the case with many commercial and most of the local RC aircraft. The decision to move to a "T-Tail" design was based on concerns from down wash of the wing. The finalized area of the tail came out to be 264 in².

4.3 Motor

It was felt that the main points of consideration for the capability for the motor were the climb rate and takeoff distance. Based on previous research and the final design, a thrust-to-weight ratio of around 0.5 would be ideal.

An initial design considered consisted of a dual-motor system. This would supply the much-appreciated extra thrust, increasing the velocity of the plane in-transit, decreasing the take-off distance, and increasing the climb rate – all ideal situations. However, it was determined that the competition-imposed penalty was undesirable, the price unreasonable, and that equipment had been found that would greatly reduce the weight of the airplane.

It was decided to use an Aveox 1415 3Y motor running off thirty-six battery cells, turning a 16 in. diameter propeller. The total thrust was determined to be 221 oz. The placement for the motor was at the logical location of the front of the fuselage, which doubled as the center pod.

4.4 Pods

Most of the initial designs considered only two pods, with the capability to hold two liters of water each. This was considered a good balance between the weight of the pods and the desire to

transport as much water as possible during each flight. The pods would be located equidistant from the center of the wings. This design was ideal for the dual-motor design.

The single-motor design required some modifications – the least not being the fact that it would be necessary to position the motor at the center of the wings, requiring a fuselage located there to house the motor. This determined that either a single pod could be used, as the fuselage could logically and efficiently double as a pod, or three with the center fuselage and two pods on the wings. It was determined that the power of the motor and strength-to-weight ration was sufficient support for three pods. The two pods on the outer wings are located 10 inches from the fuselage centerline. Further details of the pods are included in the detail design section.

5. Detail Design

5.1 Performance Data

Upon completion of our design the task of gathering data was undertaken. We have estimated 95.04 Watt-hrs, average power of approximately 712.8 watts. Other flight data is in the process of being gathered and determined and evaluated.

5.2 Final Configuration

The final configuration of the plane consisted of a high-wing, single motor, three nacelle design. The undercarriage was based on our initial torsional hypothesis, the boom was purchased from a local composites company and the T-type configuration was chosen for the empennage.

5.2.1 Wing

The final design of the wing followed from much careful consideration of the flight characteristics that it would impart. The plan form area was 1176 in², slightly tapered from 15 to 13 inches of chord and single piece construction. We chose an Eppler 214 as our airfoil as it met all of our lift, drag, and other flight characteristics quite well.

5.2.2 Nacelles

The location of the payload nacelles was at a distance of 10 inches from the centerline of the entire structure. This had a large impact on the placement of the undercarriage because of its obvious impact on stresses experienced during landings. The fuselage consisted of the motor/battery pod and was aptly located in center of the symmetric structure. These nacelles were all 21 inches long and 4 inches in diameter.

5.2.3 Undercarriage

The initial design of the landing gear was judged to be the easiest and most effective configuration. The placement was, for structural integrity reasons, chosen to be just outboard of the

payload nacelles. The forces experienced during landings were at their highest value at the payload nacelle locations. This forced us to place the gear as close to the cargo pods as possible. This distance was chosen to be at a distance of 11 inches from the centerline of the plane.

5.2.4 Empennage

Located at a distance of 38 inches from the trailing edge of the wing, the T-type configuration for the empennage would allow for good flight handling characteristics. The boom, which was attached directly to the vertical stabilizer, was a carbon fiber tube of approximately 2 oz. The area of the empennage was 88 in² and the horizontal stabilizer was 22 inches long. We chose a symmetric airfoil, which was tapered from 9 inches to 7 inches.

6. Manufacturing Plan

6.1 Manufacturing Processes

The manufacturing processes involved in the construction of a model airplane utilize various materials. These include foam, wood, lightweight metal, plastics, composite materials and combinations of them all. Model airplanes tend to be combinations of the above. We encountered many planes that utilized combinations of wood, foam, plastics and metal. Such planes used:

1. Wood as ribs and fuselages
2. Plastic as wing skins
3. Metal in places that demanded strength
4. Foam as wing/empennage cores
5. Composites as stiffeners and strengtheners

We decided that the best approach was to employ combinations of these. The individual components and their respective functional requirements would dictate what the best choice of materials would be.

6.2 Figures of Merit

The following figures of merit were used to compare the competing concepts during the manufacturing process:

- Machining skill level required (1)
Due to few of us having machining this became one of the critical FOM's
- Material availability (2)
The availability of materials was of great importance for several components.

- Material cost (3)
Cost of materials caused great concern due to our small working budget.
- Required time for fabrication (4)
Timely completion of parts would allow for room for error.
- Weight of material (5)
The weight of the entire structure would play an important role in the performance of the design.

6.3 Material Selection and Fabrication Process

6.3.1 Wings and Empennage

The wing, vertical and horizontal stabilizers were constructed from a combination of blue foam and glass fiber. The 2 lb/ft² blue foam made for an excellent core due to its light weight and surprising stiffness. Once the core was cut out we installed the necessary hard points and servos so that we could proceed to encase the entire structure in 2oz bi-directional glass fiber.

The process of cutting the foam is quite similar to what is done for surfboard foam cores. In order to cut the foam we needed to make full-scale templates with the plots obtained from the MacFoil program. Two plots of each were needed in order to create templates for the top and bottom faces of the wing. We then attached the plots to Formica so that we could cut down to where the top and bottom lines of the airfoil were exposed. The templates were then attached directly to the foam. Once attached, we utilized a wire bow with a voltage applied across opposite ends so as to heat the wire up to an appropriate temperature. The templates were used as guides for the wire as it was run through the blue foam. The bottom edge was cut first so as to ensure accuracy, then the top edge was cut in the same manner, except this time with the top template attached to the foam.

Once this was completed we installed quarter inch thick marine grade plywood in the foam to act as attachment points for the pods and landing gear. The spar was then installed at the 30% chord line where the wing was thickest. The next step was to lay the glass fiber on Mylar and evenly coat the fiber with an epoxy. We then proceeded to lay the Mylar and glass on the wing in the proper orientation. At this point we put the wing in a vacuum bag so as to ensure even and smooth adhesion of the glass to the foam and hard points.

The final step in the manufacturing of the wings was to cut out the control surfaces. The control surfaces were then reattached with the use of a high strength tape to act as a hinge. This process was repeated for the empennage structures with the only difference being the location of the hard points and the servos and a strip of carbon to add stiffness.

6.3.2 Pods

The pods for the payload and the motor/batteries were comprised entirely of glass fiber. Marine grade plywood was utilized again as material for attachment to wings. Care was taken not to cut the fibers, which would lessen the strength dramatically.

The construction process began with the production of a wooden plug on a wood lathe. Three molds of the plug were made for each pod. These molds provided a template in which to place the glass fibers. We then proceeded to incorporate the attachment points.

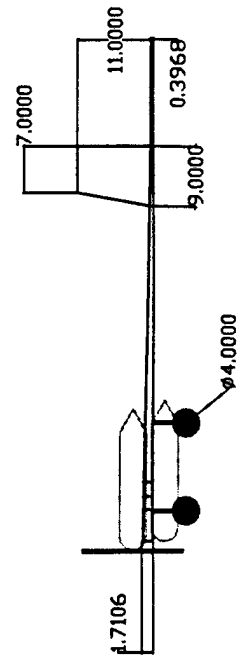
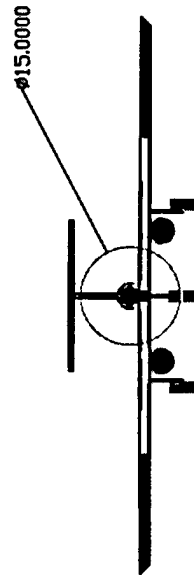
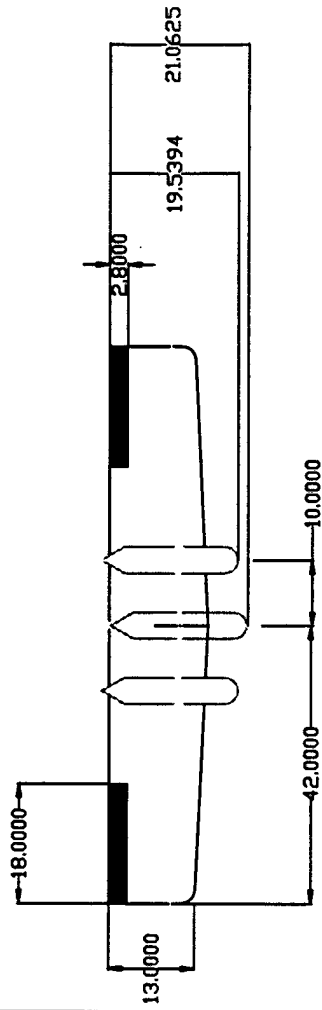
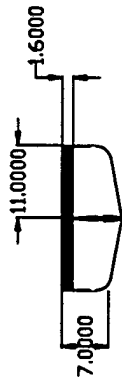
6.3.4 Undercarriage

Then landing gear structure consisted of a combination of .25 inch diameter steel piano wire and marine grade plywood. This torsional system allowed for easy construction without sacrificing durability and weight.

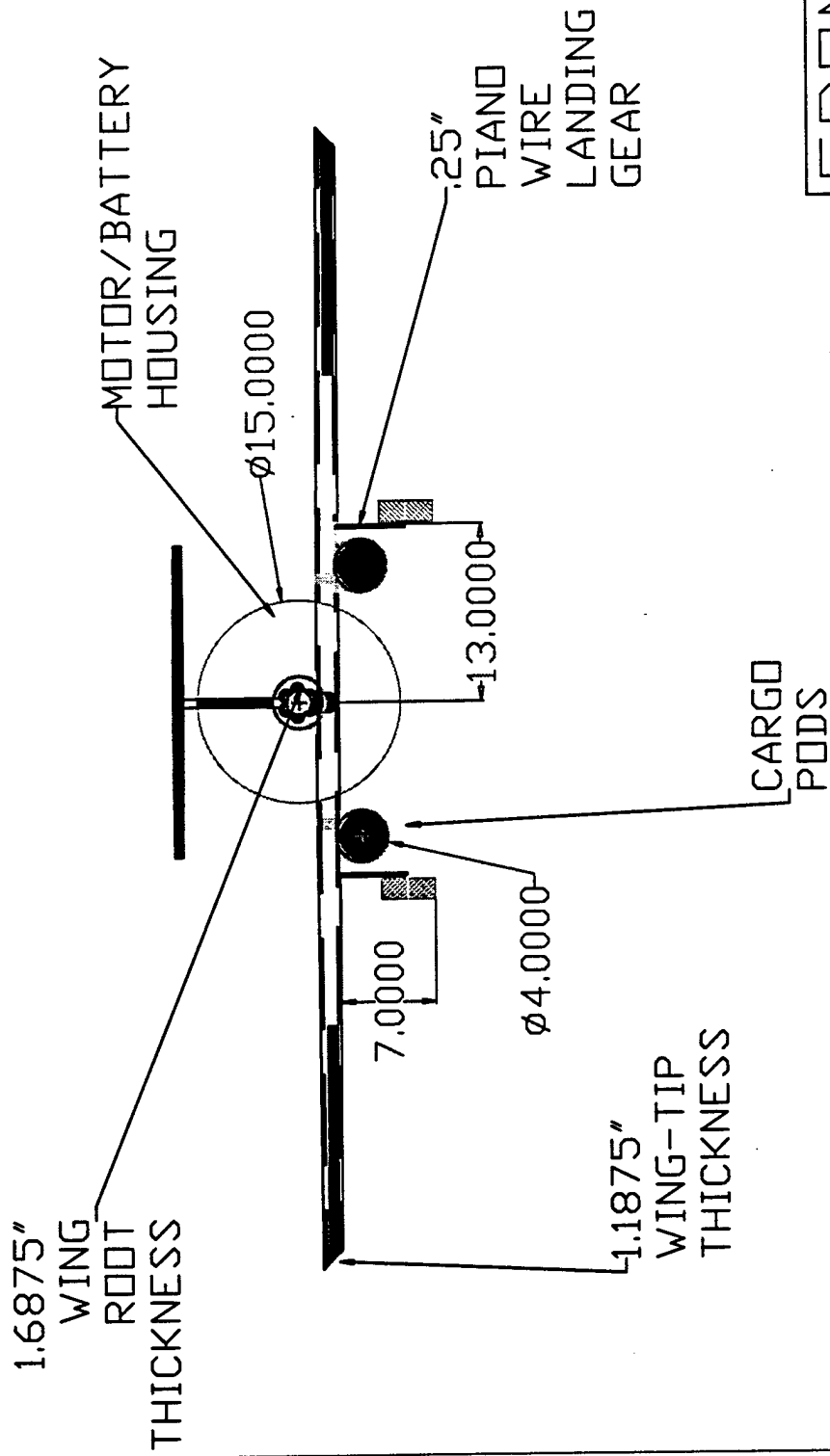
The production of this component included machining blocks of wood in the proper dimensions and gluing them together. A notch was made in the center at .25 inch depth to accommodate the wire. Brackets were then screwed in to prevent the wire from breaking free. The wheels for the plane were made of aluminum with a rubber O-ring that acted as a tire.

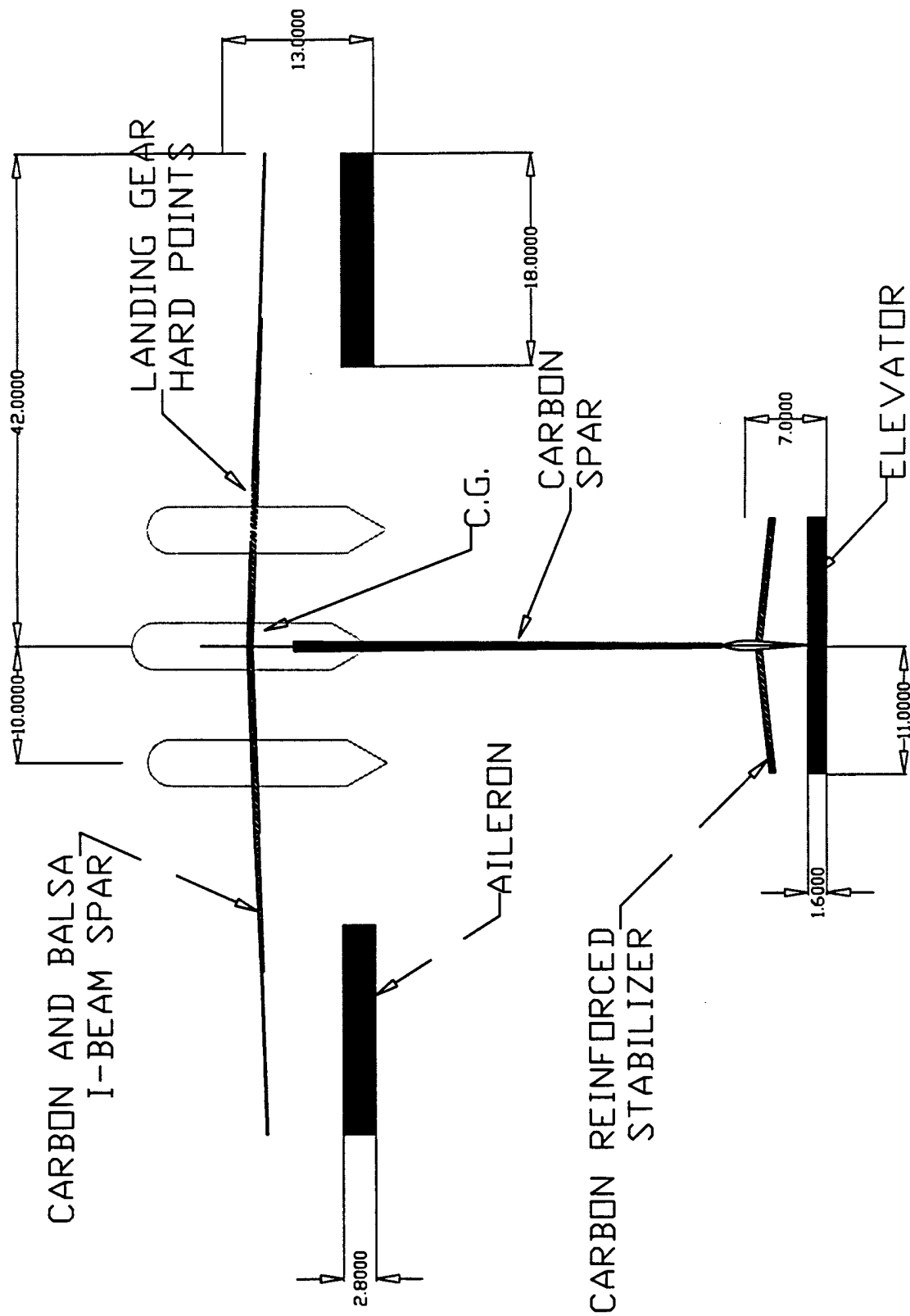
6.3.5 Spar

The spar was constructed of a combination of carbon tow and end-grain balsa in an I-beam configuration. The balsa was cut into 3-inch square parts and then glued together. Then a groove was cut into top to make room for the 2K-carbon tow, which would provide strength and stiffness. The entire structure was then inserted into a groove in the wing at the 30 % chord line. This line was the thickest point of the airfoil and thus would provide enough room to accommodate the spar. The spar was then sanded down so that it was flush with the airfoil surface.

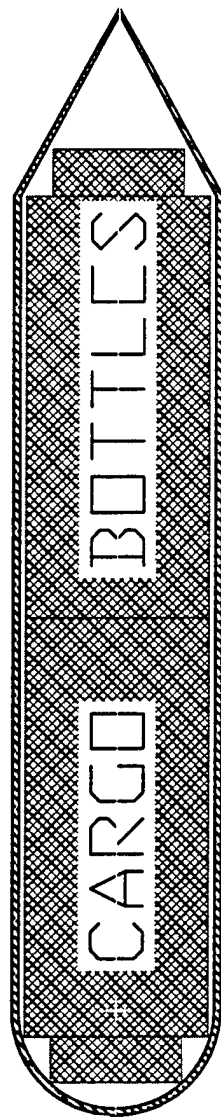


NOTE: ALL WHEELS
SAME DIMENSION





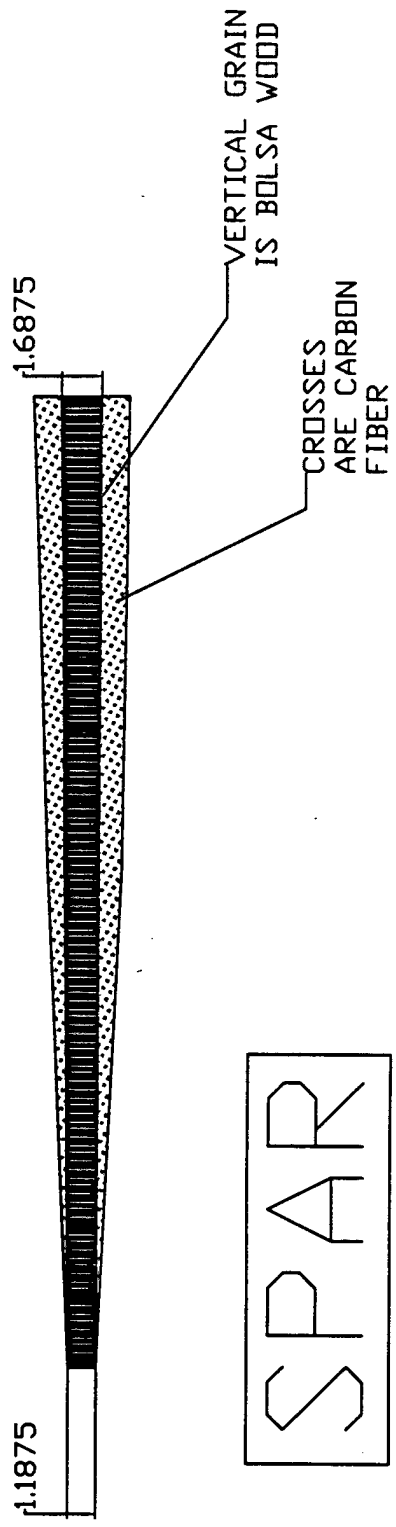
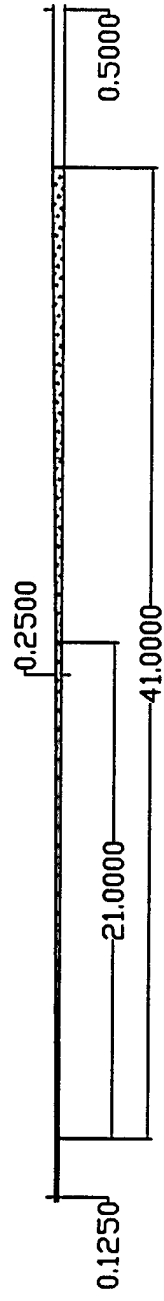
BOTTOM VIEW



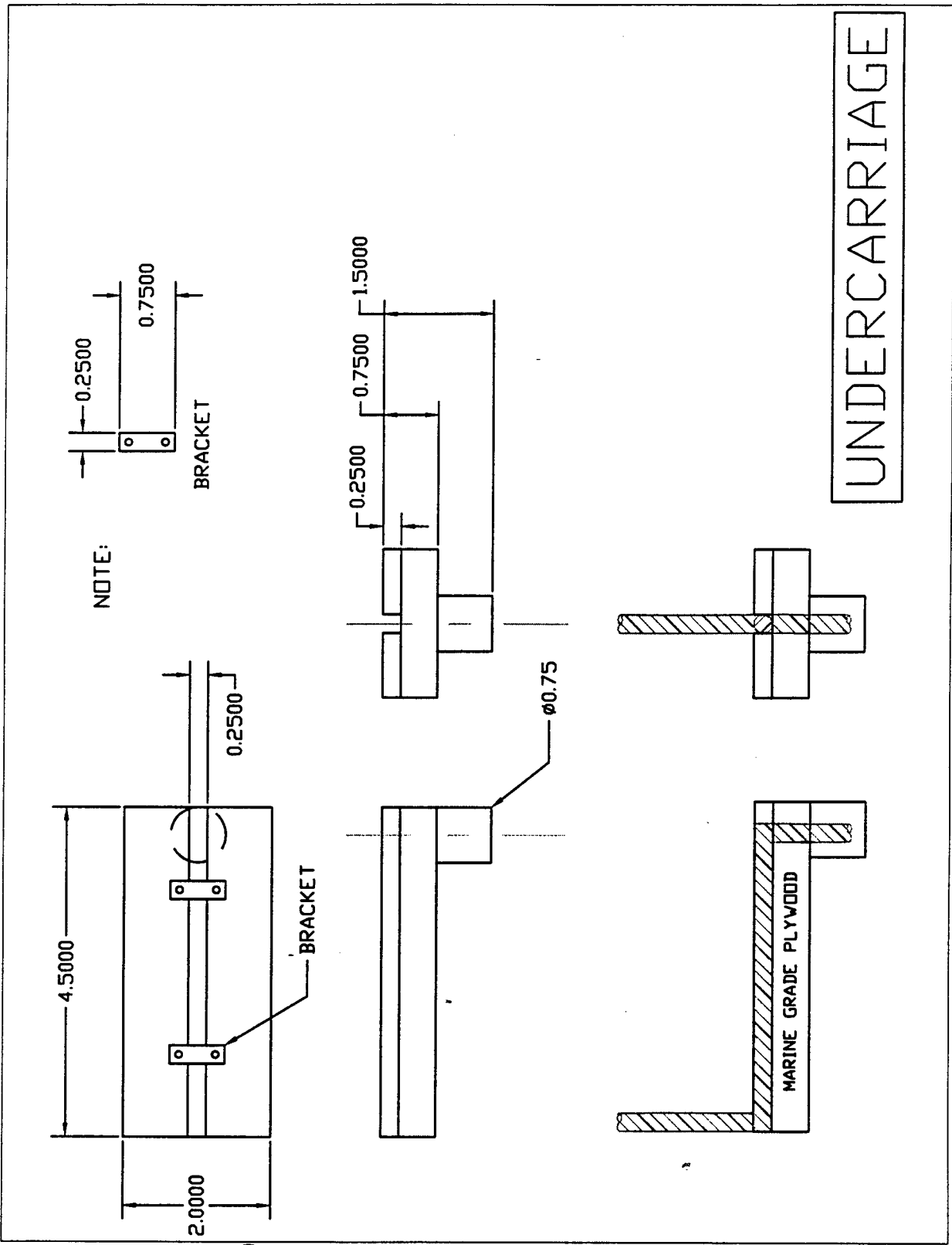
Kevlar Cargo Pods
1/8 Inch Thickness

CARGO PODS

REFER TO CARBON LAYOUT SCHEDULE
FOR ACTUAL DIMENSION



SPAR





**American Institute of
Aeronautics and Astronautics**

**AIAA Foundation/Cessna Aircraft/ONR
Student Design/Build/Fly Competition**

Design Report: Addendum Phase

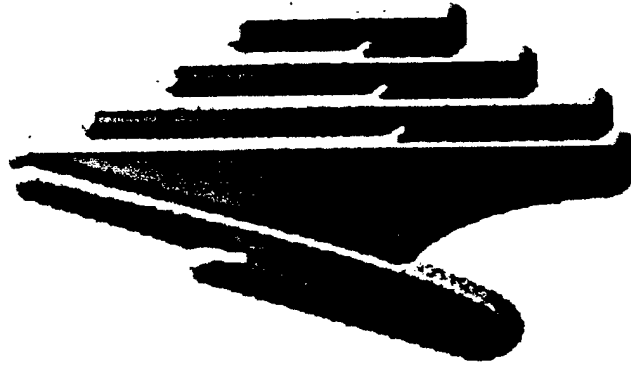
Submitted By:

**The University of California, San Diego
AIAA Student Chapter Competition Team**

April 1, 2000



*American Institute of Aeronautics
and Astronautics*



UCSD

AIAA Cessna/ONR
Student Design/Build/Fly Competition

**TEAM T.L.A.R.
ADDENDUM PHASE REPORT**

DESIGN AND DEVELOPMENT TEAM:

Andrew Mye
Joshua T. Hu
Annie Powers
Kari Goulard
John Taylor

i. Table of Contents

<u>Section 1- Executive Summary</u>	<u>Pg. 1</u>
<u>Section 2- Management Summary</u>	<u>Pg. 2</u>
<u>Section 3- Conceptual Design</u>	<u>Pg. 6</u>
<u>Section 4- Preliminary Design</u>	<u>Pg. 9</u>
<u>Section 5- Detail Design</u>	<u>Pg. 12</u>
<u>Section 6- Manufacturing Plan</u>	<u>Pg. 13</u>
<u>Section 7- Lessons Learned</u>	<u>Pg. ??</u>
<u>Section 8- Rated Aircraft Cost</u>	<u>Pg. ??</u>
<u>Section 9- Appendix</u>	<u>Pg. ??</u>

I) Table of Figures

A) Alternate Design Concepts

A1) Sketch of Dual Motors Single Wing Configuration

A2) Sketch of Single Motor Single Wing Configuration

B) VisualFoil Plots

B1) Polar Plots For Airfoils

B2) Various VisualFoil Plots of Lift and Drag Coefficients vs. Angle of Attack

C) Data Gathered of Eppler 214 Airfoil

C1) VisualFoil Plot of Lift and Moment Coefficient vs. Angle of Attack for Eppler 214

C2) VisualFoil Plot of Surface Velocity
for Eppler 214

C3) VisualFoil Plot of Surface Pressure
Distribution For Eppler 214

C4) VisualFoil Plot Pressure
Coefficient for Eppler 214

C5) MacFoil Plot of Airfoil Template
For Wing Tip for Eppler 214

II) Photo Gallery

7. LESSONS LEARNED

7.1 Major Areas of Enlightenment

Throughout the design process many important lessons were learned and much valuable experience was gained. Due to the various backgrounds and personal knowledge of each team member, lessons were learned from each other via teamwork. These included experiences with electronics, composite materials, machining techniques, use of various computer programs, teamwork skills and power supply systems. The most important lessons learned through entering a competition such as this include:

- ***Early start***

Establishing a management structure and starting the design process as early as possible allows room for error and alterations in design. Beginning early allows for time to acquire materials, sponsorship, equipment and financing thus avoiding complications due to lack of time and unavailability of necessities. Establishing a conceptual design dictates what equipment, materials and amount of money is needed and therefore should be one of the first things to be decided upon.

- ***Intricacies of design process***

The team as a whole, especially the underclassmen, was exposed to a "real world" design process. Techniques gained through taking the required design courses allowed the upperclassmen of the team to make necessary decisions and to guide the underclassmen. The major difference between projects undertaken in a classroom setting and this type of project was the fact that we were solely responsible for problems that arose. This showed us the value of self-reliance and making judgement calls based on our knowledge gained through classroom instruction.

- ***Theoretical vs. Actual***

The theoretical flight and physical characteristics of the T.L.A.R. differed from the actual characteristics. These characteristics include the location of the C.G., angle of incidence and, therefore, necessary thrust for optimum performance. The differences were found to be due to the machining processes used and using published values for weight (composites). In addition, more material was used for strengthening high stress points than was originally deemed necessary. The realization of these differences forced us to note the importance of testing the completed design. Testing also gave the team insight into what needed to be improved and/or redesigned in order to achieve satisfactory performance.

- ***Knowledge of model aircraft***

Although one of the team members had experience with RC model cars none had previous exposure to RC model airplanes. This entire experience has allowed the team as whole to understand the attraction to these recreational toys. Each individual was also able to apply knowledge gained via classes to a real world endeavor. Members of the

team with little to no background of basic aerodynamics received a crash course in this field and will no doubt benefit from the experience.

7.2 Final Configuration vs. Proposal Design

The fact that this was UCSD's first time competing in such an event, alterations in the design were necessary. Several changes were made to the various components of the T.L.A.R. due to the need for higher strength, better design ideas being generated, availability of material and ease of access and/or replacement. Initial flight-testing and analysis of flight performance data illustrated the need to make changes. Although changes were necessary, the proposal design was an excellent representation of our final configuration. The following are component-wise breakdowns of deviations from the proposal design:

- ***PODS***

The motor and cargo pods were constructed from 2-oz kevlar and epoxy. We made a wooden plug on a wood lathe and then cut one end off and split the body into two halves. These three parts were used to create molds out of hydrocal plaster in which we could lay the kevlar fiber. Once the kevlar was wetted with epoxy and opposing edges were trimmed the two halves were pinned together. This type of joint is commonly referred to as a lap joint. The original plan was to use a strip of marine grade plywood to acts as the joiner between the two halves.

The length of the motor/fuselage pod was extended because the C.G. was located 2 inches closer to the trailing edge than originally planned. This made the total length of the fuselage 28 inches as opposed to 21 inches. This also allowed room for the battery pack to be moved in order to accommodate the other equipment stored within the fuselage. One other benefit of this was that when the battery pack became hot it would not heat the other equipment, therefore reducing the chance of damaging the controller and receiver.

The method of attaching the cargo pods to the wings was also reconsidered. The team came up with the idea of using an aluminum strap to support the front of the pod. This made the fabrication process easier because it allowed us to avoid using wooden hard points as attachments. The use of aluminum straps also decreased the overall weight while maintaining the structural integrity of the kevlar pods.

- ***STABILIZERS***

The stabilizers were altered slightly to attain the required the +1.25 angle of incidence. The height of the vertical stabilizer was shortened from 11 inches to 10 inches. In order to obtain the necessary angle of incidence material was removed from the trailing edge so as to cant the horizontal stabilizer in our favor. This method helped reduce the weight further and attain good flight handling characteristics for our pilot.

- ***LANDING GEAR***

The modification to the forward landing gear was based on undesirable aspects of the original fabrication process. During the initial testing phase we noticed that the gear bent in several places and ultimately deformed and therefore needed to be modified. The .25 inch diameter piano wire, comprised entirely of 1095 cold rolled steel, is quite hard and strong. In order to attain the desired shape a heating process was utilized. This fabrication process reduced the strength while increasing the ductility of the metal, allowing us to bend it. In order to regain strength, an annealing and tempering cycle was used. This did not achieve complete return to the original strength and resulted in the deforming that was unacceptable.

In order to obtain the required strength we had to bend the wire cold, which would leave residual stress. Tempering the steel in a conventional oven at 700°F for 15 minutes helped alleviate the residual stress. We then proceeded to test the landing gear and found it to be quite strong and stiff and therefore suitable.

The team saw that it was necessary to add a tail wheel instead of the original configuration. This was necessary because the original design was not conducive to ground handling and stability during landing and taxiing. The tail wheel was purchased at local hobby store along with 3/32 piano wire to attach it to the boom. In addition, a connection to the rudder was fabricated thereby making ground handling quite smooth and efficient.

- ***WHEELS***

Substituting aluminum wheels for rubber wheels purchased at a local hobby store would reduce the overall weight of the design. This decision led to the fabrication of an aluminum rim into which a rubber o-ring could be placed to provide traction. The aluminum rim was then covered with blue MonoKote so as to reduce drag.

- ***PROPULSION SYSTEM***

The propulsion system was changed because it was determined that an AVEOX 1412 3Y motor would provide more than enough power. Switching to this motor would reduce the amount of power drained from the battery, which would allow for more sorties flown during the flight times. The importance of power management considerations would also be somewhat reduced.

- ***BOOM***

The proposal phase incorporated the use of a carbon fiber boom which was to be purchased from a local company. The dimensions of the boom did not fit our needs and therefore we decide to choose a glass fiber tube. This tube was then reinforced with 2k carbon fiber tow so as to provide stiffness and increased strength.

7.3 Possible Areas of Improvement

The team felt very confident with the design and could come up with very few areas for improvement. These areas are as follows:

- ***BRAKING SYSTEM***

Installation of a braking system was an issue that was noticed following the initial flight-testing phase. Following touchdown, T.L.A.R. rolled, on average, approximately 100 feet. This was cause of much concern considering the time necessary to taxi back to the starting line which would consume precious time and power. The idea of installing a braking system was considered but quickly dismissed due to the lack of necessary time to acquire the equipment.

- ***INTEGRATION OF MOTOR AND CARGO PODS***

Combining the motor and cargo pods would reduce the weight of the structure and decrease the drag. This configuration would require careful consideration when the necessity of quick load/unload is of the essence. The strength of the spar and the wing joiners would have to be optimized in order to support the centering of the weight. This design would make establishing the location of the C.G. easier.

- ***SHOCK ABSORBERS***

The landing gear system would have benefited from the use of shock absorbers. The use of absorbers would reduce the risk of collateral damage during landings. This design idea could possibly lead to an increase in payload capability.

7.4 Final Flight Performance Data:

Weight: 22.1 lbs

Turning radius: 25 ft

Angle of Incidence (AOI): 1.25 relative to 10" stab

Avg. Speed: 70 mph

Power: 1800 peak
718 avg.

Amp: 50A peak
18 avg.

Volt: ~36 volts under load

Peak Thrust = 82.2 Watts/ lb.

8. RATED AIRCRAFT COST

$$\text{RATED AIRCRAFT COST (RAC)} = A * \text{MEW} + B * \text{REP} + C * \text{MFHR}$$

$$A = \$100/\text{lb}$$

$$B = \$1/\text{watt}$$

$$C = \$20/\text{hour}$$

MEW = Manufacturer's Empty Weight (lb)

REP = Rated Engine Power (watts)

MFHR = Manufacturing Man Hours (hours)

$$\begin{aligned}\text{MEW} &= \text{Total weight} - \text{Battery Pack Weight} - \text{Payload weight} \\ &= 22.1 \text{ lb} - (79/16) \text{ lb} - 10.27 \text{ lb} \\ &= 6.89 \text{ lb}\end{aligned}$$

$$\begin{aligned}\text{REP} &= \text{Number of motors} * 50 \text{ Amps} * 1.2 \text{ Volts/cell} * \text{Number of cells} \\ &= 1 * 50 \text{ Amps} * 1.2 \text{ Volts/cell} * 36 \text{ cells} \\ &= 2160 \text{ watts}\end{aligned}$$

WBS Number and Type	Scoring Values	Design Description
#1-Wings	5 hr/wing + 4hr/sq. ft Projected Area (PA)	Single Wing Design PA=1176 ft ²
#2-Fuselage and/or Pods	5 hr/body + 4hr/ft of length	Two 21" Cargo Pods 28" Fuselage
#3-Empenage	5 hr (basic) + 5 hr/Vertical Surface + 10 hr/Horizontal Surface	One Vertical Surface One Horizontal Surface
#4-Flight Systems	5 hr (basic) + 1 hr/Servo	Four Servos
#5-Propulsion Systems	5 hr/Motor + 5 hr/propeller	One propeller

$$\begin{aligned}\text{MFHR} &= \text{Wing} + \text{Fuselage \& Pod} + \text{Empenage} + \text{Flight System} + \text{Propulsion System} \\ &= (5 + 4 * [1176/144]) + ([3 * 5] + 4 * [104.5/12]) + (5 + 5 + 10) + (5 + 4) + ([5 * 1] + [5 * 1]) \\ &= 126.49 \text{ hours}\end{aligned}$$

$$A * \text{MEW} = (\$100/\text{lb}) * (6.89 \text{ lb}) = \$689$$

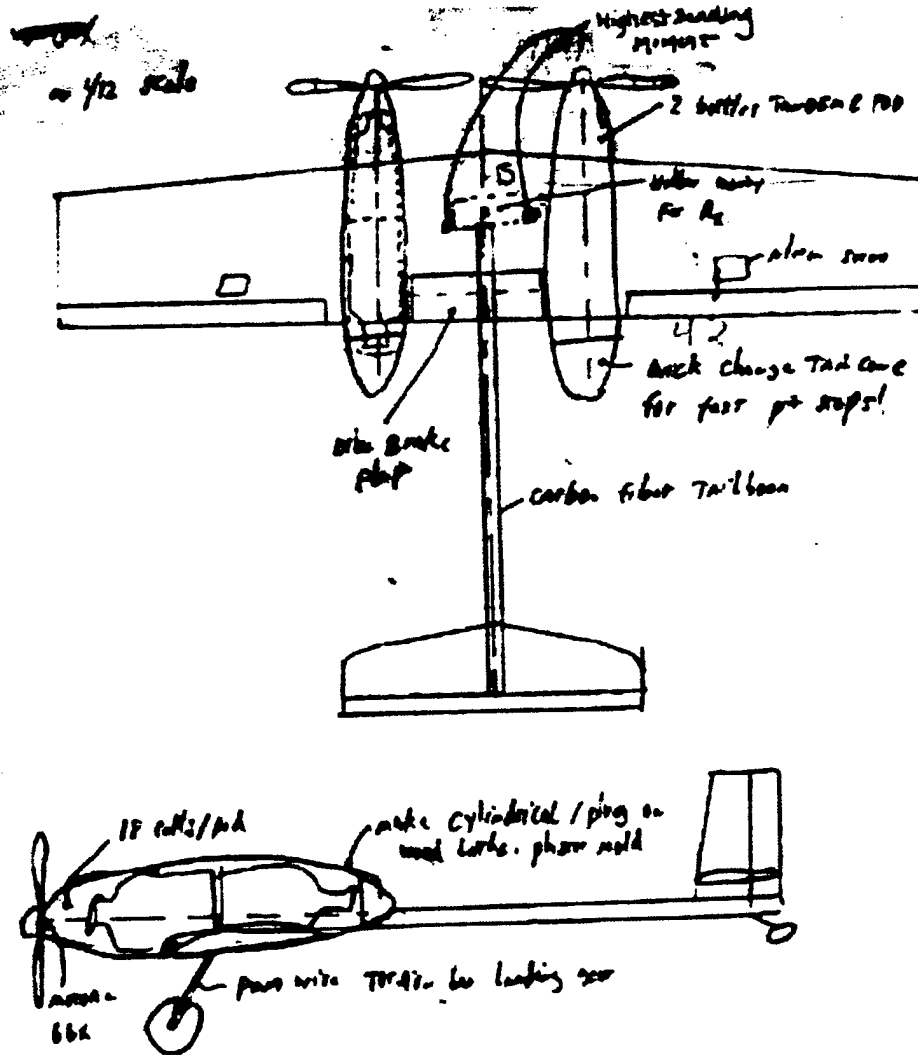
$$B * \text{REP} = (\$1/\text{watt}) * (2160 \text{ watts}) = \$2160$$

$$C * \text{MFHR} = (\$20/\text{hour}) * (126.49 \text{ hours}) = \$2529.8$$

$$\begin{aligned}\text{RAC} &= (A * \text{MEW} + B * \text{REP} + C * \text{MFHR}) * (1/1000) \\ &= (\$689 + \$2160 + \$2529.8) * (1/1000) \\ &= \underline{\underline{\$5.3788}}\end{aligned}$$

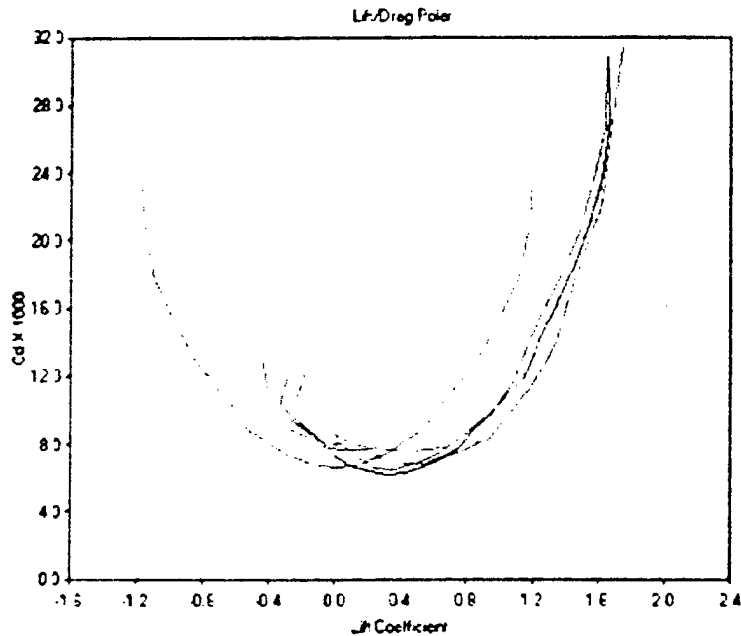
Appendix

I) Table of Figures:



A.1 Dual Motor Single Wing Design Configuration

A.2 Single Motor Single Wing Design Configuration



Airfoil	Flap	Re
E212	(0.0)	1.00e+6
-E211	(0.0)	1.00e+6
E209	(0.0)	1.00e+6
-E214	(0.0)	1.00e+6
-0012	(0.0)	1.00e+6

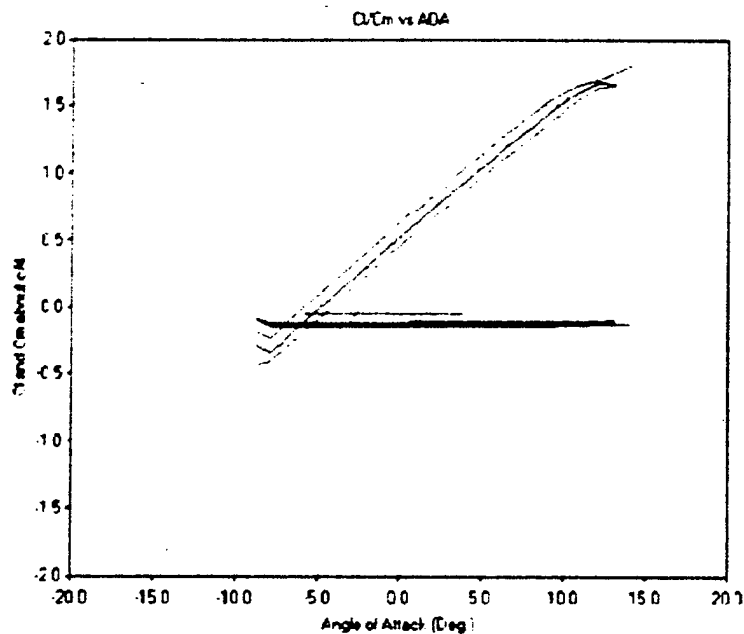
Inputs

Airfoil	0012
Angle	0.0 Deg
Disc Len	0.0 Deg
Disc Length	0.0 %
Re	1000000

Results

Lift Coeff	0.000
Moment Coeff	0.000
Cm (c/4)	0.000
Angle (Cl=0)	0.00 Deg
Cent. of Pres	N/A
Drag Coeff	0.006572
\bar{c}	2.73×10.865

B.1 Polar Plots for Various Airfoils (VisualFoil)



Airfoil	Flap	Re
-E212	(0.0)	1.00e+6
-E211	(0.0)	1.00e+6
-E209	(0.0)	1.00e+6
-E214	(0.0)	1.00e+6

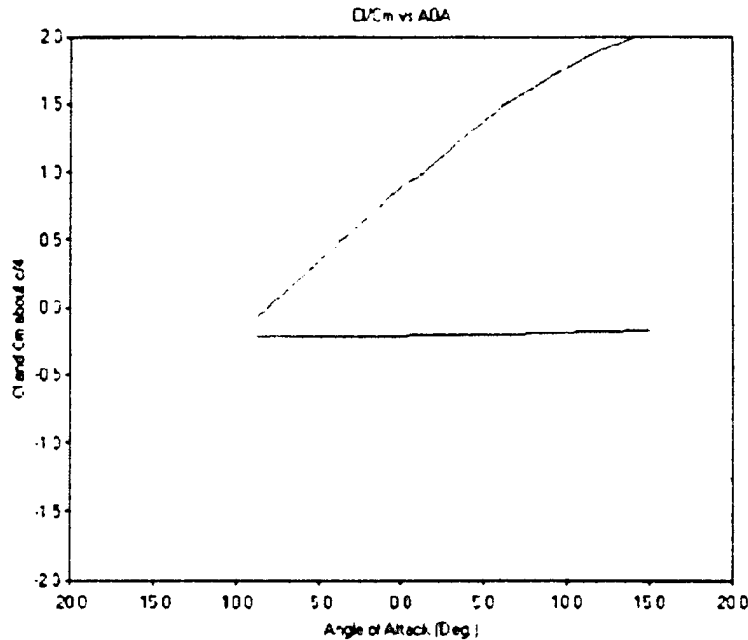
Inputs

Airfoil	E214
Angle	0.0 Deg
Disc Len	0.0 Deg
Disc Length	0.0 %
Re	1000000

Results

Lift Coeff	0.640
Moment Coeff	-0.320
Cm (c/4)	-0.160
Angle (Cl=0)	-5.84 Deg
Cent. of Pres	90 %
Drag Coeff	0.007136
\bar{c}	15.91×2.235

**B.2 Lift vs Drag Coefficients vs Angle of Attack
For Various Airfoils (VisualFoil)**



Airfoil: Eppler 214
Re: 1.00e+6

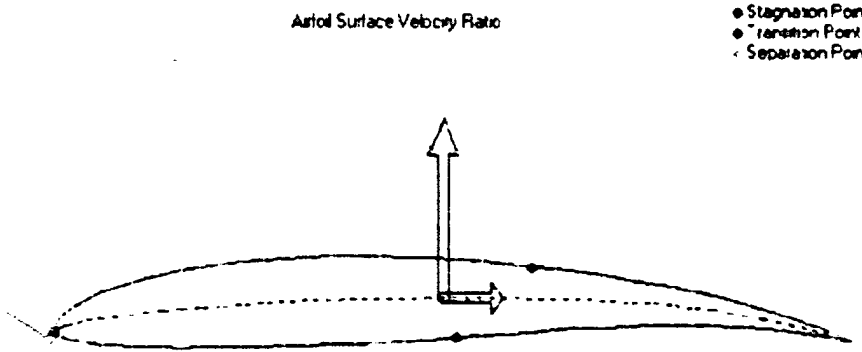
Inputs

Airfoil: Eppler 214
Angle: 0 Deg
Planform: 4 Deg
Planform: 20 %
Re: 1000000

Results

Lift Coeff: 0.897
Moment Coeff: -0.433
Cm (c/4): -0.208
Angle (Cl=0): -8.18 Deg
Cent. of Pres: 48 %
Drag Coeff: 0.007459
 $\frac{C_L}{C_D}$: 7.54 x 0.696

C.1 Lift and Moment Coefficients vs Angle of Attack for Eppler 214 (VisualFoil)



• Stagnation Point
• Transition Point
• Separation Point

Inputs

Airfoil: Eppler 214
Angle: 0 Deg
Planform: 4 Deg
Planform: 20 %
Re: 1000000

Results

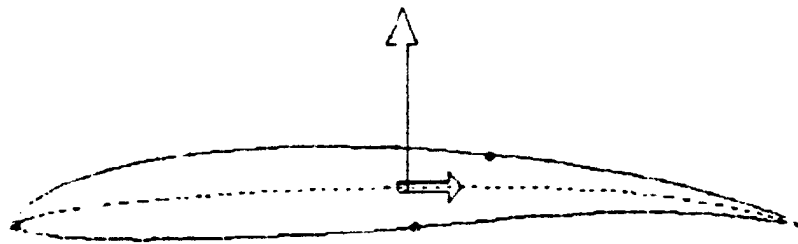
Lift Coeff: 0.897
Moment Coeff: -0.433
Cm (c/4): -0.208
Angle (Cl=0): -8.18 Deg
Cent. of Pres: 48 %
Drag Coeff: 0.007459
 $\frac{C_L}{C_D}$: 0.91 x 0.023

0.4 0.6 0.8 1.0 1.2 1.4 1.6 1.8

C.2 Surface Velocity for Eppler 214 (VisualFoil)

Airfoil Surface Pressure Coefficient

- Stagnation Point
- Transition Point
- Separation Point



Inputs

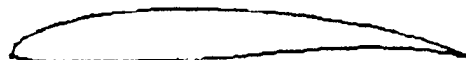
Airfoil: E214
Angle: 0 Deg
Flap Defl: 4 Deg
Flap Length: 20 %
Re: 1000000

Results

Lift Coeff: 0.897
Moment Coeff: -0.433
 $C_m(c/4)$: -0.208
Angle (Flap): -8.18 Deg
Cent. of Pres: 48 %
Drag Coeff: 0.007459
 $C_{D,0}$: 0.002 * 0.428

-1.4 -1.1 -0.8 -0.5 -0.2 0.1 0.4

C.3 Surface Pressure Distribution for Eppler 214 (VisualFoil)



Inputs

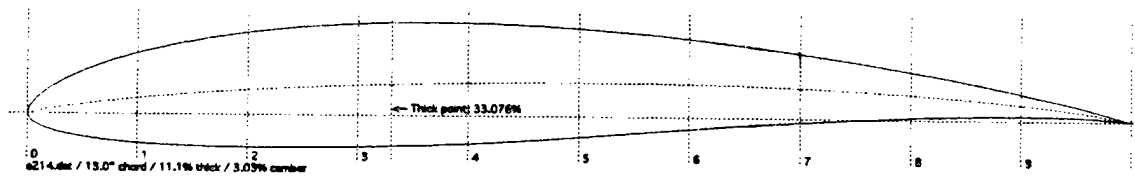
Airfoil: E214
Angle: 0 Deg
Flap Defl: 4 Deg
Flap Length: 20 %
Re: 1000000

Results

Lift Coeff: 0.897
Moment Coeff: -0.433
 $C_m(c/4)$: -0.208
Angle (Flap): -8.18 Deg
Cent. of Pres: 48 %
Drag Coeff: 0.007459
 $C_{D,0}$: 0.002 * 0.427

E214 Pressure (Red - High, Blue - Low)

C.4 Pressure Coefficient for Eppler 214 (VisualFoil)



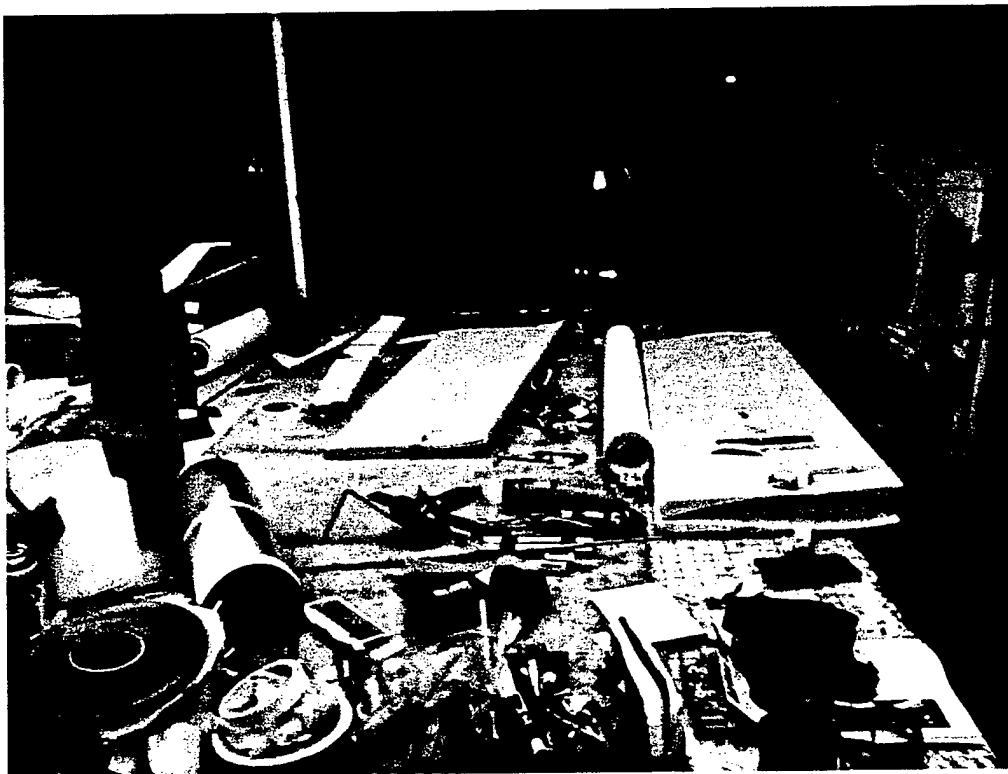
C.5 Airfoil Template for Wing Tip for Eppler 214 (MacFoil)

II) PHOTO GALLERY

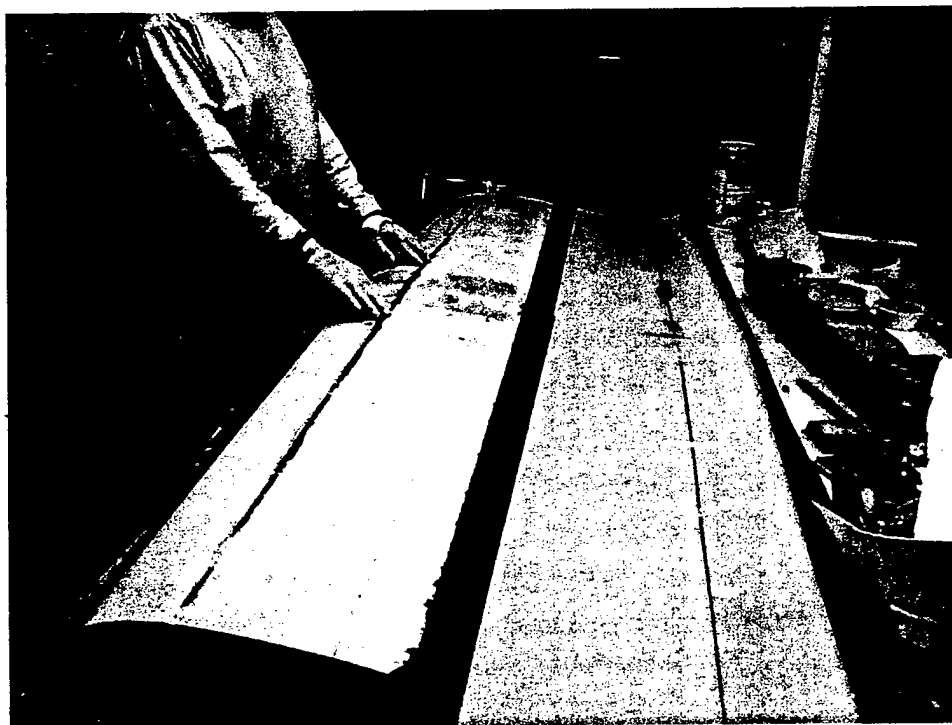


Andrew and John marking locations of spar on wing surface

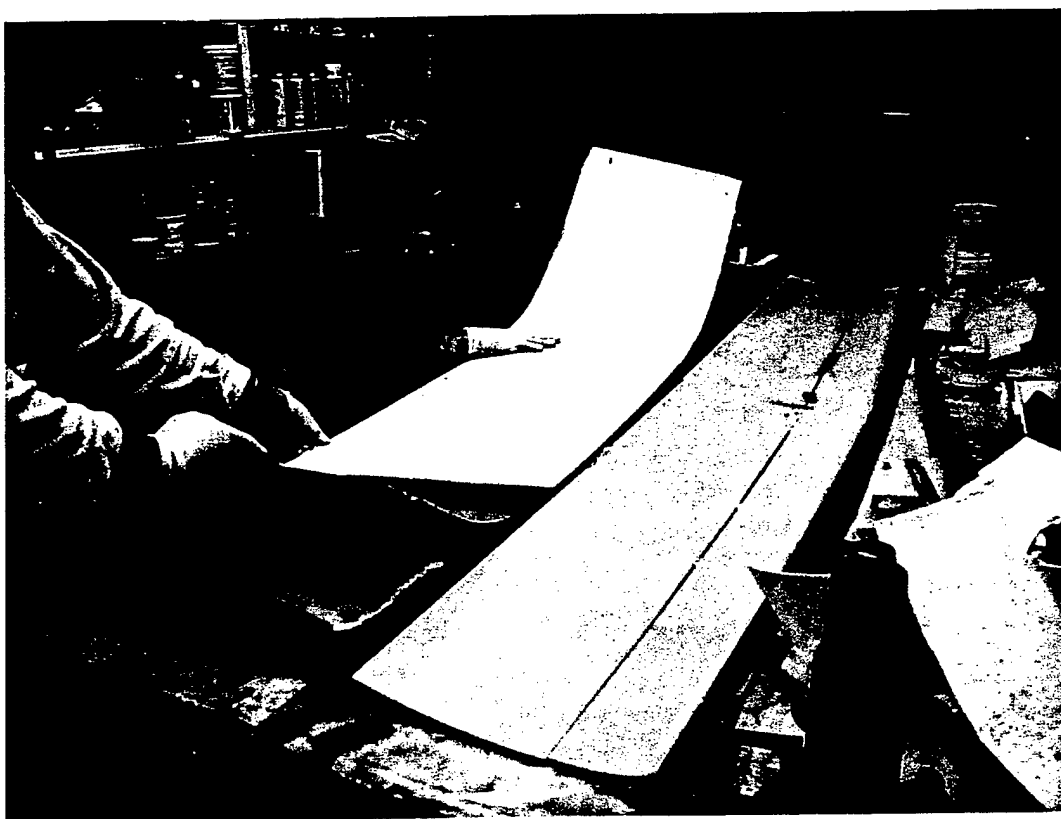




Work Bench with Rolls of Mylar and Blue Foam Cases

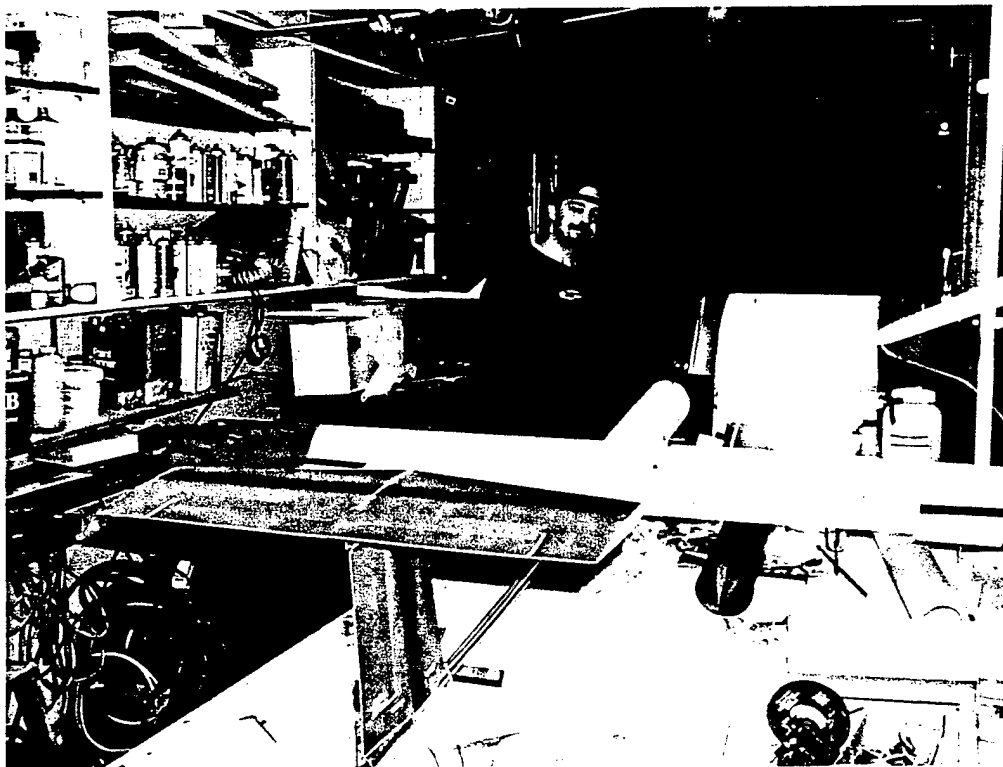


Wing w/ Spar embedded in it



Andrew and Greg laying Mylar on Wing

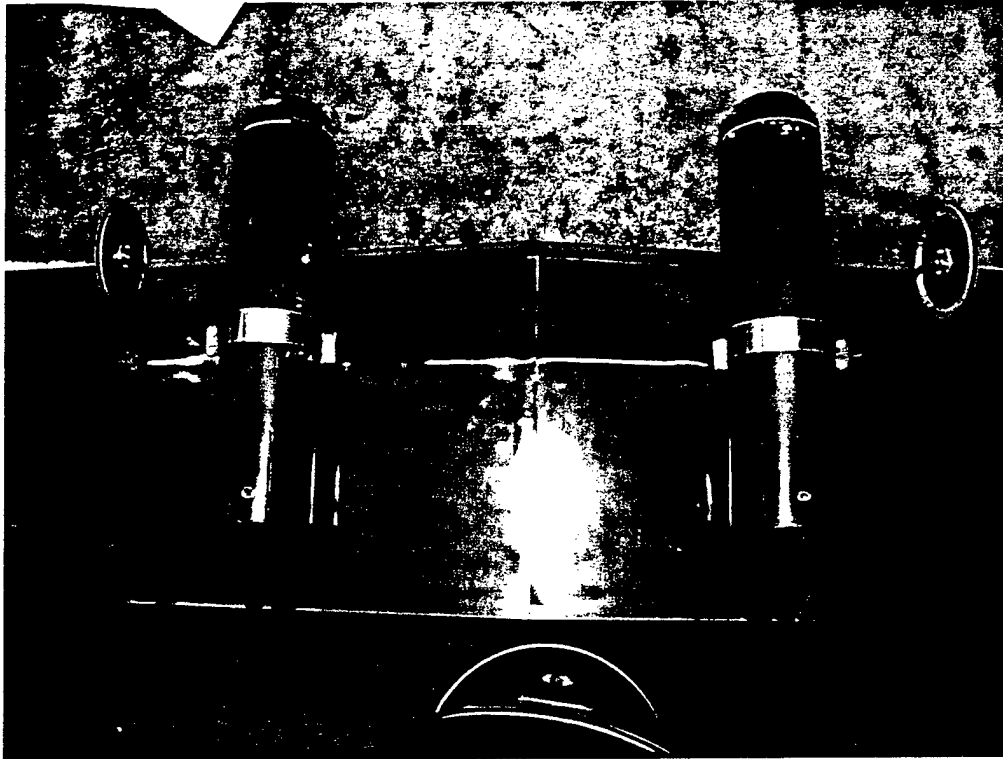




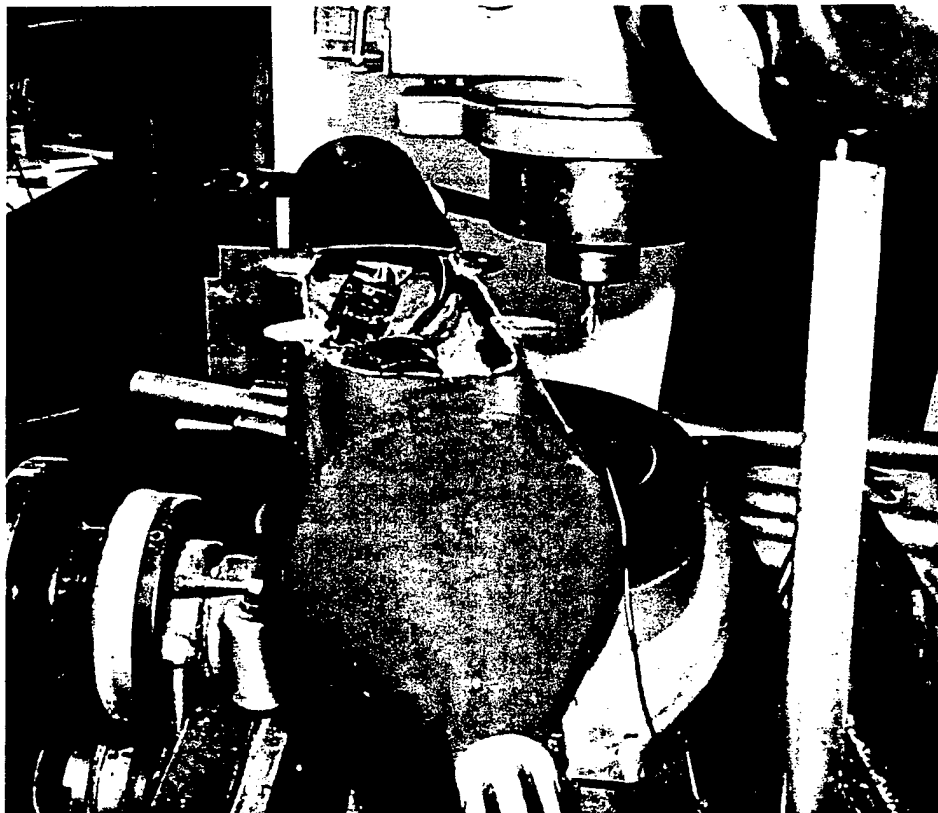
Andrew making sure vacuum bag is sealed



Photos of Final Configuration of T.L.A.R.



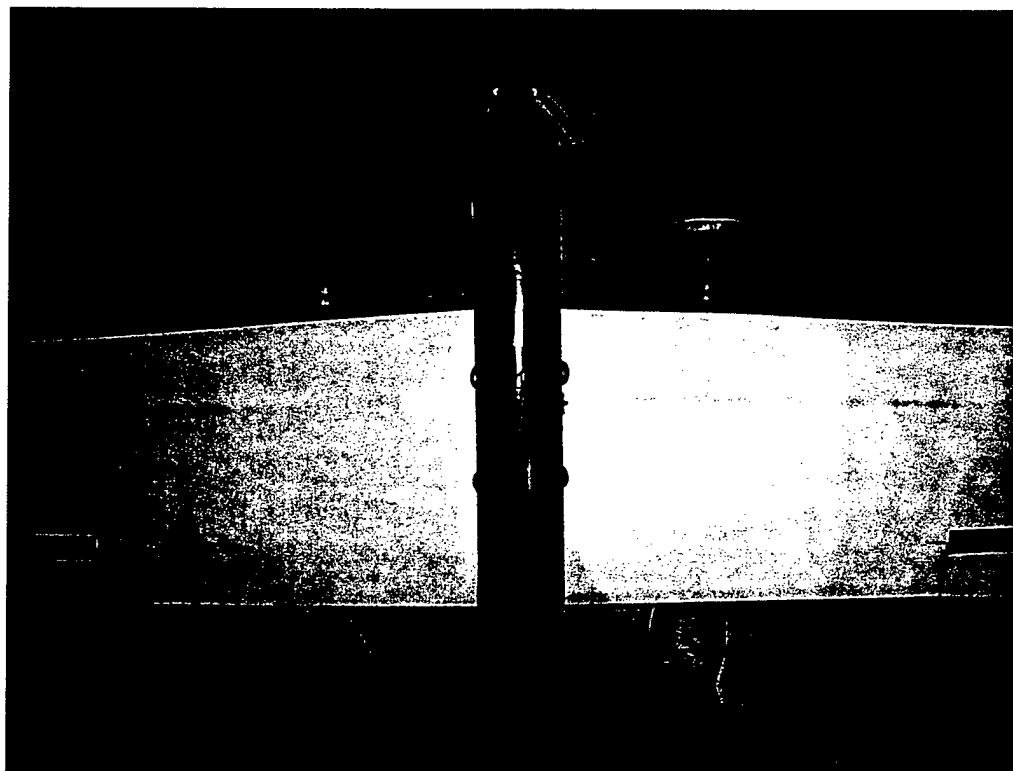
Cargo Pods

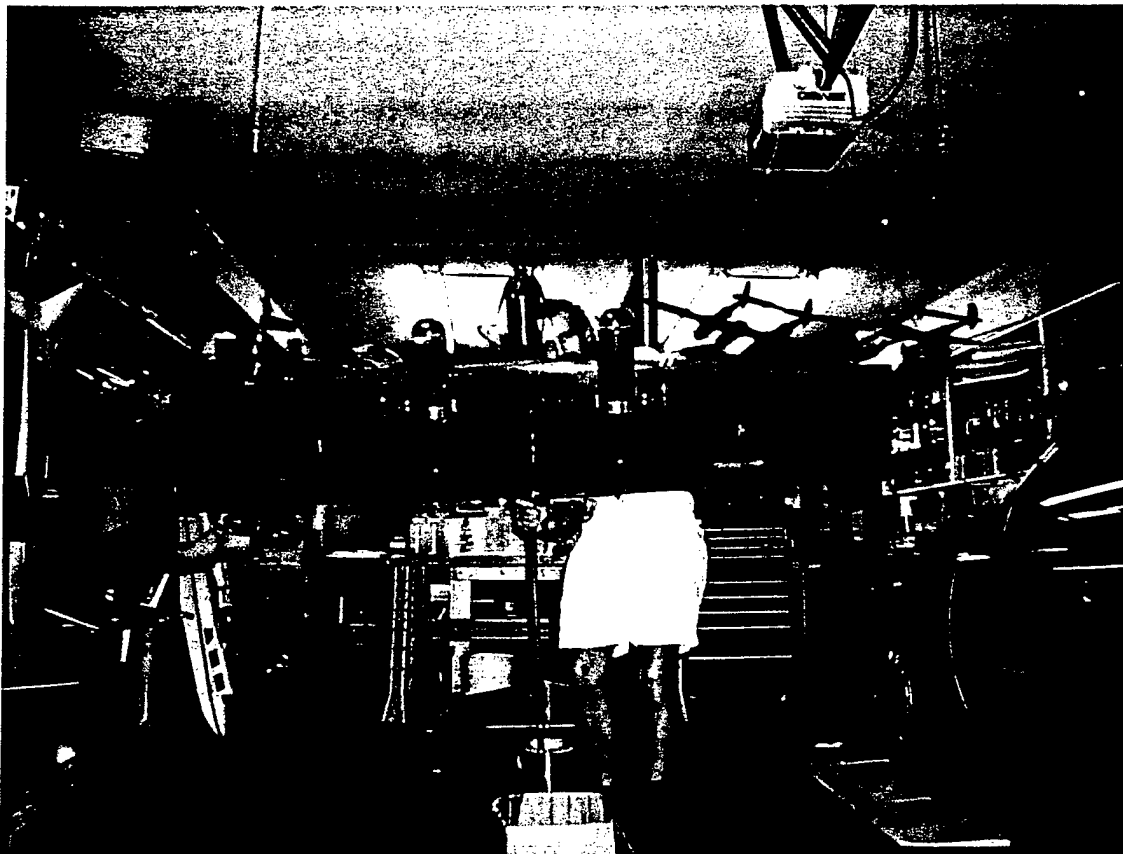


Fuselage/Motor Pod

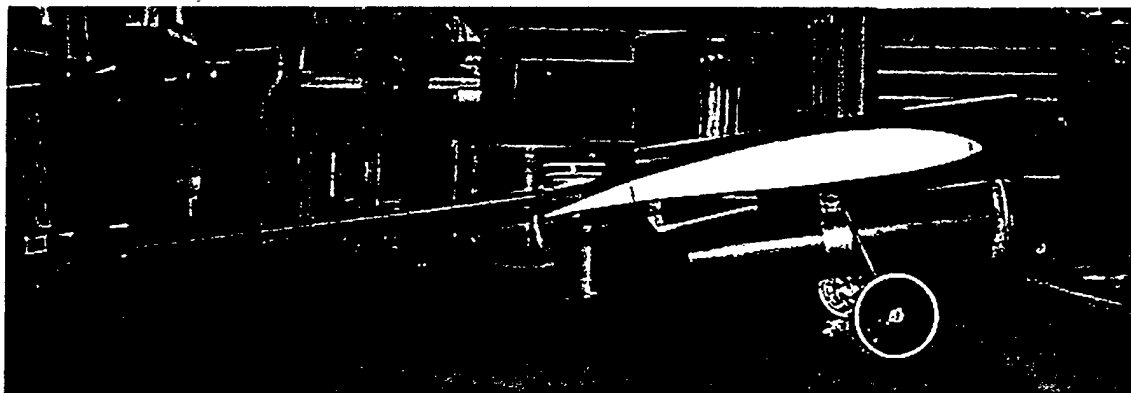


T.L.A.R. with Josh and Andrew





Bottom view of T.L.A.R.



Side view of T.L.A.R.



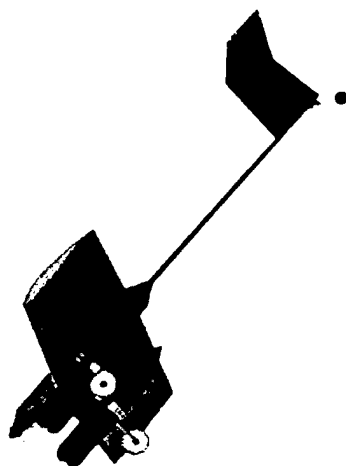
AIAA Cessna/ONR
Student Design/Build/Fly Competition

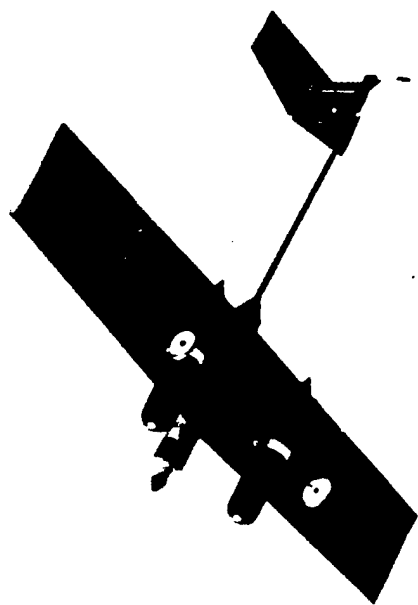
**TEAM T.L.A.R.
FLIGHT PHOTOS**

DESIGN AND DEVELOPMENT TEAM:

Andrew Mye
Joshua T. Hu
Annie Powers
Kari Goulard
John Taylor







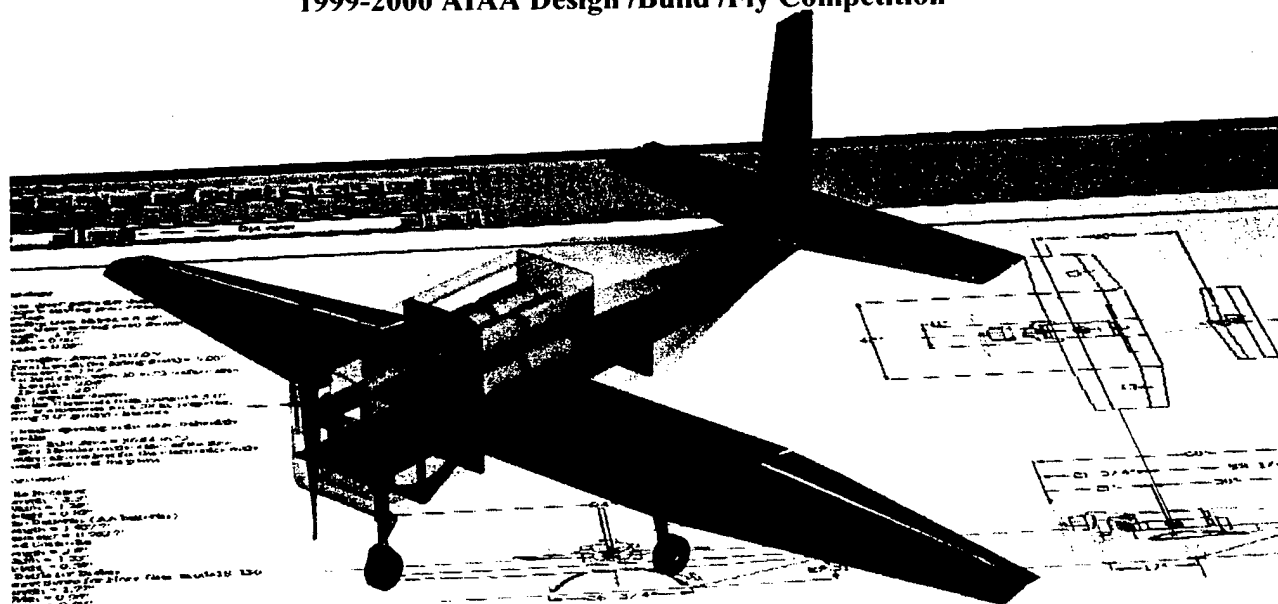




University of Southern California
Aero Design Team Presents

TSUNAMI

Design Report Proposal Phase
March 10, 2000
1999-2000 AIAA Design /Build /Fly Competition



Project Name: Tsunami	Configuration: Drawing C
------------------------------	-----------------------------



**The
Skunk
Works**



Design Report – Proposal Phase

March 11, 2000

1999/2000 AIAA Student Design/Build/Fly Competition

Project Members List

Faculty Advisor

Dr. Ron Blackwelder

Industry Advisors

Mark A. Page (All American Racing)

Blaine Rawdon (The Boeing Company)

Undergraduate Team Members

Experienced Members

Nathan Palmer

Jacob Evert

David Lazzara

Philippe Kassouf

Charles Heintz

Benjamin Hendrickson

George Sechrist

Scott Oishi

New Members

George Cano

Tim Bentley

Andrew Jamison

Ryan Dougherty

Jonathan Stair

Non-undergraduate Members

Jerry Chen

Stuart Sechrist

Pilot

Wyatt Sadler

Sponsors

Lockheed Martin Skunk Works

Northrop Grumman

Grand Wing Servo-tech Co., Ltd.

AeroVironment

Executive summary

The University of Southern California's Aero Design Team will participate in the 1999-2000 AIAA/Cessna/ONR Student Design/Build/Fly Competition. This contest draws teams of college students from across the country to compete in a remote controlled electric aircraft contest. Each year's competition brings a new set of rules, which requires a new design annually and keeps the teams from refining one design year after year. This year's contest requires teams to create a plane capable of carrying the most liters of water over a 1000-foot pylon course in 10 minutes. The plane has to take off within 100 feet, turn 180°, cruise, complete a full turn in the opposite direction, cruise to the end of the course, and then land and taxi back to the starting line. Payload removal, takeoff, two consecutive empty laps, landing, taxi and payload replacement follow each scoring lap. Figure 1.1 describes the flight profile for a loaded sortie. Figure 1.2 describes the flight profile for an unloaded sortie.

The contest also imposes severe constraints on the plane's design; for example a span limit of 7 feet and a maximum aircraft weight of 55 pounds. The contest allows only commercially available nickel cadmium batteries and limits battery pack weight to 5 pounds. It forbids motor and propeller modification and requires the propulsion system to incorporate a fuse and a disarmed lockout for safety. The judges determine the final aircraft score by multiplying the sum of the number of liters carried in the best three 10-minute periods by the report score and dividing this quantity by the rated aircraft cost. This rated aircraft cost incorporates such measures of cost and complexity as battery and motor count, gross weight, wing area and servo count. Creating a successful plane required the incorporation of many different constraints, severely impacting our design.

Our entry in this contest, the *Tsunami*, resulted from a thorough design process. Early in the year our team generated a comprehensive list of alternative configurations including a baseline high-winged monoplane, flying wings, canards, and a risky but attractive joined wing design. The configurator and other team members then developed each design for several weeks. Ultimately a design review and comparison was made between the four surviving configurations. Results from the analysis spreadsheets led to the conclusion that a conventional monoplane had the best performance to cost ratio. A set of semi-subjective comparisons of the configurations in such areas as ease of design and construction, controllability in high wind, construction risk and structural elegance buttressed this conclusion. By the end of October the plane's basic configuration had emerged: a monoplane with an empennage.

The focus then shifted into plane optimization. An interactive, multidisciplinary spreadsheet was the key analytical tool for optimization. Ongoing development of the aircraft's three-view by the configurator validated the viability of the analysis. It was evident early in the design that the cost model would heavily penalize multiple motor configurations. Multiple motors also add to aircraft weight, construction time, actual cost and flight risk. Realizing that USC's twin motor design from last year was heavier than necessary and that the new, smaller payload limit favors a smaller plane, a single motor configuration was found to be sufficient and the development of multiple motor designs ceased.

Observations from last year's contest revealed the importance of ground handling and payload access. An effective braking system significantly reduced ground time and enabled more scoring flights. A strong braking system placed on the wheels favors a tricycle landing

gear, which also improves ground controllability. Thus a tricycle landing gear arrangement with pneumatic brakes was chosen with the capability to revert to a tail-dragger configuration if problems arose. Payload access required a new design since last year's nose-loading system conflicts with this year's nose-mounted motor. A cartridge-based, top loading payload removal system was chosen similar to ones used in last year's contest. This led to a low wing design, which also allowed for a lighter attachment structure with shorter load paths.

The expected windy weather conditions near Wichita prompted an increased effort for optimizing stability and control. To aid in this analysis, the stability and control tool from the previous contest was refined. The combination of this and the main analytical spreadsheet revealed that reducing the tail length reduced model cost more than the larger tail area hurt performance. Construction and shipping concerns plus a lack of overall benefit suggested a convention tail instead of the initially favored V-tail configuration. The stability and control spreadsheet helped choose aerodynamic parameters that gave an acceptably stable plane with good stall characteristics and low gust response. To meet takeoff field requirements while minimizing drag, the use of wing flaps increased lift at takeoff and reduced wing area at cruise. The stability and control goal was to allow the pilot to fly the plane to its aerodynamic limits without to struggling to keep it aloft.

The primary analytical spreadsheet had as its main outputs the total payload per flight and vehicle cost. The ratio of payload to cost provided a single measure to evaluate each intermediate design. The team converged on two related configurations using different motors, providing a backup plan if the best motor proved unsuitable or problematic. The addition of a temperature analysis spreadsheet to the mission model allowed us to evaluate the propulsion system cooling requirements. This analysis largely determined the placement of propulsion components. When presented with a choice between increasing wing area or increasing engine requirements to meet the takeoff field length requirement, the power to the motor was increased. If flight-testing reveals a takeoff performance shortcoming, an increase in flap and aileron chord will be undertaken.

Weight and construction considerations drove the increasingly detailed design of the evolving plane. Data and experience gathered from a number of test parts constructed in the first semester aided these decisions, especially a wing structure comparison and a series of carbon fiber-Nomex honeycomb parts. The analysis spreadsheet emphasized the absolute criticality of weight to takeoff field length and overall performance. Whenever presented with a choice between durability and reduced weight, the latter was chosen creating a higher risk. A set of spare parts taken to the contest will compensate for this decreased durability.

Most components were designed for minimum weight using structural analysis spreadsheets. A wing loading analysis spreadsheet helped design a lightweight structure. The wing design featured a D section spar and a ribbed structure made of balsa-sheathed low-density foam. A composite landing gear analysis spreadsheet provided accurate prediction of the landing gear deflection and optimized its design for the required height, width, aircraft weight and design landing acceleration. The landing gear featured all-composite construction, allowing a significantly improved strength to weight ratio over aluminum. Joining the landing gear and wing mounts at a single hardpoint improved structural efficiency. A system of carbon fiber-Nomex honeycomb bulkheads formed the primary structure with the carbon composite skin providing secondary structure and torsional rigidity. The motor mount was designed to double as a heat sink. The nose gear and braking systems were chosen from commercially available

models after inconsistent performance from student-built units. To reduce servo count and weight, a single servo was chosen to drive both flaps through a system of pushrods.

The design process at USC has evolved over the last several years. This contest required a more formal and comprehensive design process that involved new areas including thermal analysis. From the beginning, the plane's design took into account critical concerns from years past such as ease of construction and maintenance. The continuing refinement of legacy design tools has also borne fruit as their reliability increases year after year. *Tsunami* is a highly optimized aircraft and is the result of much hard work.

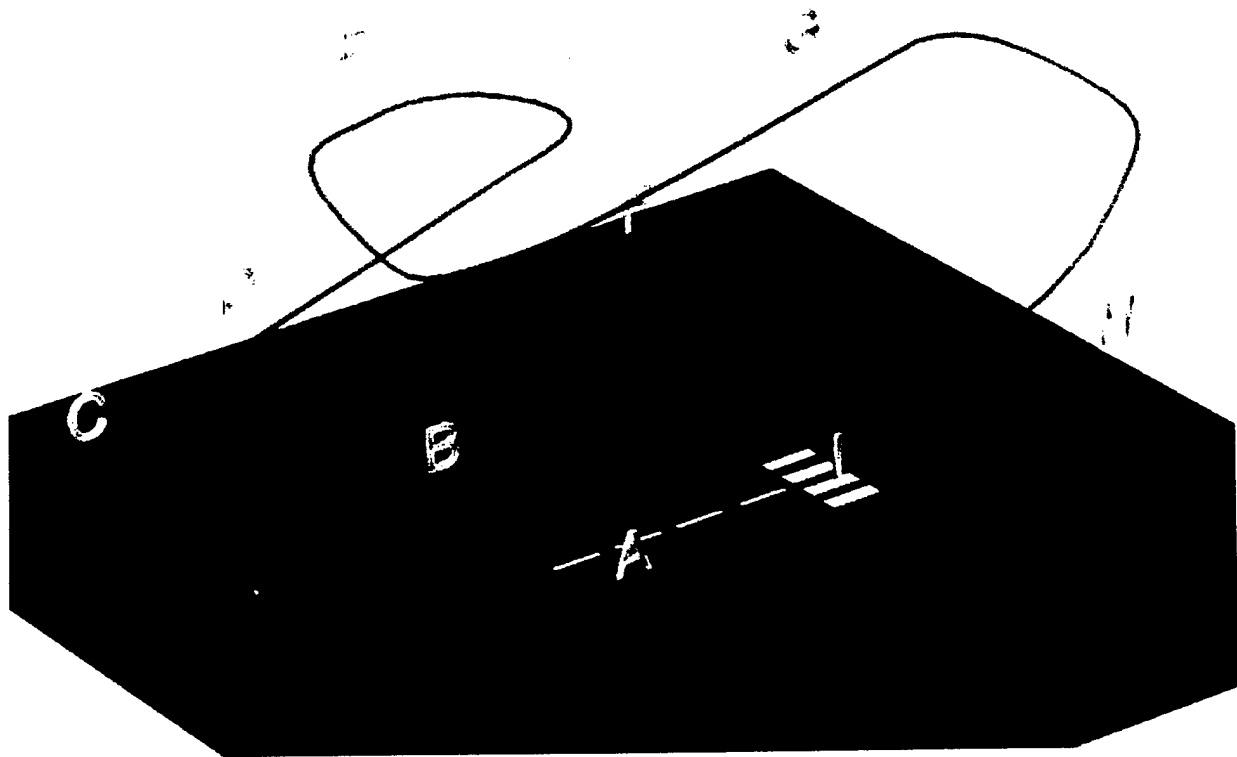


Figure 1.1- Flight profile for a loaded sortie. Loaded flights follow this sequence:

- A- Takeoff
- B- Climb
- C- 180 degree turn
- D- Cruise
- E- 360 degree turn in opposite direction
- F- Cruise
- G- 180 degree turn
- H- Descent
- I- Landing

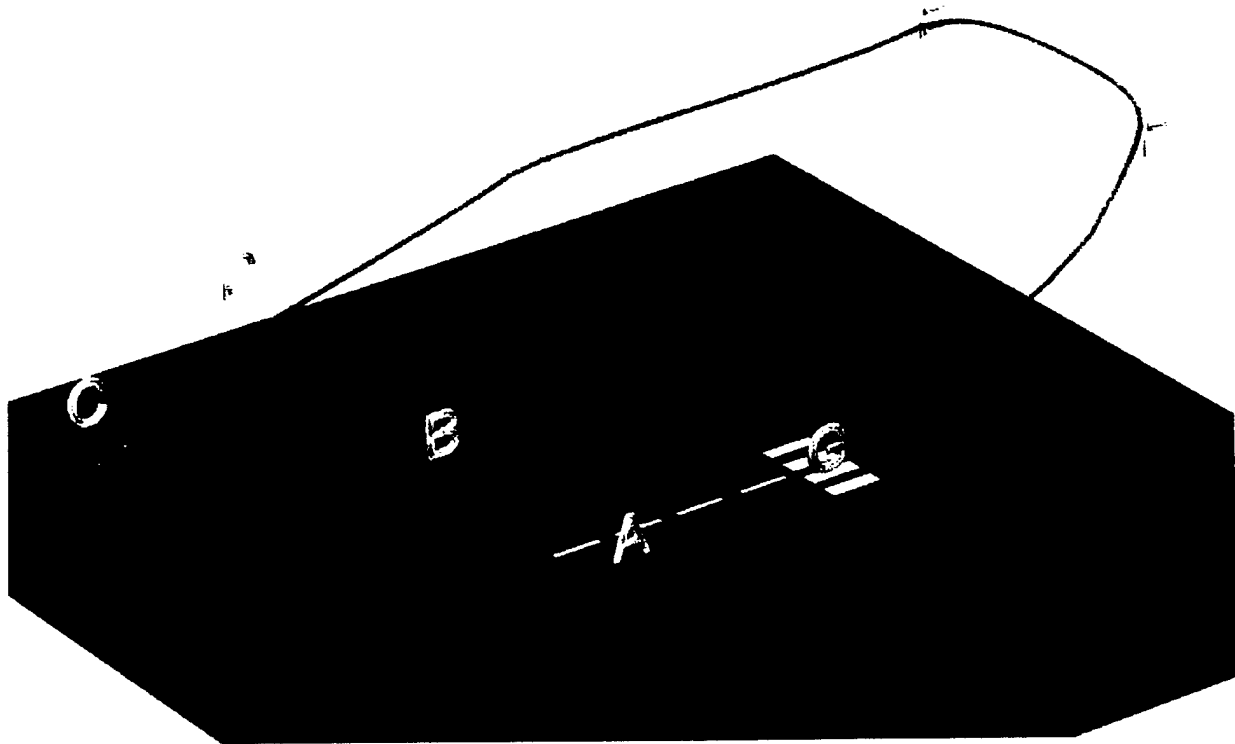
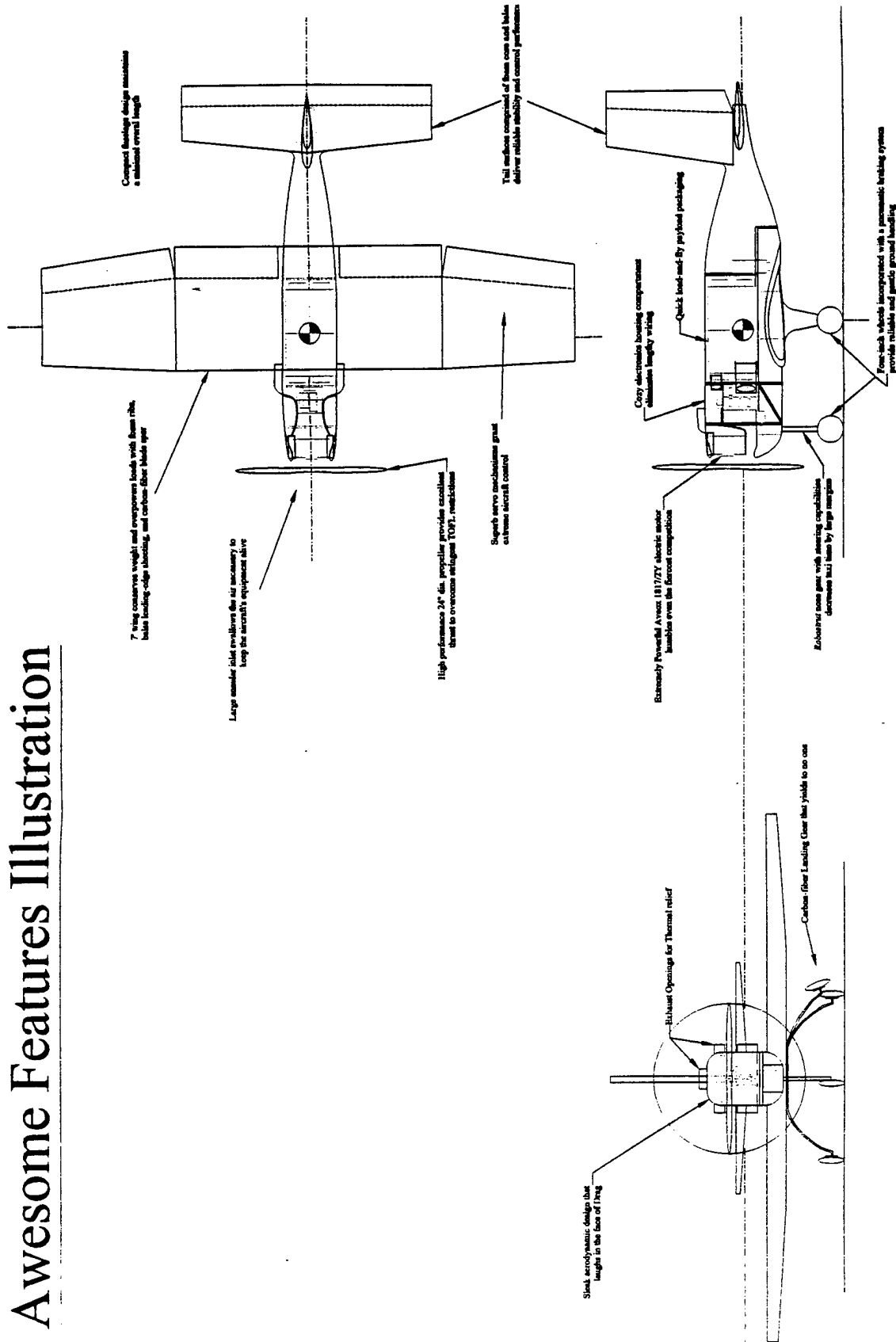


Figure 1.2- Flight profile for an empty sortie. Empty flights follow this sequence:

- A- Takeoff
- B- Climb
- C- 180 degree turn
- D- Cruise
- E- 180 degree turn
- F- Descent
- G- Landing

Awesome Features Illustration



Management Summary

USC's aero design team consists a core group of experienced students, a number of new arrivals, peripheral members and faculty and industry advisors. The core group of students consists of Nathan "Rusty" Palmer, Jake Evert, Jerry Chen, David Lazzara, Philippe Kassouf, Charles Heintz, Benjamin Hendrickson, George Sechrist, George Cano, and Scott Oishi. The faculty advisor is Dr. Ron Blackwelder of USC and our industry advisors are Blaine Rawdon from Boeing and Mark Page from All-American Racers. Stuart Sechrist from Aerovironment advised on some of the construction and Wyatt Sadler from Aerovironment is the pilot.

Our team has a semiformal command structure with positions assigned by experience and interest. The responsibilities were somewhat fluid, with team members helping out when and where needed.

-Nathaniel "Rusty" Palmer, a junior in Aerospace Engineering, was overall group leader and was responsible for making schedules and maintaining progress. He also lent his experience to others in need and supervised construction of the fuselage.

-Jacob Evert, a junior in Aerospace Engineering, was leader for the conceptual design process and aero analysis. He also was responsible for wing construction.

-Jerry Chen, a second year graduate student in Electrical Engineering, was responsible for *Tsunami's* control surfaces and also helped update our primary design tool, the Mission spreadsheet. He also was our main liaison with Grand Wing Servos, one of our sponsors.

-David Lazzara, a sophomore in Aerospace Engineering, was the configuration and determined *Tsunami's* final appearance.

-Philippe Kassouf, a sophomore in Aerospace Engineering, was responsible for structural analysis and was responsible for the team's and all of the sponsors' logos. He also was the creator of the plane renderings, and illustrations in this report, he was also a construction leader.

-Charles Heintz, a sophomore in Aerospace Engineering, was our test director and was responsible for our nose gear and braking system. He also was a construction leader.

-Benjamin Hendrickson, a sophomore in Mechanical Engineering, was our report director and labored many an hour in the computer labs

-George Sechrist, a junior in Industrial and Systems Engineering, was responsible for the design and construction of our primary landing gear and was a construction leader.

-George Cano, a sophomore in Aerospace Engineering, was responsible for our stability and control calculations.

-Scott Oishi, a sophomore in Mechanical Engineering, was responsible for determining component placement for center of gravity control.

-Dr. Ron Blackwelder was our liaison with the school. He also managed the team's finances and did much of the fundraising.

-Blaine Rawdon, a Boeing project manager and veteran modeler, gave us invaluable construction tips and shot down some of our wilder ideas. He also served as backup pilot.

-Mark Page, an aerodynamic analyst with All-American Racers who also helps run the MAYA secondary school model aircraft contest, helped run the team and construct our spreadsheet.

-Stuart Sechrist and Wyatt Saddler, both former leaders of the team, working at Aerovironment, generously donated their time and expertise in helping us. Wyatt also served as our primary pilot.

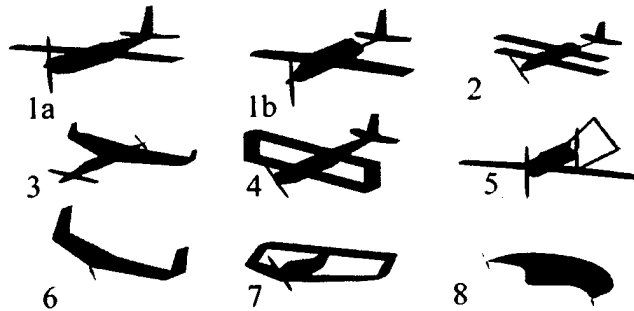
Conceptual Design

Alternative concepts investigated

List of initial design concepts

Our early design sessions identified 8 possible candidates for our plane design

1. Conventional monoplane
2. Conventional biplane
3. Canard monoplane
4. Box wing biplane
5. Tandem motor monoplane
6. Flying wing
7. Joined wing
8. "Flying flapjack"



Numerous permutations of individual attributes for these planes were developed. Some designs used V-, T-, or a conventional tails, mounted on a single or twin boom. Engines mounted to the fuselage in front, back, and both while riding on tricycle or taildragger landing gear. All of these variations were considered, but none were downselected initially.

Detail design parameters

Design Philosophy

The team design goal was to create a reliable aircraft with the highest possible ratio of liter count to aircraft cost ratio. "Cost-minded" engineering became a major design philosophy because rated cost heavily influenced the final competition score. The windy and turbulent flight conditions at the 97/98 Wichita contest also emphasized the importance of speed and especially good flying characteristics. A high thrust to weight ratio improved controllability and takeoff performance. Good ground performance and payload accessibility allowed significant reduction in ground handling time in previous contests and would apply to the 1999/00 contest.

Design Descriptions



A conventional monoplane was our baseline configuration. Its good, general quality has made it a standard industry design, and one the team has had much experience designing and successfully building. It had good handling characteristics, flight performance, and decent efficient. This design merited further analysis.



The conventional biplane configuration would have provided a greater effective aspect ratio under the 7' span limit than a single winged design. However, the extra wing joint in this concept would have made it harder to build and more difficult to stay within weight targets. Regardless, its multi wing and structural benefits provided basis for further analysis.



The canard monoplane had better stall characteristics than the baseline aircraft. This would have required a rear-mounted motor with a pusher prop, creating ground clearance issues and blade selection and supply problems. Due to these difficulties and relatively unsubstantial benefits, the canard configuration dropped from favor.



The box wing biplane configuration differed from the conventional biplane configuration in that it possesses inter-plane struts at the wingtips. Thus made it stiffer than the conventional biplane and gave it free winglets, which helped to reduce the vortex drag, subsequently increasing efficiency. However, the multiple wing joints in these concepts would have made it even harder to build and more likely to miss weight targets than the conventional biplane. These facts delayed any judgment pending an analysis of the conventional biplane configuration.



A tandem motor monoplane gave the possibility of improved energy efficiency by the use of one motor optimized for cruise flight while the other employed a folding propeller to boost power during takeoff and climb. The added weight and the increased cost penalty of a multiple engine configuration greatly reduced the attractiveness of this concept. Pusher propeller configurations created tight ground clearance problems for the aircraft while the rear motor was in operation. Its heavy weight and ground clearance issues made this configuration undesirable.



The flying wing configuration had a very high structural efficiency and low coefficient of drag. A design without a tail or a fuselage would have significantly reduced the aircraft cost. However, without a horizontal tail, its pitch control was poor and tended to be unstable. The low wing loading hurt its stability in turbulent conditions and the large wing area is penalized in the rated cost formula. Additionally, our team possesses very little experience with construction techniques needed to build a flying wing. Further analysis



A joined wing design would have reduced aircraft cost by requiring a shorter fuselage and small number of servos. Its inter-plane struts also gave similar aerodynamic and structural advantages as a box wing biplane. The joined wing's exotic nature posed controllability question, and building the complicated system of required joints would have been difficult and heavy. However, its structural elegance and potential cost reductions prompted selection for further analysis.



The flying flapjack configuration was a variant of the flying wing. The wingtip-mounted engines yielded a higher effective aspect ratio. However, two motors severely increased rated cost, added weight to the spar and power distribution system, and imposed ground clearance problems. The manifest flaws of this configuration led to its abandonment.

Subjective Figures of Merit (FOM)

Next a more detailed merit analysis was performed for the more promising configurations. The criteria used were ease of manufacturing, ease of repair, robustness of construction, elegance of structure, flight-handling qualities, ground-handling qualities, payload accessibility, and previous design experience. Each FOM is discussed followed by a numerical evaluation for the four primary conceptual designs.

Ease of Manufacturing

The configuration's complexity heavily influenced this rating. It also took into account the equipment, precision and skills required for construction. The monoplane scored highest, because of significant previous experience with this type, where as the complicated biplane and joined wing lost points.

Ease of Assembly and Repair

Contest requirements for three scoring flights made reliability especially important. The disassembling of each plane for storage, and its shipping for testing and competition were factored in. These criteria heavily favored small, simple planes with fewer parts. The simple monoplane scored well, while the complicated joined wing suffered.

Robustness of Construction

This Figure of merit was primarily a measure of structural simplicity and the expected strength of the finished plane. Other considerations also entered in, such as susceptibility to transport damage and flight crash damage. The flying wing lost points for its large, easily damageable surface, and the joined wing for its multiple joints.

Elegance of Structural Design

The elegance of the plane's structural design was a very important measure of its overall desirability. It helped determine aircraft weight and contributed to reliability. CG placement should be adjustable, for instance by alteration of the battery placement. The short nose of the flying wing hindered CG adjustment, but its deep wing and distributed structure gained points on structural efficiency. The joined wing and biplane designs lost points for their joiners.

Flight Handling Qualities

Previous competition experience in Wichita had demonstrated the importance of good handling characteristics, especially in windy conditions. The poor stability and pitch control of the flying wing hurt it seriously here.

Ground Handling Qualities

Past experience had also underscored the importance of good ground handling. Planes should not be overly tall, short in wheelbase, or long in overall length since these have proven to impede ground handling.

Payload Accessibility

Payload accessibility was deemed of such critical importance that it deserved its own section as Figure of Merit. At the last contest, several teams lost well over a minute of flight time working with difficult payload restraints. In one case, the failure of a payload restraint scuttled the plane. A low winged monoplane benefited here while the high second wing of the biplane was hurt here.

Experience with Design

One Figure of Merit that deserved special attention was our experience with the design. Using well-known, conventional designs afforded advantages over using exotic ones, since the latter tended to develop problems. Techniques for building and design were already well known for conventional planes, which gave them further advantage in this area.

Here are the scores assigned by the team to each configuration and the design's total score.

	Flying Wing	Joined Wing	Conventional Monoplane	Conventional Biplane
Ease of Manufacturing	8	3	10	6
Ease of Assembly and Repair	7	8	10	8
Robustness of Construction	6	4	10	8
Elegance of Structural Design	10	8	8	6
Flight Handling Qualities	3	6	9	10
Ground Handling Qualities	8	10	6	5
Payload Accessibility	8	8	10	7
Experience with Design	6	4	10	8
Total Scores	56	51	73	58

Table.3.1 The result of this comparison simply suggested a conventional monoplane design.

Analytic Figures of Merit (FOM)

Cost Determination Model

A model was made of the contest's cost formula. Outputs from the model were the calculated cost of each aircraft. Four separate determinations were performed to provide data to compare each competing design. The outputs of the model for the flying wing, joined wing, monoplane, and biplane are shown in Figure 3.1-3.4 respectively.

Configuration Analysis Model

A detailed, analytic, performance modeling of the conventional monoplane, biplane, joined wing and flying wing were performed. A payload of eight liters was assumed as a

reasonable amount of weight the plane could fly and score well with. The maximum wing area, battery size, and motor size were used. The contest rules governed and in turn provided numbers for other inputs like maximum wingspan and battery pack weight, which were used for motor sizing.

A reasonable C_l and C_d of a wing were assumed that allowed calculation of stall, takeoff, cruise and landing airspeeds. Knowing the airspeeds of the different legs of the sortie and the distance between the pylons allowed for the estimation of flight time. Simulation of a complete payload cycle with times for the each loaded and unloaded flight plus the ground time from previous contests was used to determine the number of laps attainable in 10 minutes.

An estimate of the total energy available used average energy densities and pack weight of nickel-cadmium batteries. Weight and C_d values led to the calculation of total drag. The sortie distance determined the work required to fly a mission cycle, which allowed estimation of the energy-limited number of cycles flyable.

The model, as shown by Figure 3.5, found total payload carried by multiplying the lesser of the time- and energy-limited cycles flyable by the payload capacity. The use of a rules-derived cost model allowed the construction of a payload to cost ratio for each configuration, providing a single Figure of merit for comparing the configurations. Ranking of the four planes by this ratio resulted in a higher score for the monoplane configuration and an adoption of the design for the competition.

(1) Flying Wing

# of Wings	1	n.d.
# of Bodies	1	n.d.
Body Length	0	ft.
# of Vertical Tails	0	n.d.
# of Horizontal Tails	0	n.d.
# of Servos	4	n.d.
# of Engines	1	n.d.
# of Props	1	n.d.



Parameter	Value	Cost	%Cost
MEW	17.84	\$1,783.67	28.72%
REPWatts	1491.42	\$1,491.42	24.01%
WBS 1.0 Wings	117.80	\$2,356.00	37.93%
WBS 2.0 Bodies	5.00	\$100.00	1.61%
WBS 3.0 Emp.	5.00	\$100.00	1.61%
WBS 4.0 Servos	9.00	\$180.00	2.90%
WBS 5.0 Prop.	10.00	\$200.00	3.22%
Total Manuf Hrs	146.80	\$2,936.00	47.27%
Rated Cost =	6.211	\$6,211.09	100.00%

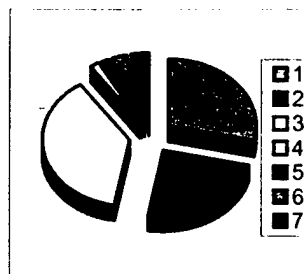


Fig.3.1 Cost model according to rough dimensions of the Flying Wing design.

(2) Jointed Wing

# of Wings	1	n.d.
# of Bodies	1	n.d.
Body Length	1	ft.
# of Vertical Tails	2	n.d.
# of Horizontal Tails	1	n.d.
# of Servos	5	n.d.
# of Engines	1	n.d.
# of Props	1	n.d.



Parameter	Value	Cost	%Cost
MEW	17.39	\$1,739.15	29.65%
REPWatts	1491.42	\$1,491.42	25.42%
WBS 1.0 Wings	77.80	\$1,556.00	26.52%
WBS 2.0 Bodies	9.00	\$180.00	3.07%
WBS 3.0 Emp.	25.00	\$500.00	8.52%
WBS 4.0 Servos	10.00	\$200.00	3.41%
WBS 5.0 Prop.	10.00	\$200.00	3.41%
Total Manuf Hrs	131.80	\$2,636.00	44.93%
Rated Cost =	5.867	\$5,866.58	100.00%

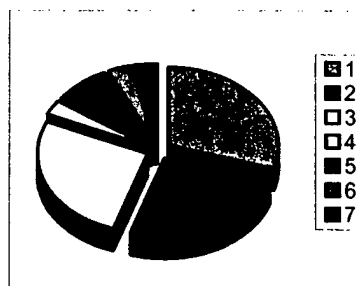
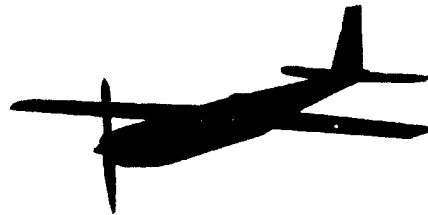


Fig.3.2 Cost model according to rough dimensions of the Jointed Wing

(3) Conventional Monoplane

# of Wings	1	n.d.
# of Bodies	1	n.d.
Body Length	2.8	ft.
# of Vertical Tails	1	n.d.
# of Horizontal Tails	1	n.d.
# of Servos	6	n.d.
# of Engines	1	n.d.
# of Props	1	n.d.



Parameter	Value	Cost	%Cost
MEW	15.51	\$1,550.80	28.82%
REPWatts	1491.42	\$1,491.42	27.72%
WBS 1.0 Wings	15.24	\$1,194.40	22.20%
WBS 2.0 Bodies	16.20	\$324.00	6.02%
WBS 3.0 Emp.	20.00	\$400.00	7.43%
WBS 4.0 Servos	11.00	\$220.00	4.09%
WBS 5.0 Prop.	10.00	\$200.00	3.72%
Total Manuf Hrs	116.92	\$2,338.40	43.46%
Rated Cost =	5.381	\$5,380.62	100.00%

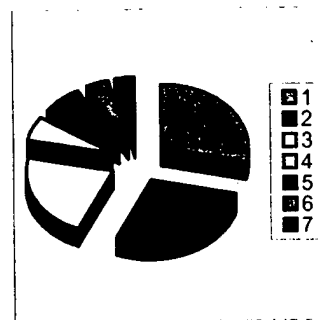


Fig.3.3 Cost model according to rough dimensions of the Conventional Monoplane

(4) Conventional Biplane

# of Wings	2	n.d.
# of Bodies	1	n.d.
Body Length	5.6	ft.
# of Vertical Tails	1	n.d.
# of Horizontal Tails	1	n.d.
# of Servos	6	n.d.
# of Engines	1	n.d.
# of Props	1	n.d.



Parameter	Value	Cost	%Cost
MEW	15.56	\$1,556.05	28.15%
REPWatts	1491.42	\$1,491.42	26.98%
WBS 1.0 Wings	55.60	\$1,112.00	20.12%
WBS 2.0 Bodies	27.40	\$548.00	9.91%
WBS 3.0 Emp.	20.00	\$400.00	7.24%
WBS 4.0 Servos	11.00	\$220.00	3.98%
WBS 5.0 Prop.	10.00	\$200.00	3.62%
Total Manuf Hrs	124.00	\$2,480.00	44.87%
Rated Cost =	5.527	\$5,527.47	100.00%

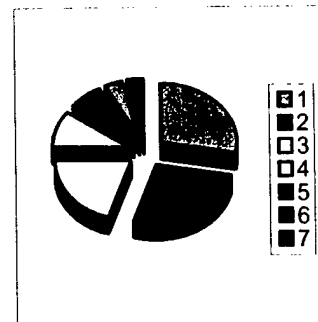


Fig.3.4 Cost model according to rough dimensions of the Conventional Biplane

Fig.3.5 Results of the cost and flight performance spreadsheet which concludes that the selection of the conventional monoplane design is most favorable

NAVJAG

Flying Wing Joined Wing Conv'Mono Conv'l Biplane

Input Parameters

Motor HP	2	2	2	2
Cargo (lbs)	18.12	18.12	18.12	18.12
CLmax	0.7	1.066	1.55	1.55
L/D Estimate	4.86	5.26	8.11	7.98
Pit Time (sec)	60	60	60	60
"Total" ARwing	0.00	0.00	0.00	0.00
Air Density	0.00228192	0.00228192	0.00228192	0.00228192
Turn G's	2	2	2	2
Battery Energy	153975.375	153975.375	153975.375	153975.375
Battery Weight	5	5	5	5
W pay*Sorties	0.00	0.00	0.00	0.00

Assumptions and Analysis

WingSweep	35	35	0	0
Lh/mac	0	1	2.8	5.6
Sh/Sw	0	0.5	0.2	0.2
Sh-tail	0	9.1	2.28	2.28
Sw-tail	0	0	1.71	2.052
Swinglet	5.64	3.64	2.28	2.28
Wing Area	28.20	18.20	11.40	11.40
Sluce	1.00	1.00	1.00	1.00

Calculations

Distance Weighted Drag (Heavy)	9.334641071	8.90	5.804729526	5.90143012
Excess Cruise Thrust Available	0.665358929	1.104265565	4.195270474	4.09856988
Swet				
Gross Weight	40.96	40.51	38.63	38.68
Swet/Swet_Conv	1.67	1.54	1.00	1.02
ARwet	1.29	1.40	2.16	2.13

Results

Energy Sortes				
Time Sortes				
Rate Cost				
Score				

General Assumptions

Propulsive Efficiency =	0.684
Ancillary Fixed Wts =	1.12
Report Score =	85

Preliminary Design

Design Tools

Mission Model

The Mission model was the primary design tool used for the D/B/F competition. It consists of an Excel workbook with several spreadsheets that were tailored to model various components of the aircraft in the design stage. This tool was used to rapidly evaluate different aircraft configurations and score the design based upon payload carried and the aircraft cost formula. Some of the most important inputs to the sheet are:

- airfoil type
- wing area
- propeller diameter and advance ratio
- motor and gearbox type and count
- battery type and count, and
- liters of water carried

This model simulates the aircraft's state at various points in the mission. It models all legs of the flight, including takeoff, cruise, turning flight, descent, landing and ground handling. The model derives its primary parameters from the mission input block, including the inputs mentioned above plus the throttle setting, airspeed, initial altitude, aircraft weight, and load factor of the leg in question. It sends these data to analysis subroutines to calculate the energy and time consumption and altitude change for each leg. The model then sums the time and energy consumed and the altitude change during the sortie and calculates the number of sorties attainable based on energy and time limits. It determines the overall score by multiplying the sorties attainable by the payload carried and dividing by the rated aircraft cost. As an aid to comparison, save and restore macros were constructed to store the critical inputs and overall score in a separate sheet. Figure 4.11 shows the input section of the Mission spreadsheet, and Figure 4.12 shows its overall structure. The following models for individual components aided the Mission spreadsheet.

Electrical model

The electrical model is designed to analyze electrical motors used for small aircraft. The actual equations follow the analysis presented by R.J. Boucher (1995) which were programmed into the spreadsheet. The inputs into the spreadsheet include the throttle settings for different stages of the flight, propeller diameter, design advance ratio, number of battery cells, volts per cell, etc. from the Mission model. Then it used the selected motor, battery, and gearbox to look up or calculate values for torque and voltage constants, resistance, no load current, and max allowable current. It sets an initial value for current, and the prop model provides prop efficiency and coefficients of thrust and power. The electrical model then feeds this data into a set of formulae to calculate thrust and motor output torque, RPM, and power. A "goal-seek" macro (an Excel spread sheet option) adjusts the current draw, and thus the voltage reaching the motor, which alters the RPM until the current drawn equals the current needed to make the prop spin at the desired rate. Using this equilibrium current, the model finds the energy consumption, thrust power produced, and total electrical system efficiency and returns it to the Mission model.

Propeller Model

This model uses the input diameter and design advance ratio to build a map of the thrust and power coefficients, C_T and C_P . It then passes this data to the electrical model.

After comparing our performance values to those generated by ECALC and our past experience, we decided that our model assumed unrealistic efficiencies of the model propellers. To make our predictions match ECALC's, the coefficient of power was multiplied by the same factor of 1.3 that ECALC uses.

Weight Model

The weight of the plane is calculated by summing the individual components. For the manufactured parts, their dimensions are entered through other spreadsheets (e.g. the aerodynamic, mission, ... spread sheets) and passed onto the weight spreadsheet. The volume of the individual materials used such as wood, carbon fiber, foam, etc. is computed and the weight calculated using stored density values for these materials. For the purchased components such as the motor, batteries, controller, etc. their weights are entered into the appropriate spreadsheets such as propulsion. The weight model then looks up the values for these components and adds them to the overall weight of the aircraft.

Cost Model

The model for calculating the cost of *Tsunami* was obtained from the rules as specified in the D/B/F website (see reference for Page, 1999). The required information, such as the fuselage area, wing area, number of motors, etc. had been entered into the different spreadsheets for other purposes. For example the area of the fuselage and wing was a component of the aerodynamics model since it was required to calculate the lift and drag. Thus the calculated cost of the aircraft was a simple program utilizing the supplied equation.

Aerodynamic Model

The aerodynamic model included two main calculations; i.e. the lift and the drag of the aircraft. The aerodynamic spreadsheet included an airfoil library consisting of typically ten airfoils that were considered for the aircraft. The raw data for the airfoils were entered from standard resources such as Selig, et al. (1995). This information and the areas of the wing were used to calculate the lift and the drag of the wing. Areas for the other components were used with standard drag coefficients were used for the drag build-up for the aircraft. This also included contributions from the landing gear, fuselage, empennage, etc. Corrections were also included for the flaps when they were used for different segments of the flight profile. For the multi-engine models, scrubbing due to the additional flow over the wings from props was also included.

Optimization Parameters

Although the variables influencing plane design are heavily interdependent, altering the inputs to the Mission model one variable at a time produces useful data. The primary Figures of Merit were:

1. Takeoff Field Length
2. Rated Cost

3. Payload Carried

The main mission parameters were separated into Mission, Wing and Propulsion inputs.

Mission Section

Payload Optimization

The payload carried per sortie has a strong effect on score. Since a high percentage of the sortie time is spent in ground operations such as taxiing, loading, unloading, etc., a simple analysis indicated that the highest score would be obtained by carrying the maximum possible payload of 8 liters of water, or 19.6 pounds. The spreadsheet results shown in Figure 4.1 confirmed this decision.

Wing Section

Airfoil Type

The takeoff field length requirement of 100 feet drove the airfoil selection. The airfoil type also influenced the score, as shown in Figure 4.2. The score in this and other Figures is the predicted weight carried (in pounds) divided by the calculated cost measured in thousands of dollars. Many of the low-camber airfoils required an increase in wing area to meet takeoff field length requirements while the large drag of the high camber airfoils made them unattractive.

Wing Area

The 7-foot span limit made it difficult to determine the plane's optimal wing area. Once again, takeoff field length was the determining factor. Large wing areas allowed the plane to meet the take off field length, but the rated cost equation favored the smallest possible wing. Figure 4.3 shows these results suggesting an optimum wing area of 10-11 ft².

Use of Winglets

Winglets slightly influence low speed performance and rated cost. Figure 4.4 reveals that very short winglets increase performance by a maximum of 1%, which was not sufficient to warrant their inclusion. The score decreased with increasing winglet size, implying that their cost penalties more than offset their performance benefits above a certain point. The change in the trend of the curve when winglet height reached 0.4 feet was caused by adding an extra battery to compensate for lack of takeoff field length capability.

Propulsion Section

Propeller Diameter

Propeller diameter strongly influenced the takeoff field length. Meeting takeoff field requirements required fairly large props, i.e. over 20", as seen in Figure 4.5. Another factor in the choice of propeller diameter was ground clearance, limiting propeller diameter to 28 inches.

Design Advance Ratio

Takeoff field length primarily determined the design advance ratio. This is shown in Figure 4-6. The lower design advance ratios would not provide sufficient thrust to meet this

requirement and the very high advance ratios demanded too much current from the batteries to make them practical options.

Motor Type

Thirty-six different motors were examined with the spreadsheet, but only four could provide sufficient power to make them practical choices. Figure 4.7 shows how the survivors stacked up.

Motor Count

Motor count heavily influenced the calculated cost. The magnitude of this effect outweighed any possible benefits of multiple motor configurations, as shown in Figure 4.8. Single motor configurations became preferred after the Mission model demonstrated their viability.

Battery Type

Battery capacity limited range and the internal resistance per cell affected takeoff distance. Optimizing the battery type traded one against the other, as shown in Figure 4-9.

Battery Cell Count

The battery pack had to provide sufficient voltage to let the plane take off in 100 feet, and enough power to enable several takeoffs and landings. Increasing cell count did not necessarily increase the airtime. The five-pound battery pack weight limit determined the maximum cell count, but several configurations did not require the full amount of cells as shown in Figure 4.10.

Configuration

The next stage of the preliminary design involved the determination of the aircraft's general configuration. This stage was governed by optimizing several parameters. The aircraft cost, weight and manufacturing time were to be minimized. At the same time, the operational features of the plane have to insure that stability and control were not compromised. The main elements of this stage of the configuration down select are discussed below.

Fuselage

The primary factor governing the fuselage shape and size was the initial component placement. Although related to other configuration considerations, it was desirable to minimize the fuselage length due to the cost function. However the size of the cargo dictated that the volume within the fuselage could not be compromised. To insure stability and control, the payload had to be located near the CG so that flight with and without the cargo was possible. The other factors in the fuselage configuration were the location of the batteries, motor and speed controller.

Motor Location

The decision to use a single motor eliminated the option of mounting the motors on the wings. The remaining options included mounting the engine in the nose, in the aft fuselage, or on a pylon above the wing. The aft mounted engine would require a longer main landing gear

to preserve ground clearance on rotation, thus increasing aircraft weight. This configuration also increases the difficulty of balancing the plane since both the motor and tail lay behind the payload. The required twin boom-mounted tail increased both manufacturing time and rated cost substantially. The pylon-mounted engine introduced a severe moment about the CG and cause additional thrust balance concerns. It also provided an undesirably high center of gravity and a potentially weighty strut. These alternative configurations have some advantage for payload access and reduced the scrubbing drag compared to the nose mounted default configuration. But these did not outweigh their manifest deficiencies. A nose mounted engine configuration was chosen.

Payload Access Method

Several payload access options were considered including nose, rear, side, and top access. The decision to use only one motor made the nose access unacceptable. Side access was considered but it interfered unacceptably with both low- and high-mounted wings. The aft loading configuration introduced severe structural concerns in the aft fuselage and would require an increase in total length to provide enough clearance for payload removal and insertion. This left, by default, top access as the method of choice for its minimal structural and cost impact and ease of construction and payload access.

Wing

The limited wingspan severely constrained the wing design. The spreadsheet analysis indicated that a wing of 10-11 ft² was required to meet the take-off field length. Although a smaller wing and dual motors could have been used, the calculated cost dictated against that choice. A LA203a airfoil was chosen since it provided a slightly favorable lift over the other choices. Also its large thickness to chord ratio allowed for a simpler spar that would be easier to construct. A constant chord was chosen for the interior wing to simplify the flap construction. A simple taper was added to the outer region but which kept a straight hinge line. Failure to meet takeoff field requirements can be resolved with small flap and aileron cord extensions. Control surfaces were sized to insure sufficient control authority.

Low or High Wing Preference

Tsunami required a payload hatch for loading and unloading the cargo. This parameter led to a discussion concerning the location of the wing. Mounting the wing high would ensure sufficient wing tip clearance and also allow an easy means to increase the wing incidence angle should that prove necessary. Nevertheless, payload accessibility retained priority and a low wing design was chosen to improve payload access. This had the additional advantage that the wing spar could be continuous across the fuselage. The lower wing had a lower tip clearance causing the landing gear to become taller.

Tail

Different tail configurations, including a V-tail, T-tail and conventional tail, were considered for this aircraft. Because of its short tail arm, *Tsunami* required large tail surfaces and careful attention to weight. Controllability required a strong and heavy vertical stabilizer that disqualified the T-tail concept. Shipping and mounting concerns made the V-tail configuration unattractive. The tail sizing was analyzed by a Stability and Control analysis before drawing the tail surfaces in the prototype blueprints.

Nose Gear and Brakes

Previous contests underscored the importance of good brakes and ground handling, making these important Figures of merit. A taildragger configuration was found to have poorer ground handling and braking characteristics, and thus was eliminated. A tricycle landing gear system with a nose gear greatly enhanced steering and allowed stronger braking systems without causing the plane to tip forward. A nose gear was purchased to decrease the amount of construction time required and to reduce the weight. Similarly, a pneumatic braking system was deemed desirable because it would reduce the time required for ground handling. The main landing gear were designed and constructed in house to leverage our strength in composite design and manufacturing.

Center of Gravity Optimization Model

The aircraft's center of gravity while unloaded marks the optimum location for the payload center of gravity since at that location its presence does not affect the aircraft's trim. To proceed in the design, an estimate of the location of the plane's empty center of gravity as calculated by the following formula:

$$X_{CG} = \frac{\sum_i W_i X_i}{\sum_i W_i},$$

where W_i and X_i represent respectively the weights of one of the plane's components and their distance from an arbitrary origin. Table 1.1 shows the moments of various components about this point and Table 2.2 shows the estimated center of gravity.

Positioning the aircraft's center of gravity at 30% of the mean aerodynamic chord of the wing minimizes the amount of elevator trim required for level flight. However, to preserve stability in the face of a possible 50% growth in tail weight we added 0.4 lb to the tail weight. This margin of error provides the ability to adapt to moderate deficiencies in the center of gravity calculation with unexpectedly weight construction techniques

MISSION 2000

DESIGNER INPUTS (input variables in red, upper inputs for heavy lap and lower inputs for light lap. All dimensions are feet, sq-ft, pounds, and slugs/cu-ft, except for prop diameter in inches.)

Airfoil # (#1-8) 8 LA 203a	Turn %CLmax % 70.00%	SW ft 10.00	Wingspan ft 7.00	Sh ft 1.65	Sv ft 1.20	Swept Fuselage Fuselage Length 5.00 5.16	Cruise Throttle % 90% 79%	T/O Throttle % 100% 60%	Climb Throttle % 100% 90%
Sweeps+frms frontal ft2 (all) 0.1	Sstruts frontal ft2 (all) 0.1	Dprop (inches) w=Wood, p=Plastic 23 W	Design Jprop (.333, .5, .666, .833, 1.000) 0.666	Motor type (#3-37) 25 18172Y	Battery type (#1-21) 22 RC-2400	# of Cells & max batt wt flag 28 OK	Gearbox Type (#1-8) or -2=2 8 3.7	Number of Motors 1	Wheel Brakes? (Y or N) Y
HEAVY → LIGHT →	Vcrz/Vstall 2.15 3.40	Top of Climb Alt 89 132	Payload Weight 18.0 0.0	Volts per Cell 1.25 (typically 1.2)	Number of packs 1	Swinglets Total 0.01	Winglet Height 0.01	Air density, p 0.002282 (80 deg F S.L.)	Speed Brake CD 1.02

Run the spreadsheet

OUTPUTS (Heavy Laps generally on top in black, Light Laps below in Blue)

Weight Breakdown									
Weight 33.62	Unpowered CL max 3-D 1.96	T/O Power CL max 3-D 1.96	CL straight 0.42	CL turn 1.37	LD straight 12.98	LD turn 9.60	n turn 3.24	Motor(s) 1.26	Batteries 3.88
Hwy Takeoff TAW & T/O SHP per eng 0.41 1.79	Hwy Crz J & Crz SHP per eng 0.60 1.11	Hwy Crz RPM (prop/motor) 4,349 16,092	Prop Efficiency (Cruise) 80.7% 79.5%	No Load Climb Voltage 35.00 21.50	No Load Cruise Voltage 31.50 27.65	No Load Takeoff Voltage 35.00 21.00	OK OK OK	Wiring+SpdC+Prop 2.02	Wing Structure 1.03
								Radio+Sensors+Batt 2.98	Ldg Gear 1.77
								Fuselage 2.09	Payload 18.00
								TOTAL 33.62	
								Peak Amp Limit = 80	
								Cont. Amp Limit = 40	
								T/O Clb, Crz Amps Hwy 57.89	T/O Clb, Crz Amps L 26.85
								55.54	49.06
								36.37	22.53
								TaxiFlag =	
Turn bank angle 72.0	VLO 46.59	Vclimb 50.47	Vtouchdown 50.47	Vcruise(fps) 83.47	TOC distance OK 445.43	Total Weight Carried (lbs) 63.89	ARw n.d. 4.90	Max Enroute Alt. 93.85	142.03
								Bad mission section?	
Top of Descent Alt 38.88	Model PROP Designation 23.0 15.3		Landed Long (good = <10s taxi)		Taxi Time 15.0		SPECIFIED		
6.99									
OK									
								PASS/FAIL?	
								PASS	
								Rated Cost	5.108
								Final Score	12.509

Fig.4.1a Image of front end of Mission analysis tool.

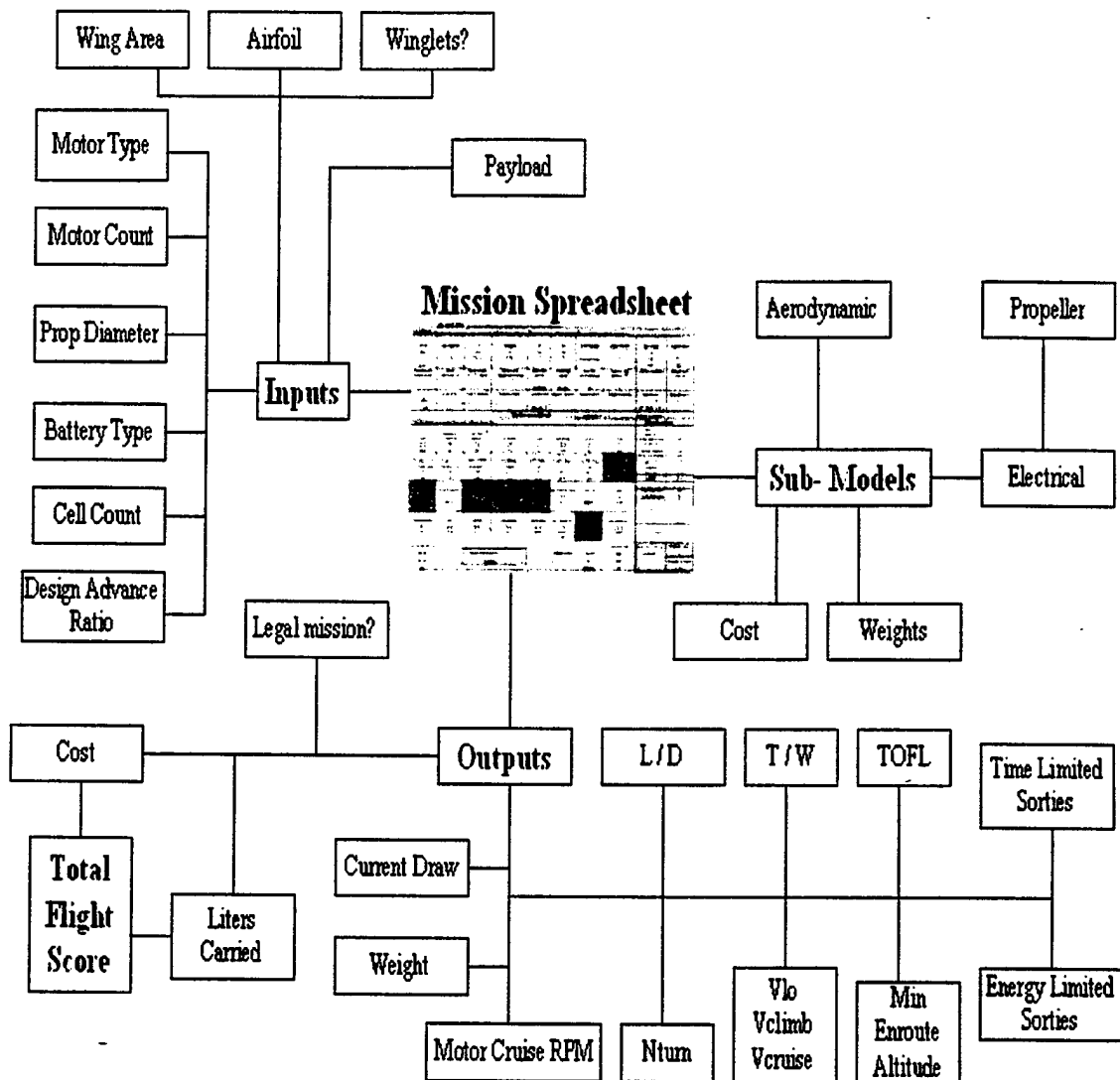


Figure 4.1b Organization of Mission model, showing inputs, sub-models, and outputs

Airfoil Type

Airfoil type	Maximum score	S_{wing}
1	4.092	10
2	4.592	8
3	4.709	11.5
4	3.689	17
5	3.886	10.5
6	4.709	11.5
7	4.946	10

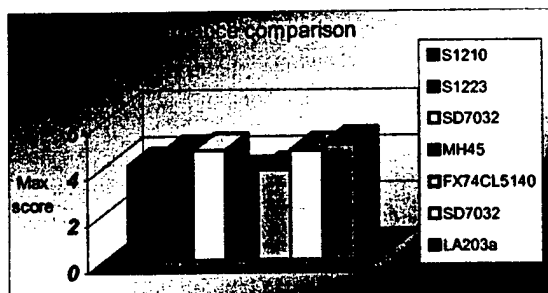


Figure 4.2 Airfoil types considered for the wing, made by optimizing wing area for maximum score.

Wing area

Wing area	max score	TOFL
5	failed TOFL	206
5.5	failed TOFL	185
6	failed TOFL	167
6.5	failed TOFL	153
7	failed TOFL	141
7.5	failed TOFL	132
8	failed TOFL	123
8.5	failed TOFL	116
9	failed TOFL	110
9.5	failed TOFL	105
10	4.946	100
10.5	4.821	97
11	4.672	93
11.5	4.517	90
12	4.378	88
12.5	4.229	85
13	4.086	83

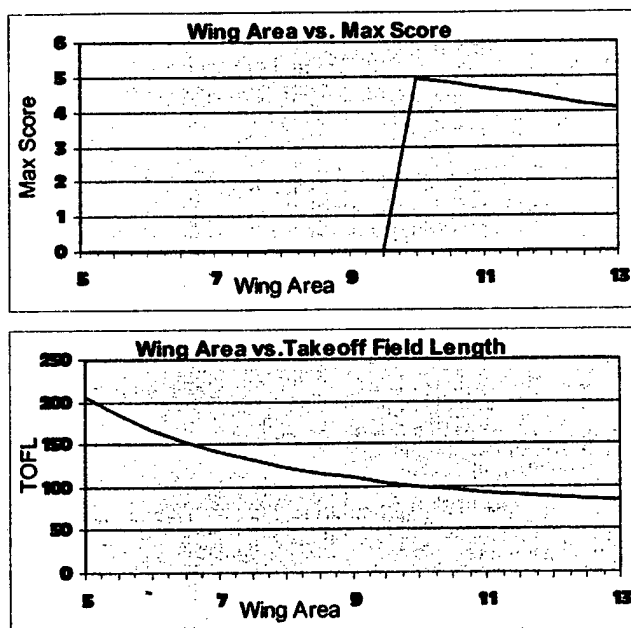


Figure 4.3 Wing area versus takeoff field length and maximum score.

Winglet/No winglet

Winglet height	S_{winglet}	Score
0.01	0.01	4.946
0.1	0.0625	4.954
0.2	0.125	4.947
0.3	0.1875	4.924
0.4	0.25	4.863
0.5	0.3125	4.851
0.6	0.375	4.841
0.7	0.4375	4.829
0.8	0.5	4.821
0.9	0.5625	4.811
1	0.625	4.803

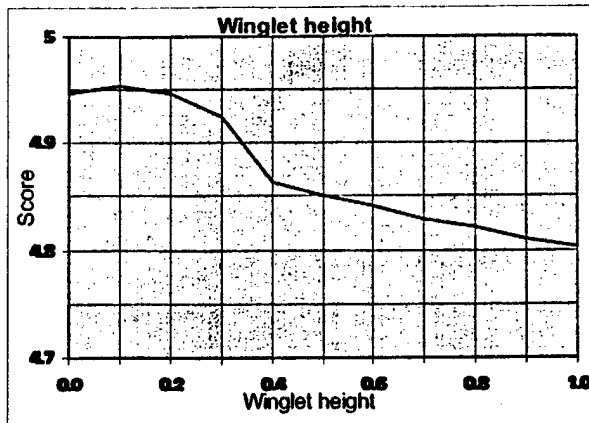


Figure 4.4 Maximum score for winglet heights. The area of the winglet is one half height times the wingtip chord of 1.25 feet.

Prop Diameter

Prop Diameter	Maximum Score	TOFL
15	failed TOFL	306
16	failed TOFL	239
17	failed TOFL	195
18	failed TOFL	166
19	failed TOFL	145
20	failed TOFL	130
21	failed TOFL	119
22	failed TOFL	111
23	failed TOFL	105
24	4.946	100
25	4.638	97
26	4.456	95
27	failed current draw	N/A
28	failed current draw	N/A
29	failed clearance	N/A
30	failed clearance	N/A

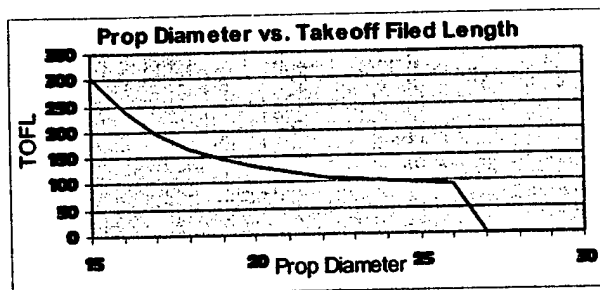
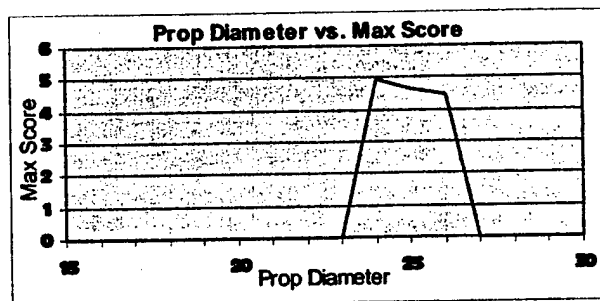


Figure 4.5 TOFL and Score as a function of propeller diameter.

Design Advance Ratio

J_{prop}	max score
0.333	failed TOFL
0.5	failed TOFL
0.666	4.946
0.833	4.258
1	failed TOFL & current

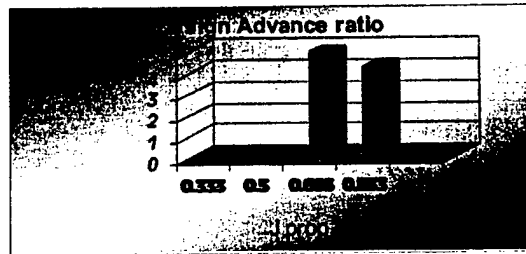


Figure 4.6 Maximum Score for different design advance. Those that did not meet TOFL requirements have a score of zero.

Motor Type

Motor number	Motor Type	Score w/32 cells
3	F10 LMR*	3.003
4	F12LMR*	4.608
6	F16 LMR*	4.551
38	Hot 1817/2Y	4.946

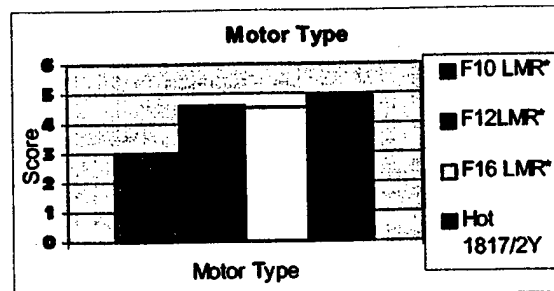


Figure 4.7 Maximum score for different motor type.

Number of motors

# of engines	Max Score
1	4.946
2	3.252
3	2.312

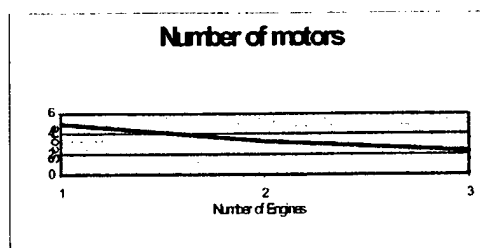


Figure 4.8 Calculated score versus the number of motors.

Battery Type

type no.	type name	# cells	Max score
1	N-4000DRL	13	failed TOFL
2	KR-5000DEL	14	failed TOFL
3	RC-2000	31	4.25
4	N-2000CR	27	failed TOFL
5	N-1700SCRC	32	3.936
6	N-1700SCR	32	3.738
7	N-1800SCR	33	3.926
8	N-1400SCR	32	3.04
9	N-1300SCR	32	2.947
10	N-1100CR	31	2.627
11	KR-2400CE	29	failed TOFL
12	KR-2300SCE	37	failed TOFL
13	KR-2800CE	30	failed TOFL
14	KR-2000SCE	37	failed TOFL
15	KR-1800SCE	46	failed TOFL
16	KR-1700AE	48	failed TOFL
17	KR-1200AE	47	2.234
18	KR-1000AEL	46	failed TOFL
19	KR-1100AEL	44	failed TOFL
20	KR-1400AE	42	failed TOFL
21	KR-1100AAE	40	failed TOFL
22	RC-2400	32	4.946

Battery Type

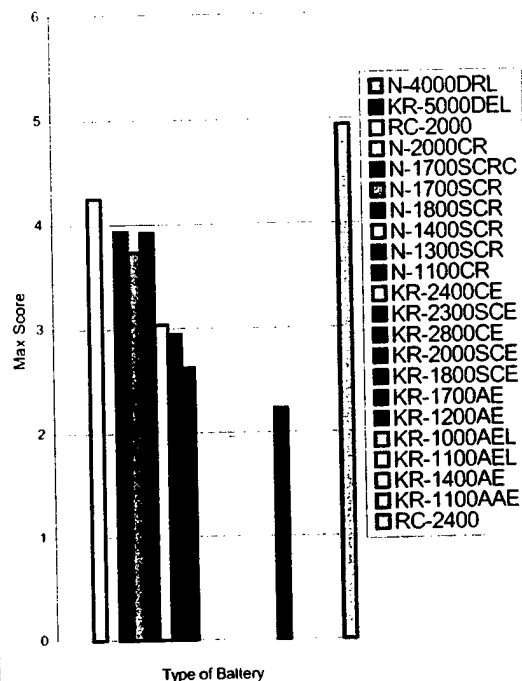


Figure 4.9 Chart for the calculated score for the different battery types.

Cell Count for RC-2400

# of cells	Score	TOFL
20	failed TOFL	175
22	failed TOFL	152
24	failed TOFL	136
26	failed TOFL	123
28	failed TOFL	114
30	failed TOFL	107
32	4.946	100
34	4.701	95
36	4.585	91
38	overweight	N/A

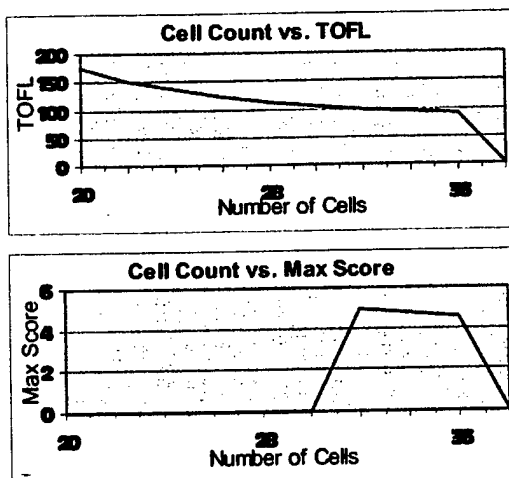


Figure 4.10 Takeoff field length and score versus the number of battery.

Parts	C.G. Distance from nose cone (in)	Weight (lb)	Moment (in-lb)
Propeller	0.75		0.26
servo for nose gear	8.75	0.40	3.50
Nosegear	6.50	0.35	2.28
Main Wheels	23.00	0.40	9.20
Horseshoe Strut (maingear)	23.00		18.86
batteries	11.25	4.43	49.84
receiver	11.25	0.18	1.97
receiver battery	12.50	0.70	8.75
motor	4.50	1.26	5.68
brakes and tubing	23.50	0.50	11.75
compressed air bottle	31.25	0.19	5.86
fuselage	33.25	2.09	69.43
speed controller	11.00	0.14	1.54
wiring	9.50	0.10	0.95
spinner	0.00	0.38	0.00
horizontal tail (65% of total tail wt)			
+servo	53.25	1.36	72.60
vertical tail (35% of total tail wt)			
+servo	50.50	0.92	46.39

Table 4.1 Estimated of moments of various components. Yellow values are estimated weights and green values are measured weights.

MAC =	18.13
Target C.G. =	30.00%
Empty Weight (no tail pad)	17.38
Payload Weight	20.60
Gross Weight (no tail pad)	37.98

Table 4.2 Outputs of center of gravity spreadsheet. "MAC" means Mean Aerodynamic Chord and XLEmac is the distance between the front of the aircraft and the front of the MAC

Detailed Design

Final Performance Data

Takeoff performance

This was perhaps the most important consideration in our design process. Optimizing takeoff performance meant getting a value for heavy TOFL that fell between 80 and 100 feet. Possible head winds at the contest and the conservative coefficients used in the propulsion model should provide better TOFL. The following methodology was used when studying the TOFL:

- ♦ Prop diameter and pitch selection were limited by the manufacturer's specifications (diameter less than 25" for the 1817/2Y motor and 3.7:1 gearbox), design constraints (less than 28" due to height of landing gear), prop availability (large props with design advance ratios above 0.7 are extremely rare), and current draw. Larger props were clear winners as long as these requirements were met since they greatly helped TOFL, did not increase the rated aircraft cost, and were not severely penalized in cruise flight. Current draw was a major issue; but the current draws were not sustained and the cooling system was designed to keep component temperatures within tolerances.
- ♦ Excessive RPM on the motor was limited by the number of batteries (limiting the 1817/2Y to 28 cells), controller rating (32 cells), and battery pack weight from the cell count limits. The excessive RPM concern was neglected after our Mission spreadsheet specified that this problem was nonexistent when using large props. The rated aircraft cost formula penalized cell count, had a dramatic impact on takeoff performance and reduced the energy limit.
- ♦ Wing area was unfavorable both in cruise performance and in the rated aircraft cost function, while providing a relatively moderate effect on TOFL. Thus increasing this parameter was our least favored strategy.

Handling Qualities

The stability and control of the aircraft was evaluated with an *Excel* spreadsheet which used standard stability and control equations from Anderson (1995). Wing area, tail areas, aspect ratios and airfoil properties were the inputs. The spreadsheet determined the handling characteristics of the aircraft as well. The most important values calculated on the spreadsheet were the static margin, directional stability, lateral stability, elevator required to stall the wing and trim in level flight.

The static margin, or pitch stability, was a very important parameter in predicting *Tsunami's* stability. A plane with a static margin of about 10% of the Mean Aerodynamic Chord was considered acceptable. If the static margin was above this threshold, the aircraft had increased stability characteristics; however, if the value became excessively higher the aircraft induced an augmented trim drag. Directional stability was also a significant aspect of the handling characteristics of the plane. A very low value indicated that the aircraft might experience a "snake-like" motion while in flight. To correct this problem, either the area of the vertical tail or its aspect ratio was increased.

As the team generated different configurations for the plane each week, the input values in the Excel Stability and Control spreadsheet needed modification in order to reflect the best results of stability and control. Of the important factors mentioned, the parameter for elevator required to stall the wing was a reoccurring problem. For many of the configurations considered, this value was greater than the hinge line stall limit on the maximum elevator deflection. This was an important factor due to its influence on values of $C_{L,max}$, which in turn was significant in the determination of TOFL. One solution for improving the elevator required to stall the wing was to move the CG of the aircraft aft. Nevertheless, the configurations incorporated a CG location approximately 30% of the wing's root chord in order to have the payload CG coincide there as well while in flight. Another option included increasing the control chord fraction of the elevator for the horizontal stabilizer. Yet if the chord fraction was greater than 30%, excessive hinge moments became an issue. Therefore, the tail aspect ratios were changed to provide acceptable values of elevator required to stall the wing.

The horizontal stabilizer was sized for 10% stability and control power to stall the wing. High aspect ratios reduced the elevator hinge moments as well. The vertical tail was sized for $0.002C_{n\beta}$ while having enough rudder power for 8-10ft/s crosswind. Dihedral was minimal for low gust response during takeoff and landing.

g load

This factor was limited by the ratio of the wing's maximum lifting capacity to the plane's weight. Aggressive turns were considered but offered no scoring benefits because of the altitude loss. Considering the loads in the turns, an acceptable g load of 4.5g was used. This was a compromise between the turning rate and the weight of the spar and wing.

Range, Endurance, and Speed

These three parameters influenced the design almost as much as TOFL. With a 5-lb battery pack weight limit, battery life was a major concern. The controlling variables were listed below:

- ♦ Using very high energy density batteries was not prudent due to their excessive weight. Moreover, reducing the cell count failed to provide sufficient energy for meeting the TOFL requirement. In addition, their characteristic high internal resistance caused their extra energy capacity to be converted into heat without benefiting the plane. The RC2400 batteries were chosen because they combined a very high energy density, very low internal resistance and a midsize capacity per cell.
- ♦ Increasing cell count allowed increased endurance at the cost of a higher rated aircraft cost—a choice which was deemed worthwhile. Nonetheless, the TOFL requirement dictated cell count.
- ♦ Even though the TOFL requirement regulated the propeller diameter, increasing the propeller diameter increased the available thrust and made the plane fly faster.
- ♦ Increasing wing area augmented energy consumption and caused the plane to fly slower due to increased drag; therefore a small, flapped wing was beneficial.
- ♦ Reducing throttle on flights without payload, where TOFL decreased, saved a small amount of energy compared to the large time lost in flying at a lower velocity setting.
- ♦ Modulating flight speed, throttle setting, turn altitude, and airbrakes allowed the pilot to arbitrarily conserve energy or save time. The optimum speed was slower than many

considered previously, causing energy savings and tighter turns.

Payload Fraction

Increasing the payload fraction generally increased the efficiency of the plane and resulted in a markedly increased score. Early iterations with the Mission model clearly predicted the largest possible payload capacity would improve the overall score. Consequently, optimizing payload fraction meant minimizing plane weight. There were efforts to meet that goal by minimizing battery pack weight and constructing the aircraft structure as light as possible. Likewise, a wing design radically different from any designs attempted before was ensued and all durability vs. weight decisions were biased towards reducing weight.

Component Selection and System Architecture

Reliability

Reliability was deemed to be a significant aspect of the competition this year because the final score will be the sum from three ten minute flight periods. Since each flight period can involve 3-4 sorties, each with multiple take-offs and landings, a large number of components must operate repeatedly without a failure. This influenced the choices for many of the components of the plane. For example, instead of machining a sophisticated braking system, commercially available pneumatic brakes were purchased after researching their compatibility and reliability when used in aircraft as large as *Tsunami*. Past experience also denoted the possibility that speed controllers did not perform as advertised by manufacturers. The chosen speed controller for *Tsunami* contained auto-adjusting capabilities and moderated the amount of current passing through it. When the amount of current surpasses a particular limit, the speed controller shuts off, saving itself and the motor from damage. The selected motors were also tested to determine their heating characteristics, in addition to that of the batteries and speed controller, in order to understand the likelihood of possible failure during the flight sequence.

During *Tsunami's* construction phase, spare parts were made of several components to prepare for the possibility of a malfunction. New methods were developed for the wing and tail construction process in order to reduce building time when a replacement was necessary. Numerous necessities were essential for creating the aircraft, such as nylon bolts, motors, batteries, propellers, tooling foam, and other accessories; furthermore, if a component was unavailable it was supplemented with a manufactured part using the materials at hand. Many tools, bolts, and foam were obtained from the Home Depot; minor building supplies, balsa wood, and batteries were purchased from Hobby Shack. The composite materials used to fabricate the aircraft were purchased from Aircraft Spruce. The Aveox 1817/2Y and Cobalt Pattern 90 motors were acquired from their respective manufacturers, as specified in their name.

More testing was accomplished to ensure the servos could withstand large loads while preserving the structural integrity of their gears. In particular, plastic gears did not perform as expected throughout the tests; thus metal gears were used and proven to function exquisitely.

Completion of the manufacturing process before the competition was a vital aspiration to uphold; otherwise, the necessity to further enhance the aircraft at the contest would deteriorate the opportunities available for improving the overall score. In addition, preliminary test flights

would assist in eliminating faulty systems, correcting defective parts, and determining other strengths and weaknesses of the aircraft.

Structure

Introduction

The integration of the various features in *Tsunami* was a critical facet of the Detailed Design stage. Extreme reliability was required as well for this year's contest in order to have confidence that the aircraft would fly at least three exceptional sorties in order to maximize the score. Alongside this concern was the necessity to construct an aircraft that upheld the predictions established by the Weights analysis that was conducted in the Preliminary Design stage. This critical aspect proved to be a large obstacle in past aircraft designs and was overcome in *Tsunami* through the use of lighter materials and more prudent manufacturing processes. Complicated structural designs were avoided to improve the reliability. In addition, a streamlined fuselage was needed to decrease the parasite drag of the aircraft; this entailed avoiding a fuselage body design that contained sharp transitions in curvature and restrained components, e.g. a speed controller, outside of the body.

Fuselage Structure

The structure of the fuselage was governed by supporting the motor, wing attachments, landing gear attachments, and payload housing. Internal bulkheads were designed to house the payload above the wing and as close to the CG of the aircraft as possible (roughly 30% of the wing chord from the leading edge as recommended by the Weights analysis). These bulkheads spanned the width of the fuselage and provided structural strength to the fuselage skin. A floor spanning approximately 90% of the fuselage length, as depicted in the Interior Profile (see the Drawing package), sealed the payload compartment and molded with the bulkheads mentioned above. Another bulkhead located near the nose and annular inlet increased strength for the nose gear attachment. An added incentive to this particular bulkhead provided the ability to separate the batteries and electrical components from the motor. A hatch beneath the internal floor provided access to the nose gear attachment and steering servo as well. The Interior Profile Drawing shows the compartment separation provided by this bulkhead, which also had a sufficient opening for air to pass through and enter the battery/electrical component compartment. The primary reason for locating the electrical components in this section included limiting the total length of wiring required to reach the motor; this reduced the electrical resistance and likewise decreased the energy lost to heat dissipation. Past experience demonstrated the necessity for having this type of electrical configuration in order to maintain the maximum possible battery life and minimal heat transfer to the electrical components. Access to these compartments was provided by a hatch on the top of the fuselage.

In particular, the floor and each bulkhead was made of honeycomb capped with carbon fiber. This lightweight combination was proven to be very strong in several tests conducted with articles that were fabricated to compare with heavy plywood and other materials. The entire fuselage was constructed of carbon fiber because it has great strength and is light weight. Several locations on the fuselage contained a cut out for a hatch, exhaust, or attachment for external components. These locations required two or three layers of carbon fiber to account for any strength lost by these openings.

Motor Mount

The motor mount was a special aspect of *Tsunami* because its creation presented a new design experience that had not been used in previous aircraft configurations. A heat analysis indicated that the motor required extensive cooling via heat sinks; therefore the heat sinks were made of lightweight aluminum and united permanently to the motor with conductive epoxy. These served a dual purpose as motor mounts. The aluminum supports were attached to the carbon fiber fuselage. An air scoop diverted a fraction of the inlet flow upward towards the motor. Thus the incoming cool air flowed over the motor and the heat sinks removing the excess heat.

Annular Inlet

The annular inlets for the cooling ducts were designed with a 10° "droop" at the opening with an elliptical lip that had a 2:1 ratio of length to width. This ensured that limited spillage of the incoming air occurred and improved the effectiveness of the cooling system as a whole. In addition, the thickness of the lip constituted about 10% of the cross-sectional width that the inlet contained while 20% of the inlet diameter was reflected in the elliptical lip length.

Location of Electrical Components and Cooling

Another influential aspect of the fuselage structure was the matter in which the electrical components (i.e., speed controller, motor, batteries, and receiver) received cooling. An analysis conducted in the Mission spreadsheet performance model found how much cross-sectional area was required for air duct inlets and exhausts. Therefore, a large annular inlet provided the most cross-sectional area that met the qualifications dictated in the thermal analysis. Smaller openings would not provide sufficient cooling. In addition, internal "false walls" would direct the incoming flow into three compartments housing the battery packs, motor, and the other electrical components. The hot air exited through an exhaust dedicated to each particular compartment. The exhausts were located on the side of the fuselage and on the top of the fuselage, as depicted in the Interior Profile Drawing. The side exhausts were prudently located above the leading edge of the wing, where the existing vacuum in that region would provide extra suction to remove the warm air inside the electrical component compartments. Furthermore, the motor was mounted within the annular inlet without a spinner in front of the prop. This characteristic assisted in allowing air to flow into the inlet with less obstruction and would likewise permit the prop wash air to enter the inlet as well.

Wing and Landing Gear Attachment

The forward section of the fuselage resulted in a confined structural geometry that distributed harsh landing loads evenly. Large loads were also predicted to concentrate in the region where the main landing gear and wing attached to the fuselage. A plan was devised that permitted the wing to attach without causing a discontinuity in its spar; in addition, the landing gear was located aft of this spar and slightly behind the CG as well to allow the aircraft to pitch upwards upon takeoff. The solution was rather simple in theory: two bulkheads attached beneath the inner floor of the fuselage and alongside the fuselage side-of-body provided the necessary attachments for the landing gear and wing. Nylon bolts provided sufficient resistance to loads from hard landings and sheared when the loads exceeded the ultimate design loads, thus

protecting the structural integrity of the wing and main landing gear. The bulkheads were made of plywood and molded into the internal floor without spanning the entire fuselage height—another form of conserving weight.

The wing required the airfoil to continue up to the fuselage side-of-body and not in the internal section of the fuselage. At the side-of-body a 1/16" balsa saddle permitted closure to this section between the fuselage skin and the adjacent airfoil. Within this cavity in the wing an air bottle, used by the pneumatic braking system, protruded from above the internal floor (where it was attached to the bulkhead housing the payload) and permitted the appropriate piping to connect it to the brakes on the wheels.

Tail Structure

The aft section of the fuselage contained a carbon fiber molded saddle for the horizontal stabilizer; moreover, it provided extra surface area for attachment as a result of the cut out required in this part of the fuselage for the stabilizer to enter. This section of the tail was removable in order to decrease the size of the shipping box required to transport *Tsunami*. The vertical fin was molded to the fuselage to ensure enough structural intensity for resisting the light loads present in that section of the aircraft. To decrease the size of the shipping box, the vertical fin was dismantled at a semi-span location; the upper section would be reattached at the contest site knowing that the small loads distributed throughout the vertical fins cannot damage that discontinuity. In contrast, though, the rudder remained as one continuous piece because it acted as a primary control surface. The tail sections were "hot-wired" from foam and covered with a think layer of balsa for structural stability.

Spar Sizing

For this airplane, the wing box had to react both torsion and vertical bending moments. In light of this, we opted for a D-section. The reasons behind this decision were:

- A tube spar would have had extremely thin walls making it prone to crippling.
- An I-beam spar would have been too thin to construct effectively, and does not react torsion well.
- The leading edge of the wing was going to be sheeted with balsa wood for aerodynamic reasons, thus making a D-section logical.

Graphical representations of the shear and moment diagrams were located at the end of the Detail Design section as Figure 5.1 and Figure 5.2, respectively. The distance from the center of the wing towards the tip was plotted on the ordinate, and the moment or the shear was plotted on the abscissa. In the shear diagram (Figure 5.1), the plot labeled 'Adjusted Shear' included the fact that the wing was mounted on the fuselage four inches from its centerline.

The goal was to create the lightest spar possible. The lay-up schedule for the spar was depicted in the table labeled Figure 5.3. The first row denoted the distance from the center of the wing while the second row provided the carbon fiber thickness, each showing values measured in inches.

Figure 5.4 shows the internal composite components of the spar. The three outer most layers represented 0° pre-preg carbon fiber. The fourth layer was 90° pre-preg carbon fiber for

buckling resistance, and the rose colored translucent material indicated thermal glue to aid the bonding between the Nomex honeycomb and the 90° pre-preg carbon fiber.

Wing Detailed Design

The wing structure incorporated balsa-capped foam ribs, where balsa sheeting was glued to the leading edge portion of the airfoil. The balsa sheeting on the wing was also responsible for providing a smooth surface for the monokote covering, in addition to adding a level of rigidity to the skin for reacting shear forces. A carbon-fiber and Nomex honeycomb blade spar provided sufficient strength for reacting loads and was positioned approximately c/4 chord; moreover, it was capable of withstanding a limit calculated load of 3.5 g's. The foam ribs were 0.5" wide and spaced four to six inches apart to prevent pillowing of the unsupported monokote. A wing structure of this caliber was designed to minimize weight for the aircraft, thus there was no necessity for extraneous foam to preside between the spaced ribs, as illustrated in Figure 5.5. The D-section, located forward of the spar at the leading edge, was also hollowed to diminish weight. The wing servos were mounted against the spar as well and deflected the control surfaces via a metal arm attached to a receiving horn positioned on the control surface. Furthermore, these control surfaces were attached to the wing with taped hinges.

Main Landing Gear Design

With the use of a Solid Landing Gear design spreadsheet designed by Blaine Rawdon, an industry adviser, a precise landing gear design was developed for the weight and strength specifications designated for reliability on *Tsunami*. The spreadsheet integrated programmed macros in *MS Excel*, which used specific input items to determine the most effective composite lay-up of the desired material and the corresponding strength needed for minimal weight requirements. The main inputs were dictated by the design, including width of the landing gear (2.0"-3.0"), distance between each wheel base (30.25"), distance between wheel axles (28.75"), distance from the ground to the attachment point with the fuselage (8.0"), landing gear track (14.22"), the angle between the CG and a wheel (48.96°), distance from the CG to the aft landing gear (1.0"), and the number of bolts required to connect the landing gear to the fuselage (4).

Inputs also designated which g-loads, sheer and stress levels, and amount of compression or decompression the landing gear needed to withstand in order to complete the mission. A pictorial representation of the input section for the spreadsheet is provided in Figure 5.6. These inputs included, aircraft weight, maximum g's allowed, ply-material, and glide slope during landing. Once these inputs were entered and a primary composite material was selected (unidirectional-carbon 0°), the spreadsheet calculated the number of layers needed to meet the established requirements. A picture of the landing gear was also produced to illustrate its geometry when static and at maximum deflection (for an estimated 36 lb. aircraft, a maximum of 8g's caused the maximum deflection), as demonstrated in Figure 5.7, as well as graphs depicting the resulting stress and tension levels at different points throughout the landing gear. An optimum number of layers was found through various iterations until stresses were described to fall below the stress and lamination limit allowed; in essence, it represented a final check for assurance that the landing gear would not delaminate or fail during landing. Another Figure was created for illustrating an isometric view of the landing gear; furthermore, a coordinate system was established by the spreadsheet in order to permit changes in landing gear appearance. The

Shear diagrams

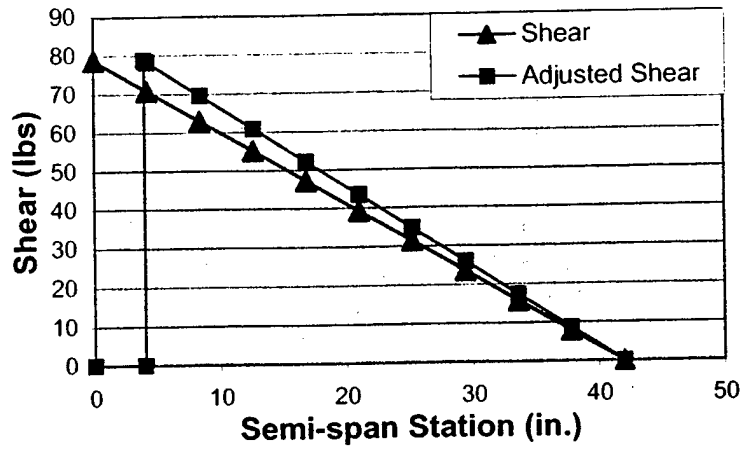


Figure 5.1

A graphical illustration of the shear stress distribution throughout the wing semi-span section.

Shear diagrams

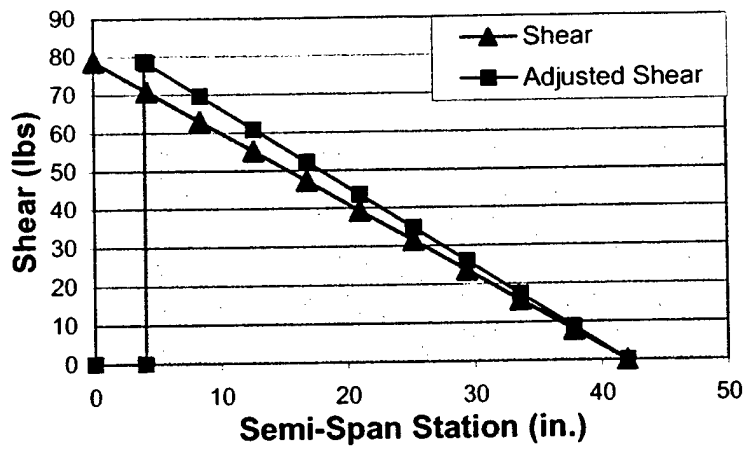


Figure 5.2

A moment diagram depicting the diminishing loads distribution along the wing semi-span section.

Side Of Body										Wing Tip
	4.2	8.4	12.6	16.8	21	25.2	29.4	33.6	37.8	42
0.0245	0.019845	0.01568	0.012005	0.00882	0.006125	0.00392	0.002205	0.00098	0.000245	7.01E-34

Figure 5.3

A table representing the lay-up schedule for the wing spar. The first row lists distance on the wing's semi-span while the second row depicts the corresponding spar thickness.

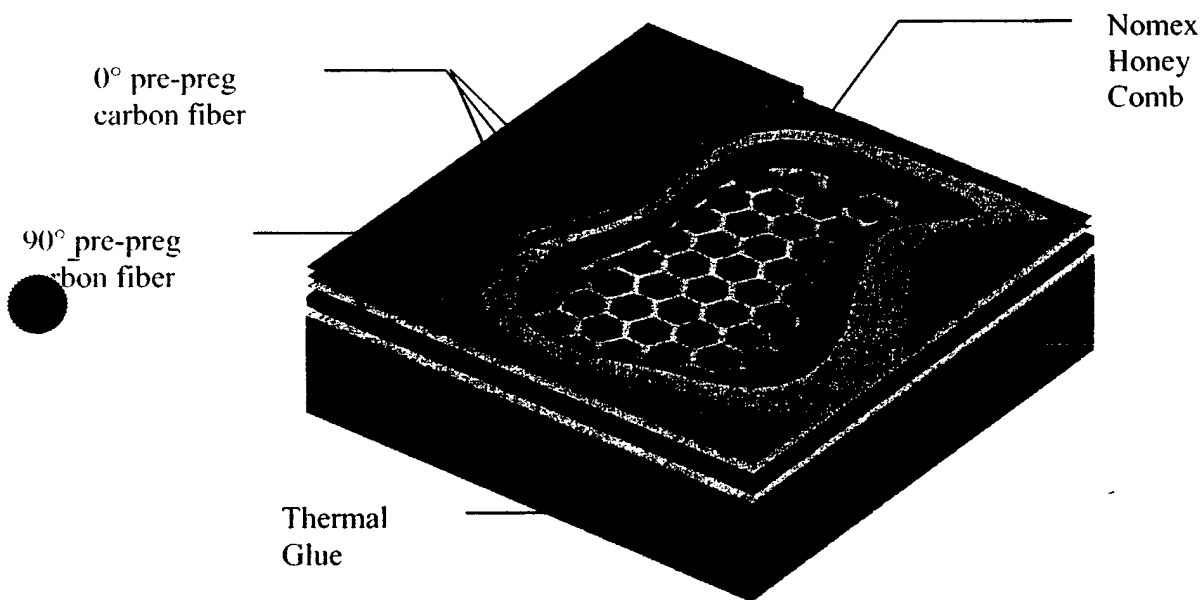


Figure 5.4

A detailed cut-away view of the spar illustrating the various composite materials implemented in its fabrication.

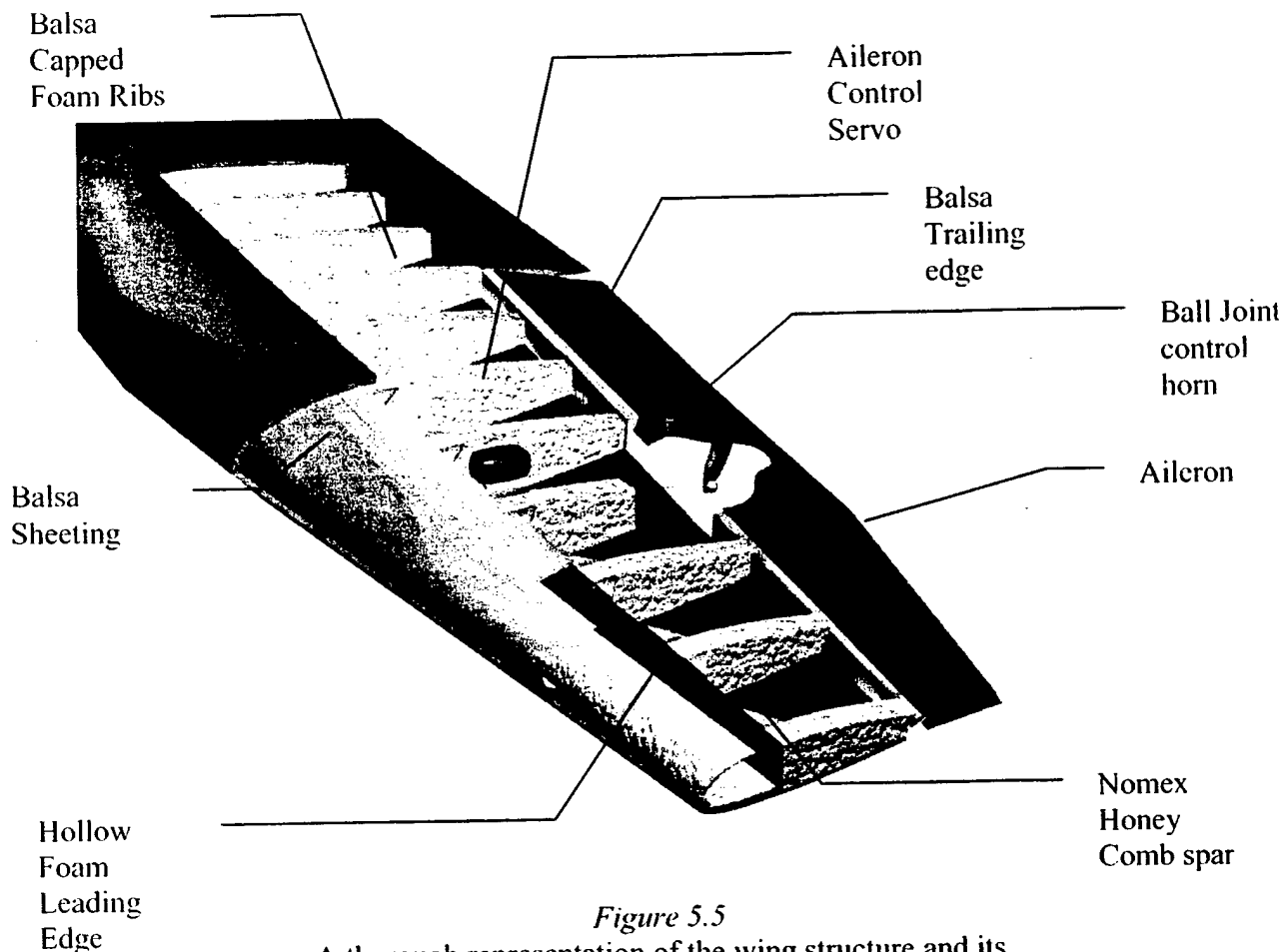


Figure 5.5

A thorough representation of the wing structure and its complicated integration of numerous features, including foam ribs, spar, balsa sheeting, servo mechanism, and control surface representation.

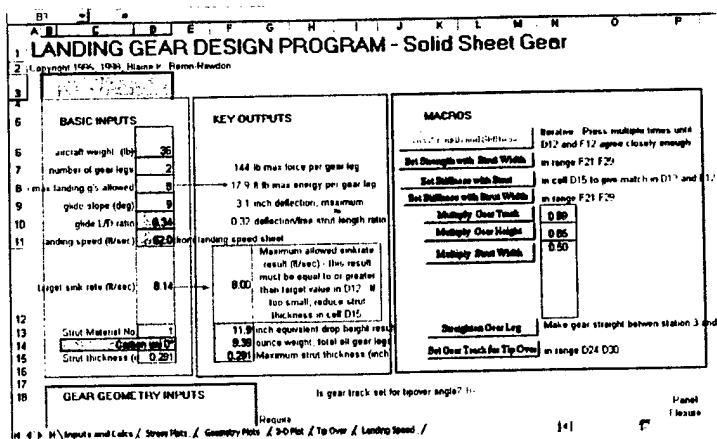
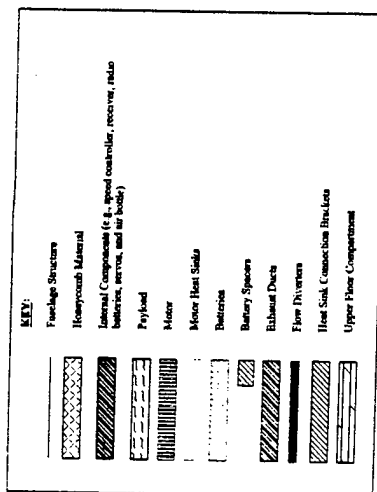
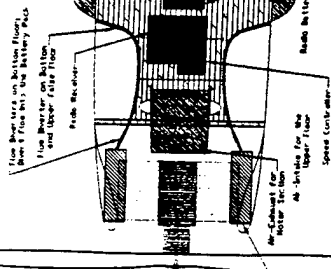


Figure 5.6

A screen snap-shot of the landing gear design spreadsheet used to analyze various landing gear configurations

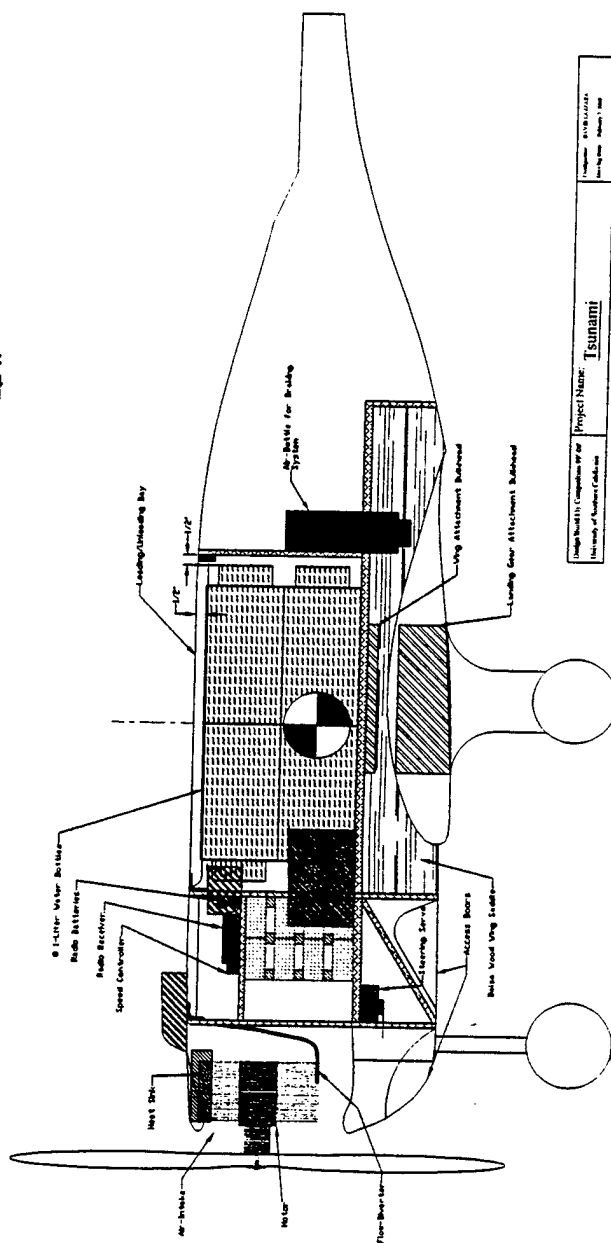
Drawing Package

INTERIOR PROFILE



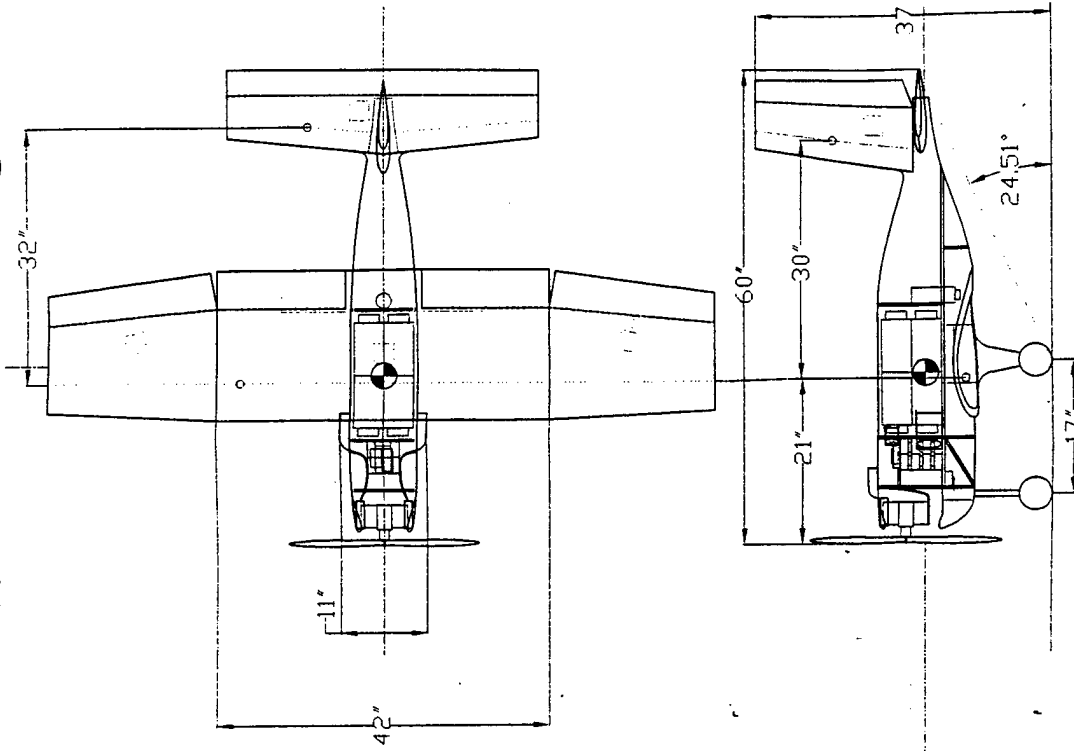
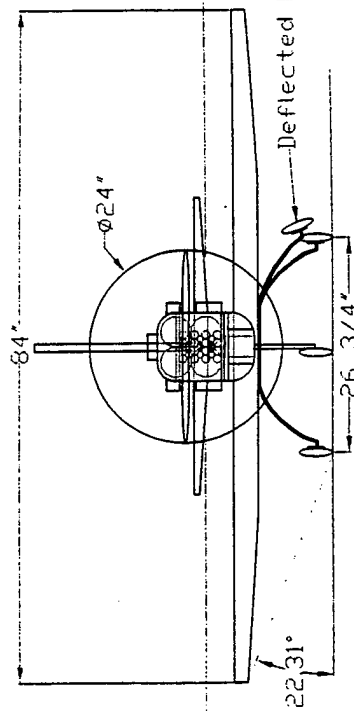
NOTE:

The mating requires 4 heat units, each with surface area = 10.0 ± 2 Length = 1.28 Height = 2.0



Design Board 11b, Comparison 99-08	Project Name: Tsunami	1. Participant: DAVID LAZARUS
This study of Southern California		2. Meeting Date: February 3, 2000

CHARACTERISTIC DATA			
	Wing Projected	Horizontal Stabilizer	Vertical Tail
• Total Area (in. ²)	1512.0	374.35	207.96
• Inner Panel	399.0	-	-
• Outer Panel	357.0	-	-
• Span (in.)	84.0	39.24	19.92
• Inner Panel	21.0	-	-
• Outer Panel	21.0	-	-
• Aspect Ratio	4.67	4.11	1.91
• Root Chord (in.)	19.0	10.56	12.0
• MAC (in.)	18.09	9.58	10.52
• Tip Chord (in.)	15.0	8.52	8.88
• Sweep C/A (deg.)	0.0	4.46	6.61
• Moment Arm (in.)	-	32.0	30.0
• Tail Volume	-	0.438	0.049
• Root V/c	0.157	0.141	0.140
• Tip V/c	0.157	0.095	0.141
• Total Taper Ratio	0.79	0.807	0.74
• Inner Panel	1.0	-	-
• Inner Panel	0.789	-	-



Design/Build/Fly Competition 99'-00'

University of Southern California

Project Name:

Tsunami

Configurator: DAVID LAZZARA

References

- Anderson, John D., Introduction to Flight. 3rd ed. New York: McGraw-Hill, Inc., 1989
- Boucher, Robert J., Electric Motor Handbook. Astroflight Inc., 1995.
- E-calc <http://www.slkelectronics.com/ecalc/index.htm>
- Hepperle, Martin. <http://beadec1.ea.bs.dlr.de/Airfoils/calcfoil.htm>
- Page, Greg, 1999, '<http://amber.aae.uiuc.edu/~aiaadbf/99rules.html>'
- Selig, Michael S., James, J. Guglielmo, Andy P. Broeren, and Philippe Giguere.
Summary of Low-speed Airfoil Data. Vol. 1 Virginia Beach, Virginia. Virginia Beach, Virginia: SoarTech Publications, 1995
- UTUC Airfoil Data Base. <http://amber.aae.uiuc.edu/~m-selig/>

Second Semester Schedule v.1

Team #	Task	Responsible	Jan 10-16	Jan 17-23	Jan 24-30	Jan 31-Feb 5	Feb 7-13	Feb 14-20	Feb 21-27	Feb 28-Mar 5	Mar 6-12	Mar 13-19	Mar 20-26	Mar 27-Apr 2	Apr 3-9	Apr 10-16
1	Fuse final design	Team Member														
2	Fuse templates															
3	Bulkhead templates															
4	Wing final design															
5	Wing spar templates															
6	Wing rib templates															
7	Wing saddle / fairing templates															
8	Landing gear templates															
9	Tail templates															
10	Plane together															
11	Bulkhead templates															
12	Report drawings															
13	Wing spar calculations															
14	Landing gear calculations															
15	Build motor mount															
16	Build first landing gear															
17	Build 2nd gear															
18	Build 3rd gear															
19	Build bulk															
20	Build mold															
21	Build luse															
22	Build and install bulkheads	Phil, Rusty, David Phil, Rusty, David Phil														
23	Control surface and servo sting	Jerry														
24	Build wing	Jake														
25	Build tail	Jerry & Jake														
26	Install servos	Jerry														
27	Cut control surfaces	Jerry														
28	2nd wing	Jake														
29	Test Landing Gear Director	Charles														
30	Get test stand operational															
31	Test Peep motor															
32	Test 1817 and P90															
33	Buy brakes															
34	Install brakes															
35	Install nose gear															
36	Electrical	Jerry and Phil														
37	Get Peep powerplant functional															
38	Reel motors arrive															
39	Batteries arrive															
40	Get 1817 and P90 functional															
41	Build light cover	Phil														
42	Report Director															
43	Initial outline															
44	Get component sections															
45	Edging															
46	Report Due															
47	Appendix Due															
48	First flight															
49	Second flight															
50	Third flight															
51	Fourth flight															
52	Ship plane															
53	CONTEST															

- Joining parts with return flanges provided stronger and more reliable joints.

The individuals involved in manufacturing *Tsunami* had much experience in composite construction techniques and used the sufficient funding for substantial amounts of wet-layup construction. A large supply of surplus Nomex honeycomb core material was obtained and constructing methods were developed that ultimately resulted in very strong and light parts. Previous experience with end grain balsa core construction demonstrated that such panels are both heavier and harder to build than Nomex core panels. An early test revealed that 1/8" thick Nomex core panels were several orders of magnitude stronger and stiffer than 1/8" thick birch plywood despite having similar aerial densities; likewise, this was our primary structural material.

Using the previous considerations and relying on experience in using this exotic material, the aircraft was established to incorporate a primarily composite fuselage. The greater strength to weight ratio of carbon fiber, in addition to the sufficient budget at the time of fabrication, replaced the use of fiberglass as the main structural material. After acquiring enough experience with Nomex honeycomb construction, it was applied to the bulkhead core and also used as a general-purpose stiffener. The final design had fairly concentrated loads and moderate fuselage moments, resulting in a system of load carrying bulkheads with stability and torsional rigidity provided by a minimal skin.

Fuselage construction originated with a set of drawings depicting fuselage templates and cross sections. These templates were used to cut the top and side fuselage geometries from a block of Styrofoam, followed by sanding that created the corner rounds. The final step in buck construction was coating it with low temperature shrink-wrap. This primarily hotwired buck required around 20 man hours vs. around 200 for the urethane-Bondo method and produced a truer, though more fragile, buck. The greater mold finish time did offset the vastly reduced buck construction time, though; but this was deemed acceptable.

Mold construction followed. The first step required releasing the buck with car wax and spray Teflon and building fences around the future mold joint. After cutting the mold materials to shape, the buck was coated in a layer of epoxy with microballoons, which provided a surface inner layer that was easily sanded, and built up the mold with layers of light and heavy fiberglass. After this first part had cured, the second half of the mold was constructed using the completed first half to provide a joint. Once these parts were completed, their inner surfaces were sanded and patched. Furthermore, bulkhead templates were used to fabricate the honeycomb panels with plywood inserts.

Final fuselage construction began after the completion of the mold halves. The first part used one layer of light bi-directional fiberglass on the outside of the mold, mainly for stiffness and a smooth outer surface, and one layer of bi-directional carbon for the interior portion of the fuselage. After cutting access holes and joining the bulkheads to one half of the fuselage part, the nascent fuselage was placed once again into the mold for alignment and attachment to the other fuselage half. Following the installation of the wing and tail saddles, front air ducting, and miscellaneous access holes, the fuselage construction was completed.

webbing and carbon fiber caps. This example proved to account for a large portion of the excessive overall weight of previously built aircraft when extreme care was not taken during the wet lay-up of the composite skin materials. Excess epoxy was the main culprit in those situations. Also, the integration of internal wiring and servo mounting became more difficult due to the wing's solid body; much time was spent creating cavities for these components and patching of the outer airfoil surface. Due to these limitations, this plan was discarded.

Experience in creating balsa ribbed wings also allowed us to discuss its effectiveness for *Tsunami's* mission. Monokote was the proposed skin for the wing as well. The subsequent analysis of the wing structure demonstrated that this configuration was not sufficiently rigid; moreover, there was concern that the wing could not be easily repaired if damaged. A modification of this fabrication method included capping each individual balsa rib with carbon fiber. This solution proved to tremendously improve the structural integrity of the wing. In both cases mentioned above, a carbon fiber capped blade spar with Nomex honeycomb interior was expected to react loads. There was concern, though, that this approach could be improved if a supplemental material was found for the ribs in order to reduce the amount of balsa throughout the wing, causing a reduction of weight.

The final solution incorporated a new design that was not undertaken in the past and yet it included facets of each proposed manufacturing process discussed above. A consensus arrived at creating a foam core and cutting numerous foam ribs. The blade spar remained the same as described above and was a continuous component spanning the wing. In addition, the leading edge of the wing, in other words the section forward of the spar, was not composed of foam; instead a D-section created with balsa was inserted and hollowed to preserve weight. The foam between each foam rib was eliminated with a small hotwire tool to eliminate unnecessary structure. Ultimately, the wing was monokoted to provide a smooth outer surface for the airfoil geometry. The control surfaces remained as the final components to create and attach to the wing; therefore the detailed information pertaining to its construction will appear in the Addendum Report.

Fuselage Manufacturing Plan

The primary goal in constructing the fuselage was to build a light and aerodynamically clean structure capable of handling the design loads. Throughout the design process the following lessons were followed in order to repeat advantageous methods and avoid past mistakes:

- The tedious, time-consuming nature of Bondo-urethane foam buck construction needed to be avoided.
- Molded, vacuum bagged composite shells give a very clean aerodynamic shape, were field repairable, and had very high torsional rigidity.
- End grain balsa absorbed epoxy, requiring very careful wet lay-up and pre-preg construction, or the use of a different core material.
- Extensive plywood inserts added significantly to the weight of the fuselage, thus careful design and the acceptance of limited mounting flexibility led to large weight savings.
- Designing for high durability allowed past aircraft to survive severe crashes. However, the critical weight parameter in this year's contest meant that each design decision should bias towards achieving the lightest possible weight.

a smooth table and pouring a small bead of epoxy; afterwards, putty scrapers were used to smear the epoxy. Once the carbon was fully coated, we took the scrapers and continuously applied heavy pressure over the fiber, thus removing the excess epoxy, and placed the material in the mold.

Twenty-nine layers were used to create the landing gear, as dictated by the landing gear analysis spreadsheet, and a simple lay-up schedule was devised as well. A layer of milar material provided a smooth outer surface as well. After vacuum bagging the part, a particular amount of time needed to transpire for it to cure. The edges of the fiber had a tendency to fray during the scraping; but this fraying was allowable because those particular portions were cut off with a Dremel tool. The landing gear strut was cut using a Dremel and a cut-off wheel. Holes were drilled for the wheel struts, as well as the holes needed for attachment to the fuselage.

Manufacturing the Tail

The tail design developed a conventional configuration that neglected sophisticated and structurally intense joints. Past experience with tail configurations such as the "T-tail" presented structural concerns at particular joints; consequently, the lack of experience with such designs were coupled with premature fabrication methods using composite materials, causing the finished product to exceed its weight limit by a large factor. Knowing that the tail surfaces did not require extensive structural support against loads, a lightweight solution was an attainable reality for its construction. Balsa ribs covered with a monokote skin was a proposed method that was eventually defeated due to the possibility of time-consuming manufacturing for the production and integration of the balsa ribs.

The only remaining concept included using 1 lb. white foam core and a carbon fiber, or fiberglass, skin; yet balsa sheeting and monokote was a sensible replacement of the composite materials due to their lower weight. The tail cores were fabricated using a CNC hotwire mechanism that relied on the dimensions provided by airfoil templates. Afterwards, balsa sheeting was glued onto the foam core and sanded in order to decrease inconsistencies throughout the airfoil shape; moreover, monokote was ironed over the balsa sheeting to compliment the smooth surface. Constructing the tail surfaces in this manner resulted in an end product that satisfied the weight requirements imposed on it while maintaining the rigidity necessary for reacting loads.

Wing Fabrication

Numerous construction concepts were debated in order to determine the most effective manner of producing a wing that its prescribed weight limits. Accomplished industry advisors provided excellent insight as to the feasibility, complexity, and effectiveness of each manufacturing proposal. In addition, an extensive amount of experience in building various wings had amounted during the construction of previous aircraft; thus the individuals involved in the wing fabrication were capable of identifying efficient construction methods and contrasting them with past mistakes in wing construction.

A particular suggestion that was often implemented in the past was using a foam core covered with carbon fiber and fiberglass while housing an I-beam spar composed of balsa

Manufacturing Plan

Introduction

This period of *Tsunami's* development was as critical, if not more so, as the conceptual, preliminary, and detailed phases. The milestones established during the initial planning stages were designated for accomplishment during manufacturing, including adapting to the prescribed methods for reducing the weight of the aircraft. A thorough schedule was developed, where each team member was assigned to complete various components of the aircraft, and was presented in *Figure 6.1*. Materials were purchased whenever necessary due to sufficient funding as well. Building sessions were scheduled throughout the weeks prior to the contest; each week included a number of evenings where team members collaborated in the construction of the various aircraft components. Team captains were also designated from among the experienced team members and were responsible for overseeing the construction process, including ensuring that the manufacturing templates were used correctly, maintaining prudent handling of the composite materials in the wet lay-up process, and providing assistance to others with little experience in the construction methods used with *Tsunami*.

Landing Gear Mold

Past experience provided confidence in landing gear designs similar to that employed in *Tsunami's* configuration. Discussion concerning retractable landing gear was considered because parasite drag decreased with the reduction of blunt external components. The structural weight required to incorporate such a system also dismayed any attempts to further pursue its implementation, though. Therefore, a conventional landing gear setup was encompassed. A landing gear spreadsheet was used to calculate the necessary layers of carbon fiber needed to withstand the loads predicted to occur on hard landing scenarios. Furthermore, the ease of construction associated with this landing gear configuration provided fast fabrication—a positive characteristic necessary for conducting repairs or creating a new part if the original failed. The skill level necessary to complete this component of the aircraft did not demand tremendous experience; nonetheless, a specific lay-up schedule was developed to ensure that the proper method was followed during the construction process.

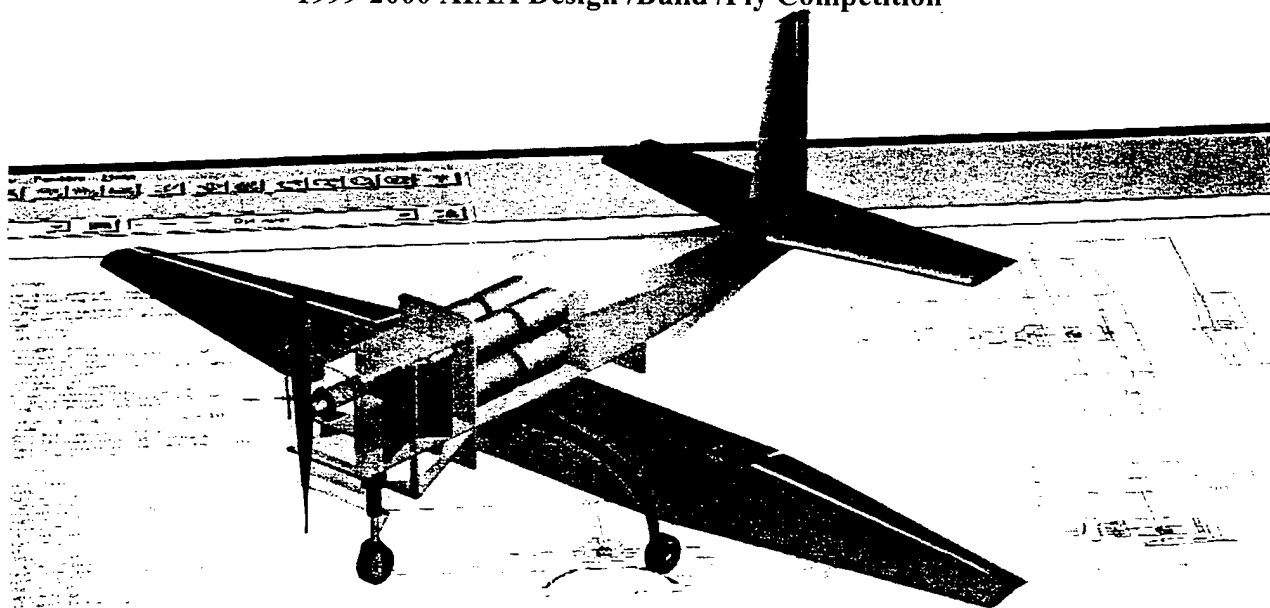
The landing gear for the aircraft consisted of a standard bowed shape manufactured with carbon fiber. The landing gear was built with multiple layers of carbon fiber cured in the shape of the desired bow. Using experience acquired from the manufacture of previous landing gear configurations, a mold was cut from a block of foam using a hotwire while referring to the interior dimensions of the gear displayed on a set of templates plotted full-scale. In continuing the efforts to decrease the necessary weight of the aircraft, care was taken to improve on the manufacturing process used in previous construction of aircraft. In order to decrease the unnecessary weight that occurs when excess epoxy dwells within the carbon fiber material, experimental parts were manufactured to find methods of reducing the amount of excess epoxy applied to the carbon fiber. The most favorable approach included spreading the carbon fiber on



University of Southern California
Aero Design Team Presents

TSUNAMI

Design Report Proposal Phase
March 10, 2000
1999-2000 AIAA Design /Build /Fly Competition



Project Name: <u>Tsunami</u>	Configuration: Drawing: 1
------------------------------	------------------------------

XF/Window/Realtime - W			
to OSNAP (MODEL TYPE	WS_FTP95 L...	Telnet	ALUDRA.US...
Adobe Apps		AutoCAD	



**The
Skunk
Works**

NORTHROP GRUMMAN



AeroVironment

GWServo

Lessons Learned

Design Changes

D Section

The initial wing design featured the removal of the foam behind the balsa sheeting on the front of the wing as a weight saving measure. The removal of excess foam from the back of the wing made clear the small size of these weight savings. Removing foam from the leading edge risked warping or otherwise damaging it for a rather minimal weight benefit. Maintaining the rigid airfoil geometry justified keeping the small excess weight in the leading edge foam.

Final Spar Location

The final location of the wing spar was moved one inch aft of the design specifications. This change from the initial design occurred to simplify the integration and attachment of the fuselage, wing, and landing gear. The new spar location lay closer to the center of gravity, increasing structural efficiency by simplifying the plane's load paths. This new position also located the spar in the thickest part of the airfoil, allowing a greater spar height and improving wing strength.

Landing Gear

The original design placed the main landing gear and wing mounts behind the wing spar. The new wing spar location required moving these mounts since they now interfered with the wing spar. The new design had the mounts straddling the spar instead of being behind it, shortening the load paths between the wing spar and the mounts. Additionally, the new mount brought the landing gear aft, easing tipback problems caused by the center of gravity being further aft than expected.

Physical Test Data

Wing Loading Test

On the 26th of March 2000 the team performed a load endurance test on the wing to determine its actual strength. A base with dimensions roughly similar to the fuselage width held the wing off of the ground while equal weights were applied to each wing tip and directly over the spar. The wing and spar easily withstood a 42.06 lb load, far exceeding the maximum calculated for a given sortie as shown in Figure 1.1.1 and 1.1.2. This testing was performed prior to applying the balsa sheeting on the leading edge, which itself increased the wing's strength even further. Therefore the wing spar alone handled all the applied stresses easily. The test results confirmed that the wing's structure could sustain significantly more than the highest calculated wing loading.

Static Thrust Test

In tests preceding the first test flight on the 2nd of April 2000 the aircraft produced a static thrust of 12-lbs. This datum was obtained by attaching a spring scale to the tail, slowly rolling the plane forward and backward under thrust, recording both weights from

the scale, and averaging the measurements. Instead of using the 24x16 propeller recommended by the Mission model, the static thrust and initial flight tests were performed using a smaller 22x12 propeller. This smaller propeller reduced the loads on the electrical system, reducing flight risk on this initial flight. The propulsion model calculated a slightly greater thrust than the test revealed, but this fell within the 1 lb. uncertainty of the measurement. These results supported the notion that using the larger competition propeller would produce adequate thrust.

Weights

The location of the aircraft's center of gravity severely affects its performance. Having the center of gravity too far forward makes the plane excessively stable, and having it too far aft makes the plane unstable. The tail's long moment arm makes excess tail weight more serious than excess nose weight. A well-balanced, light plane is easiest to fly and thus yields the best performance. Achieving this type of aircraft requires careful planning, accurate weight and moment arm estimations, and strong adaptability to changing circumstances.

The effort to estimate *Tsunami's* weight incorporated lessons learned from previous efforts. Last year's plane was grossly overweight all around, a consequence of poor weights estimation and immature manufacturing processes. Having more experience with the required construction methods aided both problems. An ongoing weight analysis also helped keep the plane within design specifications. Both manufactured and purchased components were checked against their predicted numbers to update the weight estimation. This extensive bookkeeping enabled the finding of quick solutions to weight problems during the manufacturing process. Ultimately, changes during construction improved the aircraft design without invalidating the weights model.

Proper weights estimation is very important since takeoff field length increases with the square of the weight. Figure 1.2 displays the difference between the actual and predicted locations of the center of gravity. The graph in Figure 1.3.1 and the table in Figure 1.3.2 illustrate the comparison between the predicted and the actual weights of the aircraft components.

Current Strengths and Future Potential

What did we do well this year?

One area of success was the even distribution of workload among team members. The structured division of labor prevented one team member from becoming overwhelmed, maintained morale and helped meet schedules. Organized groups operating on one facet of the design and construction process enabled the specialization of team members and the execution of concurrent projects. The flexible and temporary nature of these groups allowed the diffusion of skill and the efficient utilization of team members.

Several design concepts pervaded and aided our design process. The use of a weight-minded design philosophy encouraged the development of new construction methods. This led to the early construction of several test parts using Nomex honeycomb

and carbon fiber to estimate their weight savings over conventional materials and to create experience with these materials. Their subsequent selection resulted in a substantially lighter and stronger plane. Weight-minded design also led to the widespread use of lightening holes, the choice of the lowest possible density foam in airfoil construction, and the choice of light weight over enhanced durability wherever possible and reasonable.

Careful consideration of the contest rules and the overall goal of the competition during the design phase eliminated the possibility of constructing an aircraft that did not meet the contest specifications. The cost model, for example, severely constrained the configuration and forced the team to optimize performance while minimizing the rated cost of the aircraft. This mindset also permitted the team to focus on the overall contest objective instead of concentrating on a facet of performance such as raw battery life.

Reliability formed another cornerstone of *Tsunami's* design process since the design necessarily pushed the performance envelope. Historically, aero design competition planes have always crashed at least once, either during testing or at the contest. Component problems have also halted progress in the past. A lack of provision for later changes during the design process, a lack of flexibility in the configuration, and difficult to repair components had made workarounds difficult. To minimize risk, the team designed for repair and created numerous "back-up" plans to solve or circumvent possible component failures instead of pinning contest success on a single plan. These included a complete backup powerplant design, the ability to revert to a taildragger landing gear configuration and alternate flap designs. In the end most of the original designs held, but the flap mechanism needed alteration and the powerplant nearly did as well.

Careful consideration of the team's strengths and weaknesses influenced design decisions. Braking and nose gear systems built in-house had not fared well in the past, leading to the decision to buy rather than build. The team's industry advisors and faculty advisor provided tremendous insight and wisdom throughout the development of the aircraft. Their expertise allowed the team to provide a better design analysis and more effective execution of construction methods while the students did the majority of the design and construction.

More detailed analysis also helped *Tsunami* to fly. The thorough and detailed analysis of alternative configurations led to a well-informed decision on the final configuration. Temperature modeling aided in the detailed design process. Thrust tests led to the improvement in the mission model and substantially increased the accuracy of its predictions.

Finally, the skill and hard work of the team members enabled the construction of the plane. Without their sacrifices and hard work USC's Aero Design Team would not have a plane this year.

Improvements for Succeeding Years

Timing makes up the single biggest area of future improvement. More detailed and realistic scheduling would reduce time pressure and the mistakes it inevitably brings. Rearranging certain tasks would also help. The mission model development effort in particular held back the team's progress this year by several months. Having it completed over the summer instead of by late November would allow for much more detailed analysis during the early design stages and also permit construction to start earlier. Shortening the series of introductory lectures and combining them with the general design effort would both save time and make them more relevant. Reducing fuselage construction time by eliminating the construction of a fiberglass mold forms another area for future improvement. Also, having a more organized laboratory would reduce time wasted looking for tools.

The analysis spreadsheet still needs improvement. Its weights model relied heavily on fudge factors and did not specifically estimate joiner weight. Earlier estimation of the center of gravity would aid in the design process.

The financial aspect of this effort needs improvement. The team's faculty advisor also acted as the team's treasurer, a post better filled by a student. More careful attention to cost control would allow more team members to attend the contest, spreading enthusiasm and rewarding hard work. Building a team website would help find prospective sponsors and keep our existing ones happy.

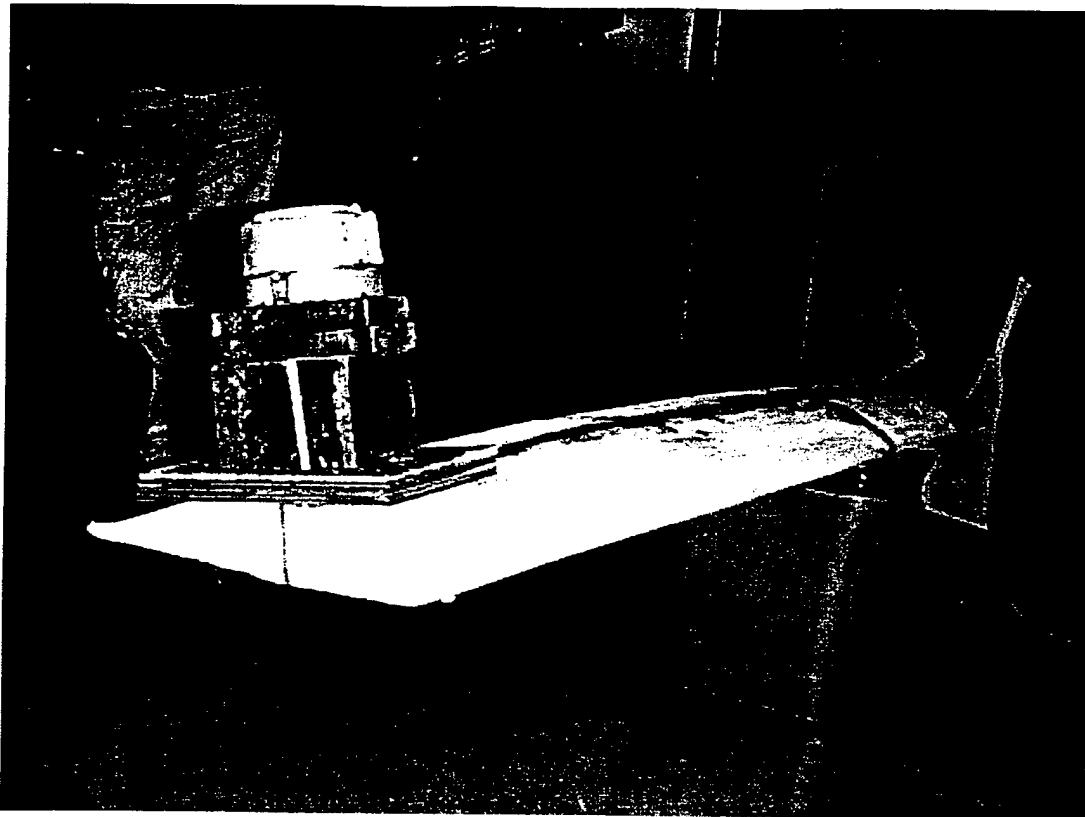


Figure 1.1.1 Wing loading test with weight centered over wing spar

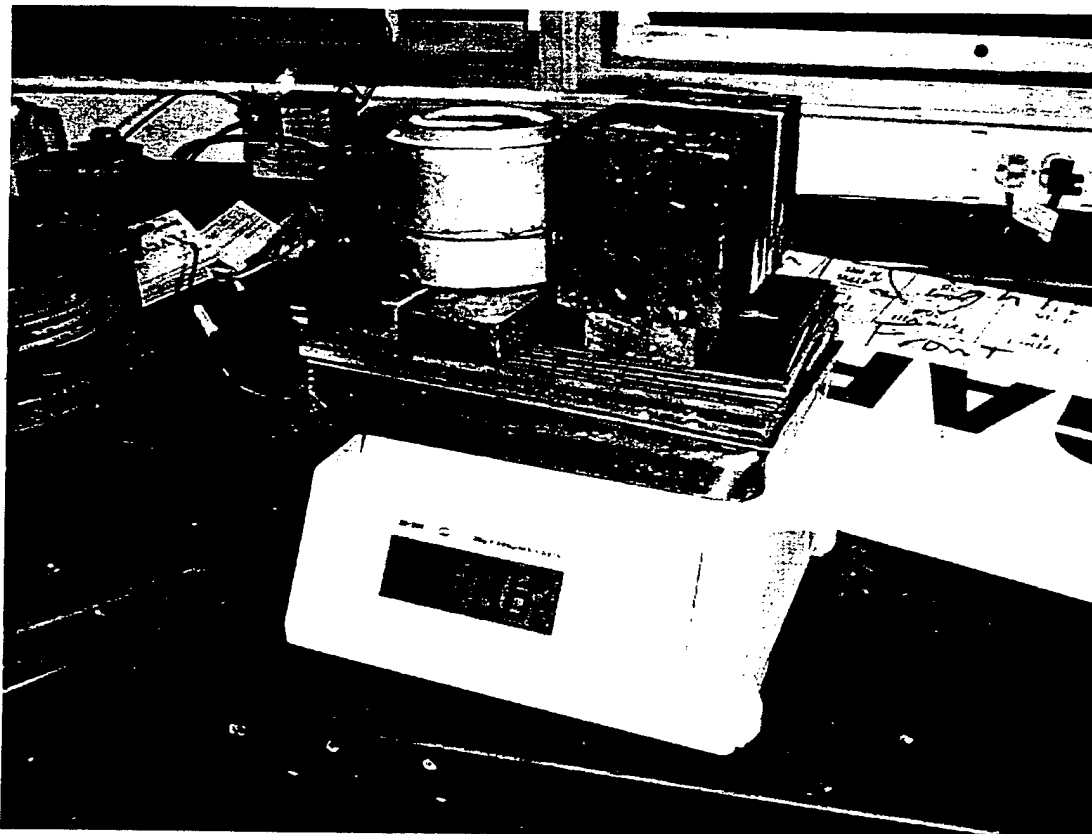


Figure 1.1.2 Measurement of test weight

Actual Weight C.G.

Actual Weight C.G.

Weight (excl wing & pay + 50% tail pad) (lbs)	15.33	Weight (excl wing & pay + 50% tail pad) (lbs)	14.41
Moment (excl wing & pay + 50% tail pad) (in-lbs)	366.30	Moment (excl wing & pay + 50% tail pad) (in-lbs)	296.72
X C.G. with 50% tail pad	23.89	X C.G. with 50% tail pad	20.59
X C.G. with NO tail pad	21.62	X C.G. with NO tail pad	19.10

MAC =	15.15	MAC =	15.15
Target C.G. =	30.00%	Target C.G. =	30.00%
required XLEmac with tail pad =	15.15	required XLEmac with tail pad =	15.15
Empty Weight (no tail pad)	17.01	Empty Weight (no tail pad)	16.58
Payload Weight	20.60	Payload Weight	20.60
Gross Weight (no tail pad)	37.61	Gross Weight (no tail pad)	37.18

Figure 1.2 Values for predicted and actual weights and C.G. location

Weights Comparison

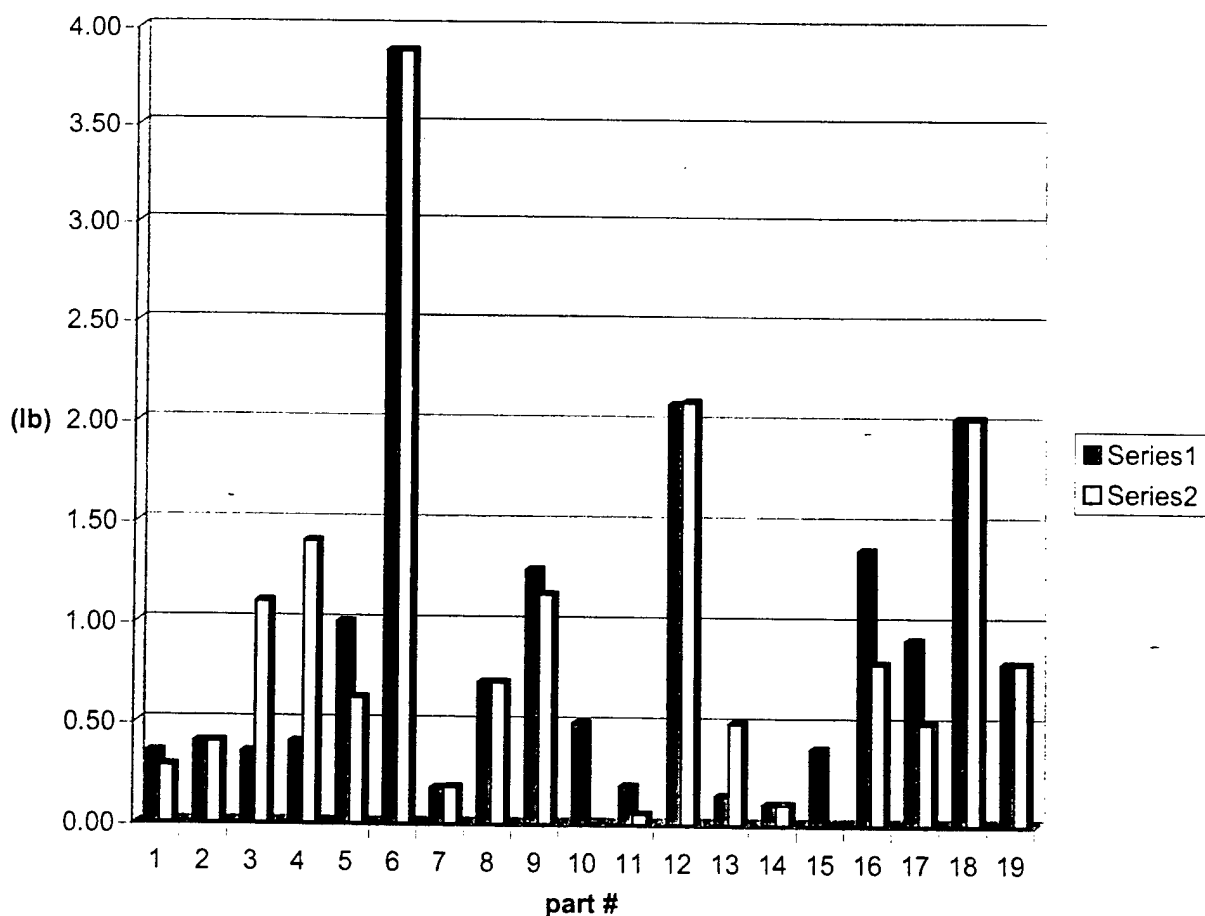


Figure 1.3.1 Graph of predicted weights (green) & actual weights (yellow)

part #	Parts	C.G. Distance from nose cone (in)	Predicted Weight (lb)	Actual Weight (lb)	Predicted Moment (in-lb)	Actual Moment (in-lb)
1	Propeller	0.75	0.35	0.28	0.26	0.21
2	servo for n	8.75	0.40	0.40	3.50	3.50
3	Nosegear	6.50	0.35	1.50	2.28	7.15
4	Main Wheel	23.00	0.10	1.50	9.20	32.20
5	Horseshoe	23.00	1.00	0.62	23.00	14.26
6	batteries	11.25	3.88	4.50	43.65	43.65
7	receiver an	11.25	0.18	0.50	1.97	2.03
8	receiver ba	12.50	0.70	0.70	8.75	8.75
9	motor	4.50	1.26	1.70	5.68	5.13
10	brakes and	23.50	0.50	0.50	11.75	0.24
11	compressor	31.25	0.10	0.10	5.86	1.56
12	fuselage	33.25	2.09	3.50	69.43	69.83
13	speed cont	11.00	0.14	0.50	1.54	5.50
14	wiring	9.50	0.10	0.10	0.95	0.95
15	spinner	0.01	0.38	0.00	0.00	0.00
16	horizontal t	53.25	1.36	1.10	72.60	42.60
17	vertical tail	50.50	0.92	0.80	46.39	25.25
18	Wing		2.02	3.10		
19	Wing Servos		0.80	0.80		
	Payload		19.60	19.60		

Figure 1.3.2 Table of predicted weights (green) & actual weights (yellow)

Aircraft Cost

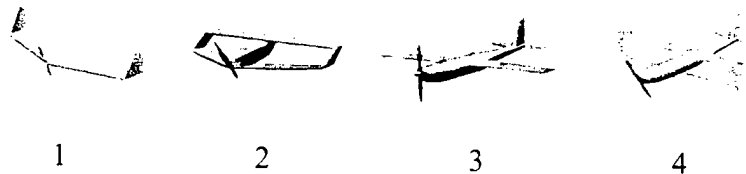
Rated aircraft cost played an important role in this year's contest. The primary goal of maximizing the total competition score required minimizing the rated cost of the aircraft. The rules caused these design parameters to affect the cost of the aircraft:

- a. Empty Weight
- b. Number of Motors
- c. Number of Propellers
- d. Number of Battery Cells
- e. Number of Wings
- f. Wing Projected Area
- g. Number of Fuselages
- h. Fuselage Length
- i. Number of Vertical Tails
- j. Number of Horizontal Tails
- k. Number of Servos.

Minimizing the aircraft's rated cost became an important part of the entire design and manufacturing process.

The conceptual design process estimated the rated cost of four different aircraft configurations:

1. Flying wing
2. Joined wing
3. Conventional monoplane
4. Conventional biplane



The conventional monoplane ultimately surpassed the other configuration models with the most cost-effective configuration for this particular mission. Figure 2.1 shows the comparison among the different configurations considered. The basic cost structures (i.e. cost parameter b, c, e, g and j) were discussed after this initial down-select process.

The finalizing of the aircraft's dimensions with the preliminary design down-select allowed the refinement of the cost model. The cost parameters that did not influence the down-select process (i.e. cost parameter a, d, f, h and k) varied throughout the remaining stages of the aircraft development. However, the cost may have possibly changed due to the construction methods used for the aircraft components. For example, the weight of the aircraft may exceed the predicted weight, making the rated cost increase in consequence. Therefore, further analysis and calculations of the cost were required during construction to give good estimates of the true performance of the aircraft. Figure 2.2 shows a component-wise cost comparison of *Tsunami* as designed and as built. The

main concern was the total aircraft weight. The ultimate empty weight of *Tsunami* measured approximately 5.7 lb. more than the predicted value. This instituted a 7.2% increase in rated cost, where the predicted cost increased from 5.73 to 6.14.

After *Tsunami's* maiden flight on April 2, 2000, a comparison between the performance of the aircraft in real flight conditions and the predicted flight performance showed more possible cost reductions. These included:

1. Weight --- cut out unstructured or unwanted weights from the fuselage (expected 0.8 lb less)
2. Number of Battery Cells --- increase or decrease the number of battery cells according to flight conditions and strategies applied at the competition (32 cells ~ 36 cells)
3. Wing Projected Area --- adding TEXs (Wing Trailing Edge Extensions) to help in fulfilling the 100 ft. TOFL limitation

Fig 2.3 shows the predicted final cost table for *Tsunami*.

(1) Flying Wing			
# of Wings	1	n.d.	
# of Bodies	1	n.d.	
Body Length	0	ft (enter "0" for no body)	
# of Vertical Tails	0	n.d.	
# of Horizontal Tails	0	n.d.	
# of Servos	4	n.d.	
# of Engines	1	n.d.	
# of Props	1	n.d.	

Parameter	Value	Cost	%Cost
MEW	17.84	\$1,783.67	28.72%
REPWatts	1491.42	\$1,491.42	24.01%
WBS 1.0 Wings	117.80	\$2,356.00	37.93%
WBS 2.0 Bodies	5.00	\$100.00	1.61%
WBS 3.0 Emp.	5.00	\$100.00	1.61%
WBS 4.0 Servos	9.00	\$180.00	2.90%
WBS 5.0 Prop.	10.00	\$200.00	3.22%
Total Manuf Hrs	146.80	\$2,936.00	47.27%
Rated Cost =	6.211	\$6,211.09	100.00%

(2) Jointed Wing			
# of Wings	1	n.d.	
# of Bodies	1	n.d.	
Body Length	1	ft (enter "0" for no body)	
# of Vertical Tails	2	n.d.	
# of Horizontal Tails	1	n.d.	
# of Servos	5	n.d.	
# of Engines	1	n.d.	
# of Props	1	n.d.	

Parameter	Value	Cost	%Cost
MEW	17.39	\$1,739.15	29.65%
REPWatts	1491.42	\$1,491.42	25.42%
WBS 1.0 Wings	77.80	\$1,556.00	26.52%
WBS 2.0 Bodies	9.00	\$180.00	3.07%
WBS 3.0 Emp.	25.00	\$500.00	8.52%
WBS 4.0 Servos	10.00	\$200.00	3.41%
WBS 5.0 Prop.	10.00	\$200.00	3.41%
Total Manuf Hrs	131.80	\$2,636.00	44.93%
Rated Cost =	5.867	\$5,866.58	100.00%

(3) Conventional Monoplane			
# of Wings	1	n.d.	
# of Bodies	1	n.d.	
Body Length	2.8	ft (enter "0" for no body)	
# of Vertical Tails	1	n.d.	
# of Horizontal Tails	1	n.d.	
# of Servos	6	n.d.	
# of Engines	1	n.d.	
# of Props	1	n.d.	

Parameter	Value	Cost	%Cost
MEW	15.51	\$1,550.80	28.82%
REPWatts	1491.42	\$1,491.42	27.72%
WBS 1.0 Wings	59.72	\$1,194.40	22.20%
WBS 2.0 Bodies	16.20	\$324.00	6.02%
WBS 3.0 Emp.	20.00	\$400.00	7.43%
WBS 4.0 Servos	11.00	\$220.00	4.09%
WBS 5.0 Prop.	10.00	\$200.00	3.72%
Total Manuf Hrs	116.92	\$2,338.40	43.46%
Rated Cost =	5.381	\$5,380.62	100.00%

(4) Conventional Biplane			
# of Wings	2	n.d.	
# of Bodies	1	n.d.	
Body Length	5.6	ft (enter "0" for no body)	
# of Vertical Tails	1	n.d.	
# of Horizontal Tails	1	n.d.	
# of Servos	6	n.d.	
# of Engines	1	n.d.	
# of Props	1	n.d.	

Parameter	Value	Cost	%Cost
MEW	15.56	\$1,556.05	28.15%
REPWatts	1491.42	\$1,491.42	26.98%
WBS 1.0 Wings	55.60	\$1,112.00	20.12%
WBS 2.0 Bodies	27.40	\$548.00	9.91%
WBS 3.0 Emp.	20.00	\$400.00	7.24%
WBS 4.0 Servos	11.00	\$220.00	3.98%
WBS 5.0 Prop.	10.00	\$200.00	3.62%
Total Manuf Hrs	124.00	\$2,480.00	44.87%
Rated Cost =	5.527	\$5,527.47	100.00%

Fig. 2.1 Cost comparison of different configurations in Conceptual Design process

Predicted Cost Table (11-30-1999)

Rated Aircraft Cost (A ₁ MEW + B ₁ REP + C ₁ MFHR)/1000		5/32/84983	5/32/84983	5/32/84983
MEW (Manufacturers Empty Weight) (lb.)		12.75	1275.25	22.24%
REP (Rated Engine Power)				
# of Engines				
# of Cells of Battery			2220	38.72%
MFHR (Manufacturing Man Hours)				
WBS1.0 (5hr/wing + 4hr/sq.ft projected area)				
# of wings			46.24	
WBS2.0 (5hr/body + 4hr/ft of length)				
Wing+Wglt Area(ft ²)			10.31	16.13%
# of Fuselages			1	
Fuselage Length (ft)			25.64	8.94%
WBS3.0 (5hr + 5hr/vertical + 10hr/horizontal)				
# of Vertical Tails			1	6.98%
# of Horizontal Tails			1	
WBS4.0 (5hr + 1hr/servo)				
# of Servos			5	3.49%
WBS5.0 (5hr/engine + 5hr/propeller)				
# of Engines			1	3.49%

Fixed Parameters

A (Manufacturers Empty Weight Multiplier) (\$/lb.)	100
B (Rated Engine Power Multiplier) (\$/Watt)	1
C (Manufacturing Cost Multiplier) (\$/hour)	20

Actual Cost Table of Tsunami (03-26-2000)

Rated Aircraft Cost (A ₂ MEW + B ₂ REP + C ₂ MFHR)/1000		6/14/47152	6/14/47152	6/14/47152
MEW (Manufacturers Empty Weight) (lb.)		18.49	1848.67	30.10%
REP (Rated Engine Power)				
# of Engines				
# of Cells of Battery			1920	31.26%
MFHR (Manufacturing Man Hours)				
WBS1.0 (5hr/wing + 4hr/sq.ft projected area)				
# of wings			32	
WBS2.0 (5hr/body + 4hr/ft of length)				
Wing+Wglt Area(ft ²)			11.51	16.62%
# of Fuselages			1	
Fuselage Length (ft)			4.90	8.01%
WBS3.0 (5hr + 5hr/vertical + 10hr/horizontal)				
# of Vertical Tails			1	6.51%
# of Horizontal Tails			1	
WBS4.0 (5hr + 1hr/servo)				
# of Servos			8	4.23%
WBS5.0 (5hr/engine + 5hr/propeller)				
# of Engines			1	3.26%

Fixed Parameters

A (Manufacturers Empty Weight Multiplier) (\$/lb.)	100
B (Rated Engine Power Multiplier) (\$/Watt)	1
C (Manufacturing Cost Multiplier) (\$/hour)	20

Figure 2.2 Cost Table of Predicted (11-30-1999) vs. Actual (3-26-2000)

Tsunami Predicted Final Cost Table 1 (32 cells, without TEX)

Rated Aircraft Cost (AxMEW + BxREP + CxMFHR)/1000						6061.472	6.061472
MEW (Manufacturers Empty Weight) (lb.)				17.69	1768.67		29.18%
REP (Rated Engine Power)				1920	1920		31.68%
	# of Engines	1					
	# of Cells of Battery	32					
MFHR (Manufacturing Man Hours)				118.64	2372.8		39.15%
WBS1.0 (5hr/wing + 4hr/sq.ft projected area)	# of wings	1	51.04			16.84%	
	Wing+Wglt Area(ft^2)	11.51					
WBS2.0 (5hr/body + 4hr/ft of length)	# of Fuselages	1	24.6			8.12%	
	Fuselage Length (ft)	4.90					
WBS3.0 (5hr + 5hr/vertical + 10hr/horizontal)	# of Vertical Tails	1	20			6.60%	
	# of Horizontal Tails	1					
WBS4.0 (5hr + 1hr/servo)	# of Servos	8	13			4.29%	
WBS5.0 (5hr/engine + 5hr/propeller)	# of Engines	1	10			3.30%	

Tsunami Predicted Final Cost Table 1 (32 cells, with TEX)

Rated Aircraft Cost (AxMEW + BxREP + CxMFHR)/1000						6125.472	6.125472
MEW (Manufacturers Empty Weight) (lb.)				17.69	1768.67		28.87%
REP (Rated Engine Power)				1920	1920		31.34%
	# of Engines	1					
	# of Cells of Battery	32					
MFHR (Manufacturing Man Hours)				121.84	2436.8		39.78%
WBS1.0 (5hr/wing + 4hr/sq.ft projected area)	# of wings	1	54.24			17.71%	
	Wing+Wglt Area(ft^2)	12.31					
WBS2.0 (5hr/body + 4hr/ft of length)	# of Fuselages	1	24.6			8.03%	
	Fuselage Length (ft)	4.90					
WBS3.0 (5hr + 5hr/vertical + 10hr/horizontal)	# of Vertical Tails	1	20			6.53%	
	# of Horizontal Tails	1					
WBS4.0 (5hr + 1hr/servo)	# of Servos	8	13			4.24%	
WBS5.0 (5hr/engine + 5hr/propeller)	# of Engines	1	10			3.27%	

Tsunami Predicted Final Cost Table 1 (36 cells, without TEX)

Rated Aircraft Cost (AxMEW + BxREP + CxMFHR)/1000						6301.472	6.301472
MEW (Manufacturers Empty Weight) (lb.)				17.69	1768.67		28.07%
REP (Rated Engine Power)				2160	2160		34.28%
	# of Engines	1					
	# of Cells of Battery	36					
MFHR (Manufacturing Man Hours)				118.64	2372.8		37.65%
WBS1.0 (5hr/wing + 4hr/sq.ft projected area)	# of wings	1	51.04			16.20%	
	Wing+Wglt Area(ft^2)	11.51					
WBS2.0 (5hr/body + 4hr/ft of length)	# of Fuselages	1	24.6			7.81%	
	Fuselage Length (ft)	4.90					
WBS3.0 (5hr + 5hr/vertical + 10hr/horizontal)	# of Vertical Tails	1	20			6.35%	
	# of Horizontal Tails	1					
WBS4.0 (5hr + 1hr/servo)	# of Servos	8	13			4.13%	
WBS5.0 (5hr/engine + 5hr/propeller)	# of Engines	1	10			3.17%	

Fig 2.3 Final cost predictions table